Editors' Suggestion

Averages of *b*-hadron, *c*-hadron, and τ-lepton properties as of 2023

Sw. Banerjee, E. Ben-Haim, F. Bernlochner, E. Bertholet, M. Bona, A. Bozek, C. Bozzi, J. Brodzicka, V. Chobanova, M. Chrzaszcz, U. Egede, M. Gersabeck, P. Goldenzweig, N. Gharbi, L. Grillo, K. Hayasaka, T. Humair, D. Johnson, T. Kuhr, O. Leroy, A. Lusiani, H.-L. Ma, M. Margoni, R. Mizuk, P. Naik, T. Nanut Petric, A. Pereiro Castro, M. Prim, M. Roney, M. Rotondo, O. Schneider, C. Schwanda, A. J. Schwartz, J. Serrano, B Schwartz, A. Soffer, M. Whitehead, and J. Yelton

(Heavy Flavor Averaging Group (HFLAV))

(Received 5 December 2024; accepted 5 June 2025; published 26 January 2026)

This paper reports world averages of measurements of *b*-hadron, *c*-hadron, and τ-lepton properties obtained by the Heavy Flavor Averaging Group using results available before October 2023. In rare cases, significant results obtained several months later are also used. For the averaging, common input parameters used in the various analyses are adjusted (rescaled) to common values, and known correlations are taken into account. The averages include branching fractions, lifetimes, neutral meson mixing parameters, *CP* violation parameters, parameters of semileptonic decays, and Cabibbo-Kobayashi-Maskawa matrix elements.

DOI: 10.1103/x87q-tld5

CONTENTS

I. EXECUTIVE SUMMARY 2
II. INTRODUCTION 6
III. AVERAGING METHODOLOGY 7
A. Treatment of correlated systematic uncertainties 7
B. Treatment of unknown correlations 10
C. Treatment of asymmetric uncertainties 10
D. Splitting uncertainty for an average into components 11
IV. *b*-HADRON PRODUCTION FRACTIONS 11
A. *b*-hadron production fractions in $\Upsilon(4S)$ decays 11
1. Discussion on measurements of f^{+-}/f^{00} 13
B. *b*-hadron production fractions at the $\Upsilon(5S)$ energy 13
C. *b*-hadron production fractions at high energy 15
V. LIFETIMES AND MIXING PARAMETERS OF *b* HADRONS 15
A. *b*-hadron lifetimes 15
1. Overview of lifetime measurements 16
2. B^0 and B^+ lifetimes and their ratio 17
3. B_s^0 lifetimes 18
4. B_c^+ lifetime 22
5. Λ_b^0 and other *b*-baryon lifetimes 23
6. Summary and comparison with theoretical predictions 23
B. Neutral *B*-meson mixing 25
1. B^0 mixing parameters $\Delta\Gamma_d$ and Δm_d 26
2. B_s^0 mixing parameters $\Delta\Gamma_s$ and Δm_s 29
3. *CP* violation in B^0 and B_s^0 mixing 33
4. Mixing-induced *CP* violation in B_s^0 decays 35
VI. SEMILEPTONIC *b* HADRON DECAYS 40
A. Exclusive CKM-favored decays 40
1. $\bar{B} \to D^* \ell^- \bar{\nu}_\ell$ 40
2. $\bar{B} \to D \ell^- \bar{\nu}_\ell$ 44
3. $\bar{B}_s^0 \to D_s^{(*)+} \mu^- \bar{\nu}_\mu$ 46
4. $\bar{B} \to D^{(*)} \pi \ell^- \bar{\nu}_\ell$ 48
5. $\bar{B} \to D^{**} \ell^- \bar{\nu}_\ell$ 48
B. Inclusive CKM-favored decays 51
1. Global analysis of $\bar{B} \to X_c \ell^- \bar{\nu}_\ell$ 51
2. Analysis using E_ℓ and M_X moments 52
3. Analysis using q^2 moments 53
4. Analysis using E_ℓ, M_X and q^2 moments 53
5. Average 53
C. Exclusive CKM-suppressed decays 53
1. $B \to \pi \ell \nu$ branching fraction and q^2 spectrum 54
2. $|V_{ub}|$ from $B \to \pi \ell \nu$ 55
3. $B \to \rho \ell \nu_\ell$ and $B \to \omega \ell \nu_\ell$ branching fraction and q^2 spectrum 56
4. Other exclusive charmless semileptonic *B* decays 57
5. Direct measurements of $|V_{ub}|/|V_{cb}|$ 58
D. Inclusive CKM-suppressed decays 60
1. BLNP 61
2. DGE 62
3. GGOU 63
4. Summary 64
E. Combined extraction of $|V_{ub}|$ and $|V_{cb}|$ 64
F. $B \to D^{(*)} \tau \nu_\tau$ decays 64
VII. DECAYS OF *b*-HADRONS INTO OPEN OR HIDDEN CHARM HADRONS 67
A. Decays of B^0 mesons 69
1. Decays to a single open charm meson 70

Published by the American Physical Society under the terms of the Creative Commons Attribution 4.0 International license. Further distribution of this work must maintain attribution to the author(s) and the published article's title, journal citation, and DOI. Funded by SCOAP³.

2. Decays to two open charm mesons 76
3. Decays to charmonium states 79
4. Decays to charm baryons 83
5. Decays to exotic states 84

B. Decays of B^+ mesons 85
1. Decays to a single open charm meson 85
2. Decays to two open charm mesons 89
3. Decays to charmonium states 92
4. Decays to charm baryons 97
5. Decays to exotic states 97

C. Decays of admixtures of B^0/B^+ mesons 99
1. Decays to two open charm mesons 99
2. Decays to charmonium states 99
3. Decays to exotic states 100

D. Decays of B_s^0 mesons 101
1. Decays to a single open charm meson 101
2. Decays to two open charm mesons 103
3. Decays to charmonium states 104
4. Decays to charm baryons 107

E. Decays of B_c^+ mesons 107
1. Decays to a single open charm meson 107
2. Decays to two open charm mesons 108
3. Decays to charmonium states 109
4. Decays to a B meson 109

F. Decays of b baryons 110
1. Decays to a single open charm meson 110
2. Decays to charmonium states 110
3. Decays to charm baryons 112
4. Decays to exotic states 114

VIII. b-HADRON DECAYS TO CHARMLESS FINAL STATES 114
A. Mesonic decays of B^+ and B^0 mesons 115
B. Baryonic decays of B^+ and B^0 mesons 143
C. Decays of b baryons 148
D. Decays of B_s^0 mesons 155
E. Decays of B_c^+ mesons 163
F. Rare decays of B^0 and B^+ mesons with photons and/or leptons 163
G. CP asymmetries in b-hadron decays 184
H. Polarization measurements in b-hadron decays 195

IX. CHARM MIXING AND CP VIOLATION 199
A. D^0-$\bar{D}^0$ mixing and CP violation 199
1. Introduction 199
2. Input measurements 200
3. Fit results 202
4. Conclusions 206

B. CP asymmetries 210
1. Introduction 210
2. Nuisance asymmetries 210
3. Measurements for charmed mesons 211
4. Measurements for charmed baryons 218
5. Sum rules 219

C. T-odd asymmetries 220
D. Interplay between direct and indirect CP violation 222

X. CHARM DECAYS 226
A. Semileptonic decays 226
1. $D \to P\ell^+\nu_\ell$ decays and $|V_{cq}|$ 226
2. $D \to V\ell^+\nu_\ell$ decays 231
3. $D \to S\ell^+\nu_\ell$ decays 235
4. $D \to A\ell^+\nu_\ell$ decays 236
5. Test of e-μ lepton flavor universality 236

B. Leptonic decays 237
1. Recent experimental results 238
2. $D^+ \to \ell^+\nu_\ell$ decays and $|V_{cd}|$ 238
3. $D_s^+ \to \ell^+\nu_\ell$ decays and $|V_{cs}|$ 239
4. Comparison with other determinations of $|V_{cd}|$ and $|V_{cs}|$ 239
5. Extraction of $D_{(s)}$ meson decay constants 243

C. Hadronic D^0 decays and final state radiation 243
1. Updates to the branching fractions 243
2. Average branching fractions for $D^0 \to K^-\pi^+$, $D^0 \to \pi^+\pi^-$ and $D^0 \to K^+K^-$ 245
3. Average branching fraction for $D^0 \to K^+\pi^-$ 247
4. Consideration of PHOTOS++ 247

D. Excited $D_{(s)}$ mesons 248
E. Excited charmed baryons 257
F. Rare and forbidden decays 261

XI. TAU LEPTON PROPERTIES 268
A. τ mass 268
B. τ lifetime 269
C. Branching fraction fit 269
1. Changes with respect to the previous report 270
2. Differences with respect to the PDG fit 270
3. Fit results 270
4. Equality constraints 270

D. Tests of lepton universality 289
E. Universality-improved values of $\mathcal{B}(\tau \to e\bar{\nu}_e\nu_\tau)$ and $R_{\rm had}$ 291
F. Measurements of $|V_{us}|$ 291
1. $|V_{us}|$ from $\mathcal{B}(\tau \to X_s\nu)$ 291
2. $|V_{us}|$ from $\mathcal{B}(\tau \to K\nu)/\mathcal{B}(\tau \to \pi\nu)$ 292
3. $|V_{us}|$ from $\mathcal{B}(\tau \to K\nu)$ 293
4. Summary of $|V_{us}|$ from τ decays 293

G. Combination of upper limits on τ lepton-flavor-violating branching fractions 294

ACKNOWLEDGMENTS 299
DATA AVAILABILITY 299

I. EXECUTIVE SUMMARY

This paper provides updated world averages of measurements of b-hadron, c-hadron, and τ-lepton properties using results available by September 2023. In a few cases, important results that appeared later are included and are clearly labeled as such. In addition, older results, including those from previous generations of experiments, are still very important and contribute to the averages that we report. Significant additional results are expected in the near future.

Since our previous paper [1], the b-hadron lifetime and mixing averages have been improved both in precision and

in the averaging procedures. In total, new B^0 results from one publication (from Belle II), new B_s^0 results from eight publications (one from ATLAS, three from CMS, and four from LHCb) and new Ξ_b^- results from one publication (from LHCb) have been incorporated into these averages.

The lifetime hierarchy for the most abundant weakly-decaying b-hadron species is well established, with a precision below 10 fs for the meson and Λ_b^0-baryon lifetimes, and is compatible with the expectations from the heavy quark expansion. However, small sample sizes still limit the precision for the lifetimes of the heavier, observed weakly decaying b baryons, namely, Ξ_b^-, Ξ_b^0, and Ω_b. A sizable value of the decay width difference in the B_s^0–$\bar{B}_s^0$ system is measured with a relative precision of 4% and is well predicted by the Standard Model (SM). In contrast, the experimental results for the decay width difference in the B^0–$\bar{B}^0$ system are not yet precise enough to distinguish the small (expected) value from zero. The mass differences in both the B^0–$\bar{B}^0$ and B_s^0–$\bar{B}_s^0$ systems are accurately known, to a few per mil or tenths of per mil, respectively. On the other hand, CP violation in the mixing of either system has not been observed yet. Although measured with uncertainties at the per mil level, the CP asymmetries are still consistent with both zero and their SM predictions. A similar conclusion holds for the CP violation induced by B_s^0 mixing in the $b \to c\bar{c}s$ transition. Many measurements are still dominated by statistical uncertainties, which will improve once new results from the LHC become available, especially from Run 3, and from Belle II.

In exclusive semileptonic b hadron decays, determinations of the CKM elements $|V_{cb}|$ and $|V_{ub}|$ are based on the decays $B \to D^{(*)}\ell\nu$, $B_s \to D_s^{(*)}\mu\nu$, $B \to \pi\ell\nu$, $B_s \to K\mu\nu$ and $\Lambda_b \to p\mu\nu$. A global fit to all exclusive results yields $|V_{cb}| = (39.77 \pm 0.46) \times 10^{-3}$ and $|V_{ub}| = (3.43 \pm 0.12) \times 10^{-3}$. The tension with the determinations from inclusive B meson decays is larger than 3σ for both $|V_{cb}|$ and $|V_{ub}|$. New measurements of $R(D^*)$ and $R(D)$, characterizing semitauonic decays $B \to D^{(*)}\tau\nu_\tau$, have been added to the averages since our previous paper. With respect to the most recent theory calculations for $R(D^*)$ and $R(D)$, the combined tension with the SM expectation persists, at 3.14σ.

We have compiled 717 measurements involving b-hadron decays into states with open or hidden charm from 305 papers by the *BABAR*, Belle, CDF, D0, LHCb, CMS, and ATLAS collaborations into 503 averages. Following the averaging procedures established in our previous paper, correlations among averages are taken into account. The large samples of b hadrons available in current experiments allow precise measurements. In addition to improvements in precision for branching fractions, new decay modes of B mesons and b baryons have been discovered.

Among charmless b-hadron decays, an important update from LHCb is tests of lepton flavor universality in $b \to s\ell^+\ell^-$ transitions. Previously seen anomalies in the measurements of the branching-fraction ratios $R_K = \mathcal{B}(B^+ \to K^+\mu^+\mu^-)/\mathcal{B}(B^+ \to K^+e^+e^-)$ and $R_{K^*} = \mathcal{B}(B^0 \to K^{*0}\mu^+\mu^-)/(B^0 \to K^{*0}e^+e^-)$ have vanished, as updated measurements based on 9 fb^{-1} are compatible with SM prediction at the level of one standard deviation. In contrast, previously seen tensions in the differential branchings fraction and angular observables of $b \to s\ell^+\ell^-$ decays persist. In addition, a handful of new limits on lepton-flavor-violating decays have been set by LHCb and Belle, especially those involving $B^{0,\pm}$ and B_s^0 meson decays into a τ lepton. Among the CP violating observable in rare decays, the "$K\pi$ CP puzzle" persists, and important new results have appeared in two- and three-body decays. LHCb has produced many other results on a wide variety of decays, including those of b-baryons, for example, a first measurement of the photon polarization in $\Lambda_b \to \Lambda\gamma$ decays.

In the area of mixing and CP violation in the charm sector, two highlights are the LHCb observation of dispersive mixing, i.e., a non-zero value for the mixing parameter $x \equiv \Delta M/\bar{\Gamma}$, and a high precision measurement from LHCb of the observable y_{CP}. A total of 63 measurements from LHCb, Belle, *BABAR*, BES III, CLEO-c, CDF, FOCUS, and Fermilab E791 of 18 observables are input into a global fit for 8–10 (depending on theoretical assumptions) mixing and CP violation parameters. From this fit, the no-mixing hypothesis is excluded at a

TABLE 1. Selected world averages. Where two uncertainties are given the first is statistical and the second is systematic.

b-hadron lifetimes	
$\tau(B^0)$	1.517 ± 0.004 ps
$\tau(B^+)$	1.638 ± 0.004 ps
$\tau(B_s^0) = 1/\Gamma_s$	1.516 ± 0.006 ps
$\tau(B_{s\mathrm{L}}^0)$	1.432 ± 0.006 ps
$\tau(B_{s\mathrm{H}}^0)$	1.612 ± 0.008 ps
$\tau(B_c^+)$	0.510 ± 0.009 ps
$\tau(\Lambda_b^0)$	1.468 ± 0.009 ps
$\tau(\Xi_b^-)$	1.578 ± 0.021 ps
$\tau(\Xi_b^0)$	1.477 ± 0.032 ps
$\tau(\Omega_b^-)$	1.64 ± 0.16 ps
B^0 and B_s^0 mixing and CP violation	
Δm_d	0.5069 ± 0.0019 ps^{-1}
$\Delta\Gamma_d/\Gamma_d$	0.001 ± 0.010
$\lvert q_d/p_d \rvert$	1.0010 ± 0.0008
Δm_s	17.766 ± 0.006 ps^{-1}
$\Delta\Gamma_s$	$+0.0781 \pm 0.0035$ ps^{-1}
$\lvert q_s/p_s \rvert$	1.0003 ± 0.0014
$\phi_s^{c\bar{c}s}$	-0.052 ± 0.013 rad

TABLE 2. Selected world averages. Where two uncertainties are given the first is statistical and the second is systematic.

Semileptonic *b*-hadron decay parameters	
$\mathcal{B}(\bar{B}^0 \to D^{*+}\ell^-\bar{\nu}_\ell)$	$(4.90 \pm 0.12)\%$
$\mathcal{B}(B^- \to D^{*0}\ell^-\bar{\nu}_\ell)$	$(5.53 \pm 0.22)\%$
$\mathcal{B}(\bar{B}^0 \to D^{+}\ell^-\bar{\nu}_\ell)$	$(2.12 \pm 0.06)\%$
$\mathcal{B}(B^- \to D^{0}\ell^-\bar{\nu}_\ell)$	$(2.21 \pm 0.06)\%$
$\mathcal{B}(\bar{B}^0 \to \pi^{+}\ell^-\bar{\nu}_\ell)$	$(1.50 \pm 0.05) \times 10^{-4}$
$\lvert V_{cb}\rvert$ from exclusive B, B_s and Λ_b decays	$(39.77 \pm 0.46) \times 10^{-3}$
$\lvert V_{ub}\rvert$ from exclusive B, B_s and Λ_b decays	$(3.43 \pm 0.12) \times 10^{-3}$
$\mathcal{B}(\bar{B} \to X_c\ell^-\bar{\nu}_\ell)$	$(10.63 \pm 0.15)\%$
$\mathcal{B}(\bar{B} \to X\ell^-\bar{\nu}_\ell)$	$(10.82 \pm 0.15)\%$
$\lvert V_{cb}\rvert$ from inclusive B decays	$(41.97 \pm 0.48) \times 10^{-3}$
$\lvert V_{ub}\rvert$ from inclusive B decays	$(4.06 \pm 0.16) \times 10^{-3}$
$\mathcal{R}(D) = \mathcal{B}(B \to D\tau\nu_\tau)/\mathcal{B}(B \to D\ell\nu_\ell)$	0.342 ± 0.026
$\mathcal{R}(D^*) = \mathcal{B}(B \to D^*\tau\nu_\tau)/\mathcal{B}(B \to D^*\ell\nu_\ell)$	0.286 ± 0.012
***b*-hadron decays to charmed hadrons**	
$\mathcal{B}(B^0 \to D^-\pi^+)$	$(2.48 \pm 0.12) \times 10^{-3}$
$\mathcal{B}(B^+ \to \bar{D}^0\pi^+)$	$(4.67 \pm 0.12) \times 10^{-3}$
$\mathcal{B}(B_s^0 \to D_s^-\pi^+)$	$(2.83 \pm 0.18) \times 10^{-3}$
$\mathcal{B}(\Lambda_b^0 \to \Lambda_c^+\pi^-)$	$(4.18 \pm 0.30) \times 10^{-3}$
$\mathcal{B}(B^0 \to J/\psi K^0)$	$(0.883 \pm 0.020) \times 10^{-3}$
$\mathcal{B}(B^+ \to J/\psi K^+)$	$(1.018 \pm 0.018) \times 10^{-3}$
$\mathcal{B}(B_s^0 \to J/\psi \phi)$	$(1.060 \pm 0.090) \times 10^{-3}$
$\mathcal{B}(\Lambda_b^0 \to J/\psi \Lambda^0)$	$(0.47 \pm 0.29) \times 10^{-3}$
$\mathcal{B}(B_c^+ \to J/\psi D_s^+)/\mathcal{B}(B_c^+ \to J/\psi \pi^+)$	3.09 ± 0.55
***b*-hadron decays to charmless final states**	
$\mathcal{B}(B \to X_s\gamma)$ $(E_\gamma > 1.6$ GeV)	$(3.49 \pm 0.19) \times 10^{-4}$
$R_K = \mathcal{B}(B^+ \to K^+\mu^+\mu^-)/\mathcal{B}(B^+ \to K^+e^+e^-)$ in $1.1 < m^2_{\ell^+\ell^-} < 6.0$ GeV$^2/c^4$	0.947 ± 0.47
$R_{K^*} = \mathcal{B}(B^0 \to K^{*0}\mu^+\mu^-)/\mathcal{B}(B^0 \to K^{*0}e^+e^-)$ in $1.1 < m^2_{\ell^+\ell^-} < 6.0$ GeV$^2/c^4$	1.028 ± 0.074
$A_{CP}(B^0 \to K^+\pi^-)$	-0.0836 ± 0.0032
$A_{CP}(B^+ \to K^+\pi^0)$	0.027 ± 0.013
$A_{CP}(B_s^0 \to K^-\pi^+)$	0.224 ± 0.012
$\mathcal{B}(B^0 \to \mu^+\tau^- + \text{c.c.})$	$< 12 \times 10^{-6}$ (CL = 90%)
$\mathcal{B}(B^0 \to e^+\tau^- + \text{c.c.})$	$< 16 \times 10^{-6}$ (CL = 90%)
$\mathcal{B}(B_s^0 \to \phi\mu^+\mu^-)$	$8.38^{+0.42}_{-0.41} \times 10^{-7}$
Observables in $B^0 \to K^{*0}\mu^+\mu^-$ decays in bins of $q^2 = m^2(\mu^+\mu^-)$	See Sec. VIII F

confidence level above 11σ. The value $x = 0$ is excluded with a statistical significance of 9.1σ. For the mixing parameter $y \equiv \Delta\Gamma/2\bar{\Gamma}$, the value $y = 0$ is excluded with a significance of 35σ, and the precision on y is improved by a factor of two from that of our previously published result [1]. The world average value for y is positive, indicating that the CP-even state has a shorter lifetime than the CP-odd state; this is similar to the K^0–$\bar{K}^0$ system. However, $x > 0$ and thus the CP-even state is heavier, in contrast to the K^0–$\bar{K}^0$ system. The CP violation parameters $|q/p|$ and ϕ are compatible with CP symmetry at the level of 2.1σ. Thus, there is no evidence yet for *indirect* CP violation arising from mixing ($|q/p| \neq 1$) or from a phase difference between the mixing amplitude and a direct decay amplitude ($\phi \neq 0$). Measurements of the time-integrated CP asymmetries in $D^0 \to K^+K^-/\pi^+\pi^-$ decays give $\Delta a_{CP}^{\text{dir}} = (-0.159 \pm 0.029)\%$. This value is similar to our previously published result [1], which established direct CP violation in singly Cabibbo-suppressed decays. For $D^0 \to \pi^+\pi^-$ decays, although the precision of the measured

TABLE 3. Selected world averages. Where two uncertainties are given the first is statistical and the second is systematic.

D^0 mixing and CP violation	
x	$(0.41 \pm 0.04)\%$
y	$(0.65 \pm 0.02)\%$
$\delta_{K\pi}$	$(11.4^{+3.5}_{-3.8})^\circ$
A_D	$(-0.77 \pm 0.35)\%$
$\lvert q/p \rvert$	0.994 ± 0.016
ϕ	$(-2.6 \pm 1.2)^\circ$
x_{12} (no direct CP violation in CF/DCS decays)	$(0.41 \pm 0.04)\%$
y_{12} (no direct CP violation in CF/DCS decays)	$(0.64 \pm 0.02)\%$
ϕ_{12} (no direct CP violation in CF/DCS decays)	$(0.65 \pm 0.91)^\circ$
ϕ_2^M (no direct CP violation in CF/DCS decays)	$(0.48 \pm 0.92)^\circ$
ϕ_2^Γ (no direct CP violation in CF/DCS decays)	$(2.4 \pm 1.5)^\circ$
a_{CP}^{ind}	$(-0.010 \pm 0.012)\%$
$\Delta a_{CP}^{\text{dir}}$	$(-0.159 \pm 0.029)\%$
Charm meson (semi-)leptonic decays	
f_D	(205.1 ± 4.4) MeV
f_{D_s}	(252.2 ± 2.5) MeV
$\lvert V_{cd} \rvert$	0.2208 ± 0.0040
$\lvert V_{cs} \rvert$	0.9701 ± 0.0081
Charm meson hadronic decays	
$\mathcal{B}(D^0 \to K^-\pi^+)$	$(3.999 \pm 0.006 \pm 0.031 \pm 0.032_{\text{FSR}})\%$
$\mathcal{B}(D^0 \to K^+\pi^-)/\mathcal{B}(D^0 \to K^-\pi^+)$	$(0.344 \pm 0.002)\%$
τ parameters, lepton universality, and $\lvert V_{us} \rvert$	
g_τ/g_μ	1.0016 ± 0.0014
g_τ/g_e	1.0018 ± 0.0014
g_μ/g_e	1.0002 ± 0.0011
$\mathcal{B}_e^{\text{uni}}$	$(17.815 \pm 0.023)\%$
$R_{\text{had}}^{\text{uni}}$	3.634 ± 0.008
$\lvert V_{us} \rvert_{\tau\text{-OPE-1}}$ using $\mathcal{B}(\tau^- \to X_s\nu_\tau)$ and OPE	0.2184 ± 0.0021
$\lvert V_{us} \rvert_{\tau\text{-latt-incl}}$ using $\mathcal{B}(\tau^- \to X_s\nu_\tau)$ and lattice QCD	0.2189 ± 0.0019
$\lvert V_{us} \rvert$ using $\mathcal{B}(\tau^- \to K^-\nu_\tau)/\mathcal{B}(\tau^- \to \pi^-\nu_\tau)$	0.2229 ± 0.0019
$\lvert V_{us} \rvert/\lvert V_{ud} \rvert$ using $\mathcal{B}(\tau^- \to K^-\nu_\tau)/\mathcal{B}(\tau^- \to \pi^-\nu_\tau)$	0.2289 ± 0.0019
$\lvert V_{us} \rvert$ using $\mathcal{B}(\tau^- \to K^-\nu_\tau)$	0.2224 ± 0.0017
$\lvert V_{us} \rvert$ τ average	0.2208 ± 0.0014

CP asymmetry has improved by more than a factor of two, the impact on an $SU(3)$ sum rule for $D \to \pi\pi$ decays is small. The sum rule remains compatible with zero at a precision of 0.3%.

The most precise measurements of $|V_{cd}|$ and $|V_{cs}|$ are obtained from leptonic $D^+ \to \mu^+\nu$ and $D_s^+ \to \mu^+\nu/\tau^+\nu$ decays, respectively. These measurements have theoretical uncertainties that arise from calculations of the decay constants. However, thanks to improvements in lattice QCD calculations, the theory uncertainties are below ~20% of the experimental uncertainties. Averages of the branching fractions for the decays $D^0 \to K^-\pi^+$, $D^0 \to K^+K^-$, and $D^0 \to \pi^+\pi^-$ must treat final state radiation correctly and consistently across measurements for the accuracy of the averages to match the measurement precision. We update the measurements to account for improvements in the simulation of final state radiation (e.g. interference between photons radiated from the two charged particles).

Our average of the τ mass includes the recent measurements from the Belle II and KEDR collaborations. In the τ branching fraction fit, the recent Belle II measurement of the ratio of the branching fractions for $\tau^- \to \mu^-\bar{\nu}_\mu\nu_\tau$ and $\tau^- \to e^-\bar{\nu}_e\nu_\tau$ has been added. The newly added measurements slightly improve the precision of the lepton universality tests. Furthermore, the modeling of the branching

fraction $\mathcal{B}(\tau^- \to a_1^-(\pi^-\gamma)\nu_\tau)$ has been improved, with a nuisance fit parameter for the branching fraction $\mathcal{B}(a_1^- \to \pi^-\gamma)$. Upper limits on lepton flavor violating τ decays are presented. These upper limits are combined for channels in which searches from multiple experimental efforts have similar sensitivities.

A small selection of highlights of the results described in Secs. V–XI are given in Tables 1–3.

II. INTRODUCTION

Flavor dynamics plays an important role in elementary particle interactions. The accurate knowledge of properties of heavy flavor hadrons, especially b hadrons, plays an essential role in determination of the elements of the Cabibbo-Kobayashi-Maskawa (CKM) quark-mixing matrix [2,3]. The operation of the Belle and *BABAR* e^+e^- B factory experiments led to a large increase in the size of available B-meson, D-hadron, and τ-lepton samples, enabling dramatic improvement in the accuracies of related measurements. The CDF and D0 experiments at the Fermilab Tevatron have also provided important results in heavy flavor physics, most notably in the B_s^0 sector. In the D-meson sector, the dedicated e^+e^- charm factory experiments CLEO-c and BESIII have made significant contributions. Run I and Run II of the CERN Large Hadron Collider delivered high luminosity, enabling the collection of even larger samples of b and c hadrons, and thus a further leap in precision in many areas, at the ATLAS, CMS, and (especially) LHCb experiments. With ongoing analyses of the LHC Run II data, further improvements are anticipated.

The Heavy Flavor Averaging Group (HFLAV)[1] was formed in 2002 to continue the activities of the LEP Heavy Flavor Steering Group [4], which was responsible for calculating averages of measurements of b-flavor related quantities. HFLAV has evolved since its inception and currently consists of seven subgroups:

(i) the "B lifetime and oscillations" subgroup provides averages for b-hadron lifetimes and various parameters governing B^0–$\bar{B}^0$ and B_s^0–$\bar{B}_s^0$ mixing and CP violation;
(ii) the "unitarity triangle angles" subgroup provides averages for parameters associated with time-dependent CP asymmetries and $B \to DK$ decays, and resulting determinations of the angles of the CKM unitarity triangle[2];
(iii) the "semileptonic B decays" subgroup provides averages for inclusive and exclusive measurements of B-decay branching fractions, and subsequent determinations of the CKM matrix element magnitudes $|V_{cb}|$ and $|V_{ub}|$;
(iv) the "B to charm decays" subgroup provides averages of branching fractions for b-hadron decays to final states involving open charm or charmonium mesons, as well as branching fractions for b-hadron production in $\Upsilon(4S)$ and $\Upsilon(5S)$ decays;
(v) the "rare b decays" subgroup provides averages of branching fractions, CP asymmetries and other observables for charmless, radiative, leptonic, and baryonic B-meson and b-baryon decays;
(vi) the "charm CP violation and oscillations" subgroup provides averages of mixing, CP-, and T-violation parameters in the D^0–$\bar{D}^0$ system;
(vii) the "charm decays" subgroup provides averages of charm-hadron branching fractions, properties of excited D^{**} and D_{sJ} mesons, properties of charm baryons, and the D^+ and D_s^+ decay constants f_D and f_{D_s};
(viii) the "tau physics" subgroup provides averages for τ branching fractions using a global fit, elaborates on the results to test lepton universality and to determine the CKM matrix element magnitude $|V_{us}|$, and lists and combines branching-fraction upper limits for τ lepton-flavor-violating decays.

Subgroups consist of representatives from experiments producing relevant results in that area, i.e., representatives from *BABAR*, Belle, Belle II, BESIII, LHCb, ATLAS, and CMS.

This article is an update of the last HFLAV publication, which used results available by March 2021 [1]. Here we report world averages using results available by September 2023. In some cases, important new results made available later are included where possible. In general, we use all publicly available results, including preliminary results that are supported by written documentation, such as conference proceedings or publicly available reports from the collaborations. However, we do not use preliminary results that remain unpublished for an extended period of time, or for which no publication is planned. Since HFLAV members are also members of the different collaborations, we exploit our close contact with analyzers to ensure that the results are prepared in a form suitable for combinations.

Section III describes the methodology used for calculating averages. In the averaging procedure, common input parameters used in the various analyses are adjusted (rescaled) to common values, and, where possible, known correlations are taken into account. Sections V–XI present world average values from each of the subgroups listed above. A complete listing of the averages and plots, including updates since this document was prepared, is available on the HFLAV web site [5].

[1]The group was originally known by the acronym "HFAG." Following feedback from the community, this was changed to HFLAV in 2017.

[2]Results from the unitarity triangle angles group have not been updated for this iteration. See Ref. [1] for the latest update.

III. AVERAGING METHODOLOGY

The main task of HFLAV is to combine independent but possibly correlated measurements of a parameter to obtain the world's best estimate of that parameter's value and uncertainty. These measurements are typically made by different experiments, or by the same experiment using different datasets, or by the same experiment using the same data but with different analysis methods. In this section, the general approach adopted by HFLAV is outlined. The software used to provide this is either the COMBOS package [6], the HFLAVAVERAGING package [7] or dedicated tools for some averages.

Our methodology focuses on the problem of combining measurements obtained with different assumptions about external (or "nuisance") parameters and with potentially correlated systematic uncertainties. Unless otherwise noted, we assume for our combinations that the quantities measured by experiments were performed in the asymptotic regime (large data samples), so that the measured estimates have a (one- or multi-dimensional) Gaussian likelihood function. We use $\boldsymbol{x}$ to represent a set of n parameters and $\boldsymbol{x}_i$ to denote the ith set of measurements of those parameters. The covariance matrix for the measurement is $\boldsymbol{V}_i$. In all fits, we ensure that $\boldsymbol{x}$ and $\boldsymbol{x}_i$ do not contain redundant information, i.e., they are vectors with n elements that represents exactly n parameters. A χ^2 statistic is constructed as

$$\chi^2(\boldsymbol{x}) = \sum_i^N (\boldsymbol{x}_i - \boldsymbol{x})^{\mathrm{T}} \boldsymbol{V}_i^{-1} (\boldsymbol{x}_i - \boldsymbol{x}), \tag{1}$$

where the sum is over the N independent determinations of the quantities $\boldsymbol{x}$, typically coming from different experiments. This is the best linear unbiased estimator with minimum variance [8] The results of the average are the central values $\hat{\boldsymbol{x}}$, which are the values of $\boldsymbol{x}$ at the minimum of $\chi^2(\boldsymbol{x})$, and their covariance matrix

$$\hat{\boldsymbol{V}}^{-1} = \sum_i^N \boldsymbol{V}_i^{-1}, \tag{2}$$

which is a generalization of the one-dimensional estimate $\sigma^{-2} = \sum_i \sigma_i^{-2}$.

The value of $\chi^2(\hat{\boldsymbol{x}})$ provides a measure of the consistency of the independent measurements of $\boldsymbol{x}$ after accounting for the number of degrees of freedom (dof), which is the difference $N - n$ between the number of measurements and the number of fitted parameters. The values of $\chi^2(\hat{\boldsymbol{x}})$ and dof are typically converted to a p-value and reported together with the averages. Unlike the Particle Data Group [9], when $\chi^2/\mathrm{dof} > 1$ we do not by default scale the resulting uncertainty. Rather, we examine the systematic uncertainties of each measurement to better understand potential sources of the discrepancy.

In many cases, publications do not quote a direct measurement of a parameter of interest, but of a quantity that is a function of multiple parameters. An example is the measurement of a ratio of branching fractions, from which a branching fraction of interest is determined using previous (and usually more precise) knowledge of the branching fraction of a "normalization mode." This leads to a correlation between the determinations of the two branching fractions that appear in the ratio. In addition, if the same normalization mode is used for measurements of different branching fraction ratios, they too become correlated. These correlations can be evaluated by performing a simultaneous fit to all averages involved. This is done by generalizing Eq. (1) to the form

$$\chi^2(\boldsymbol{p}) = \sum_i^N (\boldsymbol{f}_i(\boldsymbol{p}) - \boldsymbol{x}_i)^{\mathrm{T}} \boldsymbol{V}_i^{-1} (\boldsymbol{f}_i(\boldsymbol{p}) - \boldsymbol{x}_i), \tag{3}$$

where $\boldsymbol{p}$ are the fit parameters, including the quantities whose averages we want to determine, $\boldsymbol{x}_i$ is the set of ith measurements (e.g., of branching fractions and branching-fraction ratios), and $\boldsymbol{f}_i$ is the dependence of the measured quantities $\boldsymbol{x}_i$ on the parameters $\boldsymbol{p}$. This procedure is used for branching-fraction and related averages in Secs. VII and VIII. An alternative approach, used in Sec. XI C, is to construct the χ^2 as in Eq. (1) and minimize it subject to a list of constraints implemented with Lagrange multipliers. The two approaches are essentially identical, except that the covariance matrix is given in terms of $\boldsymbol{p}$ in the former and in terms of $\boldsymbol{x}_i$ in the latter.

If a special treatment is necessary in order to calculate an average, or if an approximation used in the calculation might not be sufficiently accurate (e.g., assuming Gaussian uncertainties when the likelihood function exhibits non-Gaussian behavior), we point this out. Further modifications to the averaging procedures for non-Gaussian situations are discussed in Sec. III C.

A. Treatment of correlated systematic uncertainties

Consider two hypothetical measurements of a parameter x, which can be summarized as

$$x_1 \pm \delta x_1 \pm \Delta x_{1,1} \pm \Delta x_{1,2} \ldots$$
$$x_2 \pm \delta x_2 \pm \Delta x_{2,1} \pm \Delta x_{2,2} \ldots,$$

where the δx_k are statistical uncertainties and the $\Delta x_{k,i}$ are contributions to the systematic uncertainty. The simplest approach is to combine statistical and systematic uncertainties in quadrature

$$x_1 \pm (\delta x_1 \oplus \Delta x_{1,1} \oplus \Delta x_{1,2} \oplus \ldots)$$
$$x_2 \pm (\delta x_2 \oplus \Delta x_{2,1} \oplus \Delta x_{2,2} \oplus \ldots),$$

and then perform a weighted average of x_1 and x_2 using their combined uncertainties, treating the measurements as

independent. This approach suffers from two potential problems that we try to address. First, the values x_k may have been obtained using different assumptions for nuisance parameters; e.g., different values of the B^0 lifetime may have been used for different measurements of the oscillation frequency Δm_d. The second potential problem is that some systematic uncertainties may be correlated between measurements. For example, different measurements of Δm_d may depend on the same branching fraction used to model a common background.

The above two problems are related. We can represent the systematic uncertainties as a set of nuisance parameters y_i upon which x_k depends. The uncertainty Δy_i, which is the uncertainty on y_i coming from external measurements, contributes $\Delta x_{k,i}$ to the systematic uncertainty on x_i. We thus use the values of y_i and Δy_i assumed by each measurement in our averaging. To properly treat correlated systematic uncertainties among measurements, requires decomposing the overall systematic uncertainties into correlated and uncorrelated components. Correlated systematic uncertainties are those that depend on a shared nuisance parameter, e.g. a lifetime as mentioned above; uncorrelated systematic uncertainties do not share a nuisance parameter, e.g. the statistical uncertainty resulting from independent limited size simulations of background components. As different measurements often quote different types of systematic uncertainties, achieving consistent definitions in order to properly treat correlations requires close coordination between HFLAV and the experiments. In some cases, a group of systematic uncertainties must be combined into a coarser description in order to obtain an average that is consistent among measurements. Systematic uncertainties that are uncorrelated with any other source of uncertainty are combined together with the statistical uncertainty, so that the only systematic uncertainties treated explicitly are those that are correlated with at least one other measurement via a consistently-defined external parameter y_i.

The fact that a measurement of x is sensitive to y_i indicates that, in principle, the data used to measure x could also be used for a simultaneous measurement of x and y_i. This is illustrated by the large contour in Fig. 1(a). However, there often exists an external measurement of y_i with uncertainty Δy_i [represented by the horizontal band in Fig. 1(a)] that is more precise than the constraint $\sigma(y_i)$ from the x data alone. In this case, the results presented in a publication can be from a simultaneous fit to x and y_i, including the external measurement as a constraint, and obtain the filled (x, y) contour and dashed one-dimensional estimate of x shown in Fig. 1(a). We call the fit without the external measurement *unconstrained*, and the fit that include the external measurement is referred to as *constrained*.

To combine two or more measurements that share a systematic uncertainty due to the same external

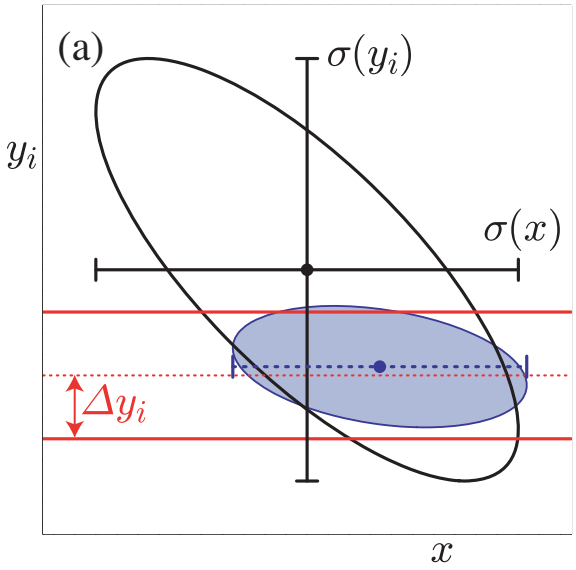


FIG. 1. Illustration of the possible dependence of a measured quantity x on a nuisance parameter y_i. The plot compares the 68% confidence level contours of a hypothetical measurement's unconstrained (large ellipse) and constrained (filled ellipse) likelihoods, using the Gaussian constraint on y_i represented by the horizontal band. The solid error bars represent the statistical uncertainties $\sigma(x)$ and $\sigma(y_i)$ of the unconstrained likelihood. The dashed error bar shows the statistical uncertainty on x from a constrained simultaneous fit to x and y_i.

parameter(s) y_i, the optimal solution is to take the unconstrained results from the publications and perform a constrained simultaneous fit of all measurements to obtain values of x and y_i. Let us consider two statistically-independent measurements, $x_1 \pm (\delta x_1 \oplus \Delta x_{1,i})$ and $x_2 \pm (\delta x_2 \oplus \Delta x_{2,i})$, of the quantity x as shown in Figs. 2(a) and 2(b). For simplicity we consider only one correlated systematic uncertainty for each external parameter y_i. Since the publications were made, our knowledge of y_i will often have improved, causing the measurements of x to shift to different central values and have different uncertainties.

If the unconstrained likelihoods $\mathcal{L}_k(x, y_1, y_2, \ldots)$ for each of the measurements are available, the exact method is to minimize the simultaneous likelihood

$$\mathcal{L}_{\text{comb}}(x, y_1, y_2, \ldots) \equiv \prod_k \mathcal{L}_k(x, y_1, y_2, \ldots) \prod_i \mathcal{L}_i(y_i), \quad (4)$$

with an independent Gaussian constraint

$$\mathcal{L}_i(y_i) = \exp\left[-\frac{1}{2}\left(\frac{y_i - y_i'}{\Delta y_i'}\right)^2\right] \quad (5)$$

for each y_i.

However, most publications do not include the full likelihood, in which case we use an approximate method

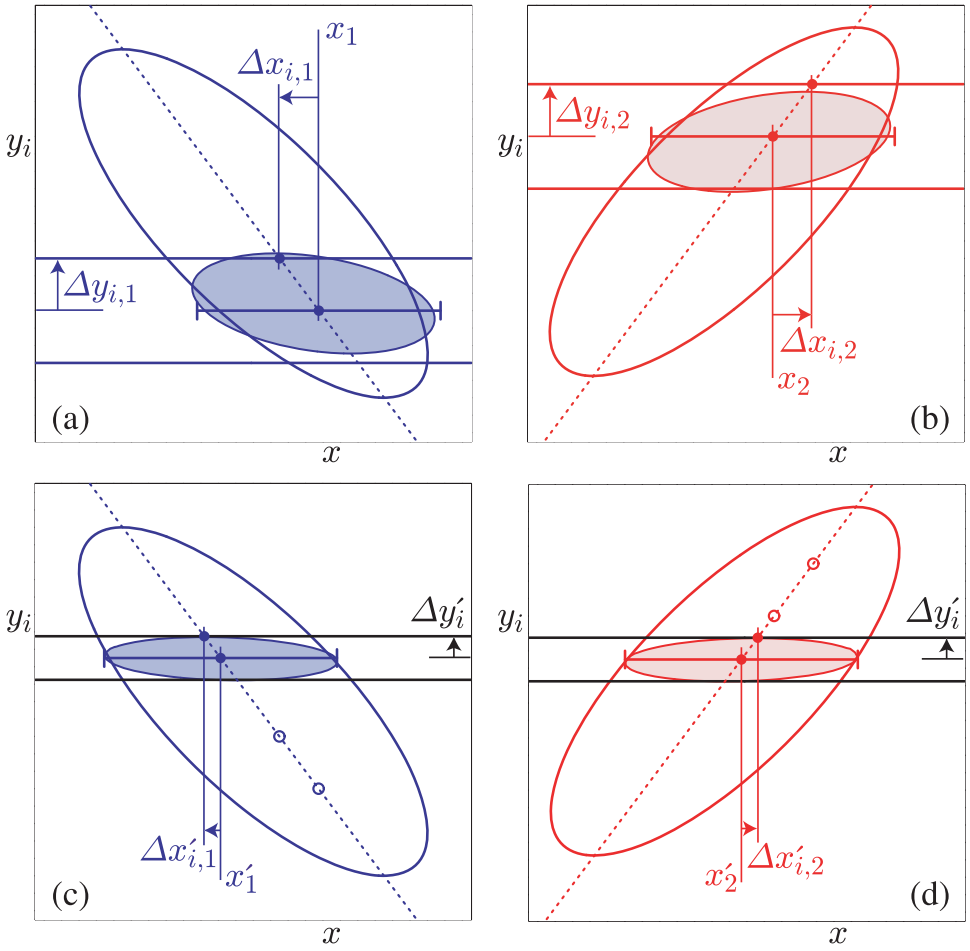


FIG. 2. Illustration of the HFLAV combination procedure for correlated systematic uncertainties. Upper plots (a) and (b) show examples of two individual measurements to be combined. The large (filled) ellipses represent their unconstrained (constrained) iso-likelihood contours, while horizontal bands indicate the different assumptions about the value and uncertainty of y_i used by each measurement. The error bars show the results of the method described in the text for obtaining x by performing fits with y_i fixed to different values. Lower plots (c) and (d) illustrate the adjustments to accommodate updated and consistent knowledge of y_i. Open circles mark the central values of the unadjusted fits to x with y fixed; these determine the dashed line used to obtain the adjusted values.

instead. The first step of our procedure is to adjust the values of each measurement to reflect the current best knowledge of the external parameters y_i' and their ranges $\Delta y_i'$, as illustrated in Figs. 2(c) and 2(d). We adjust the central values x_k and correlated systematic uncertainties $\Delta x_{k,i}$ linearly for each measurement (indexed by k) and each external parameter (indexed by i)

$$x_k' = x_k + \sum_i \frac{\Delta x_{k,i}}{\Delta y_{k,i}}(y_i' - y_{k,i}). \tag{6}$$

$$\Delta x_{k,i}' = \Delta x_{k,i}\frac{\Delta y_i'}{\Delta y_{k,i}}. \tag{7}$$

This procedure is exact in the limit that the unconstrained likelihood of each measurement is Gaussian and the linear relationships in Eqs. (6) and (7) are valid.

The second step is to combine the adjusted measurements, $x_k' \pm (\delta x_k \oplus \Delta x_{k,1}' \oplus \Delta x_{k,2}' \oplus \ldots)$ by constructing the goodness-of-fit statistic

$$\begin{aligned}&\chi^2_{\text{comb}}(x, y_1, y_2, \ldots)\\ &\equiv \sum_k \frac{1}{\delta x_k^2}\left[x_k' - \left(x + \sum\nolimits_i (y_i - y_i')\frac{\Delta x_{k,i}'}{\Delta y_i'}\right)\right]^2\\ &+ \sum_i \left(\frac{y_i - y_i'}{\Delta y_i'}\right)^2.\end{aligned} \tag{8}$$

We minimize this χ^2 to obtain the best values of x and y_i and their uncertainties, as shown in Fig. 3. Although this method determines new values for the y_i, we typically do not report them. Since the $\Delta x_{i,k}$ reported by each experiment are generally not intended for this purpose (for example, they may represent a conservative upper

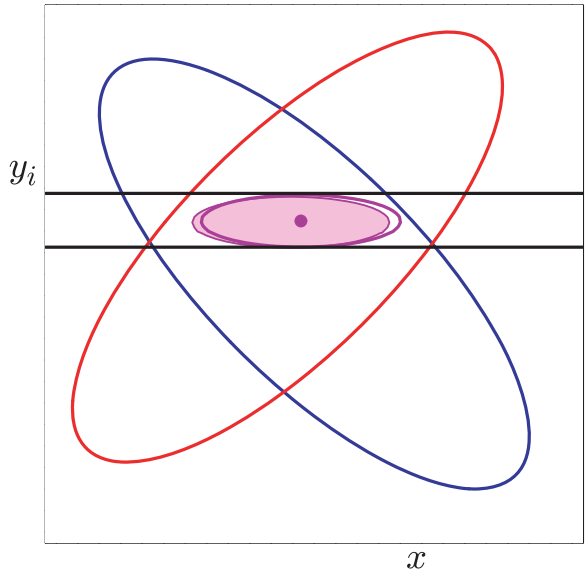


FIG. 3. Illustration of the combination of two hypothetical measurements of x using the method described in the text. The ellipses represent the unconstrained likelihoods of each measurement, and the horizontal band represents the latest knowledge about y_i that is used to adjust the individual measurements. The filled small ellipse shows the result of the exact method using $\mathcal{L}_{\text{comb}}$, and the hollow small ellipse and dot show the result of the approximate method using χ^2_{comb}.

limit rather than a true reflection of a 68% confidence level).

The results of the approximate method agree with the exact method when the $\mathcal{L}_k$ are Gaussian, $\Delta y_i' \ll \sigma(y_i)$ and the linear assumption for the approximate method is valid.

For averages where common sources of systematic uncertainty are important, central values and uncertainties are rescaled to a common set of input parameters following the prescription above. We use the most up-to-date values for common inputs, taking values for experimental constraints from within HFLAV or from the Particle Data Group when possible, and updated values of theoretical parameters from their publications.

B. Treatment of unknown correlations

Another issue that needs careful treatment is that of unknown correlations among measurements, e.g., due to use of the same decay model for intermediate states to calculate acceptances. A common practice is to set the correlation coefficient to unity to indicate full correlation. However, this is not necessarily conservative and can result in an underestimated uncertainty on the average. The most conservative choice of correlation coefficient between two measurements i and j is that which maximizes the uncertainty on $\hat{x}$ due to the pair of measurements,

$$\sigma^2_{\hat{x}(i,j)} = \frac{\sigma_i^2\sigma_j^2(1-\rho_{ij}^2)}{\sigma_i^2+\sigma_j^2-2\rho_{ij}\sigma_i\sigma_j}, \tag{9}$$

with

$$\rho_{ij} = \min\left(\frac{\sigma_i}{\sigma_j}, \frac{\sigma_j}{\sigma_i}\right). \tag{10}$$

This corresponds to setting $\sigma^2_{\hat{x}(i,j)} = \min(\sigma_i^2, \sigma_j^2)$. Setting $\rho_{ij} = 1$ when $\sigma_i \neq \sigma_j$ can lead to a significant underestimate of the uncertainty on $\hat{x}$, as can be seen from Eq. (9). In the absence of better information on the correlation, we always use Eq. (9).

C. Treatment of asymmetric uncertainties

For measurements with no correlation between them and with Gaussian uncertainties, the usual estimator for the average of a set of measurements is obtained by minimizing

$$\chi^2(x) = \sum_k^N \frac{(x_k - x)^2}{\sigma_k^2}, \tag{11}$$

where x_k is the kth measured value of x and σ_k^2 is the variance of the distribution from which x_k was drawn. The value $\hat{x}$ at minimum χ^2 is the estimate for the parameter x. The true σ_k are unknown but typically the uncertainty as assigned by the experiment σ_k^{raw} is used as an estimator for it. However, caution is advised when σ_k^{raw} depends on the measured value x_k. Examples of this are multiplicative systematic uncertainties such as those due to acceptance, or the $\sqrt{N}$ dependence of Poisson statistics for which $x_k \propto N$ and $\sigma_k \propto \sqrt{N}$. Failing to account for this type of dependence when averaging leads to a biased average. Such biases can be minimized

$$\chi^2(x) = \sum_k^N \frac{(x_k - x)^2}{\sigma_k^2(\hat{x})}, \tag{12}$$

where $\sigma_k(\hat{x})$ is the uncertainty on x_k that includes the dependence of the uncertainty on the value measured. As an example, consider the uncertainty due to detector acceptance, for which $\sigma_k(\hat{x}) = (\hat{x}/x_k) \times \sigma_k^{\text{raw}}$. Inserting this into Eq. (12) leads to the solution

$$\hat{x} = \frac{\sum_k^N x_k^3/(\sigma_k^{\text{raw}})^2}{\sum_k^N x_k^2/(\sigma_k^{\text{raw}})^2},$$

which is the correct behavior, i.e., every measurement is weighted by the inverse square of the fractional uncertainty $\sigma_k^{\text{raw}}/x_k$. When it is not possible to assess the dependence of σ_k^{raw} on $\hat{x}$ from the uncertainties quoted by the experiments, this dependence is ignored.

Another example of a non-Gaussian likelihood function is when a measurement is given with asymmetric uncertainties. In general we symmetrize them by taking their linear average, however for branching fractions and asymmetries, we take asymmetric uncertainties into account through the use of Eq. (1) with a variable value for the kth diagonal element V^{kk} of the covariance matrix for the measurement (dropping the measurement index i for simplicity). We take $V^{kk} = (\sigma^k_-)^2$ for $f^k(\boldsymbol{p}) - x^k < -\sigma_{k-}$ and $V^{kk} = (\sigma^k_+)^2$ for $f^k(\boldsymbol{p}) - x^k > \sigma^k_+$, where σ^k_- (σ^k_+) are the left- (right-side) uncertainty quoted on the measurement of x^k, and f^k is the kth element of $\boldsymbol{f}$. Between these regions, V^{kk} is interpolated linearly. While this will not fully recover the likelihood, it is the optimal solution when no further information is provided [10].

D. Splitting uncertainty for an average into components

We carefully consider the various uncertainties contributing to the overall uncertainty of an average. The covariance matrix describing the uncertainties of different measurements and their correlations is constructed, i.e., $\boldsymbol{V} = \boldsymbol{V}_{\rm stat} + \boldsymbol{V}_{\rm sys} + \boldsymbol{V}_{\rm theory}$. If the measurements are from independent data samples, then $\boldsymbol{V}_{\rm stat}$ is diagonal, but $\boldsymbol{V}_{\rm sys}$ and $\boldsymbol{V}_{\rm theory}$ may contain correlations. The variance on the average $\hat{x}$ can be written as

$$\sigma^2_{\hat{x}} = \frac{1}{\sum_{i,j}\boldsymbol{V}^{-1}_{ij}} = \frac{\sum_{i,j}(\boldsymbol{V}^{-1}\boldsymbol{V}\boldsymbol{V}^{-1})_{ij}}{(\sum_{i,j}\boldsymbol{V}^{-1}_{ij})^2} \tag{13}$$

$$= \frac{\sum_{i,j}(\boldsymbol{V}^{-1}[\boldsymbol{V}_{\rm stat} + \boldsymbol{V}_{\rm sys} + \boldsymbol{V}_{\rm theory}]\boldsymbol{V}^{-1})_{ij}}{(\sum_{i,j}\boldsymbol{V}^{-1}_{ij})^2}$$

$$= \sigma^2_{\rm stat} + \sigma^2_{\rm sys} + \sigma^2_{\rm th}. \tag{14}$$

To calculate $\sigma^2_{\rm stat}$ in the last step, the calculation is repeated without including $\boldsymbol{V}_{\rm stat}$ in $\boldsymbol{V}$ and this is then subtracted from the total. The same is done for the other two components. This breakdown of uncertainties is provided in certain cases, but usually only a single, total uncertainty is quoted for an average.

IV. b-HADRON PRODUCTION FRACTIONS

We consider here the relative fractions of the different b-hadron species produced in a specific process. These fractions are needed for characterizing the signal composition in inclusive b-hadron analyses, predicting the background composition in exclusive analyses, and converting observed event yields (or event yield ratios) into branching fraction (or branching fraction ratio) measurements. We distinguish here the following three b-hadron production processes: $\Upsilon(4S)$ decays, $\Upsilon(5S)$ decays, and high-energy collisions (including Z^0 decays).

A. b-hadron production fractions in $\Upsilon(4S)$ decays

Pairs of $b\bar{b}$ quarks produced in e^+e^- annihilations at the energy of the $\Upsilon(4S)$ resonance can hadronize into B^+B^-, $B^0\bar{B}^0$ or final states without open-beauty mesons. The latter are dominated by production of lower bottomonium levels accompanied by light hadrons, e.g. $\Upsilon(1S)\pi^+\pi^-$ or $\Upsilon(1S)\eta$. The corresponding production fractions satisfy

$$f^{+-} + f^{00} + f_{\not B} = 1. \tag{15}$$

The measurements that are used for determining the production fractions at the $\Upsilon(4S)$ are listed in Table 4.

The f^{+-}/f^{00} measurements reported in Refs. [11–14] are based on a comparison of the yields of B^+ and B^0 decays to final states related by isospin transformation, e.g., $B^+ \to J/\psi K^+$ and $B^0 \to J/\psi K^0_S$, and an assumption that corresponding partial widths are equal. The theoretical uncertainty of this assumption is considered only in the recent measurement by Belle [13], where it is conservatively estimated to be 4.4%. We assume that the same theoretical uncertainty is present in other measurements with quarkonium and $K^{(*)}$ in the final state [11,12], and that these theoretical uncertainties are correlated among the different channels.

In Ref. [15], the time dependence is studied in events where both B mesons decay semileptonically, $B \to \ell X$. The f^{+-}/f^{00} measurement is a byproduct of the $B^0\bar{B}^0$ oscillation-frequency measurement. It is assumed that $\Gamma(B^+ \to \ell X) = \Gamma(B^0 \to \ell X)$, which is expected to hold with better than 1% accuracy [22,23], and the corresponding theoretical uncertainty is neglected. In Ref. [16], the value of f^{00} is determined by comparing the numbers of events with one and with two reconstructed $B^0 \to D^{*-}\ell^+\nu_\ell$ decays. The measurement of a non-$B\bar{B}$ fraction in Ref. [17] is based on the yields of single-lepton and two-leptons events. Both of the above measurements do not rely on model assumptions and do not depend upon external parameters.

At the $\Upsilon(4S)$ energy, the *BABAR* and Belle collaborations have observed production of five final states containing bottomonium: $\Upsilon(1S)\pi^+\pi^-$, $\Upsilon(1S)\eta$, $\Upsilon(1S)\eta'$, $h_b(1P)\eta$ and $\Upsilon(2S)\pi^+\pi^-$ [18–21]. Their total production fraction is

$$f_{(b\bar{b})X} = 0.00264 \pm 0.00021, \tag{16}$$

where the contribution of channels with $\pi^0\pi^0$ are included using isospin relations. Since many transitions remain unexplored, we consider the value in Eq. (16) as a lower limit on $f_{\not B}$.

We perform a fit to all measurements shown in Table 4 using Eq. (15) as a constraint. The values and uncertainties are corrected for a change of the external parameters $\tau(B^+)/\tau(B^0)$ and $\tau(B^0)$, whose values at the time of the publication of each measurement are listed in Table 4.

TABLE 4. Measurements that are used for determining the production fractions at the $\Upsilon(4S)$, corresponding methods, external parameters, and experiments that performed them.

Measurement	Method	External parameters	Experiment
f^{+-}/f^{00}			
$1.04 \pm 0.07 \pm 0.04$	$J/\psi K^{(*)}$	$\tau(B^+)/\tau(B^0) = 1.066 \pm 0.024$	CLEO, 2001 [11]
$1.06 \pm 0.02 \pm 0.03$	$(c\bar{c})K^{(*)}$	$\tau(B^+)/\tau(B^0) = 1.086 \pm 0.017$	*BABAR*, 2005 [12]
$1.065 \pm 0.012 \pm 0.019 \pm 0.047$	$J/\psi K$	$\tau(B^+)/\tau(B^0) = 1.076 \pm 0.004$	Belle, 2023 [13]
$1.058 \pm 0.084 \pm 0.136$	$D^*\ell\nu$	$\tau(B^+)/\tau(B^0) = 1.074 \pm 0.028$	CLEO, 2002 [14]
$1.01 \pm 0.03 \pm 0.09$	Dilepton	$\tau(B^+)/\tau(B^0) = 1.083 \pm 0.017$	Belle, 2003 [15]
		$\tau(B^0) = (1.542 \pm 0.016)$ ps	
$f^{+-}/f^{00} = 1.054 \pm 0.038$	Average of the above		
f^{00}			
$0.487 \pm 0.010 \pm 0.008$			*BABAR*, 2005 [16]
f_{B^0}			
$-0.0011 \pm 0.0143 \pm 0.0107$	Semileptonic decays		CLEO, 1996 [17]
$\geq 0.00264 \pm 0.00021$	Sum of known channels		*BABAR*, Belle [18–21]

The current values are $\tau(B^+)/\tau(B^0) = 1.076 \pm 0.004$ and $\tau(B^0) = (1.519 \pm 0.004)$ ps (see Sec. V A 2). The corrections are applied with the method described in Sec. III A.

The fit is performed in two steps. First, we fit the f^{+-}/f^{00} measurements taking into account correlations of the systematic uncertainties due to $\tau(B^+)/\tau(B^0)$ and due to the isospin-conservation assumption. The result, also shown in Table 4, is $f^{+-}/f^{00} = 1.054 \pm 0.038$. Next, we perform the fit to this average and the measurements of f^{00} and f_{B^0} shown in Table 4. It is assumed that all these measurements are uncorrelated. The positive error of $f_{(b\bar{b})X}$ is set to infinity, to impose a constraint $f_{B^0} \geq f_{(b\bar{b})X}$. This constraint corresponds to the physics-motivated statement that the branching fraction of non-$B\bar{B}$ decay modes that have not yet been explored experimentally, defined as $f_{B^0}^{\text{unexplored}} = f_{B^0} - f_{(b\bar{b})X}$, must be non-negative. The results of the fit are

$$f^{+-} = 0.5113^{+0.0073}_{-0.0108}, \qquad f^{00} = 0.4861^{+0.0074}_{-0.0080},$$
$$f_{B^0} = 0.00264^{+0.0125}_{-0.0002}, \qquad \frac{f^{+-}}{f^{00}} = 1.052 \pm 0.031. \qquad (17)$$

Figure 4 shows the plane of f^{+-} vs f^{00} with their central values and 1σ and 2σ contours. The strong correlation seen in the contours is a result of the constraint $f_{B^0} \geq f_{(b\bar{b})X}$. Removing this constraint by adding $f_{B^0}^{\text{unexplored}}$ as an unconstrained parameter in the fit results in larger and symmetric uncertainties on f^{+-}, f^{00}, and f^{+-}/f^{00}, equaling ± 0.0128, ± 0.0090, and ± 0.033, respectively.

To test the ensemble behavior of the fit, we apply it to a set of parametrized experiments produced with the central values of the fit results shown in Eq. (17) and the uncorrelated uncertainties of the measurements shown in Table 4. Relative to the values shown in Eq. (17), the fit values averaged over the parametrized experiments show biases of $\Delta f^{+-} = -0.0016$, $\Delta f^{00} = -0.0015$, and $\Delta(f^{+-}/f^{00}) = -0.0044$, due to the constraint $f_{B^0} \geq f_{(b\bar{b})X}$. In terms of the fit uncertainty, the means of

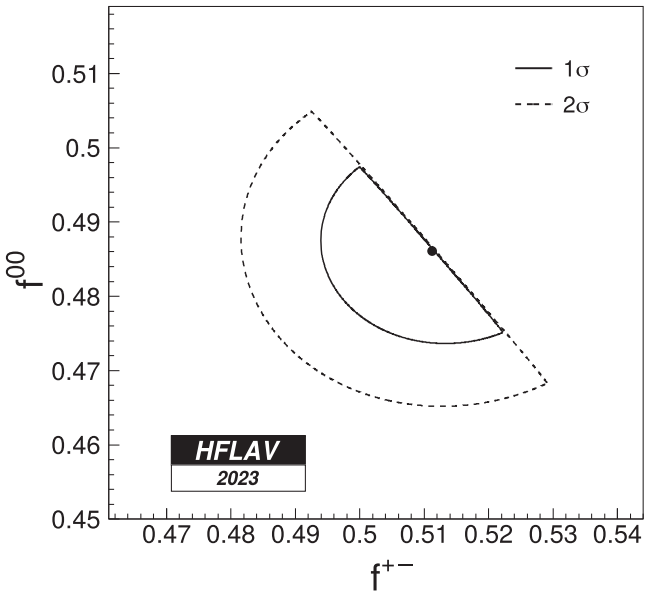


FIG. 4. The f^{00} and f^{+-} plane with the HFLAV fit results. The dot shows the central values, the solid and dashed curves show the 1σ (68% CL) and 2σ (95% CL) contours, respectively.

the pulls of these parameters are −17%, −19%, and −14%, respectively. Since the biases are small, we neglect them in our reported results.

The complex correlation between the values of f^{+-} and f^{00} cannot be represented by a correlation matrix. To obtain detailed information about the correlations, we suggest to reproduce our final fit. For this, one should express $f_{\not B}=1-f^{+-}-f^{00}$ and fit the four measurements shown in Table 4 using two parameters, f^{+-} and f^{00}.

1. Discussion on measurements of f^{+-}/f^{00}

Experimentally, the simplest method to determine f^{+-}/f^{00} is studying isospin-related decays of B^0 and B^+. However, this method suffers from theoretical uncertainty due to the assumption of isospin conservation, which is difficult to control. Thus, it is important to perform measurements that give model-independent results. Several proposals for such measurements are presented in Refs. [24,25].

It is important to note that the ratio f^{+-}/f^{00} varies with center-of-mass energy due to the different phase space of B^+B^- and $B^0\bar{B}^0$ pairs (B^0 is heavier than B^+, and phase space is proportional to p_B^3), the electromagnetic interaction, and isospin violation in the strong interaction [26]. This may introduce an additional uncertainty in f^{+-}/f^{00}, which is not included in Eq. (17), due to potential differences between the center-of-mass energies of the different experiments. Since the energy difference between the Belle and Belle II data samples collected at the $\Upsilon(4S)$ is 0.9 MeV [27,28], one can take the typical difference between the energies of the various experiments to be 1 MeV. In the *BABAR* paper on the B^0 and B^+ mass-difference measurement [29], it is assumed that the energy dependence of f^{+-}/f^{00} is entirely defined by the phase-space factor $(p_{B^+}/p_{B^0})^3$. In this case, the uncertainty in f^{+-}/f^{00} due to different energies among experiments is ±0.003, which is negligibly small relative to the total uncertainty shown in Eq. (17).

However, f^{+-}/f^{00} might have a much more pronounced dependence on energy compared to the phase-space factor $(p_{B^+}/p_{B^0})^3$, as discussed in Ref. [26] (see also references therein). If so, the uncertainty due to differences in the average collision energies between the experiments could be as high as ±0.03. Thus, it is of high interest to perform the measurement of the energy dependence of f^{+-}/f^{00}.

In addition, the different energy spreads of the experiments can result in different measured values of f^{+-}/f^{00}. Considering the typical energy spread in the range 5–6 MeV [27,28], we find that the corresponding uncertainty ranges from ±0.001 to ±0.01, depending upon the hypotheses of the f^{+-}/f^{00} energy dependence. Thus, the uncertainty in f^{+-}/f^{00} due to different energy spreads is considerably lower than the uncertainty due to different average energies in various experiments.

TABLE 5. Visible cross sections of the $e^+e^- \to B^{(*)}\bar{B}^{(*)}(\pi(\pi))$ processes measured by Belle at the $\Upsilon(5S)$ resonance ($\sqrt{s}=10.866$ GeV). The results of Ref. [31] for $[B^{(*)}\bar{B}^{(*)}]^{\pm}\pi^{\mp}$ are multiplied by 1.5 to account for the contribution of $[B^{(*)}\bar{B}^{(*)}]^0\pi^0$.

Process	$\sigma^{\rm vis}$ (pb)	Refs.
$e^+e^- \to$		
$B\bar{B}$	33.3 ± 1.2	[27]
$B\bar{B}^* + B^*\bar{B}$	68.0 ± 3.3	[27]
$B^*\bar{B}^*$	124.4 ± 5.3	[27]
$B\bar{B}\pi$	<3.2	[31]
$(B\bar{B}^* + B^*\bar{B})\pi$	16.8 ± 2.3	[31]
$B^*\bar{B}^*\pi$	8.4 ± 1.5	[31]
$B\bar{B}\pi\pi$	Not seen	[32]

B. b-hadron production fractions at the $\Upsilon(5S)$ energy

Hadronic events produced in e^+e^- collisions at the $\Upsilon(5S)$ [also known as $\Upsilon(10860)$] energy can be classified into three categories: light-quark (u, d, s, c) continuum events, $b\bar{b}$ continuum events (including $b\bar{b}\gamma$, etc., with initial-state-radiation photons), and $\Upsilon(5S)$ events. The latter two cannot be distinguished on an event-by-event basis and are referred to as $b\bar{b}$ events in the following. These $b\bar{b}$ events can hadronize into different final states. We define $f_{u,d}^{\Upsilon(5S)}$ to be the fraction of $b\bar{b}$ events at the $\Upsilon(5S)$ energy with a pair of non-strange bottom mesons, namely, $B\bar{B}$, $B\bar{B}^*$ or $B^*\bar{B}$, $B^*\bar{B}^*$, $B\bar{B}\pi$, $B\bar{B}^*\pi$ or $B^*\bar{B}\pi$, $B^*\bar{B}^*\pi$, and $B\bar{B}\pi\pi$, where B denotes a B^0 or B^+ meson and $\bar{B}$ denotes a $\bar{B}^0$ or B^- meson. The contributions of these channels are listed in Table 5. Similarly, we define $f_s^{\Upsilon(5S)}$ to be the fraction of $b\bar{b}$ events that hadronize into a pair of strange bottom mesons, $B_s^0\bar{B}_s^0$, $B_s^0\bar{B}_s^*$ or $B_s^*\bar{B}_s^0$, and $B_s^*\bar{B}_s^*$. The production fractions for the latter two channels are 0.073 ± 0.014 and 0.870 ± 0.017, respectively [30]. Note that the excited bottom-meson states decay via $B^* \to B\gamma$ and $B_s^* \to B_s^0\gamma$. Lastly, $f_{\not B}^{\Upsilon(5S)}$ is defined to be the fraction of $b\bar{b}$ events without open-bottom mesons in the final state. These events are dominated by production of bottomonium accompanied by light hadrons. By construction, these fractions satisfy

$$f_{u,d}^{\Upsilon(5S)} + f_s^{\Upsilon(5S)} + f_{\not B}^{\Upsilon(5S)} = 1. \tag{18}$$

The Belle collaboration measured $f_{u,d}^{\Upsilon(5S)}$ [27] based on the formula

$$f_{u,d}^{\Upsilon(5S)} = \frac{N_B^{\Upsilon(5S)}}{N_B^{\Upsilon(4S)}} \frac{n_{b\bar{b}}^{\Upsilon(4S)}}{n_{b\bar{b}}^{\Upsilon(5S)}}, \tag{19}$$

where $N_B^{\Upsilon(5S)}$ and $N_B^{\Upsilon(4S)}$ are the B meson yields at $\Upsilon(5S)$ and $\Upsilon(4S)$, respectively, that were measured using five clean B-decay channels; $n_{b\bar{b}}^{\Upsilon(5S)}$ and $n_{b\bar{b}}^{\Upsilon(4S)}$ are the $b\bar{b}$-event yields at $\Upsilon(5S)$ and $\Upsilon(4S)$, respectively, determined by counting hadronic events and subtracting the continuum contribution. In formula (19) it is assumed that the non-$B\bar{B}$ fraction for $\Upsilon(4S)$ decays is negligibly small. The obtained value of $f_{u,d}^{\Upsilon(5S)}$ is

$$f_{u,d}^{\Upsilon(5S)} = 0.751 \pm 0.040, \tag{20}$$

where the uncertainty in $n_{b\bar{b}}^{\Upsilon(5S)}$ dominates. This measurement supersedes the previous Belle result reported in Ref. [32].

In 2023, Belle measured $f_s^{\Upsilon(5S)}$ using inclusive production of D_s^+ mesons [33]. The $f_s^{\Upsilon(5S)}$ value was determined from the formula

$$\mathcal{B}(\Upsilon(5S) \to D_s^{\pm} X) = 2 f_s^{\Upsilon(5S)} \mathcal{B}(B_s^0 \to D_s^{\pm} X) + 2 f_{u,d}^{\Upsilon(5S)} \mathcal{B}(B \to D_s^{\pm} X), \tag{21}$$

where $\mathcal{B}(\Upsilon(5S) \to D_s^{\pm} X)$ is the D_s^+ production fraction defined as $N_{D_s^{\pm}X}^{\Upsilon(5S)}/n_{b\bar{b}}^{\Upsilon(5S)}$, where $N_{D_s^{\pm}X}^{\Upsilon(5S)}$ is the number of D_s^+ mesons produced in $b\bar{b}$ events at the $\Upsilon(5S)$ energy. The value of $N_{D_s^{\pm}X}^{\Upsilon(5S)}$ was determined by counting D_s^+ mesons and subtracting the continuum contribution [33]. The inclusive branching fraction $\mathcal{B}(B \to D_s^{\pm} X)$ is defined as $\mathcal{B}(\Upsilon(4S) \to D_s^{\pm} X)/2$; it is measured using the same approach as $\mathcal{B}(\Upsilon(5S) \to D_s^{\pm} X)$ [33]. The inclusive branching fraction $\mathcal{B}(B_s^0 \to D_s^{\pm} X)$ was measured by Belle to be $(60.2 \pm 5.8 \pm 2.3)\%$ using semileptonic tagging of the second B_s^0 in the event [34]. The obtained value of $f_s^{\Upsilon(5S)}$ is

$$f_s^{\Upsilon(5S)} = 0.230 \pm 0.002 \pm 0.028. \tag{22}$$

This measurement supersedes previous Belle results reported in Refs. [30,34]. It is important that all parameters in Eq. (21) are measured by Belle, so their systematic uncertainties partly cancel. The dominant contribution to the uncertainty of $f_s^{\Upsilon(5S)}$ originates from $\mathcal{B}(B_s^0 \to D_s^{\pm} X)$.

The CLEO collaboration performed measurements of $\mathcal{B}(\Upsilon(5S) \to D_s^{\pm} X)$ and $f_{u,d}^{\Upsilon(5S)}$ [35] that are in good agreement with corresponding Belle results but have 3–4 times lower accuracy. We do not use the CLEO results to calculate the $f_s^{\Upsilon(5S)}$ average, to ensure the partial cancellation of systematic uncertainties, mentioned above. The *BABAR* collaboration measured $f_s^{\Upsilon(5S)}$ using energy scan data [36]. This result relies on a model-dependent estimation of $\mathcal{B}(B_s^0 \to \phi X)$ and uses the constraint of Eq. (18) neglecting $f_{\not B}^{\Upsilon(5S)}$. Therefore, we do not use it in our average.

The Belle experiment observed the following bottomonium-production processes at the $\Upsilon(5S)$ energy: $e^+e^- \to \Upsilon(1S, 2S, 3S)\pi^+\pi^-$, $\Upsilon(1S, 2S, 3S)\pi^0\pi^0$, $\Upsilon(1S)K^+K^-$, $h_b(1P, 2P)\pi^+\pi^-$, $\chi_{b1,2}(1P)\pi^+\pi^-\pi^0$, $\Upsilon_J(1D)\eta$, and $\Upsilon(2S)\eta$ [37–41]. The sum of the visible (i.e., uncorrected for initial-state radiation) cross-sections into these final states, plus those of the unmeasured final states $\Upsilon(1S)K^0\bar{K}^0$ and $h_b(1P, 2P)\pi^0\pi^0$, which are obtained by assuming isospin conservation, amounts to

$$\sigma^{\rm vis}(e^+e^- \to (b\bar{b})X) = 16.1 \pm 1.5 \text{ pb}, \tag{23}$$

where $(b\bar{b}) = \Upsilon(1S, 2S, 3S)$, $\Upsilon_J(1D)$, $h_b(1P, 2P)$, $\chi_{b1,2}(1P)$; and $X = \pi\pi$, $\pi^+\pi^-\pi^0$, KK, η. We divide this by the $b\bar{b}$ production cross section, $\sigma(e^+e^- \to b\bar{b}) = 340 \pm 16$ pb [30], to obtain

$$f_{(b\bar{b})X}^{\Upsilon(5S)} = 0.0473 \pm 0.0048. \tag{24}$$

This should be taken as a lower bound for $f_{\not B}^{\Upsilon(5S)}$.

To improve accuracy, Belle performed a fit to the values of $f_{u,d}^{\Upsilon(5S)}$, $f_s^{\Upsilon(5S)}$ and $f_{\not B}^{\Upsilon(5S)}$ using Eq. (18) as a constraint [33]. For $f_{\not B}^{\Upsilon(5S)}$, Belle used the value of $f_{(b\bar{b})X}^{\Upsilon(5S)}$, setting its positive error to infinity. Correlations among the production fractions were taken into account using the method described in Sec. III A of this review. The obtained values are

$$f_{u,d}^{\Upsilon(5S)} = 0.732^{+0.020}_{-0.027}, \tag{25}$$

$$f_s^{\Upsilon(5S)} = 0.220^{+0.020}_{-0.021}, \tag{26}$$

$$f_{\not B}^{\Upsilon(5S)} = 0.048^{+0.033}_{-0.006}, \tag{27}$$

where the strongly asymmetric uncertainty on $f_{\not B}^{\Upsilon(5S)}$ is due to the one-sided constraint from the observed $(b\bar{b})X$ decays. These results, together with their correlations, imply

$$f_s^{\Upsilon(5S)}/f_{u,d}^{\Upsilon(5S)} = 0.300^{+0.036}_{-0.035}. \tag{28}$$

Further methods to measure production fractions at $\Upsilon(5S)$ are discussed in Ref. [42].

C. b-hadron production fractions at high energy

In a previous publication [43], we presented two sets of averages, one including only measurements performed at LEP, and another including only measurements performed by CDF at the Tevatron.[3] While the first set is well defined and is basically related to branching fractions of inclusive Z decays, the other set is somewhat ill-defined, since it depends on the geometrical and kinematical acceptance of the experiments over which the measurements are integrated. With the ever increasing precision in heavy flavor measurements, the b-hadron fraction averages provided by HFLAV for high-energy hadron collisions are no longer of interest, since they are not directly transferable from one experiment to the other. We have, therefore, decided to no longer maintain these averages starting in Ref. [1]. The interested reader should refer to Sec. 4.1.3 of our 2019 publication [43].

The relative fractions of b-hadron types produced in Z decays are universal and therefore still of interest. Since the averages we have reported in Ref. [43] have remained stable over the last decade and new data are not expected until a future new electron-positron collider operates again at the Z pole, they are not reported here.

V. LIFETIMES AND MIXING PARAMETERS OF b HADRONS

Quantities such as b-hadron production fractions, b-hadron lifetimes, and neutral B-meson oscillation frequencies were studied in the 1990s at LEP and SLC, at DORIS II and CESR, as well as at the Tevatron. This was followed by precise measurements of the B^0 and B^+ mesons performed at the asymmetric B factories, KEKB and PEPII, as well as measurements related to the other b hadrons, in particular B_s^0, B_c^+ and Λ_b^0, performed at the upgraded Tevatron. Currently, the most precise measurements are coming from the ATLAS, CMS, LHCb, Belle and Belle II experiments.

In many cases, these basic quantities, in addition to being interesting by themselves, are necessary ingredients for more refined measurements, for example decay-time-dependent CP-violating asymmetries. Hence, some of the averages presented in this section are used as input for the results given in subsequent sections. In the past, many b-hadron lifetime and mixing measurements had a significant dependence on the b-hadron production fractions, which themselves depended on the lifetime and mixing measurements. This circular coupling had to be dealt with carefully whenever inclusive or semiexclusive measurements of b-hadron lifetime and mixing parameters were considered. In the past decade, this dependence has reduced to a negligible level, with increasingly precise exclusive measurements becoming available and dominating practically all averages.

In addition to lifetimes and oscillation frequencies, this section also deals with CP violation in the B^0 and B_s^0 mixing amplitudes, as well as the phase $\phi_s^{c\bar{c}s}$ that describes CP violation in the interference between B_s^0 mixing and decay in $b \to c\bar{c}s$ transitions. In the absence of new physics and subleading penguin contributions, this phase is equal to $-2\beta_s = -\arg[(V_{ts}V_{tb}^*)^2/(V_{cs}V_{cb}^*)^2]$.

Throughout this section, published results that have been superseded by subsequent publications are ignored (i.e., excluded from the averages). They are only referred to if necessary.

A. b-hadron lifetimes

Lifetime calculations are performed in the framework of the heavy quark expansion (HQE) [22,44,45]. In these calculations, the total decay rate of a hadron H_b is expressed as a series of expectation values of operators of increasing dimension,

$$\Gamma_{H_b} = |\mathrm{CKM}|^2 \sum_{n,k} \frac{c_{nk}}{m_b^n} \langle H_b | O_{nk} | H_b \rangle, \tag{29}$$

where $|\mathrm{CKM}|^2$ is the relevant combination of CKM matrix elements. The coefficients c_{nk} are calculated perturbatively [46], i.e. as a series in $\alpha_s(m_b)$. The nonperturbative QCD effects are comprised in the matrix elements $\langle H_b|O_{nk}|H_b\rangle \propto \Lambda_{\mathrm{QCD}}^n$ of the operators O_{nk}. For a given dimension n, there are usually several operators, indicated by the index k. Hence the HQE predicts Γ_{H_b} in the form of an expansion in both $\Lambda_{\mathrm{QCD}}/m_b$ and $\alpha_s(m_b)$, see, e.g., Refs. [47,48]. The leading term in Eq. (29) corresponds to the weak decay of a free b quark. At this order, all b-flavored hadrons have the same lifetime. The concept of the HQE and first calculations of valence quark effects emerged in 1986 [44]. In the early 1990s experiments became sensitive enough to detect lifetime differences among various H_b species. The hypothetical existence of additional, non-powerlike, contributions to Γ_{H_b}, referred to as *violation of quark-hadron duality*, is not captured by the power series of the HQE [49,50]. The sizes of such terms can only be determined experimentally, by confronting the HQE predictions with data. Possible violation of quark-hadron duality has been shown to be severely constrained by experimental results [47,51]. The matrix elements of Eq. (29) can be calculated using lattice QCD or QCD sum rules. In some cases they can also be related to those appearing in other observables by utilizing symmetries of QCD. One may reasonably expect that powers of $\Lambda_{\mathrm{QCD}}/m_b \sim 0.1$ provide enough suppression that only

[3]The LHC production fractions results were still incomplete, lacking measurements of the production of weakly-decaying baryons heavier than Λ_b^0.

the first terms of the sum in Eq. (29) matter. However, starting from the third power the coefficients are enhanced by a factor of $16\pi^2$, so that these terms of order $16\pi^2(\Lambda_{\rm QCD}/m_b)^3$ [52] do matter when comparing lifetimes of different b-hadrons. State-of-the-art calculations of these spectator effects to the b-hadrons lifetimes predictions exist in terms of both $\Lambda_{\rm QCD}/m_b$ [53–55] and $\alpha_s(m_b)$ [56–58], with all subsequent theory papers using these results. However, it was subsequently found that the so-called Darwin contribution at order $(\Lambda_{\rm QCD}/m_b)^3$ might give very large numerical corrections, even without the $16\pi^2$ enhancement [59,60]. The exact size of this effect depends on the value of the matrix elements of the Darwin operator, which is extracted from inclusive semileptonic $b \to c$ transitions, see Refs. [61–63]. Moreover, there was recent progress in determining the non-perturbative matrix elements of the arising four-quark operators [64,65].

Theoretical predictions are usually made for the ratios of the lifetimes (with $\tau(B^0)$ often chosen as the common denominator) rather than for the individual lifetimes, since this leads to cancellation of several uncertainties. The precision of the HQE calculations (see e.g. Refs. [66,67]) is in some instances already surpassed by the measurements, e.g., in the case of $\tau(B^+)/\tau(B^0)$. Improvement in the precision of calculations requires progress along two lines. First, better nonperturbative matrix elements are needed. One expects precise calculations, especially from lattice QCD where significant advances have been made in the past decade. For the first promising steps in that direction, see Refs. [68,69]. Second, the coefficients c_{nk} must be calculated to higher orders of α_s. In particular, the α_s^2 and $\alpha_s\Lambda_{\rm QCD}/m_b$ contributions to the lifetime differences are needed to keep up with the experimental precision.

The following important conclusions, which are in agreement with experimental observation, can be drawn from the HQE, even in its present state:

(i) The larger the mass of the heavy quark, the smaller the variation in the lifetimes among different hadrons containing this quark. This is illustrated by the fact that lifetimes are rather similar in the b sector, while they differ by large factors in the charm sector (see e.g. Ref. [70]).

(ii) First corrections to the spectator model occur at order $\Lambda_{\rm QCD}^2/m_b^2$, leading to lifetime differences around one percent.

(iii) The dominant contribution to $\tau(B^+)/\tau(B^0)$ is of order $16\pi^2(\Lambda_{\rm QCD}/m_b)^3$ and typically amounts to several percent, whereas $(\Lambda_{\rm QCD}/m_b)^3$ corrections due to the Darwin operator might have a crucial role for $\tau(B_s^0)/\tau(B^0)$.

1. Overview of lifetime measurements

This section gives an overview of the types of b-hadron lifetime measurements, with details given in subsequent sections. In most cases, the decay time of an H_b state is estimated by measuring its flight distance and dividing it by the relativistic factor $\beta\gamma c$. Methods of accessing lifetime information can roughly be divided into the following five categories:

(1) *Measurements in semileptonic decays of a specific* $\boldsymbol{H_b}$. The virtual W boson from $b \to Wc$ produces a $\ell\nu_l$ pair ($\ell = e, \mu$) in about 21% of the cases. The electron or muon from such decays provides a clean and efficient trigger signature. The c quark and the H_b spectator quark(s) combine into a charm hadron H_c, which is reconstructed in one or more exclusive decay channels. Identification of the H_c species allows one to separate, at least statistically, different H_b species. The advantage of these measurements is in the sample size, which is usually larger than in the case of exclusively reconstructed hadronic H_b decays (described next). The main disadvantages are related to the difficulty of estimating the lepton + charm sample composition and to the reliance on Monte Carlo for the momentum (and hence $\beta\gamma$ factor) estimate.

(2) *Measurements in exclusively reconstructed hadronic decays*. These have the advantage of complete reconstruction of the decaying H_b state, which allows one to infer the decaying species, as well as to perform precise measurement of the $\beta\gamma$ factor. Both lead to generally smaller systematic uncertainties than semileptonic decays. The downsides are smaller branching fractions and larger combinatorial backgrounds when the signal channel involves multihadron decays, such as $H_b \to H_c\pi(\pi\pi)$ with multibody H_c decays. This problem is often more serious in a hadron collider environment, which has many hadrons and a nontrivial underlying event. Decays of the type $H_b \to J/\psi H_s$ are often used, as they are relatively clean and easy to trigger on due to the $J/\psi \to \ell^+\ell^-$ signature.

(3) *Measurements at asymmetric B factories*. In the $\Upsilon(4S) \to B\bar{B}$ decay, the B mesons (B^+ or B^0) are essentially at rest in the $\Upsilon(4S)$ frame. This makes direct lifetime measurements impossible in experiments at symmetric-energy colliders, which produce the $\Upsilon(4S)$ at rest. At asymmetric B factories the $\Upsilon(4S)$ meson is boosted, resulting in the B and $\bar{B}$ moving nearly parallel to each other with similar boosts. The decay time is inferred from the distance Δz separating the B and $\bar{B}$ decay vertices along the boost axis and from the $\Upsilon(4S)$ boost, which is known from the beam energies. In the *BABAR*, Belle and Belle II experiments, the $\Upsilon(4S)$ boosts are $\beta\gamma \approx 0.55$, 0.43 and 0.29, respectively. They result in average B decay lengths of approximately 250, 190, 130 μm.

While one B^0 or B^+ meson is fully reconstructed in a semileptonic or hadronic decay mode, the other B in the event is typically not fully reconstructed, in order to avoid loss of efficiency. Rather, only the position of its decay vertex is determined from the remaining tracks in the event. These measurements benefit from large sample sizes, but suffer from poor proper time resolution, comparable to the B lifetime itself. The resolution is dominated by the uncertainty on the decay-vertex positions, which is typically 50 (100) μm for a fully (partially) reconstructed B meson. With much larger samples in the future, the resolution and purity could be improved (and hence the systematics reduced) by fully reconstructing both B mesons in the event.

(4) *Measurement of lifetime ratios*. This method, initially applied in the measurement of $\tau(B^+)/\tau(B^0)$, is now also used for other b-hadron species at the LHC. The ratio of the lifetimes is extracted from the dependence of the ratio of the observed yields of two different b-hadron species on the proper time, i.e., the time interval between the production and the decay in the rest frame of the B meson. Subtle efficiency effects and systematic uncertainties are partially canceled in the ratio by reconstructing both the decays in similar topologies.

(5) *Inclusive (flavor-blind) measurements*. Early, low-statistics measurements were aimed at extracting the lifetime from a mixture of b-hadron decays, without distinguishing the decaying species. Often, the exact H_b composition was ill defined and analysis-dependent, and the $\beta\gamma$ factor was extracted from simulation. Nowadays, it is of little interest as it is less fundamental than the precisely measured lifetimes of the individual species. As a result, we no longer review the inclusive b-hadron lifetime measurements, the latest of which was published in 2004 [71]. The interested reader can refer to a previous publication [43].

In some analyses, measurements of two [e.g., $\tau(B^+)$ and $\tau(B^+)/\tau(B^0)$] or three [e.g. $\tau(B^+)$, $\tau(B^+)/\tau(B^0)$, and Δm_d] quantities are combined. This introduces correlations among measurements. Another source of correlations among the measurements is represented by the systematic effects, which could be common to a number of measurements in the same experiment or to an analysis technique across different experiments. When calculating the averages presented below, such known correlations are taken into account.

2. B^0 and B^+ lifetimes and their ratio

After many years of dominating the B^0 and B^+ lifetime averages, the LEP experiments yielded the scene to the asymmetric B factories and the Tevatron experiments. The B factories have been very successful in utilizing their potential—in only a few years of running, *BABAR* and, to a greater extent, Belle and Belle II, have struck a balance between the statistical and the systematic uncertainties, with both being close to (or even better than) an impressive 1% level. Meanwhile, CDF and D0 emerged as significant contributors to the field as the Tevatron Run II data flowed in. More recently, the LHC and Belle II experiments came into play, matching the precision and, in case of LHCb and CMS, even improving it by around a factor two.

At present, we have three sets of measurements (from LEP/SLC, the B factories and Tevatron/LHC) performed in different environments, obtained using substantially different techniques, and precise enough for cross-checking and comparison.

The $\tau(B^+)$, $\tau(B^0)$ and $\tau(B^+)/\tau(B^0)$ measurements, and their averages, are summarizedin Tables 6–8. For the average of $\tau(B^+)/\tau(B^0)$ we use only direct measurements of this ratio and not separate measurements of $\tau(B^+)$ and $\tau(B^0)$. In the context of the $\tau(B^0)$ average, only systematic sources originating from B-factories and LHC measurements are correlated in the averaging process within each experiment/machine. The specific sources that are correlated are outlined below:

(i) for the B-factory measurements—$\tau(B^+)$, Δm_d, length scale, machine boost, detector alignment, detector resolution, beam spot, $B\bar{B}$ fraction and analysis bias (where applicable);

(ii) for the LHC measurements—detector alignment, length scale and reconstruction effects.

A different approach is adopted for the average of $\tau(B^+)$ and $\tau(B^+)/\tau(B^0)$, for which the following systematic sources are taken into account for correlation:

(i) for the SLC and LEP measurements—D^{**} branching fraction uncertainties [4], estimation of the momentum of b mesons produced in Z^0 decays (b-quark fragmentation parameter $\langle X_E \rangle = 0.702 \pm 0.008$ [4]), B_s^0 and b-baryon lifetimes (see Secs. V A 3 and V A 5), and b-hadron production fractions at high energy [43];

(ii) for the B-factory measurements—detector alignment and length scale, machine boost, and sample composition (where applicable);

(iii) for the Tevatron and LHC measurements—detector alignment, length scale and reconstruction effects.

The resultant averages are

$$\tau(B^0) = 1.517 \pm 0.004 \text{ ps}, \tag{30}$$

$$\tau(B^+) = 1.638 \pm 0.004 \text{ ps}, \tag{31}$$

$$\tau(B^+)/\tau(B^0) = 1.076 \pm 0.004. \tag{32}$$

TABLE 6. Measurements of the B^0 lifetime with exclusive (excl.) or inclusive (incl.) decays, B charge determination from the secondary vertex (sec. vtx), or partial reconstruction. See Sec. V A for a detailed explanation of the method.

Experiment	Method	Dataset	$\tau(B^0)$ (ps)	Refs.
ALEPH	$D^{(*)}\ell$	91–95	$1.518 \pm 0.053 \pm 0.034$	[72]
ALEPH	Exclusive	91–94	$1.25^{+0.15}_{-0.13} \pm 0.05$	[73]
ALEPH	Partial rec. $\pi^+\pi^-$	91–94	$1.49^{+0.17+0.08}_{-0.15-0.06}$	[73]
DELPHI	$D^{(*)}\ell$	91–93	$1.61^{+0.14}_{-0.13} \pm 0.08$	[74]
DELPHI	Charge sec. vtx	91–93	$1.63 \pm 0.14 \pm 0.13$	[75]
DELPHI	Inclusive $D^*\ell$	91–93	$1.532 \pm 0.041 \pm 0.040$	[76]
DELPHI	Charge sec. vtx	94–95	$1.531 \pm 0.021 \pm 0.031$	[71]
L3	Charge sec. vtx	94–95	$1.52 \pm 0.06 \pm 0.04$	[77]
OPAL	$D^{(*)}\ell$	91–93	$1.53 \pm 0.12 \pm 0.08$	[78]
OPAL	Charge sec. vtx	93–95	$1.523 \pm 0.057 \pm 0.053$	[79]
OPAL	Inclusive $D^*\ell$	91–00	$1.541 \pm 0.028 \pm 0.023$	[80]
SLD	Charge sec. vtx ℓ	93–95	$1.56^{+0.14}_{-0.13} \pm 0.10$	[81][a]
SLD	Charge sec. vtx	93–95	$1.66 \pm 0.08 \pm 0.08$	[81][a]
CDF1	$D^{(*)}\ell$	92–95	$1.474 \pm 0.039^{+0.052}_{-0.051}$	[82]
CDF1	Excl. $J/\psi K^{*0}$	92–95	$1.497 \pm 0.073 \pm 0.032$	[83]
CDF2	Excl. $J/\psi K^0_S$, $J/\psi K^{*0}$	02–09	$1.507 \pm 0.010 \pm 0.008$	[84]
D0	Excl. $J/\psi K^{*0}$	03–07	$1.414 \pm 0.018 \pm 0.034$	[85]
D0	Excl. $J/\psi K^0_S$	02–11	$1.508 \pm 0.025 \pm 0.043$	[86]
D0	Inclusive $D^-\mu^+$	02–11	$1.534 \pm 0.019 \pm 0.021$	[87]
BABAR	Exclusive	99–00	$1.546 \pm 0.032 \pm 0.022$	[88]
BABAR	Inclusive $D^*\ell$	99–01	$1.529 \pm 0.012 \pm 0.029$	[89]
BABAR	Exclusive $D^*\ell$	99–02	$1.523^{+0.024}_{-0.023} \pm 0.022$	[90]
BABAR	Incl. $D^*\pi$, $D^*\rho$	99–01	$1.533 \pm 0.034 \pm 0.038$	[91]
BABAR	Inclusive $D^*\ell$	99–04	$1.504 \pm 0.013^{+0.018}_{-0.013}$	[92]
Belle	Exclusive	00–03	$1.534 \pm 0.008 \pm 0.010$	[93]
ATLAS	Excl. $J/\psi K^0_S$	2011	$1.509 \pm 0.012 \pm 0.018$	[94]
CMS	Excl. $J/\psi K^{*0}$	2012	$1.511 \pm 0.005 \pm 0.006$	[95][b]
CMS	Excl. $J/\psi K^0_S$	2012	$1.527 \pm 0.009 \pm 0.009$	[95][b]
LHCb	Excl. $J/\psi K^{*0}$	2011	$1.524 \pm 0.006 \pm 0.004$	[96]
LHCb	Excl. $J/\psi K^0_S$	2011	$1.499 \pm 0.013 \pm 0.005$	[96]
LHCb	$K^+\pi^-$	2011	$1.524 \pm 0.011 \pm 0.004$	[97]
Belle II	$D^{(*)-}\pi^+$	19–21	$1.499 \pm 0.013 \pm 0.008$	[98]
Average			1.517 ± 0.004	

[a]The combined SLD result quoted in Ref. [81] is $1.64 \pm 0.08 \pm 0.08$ ps.
[b]The combined CMS result quoted in Ref. [95] is $1.515 \pm 0.005 \pm 0.006$ ps.

3. B^0_s lifetimes

Like neutral kaons, neutral B mesons contain short- and long-lived components, since the light (L) and heavy (H) eigenstates differ not only in their masses but also in their total decay widths. While in the B^0 system the decay width difference $\Delta\Gamma_d$ can be neglected, the B^0_s system exhibits a significant value of the width difference $\Delta\Gamma_s = \Gamma_{s\mathrm{L}} - \Gamma_{s\mathrm{H}}$, where $\Gamma_{s\mathrm{L}}$ and $\Gamma_{s\mathrm{H}}$ are the total decay widths of the light eigenstate $B^0_{s\mathrm{L}}$ and the heavy eigenstate $B^0_{s\mathrm{H}}$, respectively. The sign of $\Delta\Gamma_s$ is measured to be positive [101], i.e., $B^0_{s\mathrm{H}}$ has a longer lifetime than $B^0_{s\mathrm{L}}$. Specific measurements of $\Delta\Gamma_s$ and $\Gamma_s = (\Gamma_{s\mathrm{L}} + \Gamma_{s\mathrm{H}})/2$, which are more involved than simple lifetime measurements, are explained and averaged in Sec. V B 2, but the resulting averages for $1/\Gamma_{s\mathrm{L}} = 1/(\Gamma_s + \Delta\Gamma_s/2)$, $1/\Gamma_{s\mathrm{H}} = 1/(\Gamma_s - \Delta\Gamma_s/2)$ and the mean B^0_s lifetime, defined as $\tau(B^0_s) = 1/\Gamma_s$ are also

TABLE 7. Measurements of the B^+ lifetime with exclusive (excl.) decays or with B charge determination from the secondary vertex (sec. vtx). See Sec. VA for a detailed explanation of the method.

Experiment	Method	Dataset	$\tau(B^+)$ (ps)	Refs.
ALEPH	$D^{(*)}\ell$	91–95	$1.648 \pm 0.049 \pm 0.035$	[72]
ALEPH	Exclusive	91–94	$1.58^{+0.21+0.04}_{-0.18-0.03}$	[73]
DELPHI	$D^{(*)}\ell$	91–93	$1.61 \pm 0.16 \pm 0.12$	[74][a]
DELPHI	Charge sec. vtx	91–93	$1.72 \pm 0.08 \pm 0.06$	[75][a]
DELPHI	Charge sec. vtx	94–95	$1.624 \pm 0.014 \pm 0.018$	[71]
L3	Charge sec. vtx	94–95	$1.66 \pm 0.06 \pm 0.03$	[77]
OPAL	$D^{(*)}\ell$	91–93	$1.52 \pm 0.14 \pm 0.09$	[78]
OPAL	Charge sec. vtx	93–95	$1.643 \pm 0.037 \pm 0.025$	[79]
SLD	Charge sec. vtx ℓ	93–95	$1.61^{+0.13}_{-0.12} \pm 0.07$	[81][b]
SLD	Charge sec. vtx	93–95	$1.67 \pm 0.07 \pm 0.06$	[81][b]
CDF1	$D^{(*)}\ell$	92–95	$1.637 \pm 0.058^{+0.045}_{-0.043}$	[82]
CDF1	Excl. $J/\psi K$	92–95	$1.636 \pm 0.058 \pm 0.025$	[83]
CDF2	Excl. $J/\psi K$	02–09	$1.639 \pm 0.009 \pm 0.009$	[84]
CDF2	Excl. $D^0\pi$	02–06	$1.663 \pm 0.023 \pm 0.015$	[99]
BABAR	Exclusive	99–00	$1.673 \pm 0.032 \pm 0.023$	[88]
Belle	Exclusive	00–03	$1.635 \pm 0.011 \pm 0.011$	[93]
LHCb	Excl. $J/\psi K$	2011	$1.637 \pm 0.004 \pm 0.003$	[96]
Average			1.638 ± 0.004	

[a]The combined DELPHI result quoted in [75] is 1.70 ± 0.09 ps.

[b]The combined SLD result quoted in [81] is $1.66 \pm 0.06 \pm 0.05$ ps.

TABLE 8. Measurements of the ratio $\tau(B^+)/\tau(B^0)$ from exclusive (excl.) decays modes or with B charge determination from the secondary vertex (sec. vtx). See Sec. VA for a detailed explanation of the method.

Experiment	Method	Dataset	Ratio $\tau(B^+)/\tau(B^0)$	Refs.
ALEPH	$D^{(*)}\ell$	91–95	$1.085 \pm 0.059 \pm 0.018$	[72]
ALEPH	Exclusive	91–94	$1.27^{+0.23+0.03}_{-0.19-0.02}$	[73]
DELPHI	$D^{(*)}\ell$	91–93	$1.00^{+0.17}_{-0.15} \pm 0.10$	[74]
DELPHI	Charge sec. vtx	91–93	$1.06^{+0.13}_{-0.11} \pm 0.10$	[75]
DELPHI	Charge sec. vtx	94–95	$1.060 \pm 0.021 \pm 0.024$	[71]
L3	Charge sec. vtx	94–95	$1.09 \pm 0.07 \pm 0.03$	[77]
OPAL	$D^{(*)}\ell$	91–93	$0.99 \pm 0.14^{+0.05}_{-0.04}$	[78]
OPAL	Charge sec. vtx	93–95	$1.079 \pm 0.064 \pm 0.041$	[79]
SLD	Charge sec. vtx ℓ	93–95	$1.03^{+0.16}_{-0.14} \pm 0.09$	[81][a]
SLD	Charge sec. vtx	93–95	$1.01^{+0.09}_{-0.08} \pm 0.05$	[81][a]
CDF1	$D^{(*)}\ell$	92–95	$1.110 \pm 0.056^{+0.033}_{-0.030}$	[82]
CDF1	Excl. $J/\psi K$	92–95	$1.093 \pm 0.066 \pm 0.028$	[83]
CDF2	Excl. $J/\psi K^{(*)}$	02–09	$1.088 \pm 0.009 \pm 0.004$	[84]
D0	$D^{*+}\mu D^0\mu$ ratio	02–04	$1.080 \pm 0.016 \pm 0.014$	[100]
BABAR	Exclusive	99–00	$1.082 \pm 0.026 \pm 0.012$	[88]
Belle	Exclusive	00–03	$1.066 \pm 0.008 \pm 0.008$	[93]
LHCb	Excl. $J/\psi K^{(*)}$	2011	$1.074 \pm 0.005 \pm 0.003$	[96]
Average			1.076 ± 0.004	

[a]The combined SLD result quoted in [81] is $1.01 \pm 0.07 \pm 0.06$.

quoted at the end of this section. Neglecting CP violation in $B_s^0 - \bar{B}_s^0$ mixing, which is expected [51,102–106] and measured (see Sec. V B 3) to be very small, the mass eigenstates are also CP eigenstates, with the short-lived (light) state being CP-even and the long-lived (heavy) state being CP-odd [101].

Many B_s^0 lifetime analyses, in particular the early ones performed before the nonzero value of $\Delta\Gamma_s$ was firmly established, ignore $\Delta\Gamma_s$ and fit the proper time distribution of a sample of B_s^0 candidates reconstructed in a certain final state f with a model containing a single exponential function for the signal. Such *effective lifetime* measurements, which we denote as $\tau_{\text{single}}(B_s^0 \to f)$, are estimates of the expectation value $\int_0^\infty t\Gamma(B_s(t) \to f)dt / \int_0^\infty \Gamma(B_s(t) \to f)dt$ of the decay time, where $\Gamma(B_s(t) \to f)$ is the total untagged time-dependent decay rate [107–109]. This expectation value may lie *a priori* anywhere between $1/\Gamma_{s\text{L}}$ and $1/\Gamma_{s\text{H}}$, depending on the proportion of $B_{s\text{L}}^0$ and $B_{s\text{H}}^0$ in the final state f. More recent determinations of effective lifetimes may be interpreted as measurements of the relative composition of $B_{s\text{L}}^0$ and $B_{s\text{H}}^0$ decaying to the final state f. Table 9 summarizes the effective lifetime measurements.

Averaging measurements of $\tau_{\text{single}}(B_s^0 \to f)$ over several final states f would yield a result corresponding to an ill-defined observable when the proportions of $B_{s\text{L}}^0$ and $B_{s\text{H}}^0$ differ. Therefore, the effective B_s^0 lifetime measurements are broken down into the following categories and averaged separately.

(i) $B_s^0 \to D_s^{\mp} X$ *decays* include mostly flavor-specific decays but also decays with an unknown mixture of light and heavy components. Measurements performed with such inclusive states are no longer used in our averages.

(ii) *Decays to flavor-specific final states*, i.e., decays to final states f with decay amplitudes satisfying $A(B_s^0 \to f) \neq 0$, $A(\bar{B}_s^0 \to \bar{f}) \neq 0$, $A(B_s^0 \to \bar{f}) = 0$ and $A(\bar{B}_s^0 \to f) = 0$. Since there are equal fractions of $B_{s\text{L}}^0$ and $B_{s\text{H}}^0$ at production time ($t = 0$), the corresponding effective lifetime, called the *flavor-specific lifetime*, is equal to [107]

$$\tau_{\text{single}}(B_s^0 \to \text{flavor specific}) = \frac{1/\Gamma_{s\text{L}}^2 + 1/\Gamma_{s\text{H}}^2}{1/\Gamma_{s\text{L}} + 1/\Gamma_{s\text{H}}} = \frac{1}{\Gamma_s}\frac{1 + \left(\frac{\Delta\Gamma_s}{2\Gamma_s}\right)^2}{1 - \left(\frac{\Delta\Gamma_s}{2\Gamma_s}\right)^2}. \quad (33)$$

Because of the fast $B_s^0 - \bar{B}_s^0$ oscillations, possible biases of the flavor-specific lifetime due to a combination of $B_s^0/\bar{B}_s^0$ production asymmetry, CP violation in the decay amplitudes ($|A(B_s^0 \to f)| \neq |A(\bar{B}_s^0 \to \bar{f})|$), and CP violation in $B_s^0 - \bar{B}_s^0$ mixing ($|q_s/p_s| \neq 1$, see Sec. V B) are strongly suppressed, by a factor $\sim x_s^2$ [where the definition of x_s is given in Eq. (49) and its value in Eq. (68)]. The $B_s^0/\bar{B}_s^0$ production asymmetry at LHCb and the CP asymmetry due to mixing have been measured to be compatible with zero with a precision below 3% [136] and 0.3% [see Eq. (76)], respectively. The corresponding effects on the flavor-specific lifetime, which therefore have a relative size of the order of 10^{-5} or smaller, can be neglected at the current level of experimental precision. Under the assumption of no production asymmetry and no CP violation in mixing, Eq. (33) is exact even for a flavor-specific decay with CP violation in the decay amplitudes. Hence any flavor-specific decay mode can be used to measure the flavor-specific lifetime.

The average of all flavor-specific B_s^0 lifetime measurements [87,97,114–121] is

$$\tau_{\text{single}}(B_s^0 \to \text{flavor specific}) = 1.527 \pm 0.011 \text{ ps}. \quad (34)$$

(iii) *The* $B_s^0 \to J/\psi\phi$ *decay* contains a well-measured mixture of CP-even and CP-odd states. The published $B_s^0 \to J/\psi\phi$ effective lifetime measurements [95,96,122,123] are combined into the average $\tau_{\text{single}}(B_s^0 \to J/\psi\phi) = 1.480 \pm 0.007$ ps. Analyses that separate the CP-even and CP-odd components in this decay through a full angular study, outlined in Sec. V B 2, provide directly precise measurements of $1/\Gamma_s$ and $\Delta\Gamma_s$ (see Table 20).

(iv) *The* $B_s^0 \to \mu^+\mu^-$ *decay* is predicted to be CP-odd in the Standard Model. Experimentally, a decay-time-dependent analysis can provide a measurement of the admixture of CP-even and CP-odd states. However, the statistical precision is currently too low to set any constraint on a possible CP-even contribution. Effective lifetime measurements have been published by LHCb [124], CMS [125] and ATLAS [126]. As two of the measurements have asymmetric statistical errors, different averaging procedures have been tested and due to the current central values and errors, it has been found that all of them are giving results consistent with considering the bigger of the two errors in a classic average procedure. Hence we consider 2.07 ± 0.29 ps for the LHCb input, 1.83 ± 0.23 ps for the CMS input and 0.99 ± 0.45 ps for the ATLAS input.

(v) *Decays to CP eigenstates* have also been measured. These include the CP-even modes $B_s^0 \to D_s^{(*)+} D_s^{(*)-}$ by ALEPH [127], $B_s^0 \to K^+K^-$ by LHCb [97,128] $B_s^0 \to D_s^+ D_s^-$ by LHCb [119] and $B_s^0 \to J/\psi\eta$ by LHCb [129,130], as well as the CP-odd modes $B_s^0 \to J/\psi f_0(980)$ by CDF [133] and D0 [134],

TABLE 9. Measurements of the effective B_s^0 lifetimes obtained from single exponential fits (except for the $J/\psi\pi^+\pi^-$ result of Ref. [110], obtained from a time-dependent amplitude analysis).

Experiment	Final state f		Dataset		$\tau_{\text{single}}(B_s^0 \to f)$ (ps)	Ref.
ALEPH	$D_s h$	Ill-defined	91–95		$1.47 \pm 0.14 \pm 0.08$	[111]
DELPHI	$D_s h$	Ill-defined	91–95		$1.53^{+0.16}_{-0.15} \pm 0.07$	[112]
OPAL	D_s incl.	Ill-defined	90–95		$1.72^{+0.20+0.18}_{-0.19-0.17}$	[113]
ALEPH	$D_s^- \ell^+$	Flavor-specific	91–95		$1.54^{+0.14}_{-0.13} \pm 0.04$	[114]
CDF1	$D_s^- \ell^+$	Flavor-specific	92–96		$1.36 \pm 0.09^{+0.06}_{-0.05}$	[115]
DELPHI	$D_s^- \ell^+$	Flavor-specific	92–95		$1.42^{+0.14}_{-0.13} \pm 0.03$	[116]
OPAL	$D_s^- \ell^+$	Flavor-specific	90–95		$1.50^{+0.16}_{-0.15} \pm 0.04$	[117]
D0	$D_s^- \mu^+ X$	Flavor-specific	02–11	10.4 fb^{-1}	$1.479 \pm 0.010 \pm 0.021$	[87]
CDF2	$D_s^- \pi^+(X)$	Flavor-specific	02–06	1.3 fb^{-1}	$1.518 \pm 0.041 \pm 0.027$	[118]
LHCb	$D_s^- D^+$	Flavor-specific	11–12	3 fb^{-1}	$1.52 \pm 0.15 \pm 0.01$	[119]
LHCb	$D_s^- \pi^+$	Flavor-specific	2011	1 fb^{-1}	$1.535 \pm 0.015 \pm 0.014$	[120]
LHCb	$\pi^+ K^-$	Flavor-specific	2011	1.0 fb^{-1}	$1.60 \pm 0.06 \pm 0.01$	[97]
LHCb	$D_s^{(*)-} \mu^+ \nu_\mu$	Flavor-specific	11–12	3.0 fb^{-1}	$1.547 \pm 0.013 \pm 0.011$	[121]
Average of above 10 flavor-specific lifetime measurements					1.527 ± 0.011	
CDF1	$J/\psi\phi$	CP even + odd	92–95		$1.34^{+0.23}_{-0.19} \pm 0.05$	[122]
D0	$J/\psi\phi$	CP even + odd	02–04		$1.444^{+0.098}_{-0.090} \pm 0.02$	[123]
LHCb	$J/\psi\phi$	CP even + odd	2011	1 fb^{-1}	$1.480 \pm 0.011 \pm 0.005$	[96]
CMS	$J/\psi\phi$	CP even + odd	2012	19.7 fb^{-1}	$1.481 \pm 0.007 \pm 0.005$	[95]
Average of above 4 $J/\psi\phi$ lifetime measurements					1.480 ± 0.007	
LHCb	$\mu^+\mu^-$	CP even + odd	11–18	8.7 fb^{-1}	$2.07 \pm 0.29 \pm 0.03$	[124]
CMS	$\mu^+\mu^-$	CP even + odd	16–18	140 fb^{-1}	$1.83^{+0.23}_{-0.20} \pm 0.04$	[125]
ATLAS	$\mu^+\mu^-$	CP even + odd	15–16	26.3 fb^{-1}	$0.99^{+0.42}_{-0.07} \pm 0.17$	[126]
Average of above 3 $\mu^+\mu^-$ lifetime measurements					1.79 ± 0.17	
ALEPH	$D_s^{(*)+} D_s^{(*)-}$	mostly CP even	91–95		$1.27 \pm 0.33 \pm 0.08$	[127]
LHCb	K^+K^-	CP-even	2010	0.037 fb^{-1}	$1.440 \pm 0.096 \pm 0.009$	[128]
LHCb	K^+K^-	CP-even	2011	1.0 fb^{-1}	$1.407 \pm 0.016 \pm 0.007$	[97]
Average of above 2 K^+K^- lifetime measurements					1.408 ± 0.017	
LHCb	$D_s^+ D_s^-$	CP-even	11–12	3 fb^{-1}	$1.379 \pm 0.026 \pm 0.017$	[119]
LHCb	$J/\psi\eta$	CP-even	11–12	3 fb^{-1}	$1.479 \pm 0.034 \pm 0.011$	[129]
LHCb	$J/\psi\eta$	CP-even	15–18	5.7 fb^{-1}	$1.445 \pm 0.016 \pm 0.008$	[130]
Average of above 3 measurements of $1/\Gamma_{sL}$					1.437 ± 0.014	
LHCb	$J/\psi K_S^0$	CP-odd	2011	1.0 fb^{-1}	$1.75 \pm 0.12 \pm 0.07$	[131]
CMS	$J/\psi K_S^0$	CP-odd	16–18	140 fb^{-1}	$1.59 \pm 0.07 \pm 0.03$	[132]
Average of above 2 $J/\psi K_S^0$ lifetime measurements					1.63 ± 0.07	
CDF2	$J/\psi f_0(980)$	CP-odd	02–08	3.8 fb^{-1}	$1.70^{+0.12}_{-0.11} \pm 0.03$	[133]
D0	$J/\psi f_0(980)$	CP-odd	02–11	10.4 fb^{-1}	$1.70 \pm 0.14 \pm 0.05$	[134]
LHCb	$J/\psi\pi^+\pi^-$	CP-odd	2011	1.0 fb^{-1}	$1.652 \pm 0.024 \pm 0.024$	[135]
CMS	$J/\psi\pi^+\pi^-$	CP-odd	2012	19.7 fb^{-1}	$1.677 \pm 0.034 \pm 0.011$	[95]
LHCb	$J/\psi\pi^+\pi^-$	CP-odd	15–16	1.9 fb^{-1}	$-0.050 \pm 0.004 \pm 0.004$[a]	[110]
Average of above 5 measurements of $1/\Gamma_{sH}$					1.646 ± 0.013	

[a] $\Gamma_{sH} - \Gamma_d$.

TABLE 10. Measurements of the B_c^+ lifetime.

Experiment	Method	Dataset		$\tau(B_c^+)$ (ps)	Ref.
CDF1	$J/\psi\ell$	92–95	0.11 fb^{-1}	$0.46^{+0.18}_{-0.16} \pm 0.03$	[138]
CDF2	$J/\psi e$	02–04	0.36 fb^{-1}	$0.463^{+0.073}_{-0.065} \pm 0.036$	[139]
D0	$J/\psi\mu$	02–06	1.3 fb^{-1}	$0.448^{+0.038}_{-0.036} \pm 0.032$	[140]
CDF2	$J/\psi\pi$		6.7 fb^{-1}	$0.452 \pm 0.048 \pm 0.027$	[141]
LHCb	$J/\psi\mu$	2012	2 fb^{-1}	$0.509 \pm 0.008 \pm 0.012$	[142]
LHCb	$J/\psi\pi$	11–12	3 fb^{-1}	$0.5134 \pm 0.0110 \pm 0.0057$	[143]
CMS	$J/\psi\pi$	2012	19.7 fb^{-1}	$0.541 \pm 0.026 \pm 0.014$	[95]
Average				0.510 ± 0.009	

$B_s^0 \to J/\psi\pi^+\pi^-$ by LHCb[4] [110,135] and CMS [95], and $B_s^0 \to J/\psi K_S^0$ by LHCb [131] and CMS [132]. If these decays are dominated by a single weak phase and if CP violation can be neglected, then $\tau_{\rm single}(B_s^0 \to CP\text{-even}) = 1/\Gamma_{s\rm L}$ and $\tau_{\rm single}(B_s^0 \to CP\text{-odd}) = 1/\Gamma_{s\rm H}$ (see Eqs. (63) and (64) for approximate relations in the presence of mixing-induced CP violation). However, not all these modes are pure CP eigenstates: a small CP-odd component is most probably present in $B_s^0 \to D_s^{*+}D_s^{*-}$ decays [137]. Furthermore, the decays $B_s^0 \to K^+K^-$ and $B_s^0 \to J/\psi K_S^0$ may suffer from direct CP violation due to interfering tree and loop amplitudes. The averages for the effective lifetimes obtained for decays to the (nearly) pure CP-even ($D_s^+D_s^-$, $J/\psi\eta$) and CP-odd ($J/\psi f_0(980)$, $J/\psi\pi^+\pi^-$) final states are

$$\tau_{\rm single}(B_s^0 \to CP\text{-even}) = 1.437 \pm 0.014 \text{ ps}, \quad (35)$$

$$\tau_{\rm single}(B_s^0 \to CP\text{-odd}) = 1.646 \pm 0.013 \text{ ps}. \quad (36)$$

As described in Sec. V B 2, the effective lifetime averages of Eqs. (34), (35), and (36) are used as constraints to improve the determination of $1/\Gamma_s$ and $\Delta\Gamma_s$ obtained from the full angular analyses of $B_s^0 \to J/\psi\phi$, $B_s^0 \to \psi(2S)\phi$ and $B_s^0 \to J/\psi K^+K^-$ decays. The resulting world averages for the B_s^0 lifetimes are

$$\tau(B_{s\rm L}^0) = \frac{1}{\Gamma_{s\rm L}} = \frac{1}{\Gamma_s + \Delta\Gamma_s/2} = 1.432 \pm 0.006 \text{ ps}, \quad (37)$$

$$\tau(B_{s\rm H}^0) = \frac{1}{\Gamma_{s\rm H}} = \frac{1}{\Gamma_s - \Delta\Gamma_s/2} = 1.612 \pm 0.008 \text{ ps}, \quad (38)$$

$$\tau(B_s^0) = \frac{1}{\Gamma_s} = \frac{2}{\Gamma_{s\rm L} + \Gamma_{s\rm H}} = 1.516 \pm 0.006 \text{ ps}. \quad (39)$$

4. B_c^+ lifetime

Early measurements of the B_c^+ meson lifetime, from CDF [138,139] and D0 [140], use the semileptonic decay mode $B_c^+ \to J/\psi\ell^+\nu$ and are based on a simultaneous fit to the mass and lifetime using the vertex formed with the leptons from the decay of the J/ψ and the third lepton. Correction factors are used to estimate the boost, which cannot be measured directly due to the invisible neutrino. Systematic uncertainties that are correlated among the measurements include the impact of the uncertainty of the B_c^+ transverse-momentum spectrum on the correction factors, the level of feed-down from $\psi(2S)$ decays, Monte Carlo modeling of the decay (estimated by varying the decay model from phase space to the ISGW model), and uncertainties in the B_c^+ mass. With more data, CDF2 was able to perform the first B_c^+ lifetime measurement based on fully reconstructed $B_c^+ \to J/\psi\pi^+$ decays [141], which does not suffer from a missing neutrino. More recent measurements at the LHC, both with $B_c^+ \to J/\psi\mu^+\nu$ decays from LHCb [142] and $B_c^+ \to J/\psi\pi^+$ decays from LHCb [143] and CMS [95], achieve the highest level of precision. Two of them [95,143] are made relative to the B^+ lifetime. Before averaging, they are scaled to our latest B^+ lifetime average, and the induced correlation is taken into account.

All the measurements are summarized in Table 10. The world average, dominated by the LHCb measurements, is determined to be

$$\tau(B_c^+) = 0.510 \pm 0.009 \text{ ps}, \quad (40)$$

[4]The result of Ref. [110] for the $B_s^0 \to J/\psi\pi^+\pi^-$ lifetime is not obtained through a single exponential fit of the lifetime distribution, but through a full time-dependent amplitude analysis, which concludes that the CP-odd fraction is greater than 97% at 95% CL and yields $\Gamma_{s\rm H} - \Gamma_d = -0.050 \pm 0.004 \pm 0.004$ ps^{-1}, where $1/\Gamma_d$ is the B^0 lifetime. Before being averaged with other determinations of the $B_s^0 \to J/\psi\pi^+\pi^-$ effective lifetime, this result is converted to a measurement of $1/\Gamma_{s\rm H}$ using the latest average of the B^0 lifetime.

which agrees well with the corresponding theory predictions in Refs. [144,145].

5. Λ_b^0 and other b-baryon lifetimes

The first measurements of b-baryon lifetimes, performed at LEP, originate from two classes of partially reconstructed decays. In the first class, decays with a fully reconstructed Λ_c^+ baryon and a lepton of opposite charge are used. These products are likely to occur in the decay of Λ_b^0 baryons. In the second class, more inclusive final states with a baryon (p, $\bar{p}$, Λ, or $\bar{\Lambda}$) and a lepton have been used, and these final states can generally arise from any b baryon. With the large b-hadron samples available at the Tevatron and the LHC, the most precise measurements of b baryons now come from fully reconstructed exclusive decays.

The following sources of correlated systematic uncertainties have been accounted for when averaging these measurements: experimental time resolution within a given experiment, b-quark fragmentation distribution into weakly decaying b baryons, Λ_b^0 polarization, decay model, and evaluation of the b-baryon purity in the selected event samples. In computing the averages, the central values of the masses are scaled to $M(\Lambda_b^0) = 5619.60 \pm 0.17$ MeV/c^2 [9].

For measurements with partially reconstructed decays, the meaning of the decay model systematic uncertainties and the correlation of these uncertainties between measurements are not always clear. Uncertainties related to the decay model are dominated by assumptions on the fraction of n-body semileptonic decays. To be conservative, it is assumed that these are 100% correlated whenever given as an uncertainty. DELPHI varies the fraction of four-body decays from 0.0 to 0.3. In computing the average, the DELPHI result is scaled to a value of 0.2 ± 0.2 for this fraction. Furthermore, the semileptonic decay results from LEP are scaled to a Λ_b^0 polarization of $-0.45^{+0.19}_{-0.17}$ [4] and a b fragmentation parameter $\langle x_E \rangle_b = 0.702 \pm 0.008$ [146].

The list of all measurements is given in Table 11. We do not attempt to average measurements performed with $p\ell$ or $\Lambda\ell$ combinations, which select unknown mixtures of b baryons. Measurements performed with $\Lambda_c^+\ell$ or $\Lambda\ell^+\ell^-$ combinations can be assumed to correspond to semileptonic Λ_b^0 decays. Their average ($1.247^{+0.071}_{-0.069}$ ps) is significantly different from the average using only measurements performed with exclusively reconstructed hadronic Λ_b^0 decays (1.471 ± 0.009 ps). The latter is much more precise and less prone to potential biases than the former. The discrepancy between the two averages is at the level of 3.1σ and assumed to be due to a systematic effect in the semileptonic measurements, where the Λ_b^0 momentum is not determined directly, or to a rare statistical fluctuation. Our final estimate of the Λ_b^0 lifetime is therefore based on the exclusive measurements only. The CDF $\Lambda_b^0 \to J/\psi\Lambda$ lifetime result [147] is larger than the average of all other exclusive measurements by 2.4σ. It is nonetheless kept in the combination without adjustment of input uncertainties.

For the strange b baryons, we do not include the measurements based on inclusive $\Xi^\mp\ell^\mp$ final states, which consist of a mixture of Ξ_b^- and Ξ_b^0 baryons. Rather, we only use results obtained with fully reconstructed Ξ_b^-, Ξ_b^0 and Ω_b^- baryons.

It should be noted that several b-baryon lifetime measurements from LHCb [159,161,163,164] were made with respect to the lifetime of another b hadron (i.e., the original measurement is that of a decay width difference). In particular, LHCb uses the $\Lambda_b^0 \to \Lambda_c^+\pi^-$ decay as a normalization channel for the $\tau(\Xi_b^0)$ and $\tau(\Xi_b^-)$ measurements, but does not use this decay for a measurement of $\tau(\Lambda_b^0)$. Therefore, we average Λ_c^+, Ξ_b^- and Ξ_b^0 lifetime simultaneously, taking all relevant correlations into account and constraining $\tau(B^0)$ to its average from Sec. V A 2. We subsequently average the Ω_b^- lifetime constraining the $\tau(\Xi_b^-)$ to its value obtained in the previous step. We obtain

$$\tau(\Lambda_b^0) = 1.468 \pm 0.009 \text{ ps}, \tag{41}$$

$$\tau(\Xi_b^-) = 1.578 \pm 0.021 \text{ ps}, \tag{42}$$

$$\tau(\Xi_b^0) = 1.477 \pm 0.032 \text{ ps}, \tag{43}$$

$$\tau(\Omega_b^-) = 1.64 \pm 0.16 \text{ ps}. \tag{44}$$

6. Summary and comparison with theoretical predictions

Averages of lifetimes of specific b-hadron species are collected in Table 12. As described in the introduction to Sec. V A, the HQE can be employed to explain the hierarchy $\tau(B_c^+) \ll \tau(\Lambda_b^0) < \tau(B_s^0) \approx \tau(B^0) < \tau(B^+)$, and to predict the ratios between lifetimes. Recent predictions are compared to the measured lifetime ratios in Table 13, where the experimental values have been computed as the ratio of our averages of the individual lifetimes. The ratios $\tau(\Lambda_b^0)/\tau(B^0)$, $\tau(\Xi_b^0)/\tau(\Xi_b^-)$, and $\tau(B_s^0)/\tau(B^0)$ are computed taking into account the correlation between the numerators and denominators. The ratio $\tau(B^+)/\tau(B^0)$ use only measurements of this ratio (see Sec. V A 2). The ratio $\tau(\Omega_b^-)/\tau(B^0)$ is computed neglecting the small correlation between both lifetimes.

The predictions of the ratio between the B^+ and B^0 lifetimes, 1.086 ± 0.022 [47] is in good agreement with experiment. The prediction of the ratio $\tau(B_s^0)/\tau(B^0)$ is less precise. Depending on the theoretical hypotheses, two solutions are proposed in Ref. [47]

$$\frac{\tau(B_s^0)}{\tau(B^0)} = 1.028 \pm 0.011, \tag{45}$$

$$\frac{\tau(B_s^0)}{\tau(B^0)} = 1.003 \pm 0.006. \tag{46}$$

TABLE 11. Measurements of the b-baryon lifetimes.

Experiment	Method	Dataset	Lifetime (ps)	Refs.
		b baryon admixture		
ALEPH	$\Lambda\ell$	91–95	$1.20 \pm 0.08 \pm 0.06$	[148]
DELPHI	$\Lambda\ell\pi$ vtx	91–94	$1.16 \pm 0.20 \pm 0.08$	[149][b]
DELPHI	$\Lambda\mu$ i.p.	91–94	$1.10^{+0.19}_{-0.17} \pm 0.09$	[150][b]
DELPHI	$p\ell$	91–94	$1.19 \pm 0.14 \pm 0.07$	[149][b]
OPAL	$\Lambda\ell$ i.p.	90–94	$1.21^{+0.15}_{-0.13} \pm 0.10$	[151][c]
OPAL	$\Lambda\ell$ vtx	90–94	$1.15 \pm 0.12 \pm 0.06$	[151][c]
		Ξ_b^-, Ξ_b^0 admixture		
ALEPH	$\Xi^-\ell^-X$	90–95	$1.35^{+0.37+0.15}_{-0.28-0.17}$	[152]
DELPHI	$\Xi^-\ell^-X$	91–93	$1.5^{+0.7}_{-0.4} \pm 0.3$	[153][d]
DELPHI	$\Xi^-\ell^-X$	92–95	$1.45^{+0.55}_{-0.43} \pm 0.13$	[154][d]
		Λ_b^0		
ALEPH	$\Lambda_c^+\ell$	91–95	$1.18^{+0.13}_{-0.12} \pm 0.03$	[148][a]
ALEPH	$\Lambda\ell^-\ell^+$	91–95	$1.30^{+0.26}_{-0.21} \pm 0.04$	[148][a]
DELPHI	$\Lambda_c^+\ell$	91–94	$1.11^{+0.19}_{-0.18} \pm 0.05$	[149][b]
OPAL	$\Lambda_c^+\ell$, $\Lambda\ell^-\ell^+$	90–95	$1.29^{+0.24}_{-0.22} \pm 0.06$	[117]
CDF1	$\Lambda_c^+\ell$	91–95	$1.32 \pm 0.15 \pm 0.07$	[155]
D0	$\Lambda_c^+\mu$	02–06	$1.290^{+0.119+0.087}_{-0.110-0.091}$	[156]
Average of above 6			$1.247^{+0.071}_{-0.069}$	
CDF2	$\Lambda_c^+\pi$	02–06	$1.401 \pm 0.046 \pm 0.035$	[157]
CDF2	$J/\psi\Lambda$	01–11	$1.565 \pm 0.035 \pm 0.020$	[147]
D0	$J/\psi\Lambda$	02–11	$1.303 \pm 0.075 \pm 0.035$	[86]
ATLAS	$J/\psi\Lambda$	2011	$1.449 \pm 0.036 \pm 0.017$	[94]
CMS	$J/\psi\Lambda$	2011	$1.503 \pm 0.052 \pm 0.031$	[158]
CMS	$J/\psi\Lambda$	2012	$1.477 \pm 0.027 \pm 0.009$	[95]
LHCb	$J/\psi\Lambda$	2011	$1.415 \pm 0.027 \pm 0.006$	[96]
LHCb	$J/\psi pK$ (with respect to B^0)	11–12	$1.479 \pm 0.009 \pm 0.010$	[159]
		Ξ_b^-		
CDF2	$J/\psi\Xi^-$	01–11	$1.32 \pm 0.14 \pm 0.02$	[147]
LHCb	$J/\psi\Xi^-$	11–12	$1.55^{+0.10}_{-0.09} \pm 0.03$	[160]
LHCb	$\Xi_c^0\pi^-$ (with respect to Λ_b^0)	11–12	$1.599 \pm 0.041 \pm 0.022$	[161]
LHCb	$\Xi_c^0\pi^-$ (with respect to Λ_b^0)	16–18	$1.575 \pm 0.019 \pm 0.009$	[162]
		Ξ_b^0		
LHCb	$\Xi_c^+\pi^-$ (with respect to Λ_b^0)	11–12	$1.477 \pm 0.026 \pm 0.019$	[163]
		Ω_b^-		
CDF2	$J/\psi\Omega^-$	01–11	$1.66^{+0.53}_{-0.40} \pm 0.02$	[147]
LHCb	$J/\psi\Omega^-$	11–12	$1.54^{+0.26}_{-0.21} \pm 0.05$	[160]
LHCb	$\Omega_c^0\pi^-$ (with respect to Ξ_b^-)	11–12	$1.78 \pm 0.26 \pm 0.05 \pm 0.06$	[164]
Combination of above 16 measurements with fully reconstructed decays			Λ_b^0 lifetime $= 1.468 \pm 0.008 \pm 0.005$ Ξ_b^- lifetime $= 1.578 \pm 0.019 \pm 0.009$ Ξ_b^0 lifetime $= 1.477 \pm 0.027 \pm 0.016$ Ω_b^- lifetime $= 1.64 \pm 0.16 \pm 0.03$	

[a]The combined ALEPH result quoted in [148] is 1.21 ± 0.11 ps.

[b]The combined DELPHI result quoted in [149] is $1.14 \pm 0.08 \pm 0.04$ ps.

[c]The combined OPAL result quoted in [151] is $1.16 \pm 0.11 \pm 0.06$ ps.

[d]The combined DELPHI result quoted in [154] is $1.48^{+0.40}_{-0.31} \pm 0.12$ ps.

TABLE 12. Summary of the lifetime averages for the different b-hadron species.

b-hadron species	Measured lifetime
B^+	1.638 ± 0.004 ps
B^0	1.517 ± 0.004 ps
B_s^0	$1/\Gamma_s = 1.516 \pm 0.006$ ps
B_{sL}^0	$1/\Gamma_{sL} = 1.432 \pm 0.006$ ps
B_{sH}^0	$1/\Gamma_{sH} = 1.612 \pm 0.008$ ps
B_c^+	0.510 ± 0.009 ps
Λ_b^0	1.468 ± 0.009 ps
Ξ_b^-	1.578 ± 0.021 ps
Ξ_b^0	1.477 ± 0.032 ps
Ω_b^-	1.64 ± 0.16 ps

These arise from the difference in the inputs in the calculation, taking the relevant parameters from Ref. [62] in the first and Ref. [63] in the second solutions. The second solution is much more compatible with the experimental result.

The HQE prediction for the ratio $\tau(\Lambda_b^0)/\tau(B^0)$ is now in excellent agreement with the data. Interestingly, in the 1990s a much lower experimental value for $\tau(\Lambda_b^0)$ was measured, and the world average for the ratio at the time resulted to be almost 4σ below the naive HQE prediction [44]. This large discrepancy triggered a considerable amount of interest in the theory community, see e.g. Ref. [47,50], and the validity of the HQE was put under scrutiny [165–167]. Ultimately, the experimental value of the Λ_b^0 lifetime changed and the $\tau(\Lambda_b^0)/\tau(B^0)$ ratio were found to be in agreement with the HQE result.

There is good agreement for the $\tau(\Xi_b^0)/\tau(\Xi_b^-)$ ratio and for $\tau(\Omega_b^-)/\tau(B^0)$ ratio, for which the prediction is based on the next-to-leading-order analysis of Ref. [66]. It is interesting to note that for the latter ratio, the theory precision is even higher than the experimental one.

B. Neutral B-meson mixing

The $B^0 - \bar{B}^0$ and $B_s^0 - \bar{B}_s^0$ systems both exhibit the phenomenon of particle-antiparticle mixing. For each of them, there are two mass eigenstates which are linear combinations of the two flavor states, B_q^0 and $\bar{B}_q^0$,

$$|B_{qL}^0\rangle = p_q|B_q^0\rangle + q_q|\bar{B}_q^0\rangle, \tag{47}$$

$$|B_{qH}^0\rangle = p_q|B_q^0\rangle - q_q|\bar{B}_q^0\rangle, \tag{48}$$

where the subscript $q = d$ is used for the B_d^0 $(= B^0)$ meson and $q = s$ for the B_s^0 meson. The heavier (lighter) of these mass states is denoted B_{qH}^0 (B_{qL}^0), with mass m_{qH} (m_{qL}) and total decay width Γ_{qH} (Γ_{qL}). We define

$$\Delta m_q = m_{qH} - m_{qL}, \qquad x_q = \Delta m_q/\Gamma_q, \tag{49}$$

$$\Delta\Gamma_q = \Gamma_{qL} - \Gamma_{qH}, \qquad y_q = \Delta\Gamma_q/(2\Gamma_q), \tag{50}$$

where $\Gamma_q = (\Gamma_{qH} + \Gamma_{qL})/2 = 1/\bar{\tau}(B_q^0)$ is the average decay width. By definition, Δm_q is positive, and $\Delta\Gamma_q$ is expected to be positive within the Standard Model.[5]

Four different time-dependent probabilities are needed to describe the evolution of a neutral B meson that is produced as a flavor state and decays without CP violation to a flavor-specific final state. If CPT is conserved, which will be assumed throughout, they can be written as

$$\begin{aligned}
\mathcal{P}(B_q^0 \to B_q^0) &= \frac{1}{2}e^{-\Gamma_q t}\left[\cosh\left(\frac{1}{2}\Delta\Gamma_q t\right) + \cos(\Delta m_q t)\right] \\
\mathcal{P}(B_q^0 \to \bar{B}_q^0) &= \frac{1}{2}e^{-\Gamma_q t}\left[\cosh\left(\frac{1}{2}\Delta\Gamma_q t\right) - \cos(\Delta m_q t)\right]|q_q/p_q|^2 \\
\mathcal{P}(\bar{B}_q^0 \to B_q^0) &= \frac{1}{2}e^{-\Gamma_q t}\left[\cosh\left(\frac{1}{2}\Delta\Gamma_q t\right) - \cos(\Delta m_q t)\right]|p_q/q_q|^2 \\
\mathcal{P}(\bar{B}_q^0 \to \bar{B}_q^0) &= \frac{1}{2}e^{-\Gamma_q t}\left[\cosh\left(\frac{1}{2}\Delta\Gamma_q t\right) + \cos(\Delta m_q t)\right],
\end{aligned} \tag{51}$$

where t is the proper time of the system. At the B factories *BABAR* and Belle (II), only the proper-time difference Δt between the decays of the two neutral B mesons from the $\Upsilon(4S)$ can be determined. However, since the two B mesons evolve coherently, meaning that they keep opposite flavors as long as neither of them has decayed, the above formulas remain valid if t is replaced with Δt and the production flavor is replaced by the flavor at the time of the decay of the accompanying B meson into a flavor-specific

[5]For reasons of symmetry in Eqs. (49) and (50), $\Delta\Gamma$ is sometimes defined with the opposite sign. The definition adopted in Eq. (50) is the one used in most experimental papers and many phenomenology papers on B physics.

TABLE 13. Experimental averages of b-hadron lifetime ratios and heavy-quark expansion (HQE) predictions.

Lifetime ratio	Experimental average	HQE prediction
$\tau(B^+)/\tau(B^0)$	1.076 ± 0.004	1.086 ± 0.022 [47]
$\tau(B_s^0)/\tau(B^0)$	1.0017 ± 0.0034	1.028 ± 0.011 or 1.003 ± 0.006 [47]
$\tau(\Lambda_b^0)/\tau(B^0)$	0.969 ± 0.006	0.955 ± 0.014 [47]
$\tau(\Xi_b^0)/\tau(\Xi_b^-)$	0.936 ± 0.022	0.929 ± 0.028 [47]
$\tau(\Omega_b^-)/\tau(B^0)$	1.08 ± 0.11	1.081 ± 0.042 [47]

state. As can be seen in the above expressions, the mixing probabilities depend on three mixing observables: Δm_q, $\Delta\Gamma_q$, and $|q_q/p_q|^2$. In particular, CP violation in mixing exists if $|q_q/p_q|^2 \neq 1$. Another (nonindependent) observable often used to characterize CP violation in the mixing is the so-called semileptonic asymmetry, as it is measured using B^0 semileptonic decays (see Sec. V B 3), defined as

$$\mathcal{A}_{\rm SL}^q = \frac{|p_q/q_q|^2 - |q_q/p_q|^2}{|p_q/q_q|^2 + |q_q/p_q|^2}. \tag{52}$$

All mixing observables depend on two complex numbers, M_{12}^q and Γ_{12}^q, which are the off-diagonal elements of the 2×2 mass and decay matrices describing the evolution of the $B_q^0 - \bar{B}_q^0$ system. In the Standard Model, the quantity $|\Gamma_{12}^q/M_{12}^q|$ is small, of the order of $(m_b/m_t)^2$, where m_b and m_t are the bottom and top quark masses. The following relations hold to first order in $|\Gamma_{12}^q/M_{12}^q|$:

$$\Delta m_q = 2|M_{12}^q|[1 + \mathcal{O}(|\Gamma_{12}^q/M_{12}^q|^2)], \tag{53}$$

$$\Delta\Gamma_q = 2|\Gamma_{12}^q|\cos\phi_{12}^q[1 + \mathcal{O}(|\Gamma_{12}^q/M_{12}^q|^2)], \tag{54}$$

$$\begin{aligned}\mathcal{A}_{\rm SL}^q &= {\rm Im}\,(\Gamma_{12}^q/M_{12}^q) + \mathcal{O}(|\Gamma_{12}^q/M_{12}^q|^2) \\ &= \frac{\Delta\Gamma_q}{\Delta m_q}\tan\phi_{12}^q + \mathcal{O}(|\Gamma_{12}^q/M_{12}^q|^2),\end{aligned} \tag{55}$$

where

$$\phi_{12}^q = \arg\,(-M_{12}^q/\Gamma_{12}^q), \tag{56}$$

often called the mixing phase, is the observable phase difference between $-M_{12}^q$ and Γ_{12}^q. It should be noted that the theoretical predictions for Γ_{12}^q are based on a similar HQE as the lifetime predictions, see Refs. [105,106,168–170], for perturbative corrections, and Refs. [171–176] for non-perturbative matrix elements.

In the next sections we review in turn the experimental knowledge on the B^0 decay-width and mass differences, the B_s^0 decay-width and mass differences, CP violation in B^0 and B_s^0 mixing, and mixing-induced CP violation in B_s^0 decays.

1. B^0 mixing parameters $\Delta\Gamma_d$ and Δm_d

A large number of time-dependent B^0–$\bar{B}^0$ oscillation analyses have been performed by the ALEPH, DELPHI, L3, OPAL, CDF, D0, *BABAR*, Belle, Belle II and LHCb collaborations. The corresponding measurements of Δm_d are summarized in Table 14. It is notable that the systematic uncertainties are comparable to the statistical uncertainties; they are often dominated by sample composition, mistag probability, or b-hadron lifetime contributions. Before being combined, the measurements are adjusted to a common set of input values, including the averages of the lifetimes given in this report (see Secs. IV and V A) and the b-hadron fractions of Ref. [43]. Three of the *BABAR*, four of the DELPHI, and two of the OPAL measurements have small statistical correlations among each other. Taking into account the fraction of the dataset shared among these measurements, statistical correlations are fully accounted in the combination. Systematic correlations arise both from common physics sources (fractions, lifetimes, branching fractions of b hadrons), and from purely experimental or algorithmic effects (efficiency, resolution, flavor tagging, background description). Combining all published measurements listed in Table 14 and accounting for all relevant correlations yields $\Delta m_d = 0.5069 \pm 0.0016 \pm 0.0011$ ps^{-1}. This measurement is in agreement with the latest Standard Model prediction of 0.535 ± 0.021 ps^{-1} [47].

In addition, ARGUS and CLEO have published measurements of the time-integrated mixing probability χ_d [197–199], which average to $\chi_d = 0.182 \pm 0.015$. Following Ref. [199], the decay width difference $\Delta\Gamma_d$ could in principle be extracted from the measured value of $\Gamma_d = 1/\tau(B^0)$ and the above averages for Δm_d and χ_d (provided that $\Delta\Gamma_d$ has a negligible impact on the Δm_d and $\tau(B^0)$ analyses that have assumed $\Delta\Gamma_d = 0$), using the relation

$$\chi_d = \frac{x_d^2 + y_d^2}{2(x_d^2 + 1)}. \tag{57}$$

However, $\Delta\Gamma_d/\Gamma_d$ is too small and the knowledge of χ_d too imprecise to provide useful sensitivity on $\Delta\Gamma_d/\Gamma_d$. Direct time-dependent studies provide much stronger constraints: $|\Delta\Gamma_d|/\Gamma_d < 18\%$ at 95% CL from DELPHI [179], $-6.8\% < {\rm sign}({\rm Re}\lambda_{CP})\Delta\Gamma_d/\Gamma_d < 8.4\%$ at 90% CL from

TABLE 14. Time-dependent measurements included in the Δm_d average. The results obtained from multidimensional fits involving also the B^0 (and B^+) lifetime(s) as free parameter(s) [90,92,93] have been converted into one-dimensional measurements of Δm_d. All measurements have then been adjusted to a common set of physics parameters before being combined. The label *rec.* refers to the decay channel used to reconstruct the signal B^0, and *tag* refers to the technique used to tag the initial flavor of that B^0.

	Method			
Experiment and Refs.	rec.	tag	Δm_d in ps^{-1} before adjustment	Δm_d in ps^{-1} after adjustment
ALEPH [177]	ℓ	$Q_{\rm jet}$	$0.404 \pm 0.045 \pm 0.027$	
ALEPH [177]	ℓ	ℓ	$0.452 \pm 0.039 \pm 0.044$	
ALEPH [177]	Above two combined		$0.422 \pm 0.032 \pm 0.026$	$0.439 \pm 0.032 \pm 0.019$
ALEPH [177]	D^*	$\ell, Q_{\rm jet}$	$0.482 \pm 0.044 \pm 0.024$	$0.483 \pm 0.044 \pm 0.024$
DELPHI [178]	ℓ	$Q_{\rm jet}$	$0.493 \pm 0.042 \pm 0.027$	$0.498 \pm 0.041 \pm 0.031$
DELPHI [178]	$\pi^*\ell$	$Q_{\rm jet}$	$0.499 \pm 0.053 \pm 0.015$	$0.500 \pm 0.052 \pm 0.033$
DELPHI [178]	ℓ	ℓ	$0.480 \pm 0.040 \pm 0.051$	$0.493 \pm 0.039 \pm 0.054$
DELPHI [178]	D^*	$Q_{\rm jet}$	$0.523 \pm 0.072 \pm 0.043$	$0.522 \pm 0.072 \pm 0.043$
DELPHI [179]	vtx	comb	$0.531 \pm 0.025 \pm 0.007$	$0.534 \pm 0.025 \pm 0.006$
L3 [180]	ℓ	ℓ	$0.458 \pm 0.046 \pm 0.032$	$0.464 \pm 0.046 \pm 0.028$
L3 [180]	ℓ	$Q_{\rm jet}$	$0.427 \pm 0.044 \pm 0.044$	$0.438 \pm 0.044 \pm 0.042$
L3 [180]	ℓ	ℓ(IP)	$0.462 \pm 0.063 \pm 0.053$	$0.466 \pm 0.063 \pm 0.044$
OPAL [181]	ℓ	ℓ	$0.430 \pm 0.043^{+0.028}_{-0.030}$	$0.454 \pm 0.043 \pm 0.017$
OPAL [182]	ℓ	$Q_{\rm jet}$	$0.444 \pm 0.029^{+0.020}_{-0.017}$	$0.478 \pm 0.028 \pm 0.020$
OPAL [183]	$D^*\ell$	$Q_{\rm jet}$	$0.539 \pm 0.060 \pm 0.024$	$0.544 \pm 0.060 \pm 0.023$
OPAL [183]	D^*	ℓ	$0.567 \pm 0.089^{+0.029}_{-0.023}$	$0.572 \pm 0.089 \pm 0.025$
OPAL [80]	$\pi^*\ell$	$Q_{\rm jet}$	$0.497 \pm 0.024 \pm 0.025$	$0.496 \pm 0.023 \pm 0.028$
CDF1 [184]	$D\ell$	SST	$0.471^{+0.078\,+0.033}_{-0.068\,-0.034}$	$0.470 \pm 0.073 \pm 0.034$
CDF1 [185]	μ	μ	$0.503 \pm 0.064 \pm 0.071$	$0.519 \pm 0.064 \pm 0.070$
CDF1 [186]	ℓ	$\ell, Q_{\rm jet}$	$0.500 \pm 0.052 \pm 0.043$	$0.544 \pm 0.052 \pm 0.036$
CDF1 [187]	$D^*\ell$	ℓ	$0.516 \pm 0.099^{+0.029}_{-0.035}$	$0.52 \pm 0.10 \pm 0.03$
D0 [188]	$D^{(*)}\mu$	OST	$0.506 \pm 0.020 \pm 0.016$	$0.506 \pm 0.020 \pm 0.016$
BABAR [189]	B^0	ℓ, K, NN	$0.516 \pm 0.016 \pm 0.010$	$0.521 \pm 0.016 \pm 0.008$
BABAR [190]	ℓ	ℓ	$0.493 \pm 0.012 \pm 0.009$	$0.497 \pm 0.012 \pm 0.007$
BABAR [90]	$D^*\ell\nu$	ℓ, K, NN	$0.492 \pm 0.018 \pm 0.014$	$0.493 \pm 0.018 \pm 0.013$
BABAR [92]	$D^*\ell\nu$(part)	ℓ	$0.511 \pm 0.007 \pm 0.007$	$0.5125 \pm 0.0070 \pm 0.0070$
Belle [93]	$B^0, D^*\ell\nu$	comb	$0.511 \pm 0.005 \pm 0.006$	$0.5138 \pm 0.0048 \pm 0.0063$
Belle [191]	$D^*\pi$(part)	ℓ	$0.509 \pm 0.017 \pm 0.020$	$0.514 \pm 0.017 \pm 0.019$
Belle [15]	ℓ	ℓ	$0.503 \pm 0.008 \pm 0.010$	$0.507 \pm 0.008 \pm 0.008$
Belle II [98]	B^0	comb	$0.516 \pm 0.008 \pm 0.005$	$0.5128 \pm 0.0077 \pm 0.0041$
LHCb [192]	B^0	OST	$0.499 \pm 0.032 \pm 0.003$	$0.499 \pm 0.032 \pm 0.003$
LHCb [194]	B^0	OST, SST	$0.5156 \pm 0.0051 \pm 0.0033$	$0.5156 \pm 0.0051 \pm 0.0033$
LHCb [195]	$D\mu$	OST, SST	$0.503 \pm 0.011 \pm 0.013$	$0.503 \pm 0.011 \pm 0.013$
LHCb [196]	$D^{(*)}\mu$	OST	$0.5050 \pm 0.0021 \pm 0.0010$	$0.5050 \pm 0.0021 \pm 0.0010$
World average (all above measurements included):				$0.5069 \pm 0.0016 \pm 0.0011$
—ALEPH, DELPHI, L3 and OPAL only:				$0.495 \pm 0.010 \pm 0.010$
—CDF and D0 only:				$0.509 \pm 0.017 \pm 0.013$
—*BABAR*, Belle and Belle II only:				$0.5109 \pm 0.0030 \pm 0.0034$
—LHCb only:				$0.5063 \pm 0.0019 \pm 0.0010$

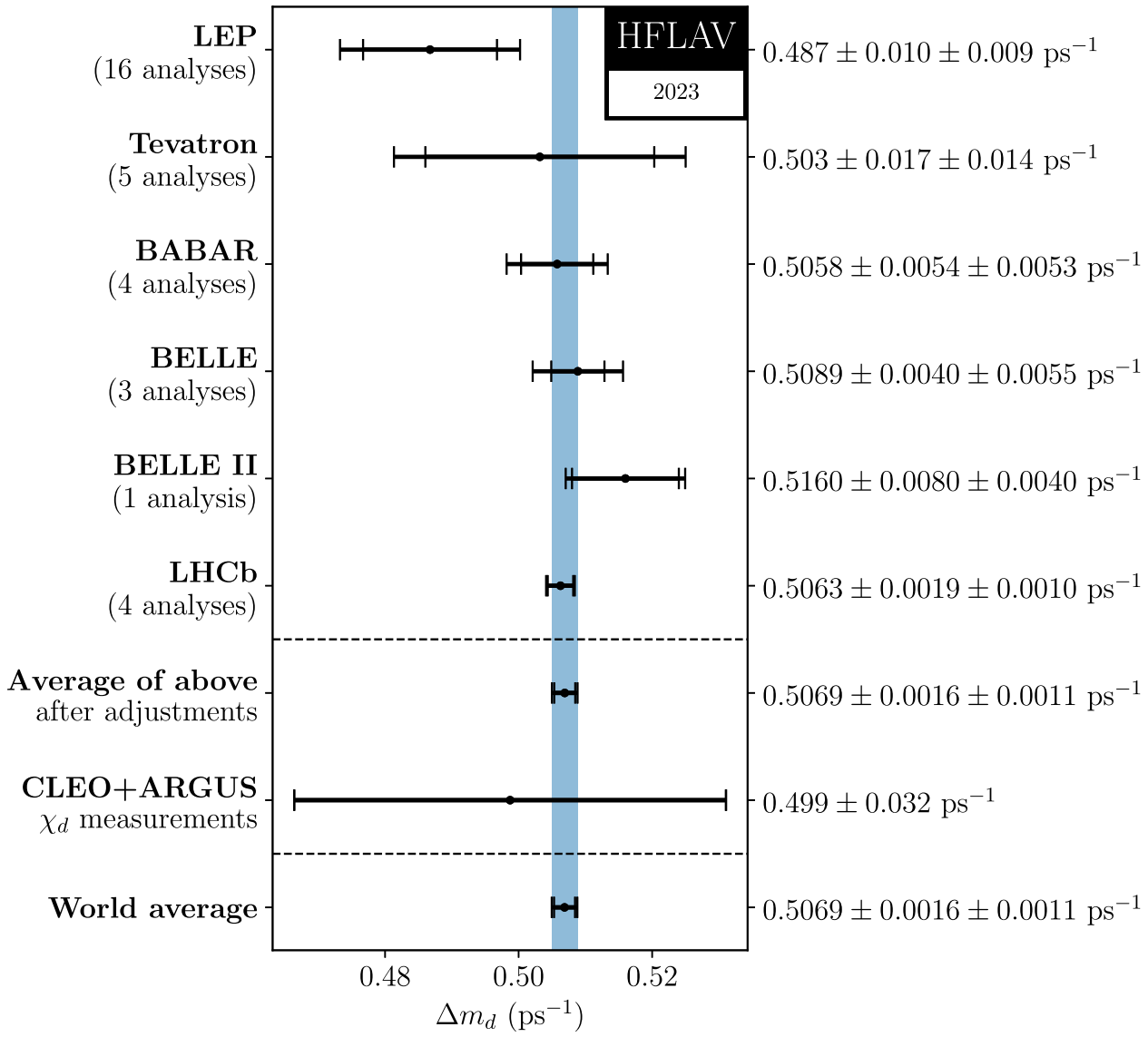


FIG. 5. The B^0–$\bar{B}^0$ oscillation frequency Δm_d as measured by the different experiments. The LEP, Tevatron, *BABAR*, Belle, Belle II and LHCb averages are computed from the individual results listed in Table 14 without performing any adjustments. The time-integrated measurements of χ_d from the symmetric B factory experiments ARGUS and CLEO are converted to a Δm_d value using $\tau(B^0) = 1.517 \pm 0.004$ ps. The two global averages are obtained after adjustments of all the individual Δm_d results of Table 14 (see text).

BABAR [200], and $\mathrm{sign}(\mathrm{Re}\lambda_{CP})\Delta\Gamma_d/\Gamma_d = (1.7 \pm 1.8 \pm 1.1)\%$ [201] from Belle, where $\lambda_{CP} = (q_d/p_d)A(\bar{B}^0 \to f_{CP})/A(B^0 \to f_{CP})$ with A denoting decays amplitudes to a CP-even final state. The sensitivity to the overall sign of $\mathrm{Re}\lambda_{CP}\Delta\Gamma_d/\Gamma_d$ comes from the use of B^0 decays to CP eigenstates. In addition, LHCb has obtained $\Delta\Gamma_d/\Gamma_d = (-4.4 \pm 2.5 \pm 1.1)\%$ [96] by comparing measurements of the lifetime for $B^0 \to J/\psi K^{*0}$ and $B^0 \to J/\psi K^0_S$ decays, following the method of Ref. [202]. Using a similar method, ATLAS and CMS have measured $\Delta\Gamma_d/\Gamma_d = (-0.1 \pm 1.1 \pm 0.9)\%$ [203] and $\Delta\Gamma_d/\Gamma_d = (+3.4 \pm 2.3 \pm 2.4)\%$ [95], respectively. Assuming $\mathrm{Re}\lambda_{CP} > 0$, as expected from the global fits of the unitarity triangle within the Standard Model [204,205], a combination of these six results (after adjusting the DELPHI and *BABAR* results to $1/\Gamma_d = \tau(B^0) = 1.517 \pm 0.004$ ps) yields

$$\Delta\Gamma_d/\Gamma_d = 0.001 \pm 0.010. \tag{58}$$

This average is consistent with zero and with the Standard Model prediction of $(3.97 \pm 0.90) \times 10^{-3}$ [103]. An independent result, $\Delta\Gamma_d/\Gamma_d = (0.50 \pm 1.38)\%$ [206], was obtained by the D0 collaboration from their measurements of the single muon and same-sign dimuon charge asymmetries, under the interpretation that the observed asymmetries are due to CP violation in neutral B-meson mixing

TABLE 15. Measurements of $\Delta\Gamma_s$ and Γ_s using $B_s^0 \to J/\psi K^+K^-$ and $B_s^0 \to \psi(2S)K^+K^-$ decays. Only the solution with $\Delta\Gamma_s > 0$ is shown, since the two-fold ambiguity has been resolved in Ref. [101]. The first error is due to statistics, the second one to systematics. The last line gives our average.

Exp.	Mode	Dataset	$\Delta\Gamma_s$ (ps^{-1})	Γ_s (ps^{-1})	Ref.
CDF	$J/\psi K^+K^-$	9.6 fb^{-1}	$+0.068 \pm 0.026 \pm 0.009$	$0.654 \pm 0.008 \pm 0.004$	[208]
D0	$J/\psi K^+K^-$	8.0 fb^{-1}	$+0.163^{+0.065}_{-0.064}$	$0.693^{+0.018}_{-0.017}$	[209]
ATLAS	$J/\psi K^+K^-$	4.9 fb^{-1}	$+0.053 \pm 0.021 \pm 0.010$	$0.677 \pm 0.007 \pm 0.004$	[210]
ATLAS	$J/\psi K^+K^-$	14.3 fb^{-1}	$+0.101 \pm 0.013 \pm 0.007$	$0.676 \pm 0.004 \pm 0.004$	[211]
ATLAS	$J/\psi K^+K^-$	80.5 fb^{-1}	$+0.0607 \pm 0.0047 \pm 0.0043$	$0.6687 \pm 0.0015 \pm 0.0022$	[212]
ATLAS	Above 3 combined		$+0.0657 \pm 0.0043 \pm 0.0037$	$0.6703 \pm 0.0014 \pm 0.0018$	[212]
CMS	$J/\psi K^+K^-$	19.7 fb^{-1}	$+0.095 \pm 0.013 \pm 0.007$	$0.6704 \pm 0.0043 \pm 0.0055$	[213]
CMS	$J/\psi K^+K^-$	96.5 fb^{-1}	$+0.0761 \pm 0.0043 \pm 0.0019$	$0.0030 \pm 0.0015 \pm 0.0022$[b]	[214]
CMS	Above 2 combined		$+0.078 \pm 0.004$	0.6640 ± 0.0028	
LHCb	$J/\psi K^+K^-$	3 fb^{-1}	$+0.0805 \pm 0.0091 \pm 0.0032$	$0.6603 \pm 0.0027 \pm 0.0015$	[215]
LHCb	$J/\psi K^+K^-$[a]	3 fb^{-1}	$+0.066 \pm 0.018 \pm 0.010$	$0.650 \pm 0.006 \pm 0.004$	[216]
LHCb	Above 2 combined		$+0.0813 \pm 0.0073 \pm 0.0036$	$0.6588 \pm 0.0022 \pm 0.0015$	[216]
LHCb	$J/\psi K^+K^-$	6 fb^{-1}	$+0.0845 \pm 0.0044 \pm 0.0025$	$-0.0056^{+0.0013}_{-0.0015} \pm 0.0014$[b]	[219]
LHCb	$J/\psi K^+K^-$[c]	3 fb^{-1}	$+0.115 \pm 0.045 \pm 0.011$	$0.608 \pm 0.018 \pm 0.012$	[218]
LHCb	$\psi(2S)K^+K^-$	3 fb^{-1}	$+0.066^{+0.041}_{-0.044} \pm 0.007$	$0.668 \pm 0.011 \pm 0.006$	[217]
LHCb	Above 5 combined		$+0.085 \pm 0.004$	0.6567 ± 0.0019	
All combined			$+0.076 \pm 0.004$	0.6632 ± 0.0034	

[a] $m(K^+K^-) > 1.05$ GeV/c^2.
[b] $\Gamma_s - \Gamma_d$.
[c] $J/\psi \to e^+e^-$.

and interference. This indirect determination was called into question [207] and is therefore not included in the above average, as explained in Sec. V B 3.

Assuming $\Delta\Gamma_d = 0$ and using $1/\Gamma_d = \tau(B^0) = 1.517 \pm 0.004$ ps, the Δm_d and χ_d results are combined through Eq. (57) to yield the world average

$$\Delta m_d = 0.5069 \pm 0.0019 \text{ ps}^{-1}, \tag{59}$$

or, equivalently,

$$x_d = 0.7697 \pm 0.0035 \quad \text{and} \quad \chi_d = 0.1860 \pm 0.0011. \tag{60}$$

Figure 5 compares the Δm_d values obtained by the different experiments.

The χ_d and x_d averages are obtained by neglecting small statistical and systematic correlations between Δm_d and $\tau(B^0)$.

2. B_s^0 mixing parameters $\Delta\Gamma_s$ and Δm_s

The best sensitivity to $\Delta\Gamma_s$ is currently achieved by the time-dependent measurements of the $B_s^0 \to J/\psi\phi$ (or more generally $B_s^0 \to (c\bar{c})K^+K^-$) decay rates performed at CDF [208], D0 [209], ATLAS [210–212], CMS [213,214] and LHCb [215–219], where the CP-even and CP-odd amplitudes are statistically separated through a full angular analysis. These studies use both untagged and tagged B_s^0 candidates and are optimized for the measurement of the CP-violating phase $\phi_s^{c\bar{c}s}$, defined later in Sec. V B 4. The LHCb collaboration analyzed the $B_s^0 \to J/\psi K^+K^-$ decay, considering that the K^+K^- system can be in a P-wave or S-wave state, and measured the dependence of the strong phase difference between the P-wave and S-wave amplitudes as a function of the K^+K^- invariant mass [101]. This allowed, for the first time, the unambiguous determination of the sign of $\Delta\Gamma_s$, which was found to be positive at the 4.7σ level.

The following averages present only the $\Delta\Gamma_s > 0$ solutions. Two degenerate solutions, differing in the values of two of the measured strong phases, $\delta_\perp$ and $\delta_\parallel$, were found in the ATLAS Run 2 analysis [212]. These show minor differences in the B_s^0 lifetime and mixing parameters, so for simplicity, the following averages only use solution (a) of Ref. [212].

The published results [208–219] are shown in Table 15. They are combined in a fit that includes all measured parameters and their correlations. These are $\phi_s^{c\bar{c}s}$, the direct CP violation parameter $|\lambda| = |(q_s/p_s)\bar{A}/A|$ ($\bar{A}$ and A are the $\bar{B}_s^0$ and B_s^0 decay amplitudes, respectively), Δm_s,

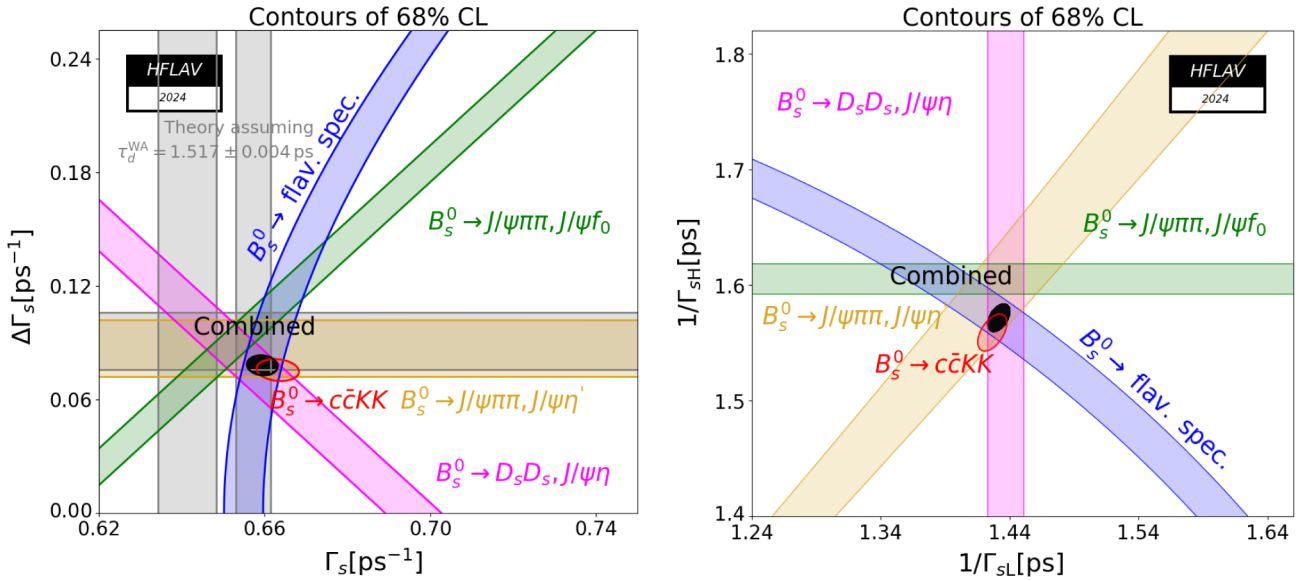


FIG. 6. Contours of 68% CL shown in the $(\Gamma_s, \Delta\Gamma_s)$ plane on the left and in the $(1/\Gamma_{sL}, 1/\Gamma_{sH})$ plane on the right. The average of all $B_s^0 \to J/\psi K^+K^-$ and $B_s^0 \to \psi(2S)K^+K^-$ results are shown as the red contour, where Γ_s and $\Delta\Gamma_s$ are scaled by factors 2.51 and 1.60. The constraints given by the effective lifetime measurements of B_s^0 to flavor-specific, pure CP-odd and pure CP-even final states are shown as the blue, green and purple bands, respectively. The constraint on $\Delta\Gamma_s$ given by the measurement of the lifetime difference between $B_s^0 \to J/\psi\pi^+\pi^-$ and $B_s^0 \to J/\psi\eta'$ is given by the golden bands. The average taking all constraints into account is shown as the dark-filled contour. The light-gray bands are theory predictions. The horizontal band is $\Delta\Gamma_s = +0.091 \pm 0.015$ ps^{-1} [47] that assumes no new physics in B_s^0 mixing. The vertical Γ_s bands are calculated from the two solutions in Ref. [47] assuming the experimental world average for the B^0 lifetime, 1.517 ± 0.004 ps. They are due to the two different sets of inputs to the theory calculation of $\tau(B_s^0)/\tau(B^0)$ according to Ref. [62] (toward lower Γ_s values) and Ref. [63] (toward higher Γ_s values).

polarization fractions and strong phases. As detailed further in Sec. V B 4, the $B_s^0 \to J/\psi K^+K^-$ measurements of ATLAS [211,212], CMS [213,214] and LHCb [215,219] are in tension at the level of several σ, driven by the time and angular parameters. To address this, the total uncertainty for each parameter in each $B_s^0 \to J/\psi K^+K^-$ set of results by ATLAS, CDF, D0, CMS and LHCb is scaled up in a way such that the results are in an agreement at the 1σ level. For the parameters already in agreement, notably ϕ_s, the uncertainties are not scaled. The covariance matrix is recomputed to preserve the correlations between the parameters. The resulting scale factors for Γ_s and $\Delta\Gamma_s$ are 2.51 and 1.60. The results, displayed as the red contours labeled "$B_s^0 \to (c\bar{c})KK$" in Fig. 6, are given in the first column of numbers of Table 16.

An alternative approach, which is directly sensitive to first order in $\Delta\Gamma_s/\Gamma_s$, is to determine the effective lifetime of untagged B_s^0 candidates decaying to pure CP eigenstates; we use here measurements with $B_s^0 \to D_s^+D_s^-$ [119], $B_s^0 \to J/\psi\eta$ [129,130], $B_s^0 \to J/\psi f_0(980)$ [133,134] and $B_s^0 \to J/\psi\pi^+\pi^-$ [95,110,135] decays. The precise extraction of $1/\Gamma_s$ and $\Delta\Gamma_s$ from such measurements, discussed in detail in Refs. [107–109], requires additional information in the form of theoretical assumptions or external inputs on weak phases and hadronic parameters. If f denotes a final state into which both B_s^0 and $\bar{B}_s^0$ can decay, the ratio of the effective $B_s^0 \to f$ lifetime τ_{single}, found by fitting the decay-time distribution to a single exponential, relative to the mean B_s^0 lifetime is [109][6]

$$\frac{\tau_{\text{single}}(B_s^0 \to f)}{\tau(B_s^0)} = \frac{1}{1-y_s^2}\left[\frac{1 - 2A_f^{\Delta\Gamma}y_s + y_s^2}{1 - A_f^{\Delta\Gamma}y_s}\right], \tag{61}$$

where

$$A_f^{\Delta\Gamma} = -\frac{2\mathrm{Re}(\lambda_f)}{1+|\lambda_f|^2}. \tag{62}$$

To include the measurements of the effective $B_s^0 \to D_s^+D_s^-$ (CP-even), $B_s^0 \to J/\psi\eta$ (CP-even), $B_s^0 \to J/\psi f_0(980)$ (CP-odd) and $B_s^0 \to J/\psi\pi^+\pi^-$ (CP-odd) lifetimes as constraints in the $\Delta\Gamma_s$ fit,[7] we neglect subleading penguin contributions and possible direct CP violation. Explicitly, in Eq. (61), we set $A_{CP\text{-even}}^{\Delta\Gamma} = \cos\phi_s^{c\bar{c}s}$ and $A_{CP\text{-odd}}^{\Delta\Gamma} = -\cos\phi_s^{c\bar{c}s}$. Given the small value of $\phi_s^{c\bar{c}s}$, we

[6]The definition of $A_f^{\Delta\Gamma}$ given in Eq. (62) has the sign opposite to that given in Ref. [109].

[7]The effective lifetimes measured in $B_s^0 \to K^+K^-$ (mostly CP-even) and $B_s^0 \to J/\psi K_S^0$ (mostly CP-odd) are not used because we cannot quantify the penguin contributions in those modes.

TABLE 16. Averages of $\Delta\Gamma_s$, Γ_s and related quantities, obtained from $B_s^0 \to J/\psi K^+K^-$ and $B_s^0 \to \psi(2S)K^+K^-$ alone (first column), adding the constraints from the effective lifetimes measured in pure CP modes $B_s^0 \to D_s^+D_s^-$, $J/\psi\eta$ and $B_s^0 \to J/\psi f_0(980)$, $J/\psi\pi^+\pi^-$ (second column), adding the $\Delta\Gamma_s$ constraint from $B_s^0 \to J/\psi\eta'$ and $B_s^0 \to J/\psi\pi^+\pi^-$, and adding the constraint from the effective lifetime measured in flavor-specific modes $B_s^0 \to D_s^-\ell^+\nu X$, $D_s^-\pi^+$, $D_s^-D^+$ (third column, recommended world averages).

	$B_s^0 \to (c\bar{c})K^+K^-$ modes only (see Table 15)	$B_s^0 \to (c\bar{c})K^+K^-$ modes +pure CP modes	$B_s^0 \to (c\bar{c})K^+K^-$ modes +pure CP modes +flavor-specific modes
Γ_s	0.6632 ± 0.0034 ps^{-1}	0.6595 ± 0.0029 ps^{-1}	0.6595 ± 0.0025 ps^{-1}
$1/\Gamma_s$	1.508 ± 0.008 ps	1.516 ± 0.007 ps	1.516 ± 0.006 ps
$1/\Gamma_{s\mathrm{L}}$	1.427 ± 0.007 ps	1.432 ± 0.006 ps	1.432 ± 0.006 ps
$1/\Gamma_{s\mathrm{H}}$	1.599 ± 0.011 ps	1.611 ± 0.010 ps	1.612 ± 0.008 ps
$\Delta\Gamma_s$	$+0.076 \pm 0.004$ ps^{-1}	$+0.078 \pm 0.004$ ps^{-1}	$+0.0781 \pm 0.0035$ ps^{-1}
$\Delta\Gamma_s/\Gamma_s$	$+0.114 \pm 0.006$	$+0.118 \pm 0.006$	$+0.119 \pm 0.005$
$\rho(\Gamma_s, \Delta\Gamma_s)$	-0.14	-0.16	-0.09

have, to first order in y_s

$$\tau_{\mathrm{single}}(B_s^0 \to CP\text{-even}) \approx \frac{1}{\Gamma_{s\mathrm{L}}}\left(1 + \frac{(\phi_s^{c\bar{c}s})^2 y_s}{2}\right), \quad (63)$$

$$\tau_{\mathrm{single}}(B_s^0 \to CP\text{-odd}) \approx \frac{1}{\Gamma_{s\mathrm{H}}}\left(1 - \frac{(\phi_s^{c\bar{c}s})^2 y_s}{2}\right). \quad (64)$$

The numerical inputs are taken from Eqs. (35) and (36), and the resulting averages, combined with the $B_s^0 \to J/\psi K^+K^-$ information, are indicated in the second column of numbers of Table 16.

Information on $\Delta\Gamma_s$ is also obtained from the study of the proper time distribution of untagged samples of flavor-specific B_s^0 decays [107], e.g. semileptonic B_s^0 decays, where the flavor (i.e., B_s^0 or $\bar{B}_s^0$) at the time of decay is determined by the decay products. Since there is an equal mix of the heavy and light mass eigenstates at production time ($t = 0$), the proper time distribution is a superposition of two exponential functions with decay constants $\Gamma_{s\mathrm{L}}$ and $\Gamma_{s\mathrm{H}}$. This provides sensitivity to both $1/\Gamma_s$ and $(\Delta\Gamma_s/\Gamma_s)^2$. Ignoring $\Delta\Gamma_s$ and fitting for a single exponential leads to an estimate of Γ_s with a relative bias proportional to $(\Delta\Gamma_s/\Gamma_s)^2$, as shown in Eq. (33). Furthermore, $\Delta\Gamma_s$ can be measured from the decay-width difference between CP-even and CP-odd B_s^0 decay final states, such as $B_s^0 \to J/\psi\eta'$ and $B_s^0 \to J/\psi\pi^+\pi^-$, respectively, as measured by LHCb [220]. The result is added as a constraint, where it is assumed to be uncorrelated with previous $B_s^0 \to J/\psi\pi^+\pi^-$ measurements, as the data overlap is expected to be small. Including the constraint from the world-average flavor-specific B_s^0 lifetime, given in Eq. (34), leads to the results shown in the last column of Table 16. These world averages are displayed as the dark-filled contours labeled "combined" in the plots of Fig. 6. They correspond to the lifetime averages $1/\Gamma_s = 1.516 \pm 0.006$ ps, $1/\Gamma_{s\mathrm{L}} = 1.432 \pm 0.006$ ps, $1/\Gamma_{s\mathrm{H}} = 1.612 \pm 0.008$ ps, and to the decay-width difference

$$\Delta\Gamma_s = +0.0781 \pm 0.0035 \text{ ps}^{-1} \quad \text{and}$$
$$\Delta\Gamma_s/\Gamma_s = +0.119 \pm 0.005. \quad (65)$$

The good agreement with the Standard Model predictions $\Delta\Gamma_s = +0.091 \pm 0.015$ ps^{-1} [47] and $\Delta\Gamma_s = +0.076 \pm 0.017$ ps^{-1} [221] excludes significant quark-hadron duality violation in the HQE [222]. Estimates of $\Delta\Gamma_s/\Gamma_s$ obtained from measurements of the $B_s^0 \to D_s^{(*)+}D_s^{(*)-}$ branching fraction [127,223–226] are not used in the average, since they are based on the questionable [54,55] assumption that these decays account for all CP-even final states. The results of early lifetime analyses that attempted to measure $\Delta\Gamma_s/\Gamma_s$ [77,112,116,122] are not used either.

The probability of B_s^0 mixing has been known to be large for more than 20 years. Indeed the time-integrated measurements of the flavor blind measurement $\bar{\chi} = f'_d\chi_d + f'_s\chi_s$, where f'_d and f'_s are the fractions of B^0 and B_s^0 hadrons in a sample of semileptonic b-hadron decays,[8] when compared to our knowledge of χ_d and the b-hadron fractions, indicated that χ_s should be close to its maximal possible value of $1/2$. Many searches of the time dependence of this mixing have been performed by ALEPH [227], DELPHI [112,116,179,228], OPAL [229,230], SLD [231,232], CDF (Run I) [233] and D0 [234] but did not have enough statistical power and proper time resolution to resolve the small period of the B_s^0 oscillations.

Oscillations of B_s^0 mesons were observed for the first time in 2006 by the CDF collaboration [235], based on samples of flavor-tagged hadronic and semileptonic B_s^0 decays in flavor-specific final states, partially or fully reconstructed in 1 fb^{-1} of data collected during Tevatron's Run II. Since then, the LHCb collaboration obtained the most precise results using fully reconstructed

[8]See Sec. 4.1.3 of our previous publication [43].

TABLE 17. Measurements of Δm_s.

Experiment	Method	Dataset		Δm_s (ps^{-1})	Ref.
CDF2	$D_s^{(*)-}\ell^+\nu$, $D_s^{(*)-}\pi^+$, $D_s^-\rho^+$		1 fb^{-1}	$17.77 \pm 0.10 \pm 0.07$	[235]
LHCb	$D_s^-\pi^+$, $D_s^-\pi^+\pi^-\pi^+$	2010	0.036 fb^{-1}	$17.63 \pm 0.11 \pm 0.02$	[193]
LHCb	$D_s^-\mu^+X$	2011	1.0 fb^{-1}	$17.93 \pm 0.22 \pm 0.15$	[195]
LHCb	$D_s^-\pi^+$	2011	1.0 fb^{-1}	$17.768 \pm 0.023 \pm 0.006$	[236]
LHCb	$J/\psi K^+K^-$	2011–2012	3.0 fb^{-1}	$17.711^{+0.055}_{-0.057} \pm 0.011$	[215]
LHCb	$J/\psi K^+K^-$	2015–2018	6 fb^{-1}	$17.743 \pm 0.033 \pm 0.009$	[219]
LHCb	Above 2 combined	2011–2018	9 fb^{-1}	17.730 ± 0.029	[219]
CMS	$J/\psi K^+K^-$	2017–2018	96.5 fb^{-1}	$17.757 \pm 0.035 \pm 0.017$	[214]
LHCb	$D_s^-\pi^+\pi^-\pi^+$	2011–2018	9 fb^{-1}	$17.757 \pm 0.007 \pm 0.008$	[237]
LHCb	$D_s^-\pi^+$	2015–2018	6 fb^{-1}	$17.768 \pm 0.005 \pm 0.003$	[238]
Average				$17.766 \pm 0.004 \pm 0.004$	

$B_s^0 \to D_s^-\pi^+$ and $B_s^0 \to D_s^-\pi^+\pi^-\pi^+$ decays [193,236–238]. LHCb has also observed B_s^0 oscillations with semileptonic $B_s^0 \to D_s^-\mu^+X$ decays [195]. In addition, measurements with non flavor-specific final states have been performed with $B_s^0 \to J/\psi K^+K^-$ decays by LHCb [215,219] and CMS [214]. The measurements of Δm_s are summarized in Table 17.

An average of all the published CDF2, LHCb and CMS results yields

$$\Delta m_s = 17.766 \pm 0.004 \pm 0.004 \text{ ps}^{-1} \tag{66}$$

and is illustrated in Fig. 7. The systematic uncertainties of the LHCb results due to the length scale (affecting all modes), the momentum scale ($B_s^0 \to D_s^-\pi^+$ Run 1 and Run

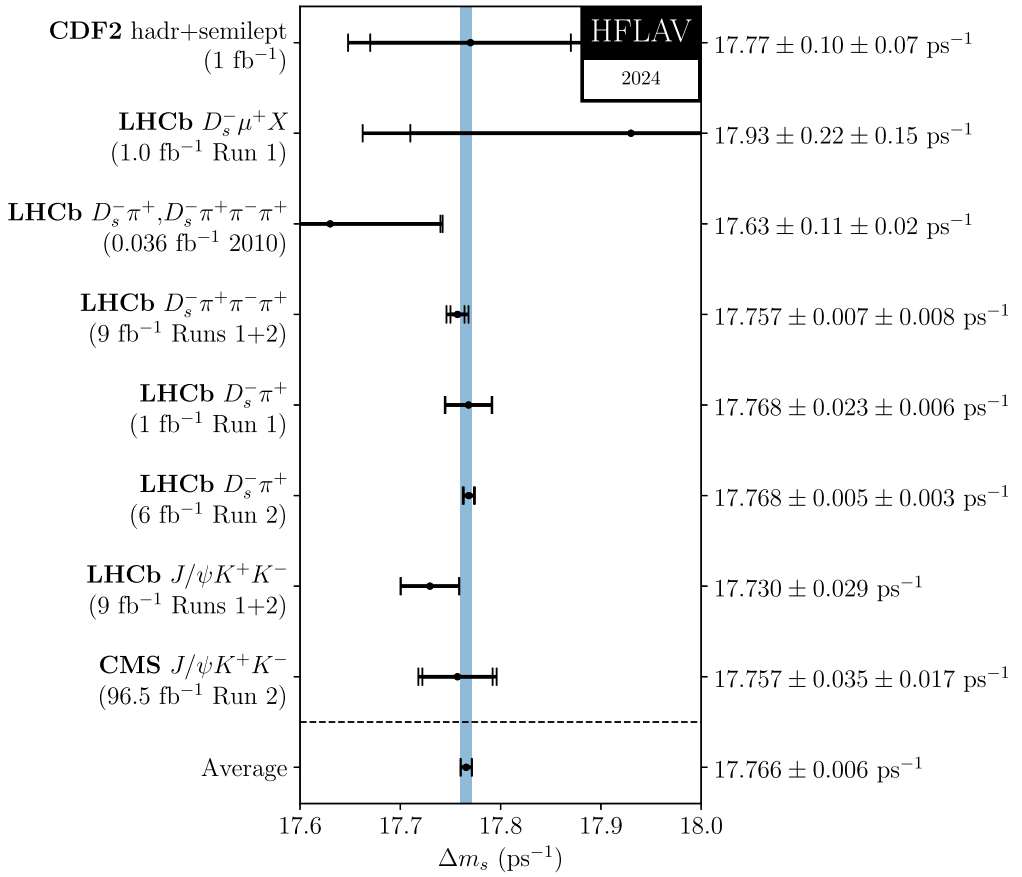


FIG. 7. Measurements of Δm_s, together with their average.

2, $B_s^0 \to D_s^- \pi^+ \pi^- \pi^+$ Run 1 and $B_s^0 \to J/\psi K^+ K^-$), the fit bias ($B_s^0 \to D_s^- \pi^+$ Run 1 and $B_s^0 \to D_s^- \pi^+ \pi^- \pi^+$ Run 1) and the decay-time bias ($B_s^0 \to D_s^- \pi^+$ Run 1 and Run 2) are considered to be 100% correlated. Furthermore, the CMS and LHCb measurements of Δm_s in $B_s^0 \to J/\psi K^+ K^-$ decays are averaged using the measured central values and uncertainties of the full set of observables determined in these studies (ϕ_s, $\Delta\Gamma_s$, Γ_s, $|\lambda|$, strong phases and polarization fractions) in order to account for their correlations with Δm_s.

The Standard Model prediction $\Delta m_s = 18.23 \pm 0.63\ \text{ps}^{-1}$ [47] is consistent with the experimental value, but has a much larger uncertainty, dominated by the uncertainty on the hadronic matrix elements determined in Refs. [64,171–175,239]. The ratio $\Delta\Gamma_s/\Delta m_s$ can be predicted more accurately to be 0.00499 ± 0.00079 [47,54,55,102,103,170,176], in good agreement with the experimental determination of

$$\Delta\Gamma_s/\Delta m_s = 0.0044 \pm 0.0002. \tag{67}$$

Multiplying the Δm_s result of Eq. (66) by the mean B_s^0 lifetime of Eq. (39), $1/\Gamma_s = 1.516 \pm 0.006$ ps, yields

$$x_s = 26.94 \pm 0.10. \tag{68}$$

With $2y_s = +0.119 \pm 0.005$ [see Eq. (65)] and under the assumption of no CP violation in B_s^0 mixing, this corresponds to

$$\chi_s = \frac{x_s^2 + y_s^2}{2(x_s^2+1)} = 0.499314 \pm 0.000005. \tag{69}$$

The ratio

$$\frac{\Delta m_d}{\Delta m_s} = 0.02853 \pm 0.00011, \tag{70}$$

of the B^0 and B_s^0 oscillation frequencies, obtained from Eqs. (59) and (66), can be used to extract the following magnitude of the ratio of CKM matrix elements,

$$\left|\frac{V_{td}}{V_{ts}}\right| = \xi \sqrt{\frac{\Delta m_d}{\Delta m_s}\frac{m(B_s^0)}{m(B^0)}} = \begin{cases} 0.2054 \pm 0.0004 \pm 0.0029\,(\text{lattice QCD}) \\ 0.2045 \pm 0.0004^{+0.0011}_{-0.0012}\,(\text{sum rules}) \end{cases}. \tag{71}$$

The first uncertainty is from experimental uncertainties (with the masses $m(B_s^0)$ and $m(B^0)$ taken from Ref. [9]). The second uncertainty arises from theoretical uncertainties in the estimation of the SU(3) flavor-symmetry breaking factor $\xi = 1.206 \pm 0.017$ [240], which is an average of three-flavor lattice QCD calculations dominated by the results of Ref. [171], or $\xi = 1.201^{+0.006}_{-0.007}$ [174] obtained from sum rules. Note that Eq. (71) assumes that Δm_s and Δm_d only receive Standard Model contributions.

3. CP violation in B^0 and B_s^0 mixing

Evidence for CP violation in B^0 mixing has been searched for, both with flavor-specific and inclusive B^0 decays, in samples where the initial flavor state is tagged. In the case of semileptonic (or other flavor-specific) decays, where the final state tag is also available, the asymmetry

$$\mathcal{A}_{\text{SL}}^d = \frac{N(\bar{B}^0(t) \to \ell^+ \nu_\ell X) - N(B^0(t) \to \ell^- \bar{\nu}_\ell X)}{N(\bar{B}^0(t) \to \ell^+ \nu_\ell X) + N(B^0(t) \to \ell^- \bar{\nu}_\ell X)} \tag{72}$$

has been measured, either in decay-time-integrated analyses at CLEO [199,241], *BABAR* [242], CDF [243] and D0 [206], or in decay-time-dependent analyses at OPAL [182], ALEPH [244], *BABAR* [200,245,246] and Belle [247]. Note that the asymmetry of time-dependent decay rates in Eq. (72) is related to $|q_d/p_d|$ through Eq. (52) and is therefore time-independent. In the inclusive case, also investigated and published by ALEPH [244] and OPAL [79], no final state tag is used, and the asymmetry [248]

$$\frac{N(B^0(t) \to \text{all}) - N(\bar{B}^0(t) \to \text{all})}{N(B^0(t) \to \text{all}) + N(\bar{B}^0(t) \to \text{all})} \simeq \mathcal{A}_{\text{SL}}^d \left[\frac{\Delta m_d}{2\Gamma_d}\sin(\Delta m_d t) - \sin^2\left(\frac{\Delta m_d t}{2}\right)\right] \tag{73}$$

must be measured as a function of the proper time to extract information on CP violation. Furthermore, D0 [249] and LHCb [250] have studied the time-dependence of the charge asymmetry of $B^0 \to D^{(*)-}\mu^+\nu_\mu X$ decays without tagging the initial state, which is equal to

$$\frac{N(D^{(*)-}\mu^+\nu_\mu X) - N(D^{(*)+}\mu^-\bar{\nu}_\mu X)}{N(D^{(*)-}\mu^+\nu_\mu X) + N(D^{(*)+}\mu^-\bar{\nu}_\mu X)} = \mathcal{A}_{\text{SL}}^d \frac{1 - \cos(\Delta m_d t)}{2} \tag{74}$$

in absence of detection and production asymmetries. Note that Eqs. (73) and (74) assume $\Delta\Gamma_d = 0$.

Table 18 summarizes the different measurements[9] of $\mathcal{A}_{\text{SL}}^d$ and $|q_d/p_d|$. In all cases asymmetries compatible with zero have been found. A simple average of all measurements performed at the B factories [199,200,241,242,245,247] yields $\mathcal{A}_{\text{SL}}^d = -0.0019 \pm 0.0027$. Adding also the D0 [249] and LHCb [250] measurements obtained with reconstructed semileptonic B^0 decays yields $\mathcal{A}_{\text{SL}}^d = +0.0001 \pm 0.0020$. As discussed in more detail later in this section, the D0 analysis with single muons and like-sign dimuons [206] separates the B^0 and B_s^0 contributions by exploiting the

[9] A low-statistics result published by CDF using the Run I data [243] is not included in our averages, nor in Table 18.

TABLE 18. Measurements[9] of CP violation in B^0 mixing and their average in terms of both $\mathcal{A}^d_{\rm SL}$ and $|q_d/p_d|$. The individual results are listed as quoted in the original publications, or converted[11] to an $\mathcal{A}^d_{\rm SL}$ value. The ALEPH and OPAL results assume no CP violation in B^0_s mixing. The abbreviation "rec." stands for reconstructed. See Sec. V 1 for a detailed explanation of the method.

Exp. and Refs.	Method	Measured $\mathcal{A}^d_{\rm SL}$	Measured $\lvert q_d/p_d\rvert$
CLEO [199]	Partial hadronic rec.	$+0.017 \pm 0.070 \pm 0.014$	
CLEO [241]	Dileptons	$+0.013 \pm 0.050 \pm 0.005$	
CLEO [241]	Average of above two	$+0.014 \pm 0.041 \pm 0.006$	
BABAR [200]	Full hadronic rec.		$1.029 \pm 0.013 \pm 0.011$
BABAR [245]	Part. rec. $D^*X\ell\nu$	$+0.0006 \pm 0.0017^{+0.0038}_{-0.0032}$	$0.99971 \pm 0.00084 \pm 0.00175$
BABAR [242]	Dileptons	$-0.0039 \pm 0.0035 \pm 0.0019$	
Belle [247]	Dileptons	$-0.0011 \pm 0.0079 \pm 0.0085$	$1.0005 \pm 0.0040 \pm 0.0043$
Average of above 6B-factory results		-0.0019 ± 0.0027 (tot)	1.0009 ± 0.0013 (tot)
D0 [249]	$B^0 \to D^{(*)-}\mu^+\nu X$	$+0.0068 \pm 0.0045 \pm 0.0014$	
LHCb [250]	$B^0 \to D^{(*)-}\mu^+\nu X$	$-0.0002 \pm 0.0019 \pm 0.0030$	
Average of above 8 pure B^0 results		$+0.0001 \pm 0.0020$ (tot)	1.0000 ± 0.0010 (tot)
D0 [206]	Muons and dimuons	-0.0062 ± 0.0043 (tot)	
Average of above 9 direct measurements		-0.0010 ± 0.0018 (tot)	1.0005 ± 0.0009 (tot)
OPAL [182]	Leptons	$+0.008 \pm 0.028 \pm 0.012$	
OPAL [79]	Inclusive [Eq. (73)]	$+0.005 \pm 0.055 \pm 0.013$	
ALEPH [244]	Leptons	$-0.037 \pm 0.032 \pm 0.007$	
ALEPH [244]	Inclusive [Eq. (73)]	$+0.016 \pm 0.034 \pm 0.009$	
ALEPH [244]	Average of above two	-0.013 ± 0.026 (tot)	
Average of above 13 results		-0.0010 ± 0.0018 (tot)	1.0005 ± 0.0009 (tot)
Best fit value from 2D combination of $\mathcal{A}^d_{\rm SL}$ and $\mathcal{A}^s_{\rm SL}$ results [see Eq. (75)]		-0.0021 ± 0.0017 (tot)	1.0010 ± 0.0008 (tot)

dependence on the muon impact parameter cut; including this $\mathcal{A}^d_{\rm SL}$ result from D0 in the average yields $\mathcal{A}^d_{\rm SL} = -0.0010 \pm 0.0018$.

All the other B^0 analyses performed at high energy, either at LEP or at the Tevatron, did not separate the contributions from the B^0 and B^0_s mesons. Under the assumption of no CP violation in B^0_s mixing ($\mathcal{A}^s_{\rm SL} = 0$), a number of these early analyses [79,182,244,251] report a measurement of $\mathcal{A}^d_{\rm SL}$ or $|q_d/p_d|$ for the B^0 meson. However, although we include them in Table 18, these imprecise determinations no longer improve the world average of $\mathcal{A}^d_{\rm SL}$. Furthermore, the assumption makes sense within the Standard Model, since $\mathcal{A}^s_{\rm SL}$ is predicted to be about a factor 20 smaller than $\mathcal{A}^d_{\rm SL}$ [102], but may not be suitable in the presence of new physics.

The Tevatron experiments have measured linear combinations of $\mathcal{A}^d_{\rm SL}$ and $\mathcal{A}^s_{\rm SL}$ using inclusive semileptonic decays of b hadrons. CDF (Run I) finds $\mathcal{A}^b_{\rm SL} = +0.0015 \pm 0.0038({\rm stat}) \pm 0.0020({\rm syst})$ [243], and D0 obtains $\mathcal{A}^b_{\rm SL} = -0.00496 \pm 0.00153({\rm stat}) \pm 0.00072({\rm syst})$ [206]. While the imprecise CDF result is compatible with no CP violation, the D0 result, obtained by measuring the single muon and like-sign dimuon charge asymmetries, differs by 2.8 standard deviations from the Standard Model expectation of $\mathcal{A}^{b,{\rm SM}}_{\rm SL} = (-2.3 \pm 0.4) \times 10^{-4}$ [54,55,206]. With a more sophisticated analysis in bins of the muon impact parameters, D0 conclude that the overall deviation of their measurements from the SM is at the level of 3.6σ. Interpreting the observed asymmetries in bins of the muon impact parameters in terms of CP violation in B-meson mixing and in interference, and using the mixing parameters and the world-average b-hadron production fractions of Ref. [252], the D0 collaboration extracts [206] values for $\mathcal{A}^d_{\rm SL}$ and $\mathcal{A}^s_{\rm SL}$ and their correlation coefficient,[10] as shown in Table 19. However, the various contributions to the total quoted uncertainties from this analysis and from the external inputs are not given, so the adjustment of these results to different or more recent values of the external inputs cannot (easily) be done.

[10]In each impact parameter bin i the measured same-sign dimuon asymmetry is interpreted as $A_i = K^s_i \mathcal{A}^s_{\rm SL} + K^d_i \mathcal{A}^d_{\rm SL} + \lambda K^{\rm int}_i \Delta\Gamma_d/\Gamma_d$, where the factors K^s_i, K^d_i and $K^{\rm int}_i$ are obtained by D0 from Monte Carlo simulation. The D0 publication [206] assumes $\lambda = 1$, but it has been demonstrated subsequently that $\lambda \leq 0.49$ [207]. This particular point invalidates the $\Delta\Gamma_d/\Gamma_d$ result published by D0, but not the $\mathcal{A}^d_{\rm SL}$ and $\mathcal{A}^s_{\rm SL}$ results. As stated by D0, their $\mathcal{A}^d_{\rm SL}$ and $\mathcal{A}^s_{\rm SL}$ results assume the above expression for A_i, i.e. that the observed asymmetries are due to CP violation in B mixing. As long as this assumption is not shown to be wrong (or withdrawn by D0), we include the $\mathcal{A}^d_{\rm SL}$ and $\mathcal{A}^s_{\rm SL}$ results in our world average.

TABLE 19. Measurements of CP violation in B^0 and B_s^0 mixing, together with their correlations $\rho(\mathcal{A}_{\rm SL}^s, \mathcal{A}_{\rm SL}^d)$ and their two-dimensional average. Only total errors are quoted.

Exp. and Refs.	Method	Measured $\mathcal{A}_{\rm SL}^d$	Measured $\mathcal{A}_{\rm SL}^s$	$\rho(\mathcal{A}_{\rm SL}^d, \mathcal{A}_{\rm SL}^s)$
B-factory average of Table 18		-0.0019 ± 0.0027		
D0 [249,253]	$B_{(s)}^0 \to D_{(s)}^{(*)-}\mu^+\nu X$	$+0.0068 \pm 0.0047$	-0.0112 ± 0.0076	$+0.$
LHCb [250,254]	$B_{(s)}^0 \to D_{(s)}^{(*)-}\mu^+\nu X$	-0.0002 ± 0.0036	$+0.0039 \pm 0.0033$	$+0.13$
Average of above		$+0.0000 \pm 0.0019$	$+0.0016 \pm 0.0030$	$+0.066$
D0 [206]	Muons and dimuons	-0.0062 ± 0.0043	-0.0082 ± 0.0099	-0.61
Average of all above		-0.0021 ± 0.0017	-0.0006 ± 0.0028	-0.054

Finally, direct determinations of $\mathcal{A}_{\rm SL}^s$, also shown in Table 19, have been obtained by D0 [253] and LHCb [254] from the time-integrated charge asymmetry of untagged $B_s^0 \to D_s^-\mu^+\nu X$ decays.

Using a two-dimensional fit, all measurements of $\mathcal{A}_{\rm SL}^d$ and $\mathcal{A}_{\rm SL}^s$ obtained by D0 and LHCb are combined with the B-factory average of Table 18. Correlations are taken into account as shown in Table 19. The results, displayed graphically in Fig. 8, are

$$\mathcal{A}_{\rm SL}^d = -0.0021 \pm 0.0017 \Leftrightarrow |q_d/p_d| = 1.0010 \pm 0.0008, \tag{75}$$

$$\mathcal{A}_{\rm SL}^s = -0.0006 \pm 0.0028 \Leftrightarrow |q_s/p_s| = 1.0003 \pm 0.0014, \tag{76}$$

$$\rho(\mathcal{A}_{\rm SL}^d, \mathcal{A}_{\rm SL}^s) = -0.054, \tag{77}$$

where $\rho(\mathcal{A}_{\rm SL}^d, \mathcal{A}_{\rm SL}^s)$ is the correlation coefficient between the two measured parameters, and the relation between $\mathcal{A}_{\rm SL}^q$ and $|q_q/p_q|$ is given in Eq. (52).[11] However, the fit χ^2 probability is only 4.5%. This is mostly due to an overall discrepancy between the D0 and LHCb averages at the level of 2.2σ. Since the assumptions underlying the inclusion of the D0 muon results in the average[10] are somewhat controversial [255], we also provide in Table 19 an average excluding these results.

The above averages show no evidence of CP violation in B^0 or B_s^0 mixing. They are consistent with the very small predictions of the Standard Model (SM), $\mathcal{A}_{\rm SL}^{d,\rm SM} = -(5.1 \pm 0.5) \times 10^{-4}$ and $\mathcal{A}_{\rm SL}^{s,\rm SM} = +(2.2 \pm 0.2) \times 10^{-5}$ [47]. Given the current experimental uncertainties, there is still significant room for a possible new physics contribution, in particular in the B_s^0 system. In this respect, the deviation of the D0 dimuon asymmetry [206] from expectation has generated significant interest. However, the recent $\mathcal{A}_{\rm SL}^s$ and $\mathcal{A}_{\rm SL}^d$ results from LHCb are not precise enough yet to settle the issue. It has been pointed out [256] that the D0 dimuon result can be reconciled with the SM expectations of $\mathcal{A}_{\rm SL}^s$ and $\mathcal{A}_{\rm SL}^d$ if there are non-SM sources of CP violation in the semileptonic decays of the b and c quarks. A Run 1 ATLAS study [257] of charge asymmetries in muon + jets $t\bar{t}$ events, in which a b-hadron decays semileptonically to a soft muon, yields results with limited statistical precision, compatible both with the D0 dimuon asymmetry and with the SM predictions.

At the more fundamental level, CP violation in B_s^0 mixing is caused by the weak phase difference ϕ_{12}^s defined in Eq. (56). The SM prediction for this phase is tiny [51,103],

$$\phi_{12}^{s,\rm SM} = 0.0046 \pm 0.0012. \tag{78}$$

However, new physics in B_s^0 mixing could change the observed phase to

$$\phi_{12}^s = \phi_{12}^{s,\rm SM} + \phi_{12}^{s,\rm NP}. \tag{79}$$

Using Eq. (55), the current knowledge of $\mathcal{A}_{\rm SL}^s$, $\Delta\Gamma_s$ and Δm_s, given in Eqs. (76), (65), and (66) respectively, yields an experimental determination of ϕ_{12}^s,

$$\tan\phi_{12}^s = \mathcal{A}_{\rm SL}^s \frac{\Delta m_s}{\Delta\Gamma_s} = -0.1 \pm 0.6, \tag{80}$$

which represents only a very weak constraint on new physics constributions.

4. Mixing-induced CP violation in B_s^0 decays

CP violation arising in the interference between $B_s^0 - \bar{B}_s^0$ mixing and decay is a very active field in which large experimental progress has been achieved in the last decade. The main observable is the phase $\phi_s^{c\bar{c}s}$, which describes CP

[11] Early analyses and the PDG use the complex parameter $\epsilon_B = (p_q - q_q)/(p_q + q_q)$ for the B^0; if CP violation in the mixing is small, $\mathcal{A}_{\rm SL}^d \cong 4{\rm Re}(\epsilon_B)/(1 + |\epsilon_B|^2)$ and the average of Eq. (75) corresponds to ${\rm Re}(\epsilon_B)/(1 + |\epsilon_B|^2) = -0.0005 \pm 0.0004$.

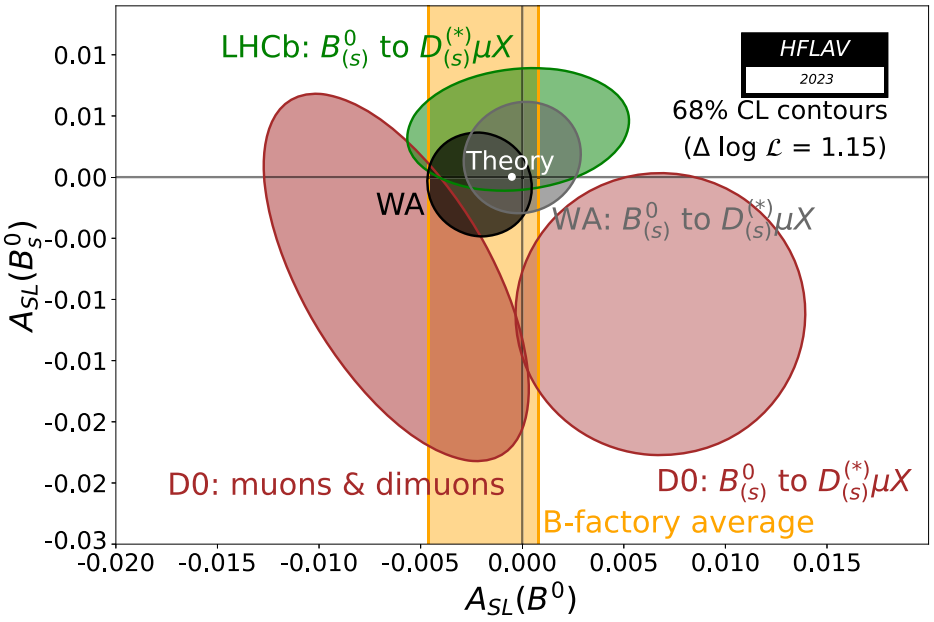


FIG. 8. Measurements of $\mathcal{A}^d_{\rm SL}$ and $\mathcal{A}^s_{\rm SL}$ listed in Table 19 (B-factory average as the orange band, D0 measurements as the brown ellipses, LHCb measurements as the green ellipse) together with their two-dimensional average (black ellipse). The gray ellipse is showing the average from D0 and LHCb results using only untagged $B^0_{(s)} \to D^{(*)-}_{(s)}\mu^+\nu X$ decays. The white point close to (0,0) is the Standard Model prediction of Ref. [47]. The prediction and the experimental world average are consistent with each other at the level of 0.5σ.

violation in the interference between B^0_s mixing and decay in $b \to c\bar{c}s$ transitions.

The golden mode for such studies is $B^0_s \to J/\psi K^+K^-$, where J/ψ decays to a muon and an anti-muon and the K^+ and K^- originate predominantly from a $\phi(1020)$ resonance, for which a full angular analysis of the decay products is performed to statistically separate the CP-even and CP-odd contributions in the final state. As already mentioned in Sec. V B 2, CDF [208], D0 [209], ATLAS [210–212], CMS [213,214] and LHCb [215–219] have used both untagged and tagged $B^0_s \to J/\psi K^+K^-$ (and more generally $B^0_s \to (c\bar{c})K^+K^-$) decays for the measurement of $\phi_s^{c\bar{c}s}$. LHCb [110,258] has used $B^0_s \to J/\psi\pi^+\pi^-$ events, analyzed with a full amplitude model including several $\pi^+\pi^-$ resonances [e.g., $f_0(980)$], although the $J/\psi\pi^+\pi^-$ final state had already been shown to have a CP-odd fraction larger than 0.977 at 95% CL [259]. In addition, LHCb has used the $B^0_s \to D^+_s D^-_s$ channel [260,261] to measure $\phi_s^{c\bar{c}s}$.

All CDF, D0, ATLAS and CMS analyses provide two mirror solutions related by the transformation $(\Delta\Gamma_s, \phi_s^{c\bar{c}s}) \to (-\Delta\Gamma_s, \pi - \phi_s^{c\bar{c}s})$. However, the LHCb analysis of $B^0_s \to J/\psi K^+K^-$ resolves this ambiguity and rules out the solution with negative $\Delta\Gamma_s$ [101], a result in agreement with the Standard Model expectation. Therefore, in what follows, we only consider the solution with $\Delta\Gamma_s > 0$.

In the $B^0_s \to J/\psi K^+K^-$ analyses, $\phi_s^{c\bar{c}s}$ and $\Delta\Gamma_s$ come from a simultaneous fit that determines also the B^0_s lifetime, the longitudinal and perpendicular ϕ polarization amplitudes $|A_0|^2$ and $|A_\perp|^2$, the S-wave amplitude $|A_S|^2$, and the strong phases. While the correlation between $\phi_s^{c\bar{c}s}$ and all other parameters is small, the correlations between $\Delta\Gamma_s$, Γ_s and the polarization amplitudes are sizeable. Therefore the full set of parameters provided by the measurements are combined in a multidimensional fit that considers the correlations between them. The combination uses the single-experiment average provided by ATLAS [212]. Both CMS and LHCb measure $\Gamma_s - \Gamma_d$ instead of Γ_s. Therefore, in order to obtain a value for Γ_s and combine it with the ATLAS result, we first perform an common average of CMS and LHCb results with the full dataset from Run 1 and Run 2. This average uses an updated world average $\tau(B^0)$ value (see Table 12).

As second-order loop processes could have different contributions to $\phi_s^{c\bar{c}s}$, we perform two combinations. In the first one, we perform a combination of all the CDF [208], D0 [209], ATLAS [210–212], CMS [213,214] and LHCb [110,215–219,258,260,261] results listed in Table 20. The second one uses only the $B^0_s \to J/\psi K^+K^-$ measurements in the vicinity of the $\phi(1020)$ resonance [208–215,218,219].

ATLAS [212] measures two solutions for the strong phases $\delta_\perp$ and $\delta_\parallel$. Using one or the other only leads to minor differences in the main parameters of interest, $\phi_s^{c\bar{c}s}$, $\Delta\Gamma_s$ and Γ_s. For simplicity, in this average, only solution (a) is used. In previous averages, the values of Δm_s and $|\lambda|$

TABLE 20. Direct experimental measurements of $\phi_s^{c\bar{c}s}$ and, wherever applicable, $\Delta\Gamma_s$ using $J/\psi K^+K^-$, $\psi(2S)K^+K^-$, $J/\psi\pi^+\pi^-$ and $D_s^+D_s^-$ decays. The first error is due to statistics, the second one to systematics. The last (last but one) line gives our averages, where the $\Delta\Gamma_s$ uncertainties have been multiplied by 1.60 (1.51) to account for inconsistencies between the $B_s^0 \to J/\psi K^+K^-$ measurements. Only solution (a) of Ref. [212] is used.

Exp.	Mode	Dataset	$\phi_s^{c\bar{c}s}$ (rad)	$\Delta\Gamma_s$ (ps^{-1})	Refs.
CDF	$J/\psi K^+K^-$	9.6 fb^{-1}	$[-0.60, +0.12]$, 68% CL	$+0.068 \pm 0.026 \pm 0.009$	[208]
D0	$J/\psi K^+K^-$	8.0 fb^{-1}	$-0.55^{+0.38}_{-0.36}$	$+0.163^{+0.065}_{-0.064}$	[209]
ATLAS	$J/\psi K^+K^-$	4.9 fb^{-1}	$+0.12 \pm 0.25 \pm 0.05$	$+0.053 \pm 0.021 \pm 0.010$	[210]
ATLAS	$J/\psi K^+K^-$	14.3 fb^{-1}	$-0.110 \pm 0.082 \pm 0.042$	$+0.101 \pm 0.013 \pm 0.007$	[211]
ATLAS	$J/\psi K^+K^-$	80.5 fb^{-1}	$-0.081 \pm 0.041 \pm 0.022$	$+0.0607 \pm 0.0047 \pm 0.0043$	[212]
ATLAS	Above 3 combined		$-0.087 \pm 0.036 \pm 0.021$	$+0.0657 \pm 0.0043 \pm 0.0037$	[212]
CMS	$J/\psi K^+K^-$	19.7 fb^{-1}	$-0.075 \pm 0.097 \pm 0.031$	$+0.095 \pm 0.013 \pm 0.007$	[213]
CMS	$J/\psi K^+K^-$	96.5 fb^{-1}	$-0.073 \pm 0.023 \pm 0.007$	$+0.0761 \pm 0.0043 \pm 0.0019$	[214]
CMS	Above 2 combined		-0.074 ± 0.023	$+0.078 \pm 0.004$	
LHCb	$J/\psi K^+K^-$	3.0 fb^{-1}	$-0.058 \pm 0.049 \pm 0.006$	$+0.0805 \pm 0.0091 \pm 0.0032$	[215]
LHCb	$J/\psi\pi^+\pi^-$	3.0 fb^{-1}	$+0.070 \pm 0.068 \pm 0.008$	…	[258]
LHCb	$J/\psi K^+K^-$[a]	3.0 fb^{-1}	$+0.119 \pm 0.107 \pm 0.034$	$+0.066 \pm 0.018 \pm 0.010$	[216]
LHCb	$\psi(2S)K^+K^-$	3.0 fb^{-1}	$+0.23^{+0.29}_{-0.28} \pm 0.02$	$+0.066^{+0.41}_{-0.44} \pm 0.007$	[217]
LHCb	$D_s^+D_s^-$	3.0 fb^{-1}	$+0.02 \pm 0.17 \pm 0.02$	…	[260]
LHCb	$D_s^+D_s^-$	6.0 fb^{-1}	$-0.09 \pm 0.11 \pm 0.03$	…	[261]
LHCb	$J/\psi\pi^+\pi^-$	1.9 fb^{-1}[b]	$-0.057 \pm 0.060 \pm 0.011$	…	[110]
LHCb	$J/\psi K^+K^-$	6 fb^{-1}[b]	$-0.039 \pm 0.022 \pm 0.006$	$+0.0845 \pm 0.0044 \pm 0.0024$	[219]
LHCb	$J/\psi K^+K^-$[c]	3.0 fb^{-1}	$+0.00 \pm 0.28 \pm 0.07$	$+0.115 \pm 0.045 \pm 0.011$	[218]
LHCb	Above 9 combined		-0.033 ± 0.018	$+0.085 \pm 0.004$	
$B_s^0 \to J/\psi K^+K^-$ combined			-0.060 ± 0.014	$+0.074 \pm 0.004$	
All combined			-0.052 ± 0.013	$+0.076 \pm 0.004$	

[a] $m(K^+K^-) > 1.05$ GeV/c^2.
[b] Run 2.
[c] $J/\psi \to e^+e^-$.

were fixed to the ones used by the ATLAS measurement. These are found to have little impact on $\phi_s^{c\bar{c}s}$, $\Delta\Gamma_s$ and Γ_s, and are now floated in the fit. Different regions of the $m(KK)$ mass are used in each measurement and the corresponding S-wave fractions and strong phases are considered independent for each experiment.

Using the same approach as discussed in Sec. V B 2 to address the tension between the $B_s^0 \to J/\psi K^+K^-$ measurements of ATLAS [211,212], CMS [213,214] and LHCb [215,219], the total uncertainty for each parameter in each $B_s^0 \to J/\psi K^+K^-$ set of results by ATLAS, CDF, D0, CMS and LHCb is scaled up in a way that results in an agreement of 1σ. The resulting scale factors are summarized in Table 21.

Given the increasing experimental precision of the LHC results, we have stopped using the two-dimensional $\Delta\Gamma_s - \phi_s^{c\bar{c}s}$ histograms provided by the CDF and D0 collaborations, and are now approximating them with two-dimensional Gaussian likelihoods.

We obtain the individual and combined contours shown in Fig. 9. Maximizing the likelihood, we find, as summarized in Table 20,

$$\Delta\Gamma_s = +0.076 \pm 0.004 \text{ ps}^{-1}, \tag{81}$$

$$\phi_s^{c\bar{c}s} = -0.052 \pm 0.013. \tag{82}$$

This $\Delta\Gamma_s$ average is consistent but highly correlated with the average of Eq. (65). Our final recommended average for $\Delta\Gamma_s$ is the one of Eq. (65), which includes all available information on this quantity. Other averaged parameters are listed in Table 21, and their correlations are in Table 22. For the sake of compactness, we exclude parameters that are used in single measurements.

In the Standard Model and ignoring subleading penguin contributions, $\phi_s^{c\bar{c}s}$ is expected to be equal to $-2\beta_s$, where $\beta_s = \arg[-(V_{ts}V_{tb}^*)/(V_{cs}V_{cb}^*)]$ is a phase analogous to the angle β of the usual CKM unitarity triangle (aside from a

TABLE 21. Results of the averaging procedure, including the fit results and the scale factors of the individual parameters, for all $b \to c\bar{c}s$ modes (second and third column) and for $B_s^0 \to J/\psi K^+K^-$ modes only (fourth and fifth column). Only parameters measured by all three LHC experiments are scaled.

	All $b \to c\bar{c}s$		$B_s^0 \to J/\psi K^+K^-$	
Parameter	Fit result	Scale factor	Fit result	Scale factor
ϕ_s	-0.052 ± 0.013	1.00	-0.060 ± 0.014	1.00
$\lvert\lambda\rvert$	0.996 ± 0.009	...	0.996 ± 0.009	...
Γ_s	0.6632 ± 0.0034 ps^{-1}	2.51	0.6637 ± 0.0033 ps^{-1}	2.42
$\Delta\Gamma_s$	$+0.076 \pm 0.004$ ps^{-1}	1.60	$+0.074 \pm 0.004$ ps^{-1}	1.51
$\lvert A_\perp^{J/\psi KK}\rvert^2$	0.259 ± 0.004	3.64	0.259 ± 0.004	3.54
$\lvert A_0^{J/\psi KK}\rvert^2$	0.5185 ± 0.0027	1.29	0.5182 ± 0.0026	1.23
$\delta_\perp^{J/\psi KK}$	3.01 ± 0.12	2.30	3.00 ± 0.12	2.36
$\delta_\parallel^{J/\psi KK}$	3.21 ± 0.07	1.72	3.20 ± 0.07	1.73
Δm_s	17.753 ± 0.021 ps^{-1}	...	17.748 ± 0.022 ps^{-1}	...

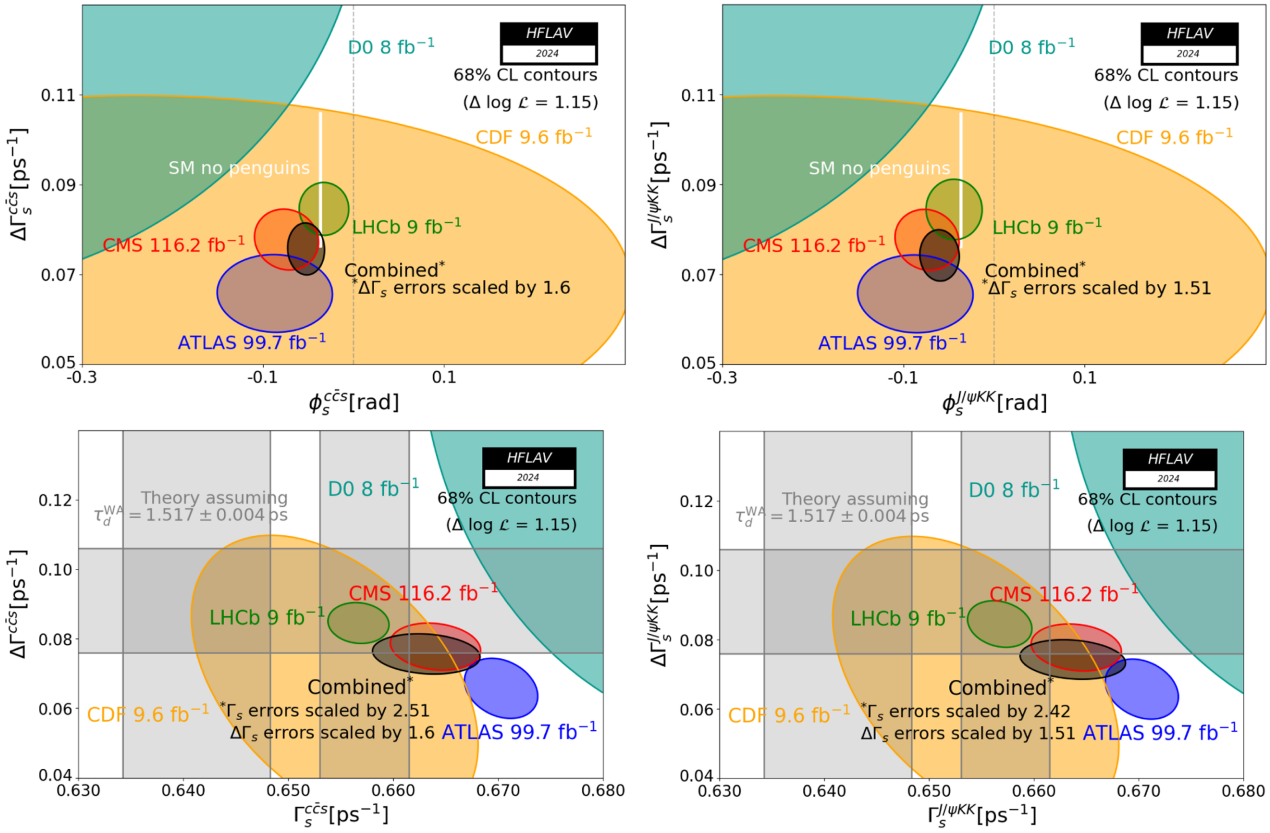


FIG. 9. Regions at 68% CL shown in the $(\phi_s^{c\bar{c}s}, \Delta\Gamma_s)$ plane on the top and in the $(\Gamma_s, \Delta\Gamma_s)$ plane on the bottom, for individual experiments and their combination. The left plots are obtained from all CDF [208], D0 [209], ATLAS [210–212], CMS [213,214] and LHCb [110,215–219,258,260,261] measurements of $B_s^0 \to J/\psi K^+K^-$, $B_s^0 \to \psi(2S)K^+K^-$, $B_s^0 \to J/\psi\pi^+\pi^-$ and $B_s^0 \to D_s^+D_s^-$ decays, while the right plots are obtained from $B_s^0 \to J/\psi K^+K^-$ measurements only [208–215,218,219]. The expectations within the Standard Model neglecting penguin contributions [47,204,205] are shown as white rectangles in the top plots. The Γ_s theory value in the bottom plots is calculated from Ref. [47] assuming the experimental world average for the B^0 lifetime, 1.517 ± 0.004 ps. The two solutions in Γ_s are due to the two different sets of inputs to the theory calculation of $\tau(B_s^0)/\tau(B^0)$ according to Ref. [62] (toward lower Γ_s values) and Ref. [63] (toward higher Γ_s values).

TABLE 22. Correlation tables of the averaged observables from the fit to all $b \to c\bar{c}s$ modes (top) and to the $B_s^0 \to J/\psi K^+K^-$ modes only (bottom).

Parameter	ϕ_s	$\lvert\lambda^{J/\psi KK}\rvert$	Γ_s	$\Delta\Gamma_s$	$\lvert A_\perp^{J/\psi KK}\rvert^2$	$\lvert A_0^{J/\psi KK}\rvert^2$	$\delta_\perp^{J/\psi KK}$	$\delta_\parallel^{J/\psi KK}$	Δm_s
ϕ_s	1.00	0.03	0.00	−0.04	0.01	−0.01	−0.01	0.00	−0.01
$\lvert\lambda^{J/\psi KK}\rvert$		1.00	0.00	−0.01	0.03	−0.03	−0.11	−0.06	−0.11
Γ_s			1.00	−0.15	0.07	−0.05	−0.01	−0.03	0.01
$\Delta\Gamma_s$				1.00	−0.24	0.17	−0.01	0.00	0.02
$\lvert A_\perp^{J/\psi KK}\rvert^2$					1.00	−0.73	−0.04	−0.05	−0.02
$\lvert A_0^{J/\psi KK}\rvert^2$						1.00	0.02	0.00	0.02
$\delta_\perp^{J/\psi KK}$							1.00	0.22	0.49
$\delta_\parallel^{J/\psi KK}$								1.00	−0.09
Δm_s									1.00

Parameter	ϕ_s	$\lvert\lambda^{J/\psi KK}\rvert$	Γ_s	$\Delta\Gamma_s$	$\lvert A_\perp^{J/\psi KK}\rvert^2$	$\lvert A_0^{J/\psi KK}\rvert^2$	$\delta_\perp$	$\delta_\parallel$	Δm_s
ϕ_s	1.00	0.02	0.00	−0.04	0.01	−0.01	0.00	0.02	0.00
$\lvert\lambda^{J/\psi KK}\rvert$		1.00	0.00	−0.01	0.04	−0.04	−0.08	−0.05	−0.07
Γ_s			1.00	−0.18	0.08	−0.06	0.00	−0.02	0.01
$\Delta\Gamma_s$				1.00	−0.25	0.18	0.00	0.01	0.03
$\lvert A_\perp^{J/\psi KK}\rvert^2$					1.00	−0.72	−0.08	−0.06	−0.06
$\lvert A_0^{J/\psi KK}\rvert^2$						1.00	0.05	0.00	0.05
$\delta_\perp^{J/\psi KK}$							1.00	0.26	0.40
$\delta_\parallel^{J/\psi KK}$								1.00	−0.12
Δm_s									1.00

sign change). An indirect determination via global fits to experimental data gives

$$(\phi_s^{c\bar{c}s})^{\mathrm{SM}} = -2\beta_s = \begin{cases} -0.0376^{+0.0006}_{-0.0005} & \text{CKMfitter [203]} \\ -0.0367 \pm 0.0010 & \text{UTfit [204].} \end{cases} \quad (83)$$

The average value of $\phi_s^{c\bar{c}s}$ from Eq. (82) is consistent with this Standard Model expectation. Penguin contributions to $\phi_s^{c\bar{c}s}$ from $B_s^0 \to J/\psi K^+K^-$ are calculated to be smaller than 0.021 in magnitude [262–264] but may become relevant if future measurements reduce the error in Eq. (82). There are no reliable estimates of the penguin contribution to $B_s^0 \to J/\psi f_0$.

From its measurements of time-dependent CP violation in $B_s^0 \to K^+K^-$ decays, the LHCb collaboration has determined the B_s^0 mixing phase to be $-2\beta_s = -0.12^{+0.14}_{-0.12}$ [265], assuming a U-spin relation (with up to 50% breaking effects) between the decay amplitudes of $B_s^0 \to K^+K^-$ and $B^0 \to \pi^+\pi^-$, and a value of the CKM angle γ of $(70.1 \pm 7.1)°$. This determination is compatible with, and less precise than, the world average of $\phi_s^{c\bar{c}s}$ from Eq. (82).

New physics could contribute to $\phi_s^{c\bar{c}s}$. Assuming that new physics only enters in M_{12}^s (rather than in Γ_{12}^s), one can write [54,55]

$$\phi_s^{c\bar{c}s} = -2\beta_s + \phi_{12}^{s,\mathrm{NP}}, \quad (84)$$

where the new physics phase $\phi_{12}^{s,\mathrm{NP}}$ is the same as that appearing in Eq. (79). In this case

$$\phi_{12}^s = \phi_{12}^{s,\mathrm{SM}} + 2\beta_s + \phi_s^{c\bar{c}s} = -0.010 \pm 0.014, \quad (85)$$

where the numerical estimation was performed with the values of Eqs. (78), (83), and (82). Note that, within the quoted precision, the same ϕ_{12}^s value is obtained with the $2\beta_s$ inputs from CKMfitter and UTfit. Keeping in mind the approximation and assumption mentioned above, this can serve as a reference value to which the measurement of Eq. (80) can be compared.

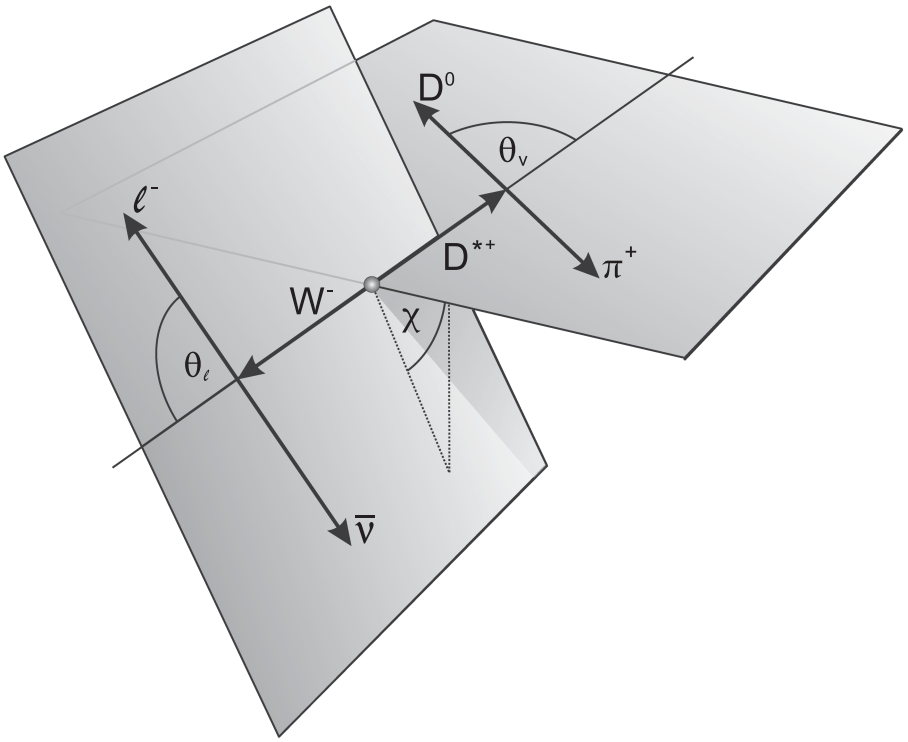


FIG. 10. Sketch of the helicity angles θ_ℓ, θ_V and χ in the decay $\bar{B} \to D^* \ell^- \bar{\nu}_\ell$.

VI. SEMILEPTONIC *b* HADRON DECAYS

In this section we present averages for semileptonic b hadron decays, i.e. decays of the type $B \to X \ell \nu_\ell$, where X refers to one or more hadrons, ℓ to a charged lepton and ν_ℓ to its associated neutrino. Unless otherwise stated, ℓ stands for an electron or a muon, lepton universality is assumed, and both charge conjugate states are combined. Some averages assume isospin symmetry which is explicitly mentioned at every instance.

Averages are presented separately for CKM favored $b \to c$ quark transitions and CKM suppressed $b \to u$ modes. We further distinguish *exclusive* decays involving a specific meson ($X = D, D^*, \pi, \rho, \ldots$) from *inclusive* decay modes, i.e. the sum over all possible hadronic states. Semileptonic decays proceed via first order weak interactions and are well described in the framework of the SM. Their decay rates are sensitive to the magnitude squared of the CKM elements V_{cb} and V_{ub}, the determination of which is one of the primary goals for the study of these decays. Semileptonic decays involving the τ lepton might be more sensitive to beyond-SM processes, because the high τ mass can result in enhanced couplings to hypothetical new particles such as a charged Higgs boson or leptoquarks.

The technique for obtaining the averages follows the general HFLAV procedure (see Sec. III) unless otherwise stated. More information on the averages, in particular on the common input parameters, is available on the HFLAV semileptonic webpage. In general, averages in this section use experimental results available through autumn 2023.

A. Exclusive CKM-favored decays

1. $\bar{B} \to D^* \ell^- \bar{\nu}_\ell$

The $\bar{B} \to D^* \ell^- \bar{\nu}_\ell$ decay rate is fully parametrized by the recoil variable $w = v_B \cdot v_{D^*}$, the product of the four-velocities of the initial and final state mesons and three decay angles θ_ℓ, θ_V and χ, defined as follows (Fig. 10):

(i) The angle θ_ℓ is the angle between the direction of the charged lepton and the direction opposite to the B meson in the virtual W boson rest frame,
(ii) The angle θ_V is the angle between the direction of the D meson and the direction opposite to the B meson in the D^* meson rest frame, and
(iii) The angle χ is the azimuthal angle between the two decay planes spanned by the W boson and D^* meson decay products, and defined in the rest frame of the B meson.

Integrating over the angles, the differential decay rate for massless fermions as a function of w is given by (see, e.g., [266])

$$\frac{d\Gamma(\bar{B} \to D^* \ell^- \bar{\nu}_\ell)}{dw} = \frac{G_F^2 m_{D^*}^3}{48\pi^3} (m_B - m_{D^*})^2 \chi(w) \eta_{EW}^2 \mathcal{F}^2(w) |V_{cb}|^2, \quad (86)$$

TABLE 23. Average of the $\bar{B}^0 \to D^{*+}\ell^-\bar{\nu}_\ell$ branching fraction measurements.

Experiment	$\mathcal{B}(\bar{B}^0 \to D^{*+}\ell^-\bar{\nu}_\ell)$ [%] (rescaled)	$\mathcal{B}(\bar{B}^0 \to D^{*+}\ell^-\bar{\nu}_\ell)$ [%] (published)
ALEPH [268]	$5.29 \pm 0.26_{\text{stat}} \pm 0.33_{\text{syst}}$	$5.53 \pm 0.26_{\text{stat}} \pm 0.52_{\text{syst}}$
OPAL incl [269]	$6.13 \pm 0.28_{\text{stat}} \pm 0.57_{\text{syst}}$	$5.92 \pm 0.27_{\text{stat}} \pm 0.68_{\text{syst}}$
OPAL excl [269]	$5.11 \pm 0.20_{\text{stat}} \pm 0.36_{\text{syst}}$	$5.11 \pm 0.19_{\text{stat}} \pm 0.49_{\text{syst}}$
DELPHI incl [270]	$4.94 \pm 0.14_{\text{stat}} \pm 0.35_{\text{syst}}$	$4.70 \pm 0.13_{\text{stat}}\,{}^{+0.36}_{-0.31}{}_{\text{syst}}$
DELPHI excl [271]	$5.05 \pm 0.20_{\text{stat}} \pm 0.42_{\text{syst}}$	$5.90 \pm 0.22_{\text{stat}} \pm 0.50_{\text{syst}}$
CLEO [272]	$5.85 \pm 0.19_{\text{stat}} \pm 0.35_{\text{syst}}$	$6.09 \pm 0.19_{\text{stat}} \pm 0.40_{\text{syst}}$
Belle untagged [273]	$4.76 \pm 0.02_{\text{stat}} \pm 0.16_{\text{syst}}$	$4.90 \pm 0.02_{\text{stat}} \pm 0.16_{\text{syst}}$
BABAR untagged [274]	$4.35 \pm 0.04_{\text{stat}} \pm 0.33_{\text{syst}}$	$4.69 \pm 0.04_{\text{stat}} \pm 0.34_{\text{syst}}$
BABAR tagged [275]	$5.08 \pm 0.16_{\text{stat}} \pm 0.31_{\text{syst}}$	$5.49 \pm 0.16_{\text{stat}} \pm 0.25_{\text{syst}}$
Belle II untagged [276]	$4.83 \pm 0.02_{\text{stat}} \pm 0.20_{\text{syst}}$	$4.922 \pm 0.023_{\text{stat}} \pm 0.220_{\text{syst}}$
Belle II tagged [277]	$5.19 \pm 0.22_{\text{stat}} \pm 0.40_{\text{syst}}$	$5.27 \pm 0.22_{\text{stat}} \pm 0.38_{\text{syst}}$
Average	$\mathbf{4.90 \pm 0.01_{stat} \pm 0.12_{syst}}$	$\boldsymbol{\chi^2/\text{dof} = 15.3/10}$ (CL = **12.2%**)

TABLE 24. Average of the $B^- \to D^{*0}\ell^-\bar{\nu}_\ell$ branching fraction measurements.

Experiment	$\mathcal{B}(B^- \to D^{*0}\ell^-\bar{\nu}_\ell)$ [%] (rescaled)	$\mathcal{B}(B^- \to D^{*0}\ell^-\bar{\nu}_\ell)$ [%] (published)
CLEO [272]	$6.12 \pm 0.20_{\text{stat}} \pm 0.26_{\text{syst}}$	$6.50 \pm 0.20_{\text{stat}} \pm 0.43_{\text{syst}}$
BABAR tagged [275]	$5.29 \pm 0.15_{\text{stat}} \pm 0.33_{\text{syst}}$	$5.83 \pm 0.15_{\text{stat}} \pm 0.30_{\text{syst}}$
BABAR untagged [278]	$4.95 \pm 0.08_{\text{stat}} \pm 0.32_{\text{syst}}$	$5.56 \pm 0.08_{\text{stat}} \pm 0.41_{\text{syst}}$
Average	$\mathbf{5.53 \pm 0.07_{stat} \pm 0.21_{syst}}$	$\boldsymbol{\chi^2/\text{dof} = 7.03/2}$ (CL = **3.0%**)

where G_{F} is Fermi's constant, m_B and m_{D^*} are the B and D^* meson masses, $\chi(w)$ is a known phase-space factor, and η_{EW} is a small electroweak correction [267]. Some authors also include a long-distance EM radiation effect (Coulomb correction) in this factor. The form factor $\mathcal{F}(w)$ for the $\bar{B} \to D^*\ell^-\bar{\nu}_\ell$ decay contains three independent functions, $h_{A_1}(w)$, $R_1(w)$ and $R_2(w)$,

$$\chi(w)\mathcal{F}^2(w) = h_{A_1}^2(w)\sqrt{w^2-1}(w+1)^2\left\{2\left[\frac{1-2wr+r^2}{(1-r)^2}\right]\times\left[1+R_1^2(w)\frac{w-1}{w+1}\right]+\left[1+(1-R_2(w))\frac{w-1}{1-r}\right]^2\right\}, \quad (87)$$

where $r = m_{D^*}/m_B$.

Branching fraction.—First, we perform separate one-dimensional averages of the $\bar{B}^0 \to D^{*+}\ell^-\bar{\nu}_\ell$ and $B^- \to D^{*0}\ell^-\bar{\nu}_\ell$ branching fractions. In the fit to the measurements listed in Tables 23 and 24, external parameters (such as the branching fractions of charmed mesons) are constrained to their latest values and the following results are obtained

$$\mathcal{B}(\bar{B}^0 \to D^{*+}\ell^-\bar{\nu}_\ell) = (4.90 \pm 0.01 \pm 0.12)\%, \quad (88)$$

$$\mathcal{B}(B^- \to D^{*0}\ell^-\bar{\nu}_\ell) = (5.53 \pm 0.07 \pm 0.21)\%, \quad (89)$$

where the first uncertainty is statistical and the second one is systematic. The results of these two fits are also shown in Fig. 11.

We combine these two averages into a result for $\mathcal{B}(\bar{B}^0 \to D^{*+}\ell^-\bar{\nu}_\ell)$ assuming isospin symmetry. Therefore, we rescale the B^+ branching fractions by the lifetime ratio $\tau_{0+} = \tau(B^0)/\tau(B^+)$ and perform a combined 1-dimensional fit over the $\bar{B}^0 \to D^{*+}\ell^-\bar{\nu}_\ell$ and $B^- \to D^{*0}\ell^-\bar{\nu}_\ell$ branching fractions. To account for isospin breaking due to the Coulomb effect in $\bar{B}^0 \to D^{*+}\ell^-\bar{\nu}_\ell$ we inflate the uncertainty in τ_{0+} by $\tau_{0+}\alpha\pi \approx 0.02123$ [279]. The result reads

$$\mathcal{B}(\bar{B}^0 \to D^{*+}\ell^-\bar{\nu}_\ell) = (4.90 \pm 0.01 \pm 0.11)\%. \quad (90)$$

The χ^2/dof of the combination is 22.56/13 (CL = 4.73%).

Average of differential distributions.—We perform an average of the normalized unfolded $\bar{B} \to D^*\ell^-\bar{\nu}_\ell$

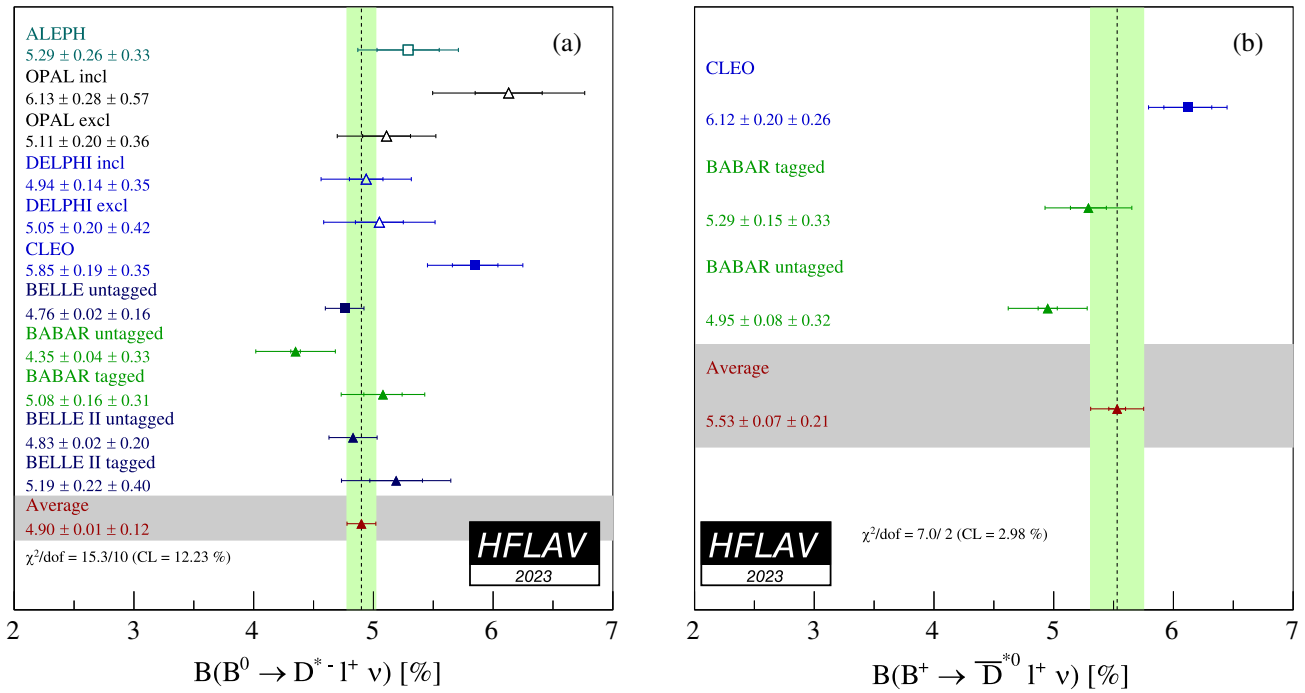


FIG. 11. Branching fractions of exclusive semileptonic B decays: (a) $\bar{B}^0 \to D^{*+}\ell^-\bar{\nu}_\ell$ (Table 23) and (b) $B^- \to D^{*0}\ell^-\bar{\nu}_\ell$ (Table 24).

differential measurements performed by the Belle [280] and Belle II [276] collaborations. We omit the Belle measurement in Ref. [273] because they do not provide unfolded spectra.

We normalize each individual measurement and drop one data point in each marginal distribution to remove the singular values in the covariance matrix C. We then minimize a χ^2 defined as

$$\chi^2(\vec{\mu}) = \sum_{\text{meas.}} \sum_x \sum_i \left(\left(\frac{\Delta\Gamma/\Gamma}{\Delta x} \right)_i - \mu_i \right) \times C_{ij}^{-1} \left(\left(\frac{\Delta\Gamma/\Gamma}{\Delta x} \right)_i - \mu_i \right), \tag{91}$$

where the first sum runs over all measurements, the second sum runs over the measured variables $x \in (w, \cos\theta_\ell, \cos\theta_V, \chi)$ and the third sum runs over the measured bins. The resulting p-value of the average is 15% and indicates good agreement between the measurements. The redundant data point in each marginal distribution is recovered via $1 = \sum_{\text{bins}} (\Delta\Gamma/\Gamma/\Delta x)_i$. The resulting spectrum is shown in Fig. 12. The central values with uncertainties are given in Table 25. The corresponding correlation matrix of the averaged normalized $\bar{B} \to D^*\ell^-\bar{\nu}_\ell$ spectrum, together with the central values and uncertainties are available at [281].

Extraction of $|V_{cb}|$ based on the BGL form factor.—To extract $|V_{cb}|$, we consider the model-independent parametrizations of the form factor functions $h_{A_1}(w)$, $R_1(w)$ and $R_2(w)$ contributing to the $\bar{B} \to D^*\ell^-\bar{\nu}_\ell$ differential decay rate by Boyd, Grinstein and Lebed (BGL) [282–284]. We use the averaged normalized differential distributions in w, $\cos\theta_\ell$, $\cos\theta_V$, and χ, the isospin average of the B^0 and B^+ absolute branching fractions, and the nonzero recoil lattice QCD calculation by Fermilab/MILC [285], HPQCD [286], and JLQCD [287] to extract the CKM matrix element $|V_{cb}|$. The Blasche factors in the BGL parametrization use $[6.730, 6.736, 7.135, 7.142]$ GeV for the axialvector poles and $[6.337, 6.899, 7.012, 7.280]$ GeV for the vector poles [288].[12] The susceptibilities are $\chi^T_{1+}(0.33) = 5.28 \times 10^{-4}$ GeV^{-2} and $\tilde{\chi}^T_{1-}(0.33) = 3.07 \times 10^{-4}$ GeV^{-2}. The χ^2 function is defined as

$$\begin{aligned}\chi^2 = &\left(\left(\frac{\Delta\vec{\Gamma}}{\Gamma} \right)^{\text{m}} - \left(\frac{\Delta\vec{\Gamma}(\vec{x})}{\Gamma(\vec{x})} \right)^{\text{p}} \right) \\ &\times C_{\text{exp}}^{-1} \left(\left(\frac{\Delta\vec{\Gamma}}{\Gamma} \right)^{\text{m}} - \left(\frac{\Delta\vec{\Gamma}(\vec{x})}{\Gamma(\vec{x})} \right)^{\text{p}} \right)^T \\ &+ (\Gamma^{\text{ext}} - \Gamma^{\text{p}}(\vec{x}))^2/\sigma(\Gamma^{\text{ext}})^2 \\ &+ (h_X^{\text{p}}(\vec{x}) - h_X^{\text{LQCD}}) C_{\text{LQCD}}^{-1} (h_X^{\text{p}}(\vec{x}) - h_X^{\text{LQCD}}),\end{aligned} \tag{92}$$

with the averaged (predicted) normalized partial decay rates $(\Delta\vec{\Gamma}/\Gamma)^{\text{m(p)}}$ in bins of w and the helicity angles, where the predicted rate is a function of the form factor coefficients $\vec{x}$

[12]Including the fourth vector resonance in the spectrum is a choice by the authors, and is sometimes treated different in the literature.

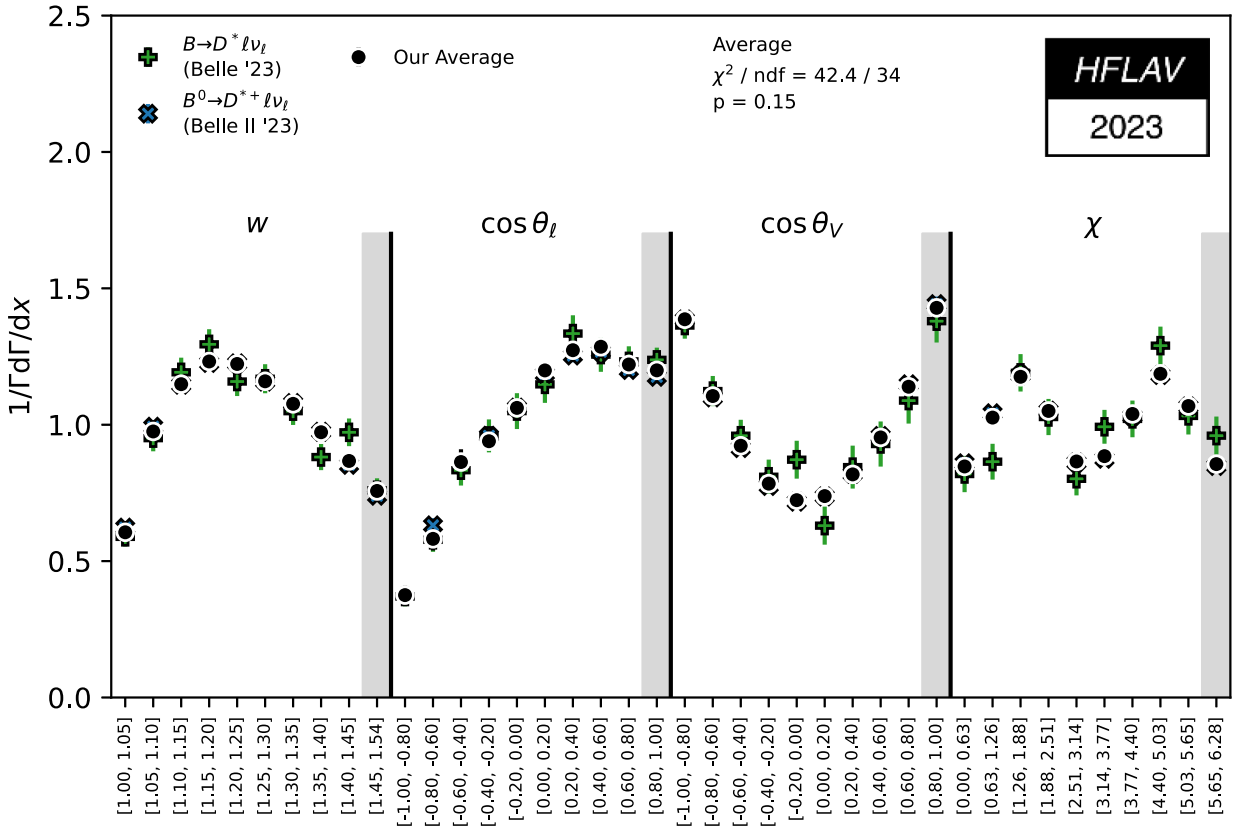


FIG. 12. The averaged normalized $\bar{B} \to D^* \ell^- \bar{\nu}_\ell$ spectrum (black data points) together with the individual measurements by Belle [280] and Belle II [276] collaborations. The gray bands indicate the omitted data point in the average (see text).

and $|V_{cb}|$. The rate is calculated assuming the meson masses of $m_B = 5.28$ GeV and $m_{D^*} = 2.01$ GeV, and the lepton as massless. The quantity $\Gamma^{\mathrm{p(ext)}}$ is the predicted (isospin averaged) absolute rate. The predicted (LQCD) form factors are $h_X^{\mathrm{p(LQCD)}}$. C_{exp} (C_{LQCD}) is the covariance matrix of the experimental (lattice) data. The BGL coefficients a_i, b_i, c_i, and d_i correspond to the form factors g, f, $\mathcal{F}_1$, $\mathcal{F}_2$ respectively. The notation $\mathrm{BGL}_{N_a N_b N_c N_d}$ corresponds to the number of free coefficients in the fit, and c_0 is always defined through the kinematical constraint. The number of BGL form factor coefficients is determined by a nested hypothesis test [289], and no unitarity bound is imposed. The impact on the uncertainty from the chosen truncation based on the NHT has not been studied in this

TABLE 25. The central values and uncertainties of the averaged normalized $\bar{B} \to D^* \ell^- \bar{\nu}_\ell$ spectrum.

w bin	$1/\Gamma\Delta\Gamma/\Delta w$	$\cos\theta_\ell$ bin	$1/\Gamma\Delta\Gamma/\Delta\cos\theta_\ell$	$\cos\theta_V$ bin	$1/\Gamma\Delta\Gamma/\Delta\cos\theta_V$	χ bin	$1/\Gamma\Delta\Gamma/\Delta\chi$
[1.00, 1.05]	0.0601 ± 0.0017	$[-1.00, -0.80]$	0.0375 ± 0.0034	$[-1.00, -0.80]$	0.1387 ± 0.0021	[0.00, 0.63]	0.0847 ± 0.0020
[1.05, 1.10]	0.0968 ± 0.0017	$[-0.80, -0.60]$	0.058 ± 0.004	$[-0.80, -0.60]$	0.1105 ± 0.0015	[0.63, 1.26]	0.1026 ± 0.0015
[1.10, 1.15]	0.1141 ± 0.0017	$[-0.60, -0.40]$	0.086 ± 0.005	$[-0.60, -0.40]$	0.0923 ± 0.0012	[1.26, 1.88]	0.1176 ± 0.0017
[1.15, 1.20]	0.1223 ± 0.0017	$[-0.40, -0.20]$	0.0940 ± 0.0018	$[-0.40, -0.20]$	0.0784 ± 0.0010	[1.88, 2.51]	0.1051 ± 0.0015
[1.20, 1.25]	0.1214 ± 0.0016	$[-0.20, 0.00]$	0.1062 ± 0.0017	$[-0.20, 0.00]$	0.0723 ± 0.0010	[2.51, 3.14]	0.0865 ± 0.0014
[1.25, 1.30]	0.1151 ± 0.0015	[0.00, 0.20]	0.1199 ± 0.0017	[0.00, 0.20]	0.0738 ± 0.0010	[3.14, 3.77]	0.0885 ± 0.0013
[1.30, 1.35]	0.1069 ± 0.0015	[0.20, 0.40]	0.1273 ± 0.0017	[0.20, 0.40]	0.0818 ± 0.0011	[3.77, 4.40]	0.1039 ± 0.0015
[1.35, 1.40]	0.0966 ± 0.0015	[0.40, 0.60]	0.1286 ± 0.0017	[0.40, 0.60]	0.0953 ± 0.0013	[4.40, 5.03]	0.1187 ± 0.0016
[1.40, 1.45]	0.0861 ± 0.0014	[0.60, 0.80]	0.1221 ± 0.0017	[0.60, 0.80]	0.1139 ± 0.0014	[5.03, 5.65]	0.1069 ± 0.0014
[1.45, 1.54]	0.0805 ± 0.0018	[0.80, 1.00]	0.1199 ± 0.0018	[0.80, 1.00]	0.1429 ± 0.0024	[5.65, 6.28]	0.0856 ± 0.0018

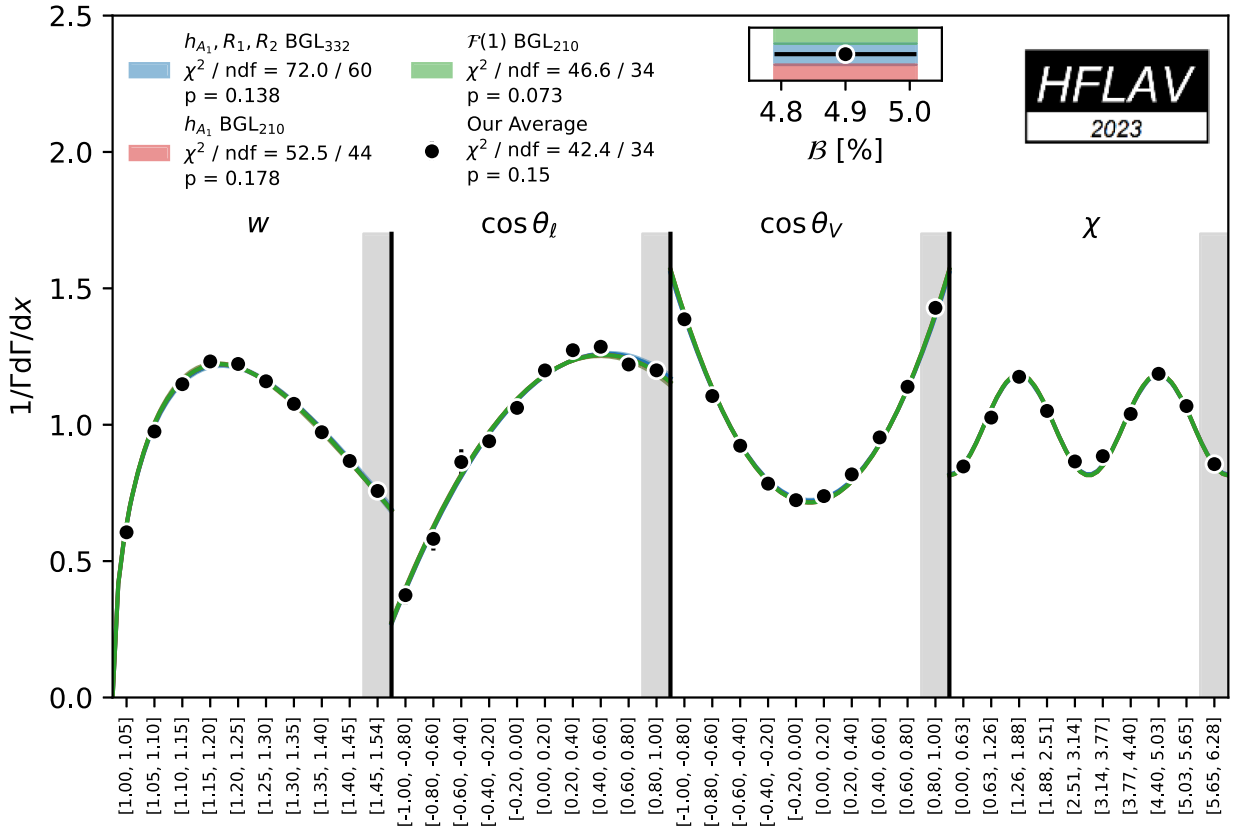


FIG. 13. The fitted $\bar{B} \to D^* \ell^- \bar{\nu}_\ell$ differential decay rate from our averaged normalized differential distribution and our isospin average of the $\bar{B} \to D^* \ell^- \bar{\nu}_\ell$ branching fraction. We find consistent fitted shapes in all three considered scenarios.

report. We consider three scenarios defined by the amount of information used from LQCD: Include all nonzero recoil form factor information, include only the nonzero recoil form factor information on $h_{A_1}(w)$, or include only the zero-recoil point $\mathcal{F}(1) = h_{A_1}(1)$. In the latter case we perform a BGL$_{332}$ fit to the beyond-zero recoil lattice data and extrapolate to zero-coil to obtain $h_{A_1}(w) = 0.895 \pm 0.007$ which is subsequently used in the fit with data. These fits yield a χ^2/ndf of 72.0/60, 52.5/44, and 46.6/34, respectively. The results of the fits are shown in Fig. 13 and the extracted values of $|V_{cb}|$ are given in Table 26. Details on the three individual fits are given in Tables 27, 28, and 29.

2. $\bar{B} \to D\ell^- \bar{\nu}_\ell$

The differential decay rate for massless fermions as a function of w (introduced in the previous section) is given by (see, e.g., [266])

$$\frac{d\Gamma(\bar{B} \to D\ell^- \bar{\nu}_\ell)}{dw} = \frac{G_F^2 m_D^3}{48\pi^3}(m_B + m_D)^2 (w^2 - 1)^{3/2} \eta_{EW}^2 \mathcal{G}^2(w) |V_{cb}|^2, \quad (93)$$

where G_F is Fermi's constant, and m_B and m_D are the B and D meson masses. Again, η_{EW} is the electroweak correction.

TABLE 26. Extracted $|V_{cb}|$ values from our averaged normalized differential distribution and our isospin average of the $\bar{B} \to D^* \ell^- \bar{\nu}_\ell$ branching fraction. For each lattice QCD input scenario we repeat the nested hypothesis test, which results in the chosen BGL parametrization (first column). We retrieve consistent $|V_{cb}|$ values in each scenario.

BGL	$\lvert V_{cb}\rvert \times 10^3$	$\lvert V_{cb}\rvert \times 10^3 \times \mathcal{F}(1)$	$\mathcal{F}(1)$	LQCD Input
332	40.0 ± 0.7	36.0 ± 0.5	0.900 ± 0.008	$h_{A_1}(w), R_1(w), R_2(w)$
210	40.2 ± 0.6	36.0 ± 0.4	0.897 ± 0.009	$h_{A_1}(w)$
210	40.2 ± 0.6	36.0 ± 0.4	0.895 ± 0.007	$h_{A_1}(1) = \mathcal{F}(1)$

TABLE 27. Fit result using all nonzero recoil form factors predicted by LQCD.

	Value	Correlation								
$a_0 \times 10^2$	3.08 ± 0.07	1.00	−0.16	−0.09	0.23	0.02	−0.12	0.14	−0.06	−0.24
$a_1 \times 10^2$	-9.27 ± 2.56	−0.16	1.00	−0.66	−0.01	0.27	−0.31	0.18	−0.11	−0.12
$a_2 \times 10^2$	6.95 ± 44.81	−0.09	−0.66	1.00	0.06	−0.36	0.60	−0.18	0.14	0.01
$b_0 \times 10^2$	1.22 ± 0.01	0.23	−0.01	0.06	1.00	−0.03	0.04	0.01	−0.03	−0.55
$b_1 \times 10^2$	1.45 ± 0.59	0.02	0.27	−0.36	−0.03	1.00	−0.70	0.57	−0.44	−0.30
$b_2 \times 10^2$	-49.74 ± 13.46	−0.12	−0.31	0.60	0.04	−0.70	1.00	−0.37	0.32	0.07
$c_1 \times 10^2$	-0.11 ± 0.13	0.14	0.18	−0.18	0.01	0.57	−0.37	1.00	−0.93	−0.32
$c_2 \times 10^2$	2.19 ± 2.47	−0.06	−0.11	0.14	−0.03	−0.44	0.32	−0.93	1.00	0.20
$\lvert V_{cb}\rvert \times 10^3$	39.97 ± 0.65	−0.24	−0.12	0.01	−0.55	−0.30	0.07	−0.32	0.20	1.00

TABLE 28. Fit result using the nonzero recoil form factor $h_{A_1}(w)$ predicted by LQCD.

	Value	Correlation			
$a_0 \times 10^2$	3.80 ± 0.43	1.00	−0.98	0.08	−0.05
$a_1 \times 10^2$	-37.81 ± 15.40	−0.98	1.00	−0.02	−0.01
$b_0 \times 10^2$	1.21 ± 0.01	0.08	−0.02	1.00	−0.64
$\lvert V_{cb}\rvert \times 10^3$	40.12 ± 0.60	−0.05	−0.01	−0.64	1.00

TABLE 29. Fit result using the zero recoil form factor $h_{A_1}(1) = \mathcal{F}(1)$ predicted by LQCD.

	Value	Correlation			
$a_0 \times 10^2$	3.79 ± 0.43	1.00	−0.98	0.07	−0.04
$a_1 \times 10^2$	-37.74 ± 15.37	−0.98	1.00	−0.02	−0.02
$b_0 \times 10^2$	1.21 ± 0.01	0.07	−0.02	1.00	−0.57
$\lvert V_{cb}\rvert \times 10^3$	40.19 ± 0.56	−0.04	−0.02	−0.57	1.00

In contrast to $\bar{B} \to D^* \ell^- \bar{\nu}_\ell$, $\mathcal{G}(w)$ contains a single form-factor function $f_+(w)$,

$$\mathcal{G}^2(w) = \frac{4r}{(1+r)^2} f_+^2(w), \tag{94}$$

where $r = m_D/m_B$.

Branching fraction.—Separate one-dimensional averages of the $\bar{B}^0 \to D^+ \ell^- \bar{\nu}_\ell$ and $B^- \to D^0 \ell^- \bar{\nu}_\ell$ branching fractions are shown in Tables 30 and 31. We obtain

$$\mathcal{B}(\bar{B}^0 \to D^+ \ell^- \bar{\nu}_\ell) = (2.12 \pm 0.02 \pm 0.06)\%, \tag{95}$$

$$\mathcal{B}(B^- \to D^0 \ell^- \bar{\nu}_\ell) = (2.21 \pm 0.02 \pm 0.06)\%, \tag{96}$$

where the first uncertainty is statistical and the second one is systematic. These fits are also shown in Fig. 14.

Again, we also calculate an average for $\mathcal{B}(\bar{B}^0 \to D^+ \ell^- \bar{\nu}_\ell)$ assuming isospin symmetry: The B^- branching fractions are rescaled by the lifetime ratio $\tau_{0-} = \tau(B^0)/\tau(B^-)$ and a combined 1-dimensional fit over the $\mathcal{B}(\bar{B}^0 \to D^+ \ell^- \bar{\nu}_\ell)$ and $\mathcal{B}(B^- \to D^0 \ell^- \bar{\nu}_\ell)$ branching fractions is performed. To account for isospin breaking due to the Coulomb effect in $\bar{B}^0 \to D^+ \ell^- \bar{\nu}_\ell$ we inflate the uncertainty in τ_{0-} by $\tau_{0-}\alpha\pi \approx 0.02123$ [279]. The result reads

$$\mathcal{B}(\bar{B}^0 \to D^+ \ell^- \bar{\nu}_\ell) = (2.11 \pm 0.01 \pm 0.05)\%. \tag{97}$$

The χ^2/dof of the combination is 8.60/10 (CL = 57.1%).

TABLE 30. Average of $\bar{B}^0 \to D^+ \ell^- \bar{\nu}_\ell$ branching fraction measurements.

Experiment	$\mathcal{B}(\bar{B}^0 \to D^+ \ell^- \bar{\nu}_\ell)$ [%] (rescaled)	$\mathcal{B}(\bar{B}^0 \to D^+ \ell^- \bar{\nu}_\ell)$ [%] (published)
ALEPH [268]	$2.16 \pm 0.18_{\text{stat}} \pm 0.35_{\text{syst}}$	$2.35 \pm 0.20_{\text{stat}} \pm 0.44_{\text{syst}}$
CLEO [290]	$2.10 \pm 0.13_{\text{stat}} \pm 0.15_{\text{syst}}$	$2.20 \pm 0.16_{\text{stat}} \pm 0.19_{\text{syst}}$
BABAR [291]	$2.15 \pm 0.11_{\text{stat}} \pm 0.14_{\text{syst}}$	$2.23 \pm 0.11_{\text{stat}} \pm 0.11_{\text{syst}}$
Belle [292]	$2.33 \pm 0.04_{\text{stat}} \pm 0.11_{\text{syst}}$	$2.39 \pm 0.04_{\text{stat}} \pm 0.11_{\text{syst}}$
Belle II $De\nu$ [293]	$1.99 \pm 0.04_{\text{stat}} \pm 0.08_{\text{syst}}$	$1.99 \pm 0.04_{\text{stat}} \pm 0.08_{\text{syst}}$
Belle II $D\mu\nu$ [293]	$2.03 \pm 0.04_{\text{stat}} \pm 0.08_{\text{syst}}$	$2.03 \pm 0.04_{\text{stat}} \pm 0.09_{\text{syst}}$
Average	$\mathbf{2.12 \pm 0.02_{stat} \pm 0.06_{syst}}$	$\boldsymbol{\chi^2/\text{dof} = 6.09/5}$ **(CL = 29.8%)**

TABLE 31. Average of $B^- \to D^0 \ell^- \bar{\nu}_\ell$ branching fraction measurements.

Experiment	$\mathcal{B}(B^- \to D^0 \ell^- \bar{\nu}_\ell)$ [%] (rescaled)	$\mathcal{B}(B^- \to D^0 \ell^- \bar{\nu}_\ell)$ [%] (published)
CLEO [290]	$2.10 \pm 0.13_{\text{stat}} \pm 0.17_{\text{syst}}$	$2.32 \pm 0.17_{\text{stat}} \pm 0.20_{\text{syst}}$
BABAR [291]	$2.14 \pm 0.08_{\text{stat}} \pm 0.13_{\text{syst}}$	$2.31 \pm 0.08_{\text{stat}} \pm 0.09_{\text{syst}}$
Belle [292]	$2.39 \pm 0.03_{\text{stat}} \pm 0.08_{\text{syst}}$	$2.54 \pm 0.04_{\text{stat}} \pm 0.13_{\text{syst}}$
Belle II $D^0 e\nu$ [293]	$2.18 \pm 0.03_{\text{stat}} \pm 0.08_{\text{syst}}$	$2.21 \pm 0.03_{\text{stat}} \pm 0.08_{\text{syst}}$
Belle II $D^0 \mu\nu$ [293]	$2.19 \pm 0.03_{\text{stat}} \pm 0.10_{\text{syst}}$	$2.22 \pm 0.03_{\text{stat}} \pm 0.10_{\text{syst}}$
Average	$\mathbf{2.21 \pm 0.02_{stat} \pm 0.06_{syst}}$	$\boldsymbol{\chi^2/\text{dof} = 2.74/4}$ (CL = **60.3%**)

Extraction of $|V_{cb}|$ based on the BGL form factor.—A model-independent expression for the $\bar{B} \to D\ell^-\bar{\nu}_\ell$ form factor is again BGL. A BGL fit allows to include available lattice QCD data at non-zero recoil $w > 1$ [294,295] to improve the extrapolation to the zero recoil point $w = 1$. A w spectrum of $\bar{B} \to D\ell^-\bar{\nu}_\ell$ has been published by *BABAR* [291] and Belle [292]. As the *BABAR* result does not include the full error matrix of the w spectrum, we perform the BGL fit to the Belle result alone.

We construct a χ^2-function similar to Eq. (92) to incorporate the normalized w spectrum from Ref. [292], and include the isospin average of the $\bar{B} \to D\ell^-\bar{\nu}_\ell$ total branching fraction. We include the nonzero recoil lattice QCD inputs for the f_0 and f_+ form factors by Fermilab/MILC [294] and HPQCD [295,296] as synthetic data points and follow the recipe in Ref. [297] for the correlation of the lattice data. Following Ref. [294], the Blaschke factors in the BGL parametrization are set to unity, which might introduce some model-dependence. We impose the kinematic constraint $f_+(w_{\max}) = f_0(w_{\max})$ on the form factors and obtain

$$|V_{cb}| = (38.9 \pm 0.7) \times 10^{-3}. \tag{98}$$

The fitted distribution is shown in Fig. 15 and the form factor coefficients and correlations are listed in Table 32.

3. $\bar{B}_s^0 \to D_s^{(*)+} \mu^- \bar{\nu}_\mu$

LHCb has extracted $|V_{cb}|$ from semileptonic $\bar{B}_s^0$ decays for the first time [298]. The measurement uses both $\bar{B}_s^0 \to D_s^+ \mu^- \bar{\nu}_\mu$ and $\bar{B}_s^0 \to D_s^{*+} \mu^- \bar{\nu}_\mu$ decays using 3 fb^{-1} collected in 2011 and 2012. The value of $|V_{cb}|$ is determined from the

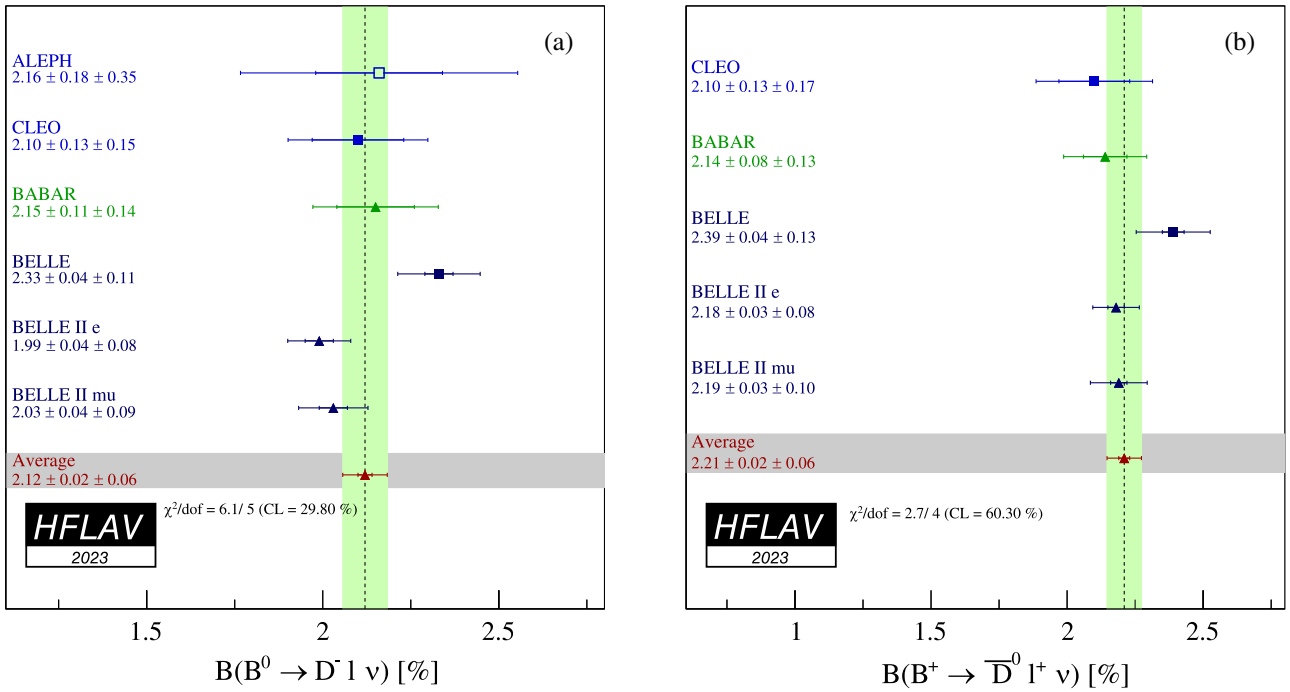


FIG. 14. Branching fractions of exclusive semileptonic B decays: (a) $\bar{B}^0 \to D^+\ell^-\bar{\nu}_\ell$ (Table 30) and (b) $B^- \to D^0\ell^-\bar{\nu}_\ell$ (Table 31).

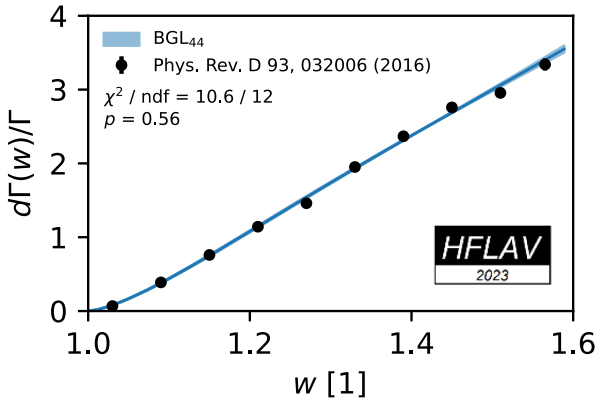


FIG. 15. The fitted $\bar{B} \to D\ell^-\bar{\nu}_\ell$ differential decay rate and our isospin average of the $\bar{B} \to D\ell^-\bar{\nu}_\ell$ branching fraction.

observed yields of $\bar{B}_s^0$ decays normalized to those of $\bar{B}^0$ decays after correcting for the relative reconstruction and selection efficiencies, and considering the known relative $\bar{B}_s^0$ and $\bar{B}^0$ fragmentation fractions, f_s/f_d, in the LHCb acceptance.

The normalization channels are $\bar{B}^0 \to D^+\mu^-\bar{\nu}_\mu$ and $\bar{B}^0 \to D^{*+}\mu^-\bar{\nu}_\mu$ decays. One of the key features of the analysis is that the D^+ is reconstructed with the same decay mode of the D_s^+ ($D_{(s)}^+ \to [K^+K^-]_\phi\pi^+$). With this choice the signal and the reference channels have the same particles in the final state and this minimizes the systematic uncertainties.

The shape of the form factors are extracted as well, exploiting the kinematic variable $p_\perp(D_s)$, which is the component of the D_s^+ momentum perpendicular to the $\bar{B}_s^0$ flight direction. This variable is highly correlated with q^2 and also slightly correlated with the helicity angles in the $\bar{B}_s^0 \to D_s^{*+}\mu^-\bar{\nu}_\mu$ decay. The D_s^{*+} is not explicitly reconstructed, but its contribution is disentangled kinematically from the D_s.

For the $\bar{B}_s^0 \to D_s^+\mu^-\bar{\nu}_\mu$ decay, $|V_{cb}|$ is connected with the measured ratio of signal yields, $N_{\rm sig}$, and the normalization channel yields, $N_{\rm ref}$, through the relation

$$\frac{N_{\rm sig}}{N_{\rm ref}} = \mathcal{K}\tau_s \int \frac{d\Gamma(\bar{B}_s^0 \to D_s^+\mu^-\bar{\nu}_\mu)}{dw} dw$$

where τ_s is the $\bar{B}_s^0$ lifetime, and the constant $\mathcal{K}$ depends on the external inputs as

$$\mathcal{K} = \xi \frac{f_s}{f_d} \frac{\mathcal{B}(D_s^+ \to K^+K^-\pi^+)}{\mathcal{B}(D^+ \to K^+K^-\pi^+)} \frac{1}{\mathcal{B}(\bar{B}^0 \to D^+\mu^-\bar{\nu}_\mu)}$$

where ξ is the efficiency ratio between the signal and the normalization. In the analogous expression for the $\bar{B}_s^0 \to D_s^{*+}\mu^-\bar{\nu}_\mu$ decay, the integral of the decay width is done on the variables $(w, \cos\theta_\ell, \cos\theta_V, \chi)$, and there is an explicit dependence on the branching fraction of the $D^{*+} \to D^+\pi^0$ decay. The analysis takes advantage of the recent results from lattice on the $\bar{B}_s^0 \to D_s^+$ and $\bar{B}_s^0 \to D_s^{*+}$ form factor calculations. In particular for the $\bar{B}_s^0 \to D_s^{*+}$, only the calculations at zero recoil, $h_{A1}^{B_s}(1)$ from Ref. [299] is used. Recently, HPQCD [286] provided calculations of form factors across for $\bar{B}_s^0 \to D_s^{*+}\mu^-\bar{\nu}_\mu$ decays in the full w-range, but these results have not been utilized and would require a re-analysis of the LHCb data, to be properly exploited. For the $\bar{B}_s^0 \to D_s^+\mu^-\bar{\nu}_\mu$ decay, the calculation of the $\bar{B}_s^0 \to D_s^+$ form factors performed in the full w-range [300] are used.

LHCb uses the BGL expansion both for $\bar{B}_s^0 \to D_s^+\mu^-\bar{\nu}_\mu$ and $\bar{B}_s^0 \to D_s^{*+}\mu^-\bar{\nu}_\mu$ decays. The form factors parameters are affected by large statistical uncertainty, but are consistent with the results from the B decays. The result for $|V_{cb}|$, updated with the most recent determination of f_s/f_d from Ref. [301], $\mathcal{B}(D_s^+ \to K^+K^-\pi^+)$ and $\mathcal{B}(D^+ \to K^+K^-\pi^+)$ from [302], and $\mathcal{B}(\bar{B}^0 \to D^{(*)+}\mu^-\bar{\nu}_\mu)$ from Secs. VI A 2 and VI A 1, is

$$|V_{cb}|_{\rm BGL} = (41.2 \pm 0.8 \pm 0.9 \pm 0.8) \times 10^{-3},$$

TABLE 32. Fit result for the $\bar{B} \to D\ell^-\bar{\nu}_\ell$ decay.

	Value	Correlation								
$a_0^+ \times 10^2$	1.265 ± 0.009	1.00	0.02	−0.12	0.00	0.78	0.17	−0.07	0.00	−0.50
$a_1^+ \times 10^2$	-9.27 ± 0.26	0.02	1.00	−0.69	0.04	0.08	0.35	0.31	−0.02	−0.41
$a_2^+ \times 10^2$	29.1 ± 3.4	−0.12	−0.69	1.00	−0.23	−0.12	−0.12	−0.22	0.01	0.10
$a_3^+ \times 10^2$	92 ± 15	0.00	0.04	−0.23	1.00	−0.00	−0.02	0.01	−0.00	−0.03
$a_0^0 \times 10^2$	1.145 ± 0.008	0.78	0.08	−0.12	−0.00	1.00	−0.03	−0.08	0.00	−0.43
$a_1^0 \times 10^2$	-5.96 ± 0.27	0.17	0.35	−0.12	−0.02	−0.03	1.00	−0.62	0.09	−0.29
$a_2^0 \times 10^2$	31 ± 13	−0.07	0.31	−0.22	0.01	−0.08	−0.62	1.00	−0.25	−0.08
$a_3^0 \times 10^2$	90 ± 90	0.00	−0.02	0.01	−0.00	0.00	0.09	−0.25	1.00	0.01
$\lvert V_{cb}\rvert \times 10^3$	38.9 ± 0.7	−0.50	−0.41	0.10	−0.03	−0.43	−0.29	−0.08	0.01	1.00

TABLE 33. Averages of the $B \to D^{(*)}\pi^-\ell^-\bar{\nu}_\ell$ branching fractions and individual results.

Experiment	$\mathcal{B}(B^- \to D^+\pi^-\ell^-\bar{\nu}_\ell)[\%]$ (rescaled)	$\mathcal{B}(B^- \to D^+\pi^-\ell^-\bar{\nu}_\ell)[\%]$ (published)
Belle [303]	$0.378 \pm 0.013_{\text{stat}} \pm 0.017_{\text{syst}}$	$0.378 \pm 0.013_{\text{stat}} \pm 0.017_{\text{syst}}$
BABAR [275]	$0.405 \pm 0.060_{\text{stat}} \pm 0.031_{\text{syst}}$	$0.42 \pm 0.06_{\text{stat}} \pm 0.03_{\text{syst}}$
Average	$\mathbf{0.380 \pm 0.020}$	$\boldsymbol{\chi^2/\text{dof} = 0.15}$ **(CL = 70%)**
Experiment	$\mathcal{B}(B^- \to D^{*+}\pi^-\ell^-\bar{\nu}_\ell)[\%]$ (rescaled)	$\mathcal{B}(B^- \to D^{*+}\pi^-\ell^-\bar{\nu}_\ell)[\%]$ (published)
Belle [303]	$0.530 \pm 0.019_{\text{stat}} \pm 0.025_{\text{syst}}$	$0.530 \pm 0.019_{\text{stat}} \pm 0.025_{\text{syst}}$
BABAR [275]	$0.566 \pm 0.050_{\text{stat}} \pm 0.045_{\text{syst}}$	$0.59 \pm 0.05_{\text{stat}} \pm 0.04_{\text{syst}}$
Average	$\mathbf{0.536 \pm 0.028}$	$\boldsymbol{\chi^2/\text{dof} = 0.25}$ **(CL = 62%)**
Experiment	$\mathcal{B}(\bar{B}^0 \to D^0\pi^+\ell^-\bar{\nu}_\ell)[\%]$ (rescaled)	$\mathcal{B}(\bar{B}^0 \to D^0\pi^+\ell^-\bar{\nu}_\ell)[\%]$ (published)
Belle [303]	$0.360 \pm 0.018_{\text{stat}} \pm 0.011_{\text{syst}}$	$0.360 \pm 0.018_{\text{stat}} \pm 0.011_{\text{syst}}$
BABAR [275]	$0.406 \pm 0.080_{\text{stat}} \pm 0.035_{\text{syst}}$	$0.43 \pm 0.08_{\text{stat}} \pm 0.03_{\text{syst}}$
Average	$\mathbf{0.363 \pm 0.021}$	$\boldsymbol{\chi^2/\text{dof} = 0.26}$ **(CL = 61%)**
Experiment	$\mathcal{B}(\bar{B}^0 \to D^{*0}\pi^+\ell^-\bar{\nu}_\ell)[\%]$ (rescaled)	$\mathcal{B}(\bar{B}^0 \to D^{*0}\pi^+\ell^-\bar{\nu}_\ell)[\%]$ (published)
Belle [303]	$0.551 \pm 0.024_{\text{stat}} \pm 0.017_{\text{syst}}$	$0.551 \pm 0.024_{\text{stat}} \pm 0.017_{\text{syst}}$
BABAR [275]	$0.461 \pm 0.080_{\text{stat}} \pm 0.044_{\text{syst}}$	$0.48 \pm 0.08_{\text{stat}} \pm 0.04_{\text{syst}}$
Average	$\mathbf{0.542 \pm 0.028}$	$\boldsymbol{\chi^2/\text{dof} = 0.87}$ **(CL = 35%)**

where the first uncertainty is statistical, the second systematic and the third due to the limited knowledge of the external inputs, in particular the constant $f_s/f_d \times \mathcal{B}(D_s^+ \to K^+K^-\pi^+)$. This result is in agreement with the exclusive determinations of $|V_{cb}|$ using the $\bar{B}^0$ and B^- decays.

4. $\bar{B} \to D^{(*)}\pi\ell^-\bar{\nu}_\ell$

The average inclusive branching fractions for $\bar{B} \to D^{(*)}\pi\ell^-\bar{\nu}_\ell$ decays, where no constraint is applied to the mass of the $D^{(*)}\pi$ system, are determined by the combination of the results provided in Table 33 for $\bar{B}^0 \to D^0\pi^+\ell^-\bar{\nu}_\ell$, $\bar{B}^0 \to D^{*0}\pi^+\ell^-\bar{\nu}_\ell$, $B^- \to D^+\pi^-\ell^-\bar{\nu}_\ell$, and $B^- \to D^{*+}\pi^-\ell^-\bar{\nu}_\ell$ decays. For the $\bar{B}^0 \to D^0\pi^+\ell^-\bar{\nu}_\ell$ decays a veto to reject the $D^{*+} \to D^0\pi^+$ decays is applied. The measurements included in the average are scaled to a consistent set of input parameters and their uncertainties. For both the *BABAR* and Belle results, the B semileptonic signal yields are extracted from a fit to the missing mass squared distribution for a sample of fully reconstructed $B\bar{B}$ events. Figure 16 shows the measurements and the resulting average for the four decay modes.

5. $\bar{B} \to D^{**}\ell^-\bar{\nu}_\ell$

In this section we report results on $\bar{B} \to D^{**}\ell^-\bar{\nu}_\ell$ decays, where D^{**} here denotes the lightest excited charm mesons above the D and D^* states. According to heavy quark symmetry (HQS) [304], the D^* mesons with a charm and anti-quark with relative angular momentum $L = 1$, form one doublet of states with angular momentum $j \equiv s_q + L = 3/2$ $[D_1(2420), D_2^*(2460)]$ and another doublet with $j = 1/2$ $[D_0^*(2300), D_1'(2430)]$, where s_q is the light quark spin.[13] Parity and angular momentum conservation constrain the decays allowed for each state. The D_1 and D_2^* states decay predominantly via D-wave to $D^*\pi$ and $D^{(*)}\pi$, respectively, and have small decay widths, while the D_0^* and D_1' states decay via S-wave to $D\pi$ and $D^*\pi$ and are very broad. For the narrow states, the averages are determined by the combination of the results provided in Table 34 and 35 for $\mathcal{B}(B^- \to D_1^0\ell^-\bar{\nu}_\ell) \times \mathcal{B}(D_1^0 \to D^{*+}\pi^-)$ and $\mathcal{B}(B^- \to D_2^0\ell^-\bar{\nu}_\ell) \times \mathcal{B}(D_2^0 \to D^{*+}\pi^-)$. For the broad states, the averages are determined by the combination of the results provided in Table 36 and 37 for $\mathcal{B}(B^- \to D_1'^0\ell^-\bar{\nu}_\ell) \times \mathcal{B}(D_1'^0 \to D^{*+}\pi^-)$ and $\mathcal{B}(B^- \to D_0^{*0}\ell^-\bar{\nu}_\ell) \times \mathcal{B}(D_0^{*0} \to D^+\pi^-)$. The measurements are scaled to a consistent set of input parameters and their uncertainties. The results are reported for B^-, and when measurements for

[13] At present only these $L = 1$ orbital excited states have been observed in the semileptonic B meson decays, but in principle also radial $2S$ excitation and states with $L = 2$, 3, observed in fully hadronic B decays, could contribute to semileptonic decays.

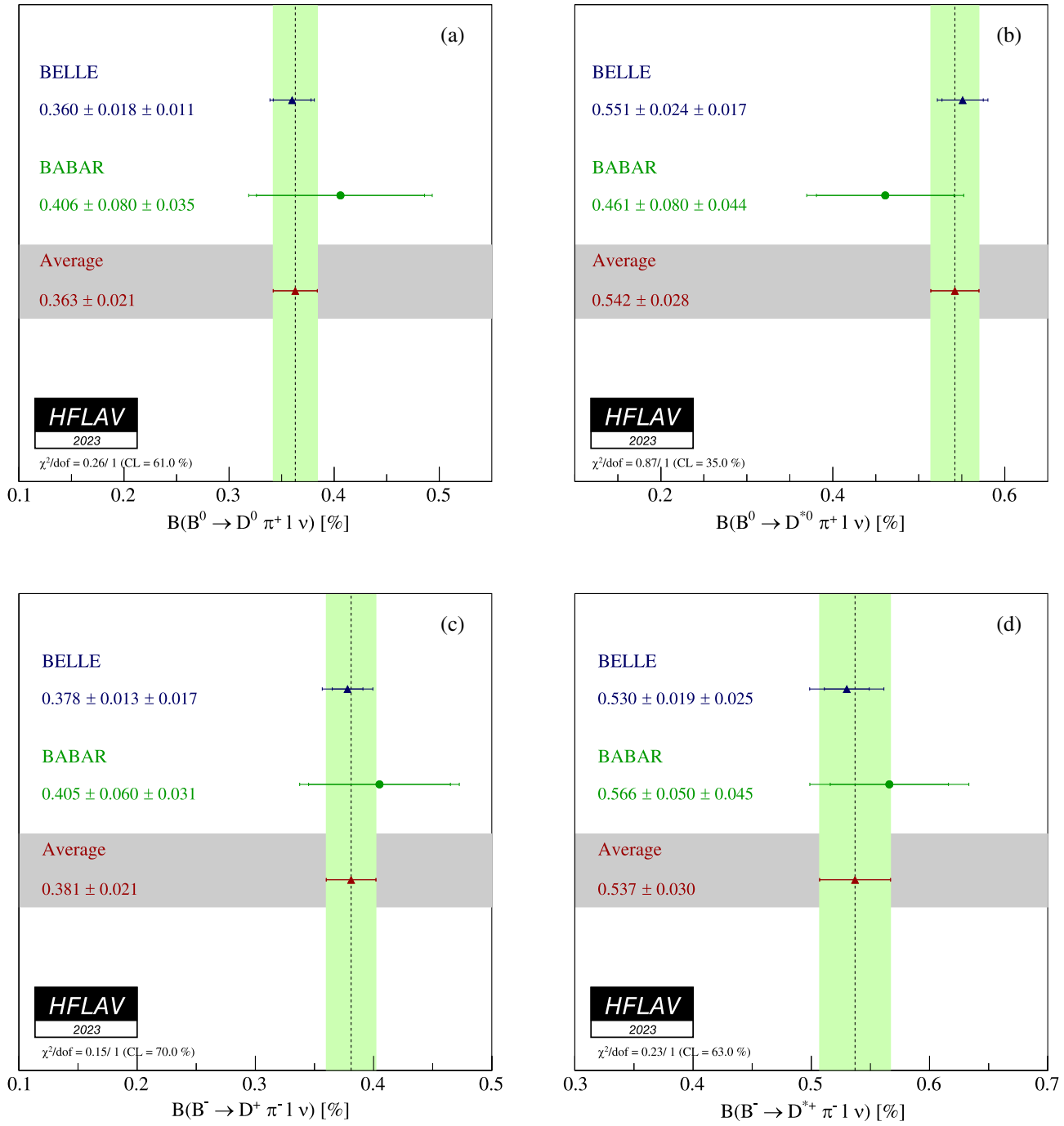


FIG. 16. Average branching fraction of exclusive semileptonic B decays (a) $\bar{B}^0 \to D^0\pi^+\ell^-\bar{\nu}_\ell$, (b) $\bar{B}^0 \to D^{*0}\pi^+\ell^-\bar{\nu}_\ell$, (c) $B^- \to D^+\pi^-\ell^-\bar{\nu}_\ell$, and (d) $B^- \to D^{*+}\pi^-\ell^-\bar{\nu}_\ell$. The corresponding individual results are also shown.

both B^0 and B^- are available, the combination assumes the isospin symmetry.

For both the B-factory and the LEP and Tevatron results, the B semileptonic signal yields are extracted from a fit to the invariant mass distribution of the $D^{(*)+}\pi^-$ system. The LEP and Tevatron measurements are for the inclusive decays $\bar{B} \to D^{**}(D^*\pi^-)X\ell^-\bar{\nu}_\ell$. In the average with the results from the B-factories, we use these measurements assuming that no particles are left in the X system. The *BABAR* tagged analysis of $\bar{B} \to D_2^*\ell^-\bar{\nu}_\ell$ was performed selecting $D_2^* \to D\pi$ decays. The *BABAR* result reported in Table 35 is translated in a branching fraction for the $D_2^* \to D^*\pi$ decay mode assuming $\mathcal{B}(D_2^* \to D\pi)/\mathcal{B}(D_2^* \to D^*\pi) = 1.52 \pm 0.14$ [9]. The Belle tagged analysis in Ref. [303], reports the branching fraction of $\bar{B} \to D_2^*\ell^-\bar{\nu}_\ell$ separated for $D_2^* \to D\pi$ and $D_2^* \to D^*\pi$. The

TABLE 34. Published and rescaled individual measurements and their averages for the branching fraction $\mathcal{B}(B^- \to D_1^0 \ell^- \bar{\nu}_\ell) \times \mathcal{B}(D_1^0 \to D^{*+}\pi^-)$.

Experiment	$\mathcal{B}(B^- \to D_1^0(D^{*+}\pi^-)\ell^-\bar{\nu}_\ell)[\%]$ (rescaled)	$\mathcal{B}(B^- \to D_1^0(D^{*+}\pi^-)\ell^-\bar{\nu}_\ell)[\%]$ (published)
ALEPH [305]	$0.436 \pm 0.098_{\text{stat}} \pm 0.067_{\text{syst}}$	$0.47 \pm 0.10_{\text{stat}} \pm 0.07_{\text{syst}}$
OPAL [306]	$0.551 \pm 0.210_{\text{stat}} \pm 0.100_{\text{syst}}$	$0.70 \pm 0.21_{\text{stat}} \pm 0.10_{\text{syst}}$
CLEO [307]	$0.347 \pm 0.085_{\text{stat}} \pm 0.056_{\text{syst}}$	$0.373 \pm 0.085_{\text{stat}} \pm 0.057_{\text{syst}}$
D0 [308]	$0.213 \pm 0.018_{\text{stat}} \pm 0.035_{\text{syst}}$	$0.219 \pm 0.018_{\text{stat}} \pm 0.035_{\text{syst}}$
Belle tagged B^- [303]	$0.249 \pm 0.023_{\text{stat}} \pm 0.015_{\text{syst}}$	$0.249 \pm 0.023_{\text{stat}} \pm 0.015_{\text{syst}}$
Belle tagged B^0 [303]	$0.329 \pm 0.054_{\text{stat}} \pm 0.031_{\text{syst}}$	$0.329 \pm 0.054_{\text{stat}} \pm 0.031_{\text{syst}}$
BABAR tagged [309]	$0.273 \pm 0.030_{\text{stat}} \pm 0.029_{\text{syst}}$	$0.29 \pm 0.03_{\text{stat}} \pm 0.03_{\text{syst}}$
BABAR untagged B^- [310]	$0.290 \pm 0.017_{\text{stat}} \pm 0.017_{\text{syst}}$	$0.30 \pm 0.02_{\text{stat}} \pm 0.02_{\text{syst}}$
BABAR untagged B^0 [310]	$0.279 \pm 0.026_{\text{stat}} \pm 0.023_{\text{syst}}$	$0.30 \pm 0.02_{\text{stat}} \pm 0.02_{\text{syst}}$
Average	$\mathbf{0.270 \pm 0.015}$	$\boldsymbol{\chi^2/\text{dof} = 9.0/8}$ (CL = **34.0%**)

TABLE 35. Published and rescaled individual measurements and their averages for $\mathcal{B}(B^- \to D_2^0 \ell^- \bar{\nu}_\ell) \times \mathcal{B}(D_2^0 \to D^{*+}\pi^-)$.

Experiment	$\mathcal{B}(B^- \to D_2^0(D^{*+}\pi^-)\ell^-\bar{\nu}_\ell)[\%]$ (rescaled)	$\mathcal{B}(B^- \to D_2^0(D^{*+}\pi^-)\ell^-\bar{\nu}_\ell)[\%]$ (published)
CLEO [307]	$0.054 \pm 0.066_{\text{stat}} \pm 0.011_{\text{syst}}$	$0.059 \pm 0.066_{\text{stat}} \pm 0.011_{\text{syst}}$
D0 [308]	$0.085 \pm 0.018_{\text{stat}} \pm 0.020_{\text{syst}}$	$0.088 \pm 0.018_{\text{stat}} \pm 0.020_{\text{syst}}$
Belle tagged B^- $(D_2 \to D^*\pi)$ [303]	$0.136 \pm 0.026_{\text{stat}} \pm 0.009_{\text{syst}}$	$0.36 \pm 0.026_{\text{stat}} \pm 0.009_{\text{syst}}$
Belle tagged B^0 $(D_2 \to D^*\pi)$ [303]	$0.054 \pm 0.043_{\text{stat}} \pm 0.011_{\text{syst}}$	$0.054 \pm 0.043_{\text{stat}} \pm 0.011_{\text{syst}}$
Belle tagged B^- $(D_2 \to D\pi)$ [303]	$0.107 \pm 0.007_{\text{stat}} \pm 0.011_{\text{syst}}$	$0.107 \pm 0.007_{\text{stat}} \pm 0.011_{\text{syst}}$
Belle tagged B^0 $(D_2 \to D^*\pi)$ [303]	$0.109 \pm 0.011_{\text{stat}} \pm 0.011_{\text{syst}}$	$0.109 \pm 0.011_{\text{stat}} \pm 0.011_{\text{syst}}$
BABAR tagged [309]	$0.075 \pm 0.013_{\text{stat}} \pm 0.009_{\text{syst}}$	$0.078 \pm 0.013_{\text{stat}} \pm 0.010_{\text{syst}}$
BABAR untagged B^- [310]	$0.088 \pm 0.009_{\text{stat}} \pm 0.007_{\text{syst}}$	$0.087 \pm 0.013_{\text{stat}} \pm 0.007_{\text{syst}}$
BABAR untagged B^0 [310]	$0.064 \pm 0.010_{\text{stat}} \pm 0.004_{\text{syst}}$	$0.087 \pm 0.013_{\text{stat}} \pm 0.007_{\text{syst}}$
Average	$\mathbf{0.085 \pm 0.006}$	$\boldsymbol{\chi^2/\text{dof} = 12.9/8}$ (CL = **11.5%**)

TABLE 36. Published and rescaled individual measurements and their averages for $\mathcal{B}(B^- \to D_1'^0 \ell^- \bar{\nu}_\ell) \times \mathcal{B}(D_1'^0 \to D^{*+}\pi^-)$.

Experiment	$\mathcal{B}(B^- \to D_1'^0(D^{*+}\pi^-)\ell^-\bar{\nu}_\ell)[\%]$ (rescaled)	$\mathcal{B}(B^- \to D_1'^0(D^{*+}\pi^-)\ell^-\bar{\nu}_\ell)[\%]$ (published)
DELPHI [311]	$0.694 \pm 0.170_{\text{stat}} \pm 0.176_{\text{syst}}$	$0.83 \pm 0.17_{\text{stat}} \pm 0.18_{\text{syst}}$
Belle tagged B^+ [303]	$0.138 \pm 0.036_{\text{stat}} \pm 0.009_{\text{syst}}$	$0.138 \pm 0.036_{\text{stat}} \pm 0.009_{\text{syst}}$
Belle tagged B^0 [303]	$0.221 \pm 0.073_{\text{stat}} \pm 0.027_{\text{syst}}$	$0.221 \pm 0.073_{\text{stat}} \pm 0.027_{\text{syst}}$
BABAR tagged [309]	$0.254 \pm 0.040_{\text{stat}} \pm 0.044_{\text{syst}}$	$0.27 \pm 0.04_{\text{stat}} \pm 0.05_{\text{syst}}$
Average	$\mathbf{0.185 \pm 0.029}$	$\boldsymbol{\chi^2/\text{dof} = 7.5/3}$ (CL = **5%**)

TABLE 37. Published and rescaled individual measurements and their averages for $\mathcal{B}(B^- \to D_0^{*0}\ell^-\bar{\nu}_\ell) \times \mathcal{B}(D_0^{*0} \to D^+\pi^-)$.

Experiment	$\mathcal{B}(B^- \to D_0^{*0}(D^+\pi^-)\ell^-\bar{\nu}_\ell)[\%]$ (rescaled)	$\mathcal{B}(B^- \to D_0^{*0}(D^+\pi^-)\ell^-\bar{\nu}_\ell)[\%]$ (published)
Belle tagged B^+ [303]	$0.054 \pm 0.022_{\text{stat}} \pm 0.005_{\text{syst}}$	$0.054 \pm 0.022_{\text{stat}} \pm 0.005_{\text{syst}}$
BABAR tagged [309]	$0.308 \pm 0.040_{\text{stat}} \pm 0.047_{\text{syst}}$	$0.26 \pm 0.05_{\text{stat}} \pm 0.04_{\text{syst}}$
Average	$\mathbf{0.084 \pm 0.021}$	$\chi^2/\text{dof} = 11./1$ (CL $< 0.1\%$)

Belle results reported in Table 35 are obtained scaling all the decays to the $D_2^* \to D^*\pi$ decay mode assuming the ratio of branching fractions reported above. Figures 17 and 18 show the measurements and the resulting averages.

It is worth noticing that, while the results for the narrow resonances are consistent between the various experiments, the measurements for $B^- \to D_0^0\ell^-\bar{\nu}_\ell$ obtained by *BABAR* [309] and Belle [303] with the hadronic tagging technique, are not compatible. Belle did not observe $\bar{B}^0 \to D_0^{*+}\ell^-\bar{\nu}_\ell$ and put an upper limit of $\mathcal{B}(\bar{B}^0 \to D_0^{*+}\ell^-\bar{\nu}_\ell) < 0.044\%$ at 90% of CL, while the corresponding mode for the B^- is observed with 3.9σ of significance. The model used to describe the D_0 state in the existing measurements, has been questioned in recent publications, as seen in [312] and [313,314]. The results for D_1' are instead consistent between *BABAR* and Belle.

B. Inclusive CKM-favored decays

1. Global analysis of $\bar{B} \to X_c\ell^-\bar{\nu}_\ell$

The semileptonic decay width $\Gamma(\bar{B} \to X_c\ell^-\bar{\nu}_\ell)$ is calculated in the framework of the operator production expansion (OPE) [22,44,45]. The result is a double-expansion in Λ_{QCD}/m_b and α_s, which depends on a number of non-perturbative parameters. These parameters describe the dynamics of the b-quark inside the B hadron and can be measured using spectral moments in inclusive $\bar{B} \to X_c\ell^-\bar{\nu}_\ell$ decays.

Recent theoretical work is done mostly in the kinetic scheme [315]. Here, the non-perturbative parameters are the quark masses m_b and m_c, μ_π^2 and μ_G^2 at $O(1/m_b^2)$, and ρ_D^3 and ρ_{LS}^3 at $O(1/m_b^3)$. To avoid proliferation of these parameters at $O(1/m_b^4)$, reparametrization invariance is

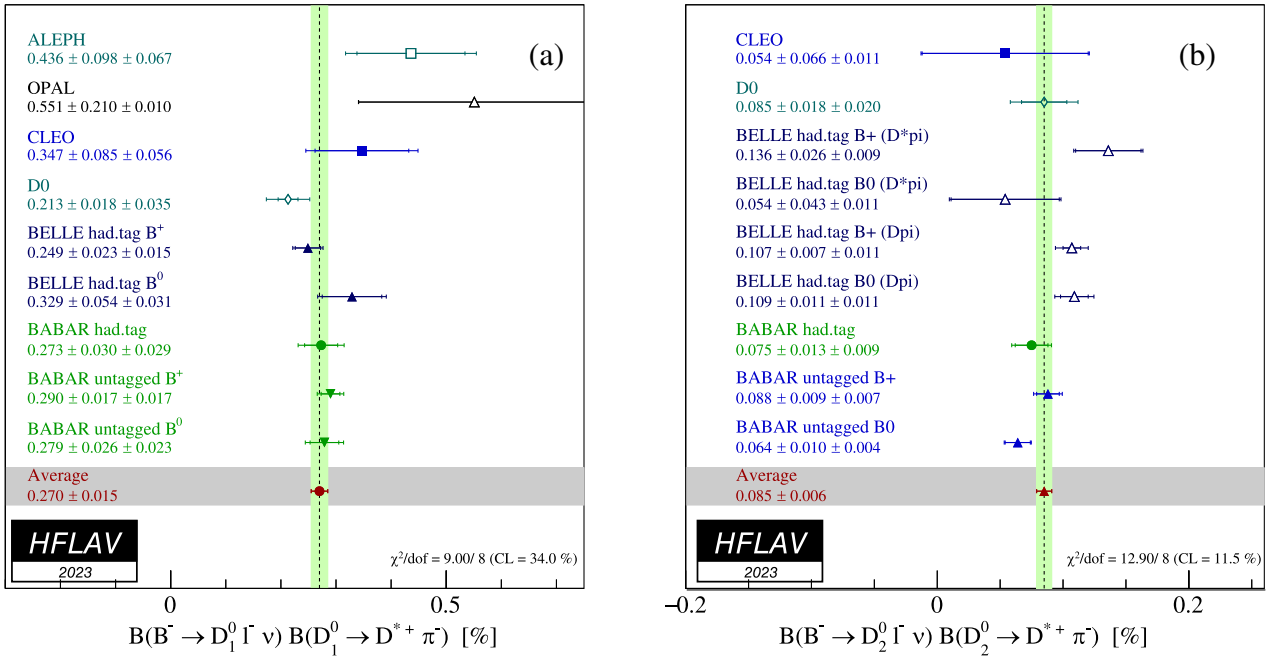


FIG. 17. Rescaled individual measurements and their averages for (a) $\mathcal{B}(B^- \to D_1^0\ell^-\bar{\nu}_\ell) \times \mathcal{B}(D_1^0 \to D^{*+}\pi^-)$ and (b) $\mathcal{B}(B^- \to D_2^0\ell^-\bar{\nu}_\ell) \times \mathcal{B}(D_2^0 \to D^{*+}\pi^-)$.

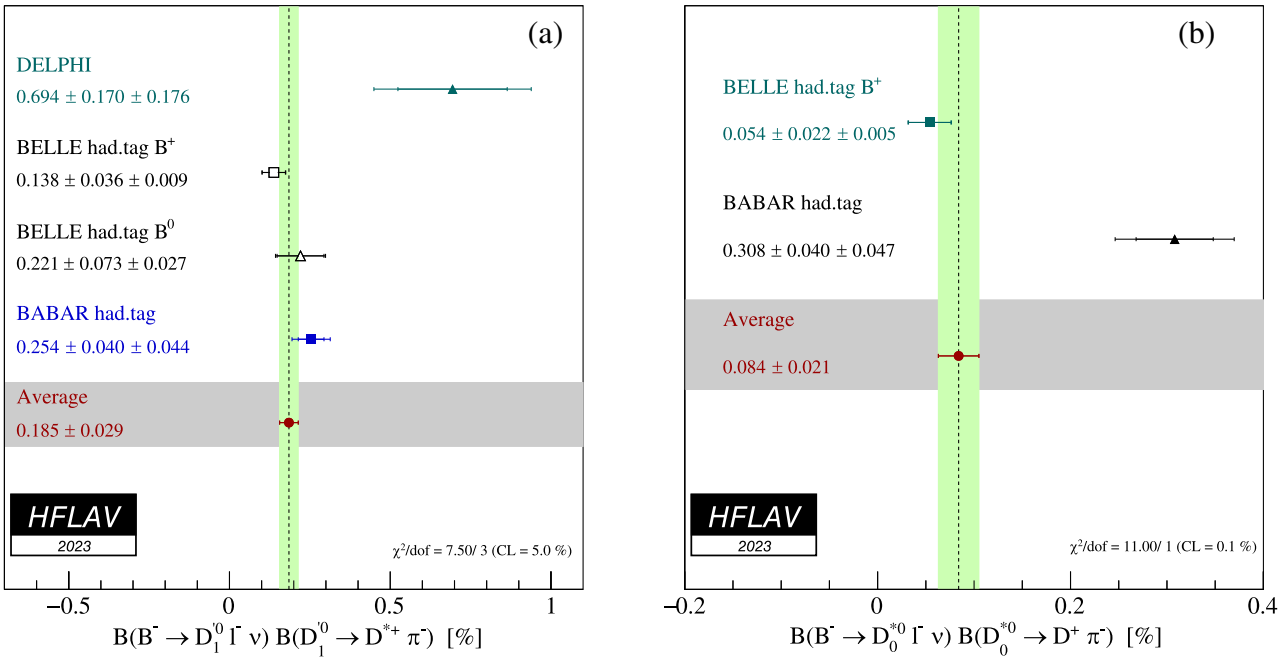


FIG. 18. Rescaled individual measurements and their averages for (a) $\mathcal{B}(B^- \to D_1'^0 \ell^- \bar{\nu}_\ell) \times \mathcal{B}(D_1'^0 \to D^{*+}\pi^-)$ and (b) $\mathcal{B}(B^- \to D_0^{*0} \ell^- \bar{\nu}_\ell) \times \mathcal{B}(D_0^{*0} \to D^+\pi^-)$.

proposed to link different operators in the heavy-quark expansion thus reducing the number of independent operators [316]. However, this limits the experimental input to certain spectral moments, such as the moments of leptonic invariant mass (q^2). An alternative expression is obtained in the 1S scheme [317].

Measurements of $\langle E_\ell^n \rangle$, $\langle M_X^n \rangle$ and $\langle q^{2n} \rangle$ have been obtained by Belle II [318], *BABAR* [319,320], Belle [321–323], CDF [324], CLEO [325] and DELPHI [311]. The moments of the E_ℓ^n and M_X^n distributions are measured for different lower threshold values $E_{\rm cut}$ of E_ℓ. For the moments of q^{2n}, the threshold is placed on q^2. As these measurements with successive $E_{\rm cut}$ values are highly correlated, global analyses typically discard a number of the experimental moments to avoid numerical issues in the fit. The region $E_{\rm cut} > 1.5$ GeV is also avoided as the quark hadron duality assumption might not be applicable anymore.

2. Analysis using E_ℓ and M_X moments

This analysis determines $|V_{cb}|$, the inclusive $\bar{B} \to X_c \ell^- \bar{\nu}_\ell$ branching fraction and the non-perturbative parameters of the kinetic scheme from a fit to the $\langle E_\ell^n \rangle$, $n = 0$, 1, 2, 3, and $\langle M_X^n \rangle$, $n = 2$, 4, 6, moments measured by *BABAR* [319,320], Belle [321,322], CDF [324], CLEO [325] and DELPHI [311] using the theoretical expressions at $O(1/m_b^3)$. Here, the zero order moment of the E_ℓ spectrum refers to the partial branching fractions. This global fit has been repeated several times [62,326,327] with Ref. [62] being the last iteration that will be reviewed here. As this analysis is known to constrain only a linear combination of m_b and m_c, the FLAG 2019 averages, $\bar{m}_c(2\ \text{GeV}) = 1.093(8)$ GeV and $m_{\rm kin}(1\ \text{GeV}) = 4.565(19)$ GeV [328], are used as constraints in the fit. Constraints are also placed on μ_G^2 and ρ_{LS}^3. Theory uncertainties and correlations included in the fit have a significant numerical impact and are estimated using the procedure described in Ref. [326] with some updates: The theory uncertainty is modeled through variations of the non-perturbative parameters around fixed values ($\pm 7\%$ for μ_π^2 and μ_G^2, $\pm 20\%$ for ρ_D^3 and ρ_{LS}^3). An irreducible uncertainty of 4 MeV is applied to the quark masses m_c and m_b, and $\alpha_s(m_b)$ is varied by ± 0.018. The theoretical correlations for different central moments are considered to be zero while correlations of predictions of the same moment at different $E_{\rm cut}$ values are modeled by the proximity of the cuts.

Reference [62] obtains

$$|V_{cb}| = (42.16 \pm 0.30(\text{th}) \pm 0.32(\text{exp}) \pm 0.25(\Gamma)) \times 10^{-3}, \tag{99}$$

where the first uncertainty originates from the variations of the theory parameters, the second from the experimental input and the third from the expression of the semileptonic width. The inclusive semileptonic branching fraction is found to be

$$\mathcal{B}(\bar{B} \to X_c \ell^- \bar{\nu}_\ell) = (10.66 \pm 0.15)\%. \tag{100}$$

The χ^2 of the fit divided by the number of degrees of freedom is 0.47.

3. Analysis using q^2 moments

Following the proposal in Ref. [316], a first analysis using terms up to $O(1/m_b^4)$ [63] has been performed using the $\langle q^{2n}\rangle$ moments measured by Belle [323] and Belle II [318]. Moments $\langle q^{2n}\rangle$ with $n = 1, 2, 3, 4$ and with different $q_{\rm cut}$ values for each moment are used. Similarly to Ref. [62], the bottom and the charm quark masses are constrained as well as μ_G^2 and ρ_{LS}^3. In addition, μ_π^2 is constrained to (0.43 ± 0.24) GeV^2 as this parameter enters the first order q^2 moments only quadratically. Theory uncertainties are again estimated by variation of the non-perturbative parameters and included in the fit.

In order to extract $|V_{cb}|$, information on the total semileptonic branching ratio is needed and the authors of Ref. [63] perform a private average of available measurements,

$$\mathcal{B}(\bar{B} \to X_c \ell^- \bar{\nu}_\ell) = (10.48 \pm 0.13)\%. \tag{101}$$

With this normalization, the resulting $|V_{cb}|$ at N3LO precision of the decay rate is

$$|V_{cb}| = (41.69 \pm 0.63) \times 10^{-3}. \tag{102}$$

The $\chi^2/\text{ndf.} = 0.15$ indicates a good fit to the data. The numerical difference to the result of Ref. [62] stems mostly from the difference in the semileptonic branching fraction. If the q^2 analysis would be rescaled to $\mathcal{B}(\bar{B} \to X_c \ell^- \bar{\nu}_\ell) = (10.63 \pm 0.19)\%$, the correspond value of $|V_{cb}|$ is $(41.99 \pm 0.65) \times 10^{-3}$.

Despite this agreement, we note a tension for the non-perturbative parameter ρ_D^3 between Refs. [62,63]: The former analysis obtains $\rho_D^3 = (0.185 \pm 0.031)$ GeV^3 while the latter obtains $\rho_D^3 = (0.03 \pm 0.02)$ GeV^3 if only terms up to $O(1/m_b^3)$ are included. However, in the perturbative calculation both analyses do not contain the same orders in α_s, which could affect the extraction of this parameter [329–331].

4. Analysis using E_ℓ, M_X and q^2 moments

Very recently, an updated calculation of the $\langle q^{2n}\rangle$ moments including $O(\alpha_s^2\beta_0)$ corrections has been published [61]. In the same publication this result is used to extend the analysis in Ref. [62] and include the $\langle q^{2n}\rangle$ moments measured by Belle [323] and Belle II [318]. The results are

$$|V_{cb}| = (41.97 \pm 0.27(\text{exp}) \pm 0.31(\text{th}) \pm 0.25(\Gamma)) \times 10^{-3} \tag{103}$$

and

$$\mathcal{B}(\bar{B} \to X_c \ell^- \bar{\nu}_\ell) = (10.63 \pm 0.15)\%, \tag{104}$$

with $\chi^2/\text{ndf.} = 0.546$. The first uncertainty on $|V_{cb}|$ is experimental, the second originates from the variations of the theory parameters and the third from the expression of the semileptonic width.

We note that here the inclusion of the $\langle q^{2n}\rangle$ moments has no significant impact on the values of the non-perturbative parameters. In particular, ρ_D^3 changes from (0.185 ± 0.031) GeV^3 to 0.167 ± 0.018 GeV^3 when including the Belle and Belle II $\langle q^{2n}\rangle$ moments.

5. Average

Due to the unknown correlations between the analyses in Refs. [61–63], we refrain from averaging the results for $|V_{cb}|$ and $\mathcal{B}(\bar{B} \to X_c \ell^- \bar{\nu}_\ell)$. Instead we use the result of Ref. [61] as our central value for $|V_{cb}|$ from inclusive decays $\bar{B} \to X_c \ell^- \bar{\nu}_\ell$,

$$|V_{cb}| = (41.97 \pm 0.48) \times 10^{-3}. \tag{105}$$

Note that this value is also very close to the arithmetic average of Refs. [62,63] assuming full correlation of the theoretical uncertainties. Consistently, we also take Ref. [61] for the central value of the charmed semileptonic branching ratio,

$$\mathcal{B}(\bar{B} \to X_c \ell^- \bar{\nu}_\ell) = (10.63 \pm 0.15)\%. \tag{106}$$

We calculate the charmless semileptonic branching ratio using Eq. 58 from Ref. [332] and the average BLNP value for $|V_{ub}|$ from Table 50 and obtain $\mathcal{B}(\bar{B} \to X_u \ell^- \bar{\nu}_\ell) = (1.92 \pm 0.21) \times 10^{-3}$. The total semileptonic branching fraction is thus

$$\mathcal{B}(\bar{B} \to X \ell^- \bar{\nu}_\ell) = (10.82 \pm 0.15)\%. \tag{107}$$

C. Exclusive CKM-suppressed decays

In this section, we give results on exclusive charmless semileptonic branching fractions and the determination of $|V_{ub}|$ based on $B \to \pi \ell \nu$ decays. The measurements are based on two different event selections: tagged events, in which the second B meson in the event is fully (or partially) reconstructed, and untagged events, for which the momentum of the undetected neutrino is inferred from measurements of the total momentum sum of the detected particles and the knowledge of the initial state.

The LHCb experiment has reported a direct measurement of $|V_{ub}|/|V_{cb}|$ [333], reconstructing the $\Lambda_b^0 \to p\mu\nu$ decays and normalizing the branching fraction to the $\Lambda_b^0 \to \Lambda_c^+(\to pK\pi)\mu\nu$ decays. Recently LHCb reported also a measurement of $|V_{ub}|/|V_{cb}|$ [334] using $B_s^0 \to K\mu\nu$ decays normalized to $B_s^0 \to D_s\mu\nu$ in two separate bins of q^2. We show a combination of $|V_{ub}|$ and $|V_{cb}|$ using the LHCb constraints on $|V_{ub}|/|V_{cb}|$, the exclusive determination of

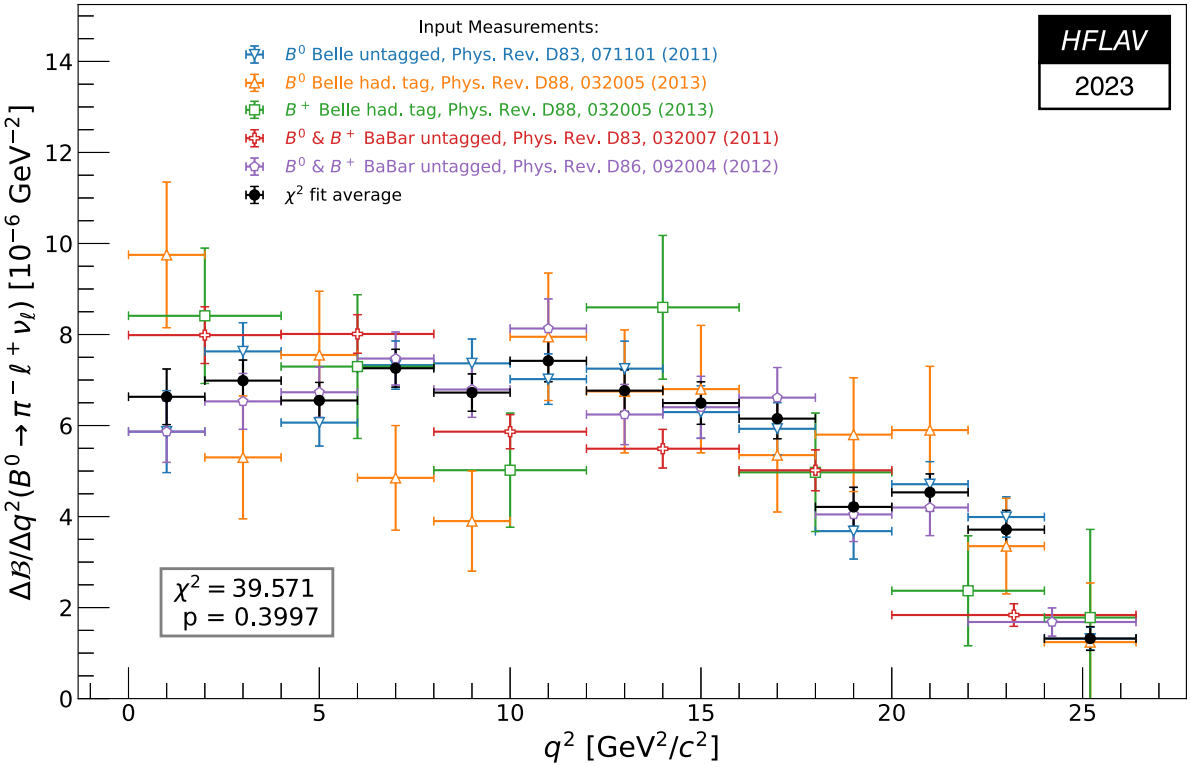


FIG. 19. The $B \to \pi\ell\nu q^2$ spectrum measurements and the average spectrum obtained from the likelihood combination (shown in black).

$|V_{ub}|$ from $B \to \pi\ell\nu$, and $|V_{cb}|$ from $B \to D^*\ell\nu$, $B \to D\ell\nu$ and $B_s \to D_s^{(*)}\mu\nu$.

We also present branching fraction averages for $B^0 \to \rho\ell^+\nu$, $B^+ \to \omega\ell^+\nu$, $B^+ \to \eta\ell^+\nu$ and $B^+ \to \eta'\ell^+\nu$. Using the available measurements of the partial branching fractions of $B^0 \to \rho\ell^+\nu$, $B^+ \to \omega\ell^+\nu$ decays, we also present for the first time the combined q^2 spectrum for these two decays.

1. $B \to \pi\ell\nu$ branching fraction and q^2 spectrum

We use the four most precise measurements of the differential $B \to \pi\ell\nu$ decay rate as a function of the four-momentum transfer squared, q^2, from *BABAR* and Belle [335–338] to obtain an average q^2 spectrum and an average for the total branching fraction. The measurements are presented in Fig. 19. From the two untagged *BABAR* analyses [337,338], the combined results for $B^0 \to \pi^-\ell^+\nu$ and $B^+ \to \pi^0\ell^+\nu$ decays based on isospin symmetry are used. The hadronic-tag analysis by Belle [336] provides results for $B^0 \to \pi^-\ell^+\nu$ and $B^+ \to \pi^0\ell^+\nu$ separately, but not for the combination of both channels. In the untagged analysis by Belle [335], only $B^0 \to \pi^-\ell^+\nu$ decays were measured. The experimental measurements use different binnings in q^2, but have matching bin edges, which allows them to be combined.

To arrive at an average q^2 spectrum, a binned maximum-likelihood fit to determine the average partial branching fraction in each q^2 interval is performed, differentiating between common and individual uncertainties and correlations for the various measurements. Shared sources of systematic uncertainty of all measurements are included in the likelihood as nuisance parameters constrained assuming Gaussian distributions. The most important shared sources of uncertainty are due to continuum subtraction, the number of B-meson pairs (only correlated among measurement by the same experiment), tracking efficiency (only correlated among measurements by the same experiment), uncertainties from modeling the $b \to u\ell\bar{\nu}_\ell$ contamination, modeling of final state radiation, and contamination from $b \to c\ell\bar{\nu}_\ell$ decays. We avoid the d'Agostini bias, described in Ref. [339], by scaling the estimated averages with the nuisance parameters. The initial combination results in a poor p-value of 0.3%, with the measurement of Ref. [337] at high q^2 being in tension with the other determinations. This kinematic region is very sensitive to the modeling of other $b \to u\ell\bar{\nu}_\ell$ processes, and Ref. [337] makes several assumptions, that no longer reflect the current knowledge. To address this, we introduce an additional scaling parameter, as suggested by Ref. [340], which we allow to enlarge the uncertainties of the offending measurement. The scaling parameter is constrained using a log-normal function with a width parameter of 0.35.

TABLE 38. Partial $B^0 \to \pi^- \ell^+ \nu_\ell$ branching fractions per GeV^2 for the input measurements and the average obtained from the likelihood fit. The uncertainties are the combined statistical and systematic uncertainties.

Δq^2 [GeV^2]	$\Delta\mathcal{B}(B^0 \to \pi^- \ell^+ \nu_\ell)/\Delta q^2 [10^{-7}]$					
	Belle untagged (B^0)	Belle tagged (B^0)	Belle tagged (B^+)	*BABAR* untagged ($B^{0,+}$, 12 bins)	*BABAR* untagged ($B^{0,+}$, 6 bins)	Average
0–2	58.7 ± 12.9	97.5 ± 16.7	84.1 ± 15.5	58.7 ± 9.4	79.9 ± 9.1	66.3 ± 6.1
2–4	76.3 ± 8.0	53.0 ± 13.8		65.3 ± 7.1		69.9 ± 4.5
4–6	60.6 ± 6.4	75.5 ± 14.5	73.0 ± 16.2	67.3 ± 6.4	80.1 ± 5.3	65.5 ± 3.9
6–8	73.3 ± 7.6	48.5 ± 11.8		74.7 ± 7.1		72.6 ± 4.2
8–10	73.7 ± 8.1	39.0 ± 11.2	50.2 ± 12.8	67.9 ± 7.8	58.7 ± 5.5	67.2 ± 4.3
10–12	70.2 ± 8.8	79.5 ± 14.6		81.3 ± 8.2		74.2 ± 4.6
12–14	72.5 ± 9.1	67.5 ± 13.9	86.0 ± 16.4	62.4 ± 7.4	54.9 ± 6.2	67.7 ± 4.6
14–16	63.0 ± 8.4	68.0 ± 14.4		64.0 ± 7.9		64.9 ± 4.7
16–18	59.3 ± 7.8	53.5 ± 12.8	49.7 ± 13.3	66.1 ± 8.2	50.2 ± 5.7	61.5 ± 4.4
18–20	36.8 ± 7.2	58.0 ± 12.8		40.5 ± 7.6		42.1 ± 4.3
20–22	47.1 ± 6.2	59.0 ± 14.3	23.7 ± 12.1	42.0 ± 7.5	18.4 ± 3.2	45.3 ± 4.0
22–24	39.9 ± 6.2	33.5 ± 10.6		16.8 ± 5.9		37.1 ± 4.2
24–26.4	13.2 ± 2.9	12.4 ± 13.0	17.8 ± 19.4			13.2 ± 2.6

TABLE 39. Correlation matrix of the averaged partial branching fractions per GeV^2 in units of 10^{-14}.

Δq^2 [GeV^2]	0–2	2–4	4–6	6–8	8–10	10–12	12–14	14–16	16–18	18–20	20–22	22–24	24–26.4
0–2	1.0	−0.009	0.233	0.176	0.136	0.17	0.145	0.184	0.159	0.133	0.167	0.15	0.106
2–4		1.0	−0.091	0.279	0.126	0.154	0.139	0.144	0.126	0.091	0.127	0.102	0.072
4–6			1.0	−0.031	0.274	0.195	0.207	0.171	0.164	0.116	0.153	0.126	0.093
6–8				1.0	−0.006	0.294	0.226	0.2	0.186	0.124	0.167	0.151	0.092
8–10					1.0	0.033	0.297	0.171	0.182	0.12	0.138	0.138	0.082
10–12						1.0	0.097	0.254	0.219	0.153	0.172	0.173	0.103
12–14							1.0	−0.011	0.196	0.094	0.146	0.13	0.079
14–16								1.0	0.139	0.194	0.146	0.161	0.103
16–18									1.0	0.076	0.149	0.13	0.087
18–20										1.0	0.043	0.111	0.057
20–22											1.0	0.073	0.094
22–24												1.0	−0.038
24–26.4													1.0

The resulting average is shown Fig. 19 (left, black data points), and the resulting p-value is 40%.

The partial branching fractions and the correlation matrix obtained from the likelihood fit are given in Tables 38 and 39. The average for the total $B^0 \to \pi^- \ell^+ \nu_\ell$ branching fraction is obtained by summing up the partial branching fractions to give

$$\mathcal{B}(B^0 \to \pi^- \ell^+ \nu_\ell) = (1.50 \pm 0.02_{\text{stat}} \pm 0.05_{\text{syst}}) \times 10^{-4}. \tag{108}$$

2. $|V_{ub}|$ from $B \to \pi \ell \nu$

The $|V_{ub}|$ average can be determined from the averaged q^2 spectrum in combination with a prediction for the normalization of the $B \to \pi$ form factor. The differential decay rate for light leptons (e, μ) is given by

$$\begin{aligned}\Delta\Gamma &= \Delta\Gamma(q^2_{\text{low}}, q^2_{\text{high}}) \\ &= \int_{q^2_{\text{low}}}^{q^2_{\text{high}}} \mathrm{d}q^2 \left[\frac{8|\vec{p}_\pi|}{3} \frac{G_F^2 |V_{ub}|^2 q^2}{256\pi^3 m_B^2} H_0^2(q^2)\right],\end{aligned} \tag{109}$$

where G_F is Fermi's constant, $|\vec{p}_\pi|$ is the magnitude of the three-momentum of the final state π (a function of q^2), m_B the B^0-meson mass, and $H_0(q^2)$ the only non-zero helicity amplitude. The helicity amplitude is a function of the form factor f_+,

$$H_0 = \frac{2m_B|\vec{p}_\pi|}{\sqrt{q^2}} f_+(q^2). \tag{110}$$

The form factor f_+ can be calculated with non-perturbative methods, but its general form can be constrained by the differential $B \to \pi\ell\nu$ spectrum. Here, we parametrize the form factor using the BCL parametrization truncated at the order z^2 [341].

The decay rate is proportional to $|V_{ub}|^2|f_+(q^2)|^2$. Thus to extract $|V_{ub}|$ one needs to determine $f_+(q^2)$ (at least at one value of q^2). In order to enhance the precision, a binned χ^2 fit is performed using a χ^2 function of the form

$$\chi^2 = \left(\vec{\mathcal{B}} - \Delta\vec{\Gamma}\tau\right)^T C^{-1}\left(\vec{\mathcal{B}} - \Delta\vec{\Gamma}\tau\right) + \chi^2_{\mathrm{LQCD}} \tag{111}$$

where C denotes the covariance matrix given in Table 39, $\vec{\mathcal{B}}$ is the vector of averaged partial branching fractions, and $\Delta\vec{\Gamma}\tau$ is the product of the vector of theoretical predictions of the partial decay rates and the B^0-meson lifetime. The form factor normalization is included in the fit by the extra term in Eq. (111): χ_{LQCD} uses the updated 2024 FLAG lattice average [342] of the Fermilab/MILC, RBC/UKQCD and JLQCD lattice QCD calculations [343–345]. The resulting constraints are quoted directly in terms of the coefficients b_j of the BCL parametrization and enter Eq. (111) as

$$\chi^2_{\mathrm{LQCD}} = \left(\vec{b} - \vec{b}_{\mathrm{LQCD}}\right)^T C^{-1}_{\mathrm{LQCD}}\left(\vec{b} - \vec{b}_{\mathrm{LQCD}}\right), \tag{112}$$

with $\vec{b}$ the vector containing the free parameters of the χ^2 fit constraining the f_+ and f_0 form factors, $\vec{b}_{\mathrm{LQCD}}$ the averaged values from Ref. [342], and C_{LQCD} their covariance matrix. Note that the coefficients of the f_0 form factor, which is only relevant to describe final states with τ leptons, introduce additional information via their correlation to the expansion coefficients of f_+. Note that we impose the exact constraint of $f_+(q^2 = 0) = f_0(q^2 = 0)$. Further, FLAG is applying a scaling of the uncertainties due to disagreements between Ref. [343,344] with Ref. [345].

For the $|V_{ub}|$ average we obtain

$$|V_{ub}| = (3.75 \pm 0.06_{\mathrm{exp}} \pm 0.19_{\mathrm{theo}}) \times 10^{-3}. \tag{113}$$

The result of the fit is shown in Fig. 20. The χ^2 probability of the fit is 37.7%. The best fit values for $|V_{ub}|$ and the BCL parameters and their correlation matrix are given in Tables 40 and 41.

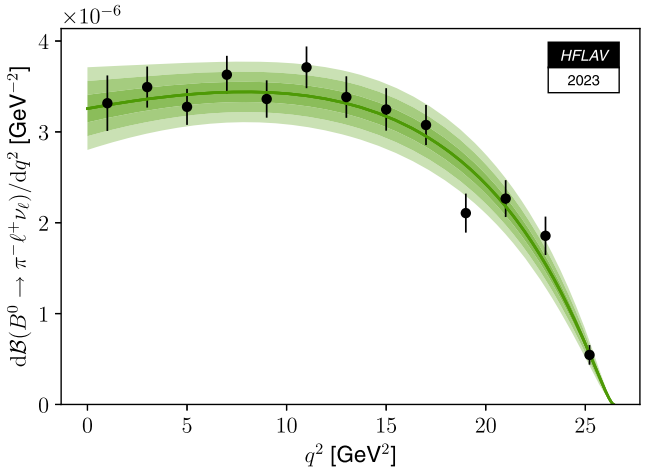


FIG. 20. Fit of the BCL parametrization to the averaged q^2 spectrum from *BABAR* and Belle and the LQCD calculations. The error bands represent the 1σ (dark green), 2σ (green), and $3\text{-}\sigma$ (light green) uncertainties of the fitted spectrum.

3. $B \to \rho\ell\nu_\ell$ and $B \to \omega\ell\nu_\ell$ branching fraction and q^2 spectrum

We report the branching fraction averages for $B \to V\ell\nu_\ell$, $V = \rho$, ω. The measurements, adjusted for common inputs, and their averages are listed in Tables 42, 43, and presented in Figs. 21.

In the $B^+ \to \rho^0\ell^+\nu$ average, both the $B^0 \to \rho^-\ell^+\nu$ and $B^+ \to \rho^0\ell^+\nu$ decays are used, where the $B^0 \to \rho^-\ell^+\nu$ are rescaled by $0.5\tau_{B^+}/\tau_{B^0}$ assuming the isospin symmetry. The $B^+ \to \rho^0\ell^+\nu$ results show significant differences, in particular the *BABAR* untagged analysis gives a branching fraction significantly lower (by about 3σ) than the Belle measurement based on the hadronic-tag. The difference is about 2σ for the $B^+ \to \rho^0\ell^+\nu$ decay modes.

We use the most precise measurements of the differential $B \to V\ell\nu_\ell$, $V = \rho$, ω decay rates as a function of the four-momentum transfer q^2 published by *BABAR* [337,350] and Belle [336]. To obtain an averaged q^2 spectrum and averaged branching fractions, we perform a χ^2 fit of the form

TABLE 40. Best fit values and uncertainties for the combined fit to data and LQCD results.

Parameter	Value
$\lvert V_{ub}\rvert$	$(3.75 \pm 0.20) \times 10^{-3}$
b_0^+	0.424 ± 0.021
b_1^+	-0.484 ± 0.043
b_2^+	-0.658 ± 0.168
b_0^0	0.561 ± 0.024
b_1^0	-1.393 ± 0.070

TABLE 41. Correlation matrix for the combined fit to data and LQCD.

Parameter	$\lvert V_{ub}\rvert$	b_0^+	b_1^+	b_2^+	b_0^0	b_1^0
$\lvert V_{ub}\rvert$	1.000	−0.913	0.164	0.308	−0.372	−0.017
b_0^+	−0.913	1.000	−0.345	−0.344	0.407	−0.035
b_1^+	0.164	−0.345	1.000	−0.597	−0.091	0.024
b_2^+	0.308	−0.344	−0.597	1.000	−0.199	0.113
b_0^0	−0.372	0.407	−0.091	−0.199	1.000	−0.817
b_1^0	−0.017	−0.035	0.024	0.113	−0.817	1.000

TABLE 42. Summary of exclusive determinations of $B^+ \to \rho^0 \ell^+ \nu$, rescaled to common inputs. The errors quoted correspond to statistical and systematic uncertainties, respectively.

	$\mathcal{B}[10^{-4}]$
CLEO (untagged) ρ^+ [346]	$1.49 \pm 0.22 \pm 0.28$
CLEO (untagged) ρ^+ [347]	$1.58 \pm 0.20 \pm 0.20$
Belle (hadronic tag) ρ^+ [336]	$1.73 \pm 0.15 \pm 0.13$
Belle (hadronic tag) ρ^0 [336]	$1.82 \pm 0.10 \pm 0.10$
Belle (semileptonic tag) ρ^+ [348]	$1.21 \pm 0.29 \pm 0.17$
Belle (semileptonic tag) ρ^0 [348]	$1.35 \pm 0.23 \pm 0.18$
BABAR (untagged) ρ^+ [337]	$1.05 \pm 0.11 \pm 0.21$
BABAR (untagged) ρ^0 [337]	$1.00 \pm 0.10 \pm 0.21$
Average	$\mathbf{1.58 \pm 0.11}$

TABLE 43. Summary of exclusive determinations of $B^+ \to \omega \ell^+ \nu$, rescaled to common inputs. The errors quoted correspond to statistical and systematic uncertainties, respectively.

	$\mathcal{B}[10^{-4}]$
Belle (untagged) [349]	$1.30 \pm 0.40 \pm 0.36$
BABAR (loose ν reco.) [338]	$1.19 \pm 0.16 \pm 0.09$
BABAR (untagged) [350]	$1.21 \pm 0.14 \pm 0.08$
Belle (hadronic tag) [336]	$1.07 \pm 0.16 \pm 0.07$
BABAR (semileptonic tag) [351]	$1.35 \pm 0.21 \pm 0.11$
Average	$\mathbf{1.19 \pm 0.10}$

$$\chi^2(\bar{\boldsymbol{x}}) = \sum_{m \in \{\text{Belle},BABAR\}} \Delta\vec{y}_m^T C_m^{-1} \Delta\vec{y}_m,$$
$$\Delta\vec{y}_m = \begin{pmatrix} \vdots \\ x_i^m - \sum_{j>N_{i-1}}^{N_i} \bar{x}_j \\ \vdots \end{pmatrix}, \tag{114}$$

where C_m is the covariance of the measurement and x_i^m is the measured differential rate in bin i multiplied by the corresponding bin width. Further, $\bar{\boldsymbol{x}}$ denotes the averaged spectrum and $(N_{i-1}, N_i]$ the range of averaged bins used to map to the ith measured bin. The binning of the averaged spectrum is chosen to match the most granular experimental binning.

For the average of the $B \to \omega \ell \bar{\nu}$ measurements from Belle and *BABAR*, we again chose the binning of the most granular spectrum, in this case *BABAR*'s. However the experimental spectra do not have a compatible binning in terms of matching bin boundaries. In order to incorporate the Belle data and create an averaged spectrum, the LCSR fit results [352] are used to create a model with which to split the second and fifth bin of the chosen binning, shown in black in Fig. 22. To match the average bin onto a measurement without matching bin edges, the average bin $\bar{x}_i$, $i = 2$ or 5, is split into two parts delimited by the lower bin edge, the q^2 value where the bin is split, and the upper bin edge. We label the two parts of the split bin as "left" and "right," respectively, in the following and define:

$$\bar{\boldsymbol{x}}_{i,\text{left}} = I_{i,\text{left}}/I_i(1 + \theta_i \varepsilon_{i,\text{left}}),$$
$$\bar{\boldsymbol{x}}_{i,\text{right}} = I_{i,\text{right}}/I_i(1 - \theta_i \varepsilon_{i,\text{right}}), \tag{115}$$

where $I_{i,\text{left}}$ ($I_{i,\text{right}}$) is the integral of the model function on the support of the left (right) part of the split bin, the sum $I_i = I_{i,\text{left}} + I_{i,\text{right}}$ is the integral over the entire bin, $\varepsilon_{i,\text{left}}$ ($\varepsilon_{i,\text{right}}$) the uncertainty of the integration given by the model uncertainty, and θ_i the nuisance parameter for the model dependence. We point out that the averaged spectrum does not depend on $|V_{ub}|$, as $|V_{ub}|$ cancels in the ratios $I_{i,\text{left}}/I_i$ ($I_{i,\text{right}}/I_i$).

The averaged spectra are shown in black in Fig. 22 and tabulated in Table 44.

4. Other exclusive charmless semileptonic B decays

We report the branching fraction averages for $B^+ \to \eta \ell^+ \nu$ and $B^+ \to \eta' \ell^+ \nu$. The measurements adjusted for common inputs, and their averages are listed in Tables 47 and 48, and presented in Fig. 23. For $B^+ \to \eta \ell^+ \nu$ decays, the agreement between the different measurements is good, while $B^+ \to \eta' \ell^+ \nu$ shows a significant discrepancy

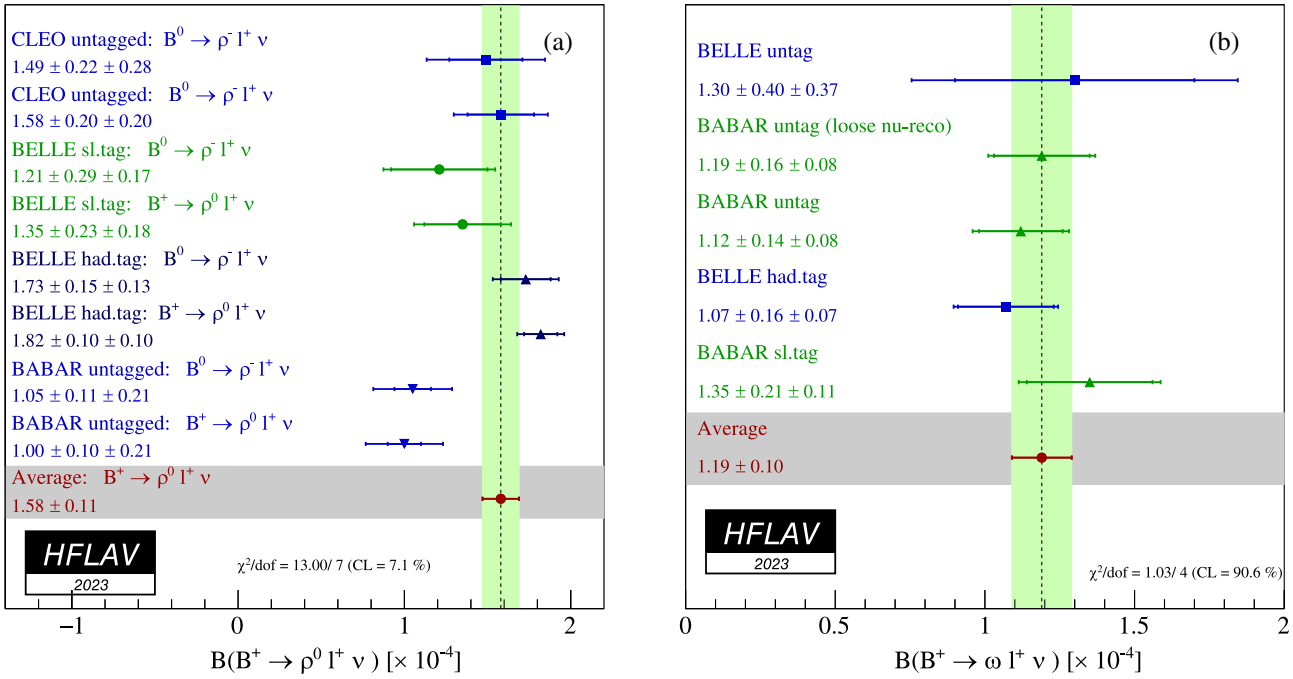


FIG. 21. (a) Summary of exclusive determinations of $\mathcal{B}(B^+ \to \rho^0 \ell^+ \nu)$ and their average. Measurements of $B^0 \to \rho^- \ell^+ \nu$ branching fractions have been scaled by $0.5\tau_{B^+}/\tau_{B^0}$ in accordance with isospin symmetry. (b) Summary of exclusive determinations of $B^+ \to \omega \ell^+ \nu$ and their average.

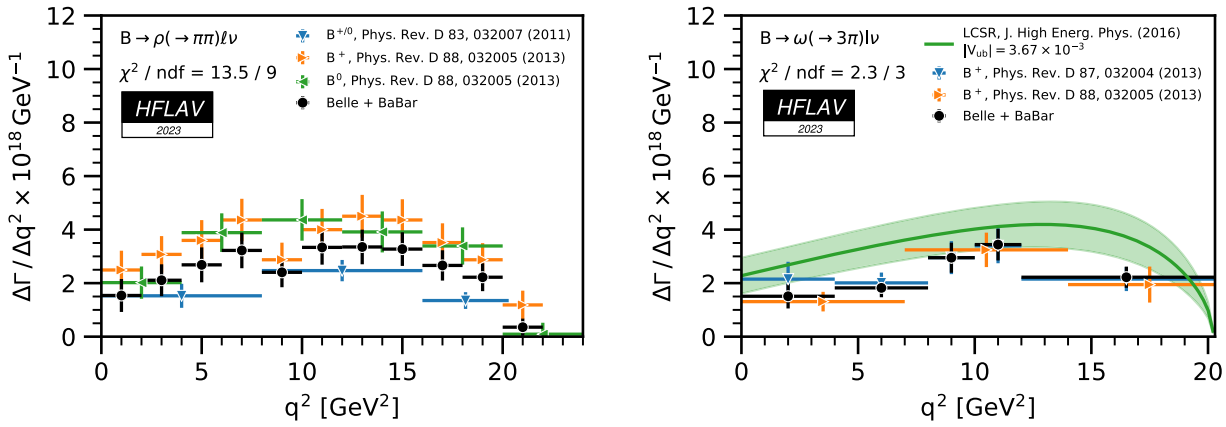


FIG. 22. The averaged q^2 spectrum of the measurements listed in the text for the ρ (left) and ω (right) final state on top of the latest Belle and *BABAR* measurements. The isospin transformation is applied to the $B^0 \to \rho^- \ell^+ \nu$ measurements. In the right figure we also show the model (green band) which was used to split the bins in the averaging procedure.

between the old CLEO measurement and the *BABAR* untagged analysis.

5. Direct measurements of $|V_{ub}|/|V_{cb}|$

The LHCb Collaboration published the direct measurement of the $|V_{ub}|/|V_{cb}|$ ratio using the $\Lambda_b \to p\mu^-\bar{\nu}_\mu$ and $\bar{B}_s^0 \to K^+\mu^-\bar{\nu}_\mu$ decays, properly normalized.

$\Lambda_b \to p\mu^-\bar{\nu}_\mu$ The first observation of the CKM-suppressed decay $\Lambda_b^0 \to p\mu^-\bar{\nu}_\mu$ has been obtained by LHCb and published in Ref. [333]. The measurement of the ratio of partial branching fractions at high q^2 for $\Lambda_b^0 \to p\mu^-\bar{\nu}_\mu$ and $\Lambda_b^0 \to \Lambda_c^+(\to pK\pi)\mu^-\bar{\nu}_\mu$ decays is

$$R = \frac{\mathcal{B}(\Lambda_b^0 \to p\mu^-\bar{\nu}_\mu)_{q^2>15\ \mathrm{GeV}^2}}{\mathcal{B}(\Lambda_b^0 \to \Lambda_c^+\mu^-\bar{\nu}_\mu)_{q^2>7\ \mathrm{GeV}^2}} = (1.00 \pm 0.04 \pm 0.08) \times 10^{-2}. \quad (116)$$

The ratio R is proportional to $(|V_{ub}|/|V_{cb}|)^2$ and sensitive to the form factors of $\Lambda_b^0 \to p$ and $\Lambda_b^0 \to \Lambda_c^+$

TABLE 44. Averaged spectra. For the corresponding correlation matrices see Tables 45 and 46.

$B \to \rho\ell\bar{\nu}$	
q^2 bin	$\Delta\Gamma/\Delta q^2 \times 10^{18}$ [GeV^{-1}]
[0, 2]	1.54 ± 0.62
[2, 4]	2.11 ± 0.60
[4, 6]	2.68 ± 0.65
[6, 8]	3.22 ± 0.67
[8, 10]	2.40 ± 0.56
[10, 12]	3.34 ± 0.65
[12, 14]	3.35 ± 0.65
[14, 16]	3.27 ± 0.63
[16, 18]	2.66 ± 0.57
[18, 20]	2.22 ± 0.52
[20, 22]	0.35 ± 0.32
$B \to \omega\ell\bar{\nu}$	
q^2 bin	$\Delta\Gamma/\Delta q^2 \times 10^{18}$ [GeV^{-1}]
[0, 4]	1.51 ± 0.46
[4, 8]	1.82 ± 0.35
[8, 10]	2.95 ± 0.56
[10, 12]	3.44 ± 0.59
[12, 21]	2.22 ± 0.40
Nuisance Parameters	
θ_2	-0.01 ± 1.00
θ_5	0.00 ± 1.00

transitions that have to be computed with non-perturbative methods, such as lattice QCD. The uncertainty on $\mathcal{B}(\Lambda_c^+ \to pK\pi)$ is the largest source of systematic uncertainties on R. Using the recent average of $\mathcal{B}(\Lambda_c^+ \to pK\pi) = (6.26 \pm 0.29)\%$ [302], the rescaled value for R is

$$R = (0.92 \pm 0.04 \pm 0.06) \times 10^{-2}. \tag{117}$$

Using the precise lattice QCD prediction [358] of the form factors in the experimentally interesting q^2 region considered, we obtain

$$\frac{|V_{ub}|}{|V_{cb}|} = 0.079 \pm 0.003_{\text{exp}} \pm 0.004_{\text{FF}} \tag{118}$$

where the first uncertainty is the total experimental uncertainty, and the second one is due to the knowledge of the form factors.

$\bar{B}_s^0 \to K^+\mu^-\bar{\nu}_\mu$ The LHCb experiment also reported the first observation of the decay $\bar{B}_s^0 \to K^+\mu^-\bar{\nu}_\mu$ and the measurements of its branching fraction normalized to the $\bar{B}_s^0 \to D_s^+\mu^-\bar{\nu}_\mu$ decays [334]. The measurement has been performed in two bins of q^2. The results of the partial branching fractions, adjusted for the recent average of $\mathcal{B}(D_s^+ \to K^+K^-\pi^-) = (5.37 \pm 0.10)\%$ [302], has been translated in measurements of $|V_{ub}|/|V_{cb}|$ using form factor calculation from LCSR for $q^2 < 7$ GeV^2 [359], and Lattice calculation for $q^2 > 7$ GeV^2 provided by FLAG [297], which is based on the calculations by HPQCD [360], FNAL/MILC [361] and RBC/UKQCD [362]. The results are

$$\frac{|V_{ub}|}{|V_{cb}|} = 0.0608 \pm 0.0020_{\text{exp}} \pm 0.0030_{\text{FF}}, \qquad q^2 < 7 \text{ GeV}^2, \tag{119}$$

$$\frac{|V_{ub}|}{|V_{cb}|} = 0.0860 \pm 0.0038_{\text{exp}} \pm 0.0037_{\text{FF}}, \qquad q^2 > 7 \text{ GeV}^2, \tag{120}$$

where the experimental uncertainties include also the uncertainties on the external inputs, and the last errors

TABLE 45. Correlation matrix of the averaged $B \to \rho\ell\nu_\ell$ spectrum.

	[0, 2]	[2, 4]	[4, 6]	[6, 8]	[8, 10]	[10, 12]	[12, 14]	[14, 16]	[16, 18]	[18, 20]	[20, 22]
[0, 2]	1.00	−0.30	0.03	0.01	0.09	0.09	0.09	0.09	0.08	0.08	0.02
[2, 4]	−0.30	1.00	−0.03	0.09	0.11	0.12	0.12	0.12	0.11	0.10	0.02
[4, 6]	0.03	−0.03	1.00	−0.18	0.13	0.13	0.15	0.14	0.13	0.12	0.03
[6, 8]	0.01	0.09	−0.18	1.00	0.06	0.18	0.18	0.18	0.16	0.14	0.04
[8, 10]	0.09	0.11	0.13	0.06	1.00	−0.21	0.05	0.04	0.12	0.10	0.03
[10, 12]	0.09	0.12	0.13	0.18	−0.21	1.00	−0.00	0.07	0.15	0.13	0.04
[12, 14]	0.09	0.12	0.15	0.18	0.05	−0.00	1.00	−0.16	0.14	0.12	0.04
[14, 16]	0.09	0.12	0.14	0.18	0.04	0.07	−0.16	1.00	0.10	0.14	0.05
[16, 18]	0.08	0.11	0.13	0.16	0.12	0.15	0.14	0.10	1.00	−0.27	−0.11
[18, 20]	0.08	0.10	0.12	0.14	0.10	0.13	0.12	0.14	−0.27	1.00	−0.13
[20, 22]	0.02	0.02	0.03	0.04	0.03	0.04	0.04	0.05	−0.11	−0.13	1.00

TABLE 46. Correlation matrix of the averaged $B \to \omega \ell \nu_\ell$ spectrum.

	[0, 4]	[4, 8]	[8, 10]	[10, 12]	[12, 21]	θ_2	θ_5
[0, 4]	1.00	−0.15	0.08	0.04	0.06	−0.01	0.00
[4, 8]	−0.15	1.00	0.09	0.09	0.15	−0.01	−0.00
[8, 10]	0.08	0.09	1.00	−0.01	0.12	−0.00	−0.00
[10, 12]	0.04	0.09	−0.01	1.00	0.15	0.00	−0.00
[12, 21]	0.06	0.15	0.12	0.15	1.00	−0.00	−0.00
θ_2	−0.01	−0.01	−0.00	0.00	−0.00	1.00	0.00
θ_5	0.00	−0.00	−0.00	−0.00	−0.00	0.00	1.00

TABLE 47. Summary of exclusive determinations of $B^+ \to \eta \ell^+ \nu$, rescaled to common inputs. The errors quoted correspond to statistical and systematic uncertainties, respectively.

	$\mathcal{B}[10^{-4}]$
CLEO [353]	$0.45 \pm 0.23 \pm 0.11$
BABAR (untagged) [354]	$0.31 \pm 0.06 \pm 0.08$
BABAR (semileptonic tag) [355]	$0.64 \pm 0.20 \pm 0.04$
BABAR (loose ν-reco.) [338]	$0.38 \pm 0.05 \pm 0.05$
Belle (hadronic tag) [356]	$0.42 \pm 0.11 \pm 0.09$
Belle (untagged) [357]	$0.283 \pm 0.055 \pm 0.034$
Average	$\mathbf{0.344 \pm 0.043}$

TABLE 48. Summary of exclusive determinations of $B^+ \to \eta' \ell^+ \nu$, rescaled to common inputs. The errors quoted correspond to statistical and systematic uncertainties, respectively.

	$\mathcal{B}[10^{-4}]$
CLEO [353]	$2.71 \pm 0.80 \pm 0.56$
BABAR (semileptonic tag) [355]	$0.04 \pm 0.22 \pm 0.04$, $(< 0.47 @ 90\%\text{CL})$
BABAR (untagged) [338]	$0.24 \pm 0.08 \pm 0.03$
Belle (hadronic tag) [356]	$0.36 \pm 0.27 \pm 0.04$
Belle (untagged) [357]	$0.279 \pm 0.129 \pm 0.030$
Average	$\mathbf{0.249 \pm 0.067}$

are due to the form factor calculations for both $B \to K$ and $B_s \to D_s$ decays. The discrepancy between the values of $|V_{ub}|/|V_{cb}|$ for the low and high q^2, requires further investigations. There are some recent efforts to combine LCSR and LQCD calculations, resulting in reduced discrepancies between low and high q^2, as shown in Ref. [363].

D. Inclusive CKM-suppressed decays

Measurements of $\bar{B} \to X_u \ell^- \bar{\nu}_\ell$ decays are very challenging because of background from the Cabibbo-favored $\bar{B} \to X_c \ell^- \bar{\nu}_\ell$ decays, whose branching fraction is about 50 times larger than that of the signal. Cuts designed to suppress this dominant background severely complicate the perturbative QCD calculations required to extract $|V_{ub}|$. Tight cuts necessitate parametrization of the so-called shape functions in order to describe the unmeasured regions of phase space. We use several theoretical calculations to extract $|V_{ub}|$ and do not advocate the use of one method over another. The authors of the different calculations have provided codes to compute the partial rates in limited regions of phase space covered by the measurements. Belle [364] and *BABAR* [365,366] produced measurements that explore large portions of phase space and thus reduce theoretical uncertainties.

In the averages reported in the following sections (VI D 1, VI D 2, VI D 3), the modeling of $\bar{B} \to X_c \ell^- \bar{\nu}_\ell$ and $\bar{B} \to X_u \ell^- \bar{\nu}_\ell$ decays and the theoretical uncertainties are taken as fully correlated among all measurements. Reconstruction-related uncertainties are taken as fully correlated within a given experiment. Measurements of partial branching fractions for $\bar{B} \to X_u \ell^- \bar{\nu}_\ell$ transitions from $\Upsilon(4S)$ decays, together with the corresponding selected region, are given in Table 49. We use all results published by *BABAR* in Ref. [365], since the statistical correlations are given. The dependence of the quoted error on the measured value for each source of uncertainty is taken into account in the calculation of the averages.

It was first suggested by Neubert [373] and later detailed by Leibovich, Low, and Rothstein (LLR) [374] and Lange, Neubert and Paz (LNP) [375], that the uncertainty of the leading shape functions can be eliminated by comparing inclusive rates for $\bar{B} \to X_u \ell^- \bar{\nu}_\ell$ decays with the inclusive photon spectrum in $\bar{B} \to X_s \gamma$, based on the assumption that the shape functions for transitions to light quarks, u or s, are the same to first order. However, shape function uncertainties are only eliminated at the leading order and they still enter via the signal models used for the determination of efficiency.

No new measurements were performed since the previous release of this work. The $|V_{ub}|$ values were recomputed from the measured partial branching fractions by recalculating the theoretical partial rates following an update of the heavy quark parameters.

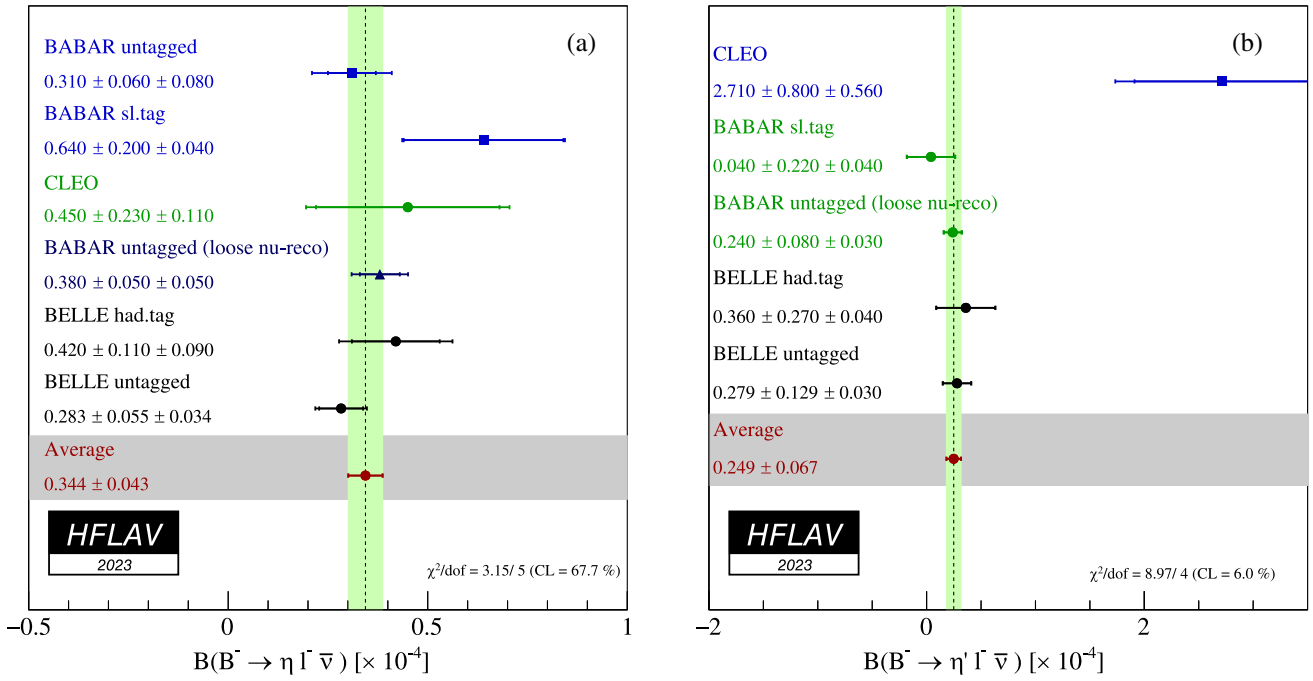


FIG. 23. (a) Summary of exclusive determinations of $\mathcal{B}(B^+ \to \eta \ell^+ \nu)$ and their average. (b) Summary of exclusive determinations of $\mathcal{B}(B^+ \to \eta' \ell^+ \nu)$ and their average.

Three theoretical calculations are used, detailed in the following. Other calculation exist [376,377], but they have not been utilized in this update.

1. BLNP

Bosch, Lange, Neubert and Paz (BLNP) [332,378–380] provide theoretical expressions for the triple differential decay rate for $\bar{B} \to X_u \ell^- \bar{\nu}_\ell$ events, incorporating all known contributions, while smoothly interpolating between the "shape-function region" of large hadronic energy and small invariant mass, and the "OPE region" in which all hadronic kinematical variables scale with the b-quark mass. BLNP assign uncertainties to the b-quark mass, which enters through the leading shape function, to sub-leading shape function forms, to possible weak annihilation contribution, and to matching scales. The BLNP calculation uses the shape function renormalization scheme; the heavy quark

TABLE 49. Summary of measurements of partial branching fractions for $\bar{B} \to X_u \ell^- \bar{\nu}_\ell$ decays. The errors quoted on $\Delta\mathcal{B}$ correspond to statistical and systematic uncertainties. E_e is the electron energy in the B rest frame, p^* the lepton momentum in the B frame and m_X is the invariant mass of the hadronic system. The light-cone momentum P_+ is defined in the B rest frame as $P_+ = E_X - |\vec{p}_X|$. The $s_h^{\max}$ variable is described in Refs. [367,368].

Measurement	Accepted region	$\Delta\mathcal{B}[10^{-4}]$	Notes
CLEO [369]	$E_e > 2.1$ GeV	$3.3 \pm 0.2 \pm 0.7$	
BABAR [368]	$E_e > 2.0$ GeV, $s_h^{\max} < 3.5$ GeV^2	$4.4 \pm 0.4 \pm 0.4$	
BABAR [366]	$E_e > 0.8$ GeV	$15.5 \pm 0.8 \pm 0.9$	Using the GGOU model
Belle [370]	$E_e > 1.9$ GeV	$8.5 \pm 0.4 \pm 1.5$	
BABAR [365]	$M_X < 1.7$ GeV/c^2, $q^2 > 8$ GeV^2/c^4	$6.9 \pm 0.6 \pm 0.4$	
Belle [371]	$M_X < 1.7$ GeV/c^2, $q^2 > 8$ GeV^2/c^4	$7.4 \pm 0.9 \pm 1.3$	
BABAR [365]	$P_+ < 0.66$ GeV	$9.9 \pm 0.9 \pm 0.8$	
BABAR [365]	$M_X < 1.7$ GeV/c^2	$11.6 \pm 1.0 \pm 0.8$	
BABAR [365]	$M_X < 1.55$ GeV/c^2	$10.9 \pm 0.8 \pm 0.6$	
Belle [372]	$p_\ell^* > 1$ GeV/c	$15.9 \pm 0.7 \pm 1.6$	
BABAR [365]	(M_X, q^2) fit, $p_\ell^* > 1$ GeV/c	$18.2 \pm 1.3 \pm 1.5$	
BABAR [365]	$p_\ell^* > 1.3$ GeV/c	$15.5 \pm 1.3 \pm 1.4$	

TABLE 50. Summary of input parameters used by the different theory calculations, corresponding inclusive determinations of $|V_{ub}|$ and their average. The errors quoted on $|V_{ub}|$ correspond to experimental and theoretical uncertainties, respectively.

	BLNP	DGE	GGOU
Input parameters			
scheme	SF	$\overline{\text{MS}}$	kinetic
Ref.	[381,382]	Ref. [383]	Ref. [61]
m_b (GeV)	4.600 ± 0.022	4.206 ± 0.040	4.573 ± 0.012
μ_π^2 (GeV^2)	$0.184^{+0.051}_{-0.062}$	⋯	0.454 ± 0.043
Ref.		$\lvert V_{ub}\rvert$ values $[10^{-3}]$	
CLEO E_e [369]	$4.10 \pm 0.48^{+0.26}_{-0.30}$	$3.77 \pm 0.44^{+0.20}_{-0.24}$	$3.94 \pm 0.46^{+0.17}_{-0.26}$
Belle M_X, q^2 [371]	$4.41 \pm 0.46^{+0.24}_{-0.26}$	$4.36 \pm 0.46^{+0.15}_{-0.17}$	$4.35 \pm 0.46^{+0.19}_{-0.23}$
Belle E_e [370]	$4.83 \pm 0.45^{+0.23}_{-0.25}$	$4.73 \pm 0.44^{+0.19}_{-0.20}$	$4.75 \pm 0.44^{+0.14}_{-0.19}$
BABAR E_e [366]	$4.38 \pm 0.12^{+0.25}_{-0.26}$	$3.79 \pm 0.10^{+0.08}_{-0.09}$	$3.90 \pm 0.09^{+0.18}_{-0.18}$
BABAR $E_e, s_{\text{h}}^{\text{max}}$ [368]	$4.57 \pm 0.31^{+0.29}_{-0.34}$	$4.05 \pm 0.20^{+0.22}_{-0.24}$	⋯
Belle E_ℓ^B, (M_X, q^2) fit [372]	$4.00 \pm 0.23^{+0.17}_{-0.19}$	$4.12 \pm 0.23^{+0.10}_{-0.11}$	$4.07 \pm 0.23^{+0.07}_{-0.09}$
BABAR M_X [365]	$4.12 \pm 0.19^{+0.22}_{-0.22}$	$4.34 \pm 0.20^{+0.17}_{-0.18}$	$4.07 \pm 0.19^{+0.17}_{-0.18}$
BABAR M_X [365]	$3.94 \pm 0.22^{+0.19}_{-0.20}$	$4.14 \pm 0.23^{+0.20}_{-0.21}$	$3.93 \pm 0.22^{+0.13}_{-0.13}$
BABAR M_X, q^2 [365]	$4.22 \pm 0.22^{+0.22}_{-0.25}$	$4.18 \pm 0.22^{+0.15}_{-0.17}$	$4.17 \pm 0.22^{+0.18}_{-0.22}$
BABAR P_+ [365]	$3.97 \pm 0.24^{+0.21}_{-0.22}$	$4.05 \pm 0.25^{+0.25}_{-0.30}$	$3.98 \pm 0.24^{+0.22}_{-0.22}$
BABAR p_ℓ^*, (M_X, q^2) fit [365]	$4.28 \pm 0.23^{+0.18}_{-0.20}$	$4.41 \pm 0.24^{+0.11}_{-0.12}$	$4.35 \pm 0.24^{+0.08}_{-0.09}$
BABAR p_ℓ^* [365]	$4.28 \pm 0.26^{+0.18}_{-0.20}$	$4.38 \pm 0.27^{+0.12}_{-0.12}$	$4.33 \pm 0.27^{+0.08}_{-0.10}$
Average	$4.25 \pm 0.13^{+0.19}_{-0.19}$	$3.87 \pm 0.10^{+0.09}_{-0.10}$	$4.06 \pm 0.12^{+0.11}_{-0.11}$

parameters determined in $b \to c$ transitions from the global fit in the kinetic scheme, published in Ref. [61], were therefore translated into the shape function scheme by using a prescription by Neubert [381,382]. The resulting parameters are $m_b(\text{SF}) = (4.600 \pm 0.012 \pm 0.018)$ GeV, $\mu_\pi^2(\text{SF}) = (0.184 \pm 0.047^{+0.020}_{-0.040})$ GeV/c^2, where the second uncertainty is due to the scheme translation. The extracted values of $|V_{ub}|$ for each measurement along with their average are given in Table 50 and illustrated in Fig. 24(a). The total uncertainty is ±5.3% and is due to: statistics (±1.5%), detector effects (±1.7%), $\bar{B} \to X_c \ell^- \bar{\nu}_\ell$ model ($^{+0.9}_{-1.0}$%), $\bar{B} \to X_u \ell^- \bar{\nu}_\ell$ model ($^{+1.6}_{-1.5}$%), heavy quark parameters (±2.4%), SF functional form ($^{+0.1}_{-0.3}$%), subleading shape functions (±0.8%), matching scales in BLNP μ, μ_i, μ_h (±3.6%), and weak annihilation ($^{+0.0}_{-1.0}$%). The error assigned to the matching scales is the source of the largest uncertainty, while the uncertainty due to HQE parameters (b-quark mass and $\mu_\pi^2(\text{SF})$) is second. The uncertainty due to weak annihilation is assumed to be asymmetric, i.e. it only tends to decrease $|V_{ub}|$.

2. DGE

Andersen and Gardi (dressed gluon exponentiation, DGE) [383] provide a framework where the on-shell b-quark calculation, converted into hadronic variables, is directly used as an approximation to the meson decay spectrum without the use of a leading-power non-perturbative function (or, in other words, a shape function). The DGE calculation uses the $\overline{\text{MS}}$ renormalization scheme. The heavy quark parameters determined in $b \to c$ transitions from the global fit in the kinetic scheme, published in Ref. [61], were therefore translated into the $\overline{\text{MS}}$ scheme by using code provided by Einan Gardi (based on Refs. [384,385]), giving $m_b(\overline{\text{MS}}) = (4.206 \pm 0.040)$ GeV. The extracted values of $|V_{ub}|$ for each measurement along with their average are given in Table 50 and illustrated in Fig. 24(b). The total error is ±3.3%, whose breakdown is: statistics (±1.5%), detector effects (±1.7%), $\bar{B} \to X_c \ell^- \bar{\nu}_\ell$ model (±0.7%), $\bar{B} \to X_u \ell^- \bar{\nu}_\ell$ model (±0.7%), strong coupling α_s (±0.3%), m_b (±2.1%), weak annihilation ($^{+0.0}_{-1.1}$%), matching scales in DGE ($^{+0.4}_{-0.5}$%). The largest

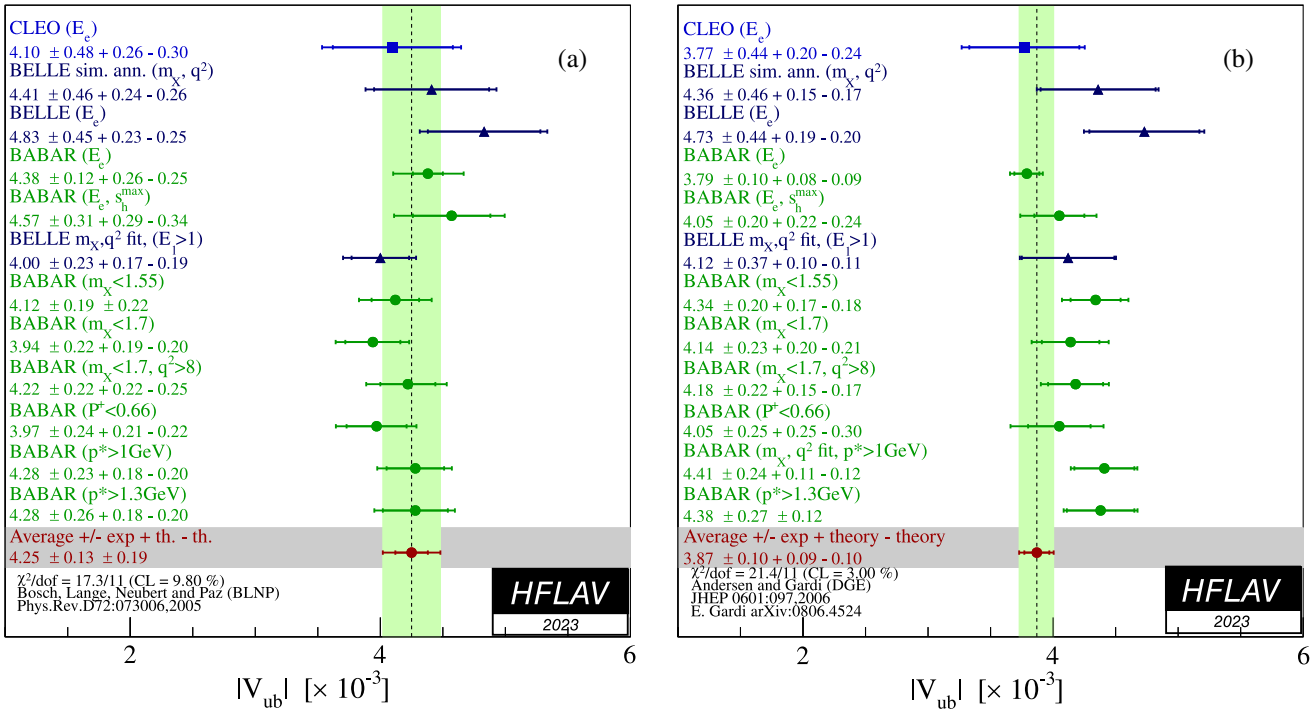


FIG. 24. Measurements of $|V_{ub}|$ from inclusive semileptonic decays and their average based on the BLNP (a) and DGE (b) prescription. The labels indicate the variables and selections used to define the signal regions in the different analyses.

contribution to the total error is due to the effect of the uncertainty on m_b. The uncertainty due to weak annihilation has been assumed to be asymmetric, i.e. it only tends to decrease $|V_{ub}|$.

3. GGOU

Gambino, Giordano, Ossola and Uraltsev (GGOU) [386] compute the triple differential decay rates of $\bar{B} \to X_u \ell^- \bar{\nu}_\ell$, including all perturbative and non-perturbative effects through $O(\alpha_s^2 \beta_0)$ and $O(1/m_b^3)$. The Fermi motion is parametrized in terms of a single light cone function for each structure function and for any value of q^2, accounting for all subleading effects. The calculations are performed in the kinetic scheme, a framework characterized by a Wilsonian treatment with a hard cutoff $\mu \sim 1$ GeV. GGOU have not included calculations for the "$(E_e, s_h^{\max})$" analysis [368]. The heavy quark parameters determined in $b \to c$ transitions from the global fit in the kinetic scheme of Ref. [61], are used as inputs: $m_b^{\rm kin} = (4.573 \pm 0.012)$ GeV, $\mu_\pi^2 = (0.454 \pm 0.043)$ GeV/c^2. The extracted values of $|V_{ub}|$ for each measurement along with their average are given in Table 50 and illustrated in Fig. 25. The total error is $\pm 3.9\%$ whose breakdown is: statistics ($\pm 1.4\%$), detector effects ($\pm 1.6\%$), $\bar{B} \to X_c \ell^- \bar{\nu}_\ell$ model ($\pm 0.9\%$), $\bar{B} \to X_u \ell^- \bar{\nu}_\ell$ model ($\pm 1.7\%$), α_s, m_b and other non-perturbative parameters ($\pm 1.6\%$), higher order

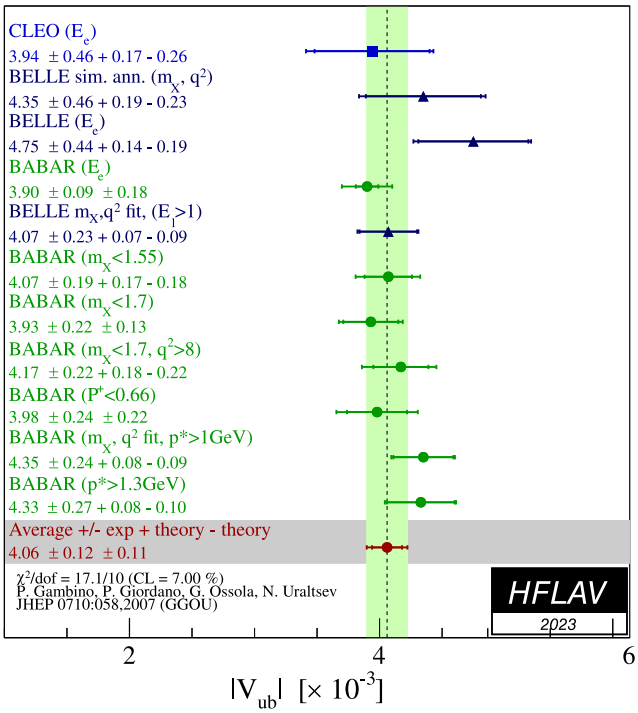


FIG. 25. Measurements of $|V_{ub}|$ from inclusive semileptonic decays and their average based on the GGOU prescription. The labels indicate the variables and selections used to define the signal regions in the different analyses.

TABLE 51. Summary of inclusive determinations of $|V_{ub}|$. The errors quoted on $|V_{ub}|$ correspond to experimental and theoretical uncertainties.

Framework	$\lvert V_{ub}\rvert[10^{-3}]$
BLNP	$4.25 \pm 0.13^{+0.19}_{-0.19}$
DGE	$3.87 \pm 0.10^{+0.09}_{-0.10}$
GGOU	$4.06 \pm 0.12^{+0.11}_{-0.11}$

perturbative and non-perturbative corrections ($\pm 1.5\%$), modeling of the q^2 tail ($\pm 1.3\%$), weak annihilations matrix element ($^{+0.0}_{-1.0}\%$), functional form of the distribution functions ($\pm 0.2\%$). The leading uncertainties on $|V_{ub}|$ are both from theory, and are due to perturbative and non-perturbative parameters and the modeling of the q^2 tail. The uncertainty due to weak annihilation has been assumed to be asymmetric, i.e. it only tends to decrease $|V_{ub}|$.

4. Summary

The averages presented in several different frameworks are presented in Table 51. In summary, we recognize that the experimental and theoretical uncertainties play out differently between the schemes and the theoretical assumptions for the theory calculations are different. Therefore, it is difficult to perform an average between the various determinations of $|V_{ub}|$. Since the methodology is similar to that used to determine the inclusive $|V_{cb}|$ average, we choose to quote as reference value the average determined by the GGOU calculation, which gives $|V_{ub}| = (4.06 \pm 0.12 \pm 0.11) \times 10^{-3}$.

E. Combined extraction of $|V_{ub}|$ and $|V_{cb}|$

In this section we report the result of a combined fit for $|V_{ub}|$ and $|V_{cb}|$ that includes the constraint from the averaged $|V_{ub}|/|V_{cb}|$, and the determination of $|V_{ub}|$ and $|V_{cb}|$ from exclusive B meson decays.

The average of the $|V_{ub}|/|V_{cb}|$ measurements from $\Lambda_b^0 \to p\mu^-\bar{\nu}_\ell$ and $\bar{B}_s^0 \to K\mu^-\bar{\nu}_\ell$, using only results at high q^2 (based on LQCD), assuming the uncertainties due to trigger selection and tracking efficiency are fully correlated, is

$$\frac{|V_{ub}|}{|V_{cb}|} = 0.0823 \pm 0.0035 \tag{121}$$

where the reported uncertainty includes both experimental and theoretical contributions. For the $\bar{B}_s^0 \to K\mu^-\bar{\nu}_\ell$ measurements, we use only the result in the high q^2 region where various calculations of the form factors from LQCD are already available. Currently, there is only a single calculation based on LCSR at low q^2 and others are underway. Once the discrepancy between the two q^2 regions is resolved, utilizing both regions will give the best estimation of $|V_{ub}|/|V_{cb}|$.

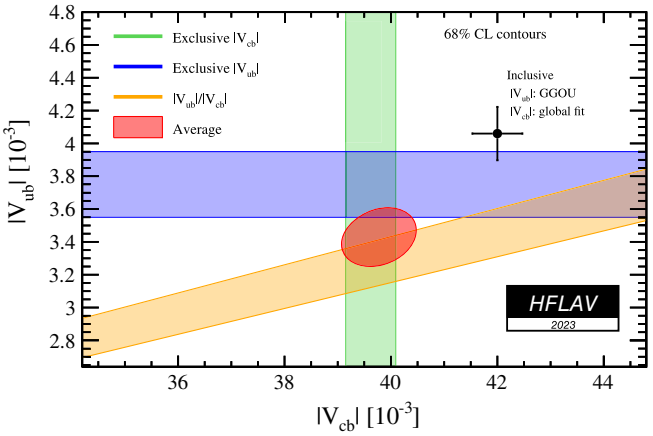


FIG. 26. Combined average on $|V_{ub}|$ and $|V_{cb}|$ including the LHCb measurements of $|V_{ub}|/|V_{cb}|$ from $\Lambda_b^0 \to p\mu^-\bar{\nu}_\mu$ and $\bar{B}_s^0 \to K\mu^-\bar{\nu}_\mu$ decays, the exclusive $|V_{ub}|$ measurement from $\bar{B} \to \pi\ell^-\bar{\nu}_\ell$, and the $|V_{cb}|$ average from $\bar{B} \to D\ell^-\bar{\nu}_\ell$, $\bar{B} \to D^*\ell^-\bar{\nu}_\ell$ and $\bar{B}_s^0 \to D_s^{(*)}\mu^-\bar{\nu}_\mu$ measurements. The point with the error bars corresponds to the inclusive $|V_{cb}|$ from from Ref. [61], and the inclusive $|V_{ub}|$ from GGOU calculation (Sec. VI D 3).

The average of the $|V_{cb}|$ results from $\bar{B} \to D\ell^-\bar{\nu}_\ell$, $\bar{B} \to D^*\ell^-\bar{\nu}_\ell$ and $\bar{B}_s^0 \to D_s^{(*)}\mu^-\bar{\nu}_\mu$, is

$$|V_{cb}| = (39.62 \pm 0.47) \times 10^{-3}, \tag{122}$$

where the uncertainty also in this case includes both experimental and theoretical contributions.

The combined fit for $|V_{ub}|$ and $|V_{cb}|$ results in

$$|V_{ub}| = (3.43 \pm 0.12) \times 10^{-3} \tag{123}$$

$$|V_{cb}| = (39.77 \pm 0.46) \times 10^{-3} \tag{124}$$

$$\rho(|V_{ub}|, |V_{cb}|) = 0.239, \tag{125}$$

where the uncertainties in the inputs are considered uncorrelated. The χ^2 of the fit is 3.9 for 1 dof, corresponding to a $P(\chi^2)$ of 4.8%. The fit result is shown in Fig. 26. The difference of $|V_{ub}|$ from the GGOU inclusive result, $(4.06 \pm 0.12^{+0.11}_{-0.11}) \times 10^{-3}$ (Table 50), taken as reference, is about 3σ. Also $|V_{cb}|$ differs from the result for inclusive $|V_{cb}|$ from the global fit reported in Ref. [61], $(41.97 \pm 0.48) \times 10^{-3}$, by more than 3σ.

F. $B \to D^{(*)}\tau\nu_\tau$ decays

In the SM, the semileptonic decays are tree level processes which proceed via the coupling to the $W^\pm$ boson. These couplings are assumed to be universal for all leptons and are well understood theoretically, (see Sec. V. A and V. B). This universality has been tested in purely

leptonic and semileptonic B meson decays involving a τ lepton, which might be sensitive to a hypothetical charged Higgs boson or other non-SM processes.

Compared to $B^- \to \tau^- \bar{\nu}_\tau$, the $B \to D^{(*)} \tau^- \bar{\nu}_\tau$ decay has advantages: the branching fraction is relatively high, because it is not Cabibbo-suppressed, and it is a three-body decay allowing access to many observables besides the branching fraction, such as $D^{(*)}$ momentum, q^2 distributions, and measurements of the D^* and τ polarizations.

Experiments have measured two ratios of branching fractions defined as

$$\mathcal{R}(D) = \frac{\mathcal{B}(\bar{B} \to D \tau^- \bar{\nu}_\tau)}{\mathcal{B}(\bar{B} \to D \ell^- \bar{\nu}_\ell)}, \tag{126}$$

$$\mathcal{R}(D^*) = \frac{\mathcal{B}(\bar{B} \to D^* \tau^- \bar{\nu}_\tau)}{\mathcal{B}(\bar{B} \to D^* \ell^- \bar{\nu}_\ell)} \tag{127}$$

where ℓ refers either to electron or μ. These ratios are independent of $|V_{cb}|$ and to a large extent, also of the $B \to D^{(*)}$ form factors. As a consequence, the SM predictions for these ratios are quite precise

(i) $\mathcal{R}(D) = 0.296 \pm 0.004$: where the central value and the uncertainty are obtained from an arithmetic average of the predictions from Refs. [297,387–391]. All these predictions are based on calculations of form factors for $B \to D \ell \nu$ at non-zero recoil from FNAL/MILC [294] and HPQCD [295]. The FLAG Collaboration, has averaged these two calculations and provides a result of $\mathcal{R}(D) = 0.2934 \pm 0.0053$ with only lattice inputs and $\mathcal{R}(D) = 0.2951 \pm 0.0031$ using also experimental inputs from B-factories [297]. The latter is used in the prediction reported above. Some calculations use inputs from LCSR calculation at low q^2, as in Refs. [388,391]. The prediction from Ref. [389] is based only on a reanalysis of the LQCD calculations.

(ii) $\mathcal{R}(D^*) = 0.254 \pm 0.005$: where the central value and the uncertainty are obtained from an arithmetic average of the predictions from Refs. [388,390–394]. These calculations are in good agreement with each other, and consistent with older predictions. They are based on Lattice QCD calculations at non-zero recoil recently available, LCSR calculations at low q^2 and experimental inputs from Belle [273]. Some predictions are the result of a combined fit of both $\mathcal{R}(D)$ and $\mathcal{R}(D^*)$, like Ref. [388,390,391]. The authors of Refs. [388,391], obtain predictions with and without using experimental inputs. In this average we use their results based on LQCD and LCSR only. The calculation in Ref. [392] is the result of the full angular analysis of $\bar{B} \to D^* \ell^- \bar{\nu}_\ell$ decay by *BABAR*, and gives an independent prediction of $\mathcal{R}(D^*) = 0.253 \pm 0.005$, which is compatible with the predictions above.

The list of calculations included in the average SM prediction, are summarized in Table 52.

The first unquenched LQCD calculation of the $\bar{B} \to D^* \ell^- \bar{\nu}_\ell$ form factors at non-zero recoil was obtained by FNAL/MILC Collaboration and it predicts a value of $\mathcal{R}(D^*) = 0.265 \pm 0.013$ [285]. More recently HPQCD and JLQCD collaborations released further calculations obtaining the predictions $\mathcal{R}(D^*) = 0.273 \pm 0.015$ [286] and $\mathcal{R}(D^*) = 0.252 \pm 0.022$ [287] respectively. These predictions, based only on LQCD, reduce the tensions with the experimental average, even if the larger uncertainty alleviates its significance. It is worth to mention that the results of joint fits between LQCD and experimental data are slightly in tension with these LQCD-only calculations. The result obtained by FNAL/MILC is $\mathcal{R}(D^*) = 0.2492 \pm 0.0012$ [285], while HPQCD obtained $\mathcal{R}(D^*) = 0.2482 \pm 0.0020$ [286]. Ongoing and future calculations of the form factors for $B \to D^*$ transitions, will provide higher precision.

On the experimental side, in the case of the leptonic τ decay, the ratios $\mathcal{R}(D^{(*)})$ can be directly measured, and many systematic uncertainties cancel in the measurement. The $\bar{B}^0 \to D^{*+} \tau^- \bar{\nu}_\tau$ decay was first observed by Belle [403] performing an "inclusive" reconstruction, which is based on the reconstruction of the $B_{\rm tag}$ from all the particles of the events, other than the $D^{(*)}$ and the lepton candidate, without looking for any specific $B_{\rm tag}$ decay chain. Since then, both *BABAR* and Belle have published improved measurements and have observed the $B^- \to D \tau^- \bar{\nu}_\tau$ decays [404,405].

The most powerful way to study these decays at the B-factories exploits the hadronic or semileptonic $B_{\rm tag}$. Using the full dataset and an improved hadronic $B_{\rm tag}$ selection, *BABAR* measured [406] $\mathcal{R}(D) = 0.440 \pm 0.058 \pm 0.042$ and $\mathcal{R}(D^*) = 0.332 \pm 0.024 \pm 0.018$, where decays to both $e^\pm$ and $\mu^\pm$ were summed, and results for B^0 and B^- decays were combined in an isospin-constrained fit. Since then other measurements have been performed. Here we report the list of measurements included in the average, where measurements from the same experiment are identified by unique superscript characters:

BABAR $R(D)$ and $R(D^*)$ with τ reconstructed in the $\tau^- \to \ell^- \bar{\nu}_\ell \nu_\tau$ mode ($\ell \in \{e, \mu\}$), and using the hadronic B-tagging approach, [406,407];

Belle[a] $R(D)$ and $R(D^*)$ with τ reconstructed in the $\tau^- \to \ell^- \bar{\nu}_\ell \nu_\tau$ mode ($\ell \in \{e, \mu\}$), and using the hadronic B-tagging approach, [408];

Belle[b] $R(D^*)$ and τ polarization with the τ reconstructed in hadronic $\tau^- \to \pi^- (\pi^0) \nu_\tau$ decay mode, and using the hadronic B-tagging, [409];

TABLE 52. Predictions for $\mathcal{R}(D^*)$ and $\mathcal{R}(D)$. Some calculations extract $\mathcal{R}(D^*)$ and $\mathcal{R}(D)$ from global fit, and provide also a correlations, but these are ignored here.

Input	$\mathcal{R}(D^*)$	$\mathcal{R}(D)$
D. Bigi, P. Gambino [387] *using:* FNAL/MILC [294], HPQCD [295], Belle [292]		0.299 ± 0.003
M. Bordone, M. Jung, D. van Dyk [388] *using:* FNAL/MILC, HPQCD [294,295,395], QCDSR [396–398], LCSR [399]	0.247 ± 0.006	0.298 ± 0.003
G. Martinelli, S. Simula, L. Vittorio [389] *using:* FNAL/MILC [294]		0.296 ± 0.008
F. Bernlochner, *et al.* [390] *using:* FNAL/MILC [294,400], HPQCD [295], Belle [273,401]	0.249 ± 0.003	0.288 ± 0.004
I. Ray, S. Nandi [391] *using:* FNAL/MILC [285,294], HPQCD [295], JLQCD [287]	0.258 ± 0.012	0.304 ± 0.003
FLAG Coll. [297] *using:* FNAL/MILC [294], HPQCD [295], Belle [292]		0.2951 ± 0.0031
BABAR Coll. [392]	0.253 ± 0.005	
P. Gambino, M. Jung, S. Schacht [393] *using:* Belle [273]	$0.254^{+0.007}_{-0.006}$	
G. Martinelli, S. Simula, L. Vittorio [402] *using:* FNAL/MILC [285], HPQCD [295], JLQCD [287]	0.262 ± 0.009	
Arithmetic average	$\mathbf{0.254 \pm 0.005}$	$\mathbf{0.296 \pm 0.004}$

Belle[c] $R(D)$ and $R(D^*)$ with $\tau^- \to \ell^- \bar{\nu}_\ell \nu_\tau$, using the semileptonic B-tagging [410] (this measurement supersedes [411], which measured only $R(D^*)$ using the same tagging approach);

LHCb[a] $R(D)$ and $R(D^*)$ with the τ^- reconstructed in $\tau^- \to \mu^- \bar{\nu}_\mu \nu_\tau$ mode [412] (this measurement supersedes [413], which measured only $R(D^*)$ using the same data and similar analysis approach).

LHCb[b] $R(D^*)$ with τ^- reconstructed in the hadronic $\tau^- \to 3\pi^-(\pi^0)\nu_\tau$ mode, obtained combining the result from Ref. [414] (based on Run 1 dataset) and the most recent from Ref. [415] (based on part of Run 2 dataset). These are direct measurements of the ratio $K(D^*) = \mathcal{B}(\bar{B}^0 \to D^* \tau^- \bar{\nu}_\tau)/\mathcal{B}(\bar{B}^0 \to D^* \pi^+ \pi^- \pi^+)$, which is translated into a measurement of $R(D^*)$ using the independently measured branching fractions of $\mathcal{B}(\bar{B}^0 \to D^* \pi^+ \pi^- \pi^+)$ and $\mathcal{B}(\bar{B}^0 \to D^* \mu^- \bar{\nu}_\mu)$.

LHCb[c] $R(D^+)$ and $R(D^{+*})$ with the τ^- reconstructed in $\tau^- \to \mu^- \bar{\nu}_\mu \nu_\tau$ mode [416].

Belle II $R(D^*)$ with $\tau^- \to \ell^- \bar{\nu}_\ell \nu_\tau$, using the hadronic B-tagging [417].

The most important source of systematic uncertainties that are correlated among the different measurement is the $\bar{B} \to D^{**}$ background components, which are difficult to disentangle from the signal. In our average, the systematic uncertainties due to the $\bar{B} \to D^{**}$ composition and kinematics are considered fully correlated among the measurements.

The results of the individual measurements, their averages and correlations are presented in Table 53 and Fig. 27. The combined results, projected separately on $\mathcal{R}(D)$ and $\mathcal{R}(D^*)$, are reported in Figs. 28(a) and 28(b) respectively.

The averaged $\mathcal{R}(D)$ and $\mathcal{R}(D^*)$ exceed the SM prediction given above, by 2.2σ and 1.9σ, respectively. Considering the $\mathcal{R}(D)$ and $\mathcal{R}(D^*)$ total correlation of -0.39, the difference with respect to the SM is about 3.14σ, and the combined $\chi^2 = 12.78$ for 2 degrees of freedom corresponds to a p-value of 1.68×10^{-3}, assuming Gaussian error distributions.

An analogous measurement using $B_c^- \to J/\psi \mu^- \bar{\nu}_\mu$ decays has been performed by LHCb, leading to $R(J\psi) = 0.71 \pm 0.17_{\text{stat}} \pm 0.18_{\text{syst}}$ [419], which lies 1.8σ above the

TABLE 53. Measurements of $\mathcal{R}(D^*)$ and $\mathcal{R}(D)$, their correlations and the combined average. The superscript character is used to distinguish the measurements taken from the same experiment.

Experiment	$\mathcal{R}(D^*)$	$\mathcal{R}(D)$	ρ
BABAR [406,407]	$0.332 \pm 0.024_{\text{stat}} \pm 0.018_{\text{syst}}$	$0.440 \pm 0.058_{\text{stat}} \pm 0.042_{\text{syst}}$	−0.27
Belle[a] [408]	$0.293 \pm 0.038_{\text{stat}} \pm 0.015_{\text{syst}}$	$0.375 \pm 0.064_{\text{stat}} \pm 0.026_{\text{syst}}$	−0.49
Belle[b] [409]	$0.270 \pm 0.035_{\text{stat}}\,{}^{+0.028}_{-0.025_{\text{syst}}}$		
Belle[c] [410]	$0.283 \pm 0.018_{\text{stat}} \pm 0.014_{\text{syst}}$	$0.307 \pm 0.037_{\text{stat}} \pm 0.016_{\text{syst}}$	−0.51
LHCb[a] [412]	$0.281 \pm 0.018_{\text{stat}} \pm 0.024_{\text{syst}}$	$0.441 \pm 0.060_{\text{stat}} \pm 0.066_{\text{syst}}$	−0.43
LHCb[b] [414,415,418]	$0.264 \pm 0.011_{\text{stat}} \pm 0.018_{\text{syst}}$		
LHCb[c] [416]	$0.402 \pm 0.081_{\text{stat}} \pm 0.085_{\text{syst}}$	$0.249 \pm 0.043_{\text{stat}} \pm 0.047_{\text{syst}}$	−0.39
Belle II [417]	$0.262^{+0.041}_{-0.039\,\text{stat}}\,{}^{+0.028}_{-0.025}\,\text{syst}$		
Average	$\mathbf{0.286 \pm 0.012}$	$\mathbf{0.342 \pm 0.026}$	−0.39

most recent SM prediction obtained by HPQCD collaboration [420]. Recently LHCb reported the first observation of the $\Lambda_b^0 \to \Lambda_c^+ \tau^- \bar{\nu}_\tau$ decay [421], exploiting the three-prong hadronic τ^- decays. The resulting ratio of semileptonic branching fractions is $\mathcal{R}(\Lambda_c) = 0.242 \pm 0.026_{\text{stat}} \pm 0.040_{\text{syst}} \pm 0.059_{\text{ext}}$, where the last term is due to the uncertainties on the external branching fractions measurement, in particular for the $\Lambda_b^0 \to \Lambda_c^+ \mu^- \bar{\nu}_\mu$ decay. This result is in agreement with the prediction of $\mathcal{R}(\Lambda_c) = 0.324 \pm 0.004$ from Ref. [422]. The first direct measurement of the ratio of inclusive semileptonic decays $\mathcal{R}(X_{\tau/\ell}) = \mathcal{B}(\bar{B} \to X\tau^-\bar{\nu}_\tau)/\mathcal{B}(\bar{B} \to X\ell^-\bar{\nu}_\ell)$ has been determined by Belle II [423]. The result, $\mathcal{R}(X_{\tau/\ell}) = 0.228 \pm 0.016_{\text{stat}} \pm 0.036_{\text{syst}}$, is compatible with SM predictions, [424,425].

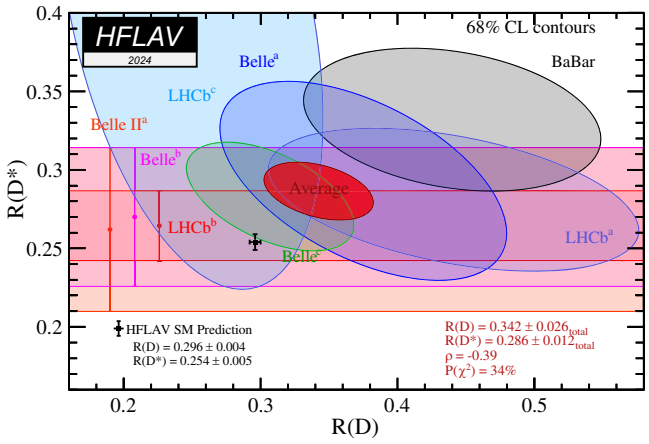


FIG. 27. Measurements of $\mathcal{R}(D)$ and $\mathcal{R}(D^*)$ listed in Table 53 and their two-dimensional average. The measurements from the same experiment are identified by the unique superscript characters as defined in the text and in Table. 53. Contours correspond to 68% CL (i.e. $\Delta\chi^2 = 2.3$). The black point with error bars, is the arithmetic average of the SM prediction for $\mathcal{R}(D^*)$ and $\mathcal{R}(D)$ reported in Table 52. More information is given in the text. An average of these predictions and the experimental average deviate from each other by about 3.14σ.

VII. DECAYS OF b-HADRONS INTO OPEN OR HIDDEN CHARM HADRONS

Ground-state B mesons and b baryons dominantly decay to particles containing a charm quark via the $b \to c$ quark transition. In this section, measurements of such decays to hadronic final states are summarized.

Since hadronic $b \to c$ decays dominate the b-hadron widths, they are an important part of the experimental program in heavy-flavor physics. Hadronic $b \to c$ decays are often used, in particular at hadron colliders, as normalization modes for measurements of rarer decays. At B-factories, hadronic $b \to c$ decays are used for the tagging of B mesons and a detailed knowledge is crucial for the optimization and calibration of the tagger performance. In addition, they are the dominant background in many analyses. To accurately model such backgrounds with simulated data, it is essential to have precise knowledge of the contributing decay modes. In particular, with the expected increase in the data samples at LHCb and Belle II, the enhanced statistical sensitivity has to be matched by low systematic uncertainties that arise from the limited understanding of the dominant b-hadron decay modes. For multibody decays, knowledge of the distribution of decays across the phase-space (e.g., the Dalitz plot density for three-body decays or the polarization amplitudes for vector-vector final states) is required in addition to the total branching fraction.

The large branching fractions of $b \to c$ decays make them ideal for studying the spectroscopy of both open and hidden charm hadrons. In particular, they have been used to both discover and measure the properties of exotic particles, such as the $X(3872)$ [426,427], $Z(4430)^+$ [428,429] and $P_c(4450)^+$ [430] states.

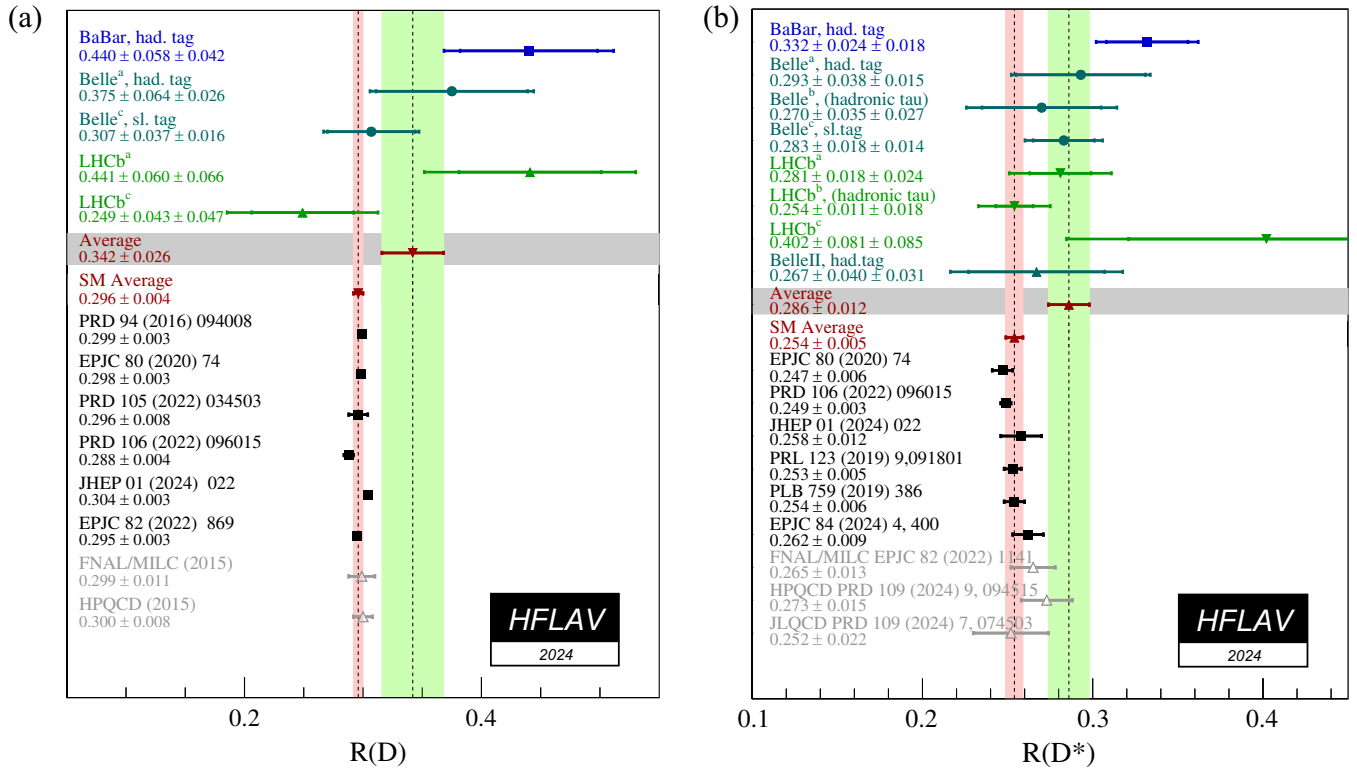


FIG. 28. (a) Measurements of $\mathcal{R}(D)$ and (b) $\mathcal{R}(D^*)$. The green (right) vertical bands are the averages obtained from the combined fit. The red (left) vertical bands are the averages of the theoretical predictions obtained as explained in the text. The theory predictions represented in gray, are based on LQCD only and are shown for comparison but not included in the SM averages.

In addition to the dominant $b \to c$ decays, there are several decays in this category that are expected to be highly suppressed in the Standard Model. These are of interest for probing particular decay amplitudes (e.g., the annihilation diagram, which dominates the $B^- \to D_s^- \phi$ decay) used to constrain effects in other hadronic decays, or in the search for new physics. There are also open charm production modes that are dominated by $b \to u$ transitions, such as $\bar{B}^0 \to D_s^- \pi^+$, which are mediated by the W emission involving the $|V_{ub}|$ CKM matrix element. Finally, $b \to c$ decays involving lepton flavor or number violation, such as $B^+ \to D^- \ell^+ \ell^+$, are extremely suppressed in the Standard Model, and therefore provide highly sensitive tests of new physics.

In this section, we give an exhaustive list of measured branching ratios of decay modes to hadrons containing charm quarks. The averaging procedure follows the methodology described in Sec. III. We perform fits of the likelihood function constructed from the quoted central values and uncertainties and do not adjust measurements as described in Sec. III A. For the cases where more than one measurement is available, in total 76 fits are performed, with on average (maximally) 4.3 (188) parameters and 7.2 (303) measurements per fit. Systematic uncertainties are taken as quoted without the scaling of multiplicative uncertainties discussed in Sec. III C. Where available, correlations between measurements are taken into account. We consider correlations not only between measurements of the same parameter, but also among parameters. The correlations among parameters are given on the HFLAV web page on hadronic B decays into open or hidden charm hadrons [431]. Limits are not included in the calculation of averages. In case only limits are available the most stringent one is quoted. If an insignificant measurement and a limit for the same parameter are provided in the same paper, the former is quoted, so that it can be included in averages. We also provide averages of the polarization amplitudes of B meson decays to vector-vector states. We do not currently provide detailed averages of quantities obtained from Dalitz plot analyses, due to the complications arising from the dependence on the model used.

The results are presented in subsections organized according to the type of decaying bottom hadron: B^0 (Sec. VII A), B^+ (Sec. VII B), B^0/B^+ admixture (Sec. VII C), B_s^0 (Sec. VII D), B_c^+ (Sec. VII E), b baryons (Sec. VII F). For each subsection, the parameters $\boldsymbol{p}$ are

arranged according to the final state into the following groups: a single charmed meson, two charmed mesons, a charmonium state, a charm baryon, or other states, e.g., $X(3872)$. In our tables, the individual measurements and average of each parameter p_j are shown in one row. We quote numerical values of all direct measurements of a parameter p_j. We also show numerical values derived from measurements of branching-fraction ratios p_j/p_k, performed with respect to the branching fraction p_k of a normalization mode, as well as measurements of products $p_j p_k$ of the branching fraction of interest with those of daughter-particle decays. In these cases, the quoted value and uncertainty of the measurement are determined with the fitted value of p_k, and the uncertainty of p_k is included in the systematic uncertainty. A footnote "using p_k" is added in these cases. Note that the fit uses p_j/p_k or $p_j p_k$ directly and not the p_j value that is quoted in the table. The p_j value is quoted to give a sense of the contribution of the measurement to the average. When the measurement depends on p_j in some other way, it is also included in our fit for p_j, but in the tables no derived value is shown. Instead, the measured function f of parameters is given in a footnote "measurement of f used in the fit." In general we prefer a directly measured function of parameters over a derived parameter if both are quoted because we do not apply corrections for updated input parameters.

In most of the tables of this section the averages are compared to those from the Particle Data Group's 2022 Review of Particle Physics (PDG 2022) [302] and 2023 update. When this is done, the "average" column quotes the PDG averages in italics only if they differ from ours. In general, such differences are due to different input parameters and measurements, differences in the averaging methods and different rounding conventions. The fit p-value is quoted if it is below 1%. Input values that are not included in the PDG average are either new results published after the closing of PDG and before the closing of this report, September 2023, or results that do not quote a direct measurement of the parameter of interest and are therefore not considered in the PDG average. Quoted upper limits are at 90% confidence level (CL), unless mentioned otherwise.

The symbol $\mathcal{B}$ is used for branching ratios, and f_X for the production fraction of hadron X or B meson with quark X (see Sec. IV C). The decay amplitudes for longitudinal, parallel, and perpendicular transverse polarization in pseudoscalar to vector-vector decays are denoted $\mathcal{A}_0$, $\mathcal{A}_\parallel$, and $\mathcal{A}_\perp$, respectively, and the definitions $\delta_\parallel = \arg(\mathcal{A}_\parallel/\mathcal{A}_0)$ and $\delta_\perp = \arg(\mathcal{A}_\perp/\mathcal{A}_0)$ are used for their relative phases. For normalized P-wave amplitudes we use the notation $f_i = |\mathcal{A}_i|^2/(|\mathcal{A}_0|^2 + |\mathcal{A}_\parallel|^2 + |\mathcal{A}_\perp|^2)$. The inclusion of charge conjugate modes is always implied.

Following the approach used by the PDG [9], for decays that involve neutral kaons we mainly quote results in terms of final states including either a K^0 or $\bar{K}^0$ meson (instead of a K^0_S or K^0_L), although the flavor of the neutral kaon is never determined experimentally. The specification as K^0 or $\bar{K}^0$ simply follows the quark model expectation for the dominant decay and the inclusion of the conjugate final state neutral kaon is implied. The exception is B^0_s decays to CP eigenstates, where the width difference between the mass eigenstates (see Sec. V) means that the measured branching fraction, integrated over decay time, is specific to the final state [432]. In such cases it is appropriate to quote the branching fraction for, e.g., $\bar{B}^0_s \to J/\psi K^0_S$ instead of $\bar{B}^0_s \to J/\psi \bar{K}^0$.

Most B-meson branching-fraction measurements assume $\Gamma(\Upsilon(4S) \to B^+B^-) = \Gamma(\Upsilon(4S) \to B^0\bar{B}^0)$. While there is no evidence for isospin violation in $\Upsilon(4S)$ decays, deviations from this assumption can be of the order of a few percent, see Sec. IV A. As the effect is negligible for many averages, we take the quoted values without applying a correction or additional systematic uncertainty. However, we note that this can be relevant for averages with percent-level uncertainty.

A. Decays of B^0 mesons

Measurements of B^0 decays to charmed hadrons are summarized in Secs. VII A 1–VII A 5.

1. Decays to a single open charm meson

Averages of B^0 decays to a single open charm meson are shown in Tables 54–62.

TABLE 54. Branching fractions for decays to a $D^{(*)}$ meson and one or more pions, I.

Parameter [10^{-3}]	Measurements		Average$^{\text{HFLAV}}_{PDG}$
$\mathcal{B}(B^0 \to D^-\pi^+)$	*BABAR* [433]	$2.55 \pm 0.05 \pm 0.16$	
	BABAR [434]	$3.03 \pm 0.23 \pm 0.23$	
	Belle [435][b]		2.48 ± 0.11
	CDF [436][a,c], [437][a,d], [438][a,e]		*2.51 ± 0.08*
	LHCb [439][f], [440][b], [441][g], [442][a,e]		
$\mathcal{B}(B^0 \to D^-\pi^+\pi^+\pi^-)$	LHCb [439][h]	$5.91 \pm 0.27 \pm 0.59$	
	CDF [437][a,i,j]		$5.78^{+0.62}_{-0.60}$
	LHCb [439][k], [443][l]		*5.98 ± 0.61*
$\mathcal{B}(B^0 \to D^*(2010)^-\pi^+)$	Belle [444][a]	$2.62 \pm 0.02 \pm 0.09$	
	Belle [445][a]	$2.22 \pm 0.04 \pm 0.19$	
	BABAR [433]	$2.79 \pm 0.08 \pm 0.17$	
	BABAR [434]	$2.99 \pm 0.23 \pm 0.24$	2.652 ± 0.064
	BABAR [446][a,m]		*2.738 ± 0.129*
	Belle [435][a,m]		
	LHCb [447][n]		
$\mathcal{B}(B^0 \to D^*(2010)^-\pi^+\pi^+\pi^-)$	LHCb [447][o]	$7.00 \pm 0.11 \pm 0.38$	
	BABAR [448]	$7.26 \pm 0.11 \pm 0.31$	7.11 ± 0.24
	Belle [449]	$6.81 \pm 0.23 \pm 0.72$	*7.21 ± 0.29*
	LHCb [447][p,q]		
$\mathcal{B}(B^0 \to \bar{D}^*(2007)^0\pi^+\pi^+\pi^-\pi^-)$	Belle [449]	$2.6 \pm 0.5 \pm 0.4$	2.60 ± 0.60
			2.72 ± 0.50
$\mathcal{B}(B^0 \to D^*(2010)^-\pi^+\pi^+\pi^+\pi^-\pi^-)$	Belle [449]	$4.72 \pm 0.59 \pm 0.71$	4.72 ± 0.92
$\mathcal{B}(B^0 \to D^*(2010)^-\omega(782)\pi^+)$	Belle [450]	$2.31 \pm 0.11 \pm 0.14$	2.41 ± 0.16
	BABAR [451]	$2.88 \pm 0.21 \pm 0.31$	*2.46 ± 0.18*

[a]Not included in PDG average.
[b]Measurement of $\mathcal{B}(B^0 \to D^-K^+)/\mathcal{B}(B^0 \to D^-\pi^+)$ used in our fit.
[c]Measurement of $\mathcal{B}(B^+ \to \bar{D}^0\pi^+)/\mathcal{B}(B^0 \to D^-\pi^+)$ used in our fit.
[d]Measurement of $\mathcal{B}(B_s^0 \to D_s^-\pi^+)/\mathcal{B}(B^0 \to D^-\pi^+)$ used in our fit.
[e]Measurement of $\mathcal{B}(\Lambda_b^0 \to \Lambda_c^+\pi^-)/\mathcal{B}(B^0 \to D^-\pi^+)$ used in our fit.
[f]Measurement of $\mathcal{B}(B^0 \to D^-\pi^+\pi^+\pi^-)/\mathcal{B}(B^0 \to D^-\pi^+)$ used in our fit.
[g]Measurement of $\mathcal{B}(B^0 \to D_s^-K^+)/\mathcal{B}(B^0 \to D^-\pi^+)$ used in our fit.
[h]Using $\mathcal{B}(B^0 \to D^-\pi^+)$.
[i]Using $f_s/f_d = 0.259 \pm 0.038$ from PDG 2006.
[j]Measurement of $\mathcal{B}(B_s^0 \to D_s^-\pi^+\pi^+\pi^-)/\mathcal{B}(B^0 \to D^-\pi^+\pi^+\pi^-)$ used in our fit.
[k]Measurement of $\mathcal{B}(B^0 \to D_1(2420)^-\pi^+) \times \mathcal{B}(D_1(2420)^+ \to D^+\pi^+\pi^-)/\mathcal{B}(B^0 \to D^-\pi^+\pi^+\pi^-)$ used in our fit.
[l]Measurement of $\mathcal{B}(B^0 \to D^-K^+\pi^+\pi^-)/\mathcal{B}(B^0 \to D^-\pi^+\pi^+\pi^-)$ used in our fit.
[m]Measurement of $\mathcal{B}(B^0 \to D^*(2010)^-K^+)/\mathcal{B}(B^0 \to D^*(2010)^-\pi^+)$ used in our fit.
[n]Measurement of $\mathcal{B}(B^0 \to D^*(2010)^-\pi^+\pi^+\pi^-)/\mathcal{B}(B^0 \to D^*(2010)^-\pi^+)$ used in our fit.
[o]Using $\mathcal{B}(B^0 \to D^*(2010)^-\pi^+)$.
[p]Measurement of $\mathcal{B}(B^0 \to D^*(2010)^-K^+\pi^+\pi^-)/\mathcal{B}(B^0 \to D^*(2010)^-\pi^+\pi^+\pi^-)$ used in our fit.
[q]Measurement of $\mathcal{B}(B^0 \to \bar{D}_1(2420)^0\pi^+\pi^-) \times \mathcal{B}(D_1(2420)^0 \to D^*(2010)^+\pi^-)/\mathcal{B}(B^0 \to D^*(2010)^-\pi^+\pi^+\pi^-)$ used in our fit.

TABLE 55. Branching fractions for decays to a $D^{(*)}$ meson and one or more pions, II.

Parameter [10^{-4}]	Measurements		Average$^{\text{HFLAV}}_{PDG}$
$\mathcal{B}(B^0 \to \bar{D}^0\pi^0)$	*BABAR* [452]	$2.69 \pm 0.09 \pm 0.13$	2.62 ± 0.15
	Belle [453]	$2.25 \pm 0.14 \pm 0.35$	*2.67 ± 0.09*
$\mathcal{B}(B^0 \to \bar{D}^*(2007)^0\pi^0)$	*BABAR* [452]	$3.05 \pm 0.14 \pm 0.28$	2.23 ± 0.22 p = 0.02%
	Belle [453]	$1.39 \pm 0.18 \pm 0.26$	*2.23 ± 0.57*
$\mathcal{B}(B^0 \to \bar{D}^0\pi^+\pi^-)$	LHCb [454][b]	$8.46 \pm 0.14 \pm 0.49$	
	Belle [445]	$8.4 \pm 0.4 \pm 0.8$	8.50 ± 0.40
	LHCb [455][c,d], [456][e]		*8.80 ± 0.46*
$\mathcal{B}(B^0 \to \bar{D}^*(2007)^0\pi^+\pi^-)$	Belle [457]	$6.2 \pm 1.2 \pm 1.8$	6.2 ± 2.1
	LHCb [458][a,f], [458][a,g]		*6.2 ± 2.2*

[a]Not included in PDG average.
[b]In phase space region $M(\bar{D}^0\pi^+) > 2.1$ GeV/c^2.
[c]Measurement of $\mathcal{B}(B_s^0 \to \bar{D}^0K^-\pi^+)/\mathcal{B}(B^0 \to \bar{D}^0\pi^+\pi^-)$ used in our fit.
[d]Measurement of $\mathcal{B}(B^0 \to \bar{D}^0K^+\pi^-)/\mathcal{B}(B^0 \to \bar{D}^0\pi^+\pi^-)$ used in our fit.
[e]Measurement of $\mathcal{B}(B^0 \to \bar{D}^0K^+K^-)/\mathcal{B}(B^0 \to \bar{D}^0\pi^+\pi^-)$ used in our fit.
[f]Measurement of $\mathcal{B}(B^0 \to \bar{D}^*(2007)^0K^+\pi^-)/\mathcal{B}(B^0 \to \bar{D}^*(2007)^0\pi^+\pi^-)$ used in our fit.
[g]Measurement of $\mathcal{B}(B_s^0 \to \bar{D}^*(2007)^0K^-\pi^+)/\mathcal{B}(B^0 \to \bar{D}^*(2007)^0\pi^+\pi^-)$ used in our fit.

TABLE 56. Branching fractions for decays to a $D^{(*)0}$ meson and a light meson.

Parameter [10^{-4}]	Measurements		Average$^{\text{HFLAV}}_{PDG}$
$\mathcal{B}(B^0 \to \bar{D}^0\rho^0(770))$	Belle [445]	$3.19 \pm 0.20 \pm 0.45$	$3.04^{+0.47}_{-0.46}$
	Belle [457][b]	$4.1 \pm 2.0 \pm 0.2$	
	LHCb [459][a,c]		*3.21 ± 0.21*
$\mathcal{B}(B^0 \to \bar{D}^*(2007)^0\rho^0(770))$	Belle [457]	< 5.1	< 5.1
$\mathcal{B}(B^0 \to \bar{D}^0\eta)$	Belle [460][a]	$2.66 \pm 0.05 \pm 0.02$	2.644 ± 0.050
	BABAR [452]	$2.53 \pm 0.09 \pm 0.11$	*2.359 ± 0.317*
$\mathcal{B}(B^0 \to \bar{D}^*(2007)^0\eta)$	*BABAR* [452]	$2.69 \pm 0.14 \pm 0.23$	2.26 ± 0.22
	Belle [453]	$1.4 \pm 0.3 \pm 0.3$	p = 0.58%
			2.26 ± 0.61
$\mathcal{B}(B^0 \to \bar{D}^0\eta')$	*BABAR* [452]	$1.48 \pm 0.13 \pm 0.07$	1.38 ± 0.12
	Belle [461]	$1.14 \pm 0.20^{+0.10}_{-0.13}$	*1.38 ± 0.16*
$\mathcal{B}(B^0 \to \bar{D}^*(2007)^0\eta')$	*BABAR* [452]	$1.48 \pm 0.22 \pm 0.13$	1.40 ± 0.22
	Belle [461]	$1.21 \pm 0.34 \pm 0.22$	
$\mathcal{B}(B^0 \to \bar{D}^0\omega(782))$	*BABAR* [452]	$2.57 \pm 0.11 \pm 0.14$	2.53 ± 0.16
	Belle [453]	$2.37 \pm 0.23 \pm 0.28$	
	LHCb [454]	$2.81 \pm 0.72 \pm 0.30$	*2.54 ± 0.16*
	Belle [457][a,d]		
$\mathcal{B}(B^0 \to \bar{D}^*(2007)^0\omega(782))$	*BABAR* [452]	$4.55 \pm 0.24 \pm 0.39$	3.64 ± 0.35
	Belle [453]	$2.29 \pm 0.39 \pm 0.40$	p = 0.18%
			3.64 ± 1.11
$\mathcal{B}(B^0 \to \bar{D}^0f_2(1270))$	LHCb [454]	$1.61 \pm 0.11 \pm 0.19$	1.52 ± 0.19
	Belle [445]	$1.2 \pm 0.2 \pm 0.4$	*1.56 ± 0.21*

[a]Not included in PDG average.
[b]Using $\mathcal{B}(B^0 \to \bar{D}^0\omega(782))$.
[c]Measurement of $\mathcal{B}(B_s^0 \to \bar{D}^0\bar{K}^*(892)^0)/\mathcal{B}(B^0 \to \bar{D}^0\rho^0(770))$ used in our fit.
[d]Measurement of $\mathcal{B}(B^0 \to \bar{D}^0\rho^0(770))/\mathcal{B}(B^0 \to \bar{D}^0\omega(782))$ used in our fit.

TABLE 57. Branching fractions for decays to a $D^{(*)+}$ meson and one or more kaons.

Parameter [10^{-4}]	Measurements		Average$^{\text{HFLAV}}_{PDG}$
$\mathcal{B}(B^0 \to D^- K^+)$	LHCb [440][c]	$2.040 \pm 0.027 \pm 0.112$	2.03 ± 0.12
	Belle [435][c]	$1.69 \pm 0.37 \pm 0.19$	*2.05 ± 0.08*
$\mathcal{B}(B^0 \to D^*(2010)^- K^+)$	Belle [444][a]	$2.22 \pm 0.06 \pm 0.08$	2.146 ± 0.079
	BABAR [446][d]	$2.058 \pm 0.090 \pm 0.091$	
	Belle [435][d]	$1.96 \pm 0.40 \pm 0.17$	*$2.117^{+0.155}_{-0.154}$*
$\mathcal{B}(B^0 \to D^- K^*(892)^+)$	*BABAR* [462]	$4.6 \pm 0.6 \pm 0.5$	4.60 ± 0.78
			4.46 ± 0.72
$\mathcal{B}(B^0 \to D^*(2010)^- K^*(892)^+)$	*BABAR* [462]	$3.2 \pm 0.6 \pm 0.3$	3.20 ± 0.67
			3.30 ± 0.61
$\mathcal{B}(B^0 \to D^- K^0 \pi^+)$	*BABAR* [462]	$4.9 \pm 0.7 \pm 0.5$	4.90 ± 0.86
$\mathcal{B}(B^0 \to D^*(2010)^- K^0 \pi^+)$	*BABAR* [462]	$3.0 \pm 0.7 \pm 0.3$	3.00 ± 0.76
$\mathcal{B}(B^0 \to D^- K^+ \bar{K}^0)$	Belle II [463][b]	$0.82 \pm 0.12 \pm 0.05$	0.82 ± 0.13
	Belle [464]	< 3.1	*< 3.10*
$\mathcal{B}(B^0 \to D^*(2010)^- K^+ \bar{K}^0)$	Belle II [463][b]	$0.91 \pm 0.19 \pm 0.05$	0.91 ± 0.20
	Belle [464]	< 4.7	*< 4.70*
$\mathcal{B}(B^0 \to D^- \bar{K}^*(892)^0 K^+)$	Belle [464][a]	$8.8 \pm 1.1 \pm 1.5$	8.8 ± 1.9
			None
$\mathcal{B}(B^0 \to D^*(2010)^- \bar{K}^*(892)^0 K^+)$	Belle [464][a]	$12.9 \pm 2.2 \pm 2.5$	12.9 ± 3.3
			None
$\mathcal{B}(B^0 \to D^- K^+ \pi^+ \pi^-)$	LHCb [443][e]	$3.41 \pm 0.64^{+0.47}_{-0.46}$	$3.41^{+0.82}_{-0.76}$
			3.53 ± 0.81
$\mathcal{B}(B^0 \to D^*(2010)^- K^+ \pi^+ \pi^-)$	LHCb [447][f]	$4.600 \pm 0.263 \pm 0.294$	4.60 ± 0.39
			4.66 ± 0.41

[a]Not included in PDG average.
[b]Preliminary result.
[c]Using $\mathcal{B}(B^0 \to D^- \pi^+)$.
[d]Using $\mathcal{B}(B^0 \to D^*(2010)^- \pi^+)$.
[e]Using $\mathcal{B}(B^0 \to D^- \pi^+ \pi^+ \pi^-)$.
[f]Using $\mathcal{B}(B^0 \to D^*(2010)^- \pi^+ \pi^+ \pi^-)$.

TABLE 58. Branching fractions for decays to a $D^{(*)0}$ meson and one or more kaons or a ϕ.

Parameter [10^{-5}]	Measurements		Average$^{\text{HFLAV}}_{PDG}$
$\mathcal{B}(B^0 \to \bar{D}^0 K^0)$	*BABAR* [465]	$5.3 \pm 0.7 \pm 0.3$	5.33 ± 0.73
	Belle [460][a]	$5.6 \pm 1.2 \pm 2.1$	$5.23^{+0.67}_{-0.66}$
$\mathcal{B}(B^0 \to \bar{D}^*(2007)^0 K^0)$	*BABAR* [465]	$3.6 \pm 1.2 \pm 0.3$	3.6 ± 1.2
	Belle [466]	< 6.6	
$\mathcal{B}(B^0 \to \bar{D}^0 K^+ \pi^-)$	LHCb [455][c]	$9.01 \pm 0.59 \pm 0.80$	$8.96^{+0.88}_{-0.86}$
	BABAR [446][d]	$8.8 \pm 1.5 \pm 0.9$	8.80 ± 1.75
$\mathcal{B}(B^0 \to \bar{D}^0 K^*(892)^0)$	*BABAR* [446][a,e]	$3.8 \pm 0.6 \pm 0.4$	$4.19^{+0.43}_{-0.42}$
	BABAR [465][a]	$4.0 \pm 0.7 \pm 0.3$	
	Belle [466][a]	$4.8^{+1.1}_{-1.0} \pm 0.5$	*None*
	LHCb [467][a,f]		
$\mathcal{B}(B^0 \to \bar{D}^*(2007)^0 K^*(892)^0)$	Belle [466]	< 6.9	< 6.9
$\mathcal{B}(B^0 \to D^*(2007)^0 K^*(892)^0)$	Belle [466]	< 4.0	< 4.0
$\mathcal{B}(B^0 \to D^0 K^+ \pi^-)$	*BABAR* [446]	< 1.9	< 1.9
			0.5 ± 0.3
$\mathcal{B}(B^0 \to D^0 K^*(892)^0)$	Belle [466][a]	< 1.8	0.00 ± 0.58
	BABAR [465][a]	$0.0 \pm 0.5 \pm 0.3$	*None*
$\mathcal{B}(B^0 \to \bar{D}^0 K^+ K^-)$	LHCb [456][c]	$5.86 \pm 0.34^{+0.38}_{-0.37}$	5.94 ± 0.39
	LHCb [456]	$6.1 \pm 0.4 \pm 0.4$	6.07 ± 0.54
	LHCb [456][g], [468][a,h,i]		
$\mathcal{B}(B^0 \to \bar{D}^0 \phi(1020))$	LHCb [468][a,h]		0.077 ± 0.022
			< 0.230
$\mathcal{B}(B^0 \to \bar{D}^*(2007)^0 K^+ \pi^-)$	LHCb [458][a,j]	$5.183 \pm 0.267 \pm 1.830$	5.2 ± 1.8
			5.2 ± 1.9
$\mathcal{B}(B^0 \to \bar{D}^*(2007)^0 \phi(1020))$	LHCb [468][a,i]		0.217 ± 0.055
			None
$\mathcal{B}(B^0 \to D^- K^+ \bar{K}^*(892)^0)$	Belle II [463][b]	$75.6 \pm 4.5 \pm 3.8$	75.6 ± 5.9
			88.0 ± 18.6
$\mathcal{B}(B^0 \to D^*(2010)^- K^+ \bar{K}^*(892)^0)$	Belle II [463][b]	$131.2 \pm 12.1 \pm 7.1$	131 ± 14
			129 ± 33

[a]Not included in PDG average.
[b]Preliminary result.
[c]Using $\mathcal{B}(B^0 \to \bar{D}^0 \pi^+ \pi^-)$.
[d]Excluding $D^*(2010)^+ K^-$.
[e]Using $\mathcal{B}(K^*(892)^0 \to K^+ \pi^-)$.
[f]Measurement of $\mathcal{B}(B_s^0 \to \bar{D}^0 \bar{K}^*(892)^0)/\mathcal{B}(B^0 \to \bar{D}^0 K^*(892)^0)$ used in our fit.
[g]Measurement of $\mathcal{B}(B_s^0 \to \bar{D}^0 K^+ K^-)/\mathcal{B}(B^0 \to \bar{D}^0 K^+ K^-)$ used in our fit.
[h]Measurement of $\mathcal{B}(B^0 \to \bar{D}^0 \phi(1020))\mathcal{B}(\phi(1020) \to K^+ K^-)/\mathcal{B}(B^0 \to \bar{D}^0 K^+ K^-)$ used in our fit.
[i]Measurement of $\mathcal{B}(B^0 \to \bar{D}^*(2007)^0 \phi(1020))\mathcal{B}(\phi(1020) \to K^+ K^-)/\mathcal{B}(B^0 \to \bar{D}^0 K^+ K^-)$ used in our fit.
[j]Using $\mathcal{B}(B^0 \to \bar{D}^*(2007)^0 \pi^+ \pi^-)$.

TABLE 59. Branching fractions for decays to a $D_s^{(*)}$ meson.

Parameter [10^{-4}]	Measurements		Average$^{\text{HFLAV}}_{PDG}$
$\mathcal{B}(B^0 \to D_s^+ \pi^-)$	Belle [469]	$0.199 \pm 0.026 \pm 0.018$	0.216 ± 0.026
	BABAR [470]	$0.25 \pm 0.04 \pm 0.02$	*0.203 ± 0.018*
$\mathcal{B}(B^0 \to D_s^{*+} \pi^-)$	Belle [471]	$0.175 \pm 0.034 \pm 0.020$	0.212 ± 0.030
	BABAR [470]	$0.26^{+0.05}_{-0.04} \pm 0.02$	*$0.212^{+0.045}_{-0.042}$*
$\mathcal{B}(B^0 \to D_s^+ \rho^-(770))$	*BABAR* [470]	$0.11^{+0.09}_{-0.08} \pm 0.03$	$0.110^{+0.095}_{-0.085}$
			< 0.240
$\mathcal{B}(B^0 \to D_s^{*+} \rho^-(770))$	*BABAR* [470]	$0.41^{+0.13}_{-0.12} \pm 0.04$	0.41 ± 0.13
			$0.41^{+0.14}_{-0.13}$
$\mathcal{B}(B^0 \to D_s^+ a_0(980)^-)$	*BABAR* [472][a]	$0.06^{+0.14}_{-0.11} \pm 0.01$	$0.06^{+0.14}_{-0.11}$
			< 0.19
$\mathcal{B}(B^0 \to D_s^{*+} a_0(980)^-)$	*BABAR* [472][a]	$0.14^{+0.21}_{-0.16} \pm 0.03$	$0.14^{+0.21}_{-0.16}$
			< 0.36
$\mathcal{B}(B^0 \to D_s^+ a_2(1320)^-)$	*BABAR* [472][a]	$0.64^{+1.04}_{-0.57} \pm 0.15$	$0.6^{+1.0}_{-0.6}$
			< 1.9
$\mathcal{B}(B^0 \to D_s^{*+} a_2(1320)^-)$	*BABAR* [472]	< 2.00	< 2.0
$\mathcal{B}(B^0 \to D_s^- K^+)$	LHCb [441][b]	$0.320 \pm 0.012 \pm 0.025$	0.273 ± 0.018
	Belle [469]	$0.191 \pm 0.024 \pm 0.017$	*0.274 ± 0.047*
	BABAR [470]	$0.29 \pm 0.04 \pm 0.02$	
$\mathcal{B}(B^0 \to D_s^{*-} K^+)$	Belle [471]	$0.202 \pm 0.033 \pm 0.022$	0.219 ± 0.030
	BABAR [470]	$0.24 \pm 0.04 \pm 0.02$	
$\mathcal{B}(B^0 \to D_s^- K^*(892)^+)$	*BABAR* [470]	$0.35^{+0.10}_{-0.09} \pm 0.04$	0.35 ± 0.10
			$0.35^{+0.11}_{-0.10}$
$\mathcal{B}(B^0 \to D_s^{*-} K^*(892)^+)$	*BABAR* [470]	$0.32^{+0.14}_{-0.12} \pm 0.04$	$0.32^{+0.15}_{-0.13}$
$\mathcal{B}(B^0 \to D_s^- K_S^0 \pi^+)$	*BABAR* [473]	$0.55 \pm 0.13 \pm 0.10$	0.55 ± 0.17
			0.97 ± 0.14
$\mathcal{B}(B^0 \to D_s^{*-} K^0 \pi^+)$	*BABAR* [473]	< 0.55	< 0.55
			< 1.10
$\mathcal{B}(B^0 \to D_s^- K^+ \pi^+ \pi^-)$	LHCb [474][c]	$1.64 \pm 0.21^{+0.41}_{-0.38}$	$1.64^{+0.49}_{-0.41}$
			1.71 ± 0.46

[a]Using *BABAR* result for $\mathcal{B}(D_s^+ \to \phi\pi^+)$ [475].
[b]Using $\mathcal{B}(B^0 \to D^-\pi^+)$.
[c]Using $\mathcal{B}(B_s^0 \to D_s^- K^+ \pi^+ \pi^-)$.

TABLE 60. Branching fractions for decays to excited D mesons.

Parameter [10^{-3}]	Measurements		Average$^{\text{HFLAV}}_{PDG}$
$\mathcal{B}(B^0 \to D^{**-} \pi^+)$[a]	*BABAR* [434]	$2.34 \pm 0.65 \pm 0.88$	2.3 ± 1.1
			1.9 ± 0.9

[a]D^{**} refers to the sum of all the non-strange charm meson states with masses in the range 2.2–2.8 GeV/c^2.

TABLE 61. Branching fractions for decays to excited D_s mesons.

Parameter [10^{-5}]	Measurements		Average$^{\text{HFLAV}}_{PDG}$
$\mathcal{B}(B^0 \to \bar{D}_1(2420)^0\pi^+\pi^-) \times \mathcal{B}(D_1(2420)^0 \to D^*(2010)^+\pi^-)$	LHCb [447][b]	$14.50 \pm 2.99 \pm 1.64$	14.5 ± 3.4 *14.7 ± 3.5*
$\mathcal{B}(B^0 \to D_1(2420)^-\pi^+) \times \mathcal{B}(D_1(2420)^+ \to D^+\pi^+\pi^-)$	Belle [476] LHCb [439][c]	$8.9 \pm 1.5^{+1.7}_{-3.1}$ $12.1 \pm 2.9^{+2.2}_{-3.2}$	$9.8^{+1.8}_{-2.3}$ $9.9^{+2.0}_{-2.5}$
$\mathcal{B}(B^0 \to \bar{D}_1(2430)^0\omega(782)) \times \mathcal{B}(D_1(2430)^0 \to D^*(2010)^+\pi^-)$	*BABAR* [451]	$41 \pm 12 \pm 11$	41 ± 16 27^{+8}_{-4}
$\mathcal{B}(B^0 \to D_0^*(2300)^-\pi^+) \times \mathcal{B}(D_0^*(2300)^+ \to \bar{D}^0\pi^+)$	Belle [445][a]	$6 \pm 1 \pm 3$	6.0 ± 3.0 *None*
$\mathcal{B}(B^0 \to D_2^*(2460)^-\pi^+) \times \mathcal{B}(D_2^*(2460)^+ \to \bar{D}^0\pi^+)$	Belle [445]	$21.5 \pm 1.7 \pm 3.1$	21.5 ± 3.6 *23.8 ± 1.6*
$\mathcal{B}(B^0 \to D_1(2420)^-\pi^+) \times \mathcal{B}(D_1(2420)^+ \to D^*(2010)^+\pi^+\pi^-)$	Belle [476]	< 3.3	< 3.3
$\mathcal{B}(B^0 \to D_2^*(2460)^-\pi^+) \times \mathcal{B}(D_2^*(2460)^+ \to D^*(2010)^+\pi^+\pi^-)$	Belle [476]	< 2.4	< 2.4
$\mathcal{B}(B^0 \to D_2^*(2460)^-K^+) \times \mathcal{B}(D_2^*(2460)^+ \to D^0\pi^+)$	*BABAR* [446][a]	$1.83 \pm 0.40 \pm 0.31$	1.83 ± 0.51 *None*
$\mathcal{B}(B^0 \to D_{s1}(2460)^-\pi^+)$	Belle [477][a,d]	< 2.2	< 2.2 *None*
$\mathcal{B}(B^0 \to D_{s1}(2460)^-K^+)$	Belle [477][a,d]	< 5.12	< 5.1 *None*
$\mathcal{B}(B^0 \to D_{s0}^*(2317)^-\pi^+)$	Belle [477][e]	< 2.5	< 2.5 *< 0.4*
$\mathcal{B}(B^0 \to D_{s0}^*(2317)^-K^+)$	Belle [477][a,e]	$5.3^{+1.5+1.6}_{-1.3-1.9}$	$5.3^{+2.3}_{-2.0}$ *None*

[a]Not included in PDG average.
[b]Using $\mathcal{B}(B^0 \to D^*(2010)^-\pi^+\pi^+\pi^-)$.
[c]Using $\mathcal{B}(B^0 \to D^-\pi^+\pi^+\pi^-)$.
[d]Using $\mathcal{B}(D_{s1}(2460)^+ \to D_s^+\gamma)$.
[e]Using $\mathcal{B}(D_{s0}^*(2317)^+ \to D_s^+\pi^0)$.

TABLE 62. Branching fractions for decays to a $D^{(*)}$ meson and baryons.

Parameter [10^{-4}]	Measurements		Average$^{\text{HFLAV}}_{PDG}$
$\mathcal{B}(B^0 \to D^- p\bar{p}\pi^+)$	*BABAR* [478]	$3.32 \pm 0.10 \pm 0.29$	3.32 ± 0.31
$\mathcal{B}(B^0 \to D^*(2010)^- p\bar{p}\pi^+)$	*BABAR* [478]	$4.55 \pm 0.16 \pm 0.39$	4.55 ± 0.42 *4.68 ± 0.49*
$\mathcal{B}(B^0 \to \bar{D}^0 p\bar{p}\pi^+\pi^-)$	*BABAR* [478]	$2.99 \pm 0.21 \pm 0.45$	2.99 ± 0.50
$\mathcal{B}(B^0 \to \bar{D}^*(2007)^0 p\bar{p}\pi^+\pi^-)$	*BABAR* [478]	$1.91 \pm 0.36 \pm 0.29$	1.91 ± 0.46
$\mathcal{B}(B^0 \to \bar{D}^0 p\bar{p})$	*BABAR* [478] Belle [479]	$1.02 \pm 0.04 \pm 0.06$ $1.18 \pm 0.15 \pm 0.16$	1.036 ± 0.069
$\mathcal{B}(B^0 \to \bar{D}^*(2007)^0 p\bar{p})$	*BABAR* [478] Belle [479]	$0.97 \pm 0.07 \pm 0.09$ $1.2 \pm 0.3 \pm 0.2$	0.99 ± 0.11
$\mathcal{B}(B^0 \to D_s^- \bar{\Lambda}^0 p)$	Belle [480]	$0.29 \pm 0.07 \pm 0.06$	0.306 ± 0.091 *0.284 ± 0.088*
$\mathcal{B}(B^0 \to \bar{D}^0 \Lambda^0 \bar{\Lambda}^0)$	*BABAR* [481] Belle [482]	$0.098^{+0.029}_{-0.026} \pm 0.019$ $0.105^{+0.057}_{-0.044} \pm 0.014$	0.100 ± 0.028 $0.100^{+0.030}_{-0.026}$
$\mathcal{B}(B^0 \to \bar{D}^0 \bar{\Sigma}^0 \Lambda^0 + \text{c.c.})$	*BABAR* [481]	$0.150^{+0.090}_{-0.080} \pm 0.030$	$0.150^{+0.095}_{-0.085}$ *< 0.310*
$\mathcal{B}(B^0 \to D^- \bar{\Lambda}^0 p)$	Belle [483]	$0.336 \pm 0.063 \pm 0.044$	0.336 ± 0.077 *0.251 ± 0.044*
$\mathcal{B}(B^0 \to D^*(2010)^- \bar{\Lambda}^0 p)$	Belle [483]	$0.251 \pm 0.026 \pm 0.035$	0.251 ± 0.044 *0.336 ± 0.077*

2. Decays to two open charm mesons

Averages of B^0 decays to two open charm mesons are shown in Tables 63–67.

TABLE 63. Branching fractions for decays to $D^{(*)}\bar{D}^{(*)}$.

Parameter [10^{-4}]	Measurements		Average$^{\text{HFLAV}}_{PDG}$
$\mathcal{B}(B^0 \to D^+ D^-)$	Belle [484] *BABAR* [485] LHCb [486][a,b]	$2.12 \pm 0.16 \pm 0.18$ $2.8 \pm 0.4 \pm 0.5$	2.20 ± 0.23 *2.11 ± 0.18*
$\mathcal{B}(B^0 \to D^*(2010)^+ D^-)$	Belle [484] *BABAR* [485][a,c]	$6.14 \pm 0.29 \pm 0.50$ $5.7 \pm 0.7 \pm 0.7$	6.03 ± 0.50 *6.14 ± 0.58*
$\mathcal{B}(B^0 \to D^*(2010)^+ D^*(2010)^-)$	Belle [487] *BABAR* [485] LHCb [488][a,d]	$7.82 \pm 0.38 \pm 0.60$ $8.1 \pm 0.6 \pm 1.0$	7.90 ± 0.61 $7.96^{+0.62}_{-0.61}$
$\mathcal{B}(B^0 \to D^0 \bar{D}^0)$	LHCb [486][e] Belle [489] *BABAR* [485]	$0.136 \pm 0.058 \pm 0.021$ < 0.43 < 0.6	0.136 ± 0.061 *0.140 ± 0.067*
$\mathcal{B}(B^0 \to D^*(2007)^0 \bar{D}^0)$	*BABAR* [485]	< 2.9	< 2.9
$\mathcal{B}(B^0 \to D^*(2007)^0 \bar{D}^*(2007)^0)$	*BABAR* [485]	< 0.9	< 0.90

[a]Not included in PDG average.
[b]Measurement of $\mathcal{B}(B_s^0 \to D^+ D^-)/\mathcal{B}(B^0 \to D^+ D^-)$ used in our fit.
[c]Including the charge-conjugate final state.
[d]Measurement of $\mathcal{B}(B_s^0 \to D^*(2010)^+ D^*(2010)^-)/\mathcal{B}(B^0 \to D^*(2010)^+ D^*(2010)^-)$ used in our fit.
[e]Using $\mathcal{B}(B^+ \to D_s^+ \bar{D}^0)$.

TABLE 64. Branching fractions for decays to two D mesons and a kaon.

Parameter [10^{-3}]	Measurements		Average$^{\text{HFLAV}}_{PDG}$
$\mathcal{B}(B^0 \to D^*(2010)^- D^+ K^0)$	*BABAR* [490]	$6.41 \pm 0.36 \pm 0.39$	6.41 ± 0.53
$\mathcal{B}(B^0 \to D^*(2010)^+ D^*(2010)^- K^0)$	*BABAR* [490] *BABAR* [491][b,c] Belle [492][b]	$8.26 \pm 0.43 \pm 0.67$	8.33 ± 0.64 *8.11 ± 0.65*
$\mathcal{B}(B^0 \to D^*(2010)^- D^0 K^+)$	*BABAR* [490]	$2.47 \pm 0.10 \pm 0.18$	2.47 ± 0.21
$\mathcal{B}(B^0 \to D^*(2007)^0 D^- K^+)$	*BABAR* [490]	$3.46 \pm 0.18 \pm 0.37$	3.46 ± 0.41
$\mathcal{B}(B^0 \to D_s^- D^*(2007)^0 K^+)$	*BABAR* [490][a]	$10.6 \pm 0.3 \pm 0.9$	10.60 ± 0.92 *None*
$\mathcal{B}(B^0 \to D^*(2007)^0 \bar{D}^0 K^0)$	*BABAR* [490]	$1.08 \pm 0.32 \pm 0.36$	1.08 ± 0.48
$\mathcal{B}(B^0 \to D^*(2007)^0 \bar{D}^*(2007)^0 K^0)$	*BABAR* [490]	$2.4 \pm 0.6 \pm 0.7$	2.40 ± 0.87
$\mathcal{B}(B^0 \to D^+ D^- K^0)$	*BABAR* [490]	$0.75 \pm 0.12 \pm 0.12$	0.75 ± 0.17
$\mathcal{B}(B^0 \to D^- D^0 K^+)$	*BABAR* [490]	$1.07 \pm 0.07 \pm 0.09$	1.07 ± 0.11
$\mathcal{B}(B^0 \to D^0 \bar{D}^0 K^0)$	*BABAR* [490]	$0.27 \pm 0.10 \pm 0.05$	0.27 ± 0.11
$\mathcal{B}(B^0 \to D^0 \bar{D}^0 K^0 \pi^0)$	Belle [493][a]	$0.173 \pm 0.070^{+0.031}_{-0.053}$	$0.173^{+0.077}_{-0.088}$ *None*

[a]Not included in PDG average.
[b]Measurement of $\mathcal{B}(B^0 \to D^*(2010)^+ D^*(2010)^- K^0)/2$ used in our fit.
[c]Measurement of $\mathcal{B}(B^0 \to D_{s1}(2536)^+ D^*(2010)^-)/\mathcal{B}(B^0 \to D^*(2010)^+ D^*(2010)^- K^0)2$ used in our fit.

TABLE 65. Branching fractions for decays to $D_s^{(*)-} D^{(*)+}$.

Parameter [10^{-3}]	Measurements		Average$^{\text{HFLAV}}_{PDG}$
$\mathcal{B}(B^0 \to D_s^+ D^-)$	Belle [494]	$7.5 \pm 0.2 \pm 1.1$	
	Belle II [463][a]	$8.9 \pm 0.5 \pm 0.5$	$8.16^{+0.43}_{-0.42}$
	BABAR [495][c]	$5.97 \pm 1.36 \pm 1.13$	*7.24 ± 0.77*
	BABAR [495]	$9 \pm 2 \pm 1$	
	LHCb [486][b,d,e,f], [496][b,g,h]		
$\mathcal{B}(B^0 \to D_s^+ D^*(2010)^-)$	Belle II [463][a]	$8.3 \pm 1.0 \pm 0.6$	
	BABAR [497]	$10.3 \pm 1.4 \pm 2.9$	8.20 ± 0.89
	BABAR [495]	$5.7 \pm 1.6 \pm 0.9$	*8.04 ± 1.10*
	BABAR [495][c]	$11.43 \pm 2.10 \pm 1.79$	
$\mathcal{B}(B^0 \to D_s^{*+} D^*(2010)^-)$	*BABAR* [475]	$18.8 \pm 0.9 \pm 1.7$	
	BABAR [497]	$19.7 \pm 1.5 \pm 5.7$	18.7 ± 1.5
	BABAR [495]	$16.5 \pm 2.3 \pm 1.9$	*17.7 ± 1.4*
	BABAR [495][c]	$27.3 \pm 4.9 \pm 5.3$	
$\mathcal{B}(B^0 \to D_s^{*+} D^-)$	*BABAR* [495]	$6.7 \pm 2.0 \pm 1.1$	7.5 ± 1.9
	BABAR [495][c]	$9.26 \pm 2.66 \pm 2.20$	*7.4 ± 1.6*

[a]Preliminary result.
[b]Not included in PDG average.
[c]Using $\mathcal{B}(D_s^+ \to \phi(1020)\pi^+)$.
[d]Measurement of $\mathcal{B}(B_s^0 \to D_s^- D^+)/\mathcal{B}(B^0 \to D_s^+ D^-)$ used in our fit.
[e]Measurement of $\mathcal{B}(B_s^0 \to D_s^+ D_s^-)/\mathcal{B}(B^0 \to D_s^+ D^-)$ used in our fit.
[f]Measurement of $\mathcal{B}(B^+ \to D_s^+ \bar{D}^0)/\mathcal{B}(B^0 \to D_s^+ D^-)$ used in our fit.
[g]At CL = 95%.
[h]Measurement of $\mathcal{B}(B^0 \to \Lambda_c^+ \bar{\Lambda}_c^-)/\mathcal{B}(B^0 \to D_s^+ D^-)$ used in our fit.

TABLE 66. Branching fractions for decays to $D_s^{(*)+}D_s^{(*)-}$.

Parameter [10^{-4}]	Measurements		Average$^{\text{HFLAV}}_{PDG}$
$\mathcal{B}(B^0 \to D_s^+ D_s^-)$	Belle [494]	< 0.36	< 0.36
	BABAR [498]	< 1.0	
$\mathcal{B}(B^0 \to D_s^{*-} D_s^+)$	*BABAR* [498]	< 1.3	< 1.3
$\mathcal{B}(B^0 \to D_s^{*+} D_s^{*-})$	*BABAR* [498]	< 2.4	< 2.4

TABLE 67. Branching fractions for decays to excited D_s mesons.

Parameter [10^{-3}]	Measurements		Average$^{\text{HFLAV}}_{PDG}$
$\mathcal{B}(B^0 \to D_{s0}^*(2317)^+ D^-)$	Belle [499][a,b]	$1.02^{+0.13\,+0.11}_{-0.12\,-0.23}$	$1.07^{+0.30}_{-0.16}$
	BABAR [500][a,b]	$1.8 \pm 0.4^{+0.7}_{-0.6}$	*< 0.95*
$\mathcal{B}(B^0 \to D_{s0}^*(2317)^+ D^*(2010)^-)$	*BABAR* [500][b]	$1.5 \pm 0.4 \pm 0.5$	$1.50^{+0.70}_{-0.54}$ *$1.50^{+0.64}_{-0.57}$*
$\mathcal{B}(B^0 \to D_{s1}(2460)^+ D^-)$	*BABAR* [500][c]	$4.4 \pm 1.1^{+1.8}_{-1.4}$	4.07 ± 0.86 *$3.55^{+1.14}_{-1.07}$*
	Belle [501][c]	$4.47^{+1.20}_{-1.04} \pm 1.53$	
	Belle [501][d]	$4.25^{+1.37}_{-1.16} \pm 1.43$	
	BABAR [500][d]	$5.2 \pm 1.5^{+2.2}_{-1.7}$	
	BABAR [495]	$2.6 \pm 1.5 \pm 0.7$	
	Belle [501][e]	< 4.7	
$\mathcal{B}(B^0 \to D_{s1}(2460)^+ D^*(2010)^-)$	*BABAR* [500][c]	$12.5 \pm 1.6^{+5.0}_{-3.7}$	10.0 ± 1.8 *$9.3^{+2.3}_{-2.2}$*
	BABAR [495]	$8.8 \pm 2.0 \pm 1.4$	
	BABAR [500][d]	$10.3 \pm 2.2^{+4.3}_{-3.3}$	
$\mathcal{B}(B^0 \to D_{s1}(2536)^+ D^-)$	*BABAR* [502][a,f]	$0.359 \pm 0.101 \pm 0.083$	0.39 ± 0.11 *0.28 ± 0.07*
	BABAR [502][a,g]	$0.464 \pm 0.183 \pm 0.078$	
$\mathcal{B}(B^0 \to D_{s1}(2536)^+ D^*(2010)^-)$	*BABAR* [502][a,f]	$0.696 \pm 0.185 \pm 0.167$	0.473 ± 0.094 *None*
	BABAR [491][a,h]	$0.766 \pm 0.200 \pm 0.059$	
	BABAR [502][a,g]	$0.89 \pm 0.27 \pm 0.16$	
$\mathcal{B}(B^0 \to D_{s1}(2536)^- D^+)$	Belle [503][a,i]		0.265 ± 0.073 *None*
$\mathcal{B}(B^0 \to D_{s1}(2536)^- D^*(2010)^+)$	Belle [503][j], [492][a,k]		0.48 ± 0.14 *0.50 ± 0.14*

[a]Not included in PDG average.
[b]Using $\mathcal{B}(D_{s0}^*(2317)^+ \to D_s^+ \pi^0)$.
[c]Using $\mathcal{B}(D_{s1}(2460)^+ \to D_s^+ \gamma)$.
[d]Using $\mathcal{B}(D_{s1}(2460)^+ \to D_s^{*+} \pi^0)$.
[e]Using $\mathcal{B}(D_{s1}(2460)^+ \to D_s^+ \pi^+ \pi^-)$.
[f]Using $\mathcal{B}(D_{s1}(2536)^+ \to D^*(2007)^0 K^+)$.
[g]Using $\mathcal{B}(D_{s1}(2536)^+ \to D^*(2010)^+ K^0)$.
[h]Using $\mathcal{B}(B^0 \to D^*(2010)^+ D^*(2010)^- K^0)$.
[i]Measurement of $\mathcal{B}(B^0 \to D_{s1}(2536)^- D^+)(\mathcal{B}(D_{s1}(2536)^+ \to D^*(2007)^0 K^+) + \mathcal{B}(D_{s1}(2536)^+ \to D^*(2010)^+ K^0))$ used in our fit.
[j]Measurement of $\mathcal{B}(B^0 \to D_{s1}(2536)^- D^*(2010)^+)(\mathcal{B}(D_{s1}(2536)^+ \to D^*(2007)^0 K^+) + \mathcal{B}(D_{s1}(2536)^+ \to D^*(2010)^+ K^0))$ used in our fit.
[k]Measurement of $\mathcal{B}(B^0 \to D_{s1}(2536)^- D^*(2010)^+) BR_D s1(2536) *_D * +_K 0S$ used in our fit.

3. Decays to charmonium states

Averages of B^0 decays to charmonium states are shown in Tables 68–73.

TABLE 68. Branching fractions for decays to J/ψ and one kaon.

Parameter [10^{-4}]	Measurements		Average$^{\text{HFLAV}}_{PDG}$
$\mathcal{B}(B^0 \to J/\psi K^0)$	BELLE [504]	$9.02 \pm 0.10 \pm 0.26$	
	BABAR [12]	$8.69 \pm 0.22 \pm 0.30$	
	Belle [505]	$7.9 \pm 0.4 \pm 0.9$	
	CDF [506]	$11.5 \pm 2.3 \pm 1.7$	8.83 ± 0.20
	BABAR [507][b], [12][c]		*8.91 ± 0.21*
	Belle [508][d]		
	CDF [509][c]		
	LHCb [510][a,e], [511][f,g]		
$\mathcal{B}(B^0 \to J/\psi K^+\pi^-)$	Belle [512]		11.50 ± 0.51
	LHCb [513][h]	$11.5 \pm 0.1 \pm 0.5$	
$\mathcal{B}(B^0 \to J/\psi K^*(892)^0)$	Belle [512]	$11.9 \pm 0.1 \pm 0.8$	
	BABAR [12]	$13.09 \pm 0.26 \pm 0.77$	
	BABAR [12][i]	$13.33 \pm 0.44 \pm 0.77$	$12.78^{+0.44}_{-0.43}$
	CDF [514]	$17.4 \pm 2.0 \pm 1.8$	*12.65 ± 0.46*
	CDF [509][i]	$12.27 \pm 3.18 \pm 0.92$	
	LHCb [515][j]		
$\mathcal{B}(B^0 \to J/\psi K^0\pi^+\pi^-)$	LHCb [511]	$4.30 \pm 0.30 \pm 0.37$	
	LHCb [511][i]	$4.352 \pm 0.300^{+0.258}_{-0.257}$	$4.37^{+0.31}_{-0.30}$
	CDF [516]	$10.3 \pm 3.3 \pm 1.5$	*4.46 ± 0.40*
	LHCb [511][k]		
$\mathcal{B}(B^0 \to J/\psi K^0\rho^0(770))$	CDF [516]	$5.4 \pm 2.9 \pm 0.9$	5.4 ± 3.0
$\mathcal{B}(B^0 \to J/\psi K^*(892)^+\pi^-)$	CDF [516]	$7.7 \pm 4.1 \pm 1.3$	7.7 ± 4.3
$\mathcal{B}(B^0 \to J/\psi\omega(782)K^0)$	*BABAR* [517]	$2.3 \pm 0.3 \pm 0.3$	2.28 ± 0.34
	BABAR [517][l]	$2.3 \pm 0.3^{+0.5}_{-0.4}$	*2.30 ± 0.42*
$\mathcal{B}(B^0 \to J/\psi\phi(1020)K^0)$	*BABAR* [518]	$1.02 \pm 0.38 \pm 0.10$	1.02 ± 0.39
			0.49 ± 0.10
$\mathcal{B}(B^0 \to J/\psi K_1(1270)^0)$	Belle [519][m]	$13 \pm 3 \pm 3$	13.2 ± 4.5
			13.0 ± 4.7
$\mathcal{B}(B^0 \to J/\psi\eta K_S^0)$	Belle [520]	$0.522 \pm 0.078 \pm 0.049$	0.540 ± 0.089
	BABAR [521]	$0.84 \pm 0.26 \pm 0.27$	
$\mathcal{B}(B^0 \to J/\psi K^*(892)^0\pi^+\pi^-)$	CDF [516]	$6.6 \pm 1.9 \pm 1.1$	6.6 ± 2.2
	LHCb [511][a,n]		

[a]Not included in PDG average.
[b]Measurement of $\mathcal{B}(B^0 \to \eta_c K^0)/\mathcal{B}(B^0 \to J/\psi K^0)$ used in our fit.
[c]Measurement of $\mathcal{B}(B^0 \to J/\psi K^*(892)^0)/\mathcal{B}(B^0 \to J/\psi K^0)$ used in our fit.
[d]Measurement of $0.5\mathcal{B}(B^0 \to J/\psi K^0)\mathcal{B}(J/\psi \to p\bar{p}\pi^+\pi^-)$ used in our fit.
[e]Measurement of $2\mathcal{B}(B_s^0 \to J/\psi K_S^0)/\mathcal{B}(B^0 \to J/\psi K^0)$ used in our fit.
[f]Measurement of $\mathcal{B}(B^0 \to J/\psi K^0\pi^+\pi^-)/\mathcal{B}(B^0 \to J/\psi K^0)$ used in our fit.
[g]Measurement of $\mathcal{B}(B^0 \to \psi(2S)K^0)\mathcal{B}(\psi(2S) \to J/\psi\pi^+\pi^-)/\mathcal{B}(B^0 \to J/\psi K^0)$ used in our fit.
[h]Measurement of $(\mathcal{B}(B^0 \to \eta_c K^+\pi^-)\mathcal{B}(\eta_c \to p\bar{p}))/(\mathcal{B}(B^0 \to J/\psi K^+\pi^-)\mathcal{B}(J/\psi \to p\bar{p}))$ used in our fit.
[i]Using $\mathcal{B}(B^0 \to J/\psi K^0)$.
[j]Measurement of $\mathcal{B}(B^0 \to \psi(2S)K^*(892)^0)/\mathcal{B}(B^0 \to J/\psi K^*(892)^0)$ used in our fit.
[k]Measurement of $\mathcal{B}(B_s^0 \to J/\psi K^0 K^-\pi^+ + \text{c.c.})/\mathcal{B}(B^0 \to J/\psi K^0\pi^+\pi^-)$ used in our fit.
[l]Using $\mathcal{B}(B^+ \to J/\psi\omega(782)K^+)$.
[m]Using $\mathcal{B}(B^+ \to J/\psi K^+)$.
[n]Measurement of $\mathcal{B}(B^0 \to J/\psi K^*(892)^0 K^+K^-)/\mathcal{B}(B^0 \to J/\psi K^*(892)^0\pi^+\pi^-)$ used in our fit.

TABLE 69. Branching fractions for decays to charmonium other than J/ψ and one kaon.

Parameter [10^{-4}]	Measurements		Average$^{\text{HFLAV}}_{PDG}$
$\mathcal{B}(B^0 \to \psi(2S)K^0)$	*BABAR* [12]	$6.46 \pm 0.65 \pm 0.51$	
	LHCb [511]	$4.7 \pm 0.7 \pm 0.7$	
	Belle [505]	6.7 ± 1.1	
	Belle [522][a]	$6.8 \pm 1.0 \pm 0.7$	5.72 ± 0.38
	Belle [522][a]	$4.7 \pm 1.6 \pm 0.8$	*5.85 ± 0.46*
	BABAR [12][b]		
	Belle [508][a,c]		
	LHCb [511][d]		
$\mathcal{B}(B^0 \to \psi(2S)K^*(892)^0)$	LHCb [515][e]	$6.08 \pm 0.18 \pm 0.29$	
	Belle [523]	$5.52^{+0.35+0.53}_{-0.32-0.58}$	
	BABAR [12]	$6.49 \pm 0.59 \pm 0.97$	6.08 ± 0.28
	BABAR [12][f]	$5.7 \pm 0.8 \pm 0.6$	$5.94^{+0.41}_{-0.45}$
	CDF [514]	$9.0 \pm 2.2 \pm 0.9$	
	LHCb [524][a,g]		
$\mathcal{B}(B^0 \to \eta_c K^0)$	*BABAR* [507][h]	$9.2 \pm 1.4 \pm 0.9$	
	BABAR [507]	$11.4 \pm 1.5 \pm 3.4$	
	BABAR [507][i]	$11.83 \pm 1.68 \pm 3.56$	8.8 ± 1.1
	BABAR [525][j]	$6.4^{+2.2}_{-2.0} \pm 2.8$	*8.2 ± 1.1*
	Belle [526]	$12.3 \pm 2.3^{+4.0}_{-4.1}$	
	Belle [508][k], [526][l]		
$\mathcal{B}(B^0 \to \eta_c K^*(892)^0)$	*BABAR* [527]	$5.7 \pm 0.6 \pm 0.9$	
	BABAR [527][h]	$6.6 \pm 0.6 \pm 0.7$	
	BABAR [525][j]	$8 \pm 2 \pm 4$	6.63 ± 0.66
	Belle [526][m]	$11.72 \pm 3.17^{+2.57}_{-3.25}$	$5.20^{+0.80}_{-0.90}$
	Belle [526]	$16.2 \pm 3.2^{+5.5}_{-6.0}$	
$\mathcal{B}(B^0 \to \eta_c K^+\pi^-)$	LHCb [513][n]		$6.86^{+0.69}_{-0.64}$
			$6.44^{+0.74}_{-0.75}$
$\mathcal{B}(B^0 \to \eta_c(2S)K^*(892)^0)$	*BABAR* [527]	< 3.9	< 3.9
$\mathcal{B}(B^0 \to h_c K^*(892)^0)$	*BABAR* [527][o]	< 3.9	< 3.9
	BABAR [527][p]		*< 4.0*
$\mathcal{B}(B^0 \to \psi(3770)K^0)$	*BABAR* [502][a,q]	< 2.35	< 2.3
	BABAR [502][a,r]	< 4.64	*None*

[a]Not included in PDG average.
[b]Measurement of $\mathcal{B}(B^0 \to \psi(2S)K^*(892)^0)/\mathcal{B}(B^0 \to \psi(2S)K^0)$ used in our fit.
[c]Measurement of $0.5\mathcal{B}(B^0 \to \psi(2S)K^0)\mathcal{B}(\psi(2S) \to p\bar{p}\pi^+\pi^-)$ used in our fit.
[d]Measurement of $\mathcal{B}(B^0 \to \psi(2S)K^0)\mathcal{B}(\psi(2S) \to J/\psi\pi^+\pi^-)/\mathcal{B}(B^0 \to J/\psi K^0)$ used in our fit.
[e]Using $\mathcal{B}(B^0 \to J/\psi K^*(892)^0)$.
[f]Using $\mathcal{B}(B^0 \to \psi(2S)K^0)$.
[g]Measurement of $\mathcal{B}(B_s^0 \to \psi(2S)\bar{K}^*(892)^0)/\mathcal{B}(B^0 \to \psi(2S)K^*(892)^0)$ used in our fit.
[h]Using $\mathcal{B}(B^+ \to \eta_c K^+)$.
[i]Using $\mathcal{B}(B^0 \to J/\psi K^0)$.
[j]Calculated using $\mathcal{B}(\eta_c \to p\bar{p})$.
[k]Measurement of $0.5\mathcal{B}(B^0 \to \eta_c K^0)\mathcal{B}(\eta_c \to p\bar{p}\pi^+\pi^-)$ used in our fit.
[l]Measurement of $\mathcal{B}(B^0 \to \eta_c K^*(892)^0)/\mathcal{B}(B^0 \to \eta_c K^0)$ used in our fit.
[m]Using $\mathcal{B}(B^0 \to \eta_c K^0)$.
[n]Measurement of $(\mathcal{B}(B^0 \to \eta_c K^+\pi^-)\mathcal{B}(\eta_c \to p\bar{p}))/(\mathcal{B}(B^0 \to J/\psi K^+\pi^-)\mathcal{B}(J/\psi \to p\bar{p}))$ used in our fit.
[o]Using $\mathcal{B}(h_c \to \eta_c\gamma)$.
[p]Measurement of $\mathcal{B}(B^0 \to h_c K^*(892)^0)\mathcal{B}(h_c \to \eta_c\gamma)/\mathcal{B}(B^+ \to \eta_c K^+)$ used in our fit.
[q]Using $\mathcal{B}(\psi(3770) \to D^0\bar{D}^0)$.
[r]Using $\mathcal{B}(\psi(3770) \to D^+D^-)$.

TABLE 70. Branching fractions for decays to χ_c and one kaon.

Parameter [10^{-4}]	Measurements		Average$^{\text{HFLAV}}_{PDG}$
$\mathcal{B}(B^0 \to \chi_{c0} K^0)$	*BABAR* [528]	< 12.4	< 12 2 ± 0
$\mathcal{B}(B^0 \to \chi_{c0} K^*(892)^0)$	*BABAR* [529] *BABAR* [528]	$1.7 \pm 0.3 \pm 0.2$ < 7.7	1.70 ± 0.36
$\mathcal{B}(B^0 \to \chi_{c1} K^0)$	Belle [530] *BABAR* [531] *BABAR* [12][a]	$3.78^{+0.17}_{-0.16} \pm 0.33$ $4.2 \pm 0.3 \pm 0.3$	3.93 ± 0.27 3.95 ± 0.27
$\mathcal{B}(B^0 \to \chi_{c1} K^+ \pi^-)$	Belle [532] *BABAR* [533]	$4.97 \pm 0.12 \pm 0.28$ $5.11 \pm 0.14 \pm 0.58$	5.00 ± 0.27 4.97 ± 0.30
$\mathcal{B}(B^0 \to \chi_{c1} K^*(892)^0)$	*BABAR* [531] Belle [534] *BABAR* [12][b]	$2.5 \pm 0.2 \pm 0.2$ $3.1 \pm 0.3 \pm 0.7$ $2.83 \pm 0.43 \pm 0.51$	2.61 ± 0.25 $2.38^{+0.20}_{-0.19}$
$\mathcal{B}(B^0 \to \chi_{c1} K^+ \pi^- \pi^0)$	Belle [532]	$3.52 \pm 0.52 \pm 0.24$	3.52 ± 0.57
$\mathcal{B}(B^0 \to \chi_{c1} K^0 \pi^+ \pi^-)$	Belle [532]	$3.16 \pm 0.35 \pm 0.32$	3.16 ± 0.47
$\mathcal{B}(B^0 \to \chi_{c2} K^0)$	*BABAR* [531] Belle [530]	$0.15 \pm 0.09 \pm 0.03$ < 0.15	0.150 ± 0.095 < 0.150
$\mathcal{B}(B^0 \to \chi_{c2} K^*(892)^0)$	*BABAR* [531]	$0.66 \pm 0.18 \pm 0.05$	0.66 ± 0.19 0.49 ± 0.12
$\mathcal{B}(B^0 \to \chi_{c2} K^+ \pi^-)$	Belle [532]	$0.72 \pm 0.09 \pm 0.05$	0.72 ± 0.10

[a]Measurement of $\mathcal{B}(B^0 \to \chi_{c1} K^*(892)^0)/\mathcal{B}(B^0 \to \chi_{c1} K^0)$ used in our fit.
[b]Using $\mathcal{B}(B^0 \to \chi_{c1} K^0)$.

TABLE 71. Branching fractions for decays to charmonium and light mesons.

Parameter [10^{-5}]	Measurements		Average$^{\text{HFLAV}}_{PDG}$
$\mathcal{B}(B^0 \to J/\psi \pi^0)$	*BABAR* [535] Belle [505]	$1.69 \pm 0.14 \pm 0.07$ $2.3 \pm 0.5 \pm 0.2$	1.74 ± 0.15 1.66 ± 0.10
$\mathcal{B}(B^0 \to J/\psi \pi^+ \pi^-)$	*BABAR* [536] LHCb [537][b]	$4.6 \pm 0.7 \pm 0.6$	4.60 ± 0.92 4.00 ± 0.15
$\mathcal{B}(B^0 \to J/\psi \pi^+ \pi^-(\text{NR}))$	*BABAR* [538][c]	< 1.2	< 1.2
$\mathcal{B}(B^0 \to J/\psi \rho^0(770))$	*BABAR* [538] LHCb [539][d], [539][e], [539][f]	$2.7 \pm 0.3 \pm 0.2$	2.96 ± 0.28 $2.55^{+0.18}_{-0.16}$
$\mathcal{B}(B^0 \to J/\psi \eta)$	Belle [540] LHCb [541][g] *BABAR* [518]	$1.23^{+0.18}_{-0.17} \pm 0.07$ $0.848 \pm 0.280^{+0.123}_{-0.114}$ < 2.7	1.12 ± 0.16 $1.08^{+0.24}_{-0.23}$
$\mathcal{B}(B^0 \to J/\psi \eta')$	LHCb [541][h] Belle [540] *BABAR* [518]	$0.855 \pm 0.244^{+0.134}_{-0.124}$ < 0.74 < 6.3	0.86 ± 0.28 $0.76^{+0.24}_{-0.25}$
$\mathcal{B}(B^0 \to J/\psi \omega(782))$	LHCb [539][i]	$2.63 \pm 0.56^{+0.33}_{-0.46}$	2.63 ± 0.69 $1.76^{+0.70}_{-0.53}$
$\mathcal{B}(B^0 \to J/\psi f_0(980))$	LHCb [542][j]		< 0.11
$\mathcal{B}(B^0 \to J/\psi f_1(1285))$	LHCb [543][k]	$0.8450 \pm 0.1963 \pm 0.0752$	0.84 ± 0.21
$\mathcal{B}(B^0 \to J/\psi f_2(1270))$	*BABAR* [538]	< 0.46	< 0.46 $0.33^{+0.05}_{-0.06}$

(Table continued)

TABLE 71. *(Continued)*

Parameter [10^{-5}]	Measurements		Average$^{\text{HFLAV}}_{PDG}$
$\mathcal{B}(B^0 \to J/\psi K^0 K^+ \pi^- + \text{c.c.})$	LHCb [511]	< 2.10	< 2.1
$\mathcal{B}(B^0 \to J/\psi K^0 K^+ K^-)$	LHCb [511]	$2.02 \pm 0.43 \pm 0.19$	2.02 ± 0.47 *2.49 ± 0.69*
$\mathcal{B}(B^0 \to J/\psi K^*(892)^0 K^+ K^-)$	LHCb [511][a,l]	$3.10 \pm 0.66 \pm 1.07$	$3.1^{+1.4}_{-1.2}$ *None*
$\mathcal{B}(B^0 \to J/\psi a_0(980)^0) \times \mathcal{B}(a_0(980)^0 \to K^+ K^-)$	LHCb [544]	< 0.090	< 0.090 *0.047 ± 0.034*
$\mathcal{B}(B^0 \to J/\psi K^+ K^-)$	LHCb [544]	$0.253 \pm 0.031 \pm 0.019$	0.253 ± 0.036 *0.254 ± 0.035*
$\mathcal{B}(B^0 \to J/\psi \phi(1020))$	LHCb [544] Belle [545] *BABAR* [518]	< 0.019 < 0.094 < 0.9	< 0.019 *< 0.011*
$\mathcal{B}(B^0 \to \psi(2S)\pi^+\pi^-)$	LHCb [537][m]	$2.57 \pm 0.32 \pm 0.57$	$2.59^{+0.69}_{-0.61}$ *2.24 ± 0.35*
$\mathcal{B}(B^0 \to \chi_{c1}\pi^0)$	Belle [546]	$1.12 \pm 0.25 \pm 0.12$	1.12 ± 0.28

[a]Not included in PDG average.
[b]Measurement of $\mathcal{B}(B^0 \to \psi(2S)\pi^+\pi^-)/\mathcal{B}(B^0 \to J/\psi\pi^+\pi^-)$ used in our fit.
[c]Non resonant only: K^0_S, ρ and f_2 contributions have been subtracted out.
[d]Measurement of $\mathcal{B}(B^0 \to J/\psi\omega(782))/\mathcal{B}(B^0 \to J/\psi\rho^0(770))$ used in our fit.
[e]Measurement of $\mathcal{B}(B^0_s \to J/\psi\eta)/\mathcal{B}(B^0 \to J/\psi\rho^0(770))$ used in our fit.
[f]Measurement of $\mathcal{B}(B^0_s \to J/\psi\eta')/\mathcal{B}(B^0 \to J/\psi\rho^0(770))$ used in our fit.
[g]Using $\mathcal{B}(B^0_s \to J/\psi\eta)$.
[h]Using $\mathcal{B}(B^0_s \to J/\psi\eta')$.
[i]Using $\mathcal{B}(B^0 \to J/\psi\rho^0(770))$.
[j]Measurement of $\mathcal{B}(B^0 \to J/\psi f_0(980))BR_f 0_p i +_p i-$ used in our fit.
[k]Using $\mathcal{B}(f_1(1285) \to \pi^+\pi^+\pi^-\pi^-)$.
[l]Using $\mathcal{B}(B^0 \to J/\psi K^*(892)^0\pi^+\pi^-)$.
[m]Using $\mathcal{B}(B^0 \to J/\psi\pi^+\pi^-)$.

TABLE 72. Branching fractions for decays to J/ψ and photons, baryons, or heavy mesons.

Parameter [10^{-6}]	Measurements		Average$^{\text{HFLAV}}_{PDG}$
$\mathcal{B}(B^0 \to J/\psi\gamma)$	LHCb [547]	< 1.5	< 1.5
	BABAR [548]	< 1.6	
$\mathcal{B}(B^0 \to J/\psi p\bar{p})$	LHCb [549]	$0.451 \pm 0.040 \pm 0.044$	0.451 ± 0.059
	LHCb [550]	< 0.52	
	Belle [551]	< 0.83	
	BABAR [552]	< 1.9	
$\mathcal{B}(B^0 \to J/\psi\bar{D}^0)$	*BABAR* [553]	< 13	< 13
	Belle [554]	< 20	

TABLE 73. Branching fraction ratios for decays to J/ψ.

Parameter [10^{-2}]	Measurements		Average
$\frac{\mathcal{B}(B^0 \to J/\psi K^0_S K^+\pi^- + \text{c.c.})}{\mathcal{B}(B^0 \to J/\psi K^0_S \pi^+\pi^-)}$	LHCb [511]	< 4.8	< 4.8

4. Decays to charm baryons

Averages of B^0 decays to charm baryons are shown in Tables 74 and 75.

TABLE 74. Branching fractions for decays to charm baryons, I.

Parameter [10^{-4}]	Measurements		Average$^{\text{HFLAV}}_{PDG}$
$\mathcal{B}(B^0 \to \bar{\Lambda}_c^- p\pi^0)$	*BABAR* [555]	$1.94 \pm 0.17 \pm 0.52$	1.94 ± 0.55 *1.55 ± 0.18*
$\mathcal{B}(B^0 \to \bar{\Lambda}_c^- p\pi^+\pi^-)$	*BABAR* [556] Belle [557]	$12.30 \pm 0.50 \pm 3.28$ $11.0 \pm 1.2 \pm 3.5$	11.7 ± 2.5 *10.2 ± 1.4*
$\mathcal{B}(B^0 \to \bar{\Lambda}_c^- p\pi^+\pi^-(\text{NR}))$	*BABAR* [556]	$7.90 \pm 0.40 \pm 2.04$	7.9 ± 2.1 *5.5 ± 1.0*
$\mathcal{B}(B^0 \to \bar{\Sigma}_c(2455)^0 p\pi^-)$	*BABAR* [556] Belle [558]	$0.91 \pm 0.07 \pm 0.24$ $1.4 \pm 0.2 \pm 0.4$	1.01 ± 0.22 *1.08 ± 0.16*
$\mathcal{B}(B^0 \to \bar{\Sigma}_c(2455)^{--} p\pi^+)$	*BABAR* [556] Belle [558]	$2.13 \pm 0.10 \pm 0.56$ $2.1 \pm 0.2 \pm 0.6$	2.12 ± 0.42 *1.84 ± 0.24*
$\mathcal{B}(B^0 \to \bar{\Sigma}_c(2520)^{--} p\pi^+)$	*BABAR* [556] Belle [558]	$1.15 \pm 0.10 \pm 0.30$ $1.2 \pm 0.1 \pm 0.4$	1.17 ± 0.24 *1.02 ± 0.18*
$\mathcal{B}(B^0 \to \Lambda_c^+ \bar{\Lambda}_c^-)$	LHCb [496][b,c] Belle [559]	< 0.16 < 0.57	< 0.16
$\mathcal{B}(B^0 \to \Lambda_c^+ \bar{\Lambda}_c^- K^0)$	Belle [560] *BABAR* [561]	$7.9^{+2.9}_{-2.3} \pm 4.3$ $3.8 \pm 3.1 \pm 2.1$	5.3 ± 2.9 *4.0 ± 0.9*
$\mathcal{B}(B^0 \to \bar{\Xi}_c^- \Lambda_c^+)$	*BABAR* [561][a,d] Belle [562][a,d]	$5.2 \pm 3.7 \pm 2.8$ $32.0^{+12.7}_{-9.6} \pm 17.9$	$7.1^{+7.7}_{-4.1}$ *11.6 ± 8.1*

[a]Not included in PDG average.
[b]At CL = 95%.
[c]Using $\mathcal{B}(B^0 \to D_s^+ D^-)$.
[d]Using $\mathcal{B}(\Xi_c^+ \to \Xi^- \pi^+ \pi^+)$.

TABLE 75. Branching fractions for decays to charm baryons, II.

Parameter [10^{-5}]	Measurements		Average$^{\text{HFLAV}}_{PDG}$
$\mathcal{B}(B^0 \to \bar{\Lambda}_c^- pK^+K^-)$	*BABAR* [563]	$2.5 \pm 0.4 \pm 0.6$	2.50 ± 0.75 *2.00 ± 0.37*
$\mathcal{B}(B^0 \to \bar{\Lambda}_c^- p\phi(1020))$	*BABAR* [563]	< 1.2	< 1.2 *< 1.0*
$\mathcal{B}(B^0 \to \bar{\Lambda}_c^- p)$	*BABAR* [564] Belle [565] *BABAR* [564][a]	$1.89 \pm 0.21 \pm 0.49$ $2.19^{+0.56}_{-0.49} \pm 0.65$	1.80 ± 0.31 *$1.54^{+0.17}_{-0.18}$*
$\mathcal{B}(B^0 \to \bar{\Lambda}_c^- pK^*(892)^0)$	*BABAR* [566]	$1.6 \pm 0.6 \pm 0.4$	1.60 ± 0.75 *< 2.42*
$\mathcal{B}(B^0 \to \bar{\Lambda}_c^- \Lambda^0 K^+)$	*BABAR* [567]	$3.8 \pm 0.8 \pm 1.0$	3.8 ± 1.3 *4.8 ± 1.1*
$\mathcal{B}(B^0 \to \bar{\Lambda}_c^- pK^+\pi^-)$	*BABAR* [566]	$4.33 \pm 0.82 \pm 1.18$	4.3 ± 1.4 *3.5 ± 0.7*
$\mathcal{B}(B^0 \to \bar{\Sigma}_c(2455)^- p)$	*BABAR* [555][b]	< 2.3	< 2.3 *< 2.4*
$\mathcal{B}(B^0 \to \bar{\Sigma}_c(2455)^{--} pK^+)$	*BABAR* [566]	$1.11 \pm 0.30 \pm 0.30$	1.11 ± 0.43 *0.89 ± 0.25*
$\mathcal{B}(B^0 \to \bar{\Sigma}_c(2520)^0 p\pi^-)$	*BABAR* [556] Belle [558]	$2.2 \pm 0.7 \pm 0.6$ < 3.3	2.20 ± 0.93 *< 3.10*
$\mathcal{B}(B^0 \to \bar{\Lambda}_c^- pp\bar{p})$	*BABAR* [568][b]	< 0.22	< 0.22 *< 0.28*

[a]Measurement of $\mathcal{B}(B^+ \to \bar{\Lambda}_c^- p\pi^+)/\mathcal{B}(B^0 \to \bar{\Lambda}_c^- p)$ used in our fit.
[b]Using $\mathcal{B}(\Lambda_c^+ \to pK^-\pi^+)$.

5. Decays to exotic states

Averages of B^0 decays to exotic states are shown in Tables 76–79.

TABLE 76. Branching fractions for decays to $X(3872)$.

Parameter [10^{-5}]	Measurements		Average$^{\text{HFLAV}}_{PDG}$
$\mathcal{B}(B^0 \to X(3872)K^0)$	Belle [569][b]	$9.7 \pm 2.7 \pm 2.6$	$9.8^{+3.2}_{-2.8}$ *11.1*$^{+4.2}_{-4.1}$
	BABAR [570][b]	$7.9 \pm 4.6^{+2.3}_{-2.2}$	
	BABAR [570][c]	$9.4 \pm 5.1^{+3.0}_{-2.8}$	
	BABAR [517][d]	$12 \pm 6 \pm 5$	
	BABAR [517][b]	19^{+15+5}_{-12-6}	
	BABAR [502][e]	< 118.1	
$\mathcal{B}(B^0 \to X(3872)K^+\pi^-)$	Belle [571][c]	$21.2 \pm 3.5^{+6.3}_{-6.1}$	$21.2^{+9.3}_{-5.8}$ *20.6 ± 7.6*
$\mathcal{B}(B^0 \to X(3872)K^0) \times \mathcal{B}(X(3872) \to \chi_{c1}\gamma)$	Belle [522][a]	< 0.96	< 0.96 *None*
$\mathcal{B}(B^0 \to X(3872)K^0) \times \mathcal{B}(X(3872) \to \chi_{c2}\gamma)$	Belle [522][a]	< 1.22	< 1.2 *None*

[a]Not included in PDG average.
[b]Using $\mathcal{B}(B^+ \to X(3872)K^+)$.
[c]Using $\mathcal{B}(X(3872) \to J/\psi\pi^+\pi^-)$.
[d]Using $\mathcal{B}(X(3872) \to J/\psi\omega(782))$.
[e]Using $\mathcal{B}(X(3872) \to \bar{D}^*(2007)^0 D^0)$.

TABLE 77. Branching fractions for decays to neutral states other than $X(3872)$.

Parameter [10^{-5}]	Measurements		Average$^{\text{HFLAV}}_{PDG}$
$\mathcal{B}(B^0 \to \psi_2(3823)K^0) \times \mathcal{B}(\psi_2(3823) \to \chi_{c1}\gamma)$	Belle [522][a]	< 0.99	< 0.99 *None*
$\mathcal{B}(B^0 \to \psi_2(3823)K^0) \times \mathcal{B}(\psi_2(3823) \to \chi_{c2}\gamma)$	Belle [522][a]	< 2.28	< 2.3 *None*
$\mathcal{B}(B^0 \to Y(3940)K^0) \times \mathcal{B}(Y(3940) \to J/\psi\omega(782))$	*BABAR* [517][a]	$2.1 \pm 0.9 \pm 0.3$	2.10 ± 0.95 *None*
$\mathcal{B}(B^0 \to X(4050)^+K^+) \times \mathcal{B}(X(4050)^+ \to \chi_{c1}\pi^+)$	Belle [572] *BABAR* [533]	$3.0^{+1.5+3.7}_{-0.8-1.6}$ < 1.8	$3.0^{+4.0}_{-1.8}$
$\mathcal{B}(B^0 \to X(4250)^-K^+) \times \mathcal{B}(X(4250)^+ \to \chi_{c1}\pi^+)$	Belle [572] *BABAR* [533]	$4.0^{+2.3+19.7}_{-0.9-0.5}$ < 4.7	4^{+20}_{-1}

[a]Not included in PDG average.

TABLE 78. Branching fractions for decays to charged states.

Parameter [10^{-5}]	Measurements		Average$^{\text{HFLAV}}_{PDG}$
$\mathcal{B}(B^0 \to X(3872)^- K^+)$	*BABAR* [573]	< 50	< 50
$\mathcal{B}(B^0 \to X(3872)^- K^+) \times \mathcal{B}(X(3872)^+ \to J/\psi\pi^+\pi^0)$	*BABAR* [574][a]	< 0.54	< 0.54 *None*
$\mathcal{B}(B^0 \to Z_c(4430)^- K^+) \times \mathcal{B}(Z_c(4430)^+ \to J/\psi\pi^+)$	Belle [512]	$0.54^{+0.40+0.11}_{-0.10-0.09}$	$0.54^{+0.41}_{-0.13}$
	BABAR [575]	< 0.4	$\mathit{0.54^{+0.41}_{-0.12}}$
	LHCb [429][a,b]	$3.4 \pm 0.5^{+0.9}_{-1.9}$	$3.4^{+1.1}_{-1.5}$
$\mathcal{B}(B^0 \to Z_c(4430)^- K^+) \times \mathcal{B}(Z_c(4430)^+ \to \psi(2S)\pi^+)$	Belle [523]	$3.2^{+1.8+5.3}_{-0.9-1.6}$	$\mathit{6.0^{+3.0}_{-2.4}}$
	BABAR [575]	< 3.1	
$\mathcal{B}(B^0 \to Z_c(3900)^- K^+) \times \mathcal{B}(Z_c(3900)^+ \to J/\psi\pi^+)$	Belle [512]	< 0.090	< 0.090
$\mathcal{B}(B^0 \to Z_c(4200)^- K^+) \times \mathcal{B}(Z_c(4200)^+ \to J/\psi\pi^+)$	Belle [512]	$2.2^{+0.7+1.1}_{-0.5-0.6}$	$2.2^{+1.3}_{-0.8}$

[a]Not included in PDG average.

[b]The quoted amplitude fraction is multiplied by $\mathcal{B}(B^0 \to \psi(2S)K^+\pi^-) = (5.80 \pm 0.39) \times 10^{-4}$.

TABLE 79. Branching fraction ratios for decays to exotic states.

Parameter	Measurements		Average
$\frac{\mathcal{B}(B^0 \to Y(3940)K^0)}{\mathcal{B}(B^+ \to Y(3940)K^+)}$	*BABAR* [517]	$0.7^{+0.4}_{-0.3} \pm 0.1$	$0.70^{+0.41}_{-0.32}$

B. Decays of B^+ mesons

Measurements of B^+ decays to charmed hadrons are summarized in Secs. VII B 1–VII B 5.

1. Decays to a single open charm meson

Averages of B^+ decays to a single open charm meson are shown in Tables 80–86.

TABLE 80. Branching fractions for decays to a $\bar{D}^{(*)}$ meson and one or more light mesons.

Parameter [10^{-3}]	Measurements		Average$^{\text{HFLAV}}_{PDG}$
$\mathcal{B}(B^+ \to \bar{D}^0\pi^+)$	*BABAR* [433]	$4.90 \pm 0.07 \pm 0.22$	
	Belle [576]	$4.34 \pm 0.10 \pm 0.25$	
	BABAR [434]	$4.49 \pm 0.21 \pm 0.23$	4.66 ± 0.14
	CDF [436][b]	$4.89 \pm 0.25 \pm 0.57$	$\mathit{4.61 \pm 0.10}$
	BABAR [577][c,d]		
	Belle [578][d], [579][d]		
	LHCb [439][e], [580][d], [581][d]		
$\mathcal{B}(B^+ \to \bar{D}^0\rho^+(770))$	Belle II [582][a]	$9.39 \pm 0.21 \pm 0.50$	9.39 ± 0.54 $\mathit{13.45 \pm 1.82}$
$\mathcal{B}(B^+ \to \bar{D}^*(2007)^0\pi^+)$	LHCb [583]	$4.664 \pm 0.029 \pm 0.268$	
	Belle [576]	$4.82 \pm 0.12 \pm 0.35$	
	BABAR [433]	$5.52 \pm 0.17 \pm 0.42$	4.84 ± 0.16
	BABAR [434]	$5.13 \pm 0.22 \pm 0.28$	$\mathit{5.17 \pm 0.15}$
	BABAR [584][a,c,f]		
	Belle [435][a,f]		
	LHCb [581][f]		

(Table continued)

TABLE 80. *(Continued)*

Parameter [10^{-3}]	Measurements		Average$^{\text{HFLAV}}_{PDG}$
$\mathcal{B}(B^+ \to \bar{D}^*(2007)^0\pi^+\pi^+\pi^-)$	Belle [449]	$10.55 \pm 0.47 \pm 1.29$	10.6 ± 1.4 *10.3 ± 1.2*
$\mathcal{B}(B^+ \to \bar{D}^*(2007)^0\pi^+\pi^+\pi^+\pi^-\pi^-)$	Belle [449]	$5.67 \pm 0.91 \pm 0.85$	5.7 ± 1.2
$\mathcal{B}(B^+ \to D^-\pi^+\pi^+)$	*BABAR* [585] Belle [586]	$1.08 \pm 0.03 \pm 0.05$ $1.02 \pm 0.04 \pm 0.15$	1.073 ± 0.055
$\mathcal{B}(B^+ \to D^*(2010)^-\pi^+\pi^+)$	Belle [586] LHCb [587][g]	$1.25 \pm 0.08 \pm 0.22$	1.25 ± 0.23 *1.35 ± 0.22*
$\mathcal{B}(B^+ \to D^*(2010)^-\pi^+\pi^+\pi^+\pi^-)$	Belle [449]	$2.56 \pm 0.26 \pm 0.33$	2.56 ± 0.42

[a]Not included in PDG average.
[b]Using $\mathcal{B}(B^0 \to D^-\pi^+)$.
[c]Using non-CP modes for the D^0.
[d]Measurement of $\mathcal{B}(B^+ \to \bar{D}^0K^+)/\mathcal{B}(B^+ \to \bar{D}^0\pi^+)$ used in our fit.
[e]Measurement of $\mathcal{B}(B^+ \to \bar{D}^0\pi^+\pi^+\pi^-)/\mathcal{B}(B^+ \to \bar{D}^0\pi^+)$ used in our fit.
[f]Measurement of $\mathcal{B}(B^+ \to \bar{D}^*(2007)^0K^+)/\mathcal{B}(B^+ \to \bar{D}^*(2007)^0\pi^+)$ used in our fit.
[g]Measurement of $\mathcal{B}(B^+ \to D^*(2010)^-K^+\pi^+)/\mathcal{B}(B^+ \to D^*(2010)^-\pi^+\pi^+)$ used in our fit.

TABLE 81. Branching fractions for decays to a $\bar{D}^{(*)}$ meson and one or more kaons.

Parameter [10^{-4}]	Measurements		Average$^{\text{HFLAV}}_{PDG}$
$\mathcal{B}(B^+ \to \bar{D}^0K^+)$	LHCb [581][c]	$3.711 \pm 0.014 \pm 0.126$	3.67 ± 0.12 *3.64 ± 0.15*
	LHCb [580][c]	$3.632 \pm 0.028^{+0.140}_{-0.139}$	
	Belle [578][c]	$3.156 \pm 0.107^{+0.169}_{-0.168}$	
	BABAR [577][d,c]	$3.874 \pm 0.163^{+0.149}_{-0.148}$	
	Belle [579][c]	$3.59 \pm 0.23 \pm 0.30$	
	Belle [578][e]		
	LHCb [583][f,g]		
$\mathcal{B}(B^+ \to \bar{D}^0K^*(892)^+)$	*BABAR* [588]	$5.29 \pm 0.30 \pm 0.34$	5.29 ± 0.45 *5.32 ± 0.45*
$\mathcal{B}(B^+ \to \bar{D}^0K^+\pi^+\pi^-)$	LHCb [443][h]	$5.02 \pm 0.69^{+0.72}_{-0.71}$	5.0 ± 1.0 *5.2 ± 2.1*
$\mathcal{B}(B^+ \to \bar{D}^0K^+\bar{K}^0)$	Belle [464] Belle II [463][a,i]	$5.5 \pm 1.4 \pm 0.8$	3.73 ± 0.35 *5.50 ± 1.61*
$\mathcal{B}(B^+ \to \bar{D}^0\bar{K}^*(892)^0K^+)$	Belle [464][b]	$7.5 \pm 1.3 \pm 1.1$	7.5 ± 1.7 *None*
$\mathcal{B}(B^+ \to \bar{D}^*(2007)^0K^+)$	LHCb [581][b,j]	$4.122 \pm 0.058 \pm 0.270$	3.92 ± 0.18 *None*
	BABAR [584][b,d,j]	$3.938 \pm 0.194^{+0.242}_{-0.199}$	
	LHCb [583][b,f,k]	$3.637 \pm 0.282^{+0.117}_{-0.115}$	
	Belle [435][b,j]	$3.78 \pm 0.92 \pm 0.45$	
$\mathcal{B}(B^+ \to \bar{D}^*(2007)^0K^*(892)^+)$	*BABAR* [589]	$8.3 \pm 1.1 \pm 1.0$	8.3 ± 1.5 *8.1 ± 1.4*
$\mathcal{B}(B^+ \to \bar{D}^*(2007)^0K^+\bar{K}^0)$	Belle [464] Belle II [463][a,l]	< 10.6	2.94 ± 0.58 *< 10.60*

(Table continued)

TABLE 81. *(Continued)*

Parameter [10^{-4}]	Measurements		Average$^{\text{HFLAV}}_{PDG}$
$\mathcal{B}(B^+ \to \bar{D}^*(2007)^0 \bar{K}^*(892)^0 K^+)$	Belle [464][b]	$15.3 \pm 3.1 \pm 2.9$	15.3 ± 4.2 *None*
$\mathcal{B}(B^+ \to D^- K^+ \pi^+)$	LHCb [590]	$0.731 \pm 0.019 \pm 0.045$	0.731 ± 0.049 *0.772 ± 0.050*
$\mathcal{B}(B^+ \to D^*(2010)^- K^+ \pi^+)$	LHCb [587][m]	$0.799 \pm 0.034 \pm 0.161$	0.80 ± 0.16 *0.82 ± 0.14*
$\mathcal{B}(B^0 \to D^- K^+ \bar{K}^*(892)^0)$	Belle II [463][a]	$7.56 \pm 0.45 \pm 0.38$	7.56 ± 0.59 *8.80 ± 1.86*
$\mathcal{B}(B^0 \to D^*(2010)^- K^+ \bar{K}^*(892)^0)$	Belle II [463][a]	$13.12 \pm 1.21 \pm 0.71$	13.1 ± 1.4 *12.9 ± 3.3*

[a]Preliminary result.
[b]Not included in PDG average.
[c]Using $\mathcal{B}(B^+ \to \bar{D}^0 \pi^+)$.
[d]Using non-CP modes for the D^0.
[e]Measurement of $\mathcal{B}(B^+ \to D^0 K^+)/\mathcal{B}(B^+ \to \bar{D}^0 K^+)$ used in our fit.
[f]Statistical and systematic uncertainties are combined.
[g]Measurement of $\mathcal{B}(B^+ \to \bar{D}^*(2007)^0 K^+)/\mathcal{B}(B^+ \to \bar{D}^0 K^+)$ used in our fit.
[h]Using $\mathcal{B}(B^+ \to \bar{D}^0 \pi^+ \pi^+ \pi^-)$.
[i]Measurement of $\mathcal{B}(B^+ \to \bar{D}^0 K^+ \bar{K}^0)/2$ used in our fit.
[j]Using $\mathcal{B}(B^+ \to \bar{D}^*(2007)^0 \pi^+)$.
[k]Using $\mathcal{B}(B^+ \to \bar{D}^0 K^+)$.
[l]Measurement of $\mathcal{B}(B^+ \to \bar{D}^*(2007)^0 K^+ \bar{K}^0)/2$ used in our fit.
[m]Using $\mathcal{B}(B^+ \to D^*(2010)^- \pi^+ \pi^+)$.

TABLE 82. Branching fractions for decays to a $D^{(*)}$ meson.

Parameter [10^{-6}]	Measurements		Average$^{\text{HFLAV}}_{PDG}$
$\mathcal{B}(B^+ \to D^0 K^+)$	Belle [578][a,b]	< 70	< 70 *4 ± 0*
$\mathcal{B}(B^+ \to D^+ K^0)$	*BABAR* [591] Belle [460][a]	$-3.8^{+2.2+1.2}_{-1.8-1.6}$ < 2	-3.8 ± 2.5 *< 2.9*
$\mathcal{B}(B^+ \to D^+ K^*(892)^0)$	*BABAR* [591]	$-5.3^{+2.3+1.4}_{-2.0-1.8}$	-5.3 ± 2.7 *< 0.5*
$\mathcal{B}(B^+ \to D^+ K^+ \pi^-)$	LHCb [592]	$5.31 \pm 0.90 \pm 0.59$	5.3 ± 1.1 *5.6 ± 1.1*
$\mathcal{B}(B^+ \to D^*(2010)^+ K^0)$	*BABAR* [593]	< 9.0	< 9.0
$\mathcal{B}(B^+ \to D^*(2010)^+ \pi^0)$	Belle [594]	< 3.6	< 3.6

[a]Not included in PDG average.
[b]Using $\mathcal{B}(B^+ \to \bar{D}^0 K^+)$.

TABLE 83. Branching fractions for decays to excited D mesons.

Parameter [10^{-4}]	Measurements		Average$^{\text{HFLAV}}_{PDG}$
$\mathcal{B}(B^+ \to \bar{D}^{**0}\pi^+)$[1]	*BABAR* [434]	$55 \pm 5 \pm 10$	55 ± 12 *56 ± 12*
$\mathcal{B}(B^+ \to \bar{D}_0^*(2300)^0\pi^+) \times \mathcal{B}(D_0^*(2300)^0 \to D^+\pi^-)$	*BABAR* [585] Belle [586]	$6.8 \pm 0.3 \pm 2.0$ $6.1 \pm 0.6 \pm 1.8$	6.4 ± 1.4
$\mathcal{B}(B^+ \to \bar{D}_1(2420)^0\pi^+) \times \mathcal{B}(D_1(2420)^0 \to D^*(2010)^+\pi^-)$	Belle [586]	$6.8 \pm 0.7 \pm 1.3$	6.8 ± 1.5 *7.4 ± 1.0*
$\mathcal{B}(B^+ \to \bar{D}_1(2420)^0\pi^+) \times \mathcal{B}(D_1(2420)^0 \to D^0\pi^+\pi^-)$	Belle [476] LHCb [439][c]	$1.85 \pm 0.29^{+0.35}_{-0.58}$ $5.50 \pm 0.80^{+0.76}_{-0.74}$	$2.55^{+0.41}_{-0.42}$ $2.55^{+1.59}_{-1.42}$
$\mathcal{B}(B^+ \to \bar{D}_1(2420)^0\pi^+) \times \mathcal{B}(D_1(2420)^0 \to D^0\pi^+\pi^-(\text{NR}))$	LHCb [439][d,c]	$2.14 \pm 0.37 \pm 0.35$	$2.14^{+0.53}_{-0.49}$ *2.20 ± 0.93*
$\mathcal{B}(B^+ \to \bar{D}_1(2420)^0\pi^+) \times \mathcal{B}(D_1(2420)^0 \to D^*(2007)^0\pi^+\pi^-)$	Belle [476]	< 0.06	< 0.060
$\mathcal{B}(B^+ \to \bar{D}_1(2430)^0\pi^+) \times \mathcal{B}(D_1(2430)^0 \to D^*(2010)^+\pi^-)$	Belle [586][a] LHCb [439][a,c]	$5.0 \pm 0.4 \pm 1.1$ $4.97 \pm 0.85^{+0.72}_{-0.70}$	$4.98^{+0.82}_{-0.79}$ *3.51 ± 0.61*
$\mathcal{B}(B^+ \to \bar{D}_2^*(2460)^0\pi^+) \times \mathcal{B}(D_2^*(2460)^0 \to D^+\pi^-)$	*BABAR* [585] Belle [586]	$3.5 \pm 0.2 \pm 0.4$ $3.4 \pm 0.3 \pm 0.7$	3.47 ± 0.42 *3.56 ± 0.24*
$\mathcal{B}(B^+ \to \bar{D}_2^*(2460)^0\pi^+) \times \mathcal{B}(D_2^*(2460)^0 \to D^*(2010)^+\pi^-)$	Belle [586] LHCb [439][a,c]	$1.8 \pm 0.3 \pm 0.4$ $2.08 \pm 0.64^{+0.31}_{-0.30}$	1.89 ± 0.39 *1.98 ± 0.30*
$\mathcal{B}(B^+ \to \bar{D}_2^*(2460)^0\pi^+) \times \mathcal{B}(D_2^*(2460)^0 \to D^0\pi^+\pi^-)$	LHCb [439][d,c] LHCb [439][c]	$0.75 \pm 0.32 \pm 0.13$ $2.14 \pm 0.53 \pm 0.31$	$1.10^{+0.33}_{-0.30}$ *2.20 ± 1.00*
$\mathcal{B}(B^+ \to \bar{D}_2^*(2460)^0\pi^+) \times \mathcal{B}(D_2^*(2460)^0 \to D^*(2007)^0\pi^+\pi^-)$	Belle [476]	< 0.22	< 0.22

[a]Not included in PDG average.
[b]D^{**} refers to the sum of all the non-strange charm meson states with masses in the range 2.2–2.8 GeV/c^2.
[c]Using $\mathcal{B}(B^+ \to \bar{D}^0\pi^+\pi^+\pi^-)$.
[d]Non-D^*.

TABLE 84. Branching fractions for decays to $D_s^{(*)}$ mesons.

Parameter [10^{-5}]	Measurements		Average$^{\text{HFLAV}}_{PDG}$
$\mathcal{B}(B^+ \to D_s^- K^+\pi^+)$	Belle [595] *BABAR* [473]	$19.4^{+0.9}_{-0.8} \pm 2.6$ $20.2 \pm 1.3 \pm 3.8$	19.7 ± 2.3 *18.0 ± 2.2*
$\mathcal{B}(B^+ \to D_s^- K^+K^+)$	*BABAR* [473]	$1.1 \pm 0.4 \pm 0.2$	1.10 ± 0.45 *0.97 ± 0.21*
$\mathcal{B}(B^+ \to D_s^{*-} K^+\pi^+)$	Belle [595] *BABAR* [473]	$14.7^{+1.5}_{-1.4} \pm 2.3$ $16.7 \pm 1.6 \pm 3.5$	15.4 ± 2.2 *14.5 ± 2.4*
$\mathcal{B}(B^+ \to D_s^{*-} K^+K^+)$	*BABAR* [473]	< 1.5	< 1.5
$\mathcal{B}(B^+ \to D_s^+\pi^0)$	*BABAR* [596]	$1.5^{+0.5}_{-0.4} \pm 0.2$	$1.50^{+0.55}_{-0.46}$ $1.56^{+0.57}_{-0.52}$
$\mathcal{B}(B^+ \to D_s^+ K^+K^-)$	LHCb [597][a]		0.79 ± 0.10 *0.72 ± 0.11*
$\mathcal{B}(B^+ \to D_s^+\phi(1020))$	LHCb [597] *BABAR* [598]	$0.012^{+0.016}_{-0.014} \pm 0.008$ < 0.19	$0.012^{+0.018}_{-0.016}$ *< 0.042*
$\mathcal{B}(B^+ \to D_s^{*+}\phi(1020))$	*BABAR* [598]	< 1.2	< 1.2

[a]Measurement of $\mathcal{B}(B^+ \to D_s^+ K^+K^-)/(\mathcal{B}(B^+ \to D_s^+\bar{D}^0)\mathcal{B}(D^0 \to K^+K^-))$ used in our fit.

TABLE 85. Branching fractions for decays to a $D^{(*)}$ meson and baryons.

Parameter [10^{-4}]	Measurements		Average$^{\text{HFLAV}}_{PDG}$
$\mathcal{B}(B^+ \to \bar{D}^0 p\bar{p}\pi^+)$	*BABAR* [478]	$3.72 \pm 0.11 \pm 0.25$	3.72 ± 0.27
$\mathcal{B}(B^+ \to \bar{D}^0 \bar{\Lambda}^0 p)$	Belle [599]	$0.143^{+0.028}_{-0.025} \pm 0.018$	0.143 ± 0.032 $0.143^{+0.033}_{-0.031}$
$\mathcal{B}(B^+ \to \bar{D}^*(2007)^0 p\bar{p}\pi^+)$	*BABAR* [478]	$3.73 \pm 0.17 \pm 0.27$	3.73 ± 0.32
$\mathcal{B}(B^+ \to \bar{D}^*(2007)^0 \bar{\Lambda}^0 p)$	Belle [599]	< 0.48	< 0.48 < 0.50
$\mathcal{B}(B^+ \to D^- p\bar{p}\pi^+\pi^+)$	*BABAR* [478]	$1.66 \pm 0.13 \pm 0.27$	1.66 ± 0.30
$\mathcal{B}(B^+ \to D^*(2010)^- p\bar{p}\pi^+\pi^+)$	*BABAR* [478]	$1.86 \pm 0.16 \pm 0.19$	1.86 ± 0.25
$\mathcal{B}(B^+ \to D^+ p\bar{p})$	Belle [479]	< 0.15	< 0.15
$\mathcal{B}(B^+ \to D^*(2010)^+ p\bar{p})$	Belle [479]	< 0.15	< 0.15

TABLE 86. Branching fractions of lepton number violating decays.

Parameter [10^{-6}]	Measurements		Average$^{\text{HFLAV}}_{PDG}$
$\mathcal{B}(B^+ \to D^- e^+ e^+)$	Belle [600]	< 2.6	< 2.6
$\mathcal{B}(B^+ \to D^- \mu^+ e^+)$	Belle [600]	< 1.8	< 1.8
$\mathcal{B}(B^+ \to D^- \mu^+ \mu^+)$	Belle [600]	< 1.0	< 1.0 < 0.7

2. Decays to two open charm mesons

Averages of B^+ decays to two open charm mesons are shown in Tables 87–90.

TABLE 87. Branching fractions for decays to $D^{(*)-}D^{(*)0}$.

Parameter [10^{-4}]	Measurements		Average$^{\text{HFLAV}}_{PDG}$
$\mathcal{B}(B^+ \to D^+ \bar{D}^0)$	Belle [489]	$3.85 \pm 0.31 \pm 0.38$	4.03 ± 0.21
	BABAR [485]	$3.8 \pm 0.6 \pm 0.5$	*3.84 ± 0.42*
	LHCb [601][a,b,c,d,e,f,g], [602][a,h,i]		
$\mathcal{B}(B^+ \to \bar{D}^*(2007)^0 D^+)$	*BABAR* [485]	$6.3 \pm 1.4 \pm 1.0$	6.3 ± 1.7
$\mathcal{B}(B^+ \to D^*(2010)^+ \bar{D}^0)$	*BABAR* [485]	$3.6 \pm 0.5 \pm 0.4$	3.80 ± 0.22
	Belle [603]	$4.59 \pm 0.72 \pm 0.56$	*3.92 ± 0.52*
	LHCb [602][a,i]		
$\mathcal{B}(B^+ \to D^*(2010)^+ \bar{D}^*(2007)^0)$	*BABAR* [485]	$8.1 \pm 1.2 \pm 1.2$	8.1 ± 1.7

[a]Not included in PDG average.

[b]Measurement of $f_c \times \mathcal{B}(B_c^+ \to D^+\bar{D}^0)/(f_u \mathcal{B}(B^+ \to D^+\bar{D}^0))$ used in our fit.

[c]Measurement of $f_c \times \mathcal{B}(B_c^+ \to D^+ D^0)/(f_u \mathcal{B}(B^+ \to D^+\bar{D}^0))$ used in our fit.

[d]Measurement of $f_c \times (\mathcal{B}(B_c^- \to D^{*-}D^0) \times \mathcal{B}(D^{*-} \to D^-(\pi^0,\gamma)) + \mathcal{B}(B_c^- \to D^- D^{*0}))/(f_u \mathcal{B}(B^+ \to D^+\bar{D}^0))$ used in our fit.

[e]Measurement of $f_c \times (\mathcal{B}(B_c^- \to D^{*-}\bar{D}^0) \times \mathcal{B}(D^{*-} \to D^-(\pi^0,\gamma)) + \mathcal{B}(B_c^- \to D^-\bar{D}^{*0}))/(f_u \mathcal{B}(B^+ \to D^+\bar{D}^0))$ used in our fit.

[f]Measurement of $f_c \times \mathcal{B}(B_c^+ \to D^*(2010)^+\bar{D}^*(2007)^0)/(f_u \mathcal{B}(B^+ \to D^+\bar{D}^0))$ used in our fit.

[g]Measurement of $f_c \times \mathcal{B}(B_c^+ \to D^*(2010)^+ D^*(2007)^0)/(f_u \mathcal{B}(B^+ \to D^+\bar{D}^0))$ used in our fit.

[h]Measurement of $\mathcal{B}(B^+ \to D^+\bar{D}^0)\mathcal{B}(D^+ \to K^-\pi^+\pi^+)/(\mathcal{B}(B^+ \to D_s^+\bar{D}^0)\mathcal{B}(D_s^+ \to K^-K^+\pi^+))$ used in our fit.

[i]Measurement of $\mathcal{B}(B^+ \to D^*(2010)^+\bar{D}^0)\mathcal{B}(D^*(2010)^+ \to D^0\pi^+)\mathcal{B}(D^0 \to K^-\pi^+)/(\mathcal{B}(B^+ \to D^+\bar{D}^0)\mathcal{B}(D^+ \to K^-\pi^+\pi^+))$ used in our fit.

TABLE 88. Branching fractions for decays to two D mesons and a kaon.

Parameter [10^{-3}]	Measurements		Average$^{\text{HFLAV}}_{PDG}$
$\mathcal{B}(B^+ \to \bar{D}^*(2007)^0 D^0 K^+)$	*BABAR* [490]	$2.26 \pm 0.16 \pm 0.17$	2.26 ± 0.23
$\mathcal{B}(B^+ \to D^*(2007)^0 \bar{D}^0 K^+)$	*BABAR* [490]	$6.32 \pm 0.19 \pm 0.45$	6.32 ± 0.49
$\mathcal{B}(B^+ \to D^*(2007)^0 \bar{D}^*(2007)^0 K^+)$	*BABAR* [490]	$11.23 \pm 0.36 \pm 1.26$	11.2 ± 1.3
$\mathcal{B}(B^+ \to \bar{D}^*(2007)^0 D^+ K^0)$	*BABAR* [490]	$2.06 \pm 0.38 \pm 0.30$	2.06 ± 0.48
$\mathcal{B}(B^+ \to D^*(2010)^+ \bar{D}^0 K^0)$	*BABAR* [490]	$3.81 \pm 0.31 \pm 0.23$	3.81 ± 0.39
$\mathcal{B}(B^+ \to D^*(2010)^+ \bar{D}^*(2007)^0 K^0)$	*BABAR* [490]	$9.17 \pm 0.83 \pm 0.90$	9.2 ± 1.2
$\mathcal{B}(B^+ \to D^0 \bar{D}^0 K^+)$	*BABAR* [490]	$1.31 \pm 0.07 \pm 0.12$	1.45 ± 0.13
	Belle [604]	$2.22 \pm 0.22^{+0.26}_{-0.24}$	*1.45 ± 0.33*
$\mathcal{B}(B^+ \to D^0 \bar{D}^0 K^+ \pi^0)$	Belle [493][a]	$0.107 \pm 0.031^{+0.019}_{-0.033}$	$0.107^{+0.036}_{-0.045}$ *None*
$\mathcal{B}(B^+ \to D^+ D^- K^+)$	*BABAR* [490]	$0.22 \pm 0.05 \pm 0.05$	$0.219^{+0.072}_{-0.070}$
	Belle [605]	< 0.9	*0.220 ± 0.071*
	LHCb [606][a,b]		
$\mathcal{B}(B^+ \to D^*(2010)^- D^+ K^+)$	*BABAR* [490]	$0.6 \pm 0.1 \pm 0.1$	0.60 ± 0.13
$\mathcal{B}(B^+ \to D^*(2010)^+ D^- K^+)$	*BABAR* [490]	$0.63 \pm 0.09 \pm 0.06$	0.63 ± 0.11
$\mathcal{B}(B^+ \to D^*(2010)^+ D^*(2010)^- K^+)$	*BABAR* [490]	$1.32 \pm 0.13 \pm 0.12$	1.32 ± 0.18
$\mathcal{B}(B^+ \to D^+ \bar{D}^0 K^0)$	*BABAR* [490]	$1.55 \pm 0.17 \pm 0.13$	1.55 ± 0.21
$\mathcal{B}(B^+ \to D_s^+ D_s^- K^+)$	LHCb [606][a,c]	$0.1150 \pm 0.0072^{+0.0386}_{-0.0376}$	$0.115^{+0.041}_{-0.038}$ *None*

[a]Not included in PDG average.
[b]Measurement of $\mathcal{B}(B^+ \to D_s^+ D_s^- K^+)/\mathcal{B}(B^+ \to D^+ D^- K^+)$ used in our fit.
[c]Using $\mathcal{B}(B^+ \to D^+ D^- K^+)$.

TABLE 89. Branching fractions for decays to $D_s^{(*)-} D^{(*)+}$.

Parameter [10^{-3}]	Measurements		Average$^{\text{HFLAV}}_{PDG}$
$\mathcal{B}(B^+ \to D_s^+ \bar{D}^0)$	LHCb [486][c]	$9.96 \pm 0.16 \pm 0.77$	
	Belle II [463][a]	$9.5 \pm 0.6 \pm 0.5$	$9.74^{+0.46}_{-0.47}$
	BABAR [495][d]	$8.9 \pm 1.4 \pm 1.5$	*9.01 ± 0.94*
	BABAR [495]	$13.3 \pm 1.8 \pm 3.2$	
	LHCb [486][e,f], [597][g], [601][b,h,i,j,k,l,m], [602][b,n]		
$\mathcal{B}(B^+ \to D_s^+ \bar{D}^*(2007)^0)$	Belle II [463][a]	$6.5 \pm 1.0 \pm 0.6$	7.03 ± 0.91
	BABAR [495][d]	$6.60 \pm 1.45 \pm 0.92$	*8.22 ± 1.72*
	BABAR [495]	$12.1 \pm 2.3 \pm 2.0$	
$\mathcal{B}(B^+ \to D_s^{*+} \bar{D}^0)$	*BABAR* [495]	$9.3 \pm 1.8 \pm 1.9$	8.3 ± 2.0
	BABAR [495][d]	$7.00 \pm 2.66 \pm 1.38$	*7.6 ± 1.6*

(Table continued)

TABLE 89. *(Continued)*

Parameter $[10^{-3}]$	Measurements		Average$^{\text{HFLAV}}_{PDG}$
$\mathcal{B}(B^+ \to D_s^{*+}\bar{D}^*(2007)^0)$	*BABAR* [495]	$17 \pm 3 \pm 2$	17.9 ± 2.7
	BABAR [495][d]	$19.17 \pm 3.31^{+2.83}_{-2.82}$	*17.1 ± 2.4*

[a]Preliminary result.
[b]Not included in PDG average.
[c]Using $\mathcal{B}(B^0 \to D_s^+ D^-)$.
[d]Using $\mathcal{B}(D_s^+ \to \phi(1020)\pi^+)$.
[e]Measurement of $\mathcal{B}(B_s^0 \to D^0\bar{D}^0)/\mathcal{B}(B^+ \to D_s^+\bar{D}^0)$ used in our fit.
[f]Measurement of $\mathcal{B}(B^0 \to D^0\bar{D}^0)/\mathcal{B}(B^+ \to D_s^+\bar{D}^0)$ used in our fit.
[g]Measurement of $\mathcal{B}(B^+ \to D_s^+K^+K^-)/(\mathcal{B}(B^+ \to D_s^+\bar{D}^0)\mathcal{B}(D^0 \to K^+K^-))$ used in our fit.
[h]Measurement of $f_c \times \mathcal{B}(B_c^+ \to D_s^+\bar{D}^0)/(f_u\mathcal{B}(B^+ \to D_s^+\bar{D}^0))$ used in our fit.
[i]Measurement of $f_c \times \mathcal{B}(B_c^+ \to D_s^+D^0)/(f_u\mathcal{B}(B^+ \to D_s^+\bar{D}^0))$ used in our fit.
[j]Measurement of $f_c \times \mathcal{B}(B_c^+ \to D_s^{*+}\bar{D}^0 + D_s^+\bar{D}^*(2007)^0)/(f_u\mathcal{B}(B^+ \to D_s^+\bar{D}^0))$ used in our fit.
[k]Measurement of $f_c \times \mathcal{B}(B_c^+ \to D_s^{*+}D^0 + D_s^+D^*(2007)^0)/(f_u\mathcal{B}(B^+ \to D_s^+\bar{D}^0))$ used in our fit.
[l]Measurement of $f_c \times \mathcal{B}(B_c^+ \to D_s^{*+}\bar{D}^*(2007)^0)/(f_u\mathcal{B}(B^+ \to D_s^+\bar{D}^0))$ used in our fit.
[m]Measurement of $f_c \times \mathcal{B}(B_c^+ \to D_s^{*+}D^*(2007)^0)/(f_u\mathcal{B}(B^+ \to D_s^+\bar{D}^0))$ used in our fit.
[n]Measurement of $\mathcal{B}(B^+ \to D^+\bar{D}^0)\mathcal{B}(D^+ \to K^-\pi^+\pi^+)/(\mathcal{B}(B^+ \to D_s^+\bar{D}^0)\mathcal{B}(D_s^+ \to K^-K^+\pi^+))$ used in our fit.

TABLE 90. Branching fractions for decays to excited D_s mesons.

Parameter $[10^{-3}]$	Measurements		Average$^{\text{HFLAV}}_{PDG}$
$\mathcal{B}(B^+ \to D_{s0}^*(2317)^+\bar{D}^0)$	Belle [499][b]	$0.80^{+0.13+0.12}_{-0.12-0.20}$	$0.83^{+0.25}_{-0.15}$
	BABAR [500][b]	$1.0 \pm 0.3^{+0.4}_{-0.3}$	*0.80*$^{+0.16}_{-0.13}$
$\mathcal{B}(B^+ \to D_{s0}^*(2317)^+\bar{D}^*(2007)^0)$	*BABAR* [500][a,b]	$0.9 \pm 0.6^{+0.4}_{-0.3}$	0.90 ± 0.68 *None*
$\mathcal{B}(B^+ \to D_{s1}(2460)^+\bar{D}^0)$	Belle [501][c]	$3.05^{+0.87}_{-0.82} \pm 1.04$	
	Belle [501][d]	$2.23^{+1.14}_{-0.92} \pm 0.76$	
	BABAR [500][c]	$3.3 \pm 1.1^{+1.3}_{-0.9}$	3.28 ± 0.78
	BABAR [500][d]	$5.1 \pm 1.3^{+2.1}_{-1.7}$	*3.09*$^{+0.97}_{-0.87}$
	BABAR [495]	$4.3 \pm 1.6 \pm 1.3$	
	Belle [501][e]	< 5.1	
$\mathcal{B}(B^+ \to D_{s1}(2460)^+\bar{D}^*(2007)^0)$	*BABAR* [500][c]	$7.6 \pm 2.2^{+3.4}_{-2.6}$	10.5 ± 2.4
	BABAR [495]	$11.2 \pm 2.6 \pm 2.0$	*12.0*$^{+3.1}_{-3.0}$
	BABAR [500][d]	$14.2 \pm 3.2^{+6.3}_{-5.0}$	
$\mathcal{B}(B^+ \to D_{s1}(2536)^+\bar{D}^0)$	*BABAR* [502][1,f]	$0.453 \pm 0.109 \pm 0.112$	0.405 ± 0.084
	BABAR [502][a,g]	$0.41 \pm 0.17 \pm 0.09$	*None*
	Belle [503][a,h]		
$\mathcal{B}(B^+ \to D_{s1}(2536)^+\bar{D}^*(2007)^0)$	*BABAR* [502][a,f]	$1.145 \pm 0.245 \pm 0.267$	$1.15^{+0.38}_{-0.35}$
	BABAR [502][a,g]	< 1.901	*None*

[a]Not included in PDG average.
[b]Using $\mathcal{B}(D_{s0}^*(2317)^+ \to D_s^+\pi^0)$.
[c]Using $\mathcal{B}(D_{s1}(2460)^+ \to D_s^+\gamma)$.
[d]Using $\mathcal{B}(D_{s1}(2460)^+ \to D_s^{*+}\pi^0)$.
[e]Using $\mathcal{B}(D_{s1}(2460)^+ \to D_s^+\pi^+\pi^-)$.
[f]Using $\mathcal{B}(D_{s1}(2536)^+ \to D^*(2007)^0K^+)$.
[g]Using $\mathcal{B}(D_{s1}(2536)^+ \to D^*(2010)^+K^0)$.
[h]Measurement of $\mathcal{B}(B^+ \to D_{s1}(2536)^+\bar{D}^0)(\mathcal{B}(D_{s1}(2536)^+ \to D^*(2007)^0K^+) + \mathcal{B}(D_{s1}(2536)^+ \to D^*(2010)^+K^0))$ used in our fit.

3. Decays to charmonium states

Averages of B^+ decays to charmonium states are shown in Tables 91–97.

TABLE 91. Branching fractions for decays to J/ψ and one kaon.

Parameter $[10^{-4}]$	Measurements		Average$^{\text{HFLAV}}_{PDG}$
$\mathcal{B}(B^+ \to J/\psi K^+)$	BELLE [504]	$10.32 \pm 0.07 \pm 0.24$	
	BABAR [12]	$10.61 \pm 0.15 \pm 0.48$	
	Belle [505]	$10.1 \pm 0.2 \pm 0.7$	
	Belle [508][b]	$9.93^{+0.58+0.69}_{-0.56-0.68}$	
	Belle [576]	$8.9 \pm 0.6 \pm 0.5$	
	Belle [607][a,c]	$10.38 \pm 0.61 \pm 0.49$	
	BABAR [608][c]	$10.3 \pm 0.9 \pm 0.5$	10.18 ± 0.18
	BABAR [573]	$8.1 \pm 1.3 \pm 0.7$	*10.20 ± 0.19*
	Belle [607][a,d]	$10.6^{+1.8}_{-1.5} \pm 1.9$	
	BABAR [507][e], [609][f], [12][g], [573][e]		
	Belle [610][a,h], [519][a,i,j]		
	CDF [509][g], [611][f], [612][f]		
	CMS [613][a,k]		
	D0 [614][l]		
	LHCb [615][a,m,k], [515][l], [616][n], [617][a,o,k]		
$\mathcal{B}(B^+ \to J/\psi K^*(892)^+)$	*BABAR* [12][p]	$13.9 \pm 0.5^{+0.9}_{-0.8}$	
	Belle [618]	$12.8 \pm 0.7 \pm 1.4$	13.77 ± 0.81
	CDF [506]	$15.8 \pm 4.7 \pm 2.7$	*14.30 ± 0.81*
	CDF [509][p]	$19.5 \pm 6.1 \pm 1.8$	
$\mathcal{B}(B^+ \to J/\psi K_1(1270)^+)$	Belle [519][p]	$18 \pm 3 \pm 3$	18.3 ± 4.9
	Belle [519][q]		*18.0 ± 5.2*
$\mathcal{B}(B^+ \to J/\psi K_1(1400)^+)$	Belle [519][r]	< 5	< 5.5
			< 5.0
$\mathcal{B}(B^+ \to J/\psi K^+\pi^+\pi^-)$	Belle [619]	$7.16 \pm 0.10 \pm 0.60$	8.07 ± 0.52
	BABAR [620]	$11.6 \pm 0.7 \pm 0.9$	p = 0.23%
	CDF [621]	$6.9 \pm 1.8 \pm 1.2$	*8.11 ± 1.28*
$\mathcal{B}(B^+ \to J/\psi \eta K^+)$	Belle [520]	$1.27 \pm 0.11 \pm 0.11$	1.24 ± 0.14
	BABAR [521]	$1.08 \pm 0.23 \pm 0.24$	
$\mathcal{B}(B^+ \to J/\psi \omega(782) K^+)$	*BABAR* [517]	$3.2 \pm 0.1^{+0.6}_{-0.3}$	$3.22^{+0.51}_{-0.31}$
	BABAR [517][s]		$3.20^{+0.61}_{-0.32}$

(Table continued)

TABLE 91. *(Continued)*

Parameter $[10^{-4}]$	Measurements		Average$^{\text{HFLAV}}_{PDG}$
$\mathcal{B}(B^+ \to J/\psi\phi(1020)K^+)$	*BABAR* [518]	$0.44 \pm 0.14 \pm 0.05$	0.44 ± 0.15
	D0 [622][t]		*0.50 ± 0.04*
	LHCb [623][a,u,t], [623][a,u,v]		

[a]Not included in PDG average.
[b]Using $\mathcal{B}(J/\psi \to p\bar{p}\pi^+\pi^-)$.
[c]Using $\mathcal{B}(J/\psi \to p\bar{p})$.
[d]Using $\mathcal{B}(J/\psi \to \Lambda^0\bar{\Lambda}^0)$.
[e]Measurement of $\mathcal{B}(B^+ \to \eta_c K^+)/\mathcal{B}(B^+ \to J/\psi K^+)$ used in our fit.
[f]Measurement of $\mathcal{B}(B^+ \to J/\psi\pi^+)/\mathcal{B}(B^+ \to J/\psi K^+)$ used in our fit.
[g]Measurement of $\mathcal{B}(B^+ \to J/\psi K^*(892)^+)/\mathcal{B}(B^+ \to J/\psi K^+)$ used in our fit.
[h]Measurement of $\mathcal{B}(B^+ \to \chi_{c0}K^+)/\mathcal{B}(B^+ \to J/\psi K^+)$ used in our fit.
[i]Measurement of $\mathcal{B}(B^+ \to J/\psi K_1(1270)^+)/\mathcal{B}(B^+ \to J/\psi K^+)$ used in our fit.
[j]Measurement of $\mathcal{B}(B^0 \to J/\psi K_1(1270)^0)/\mathcal{B}(B^+ \to J/\psi K^+)$ used in our fit.
[k]Measurement of $f_c \times \mathcal{B}(B_c^+ \to J/\psi\pi^+)/(f_u\mathcal{B}(B^+ \to J/\psi K^+))$ used in our fit.
[l]Measurement of $\mathcal{B}(B^+ \to \psi(2S)K^+)/\mathcal{B}(B^+ \to J/\psi K^+)$ used in our fit.
[m]$\sqrt{s} = 7$ TeV, $p_T > 4$ GeV and $2.5 < y < 4.5$.
[n]Measurement of $(\mathcal{B}(B^+ \to \eta_c K^+)\mathcal{B}(\eta_c \to p\bar{p}))/(\mathcal{B}(B^+ \to J/\psi K^+)\mathcal{B}(J/\psi \to p\bar{p}))$ used in our fit.
[o]$\sqrt{s} = 8$ TeV, $0 < p_T < 20$ GeV and $2.0 < y < 4.5$.
[p]Using $\mathcal{B}(B^+ \to J/\psi K^+)$.
[q]Measurement of $\mathcal{B}(B^+ \to J/\psi K_1(1400)^+)/\mathcal{B}(B^+ \to J/\psi K_1(1270)^+)$ used in our fit.
[r]Using $\mathcal{B}(B^+ \to J/\psi K_1(1270)^+)$.
[s]Measurement of $\mathcal{B}(B^0 \to J/\psi\omega(782)K^0)/\mathcal{B}(B^+ \to J/\psi\omega(782)K^+)$ used in our fit.
[t]Measurement of $\mathcal{B}(B^+ \to \chi_{c1}(4140)K^+) \times \mathcal{B}(\chi_{c1}(4140) \to J/\psi\phi(1020))/\mathcal{B}(B^+ \to J/\psi\phi(1020)K^+)$ used in our fit.
[u]The quoted value is a fit fraction from a Dalitz plot fit.
[v]Measurement of $\mathcal{B}(B^+ \to \chi_{c1}(4274)K^+) \times \mathcal{B}(\chi_{c1}(4274) \to J/\psi\phi(1020))/\mathcal{B}(B^+ \to J/\psi\phi(1020)K^+)$ used in our fit.

TABLE 92. Branching fractions for decays to charmonium other than J/ψ and one kaon.

Parameter $[10^{-4}]$	Measurements		Average$^{\text{HFLAV}}_{PDG}$
$\mathcal{B}(B^+ \to \psi(2S)K^+)$	LHCb [515][b]	$6.05 \pm 0.06 \pm 0.25$	6.17 ± 0.20
	BABAR [12]	$6.17 \pm 0.32 \pm 0.44$	
	D0 [614][b]	$6.6 \pm 0.4 \pm 0.8$	
	Belle [505]	6.9 ± 0.6	
	Belle [522][a]	$7.7 \pm 0.8 \pm 0.9$	
	Belle [522][a]	$6.3 \pm 0.9 \pm 0.6$	*6.24 ± 0.20*
	CDF [514]	$5.5 \pm 1.0 \pm 0.6$	
	Belle [576]	$6.4 \pm 1.0 \pm 0.4$	
	BABAR [573]	$4.9 \pm 1.6 \pm 0.4$	
	BABAR [12][c]		
	LHCb [624][a,d]		
$\mathcal{B}(B^+ \to \psi(2S)K^*(892)^+)$	*BABAR* [12][e]	$5.93 \pm 0.93 \pm 0.59$	5.9 ± 1.1
			6.7 ± 1.4
$\mathcal{B}(B^+ \to \psi(2S)K^+\pi^+\pi^-)$	Belle [619]	$4.31 \pm 0.20 \pm 0.50$	4.31 ± 0.54
			4.34 ± 0.54

(Table continued)

TABLE 92. *(Continued)*

Parameter $[10^{-4}]$	Measurements		Average$^{\text{HFLAV}}_{PDG}$
$\mathcal{B}(B^+ \to \psi(2S)\phi(1020)K^+)$	CMS [625]	$0.040 \pm 0.004 \pm 0.006$	0.0400 ± 0.0075 *0.0400 ± 0.0072*
$\mathcal{B}(B^+ \to \psi(3770)K^+)$	*BABAR* [502][a,f]	$2.69 \pm 0.57^{+0.46}_{-0.48}$	
	BABAR [502][a,g]	$2.07 \pm 0.79 \pm 0.56$	2.51 ± 0.49
	Belle [605][h]	$4.8 \pm 1.1 \pm 0.7$	*4.34 ± 1.10*
	Belle [576]	$-0.2 \pm 1.4 \pm -0.0$	
	BABAR [573]	$3.5 \pm 2.5 \pm 0.3$	
	Belle [626][a,i]	$3.80 \pm 0.20^{+0.84}_{-0.82}$	
	Belle [576]	$12.0 \pm 0.8 \pm 0.7$	
	Belle [607][a,j]	$11.14 \pm 0.86^{+1.50}_{-1.75}$	
	BABAR [507]	$12.9 \pm 0.9 \pm 3.8$	
	BABAR [507][b]	$13.0 \pm 1.0 \pm 3.9$	
$\mathcal{B}(B^+ \to \eta_c K^+)$	Belle [508][k]	$10.22^{+1.06+1.42}_{-1.01-1.28}$	$10.63^{+0.68}_{-0.66}$
	Belle [526]	$12.5 \pm 1.4^{+3.9}_{-4.0}$	*$10.84^{+0.84}_{-0.83}$*
	BABAR [608][j]	$14.1^{+2.4}_{-1.6} \pm 1.9$	
	BABAR [573][b]	$10.8 \pm 2.3 \pm 0.4$	
	Belle [607][a,l]	$9.7^{+2.5+1.9}_{-2.2-2.0}$	
	BABAR [507][m], [527][a,n,o,p]		
	LHCb [616][q]		
$\mathcal{B}(B^+ \to \eta_c K^*(892)^+)$	*BABAR* [525][r]	$12.1^{+4.3+6.4}_{-3.5-6.1}$	$12.5^{+6.0}_{-5.2}$ *$11.6^{+5.4}_{-4.5}$*
$\mathcal{B}(B^+ \to \eta_c(2S)K^+)$	Belle [626][a,s]	$1.63^{+1.05+0.75}_{-0.72-0.64}$	4.47 ± 0.93
	Belle [576]	$4.8 \pm 1.1 \pm 0.3$	*4.42 ± 0.96*
	BABAR [573]	$3.4 \pm 1.8 \pm 0.3$	
	Belle [508]	$0.37^{+0.10}_{-0.09} \pm 0.08$	0.37 ± 0.12
$\mathcal{B}(B^+ \to h_c K^+)$	Belle [627]	< 0.038	*$0.37^{+0.13}_{-0.12}$*
	BABAR [527][p]		

[a]Not included in PDG average.
[b]Using $\mathcal{B}(B^+ \to J/\psi K^+)$.
[c]Measurement of $\mathcal{B}(B^+ \to \psi(2S)K^*(892)^+)/\mathcal{B}(B^+ \to \psi(2S)K^+)$ used in our fit.
[d]Measurement of $\mathcal{B}(B^+ \to J/\psi\eta' K^+)/\mathcal{B}(B^+ \to \psi(2S)K^+)$ used in our fit.
[e]Using $\mathcal{B}(B^+ \to \psi(2S)K^+)$.
[f]Using $\mathcal{B}(\psi(3770) \to D^0\bar{D}^0)$.
[g]Using $\mathcal{B}(\psi(3770) \to D^+D^-)$.
[h]Assumed $\mathcal{B}(\psi(3770) \to D^+D^-) + \mathcal{B}(\psi(3770) \to D^0\bar{D}^0) = 1$.
[i]Using $\mathcal{B}(\eta_c \to K\bar{K}\pi)$.
[j]Using $\mathcal{B}(\eta_c \to p\bar{p})$.
[k]Using $\mathcal{B}(\eta_c \to p\bar{p}\pi^+\pi^-)$.
[l]Using $\mathcal{B}(\eta_c \to \Lambda^0\bar{\Lambda}^0)$.
[m]Measurement of $\mathcal{B}(B^0 \to \eta_c K^0)/\mathcal{B}(B^+ \to \eta_c K^+)$ used in our fit.
[n]Measurement of $\mathcal{B}(B^0 \to \eta_c K^*(892)^0)/\mathcal{B}(B^+ \to \eta_c K^+)$ used in our fit.
[o]Measurement of $\mathcal{B}(B^0 \to h_c K^*(892)^0)\mathcal{B}(h_c \to \eta_c\gamma)/\mathcal{B}(B^+ \to \eta_c K^+)$ used in our fit.
[p]Measurement of $\mathcal{B}(B^+ \to h_c K^+)\mathcal{B}(h_c \to \eta_c\gamma)/\mathcal{B}(B^+ \to \eta_c K^+)$ used in our fit.
[q]Measurement of $(\mathcal{B}(B^+ \to \eta_c K^+)\mathcal{B}(\eta_c \to p\bar{p}))/(\mathcal{B}(B^+ \to J/\psi K^+)\mathcal{B}(J/\psi \to p\bar{p}))$ used in our fit.
[r]Calculated using $\mathcal{B}(\eta_c \to p\bar{p})$.
[s]Using $\mathcal{B}(\eta_c(2S) \to K\bar{K}\pi)$.

TABLE 93. Branching fractions for decays to χ_c and one kaon.

Parameter [10^{-4}]	Measurements		Average$^{\text{HFLAV}}_{PDG}$
$\mathcal{B}(B^+ \to \chi_{c0}K^+)$	*BABAR* [628]	$1.84 \pm 0.32 \pm 0.31$	
	Belle [576]	$2.0 \pm 0.9 \pm 0.1$	2.16 ± 0.38
	Belle [610]	$6.0^{+2.1}_{-1.8} \pm 1.1$	$1.51^{+0.15}_{-0.13}$
	Belle [610][a]	$6 \pm 2 \pm 1$	
	BABAR [573]	< 1.8	
$\mathcal{B}(B^+ \to \chi_{c0}K^*(892)^+)$	*BABAR* [529]	$1.4 \pm 0.5 \pm 0.2$	1.40 ± 0.54
	BABAR [528]	< 28.6	< 2.10
$\mathcal{B}(B^+ \to \chi_{c1}K^+)$	*BABAR* [531]	$4.5 \pm 0.1 \pm 0.3$	
	Belle [530]	$4.94 \pm 0.11 \pm 0.33$	
	Belle [576]	$5.8 \pm 0.9 \pm 0.5$	4.85 ± 0.22
	BABAR [573]	$8.0 \pm 1.4 \pm 0.7$	4.74 ± 0.22
	CDF [621]	$15.5 \pm 5.4 \pm 2.0$	
	BABAR [12][b]		
	Belle [629][c]		
$\mathcal{B}(B^+ \to \chi_{c1}K^*(892)^+)$	*BABAR* [531]	$2.6 \pm 0.5 \pm 0.4$	2.89 ± 0.50
	Belle [534]	$4.1 \pm 0.6 \pm 0.9$	2.96 ± 0.63
	BABAR [12][d]	$2.48 \pm 0.83 \pm 0.78$	
$\mathcal{B}(B^+ \to \chi_{c1}K^+\pi^0)$	Belle [532]	$3.29 \pm 0.29 \pm 0.19$	3.29 ± 0.35
$\mathcal{B}(B^+ \to \chi_{c1}K^0\pi^+)$	*BABAR* [533]	$5.52 \pm 0.26 \pm 0.61$	5.69 ± 0.35
	Belle [532]	$5.75 \pm 0.26 \pm 0.32$	5.75 ± 0.41
$\mathcal{B}(B^+ \to \chi_{c1}K^+\pi^+\pi^-)$	Belle [532]	$3.74 \pm 0.18 \pm 0.24$	3.74 ± 0.30
$\mathcal{B}(B^+ \to \chi_{c2}K^+)$	Belle [530]	$0.111^{+0.036}_{-0.034} \pm 0.009$	0.108 ± 0.031
	BABAR [531]	$0.10 \pm 0.06 \pm 0.01$	$0.111^{+0.037}_{-0.035}$
$\mathcal{B}(B^+ \to \chi_{c2}K^*(892)^+)$	*BABAR* [531]	$0.11 \pm 0.43 \pm 0.55$	0.11 ± 0.70
			< 1.20
$\mathcal{B}(B^+ \to \chi_{c2}K^0\pi^+)$	Belle [532]	$1.16 \pm 0.22 \pm 0.12$	1.16 ± 0.25
$\mathcal{B}(B^+ \to \chi_{c2}K^+\pi^+\pi^-)$	Belle [532]	$1.34 \pm 0.17 \pm 0.09$	1.34 ± 0.19

[a]Using $\mathcal{B}(B^+ \to J/\psi K^+)$.
[b]Measurement of $\mathcal{B}(B^+ \to \chi_{c1}K^*(892)^+)/\mathcal{B}(B^+ \to \chi_{c1}K^+)$ used in our fit.
[c]Measurement of $\mathcal{B}(B^+ \to \chi_{c1}\pi^+)/\mathcal{B}(B^+ \to \chi_{c1}K^+)$ used in our fit.
[d]Using $\mathcal{B}(B^+ \to \chi_{c1}K^+)$.

TABLE 94. Branching fractions for decays to charmonium and light mesons.

Parameter [10^{-5}]	Measurements		Average$^{\text{HFLAV}}_{PDG}$
$\mathcal{B}(B^+ \to J/\psi\pi^+)$	LHCb [630]	$3.88 \pm 0.11 \pm 0.15$	
	BABAR [609][a]	$5.47 \pm 0.46 \pm 0.15$	
	Belle [505]	$3.8 \pm 0.6 \pm 0.3$	4.12 ± 0.16
	CDF [612][a]	$4.95 \pm 0.83 \pm 0.18$	3.92 ± 0.08
	CDF [611][a]	$5 \pm 2 \pm 0$	
$\mathcal{B}(B^+ \to J/\psi\pi^+\pi^0)$	*BABAR* [538][b]	< 0.73	< 0.73

(Table continued)

TABLE 94. *(Continued)*

Parameter [10^{-5}]	Measurements		Average$^{\text{HFLAV}}_{PDG}$
$\mathcal{B}(B^+ \to J/\psi\rho^+(770))$	LHCb [631]	$3.81^{+0.25}_{-0.24} \pm 0.35$	4.10 ± 0.38
	BABAR [538]	$5.0 \pm 0.7 \pm 0.3$	$4.10^{+0.51}_{-0.50}$
$\mathcal{B}(B^+ \to \psi(2S)\pi^+)$	LHCb [630]	$2.52 \pm 0.26 \pm 0.15$	2.52 ± 0.30
			2.44 ± 0.30
$\mathcal{B}(B^+ \to \chi_{c0}\pi^+)$	*BABAR* [632][c]	< 6.1	< 6.1
			< 0.0
$\mathcal{B}(B^+ \to \chi_{c1}\pi^+)$	Belle [629][d]	$2.09 \pm 0.39 \pm 0.17$	2.13 ± 0.32
	Belle [629]	$2.2 \pm 0.4 \pm 0.3$	2.20 ± 0.50

[a]Using $\mathcal{B}(B^+ \to J/\psi K^+)$.
[b]Non resonant only.
[c]Computed using PDG2004 value of $\mathcal{B}(\chi_{c0} \to \pi\pi)$.
[d]Using $\mathcal{B}(B^+ \to \chi_{c1}K^+)$.

TABLE 95. Branching fractions for decays to J/ψ and a heavy mesons.

Parameter [10^{-4}]	Measurements		Average$^{\text{HFLAV}}_{PDG}$
$\mathcal{B}(B^+ \to J/\psi D^+)$	*BABAR* [553]	< 1.2	< 1.2
$\mathcal{B}(B^+ \to J/\psi \bar{D}^0\pi^+)$	Belle [554]	< 0.25	< 0.25
	BABAR [620]	< 0.52	

TABLE 96. Branching fractions for decays to J/ψ and baryons.

Parameter [10^{-6}]	Measurements		Average$^{\text{HFLAV}}_{PDG}$
$\mathcal{B}(B^+ \to J/\psi\bar{\Lambda}^0 p)$	Belle [551]	$11.6 \pm 2.8^{+1.8}_{-2.3}$	11.6 ± 3.1
	BABAR [552]	$11.6^{+7.4+4.2}_{-5.3-1.8}$	14.6 ± 1.2
$\mathcal{B}(B^+ \to J/\psi\bar{\Sigma}^0 p)$	Belle [551]	< 11	< 11
$\mathcal{B}(B^+ \to J/\psi p\bar{p}\pi^+)$	LHCb [550]	< 0.50	< 0.50

TABLE 97. Direct *CP* violation parameters for decays to J/ψ.

Parameter	Measurements		Average
$A_{CP}(B^+ \to J/\psi K^+)$	D0 [633]	$0.0059 \pm 0.0036 \pm 0.0007$	0.0059 ± 0.0037
$A_{CP}(B^+ \to J/\psi\pi^+)$	D0 [633]	$-0.042 \pm 0.044 \pm 0.009$	-0.042 ± 0.045
$A_{CP}(B^+ \to J/\psi\rho^+(770))$	LHCb [631]	$-0.045^{+0.056}_{-0.057} \pm 0.008$	-0.054 ± 0.053
	BABAR [538]	$-0.11 \pm 0.12 \pm 0.08$	

4. Decays to charm baryons

Averages of B^+ decays to charm baryons are shown in Table 98.

TABLE 98. Branching fractions for decays to charm baryons.

Parameter [10^{-4}]	Measurements		Average$^{\text{HFLAV}}_{PDG}$
$\mathcal{B}(B^+ \to \bar{\Lambda}_c^- p\pi^+)$	*BABAR* [564]	$3.38 \pm 0.12 \pm 0.89$	
	BABAR [564][b]	$2.77 \pm 0.32 \pm 0.48$	2.71 ± 0.43
	Belle [557]	$1.87^{+0.43}_{-0.40} \pm 0.56$	*$2.27^{+0.37}_{-0.38}$*
	BABAR [564][c,d]		
$\mathcal{B}(B^+ \to \Lambda_c^+ \bar{\Lambda}_c^- K^+)$	Belle [634]	$4.8 \pm 0.4 \pm 0.6$	4.89 ± 0.73
	BABAR [561]	$11.4 \pm 1.5 \pm 6.2$	*4.91 ± 0.73*
$\mathcal{B}(B^+ \to \bar{\Xi}_c^0 \Lambda_c^+)$	*BABAR* [561][a,e]	$14.54 \pm 4.54 \pm 5.39$	$18.1^{+8.2}_{-6.2}$
	Belle [562][a,e]	$33.6^{+7.0}_{-6.3} \pm 13.6$	*9.5 ± 2.3*
$\mathcal{B}(B^+ \to \bar{\Xi}_c(2930)^+ \Lambda_c^+)$	Belle [634][a,f]	$3.46 \pm 0.90 \pm 3.49$	3.5 ± 3.9
			None
$\mathcal{B}(B^+ \to \bar{\Sigma}_c(2455)^0 p)$	*BABAR* [564][g]	$0.333 \pm 0.032 \pm 0.057$	0.336 ± 0.065
	Belle [557]	$0.45^{+0.26}_{-0.19} \pm 0.14$	*0.296 ± 0.066*
$\mathcal{B}(B^+ \to \bar{\Sigma}_c(2520)^0 p)$	Belle [557]	< 0.46	< 0.46
			< 0.03
$\mathcal{B}(B^+ \to \bar{\Sigma}_c(2455)^{--} p\pi^+\pi^+)$	*BABAR* [635]	$2.98 \pm 0.16 \pm 0.78$	2.98 ± 0.80
			2.38 ± 0.19
$\mathcal{B}(B^+ \to \bar{\Sigma}_c(2800)^0 p)$	*BABAR* [564][g]	$0.317 \pm 0.062 \pm 0.082$	$0.32^{+0.11}_{-0.10}$
			0.27 ± 0.09

[a]Not included in PDG average.
[b]Using $\mathcal{B}(B^0 \to \bar{\Lambda}_c^- p)$.
[c]Measurement of $\mathcal{B}(B^+ \to \bar{\Sigma}_c(2455)^0 p)/\mathcal{B}(B^+ \to \bar{\Lambda}_c^- p\pi^+)$ used in our fit.
[d]Measurement of $\mathcal{B}(B^+ \to \bar{\Sigma}_c(2800)^0 p)/\mathcal{B}(B^+ \to \bar{\Lambda}_c^- p\pi^+)$ used in our fit.
[e]Using $\mathcal{B}(\Xi_c^0 \to \Xi^- \pi^+)$.
[f]Using $\mathcal{B}(\Xi_c(2930)^+ \to \Lambda_c^+ K^-)$.
[g]Using $\mathcal{B}(B^+ \to \bar{\Lambda}_c^- p\pi^+)$.

5. Decays to exotic states

Averages of B^+ decays to exotic states are shown in Tables 99–102.

TABLE 99. Branching fractions for decays to exotic states.

Parameter [10^{-4}]	Measurements		Average$^{\text{HFLAV}}_{PDG}$
$\mathcal{B}(B^+ \to X(3872)K^+)$	*BABAR* [636]	$2.1 \pm 0.6 \pm 0.3$	
	Belle [576]	$1.2 \pm 1.1 \pm 0.1$	$1.93^{+0.51}_{-0.49}$
	BABAR [570][a,b], [517][a,b]		*2.10 ± 0.68*
	Belle [569][a,b]		
$\mathcal{B}(B^+ \to X(3872)K^0\pi^+)$	Belle [571][c]	$2.84 \pm 0.80^{+0.87}_{-0.83}$	$2.8^{+1.5}_{-1.0}$
			2.8 ± 1.2
$\mathcal{B}(B^+ \to X(3915)K^+)$	Belle [576]	$0.4 \pm 1.6 \pm -0.0$	0.4 ± 1.6
			< 2.8

[a]Not included in PDG average.
[b]Measurement of $\mathcal{B}(B^0 \to X(3872)K^0)/\mathcal{B}(B^+ \to X(3872)K^+)$ used in our fit.
[c]Using $\mathcal{B}(X(3872) \to J/\psi\pi^+\pi^-)$.

TABLE 100. Product branching fractions for decays to $X(3872)$.

Parameter $[10^{-5}]$	Measurements		Average$^{\text{HFLAV}}_{PDG}$
$\mathcal{B}(B^+ \to X(3872)K^+) \times \mathcal{B}(X(3872) \to D^*(2007)^0\bar{D}^0)$			
	BABAR [502][a]	$16.7 \pm 3.6 \pm 4.7$	16.7 ± 5.9 *None*
$\mathcal{B}(B^+ \to X(3872)K^+) \times \mathcal{B}(X(3872) \to D^0\bar{D}^0\pi^0)$			
	Belle [605][a]	< 6.0	< 6.0 *None*
$\mathcal{B}(B^+ \to X(3872)K^+) \times \mathcal{B}(X(3872) \to D^0\bar{D}^0)$			
	Belle [605][a]	< 6.0	< 6.0 *None*
$\mathcal{B}(B^+ \to X(3872)K^+) \times \mathcal{B}(X(3872) \to D^+D^-)$			
	Belle [605][a]	< 4.0	< 4.0 *None*
$\mathcal{B}(B^+ \to X(3872)K^+) \times \mathcal{B}(X(3872) \to J/\psi\pi^+\pi^-)$			
	Belle [569][a]	$0.861 \pm 0.062 \pm 0.052$	0.857 ± 0.073
	BABAR [570][a]	$0.84 \pm 0.15 \pm 0.07$	*None*
$\mathcal{B}(B^+ \to X(3872)K^+) \times \mathcal{B}(X(3872) \to J/\psi\omega(782))$			
	BABAR [517][a]	$0.6 \pm 0.2 \pm 0.1$	0.60 ± 0.22 *None*
$\mathcal{B}(B^+ \to X(3872)K^+) \times \mathcal{B}(X(3872) \to J/\psi\eta)$			
	BABAR [521][a]	< 0.77	< 0.77 *None*
$\mathcal{B}(B^+ \to X(3872)K^+) \times \mathcal{B}(X(3872) \to \chi_{c1}\gamma)$			
	Belle [522][a]	< 0.19	< 0.19 *None*
$\mathcal{B}(B^+ \to X(3872)K^+) \times \mathcal{B}(X(3872) \to \chi_{c2}\gamma)$			
	Belle [522][a]	< 0.67	< 0.67 *None*

[a]Not included in PDG average.

TABLE 101. Product branching fractions to neutral states other than $X(3872)$.

Parameter $[10^{-5}]$	Measurements		Average$^{\text{HFLAV}}_{PDG}$
$\mathcal{B}(B^+ \to \psi_2(3823)K^+) \times \mathcal{B}(\psi_2(3823) \to \chi_{c1}\gamma)$	Belle [522][a]	$0.97 \pm 0.28 \pm 0.11$	0.97 ± 0.30 *None*
$\mathcal{B}(B^+ \to \psi_2(3823)K^+) \times \mathcal{B}(\psi_2(3823) \to \chi_{c2}\gamma)$	Belle [522][a]	< 0.36	< 0.36 *None*
$\mathcal{B}(B^+ \to Y(3940)K^+) \times \mathcal{B}(Y(3940) \to J/\psi\gamma)$	*BABAR* [637][a]	< 1.4	< 1.4 *None*
$\mathcal{B}(B^+ \to Y(3940)K^+) \times \mathcal{B}(Y(3940) \to J/\psi\omega(782))$	*BABAR* [517][a]	$3.0^{+0.7+0.5}_{-0.6-0.3}$	$3.00^{+0.86}_{-0.67}$ *None*
$\mathcal{B}(B^+ \to \psi(4260)K^+) \times \mathcal{B}(\psi(4260) \to J/\psi\pi^+\pi^-)$	*BABAR* [638]	$2.0 \pm 0.7 \pm 0.2$	2.00 ± 0.73 *< 1.56*

(Table continued)

TABLE 101. *(Continued)*

Parameter [10^{-5}]	Measurements		Average$^{\text{HFLAV}}_{PDG}$
$\mathcal{B}(B^+ \to \psi(4660)K^+) \times \mathcal{B}(\psi(4660) \to \Lambda_c^+ \bar{\Lambda}_c^-)$	Belle [634][a]	< 12	< 12 *None*
$\mathcal{B}(B^+ \to Y_\eta K^+) \times \mathcal{B}(Y_\eta \to \Lambda_c^+ \bar{\Lambda}_c^-)$	Belle [634][a]	< 20	< 20 *None*
$\mathcal{B}(B^+ \to \chi_{c1}(4140)K^+) \times \mathcal{B}(\chi_{c1}(4140) \to J/\psi\phi(1020))$	LHCb [623][a,b,c] D0 [622][a,c]	$0.57 \pm 0.14^{+0.28}_{-0.21}$ $0.925 \pm 0.353 \pm 0.358$	$0.66^{+0.36}_{-0.27}$ *None*
$\mathcal{B}(B^+ \to \chi_{c1}(4274)K^+) \times \mathcal{B}(\chi_{c1}(4274) \to J/\psi\phi(1020))$	LHCb [623][a,b,c]	$0.313 \pm 0.110^{+0.187}_{-0.149}$	$0.31^{+0.24}_{-0.16}$ $0.36^{+0.22}_{-0.18}$

[a]Not included in PDG average.
[b]The quoted value is a fit fraction from a Dalitz plot fit.
[c]Using $\mathcal{B}(B^+ \to J/\psi\phi(1020)K^+)$.

TABLE 102. Product branching fractions to charged exotic states.

Parameter [10^{-5}]	Measurements		Average$^{\text{HFLAV}}_{PDG}$
$\mathcal{B}(B^+ \to X(3872)^+K^0) \times \mathcal{B}(X(3872)^+ \to J/\psi\pi^+\pi^0)$	*BABAR* [574]	< 2.2	< 2.2 < 0.6
$\mathcal{B}(B^+ \to Z_c(4430)^+K^0) \times \mathcal{B}(Z_c(4430)^+ \to J/\psi\pi^+)$	*BABAR* [575]	< 1.5	< 1.5
$\mathcal{B}(B^+ \to Z_c(4430)^+K^0) \times \mathcal{B}(Z_c(4430)^+ \to \psi(2S)\pi^+)$	*BABAR* [575]	< 4.7	< 4.7

C. Decays of admixtures of B^0/B^+ mesons

Measurements of B^0/B^+ decays to charmed hadrons are summarized in Secs. VII C 1 to VII C 3.

1. Decays to two open charm mesons

Averages of B^0/B^+ decays to two open charm mesons are shown in Table 103.

TABLE 103. Branching fractions for decays to double charm.

Parameter [10^{-4}]	Measurements		Average
$\mathcal{B}(B \to D^0\bar{D}^0K\pi^0)$	Belle [493]	$1.27 \pm 0.31^{+0.22}_{-0.39}$	$1.27^{+0.38}_{-0.50}$

2. Decays to charmonium states

Averages of B^0/B^+ decays to charmonium states are shown in Tables 104–108.

TABLE 104. Decay amplitudes for parallel transverse polarization of decays to charmonia.

Parameter	Measurements		Average
$A_\parallel(B \to J/\psi K^*)$	LHCb [639]	$0.227 \pm 0.004 \pm 0.011$	0.2219 ± 0.0072
	BABAR [640]	$0.211 \pm 0.010 \pm 0.006$	
	Belle [641]	$0.231 \pm 0.012 \pm 0.008$	
$A_\parallel(B \to \chi_{c1}K^*)$	*BABAR* [640]	$0.2 \pm 0.1 \pm 0.0$	0.200 ± 0.081
$A_\parallel(B \to \psi(2S)K^*)$	*BABAR* [640]	$0.22 \pm 0.06 \pm 0.02$	0.220 ± 0.063

TABLE 105. Decay amplitudes for perpendicular transverse polarization of decays to charmonia.

Parameter	Measurements		Average
$A_\perp(B \to J/\psi K^*)$	LHCb [639]	$0.201 \pm 0.004 \pm 0.008$	0.2100 ± 0.0063
	BABAR [640]	$0.233 \pm 0.010 \pm 0.005$	
	Belle [641]	$0.195 \pm 0.012 \pm 0.008$	
$A_\perp(B \to \chi_{c1} K^*)$	*BABAR* [640]	$0.03 \pm 0.04 \pm 0.02$	0.030 ± 0.045
$A_\perp(B \to \psi(2S) K^*)$	*BABAR* [640]	$0.3 \pm 0.1 \pm 0.0$	0.300 ± 0.063

TABLE 106. Decay amplitudes for longitudinal polarization of decays to charmonia.

Parameter	Measurements		Average
$A_0(B \to J/\psi K^*)$	*BABAR* [640]	$0.556 \pm 0.009 \pm 0.010$	0.564 ± 0.010
	Belle [641]	$0.574 \pm 0.012 \pm 0.009$	
$A_0(B \to \chi_{c1} K^*)$	*BABAR* [640]	$0.77 \pm 0.07 \pm 0.04$	0.770 ± 0.081
$A_0(B \to \psi(2S) K^*)$	*BABAR* [640]	$0.48 \pm 0.05 \pm 0.02$	0.480 ± 0.054

TABLE 107. Relative phases of parallel transverse polarization decay amplitudes of decays to charmonia.

Parameter	Measurements		Average
$\delta_\parallel(B \to J/\psi K^*)$	LHCb [639]	$-2.94 \pm 0.02 \pm 0.03$	-2.932 ± 0.031
	BABAR [640]	$-2.93 \pm 0.08 \pm 0.04$	
	Belle [641]	$-2.887 \pm 0.090 \pm 0.008$	
$\delta_\parallel(B \to \chi_{c1} K^*)$	*BABAR* [640]	$0.0 \pm 0.3 \pm 0.1$	0.00 ± 0.32
$\delta_\parallel(B \to \psi(2S) K^*)$	*BABAR* [640]	$-2.8 \pm 0.4 \pm 0.1$	-2.80 ± 0.41

TABLE 108. Relative phases of perpendicular transverse polarization decay amplitudes of decays to charmonia.

Parameter	Measurements		Average
$\delta_\perp(B \to J/\psi K^*)$	LHCb [639]	$2.94 \pm 0.02 \pm 0.02$	
	BABAR [640]	$2.91 \pm 0.05 \pm 0.03$	2.935 ± 0.024
	Belle [641]	$2.938 \pm 0.064 \pm 0.010$	
$\delta_\perp(B \to \psi(2S) K^*)$	*BABAR* [640]	$2.8 \pm 0.3 \pm 0.1$	2.80 ± 0.32

3. Decays to exotic states

Averages of B^0/B^+ decays to exotic states are shown in Table 109.

TABLE 109. Branching fractions for decays to exotic states.

Parameter [10^{-4}]	Measurements		Average$^{\text{HFLAV}}_{PDG}$
$\mathcal{B}(B \to Y(3940)K) \times \mathcal{B}(Y(3940) \to D^*(2007)^0 \bar{D}^*(2007)^0)$			
	Belle [642]	< 0.67	< 0.67
$\mathcal{B}(B \to Y(3940)K) \times \mathcal{B}(Y(3940) \to J/\psi\omega(782))$			
	Belle [643]	$0.71 \pm 0.13 \pm 0.31$	0.71 ± 0.34

D. Decays of B_s^0 mesons

Measurements of B_s^0 decays to charmed hadrons are summarized in Secs. VII D 1–VII D 4.

1. Decays to a single open charm meson

Averages of B_s^0 decays to a single open charm meson are shown in Tables 110–113.

TABLE 110. Branching fractions for decays to a $D_s^{(*)}$.

Parameter [10^{-3}]	Measurements		Average$^{\text{HFLAV}}_{PDG}$
$\mathcal{B}(B_s^0 \to D_s^- \pi^+)$	LHCb [644]	$2.95 \pm 0.05^{+0.25}_{-0.28}$	
	CDF [437][b]	$2.80 \pm 0.20 \pm 0.59$	$2.83^{+0.18}_{-0.19}$
	Belle [645]	$3.67^{+0.35}_{-0.33} \pm 0.65$	*2.98 ± 0.14*
	CDF [646][c]		
	LHCb [439][d], [441][c]		
$\mathcal{B}(B_s^0 \to D_s^{*-} \pi^+)$	Belle [647]	$2.4^{+0.5}_{-0.4} \pm 0.4$	$2.20^{+0.61}_{-0.54}$
	LHCb [648][a,e]		*$1.93^{+0.50}_{-0.45}$*
$\mathcal{B}(B_s^0 \to D_s^- \rho^+(770))$	Belle [647]	$8.5^{+1.3}_{-1.2} \pm 1.7$	$7.6^{+1.9}_{-1.8}$
			6.8 ± 1.4
$\mathcal{B}(B_s^0 \to D_s^{*-} \rho^+(770))$	Belle [647]	$11.8^{+2.2}_{-2.0} \pm 2.5$	$10.6^{+3.0}_{-2.9}$
			9.5 ± 2.0
$\mathcal{B}(B_s^0 \to D_s^- \pi^+ \pi^+ \pi^-)$	CDF [437][f,g]	$6.07 \pm 0.58^{+1.43}_{-1.42}$	
	LHCb [439][h]	$5.69 \pm 1.05 \pm 0.68$	$5.85^{+1.00}_{-0.95}$
	LHCb [474][i,j]		*6.10 ± 0.99*
$\mathcal{B}(B_s^0 \to D_s^{\mp} K^{\pm})$	LHCb [441][h]	$0.2130 \pm 0.0042^{+0.0148}_{-0.0151}$	
	LHCb [644]	$0.19 \pm 0.01 \pm 0.02$	0.212 ± 0.014
	CDF [646][h]	$0.275 \pm 0.051 \pm 0.031$	*0.225 ± 0.012*
	Belle [645]	$0.24^{+0.12}_{-0.10} \pm 0.04$	
$\mathcal{B}(B_s^0 \to D_s^{*\mp} K^{\pm})$	LHCb [648][a,k]	$0.150 \pm 0.011^{+0.042}_{-0.037}$	$0.150^{+0.044}_{-0.038}$
			$0.132^{+0.036}_{-0.032}$
$\mathcal{B}(B_s^0 \to D_s^- K^+ \pi^+ \pi^-)$	LHCb [474][l]	$0.304 \pm 0.029^{+0.055}_{-0.053}$	$0.304^{+0.065}_{-0.058}$
	LHCb [474][m]		*0.317 ± 0.063*

[a]Not included in PDG average.
[b]Using $\mathcal{B}(B^0 \to D^- \pi^+)$.
[c]Measurement of $\mathcal{B}(B_s^0 \to D_s^{\mp} K^{\pm})/\mathcal{B}(B_s^0 \to D_s^- \pi^+)$ used in our fit.
[d]Measurement of $\mathcal{B}(B_s^0 \to D_s^- \pi^+ \pi^+ \pi^-)/\mathcal{B}(B_s^0 \to D_s^- \pi^+)$ used in our fit.
[e]Measurement of $\mathcal{B}(B_s^0 \to D_s^{*\mp} K^{\pm})/\mathcal{B}(B_s^0 \to D_s^{*-} \pi^+)$ used in our fit.
[f]Using $f_s/f_d = 0.259 \pm 0.038$ from PDG 2006.
[g]Using $\mathcal{B}(B^0 \to D^- \pi^+ \pi^+ \pi^-)$.
[h]Using $\mathcal{B}(B_s^0 \to D_s^- \pi^+)$.
[i]Measurement of $\mathcal{B}(B_s^0 \to D_s^- K^+ \pi^+ \pi^-)/\mathcal{B}(B_s^0 \to D_s^- \pi^+ \pi^+ \pi^-)$ used in our fit.
[j]Measurement of $\mathcal{B}(B_s^0 \to D_{s1}(2536)^- \pi^+) \times \mathcal{B}(D_{s1}(2536)^+ \to D_s^+ \pi^+ \pi^-)/\mathcal{B}(B_s^0 \to D_s^- \pi^+ \pi^+ \pi^-)$ used in our fit.
[k]Using $\mathcal{B}(B_s^0 \to D_s^{*-} \pi^+)$.
[l]Using $\mathcal{B}(B_s^0 \to D_s^- \pi^+ \pi^+ \pi^-)$.
[m]Measurement of $\mathcal{B}(B^0 \to D_s^- K^+ \pi^+ \pi^-)/\mathcal{B}(B_s^0 \to D_s^- K^+ \pi^+ \pi^-)$ used in our fit.

TABLE 111. Branching fractions for decays to a $D^{(*)}$.

Parameter [10^{-4}]	Measurements		Average$^{\text{HFLAV}}_{PDG}$
$\mathcal{B}(B_s^0 \to \bar{D}^0 \bar{K}^0)$	LHCb [649]	$4.3 \pm 0.5 \pm 0.5$	4.30 ± 0.71 *4.30 ± 0.86*
$\mathcal{B}(B_s^0 \to \bar{D}^*(2007)^0 \bar{K}^0)$	LHCb [649]	$2.8 \pm 1.0 \pm 0.4$	2.8 ± 1.1
$\mathcal{B}(B_s^0 \to \bar{D}^0 \bar{K}^*(892)^0)$	LHCb [467][b] LHCb [459][c] LHCb [467][d]	$3.27 \pm 0.29^{+0.44}_{-0.43}$ $4.49 \pm 1.03^{+0.91}_{-0.89}$	$3.38^{+0.46}_{-0.42}$ *4.38 ± 0.58*
$\mathcal{B}(B_s^0 \to \bar{D}^0 \phi(1020))$	LHCb [468][a] LHCb [467][e]	$0.230 \pm 0.010 \pm 0.023$ $0.233 \pm 0.044^{+0.040}_{-0.037}$	0.231 ± 0.023 *0.299 ± 0.047*
$\mathcal{B}(B_s^0 \to \bar{D}^*(2007)^0 \phi(1020))$	LHCb [468][a]	$0.317 \pm 0.016 \pm 0.032$	0.317 ± 0.036 *0.370 ± 0.060*
$\mathcal{B}(B_s^0 \to D^{*\mp} \pi^{\pm})$	LHCb [650]	< 0.061	< 0.061
$\mathcal{B}(B_s^0 \to \bar{D}^0 f_0(980))$	LHCb [651]	< 0.031	< 0.031
$\mathcal{B}(B_s^0 \to \bar{D}^0 K^+ K^-)$	LHCb [456][f]	$0.5529 \pm 0.0529^{+0.0550}_{-0.0545}$	$0.553^{+0.078}_{-0.074}$ *0.565 ± 0.085*
$\mathcal{B}(B_s^0 \to \bar{D}^0 K^- \pi^+)$	LHCb [455][g]	$10.03 \pm 0.42 \pm 1.12$	10.0 ± 1.2 *10.4 ± 1.3*
$\mathcal{B}(B_s^0 \to \bar{D}^*(2007)^0 K^- \pi^+)$	LHCb [458][a,h]	$7.304 \pm 0.180 \pm 2.596$	7.3 ± 2.6

[a]Not included in PDG average.
[b]Using $\mathcal{B}(B^0 \to \bar{D}^0 K^*(892)^0)$.
[c]Using $\mathcal{B}(B^0 \to \bar{D}^0 \rho^0(770))$.
[d]Measurement of $\mathcal{B}(B_s^0 \to \bar{D}^0 \phi(1020))/\mathcal{B}(B_s^0 \to \bar{D}^0 \bar{K}^*(892)^0)$ used in our fit.
[e]Using $\mathcal{B}(B_s^0 \to \bar{D}^0 \bar{K}^*(892)^0)$.
[f]Using $\mathcal{B}(B^0 \to \bar{D}^0 K^+ K^-)$.
[g]Using $\mathcal{B}(B^0 \to \bar{D}^0 \pi^+ \pi^-)$.
[h]Using $\mathcal{B}(B^0 \to \bar{D}^*(2007)^0 \pi^+ \pi^-)$.

TABLE 112. Branching fractions for decays to excited D_s mesons.

Parameter [10^{-5}]	Measurements		Average$^{\text{HFLAV}}_{PDG}$
$\mathcal{B}(B_s^0 \to D_{s1}(2536)^- \pi^+) \times \mathcal{B}(D_{s1}(2536)^+ \to D_s^+ \pi^+ \pi^-)$			
	LHCb [474][a]	$2.34 \pm 0.58^{+0.46}_{-0.45}$	$2.34^{+0.79}_{-0.69}$ *2.44 ± 0.77*

[a]Using $\mathcal{B}(B_s^0 \to D_s^- \pi^+ \pi^+ \pi^-)$.

TABLE 113. Longitudinal polarization fraction for decays to a D^*.

Parameter	Measurements		Average
$f_L(B_s^0 \to \bar{D}^*(2007)^0 \phi(1020))$	LHCb [468]	$0.531 \pm 0.060 \pm 0.019$	0.531 ± 0.063

2. Decays to two open charm mesons

Averages of B_s^0 decays to two open charm mesons are shown in Table 114.

TABLE 114. Branching fractions for decays to two $D_{(s)}^{(*)}$ mesons.

Parameter [10^{-4}]	Measurements		Average$^{\text{HFLAV}}_{PDG}$
$\mathcal{B}(B_s^0 \to D_s^+ D_s^-)$	LHCb [486][b]	$45.7 \pm 2.4 \pm 4.0$	$46.7^{+4.3}_{-4.2}$ *44.0 ± 4.8*
	CDF [226][c]	$49 \pm 6 \pm 9$	
	Belle [30]	$58^{+11}_{-9} \pm 13$	
	D0 [224][a,d]		
	LHCb [652][a,d]		
$\mathcal{B}(B_s^0 \to D_s^{*+} D_s^- + D_s^{*-} D_s^+)$	LHCb [652]	$135 \pm 6 \pm 17$	130 ± 13 *139 ± 17*
	CDF [226][c]	$113 \pm 12 \pm 21$	
	Belle [30]	$176^{+23}_{-22} \pm 40$	
	D0 [224][a,d]		
	LHCb [652][d]		
$\mathcal{B}(B_s^0 \to D_s^{*+} D_s^{*-})$	LHCb [652]	$127 \pm 8 \pm 17$	140 ± 15 *144 ± 21*
	CDF [226][c]	$175 \pm 19 \pm 34$	
	Belle [30]	198^{+33+51}_{-31-50}	
	D0 [224][a,d]		
	LHCb [652][d]		
$\mathcal{B}(B_s^0 \to D_s^- D^+)$	LHCb [486][b]	$4.1 \pm 0.7 \pm 0.4$	4.08 ± 0.76 *2.75 ± 0.46*
	LHCb [496][e,f]		
$\mathcal{B}(B_s^0 \to D^+ D^-)$	LHCb [486][g]	$2.38 \pm 0.44 \pm 0.33$	2.38 ± 0.55 *2.20 ± 0.57*
$\mathcal{B}(B_s^0 \to D^0 \bar{D}^0)$	LHCb [486][h]	$1.85 \pm 0.29 \pm 0.31$	1.85 ± 0.42 *1.90 ± 0.50*

[a]Not included in PDG average.
[b]Using $\mathcal{B}(B^0 \to D_s^+ D^-)$.
[c]Using $f_s/f_d = 0.269 \pm 0.033$ and $\mathcal{B}(B^0 \to D_s^+ D^-) = (7.2 \pm 0.8) \times 10^{-3}$.
[d]Measurement of $\mathcal{B}(B_s^0 \to D_s^+ D_s^-) + \mathcal{B}(B_s^0 \to D_s^{*+} D_s^- + D_s^{*-} D_s^+) + \mathcal{B}(B_s^0 \to D_s^{*+} D_s^{*-})$ used in our fit.
[e]At CL = 95%.
[f]Measurement of $\mathcal{B}(B_s^0 \to \Lambda_c^+ \bar{\Lambda}_c^-)/\mathcal{B}(B_s^0 \to D_s^- D^+)$ used in our fit.
[g]Using $\mathcal{B}(B^0 \to D^+ D^-)$.
[h]Using $\mathcal{B}(B^+ \to D_s^+ \bar{D}^0)$.

3. Decays to charmonium states

Averages of B_s^0 decays to charmonium states are shown in Tables 115–119.

TABLE 115. Branching fractions for decays to J/ψ, I.

Parameter [10^{-4}]	Measurements		Average$^{\text{HFLAV}}_{PDG}$
$\mathcal{B}(B_s^0 \to J/\psi\phi(1020))$	LHCb [653]	$10.5 \pm 0.1 \pm 1.0$	
	Belle [654]	$12.5 \pm 0.7 \pm 2.3$	
	CDF [509]	$9.3 \pm 2.8 \pm 1.7$	
	CDF [133][a], [655][b]		
	CMS [656][a]		10.61 ± 0.90
	D0 [614][b], [657][a], [658][c]		*10.44 ± 0.38*
	LHCb [659][d], [515][b], [660][e], [661][a], [259][f]		
$\mathcal{B}(B_s^0 \to J/\psi K^0 K^- \pi^+ + \text{c.c.})$	LHCb [511][g]	$9.26 \pm 0.66^{+0.96}_{-0.95}$	$9.3^{+1.2}_{-1.1}$ *9.5 ± 1.3*
$\mathcal{B}(B_s^0 \to J/\psi\eta)$	LHCb [539][h]	$4.14 \pm 0.35^{+0.61}_{-0.66}$	
	Belle [662]	$5.1 \pm 0.5^{+1.2}_{-0.8}$	$4.58^{+0.56}_{-0.51}$
	LHCb [541][i]		*3.95 ± 0.70*
$\mathcal{B}(B_s^0 \to J/\psi\eta')$	LHCb [539][h]	$3.76 \pm 0.33^{+0.49}_{-0.45}$	
	Belle [662]	$3.71 \pm 0.61^{+0.85}_{-0.60}$	$3.75^{+0.52}_{-0.47}$
	LHCb [541][j]		$3.34^{+0.42}_{-0.45}$
$\mathcal{B}(B_s^0 \to J/\psi\phi(1020)\phi(1020))$	LHCb [660][k]	$0.122 \pm 0.013^{+0.012}_{-0.014}$	0.122 ± 0.018 $0.120^{+0.014}_{-0.016}$
$\mathcal{B}(B_s^0 \to J/\psi K_S^0)$	CDF [663][l,m]		0.182 ± 0.023
	LHCb [510][n]		*0.192 ± 0.014*
$\mathcal{B}(B_s^0 \to J/\psi \bar{K}^*(892)^0)$	LHCb [264]	$0.417 \pm 0.018 \pm 0.035$	0.422 ± 0.039
	CDF [663][l]	$0.83 \pm 0.12 \pm 0.35$	*0.414 ± 0.039*
$\mathcal{B}(B_s^0 \to J/\psi \bar{K}^0 \pi^+ \pi^-)$	LHCb [511]	< 0.44	< 0.44
$\mathcal{B}(B_s^0 \to J/\psi \bar{K}^0 K^+ K^-)$	LHCb [511]	< 0.120	< 0.12

[a]Measurement of $\mathcal{B}(B_s^0 \to J/\psi f_0(980)) \times \mathcal{B}(f_0(980) \to \pi^+\pi^-)/\mathcal{B}(B_s^0 \to J/\psi\phi(1020))/\mathcal{B}(\phi(1020) \to K^+K^-)$ used in our fit.

[b]Measurement of $\mathcal{B}(B_s^0 \to \psi(2S)\phi(1020))/\mathcal{B}(B_s^0 \to J/\psi\phi(1020))$ used in our fit.

[c]Measurement of $\mathcal{B}(B_s^0 \to J/\psi f_2'(1525))\mathcal{B}(f_2'(1525) \to K^+K^-)/\mathcal{B}(B_s^0 \to J/\psi\phi(1020))/\mathcal{B}(\phi(1020) \to K^+K^-)$ used in our fit.

[d]Measurement of $\mathcal{B}(B_s^0 \to J/\psi f_2'(1525))/\mathcal{B}(B_s^0 \to J/\psi\phi(1020))$ used in our fit.

[e]Measurement of $\mathcal{B}(B_s^0 \to J/\psi\phi(1020)\phi(1020))/\mathcal{B}(B_s^0 \to J/\psi\phi(1020))$ used in our fit.

[f]Measurement of $\mathcal{B}(B_s^0 \to J/\psi\pi^+\pi^-)/\mathcal{B}(B_s^0 \to J/\psi\phi(1020))$ used in our fit.

[g]Using $\mathcal{B}(B^0 \to J/\psi K^0\pi^+\pi^-)$.

[h]Using $\mathcal{B}(B^0 \to J/\psi\rho^0(770))$.

[i]Measurement of $\mathcal{B}(B^0 \to J/\psi\eta)/\mathcal{B}(B_s^0 \to J/\psi\eta)$ used in our fit.

[j]Measurement of $\mathcal{B}(B^0 \to J/\psi\eta')/\mathcal{B}(B_s^0 \to J/\psi\eta')$ used in our fit.

[k]Using $\mathcal{B}(B_s^0 \to J/\psi\phi(1020))$.

[l]Using $f_s/f_d = 0.269 \pm 0.033$.

[m]Measurement of $2\mathcal{B}(B_s^0 \to J/\psi K_S^0)$ used in our fit.

[n]Measurement of $2\mathcal{B}(B_s^0 \to J/\psi K_S^0)/\mathcal{B}(B^0 \to J/\psi K^0)$ used in our fit.

TABLE 116. Branching fractions for decays to J/ψ, II.

Parameter [10^{-5}]	Measurements		Average$^{\text{HFLAV}}_{PDG}$
$\mathcal{B}(B_s^0 \to J/\psi\pi^+\pi^-)$	LHCb [259][a,b]	$20.87 \pm 0.50^{+1.84}_{-1.88}$	20.9 ± 1.9
	LHCb [537][c]		*20.2 ± 1.7*
$\mathcal{B}(B_s^0 \to J/\psi f_0(980)) \times \mathcal{B}(f_0(980) \to \pi^+\pi^-)$	Belle [664]	$11.6^{+3.1+3.0}_{-1.9-3.1}$	
	CDF [133][d]		10.8 ± 1.2
	CMS [656][d]		*$12.4^{+1.5}_{-1.6}$*
	D0 [657][d]		
	LHCb [665][e], [661][d]		
$\mathcal{B}(B_s^0 \to J/\psi f_0(1370)) \times \mathcal{B}(f_0(1370) \to \pi^+\pi^-)$	Belle [664]	$3.4^{+1.1+0.9}_{-1.4-0.8}$	$2.9^{+1.3}_{-1.5}$
			$4.4^{+0.6}_{-3.9}$
$\mathcal{B}(B_s^0 \to J/\psi f_1(1285))$	LHCb [543][f]	$7.202 \pm 1.000^{+0.906}_{-1.009}$	7.2 ± 1.4
$\mathcal{B}(B_s^0 \to J/\psi f_2'(1525))$	LHCb [659][a]	$28.0 \pm 2.9 \pm 3.5$	$26.9^{+4.3}_{-4.0}$
	D0 [658][g]		*$26.1^{+5.9}_{-5.4}$*
$\mathcal{B}(B_s^0 \to J/\psi f_0(500)) \times \mathcal{B}(f_0(500) \to \pi^+\pi^-)$	LHCb [665][h]	< 0.37	< 0.37
			< 0.40
$\mathcal{B}(B_s^0 \to J/\psi p\bar{p})$	LHCb [549]	$0.358 \pm 0.019 \pm 0.033$	0.358 ± 0.038
	LHCb [550]	< 0.48	*0.358 ± 0.043*
$\mathcal{B}(B_s^0 \to J/\psi\gamma)$	LHCb [547]	< 0.73	< 0.73

[a]Using $\mathcal{B}(B_s^0 \to J/\psi\phi(1020))$.

[b]Corrected for updates of $\mathcal{B}(\phi(1020) \to K^+K^-)$.

[c]Measurement of $\mathcal{B}(B_s^0 \to \psi(2S)\pi^+\pi^-)/\mathcal{B}(B_s^0 \to J/\psi\pi^+\pi^-)$ used in our fit.

[d]Measurement of $\mathcal{B}(B_s^0 \to J/\psi f_0(980)) \times \mathcal{B}(f_0(980) \to \pi^+\pi^-)/\mathcal{B}(B_s^0 \to J/\psi\phi(1020))/\mathcal{B}(\phi(1020) \to K^+K^-)$ used in our fit.

[e]Measurement of $\mathcal{B}(B_s^0 \to J/\psi f_0(500)) \times \mathcal{B}(f_0(500) \to \pi^+\pi^-)/\mathcal{B}(B_s^0 \to J/\psi f_0(980)) \times \mathcal{B}(f_0(980) \to \pi^+\pi^-)$ used in our fit.

[f]Using $\mathcal{B}(f_1(1285) \to \pi^+\pi^+\pi^-\pi^-)$.

[g]Measurement of $\mathcal{B}(B_s^0 \to J/\psi f_2'(1525))\mathcal{B}(f_2'(1525) \to K^+K^-)/\mathcal{B}(B_s^0 \to J/\psi\phi(1020))/\mathcal{B}(\phi(1020) \to K^+K^-)$ used in our fit.

[h]Using $\mathcal{B}(B_s^0 \to J/\psi f_0(980)) \times \mathcal{B}(f_0(980) \to \pi^+\pi^-)$.

TABLE 117. Branching fractions for decays to charmonium other than J/ψ.

Parameter [10^{-4}]	Measurements		Average$^{\text{HFLAV}}_{PDG}$
$\mathcal{B}(B_s^0 \to \psi(2S)\phi(1020))$	LHCb [515][b]	$5.19 \pm 0.28 \pm 0.51$	$5.27^{+0.58}_{-0.56}$ *5.25 ± 0.40*
	D0 [614][b]	$5.8 \pm 1.2 \pm 1.1$	
	CDF [655][b]	$5.5 \pm 1.4 \pm 0.9$	
	LHCb [666][c,d]		
$\mathcal{B}(B_s^0 \to \psi(2S)K^-\pi^+)$	LHCb [524][e]	$0.3120 \pm 0.0209 \pm 0.0304$	0.312 ± 0.037
$\mathcal{B}(B_s^0 \to \psi(2S)\bar{K}^*(892)^0)$	LHCb [524][f]	$0.3272 \pm 0.0347^{+0.0347}_{-0.0345}$	$0.327^{+0.050}_{-0.048}$ *$0.331^{+0.051}_{-0.052}$*
$\mathcal{B}(B_s^0 \to \psi(2S)\pi^+\pi^-)$	LHCb [537][g]	$0.71 \pm 0.08 \pm 0.09$	$0.72^{+0.13}_{-0.12}$ *0.69 ± 0.12*
	LHCb [667][a,h]		

[a]Not included in PDG average.
[b]Using $\mathcal{B}(B_s^0 \to J/\psi\phi(1020))$.
[c]Measurement of $\mathcal{B}(B_s^0 \to X(3872)\phi(1020))\mathcal{B}(X(3872) \to J/\psi\pi^+\pi^-)/\mathcal{B}(B_s^0 \to \psi(2S)\phi(1020))/\mathcal{B}(\psi(2S) \to J/\psi\pi^+\pi^-)$ used in our fit.
[d]Measurement of $\mathcal{B}(B_s^0 \to J/\psi K^*(892)^0\bar{K}^*(892)^0)\mathcal{B}(K^*(892)^0 \to K^+\pi^-) * *2/\mathcal{B}(B_s^0 \to \psi(2S)\phi(1020))/\mathcal{B}(\psi(2S) \to J/\psi\pi^+\pi^-)/\mathcal{B}(\phi(1020) \to K^+K^-)$ used in our fit.
[e]Using $\mathcal{B}(B^0 \to \psi(2S)K^+\pi^-)$.
[f]Using $\mathcal{B}(B^0 \to \psi(2S)K^*(892)^0)$.
[g]Using $\mathcal{B}(B_s^0 \to J/\psi\pi^+\pi^-)$.
[h]Measurement of $\mathcal{B}(B_s^0 \to X(3872)\pi^+\pi^-)\mathcal{B}(X(3872) \to J/\psi\pi^+\pi^-)/\mathcal{B}(B_s^0 \to \psi(2S)\pi^+\pi^-)/\mathcal{B}(\psi(2S) \to J/\psi\pi^+\pi^-)$ used in our fit.

TABLE 118. Branching fraction ratios for decays to charmonium.

Parameter	Measurements		Average
$\frac{\mathcal{B}(B_s^0 \to \chi_{c2}K^+K^-)}{\mathcal{B}(B_s^0 \to \chi_{c1}K^+K^-)}$	LHCb [668]	$0.171 \pm 0.031 \pm 0.010$	0.171 ± 0.033

TABLE 119. Decay amplitudes and relative phases for decays to $J/\psi K^*$ (see Sec. V for decays to $J/\psi\phi$).

Parameter	Measurements		Average
$f_0(B_s^0 \to J/\psi\bar{K}^*(892)^0)$	LHCb [264]	$0.497 \pm 0.025 \pm 0.025$	0.497 ± 0.035
$f_\parallel(B_s^0 \to J/\psi\bar{K}^*(892)^0)$	LHCb [264]	$0.179 \pm 0.027 \pm 0.013$	0.179 ± 0.030
$\delta_\parallel(B_s^0 \to J/\psi\bar{K}^*(892)^0)$	LHCb [264]	$-2.7 \pm 0.2 \pm 0.2$	-2.70 ± 0.25
$\delta_\perp(B_s^0 \to J/\psi\bar{K}^*(892)^0)$	LHCb [264]	$0.01 \pm 0.11^{+0.12}_{-0.13}$	0.01 ± 0.17

4. Decays to charm baryons

Averages of B_s^0 decays to charm baryons are shown in Tables 120 and 121.

TABLE 120. Branching fractions for decays to one charm baryon.

Parameter [10^{-4}]	Measurements		Average$^{\text{HFLAV}}_{PDG}$
$\mathcal{B}(B_s^0 \to \bar{\Lambda}_c^- \Lambda^0 \pi^+)$	Belle [669]	$3.6 \pm 1.1^{+0.9}_{-1.0}$	3.6 ± 1.5 *3.6 ± 1.6*

TABLE 121. Branching fractions for decays to two charm baryons.

Parameter [10^{-4}]	Measurements		Average$^{\text{HFLAV}}_{PDG}$
$\mathcal{B}(B_s^0 \to \Lambda_c^+ \bar{\Lambda}_c^-)$	LHCb [496][a,b]	< 1.2	< 1.2 *< 0.8*

[a]At CL = 95%.
[b]Using $\mathcal{B}(B_s^0 \to D_s^- D^+)$.

E. Decays of B_c^+ mesons

Measurements of B_c^+ decays to charmed hadrons are summarized in Secs. VII E 1–VII E 4.

1. Decays to a single open charm meson

Averages of B_c^+ decays to a single open charm meson are shown in Table 122.

TABLE 122. Branching fractions for decays to one charm meson.

Parameter [10^{-7}]	Measurements		Average
$f_c \times \mathcal{B}(B_c^+ \to D^0 K^+)$	LHCb [670][a]	$3.79^{+1.14}_{-1.02} \pm 0.25$	$3.8^{+1.2}_{-1.1}$

[a]Using f_u.

2. Decays to two open charm mesons

Averages of B_c^+ decays to two open charm mesons are shown in Table 123.

TABLE 123. Branching fractions for decays to two D mesons.

Parameter [10^{-6}]	Measurements	Average
$f_c \times \mathcal{B}(B_c^+ \to D_s^+ \bar{D}^0)$	LHCb [601][a]	1.2 ± 1.5
$f_c \times \mathcal{B}(B_c^+ \to D_s^+ D^0)$	LHCb [601][b]	-1.5 ± 1.0
$f_c \times \mathcal{B}(B_c^+ \to D^+ \bar{D}^0)$	LHCb [601][c]	1.3 ± 1.2
$f_c \times \mathcal{B}(B_c^+ \to D^+ D^0)$	LHCb [601][d]	0.48 ± 0.87
$f_c \times \mathcal{B}(B_c^+ \to D_s^{*+} \bar{D}^0 + D_s^+ \bar{D}^*(2007)^0)$	LHCb [601][e]	-0.4 ± 5.9
$f_c \times \mathcal{B}(B_c^+ \to D_s^{*+} D^0 + D_s^+ D^*(2007)^0)$	LHCb [601][f]	-1.2 ± 7.5
$f_c \times \mathcal{B}(B_c^+ \to D_s^{*+} \bar{D}^*(2007)^0)$	LHCb [601][g]	13 ± 17
$f_c \times \mathcal{B}(B_c^+ \to D_s^{*+} D^*(2007)^0)$	LHCb [601][h]	28 ± 36
$f_c \times (\mathcal{B}(B_c^- \to D^{*-} D^0) \times \mathcal{B}(D^{*-} \to D^-(\pi^0, \gamma)) + \mathcal{B}(B_c^- \to D^- D^{*0}))$	LHCb [601][i]	0.3 ± 5.3
$f_c \times (\mathcal{B}(B_c^- \to D^{*-} \bar{D}^0) \times \mathcal{B}(D^{*-} \to D^-(\pi^0, \gamma)) + \mathcal{B}(B_c^- \to D^- \bar{D}^{*0}))$	LHCb [601][j]	-2.5 ± 2.8
$f_c \times \mathcal{B}(B_c^+ \to D^*(2010)^+ D^*(2007)^0)$	LHCb [601][k]	-7 ± 15
$f_c \times \mathcal{B}(B_c^+ \to D^*(2010)^+ \bar{D}^*(2007)^0)$	LHCb [601][l]	56 ± 38

[a]Measurement of $f_c \times \mathcal{B}(B_c^+ \to D_s^+ \bar{D}^0)/(f_u \mathcal{B}(B^+ \to D_s^+ \bar{D}^0))$ used in our fit.
[b]Measurement of $f_c \times \mathcal{B}(B_c^+ \to D_s^+ D^0)/(f_u \mathcal{B}(B^+ \to D_s^+ \bar{D}^0))$ used in our fit.
[c]Measurement of $f_c \times \mathcal{B}(B_c^+ \to D^+ \bar{D}^0)/(f_u \mathcal{B}(B^+ \to D^+ \bar{D}^0))$ used in our fit.
[d]Measurement of $f_c \times \mathcal{B}(B_c^+ \to D^+ D^0)/(f_u \mathcal{B}(B^+ \to D^+ \bar{D}^0))$ used in our fit.
[e]Measurement of $f_c \times \mathcal{B}(B_c^+ \to D_s^{*+} \bar{D}^0 + D_s^+ \bar{D}^*(2007)^0)/(f_u \mathcal{B}(B^+ \to D_s^+ \bar{D}^0))$ used in our fit.
[f]Measurement of $f_c \times \mathcal{B}(B_c^+ \to D_s^{*+} D^0 + D_s^+ D^*(2007)^0)/(f_u \mathcal{B}(B^+ \to D_s^+ \bar{D}^0))$ used in our fit.
[g]Measurement of $f_c \times \mathcal{B}(B_c^+ \to D_s^{*+} \bar{D}^*(2007)^0)/(f_u \mathcal{B}(B^+ \to D_s^+ \bar{D}^0))$ used in our fit.
[h]Measurement of $f_c \times \mathcal{B}(B_c^+ \to D_s^{*+} D^*(2007)^0)/(f_u \mathcal{B}(B^+ \to D_s^+ \bar{D}^0))$ used in our fit.
[i]Measurement of $f_c \times (\mathcal{B}(B_c^- \to D^{*-} D^0) \times \mathcal{B}(D^{*-} \to D^-(\pi^0, \gamma)) + \mathcal{B}(B_c^- \to D^- D^{*0}))/(f_u \mathcal{B}(B^+ \to D^+ \bar{D}^0))$ used in our fit.
[j]Measurement of $f_c \times (\mathcal{B}(B_c^- \to D^{*-} \bar{D}^0) \times \mathcal{B}(D^{*-} \to D^-(\pi^0, \gamma)) + \mathcal{B}(B_c^- \to D^- \bar{D}^{*0}))/(f_u \mathcal{B}(B^+ \to D^+ \bar{D}^0))$ used in our fit.
[k]Measurement of $f_c \times \mathcal{B}(B_c^+ \to D^*(2010)^+ D^*(2007)^0)/(f_u \mathcal{B}(B^+ \to D^+ \bar{D}^0))$ used in our fit.
[l]Measurement of $f_c \times \mathcal{B}(B_c^+ \to D^*(2010)^+ \bar{D}^*(2007)^0)/(f_u \mathcal{B}(B^+ \to D^+ \bar{D}^0))$ used in our fit.

3. Decays to charmonium states

Averages of B_c^+ decays to charmonium states are shown in Tables 124 and 125.

TABLE 124. Branching fractions for decays to charmonium.

Parameter [10^{-6}]	Measurements		Average
$f_c \times \mathcal{B}(B_c^+ \to J/\psi\pi^+)$	CMS [613][a] LHCb [615][b,a], [617][c,a]		$2.79^{+0.11}_{-0.10}$
$f_c \times \mathcal{B}(B_c^+ \to \chi_{c0}\pi^+)$	LHCb [671][d]	$4.00^{+1.39}_{-1.22} \pm 0.33$	$4.0^{+1.4}_{-1.3}$

[a]Measurement of $f_c \times \mathcal{B}(B_c^+ \to J/\psi\pi^+)/(f_u \mathcal{B}(B^+ \to J/\psi K^+))$ used in our fit.
[b]$\sqrt{s} = 7$ TeV, $p_T > 4$ GeV and $2.5 < y < 4.5$.
[c]$\sqrt{s} = 8$ TeV, $0 < p_T < 20$ GeV and $2.0 < y < 4.5$.
[d]Using f_u.

TABLE 125. Branching fraction ratios for decays to charmonium.

Parameter	Measurements		Average
$\frac{\mathcal{B}(B_c^+ \to J/\psi D_s^+)}{\mathcal{B}(B_c^+ \to J/\psi\pi^+)}$	LHCb [672] ATLAS [673]	$2.9 \pm 0.6 \pm 0.2$ $3.8 \pm 1.1 \pm 0.4$	3.09 ± 0.55
$\frac{\mathcal{B}(B_c^+ \to J/\psi D_s^{*+})}{\mathcal{B}(B_c^+ \to J/\psi D_s^+)}$	ATLAS [673]	$2.8^{+1.2}_{-0.8} \pm 0.3$	$2.8^{+1.2}_{-0.9}$
$\frac{\mathcal{B}(B_c^+ \to J/\psi D_s^{*+})}{\mathcal{B}(B_c^+ \to J/\psi\pi^+)}$	ATLAS [673]	$10.4 \pm 3.1 \pm 1.6$	10.4 ± 3.5
$\frac{\mathcal{B}(B_c^+ \to J/\psi\pi^+\pi^+\pi^-)}{\mathcal{B}(B_c^+ \to J/\psi\pi^+)}$	LHCb [674] CMS [613]	$2.41 \pm 0.30 \pm 0.33$ $2.55 \pm 0.80 \pm 0.33$	2.45 ± 0.40
$\frac{\mathcal{B}(B_c^+ \to J/\psi D^*(2007)^0 K^+)}{\mathcal{B}(B_c^+ \to J/\psi D^0 K^+)}$	LHCb [675]	$5.1 \pm 1.8 \pm 0.4$	5.1 ± 1.8
$\frac{\mathcal{B}(B_c^+ \to J/\psi D^*(2010)^+ K^*(892)^0)}{\mathcal{B}(B_c^+ \to J/\psi D^0 K^+)}$	LHCb [675]	$2.1 \pm 1.1 \pm 0.3$	2.1 ± 1.1
$\frac{\mathcal{B}(B_c^+ \to J/\psi K^+)}{\mathcal{B}(B_c^+ \to J/\psi\pi^+)}$	LHCb [676]	$0.069 \pm 0.019 \pm 0.005$	0.069 ± 0.020
$\frac{\mathcal{B}(B_c^+ \to J/\psi K^+ K^-\pi^+)}{\mathcal{B}(B_c^+ \to J/\psi\pi^+)}$	LHCb [677]	$0.53 \pm 0.10 \pm 0.05$	0.53 ± 0.11
$\frac{\mathcal{B}(B_c^+ \to \psi(2S)\pi^+)}{\mathcal{B}(B_c^+ \to J/\psi\pi^+)}$	LHCb [678]	$0.268 \pm 0.032 \pm 0.009$	0.270 ± 0.033
$\frac{\mathcal{B}(B_c^+ \to J/\psi D^0 K^+)}{\mathcal{B}(B_c^+ \to J/\psi\pi^+)}$	LHCb [675]	$0.432 \pm 0.136 \pm 0.028$	0.43 ± 0.14
$\frac{\mathcal{B}(B_c^+ \to J/\psi D^+ K^*(892)^0)}{\mathcal{B}(B_c^+ \to J/\psi D^0 K^+)}$	LHCb [675]	$0.63 \pm 0.39 \pm 0.08$	0.63 ± 0.40

4. Decays to a B meson

Averages of B_c^+ decays to a B meson are shown in Table 126.

TABLE 126. Branching fractions for decays to B_s^0 meson.

Parameter [10^{-4}]	Measurements		Average
$f_c \times \mathcal{B}(B_c^+ \to B_s^0\pi^+)$	LHCb [679][a]	$2.323 \pm 0.304^{+0.291}_{-0.271}$	$2.32^{+0.43}_{-0.39}$

[a]Using f_s.

F. Decays of b baryons

Measurements of b baryon decays to charmed hadrons are summarized in Secs. VII F 1–VII F 4.

1. Decays to a single open charm meson

Averages of b baryon decays to a single open charm meson are shown in Table 127.

TABLE 127. Branching fractions for decays to $D_{(s)}$ mesons.

Parameter [10^{-5}]	Measurements		Average$^{\text{HFLAV}}_{PDG}$
$\mathcal{B}(\Lambda_b^0 \to D^0 p K^-)$	LHCb [680][b]	$4.04 \pm 0.44^{+0.44}_{-0.47}$	$4.04^{+0.65}_{-0.63}$
	LHCb [680][c]		*$4.55^{+0.75}_{-0.77}$*
$\mathcal{B}(\Lambda_b^0 \to D_s^- p)$	LHCb [681][a,d]	$1.070 \pm 0.042^{+0.099}_{-0.097}$	1.09 ± 0.10
			None
$\frac{f_{\Xi_b^0}}{f_{\Lambda_b^0}} \times \mathcal{B}(\Xi_b^0 \to D^0 p K^-)$	LHCb [680][a,e]	$1.78 \pm 0.36 \pm 0.37$	$1.78^{+0.55}_{-0.49}$
			None

[a]Not included in PDG average.
[b]Using $\mathcal{B}(\Lambda_b^0 \to D_s^0 p\pi^-)$.
[c]Measurement of $\frac{f_{\Xi_b^0}}{f_{\Lambda_b^0}} \times \mathcal{B}(\Xi_b^0 \to D^0 p K^-)/\mathcal{B}(\Lambda_b^0 \to D^0 p K^-)$ used in our fit.
[d]Using $\mathcal{B}(\Lambda_b^0 \to \Lambda_c^+ \pi^-)$.
[e]Using $\mathcal{B}(\Lambda_b^0 \to D^0 p K^-)$.

2. Decays to charmonium states

Averages of b baryon decays to charmonium states are shown in Tables 128–131.

TABLE 128. Λ_b^0 branching fractions to charmonium.

Parameter [10^{-4}]	Measurements		Average$^{\text{HFLAV}}_{PDG}$
$\mathcal{B}(\Lambda_b^0 \to J/\psi p K^-)$	LHCb [682]	$3.17 \pm 0.04^{+0.57}_{-0.45}$	$3.18^{+0.56}_{-0.45}$
	LHCb [683][b], [684][c,d], [685][a,e,f,g], [686][h,i]		*$3.17^{+0.57}_{-0.45}$*
$\mathcal{B}(\Lambda_b^0 \to J/\psi p K^- \pi^+ \pi^-)$	LHCb [684][j]	$0.6625 \pm 0.0305^{+0.1251}_{-0.1038}$	$0.66^{+0.13}_{-0.11}$
$\mathcal{B}(\Lambda_b^0 \to J/\psi p \pi^-)$	LHCb [683][j]	$0.2617 \pm 0.0079^{+0.0483}_{-0.0397}$	$0.262^{+0.050}_{-0.040}$
			$0.261^{+0.050}_{-0.040}$
$\mathcal{B}(\Lambda_b^0 \to J/\psi \Lambda^0)$	CDF [687][a]	$4.7 \pm 2.1 \pm 1.9$	
	ATLAS [688][k]		$4.7^{+2.9}_{-2.8}$
	CDF [689][a,l]		*None*
	LHCb [690][k]		
$f_{\Lambda_b^0} \times \mathcal{B}(\Lambda_b^0 \to J/\psi \Lambda^0)$	D0 [691]	$0.601 \pm 0.060 \pm 0.064$	0.601 ± 0.088
	CDF [689][a,m]		*0.585 ± 0.083*
$\mathcal{B}(\Lambda_b^0 \to \psi(2S) p K^-)$	LHCb [684][j]	$0.6574 \pm 0.0241^{+0.1182}_{-0.0958}$	$0.66^{+0.12}_{-0.10}$
	LHCb [692][n], [693][o]		
$\mathcal{B}(\Lambda_b^0 \to \psi(2S) \Lambda^0)$	LHCb [690][p]	$2.394 \pm 0.107^{+1.472}_{-1.439}$	$2.4^{+1.5}_{-1.4}$
	ATLAS [688][p]	$2.338 \pm 0.154^{+1.438}_{-1.405}$	*None*

(Table continued)

TABLE 128. *(Continued)*

Parameter [10^{-4}]	Measurements		Average$^{\text{HFLAV}}_{PDG}$
$\mathcal{B}(\Lambda_b^0 \to \chi_{c1} p K^-)$	LHCb [686][j]	$0.769 \pm 0.044^{+0.145}_{-0.121}$	$0.77^{+0.15}_{-0.12}$
	LHCb [686][q]		$0.76^{+0.15}_{-0.13}$
$\mathcal{B}(\Lambda_b^0 \to \chi_{c2} p K^-)$	LHCb [686][j]	$0.788 \pm 0.064^{+0.149}_{-0.124}$	$0.79^{+0.16}_{-0.13}$
	LHCb [686][r]	$0.785 \pm 0.077^{+0.158}_{-0.131}$	$0.79^{+0.16}_{-0.14}$

[a]Not included in PDG average.
[b]Measurement of $\mathcal{B}(\Lambda_b^0 \to J/\psi p\pi^-)/\mathcal{B}(\Lambda_b^0 \to J/\psi p K^-)$ used in our fit.
[c]Measurement of $\mathcal{B}(\Lambda_b^0 \to \psi(2S) p K^-)/\mathcal{B}(\Lambda_b^0 \to J/\psi p K^-)$ used in our fit.
[d]Measurement of $\mathcal{B}(\Lambda_b^0 \to J/\psi p K^-\pi^+\pi^-)/\mathcal{B}(\Lambda_b^0 \to J/\psi p K^-)$ used in our fit.
[e]Measurement of $\mathcal{B}(\Lambda_b^0 \to P_c(4380)^+\pi^-)/\mathcal{B}(\Lambda_b^0 \to J/\psi p K^-)$ used in our fit.
[f]Measurement of $\mathcal{B}(\Lambda_b^0 \to P_c(4457)^+\pi^-)/\mathcal{B}(\Lambda_b^0 \to J/\psi p K^-)$ used in our fit.
[g]Measurement of $\mathcal{B}(\Lambda_b^0 \to Z_c(4200)^- p)/\mathcal{B}(\Lambda_b^0 \to J/\psi p K^-)$ used in our fit.
[h]Measurement of $\mathcal{B}(\Lambda_b^0 \to \chi_{c1} p K^-)/\mathcal{B}(\Lambda_b^0 \to J/\psi p K^-)$ used in our fit.
[i]Measurement of $\mathcal{B}(\Lambda_b^0 \to \chi_{c2} p K^-)/\mathcal{B}(\Lambda_b^0 \to J/\psi p K^-)$ used in our fit.
[j]Using $\mathcal{B}(\Lambda_b^0 \to J/\psi p K^-)$.
[k]Measurement of $\mathcal{B}(\Lambda_b^0 \to \psi(2S)\Lambda^0)/\mathcal{B}(\Lambda_b^0 \to J/\psi\Lambda^0)$ used in our fit.
[l]Measurement of $\frac{f_{\Xi_b^-}}{f_{\Lambda_b^0}} \times \mathcal{B}(\Xi_b^- \to J/\psi\Xi^-)/\mathcal{B}(\Lambda_b^0 \to J/\psi\Lambda^0)$ used in our fit.
[m]Measurement of $f_{\Omega_b^-} \times \mathcal{B}(\Omega_b^- \to J/\psi\Omega^-)/f_{\Lambda_b^0} \times \mathcal{B}(\Lambda_b^0 \to J/\psi\Lambda^0)$ used in our fit.
[n]Measurement of $\mathcal{B}(\Lambda_b^0 \to \psi(2S) p\pi^-)/\mathcal{B}(\Lambda_b^0 \to \psi(2S) p K^-)$ used in our fit.
[o]Measurement of $\mathcal{B}(\Lambda_b^0 \to X(3872) p K^-)\mathcal{B}(X(3872) \to J/\psi\pi^+\pi^-)/\mathcal{B}(\Lambda_b^0 \to \psi(2S) p K^-)/\mathcal{B}(\psi(2S) \to J/\psi\pi^+\pi^-)$ used in our fit.
[p]Using $\mathcal{B}(\Lambda_b^0 \to J/\psi\Lambda^0)$.
[q]Measurement of $\mathcal{B}(\Lambda_b^0 \to \chi_{c2} p K^-)/\mathcal{B}(\Lambda_b^0 \to \chi_{c1} p K^-)$ used in our fit.
[r]Using $\mathcal{B}(\Lambda_b^0 \to \chi_{c1} p K^-)$.

TABLE 129. Ξ_b^- and Ω_b^- branching fractions to charmonium.

Parameter [10^{-5}]	Measurements		Average$^{\text{HFLAV}}_{PDG}$
$\frac{f_{\Xi_b^-}}{f_{\Lambda_b^0}} \times \mathcal{B}(\Xi_b^- \to J/\psi\Xi^-)$	CDF [689][a,b]	$7.79^{+1.73+4.82}_{-1.17-4.71}$	$7.8^{+5.4}_{-4.7}$ *None*
$f_{\Omega_b^-} \times \mathcal{B}(\Omega_b^- \to J/\psi\Omega^-)$	CDF [689][c]	$0.270^{+0.102}_{-0.072} \pm 0.046$	$0.27^{+0.12}_{-0.08}$ $0.29^{+0.11}_{-0.08}$

[a]Not included in PDG average.
[b]Using $\mathcal{B}(\Lambda_b^0 \to J/\psi\Lambda^0)$.
[c]Using $f_{\Lambda_b^0} \times \mathcal{B}(\Lambda_b^0 \to J/\psi\Lambda^0)$.

TABLE 130. Parity-violating asymmetry in Λ_b^0 decays to charmonium.

Parameter	Measurements		Average$^{\text{HFLAV}}_{PDG}$
$\alpha(\Lambda_b^0 \to J/\psi\Lambda^0)$	CMS [694][a]	$-0.14 \pm 0.14 \pm 0.10$	0.07 ± 0.10
	ATLAS [695][a]	$0.3 \pm 0.2 \pm 0.1$	*None*
	LHCb [696][a]	$0.050 \pm 0.170 \pm 0.070$	

[a]Not included in PDG average.

TABLE 131. Transverse polarization of Λ_b^0 produced in pp collisions.

Parameter	Measurements		Average$^{\text{HFLAV}}_{PDG}$
$P(\Lambda_b^0 \to J/\psi\Lambda^0)$	LHCb [696][a]	$0.060 \pm 0.070 \pm 0.020$	0.035 ± 0.055
	CMS [694][a]	$0.0 \pm 0.1 \pm 0.1$	*None*

[a]Not included in PDG average.

3. Decays to charm baryons

Averages of b baryon decays to charm baryons are shown in Tables 132–135.

TABLE 132. Λ_b branching fractions.

Parameter [10^{-3}]	Measurements		Average$^{\text{HFLAV}}_{PDG}$
$\mathcal{B}(\Lambda_b^0 \to \Lambda_c^+\pi^-)$	LHCb [442][b]	$3.981 \pm 0.027^{+0.322}_{-0.319}$	
	CDF [438][b]	$8.2 \pm 0.7 \pm 2.9$	$4.18^{+0.30}_{-0.29}$
	CDF [697][a,c]		$\mathit{4.88^{+0.36}_{-0.35}}$
	LHCb [439][c], [680][d,e], [698][f], [681][a,g]		
$\mathcal{B}(\Lambda_b^0 \to \Lambda_c^+\pi^+\pi^-\pi^-)$	LHCb [439][h]	$5.98 \pm 0.67 \pm 0.69$	
	CDF [697][h]	$12.70 \pm 1.38^{+3.07}_{-2.46}$	6.71 ± 0.95
	CDF [697]	$26.8 \pm 2.9^{+11.5}_{-10.9}$	$\mathit{7.64 \pm 1.10}$
	LHCb [439][i,j,k,l]		
$\mathcal{B}(\Lambda_b^0 \to \Lambda_c^+K^-)$	LHCb [680][h]	$0.3055 \pm 0.0067^{+0.0230}_{-0.0224}$	$0.305^{+0.024}_{-0.023}$
			$\mathit{0.356 \pm 0.028}$
$\mathcal{B}(\Lambda_b^0 \to \Lambda_c^+p\bar{p}\pi^-)$	LHCb [698][h]	$0.22567 \pm 0.00961^{+0.02104}_{-0.02068}$	0.226 ± 0.023
	LHCb [698][m,n]		$\mathit{0.263 \pm 0.027}$

[a]Not included in PDG average.
[b]Using $\mathcal{B}(B^0 \to D^-\pi^+)$.
[c]Measurement of $\mathcal{B}(\Lambda_b^0 \to \Lambda_c^+\pi^+\pi^-\pi^-)/\mathcal{B}(\Lambda_b^0 \to \Lambda_c^+\pi^-)$ used in our fit.
[d]Measurement of $\mathcal{B}(\Lambda_b^0 \to \Lambda_c^+K^-)/\mathcal{B}(\Lambda_b^0 \to \Lambda_c^+\pi^-)$ used in our fit.
[e]Measurement of $\mathcal{B}(\Lambda_b^0 \to D^0p\pi^-)\mathcal{B}(D^0 \to K^-\pi^+)/(\mathcal{B}(\Lambda_b^0 \to \Lambda_c^+\pi^-)\mathcal{B}(\Lambda_c^+ \to pK^-\pi^+))$ used in our fit.
[f]Measurement of $\mathcal{B}(\Lambda_b^0 \to \Lambda_c^+p\bar{p}\pi^-)/\mathcal{B}(\Lambda_b^0 \to \Lambda_c^+\pi^-)$ used in our fit.
[g]Measurement of $\mathcal{B}(\Lambda_b^0 \to D_s^-p)/\mathcal{B}(\Lambda_b^0 \to \Lambda_c^+\pi^-)$ used in our fit.
[h]Using $\mathcal{B}(\Lambda_b^0 \to \Lambda_c^+\pi^-)$.
[i]Measurement of $\mathcal{B}(\Lambda_b^0 \to \Sigma_c(2455)^0\pi^+\pi^-) \times \mathcal{B}(\Sigma_c(2455)^0 \to \Lambda_c^+\pi^-)/\mathcal{B}(\Lambda_b^0 \to \Lambda_c^+\pi^+\pi^-\pi^-)$ used in our fit.
[j]Measurement of $\mathcal{B}(\Lambda_b^0 \to \Sigma_c(2455)^{++}\pi^-\pi^-) \times \mathcal{B}(\Sigma_c(2455)^{++} \to \Lambda_c^+\pi^+)/\mathcal{B}(\Lambda_b^0 \to \Lambda_c^+\pi^+\pi^-\pi^-)$ used in our fit.
[k]Measurement of $\mathcal{B}(\Lambda_b^0 \to \Lambda_c(2595)^+\pi^-) \times \mathcal{B}(\Lambda_c(2595)^+ \to \Lambda_c^+\pi^+\pi^-)/\mathcal{B}(\Lambda_b^0 \to \Lambda_c^+\pi^+\pi^-\pi^-)$ used in our fit.
[l]Measurement of $\mathcal{B}(\Lambda_b^0 \to \Lambda_c(2625)^+\pi^-) \times \mathcal{B}(\Lambda_c(2625)^+ \to \Lambda_c^+\pi^+\pi^-)/\mathcal{B}(\Lambda_b^0 \to \Lambda_c^+\pi^+\pi^-\pi^-)$ used in our fit.
[m]Measurement of $\mathcal{B}(\Lambda_b^0 \to \Sigma_c(2455)^0p\bar{p}) \times \mathcal{B}(\Sigma_c(2455)^0 \to \Lambda_c^+\pi^-)/\mathcal{B}(\Lambda_b^0 \to \Lambda_c^+p\bar{p}\pi^-)$ used in our fit.
[n]Measurement of $\mathcal{B}(\Lambda_b^0 \to \Sigma_c(2520)^0p\bar{p}) \times \mathcal{B}(\Sigma_c(2520)^0 \to \Lambda_c^+\pi^-)/\mathcal{B}(\Lambda_b^0 \to \Lambda_c^+p\bar{p}\pi^-)$ used in our fit.

TABLE 133. Ξ_b branching fractions.

Parameter [10^{-4}]	Measurements		Average$^{\text{HFLAV}}_{PDG}$
$\frac{f_{\Xi_b^-}}{f_{\Lambda_b^0}} \times \mathcal{B}(\Xi_b^- \to \Lambda_b^0 \pi^-)$	LHCb [699][a]	$5.7 \pm 1.8^{+0.8}_{-0.9}$	5.7 ± 2.0 *None*

[a]Not included in PDG average.

TABLE 134. Branching fraction ratios of b baryons.

Parameter	Measurements		Average$^{\text{HFLAV}}_{PDG}$
$\frac{\mathcal{B}(\Lambda_b^0 \to \Lambda_c^+ D^-)}{\mathcal{B}(\Lambda_b^0 \to \Lambda_c^+ D_s^-)}$	LHCb [496][a]	$0.042 \pm 0.003 \pm 0.003$	0.0420 ± 0.0042 *None*
$\frac{\mathcal{B}(\Lambda_b^0 \to \Lambda_c(2860)^+ \pi^-) \times \mathcal{B}(\Lambda_c(2860)^+ \to D^0 p)}{\mathcal{B}(\Lambda_b^0 \to \Lambda_c(2880)^+ \pi^-) \times \mathcal{B}(\Lambda_c(2880)^+ \to D^0 p)}$	LHCb [700]	$4.51^{+0.51}_{-0.39}{}^{+0.21}_{-0.45}$	4.51 ± 0.57 *None*
$\frac{\mathcal{B}(\Lambda_b^0 \to \Lambda_c(2940)^+ \pi^-) \times \mathcal{B}(\Lambda_c(2940)^+ \to D^0 p)}{\mathcal{B}(\Lambda_b^0 \to \Lambda_c(2880)^+ \pi^-) \times \mathcal{B}(\Lambda_c(2880)^+ \to D^0 p)}$	LHCb [700]	$0.83^{+0.31}_{-0.10}{}^{+0.18}_{-0.43}$	$0.83^{+0.36}_{-0.45}$ *None*
$\frac{\mathcal{B}(\Xi_b^0 \to \Lambda_c^+ K^-)}{\mathcal{B}(\Xi_b^0 \to D^0 p K^-)}$	LHCb [680][a,b]		0.35 ± 0.19 *None*

[a]Not included in PDG average.
[b]Measurement of $\frac{\mathcal{B}(\Xi_b^0 \to \Lambda_c^+ K^-)}{\mathcal{B}(\Xi_b^0 \to D^0 p K^-)} \mathcal{B}(\Lambda_c^+ \to p K^- \pi^+)/\mathcal{B}(D^0 \to K^- \pi^+)$ used in our fit.

TABLE 135. Product branching fractions of b baryons.

Parameter [10^{-4}]	Measurements		Average$^{\text{HFLAV}}_{PDG}$
$\mathcal{B}(\Lambda_b^0 \to \Sigma_c(2455)^0 p \bar{p}) \times \mathcal{B}(\Sigma_c(2455)^0 \to \Lambda_c^+ \pi^-)$	LHCb [698][a]	$0.2009 \pm 0.0339 \pm 0.0245$	$0.201^{+0.044}_{-0.040}$ *0.234 ± 0.049*
$\mathcal{B}(\Lambda_b^0 \to \Sigma_c(2520)^0 p \bar{p}) \times \mathcal{B}(\Sigma_c(2520)^0 \to \Lambda_c^+ \pi^-)$	LHCb [698][a]	$0.2686 \pm 0.0451 \pm 0.0417$	$0.269^{+0.064}_{-0.059}$ *0.313 ± 0.072*
$\mathcal{B}(\Lambda_b^0 \to \Lambda_c(2595)^+ \pi^-) \times \mathcal{B}(\Lambda_c(2595)^+ \to \Lambda_c^+ \pi^+ \pi^-)$	LHCb [439][b]	$2.95 \pm 1.14^{+0.58}_{-0.50}$	$3.0^{+1.3}_{-1.2}$ $3.4^{+1.5}_{-1.4}$
$\mathcal{B}(\Lambda_b^0 \to \Lambda_c(2625)^+ \pi^-) \times \mathcal{B}(\Lambda_c(2625)^+ \to \Lambda_c^+ \pi^+ \pi^-)$	LHCb [439][b]	$2.89 \pm 1.01 \pm 0.49$	$2.9^{+1.2}_{-1.1}$ *3.3 ± 1.3*
$\mathcal{B}(\Lambda_b^0 \to \Sigma_c(2455)^0 \pi^+ \pi^-) \times \mathcal{B}(\Sigma_c(2455)^0 \to \Lambda_c^+ \pi^-)$	LHCb [439][b]	$4.97 \pm 1.61 \pm 1.07$	5.0 ± 2.0 *5.7 ± 2.2*
$\mathcal{B}(\Lambda_b^0 \to \Sigma_c(2455)^{++} \pi^- \pi^-) \times \mathcal{B}(\Sigma_c(2455)^{++} \to \Lambda_c^+ \pi^+)$	LHCb [439][b]	$2.82 \pm 1.21 \pm 0.62$	2.8 ± 1.4 *3.2 ± 1.5*

[a]Using $\mathcal{B}(\Lambda_b^0 \to \Lambda_c^+ p \bar{p} \pi^-)$.
[b]Using $\mathcal{B}(\Lambda_b^0 \to \Lambda_c^+ \pi^+ \pi^- \pi^-)$.

4. Decays to exotic states

Averages of b baryon decays to $XYZP$ states are shown in Table 136.

TABLE 136. Branching fractions for decays to pentaquarks.

Parameter [10^{-4}]	Measurements		Average$^{\mathrm{HFLAV}}_{PDG}$
$\mathcal{B}(\Lambda_b^0 \to P_c(4380)^+\pi^-)$	LHCb [685][a,b]	$0.162 \pm 0.048^{+0.087}_{-0.056}$	$0.16^{+0.10}_{-0.07}$
	LHCb [685][a,c]	$0.162 \pm 0.052^{+0.389}_{-0.133}$	*None*
$\mathcal{B}(\Lambda_b^0 \to P_c(4380)^+K^-)$	LHCb [685][a,d]		$3.2^{+7.4}_{-1.8}$
			None
$\mathcal{B}(\Lambda_b^0 \to P_c(4457)^+\pi^-)$	LHCb [685][a,b]	$0.051^{+0.025+0.021}_{-0.019-0.017}$	$0.051^{+0.034}_{-0.025}$
	LHCb [685][a,e]	$0.051^{+0.025+0.090}_{-0.022-0.036}$	*None*
$\mathcal{B}(\Lambda_b^0 \to P_c(4457)^+K^-)$	LHCb [685][a,f]		$1.5^{+2.6}_{-0.9}$
			None
$\mathcal{B}(\Lambda_b^0 \to Z_c(4200)^- p)$	LHCb [685][a,b]	$0.245 \pm 0.089^{+0.116}_{-0.132}$	0.24 ± 0.15
			None

[a]Not included in PDG average.
[b]Using $\mathcal{B}(\Lambda_b^0 \to J/\psi p K^-)$.
[c]Using $\mathcal{B}(\Lambda_b^0 \to P_c(4380)^+K^-)$.
[d]Measurement of $\mathcal{B}(\Lambda_b^0 \to P_c(4380)^+\pi^-)/\mathcal{B}(\Lambda_b^0 \to P_c(4380)^+K^-)$ used in our fit.
[e]Using $\mathcal{B}(\Lambda_b^0 \to P_c(4457)^+K^-)$.
[f]Measurement of $\mathcal{B}(\Lambda_b^0 \to P_c(4457)^+\pi^-)/\mathcal{B}(\Lambda_b^0 \to P_c(4457)^+K^-)$ used in our fit.

VIII. *b*-HADRON DECAYS TO CHARMLESS FINAL STATES

This section provides branching fractions (BF), polarization fractions, CP asymmetries (A_{CP}) and other observables of b-hadron decays to final states that do not contain charm hadrons or charmonium mesons,[14] except for a few lepton-flavor- and lepton-number-violating decays reported in Sec. VIII F. Four categories of B^0 and B^+ decays are reported: mesonic (i.e., final states containing only mesons), baryonic (hadronic final states with baryon-antibaryon pairs), radiative (including a photon or a lepton-antilepton pair) and semileptonic/leptonic (including/only leptons). We also report measurements of B_s^0, B_c^+ and b-baryon decays, and measurements of final-state polarization in b-hadron decays. As discussed in Sec. II, measurements included in our averages are those supported with public notes, including journal papers, conference-contributed papers, preprints or conference proceedings, except when a result has not led to a journal publication after an extended period of time.

The largest improvements since our last report [1] have come from a variety of new measurements from LHCb and Belle-II. This includes LHCb's update of the ratio R_{K^*}, which is now consistent with the standard model prediction at the level of 0.6 standard deviations, as well as the first evidence of the decay $B \to K\nu\bar{\nu}$ from Belle II.

The averaging procedure follows the methodology described in Sec. III. We perform fits of the full likelihood function and do not use the approximation described in Sec. III A. Thus, observables that are related to each other, e.g., by ratios of branching fractions, are fitted jointly. Details about all the observables involved in each average, as well as the induced correlation coefficients and p-values, are available via clickable links from each average in the tables on our web page [701].[15] In total 404 fits are performed, with on average (maximally) 1.2 (37) parameters and 4.1 (20) measurements per fit. In our tables, each group of rows contains the individual measurements and the average corresponding to a given parameter p_j.

[14]The treatment of intermediate charm or charmonium states differs between observables and sometimes among results for the same observable. In the latter case, when these results are averaged, we indicate the differences by footnotes.

[15]Where available, other sources of correlations between measurements of the same observable and among different observables are also taken into account.

The cases where the fits incorporate measurements that are functions of p_j, which are used as direct inputs to the fits, are indicated with a footnote. In general, a value of p_j is not quoted in the tables. There are two exceptions to this: a ratio of branching fractions, p_j/p_k, where p_k is the branching fraction of a normalization mode, and a product, $p_j p_k$ of the branching fraction of interest with that of a daughter decay. In these two cases the numerical value of p_j, naively obtained using the known value of p_k, is quoted in the tables for reference, and the uncertainty on p_k is included in the systematic uncertainty on p_j.

Systematic uncertainties are taken as quoted in the original publications, without the scaling of multiplicative uncertainties discussed in Sec. III C. When several systematic uncertainties are given separately, we sum them in quadrature and quote a single systematic uncertainty. These cases are marked by a footnote.

If one or more experiments report a BF measurement with a significance of more than three standard deviations (σ), all available central values for that BF are used in our average. For BFs that do not satisfy this criterion, the most stringent limit is used. Quoted upper limits are at 90% confidence level (CL), unless mentioned otherwise. For observables that are not BFs, such as A_{CP} or polarization fractions, we include in our averages all the available results, regardless of their significance.

Many of the branching fractions from *BABAR* and Belle assume equal production of charged and neutral B-meson pairs. The best measurements to date show that this is still a reasonable approximation (see Sec. IV), and thus, we do not correct for it and simply quote the results from the original publications.

At the end of some of the sections, we list results that were not included in the tables. Typical cases are measurements of distributions, such as differential branching fractions or longitudinal polarizations, which are measured in different binning schemes by the different collaborations, and thus cannot be directly used to obtain averages.

Observables obtained by Dalitz-plot analyses are marked by footnotes. In these analyses, different experimental collaborations often use different models, in particular for the nonresonant component. When applicable, we detail the model used for the nonresonant component in a footnote. In addition to this, Dalitz-plot analyses often yield multiple solutions. In this case, we take the results corresponding to the global minimum and follow the conclusions of the papers.

In most of the tables, the averages are compared to those from the PDG 2022 and 2023 updates [302]. When this is done, the "average" column quotes the PDG averages (in italic characters) only if they differ from ours. In general, such differences are due to different input parameters, differences in the averaging methods and different rounding conventions. Unlike the PDG, no error scaling is applied in our averages when the fit χ^2 is greater than 1. On the other hand, the fit p-value is quoted if it is below 1%. Input values that are not included in the PDG 2023 average are marked with footnotes. These are new results published since the closing of PDG 2023 and before the closing of this report in September 2023. Input values that were unpublished at the closing of this report (unpublished results are never included in the PDG averages) are also marked with footnotes.

Sections VIII A and VIII B provide compilations of branching fractions of B^0 and B^+ to mesonic and baryonic charmless final states, respectively. Sections VIII C, VIII D and VIII E give branching fractions of b-baryon, B_s^0-meson, and B_c^+ meson decays to charmless final states, respectively.[16] In Sec. VIII F observables of interest are given for radiative decays and FCNC decays with leptons of B^0 and B^+ mesons, including limits from searches for lepton-flavor/number-violating decays. Finally, Secs. VIII G and VIII H give CP asymmetries and results of polarization measurements, respectively, in various b-hadron charmless decays.

A. Mesonic decays of B^+ and B^0 mesons

This section provides branching fractions of charmless mesonic decays. Tables 137–148 are for B^+ and Tables 149–163 are for B^0 mesons. For both, decay modes with and without strange mesons in the final state appear in different tables. Finally, Tables 164 and 165 detail several relative branching fractions of B^+ and B^0 decays, respectively. Figure 29 gives a graphic representation of a selection of high-precision branching fractions given in this section.

[16]Except for decays of B_c^+ mesons to final states containing B_s^0 mesons, which are quoted in Sec. VII E.

TABLE 137. Branching fractions of charmless mesonic B^+ decays with strange mesons (part 1).

Parameter [10^{-6}]	Measurements		Average$^{\text{HFLAV}}_{PDG}$
$\mathcal{B}(B^+ \to K^0\pi^+)$[c]	Belle [702]	$23.97 \pm 0.53 \pm 0.71$	23.9 ± 0.6 *23.7 ± 0.8*
	Belle II [703][a]	$24.4 \pm 0.7 \pm 0.9$	
	BABAR [704]	$23.9 \pm 1.1 \pm 1.0$	
	CLEO [705]	$18.8^{+3.7+2.1}_{-3.3-1.8}$	
	LHCb [706][d]		
$\mathcal{B}(B^+ \to K^+\pi^0)$	Belle [702]	$12.62 \pm 0.31 \pm 0.56$	13.2 ± 0.4 *12.9 ± 0.5*
	Belle II [703][a]	$13.9 \pm 0.4 \pm 0.7$	
	BABAR [707]	$13.6 \pm 0.6 \pm 0.7$	
	CLEO [705]	$12.9^{+2.4+1.2}_{-2.2-1.1}$	
$\mathcal{B}(B^+ \to \eta' K^+)$	*BABAR* [708]	$71.5 \pm 1.3 \pm 3.2$	68.9 ± 2.3 *70.4 ± 2.5*
	Belle [709]	$69.2 \pm 2.2 \pm 3.7$	
	Belle II [710][a]	$63.4^{+3.4}_{-3.3} \pm 3.4$	
	Belle [711]	$61^{+10}_{-8} \pm 1$	
	CLEO [712]	$80^{+10}_{-9} \pm 7$	
	LHCb [713][b,e]		
$\mathcal{B}(B^+ \to \eta' K^*(892)^+)$	*BABAR* [714]	$4.8^{+1.6}_{-1.4} \pm 0.8$	$4.8^{+1.8}_{-1.6}$
	Belle [715]	< 2.9	
$\mathcal{B}(B^+ \to \eta'(K\pi)^{*+}_0)$	*BABAR* [714]	$6.0^{+2.2}_{-2.0} \pm 0.9$	6.0 ± 2.3 *None*
$\mathcal{B}(B^+ \to \eta' K^*_0(1430)^+)$	*BABAR* [714][f]	$5.2 \pm 1.9 \pm 1.0$	5.2 ± 2.1
$\mathcal{B}(B^+ \to \eta' K^*_2(1430)^+)$	*BABAR* [714]	$28.0^{+4.6}_{-4.3} \pm 2.6$	28.0 ± 5.2 $28.0^{+5.3}_{-5.0}$

[a]Preliminary result.
[b]Not included in PDG average.
[c]The PDG average is a result of a fit including input from other measurements.
[d]Measurement of $\mathcal{B}(B^+ \to K^+\bar{K}^0)/\mathcal{B}(B^+ \to K^0\pi^+)$ used in our fit.
[e]Measurement of $\mathcal{B}(B^0_s \to \eta'\eta')/\mathcal{B}(B^+ \to \eta' K^+)$ used in our fit.
[f]Multiple systematic uncertainties are added in quadrature.

TABLE 138. Branching fractions of charmless mesonic B^+ decays with strange mesons (part 2).

Parameter [10^{-6}]	Measurements		Average$^{\text{HFLAV}}_{PDG}$
$\mathcal{B}(B^+ \to \eta K^+)$[a]	Belle [716]	$2.12 \pm 0.23 \pm 0.11$	
	BABAR [708]	$2.94^{+0.39}_{-0.34} \pm 0.21$	2.36 ± 0.21
	CLEO [712]	$2.2^{+2.8}_{-2.2}$	$\mathit{2.36^{+0.38}_{-0.37}}$
$\mathcal{B}(B^+ \to \eta K^*(892)^+)$	*BABAR* [717]	$18.9 \pm 1.8 \pm 1.3$	
	Belle [718]	$19.3^{+2.0}_{-1.9} \pm 1.5$	19.2 ± 1.3
	CLEO [712]	$26.4^{+9.6}_{-8.2} \pm 3.3$	$\mathit{19.3 \pm 1.6}$
$\mathcal{B}(B^+ \to \eta(K\pi)^{*+}_0)$	*BABAR* [717]	$18.2 \pm 2.6 \pm 2.6$	18.2 ± 2.6 *None*
$\mathcal{B}(B^+ \to \eta K^*_0(1430)^+)$[b]	*BABAR* [717][c]	$12.9 \pm 1.8 \pm 1.8$	12.9 ± 1.8 $\mathit{18.2 \pm 3.7}$
$\mathcal{B}(B^+ \to \eta K^*_2(1430)^+)$	*BABAR* [717]	$9.1 \pm 2.7 \pm 1.4$	9.1 ± 2.2 $\mathit{9.1 \pm 3.0}$
$\mathcal{B}(B^+ \to \eta(1295)K^+) \times \mathcal{B}(\eta(1295) \to \eta\pi\pi)$	*BABAR* [719]	$2.9^{+0.8}_{-0.7} \pm 0.2$	$2.9^{+0.8}_{-0.7}$
$\mathcal{B}(B^+ \to \eta(1405)K^+) \times \mathcal{B}(\eta(1405) \to \eta\pi\pi)$	*BABAR* [719]	< 1.3	< 1.3
$\mathcal{B}(B^+ \to \eta(1405)K^+) \times \mathcal{B}(\eta(1405) \to K^*K)$	*BABAR* [719]	< 1.2	< 1.2
$\mathcal{B}(B^+ \to \eta(1475)K^+) \times \mathcal{B}(\eta(1475) \to K^*K)$	*BABAR* [719]	$13.8^{+1.8+1.0}_{-1.7-0.6}$	$13.8^{+2.1}_{-1.8}$
$\mathcal{B}(B^+ \to f_1(1285)K^+) \times \mathcal{B}(f_1(1285) \to \eta\pi\pi)$	*BABAR* [719]	< 0.8	< 0.80 *None*
$\mathcal{B}(B^+ \to f_1(1420)K^+) \times \mathcal{B}(f_1(1420) \to \eta\pi\pi)$	*BABAR* [719]	< 2.9	< 2.9
$\mathcal{B}(B^+ \to f_1(1420)K^+) \times \mathcal{B}(f_1(1420) \to K^*K)$	*BABAR* [719]	< 4.1	< 4.1
$\mathcal{B}(B^+ \to \phi(1680)K^+) \times \mathcal{B}(\phi(1680) \to K^*K)$	*BABAR* [719]	< 3.4	< 3.4
$\mathcal{B}(B^+ \to f_0(1500)K^+)$	*BABAR* [720][d]	$17 \pm 4 \pm 12$	17 ± 12
	BABAR [720][e]	$20 \pm 10 \pm 27$	$\mathit{4 \pm 2}$

[a]The PDG uncertainty includes a scale factor.
[b]The PDG entry corresponds to $\mathcal{B}(B^+ \to \eta(K\pi)^{*+}_0)$.
[c]Multiple systematic uncertainties are added in quadrature.
[d]Result extracted from Dalitz-plot analysis of $B^+ \to K^+K^+K^-$ decays.
[e]Result extracted from Dalitz-plot analysis of $B^+ \to K^0_S K^0_S K^+$ decays.

TABLE 139. Branching fractions of charmless mesonic B^+ decays with strange mesons (part 3).

Parameter [10^{-6}]	Measurements		Average$^{\text{HFLAV}}_{PDG}$
$\mathcal{B}(B^+ \to \omega(782)K^+)$[b]	Belle [721]	$6.8 \pm 0.4 \pm 0.4$	
	BABAR [722]	$6.3 \pm 0.5 \pm 0.3$	6.47 ± 0.40
	CLEO [723]	$3.2^{+2.4}_{-1.9} \pm 0.8$	
$\mathcal{B}(B^+ \to \omega(782)K^*(892)^+)$	*BABAR* [724]	< 7.4	< 7.4
$\mathcal{B}(B^+ \to \omega(782)(K\pi)^{*+}_0)$	*BABAR* [724]	$27.5 \pm 3.0 \pm 2.6$	27.5 ± 4.0
$\mathcal{B}(B^+ \to \omega(782)K^*_0(1430)^+)$	*BABAR* [724]	$24.0 \pm 2.6 \pm 4.4$	24.0 ± 5.1
$\mathcal{B}(B^+ \to \omega(782)K^*_2(1430)^+)$	*BABAR* [724]	$21.5 \pm 3.6 \pm 2.4$	21.5 ± 4.3
$\mathcal{B}(B^+ \to a_0(980)^+K^0) \times \mathcal{B}(a_0(980)^+ \to \eta\pi^+)$	*BABAR* [725]	< 3.9	< 3.9
$\mathcal{B}(B^+ \to a_0(980)^0K^+) \times \mathcal{B}(a_0(980)^0 \to \eta\pi^0)$	*BABAR* [725]	< 2.5	< 2.5
$\mathcal{B}(B^+ \to K^*(892)^0\pi^+)$	*BABAR* [726][c]	$10.8 \pm 0.6^{+1.2}_{-1.4}$	
	Belle [727][c]	$9.67 \pm 0.64^{+0.81}_{-0.89}$	10.4 ± 0.8
	BABAR [728][d,e]	$14.6 \pm 2.4^{+1.4}_{-1.5}$	*10.1 ± 0.8*
$\mathcal{B}(B^+ \to K^*(892)^+\pi^0)$	*BABAR* [728][d,e]	$9.2 \pm 1.3^{+0.7}_{-0.8}$	
	BABAR [729]	$8.2 \pm 1.5 \pm 1.1$	8.8 ± 1.2
	CLEO [723]	$7.1^{+11.4}_{-7.1} \pm 1.0$	*6.8 ± 0.9*
$\mathcal{B}(B^+ \to K^+\pi^+\pi^-)$	LHCb [730][f]	$57.71 \pm 0.37 \pm 1.45$	
	BABAR [726][c]	$54.4 \pm 1.1 \pm 4.6$	57.6 ± 1.4
	Belle [727][c]	$48.8 \pm 1.1 \pm 3.6$	*51.0 ± 2.9*
	Belle II [731][a]	$67.0 \pm 3.3 \pm 2.3$	
$\mathcal{B}(B^+ \to K^+\pi^+\pi^-(\text{NR}))$	*BABAR* [726][c,g]	$9.3 \pm 1.0^{+6.9}_{-1.7}$	$16.3^{+2.0}_{-1.8}$
	Belle [727][c]	$16.9 \pm 1.3^{+1.7}_{-1.6}$	$16.3^{+2.1}_{-1.5}$

[a]Preliminary result.

[b]The measurement from the Dalitz-plot analysis of $B^+ \to K^+\pi^+\pi^-$ decays [726] was not included in this average. It is quoted as a separate entry.

[c]Result extracted from Dalitz-plot analysis of $B^+ \to K^+\pi^+\pi^-$ decays.

[d]Result extracted from Dalitz-plot analysis of $B^+ \to K^0_S\pi^+\pi^0$ decays.

[e]Multiple systematic uncertainties are added in quadrature.

[f]Using $\mathcal{B}(B^+ \to K^+K^+K^-)$.

[g]The total nonresonant contribution is obtained by combining a exponential nonresonant component with the effective-range part of the LASS line shape.

TABLE 140. Branching fractions of charmless mesonic B^+ decays with strange mesons (part 4).

Parameter [10^{-6}]	Measurements		Average$^{\text{HFLAV}}_{PDG}$
$\mathcal{B}(B^+ \to \omega(782)K^+(K^+\pi^+\pi^-))$[a]	*BABAR* [726][b]	$5.9^{+8.8+0.5}_{-9.0-0.4}$	5.9 ± 8.9 *$5.9^{+8.8}_{-9.0}$*
$\mathcal{B}(B^+ \to f_0(980)K^+) \times \mathcal{B}(f_0(980) \to \pi^+\pi^-)$	*BABAR* [726][b] Belle [727][b]	$10.3 \pm 0.5^{+2.0}_{-1.4}$ $8.78 \pm 0.82^{+0.85}_{-1.76}$	$9.40^{+0.84}_{-0.92}$ *$9.40^{+1.02}_{-1.18}$*
$\mathcal{B}(B^+ \to f_2(1270)K^+)$	Belle [727][b] *BABAR* [726][b]	$1.33 \pm 0.30^{+0.23}_{-0.34}$ $0.89^{+0.38+0.01}_{-0.33-0.03}$	1.07 ± 0.31 *1.07 ± 0.27*
$\mathcal{B}(B^+ \to f_0(1370)K^+) \times \mathcal{B}(f_0(1370) \to \pi^+\pi^-)$	*BABAR* [732][b]	< 10.7	< 11
$\mathcal{B}(B^+ \to \rho(1450)^0K^+) \times \mathcal{B}(\rho(1450)^0 \to \pi^+\pi^-)$	*BABAR* [732][b]	< 11.7	< 12
$\mathcal{B}(B^+ \to f_2'(1525)K^+) \times \mathcal{B}(f_2'(1525) \to \pi^+\pi^-)$	*BABAR* [732][b]	< 3.4	< 3.4
$\mathcal{B}(B^+ \to \rho^0(770)K^+)$	*BABAR* [726][b] Belle [727][b]	$3.56 \pm 0.45^{+0.57}_{-0.46}$ $3.89 \pm 0.47^{+0.43}_{-0.41}$	3.74 ± 0.47 *$3.74^{+0.48}_{-0.45}$*
$\mathcal{B}(B^+ \to K_0^*(1430)^0\pi^+)$[3c]	*BABAR* [726][b] Belle [727][b] *BABAR* [728][d,e]	$32.0 \pm 1.2^{+10.8}_{-6.0}$ $51.6 \pm 1.7^{+7.0}_{-7.5}$ $50.0 \pm 4.8^{+6.7}_{-6.6}$	46.9 ± 5.0 *$39.0^{+5.7}_{-5.0}$*
$\mathcal{B}(B^+ \to K_2^*(1430)^0\pi^+)$	*BABAR* [726][b] Belle [733][b]	$5.6 \pm 1.2^{+1.8}_{-0.8}$ < 6.9	$5.6^{+2.2}_{-1.4}$ *$5.6^{+2.2}_{-1.5}$*
$\mathcal{B}(B^+ \to K^*(1410)^0\pi^+)$	Belle [733][b]	< 45.0	< 45
$\mathcal{B}(B^+ \to K^*(1680)^0\pi^+)$	Belle [733][b] *BABAR* [732][b]	< 12.0 < 15.0	< 12
$\mathcal{B}(B^+ \to K^+\pi^0\pi^0)$	*BABAR* [729]	$16.2 \pm 1.2 \pm 1.5$	16.2 ± 1.9
$\mathcal{B}(B^+ \to f_0(980)K^+) \times \mathcal{B}(f_0(980) \to \pi^0\pi^0)$	*BABAR* [729]	$2.8 \pm 0.6 \pm 0.5$	2.8 ± 0.8

[a]This result was not included in the main entry of $\mathcal{B}(B^+ \to \omega(782)K^+)$.
[b]Result extracted from Dalitz-plot analysis of $B^+ \to K^+\pi^+\pi^-$ decays.
[c]The PDG uncertainty includes a scale factor.
[d]Result extracted from Dalitz-plot analysis of $B^+ \to K_S^0\pi^+\pi^0$ decays.
[e]Multiple systematic uncertainties are added in quadrature.

TABLE 141. Branching fractions of charmless mesonic B^+ decays with strange mesons (part 5).

Parameter [10^{-6}]	Measurements		Average$^{\text{HFLAV}}_{PDG}$
$\mathcal{B}(B^+ \to K^-\pi^+\pi^+)$	LHCb [734]	< 0.046	< 0.046
	BABAR [735]	< 0.95	
	Belle [736]	< 4.5	
$\mathcal{B}(B^+ \to K^-\pi^+\pi^+(\text{NR}))$	CLEO [737]	< 56	< 56
$\mathcal{B}(B^+ \to K_1(1270)^0\pi^+)$	*BABAR* [738]	< 40	< 40
$\mathcal{B}(B^+ \to K_1(1400)^0\pi^+)$	*BABAR* [738]	< 39	< 39
$\mathcal{B}(B^+ \to K^0\pi^+\pi^0)$	CLEO [739]	< 66.0	< 66
$\mathcal{B}(B^+ \to K_0^*(1430)^+\pi^0)$	*BABAR* [728][a,b]	$17.2 \pm 2.4^{+1.5}_{-3.0}$	$17.2^{+2.8}_{-3.8}$ *$11.9^{+2.0}_{-2.3}$*
$\mathcal{B}(B^+ \to \rho^+(770)K^0)$	*BABAR* [728][a,b]	$9.4 \pm 1.6^{+1.1}_{-2.8}$	$9.4^{+1.9}_{-3.2}$ *$7.3^{+1.0}_{-1.2}$*
$\mathcal{B}(B^+ \to K^*(892)^+\pi^+\pi^-)$	*BABAR* [740]	$75.3 \pm 6.0 \pm 8.1$	75 ± 10
$\mathcal{B}(B^+ \to K^*(892)^+\rho^0(770))$	*BABAR* [741]	$4.6 \pm 1.0 \pm 0.4$	4.6 ± 1.1
$\mathcal{B}(B^+ \to f_0(980)K^*(892)^+) \times \mathcal{B}(f_0(980) \to \pi^+\pi^-)$	*BABAR* [741]	$4.2 \pm 0.6 \pm 0.3$	4.2 ± 0.7
$\mathcal{B}(B^+ \to a_1(1260)^+K^0)$	*BABAR* [742]	$34.9 \pm 5.0 \pm 4.4$	34.9 ± 6.7
$\mathcal{B}(B^+ \to b_1(1235)^+K^0) \times \mathcal{B}(b_1(1235)^0 \to \omega(782)\pi^+)$	*BABAR* [743]	$9.6 \pm 1.7 \pm 0.9$	9.6 ± 1.9
$\mathcal{B}(B^+ \to K^*(892)^0\rho^+(770))$	*BABAR* [744]	$9.6 \pm 1.7 \pm 1.5$	
	Belle [745][c]	$8.9 \pm 1.7 \pm 1.2$	9.2 ± 1.5
$\mathcal{B}(B^+ \to K_1(1400)^+\rho^0(770))$	ARGUS [746]	< 780	< 780
$\mathcal{B}(B^+ \to K_2^*(1430)^+\rho^0(770))$	ARGUS [746]	< 1500	< 1500

[a]Result extracted from Dalitz-plot analysis of $B^+ \to K^0_S\pi^+\pi^0$ decays.
[b]Multiple systematic uncertainties are added in quadrature.
[c]See also Ref. [747].

TABLE 142. Branching fractions of charmless mesonic B^+ decays with strange mesons (part 6).

Parameter [10^{-6}]	Measurements		Average$^{\text{HFLAV}}_{PDG}$
$\mathcal{B}(B^+ \to b_1(1235)^0 K^+) \times \mathcal{B}(b_1(1235)^0 \to \omega(782)\pi^0)$	*BABAR* [748]	$9.1 \pm 1.7 \pm 1.0$	9.1 ± 2.0
$\mathcal{B}(B^+ \to b_1(1235)^+ K^*(892)^0) \times \mathcal{B}(b_1(1235)^+ \to \omega(782)\pi^+)$	*BABAR* [749]	< 5.9	< 5.9
$\mathcal{B}(B^+ \to b_1(1235)^0 K^*(892)^+) \times \mathcal{B}(b_1(1235)^0 \to \omega(782)\pi^0)$	*BABAR* [749]	< 6.7	< 6.7
$\mathcal{B}(B^+ \to K^+ \bar{K}^0)$[a]	Belle [702]	$1.11 \pm 0.19 \pm 0.05$	
	LHCb [706][b]	$1.53 \pm 0.22 \pm 0.10$	1.32 ± 0.14
	BABAR [704]	$1.61 \pm 0.44 \pm 0.09$	*1.31 ± 0.17*
$\mathcal{B}(B^+ \to \bar{K}^0 K^+ \pi^0)$	CLEO [739]	< 24.0	< 24
$\mathcal{B}(B^+ \to K^+ K_S^0 K_S^0)$[c]	Belle [750]	$10.42 \pm 0.43 \pm 0.22$	10.29 ± 0.37
	BABAR [720][d,e]	$10.1 \pm 0.5 \pm 0.3$	*10.49 ± 0.37*
$\mathcal{B}(B^+ \to f_0(980) K^+) \times \mathcal{B}(f_0(980) \to K_S^0 K_S^0)$	*BABAR* [720][d]	$14.7 \pm 2.8 \pm 1.8$	14.7 ± 3.3
$\mathcal{B}(B^+ \to f_0(1710) K^+) \times \mathcal{B}(f_0(1710) \to K_S^0 K_S^0)$	*BABAR* [720][d]	$0.48^{+0.40}_{-0.24} \pm 0.11$	$0.48^{+0.41}_{-0.26}$
$\mathcal{B}(B^+ \to K^+ K_S^0 K_S^0(\text{NR}))$	*BABAR* [720][f,d]	$19.8 \pm 3.7 \pm 2.5$	19.8 ± 4.5
$\mathcal{B}(B^+ \to K_S^0 K_S^0 \pi^+)$	*BABAR* [751]	< 0.51	< 0.51
	Belle [750]	< 0.87	

[a]The PDG average is a result of a fit including input from other measurements.

[b]Using $\mathcal{B}(B^+ \to K^0 \pi^+)$.

[c]PDG uses the *BABAR* result including the χ_{c0} intermediate state.

[d]Result extracted from Dalitz-plot analysis of $B^+ \to K_S^0 K_S^0 K^+$ decays.

[e]All charmonium resonances are vetoed. The analysis also reports $\mathcal{B}(B^+ \to K_S^0 K_S^0 K^+) = (10.6 \pm 0.5 \pm 0.3) \times 10^{-6}$ including the χ_{c0} intermediate state.

[f]The nonresonant amplitude is modeled using a polynomial function of order 2.

TABLE 143. Branching fractions of charmless mesonic B^+ decays with strange mesons (part 7).

Parameter [10^{-6}]	Measurements		Average$^{\text{HFLAV}}_{PDG}$
$\mathcal{B}(B^+ \to K^+K^-\pi^+)$	LHCb [730][b]	$5.12 \pm 0.14 \pm 0.29$	
	Belle [752][a,c]	$5.38 \pm 0.40 \pm 0.35$	5.16 ± 0.26
	BABAR [753]	$5.0 \pm 0.5 \pm 0.5$	*5.24 ± 0.42*
$\mathcal{B}(B^+ \to K^+K^-\pi^+(\text{NR}))$	LHCb [754][d,e]	$1.625 \pm 0.075 \pm 0.221$	$1.62^{+0.24}_{-0.23}$ *1.68 ± 0.26*
$\mathcal{B}(B^+ \to \bar{K}^*(892)^0K^+)$	*BABAR* [755]	< 1.1	$0.57^{+0.07}_{-0.06}$
	LHCb [754][f,g]		*0.59 ± 0.08*
$\mathcal{B}(B^+ \to \bar{K}^*_0(1430)^0K^+)$	*BABAR* [755]	< 2.2	$0.37^{+0.13}_{-0.12}$
	LHCb [754][f,h]		*0.38 ± 0.13*
$\mathcal{B}(B^+ \to K^+K^-\pi^+)\pi\pi \leftrightarrow KK$rescattering	LHCb [754][i,e]	$0.825 \pm 0.040 \pm 0.065$	$0.825^{+0.078}_{-0.075}$ *0.853 ± 0.094*
$\mathcal{B}(B^+ \to K^+K^+\pi^-)$	LHCb [734]	< 0.011	
	BABAR [735]	< 0.16	< 0.011
	Belle [736]	< 2.4	
$\mathcal{B}(B^+ \to f'_2(1525)K^+)$[j]	*BABAR* [720][k]	$1.56 \pm 0.36 \pm 0.30$	
	BABAR [720][l]	$2.8 \pm 0.9^{+0.5}_{-0.4}$	1.79 ± 0.42
	Belle [733][k]	< 8.0	*1.79 ± 0.48*
$\mathcal{B}(B^+ \to f_J(2220)K^+) \times \mathcal{B}(f_J(2220) \to p\bar{p})$	Belle [756]	< 0.41	< 0.41
$\mathcal{B}(B^+ \to K^*(892)^+\pi^+K^-)$	*BABAR* [740]	< 11.8	< 12
$\mathcal{B}(B^+ \to K^*(892)^+\bar{K}^*(892)^0)$	Belle [757]	$0.77^{+0.35}_{-0.30} \pm 0.12$	0.91 ± 0.30
	BABAR [758]	$1.2 \pm 0.5 \pm 0.1$	$0.91^{+0.30}_{-0.27}$
$\mathcal{B}(B^+ \to K^*(892)^+K^+\pi^-)$	*BABAR* [740]	< 6.1	< 6.1

[a]Not included in PDG average.

[b]Using $\mathcal{B}(B^+ \to K^+K^+K^-)$.

[c]Also measured in bins of $m_{K^+K^-}$ and $m_{K^+\pi^-}$.

[d]LHCb uses a model of the nonresonant contribution obtained from a phenomenological description of the partonic interaction that produces the final state. This contribution is referred to as the single pole in the paper; see Ref. [754] for details.

[e]Using $\mathcal{B}(B^+ \to K^+K^-\pi^+)$.

[f]Result extracted from Dalitz-plot analysis of $B^+ \to K^+K^-\pi^+$ decays.

[g]Measurement of $(\mathcal{B}(B^+ \to \bar{K}^*(892)^0K^+)\mathcal{B}(K^*(892)^0 \to K\pi)2/3)/\mathcal{B}(B^+ \to K^+K^-\pi^+)$ used in our fit.

[h]Measurement of $(\mathcal{B}(B^+ \to \bar{K}^*_0(1430)^0K^+)\mathcal{B}(K^*(1430) \to K\pi)2/3)/\mathcal{B}(B^+ \to K^+K^-\pi^+)$ used in our fit.

[i]LHCb uses a dedicated lineshape to take into account $\pi\pi \leftrightarrow KK$ rescattering, which is particularly significant in the region $1 < m_{KK} < 1.5$ GeV/c^2. See Ref. [754] for details.

[j]The PDG uncertainty includes a scale factor.

[k]Result extracted from Dalitz-plot analysis of $B^+ \to K^+K^+K^-$ decays.

[l]Result extracted from Dalitz-plot analysis of $B^+ \to K^0_SK^0_SK^+$ decays.

TABLE 144. Branching fractions of charmless mesonic B^+ decays with strange mesons (part 8).

Parameter [10^{-6}]	Measurements		Average$^{\text{HFLAV}}_{PDG}$
$\mathcal{B}(B^+ \to K^+K^+K^-)$[b,c]	*BABAR* [720][d,e]	$34.6 \pm 0.6 \pm 0.9$	
	Belle [733][d]	$30.6 \pm 1.2 \pm 2.3$	33.9 ± 0.7
	Belle II [731][a]	$35.8 \pm 1.6 \pm 1.4$	*34.0 ± 1.4*
	LHCb [759][f,g,h], [730][i,j,k]		
$\mathcal{B}(B^+ \to \phi(1020)K^+)$[b]	*BABAR* [720][d]	$9.2 \pm 0.4^{+0.7}_{-0.5}$	
	Belle [733][d]	$9.60 \pm 0.92^{+1.05}_{-0.85}$	
	Belle II [760][a]	$6.7 \pm 1.1 \pm 0.5$	8.53 ± 0.47
	CDF [761]	$7.6 \pm 1.3 \pm 0.6$	$8.83^{+0.67}_{-0.57}$
	CLEO [762]	$5.5^{+2.1}_{-1.8} \pm 0.6$	
$\mathcal{B}(B^+ \to f_0(980)K^+) \times \mathcal{B}(f_0(980) \to K^+K^-)$	*BABAR* [720][d]	$9.4 \pm 1.6 \pm 2.8$	9.4 ± 3.2
$\mathcal{B}(B^+ \to a_2(1320)^0K^+) \times \mathcal{B}(a_2(1320)^0 \to K^+K^-)$	Belle [733][d]	< 1.1	< 1.1
$\mathcal{B}(B^+ \to \phi(1680)K^+) \times \mathcal{B}(\phi(1680) \to K^+K^-)$	Belle [733][d]	< 0.8	< 0.8
$\mathcal{B}(B^+ \to f_0(1710)K^+) \times \mathcal{B}(f_0(1710) \to K^+K^-)$	*BABAR* [720][d]	$1.12 \pm 0.25 \pm 0.50$	1.12 ± 0.56
$\mathcal{B}(B^+ \to K^+K^+K^-(\text{NR}))$	Belle [733][d]	$24.0 \pm 1.5^{+2.6}_{-6.0}$	$23.7^{+3.0}_{-4.9}$
	BABAR [720][l,d]	$22.8 \pm 2.7 \pm 7.6$	$23.8^{+2.8}_{-4.9}$

[a]Preliminary result.

[b]The PDG uncertainty includes a scale factor.

[c]Treatment of charmonium intermediate components differs between the results.

[d]Result extracted from Dalitz-plot analysis of $B^+ \to K^+K^+K^-$ decays.

[e]All charmonium resonances are vetoed, except for χ_{c0}. The analysis also reports $\mathcal{B}(B^+ \to K^+K^+K^-) = (33.4 \pm 0.5 \pm 0.9) \times 10^{-6}$ excluding χ_{c0}.

[f]Measurement of $\frac{f_{\Omega_b^-}}{f_u} \times \mathcal{B}(\Omega_b^- \to pK^-K^-)/\mathcal{B}(B^+ \to K^+K^+K^-)$ used in our fit.

[g]Measurement of $\frac{f_{\Omega_b^-}}{f_u} \times \mathcal{B}(\Omega_b^- \to pK^-\pi^-)/\mathcal{B}(B^+ \to K^+K^+K^-)$ used in our fit.

[h]Measurement of $\frac{f_{\Omega_b^-}}{f_u} \times \mathcal{B}(\Omega_b^- \to p\pi^-\pi^-)/\mathcal{B}(B^+ \to K^+K^+K^-)$ used in our fit.

[i]Measurement of $\mathcal{B}(B^+ \to K^+K^-\pi^+)/\mathcal{B}(B^+ \to K^+K^+K^-)$ used in our fit.

[j]Measurement of $\mathcal{B}(B^+ \to K^+\pi^+\pi^-)/\mathcal{B}(B^+ \to K^+K^+K^-)$ used in our fit.

[k]Measurement of $\mathcal{B}(B^+ \to \pi^+\pi^+\pi^-)/\mathcal{B}(B^+ \to K^+K^+K^-)$ used in our fit.

[l]The nonresonant amplitude is modeled using a polynomial function including S-wave and P-wave terms.

TABLE 145. Branching fractions of charmless mesonic B^+ decays with strange mesons (part 9).

Parameter [10^{-6}]	Measurements		Average$^{\text{HFLAV}}_{PDG}$
$\mathcal{B}(B^+ \to K^*(892)^+K^+K^-)$	*BABAR* [740]	$36.2 \pm 3.3 \pm 3.6$	36.2 ± 4.9
	BABAR [763][c]	$11.2 \pm 1.0 \pm 0.9$	
$\mathcal{B}(B^+ \to \phi(1020)K^*(892)^+)$[b]	Belle [764]	$6.7^{+2.1+0.7}_{-1.9-1.0}$	10.6 ± 1.1
	Belle II [760][a]	$21.7 \pm 4.6 \pm 1.9$	*10.0 ± 2.0*
	CLEO [762]	$10.6^{+6.4+1.8}_{-4.9-1.6}$	
$\mathcal{B}(B^+ \to \phi(1020)(K\pi)^{*+}_0)$	*BABAR* [765]	$8.3 \pm 1.4 \pm 0.8$	8.3 ± 1.6
$\mathcal{B}(B^+ \to K_1(1270)^+\phi(1020))$	*BABAR* [765]	$6.1 \pm 1.6 \pm 1.1$	6.1 ± 1.9
$\mathcal{B}(B^+ \to K_1(1400)^+\phi(1020))$	*BABAR* [765]	< 3.2	< 3.2
$\mathcal{B}(B^+ \to K^*(1410)^+\phi(1020))$	*BABAR* [765]	< 4.3	< 4.3
$\mathcal{B}(B^+ \to K^*_0(1430)^+\phi(1020))$	*BABAR* [765]	$7.0 \pm 1.3 \pm 0.9$	7.0 ± 1.6
$\mathcal{B}(B^+ \to K^*_2(1430)^+\phi(1020))$	*BABAR* [765]	$8.4 \pm 1.8 \pm 1.0$	8.4 ± 2.1
$\mathcal{B}(B^+ \to K_2(1770)^+\phi(1020))$	*BABAR* [765]	< 15.0	< 15
$\mathcal{B}(B^+ \to \phi(1020)K_2(1820)^+)$	*BABAR* [765]	< 16.3	< 16
$\mathcal{B}(B^+ \to a_1(1260)^+K^*(892)^0)$	*BABAR* [766]	< 3.6	< 3.6
$\mathcal{B}(B^+ \to \phi(1020)\phi(1020)K^+)$[b]	*BABAR* [767][d]	$5.6 \pm 0.5 \pm 0.3$	4.98 ± 0.52
	Belle [768][d]	$2.6^{+1.1}_{-0.9} \pm 0.3$	$4.22^{+0.82}_{-0.79}$
$\mathcal{B}(B^+ \to \eta'\eta'K^+)$	*BABAR* [769]	< 25.0	< 25
$\mathcal{B}(B^+ \to \phi(1020)\omega(782)K^+)$	Belle [770]	< 1.9	< 1.9
$\mathcal{B}(B^+ \to X(1812)K^+) \times \mathcal{B}(X(1812) \to \phi(1020)\omega(782))$	Belle [770]	< 0.32	< 0.32
$\mathcal{B}(B^+ \to h^+X^0(\text{Familon}))$[e]	CLEO [771]	< 49	< 49

[a]Preliminary result.

[b]The PDG uncertainty includes a scale factor.

[c]Combination of two final states of the $K^*(892)^\pm$, $K^0_S\pi^\pm$ and $K^\pm\pi^0$. In addition to the combined results, the paper reports separately the results for each individual final state.

[d]Measured in the $\phi\phi$ invariant mass range below the η_c resonance ($m_{\phi\phi} < 2.85$ GeV/c^2).

[e]$h = \pi$, K.

TABLE 146. Branching fractions of charmless mesonic B^+ decays without strange mesons (part 1).

Parameter [10^{-6}]	Measurements		Average$^{\text{HFLAV}}_{PDG}$
$\mathcal{B}(B^+ \to \pi^+\pi^0)$[c]	Belle [702]	$5.86 \pm 0.26 \pm 0.38$	
	Belle II [703][a]	$5.1 \pm 0.3 \pm 0.3$	5.33 ± 0.27
	BABAR [707]	$5.02 \pm 0.46 \pm 0.29$	*5.48 ± 0.41*
	CLEO [705]	$4.6^{+1.8\,+0.6}_{-1.6\,-0.7}$	
$\mathcal{B}(B^+ \to \pi^+\pi^+\pi^-)$	LHCb [730][d]	$16.54 \pm 0.17 \pm 0.47$	16.46 ± 0.48
	BABAR [772][e,f,g]	$15.2 \pm 0.6^{+1.3}_{-1.2}$	*$15.20^{+1.43}_{-1.34}$*
$\mathcal{B}(B^+ \to \rho^0(770)\pi^+)$	LHCb [773][b,e,h,g,i]	$8.82 \pm 0.10 \pm 0.50$	
	BABAR [772][e,g]	$8.1 \pm 0.7^{+1.3}_{-1.6}$	8.76 ± 0.48
	Belle [774]	$8.0^{+2.3}_{-2.0} \pm 0.7$	*$8.29^{+1.20}_{-1.28}$*
	CLEO [723]	$10.4^{+3.3}_{-3.4} \pm 2.1$	
$\mathcal{B}(B^+ \to f_0(980)\pi^+) \times \mathcal{B}(f_0(980) \to \pi^+\pi^-)$	*BABAR* [772][e]	< 1.5	< 1.5
$\mathcal{B}(B^+ \to f_2(1270)\pi^+) \times \mathcal{B}(f_2(1270) \to \pi^+\pi^-)$	LHCb [773][e,h,g,i]	$1.43 \pm 0.05 \pm 0.27$	$1.27^{+0.20}_{-0.23}$
	BABAR [772][e,g]	$0.9 \pm 0.2^{+0.3}_{-0.1}$	*None*
$\mathcal{B}(B^+ \to f_2(1270)\pi^+) \times \mathcal{B}(f_2(1270) \to K^+K^-)$	LHCb [754][j,k]	$0.377 \pm 0.040 \pm 0.040$	$0.377^{+0.058}_{-0.056}$ *None*
$\mathcal{B}(B^+ \to \rho(1450)^0\pi^+) \times \mathcal{B}(\rho(1450)^0 \to \pi^+\pi^-)$	LHCb [773][b,e,h,g,i]	$0.83 \pm 0.05 \pm 0.89$	$1.14^{+0.59}_{-0.67}$
	BABAR [772][e,g]	$1.4 \pm 0.4^{+0.5}_{-0.8}$	*$1.40^{+0.64}_{-0.89}$*
$\mathcal{B}(B^+ \to \rho(1450)^0\pi^+) \times \mathcal{B}(\rho(1450)^0 \to K^+K^-)$	LHCb [754][j,k]	$1.544 \pm 0.060 \pm 0.089$	1.54 ± 0.11 *1.60 ± 0.14*
$\mathcal{B}(B^+ \to \rho_3(1690)^0\pi^+) \times \mathcal{B}(\rho_3(1690)^0 \to \pi^+\pi^-)$	LHCb [773][e,h,g,i]	$0.08 \pm 0.02 \pm 0.16$	0.08 ± 0.16 *None*

[a]Preliminary result.

[b]Not included in PDG average.

[c]The PDG uncertainty includes a scale factor.

[d]Using $\mathcal{B}(B^+ \to K^+K^+K^-)$.

[e]Result extracted from Dalitz-plot analysis of $B^+ \to \pi^+\pi^+\pi^-$ decays.

[f]Charm and charmonium contributions are subtracted.

[g]Multiple systematic uncertainties are added in quadrature.

[h]This analysis uses three different approaches: isobar, K-matrix and quasi-model-independent, to describe the S-wave component. The results are taken from the isobar model with an additional error accounting for the different S-wave methods as reported in Appendix D of Ref. [775].

[i]Using $\mathcal{B}(B^+ \to \pi^+\pi^+\pi^-)$.

[j]Result extracted from Dalitz-plot analysis of $B^+ \to K^+K^-\pi^+$ decays.

[k]Using $\mathcal{B}(B^+ \to K^+K^-\pi^+)$.

TABLE 147. Branching fractions of charmless mesonic B^+ decays without strange mesons (part 2).

Parameter [10^{-6}]	Measurements		Average$^{\text{HFLAV}}_{PDG}$
$\mathcal{B}(B^+ \to \pi^+\pi^+\pi^-)$ S-wave	LHCb [773][c,d,e,f]	$4.04 \pm 0.08 \pm 0.64$	4.04 ± 0.64 *None*
$\mathcal{B}(B^+ \to f_0(1370)\pi^+) \times \mathcal{B}(f_0(1370) \to \pi^+\pi^-)$	*BABAR* [772][g]	< 4.0	< 4.0
$\mathcal{B}(B^+ \to \pi^+\pi^-\pi^+(\text{NR}))$	*BABAR* [772][h,e]	$5.3 \pm 0.7^{+1.3}_{-0.8}$	$5.3^{+1.4}_{-1.0}$ $5.3^{+1.5}_{-1.1}$
$\mathcal{B}(B^+ \to \pi^+\pi^0\pi^0)$	Belle [776][a] ARGUS [777]	$19.0 \pm 1.5 \pm 1.4$ < 890	19.0 ± 2.1 < 890.0
$\mathcal{B}(B^+ \to X_{\pi^0\pi^0}\pi^+) \times \mathcal{B}(X(\pi^0\pi^0) \to \pi^0\pi^0)$	Belle [776][i]	$6.9 \pm 0.9 \pm 0.6$	6.9 ± 1.1 *None*
$\mathcal{B}(B^+ \to \pi^+\pi^0\pi^0(\text{NR}))$	Belle [776]	< 0.6	< 0.60 *None*
$\mathcal{B}(B^+ \to \rho^+(770)\pi^0)$	Belle [776][a,e] *BABAR* [778]	$11.2 \pm 1.1^{+1.2}_{-1.8}$ $10.2 \pm 1.4 \pm 0.9$	10.6 ± 1.3 $10.9^{+1.4}_{-1.5}$
$\mathcal{B}(B^+ \to \pi^+\pi^+\pi^-\pi^0)$	ARGUS [777]	< 4000	< 4000
$\mathcal{B}(B^+ \to \rho^+(770)\rho^0(770))$	*BABAR* [779] Belle II [780][b] Belle [781]	$23.7 \pm 1.4 \pm 1.4$ $23.2^{+2.2}_{-2.1} \pm 2.7$ $31.7 \pm 7.1^{+3.8}_{-6.7}$	23.8 ± 1.7 24.0 ± 1.9
$\mathcal{B}(B^+ \to f_0(980)\rho^+(770)) \times \mathcal{B}(f_0(980) \to \pi^+\pi^-)$	*BABAR* [779]	< 2.0	< 2.0
$\mathcal{B}(B^+ \to a_1(1260)^+\pi^0)$	*BABAR* [782]	$26.4 \pm 5.4 \pm 4.1$	26.4 ± 6.8
$\mathcal{B}(B^+ \to a_1(1260)^0\pi^+)$	*BABAR* [782]	$20.4 \pm 4.7 \pm 3.4$	20.4 ± 5.8
$\mathcal{B}(B^+ \to \omega(782)\pi^+)$	*BABAR* [722] Belle [783] CLEO [723] LHCb [773][a,g,d,e,j]	$6.7 \pm 0.5 \pm 0.4$ $6.9 \pm 0.6 \pm 0.5$ $11.3^{+3.3}_{-2.9} \pm 1.4$	$6.60^{+0.46}_{-0.45}$ 6.88 ± 0.49
$\mathcal{B}(B^+ \to \omega(782)\rho^+(770))$	*BABAR* [724]	$15.9 \pm 1.6 \pm 1.4$	15.9 ± 2.1

[a]Not included in PDG average.

[b]Preliminary result.

[c]LHCb accounts for the S-wave component using a model that comprises the coherent sum of a σ pole and a rescattering amplitude. See Ref. [773] for details.

[d]This analysis uses three different approaches: isobar, K-matrix and quasi-model-independent, to describe the S-wave component. The results are taken from the isobar model with an additional error accounting for the different S-wave methods as reported in Appendix D of Ref. [775].

[e]Multiple systematic uncertainties are added in quadrature.

[f]Using $\mathcal{B}(B^+ \to \pi^+\pi^+\pi^-)$.

[g]Result extracted from Dalitz-plot analysis of $B^+ \to \pi^+\pi^+\pi^-$ decays.

[h]The nonresonant amplitude is modeled using a sum of exponential functions.

[i]$X_{\pi^0\pi^0}$ corresponds to a structure observed in Ref. [776], likely arising due to multiple resonances.

[j]Measurement of $(\mathcal{B}(B^+ \to \omega(782)\pi^+)\mathcal{B}(\omega(782) \to \pi^+\pi^-))/\mathcal{B}(B^+ \to \pi^+\pi^+\pi^-)$ used in our fit.

TABLE 148. Branching fractions of charmless mesonic B^+ decays without strange mesons (part 3).

Parameter [10^{-6}]	Measurements		Average$^{\text{HFLAV}}_{PDG}$
$\mathcal{B}(B^+ \to \eta\pi^+)$	Belle [716]	$4.07 \pm 0.26 \pm 0.21$	4.02 ± 0.27
	BABAR [708]	$4.00 \pm 0.40 \pm 0.24$	
	CLEO [712]	$1.2^{+2.8}_{-1.2}$	$\mathit{4.02^{+0.27}_{-0.26}}$
$\mathcal{B}(B^+ \to \eta\rho^+(770))$[a]	*BABAR* [784]	$9.9 \pm 1.2 \pm 0.8$	6.9 ± 1.0
	Belle [718]	$4.1^{+1.4}_{-1.3} \pm 0.4$	
	CLEO [712]	$4.8^{+5.2}_{-3.8}$	$\mathit{7.0^{+2.9}_{-2.8}}$
$\mathcal{B}(B^+ \to \eta'\pi^+)$[a]	*BABAR* [708]	$3.5 \pm 0.6 \pm 0.2$	2.68 ± 0.46
	Belle [709]	$1.76^{+0.67+0.15}_{-0.62-0.14}$	
	CLEO [712]	$1.0^{+5.8}_{-1.0}$	$\mathit{2.70^{+0.87}_{-0.84}}$
$\mathcal{B}(B^+ \to \eta'\rho^+(770))$	*BABAR* [714]	$9.7^{+1.9}_{-1.8} \pm 1.1$	9.8 ± 2.1
	CLEO [712]	$11.2^{+11.9}_{-7.0}$	
	Belle [715]	< 5.8	$\mathit{9.7^{+2.2}_{-2.1}}$
$\mathcal{B}(B^+ \to \phi(1020)\pi^+)$	*BABAR* [785]	< 0.24	0.031 ± 0.014
	Belle [786]	< 0.33	
	LHCb [754][b,c]		$\mathit{0.032 \pm 0.015}$
$\mathcal{B}(B^+ \to \phi(1020)\rho^+(770))$	*BABAR* [787]	< 3.0	< 3.0
$\mathcal{B}(B^+ \to a_0(980)^0\pi^+) \times \mathcal{B}(a_0(980)^0 \to \eta\pi^0)$	*BABAR* [725]	< 5.8	< 5.8
$\mathcal{B}(B^+ \to \pi^+\pi^+\pi^+\pi^-\pi^-)$	ARGUS [777]	< 860	< 860
$\mathcal{B}(B^+ \to a_1(1260)^+\rho^0(770))$	CLEO [788][d]	< 620.0	< 620
$\mathcal{B}(B^+ \to a_2(1320)^+\rho^0(770))$	CLEO [788][d]	< 720.0	< 720
$\mathcal{B}(B^+ \to b_1(1235)^0\pi^+) \times \mathcal{B}(b_1(1235)^0 \to \omega(782)\pi^0)$	*BABAR* [748]	$6.7 \pm 1.7 \pm 1.0$	6.7 ± 2.0
$\mathcal{B}(B^+ \to b_1^+\pi^0)$	*BABAR* [743]	< 3.3	< 3.3
$\mathcal{B}(B^+ \to \pi^+\pi^+\pi^+\pi^-\pi^-\pi^0)$	ARGUS [777]	< 6300	< 6300
$\mathcal{B}(B^+ \to b_1(1235)^+\rho^0(770)) \times \mathcal{B}(b_1(1235)^0 \to \omega(782)\pi^+)$	*BABAR* [749]	< 5.2	< 5.2
$\mathcal{B}(B^+ \to a_1(1260)^+a_1(1260)^0)$	ARGUS [777]	< 13000	< 13000
$\mathcal{B}(B^+ \to b_1(1235)^0\rho^+(770)) \times \mathcal{B}(b_1(1235)^0 \to \omega(782)\pi^0)$	*BABAR* [749]	< 3.3	< 3.3

[a]The PDG uncertainty includes a scale factor.

[b]Result extracted from Dalitz-plot analysis of $B^+ \to K^+K^-\pi^+$ decays.

[c]Measurement of $(\mathcal{B}(B^+ \to \phi(1020)\pi^+)\mathcal{B}(\phi(1020) \to K^+K^-))/\mathcal{B}(B^+ \to K^+K^-\pi^+)$ used in our fit.

[d]CLEO assumes $\mathcal{B}(\Upsilon(4S) \to B^0\bar{B}^0) = 0.43$. The result has been modified to account for a branching fraction of 0.50.

TABLE 149. Branching fractions of charmless mesonic B^0 decays with strange mesons (part 1).

Parameter [10^{-6}]	Measurements		Average$^{\text{HFLAV}}_{PDG}$
$\mathcal{B}(B^0 \to K^+\pi^-)$	Belle [702]	$20.00 \pm 0.34 \pm 0.60$	20.1 ± 0.4 *19.6 ± 0.5*
	Belle II [703][a]	$20.7 \pm 0.4 \pm 0.6$	
	BABAR [789]	$19.1 \pm 0.6 \pm 0.6$	
	CLEO [705]	$18.0^{+2.3+1.2}_{-2.1-0.9}$	
	CDF [790][b,c,d], [791][e,f], [792][b,g,h]		
	LHCb [793][e,f,c], [794][b,g,h]		
$\mathcal{B}(B^0 \to K^0\pi^0)$	Belle [702]	$9.68 \pm 0.46 \pm 0.50$	10.12 ± 0.43 *9.93 ± 0.49*
	BABAR [795]	$10.1 \pm 0.6 \pm 0.4$	
	Belle II [703][a,i]	$10.73 \pm 0.63 \pm 0.62$	
	CLEO [705]	$12.8^{+4.0+1.7}_{-3.3-1.4}$	
$\mathcal{B}(B^0 \to \eta' K^0)$[j]	*BABAR* [708]	$68.5 \pm 2.2 \pm 3.1$	65.0 ± 2.8 $66.1^{+4.5}_{-4.4}$
	Belle [709]	$58.9^{+3.6}_{-3.5} \pm 4.3$	
	Belle II [710][a]	$59.9^{+5.8}_{-5.5} \pm 2.7$	
	CLEO [712]	$89.0^{+18.0}_{-16.0} \pm 9.0$	
	LHCb [796][b,k,l]		
$\mathcal{B}(B^0 \to \eta' K^*(892)^0)$	Belle [797]	$2.6 \pm 0.7 \pm 0.2$	2.8 ± 0.6
	BABAR [714]	$3.1^{+0.9}_{-0.8} \pm 0.3$	
$\mathcal{B}(B^0 \to \eta' K_0^*(1430)^0)$	*BABAR* [714][m]	$6.3 \pm 1.3 \pm 0.9$	6.3 ± 1.6
$\mathcal{B}(B^0 \to \eta'(K\pi)_0^{*0})$	*BABAR* [714]	$7.4^{+1.5}_{-1.4} \pm 0.6$	7.4 ± 1.6 *None*
$\mathcal{B}(B^0 \to \eta' K_2^*(1430)^0)$	*BABAR* [714]	$13.7^{+3.0}_{-2.9} \pm 1.2$	13.7 ± 3.2 $13.7^{+3.2}_{-3.1}$

[a]Preliminary result.
[b]Not included in PDG average.
[c]Measurement of $(\mathcal{B}(B_s^0 \to K^-\pi^+)/\mathcal{B}(B^0 \to K^+\pi^-))\frac{f_s}{f_d}$ used in our fit.
[d]Measurement of $(\mathcal{B}(\Lambda_b^0 \to p\pi^-)/\mathcal{B}(B^0 \to K^+\pi^-))(f_{\Lambda_b^0}/f_d)$ used in our fit.
[e]Measurement of $\mathcal{B}(B^0 \to \pi^+\pi^-)/\mathcal{B}(B^0 \to K^+\pi^-)$ used in our fit.
[f]Measurement of $(\mathcal{B}(B_s^0 \to K^+K^-)/\mathcal{B}(B^0 \to K^+\pi^-))\frac{f_s}{f_d}$ used in our fit.
[g]Measurement of $\mathcal{B}(B^0 \to K^+K^-)/\mathcal{B}(B^0 \to K^+\pi^-)$ used in our fit.
[h]Measurement of $(\mathcal{B}(B_s^0 \to \pi^+\pi^-)/\mathcal{B}(B^0 \to K^+\pi^-))\frac{f_s}{f_d}$ used in our fit.
[i]Combination of time-integrated and time-dependent analyses using the best linear unbiased estimator Ref. [798].
[j]The PDG uncertainty includes a scale factor.
[k]Measurement of $\mathcal{B}(\Lambda_b^0 \to \Lambda^0\eta)/\mathcal{B}(B^0 \to \eta' K^0)$ used in our fit.
[l]Measurement of $\mathcal{B}(\Lambda_b^0 \to \Lambda^0\eta')/\mathcal{B}(B^0 \to \eta' K^0)$ used in our fit.
[m]Multiple systematic uncertainties are added in quadrature.

TABLE 150. Branching fractions of charmless mesonic B^0 decays with strange mesons (part 2).

Parameter [10^{-6}]	Measurements		Average$^{\text{HFLAV}}_{PDG}$
$\mathcal{B}(B^0 \to \eta K^0)$	Belle [716]	$1.27^{+0.33}_{-0.29} \pm 0.08$	1.23 ± 0.25
	BABAR [708]	$1.15^{+0.43}_{-0.38} \pm 0.09$	$\mathit{1.23^{+0.27}_{-0.24}}$
$\mathcal{B}(B^0 \to \eta K^*(892)^0)$	*BABAR* [717]	$16.5 \pm 1.1 \pm 0.8$	16.09 ± 0.81
	Belle [718]	$15.2 \pm 1.2 \pm 1.0$	$\mathit{15.87^{+1.01}_{-1.00}}$
	CLEO [712]	$13.8^{+5.5}_{-4.6} \pm 1.6$	
$\mathcal{B}(B^0 \to \eta(K\pi)^{*0}_0)$	*BABAR* [717]	$11.0 \pm 1.6 \pm 1.5$	11.0 ± 1.6 *None*
$\mathcal{B}(B^0 \to \eta K^*_0(1430)^0)$	*BABAR* [717][a]	$7.8 \pm 1.1 \pm 1.1$	7.8 ± 1.1 $\mathit{11.0 \pm 2.2}$
$\mathcal{B}(B^0 \to \eta K^*_2(1430)^0)$	*BABAR* [717]	$9.6 \pm 1.8 \pm 1.1$	9.6 ± 1.5 $\mathit{9.6 \pm 2.1}$
$\mathcal{B}(B^0 \to \omega(782)K^0)$	Belle [721]	$4.5 \pm 0.4 \pm 0.3$	4.78 ± 0.43
	BABAR [722]	$5.4 \pm 0.8 \pm 0.3$	
	CLEO [723]	$10.0^{+5.4}_{-4.2} \pm 1.4$	
$\mathcal{B}(B^0 \to a_0(980)^0 K^0) \times \mathcal{B}(a_0(980)^0 \to \eta\pi^0)$	*BABAR* [725]	< 7.8	< 7.8
$\mathcal{B}(B^0 \to b_1(1235)^0 K^0) \times \mathcal{B}(b_1(1235)^0 \to \omega(782)\pi^0)$	*BABAR* [743]	< 7.8	< 7.8
$\mathcal{B}(B^0 \to a_0(980)^- K^+) \times \mathcal{B}(a_0(980)^- \to \eta\pi^-)$	*BABAR* [799]	< 1.9	< 1.9
$\mathcal{B}(B^0 \to b_1(1235)^- K^+) \times \mathcal{B}(b_1(1235)^- \to \omega(782)\pi^-)$	*BABAR* [748]	$7.4 \pm 1.0 \pm 1.0$	7.4 ± 1.4
$\mathcal{B}(B^0 \to b_1(1235)^0 K^*(892)^0) \times \mathcal{B}(b_1(1235)^0 \to \omega(782)\pi^0)$	*BABAR* [749]	< 8.0	< 8.0
$\mathcal{B}(B^0 \to b_1(1235)^- K^*(892)^+) \times \mathcal{B}(b_1(1235)^- \to \omega(782)\pi^-)$	*BABAR* [749]	< 5.0	< 5.0
$\mathcal{B}(B^0 \to a_0(1450)^- K^+) \times \mathcal{B}(a_0(1450)^- \to \eta\pi^-)$	*BABAR* [799]	< 3.1	< 3.1
$\mathcal{B}(B^0 \to K^0_S X^0(\text{Familon}))$	CLEO [771]	< 53	< 53

[a]Multiple systematic uncertainties are added in quadrature.

TABLE 151. Branching fractions of charmless mesonic B^0 decays with strange mesons (part 3).

Parameter [10^{-6}]	Measurements		Average$^{\text{HFLAV}}_{PDG}$
$\mathcal{B}(B^0 \to \omega(782)K^*(892)^0)$	*BABAR* [724]	$2.2 \pm 0.6 \pm 0.2$	2.04 ± 0.49
	Belle [800]	$1.8 \pm 0.7 \pm 0.3$	
$\mathcal{B}(B^0 \to \omega(782)(K\pi)_0^{*0})$	*BABAR* [724]	$18.4 \pm 1.8 \pm 1.7$	18.4 ± 2.5
$\mathcal{B}(B^0 \to \omega(782)K_0^*(1430)^0)$	*BABAR* [724]	$16.0 \pm 1.6 \pm 3.0$	16.0 ± 3.4
$\mathcal{B}(B^0 \to \omega(782)K_2^*(1430)^0)$	*BABAR* [724]	$10.1 \pm 2.0 \pm 1.1$	10.1 ± 2.3
$\mathcal{B}(B^0 \to \omega(782)K^+\pi^-(\text{NR}))$	Belle [800][b]	$5.1 \pm 0.7 \pm 0.7$	5.1 ± 1.0
$\mathcal{B}(B^0 \to K^+\pi^-\pi^0)$	*BABAR* [801][c]	$38.5 \pm 1.0 \pm 3.9$	37.9 ± 2.7
	Belle II [731][a]	$38.1 \pm 3.5 \pm 3.9$	*37.8 ± 3.2*
	Belle [802]	$36.6^{+4.2}_{-4.1} \pm 3.0$	
$\mathcal{B}(B^0 \to \rho^-(770)K^+)$	*BABAR* [801][c]	$6.6 \pm 0.5 \pm 0.8$	7.01 ± 0.92
	Belle [802][d]	$15.1^{+3.4+2.4}_{-3.3-2.6}$	
$\mathcal{B}(B^0 \to \rho(1450)^-K^+)$	*BABAR* [801][c]	$2.4 \pm 1.0 \pm 0.6$	2.4 ± 1.2
$\mathcal{B}(B^0 \to \rho(1700)^-K^+)$	*BABAR* [801][c]	$0.6 \pm 0.6 \pm 0.4$	0.6 ± 0.7
$\mathcal{B}(B^0 \to K^+\pi^-\pi^0(\text{NR}))$	*BABAR* [801][e]	$2.8 \pm 0.5 \pm 0.4$	2.8 ± 0.6
	Belle [802]	< 9.4	
$\mathcal{B}(B^0 \to (K\pi)_0^{*+}\pi^-) \times \mathcal{B}((K\pi)_0^{*+} \to K^+\pi^0)$	*BABAR* [801][c]	$34.2 \pm 2.4 \pm 4.1$	34.2 ± 4.8
$\mathcal{B}(B^0 \to (K\pi)_0^{*0}\pi^0) \times \mathcal{B}((K\pi)_0^{*0} \to K^+\pi^-)$	*BABAR* [801][c]	$8.6 \pm 1.1 \pm 1.3$	8.6 ± 1.7
$\mathcal{B}(B^0 \to K_2^*(1430)^0\pi^0)$	*BABAR* [803][c]	< 4.0	< 4.0
$\mathcal{B}(B^0 \to K^*(1680)^0\pi^0)$	*BABAR* [803][c]	< 7.5	< 7.5
$\mathcal{B}(B^0 \to K_x^{*0}\pi^0)$	Belle [802][f,g]	$6.1^{+1.6+0.5}_{-1.5-0.6}$	6.1 ± 1.6
			$6.1^{+1.7}_{-1.6}$

[a]Preliminary result.
[b]$0.755 < m_{K\pi} < 1.250$ GeV/c^2.
[c]Result extracted from Dalitz-plot analysis of $B^0 \to K^+\pi^-\pi^0$ decays.
[d]Multiple systematic uncertainties are added in quadrature.
[e]The nonresonant amplitude is taken to be constant across the Dalitz plane.
[f]$1.1 < m_{K\pi} < 1.6$ GeV/c^2.
[g]K_x^* stands for the possible candidates of $K^*(1410)$, $K_0^*(1430)$ and $K_2^*(1430)$.

TABLE 152. Branching fractions of charmless mesonic B^0 decays with strange mesons (part 4).

Parameter [10^{-6}]	Measurements		Average$^{\text{HFLAV}}_{PDG}$
$\mathcal{B}(B^0 \to K^0\pi^+\pi^-)$[b,c]	*BABAR* [804][d,e]	$50.15 \pm 1.47 \pm 1.76$	49.7 ± 1.8
	Belle [805][d]	$47.5 \pm 2.4 \pm 3.7$	
	CLEO [739]	$50.0^{+10.0}_{-9.0} \pm 7.0$	
	LHCb [806][a,e,f,g,h,i], [807][a,j], [808][k,l], [808][k,m], [808][k,n], [808][k,o], [808][k,p]		
$\mathcal{B}(B^0 \to K^0\pi^+\pi^-(\text{NR}))$[q]	LHCb [809][d,r,e,s]	$12.60 \pm 0.67 \pm 3.05$	14.0 ± 1.7
	BABAR [804][d,t,e]	$11.07^{+2.51}_{-0.99} \pm 0.90$	$p = 0.16\%$
	Belle [805][d,u]	$19.9 \pm 2.5^{+1.7}_{-2.0}$	$\mathit{13.9}^{+2.6}_{-1.8}$
$\mathcal{B}(B^0 \to \rho^0(770)K^0)$[q]	*BABAR* [804][d,e]	$4.36^{+0.71}_{-0.62} \pm 0.31$	3.45 ± 0.48
	LHCb [809][d,e,s]	$1.97^{+0.57}_{-0.83} \pm 0.42$	$p = 0.16\%$
	Belle [805][d]	$6.1 \pm 1.0^{+1.1}_{-1.2}$	$\mathit{3.41}^{+1.08}_{-1.14}$
$\mathcal{B}(B^0 \to K^*(892)^+\pi^-)$	*BABAR* [804][d,e]	$8.29^{+0.92}_{-0.81} \pm 0.82$	7.64 ± 0.44
	BABAR [801][v]	$8.0 \pm 1.1 \pm 0.8$	$p = 0.16\%$
	Belle [805][d]	$8.4 \pm 1.1^{+1.0}_{-0.9}$	$\mathit{7.50 \pm 0.44}$
	CLEO [739]	$16.0^{+6.0}_{-5.0} \pm 2.0$	
	LHCb [810][a,w,x], [809][d,e,y]		

[a]Not included in PDG average.

[b]The PDG average is a result of a fit including input from other measurements.

[c]Treatment of charmonium intermediate components differs between the results.

[d]Result extracted from Dalitz-plot analysis of $B^0 \to K^0_S\pi^+\pi^-$ decays.

[e]Multiple systematic uncertainties are added in quadrature.

[f]Measurement of $\mathcal{B}(\Lambda^0_b \to p\bar{K}^0\pi^-)/\mathcal{B}(B^0 \to K^0\pi^+\pi^-)$ used in our fit.

[g]Measurement of $\mathcal{B}(\Lambda^0_b \to pK^0K^-)/\mathcal{B}(B^0 \to K^0\pi^+\pi^-)$ used in our fit.

[h]Measurement of $\frac{f_{\Xi^0_b}}{f_d}\mathcal{B}(\Xi^0_b \to p\bar{K}^0\pi^-)/\mathcal{B}(B^0 \to K^0\pi^+\pi^-)$ used in our fit.

[i]Measurement of $\frac{f_{\Xi^0_b}}{f_d}\mathcal{B}(\Xi^0_b \to p\bar{K}^0K^-)/\mathcal{B}(B^0 \to K^0\pi^+\pi^-)$ used in our fit.

[j]Measurement of $\mathcal{B}(B^0 \to K^*(892)^0\bar{K}^0\text{+c.c.})/\mathcal{B}(B^0 \to K^0\pi^+\pi^-)$ used in our fit.

[k]Regions corresponding to D, Λ^+_c and charmonium resonances are vetoed in this analysis.

[l]Measurement of $\mathcal{B}(B^0 \to K^0K^+\pi^-\text{+c.c.})/\mathcal{B}(B^0 \to K^0\pi^+\pi^-)$ used in our fit.

[m]Measurement of $\mathcal{B}(B^0 \to K^0K^+K^-)/\mathcal{B}(B^0 \to K^0\pi^+\pi^-)$ used in our fit.

[n]Measurement of $\mathcal{B}(B^0_s \to K^0\pi^+\pi^-)/\mathcal{B}(B^0 \to K^0\pi^+\pi^-)$ used in our fit.

[o]Measurement of $\mathcal{B}(B^0_s \to K^0K^+\pi^-\text{+c.c.})/\mathcal{B}(B^0 \to K^0\pi^+\pi^-)$ used in our fit.

[p]Measurement of $\mathcal{B}(B^0_s \to K^0K^+K^-)/\mathcal{B}(B^0 \to K^0\pi^+\pi^-)$ used in our fit.

[q]The PDG uncertainty includes a scale factor.

[r]The nonresonant component is modeled as a flat contribution over the Dalitz plane.

[s]Using $\mathcal{B}(B^0 \to K^0\pi^+\pi^-)$.

[t]This value includes the flat NR component and the effective range of the LASS line shape. The value corresponding to the flat component alone is also given in the article.

[u]The nonresonant component is modeled using a sum of two exponential functions.

[v]Result extracted from Dalitz-plot analysis of $B^0 \to K^+\pi^-\pi^0$ decays.

[w]Measurement of $\mathcal{B}(B^0_s \to K^*(892)^-\pi^+)/\mathcal{B}(B^0 \to K^*(892)^+\pi^-)$ used in our fit.

[x]Measurement of $\mathcal{B}(B^0 \to K^*(892)^-K^+\text{+c.c.})/\mathcal{B}(B^0 \to K^*(892)^+\pi^-)$ used in our fit.

[y]Measurement of $(\mathcal{B}(B^0 \to K^*(892)^+\pi^-)2/3)/\mathcal{B}(B^0 \to K^0\pi^+\pi^-)$ used in our fit.

TABLE 153. Branching fractions of charmless mesonic B^0 decays with strange mesons (part 5).

Parameter [10^{-6}]	Measurements		Average$^{\text{HFLAV}}_{PDG}$
$\mathcal{B}(B^0 \to K_0^*(1430)^+\pi^-)$[b]	*BABAR* [804][c,d]	$29.9^{+2.3}_{-1.7} \pm 3.6$	$33.6^{+3.8}_{-4.0}$
	Belle [805][c]	$49.7 \pm 3.8^{+6.8}_{-8.2}$	$\mathit{33.5}^{+7.4}_{-7.2}$
$\mathcal{B}(B^0 \to K_x^{*+}\pi^-)$	Belle [802][e,f]	$5.1 \pm 1.5^{+0.6}_{-0.7}$	5.1 ± 1.6 $\mathit{5.1}^{+1.6}_{-1.7}$
$\mathcal{B}(B^0 \to K^*(1410)^+\pi^-) \times \mathcal{B}(K^*(1410)^+ \to K^0\pi^+)$	Belle [805][c]	< 3.8	< 3.8
$\mathcal{B}(B^0 \to (K\pi)_0^{*+}\pi^-) \times \mathcal{B}((K\pi)_0^{*+} \to K^0\pi^+)$	LHCb [809][c,d,g]	$16.95 \pm 0.73 \pm 1.12$	18.6 ± 1.1
	BABAR [804][a,c,d]	$22.7^{+1.7}_{-1.3} \pm 1.3$	p = 0.16% *16.2 ± 1.3*
$\mathcal{B}(B^0 \to f_0(980)K^0) \times \mathcal{B}(f_0(980) \to \pi^+\pi^-)$[b]	LHCb [809][c,d,g]	$9.64 \pm 0.41 \pm 0.79$	8.38 ± 0.61
	BABAR [804][c,d]	$6.92 \pm 0.77 \pm 0.56$	p = 0.16%
	Belle [805][c]	$7.6 \pm 1.7^{+0.9}_{-1.3}$	$\mathit{8.15}^{+0.78}_{-0.79}$
$\mathcal{B}(B^0 \to f_0(500)K^0)$	LHCb [809][c,d,g]	$0.166^{+0.207}_{-0.041} \pm 0.155$	$0.17^{+0.26}_{-0.16}$ p = 0.16% $\mathit{0.16}^{+0.25}_{-0.16}$
$\mathcal{B}(B^0 \to f_0(1500)K^0) \times \mathcal{B}(f_0(1500) \to \pi^+\pi^-)$	LHCb [809][c,d,g]	$1.348 \pm 0.280 \pm 0.734$	1.35 ± 0.79 p = 0.16% *1.29 ± 0.75*
$\mathcal{B}(B^0 \to f_2(1270)K^0)$	*BABAR* [804][c,d]	$2.71^{+0.99}_{-0.83} \pm 0.87$	2.7 ± 1.3
	Belle [805][c,h]	< 2.5	$\mathit{2.7}^{+1.3}_{-1.2}$
$\mathcal{B}(B^0 \to f_x(1300)^0K^0) \times \mathcal{B}(f_x(1300)^0 \to \pi^+\pi^-)$	*BABAR* [804][c,d]	$1.81^{+0.55}_{-0.45} \pm 0.48$	$1.81^{+0.73}_{-0.66}$

[a]Not included in PDG average.
[b]The PDG uncertainty includes a scale factor.
[c]Result extracted from Dalitz-plot analysis of $B^0 \to K^0_S\pi^+\pi^-$ decays.
[d]Multiple systematic uncertainties are added in quadrature.
[e]$1.1 < m_{K\pi} < 1.6$ GeV/c^2.
[f]K_x^* stands for the possible candidates of $K^*(1410)$, $K_0^*(1430)$ and $K_2^*(1430)$.
[g]Using $\mathcal{B}(B^0 \to K^0\pi^+\pi^-)$.
[h]Using $\mathcal{B}(f_2(1270) \to \pi^+\pi^-)$.

TABLE 154. Branching fractions of charmless mesonic B^0 decays with strange mesons (part 6).

Parameter [10^{-6}]	Measurements		Average$^{\text{HFLAV}}_{PDG}$
$\mathcal{B}(B^0 \to K^*(892)^0\pi^0)$	*BABAR* [801][a]	$3.3 \pm 0.5 \pm 0.4$	3.3 ± 0.6
	Belle [802]	< 3.5	
$\mathcal{B}(B^0 \to K_2^*(1430)^+\pi^-)$	Belle [805][b]	< 6.3	3.82 ± 0.36
	BABAR [803][a]	< 16.2	p = 0.16%
	LHCb [809][b,c,d]		*$3.65^{+0.34}_{-0.33}$*
$\mathcal{B}(B^0 \to K^*(1680)^+\pi^-)$	Belle [805][b]	< 10.1	$14.7^{+1.5}_{-1.3}$
	BABAR [803][a]	< 25.0	p = 0.16%
	LHCb [809][b,c,e]		*14.1 ± 1.0*
$\mathcal{B}(B^0 \to K^+\pi^-\pi^+\pi^-)$	DELPHI [811]	< 230	< 230
$\mathcal{B}(B^0 \to \rho^0(770)K^+\pi^-)$	Belle [812][f]	$2.8 \pm 0.5 \pm 0.5$	2.8 ± 0.7
$\mathcal{B}(B^0 \to f_0(980)K^+\pi^-) \times \mathcal{B}(f_0(980) \to \pi\pi)$	Belle [812][f]	$1.4 \pm 0.4^{+0.3}_{-0.4}$	$1.4^{+0.5}_{-0.6}$
$\mathcal{B}(B^0 \to K^+\pi^-\pi^+\pi^-(\text{NR}))$	Belle [812][f,g]	< 2.1	< 2.1
$\mathcal{B}(B^0 \to K^*(892)^0\pi^+\pi^-)$	*BABAR* [813]	$54.5 \pm 2.9 \pm 4.3$	54.5 ± 5.2
$\mathcal{B}(B^0 \to K^*(892)^0\rho^0(770))$[h]	*BABAR* [814]	$5.1 \pm 0.6^{+0.6}_{-0.8}$	3.88 ± 0.77
	Belle [812]	$2.1^{+0.8\,+0.9}_{-0.7\,-0.5}$	*$3.88^{+1.33}_{-1.25}$*
$\mathcal{B}(B^0 \to f_0(980)K_0^*(892)^0) \times \mathcal{B}(f_0(980) \to \pi\pi)$[h]	Belle [812]	$1.4^{+0.6\,+0.6}_{-0.5\,-0.4}$	3.90 ± 0.55
	BABAR [814]	$5.7 \pm 0.6 \pm 0.4$	p = 0.01%
			$3.90^{+2.12}_{-1.85}$

[a]Result extracted from Dalitz-plot analysis of $B^0 \to K^+\pi^-\pi^0$ decays.
[b]Result extracted from Dalitz-plot analysis of $B^0 \to K^0_S\pi^+\pi^-$ decays.
[c]Multiple systematic uncertainties are added in quadrature.
[d]Measurement of $(\mathcal{B}(B^0 \to K_2^*(1430)^+\pi^-)\mathcal{B}(K_2^*(1430)^+ \to K\pi) \times 2/3)/\mathcal{B}(B^0 \to K^0\pi^+\pi^-)$ used in our fit.
[e]Measurement of $(\mathcal{B}(B^0 \to K^*(1680)^+\pi^-)\mathcal{B}(K^*(1680)^+ \to K\pi) \times 2/3)/\mathcal{B}(B^0 \to K^0\pi^+\pi^-)$ used in our fit.
[f]$0.75 < m_{K\pi} < 1.20$ GeV/c^2.
[g]$0.55 < m_{\pi\pi} < 1.20$ GeV/c^2.
[h]The PDG uncertainty includes a scale factor.

TABLE 155. Branching fractions of charmless mesonic B^0 decays with strange mesons (part 7).

Parameter [10^{-6}]	Measurements		Average$^{\text{HFLAV}}_{PDG}$
$\mathcal{B}(B^0 \to K_1(1270)^+\pi^-)$	*BABAR* [738]	< 30	< 30
$\mathcal{B}(B^0 \to K_1(1400)^+\pi^-)$	*BABAR* [738]	< 27	< 27
$\mathcal{B}(B^0 \to a_1(1260)^-K^+)$	*BABAR* [742]	$16.3 \pm 2.9 \pm 2.3$	16.3 ± 3.7
$\mathcal{B}(B^0 \to K^*(892)^+\rho^-(770))$	*BABAR* [814]	$10.3 \pm 2.3 \pm 1.3$	10.3 ± 2.6
$\mathcal{B}(B^0 \to (K\pi)_0^{*+}\rho^-(770)) \times \mathcal{B}((K\pi)_0^* \to K\pi)$	*BABAR* [814]	< 48	< 48 *None*
$\mathcal{B}(B^0 \to K_0^*(1430)^+\rho^-(770))$	*BABAR* [814][a]	$28 \pm 10 \pm 6$	28 ± 12
$\mathcal{B}(B^0 \to K_1(1400)^0\rho^0(770))$	ARGUS [746]	< 3000	< 3000
$\mathcal{B}(B^0 \to (K\pi)_0^{*0}\rho^0(770)) \times \mathcal{B}((K\pi)_0^* \to K\pi)$	*BABAR* [814]	$31 \pm 4 \pm 3$	31.0 ± 5.0 *None*
$\mathcal{B}(B^0 \to K_0^*(1430)^0\rho^0(770))$	*BABAR* [814][a]	$27 \pm 4 \pm 4$	27.0 ± 5.4 *27.0 ± 5.7*
$\mathcal{B}(B^0 \to (K\pi)_0^{*0}f_0(980)) \times \mathcal{B}(f_0(980) \to \pi\pi) \times \mathcal{B}((K\pi)_0^* \to K\pi)$	*BABAR* [814]	$3.1 \pm 0.8 \pm 0.7$	3.1 ± 1.1 *None*
$\mathcal{B}(B^0 \to K_0^*(1430)^0f_0(980)) \times \mathcal{B}(f_0(980) \to \pi\pi)$	*BABAR* [814][a]	$2.7 \pm 0.7 \pm 0.6$	2.7 ± 0.9
$\mathcal{B}(B^0 \to K_2^*(1430)^0f_0(980)) \times \mathcal{B}(f_0(980) \to \pi\pi)$	*BABAR* [814]	$8.6 \pm 1.7 \pm 1.0$	8.6 ± 2.0
$\mathcal{B}(B^0 \to K^+K^-)$	LHCb [794][b] Belle [702] CDF [792][b] *BABAR* [798]	$0.0799 \pm 0.0130 \pm 0.0086$ $0.10 \pm 0.08 \pm 0.04$ $0.24 \pm 0.10 \pm 0.10$ < 0.5	0.082 ± 0.015 *0.078 ± 0.015*
$\mathcal{B}(B^0 \to K^0\bar{K}^0)$	Belle [702] *BABAR* [704]	$1.26 \pm 0.19 \pm 0.05$ $1.08 \pm 0.28 \pm 0.11$	1.21 ± 0.16
$\mathcal{B}(B^0 \to K^0K^+\pi^-+\text{c.c.})$	LHCb [808][c,d] Belle [815] *BABAR* [816]	$6.11 \pm 0.45 \pm 0.78$ $7.20 \pm 0.66 \pm 0.30$ $6.4 \pm 1.0 \pm 0.6$	6.7 ± 0.5
$\mathcal{B}(B^0 \to K^*(892)^-K^+ + \text{c.c.})$	LHCb [810][e]	< 0.38	< 0.4
$\mathcal{B}(B^0 \to K^*(892)^0\bar{K}^0 + \text{c.c.})$[f]	LHCb [807][d] *BABAR* [817]	< 1.0 < 1.9	< 0.99 *< 0.96*

[a]Multiple systematic uncertainties are added in quadrature.
[b]Using $\mathcal{B}(B^0 \to K^+\pi^-)$.
[c]Regions corresponding to D, Λ_c^+ and charmonium resonances are vetoed in this analysis.
[d]Using $\mathcal{B}(B^0 \to K^0\pi^+\pi^-)$.
[e]Using $\mathcal{B}(B^0 \to K^*(892)^+\pi^-)$.
[f]$0.75 < m_{K\pi} < 1.20$ GeV/c^2.

TABLE 156. Branching fractions of charmless mesonic B^0 decays with strange mesons (part 8).

Parameter [10^{-6}]	Measurements		Average$^{\text{HFLAV}}_{PDG}$
$\mathcal{B}(B^0 \to K^+K^-\pi^0)$	Belle [818]	$2.17 \pm 0.60 \pm 0.24$	2.17 ± 0.65
$\mathcal{B}(B^0 \to K^0_S K^0_S \pi^0)$	*BABAR* [819]	< 0.9	< 0.9
$\mathcal{B}(B^0 \to K^0_S K^0_S \eta)$	*BABAR* [819]	< 1.0	< 1.0
$\mathcal{B}(B^0 \to K^0_S K^0_S \eta')$	*BABAR* [819]	< 2.0	< 2.0
$\mathcal{B}(B^0 \to K^0 K^+ K^-)$	LHCb [808][c,d]	$27.29 \pm 0.89 \pm 1.90$	26.8 ± 1.0
	BABAR [720][e,f]	$26.5 \pm 0.9 \pm 0.8$	*26.8 ± 1.1*
	Belle [736]	$28.3 \pm 3.3 \pm 4.0$	
$\mathcal{B}(B^0 \to \phi(1020)K^0)$	*BABAR* [720][e]	$7.1 \pm 0.6^{+0.4}_{-0.3}$	7.24 ± 0.60
	Belle II [760][a]	$5.9 \pm 1.8 \pm 0.7$	$7.32^{+0.69}_{-0.63}$
	Belle [764]	$9.0^{+2.2}_{-1.8} \pm 0.7$	
	LHCb [820][b,g], [821][h,i]		
$\mathcal{B}(B^0 \to f_0(980)K^0) \times \mathcal{B}(f_0(980) \to K^+K^-)$	*BABAR* [720][e]	$7.0^{+2.6}_{-1.8} \pm 2.4$	$7.0^{+3.5}_{-3.0}$
$\mathcal{B}(B^0 \to f_0(1500)K^0)$	*BABAR* [720][e]	$13.3^{+5.8}_{-4.4} \pm 3.2$	$13.3^{+6.6}_{-5.4}$
$\mathcal{B}(B^0 \to f'_2(1525)K^0)$	*BABAR* [720][e]	$0.29^{+0.27}_{-0.18} \pm 0.36$	$0.29^{+0.45}_{-0.40}$
$\mathcal{B}(B^0 \to f_0(1710)K^0) \times \mathcal{B}(f_0(1710) \to K^+K^-)$	*BABAR* [720][e]	$4.4 \pm 0.7 \pm 0.5$	4.4 ± 0.9
$\mathcal{B}(B^0 \to K^0K^+K^-(\text{NR}))$	*BABAR* [720][j]	$33 \pm 5 \pm 9$	33 ± 10

[a]Preliminary result.

[b]Not included in PDG average.

[c]Regions corresponding to D, Λ_c^+ and charmonium resonances are vetoed in this analysis.

[d]Using $\mathcal{B}(B^0 \to K^0\pi^+\pi^-)$.

[e]Result extracted from Dalitz-plot analysis of $B^0 \to K^0_S K^+K^-$ decays.

[f]All charmonium resonances are vetoed, except for χ_{c0}. The analysis also reports $\mathcal{B}(B^0 \to K^0K^+K^-) = (25.4 \pm 0.9 \pm 0.8) \times 10^{-6}$ excluding χ_{c0}.

[g]Measurement of $(\mathcal{B}(\Lambda_b^0 \to \Lambda^0\phi(1020))/\mathcal{B}(B^0 \to \phi(1020)K^0))(f_{\Lambda_b^0}/f_d) \times 2$ used in our fit.

[h]Multiple systematic uncertainties are added in quadrature.

[i]Measurement of $\mathcal{B}(B_s^0 \to K^0\bar{K}^0)/\mathcal{B}(B^0 \to \phi(1020)K^0)$ used in our fit.

[j]The nonresonant amplitude is modeled using a polynomial function including S-wave and P-wave terms.

TABLE 157. Branching fractions of charmless mesonic B^0 decays with strange mesons (part 9).

Parameter [10^{-6}]	Measurements		Average$^{\text{HFLAV}}_{PDG}$
$\mathcal{B}(B^0 \to K^0_S K^0_S K^0_S)$[a]	*BABAR* [822][b,c]	$6.19 \pm 0.48 \pm 0.19$	6.04 ± 0.50
	Belle [736]	$4.2^{+1.6}_{-1.3} \pm 0.8$	$\mathit{6.04}^{+0.53}_{-0.52}$
$\mathcal{B}(B^0 \to f_0(980)K^0_S) \times \mathcal{B}(f_0(980) \to K^0_S K^0_S)$	*BABAR* [822][b,c]	$2.7^{+1.3}_{-1.2} \pm 1.3$	2.7 ± 1.8
$\mathcal{B}(B^0 \to f_0(1710)K^0_S) \times \mathcal{B}(f_0(1710) \to K^0_S K^0_S)$	*BABAR* [822][b,c]	$0.50^{+0.46}_{-0.24} \pm 0.11$	$0.50^{+0.47}_{-0.26}$
$\mathcal{B}(B^0 \to f_2(2010)K^0_S) \times \mathcal{B}(f_2(2010) \to K^0_S K^0_S)$	*BABAR* [822][b,c]	$0.54^{+0.21}_{-0.20} \pm 0.52$	0.54 ± 0.56
$\mathcal{B}(B^0 \to K^0_S K^0_S K^0_S(\text{NR}))$	*BABAR* [822][d,c]	$13.3^{+2.2}_{-2.3} \pm 0.6$	13.3 ± 2.3
			$\mathit{13.3}^{+3.1}_{-3.2}$
$\mathcal{B}(B^0 \to K^0_S K^0_S K^0_L)$	*BABAR* [823][e]	<16	<16

[a]The PDG uncertainty includes a scale factor.
[b]Result extracted from Dalitz-plot analysis of $B^0 \to K^0_S K^0_S K^0_S$ decays.
[c]Multiple systematic uncertainties are added in quadrature.
[d]The nonresonant amplitude is modeled using an exponential function.
[e]$0.75 < m_{K\pi} < 1.20$ GeV/c^2.

TABLE 158. Branching fractions of charmless mesonic B^0 decays with strange mesons (part 10).

Parameter [10^{-6}]	Measurements		Average$^{\text{HFLAV}}_{PDG}$
$\mathcal{B}(B^0 \to K^*(892)^0 K^+ K^-)$	*BABAR* [813]	$27.5 \pm 1.3 \pm 2.2$	27.5 ± 2.6
$\mathcal{B}(B^0 \to \phi(1020)K^*(892)^0)$	*BABAR* [824]	$9.7 \pm 0.5 \pm 0.5$	
	Belle [825]	$10.4 \pm 0.5 \pm 0.6$	10.08 ± 0.48
	Belle II [760][a]	$11.0 \pm 2.1 \pm 1.1$	$\mathit{10.04 \pm 0.52}$
	CLEO [762]	$11.5^{+4.5+1.8}_{-3.7-1.7}$	
	LHCb [826][b,c,d], [827][b,c,e], [828][b,c,f], [829][g]		
$\mathcal{B}(B^0 \to K^+\pi^-\pi^+K^-(\text{NR}))$	Belle [830][h]	< 71.7	< 72
$\mathcal{B}(B^0 \to K^*(892)^0\pi^+K^-)$	*BABAR* [813]	$4.6 \pm 1.1 \pm 0.8$	4.5 ± 1.3
	Belle [830][h]	$2.11^{+5.63+4.85}_{-5.26-4.75}$	
$\mathcal{B}(B^0 \to K^*(892)^0 \bar{K}^*(892)^0)$[i]	LHCb [831][c,j]	$0.832 \pm 0.063 \pm 0.156$	0.83 ± 0.15
	Belle [830]	$0.26^{+0.33+0.10}_{-0.29-0.08}$	$\mathit{0.83}^{+0.25}_{-0.23}$
	BABAR [832]	$1.28^{+0.35}_{-0.30} \pm 0.11$	
$\mathcal{B}(B^0 \to K^+\pi^-K^+\pi^-(\text{NR}))$	Belle [830][h]	< 6.0	< 6.0
$\mathcal{B}(B^0 \to K^*(892)^0 K^+\pi^-)$	*BABAR* [813]	< 2.2	< 2.2
	Belle [830][h]	< 7.6	
$\mathcal{B}(B^0 \to K^*(892)^0 K^*(892)^0)$	Belle [830]	< 0.20	< 0.2
	BABAR [832]	< 0.41	
$\mathcal{B}(B^0 \to K^*(892)^+ K^*(892)^-)$	*BABAR* [833]	< 2.0	< 2.0

(Table continued)

TABLE 158. *(Continued)*

Parameter [10^{-6}]	Measurements		Average$^{\text{HFLAV}}_{PDG}$
$\mathcal{B}(B^0 \to K_1(1400)^0\phi(1020))$	ARGUS [746]	< 5000	< 5000
$\mathcal{B}(B^0 \to (K\pi)_0^{*0}\phi(1020))$	Belle [825]	$4.3 \pm 0.4 \pm 0.4$	4.30 ± 0.45
	BABAR [824]	$4.3 \pm 0.6 \pm 0.4$	
$\mathcal{B}(B^0 \to (K\pi)_0^{*0}\phi)$, $1.60 < m_{K\pi} < 2.15$ GeV/c^2.	*BABAR* [834]	< 1.7	< 1.7

[a]Preliminary result.
[b]Not included in PDG average.
[c]Multiple systematic uncertainties are added in quadrature.
[d]Measurement of $\mathcal{B}(B_s^0 \to \phi(1020)\bar{K}^*(892)^0)/\mathcal{B}(B^0 \to \phi(1020)K^*(892)^0)$ used in our fit.
[e]Measurement of $\mathcal{B}(B_s^0 \to K^*(892)^0\bar{K}^*(892)^0)/\mathcal{B}(B^0 \to \phi(1020)K^*(892)^0)$ used in our fit.
[f]Measurement of $\mathcal{B}(B_s^0 \to \phi(1020)\phi(1020))/\mathcal{B}(B^0 \to \phi(1020)K^*(892)^0)$ used in our fit.
[g]Measurement of $\mathcal{B}(B^0 \to \rho^0(770)\rho^0(770))/\mathcal{B}(B^0 \to \phi(1020)K^*(892)^0)$ used in our fit.
[h]$0.70 < m_{K\pi} < 1.70$ GeV/c^2.
[i]The PDG uncertainty includes a scale factor.
[j]Using $\mathcal{B}(B_s^0 \to K^*(892)^0\bar{K}^*(892)^0)$.

TABLE 159. Branching fractions of charmless mesonic B^0 decays with strange mesons (part 11).

Parameter [10^{-6}]	Measurements		Average$^{\text{HFLAV}}_{PDG}$
$\mathcal{B}(B^0 \to K_0^*(1430)^0\pi^+K^-)$	Belle [830][a]	< 31.8	< 32
$\mathcal{B}(B^0 \to K_0^*(1430)^0\bar{K}^*(892)^0)$	Belle [830]	< 3.3	< 3.3
$\mathcal{B}(B^0 \to K_0^*(1430)^0\bar{K}_0^*(1430)^0)$	Belle [830]	< 8.4	< 8.4
$\mathcal{B}(B^0 \to \phi(1020)K_0^*(1430)^0)$	*BABAR* [824]	$3.9 \pm 0.5 \pm 0.6$	3.90 ± 0.78
$\mathcal{B}(B^0 \to K_0^*(1430)^0K^*(892)^0)$	Belle [830]	< 1.7	< 1.7
$\mathcal{B}(B^0 \to K_0^*(1430)^0K_0^*(1430)^0)$	Belle [830]	< 4.7	< 4.7
$\mathcal{B}(B^0 \to \phi(1020)K^*(1680)^0)$	*BABAR* [834]	< 3.5	< 3.5
$\mathcal{B}(B^0 \to \phi(1020)K_3^*(1780)^0)$	*BABAR* [834]	< 2.7	< 2.7
$\mathcal{B}(B^0 \to \phi(1020)K_4^*(2045)^0)$	*BABAR* [834]	< 15.3	< 15
$\mathcal{B}(B^0 \to \rho^0(770)K_2^*(1430)^0)$	ARGUS [746]	< 1100	< 1100
$\mathcal{B}(B^0 \to \phi(1020)K_2^*(1430)^0)$[b]	Belle [825]	$5.5^{+0.9}_{-0.7} \pm 1.0$	6.8 ± 0.8
	BABAR [824]	$7.5 \pm 0.9 \pm 0.5$	$6.8^{+1.0}_{-0.9}$
$\mathcal{B}(B^0 \to \phi(1020)\phi(1020)K^0)$	*BABAR* [767][c]	$4.5 \pm 0.8 \pm 0.3$	4.5 ± 0.9
			3.7 ± 0.7
$\mathcal{B}(B^0 \to \eta'\eta'K^0)$	*BABAR* [769]	< 31.0	< 31

[a]$0.70 < m_{K\pi} < 1.70$ GeV/c^2.
[b]The PDG uncertainty includes a scale factor.
[c]Measured in the $\phi\phi$ invariant mass range below the η_c resonance ($m_{\phi\phi} < 2.85$ GeV/c^2).

TABLE 160. Branching fractions of charmless mesonic B^0 decays without strange mesons (part 1).

Parameter [10^{-6}]	Measurements		Average$^{\text{HFLAV}}_{PDG}$
$\mathcal{B}(B^0 \to \pi^+\pi^-)$	LHCb [793][c]	$5.26 \pm 0.18 \pm 0.36$	5.36 ± 0.16
	Belle II [703][a]	$5.8 \pm 0.2 \pm 0.2$	*5.12 ± 0.19*
	Belle [702]	$5.04 \pm 0.21 \pm 0.18$	
	CDF [791][c]	$5.20 \pm 0.34 \pm 0.34$	
	BABAR [789]	$5.5 \pm 0.4 \pm 0.3$	
	CLEO [705]	$4.5^{+1.4+0.5}_{-1.2-0.4}$	
$\mathcal{B}(B^0 \to \pi^0\pi^0)$[d]	Belle [835]	$1.31 \pm 0.19 \pm 0.19$	1.55 ± 0.16
	BABAR [795]	$1.83 \pm 0.21 \pm 0.13$	*1.59 ± 0.26*
	Belle II [836][b]	$1.38 \pm 0.27 \pm 0.22$	
$\mathcal{B}(B^0 \to \eta\pi^0)$	Belle [837]	$0.41^{+0.17+0.05}_{-0.15-0.07}$	0.41 ± 0.17
	BABAR [784]	< 1.5	*$0.41^{+0.18}_{-0.17}$*
	CLEO [712]	< 2.9	
$\mathcal{B}(B^0 \to \eta\eta)$	*BABAR* [708]	< 1.0	< 1.0
$\mathcal{B}(B^0 \to \eta'\pi^0)$[d]	*BABAR* [784]	$0.9 \pm 0.4 \pm 0.1$	1.2 ± 0.4
	Belle [709]	$2.79^{+1.02+0.25}_{-0.96-0.34}$	*1.2 ± 0.6*
$\mathcal{B}(B^0 \to \eta'\eta')$	*BABAR* [708]	< 1.7	< 1.7
	Belle [715]	< 6.5	
$\mathcal{B}(B^0 \to \eta'\eta)$	*BABAR* [784]	< 1.2	< 1.2
	Belle [715]	< 4.5	
$\mathcal{B}(B^0 \to \eta'\rho^0(770))$	Belle [715]	< 1.3	< 1.3
	BABAR [714]	< 2.8	
$\mathcal{B}(B^0 \to f_0(980)\eta') \times \mathcal{B}(f_0(980) \to \pi^+\pi^-)$	*BABAR* [714]	< 0.9	< 0.9
$\mathcal{B}(B^0 \to \eta\rho^0(770))$	*BABAR* [799]	< 1.5	< 1.5
	Belle [718]	< 1.9	
$\mathcal{B}(B^0 \to f_0(980)\eta) \times \mathcal{B}(f_0(980) \to \pi^+\pi^-)$	*BABAR* [799]	< 0.4	< 0.4
$\mathcal{B}(B^0 \to \omega(782)\eta)$	*BABAR* [708]	$0.94^{+0.35}_{-0.30} \pm 0.09$	$0.94^{+0.36}_{-0.31}$

[a]Preliminary result.
[b]Not included in PDG average.
[c]Using $\mathcal{B}(B^0 \to K^+\pi^-)$.
[d]The PDG uncertainty includes a scale factor.

TABLE 161. Branching fractions of charmless mesonic B^0 decays without strange mesons (part 2).

Parameter [10^{-6}]	Measurements		Average$^{\text{HFLAV}}_{PDG}$
$\mathcal{B}(B^0 \to \omega(782)\eta')$	*BABAR* [708]	$1.01^{+0.46}_{-0.38} \pm 0.09$	$1.01^{+0.47}_{-0.39}$
	Belle [715]	< 2.2	
$\mathcal{B}(B^0 \to \omega(782)\rho^0(770))$	*BABAR* [724]	< 1.6	< 1.6
$\mathcal{B}(B^0 \to f_0(980)\omega(782)) \times \mathcal{B}(f_0(980) \to \pi^+\pi^-)$	*BABAR* [724]	< 1.5	< 1.5
$\mathcal{B}(B^0 \to \omega(782)\omega(782))$	*BABAR* [838]	$1.2 \pm 0.3^{+0.3}_{-0.2}$	1.2 ± 0.4
$\mathcal{B}(B^0 \to \phi(1020)\pi^0)$	Belle [786]	< 0.15	< 0.15
	BABAR [785]	< 0.28	
$\mathcal{B}(B^0 \to \phi(1020)\eta)$	*BABAR* [708]	< 0.5	< 0.5
$\mathcal{B}(B^0 \to \phi(1020)\eta')$	Belle [715]	< 0.5	< 0.5
	BABAR [708]	< 1.1	
$\mathcal{B}(B^0 \to \phi(1020)\pi^+\pi^-)$	LHCb [839][a,b]	$0.182 \pm 0.025 \pm 0.043$	0.182 ± 0.050
$\mathcal{B}(B^0 \to \phi(1020)\rho^0(770))$	*BABAR* [787]	< 0.33	< 0.33
$\mathcal{B}(B^0 \to f_0(980)\phi(1020)) \times \mathcal{B}(f_0(980) \to \pi^+\pi^-)$	*BABAR* [787]	< 0.38	< 0.38
$\mathcal{B}(B^0 \to \omega(782)\phi(1020))$	*BABAR* [838]	< 0.7	< 0.7
$\mathcal{B}(B^0 \to \phi(1020)\phi(1020))$	LHCb [840]	< 0.027	< 0.027
	BABAR [787]	< 0.2	
$\mathcal{B}(B^0 \to a_0(980)^+\pi^- + \text{c.c.}) \times \mathcal{B}(a_0(980)^+ \to \eta\pi^+)$	*BABAR* [799]	< 3.1	< 3.1
$\mathcal{B}(B^0 \to a_0(1450)^+\pi^- + \text{c.c.}) \times \mathcal{B}(a_0(1450)^+ \to \eta\pi^+)$	*BABAR* [799]	< 2.3	< 2.3

[a] $400 < m_{\pi^+\pi^-} < 1600$ MeV/c^2.

[b] Multiple systematic uncertainties are added in quadrature.

TABLE 162. Branching fractions of charmless mesonic B^0 decays without strange mesons (part 3).

Parameter [10^{-6}]	Measurements		Average$^{\text{HFLAV}}_{PDG}$
$\mathcal{B}(B^0 \to \pi^+\pi^-\pi^0)$	ARGUS [777]	< 720	< 720
$\mathcal{B}(B^0 \to \rho^0(770)\pi^0)$	Belle [841][a]	$3.0 \pm 0.5 \pm 0.7$	2.0 ± 0.5
	BABAR [842]	$1.4 \pm 0.6 \pm 0.3$	
	CLEO [723]	$1.6^{+2.0}_{-1.4} \pm 0.8$	
$\mathcal{B}(B^0 \to \rho^+(770)\pi^- + \text{c.c.})$	Belle [841][a]	$22.6 \pm 1.1 \pm 4.4$	23.0 ± 2.3
	BABAR [843]	$22.6 \pm 1.8 \pm 2.2$	
	CLEO [723]	$27.6^{+8.4}_{-7.4} \pm 4.2$	
$\mathcal{B}(B^0 \to \pi^+\pi^-\pi^+\pi^-)$	Belle [844][b]	< 11.2	< 11
	BABAR [845][c]	< 23.1	
$\mathcal{B}(B^0 \to \rho^0(770)\pi^+\pi^-)$	*BABAR* [845][c]	< 8.8	< 8.8
	Belle [844][b]	< 12.0	
$\mathcal{B}(B^0 \to \rho^0(770)\rho^0(770))$	LHCb [829][d]	$0.95 \pm 0.17 \pm 0.10$	0.96 ± 0.15
	Belle [844]	$1.02 \pm 0.30 \pm 0.15$	
	BABAR [845]	$0.92 \pm 0.32 \pm 0.14$	

(Table continued)

TABLE 162. *(Continued)*

Parameter [10^{-6}]	Measurements		Average$^{\text{HFLAV}}_{PDG}$
$\mathcal{B}(B^0 \to f_0(980)\pi^+\pi^-) \times \mathcal{B}(f_0(980) \to \pi^+\pi^-)$	Belle [844][b]	< 3.0	< 3.0
$\mathcal{B}(B^0 \to f_0(980)\rho^0(770)) \times \mathcal{B}(f_0(980) \to \pi^+\pi^-)$	Belle [844] *BABAR* [845]	$0.78 \pm 0.22 \pm 0.11$ < 0.40	0.78 ± 0.25
$\mathcal{B}(B^0 \to f_0(980)f_0(980)) \times \mathcal{B}(f_0(980) \to \pi^+\pi^-) \times \mathcal{B}(f_0(980) \to \pi^+\pi^-)$	*BABAR* [845] Belle [844]	< 0.19 < 0.2	< 0.19
$\mathcal{B}(B^0 \to f_0(980)f_0(980)) \times \mathcal{B}(f_0(980) \to \pi^+\pi^-) \times \mathcal{B}(f_0(980) \to K^+K^-)$	*BABAR* [787]	< 0.23	< 0.23

[a]Result extracted from Dalitz-plot analysis of $B^0 \to \pi^+\pi^-\pi^0$ decays.
[b]$0.52 < m_{\pi^+\pi^-} < 1.15$ GeV/c^2.
[c]$0.55 < m_{\pi^+\pi^-} < 1.050$ GeV/c^2.
[d]Using $\mathcal{B}(B^0 \to \phi(1020)K^*(892)^0)$.

TABLE 163. Branching fractions of charmless mesonic B^0 decays without strange mesons (part 4).

Parameter [10^{-6}]	Measurements		Average$^{\text{HFLAV}}_{PDG}$
$\mathcal{B}(B^0 \to a_1(1260)^+\pi^- + \text{c.c.})$[b]	Belle [846] *BABAR* [847]	$22.2 \pm 2.0 \pm 2.8$ $33.2 \pm 3.8 \pm 3.0$	25.9 ± 2.8 *25.9 ± 5.2*
$\mathcal{B}(B^0 \to a_2(1320)^+\pi^- + \text{c.c.})$	Belle [846]	< 6.3	< 6.3
$\mathcal{B}(B^0 \to \pi^+\pi^-\pi^0\pi^0)$	ARGUS [777]	< 3100	< 3100
$\mathcal{B}(B^0 \to \rho^+(770)\rho^-(770))$	Belle [848] *BABAR* [849] Belle II [850][a]	$28.3 \pm 1.5 \pm 1.5$ $25.5 \pm 2.1^{+3.6}_{-3.9}$ $26.7 \pm 2.8 \pm 2.8$	27.5 ± 1.7 *27.7 ± 1.9*
$\mathcal{B}(B^0 \to a_1(1260)^0\pi^0)$	ARGUS [777]	< 1100	< 1100
$\mathcal{B}(B^0 \to \omega(782)\pi^0)$	*BABAR* [784] Belle [783]	< 0.5 < 2.0	< 0.5
$\mathcal{B}(B^0 \to \pi^+\pi^+\pi^-\pi^-\pi^0)$	ARGUS [777]	< 9000	< 9000
$\mathcal{B}(B^0 \to a_1(1260)^+\rho^-(770) + \text{c.c.})$	*BABAR* [851]	< 61.0	< 61
$\mathcal{B}(B^0 \to a_1(1260)^0\rho^0(770))$	ARGUS [777]	< 2400	< 2400
$\mathcal{B}(B^0 \to b_1(1235)^+\pi^- + \text{c.c.}) \times \mathcal{B}(b_1(1235)^+ \to \omega(782)\pi^+)$	*BABAR* [748]	$10.9 \pm 1.2 \pm 0.9$	10.9 ± 1.5
$\mathcal{B}(B^0 \to b_1(1235)^0\pi^0) \times \mathcal{B}(b_1(1235)^0 \to \omega(782)\pi^0)$	*BABAR* [743]	< 1.9	< 1.9
$\mathcal{B}(B^0 \to b_1(1235)^-\rho^+(770)) \times \mathcal{B}(b_1(1235)^- \to \omega(782)\pi^-)$	*BABAR* [749]	< 1.4	< 1.4
$\mathcal{B}(B^0 \to b_1(1235)^0\rho^0(770)) \times \mathcal{B}(b_1(1235)^0 \to \omega(782)\pi^0)$	*BABAR* [749]	< 3.4	< 3.4
$\mathcal{B}(B^0 \to \pi^+\pi^+\pi^+\pi^-\pi^-\pi^-)$	ARGUS [777]	< 3000	< 3000
$\mathcal{B}(B^0 \to a_1(1260)^+a_1(1260)^-) \times \mathcal{B}(a_1(1260)^+ \to \pi^+\pi^+\pi^-)$ $\times \mathcal{B}(a_1(1260)^- \to \pi^-\pi^-\pi^+)$	*BABAR* [852]	$11.8 \pm 2.6 \pm 1.6$	11.8 ± 3.1
$\mathcal{B}(B^0 \to \pi^+\pi^+\pi^+\pi^-\pi^-\pi^-\pi^0)$	ARGUS [777]	< 11000	< 11000

[a]Preliminary result.
[b]The PDG uncertainty includes a scale factor.

TABLE 164. Relative branching fractions of mesonic B^+ decays.

Parameter	Measurements		Average
$\frac{\mathcal{B}(B^+ \to K^+K^-\pi^+)}{\mathcal{B}(B^+ \to K^+K^+K^-)}$	LHCb [730]	$0.151 \pm 0.004 \pm 0.008$	0.151 ± 0.009
$\frac{\mathcal{B}(B^+ \to K^+\pi^+\pi^-)}{\mathcal{B}(B^+ \to K^+K^+K^-)}$	LHCb [730]	$1.703 \pm 0.011 \pm 0.022$	1.703 ± 0.025
$\frac{\mathcal{B}(B^+ \to \pi^+\pi^+\pi^-)}{\mathcal{B}(B^+ \to K^+K^+K^-)}$	LHCb [730]	$0.488 \pm 0.005 \pm 0.009$	0.488 ± 0.010

TABLE 165. Relative branching fractions of mesonic B^0 decays.

Parameter	Measurements		Average
$\frac{\mathcal{B}(B^0 \to K^+K^-)}{\mathcal{B}(B^0 \to K^+\pi^-)}$ $[10^{-3}]$	LHCb [794] CDF [792]	$3.98 \pm 0.65 \pm 0.42$ $12 \pm 5 \pm 5$	4.07 ± 0.77
$\frac{\mathcal{B}(B^0 \to K^*(892)^+K^-+\text{c.c.})}{\mathcal{B}(B^0 \to K^*(892)^+\pi^-)}$ $[10^{-2}]$	LHCb [810]	< 5	< 5.0
$\frac{\mathcal{B}(B^0 \to K^0_S K^*(892)^0+\text{c.c.})}{\mathcal{B}(B^0 \to K^0_S\pi^+\pi^-)}$ $[10^{-2}]$	LHCb [807]	< 2	< 2.0
$\frac{\mathcal{B}(B^0 \to \pi^+\pi^-)}{\mathcal{B}(B^0 \to K^+\pi^-)}$	LHCb [793] CDF [791]	$0.262 \pm 0.009 \pm 0.017$ $0.259 \pm 0.017 \pm 0.016$	0.261 ± 0.015
$\frac{\mathcal{B}(B^0 \to K^0K^+\pi^-+\text{c.c.})}{\mathcal{B}(B^0 \to K^0\pi^+\pi^-)}$	LHCb [808][a]	$0.123 \pm 0.009 \pm 0.015$	0.123 ± 0.017
$\frac{\mathcal{B}(B^0 \to K^0K^+K^-)}{\mathcal{B}(B^0 \to K^0\pi^+\pi^-)}$	LHCb [808][a]	$0.549 \pm 0.018 \pm 0.033$	0.549 ± 0.038
$\frac{\mathcal{B}(B^0 \to K^*(892)^0\bar{K}^*(892)^0)}{\mathcal{B}(B^0_s \to K^*(892)^0\bar{K}^*(892)^0)}$ $[10^{-2}]$	LHCb [831][b]	$7.58 \pm 0.57 \pm 0.30$	7.58 ± 0.64
$\frac{f_s}{f_d}\frac{\mathcal{B}(B^0 \to K^+K^-)}{\mathcal{B}(B^0_s \to K^+K^-)}$ $[10^{-2}]$	LHCb [793]	$1.8^{+0.8}_{-0.7} \pm 0.9$	1.8 ± 1.2
$\frac{\mathcal{B}(B^0 \to \rho^0(770)\rho^0(770))}{\mathcal{B}(B^0 \to \phi(1020)K^*(892)^0)}$ $[10^{-2}]$	LHCb [829]	$9.4 \pm 1.7 \pm 0.9$	9.4 ± 1.9
$\frac{\mathcal{B}(B^0 \to K^0\bar{K}^0)}{\mathcal{B}(B^0_s \to K^0\bar{K}^0)}$ $[10^{-2}]$	LHCb [821][b]	$7.5 \pm 3.1 \pm 0.6$	7.5 ± 3.2
$\frac{\mathcal{B}(B^0 \to K^0\bar{K}^0)}{\mathcal{B}(B^0 \to \phi(1020)K^0)}$	LHCb [821]	$0.17 \pm 0.08 \pm 0.02$	0.17 ± 0.08

[a]Regions corresponding to D, Λ_c^+ and charmonium resonances are vetoed in this analysis.
[b]Multiple systematic uncertainties are added in quadrature.

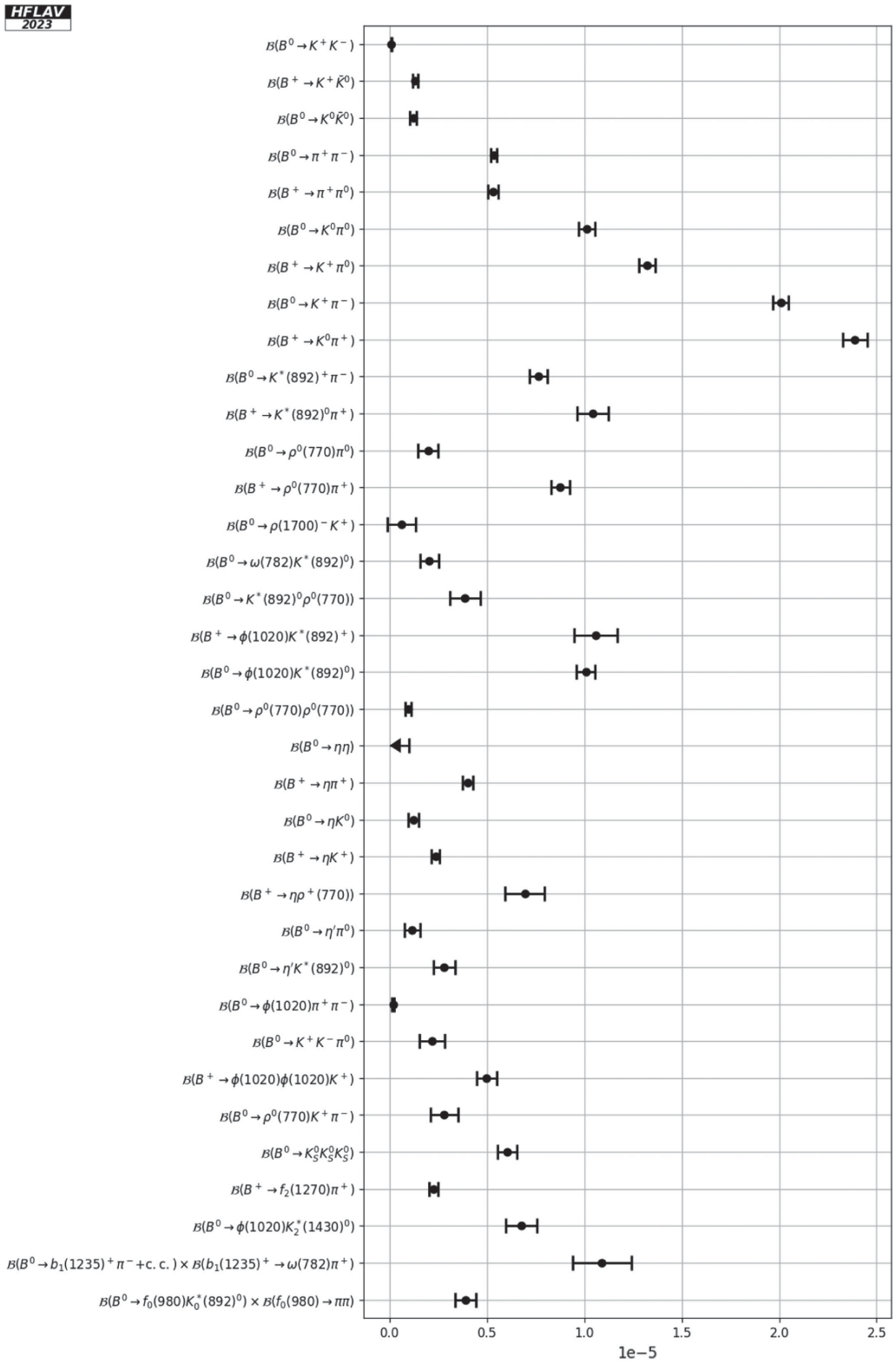


FIG. 29. A selection of high-precision measurements of Branching Fractions of B-meson decays into charmless mesonic final states.

B. Baryonic decays of B^+ and B^0 mesons

This section provides branching fractions of charmless baryonic decays of B^+ and B^0 mesons in Tables 166–170, respectively. Relative branching fractions are given in Table 171. Figures 30 and 31 show graphic representations of a selection of results given in this section.

TABLE 166. Branching fractions of charmless baryonic B^+ decays (part 1).

Parameter [10^{-6}]	Measurements		Average$^{\text{HFLAV}}_{PDG}$
$\mathcal{B}(B^+ \to p\bar{n}\pi^0)$	Belle [854]	< 6.1	< 6.1 *None*
$\mathcal{B}(B^+ \to p\bar{p}\pi^+)$	Belle [855][a] *BABAR* [525][b]	$1.60^{+0.22}_{-0.19} \pm 0.12$ $1.69 \pm 0.29 \pm 0.26$	1.62 ± 0.21 $1.62^{+0.21}_{-0.19}$
$\mathcal{B}(B^+ \to p\bar{p}\pi^+), m_{p\bar{p}} < 2.85$ GeV/c^2	LHCb [856][c]		1.00 ± 0.10 *None*
$\mathcal{B}(B^+ \to p\bar{p}\pi^+(\text{NR}))$	CLEO [737]	< 53	< 53
$\mathcal{B}(B^+ \to p\bar{p}\pi^+\pi^0)$	Belle [857][d]	$4.58 \pm 1.17 \pm 0.67$	4.6 ± 1.3
$\mathcal{B}(B^+ \to p\bar{p}\pi^+\pi^+\pi^-)$	ARGUS [858]	< 520	< 520 *None*

[a]The charmonium mass regions are vetoed.
[b]Charmonium decays to $p\bar{p}$ have been statistically subtracted.
[c]Measurement of $\mathcal{B}(B^+ \to p\bar{p}\pi^+), m_{p\bar{p}} < 2.85$ GeV/c^2/$(\mathcal{B}(B^+ \to J/\psi\pi^+)\mathcal{B}(J/\psi \to p\bar{p}))$ used in our fit.
[d]$m_{\pi^+\pi^0} < 1.3$ GeV/c^2.

TABLE 167. Branching fractions of charmless baryonic B^+ decays (part 2).

Parameter [10^{-6}]	Measurements		Average$^{\text{HFLAV}}_{PDG}$
$\mathcal{B}(B^+ \to p\bar{p}K^+)$[a]	Belle [855][b] *BABAR* [608][c]	$5.54^{+0.27}_{-0.25} \pm 0.36$ $6.7 \pm 0.5 \pm 0.4$	5.9 ± 0.4 *5.9 ± 0.5*
$\mathcal{B}(B^+ \to p\bar{p}K^+), m_{p\bar{p}} < 2.85$ GeV/c^2	LHCb [616][d]		4.37 ± 0.29 *None*
$\mathcal{B}(B^+ \to \Theta^{++}(1710)\bar{p}) \times \mathcal{B}(\Theta^{++}(1710) \to pK^+)$[e]	Belle [756]	< 0.091	< 0.091
$\mathcal{B}(B^+ \to f_J(2220)K^+) \times \mathcal{B}(f_J(2220) \to p\bar{p})$	Belle [756]	< 0.41	< 0.41
$\mathcal{B}(B^+ \to p\bar{\Lambda}(1520))$	*BABAR* [608] LHCb [856][f]	< 1.5	$0.305^{+0.084}_{-0.081}$ *0.315 ± 0.055*
$\mathcal{B}(B^+ \to p\bar{p}K^+(\text{NR}))$	CLEO [737]	< 89	< 89
$\mathcal{B}(B^+ \to p\bar{p}K^*(892)^+)$	Belle [859][g] *BABAR* [525][c]	$3.38^{+0.73}_{-0.60} \pm 0.39$ $5.3 \pm 1.5 \pm 1.3$	$3.6^{+0.8}_{-0.7}$
$\mathcal{B}(B^+ \to f_J(2220)K^*(892)^+) \times \mathcal{B}(f_J(2220) \to p\bar{p})$	*BABAR* [525]	< 0.77	< 0.77
$\mathcal{B}(B^+ \to p\bar{\Lambda}^0)$	LHCb [860] Belle [861]	$0.24^{+0.10}_{-0.08} \pm 0.03$ < 0.32	$0.24^{+0.10}_{-0.09}$

(Table continued)

TABLE 167. *(Continued)*

Parameter [10^{-6}]	Measurements		Average$^{\text{HFLAV}}_{PDG}$
$\mathcal{B}(B^+ \to p\bar{\Lambda}^0\pi^0)$	Belle [862]	$3.00^{+0.61}_{-0.53} \pm 0.33$	$3.00^{+0.69}_{-0.62}$
$\mathcal{B}(B^+ \to p\bar{\Sigma}(1385)^0)$	Belle [862]	< 0.47	< 0.47
$\mathcal{B}(B^+ \to \Delta(1232)^+\bar{\Lambda}^0)$	Belle [862]	< 0.82	< 0.82

[a]The PDG uncertainty includes a scale factor.
[b]The charmonium mass regions are vetoed.
[c]Charmonium decays to $p\bar{p}$ have been statistically subtracted.
[d]Measurement of $\mathcal{B}(B^+ \to p\bar{p}K^+), m_{p\bar{p}} < 2.85\ \text{GeV}/c^2/(\mathcal{B}(B^+ \to J/\psi K^+)\mathcal{B}(J/\psi \to p\bar{p}))$ used in our fit.
[e]Pentaquark candidate.
[f]Measurement of $(\mathcal{B}(B^+ \to p\bar{\Lambda}(1520))\mathcal{B}(\overline{\Lambda(1520)} \to K^+p))/(\mathcal{B}(B^+ \to J/\psi K^+)\mathcal{B}(J/\psi \to p\bar{p}))$ used in our fit.
[g]The charmonium mass region has been vetoed.

TABLE 168. Branching fractions of charmless baryonic B^+ decays (part 3).

Parameter [10^{-6}]	Measurements		Average$^{\text{HFLAV}}_{PDG}$
$\mathcal{B}(B^+ \to p\bar{\Lambda}^0\pi^+\pi^-)$	Belle [863]	$11.28^{+0.91}_{-0.72} \pm 1.03$	11.3 ± 1.3 $11.3^{+1.4}_{-1.3}$
$\mathcal{B}(B^+ \to p\bar{\Lambda}^0\pi^+\pi^-(\text{NR}))$	Belle [863]	$5.92^{+0.88}_{-0.84} \pm 0.69$	5.9 ± 1.1
$\mathcal{B}(B^+ \to p\bar{\Lambda}^0\rho^0(770)) \times \mathcal{B}(\rho^0(770) \to \pi^+\pi^-)$	Belle [863]	$4.78^{+0.67}_{-0.64} \pm 0.60$	4.8 ± 0.9
$\mathcal{B}(B^+ \to p\bar{\Lambda}^0 f_2(1270)) \times \mathcal{B}(f_2(1270) \to \pi^+\pi^-)$	Belle [863]	$2.03^{+0.77}_{-0.72} \pm 0.27$	2.0 ± 0.8
$\mathcal{B}(B^+ \to p\bar{\Lambda}^0K^+K^-)$	Belle [864]	$4.10^{+0.45}_{-0.43} \pm 0.50$	4.1 ± 0.7
$\mathcal{B}(B^+ \to p\bar{\Lambda}^0\phi(1020))$	Belle [864]	$0.795 \pm 0.209 \pm 0.077$	0.80 ± 0.22
$\mathcal{B}(B^+ \to \bar{p}\Lambda^0K^+K^-)$	Belle [864]	$3.70^{+0.39}_{-0.37} \pm 0.44$	3.7 ± 0.6
$\mathcal{B}(B^+ \to \Lambda^0\bar{\Lambda}^0\pi^+)$	Belle [482][a,b]	< 0.94	< 0.94
$\mathcal{B}(B^+ \to \Lambda^0\bar{\Lambda}^0K^+)$	Belle [482][a]	$3.38^{+0.41}_{-0.36} \pm 0.41$	3.4 ± 0.6 $3.4^{+0.6}_{-0.5}$
$\mathcal{B}(B^+ \to \Lambda^0\bar{\Lambda}^0K^*(892)^+)$	Belle [482][a,b]	$2.19^{+1.13}_{-0.88} \pm 0.33$	$2.2^{+1.2}_{-0.9}$
$\mathcal{B}(B^+ \to \Lambda(1520)\bar{\Lambda}^0K^+)$	Belle [864]	$2.23 \pm 0.63 \pm 0.25$	2.2 ± 0.7
$\mathcal{B}(B^+ \to \bar{\Lambda}(1520)\Lambda^0K^+)$	Belle [864]	< 2.08	< 2.1
$\mathcal{B}(B^+ \to \bar{\Delta}(1232)^0p)$	Belle [855]	< 1.38	< 1.4
$\mathcal{B}(B^+ \to \Delta^{++}\bar{p})$	Belle [855]	< 0.14	< 0.14

[a]The charmonium mass regions are vetoed.
[b]$m_{\Lambda^0\overline{\Lambda^0}} < 2.85\ \text{GeV}/c^2$.

TABLE 169. Branching fractions of charmless baryonic B^0 decays (part 1).

Parameter [10^{-6}]	Measurements		Average$^{\text{HFLAV}}_{PDG}$
$\mathcal{B}(B^0 \to p\bar{p})$	LHCb [865][a,b,c]	$0.0127 \pm 0.0013 \pm 0.0006$	0.0127 ± 0.0014
	Belle [861]	< 0.11	*0.0125 ± 0.0032*
	BABAR [866]	< 0.27	
$\mathcal{B}(B^0 \to p\bar{p}\pi^+\pi^-)$	LHCb [867][d,c]	$2.7 \pm 0.1 \pm 0.2$	2.7 ± 0.2
			2.9 ± 0.2
$\mathcal{B}(B^0 \to p\bar{p}\pi^+\pi^-), m_{\pi^+\pi^-} < 1.22$ GeV/c^2	Belle [857][e]	$0.83 \pm 0.17 \pm 0.17$	0.8 ± 0.2
			None
$\mathcal{B}(B^0 \to p\bar{p}K^+\pi^-)$	LHCb [867][d,c]	$5.9 \pm 0.3 \pm 0.5$	5.90 ± 0.58
			6.27 ± 0.52
$\mathcal{B}(B^0 \to p\bar{p}K^0)$	Belle [859][f]	$2.51^{+0.35}_{-0.29} \pm 0.21$	2.7 ± 0.3
	BABAR [525][g]	$3.0 \pm 0.5 \pm 0.3$	
$\mathcal{B}(B^0 \to \Theta(1540)^+\bar{p}) \times \mathcal{B}(\Theta(1540)^+ \to pK^0_S)$[h]	*BABAR* [525]	< 0.05	< 0.05
	Belle [756]	< 0.23	
$\mathcal{B}(B^0 \to f_J(2220)K^0) \times \mathcal{B}(f_J(2220) \to p\bar{p})$	*BABAR* [525]	< 0.45	< 0.45
$\mathcal{B}(B^0 \to p\bar{p}K^*(892)^0)$	Belle [859][f]	$1.18^{+0.29}_{-0.25} \pm 0.11$	1.24 ± 0.27
	BABAR [525][g]	$1.47 \pm 0.45 \pm 0.40$	*$1.24^{+0.28}_{-0.25}$*
$\mathcal{B}(B^0 \to f_J(2220)K^*(892)^0) \times \mathcal{B}(f_J(2220) \to p\bar{p})$	*BABAR* [525]	< 0.15	< 0.15

[a]Not included in PDG average.
[b]Run I and run II combination.
[c]Multiple systematic uncertainties are added in quadrature.
[d]$m_{p\bar{p}} < 2.85$ GeV/c^2.
[e]$0.46 < m_{\pi^+\pi^-} < 0.53$ GeV/c^2 invariant mass region has been excluded.
[f]The charmonium mass region has been vetoed.
[g]Charmonium decays to $p\bar{p}$ have been statistically subtracted.
[h]Pentaquark candidate.

TABLE 170. Branching fractions of charmless baryonic B^0 decays (part 2).

Parameter [10^{-6}]	Measurements		Average$^{\text{HFLAV}}_{PDG}$
$\mathcal{B}(B^0 \to p\bar{p}K^+K^-)$	LHCb [867][b,c]	$0.113 \pm 0.028 \pm 0.014$	0.113 ± 0.031
			0.121 ± 0.032
$\mathcal{B}(B^0 \to p\bar{p}\pi^0)$	Belle [868]	$0.50 \pm 0.18 \pm 0.06$	0.50 ± 0.19
$\mathcal{B}(B^0 \to pp\bar{p}\,\bar{p})$	*BABAR* [869]	< 0.2	< 0.2
$\mathcal{B}(B^0 \to p\bar{\Lambda}^0\pi^-)$	Belle [870][a]	$3.21^{+0.28}_{-0.25} \pm 0.16$	3.16 ± 0.24
	BABAR [871]	$3.07 \pm 0.31 \pm 0.23$	*$3.14^{+0.29}_{-0.28}$*
$\mathcal{B}(B^0 \to p\bar{\Sigma}(1385)^-)$	Belle [862]	< 0.26	< 0.26
$\mathcal{B}(B^0 \to \Delta(1232)^+\bar{p}+\text{c.c.})$	Belle [868]	< 1.6	< 1.6
$\mathcal{B}(B^0 \to \Delta(1232)^0\bar{\Lambda}^0)$	Belle [862]	< 0.93	< 0.93
$\mathcal{B}(B^0 \to p\bar{\Lambda}^0K^-)$	Belle [872]	< 0.82	< 0.82

(Table continued)

TABLE 170. *(Continued)*

Parameter [10^{-6}]	Measurements		Average$^{\text{HFLAV}}_{PDG}$
$\mathcal{B}(B^0 \to p\bar{\Sigma}^0\pi^-)$	Belle [870][a]	$1.17^{+0.43}_{-0.40} \pm 0.07$	1.17 ± 0.42 *< 3.80*
$\mathcal{B}(B^0 \to \bar{\Lambda}^0\Lambda^0)$	Belle [861]	< 0.32	< 0.32
$\mathcal{B}(B^0 \to \bar{\Lambda}^0\Lambda^0 K^0)$	Belle [482][d]	$4.76^{+0.84}_{-0.68} \pm 0.61$	$4.8^{+1.0}_{-0.9}$
$\mathcal{B}(B^0 \to \Lambda^0\bar{\Lambda}^0 K^*(892)^0)$	Belle [482][d]	$2.46^{+0.87}_{-0.72} \pm 0.34$	$2.46^{+0.93}_{-0.80}$
$\mathcal{B}(B^0 \to \Delta(1232)^0\bar{\Delta}(1232)^0)$	CLEO [788][e]	< 1500	< 1500
$\mathcal{B}(B^0 \to \Delta^{++}\bar{\Delta}^{--})$	CLEO [788][e]	< 110	< 110
$\mathcal{B}(B^0 \to p\bar{p}p\bar{p})$	LHCb [873][f]		$0.0222^{+0.0040}_{-0.0039}$ *None*

[a]Not included in PDG average.
[b]$m_{p\bar{p}} < 2.85$ GeV/c^2.
[c]Multiple systematic uncertainties are added in quadrature.
[d]The charmonium mass regions are vetoed.
[e]CLEO assumes $\mathcal{B}(\Upsilon(4S) \to B^0\bar{B}^0) = 0.43$. The result has been modified to account for a branching fraction of 0.50.
[f]Measurement of $\mathcal{B}(B^0 \to p\bar{p}p\bar{p})/(\mathcal{B}(B^0 \to J/\psi K^*(892)^0)\mathcal{B}(J/\psi \to p\bar{p})\mathcal{B}(K^*(892)^0 \to K\pi) \times 2/3)$ used in our fit.

TABLE 171. Baryonic relative branching fractions.

Parameter	Measurements		Average
$\frac{\mathcal{B}(B^+ \to p\bar{p}\pi^+, m_{p\bar{p}} < 2.85\ \text{GeV/c}^2)}{\mathcal{B}(B^+ \to J/\psi\pi^+) \times \mathcal{B}(J/\psi \to p\bar{p})}$	LHCb [856]	$12.0 \pm 1.2 \pm 0.3$	12.0 ± 1.2
$\frac{\mathcal{B}(B^+ \to p\bar{p}K^+)}{\mathcal{B}(B^+ \to J/\psi K^+) \times \mathcal{B}(J/\psi \to p\bar{p})}$	LHCb [616][a]	$4.91 \pm 0.19 \pm 0.14$	4.91 ± 0.24
$\frac{\mathcal{B}(B^+ \to p\bar{p}K^+, m_{p\bar{p}} < 2.85\ \text{GeV/c}^2)}{\mathcal{B}(B^+ \to J/\psi\pi^+) \times \mathcal{B}(J/\psi \to p\bar{p})}$	LHCb [616]	$2.02 \pm 0.10 \pm 0.08$	2.02 ± 0.13
$\frac{\mathcal{B}(B^+ \to \bar{\Lambda}(1520)p) \times \mathcal{B}(\bar{\Lambda}(1520) \to K^+\bar{p}))}{\mathcal{B}(B^+ \to J/\psi\pi^+) \times \mathcal{B}(J/\psi \to p\bar{p})}$	LHCb [856]	$0.033 \pm 0.005 \pm 0.007$	0.033 ± 0.009
$\frac{\mathcal{B}(B^0 \to p\bar{p}K^+K^-)}{\mathcal{B}(B^0 \to p\bar{p}K^+\pi^-)}$	LHCb [867][b]	$0.019 \pm 0.005 \pm 0.002$	0.019 ± 0.005
$\frac{\mathcal{B}(B^0 \to p\bar{p}\pi^+\pi^-)}{\mathcal{B}(B^0 \to p\bar{p}K^+\pi^-)}$	LHCb [867][b]	$0.46 \pm 0.02 \pm 0.02$	0.46 ± 0.03
$\frac{\mathcal{B}(B^0 \to p\bar{p}p\bar{p})}{\mathcal{B}(B^0 \to J/\psi K^{*0})\mathcal{B}(J/\psi \to p\bar{p})\mathcal{B}(K^{*0} \to K^+\pi^-)}$	LHCb [873]	$0.0124 \pm 0.0021 \pm 0.0004$	0.0124 ± 0.0021
$\frac{\mathcal{B}(B^0 \to p\bar{p}p\bar{p})}{\mathcal{B}(B^0 \to J/\psi\phi)\mathcal{B}(J/\psi \to p\bar{p})\mathcal{B}(\phi \to K^+K^-)}$	LHCb [873]	$0.021 \pm 0.009 \pm 0.002$	0.0210 ± 0.0092

[a]Includes contribution where $p\bar{p}$ is produced in charmonium decays.
[b]$m_{p\bar{p}} < 2.85$ GeV/c^2.

Measurements that are not included in the tables:

(i) In Ref. [853], Belle searches for B^0 mesons decaying into a final state containing a Λ baryon and missing energy. Upper limits on the branching fractions are set in the range $2.1 - 3.8 \times 10^{-5}$.

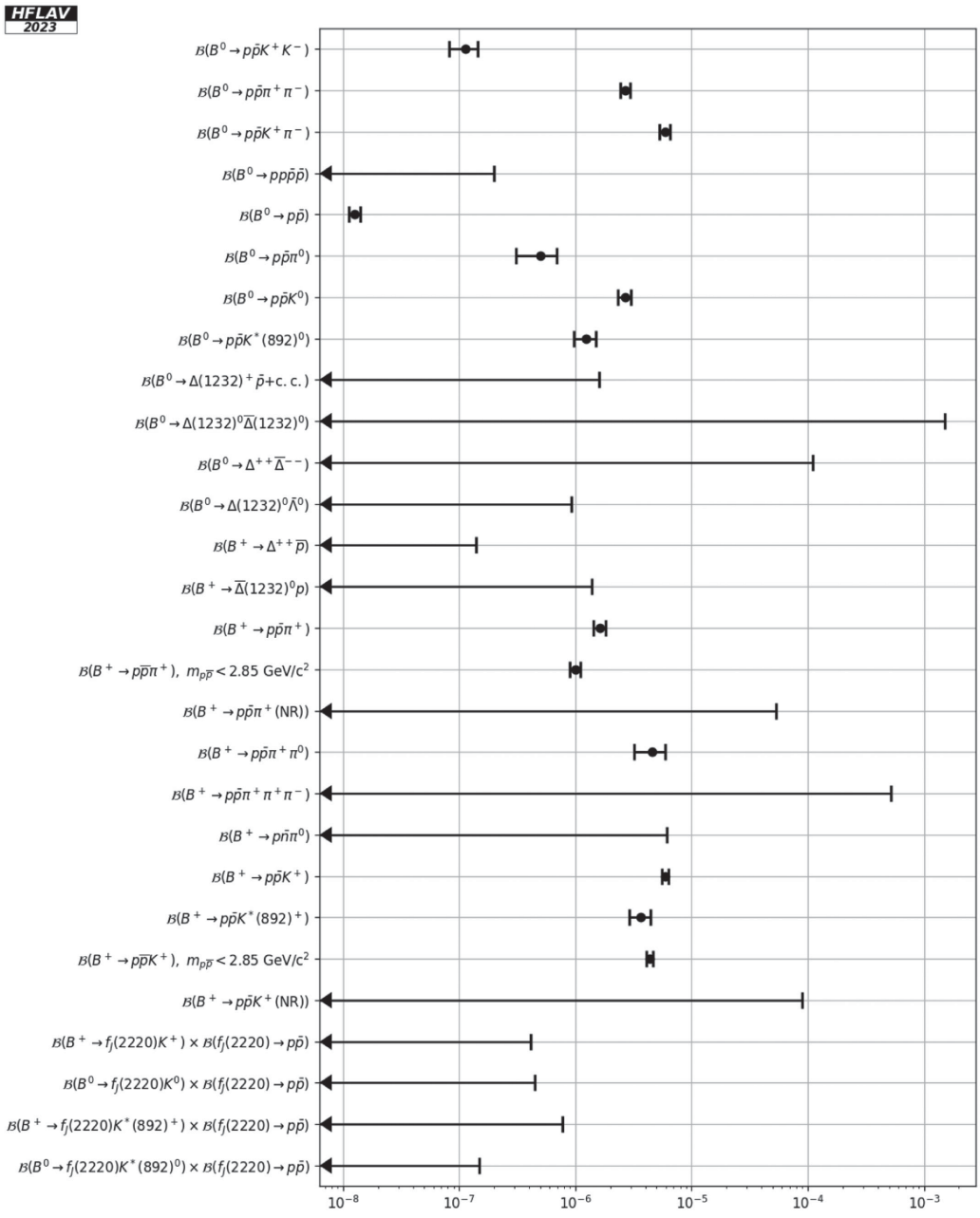


FIG. 30. Branching fractions of charmless B^+ and B^0 decays into nonstrange baryons.

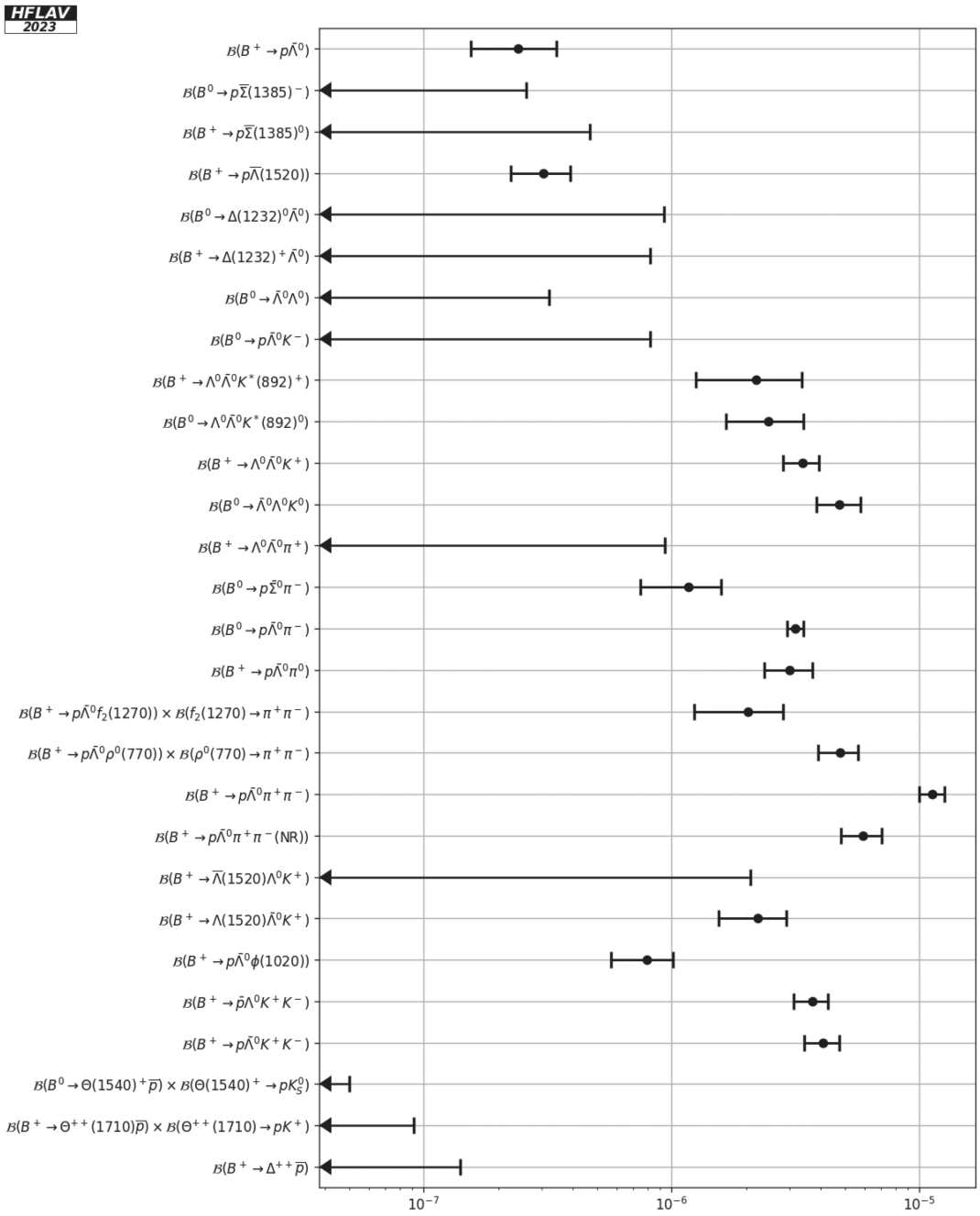


FIG. 31. Branching fractions of charmless B^+ and B^0 decays into strange baryons.

C. Decays of b baryons

A compilation of branching fractions of Λ_b^0 baryon decays is given in Tables 172–174. Table 175 provides the partial branching fractions of $\Lambda_b^0 \to \Lambda\mu^+\mu^-$ decays in intervals of $q^2 = m^2(\mu^+\mu^-)$. Compilations of branching fractions of Ξ_b^0, Ξ_b^- and Ω_b^- baryon decays are given in Tables 176, 177, and 178, respectively. Finally, ratios of branching fractions of Λ_b^0, Ξ_b^0, Ξ_b^- and Ω_b^- baryon decays are detailed in Tables 179–183. Figure 32 shows a graphic representation of branching fractions of Λ_b^0 decays.

Measurements that are not included in the tables:

(i) In Ref. [874], LHCb measures angular observables of the decay $\Lambda_b^0 \to \Lambda\mu^+\mu^-$, including the lepton-side, hadron-side and combined forward-backward asymmetries of the decay in the low recoil region $15 < m^2(\ell\ell) < 20\ \mathrm{GeV}^2/\mathrm{c}^4$.

(ii) In Ref. [875], LHCb performs a search for baryon-number-violating Ξ_b^0 oscillations and set an upper limit of $\omega < 0.08\ \mathrm{ps}^{-1}$ on the oscillation rate.

(iii) In Ref. [876], LHCb measures the photon polarization in $\Lambda_b \to \Lambda\gamma$ decays to be $\alpha_\gamma = 0.82^{+0.17+0.04}_{-0.26-0.13}$.

TABLE 172. Branching fractions of charmless Λ_b^0 decays (part 1).

Parameter [10^{-6}]	Measurements		Average$^{\text{HFLAV}}_{PDG}$
$\mathcal{B}(\Lambda_b^0 \to p\bar{K}^0\pi^-)$	LHCb [806][a,b]	$12.4 \pm 2.0 \pm 3.6$	12.4 ± 4.2 *12.6 ± 4.1*
$\mathcal{B}(\Lambda_b^0 \to pK^0K^-)$	LHCb [806][b]	< 3.5	< 3.5
$\mathcal{B}(\Lambda_b^0 \to p\pi^-)$[c]	LHCb [793][d] CDF [790][e]	$4.76 \pm 0.44 \pm 0.95$	$4.6^{+0.9}_{-0.8}$ *4.5 ± 0.8*
$\mathcal{B}(\Lambda_b^0 \to pK^-)$[c]	CDF [790] LHCb [793][f]	$6.3 \pm 1.2 \pm 0.8$	5.5 ± 1.1 *5.4 ± 1.0*
$\mathcal{B}(\Lambda_b^0 \to \Lambda^0\mu^+\mu^-)$	LHCb [877][a,g] CDF [878][g]	$0.955 \pm 0.186 \pm 0.248$ $1.520 \pm 0.366 \pm 0.386$	$1.09^{+0.34}_{-0.29}$ *1.08 ± 0.28*
$\mathcal{B}(\Lambda_b^0 \to p\pi^-\mu^+\mu^-)$	LHCb [879][h]		$0.068^{+0.027}_{-0.023}$ *$0.069^{+0.025}_{-0.024}$*
$\mathcal{B}(\Lambda_b^0 \to pK^-e^+e^-)$	LHCb [880][i,j]	$0.314^{+0.045+0.064}_{-0.042-0.055}$	$0.31^{+0.08}_{-0.07}$ *$0.31^{+0.07}_{-0.06}$*
$\mathcal{B}(\Lambda_b^0 \to pK^-\mu^+\mu^-)$	LHCb [880][i,j]	$0.269 \pm 0.013^{+0.052}_{-0.044}$	$0.269^{+0.054}_{-0.045}$ *$0.265^{+0.051}_{-0.041}$*

[a]Multiple systematic uncertainties are added in quadrature.
[b]Using $\mathcal{B}(B^0 \to K^0\pi^+\pi^-)$.
[c]The PDG average is a result of a fit including input from other measurements.
[d]Using $\mathcal{B}(\Lambda_b^0 \to pK^-)$.
[e]Measurement of $(\mathcal{B}(\Lambda_b^0 \to p\pi^-)/\mathcal{B}(B^0 \to K^+\pi^-))(f_{\Lambda_b^0}/f_d)$ used in our fit.
[f]Measurement of $\mathcal{B}(\Lambda_b^0 \to p\pi^-)/\mathcal{B}(\Lambda_b^0 \to pK^-)$ used in our fit.
[g]Using $\mathcal{B}(\Lambda_b^0 \to J/\psi\Lambda^0)$.
[h]Measurement of $\mathcal{B}(\Lambda_b^0 \to p\pi^-\mu^+\mu^-)/(\mathcal{B}(\Lambda_b^0 \to J/\psi p\pi^-)\mathcal{B}(J/\psi \to \mu^+\mu^-))$ used in our fit.
[i]Measured in the $m^2_{\ell^+\ell^-}$ bin $[0.1, 6.0]$ GeV^2/c^4 and for $m_{pK} < 2.6$ GeV/c^2.
[j]Using $\mathcal{B}(\Lambda_b^0 \to J/\psi pK^-)$.

TABLE 173. Branching fractions of charmless Λ_b^0 decays (part 2).

Parameter [10^{-6}]	Measurements		Average$^{\text{HFLAV}}_{PDG}$
$\mathcal{B}(\Lambda_b^0 \to \Lambda^0\gamma)$	LHCb [881][a]		6.9 ± 1.5 *7.1 ± 1.7*
$\mathcal{B}(\Lambda_b^0 \to \Lambda^0\eta)$	LHCb [796][b]	$9.23^{+7.15}_{-5.20} \pm 0.40$	$9.2^{+7.2}_{-5.2}$ *$9.4^{+7.3}_{-5.3}$*
$\mathcal{B}(\Lambda_b^0 \to \Lambda^0\eta')$	LHCb [796][b]	< 3.05	< 3.1
$\mathcal{B}(\Lambda_b^0 \to \Lambda^0\pi^+\pi^-)$	LHCb [882][c]		$4.7^{+2.0}_{-1.9}$ *4.6 ± 1.9*
$\mathcal{B}(\Lambda_b^0 \to \Lambda^0K^+\pi^-)$	LHCb [882][d]		$5.7^{+1.3}_{-1.2}$ *5.6 ± 1.2*

(Table continued)

TABLE 173. *(Continued)*

Parameter [10^{-6}]	Measurements	Average$^{\text{HFLAV}}_{PDG}$
$\mathcal{B}(\Lambda_b^0 \to \Lambda^0 K^+ K^-)$	LHCb [882][e]	$16.1^{+2.4}_{-2.2}$ *16.0 ± 2.2*
$\mathcal{B}(\Lambda_b^0 \to \Lambda^0 \phi(1020))$	LHCb [820][f]	$10.0^{+2.9}_{-2.4}$ *9.8 ± 2.6*

[a]Measurement of $(\mathcal{B}(\Lambda_b^0 \to \Lambda^0\gamma)/\mathcal{B}(B^0 \to K^*(892)^0\gamma))\frac{f_{\Lambda_b^0}}{f_d}$ used in our fit.
[b]Using $\mathcal{B}(B^0 \to \eta' K^0)$.
[c]Measurement of $\mathcal{B}(\Lambda_b^0 \to \Lambda^0\pi^+\pi^-)/(\mathcal{B}(\Lambda_b^0 \to \Lambda_c^+\pi^-)\mathcal{B}(\Lambda_c^+ \to \Lambda^0\pi^+))$ used in our fit.
[d]Measurement of $\mathcal{B}(\Lambda_b^0 \to \Lambda^0 K^+\pi^-)/(\mathcal{B}(\Lambda_b^0 \to \Lambda_c^+\pi^-)\mathcal{B}(\Lambda_c^+ \to \Lambda^0\pi^+))$ used in our fit.
[e]Measurement of $\mathcal{B}(\Lambda_b^0 \to \Lambda^0 K^+ K^-)/(\mathcal{B}(\Lambda_b^0 \to \Lambda_c^+\pi^-)\mathcal{B}(\Lambda_c^+ \to \Lambda^0\pi^+))$ used in our fit.
[f]Measurement of $(\mathcal{B}(\Lambda_b^0 \to \Lambda^0\phi(1020))/\mathcal{B}(B^0 \to \phi(1020)K^0) \times 2)(f_{\Lambda_b^0}/f_d)$ used in our fit.

TABLE 174. Branching fractions of charmless Λ_b^0 decays (part 3).

Parameter [10^{-6}]	Measurements	Average$^{\text{HFLAV}}_{PDG}$
$\mathcal{B}(\Lambda_b^0 \to p\pi^+\pi^-\pi^-)$	LHCb [883][a,b,c]	$21.1^{+2.4}_{-2.3}$ *20.9 ± 2.1*
$\mathcal{B}(\Lambda_b^0 \to pK^-K^+\pi^-)$	LHCb [883][b,d]	$4.06^{+0.66}_{-0.61}$ *4.03 ± 0.60*
$\mathcal{B}(\Lambda_b^0 \to pK^-\pi^+\pi^-)$	LHCb [883][b,e]	$50.5^{+5.6}_{-5.3}$ *50.0 ± 4.9*
$\mathcal{B}(\Lambda_b^0 \to pK^-K^+K^-)$	LHCb [883][b,f]	$12.6^{+1.5}_{-1.4}$ *12.5 ± 1.3*

[a]Vetoes on charm and charmonium resonances are applied.
[b]Multiple systematic uncertainties are added in quadrature.
[c]Measurement of $\mathcal{B}(\Lambda_b^0 \to p\pi^+\pi^-\pi^-)/(\mathcal{B}(\Lambda_b^0 \to \Lambda_c^+\pi^-)\mathcal{B}(\Lambda_c^+ \to pK^-\pi^+))$ used in our fit.
[d]Measurement of $\mathcal{B}(\Lambda_b^0 \to pK^-K^+\pi^-)/(\mathcal{B}(\Lambda_b^0 \to \Lambda_c^+\pi^-)\mathcal{B}(\Lambda_c^+ \to pK^-\pi^+))$ used in our fit.
[e]Measurement of $\mathcal{B}(\Lambda_b^0 \to pK^-\pi^+\pi^-)/(\mathcal{B}(\Lambda_b^0 \to \Lambda_c^+\pi^-)\mathcal{B}(\Lambda_c^+ \to pK^-\pi^+))$ used in our fit.
[f]Measurement of $\mathcal{B}(\Lambda_b^0 \to pK^-K^+K^-)/(\mathcal{B}(\Lambda_b^0 \to \Lambda_c^+\pi^-)\mathcal{B}(\Lambda_c^+ \to pK^-\pi^+))$ used in our fit.

TABLE 175. Partial branching fractions of $\Lambda_b^0 \to \Lambda\mu^+\mu^-$ decays in intervals of $m^2_{\mu^+\mu^-}$.

Parameter $[10^{-7}]$	Measurements		Average$^{\text{HFLAV}}_{PDG}$
$m^2_{\mu^+\mu^-} < 2.0\ \text{GeV}^2/c^4$	LHCb [884]	$0.72^{+0.24}_{-0.22} \pm 0.14$	0.7 ± 0.3
	CDF [878]	$0.15 \pm 2.01 \pm 0.05$	
$2.0 < m^2_{\mu^+\mu^-} < 4.3\ \text{GeV}^2/c^4$	LHCb [884]	$0.253^{+0.276}_{-0.207} \pm 0.046$	$0.3^{+0.3}_{-0.2}$
	CDF [878]	$1.84 \pm 1.66 \pm 0.59$	
$4.3 < m^2_{\mu^+\mu^-} < 8.68\ \text{GeV}^2/c^4$	LHCb [877]	$0.66 \pm 0.72 \pm 0.16$	0.5 ± 0.7
	CDF [878]	$-0.20 \pm 1.64 \pm 0.08$	
$10.09 < m^2_{\mu^+\mu^-} < 12.86\ \text{GeV}^2/c^4$	LHCb [884]	$2.08^{+0.42}_{-0.39} \pm 0.42$	2.2 ± 0.6
	CDF [878]	$2.97 \pm 1.47 \pm 0.95$	$2.2^{+0.6}_{-0.5}$
$14.18 < m^2_{\mu^+\mu^-} < 16.00\ \text{GeV}^2/c^4$	LHCb [884]	$2.04^{+0.35}_{-0.33} \pm 0.42$	1.7 ± 0.4
	CDF [878]	$0.96 \pm 0.73 \pm 0.31$	1.7 ± 0.5
$m^2_{\mu^+\mu^-} > 16.00\ \text{GeV}^2/c^4$	CDF [878]	$6.97 \pm 1.88 \pm 2.23$	7.0 ± 2.9

TABLE 176. Branching fractions of charmless Ξ_b^0 decays.

Parameter $[10^{-6}]$	Measurements		Average$^{\text{HFLAV}}_{PDG}$
$\frac{f_{\Xi_b^0}}{f_d}\mathcal{B}(\Xi_b^0 \to p\bar{K}^0\pi^-)$	LHCb [806][a]	< 1.5	< 1.5
			< 1.6
$\frac{f_{\Xi_b^0}}{f_d}\mathcal{B}(\Xi_b^0 \to p\bar{K}^0K^-)$	LHCb [806][a]	< 1.0	< 0.99
			< 1.10
$\frac{f_{\Xi_b^0}}{f_{\Lambda_b^0}}\mathcal{B}(\Xi_b^0 \to \Lambda\pi^+\pi^-)$	LHCb [882]	< 1.7	< 1.7
$\frac{f_{\Xi_b^0}}{f_{\Lambda_b^0}}\mathcal{B}(\Xi_b^0 \to \Lambda K^-\pi^+)$	LHCb [882]	< 0.8	< 0.8
$\frac{f_{\Xi_b^0}}{f_{\Lambda_b^0}}\mathcal{B}(\Xi_b^0 \to \Lambda K^+K^-)$	LHCb [882]	< 0.3	< 0.3
$\frac{f_{\Xi_b^0}}{f_{\Lambda_b^0}}\mathcal{B}(\Xi_b^0 \to pK^-\pi^+\pi^-)$	LHCb [883][b,c]		$1.91^{+0.41}_{-0.38}$
			1.89 ± 0.39
$\frac{f_{\Xi_b^0}}{f_{\Lambda_b^0}}\mathcal{B}(\Xi_b^0 \to pK^-K^-\pi^+)$	LHCb [883][b,d]		$1.72^{+0.33}_{-0.30}$
			1.71 ± 0.31
$\frac{f_{\Xi_b^0}}{f_{\Lambda_b^0}}\mathcal{B}(\Xi_b^0 \to pK^+K^-K^-)$	LHCb [883][b,e]		0.18 ± 0.10
			0.17 ± 0.10

[a]Using $\mathcal{B}(B^0 \to K^0\pi^+\pi^-)$.

[b]Multiple systematic uncertainties are added in quadrature.

[c]Measurement of $\frac{f_{\Xi_b^0}}{f_{\Lambda_b^0}}\mathcal{B}(\Xi_b^0 \to pK^-\pi^+\pi^-)/(\mathcal{B}(\Lambda_b^0 \to \Lambda_c^+\pi^-)\mathcal{B}(\Lambda_c^+ \to pK^-\pi^+))$ used in our fit.

[d]Measurement of $\frac{f_{\Xi_b^0}}{f_{\Lambda_b^0}}\mathcal{B}(\Xi_b^0 \to pK^-K^-\pi^+)/(\mathcal{B}(\Lambda_b^0 \to \Lambda_c^+\pi^-)\mathcal{B}(\Lambda_c^+ \to pK^-\pi^+))$ used in our fit.

[e]Measurement of $\frac{f_{\Xi_b^0}}{f_{\Lambda_b^0}}\mathcal{B}(\Xi_b^0 \to pK^+K^-K^-)/(\mathcal{B}(\Lambda_b^0 \to \Lambda_c^+\pi^-)\mathcal{B}(\Lambda_c^+ \to pK^-\pi^+))$ used in our fit.

TABLE 177. Branching fractions of charmless Ξ_b^- decays.

Parameter [10^{-6}]	Measurements		Average$^{\text{HFLAV}}_{PDG}$
$\mathcal{B}(\Xi_b^- \to \Sigma(1385)^0 K^-)$	LHCb [885][a,b]	$0.26 \pm 0.11 \pm 0.20$	0.26 ± 0.23 *None*
$\mathcal{B}(\Xi_b^- \to \Lambda(1405) K^-)$	LHCb [885][a,b]	$0.19 \pm 0.06 \pm 0.10$	0.19 ± 0.12 *None*
$\mathcal{B}(\Xi_b^- \to \Lambda(1520) K^-)$	LHCb [885][a,b]	$0.76 \pm 0.09 \pm 0.31$	0.76 ± 0.32 *None*
$\mathcal{B}(\Xi_b^- \to \Lambda(1670) K^-)$	LHCb [885][a,b]	$0.45 \pm 0.07 \pm 0.22$	0.45 ± 0.23 *None*
$\mathcal{B}(\Xi_b^- \to \Sigma(1775) K^-)$	LHCb [885][a,b]	$0.22 \pm 0.08 \pm 0.13$	0.22 ± 0.15 *None*
$\mathcal{B}(\Xi_b^- \to \Sigma(1915) K^-)$	LHCb [885][a,b]	$0.26 \pm 0.09 \pm 0.23$	0.26 ± 0.25 *None*

[a]Result extracted from Dalitz plot analysis of $\Xi_b^- \to pK^-K^-$.
[b]Multiple systematic uncertainties are added in quadrature.

TABLE 178. Branching fractions of charmless Ω_b^- decays.

Parameter [10^{-8}]	Measurements		Average
$\frac{f_{\Omega_b^-}}{f_u} \times \mathcal{B}(\Omega_b^- \to pK^-K^-)$	LHCb [759][a]	< 0.61	< 0.61
$\frac{f_{\Omega_b^-}}{f_u} \times \mathcal{B}(\Omega_b^- \to pK^-\pi^-)$	LHCb [759][a]	< 1.73	< 1.7
$\frac{f_{\Omega_b^-}}{f_u} \times \mathcal{B}(\Omega_b^- \to p\pi^-\pi^-)$	LHCb [759][a]	< 3.69	< 3.7

[a]Using $\mathcal{B}(B^+ \to K^+K^+K^-)$.

TABLE 179. Relative branching fractions of Λ_b^0 decays (part 1).

Parameter	Measurements		Average
$\frac{\mathcal{B}(\Lambda_b^0 \to p\pi^-)}{\mathcal{B}(\Lambda_b^0 \to pK^-)}$	LHCb [793]	$0.86 \pm 0.08 \pm 0.05$	0.86 ± 0.09
$\frac{\mathcal{B}(\Lambda_b^0 \to \Lambda^0\eta)}{\mathcal{B}(B^0 \to \eta' K^0)}$	LHCb [796]	$0.142^{+0.110}_{-0.080}$	$0.14^{+0.11}_{-0.08}$
$\frac{f_{\Lambda_b^0}}{f_d}\frac{\mathcal{B}(\Lambda_b^0 \to p\pi^-)}{\mathcal{B}(B^0 \to K^+\pi^-)}$	CDF [790]	$0.042 \pm 0.007 \pm 0.006$	0.042 ± 0.009
$\frac{f_{\Lambda_b^0}}{f_d}\frac{\mathcal{B}(\Lambda_b^0 \to pK^-)}{\mathcal{B}(B^0 \to K^+\pi^-)}$	CDF [790]	$0.066 \pm 0.009 \pm 0.008$	0.066 ± 0.012
$\frac{f_{\Lambda_b^0}}{f_d}\frac{\mathcal{B}(\Lambda_b^0 \to \Lambda^0\phi)}{\mathcal{B}(B^0 \to K_S^0\phi)}$	LHCb [820]	$0.55 \pm 0.11 \pm 0.04$	0.55 ± 0.12
$\frac{\mathcal{B}(\Lambda_b^0 \to p\pi^-\mu^+\mu^-)}{\mathcal{B}(\Lambda_b^0 \to J/\psi p\pi^-) \times \mathcal{B}(J/\psi \to \mu^+\mu^-)}$	LHCb [879]	$0.044 \pm 0.012 \pm 0.007$	0.044 ± 0.014
$\frac{\mathcal{B}(\Lambda_b^0 \to \Lambda^0\pi^+\pi^-)}{\mathcal{B}(\Lambda_b^0 \to \Lambda_c^+\pi^-) \times \mathcal{B}(\Lambda_c^+ \to \Lambda^0\pi^+)}$	LHCb [882]	$0.073 \pm 0.019 \pm 0.022$	0.073 ± 0.029
$\frac{\mathcal{B}(\Lambda_b^0 \to \Lambda^0 K^+\pi^-)}{\mathcal{B}(\Lambda_b^0 \to \Lambda_c^+\pi^-) \times \mathcal{B}(\Lambda_c^+ \to \Lambda^0\pi^+)}$	LHCb [882]	$0.089 \pm 0.012 \pm 0.013$	0.089 ± 0.018
$\frac{\mathcal{B}(\Lambda_b^0 \to \Lambda^0 K^+K^-)}{\mathcal{B}(\Lambda_b^0 \to \Lambda_c^+\pi^-) \times \mathcal{B}(\Lambda_c^+ \to \Lambda^0\pi^+)}$	LHCb [882]	$0.253 \pm 0.019 \pm 0.019$	0.253 ± 0.027

TABLE 180. Relative branching fractions of Λ_b^0 decays (part 2).

Parameter	Measurements		Average
$\frac{\mathcal{B}(\Lambda_b^0 \to p\pi^-\pi^+\pi^-)}{\mathcal{B}(\Lambda_b^0 \to \Lambda_c^+\pi^-)\times\mathcal{B}(\Lambda_c^+ \to pK^-\pi^+)}$	LHCb [883][a]	$0.0685 \pm 0.0019 \pm 0.0033$	0.0685 ± 0.0038
$\frac{\mathcal{B}(\Lambda_b^0 \to pK^-\pi^+\pi^-)}{\mathcal{B}(\Lambda_b^0 \to \Lambda_c^+\pi^-)\times\mathcal{B}(\Lambda_c^+ \to pK^-\pi^+)}$	LHCb [883][a]	$0.164 \pm 0.003 \pm 0.007$	0.164 ± 0.008
$\frac{\mathcal{B}(\Lambda_b^0 \to pK^-K^+\pi^-)}{\mathcal{B}(\Lambda_b^0 \to \Lambda_c^+\pi^-)\times\mathcal{B}(\Lambda_c^+ \to pK^-\pi^+)}$	LHCb [883][a]	$0.0132 \pm 0.0009 \pm 0.0013$	0.0132 ± 0.0016
$\frac{\mathcal{B}(\Lambda_b^0 \to pK^-K^+K^-)}{\mathcal{B}(\Lambda_b^0 \to \Lambda_c^+\pi^-)\times\mathcal{B}(\Lambda_c^+ \to pK^-\pi^+)}$	LHCb [883][a]	$0.0411 \pm 0.0012 \pm 0.0020$	0.0411 ± 0.0023
$\frac{\mathcal{B}(\Lambda_b^0 \to p\bar{K}^0\pi^-)}{\mathcal{B}(B^0 \to K^0\pi^+\pi^-)}$	LHCb [806][a]	$0.25 \pm 0.04 \pm 0.07$	0.25 ± 0.08
$\frac{\mathcal{B}(\Lambda_b^0 \to p\bar{K}^0K^-)}{\mathcal{B}(B^0 \to K^0\pi^+\pi^-)}$	LHCb [806]	< 0.07	< 0.07
$\frac{\mathcal{B}(\Lambda_b^0 \to \Lambda^0\mu^+\mu^-)}{\mathcal{B}(\Lambda_b^0 \to J/\psi\Lambda^0)}$	LHCb [877][a]	$0.00154 \pm 0.00030 \pm 0.00020$	0.00154 ± 0.00036
$\frac{\mathcal{B}(\Lambda_b^0 \to pK^-e^+e^-)}{\mathcal{B}(\Lambda_b^0 \to J/\psi pK^-)}$	LHCb [880][b]	$0.00098^{+0.00014}_{-0.00013} \pm 0.00008$	0.00098 ± 0.00016
$\frac{\mathcal{B}(\Lambda_b^0 \to pK^-\mu^+\mu^-)}{\mathcal{B}(\Lambda_b^0 \to J/\psi pK^-)}$	LHCb [880][b]	$0.00084 \pm 0.00004 \pm 0.00004$	0.000840 ± 0.000057
$\frac{\mathcal{B}(\Lambda_b^0 \to pK^-e^+e^-)}{\mathcal{B}(\Lambda_b^0 \to pK^-\mu^+\mu^-)}$	LHCb [880][b]	$1.17^{+0.18}_{-0.16} \pm 0.07$	$1.17^{+0.19}_{-0.17}$

[a]Multiple systematic uncertainties are added in quadrature.

[b]Measured in the $m^2_{\ell^+\ell^-}$ bin $[0.1, 6.0]$ GeV^2/c^4 and for $m_{pK} < 2.6$ GeV/c^2.

TABLE 181. Relative branching fractions of Ξ_b^0 decays.

Parameter $[10^{-2}]$	Measurements		Average
$\frac{f_{\Xi_b^0}}{f_d} \times \frac{\mathcal{B}(\Xi_b^0 \to p\overline{K^0}\pi^-)}{\mathcal{B}(B^0 \to K^0\pi^+\pi^-)}$	LHCb [806]	< 3	< 3.0
$\frac{f_{\Xi_b^0}}{f_d} \times \frac{\mathcal{B}(\Xi_b^0 \to p\overline{K^0}K^-)}{\mathcal{B}(B^0 \to K^0\pi^+\pi^-)}$	LHCb [806]	< 2	< 2.0
$\frac{f_{\Xi_b^0}}{f_{\Lambda_b^0}} \times \frac{\mathcal{B}(\Xi_b^0 \to pK^-K^+K^-)}{\mathcal{B}(\Lambda_b^0 \to \Lambda_c^+\pi^-)\times\mathcal{B}(\Lambda_c^+ \to pK^-\pi^+)}$	LHCb [883][a]	$0.057 \pm 0.028 \pm 0.013$	0.057 ± 0.031
$\frac{f_{\Xi_b^0}}{f_{\Lambda_b^0}} \times \frac{\mathcal{B}(\Xi_b^0 \to pK^-\pi^+\pi^-)}{\mathcal{B}(\Lambda_b^0 \to \Lambda_c^+\pi^-)\times\mathcal{B}(\Lambda_c^+ \to pK^-\pi^+)}$	LHCb [883][a]	$0.62 \pm 0.08 \pm 0.08$	0.62 ± 0.11
$\frac{f_{\Xi_b^0}}{f_{\Lambda_b^0}} \times \frac{\mathcal{B}(\Xi_b^0 \to pK^-\pi^+K^-)}{\mathcal{B}(\Lambda_b^0 \to \Lambda_c^+\pi^-)\times\mathcal{B}(\Lambda_c^+ \to pK^-\pi^+)}$	LHCb [883][a]	$0.56 \pm 0.06 \pm 0.06$	0.560 ± 0.088

[a]Multiple systematic uncertainties are added in quadrature.

TABLE 182. Relative branching fractions of Ξ_b^- decays.

Parameter $[10^{-2}]$	Measurements		Average
$\frac{f_{\Xi_b^-}}{f_u}\frac{\mathcal{B}(\Xi_b^-\to pK^-K^-)}{\mathcal{B}(B^-\to K^+K^-K^-)}$	LHCb [759]	$0.2650 \pm 0.0350 \pm 0.0470$	0.265 ± 0.059
$\frac{f_{\Xi_b^-}}{f_u}\frac{\mathcal{B}(\Xi_b^-\to p\pi^-\pi^-)}{\mathcal{B}(B^-\to K^+K^-K^-)}$	LHCb [759]	< 0.1470	< 0.15
$\frac{f_{\Xi_b^-}}{f_u}\frac{\mathcal{B}(\Xi_b^-\to pK^-\pi^-)}{\mathcal{B}(B^-\to K^+K^-K^-)}$	LHCb [759]	$0.2590 \pm 0.0640 \pm 0.0490$	0.259 ± 0.081
$\frac{\mathcal{B}(\Xi_b^-\to p\pi^-\pi^-)}{\mathcal{B}(\Xi_b^-\to pK^-K^-)}$	LHCb [759]	< 56	< 56
$\frac{\mathcal{B}(\Xi_b^-\to pK^-\pi^-)}{\mathcal{B}(\Xi_b^-\to pK^-K^-)}$	LHCb [759]	$98 \pm 27 \pm 9$	98 ± 28
$\frac{\mathcal{B}(\Xi_b^-\to \Xi^-\gamma)}{\mathcal{B}(\Xi_b^-\to \Xi^- J/\psi)}$	LHCb [886]	< 8	< 8.0

TABLE 183. Relative branching fractions of Ω_b^- decays.

Parameter $[10^{-3}]$	Measurements		Average
$\frac{f_{\Omega_b^-}}{f_u}\frac{\mathcal{B}(\Omega_b^-\to pK^-K^-)}{\mathcal{B}(B^-\to K^+K^-K^-)}$	LHCb [759]	< 0.180	< 0.18
$\frac{f_{\Omega_b^-}}{f_u}\frac{\mathcal{B}(\Omega_b^-\to p\pi^-\pi^-)}{\mathcal{B}(B^-\to K^+K^-K^-)}$	LHCb [759]	< 1.090	< 1.1
$\frac{f_{\Omega_b^-}}{f_u}\frac{\mathcal{B}(\Omega_b^-\to pK^-\pi^-)}{\mathcal{B}(B^-\to K^+K^-K^-)}$	LHCb [759]	< 0.510	< 0.51

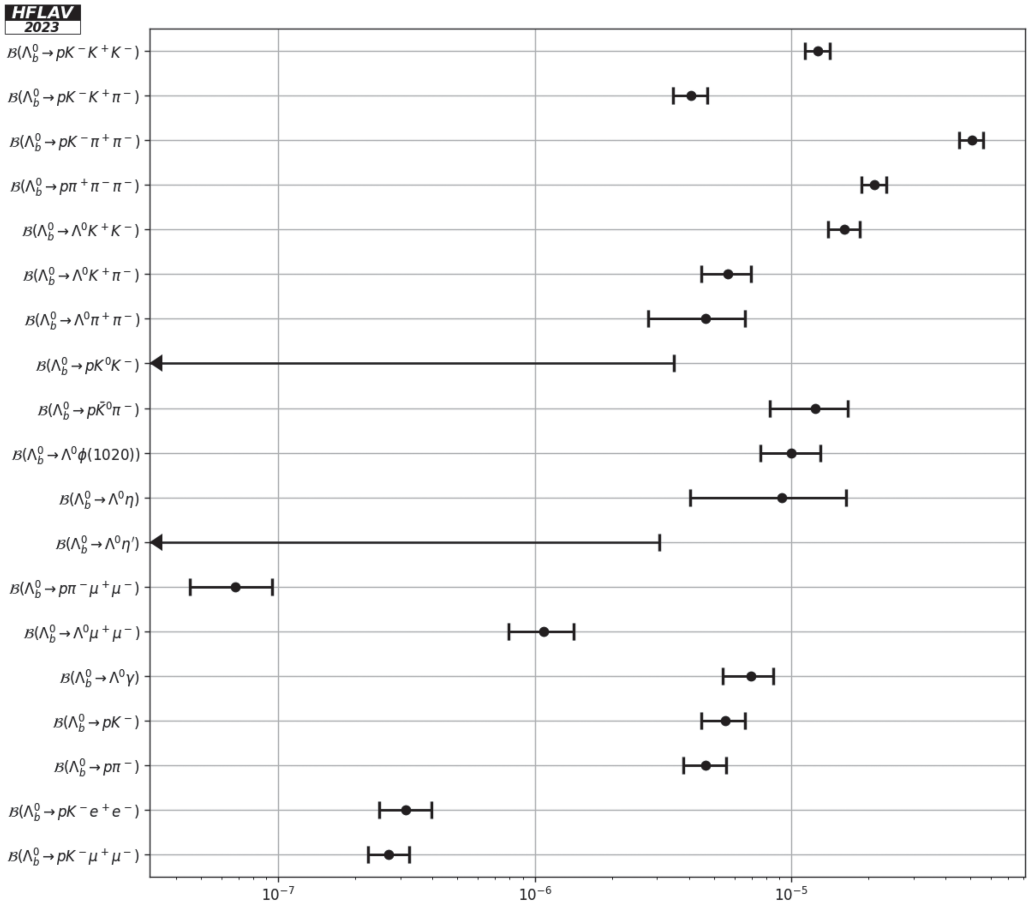


FIG. 32. Branching fractions of charmless Λ_b^0 decays.

D. Decays of B_s^0 mesons

Tables 184–189 and 190 to 191 detail branching fractions and relative branching fractions of B_s^0 meson decays, respectively. Figures 33 and 34 show graphic representations of a selection of results given in this section.

TABLE 184. Branching fractions of charmless B_s^0 decays (part 1).

Parameter [10^{-6}]	Measurements		Average$^{\text{HFLAV}}_{PDG}$
$\mathcal{B}(B_s^0 \to \pi^+\pi^-)$	Belle [887]	< 12	$0.74^{+0.12}_{-0.10}$
	CDF [792][b]		*0.70 ± 0.10*
	LHCb [794][b]		
$\mathcal{B}(B_s^0 \to \pi^0\pi^0)$	Belle [888][a]	< 7.7	< 7.7
			< 210.0
$\mathcal{B}(B_s^0 \to \eta\pi^0)$	L3 [889]	< 1000	< 1000
$\mathcal{B}(B_s^0 \to \eta\eta)$	Belle [890][a,c]	< 144	< 144
			< 143
$f_s \times \mathcal{B}(B_s^0 \to \eta\eta)$	Belle [890]	< 29	< 29
			None
$\mathcal{B}(B_s^0 \to \rho^0(770)\rho^0(770))$	SLD [891]	< 320	< 320
$\mathcal{B}(B_s^0 \to \eta'\eta')$	LHCb [713][d]	$32.4 \pm 6.2 \pm 3.0$	32 ± 7
			33 ± 7
$\mathcal{B}(B_s^0 \to \eta'\phi(1020))$	LHCb [892]	< 0.82	< 0.82
$\mathcal{B}(B_s^0 \to \phi(1020)f_0(980)) \times \mathcal{B}(f_0(980) \to \pi^+\pi^-)$	LHCb [839][e]	$1.12 \pm 0.16 \pm 0.14$	1.12 ± 0.21
$\mathcal{B}(B_s^0 \to f_2(1270)\phi(1020)) \times \mathcal{B}(f_2(1270) \to \pi^+\pi^-)$	LHCb [839][e]	$0.61 \pm 0.13^{+0.13}_{-0.08}$	$0.61^{+0.19}_{-0.15}$
			$0.61^{+0.18}_{-0.15}$
$\mathcal{B}(B_s^0 \to \phi(1020)\rho^0(770))$	LHCb [839][e]	$0.27 \pm 0.07 \pm 0.03$	0.27 ± 0.08
$\mathcal{B}(B_s^0 \to \phi(1020)\pi^+\pi^-)$	LHCb [839][f,e]	$3.48 \pm 0.23 \pm 0.39$	3.48 ± 0.45
$\mathcal{B}(B_s^0 \to \phi(1020)\phi(1020))$	LHCb [828][e,g]	$18.5 \pm 0.5 \pm 1.6$	18.5 ± 1.4
	CDF [893][h]	$18.5 \pm 1.5 \pm 2.2$	

[a]Not included in PDG average.
[b]Measurement of $(\mathcal{B}(B_s^0 \to \pi^+\pi^-)/\mathcal{B}(B^0 \to K^+\pi^-))\frac{f_s}{f_d}$ used in our fit.
[c]Using f_s.
[d]Using $\mathcal{B}(B^+ \to \eta' K^+)$.
[e]Multiple systematic uncertainties are added in quadrature.
[f]$400 < m_{\pi^+\pi^-} < 1600$ MeV/c^2.
[g]Using $\mathcal{B}(B^0 \to \phi(1020)K^*(892)^0)$.
[h]Using $\mathcal{B}(B_s^0 \to J/\psi\phi(1020))$.

TABLE 185. Branching fractions of charmless B_s^0 decays (part 2).

Parameter [10^{-6}]	Measurements		Average$^{\text{HFLAV}}_{PDG}$
$\mathcal{B}(B_s^0 \to K^-\pi^+)$	Belle [887]	< 26	$6.1^{+0.9}_{-0.8}$
	CDF [790][a]		*5.8 ± 0.7*
	LHCb [793][a]		
$\mathcal{B}(B_s^0 \to K^+K^-)$	Belle [887][b]	$38^{+10}_{-9} \pm 7$	$27.4^{+3.2}_{-2.8}$
	CDF [791][c]		*26.6 ± 2.2*
	LHCb [793][c]		
$\mathcal{B}(B_s^0 \to K^0\bar{K}^0)$	LHCb [821][b,d]	$16.7 \pm 2.9 \pm 2.1$	17.4 ± 3.1
	Belle [894][b]	$19.6^{+5.8}_{-5.1} \pm 2.2$	$17.6^{+3.2}_{-3.1}$
$\mathcal{B}(B_s^0 \to K^0\pi^+\pi^-)$	LHCb [808][e,f]	$9.49 \pm 1.34 \pm 1.67$	9.5 ± 2.1
$\mathcal{B}(B_s^0 \to K^0K^+\pi^-+\text{c.c.})$	LHCb [808][e,f]	$84.5 \pm 3.5 \pm 8.0$	84.5 ± 8.7
			84.5 ± 8.8
$\mathcal{B}(B_s^0 \to K^*(892)^-\pi^+)$	LHCb [810][g]	$2.98 \pm 0.99 \pm 0.42$	3.0 ± 1.1
			p = 0.16%
			2.9 ± 1.1

[a]Measurement of $(\mathcal{B}(B_s^0 \to K^-\pi^+)/\mathcal{B}(B^0 \to K^+\pi^-))\frac{f_s}{f_d}$ used in our fit.
[b]Multiple systematic uncertainties are added in quadrature.
[c]Measurement of $(\mathcal{B}(B_s^0 \to K^+K^-)/\mathcal{B}(B^0 \to K^+\pi^-))\frac{f_s}{f_d}$ used in our fit.
[d]Using $\mathcal{B}(B^0 \to \phi(1020)K^0)$.
[e]Regions corresponding to D, Λ_c^+ and charmonium resonances are vetoed in this analysis.
[f]Using $\mathcal{B}(B^0 \to K^0\pi^+\pi^-)$.
[g]Using $\mathcal{B}(B^0 \to K^*(892)^+\pi^-)$.

TABLE 186. Branching fractions of charmless B_s^0 decays (part 3).

Parameter [10^{-6}]	Measurements		Average$^{\text{HFLAV}}_{PDG}$
$\mathcal{B}(B_s^0 \to K^*(892)^+K^-+\text{c.c.})$	LHCb [895][b,c]	$18.6 \pm 1.2 \pm 4.5$	18.6 ± 4.7
$\mathcal{B}(B_s^0 \to (K\pi)_0^{*+}K^-+\text{c.c.})$	LHCb [895][b,c]	$24.9 \pm 1.8 \pm 20.2$	25 ± 20
			None
$\mathcal{B}(B_s^0 \to K_0^*(1430)^+K^-+\text{c.c.})$	LHCb [895][b,c]	$31.3 \pm 2.3 \pm 25.3$	31 ± 25
$\mathcal{B}(B_s^0 \to K_2^*(1430)^+K^-+\text{c.c.})$	LHCb [895][b,c]	$10.3 \pm 2.5 \pm 16.4$	10 ± 17
$\mathcal{B}(B_s^0 \to K^*(892)^0\bar{K}^0+\text{c.c.})$	LHCb [895][b,c]	$19.8 \pm 2.8 \pm 5.0$	19.8 ± 5.7
$\mathcal{B}(B_s^0 \to (K\pi)_0^{*0}\bar{K}^0+\text{c.c.})$	LHCb [895][b,c]	$26.2 \pm 2.0 \pm 7.8$	26.2 ± 8.1
			None
$\mathcal{B}(B_s^0 \to K_0^*(1430)^0\bar{K}^0+\text{c.c.})$	LHCb [895][b,c]	$33.0 \pm 2.5 \pm 9.8$	33 ± 10
$\mathcal{B}(B_s^0 \to K_2^*(1430)^0\bar{K}^0+\text{c.c.})$	LHCb [895][b,c]	$16.8 \pm 4.5 \pm 21.3$	17 ± 22
$\mathcal{B}(B_s^0 \to K_S^0K^*(892)^0+\text{c.c.})$	LHCb [807][c,d]	$17.1 \pm 3.6 \pm 2.4$	17.1 ± 4.3
			p = 0.16%
			16.4 ± 4.1
$\mathcal{B}(B_s^0 \to K^0K^+K^-)$	LHCb [808][e,f]	$1.29 \pm 0.55 \pm 0.36$	1.29 ± 0.66
			1.29 ± 0.65

(Table continued)

TABLE 186. *(Continued)*

Parameter [10^{-6}]	Measurements		Average$^{\text{HFLAV}}_{PDG}$
$\mathcal{B}(B_s^0 \to \bar{K}^*(892)^0\rho^0(770))$	SLD [891]	< 767	< 767
$\mathcal{B}(B_s^0 \to K^*(892)^0\bar{K}^*(892)^0)$	LHCb [827][c,g] LHCb [831][a,c,h]	$11.2 \pm 2.2 \pm 1.5$	11.0 ± 2.0 *11.1 ± 2.7*
$\mathcal{B}(B_s^0 \to \phi(1020)\bar{K}^*(892)^0)$	LHCb [826][c,g]	$1.14 \pm 0.24 \pm 0.17$	1.14 ± 0.29 *1.14 ± 0.30*

[a]Not included in PDG average.
[b]Result extracted from Dalitz-plot analysis of $B_s^0 \to K_S^0 K^+\pi^-$ decays.
[c]Multiple systematic uncertainties are added in quadrature.
[d]Using $\mathcal{B}(B^0 \to K^0\pi^+\pi^-)$.
[e]Regions corresponding to D, Λ_c^+ and charmonium resonances are vetoed in this analysis.
[f]Using $\mathcal{B}(B^0 \to K^0\pi^+\pi^-)$.
[g]Using $\mathcal{B}(B^0 \to \phi(1020)K^*(892)^0)$.
[h]Measurement of $\mathcal{B}(B^0 \to K^*(892)^0\bar{K}^*(892)^0)/\mathcal{B}(B_s^0 \to K^*(892)^0\bar{K}^*(892)^0)$ used in our fit.

TABLE 187. Branching fractions of charmless B_s^0 decays (part 4).

Parameter [10^{-6}]	Measurements		Average$^{\text{HFLAV}}_{PDG}$
$\mathcal{B}(B_s^0 \to p\bar{p})$	LHCb [865][a]	< 0.0044	< 0.0044 *< 0.0150*
$\mathcal{B}(B_s^0 \to p\bar{p}K^+K^-)$	LHCb [867][b,c]	$4.2 \pm 0.3 \pm 0.4$	4.2 ± 0.5 *4.5 ± 0.5*
$\mathcal{B}(B_s^0 \to p\bar{p}K^+\pi^-)$	LHCb [867][b,c]	$1.3 \pm 0.2 \pm 0.2$	1.3 ± 0.3 *1.4 ± 0.3*
$\mathcal{B}(B_s^0 \to p\bar{p}\pi^+\pi^-)$	LHCb [867][b]	< 0.66	< 0.66 *0.43 ± 0.20*
$\mathcal{B}(B_s^0 \to p\bar{\Lambda}^0K^-+\text{c.c.})$	LHCb [896][c]	$5.46 \pm 0.61 \pm 0.82$	5.5 ± 1.0
$\mathcal{B}(B_s^0 \to \gamma\gamma)$	Belle [897]	< 3.1	< 3.1
$\mathcal{B}(B_s^0 \to \phi(1020)\gamma)$	LHCb [898][d] Belle [897]	$34.1 \pm 1.7 \pm 3.1$ $36.0 \pm 5.0 \pm 7.0$	34.4 ± 3.3 *34.2 ± 3.6*

[a]Not included in PDG average.
[b]$m_{p\bar{p}} < 2.85$ GeV/c^2.
[c]Multiple systematic uncertainties are added in quadrature.
[d]Using $\mathcal{B}(B^0 \to K^*(892)^0\gamma)$.

TABLE 188. Branching fractions of charmless B_s^0 decays (part 5).

Parameter [10^{-6}]	Measurements		Average$^{\text{HFLAV}}_{PDG}$
$\mathcal{B}(B_s^0 \to e^+e^-)$	LHCb [899]	< 0.0094	< 0.0094
	CDF [900]	< 0.28	
	Belle [901][a]	< 15.3	
$\mathcal{B}(B_s^0 \to \tau^+\tau^-)$[b]	LHCb [902]	< 5200	< 5200
			< 6800
$\mathcal{B}(B_s^0 \to \mu^+\mu^-\gamma)$	LHCb [903][c]	< 0.0015	< 0.0015
			None
$\mathcal{B}(B_s^0 \to \mu^+\mu^-\mu^+\mu^-)$	LHCb [904][d]	< 0.00086	< 0.00086
$\mathcal{B}(B_s^0 \to aa) \times \mathcal{B}(a \to \mu^+\mu^-) \times \mathcal{B}(a \to \mu^+\mu^-)$	LHCb [904][e,f,d]	< 0.00058	< 0.00058
			None
$\mathcal{B}(B_s^0 \to \phi(1020)\mu^+\mu^-)$[g,h]	LHCb [905][a,i,j]	$0.832 \pm 0.022^{+0.035}_{-0.036}$	$0.838^{+0.042}_{-0.041}$
	CDF [878][j]	$1.18 \pm 0.20^{+0.08}_{-0.09}$	*0.841 ± 0.041*
$\mathcal{B}(B_s^0 \to \bar{K}^*(892)^0\mu^+\mu^-)$	LHCb [906][i]	$0.029 \pm 0.010 \pm 0.004$	0.029 ± 0.011
$\mathcal{B}(B_s^0 \to \pi^+\pi^-\mu^+\mu^-)$	LHCb [907][k,l]		0.084 ± 0.016
			0.084 ± 0.017
$\mathcal{B}(B_s^0 \to \phi(1020)\nu\bar{\nu})$	DELPHI [811]	< 5400	< 5400

[a]Not included in PDG average.
[b]PDG shows the result obtained at 95% CL.
[c]$m_{\mu^+\mu^-} > 4.9$ GeV/c^2.
[d]At CL = 95%.
[e]The mass windows corresponding to ϕ and charmonium resonances decaying to $\mu\mu$ are vetoed.
[f]a is a promptly decaying scalar particle with a mass of 1 GeV/c^2.
[g]The PDG uncertainty includes a scale factor.
[h]Treatment of charmonium intermediate components differs between the results.
[i]Multiple systematic uncertainties are added in quadrature.
[j]Using $\mathcal{B}(B_s^0 \to J/\psi\phi(1020))$.
[k]$0.5 < m_{\pi^+\pi^-} < 1.3$ GeV/c^2.
[l]Measurement of $\mathcal{B}(B_s^0 \to \pi^+\pi^-\mu^+\mu^-)/(\mathcal{B}(B^0 \to J/\psi K^*(892)^0)\mathcal{B}(J/\psi \to \mu^+\mu^-)\mathcal{B}(K^*(892)^0 \to K\pi) \times 2/3)$ used in our fit.

TABLE 189. Branching fractions of charmless B_s^0 decays (part 6).

Parameter [10^{-6}]	Measurements		Average$_{PDG}^{HFLAV}$
$\mathcal{B}(B_s^0 \to e^+\mu^- + \text{c.c.})$	LHCb [908] CDF [900]	< 0.0054 < 0.2	< 0.0054
$\mathcal{B}(B_s^0 \to \tau^+ e^- + \text{c.c.})$	Belle [909]	< 1410	< 1410 *None*
$\mathcal{B}(B_s^0 \to \tau^+\mu^- + \text{c.c.})$[c]	LHCb [910] Belle [909][a]	< 34 < 730	< 34 *< 42*
$\mathcal{B}(B_s^0 \to \phi(1020)e^+\mu^- + \text{c.c.})$	LHCb [911][b]	< 0.0160	< 0.016 *None*
$\mathcal{B}(B_s^0 \to p\mu^-)$	LHCb [912]	< 0.0121	< 0.012 *None*
$\mathcal{B}(B_s^0 \to \eta'\eta)$	Belle [913]	< 65	< 65
$\mathcal{B}(B_s^0 \to f_2'(1525)\mu^+\mu^-)$	LHCb [905][d,e]	$0.161 \pm 0.020 \pm 0.011$	0.161 ± 0.022 *None*
$\mathcal{B}(B_s^0 \to \eta' X_{s\bar{s}})$	Belle [914][f]	< 1400	< 1400 *None*
$\mathcal{B}(B_s^0 \to \eta' K_S^0)$	Belle [915][g]	< 8.16	< 8.2 *None*
$\mathcal{B}(B_s^0 \to p\bar{p}p\bar{p})$	LHCb [873][h,i]		0.0227 ± 0.0100 *None*

[a]Not included in PDG average.
[b]Preliminary result.
[c]PDG shows the result obtained at 95% CL.
[d]Multiple systematic uncertainties are added in quadrature.
[e]Using $\mathcal{B}(B_s^0 \to J/\psi\phi(1020))$.
[f]$m_{X_{ss}} < 2.4$ GeV/c^2.
[g]Using f_s.
[h]black.
[i]Measurement of $\mathcal{B}(B_s^0 \to p\bar{p}p\bar{p})/(\mathcal{B}(B_s^0 \to J/\psi\phi(1020))\mathcal{B}(J/\psi \to p\bar{p})\mathcal{B}(\phi(1020) \to K^+K^-))$ used in our fit.

TABLE 190. Relative branching fractions of B_s^0 decays (part 1).

Parameter [10^{-2}]	Measurements		Average
$\frac{f_s}{f_d}\frac{\mathcal{B}(B_s^0 \to \pi^+\pi^-)}{\mathcal{B}(B^0 \to K^+\pi^-)}$	LHCb [794]	$0.915 \pm 0.071 \pm 0.083$	0.893 ± 0.098
	CDF [792]	$0.8 \pm 0.2 \pm 0.1$	
$\frac{f_s}{f_d}\frac{\mathcal{B}(B_s^0 \to \pi^+\pi^-)}{\mathcal{B}(B^0 \to \pi^+\pi^-)}$	LHCb [793]	$5.0^{+1.1}_{-0.9} \pm 0.4$	$5.0^{+1.2}_{-1.0}$
$\frac{\mathcal{B}(B_s^0 \to \phi(1020)\phi(1020))_a}{\mathcal{B}(B_s^0 \to J/\psi\phi(1020))}$	CDF [893]	$1.78 \pm 0.14 \pm 0.20$	1.78 ± 0.24
$\frac{\mathcal{B}(B_s^0 \to \phi(1020)\phi(1020))}{\mathcal{B}(B^0 \to \phi(1020)K^*(892)^0)}$	LHCb [828][b]	$184 \pm 5 \pm 13$	184 ± 14
$\frac{f_s}{f_d}\frac{\mathcal{B}(B_s^0 \to K^+\pi^-)}{\mathcal{B}(B_d^0 \to K^+\pi^-)}$	LHCb [793]	$7.4 \pm 0.6 \pm 0.6$	7.30 ± 0.70
	CDF [790]	$7.1 \pm 1.0 \pm 0.7$	
$\frac{f_s}{f_d}\frac{\mathcal{B}(B_s^0 \to K^+K^-)}{\mathcal{B}(B_d^0 \to K^+\pi^-)}$	LHCb [793]	$31.6 \pm 0.9 \pm 1.9$	32.7 ± 1.7
	CDF [791]	$34.7 \pm 2.0 \pm 2.1$	
$\frac{\mathcal{B}(B_s^0 \to K^0\pi^+\pi^-)}{\mathcal{B}(B^0 \to K^0\pi^+\pi^-)}$	LHCb [808][c,b]	$19.1 \pm 2.7 \pm 3.3$	19.1 ± 4.3
$\frac{\mathcal{B}(B_s^0 \to K^0K^+\pi^- + \text{c.c.})}{\mathcal{B}(B^0 \to K^0\pi^+\pi^-)}$	LHCb [808][c,b]	$170 \pm 7 \pm 15$	170 ± 16
$\frac{\mathcal{B}(B_s^0 \to K^0K^+K^-)}{\mathcal{B}(B^0 \to K^0\pi^+\pi^-)}$	LHCb [808][c]	< 5.1	< 5.1
$\frac{\mathcal{B}(B_s^0 \to K^*(892)^-\pi^+)}{\mathcal{B}(B^0 \to K^*(892)^+\pi^-)}$	LHCb [810]	$39 \pm 13 \pm 5$	39 ± 14
$\frac{\mathcal{B}(B_s^0 \to K^*(892)^0\bar{K}^*(892)^0)}{\mathcal{B}(B^0 \to \phi(1020)K^*(892)^0)}$	LHCb [827][b]	$111 \pm 22 \pm 13$	111 ± 26
$\frac{\mathcal{B}(B_s^0 \to \phi(1020)\bar{K}^*(892)^0)}{\mathcal{B}(B^0 \to \phi(1020)K^*(892)^0)}$	LHCb [826][b]	$11.3 \pm 2.4 \pm 1.6$	11.3 ± 2.9
$\frac{\mathcal{B}(B_s^0 \to \phi(1020)\mu^+\mu^-)}{\mathcal{B}(B_s^0 \to J/\psi\phi(1020))}$	LHCb [905][b]	$0.0800 \pm 0.0021 \pm 0.0016$	0.0806 ± 0.0026
	CDF [878]	$0.113 \pm 0.019 \pm 0.007$	

[a]The PDG average is a result of a fit including input from other measurements.

[b]Multiple systematic uncertainties are added in quadrature.

[c]Regions corresponding to D, Λ_c^+ and charmonium resonances are vetoed in this analysis.

TABLE 191. Relative branching fractions of B_s^0 decays (part 2).

Parameter [10^{-2}]	Measurements		Average
$\frac{\mathcal{B}(B_s^0 \to p\bar{p}K^+\pi^-)}{\mathcal{B}(B^0 \to p\bar{p}K^+\pi^-)}$	LHCb [867][a,b]	$22 \pm 4 \pm 2$	22 ± 5
$\frac{\mathcal{B}(B_s^0 \to p\bar{p}K^+\pi^-)}{\mathcal{B}(B_s^0 \to p\bar{p}K^+K^-)}$	LHCb [867][a]	$31 \pm 5 \pm 2$	31 ± 5
$\frac{\mathcal{B}(B_s^0 \to \bar{K}^*(892)^0\mu^+\mu^-)}{\mathcal{B}(B_s^0 \to J/\psi\bar{K}^*(892)^0) \times \mathcal{B}(J/\psi \to \mu^+\mu^-)}$	LHCb [906][b]	$1.4 \pm 0.4 \pm 0.1$	1.4 ± 0.4
$\frac{\mathcal{B}(B_s^0 \to \bar{K}^*(892)^0\mu^+\mu^-)}{\mathcal{B}(\bar{B}^0 \to \bar{K}^*(892)^0\mu^+\mu^-)}$	LHCb [906][b]	$3.3 \pm 1.1 \pm 0.4$	3.3 ± 1.2
$\frac{\mathcal{B}(B_s^0 \to \phi(1020)\phi(1020)\phi(1020))}{\mathcal{B}(B_s^0 \to \phi(1020)\phi(1020))}$	LHCb [916]	$11.7 \pm 3.0 \pm 1.5$	11.7 ± 3.4
$\frac{\mathcal{B}(B_s^0 \to K^0\bar{K}^0)}{\mathcal{B}(B^0 \to \phi(1020)K^0)}$	LHCb [821][b]	$230 \pm 40 \pm 22$	230 ± 46
$\frac{\mathcal{B}(B_s^0 \to K_S^0K^*(892)^0+\text{c.c.})}{\mathcal{B}(B^0 \to K_S^0\pi^+\pi^-)}$	LHCb [807][b]	$33 \pm 7 \pm 4$	33 ± 8
$\frac{\mathcal{B}(B_s^0 \to f_2'(1525)\mu^+\mu^-)}{\mathcal{B}(B_s^0 \to J/\psi\phi(1020))}$	LHCb [905][b]	$0.0155 \pm 0.0019 \pm 0.0008$	0.0155 ± 0.0021
$\frac{\mathcal{B}(B_s^0 \to \pi^+\pi^-\mu^+\mu^-)}{\mathcal{B}(B^0 \to J/\psi K^{*0}) \times \mathcal{B}(J/\psi \to \mu^+\mu^-) \times \mathcal{B}(K^{*0} \to K^+\pi^-)}$	LHCb [907][c]	$0.167 \pm 0.029 \pm 0.013$	0.167 ± 0.032
$\frac{\mathcal{B}(B^0 \to p\bar{p}p\bar{p})}{\mathcal{B}(B^0 \to J/\psi\phi)\mathcal{B}(J/\psi \to p\bar{p})\mathcal{B}(\phi \to K^+K^-)}$	LHCb [873]	$2.1 \pm 0.9 \pm 0.2$	2.10 ± 0.92

[a] $m_{p\bar{p}} < 2.85$ GeV/c^2.
[b] Multiple systematic uncertainties are added in quadrature.
[c] $0.5 < m_{\pi^+\pi^-} < 1.3$ GeV/c^2.

Measurements that are not included in the tables (the definitions of observables can be found in the corresponding experimental papers):

(i) In Ref. [905], LHCb reports the differential $B_s^0 \to \phi\mu^+\mu^-$ branching fraction in bins of $m^2(\mu^+\mu^-)$.

(ii) In Ref. [917], LHCb performs an angular analysis of $B_s^0 \to \phi\mu^+\mu^-$ decays and reports F_L, S_3, S_4, S_7, A_5, A_{FB}^{CP}, A_8 and A_9 in bins of $m^2(\mu^+\mu^-)$.

(iii) In Ref. [918], LHCb reports the photon polarization in $B_s^0 \to \phi\gamma$ decays.

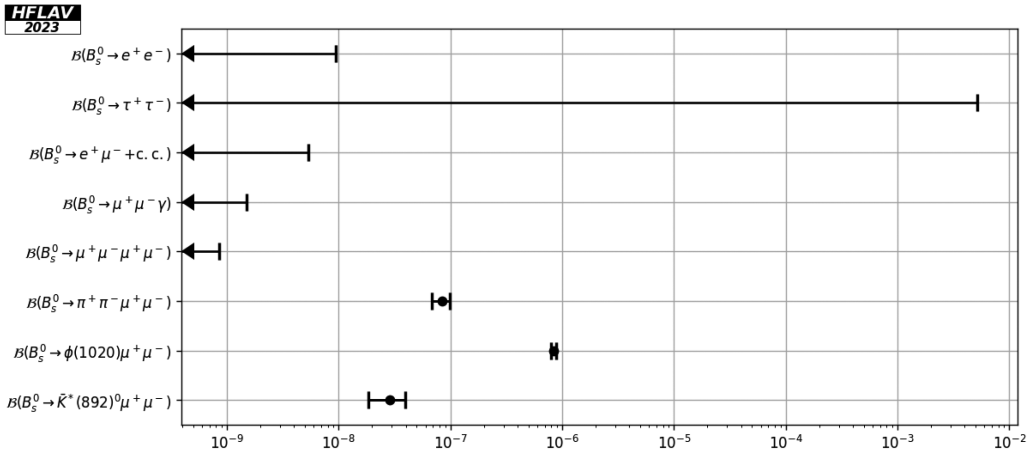


FIG. 33. Branching fractions of charmless leptonic B_s^0 decays.

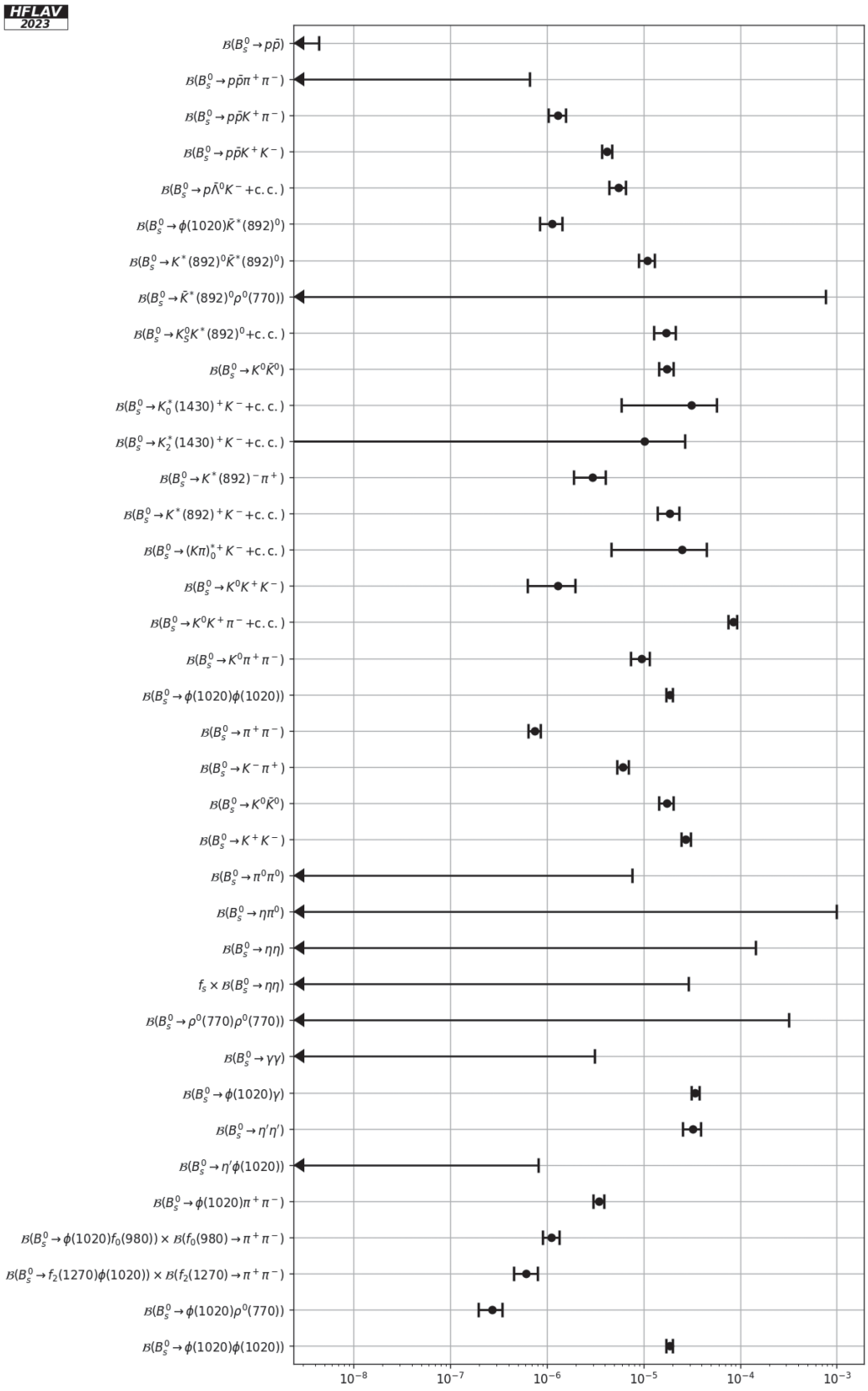


FIG. 34. Branching fractions of charmless nonleptonic B_s^0 decays.

(iv) We do not perform the average of the branching fraction of $B \to \mu^+\mu^-$ decays, which is taken care of by the LHC Heavy Flavor Working Group [919], taking into account the correlations between the $B^0 \to \mu^+\mu^-$ and $B_s^0 \to \mu^+\mu^-$ branching fractions. The latest results from ATLAS, CMS and LHCb are in Refs. [125,903,920], respectively.

E. Decays of B_c^+ mesons

Table 192 details branching fractions and ratios of branching fractions of B_c^+ meson decays to charmless hadronic final states, except for decays to final states containing B_s^0 mesons that are quoted in Sec. VII E.

F. Rare decays of B^0 and B^+ mesons with photons and/or leptons

This section reports different observables for radiative decays, lepton-flavor/number-violating (LFV/LNV) decays and flavor-changing-neutral-current (FCNC) decays with leptons of B^0 and B^+ mesons. In all decays listed in this section, charmonium intermediate states are vetoed. Tables 193–197, 198–202 and 203–205 provide compilations of branching fractions of radiative and FCNC decays with leptons of B^+ mesons, B^0 mesons and their admixture, respectively. Tables 202 and 205 also include LFV/LNV decays. Tables 206 and 207 contain branching fractions of leptonic and radiative-leptonic B^+ and B^0 decays. These are followed by Tables 208–210, which give relative branching fractions of B^+ and B^0 decays, then Table 211, which gives a compilation of inclusive decays. In the modes listed in Table 211, the radiated particle is a gluon, which is an exception in this section. Table 212 contains isospin asymmetry measurements. Finally, Tables 213–215 and 216 provide compilations of branching fractions of B^+ and B^0 mesons to lepton-flavor/number-violating final states, respectively. The average of Figs. 35–40 show graphic representations of a selection of results given in this section.

Measurements that are not included in the tables (the definitions of observables can be found in the corresponding experimental papers):

(1) In Ref. [1023], LHCb reports the up-down asymmetries in bins of the $K\pi\pi\gamma$ mass of the $B^+ \to K^+\pi^-\pi^+\gamma$ decay.

(2) For the $B \to K\ell^-\ell^+$ channel, LHCb measures F_H and $A_{\rm FB}$ in 17 (5) bins of $m^2(\ell^+\ell^-)$ for the K^+ (K_S^0) final state [1024]. Belle measures F_L and $A_{\rm FB}$ in 6 $m^2(\ell^+\ell^-)$ [952].

(3) For the $B \to K^*\ell^-\ell^+$ analyses, partial branching fractions and angular observables in bins of $m^2(\ell^+\ell^-)$ are also available:

(a) $B^0 \to K^{*0}e^-e^+$: LHCb reports F_L, $A_T^{(2)}$, $A_T^{\rm Im}$, $A_T^{\rm Re}$ in the $[0.0008, 0.257]$ GeV^2/c^4 bin of $m^2(\ell^+\ell^-)$ putting constraints on the $B \to K^{*0}\gamma$ photon polarization [1025]. In Ref. [1026], LHCb determines the branching fraction in the dilepton mass region $[0.0009, 1.0]$ GeV^2/c^4.

(b) $B \to K^*\ell^-\ell^+$: Belle measures F_L, $A_{\rm FB}$, isospin asymmetry in 6 $m^2(\ell^+\ell^-)$ bins [952] and P_4', P_5', P_6', P_8' in 4 $m^2(\ell^+\ell^-)$ bins [1027]. In a more recent paper [1028], they report measurements of P_4' and P_5', separately for $\ell = \mu$ or e, in 4 $m^2(\ell^+\ell^-)$ bins and in the region $[1, 6]$ GeV^2/c^4. The measurements use both B^0 and B^+ decays. They also measure the LFU observables $Q_i = P_i^\mu - P_i^e$, for $i = 4, 5$. *BABAR* reports F_L, $A_{\rm FB}$, P_2 in 5 $m^2(\ell^+\ell^-)$ bins [1029].

(c) $B^0 \to K^{*0}\mu^-\mu^+$: LHCb measures F_L, $A_{\rm FB}$, $S_3 - S_9$, $A_3 - A_9$, $P_1 - P_3$, $P_4' - P_8'$ in 8 $m^2(\ell^+\ell^-)$ bins [1030]. An updated measurement of the CP-averaged observables is presented in Ref. [1031]. CMS measures F_L and $A_{\rm FB}$ in 7 $m^2(\ell^+\ell^-)$ bins [1032], as well as P_1, P_5' [1033]. ATLAS measures F_L, $S_{3,4,5,7,8}$ and $P'_{1,4,5,6,8}$ in 6 $m^2(\ell^+\ell^-)$ bins [1034].

(d) $B^+ \to K^{*+}\mu^-\mu^+$: LHCb reports the full set of CP-averaged angular observables in

TABLE 192. Branching fractions and relative branching fractions of B_c^+ decays.

Parameter	Measurements		Average
$\mathcal{B}(B_c^+ \to p\bar{p}\pi^+) \times \frac{f_c}{f_u}$ [10^{-8}]	LHCb [921][a]	< 2.8	< 2.8
$\frac{\mathcal{B}(B_c^+ \to K^+K_S^0)}{\mathcal{B}(B^+ \to K_S^0\pi^+)} \times \frac{f_c}{f_u}$ [10^{-2}]	LHCb [706]	< 5.8	< 5.8
$\mathcal{B}(B_c^+ \to K^+\bar{K}^0)$[b] [$10^{-4}$]	LHCb [706]	< 4.6	< 4.6
$\mathcal{B}(B_c^+ \to K^+K^-\pi^+) \times \frac{f_c}{f_u}$ [10^{-7}]	LHCb [671][c]	< 1.50	< 1.5

[a]Measured in the region $p\bar{p} < 2.85$ GeV/c^2, $p_T(B) < 20$ GeV/c and $2.0 < y(B) < 4.5$.

[b]Derived from the ratio in the previous entry using $\mathcal{B}(B^+ \to K^0\pi^+) = (23.97 \pm 0.53 \pm 0.71) \times 10^{-6}$, $f_u = 0.33$ and $f_c = 0.001$.

[c]Measured in the annihilation region $m_{K^+\pi^+} < 1.834$ GeV/c^2, and in the fiducial region $p_T(B) < 20$ GeV/c and $2.0 < y(B) < 4.5$.

TABLE 193. Branching fractions of B^+ radiative and FCNC decays with leptons (part 1).

Parameter [10^{-6}]	Measurements		Average$^{\text{HFLAV}}_{PDG}$
$\mathcal{B}(B^+ \to K^*(892)^+\gamma)$[b]	Belle [922]	$37.6 \pm 1.0 \pm 1.2$	39.9 ± 1.2
	BABAR [923]	$42.2 \pm 1.4 \pm 1.6$	*39.2 ± 2.2*
	Belle II [924][a]	$52 \pm 4 \pm 3$	
	CLEO [925]	$37.6^{+8.9}_{-8.3} \pm 2.8$	
$\mathcal{B}(B^+ \to K^+\pi^0\gamma)$	Belle [922][c]	$39.1 \pm 1.6 \pm 1.6$	40.7 ± 1.9
	BABAR [923][d]	$43.8 \pm 1.9 \pm 2.6$	*None*
$\mathcal{B}(B^+ \to K^0_S\pi^+\gamma)$	Belle [922][c]	$36.9 \pm 1.2 \pm 1.2$	38.4 ± 1.4
	BABAR [923][d]	$41.3 \pm 1.8 \pm 1.6$	*None*
$\mathcal{B}(B^+ \to K_1(1270)^+\gamma)$	*BABAR* [926][e]	$44.1^{+6.3}_{-4.4} \pm 5.8$	$43.8^{+7.0}_{-6.3}$
	Belle [927][f]	$43.0 \pm 9.0 \pm 9.0$	$43.8^{+7.1}_{-6.3}$
$\mathcal{B}(B^+ \to \eta K^+\gamma)$	*BABAR* [928][g]	$7.7 \pm 1.0 \pm 0.4$	7.89 ± 0.92
	Belle [929][h]	$8.4 \pm 1.5^{+1.2}_{-0.9}$	$7.88^{+0.94}_{-0.92}$
$\mathcal{B}(B^+ \to \eta' K^+\gamma)$	Belle [930][i]	$3.6 \pm 1.2 \pm 0.4$	2.9 ± 1.0
	BABAR [931][g]	$1.9^{+1.5}_{-1.2} \pm 0.1$	$2.9^{+1.0}_{-0.9}$
$\mathcal{B}(B^+ \to \phi(1020)K^+\gamma)$[b]	Belle [932]	$2.48 \pm 0.30 \pm 0.24$	2.71 ± 0.34
	BABAR [933][j]	$3.5 \pm 0.6 \pm 0.4$	*2.71 ± 0.42*

[a]Preliminary result.
[b]The PDG uncertainty includes a scale factor.
[c]$m_{K\pi} < 2.0$ GeV/c^2.
[d]$0.79 < m_{K\pi} < 1.0$ GeV/c^2.
[e]Multiple systematic uncertainties are added in quadrature.
[f]$1 < m_{K\pi\pi} < 2$ GeV/c^2.
[g]$m_{K\eta^{(\prime)}} < 3.25$ GeV/c^2.
[h]$m_{K\eta} < 2.4$ GeV/c^2.
[i]$m_{K\eta'} < 3.4$ GeV/c^2.
[j]$m_{\phi K} < 3.0$ GeV/c^2.

TABLE 194. Branching fractions of B^+ radiative and FCNC decays with leptons (part 2).

Parameter [10^{-6}]	Measurements		Average$^{\text{HFLAV}}_{PDG}$
$\mathcal{B}(B^+ \to K^+\pi^-\pi^+\gamma)$[a]	*BABAR* [926][b]	$24.5 \pm 0.9 \pm 1.2$	24.6 ± 1.3
	Belle [927][c]	$25.0 \pm 1.8 \pm 2.2$	*25.8 ± 1.5*
$\mathcal{B}(B^+ \to K^*(892)^0\pi^+\gamma)$	*BABAR* [926][b]	$23.4 \pm 0.9^{+0.8}_{-0.7}$	23.3 ± 1.2
	Belle [934][d]	$20.0^{+7.0}_{-6.0} \pm 2.0$	$23.3^{+1.2}_{-1.1}$
$\mathcal{B}(B^+ \to K^+\rho^0(770)\gamma)$	*BABAR* [926][b]	$8.2 \pm 0.4 \pm 0.8$	8.2 ± 0.9
	Belle [934][d]	< 20.0	
$\mathcal{B}(B^+ \to (K\pi)^{*0}_0\pi^+\gamma) \times \mathcal{B}((K\pi)^{*0}_0 \to K^+\pi^-)$[e]	*BABAR* [926][b]	$10.3^{+0.7+1.5}_{-0.8-2.0}$	$10.3^{+1.7}_{-2.2}$
			None
$\mathcal{B}(B^+ \to K^+\pi^-\pi^+\gamma(\text{NR}))$	*BABAR* [926][b,f]	$9.9 \pm 0.7^{+1.5}_{-1.9}$	$9.9^{+1.7}_{-2.0}$
	Belle [934][g]	< 9.2	
$\mathcal{B}(B^+ \to K^0\pi^+\pi^0\gamma)$	*BABAR* [935][b]	$45.6 \pm 4.2 \pm 3.1$	45.6 ± 5.2
$\mathcal{B}(B^+ \to K_1(1400)^+\gamma)$	*BABAR* [926][b,h]	$9.7^{+4.6+2.9}_{-2.9-2.4}$	$9.7^{+5.4}_{-3.8}$
	Belle [927]	< 15.0	
$\mathcal{B}(B^+ \to K^*(1410)^+\gamma)$	*BABAR* [926][b,h]	$27.1^{+5.4+5.9}_{-4.8-3.7}$	$27.1^{+8.0}_{-6.1}$
$\mathcal{B}(B^+ \to K^*_0(1430)^0\pi^+\gamma)$	*BABAR* [926][b,h]	$1.32^{+0.09+0.24}_{-0.10-0.30}$	$1.32^{+0.26}_{-0.31}$
			$1.32^{+0.26}_{-0.32}$
$\mathcal{B}(B^+ \to K^*_2(1430)^+\gamma)$	*BABAR* [936]	$14.5 \pm 4.0 \pm 1.5$	13.8 ± 4.0
	BABAR [926][b,h]	$8.7^{+7.0+8.7}_{-5.3-10.4}$	
$\mathcal{B}(B^+ \to K^*(1680)^+\gamma)$	*BABAR* [926][b,h]	$66.7^{+9.3+14.4}_{-7.8-11.4}$	67^{+17}_{-14}
$\mathcal{B}(B^+ \to K^*_3(1780)^+\gamma)$	Belle [929]	< 14	< 14
			< 39
$\mathcal{B}(B^+ \to K^*_4(2045)^+\gamma)$	ARGUS [937]	< 9900	< 9900

[a]The PDG uncertainty includes a scale factor.
[b]$m_{K\pi\pi} < 1.8$ GeV/c^2.
[c]$1 < m_{K\pi\pi} < 2$ GeV/c^2.
[d]$m_{K\pi\pi} < 2.4$ GeV/c^2.
[e]This corresponds to the $(K\pi)S$-wave obtained with LASS parametrization [938].
[f]$m_{K\pi} < 1.6$ GeV/c^2.
[g]$1.25 < m_{K\pi} < 1.6$ GeV/c^2 and $m_{K\pi\pi} < 2.4$ GeV/c^2.
[h]Multiple systematic uncertainties are added in quadrature.

TABLE 195. Branching fractions of B^+ radiative and FCNC decays with leptons (part 3).

Parameter [10^{-6}]	Measurements		Average$^{\text{HFLAV}}_{PDG}$
$\mathcal{B}(B^+ \to \rho^+(770)\gamma)$	Belle [939]	$0.87^{+0.29+0.09}_{-0.27-0.11}$	0.98 ± 0.24
	BABAR [940]	$1.2 \pm 0.4 \pm 0.2$	$0.98^{+0.25}_{-0.24}$
$\mathcal{B}(B^+ \to p\bar{\Lambda}^0\gamma)$	Belle [862]	$2.45^{+0.44}_{-0.38} \pm 0.22$	$2.45^{+0.49}_{-0.44}$
$\mathcal{B}(B^+ \to p\bar{\Sigma}^0\gamma)$	Belle [941]	< 4.6	< 4.6

TABLE 196. Branching fractions of B^+ radiative and FCNC decays with leptons (part 4).

Parameter [10^{-6}]	Measurements		Average$^{\text{HFLAV}}_{PDG}$
$\mathcal{B}(B^+ \to \pi^+\ell^+\ell^-)$[a]	Belle [942]	< 0.049	< 0.049
	BABAR [943]	< 0.066	
$\mathcal{B}(B^+ \to \pi^+e^+e^-)$[a]	Belle [942]	< 0.08	< 0.08
	BABAR [943]	< 0.125	
$\mathcal{B}(B^+ \to \pi^+\mu^+\mu^-)$[a]	*BABAR* [943]	< 0.055	0.0178 ± 0.0023
	Belle [942]	< 0.069	
	LHCb [944][b,c]		
$\mathcal{B}(B^+ \to \pi^+\nu\bar{\nu})$	Belle [945]	< 14.0	< 14
	BABAR [946]	< 100.0	

[a]Treatment of charmonium intermediate components differs between the results.

[b]LHCb also reports the branching fraction in bins of $m^2_{\ell^+\ell^-}$.

[c]Measurement of $\mathcal{B}(B^+ \to \pi^+\mu^+\mu^-)/(\mathcal{B}(B^+ \to J/\psi K^+)\mathcal{B}(J/\psi \to \mu^+\mu^-))$ used in our fit.

$8\, m^2(\ell^+\ell^-)$ bins [1035]. CMS measures F_L and A_{FB} in 3 $m^2(\ell^+\ell^-)$ bins [1036].

(4) $B \to X_s\ell^-\ell^+$ (where X_s is a hadronic system with an s quark): Belle measures A_{FB} in bins of $m^2(\ell^+\ell^-)$ with a sum of 10 exclusive final states [1037].

(5) $B^0 \to K^+\pi^-\mu^+\mu^-$, with $1330 < m(K^+\pi^-) < 1530$ GeV/c^2: LHCb measures the partial branching fraction in bins of $m^2(\mu^+\mu^-)$ in the range $[0.1, 8.0]$ GeV^2/c^4, and reports angular moments [1038].

(6) In Ref. [1039], LHCb measures the phase difference between the short- and long-distance contributions to the $B^+ \to K^+\mu^+\mu^-$ decay. The measurement is based on the analysis of the dimuon mass distribution in the regions of the J/ψ and $\psi(2S)$ resonances and far from their poles, to probe long and short distance effects, respectively.

(7) In Ref. [1040], CMS performs the study of the angular distribution of the $B^+ \to K^+\mu^+\mu^-$ channel and measures, in 7 $m^2(\mu^+\mu^-)$ bins, A_{FB} and the contribution F_{H} from the pseudoscalar, scalar and tensor amplitudes to the decay.

(8) In Ref. [1041], LHCb performs a search for a hidden-sector boson χ decaying into two muons in $B^0 \to K^{*0}\mu^+\mu^-$ decays. Results are given as function of mass and lifetime in the range $214 < m(\chi) < 4350$ MeV/c^2 and $0 < \tau(\chi) < 1000$ ps.

(9) In Ref. [1042], LHCb performs a search for a hypothetical new scalar particle χ, assumed to have a narrow width, through the decay $B^+ \to K^+\chi(\mu^+\mu^-)$ in the ranges of mass $250 < m(\chi) < 4700$ MeV/c^2 and lifetime $0.1 < \tau(\chi) < 1000$ ps. Upper limits are given as a function of $m(\chi)$ and $\tau(\chi)$.

(10) In Ref. [1043] LHCb reports the differential branching fraction of $\Lambda_b^0 \to \Lambda(1520)\mu^+\mu^-$ in 5 $m(\mu^+\mu^-)$ intervals in the range $[0.1, 17]$ GeV^2/c^4. It also reports the branching fraction in the interval $1.1 < m^2(\mu^+\mu^-) < 6$ GeV^2/c^4.

(11) In Ref. [1044], Belle-II performs a search for long-lived spin-0 particles (S) in B-meson decays mediated by a $b \to s$ quark transition. They set model-independent upper limits, at the level of 10^{-7}, on the products of branching fractions $\mathcal{B}(B^0 \to K^*(892)^0S) \times \mathcal{B}(S \to x^+x^-)$ and $\mathcal{B}(B^+ \to K^+S) \times \mathcal{B}(S \to x^+x^-)$, where x^+x^- indicates e^+e^-, $\mu^+\mu^-$, $\pi^+\pi^-$, or K^+K^-, as functions of the S mass and lifetime.

(12) We do not perform the average of the branching fraction of $B \to \mu^+\mu^-$ decays, which is taken care of

TABLE 197. Branching fractions of B^+ radiative and FCNC decays with leptons (part 5).

Parameter [10^{-6}]	Measurements		Average$^{\text{HFLAV}}_{PDG}$
$\mathcal{B}(B^+ \to K^+\ell^+\ell^-)$[b]	Belle [504]	$0.599^{+0.045}_{-0.043} \pm 0.014$	0.576 ± 0.040
	BABAR [947]	$0.476^{+0.092}_{-0.086} \pm 0.022$	*0.471 ± 0.046*
$\mathcal{B}(B^+ \to K^+e^+e^-)$[b]	Belle [504]	$0.575^{+0.064}_{-0.061} \pm 0.015$	0.561 ± 0.056
	BABAR [947]	$0.51^{+0.12}_{-0.11} \pm 0.02$	$0.560^{+0.058}_{-0.055}$
$\mathcal{B}(B^+ \to K^+\mu^+\mu^-)$[c,b]	LHCb [948]	$0.429 \pm 0.007 \pm 0.021$	0.450 ± 0.021
	Belle [504]	$0.624^{+0.065}_{-0.061} \pm 0.016$	*0.453 ± 0.035*
	BABAR [947]	$0.41^{+0.16}_{-0.15} \pm 0.02$	
$\mathcal{B}(B^+ \to K^+\tau^+\tau^-)$	*BABAR* [949]	< 2250.0	< 2250
$\mathcal{B}(B^+ \to K^+\nu\bar{\nu})$	*BABAR* [950]	< 16.0	< 16
	Belle [945]	< 19.0	
	Belle II [951][a]	< 41.0	
$\mathcal{B}(B^+ \to \rho^+(770)\nu\bar{\nu})$	Belle [945]	< 30.0	< 30
$\mathcal{B}(B^+ \to K^*(892)^+\ell^+\ell^-)$[c,b]	LHCb [948][d]	$0.924 \pm 0.093 \pm 0.067$	1.010 ± 0.099
	Belle [952]	$1.24^{+0.23}_{-0.21} \pm 0.13$	$1.009^{+0.113}_{-0.112}$
	BABAR [947]	$1.40^{+0.40}_{-0.37} \pm 0.09$	
$\mathcal{B}(B^+ \to K^*(892)^+e^+e^-)$[b]	*BABAR* [947]	$1.38^{+0.47}_{-0.42} \pm 0.08$	1.55 ± 0.33
	Belle [952]	$1.73^{+0.50}_{-0.42} \pm 0.20$	$1.55^{+0.36}_{-0.31}$
$\mathcal{B}(B^+ \to K^*(892)^+\mu^+\mu^-)$[b]	LHCb [948]	$0.924 \pm 0.093 \pm 0.067$	0.96 ± 0.10
	Belle [952]	$1.11^{+0.32}_{-0.27} \pm 0.10$	
	BABAR [947]	$1.46^{+0.79}_{-0.75} \pm 0.12$	
$\mathcal{B}(B^+ \to K^*(892)^+\nu\bar{\nu})$	Belle [953]	< 40.0	< 40
	Belle [945]	< 61.0	
	BABAR [950]	< 64.0	
$\mathcal{B}(B^+ \to K^+\pi^+\pi^-\mu^+\mu^-)$	LHCb [954][e]	$0.4337^{+0.0287}_{-0.0268} \pm 0.0254$	0.434 ± 0.038
			$0.433^{+0.038}_{-0.037}$
$\mathcal{B}(B^+ \to \phi(1020)K^+\mu^+\mu^-)$	LHCb [954][f]	$0.0790^{+0.0180+0.0114}_{-0.0160-0.0072}$	$0.079^{+0.022}_{-0.017}$
			$0.079^{+0.021}_{-0.017}$
$\mathcal{B}(B^+ \to \bar{\Lambda}^0 p\nu\bar{\nu})$	*BABAR* [955]	< 30.0	< 30

[a]Not included in PDG average.
[b]Treatment of charmonium intermediate components differs between the results.
[c]The PDG uncertainty includes a scale factor.
[d]Only muons are used.
[e]Using $\mathcal{B}(B^+ \to \psi(2S)K^+)$.
[f]Using $\mathcal{B}(B^+ \to J/\psi\phi(1020)K^+)$.

TABLE 198. Branching fractions of B^0 radiative and FCNC decays with leptons (part 1).

Parameter [10^{-6}]	Measurements		Average$^{\text{HFLAV}}_{PDG}$
$\mathcal{B}(B^0 \to K^*(892)^0\gamma)$[c]	Belle [922]	$39.6 \pm 0.7 \pm 1.4$	42.1 ± 1.1
	BABAR [923]	$44.7 \pm 1.0 \pm 1.6$	*41.8 ± 2.5*
	Belle II [924][a]	$45 \pm 3 \pm 2$	
	CLEO [925]	$45.5^{+7.2}_{-6.8} \pm 3.4$	
	LHCb [898][b,d], [881][b,e]		
$\mathcal{B}(B^0 \to K^+\pi^-\gamma)$	Belle [922][b,f]	$39.5 \pm 0.7 \pm 1.4$	41.4 ± 1.2
	BABAR [923][b,g]	$44.5 \pm 1.0 \pm 1.7$	*4.6 ± 1.4*
$\mathcal{B}(B^0 \to K^0_S\pi^0\gamma)$	Belle [922][f]	$40.0 \pm 2.7 \pm 2.4$	42.2 ± 2.9
	BABAR [923][h]	$46.6 \pm 3.7 \pm 3.5$	*None*
$\mathcal{B}(B^0 \to K^*(1410)^0\gamma)$	Belle [934][i]	< 130.0	< 130
$\mathcal{B}(B^0 \to K^+\pi^-\gamma(\text{NR}))$	Belle [934][i]	< 2.6	< 2.6
$\mathcal{B}(B^0 \to \eta K^0\gamma)$	*BABAR* [928][j]	$7.1^{+2.1}_{-2.0} \pm 0.4$	7.6 ± 1.8
	Belle [929][k]	$8.7^{+3.1+1.9}_{-2.7-1.6}$	$7.6^{+1.8}_{-1.7}$
$\mathcal{B}(B^0 \to \eta' K^0\gamma)$	Belle [930][l]	< 6.4	< 6.4
	BABAR [931][j]	< 6.6	
$\mathcal{B}(B^0 \to \phi(1020)K^0\gamma)$	Belle [932]	$2.74 \pm 0.60 \pm 0.32$	2.74 ± 0.68
	BABAR [933][m]	< 27	
$\mathcal{B}(K^{*0}X(214)) \times \mathcal{B}(X(214) \to \mu^+\mu^-)$	Belle [956][n]	< 0.0226	< 0.023

[a]Preliminary result.
[b]Not included in PDG average.
[c]The PDG uncertainty includes a scale factor.
[d]Measurement of $\mathcal{B}(B^0_s \to \phi(1020)\gamma)/\mathcal{B}(B^0 \to K^*(892)^0\gamma)$ used in our fit.
[e]Measurement of $(\mathcal{B}(\Lambda^0_b \to \Lambda^0\gamma)/\mathcal{B}(B^0 \to K^*(892)^0\gamma))\frac{f_{\Lambda^0_b}}{f_d}$ used in our fit.
[f]$m_{K\pi} < 2.0$ GeV/c^2.
[g]$0.78 < m_{K\pi} < 1.1$ GeV/c^2.
[h]$0.82 < m_{K\pi} < 1.0$ GeV/c^2.
[i]$1.25 < m_{K\pi} < 1.6$ GeV/c^2.
[j]$m_{K\eta^{(\prime)}} < 3.25$ GeV/c^2.
[k]$m_{K\eta} < 2.4$ GeV/c^2.
[l]$m_{K\eta'} < 3.4$ GeV/c^2.
[m]$m_{\phi K} < 3.0$ GeV/c^2.
[n]$X(214)$ is searched for in the mass range $[212, 300]$ MeV/c^2.

TABLE 199. Branching fractions of B^0 radiative and FCNC decays with leptons (part 2).

Parameter [10^{-6}]	Measurements		Average$^{\text{HFLAV}}_{PDG}$
$\mathcal{B}(B^0 \to K^0\pi^+\pi^-\gamma)$	*BABAR* [926][a]	$20.5 \pm 2.0^{+2.6}_{-2.2}$	19.9 ± 1.8
	BABAR [935][a]	$18.5 \pm 2.1 \pm 1.2$	
	Belle [927][b]	$24.0 \pm 4.0 \pm 3.0$	
$\mathcal{B}(B^0 \to K^+\pi^-\pi^0\gamma)$	*BABAR* [935][a]	$40.7 \pm 2.2 \pm 3.1$	40.7 ± 3.8
$\mathcal{B}(B^0 \to K_1(1270)^0\gamma)$	Belle [927]	< 58.0	< 58
$\mathcal{B}(B^0 \to K^0_S K^0_S \gamma)$	Belle [957][c]	< 0.58	< 0.58 *None*
$\mathcal{B}(B^0 \to f_2(1270)\gamma) \times \mathcal{B}(f_2(1270) \to K^0_S K^0_S)$	Belle [957][d]	< 0.31	< 0.31 *None*
$\mathcal{B}(B^0 \to f'_2(1525)\gamma) \times \mathcal{B}(f'_2(1525) \to K^0_S K^0_S)$	Belle [957][e]	< 0.21	< 0.21 *None*
$\mathcal{B}(B^0 \to K_1(1400)^0\gamma)$	Belle [927]	< 12.0	< 12
$\mathcal{B}(B^0 \to K^*_2(1430)^0\gamma)$	*BABAR* [936]	$12.2 \pm 2.5 \pm 1.0$	12.4 ± 2.4
	Belle [934]	$13.0 \pm 5.0 \pm 1.0$	
$\mathcal{B}(B^0 \to K^*_3(1780)^0\gamma)$	Belle [929]	< 30	< 30 < 83

[a] $m_{K\pi\pi} < 1.8$ GeV/c^2.
[b] $1 < m_{K\pi\pi} < 2$ GeV/c^2.
[c] Measured in bins of $m_{K^0_S K^0_S}$. We report the result for the full range, 1.0 GeV/c^2 $< m_{K^0_S K^0_S} <$ 3.0 GeV/c^2.
[d] Measured in bins of $m_{K^0_S K^0_S}$. We report the result for the full range, 1.00 GeV/c^2 $< m_{K^0_S K^0_S} <$ 1.44 GeV/c^2.
[e] Measured in bins of $m_{K^0_S K^0_S}$. We report the result for the full range, 1.44 GeV/c^2 $< m_{K^0_S K^0_S} <$ 1.63 GeV/c^2.

TABLE 200. Branching fractions of B^0 radiative and FCNC decays with leptons (part 3).

Parameter [10^{-6}]	Measurements		Average$^{\text{HFLAV}}_{PDG}$
$\mathcal{B}(B^0 \to \rho^0(770)\gamma)$	Belle [939]	$0.78^{+0.17+0.09}_{-0.16-0.10}$	0.86 ± 0.15
	BABAR [940]	$0.97^{+0.24}_{-0.22} \pm 0.06$	
$\mathcal{B}(\rho^0 X(214)) \times \mathcal{B}(X(214) \to \mu^+\mu^-)$	Belle [956][a]	< 0.0173	< 0.017
$\mathcal{B}(B^0 \to \omega(782)\gamma)$	Belle [939]	$0.40^{+0.19}_{-0.17} \pm 0.13$	0.44 ± 0.17
	BABAR [940]	$0.50^{+0.27}_{-0.23} \pm 0.09$	$0.44^{+0.18}_{-0.16}$
$\mathcal{B}(B^0 \to \phi(1020)\gamma)$	Belle [958]	< 0.1	< 0.1
	BABAR [959]	< 0.85	
$\mathcal{B}(B^0 \to p\bar{\Lambda}^0\pi^-\gamma)$	Belle [960]	< 0.65	< 0.65
$\mathcal{B}(B^0 \to \pi^0\ell^+\ell^-)$[b]	*BABAR* [943]	< 0.053	< 0.053
	Belle [942]	< 0.154	
$\mathcal{B}(B^0 \to \pi^0 e^+ e^-)$[b]	*BABAR* [943]	< 0.084	< 0.084
	Belle [942]	< 0.227	
$\mathcal{B}(B^0 \to \pi^0\mu^+\mu^-)$[b]	*BABAR* [943]	< 0.069	< 0.069
	Belle [942]	< 0.184	

[a] $X(214)$ is searched for in the mass range $[212, 300]$ MeV/c^2.
[b] Treatment of charmonium intermediate components differs between the results.

TABLE 201. Branching fractions of B^0 radiative and FCNC decays with leptons (part 4).

Parameter [10^{-6}]	Measurements		Average$^{\text{HFLAV}}_{PDG}$
$\mathcal{B}(B^0 \to \eta \ell^+ \ell^-)$	*BABAR* [943]	< 0.064	< 0.064
$\mathcal{B}(B^0 \to \eta e^+ e^-)$	*BABAR* [943]	< 0.108	< 0.11
$\mathcal{B}(B^0 \to \eta \mu^+ \mu^-)$	*BABAR* [943]	< 0.112	< 0.11
$\mathcal{B}(B^0 \to \pi^0 \nu\bar{\nu})$	Belle [945]	< 9.0	< 9.0
$\mathcal{B}(B^0 \to K^0 \ell^+ \ell^-)$[b]	LHCb [948][a,c]	$0.327 \pm 0.034 \pm 0.017$	0.328 ± 0.032
	Belle [504]	$0.351^{+0.069}_{-0.060} \pm 0.010$	$\mathit{0.329^{+0.063}_{-0.055}}$
	BABAR [947]	$0.21^{+0.15}_{-0.13} \pm 0.02$	
$\mathcal{B}(B^0 \to K^0 e^+ e^-)$[b]	Belle [504]	$0.306^{+0.098}_{-0.086} \pm 0.008$	0.249 ± 0.072
	BABAR [947]	$0.08^{+0.15}_{-0.12} \pm 0.01$	$\mathit{0.247^{+0.109}_{-0.094}}$
$\mathcal{B}(B^0 \to K^0 \mu^+ \mu^-)$[b]	LHCb [948]	$0.327 \pm 0.034 \pm 0.017$	0.341 ± 0.034
	Belle [504]	$0.394^{+0.096}_{-0.084} \pm 0.012$	$\mathit{0.339 \pm 0.035}$
	BABAR [947]	$0.49^{+0.29}_{-0.25} \pm 0.03$	
$\mathcal{B}(B^0 \to K^0 \nu\bar{\nu})$	Belle [945]	< 26.0	< 26
	BABAR [950]	< 49.0	
$\mathcal{B}(B^0 \to \rho^0(770) \nu\bar{\nu})$	Belle [945]	< 40.0	< 40
$\mathcal{B}(B^0 \to K^*(892)^0 \ell^+ \ell^-)$[b]	Belle [952]	$0.97^{+0.13}_{-0.11} \pm 0.07$	0.99 ± 0.12
	BABAR [947]	$1.03^{+0.22}_{-0.21} \pm 0.07$	$\mathit{0.99^{+0.12}_{-0.11}}$
$\mathcal{B}(B^0 \to K^*(892)^0 e^+ e^-)$[b]	Belle [952]	$1.18^{+0.27}_{-0.22} \pm 0.09$	1.04 ± 0.17
	BABAR [947]	$0.86^{+0.26}_{-0.24} \pm 0.05$	$\mathit{1.03^{+0.19}_{-0.17}}$
$\mathcal{B}(B^0 \to K^*(892)^0 \mu^+ \mu^-)$[b]	LHCb [961][d]	$0.904^{+0.016}_{-0.015} \pm 0.062$	0.94 ± 0.06
	Belle [952]	$1.06^{+0.19}_{-0.14} \pm 0.07$	$\mathit{0.94 \pm 0.05}$
	BABAR [947]	$1.35^{+0.40}_{-0.37} \pm 0.10$	
$\mathcal{B}(B^0 \to K^*(892)^0 \tau^+ \tau^-)$	Belle [962]	< 3100	< 3100
			None

[a]Not included in PDG average.

[b]Treatment of charmonium intermediate components differs between the results.

[c]Only muons are used.

[d]Multiple systematic uncertainties are added in quadrature.

TABLE 202. Branching fractions of B^0 radiative and FCNC decays with leptons (part 5).

Parameter [10^{-6}]	Measurements		Average$^{\text{HFLAV}}_{PDG}$
$\mathcal{B}(B^0 \to \pi^+\pi^-\mu^+\mu^-)$	LHCb [907][b,c,d]		0.021 ± 0.005
$\mathcal{B}(B^0 \to K^*(892)^0\nu\bar{\nu})$	Belle [945]	< 18.0	< 18
	Belle [953]	< 55.0	
	BABAR [950]	< 120.0	
$\mathcal{B}(B^0 \to \phi(1020)\nu\bar{\nu})$	Belle [953]	< 127.0	< 127
$\mathcal{B}(B^0 \to \pi^0 e^+\mu^-+\text{c.c.})$	*BABAR* [963]	< 0.14	< 0.14
$\mathcal{B}(B^0 \to K^0 e^+\mu^-+\text{c.c.})$	Belle [504]	< 0.038	< 0.038
	BABAR [964]	< 0.27	
$\mathcal{B}(B^0 \to K^*(892)^0 e^+\mu^-)$	LHCb [911][a]	< 0.0068	< 0.0068
	Belle [965]	< 0.16	*< 0.1600*
	BABAR [964]	< 0.53	
$\mathcal{B}(B^0 \to K^*(892)^0 e^-\mu^+)$	LHCb [911][a]	< 0.0057	< 0.0057
	Belle [965]	< 0.12	*< 0.1200*
	BABAR [964]	< 0.34	
$\mathcal{B}(B^0 \to K^*(892)^0 e^+\mu^-+\text{c.c.})$	LHCb [911][a]	< 0.0101	< 0.010
	Belle [965]	< 0.18	*< 0.180*
	BABAR [964]	< 0.58	
$\mathcal{B}(B^0 \to \Lambda_c^+\mu^-)$	*BABAR* [966]	< 1.4	< 1.4
$\mathcal{B}(B^0 \to \Lambda_c^+ e^-)$	*BABAR* [966]	< 4.0	< 4.0
$\mathcal{B}(B^0 \to \phi(1020)\mu^+\mu^-)$	LHCb [967][e]	< 0.0032	< 0.0032 *None*

[a]Preliminary result.
[b]The mass windows corresponding to ϕ and charmonium resonances decaying to $\mu\mu$ are vetoed.
[c]$0.5 < m_{\pi^+\pi^-} < 1.3$ GeV/c^2.
[d]Measurement of $\mathcal{B}(B^0 \to \pi^+\pi^-\mu^+\mu^-)/(\mathcal{B}(B^0 \to J/\psi K^*(892)^0)\mathcal{B}(J/\psi \to \mu^+\mu^-)\mathcal{B}(K^*(892)^0 \to K\pi) \times 2/3)$ used in our fit.
[e]LHCb also reports an upper limit at 2.3×10^{-9} excluding the ϕ and charmonium regions.

TABLE 203. Branching fractions of radiative, FCNC decays with leptons and LFV/LNV decays of $B^\pm/B^0$ admixture (part 1).

Parameter [10^{-6}]	Measurements		Average$^{\text{HFLAV}}_{PDG}$
$\mathcal{B}(B \to K\eta\gamma)$	Belle [929][b]	$8.5 \pm 1.3^{+1.2}_{-0.9}$	$8.5^{+1.8}_{-1.6}$
$\mathcal{B}(B \to K_1(1400)\gamma)$	CLEO [925]	< 127	< 127
$\mathcal{B}(B \to K_2^*(1430)\gamma)$	CLEO [925]	$16.6^{+5.9}_{-5.3} \pm 1.3$	$16.6^{+6.0}_{-5.5}$
$\mathcal{B}(B \to K_3^*(1780)\gamma)$	Belle [929]	< 14	< 14 *< 37*
$\mathcal{B}(B \to X_s\gamma)$	Belle [968][c,d]	$351 \pm 15 \pm 41$	349 ± 19
	BABAR [969][c,e]	$331 \pm 16 \pm 31$	
	Belle [970][c,f]	$375 \pm 18 \pm 35$	
	BABAR [971][c,f]	$352 \pm 20 \pm 51$	
	CLEO [972][c,g]	$328 \pm 44 \pm 28$	
	Belle II [973][a,c,e]	$366 \pm 81 \pm 86$	
	BABAR [974][c,f]	$390 \pm 91 \pm 64$	

(Table continued)

TABLE 203. *(Continued)*

Parameter [10^{-6}]	Measurements		Average$^{\text{HFLAV}}_{PDG}$
$\mathcal{B}(B \to X_d\gamma)$	*BABAR* [975]	$9.2 \pm 2.0 \pm 2.3$	9.2 ± 3.0
$\mathcal{B}(B \to \rho\gamma)$[h]	Belle [939]	$1.21^{+0.24}_{-0.22} \pm 0.12$	1.40 ± 0.22
	BABAR [940]	$1.73^{+0.34}_{-0.32} \pm 0.17$	$\mathit{1.39^{+0.25}_{-0.24}}$
$\mathcal{B}(B \to \rho/\omega\gamma)$[h]	Belle [939]	$1.14 \pm 0.20^{+0.10}_{-0.12}$	1.30 ± 0.18
	BABAR [940]	$1.63^{+0.30}_{-0.28} \pm 0.16$	$\mathit{1.30^{+0.23}_{-0.24}}$
$\mathcal{B}(B \to X_s e^+e^-)$[h,i,j]	*BABAR* [976][k]	$7.69^{+0.82+0.71}_{-0.77-0.60}$	6.67 ± 0.83
	Belle [977]	$4.04 \pm 1.30^{+0.87}_{-0.83}$	$\mathit{6.67^{+1.76}_{-1.63}}$
$\mathcal{B}(B \to X_s\mu^+\mu^-)$[i,j]	Belle [977]	$4.13 \pm 1.05^{+0.85}_{-0.81}$	4.27 ± 0.95
	BABAR [976][k]	$4.41^{+1.31+0.63}_{-1.17-0.50}$	$\mathit{4.27^{+0.99}_{-0.92}}$
$\mathcal{B}(B \to X_s\ell^+\ell^-)$[i,h,j]	*BABAR* [976][k]	$6.73^{+0.70+0.60}_{-0.64-0.56}$	5.84 ± 0.69
	Belle [977]	$4.11 \pm 0.83^{+0.85}_{-0.81}$	$\mathit{5.84^{+1.31}_{-1.23}}$

[a]Preliminary result.
[b]$m_{K\eta} < 2.4$ GeV$/c^2$.
[c]Measurement extrapolated to $E_\gamma > 1.6$ GeV using the method from Ref. [978].
[d]The systematic error includes a shape-function systematic of 0.01.
[e]The systematic error includes a shape-function systematic of 0.02.
[f]The systematic error includes a shape-function systematic of 0.04.
[g]The systematic error includes a shape-function systematic of 0.06.
[h]The PDG uncertainty includes a scale factor.
[i]Belle uses $m_{\ell^+\ell^-} > 0.2$ GeV$/c^2$, *BABAR* uses $m_{\ell^+\ell^-} > 0.1$ GeV$/c^2$.
[j]Treatment of charmonium intermediate components differs between the results.
[k]Multiple systematic uncertainties are added in quadrature.

TABLE 204. Branching fractions of radiative, FCNC decays with leptons and LFV/LNV decays of $B^\pm/B^0$ admixture (part 2).

Parameter [10^{-6}]	Measurements		Average$^{\text{HFLAV}}_{PDG}$
$\mathcal{B}(B \to \pi\ell^+\ell^-)$[b]	*BABAR* [943]	< 0.059	< 0.059
	Belle [942]	< 0.062	
$\mathcal{B}(B \to \pi e^+e^-)$	*BABAR* [943]	< 0.11	< 0.11
$\mathcal{B}(B \to \pi\mu^+\mu^-)$	*BABAR* [943]	< 0.05	< 0.05
$\mathcal{B}(B \to Ke^+e^-)$[b]	Belle [952]	$0.48^{+0.08}_{-0.07} \pm 0.03$	0.44 ± 0.06
	BABAR [947]	$0.388^{+0.090}_{-0.083} \pm 0.020$	
$\mathcal{B}(B \to K^*e^+e^-)$[c,b]	Belle [952]	$1.39^{+0.23}_{-0.20} \pm 0.12$	1.22 ± 0.16
	BABAR [947]	$0.99^{+0.23}_{-0.21} \pm 0.06$	$\mathit{1.19^{+0.21}_{-0.19}}$
	Belle II [979][a,d,e]	$1.42 \pm 0.48 \pm 0.09$	
$\mathcal{B}(B \to K\mu^+\mu^-)$[b]	CDF [878]	$0.42 \pm 0.04 \pm 0.02$	0.442 ± 0.036
	Belle [952]	$0.50 \pm 0.06 \pm 0.03$	
	BABAR [947]	$0.41^{+0.13}_{-0.12} \pm 0.02$	
$\mathcal{B}(B \to K^*\mu^+\mu^-)$[b]	CDF [878]	$1.01 \pm 0.10 \pm 0.05$	1.07 ± 0.09
	Belle [952]	$1.10^{+0.16}_{-0.14} \pm 0.08$	$\mathit{1.06 \pm 0.09}$
	Belle II [979][a,d]	$1.19 \pm 0.31^{+0.08}_{-0.07}$	
	BABAR [947]	$1.35^{+0.35}_{-0.33} \pm 0.10$	

(Table continued)

TABLE 204. *(Continued)*

Parameter [10^{-6}]	Measurements		Average$^{\text{HFLAV}}_{PDG}$
$\mathcal{B}(B \to K\ell^+\ell^-)$[b]	Belle [952]	$0.48^{+0.05}_{-0.04} \pm 0.03$	0.48 ± 0.04
	BABAR [980]	$0.47 \pm 0.06 \pm 0.02$	
$\mathcal{B}(B \to K^*\ell^+\ell^-)$[b]	Belle [952]	$1.07^{+0.11}_{-0.10} \pm 0.09$	1.07 ± 0.10
	BABAR [980]	$1.02^{+0.14}_{-0.13} \pm 0.05$	*1.05 ± 0.10*
	Belle II [979][a,d,e]	$1.25 \pm 0.30^{+0.08}_{-0.07}$	

[a]Preliminary result.
[b]Treatment of charmonium intermediate components differs between the results.
[c]The PDG uncertainty includes a scale factor.
[d]J/ψ and $\psi(2S)$ regions are vetoed.
[e]$m_{e^+e^-} > 0.14$ GeV/c^2.

TABLE 205. Branching fractions of radiative, FCNC decays with leptons and LFV/LNV decays of $B^\pm/B^0$ admixture (part 3).

Parameter [10^{-6}]	Measurements		Average$^{\text{HFLAV}}_{PDG}$
$\mathcal{B}(B \to K\nu\bar{\nu})$	Belle [945]	< 16.0	< 16
	BABAR [950]	< 17.0	
$\mathcal{B}(B \to K^*\nu\bar{\nu})$	Belle [945]	< 27.0	< 27
	BABAR [950]	< 76.0	
$\mathcal{B}(B \to \pi\nu\bar{\nu})$	Belle [945]	< 8.0	< 8.0
$\mathcal{B}(B \to \rho\nu\bar{\nu})$	Belle [945]	< 28.0	< 28
$\mathcal{B}(B \to \pi e^\pm\mu^\mp)$	*BABAR* [963]	< 0.092	< 0.092
$\mathcal{B}(B \to \rho e^\pm\mu^\mp)$	CLEO [981]	< 3.2	< 3.2
$\mathcal{B}(B \to K e^\pm\mu^\mp)$	*BABAR* [964]	< 0.038	< 0.038
$\mathcal{B}(B \to K^* e^\pm\mu^\mp)$	*BABAR* [964]	< 0.51	< 0.51

TABLE 206. Branching fractions of leptonic and radiative-leptonic B^+ and B^0 decays (part 1).

Parameter [10^{-7}]	Measurements		Average$^{\text{HFLAV}}_{PDG}$
$\mathcal{B}(B^+ \to e^+\nu_e)$	Belle [982]	< 9.8	< 9.8
	BABAR [983]	< 19	
$\mathcal{B}(B^+ \to \mu^+\nu_\mu)$	Belle [984]	< 8.6	< 8.6
	BABAR [983]	< 10	
	Belle [985]	< 10.7	
$\mathcal{B}(B^+ \to \tau^+\nu_\tau)$[a]	Belle [986]	$720^{+270}_{-250} \pm 110$	1094 ± 208
	Belle [987]	$1250 \pm 280 \pm 270$	*1094^{+247}_{-236}*
	BABAR [988]	$1830^{+530}_{-490} \pm 240$	
	BABAR [989]	$1700 \pm 800 \pm 200$	
$\mathcal{B}(B^+ \to \ell^+\nu_\ell\gamma)$	Belle [990][b]	< 30	< 30
	BABAR [991]	< 156	

(Table continued)

TABLE 206. *(Continued)*

Parameter [10^{-7}]	Measurements		Average$^{\text{HFLAV}}_{PDG}$
$\mathcal{B}(B^+ \to e^+\nu_e\gamma)$	Belle [990][b]	< 43	< 43
	BABAR [991]	< 170	
$\mathcal{B}(B^+ \to \mu^+\nu_\mu\gamma)$	Belle [990][b]	< 34	< 34
	BABAR [991]	< 260	
$\mathcal{B}(B^0 \to \gamma\gamma)$	*BABAR* [992]	< 3.3	< 3.3
	Belle [993]	< 6.2	< 3.2
$\mathcal{B}(B^0 \to e^+e^-)$	LHCb [899]	< 0.025	< 0.025
	CDF [900]	< 0.83	
	BABAR [994]	< 1.13	
	Belle [995]	< 1.9	
$\mathcal{B}(B^0 \to e^+e^-\gamma)$	*BABAR* [996]	< 1.2	< 1.2

[a]The PDG uncertainty includes a scale factor.
[b]$E_\gamma > 1$ GeV.

TABLE 207. Branching fractions of leptonic and radiative-leptonic B^+ and B^0 decays (part 2).

Parameter [10^{-7}]	Measurements		Average$^{\text{HFLAV}}_{PDG}$
$\mathcal{B}(B^0 \to \mu^+\mu^-\gamma)$	*BABAR* [996]	< 1.5	< 1.5 *None*
$\mathcal{B}(B^0 \to \mu^+\mu^-\mu^+\mu^-)$	LHCb [904][a,b,c]	< 0.0018	< 0.0018
$\mathcal{B}(B^0 \to SP) \times \mathcal{B}(S \to \mu^+\mu^-) \times \mathcal{B}(P \to \mu^+\mu^-)$	LHCb [997][b,c]	< 0.006	< 0.0060
$\mathcal{B}(B^0 \to aa) \times \mathcal{B}(a \to \mu^+\mu^-) \times \mathcal{B}(a \to \mu^+\mu^-)$	LHCb [904][b,d,c]	< 0.0023	< 0.0023 *None*
$\mathcal{B}(B^0 \to \tau^+\tau^-)$[e]	LHCb [902]	< 16000	< 16000
	BABAR [998]	< 41000	< 21000
$\mathcal{B}(B^0 \to \nu\bar{\nu})$	*BABAR* [999]	< 240	< 240
	Belle [1000]	< 780	
$\mathcal{B}(B^0 \to \nu\bar{\nu}\gamma)$	Belle [1000][f]	< 160	< 160
	BABAR [999][g]	< 170	
$\mathcal{B}(B^+ \to \mu^+\mu^-\mu^+\nu_\mu)$	LHCb [1001][c]	< 0.16	< 0.16

[a]Not included in PDG average.
[b]The mass windows corresponding to ϕ and charmonium resonances decaying to $\mu\mu$ are vetoed.
[c]At CL $= 95\%$.
[d]a is a promptly decaying scalar particle with a mass of 1 GeV$/c^2$.
[e]PDG shows the result obtained at 95% CL.
[f]$E_\gamma > 0.5$ GeV.
[g]$E_\gamma > 1.2$ GeV.

TABLE 208. Relative branching fractions of B radiative and FCNC decays with leptons (part 1).

Parameter	Measurements		Average
$\frac{\mathcal{B}(B^+\to\pi^+\mu^+\mu^-)}{\mathcal{B}(B^+\to K^+\mu^+\mu^-)}$, $1.0 < m^2_{\ell^+\ell^-} < 6.0$ GeV^2/c^4	LHCb [944]	$0.038 \pm 0.009 \pm 0.001$	0.038 ± 0.009
$\frac{\mathcal{B}(B^+\to K^+\mu^+\mu^-)}{\mathcal{B}(B^+\to K^+e^+e^-)}$, Full $m^2_{\ell^+\ell^-}$range	Belle [504]	$1.08^{+0.16}_{-0.15} \pm 0.02$	1.08 ± 0.16
$\frac{\mathcal{B}(B^+\to K^+\mu^+\mu^-)}{\mathcal{B}(B^+\to K^+e^+e^-)}$, $0.1 < m^2_{\ell^+\ell^-} < 1.1$ GeV^2/c^4	LHCb [1002]	$0.994^{+0.090+0.029}_{-0.082-0.027}$	0.994 ± 0.090
$\frac{\mathcal{B}(B^+\to K^+\mu^+\mu^-)}{\mathcal{B}(B^+\to K^+e^+e^-)}$, $1.1 < m^2_{\ell^+\ell^-} < 6.0$ GeV^2/c^4	LHCb [1002] CMS[a]	$0.949^{+0.042}_{-0.041} \pm 0.022$ $0.78^{+0.47}_{-0.23}$	0.947 ± 0.047
$\frac{\mathcal{B}(B^+\to K^+\mu^+\mu^-)}{\mathcal{B}(B^+\to K^+e^+e^-)}$, $0.10 < m^2_{\ell^+\ell^-} < 8.12$ GeV^2/c^4 and $m^2_{\ell^+\ell^-} > 10.11$ GeV^2/c^4	*BABAR* [980]	$1.00^{+0.31}_{-0.25} \pm 0.07$	$1.00^{+0.32}_{-0.26}$
$\frac{\mathcal{B}(B^+\to K^+\mu^+\mu^-)}{\mathcal{B}(B^+\to K^+e^+e^-)}$, $1.0 < m^2_{\ell^+\ell^-} < 6.0$ GeV^2/c^4[b]	Belle [504]	$1.39^{+0.36}_{-0.33} \pm 0.02$	1.39 ± 0.35
$\frac{\mathcal{B}(B^0\to K^0_S\mu^+\mu^-)}{\mathcal{B}(B^0\to K^0_S e^+e^-)}$, Full$m^2_{\ell^+\ell^-}$range	Belle [504]	$1.29^{+0.52}_{-0.45} \pm 0.01$	$1.29^{+0.52}_{-0.45}$
$\frac{\mathcal{B}(B^0\to K^0_S\mu^+\mu^-)}{\mathcal{B}(B^0\to K^0_S e^+e^-)}$, $1.0 < m^2_{\ell^+\ell^-} < 6.0$ GeV^2/c^4[b]	Belle [504]	$0.55^{+0.46}_{-0.34} \pm 0.01$	$0.55^{+0.46}_{-0.34}$
$\frac{\mathcal{B}(B^0\to K^0_S\mu^+\mu^-)}{\mathcal{B}(B^0\to K^0_S e^+e^-)}$, $1.1 < m^2_{\ell^+\ell^-} < 6.0$ GeV^2/c^4	LHCb [1003]	$0.66^{+0.20+0.02}_{-0.14-0.04}$	$0.66^{+0.20}_{-0.15}$
$\frac{\mathcal{B}(B\to K\mu^+\mu^-)}{\mathcal{B}(B\to Ke^+e^-)}$, Full $m^2_{\ell^+\ell^-}$ range	Belle [504]	$1.10^{+0.16}_{-0.15} \pm 0.02$	1.10 ± 0.16
$\frac{\mathcal{B}(B\to K\mu^+\mu^-)}{\mathcal{B}(B\to Ke^+e^-)}$, $1.0 < m^2_{\ell^+\ell^-} < 6.0$ GeV^2/c^4[b]	Belle [504]	$1.03^{+0.28}_{-0.24} \pm 0.01$	$1.03^{+0.28}_{-0.24}$

[a]Preliminary result.

[b]For the other bins see the article.

TABLE 209. Relative branching fractions of B radiative and FCNC decays with leptons (part 2).

Parameter	Measurements		Average
$\frac{\mathcal{B}(B\to K^*\mu^+\mu^-)}{\mathcal{B}(B\to K^*e^+e^-)}$, Full $m^2_{\ell^+\ell^-}$range	Belle [952]	$0.83 \pm 0.17 \pm 0.08$	0.83 ± 0.19
$\frac{\mathcal{B}(B\to K^*\mu^+\mu^-)}{\mathcal{B}(B\to K^*e^+e^-)}$, $0.10 < m^2_{\ell^+\ell^-} < 8.12$ GeV^2/c^4 and $m^2_{\ell^+\ell^-} > 10.11$ GeV^2/c^4	*BABAR* [980]	$1.13^{+0.34}_{-0.26} \pm 0.10$	$1.13^{+0.35}_{-0.28}$
$\frac{\mathcal{B}(B\to K^*\mu^+\mu^-)}{\mathcal{B}(B\to K^*e^+e^-)}$, $0.045 < m^2_{\ell^+\ell^-} < 1.1$ GeV^2/c^4	Belle [1004]	$0.52^{+0.36}_{-0.26} \pm 0.06$	$0.52^{+0.36}_{-0.27}$
$\frac{\mathcal{B}(B\to K^*\mu^+\mu^-)}{\mathcal{B}(B\to K^*e^+e^-)}$, $1.1 < m^2_{\ell^+\ell^-} < 6.0$ GeV^2/c^4	Belle [1004]	$0.96^{+0.45}_{-0.29} \pm 0.11$	$0.96^{+0.46}_{-0.31}$
$\frac{\mathcal{B}(B\to K^*\mu^+\mu^-)}{\mathcal{B}(B\to K^*e^+e^-)}$, $15 < m^2_{\ell^+\ell^-} < 19$ GeV^2/c^4	Belle [1004]	$1.18^{+0.52}_{-0.32} \pm 0.11$	$1.18^{+0.53}_{-0.34}$
$\frac{\mathcal{B}(B^0\to K^*(892)^0\mu^+\mu^-)}{\mathcal{B}(B^0\to K^*(892)^0e^+e^-)}$, $0.045 < m^2_{\ell^+\ell^-} < 1.1$ GeV^2/c^4	Belle [1004]	$0.46^{+0.55}_{-0.27} \pm 0.13$	$0.46^{+0.56}_{-0.30}$
$\frac{\mathcal{B}(B^0\to K^*(892)^0\mu^+\mu^-)}{\mathcal{B}(B^0\to K^*(892)^0e^+e^-)}$, $1.1 < m^2_{\ell^+\ell^-} < 6.0$ GeV^2/c^4	LHCb [1002] Belle [1004]	$1.027^{+0.072+0.027}_{-0.068-0.026}$ $1.06^{+0.63}_{-0.38} \pm 0.14$	1.028 ± 0.074
$\frac{\mathcal{B}(B^0\to K^*(892)^0\mu^+\mu^-)}{\mathcal{B}(B^0\to K^*(892)^0e^+e^-)}$, $15 < m^2_{\ell^+\ell^-} < 19$ GeV^2/c^4	Belle [1004]	$1.12^{+0.61}_{-0.36} \pm 0.10$	$1.12^{+0.62}_{-0.37}$
$\frac{\mathcal{B}(B^0\to K^*(892)^0\mu^+\mu^-)}{\mathcal{B}(B^0\to K^*(892)^0e^+e^-)}$, $0.1 < m^2_{\ell^+\ell^-} < 1.1$ GeV^2/c^4	LHCb [1002]	$0.927^{+0.093+0.036}_{-0.087-0.035}$	0.927 ± 0.097
$\frac{\mathcal{B}(B^+\to K^*(892)^+\mu^+\mu^-)}{\mathcal{B}(B^+\to K^*(892)^+e^+e^-)}$, $0.045 < m^2_{\ell^+\ell^-} < 1.1$ GeV^2/c^4	Belle [1004]	$0.62^{+0.60}_{-0.36} \pm 0.09$	$0.62^{+0.61}_{-0.37}$
$\frac{\mathcal{B}(B^+\to K^*(892)^+\mu^+\mu^-)}{\mathcal{B}(B^+\to K^*(892)^+e^+e^-)}$, $1.1 < m^2_{\ell^+\ell^-} < 6.0$ GeV^2/c^4	Belle [1004]	$0.72^{+0.99}_{-0.44} \pm 0.15$	$0.7^{+1.0}_{-0.5}$
$\frac{\mathcal{B}(B^+\to K^*(892)^+\mu^+\mu^-)}{\mathcal{B}(B^+\to K^*(892)^+e^+e^-)}$, $15 < m^2_{\ell^+\ell^-} < 19$ GeV^2/c^4	Belle [1004]	$1.40^{+1.99}_{-0.68} \pm 0.12$	$1.4^{+2.0}_{-0.7}$
$\frac{\mathcal{B}(B^+\to K^*(892)^+\mu^+\mu^-)}{\mathcal{B}(B^+\to K^*(892)^+e^+e^-)}$, $0.045 < m^2_{\ell^+\ell^-} < 6.0$ GeV^2/c^4	LHCb [1003]	$0.70^{+0.18+0.03}_{-0.13-0.04}$	$0.70^{+0.18}_{-0.14}$

TABLE 210. Relative branching fractions of B radiative and FCNC decays with leptons (part 3).

Parameter	Measurements		Average
$\frac{\mathcal{B}(B^0\to K^*(892)^0\gamma)}{\mathcal{B}(B_s^0\to\phi(1020)\gamma)}$	LHCb [898][a]	$1.23 \pm 0.06 \pm 0.11$	1.21 ± 0.11
	Belle [922][a]	$1.10 \pm 0.16 \pm 0.20$	
$\frac{\mathcal{B}(B^0\to\mu^+\mu^-)}{\mathcal{B}(B_s^0\to\mu^+\mu^-)}$ $[10^{-2}]$	LHCb [903]	< 8.1	< 8.1
$\frac{\mathcal{B}(B^0\to\phi(1020)\mu^+\mu^-)}{\mathcal{B}(B_s^0\to\phi(1020)\mu^+\mu^-)}$ $[10^{-3}]$	LHCb [967][b]	< 4.4	< 4.4
$\frac{\mathcal{B}(B^0\to\pi^+\pi^-\mu^+\mu^-)}{\mathcal{B}(B^0\to J/\psi K^{*0})\times\mathcal{B}(J/\psi\to\mu^+\mu^-)\times\mathcal{B}(K^{*0}\to K^+\pi^-)}$ $[10^{-4}]$	LHCb [907][c,d]	$4.1 \pm 1.0 \pm 0.3$	4.1 ± 1.0

[a]Multiple systematic uncertainties are added in quadrature.
[b]ϕ and charmonium regions excluded from the dimuon spectrum.
[c]The mass windows corresponding to ϕ and charmonium resonances decaying to $\mu\mu$ are vetoed.
[d]$0.5 < m_{\pi^+\pi^-} < 1.3$ GeV/c^2.

TABLE 211. Branching fractions of $B^+/B^0 \to q\bar{q}'$ gluon decays.

Parameter $[10^{-4}]$	Measurements		Average$^{\text{HFLAV}}_{PDG}$
$\mathcal{B}(B \to \eta X)$	Belle [1005][a]	$2.610 \pm 0.300^{+0.440}_{-0.740}$	$2.61^{+0.53}_{-0.80}$
	CLEO [1006][b]	< 4.400	
$\mathcal{B}(B \to \eta' X)$	*BABAR* [1007][c]	$3.90 \pm 0.80 \pm 0.90$	4.24 ± 0.87
	CLEO [1008][c]	$4.60 \pm 1.10 \pm 0.60$	
$\mathcal{B}(B \to K^+ X)$	*BABAR* [1009][d]	< 1.87	< 1.9
$\mathcal{B}(B \to K^0 X)$	*BABAR* [1009][d]	$1.95^{+0.51}_{-0.45} \pm 0.50$	1.95 ± 0.69
			$1.95^{+0.71}_{-0.67}$
$\mathcal{B}(B \to \pi^+ X)$	*BABAR* [1009][e]	$3.72^{+0.50}_{-0.47} \pm 0.59$	3.72 ± 0.76
			$3.72^{+0.77}_{-0.75}$

[a]$0.4 < m_X < 2.6$ GeV/c^2.
[b]$2.1 < p_\eta < 2.7$ GeV/c.
[c]$2.0 < p^*(\eta') < 2.7$ GeV/c.
[d]$p^*(K) < 2.34$ GeV/c.
[e]$p^*(\pi^+) < 2.36$ GeV/c.

TABLE 212. Isospin asymmetry in B mesons radiative and FCNC decays with leptons. In some of the B-factory results it is assumed that $\mathcal{B}(\Upsilon(4S) \to B^+B^-) = \mathcal{B}(\Upsilon(4S) \to B^0\bar{B}^0)$, and in others a measured value of the ratio of branching fractions is used. See original papers for details. The averages quoted here are computed naively and should be treated with caution.

Parameter	Measurements		Average$^{\text{HFLAV}}_{PDG}$
$\Delta_{0^-}(B \to X_s\gamma)$	Belle [1010][a,b]	$-0.0048 \pm 0.0149 \pm 0.0150$	-0.005 ± 0.020
	BABAR [1011][a,b]	$-0.006 \pm 0.058 \pm 0.026$	
$\Delta_{0^-}(B \to X_{s+d}\gamma)$	*BABAR* [974][c]	$-0.06 \pm 0.15 \pm 0.07$	-0.06 ± 0.17
$\Delta_{0^+}(B \to K^*\gamma)$	Belle [922][b]	$0.062 \pm 0.015 \pm 0.013$	0.063 ± 0.017
	BABAR [923]	$0.066 \pm 0.021 \pm 0.022$	

(Table continued)

TABLE 212. *(Continued)*

Parameter	Measurements		Average$^{\text{HFLAV}}_{PDG}$
$\frac{\Gamma(B^+\to\rho^+\gamma)}{2\Gamma(B^0\to\rho^0\gamma)}-1$	Belle [939]	$-0.48^{+0.21+0.08}_{-0.19-0.09}$	-0.46 ± 0.17
	BABAR [940]	$-0.43^{+0.25}_{-0.22}\pm0.10$	$\mathit{-0.46^{+0.17}_{-0.16}}$
$\Delta_{0-}(B\to K\ell^+\ell^-)$[d]	LHCb [948][e]	$-0.10^{+0.08}_{-0.09}\pm0.02$	$-0.191^{+0.073}_{-0.071}$
	Belle [504][f]	$-0.31^{+0.13}_{-0.11}\pm0.01$	$\mathit{-0.148^{+0.064}_{-0.065}}$
	BABAR [980][f]	$-0.41\pm0.25\pm0.01$	
$\Delta_{0-}(B\to K^*\ell^+\ell^-)$[d]	*BABAR* [980][f]	$-0.20^{+0.30}_{-0.23}\pm0.03$	$-0.01^{+0.11}_{-0.09}$
	Belle [952][f]	$0.33^{+0.37}_{-0.43}\pm0.08$	$\mathit{-0.03^{+0.08}_{-0.07}}$
	LHCb [948][e]	$0.00^{+0.12}_{-0.10}\pm0.02$	
$\Delta_{0^-}(B\to K^{(*)}\ell^+\ell^-)$[d]	Belle [952][g]	$-0.30^{+0.12}_{-0.11}\pm0.08$	-0.45 ± 0.10
	BABAR [947][h]	$-0.64^{+0.15}_{-0.14}\pm0.03$	$\mathit{-0.45^{+0.17}_{-0.16}}$

[a] $m_{X_s}<2.8$ GeV/c^2.
[b] Multiple systematic uncertainties are added in quadrature.
[c] $E_\gamma>2.2$ GeV.
[d] The PDG uncertainty includes a scale factor.
[e] Only muons are used, $1.1<m^2_{\ell^+\ell^-}<6.0$ GeV^2/c^4.
[f] $1.0<m^2_{\ell^+\ell^-}<6.0$ GeV^2/c^4.
[g] $m^2_{\ell^+\ell^-}<8.68$ GeV^2/c^4.
[h] $0.1<m^2_{\ell^+\ell^-}<7.02$ GeV^2/c^4.

TABLE 213. Branching fractions of semileptonic B^+ decays to LFV and LNV final states (part 1).

Parameter [10^{-6}]	Measurements		Average$^{\text{HFLAV}}_{PDG}$
$\mathcal{B}(B^+\to\pi^+e^+\mu^-+\text{c.c.})$	*BABAR* [963]	<0.17	<0.17
$\mathcal{B}(B^+\to\pi^+e^+\tau^-)$	*BABAR* [1012]	<74.0	<74
$\mathcal{B}(B^+\to\pi^+e^-\tau^+)$	*BABAR* [1012]	<20.0	<20
$\mathcal{B}(B^+\to\pi^+e^+\tau^-+\text{c.c.})$	*BABAR* [1012]	<75.0	<75
$\mathcal{B}(B^+\to\pi^+\mu^+\tau^-)$	*BABAR* [1012]	<62.0	<62
$\mathcal{B}(B^+\to\pi^+\mu^-\tau^+)$	*BABAR* [1012]	<45.0	<45
$\mathcal{B}(B^+\to\pi^+\mu^+\tau^-+\text{c.c.})$	*BABAR* [1012]	<72.0	<72
$\mathcal{B}(B^+\to K^+e^+\mu^-)$	LHCb [1013]	<0.0070	<0.007
	Belle [504]	<0.03	
	BABAR [964]	<0.091	
$\mathcal{B}(B^+\to K^+e^-\mu^+)$	LHCb [1013]	<0.0064	<0.0064
	Belle [504]	<0.085	
	BABAR [964]	<0.13	

(Table continued)

TABLE 213. *(Continued)*

Parameter [10^{-6}]	Measurements		Average$^{\text{HFLAV}}_{PDG}$
$\mathcal{B}(B^+ \to K^+ e^+ \mu^- + \text{c.c.})$	*BABAR* [964]	< 0.091	< 0.091
$\mathcal{B}(B^+ \to K^+ e^+ \tau^-)$	*BABAR* [1012]	< 43.0	< 43
$\mathcal{B}(B^+ \to K^+ e^- \tau^+)$	*BABAR* [1012]	< 15.0	< 15
	Belle [901][a]	< 15.1	
$\mathcal{B}(B^+ \to K^+ e^+ \tau^- + \text{c.c.})$	*BABAR* [1012]	< 30.0	< 30
$\mathcal{B}(B^+ \to K^+ \mu^+ \tau^-)$	Belle [901][a]	< 24.5	< 24
	BABAR [1012]	< 45.0	*< 45*
$\mathcal{B}(B^+ \to K^+ \mu^- \tau^+)$	Belle [901][a]	< 5.9	< 5.9
	BABAR [1012]	< 28.0	*< 28.0*
	LHCb [1014]	< 39.0	
$\mathcal{B}(B^+ \to K^+ \mu^+ \tau^- + \text{c.c.})$	*BABAR* [1012]	< 48.0	< 48

[a]Not included in PDG average.

TABLE 214. Branching fractions of semileptonic B^+ decays to LFV and LNV final states (part 2).

Parameter [10^{-6}]	Measurements		Average$^{\text{HFLAV}}_{PDG}$
$\mathcal{B}(B^+ \to K^*(892)^+ e^+ \mu^-)$	*BABAR* [964]	< 1.30	< 1.3
$\mathcal{B}(B^+ \to K^*(892)^+ e^- \mu^+)$	*BABAR* [964]	< 0.99	< 0.99
$\mathcal{B}(B^+ \to K^*(892)^+ e^+ \mu^- + \text{c.c.})$	*BABAR* [964]	< 1.40	< 1.4
$\mathcal{B}(B^+ \to \pi^- e^+ e^+)$	*BABAR* [1015]	< 0.023	< 0.023
$\mathcal{B}(B^+ \to \pi^- \mu^+ \mu^+)$	LHCb [1016][a]	< 0.0040	< 0.004
	BABAR [1015]	< 0.107	
$\mathcal{B}(B^+ \to \pi^- e^+ \mu^+)$	*BABAR* [1017]	< 0.15	< 0.15
$\mathcal{B}(B^+ \to \rho^-(770) e^+ e^+)$	*BABAR* [1017]	< 0.17	< 0.17
$\mathcal{B}(B^+ \to \rho^-(770) \mu^+ \mu^+)$	*BABAR* [1017]	< 0.42	< 0.42
$\mathcal{B}(B^+ \to \rho^-(770) e^+ \mu^+)$	*BABAR* [1017]	< 0.47	< 0.47

[a]At CL $= 95\%$.

TABLE 215. Branching fractions of semileptonic B^+ decays to LFV and LNV final states (part 3).

Parameter [10^{-6}]	Measurements		Average$^{\text{HFLAV}}_{PDG}$
$\mathcal{B}(B^+ \to K^- e^+ e^+)$	*BABAR* [1015]	< 0.030	< 0.030
$\mathcal{B}(B^+ \to K^- \mu^+ \mu^+)$	LHCb [1018]	< 0.041	< 0.041
	BABAR [1015]	< 0.067	
$\mathcal{B}(B^+ \to K^- e^+ \mu^+)$	*BABAR* [1017]	< 0.16	< 0.16
$\mathcal{B}(B^+ \to K^*(892)^- e^+ e^+)$	*BABAR* [1017]	< 0.40	< 0.40
$\mathcal{B}(B^+ \to K^*(892)^- \mu^+ \mu^+)$	*BABAR* [1017]	< 0.59	< 0.59
$\mathcal{B}(B^+ \to K^*(892)^- e^+ \mu^+)$	*BABAR* [1017]	< 0.30	< 0.30
$\mathcal{B}(B^+ \to D^- e^+ e^+)$	*BABAR* [1017]	< 2.6	< 2.6
	Belle [600]	< 2.6	

(Table continued)

TABLE 215. *(Continued)*

Parameter [10^{-6}]	Measurements		Average$^{\text{HFLAV}}_{PDG}$
$\mathcal{B}(B^+ \to D^- e^+ \mu^+)$	Belle [600]	< 1.8	< 1.8
	BABAR [1017]	< 2.1	
	LHCb [1019][a]	< 0.69	
$\mathcal{B}(B^+ \to D^- \mu^+ \mu^+)$	Belle [600]	< 1.0	< 0.69
	BABAR [1017]	< 1.7	
$\mathcal{B}(B^+ \to D^*(2010)^- \mu^+ \mu^+)$	LHCb [1019][a]	< 2.4	< 2.4
$\mathcal{B}(B^+ \to D_s^- \mu^+ \mu^+)$	LHCb [1019][a]	< 0.58	< 0.58
$\mathcal{B}(B^+ \to \bar{D}^0 \pi^- \mu^+ \mu^+)$	LHCb [1019][a]	< 1.5	< 1.5
$\mathcal{B}(B^+ \to \Lambda^0 \mu^+)$	*BABAR* [966]	< 0.061	< 0.061 < 0.060
$\mathcal{B}(B^+ \to \Lambda^0 e^+)$	*BABAR* [966]	< 0.032	< 0.032
$\mathcal{B}(B^+ \to \bar{\Lambda}^0 \mu^+)$	*BABAR* [966]	< 0.062	< 0.062 < 0.060
$\mathcal{B}(B^+ \to \bar{\Lambda}^0 e^+)$	*BABAR* [966]	< 0.081	< 0.081 < 0.080

[a]At CL = 95%.

TABLE 216. Branching fractions of semileptonic B^0 decays to LFV and LNV final states.

Parameter [10^{-6}]	Measurements		Average$^{\text{HFLAV}}_{PDG}$
$\mathcal{B}(B^0 \to K^*(892)^0 e^- \mu^+)$	LHCb [911][a]	< 0.0057	< 0.0057 < 0.1200
	Belle [965]	< 0.12	
	BABAR [964]	< 0.34	
$\mathcal{B}(B^0 \to K^*(892)^0 e^+ \mu^-)$	LHCb [911][a]	< 0.0068	< 0.0068 < 0.1600
	Belle [965]	< 0.16	
	BABAR [964]	< 0.53	
$\mathcal{B}(B^0 \to K^*(892)^0 e^+ \mu^- + \text{c.c.})$	LHCb [911][a]	< 0.0101	< 0.010 < 0.180
	Belle [965]	< 0.18	
	BABAR [964]	< 0.58	
$\mathcal{B}(B^0 \to K^0 e^+ \mu^- + \text{c.c.})$	Belle [504]	< 0.038	< 0.038
	BABAR [964]	< 0.27	
$\mathcal{B}(B^0 \to \pi^0 e^+ \mu^- + \text{c.c.})$	*BABAR* [963]	< 0.14	< 0.14
$\mathcal{B}(B^0 \to e^+ \mu^- + \text{c.c.})$	LHCb [908]	< 0.0010	< 0.001
	CDF [900]	< 0.064	
	BABAR [994]	< 0.092	
	Belle [995]	< 0.17	
$\mathcal{B}(B^0 \to K^*(892)^0 \tau^+ \mu^-)$	LHCb [1020]	< 10	< 10 *None*
$\mathcal{B}(B^0 \to K^*(892)^0 \tau^- \mu^+)$	LHCb [1020]	< 8.2	< 8.2 *None*

(Table continued)

TABLE 216. *(Continued)*

Parameter [10^{-6}]	Measurements		Average$^{\text{HFLAV}}_{PDG}$
$\mathcal{B}(B^0 \to \tau^{\pm}\mu^{\mp})$[c]	LHCb [910]	< 12	
	Belle [1021][b]	< 15	< 12
	BABAR [1022]	< 22.0	*< 14*
$\mathcal{B}(B^0 \to \tau^{\pm}e^{\mp})$	Belle [1021][b]	< 16	< 16
	BABAR [1022]	< 28.0	
$\mathcal{B}(B^0 \to p\mu^-)$	LHCb [912]	< 0.0026	< 0.0026
			None

[a]Preliminary result.
[b]Not included in PDG average.
[c]PDG shows the result obtained at 95% CL.

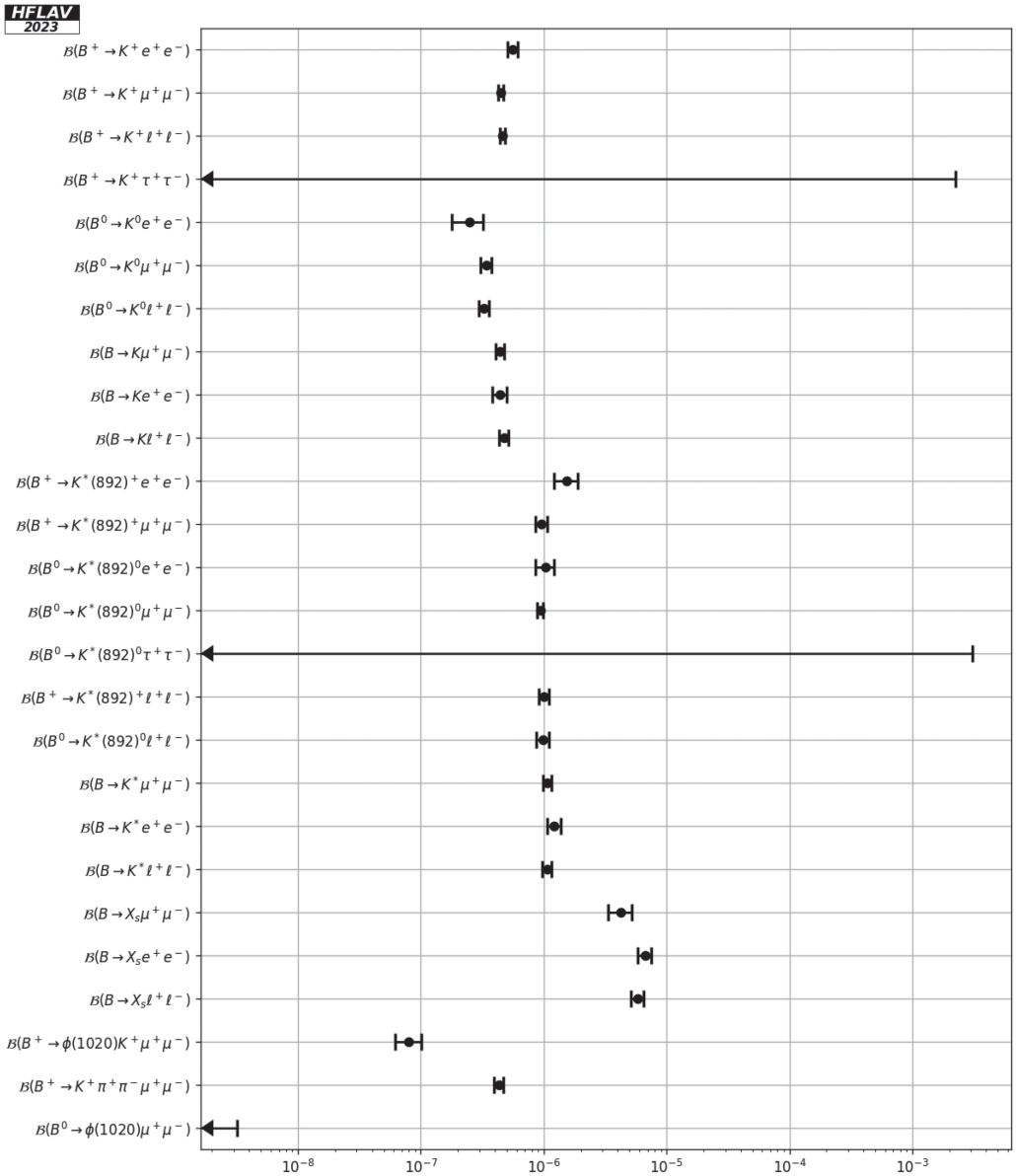


FIG. 35. Branching fractions of B^+ and B^0 decays of the type $b \to s\ell^+\ell^-$.

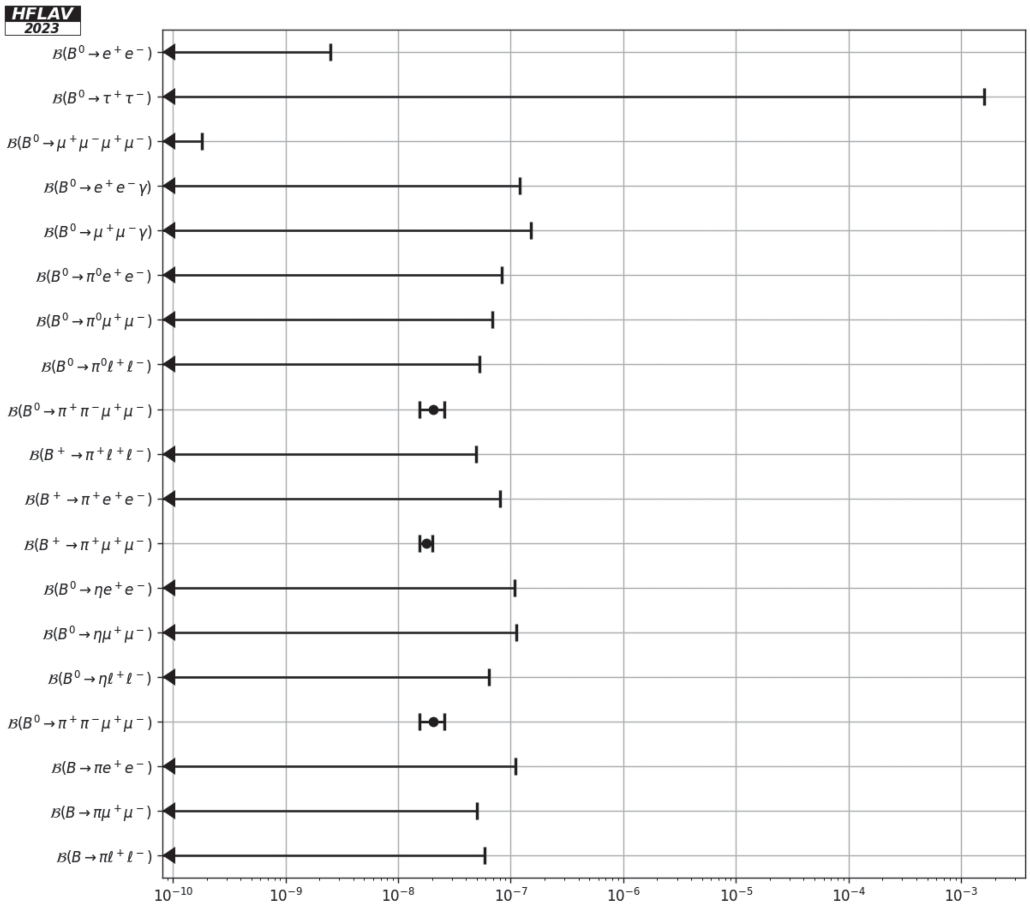


FIG. 36. Branching fractions of B^+ and B^0 decays of the type $b \to u\ell^+\ell^-$, purely leptonic and leptonic radiative.

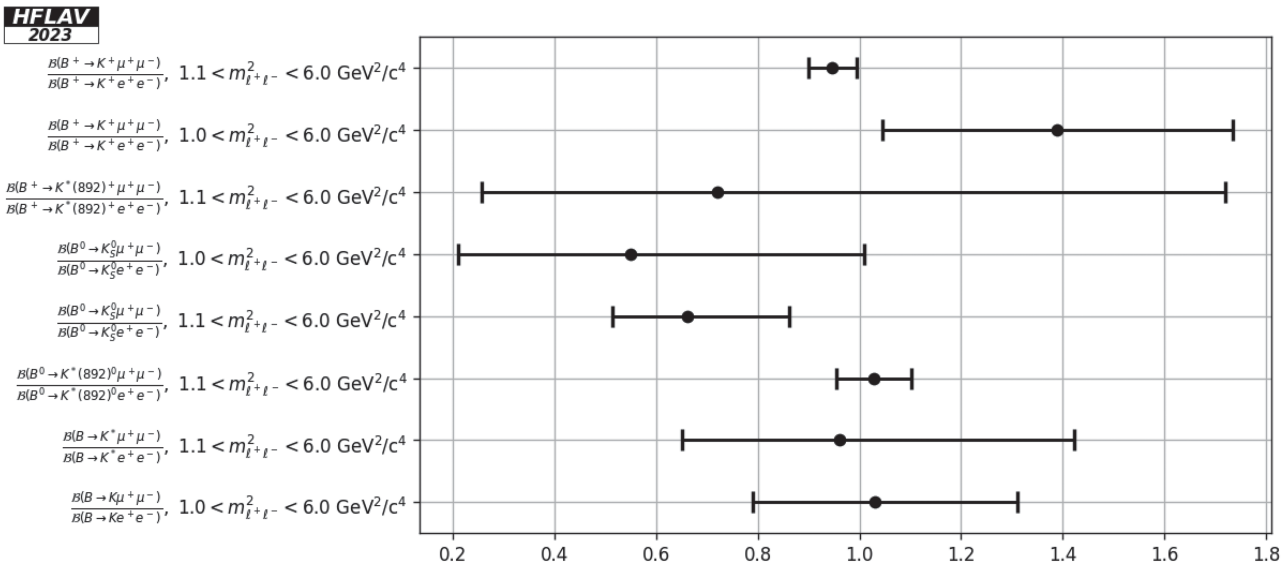


FIG. 37. Compilation of $R_K^{(*)}$ ratios in the low dilepton invariant-mass region. These are ratios between branching fractions of B-meson decays to $K^{(*)}\mu^+\mu^-$ and $K^{(*)}e^+e^-$, which provide information on lepton universality.

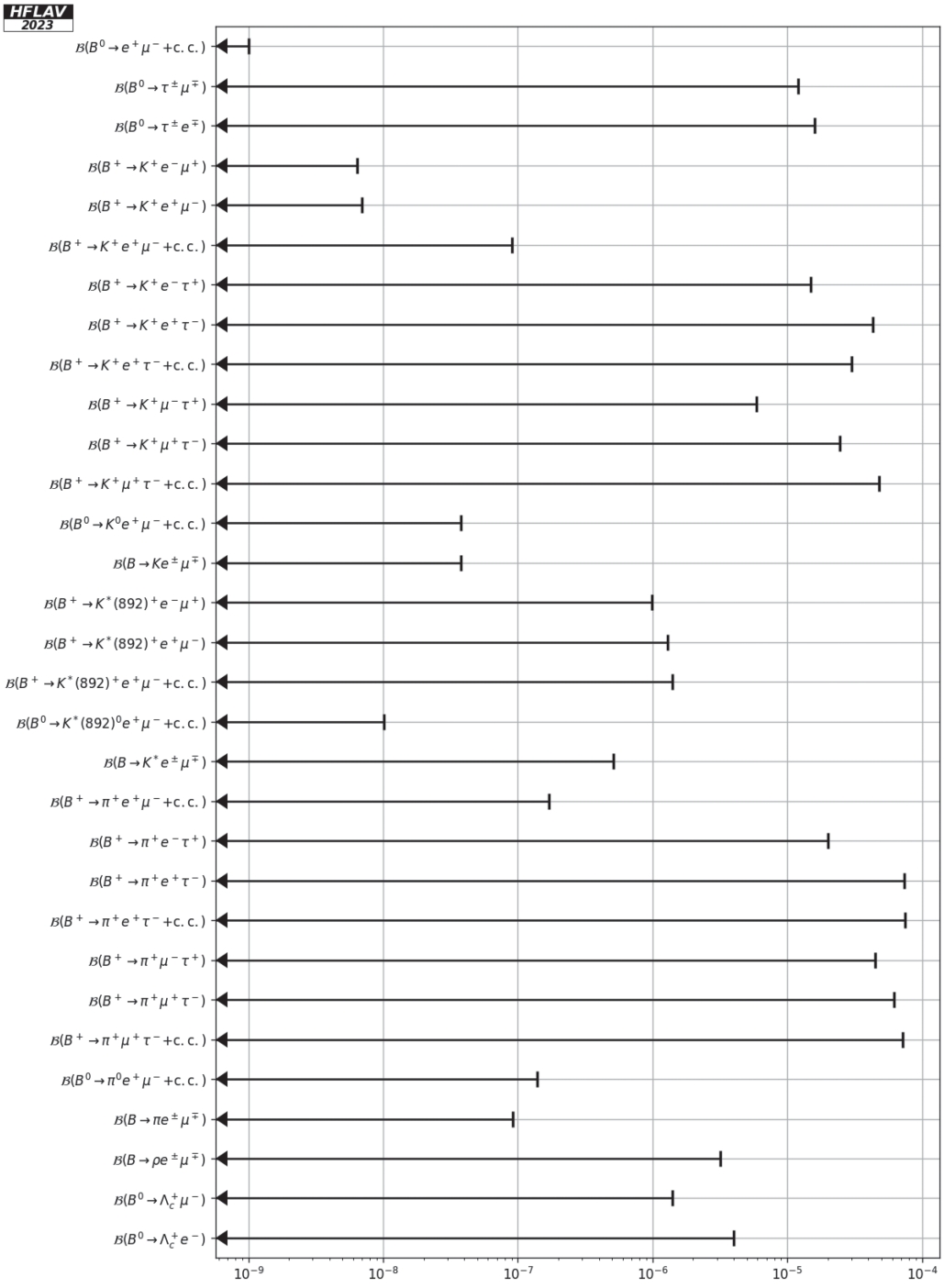


FIG. 38. Limits on branching fractions of lepton-flavor-violating B^+ and B^0 decays.

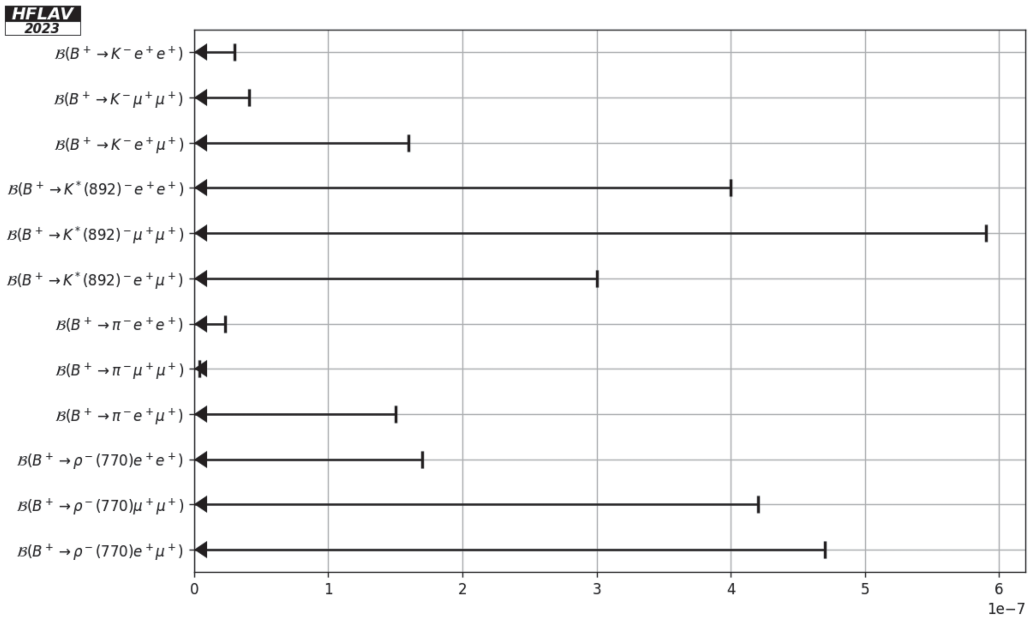


FIG. 39. Limits on branching fractions of lepton-number-violating B^+ and B^0 decays.

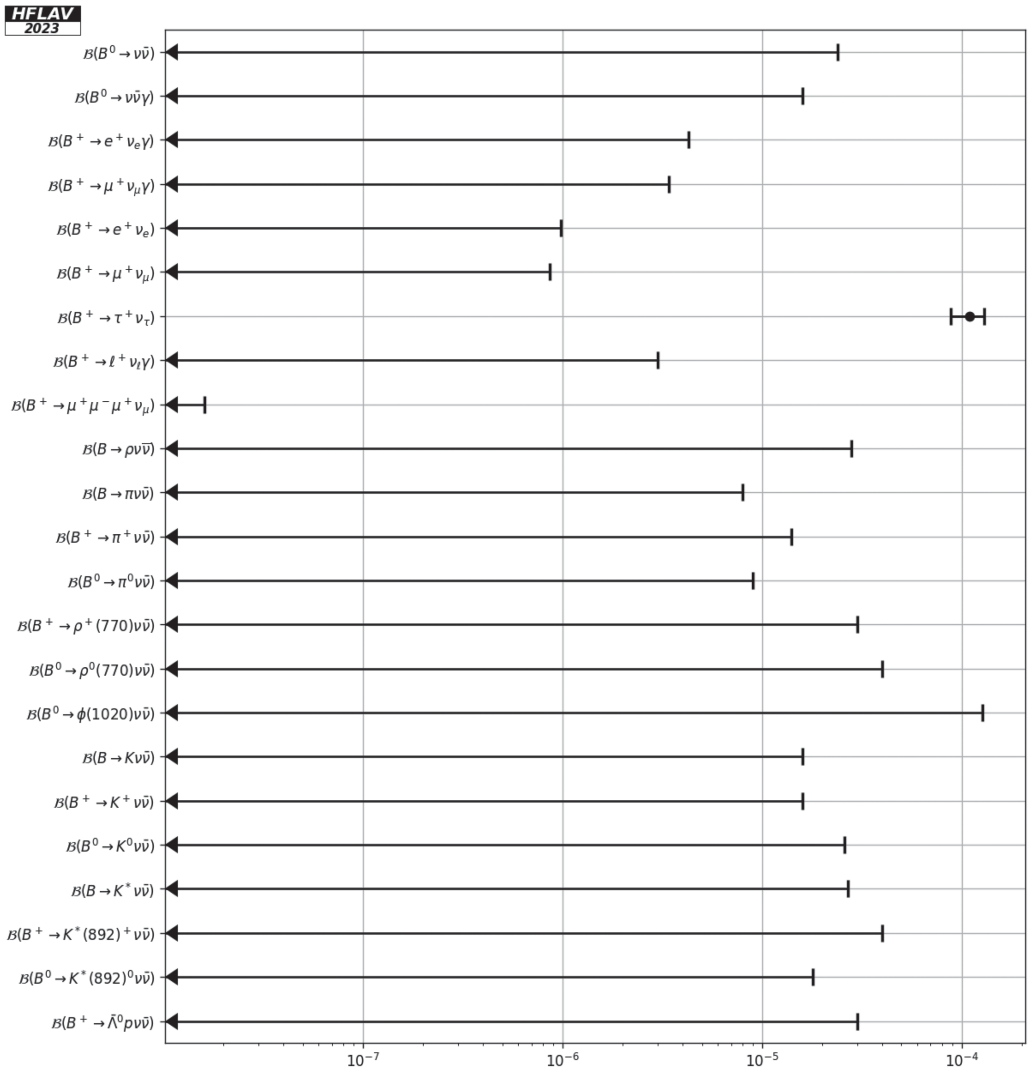


FIG. 40. Branching fractions of charmless B decays with neutrinos.

by the LHC Heavy Flavor Working Group [919], taking into account the correlations between the $B^0 \to \mu^+\mu^-$ and $B_s^0 \to \mu^+\mu^-$ branching fractions. The latest results from ATLAS, CMS and LHCb are in Refs. [125,903,920], respectively.

G. *CP* asymmetries in *b*-hadron decays

This section contains, in Tables 217–235, compilations of *CP* asymmetries in decays of various *b*-hadrons: B^+, B^0 mesons, $B^\pm/B^0$ admixtures, B_s^0 mesons and finally Λ_b^0 baryons. The *CP* asymmetry is defined as

$$A_{CP} = \frac{N_b - N_{\bar{b}}}{N_b + N_{\bar{b}}}, \tag{128}$$

where N_b ($N_{\bar{b}}$) is the number of hadrons containing a b ($\bar{b}$) quark decaying into a specific final state (the *CP*-conjugate state). Figure 41 shows a graphic representation of a selection of results given in this section.

Measurements that are not included in the tables (the definitions of observables can be found in the corresponding experimental papers):

(i) In Ref. [1058], LHCb reports the triple-product asymmetries ($a_{CP}^{\hat{T}-\text{odd}}$, $a_P^{\hat{T}-\text{odd}}$) for the decays $\Lambda_b^0 \to p\pi^-\pi^+\pi^-$ and $\Lambda_b^0 \to p\pi^-K^+K^-$.

(ii) In Ref. [1059], LHCb reports $a_{CP}^{\hat{T}-\text{odd}}$, $a_P^{\hat{T}-\text{odd}}$ and $\Delta(A_{CP}) = A_{CP}(\Lambda_b^0 \to pK^-\mu^+\mu^-) - A_{CP}(\Lambda_b^0 \to pK^-J/\psi)$.

(iii) In Ref. [1060], LHCb reports $a_{CP}^{\hat{T}-\text{odd}}$ and $a_P^{\hat{T}-\text{odd}}$ for the decays $\Lambda_b^0 \to pK^-\pi^+\pi^-$, $\Lambda_b^0 \to pK^-K^+K^-$ and $\Xi_b^0 \to pK^-K^-\pi^+$.

(iv) In Ref. [1061] LHCb measures differences of *CP* asymmetries between Λ_b^0 and Ξ_b^0 charmless decays into a proton and three charged mesons and the

TABLE 217. *CP* asymmetries of charmless hadronic B^+ decays (part 1).

Parameter	Measurements		Average
$A_{CP}(B^+ \to K_S^0\pi^+)$	Belle [702]	$-0.011 \pm 0.021 \pm 0.006$	-0.023 ± 0.014
	LHCb [706]	$-0.022 \pm 0.025 \pm 0.010$	
	Belle II [703][a]	$-0.05 \pm 0.03 \pm 0.01$	
	BABAR [704]	$-0.029 \pm 0.039 \pm 0.010$	
	CLEO [1045]	$0.18 \pm 0.24 \pm 0.02$	
$A_{CP}(B^+ \to K^+\pi^0)$	LHCb [1046][b]	$0.025 \pm 0.015 \pm 0.007$	0.027 ± 0.012
	Belle [702]	$0.043 \pm 0.024 \pm 0.002$	
	Belle II [703][a]	$0.01 \pm 0.03 \pm 0.01$	
	BABAR [707]	$0.030 \pm 0.039 \pm 0.010$	
	CLEO [1045]	$-0.29 \pm 0.23 \pm 0.02$	
$A_{CP}(B^+ \to \eta' K^+)$	LHCb [713][b]	$-0.002 \pm 0.012 \pm 0.006$	0.004 ± 0.011
	BABAR [708]	$0.008^{+0.017}_{-0.018} \pm 0.009$	
	Belle [709]	$0.028 \pm 0.028 \pm 0.021$	
	CLEO [1045]	$0.03 \pm 0.12 \pm 0.02$	
$A_{CP}(B^+ \to \eta' K^*(892)^+)$	*BABAR* [714]	$-0.26 \pm 0.27 \pm 0.02$	-0.26 ± 0.27
$A_{CP}(B^+ \to \eta'(K\pi)_0^{*+})$	*BABAR* [714]	$0.06 \pm 0.20 \pm 0.02$	0.06 ± 0.20
$A_{CP}(B^+ \to \eta' K_2^*(1430)^+)$	*BABAR* [714]	$0.15 \pm 0.13 \pm 0.02$	0.15 ± 0.13
$A_{CP}(B^+ \to \eta K^+)$	*BABAR* [708]	$-0.36 \pm 0.11 \pm 0.03$	-0.37 ± 0.08
	Belle [716]	$-0.38 \pm 0.11 \pm 0.01$	
$A_{CP}(B^+ \to \eta K^*(892)^+)$	*BABAR* [717]	$0.01 \pm 0.08 \pm 0.02$	0.02 ± 0.05
	Belle [718]	$0.03 \pm 0.10 \pm 0.01$	
$A_{CP}(B^+ \to \eta(K\pi)_0^{*+})$	*BABAR* [717]	$0.05 \pm 0.13 \pm 0.02$	0.050 ± 0.093
$A_{CP}(B^+ \to \eta K_2^*(1430)^+)$	*BABAR* [717]	$-0.45 \pm 0.30 \pm 0.02$	-0.45 ± 0.21

[a]Preliminary result.

[b]Multiple systematic uncertainties are added in quadrature.

TABLE 218. CP asymmetries of charmless hadronic B^+ decays (part 2).

Parameter	Measurements		Average
$A_{CP}(B^+ \to \omega(782)K^+)$	Belle [721]	$-0.03 \pm 0.04 \pm 0.01$	-0.025 ± 0.036
	BABAR [722]	$-0.01 \pm 0.07 \pm 0.01$	
$A_{CP}(B^+ \to \omega(782)K^*(892)^+)$	*BABAR* [724]	$0.29 \pm 0.35 \pm 0.02$	0.29 ± 0.35
$A_{CP}(B^+ \to \omega(782)(K\pi)_0^{*+})$	*BABAR* [724]	$-0.10 \pm 0.09 \pm 0.02$	-0.10 ± 0.09
$A_{CP}(B^+ \to \omega(782)K_2^*(1430)^+)$	*BABAR* [724]	$0.14 \pm 0.15 \pm 0.02$	0.14 ± 0.15
$A_{CP}(B^+ \to K^*(892)^0\pi^+)$	*BABAR* [726][b,c]	$0.032 \pm 0.052^{+0.016}_{-0.013}$	-0.04 ± 0.04
	Belle [727][b,c]	$-0.149 \pm 0.064 \pm 0.022$	
	BABAR [728][d,c]	$-0.12 \pm 0.21^{+0.08}_{-0.14}$	
$A_{CP}(B^+ \to K^*(892)^+\pi^0)$	*BABAR* [728][d,c]	$-0.52 \pm 0.14^{+0.06}_{-0.04}$	-0.39 ± 0.13
	BABAR [729]	$-0.06 \pm 0.24 \pm 0.04$	
$A_{CP}(B^+ \to K^+\pi^+\pi^-)$[e]	LHCb [1047][f,g,c]	$0.011 \pm 0.002 \pm 0.004$	0.0146 ± 0.0041
	LHCb [1048][h,c]	$0.025 \pm 0.004 \pm 0.008$	
	BABAR [726][b,c]	$0.028 \pm 0.020 \pm 0.023$	
	Belle [727][b]	$0.049 \pm 0.026 \pm 0.020$	
	Belle II [731][a]	$-0.010 \pm 0.050 \pm 0.021$	
$A_{CP}(B^+ \to K^+K^+K^-(\mathrm{NR}))$	*BABAR* [720][i]	$0.060 \pm 0.044 \pm 0.019$	0.06 ± 0.05

[a]Preliminary result.

[b]Result extracted from Dalitz-plot analysis of $B^+ \to K^+\pi^+\pi^-$ decays.

[c]Multiple systematic uncertainties are added in quadrature.

[d]Result extracted from Dalitz-plot analysis of $B^+ \to K_S^0\pi^+\pi^0$ decays.

[e]Treatment of charmonium intermediate components differs between the results.

[f]Using run II dataset, corresponding to an integrated luminosity of 5.9 fb^{-1} collected at a center-of-mass energy of 13 TeV (2015–2018).

[g]Also measured in several invariant mass regions.

[h]Using run I dataset, corresponding to an integrated luminosity of 3.0 fb^{-1} collected at a center-of-mass energy of 7 TeV (2011) and 8 TeV (2012).

[i]The nonresonant amplitude is modeled using a polynomial function including S-wave and P-wave terms.

TABLE 219. CP asymmetries of charmless hadronic B^+ decays (part 3).

Parameter	Measurements		Average
$A_{CP}(B^+ \to f_0(980)K^+)$	*BABAR* [726][a,b]	$-0.106 \pm 0.050^{+0.036}_{-0.015}$	-0.08 ± 0.04
	Belle [727][a,b]	$-0.077 \pm 0.065^{+0.046}_{-0.026}$	
	BABAR [720][c]	$-0.08 \pm 0.08 \pm 0.04$	
	BABAR [729]	$0.18 \pm 0.18 \pm 0.04$	
$A_{CP}(B^+ \to f_2(1270)K^+)$	*BABAR* [726][a,b]	$-0.85 \pm 0.22^{+0.26}_{-0.13}$	-0.67 ± 0.19
	Belle [727][a,b]	$-0.59 \pm 0.22 \pm 0.04$	
$A_{CP}(B^+ \to f_2'(1525)K^+)$	*BABAR* [720][c]	$0.14 \pm 0.10 \pm 0.04$	0.14 ± 0.11
$A_{CP}(B^+ \to \rho^0(770)K^+)$	*BABAR* [726][a,b]	$0.44 \pm 0.10^{+0.06}_{-0.14}$	0.37 ± 0.12
	Belle [727][a,b]	$0.30 \pm 0.11^{+0.11}_{-0.04}$	
$A_{CP}(B^+ \to K^0\pi^+\pi^0)$	*BABAR* [728][d,b]	$0.07 \pm 0.05 \pm 0.04$	0.07 ± 0.06
$A_{CP}(B^+ \to K_0^*(1430)^0\pi^+)$	Belle [727][a,b]	$0.076 \pm 0.038^{+0.028}_{-0.022}$	0.084 ± 0.043
	BABAR [728][d,b]	$0.14 \pm 0.10^{+0.14}_{-0.06}$	

(Table continued)

TABLE 219. *(Continued)*

Parameter	Measurements		Average
$A_{CP}(B^+ \to (K\pi)_0^{*0}\pi^+)$	*BABAR* [726][a,b]	$0.032 \pm 0.035^{+0.034}_{-0.028}$	0.032 ± 0.046
$A_{CP}(B^+ \to K_0^*(1430)^+\pi^0)$	*BABAR* [728][d,b]	$0.26 \pm 0.12^{+0.14}_{-0.08}$	$0.26^{+0.19}_{-0.14}$
$A_{CP}(B^+ \to K_2^*(1430)^0\pi^+)$	*BABAR* [726][a,b]	$0.05 \pm 0.23^{+0.18}_{-0.08}$	$0.05^{+0.29}_{-0.24}$
$A_{CP}(B^+ \to K^+\pi^0\pi^0)$	*BABAR* [729]	$-0.06 \pm 0.06 \pm 0.04$	-0.06 ± 0.07
$A_{CP}(B^+ \to \rho^+(770)K^0)$	*BABAR* [728][d,b]	$0.21 \pm 0.19^{+0.24}_{-0.20}$	$0.21^{+0.31}_{-0.28}$
$A_{CP}(B^+ \to K^*(892)^+\pi^+\pi^-)$	*BABAR* [740]	$0.07 \pm 0.07 \pm 0.04$	0.07 ± 0.08
$A_{CP}(B^+ \to K^*(892)^+\rho^0(770))$	*BABAR* [741]	$0.31 \pm 0.13 \pm 0.03$	0.31 ± 0.13
$A_{CP}(B^+ \to f_0(980)K^*(892)^+)$	*BABAR* [741]	$-0.15 \pm 0.12 \pm 0.03$	-0.15 ± 0.12
$A_{CP}(B^+ \to X_{\pi^0\pi^0}\pi^+)$	Belle [776][e]	$0.182 \pm 0.116 \pm 0.007$	0.18 ± 0.12

[a]Result extracted from Dalitz-plot analysis of $B^+ \to K^+\pi^+\pi^-$ decays.

[b]Multiple systematic uncertainties are added in quadrature.

[c]Result extracted from Dalitz-plot analysis of $B^+ \to K^+K^+K^-$ decays.

[d]Result extracted from Dalitz-plot analysis of $B^+ \to K_S^0\pi^+\pi^0$ decays.

[e]$X_{\pi^0\pi^0}$ corresponds to a structure observed in Ref. [776], likely arising due to multiple resonances.

TABLE 220. *CP* asymmetries of charmless hadronic B^+ decays (part 4).

Parameter	Measurements		Average
$A_{CP}(B^+ \to a_1(1260)^+K^0)$	*BABAR* [742]	$0.12 \pm 0.11 \pm 0.02$	0.12 ± 0.11
$A_{CP}(B^+ \to b_1(1235)^+K^0)$	*BABAR* [743]	$-0.03 \pm 0.15 \pm 0.02$	-0.03 ± 0.15
$A_{CP}(B^+ \to K^*(892)^0\rho^+(770))$	*BABAR* [744]	$-0.01 \pm 0.16 \pm 0.02$	-0.01 ± 0.16
$A_{CP}(B^+ \to b_1(1235)^0K^+)$	*BABAR* [748]	$-0.46 \pm 0.20 \pm 0.02$	-0.46 ± 0.20
$A_{CP}(B^+ \to K^+K_S^0)$	LHCb [706]	$-0.21 \pm 0.14 \pm 0.01$	-0.086 ± 0.100
	Belle [702]	$0.014 \pm 0.168 \pm 0.002$	
	BABAR [704]	$0.10 \pm 0.26 \pm 0.03$	
$A_{CP}(B^+ \to K^+K_S^0K_S^0)$[a]	Belle [750][b]	$0.016 \pm 0.039 \pm 0.009$	0.025 ± 0.032
	BABAR [720][c]	$0.04^{+0.04}_{-0.05} \pm 0.02$	
$A_{CP}(B^+ \to K^+K^-\pi^+)$[a]	LHCb [1047][d,e,f]	$-0.114 \pm 0.007 \pm 0.004$	-0.1151 ± 0.0076
	LHCb [1048][g,f]	$-0.123 \pm 0.017 \pm 0.014$	
	Belle [752][h]	$-0.170 \pm 0.073 \pm 0.017$	
	BABAR [753]	$0.00 \pm 0.10 \pm 0.03$	
$A_{CP}(B^+ \to K^+K^-\pi^+(\mathrm{NR}))$	LHCb [754][i]	$-0.107 \pm 0.053 \pm 0.035$	-0.107 ± 0.064
$A_{CP}(B^+ \to \bar{K}^*(892)^0K^+)$	LHCb [754][j]	$0.123 \pm 0.087 \pm 0.045$	0.123 ± 0.098
$A_{CP}(B^+ \to \bar{K}_0^*(1430)^0K^+)$	LHCb [754][j]	$0.104 \pm 0.149 \pm 0.088$	0.10 ± 0.17
$A_{CP}(B^+ \to \phi(1020)\pi^+)$	LHCb [754][j]	$0.098 \pm 0.436 \pm 0.266$	0.10 ± 0.51
$A_{CP}(B^+ \to K^+K^-\pi^+)\pi\pi \leftrightarrow KK$ rescattering	LHCb [754][j]	$-0.664 \pm 0.038 \pm 0.019$	-0.664 ± 0.042

[a]Treatment of charmonium intermediate components differs between the results.

[b]A_{CP} is also measured in bins of $m_{K_S^0K_S^0}$.

[c]Result extracted from Dalitz-plot analysis of $B^0 \to K_S^0K^+K^-$ decays.

[d]Using run II dataset, corresponding to an integrated luminosity of 5.9 fb^{-1} collected at a center-of-mass energy of 13 TeV (2015–2018).

[e]Also measured in several invariant mass regions.

[f]Multiple systematic uncertainties are added in quadrature.

[g]Using run I dataset, corresponding to an integrated luminosity of 3.0 fb^{-1} collected at a center-of-mass energy of 7 TeV (2011) and 8 TeV (2012).

[h]Also measured in bins of $m_{K^+K^-}$.

[i]LHCb uses a model of the nonresonant contribution obtained from a phenomenological description of the partonic interaction that produces the final state. This contribution is referred to as the single pole in the paper; see Ref. [754] for details.

[j]Result extracted from Dalitz-plot analysis of $B^+ \to K^+K^-\pi^+$ decays.

TABLE 221. CP asymmetries of charmless hadronic B^+ decays (part 5).

Parameter	Measurements		Average
$A_{CP}(B^+ \to K^+K^+K^-)$	LHCb [1047][b,c,d]	$-0.037 \pm 0.002 \pm 0.004$	-0.036 ± 0.004
	LHCb [1048][e,d]	$-0.036 \pm 0.004 \pm 0.007$	
	BABAR [720][f]	$-0.017^{+0.019}_{-0.014} \pm 0.014$	
	Belle II [731][a]	$-0.103 \pm 0.042 \pm 0.020$	
$A_{CP}(B^+ \to \phi(1020)K^+)$	LHCb [713][e,d]	$0.017 \pm 0.011 \pm 0.006$	0.024 ± 0.012
	BABAR [720][f]	$0.128 \pm 0.044 \pm 0.013$	
	Belle [764]	$0.01 \pm 0.12 \pm 0.05$	
	CDF [761]	$-0.07 \pm 0.17^{+0.03}_{-0.02}$	
$A_{CP}(B^+ \to K^*(892)^+K^+K^-)$	*BABAR* [740]	$0.11 \pm 0.08 \pm 0.03$	0.11 ± 0.09
$A_{CP}(B^+ \to \phi(1020)K^*(892)^+)$	Belle [1049]	$-0.02 \pm 0.14 \pm 0.03$	-0.01 ± 0.08
	BABAR [763][g]	$0.00 \pm 0.09 \pm 0.04$	
$A_{CP}(B^+ \to (K\pi)_0^{*+}\phi(1020))$	*BABAR* [765]	$0.04 \pm 0.15 \pm 0.04$	0.04 ± 0.16
$A_{CP}(B^+ \to K_1(1270)^+\phi(1020))$	*BABAR* [765]	$0.15 \pm 0.19 \pm 0.05$	0.15 ± 0.20
$A_{CP}(B^+ \to K_2^*(1430)^+\phi(1020))$	*BABAR* [765]	$-0.23 \pm 0.19 \pm 0.06$	-0.23 ± 0.20
$A_{CP}(B^+ \to \phi(1020)\phi(1020)K^+)$	*BABAR* [767][h]	$-0.10 \pm 0.08 \pm 0.02$	-0.10 ± 0.08

[a]Preliminary result.

[b]Using run II dataset, corresponding to an integrated luminosity of 5.9 fb^{-1} collected at a center-of-mass energy of 13 TeV (2015–2018).

[c]Also measured in several invariant mass regions.

[d]Multiple systematic uncertainties are added in quadrature.

[e]Using run I dataset, corresponding to an integrated luminosity of 3.0 fb^{-1} collected at a center-of-mass energy of 7 TeV (2011) and 8 TeV (2012).

[f]Result extracted from Dalitz-plot analysis of $B^+ \to K^+K^+K^-$ decays.

[g]Combination of two final states of the $K^*(892)^\pm$, $K^0_S\pi^\pm$ and $K^\pm\pi^0$. In addition to the combined results, the paper reports separately the results for each individual final state.

[h]Measured in the $\phi\phi$ invariant mass range below the η_c resonance ($m_{\phi\phi} < 2.85$ GeV/c^2).

TABLE 222. CP asymmetries of charmless hadronic B^+ decays (part 6).

Parameter	Measurements		Average
$A_{CP}(B^+ \to K^*(892)^+\gamma)$	Belle [922]	$0.011 \pm 0.023 \pm 0.003$	0.014 ± 0.018
	BABAR [923]	$0.018 \pm 0.028 \pm 0.007$	
$A_{CP}(B^+ \to K^+\pi^0\gamma)$	Belle [922][a]	$0.010 \pm 0.036 \pm 0.003$	0.024 ± 0.027
	BABAR [923][b]	$0.040 \pm 0.039 \pm 0.007$	
$A_{CP}(B^+ \to K^0_S\pi^+\gamma)$	Belle [922][a]	$0.013 \pm 0.029 \pm 0.004$	0.007 ± 0.024
	BABAR [923][b]	$-0.006 \pm 0.041 \pm 0.007$	
$A_{CP}(B^+ \to X_s\gamma)$	Belle [1010][c]	$0.0275 \pm 0.0184 \pm 0.0032$	0.028 ± 0.019
$A_{CP}(B^+ \to \eta K^+\gamma)$	Belle [929][d]	$-0.16 \pm 0.09 \pm 0.06$	-0.12 ± 0.07
	BABAR [928][e]	$-0.090^{+0.104}_{-0.098} \pm 0.014$	
$A_{CP}(B^+ \to \phi(1020)K^+\gamma)$	Belle [932][f]	$-0.03 \pm 0.11 \pm 0.08$	-0.13 ± 0.10
	BABAR [933][g]	$-0.26 \pm 0.14 \pm 0.05$	
$A_{CP}(B^+ \to \rho^+(770)\gamma)$	Belle [939]	$-0.11 \pm 0.32 \pm 0.09$	-0.11 ± 0.33

[a]$m_{K\pi} < 2.0$ GeV/c^2.

[b]$0.79 < m_{K\pi} < 1.0$ GeV/c^2.

[c]$m_{X_s} < 2.8$ GeV/c^2.

[d]$m_{K\eta} < 2.4$ GeV/c^2.

[e]$m_{K\eta^{(\prime)}} < 3.25$ GeV/c^2.

[f]$1.4 \le E^*_\gamma \le 3.4$ GeV/c^2, where E^*_γ is the photon energy in the center-of-mass frame.

[g]$m_{\phi K} < 3.0$ GeV/c^2.

TABLE 223. *CP* asymmetries of charmless hadronic B^+ decays (part 7).

Parameter	Measurements		Average
$A_{CP}(B^+ \to \pi^+\pi^0)$	Belle [702]	$0.025 \pm 0.043 \pm 0.007$	-0.01 ± 0.03
	Belle II [703][a]	$-0.08 \pm 0.05 \pm 0.01$	
	BABAR [707]	$0.03 \pm 0.08 \pm 0.01$	
$A_{CP}(B^+ \to \pi^+\pi^+\pi^-)$[b]	LHCb [1047][c,d,e]	$0.080 \pm 0.004 \pm 0.004$	0.0764 ± 0.0054
	LHCb [1048][f,e]	$0.058 \pm 0.008 \pm 0.011$	
	BABAR [772][g,e]	$0.032 \pm 0.044^{+0.040}_{-0.037}$	
$A_{CP}(B^+ \to \rho^0(770)\pi^+)$	LHCb [773][f,g,h,e]	$0.007 \pm 0.011 \pm 0.040$	$0.016^{+0.041}_{-0.039}$
	BABAR [772][g,e]	$0.18 \pm 0.07^{+0.05}_{-0.15}$	
$A_{CP}(B^+ \to f_2(1270)\pi^+)$	LHCb [773][g,h,e]	$0.468 \pm 0.061 \pm 0.103$	0.365 ± 0.079
	LHCb [754][i]	$0.267 \pm 0.102 \pm 0.048$	
	BABAR [772][g,e]	$0.41 \pm 0.25^{+0.18}_{-0.15}$	
$A_{CP}(B^+ \to \rho(1450)^0\pi^+)$	LHCb [773][g,h,e]	$-0.129 \pm 0.033 \pm 0.421$	-0.109 ± 0.049
	LHCb [754][i]	$-0.109 \pm 0.044 \pm 0.024$	
	BABAR [772][g,e]	$-0.06 \pm 0.28^{+0.23}_{-0.40}$	
$A_{CP}(B^+ \to \rho_3(1690)^0\pi^+)$	LHCb [773][g,h,e]	$-0.801 \pm 0.114 \pm 0.511$	-0.80 ± 0.52
$A_{CP}(B^+ \to f_0(1370)\pi^+)$	*BABAR* [772][g,e]	$0.72 \pm 0.15 \pm 0.16$	0.72 ± 0.22
$A_{CP}(B^+ \to \pi^+\pi^+\pi^-), S-$ wave	LHCb [773][g,h,e]	$0.144 \pm 0.018 \pm 0.026$	0.144 ± 0.032
$A_{CP}(B^+ \to \pi^+\pi^+\pi^-(\mathrm{NR}))$	*BABAR* [772][j,e]	$-0.14 \pm 0.14^{+0.18}_{-0.08}$	$-0.14^{+0.23}_{-0.16}$
$A_{CP}(B^+ \to \rho^+(770)\pi^0)$	*BABAR* [778]	$-0.01 \pm 0.13 \pm 0.02$	0.03 ± 0.10
	Belle [776]	$0.080 \pm 0.150^{+0.023}_{-0.075}$	

[a]Preliminary result.

[b]Treatment of charmonium intermediate components differs between the results.

[c]Using run II dataset, corresponding to an integrated luminosity of 5.9 fb^{-1} collected at a center-of-mass energy of 13 TeV (2015–2018).

[d]Also measured in several invariant mass regions.

[e]Multiple systematic uncertainties are added in quadrature.

[f]Using run I dataset, corresponding to an integrated luminosity of 3.0 fb^{-1} collected at a center-of-mass energy of 7 TeV (2011) and 8 TeV (2012).

[g]Result extracted from Dalitz-plot analysis of $B^+ \to \pi^+\pi^+\pi^-$ decays.

[h]This analysis uses three different approaches: isobar, K-matrix and quasi-model-independent, to describe the S-wave component. The A_{CP} results are taken from the isobar model with an additional error accounting for the different S-wave methods as reported in Appendix D of Ref. [775].

[i]Result extracted from Dalitz-plot analysis of $B^+ \to K^+K^-\pi^+$ decays.

[j]The nonresonant amplitude is modeled using a sum of exponential functions.

TABLE 224. CP asymmetries of charmless hadronic B^+ decays (part 8).

Parameter	Measurements		Average
$A_{CP}(B^+ \to \rho^+(770)\rho^0(770))$	*BABAR* [779]	$-0.054 \pm 0.055 \pm 0.010$	-0.056 ± 0.047
	Belle II [780][a]	$-0.069 \pm 0.068 \pm 0.060$	
	Belle [781]	$0.00 \pm 0.22 \pm 0.03$	
$A_{CP}(B^+ \to \omega(782)\pi^+)$	LHCb [773][b,c,d]	$-0.048 \pm 0.065 \pm 0.049$	-0.041 ± 0.048
	BABAR [722]	$-0.02 \pm 0.08 \pm 0.01$	
	Belle [783]	$-0.02 \pm 0.09 \pm 0.01$	
	CLEO [1045]	$-0.34 \pm 0.25 \pm 0.02$	
$A_{CP}(B^+ \to \omega(782)\rho^+(770))$	*BABAR* [724]	$-0.20 \pm 0.09 \pm 0.02$	-0.20 ± 0.09
$A_{CP}(B^+ \to \pi^+\pi^0\pi^0)$	Belle [776]	$0.092 \pm 0.068 \pm 0.007$	0.092 ± 0.068
$A_{CP}(B^+ \to \eta\pi^+)$	Belle [716]	$-0.19 \pm 0.06 \pm 0.01$	-0.14 ± 0.05
	BABAR [708]	$-0.03 \pm 0.09 \pm 0.03$	
$A_{CP}(B^+ \to \eta\rho^+(770))$	*BABAR* [784]	$0.13 \pm 0.11 \pm 0.02$	0.11 ± 0.11
	Belle [718]	$-0.04^{+0.34}_{-0.32} \pm 0.01$	
$A_{CP}(B^+ \to \eta'\pi^+)$	*BABAR* [708]	$0.03 \pm 0.17 \pm 0.02$	0.06 ± 0.15
	Belle [709]	$0.20^{+0.37}_{-0.36} \pm 0.04$	
$A_{CP}(B^+ \to \eta'\rho^+(770))$	*BABAR* [714]	$0.26 \pm 0.17 \pm 0.02$	0.26 ± 0.17
$A_{CP}(B^+ \to b_1(1235)^0\pi^+)$	*BABAR* [748]	$0.05 \pm 0.16 \pm 0.02$	0.05 ± 0.16

[a]Preliminary result.

[b]Result extracted from Dalitz-plot analysis of $B^+ \to \pi^+\pi^+\pi^-$ decays.

[c]This analysis uses three different approaches: isobar, K-matrix and quasi-model-independent, to describe the S-wave component. The A_{CP} results are taken from the isobar model with an additional error accounting for the different S-wave methods as reported in Appendix D of Ref. [775].

[d]Multiple systematic uncertainties are added in quadrature.

TABLE 225. CP asymmetries of charmless hadronic B^+ decays (part 9).

Parameter	Measurements		Average
$A_{CP}(B^+ \to p\bar{p}\pi^+)$	*BABAR* [525]	$0.04 \pm 0.07 \pm 0.04$	0.04 ± 0.08
$A_{CP}(B^+ \to p\bar{p}\pi^+), m_{p\bar{p}} < 2.85$ GeV/c^2	LHCb [856]	$-0.041 \pm 0.039 \pm 0.005$	-0.058 ± 0.037
	Belle [855]	$-0.17 \pm 0.10 \pm 0.02$	
$A_{CP}(B^+ \to p\bar{p}K^+), m_{p\bar{p}} < 2.85$ GeV/c^2	LHCb [856]	$0.021 \pm 0.020 \pm 0.004$	0.007 ± 0.019
	Belle [855]	$-0.02 \pm 0.05 \pm 0.02$	
	BABAR [608]	$-0.16^{+0.07}_{-0.08} \pm 0.04$	
$A_{CP}(B^+ \to p\bar{p}K^*(892)^+)$[a]	*BABAR* [525]	$0.32 \pm 0.13 \pm 0.05$	0.21 ± 0.11
	Belle [859]	$-0.01 \pm 0.19 \pm 0.02$	
$A_{CP}(B^+ \to p\bar{\Lambda}^0\gamma)$	Belle [862]	$0.17 \pm 0.16 \pm 0.05$	0.17 ± 0.17
$A_{CP}(B^+ \to p\bar{\Lambda}^0\pi^0)$	Belle [862]	$0.01 \pm 0.17 \pm 0.04$	0.01 ± 0.17

[a]Treatment of charmonium intermediate components differs between the results.

TABLE 226. *CP* asymmetries of charmless hadronic B^+ decays (part 10).

Parameter	Measurements		Average
$A_{CP}(B^+ \to K^+\ell^+\ell^-)$	Belle [952]	$0.04 \pm 0.10 \pm 0.02$	0.02 ± 0.08
	BABAR [980]	$-0.03 \pm 0.14 \pm 0.01$	
$A_{CP}(B^+ \to K^+e^+e^-)$	Belle [952]	$0.14 \pm 0.14 \pm 0.03$	0.14 ± 0.14
$A_{CP}(B^+ \to K^+\mu^+\mu^-)$	LHCb [1050][a,b]	$0.012 \pm 0.017 \pm 0.001$	0.011 ± 0.017
	Belle [952][c]	$-0.05 \pm 0.13 \pm 0.03$	
$A_{CP}(B^+ \to \pi^+\mu^+\mu^-)$	LHCb [944]	$-0.11 \pm 0.12 \pm 0.01$	-0.11 ± 0.12
$A_{CP}(B^+ \to K^*(892)^+\ell^+\ell^-)$	Belle [952]	$-0.13^{+0.17}_{-0.16} \pm 0.01$	-0.09 ± 0.14
	BABAR [947]	$0.01^{+0.26}_{-0.24} \pm 0.02$	
$A_{CP}(B^+ \to K^*(892)^+e^+e^-)$	Belle [952]	$-0.14^{+0.23}_{-0.22} \pm 0.02$	-0.14 ± 0.23
$A_{CP}(B^+ \to K^*(892)^+\mu^+\mu^-)$	Belle [952]	$-0.12 \pm 0.24 \pm 0.02$	-0.12 ± 0.24

[a]A_{CP} is also measured in bins of $m_{\mu^+\mu^-}$.
[b]Mass regions corresponding to ϕ, J/ψ and $\psi(2S)$ are vetoed.
[c]Mass regions corresponding to J/ψ and $\psi(2S)$ are vetoed.

TABLE 227. *CP* asymmetries of charmless hadronic B^0 decays (part 1).

Parameter	Measurements		Average
$A_{CP}(B^0 \to \pi^0\pi^0)$	*BABAR* [795]	$0.43 \pm 0.26 \pm 0.05$	0.30 ± 0.20
	Belle [835]	$0.14 \pm 0.36 \pm 0.10$	
	Belle II [836]	$0.14 \pm 0.46 \pm 0.07$	
$A_{CP}(B^0 \to K^+\pi^-)$	LHCb [1051][b]	-0.0831 ± 0.0034	-0.0831 ± 0.0031
	CDF [1052]	$-0.083 \pm 0.013 \pm 0.004$	
	Belle [702]	$-0.069 \pm 0.014 \pm 0.007$	
	BABAR [795]	$-0.107 \pm 0.016^{+0.006}_{-0.004}$	
	Belle II [703][a]	$-0.07 \pm 0.02 \pm 0.01$	
$A_{CP}(B^0 \to K^0\pi^0)$	Belle II [703][a,c]	$-0.01 \pm 0.12 \pm 0.04$	-0.01 ± 0.13
$A_{CP}(B^0 \to \eta' K^*(892)^0)$	*BABAR* [714]	$0.02 \pm 0.23 \pm 0.02$	-0.07 ± 0.18
	Belle [797]	$-0.22 \pm 0.29 \pm 0.07$	
$A_{CP}(B^0 \to \eta'(K\pi)_0^{*0})$	*BABAR* [714]	$-0.19 \pm 0.17 \pm 0.02$	-0.19 ± 0.17
$A_{CP}(B^0 \to \eta' K_2^*(1430)^0)$	*BABAR* [714]	$0.14 \pm 0.18 \pm 0.02$	0.14 ± 0.18
$A_{CP}(B^0 \to \eta K^*(892)^0)$	*BABAR* [717]	$0.21 \pm 0.06 \pm 0.02$	0.20 ± 0.04
	Belle [718]	$0.17 \pm 0.08 \pm 0.01$	
$A_{CP}(B^0 \to \eta(K\pi)_0^{*0})$	*BABAR* [717]	$0.06 \pm 0.13 \pm 0.02$	0.060 ± 0.093
$A_{CP}(B^0 \to \eta K_2^*(1430)^0)$	*BABAR* [717]	$-0.07 \pm 0.19 \pm 0.02$	-0.07 ± 0.14
$A_{CP}(B^0 \to b_1(1235)^- K^+)$	*BABAR* [748]	$-0.07 \pm 0.12 \pm 0.02$	-0.07 ± 0.12
$A_{CP}(B^0 \to \omega(782)K^*(892)^0)$	*BABAR* [724]	$0.45 \pm 0.25 \pm 0.02$	0.45 ± 0.25
$A_{CP}(B^0 \to \omega(782)(K\pi)_0^{*0})$	*BABAR* [724]	$-0.07 \pm 0.09 \pm 0.02$	-0.07 ± 0.09
$A_{CP}(B^0 \to \omega(782)K_2^*(1430)^0)$	*BABAR* [724]	$-0.37 \pm 0.17 \pm 0.02$	-0.37 ± 0.17

[a]Peliminary result.
[b]LHCb combines results of the 1.9 fb^{-1} run 2 data analysis with those based on Run 1 dataset [1053]. The full statistical and systematic covariance matrices are used in the combination.
[c]Combination of time-integrated and time-dependent analyses using the best linear unbiased estimator Ref. [798].

TABLE 228. CP asymmetries of charmless hadronic B^0 decays (part 2).

Parameter	Measurements		Average
$A_{CP}(B^0 \to K^+\pi^-\pi^0)$	*BABAR* [803][b]	$-0.030^{+0.045}_{-0.051} \pm 0.055$	0.06 ± 0.05
	Belle II [731][a]	$0.207 \pm 0.088 \pm 0.011$	
	Belle [802]	$0.07 \pm 0.11 \pm 0.01$	
$A_{CP}(B^0 \to \rho^-(770)K^+)$	*BABAR* [801][b]	$0.20 \pm 0.09 \pm 0.08$	0.20 ± 0.11
	Belle [802]	$0.22^{+0.22+0.06}_{-0.23-0.02}$	
$A_{CP}(B^0 \to \rho(1450)^-K^+)$	*BABAR* [801][b]	$-0.10 \pm 0.32 \pm 0.09$	-0.10 ± 0.33
$A_{CP}(B^0 \to \rho(1700)^-K^+)$	*BABAR* [801][b]	$-0.36 \pm 0.57 \pm 0.23$	-0.36 ± 0.61
$A_{CP}(B^0 \to K^+\pi^-\pi^0(\mathrm{NR}))$	*BABAR* [801][c]	$0.10 \pm 0.16 \pm 0.08$	0.10 ± 0.18
$A_{CP}(B^0 \to K^0\pi^+\pi^-)$	*BABAR* [804][d]	$-0.01 \pm 0.05 \pm 0.01$	-0.01 ± 0.05
$A_{CP}(B^0 \to K^*(892)^+\pi^-)$	LHCb [809][d,e]	$-0.308 \pm 0.060 \pm 0.016$	-0.274 ± 0.045
	BABAR [804][d,e]	$-0.21 \pm 0.10 \pm 0.02$	
	BABAR [801][b]	$-0.29 \pm 0.11 \pm 0.02$	
	Belle [1054][d]	$-0.21 \pm 0.11 \pm 0.07$	
$A_{CP}(B^0 \to (K\pi)_0^{*+}\pi^-)$	LHCb [809][d,e]	$-0.032 \pm 0.047 \pm 0.031$	0.017 ± 0.043
	BABAR [804][d,e]	$0.09 \pm 0.07 \pm 0.03$	
	BABAR [801][b]	$0.07 \pm 0.14 \pm 0.01$	
$A_{CP}(B^0 \to K_2^*(1430)^+\pi^-)$	LHCb [809][d,e]	$-0.29 \pm 0.22 \pm 0.09$	-0.29 ± 0.24
$A_{CP}(B^0 \to K^*(1680)^+\pi^-)$	LHCb [809][d,e]	$-0.07 \pm 0.13 \pm 0.04$	-0.07 ± 0.13
$A_{CP}(B^0 \to f_0(980)K_S^0)$[f]	LHCb [809][d,e]	$0.28 \pm 0.27 \pm 0.15$	0.28 ± 0.31
$A_{CP}(B^0 \to (K\pi)_0^{*0}\pi^0)$	*BABAR* [801][b]	$-0.15 \pm 0.10 \pm 0.04$	-0.15 ± 0.11
$A_{CP}(B^0 \to K^*(892)^0\pi^0)$	*BABAR* [801][b]	$-0.15 \pm 0.12 \pm 0.04$	-0.15 ± 0.13

[a]Preliminary result.

[b]Result extracted from Dalitz-plot analysis of $B^0 \to K^+\pi^-\pi^0$ decays.

[c]The nonresonant amplitude is taken to be constant across the Dalitz plane.

[d]Result extracted from Dalitz-plot analysis of $B^0 \to K_S^0\pi^+\pi^-$ decays.

[e]Multiple systematic uncertainties are added in quadrature.

[f]The official HFLAV average includes results from time-dependent analyses and is given in the section Measurements related to Unitarity Triangle angles.

TABLE 229. CP asymmetries of charmless hadronic B^0 decays (part 3).

Parameter	Measurements		Average
$A_{CP}(B^0 \to K^*(892)^0\pi^+\pi^-)$	*BABAR* [813]	$0.07 \pm 0.04 \pm 0.03$	0.07 ± 0.05
$A_{CP}(B^0 \to K^*(892)^0\rho^0(770))$	*BABAR* [814]	$-0.06 \pm 0.09 \pm 0.02$	-0.06 ± 0.09
$A_{CP}(B^0 \to f_0(980)K^*(892)^0)$	*BABAR* [814]	$0.07 \pm 0.10 \pm 0.02$	0.07 ± 0.10
$A_{CP}(B^0 \to K^*(892)^+\rho^-(770))$	*BABAR* [814]	$0.21 \pm 0.15 \pm 0.02$	0.21 ± 0.15
$A_{CP}(B^0 \to K^*(892)^0K^+K^-)$	*BABAR* [813]	$0.01 \pm 0.05 \pm 0.02$	0.01 ± 0.05
$A_{CP}(B^0 \to a_1(1260)^-K^+)$	*BABAR* [742]	$-0.16 \pm 0.12 \pm 0.01$	-0.16 ± 0.12
$A_{CP}(B^0 \to \phi(1020)K^*(892)^0)$	Belle [825]	$-0.007 \pm 0.048 \pm 0.021$	-0.001 ± 0.041
	BABAR [824]	$0.01 \pm 0.06 \pm 0.03$	
$A_{CP}(B^0 \to K^*(892)^0\pi^+K^-)$	*BABAR* [813]	$0.22 \pm 0.33 \pm 0.20$	0.22 ± 0.39
$A_{CP}(B^0 \to (K\pi)_0^{*0}\phi(1020))$	Belle [825]	$0.093 \pm 0.094 \pm 0.017$	0.123 ± 0.081
	BABAR [824]	$0.20 \pm 0.14 \pm 0.06$	
$A_{CP}(B^0 \to K_2^*(1430)^0\phi(1020))$	*BABAR* [824]	$-0.08 \pm 0.12 \pm 0.05$	-0.112 ± 0.099
	Belle [825]	$-0.155^{+0.152}_{-0.133} \pm 0.033$	

TABLE 230. *CP* asymmetries of charmless hadronic B^0 decays (part 4).

Parameter	Measurements		Average
$A_{\rm CP}(B^0 \to K^*(892)^0\gamma)$	LHCb [898]	$0.008 \pm 0.017 \pm 0.009$	-0.006 ± 0.011
	Belle [922]	$-0.013 \pm 0.017 \pm 0.004$	
	BABAR [923]	$-0.016 \pm 0.022 \pm 0.007$	
$A_{\rm CP}(B^0 \to K^+\pi^-\gamma)$	Belle [922][a]	$-0.013 \pm 0.017 \pm 0.004$	-0.014 ± 0.014
	BABAR [923][b]	$-0.016 \pm 0.022 \pm 0.007$	
$A_{\rm CP}(B^0 \to K_2^*(1430)^0\gamma)$	*BABAR* [936]	$-0.08 \pm 0.15 \pm 0.01$	-0.08 ± 0.15
$A_{CP}(B^0 \to X_s\gamma)$	Belle [1010][c]	$-0.0094 \pm 0.0174 \pm 0.0047$	-0.009 ± 0.018

[a] $m_{K\pi} < 2.0$ GeV/c^2.
[b] $0.78 < m_{K\pi} < 1.1$ GeV/c^2.
[c] $m_{X_s} < 2.8$ GeV/c^2.

TABLE 231. *CP* asymmetries of charmless hadronic B^0 decays (part 5).

Parameter	Measurements		Average
$A_{\rm CP}(B^0 \to b_1(1235)^+\pi^- + \text{c.c.})$	*BABAR* [748]	$-0.05 \pm 0.10 \pm 0.02$	-0.05 ± 0.10
$A_{\rm CP}(B^0 \to p\bar{p}K^*(892)^0)$[a]	*BABAR* [525]	$0.11 \pm 0.13 \pm 0.06$	0.05 ± 0.12
	Belle [859]	$-0.08 \pm 0.20 \pm 0.02$	
$A_{\rm CP}(B^0 \to p\bar{\Lambda}^0\pi^-)$	*BABAR* [871]	$-0.10 \pm 0.10 \pm 0.02$	-0.06 ± 0.07
	Belle [862]	$-0.02 \pm 0.10 \pm 0.03$	
$A_{\rm CP}(B^0 \to K^*(892)^0\ell^+\ell^-)$	Belle [952]	$-0.08 \pm 0.12 \pm 0.02$	-0.05 ± 0.10
	BABAR [947]	$0.02 \pm 0.20 \pm 0.02$	
$A_{\rm CP}(B^0 \to K^*(892)^0 e^+e^-)$	Belle [952]	$-0.21 \pm 0.19 \pm 0.02$	-0.21 ± 0.19
$A_{\rm CP}(B^0 \to K^*(892)^0\mu^+\mu^-)$	LHCb [1050][b,c]	$-0.035 \pm 0.024 \pm 0.003$	-0.034 ± 0.024
	Belle [952][d]	$0.00 \pm 0.15 \pm 0.03$	

[a] Treatment of charmonium intermediate components differs between the results.
[b] A_{CP} is also measured in bins of $m_{\mu^+\mu^-}$.
[c] Mass regions corresponding to ϕ, J/ψ and $\psi(2S)$ are vetoed.
[d] Mass regions corresponding to J/ψ and $\psi(2S)$ are vetoed.

TABLE 232. *CP* asymmetries of charmless hadronic decays of $B^\pm/B^0$ admixture.

Parameter	Measurements		Average
$A_{\rm CP}(B \to K^*\gamma)$	Belle [922]	$-0.004 \pm 0.014 \pm 0.003$	-0.004 ± 0.011
	BABAR [923]	$-0.003 \pm 0.017 \pm 0.007$	
$A_{CP}(B \to X_s\gamma)$	Belle [1010][a]	$0.0144 \pm 0.0128 \pm 0.0011$	0.015 ± 0.011
	BABAR [1055][b]	$0.017 \pm 0.019 \pm 0.010$	
$A_{CP}(B \to X_{s+d}\gamma)$	Belle [1056][c]	$0.022 \pm 0.039 \pm 0.009$	0.032 ± 0.034
	BABAR [969][d]	$0.057 \pm 0.060 \pm 0.018$	
$A_{CP}(B \to X_s\ell^+\ell^-)$	*BABAR* [976]	$0.04 \pm 0.11 \pm 0.01$	0.04 ± 0.11

(Table continued)

TABLE 232. *(Continued)*

Parameter	Measurements		Average
$A_{\rm CP}(B \to K^* e^+ e^-)$	Belle [952]	$-0.18 \pm 0.15 \pm 0.01$	-0.18 ± 0.15
$A_{\rm CP}(B \to K^* \mu^+ \mu^-)$	Belle [952]	$-0.03 \pm 0.13 \pm 0.02$	-0.03 ± 0.13
$A_{\rm CP}(B \to K^* \ell^+ \ell^-)$	Belle [952] *BABAR* [980]	$-0.10 \pm 0.10 \pm 0.01$ $0.03 \pm 0.13 \pm 0.01$	-0.05 ± 0.08
$A_{CP}(B \to X_s \eta)$	Belle [1005][e]	$-0.13 \pm 0.04^{+0.02}_{-0.03}$	$-0.13^{+0.04}_{-0.05}$
$A_{\rm CP}(B \to K \ell^+ \ell^-)$	*BABAR* [980]	$-0.03 \pm 0.14 \pm 0.01$	-0.03 ± 0.14

[a]$m_{X_s} < 2.8$ GeV/c^2.
[b]$0.6 < m_{X_s} < 2.0$ GeV/c^2.
[c]$E^*_\gamma \geq 2.1$ GeV where E^*_γ is the photon energy in the center-of-mass frame.
[d]$2.1 < E^*_\gamma < 2.8$ GeV where E^*_γ is the photon energy in the center-of-mass frame.
[e]$0.4 < m_X < 2.6$ GeV/c^2.

TABLE 233. CP asymmetries of charmless hadronic B^0_s decays.

Parameter	Measurements		Average
$A_{CP}(B^0_s \to \pi^+ K^-)$	LHCb [1051][a] CDF [1052]	0.225 ± 0.012 $0.22 \pm 0.07 \pm 0.02$	0.225 ± 0.012

[a]LHCb combines results of the 1.9 fb^{-1} run 2 data analysis with those based on Run 1 dataset [1053]. The full statistical and systematic covariance matrices are used in the combination.

TABLE 234. CP asymmetries of charmless hadronic Λ^0_b decays.

Parameter	Measurements		Average
$A_{\rm CP}(\Lambda^0_b \to p\pi^-)$	LHCb [1057] CDF [1052]	$-0.035 \pm 0.017 \pm 0.020$ $0.06 \pm 0.07 \pm 0.03$	-0.025 ± 0.025
$A_{\rm CP}(\Lambda^0_b \to pK^-)$	LHCb [1057] CDF [1052]	$-0.020 \pm 0.013 \pm 0.019$ $-0.10 \pm 0.08 \pm 0.04$	-0.025 ± 0.022
$A_{\rm CP}(\Lambda^0_b \to p\bar{K}^0\pi^-)$	LHCb [806]	$0.22 \pm 0.13 \pm 0.03$	0.22 ± 0.13
$A_{\rm CP}(\Lambda^0_b \to \Lambda^0 K^+\pi^-)$	LHCb [882]	$-0.53 \pm 0.23 \pm 0.11$	-0.53 ± 0.25
$A_{\rm CP}(\Lambda^0_b \to \Lambda^0 K^+ K^-)$	LHCb [882]	$-0.28 \pm 0.10 \pm 0.07$	-0.28 ± 0.12

TABLE 235. CP asymmetries of charmless hadronic Ξ^-_b decays.

Parameter	Measurements		Average
$A_{\rm CP}(\Xi^-_b \to \Sigma(1385)^0 K^-)$	LHCb [885]	$-0.01 \pm 0.24 \pm 0.32$	-0.01 ± 0.40
$A_{CP}(\Xi^-_b \to \Lambda(1405) K^-)$	LHCb [885]	$-0.27 \pm 0.34 \pm 0.73$	-0.27 ± 0.81
$A_{CP}(\Xi^-_b \to \Lambda(1520) K^-)$	LHCb [885]	$-0.05 \pm 0.09 \pm 0.08$	-0.05 ± 0.12
$A_{CP}(\Xi^-_b \to \Lambda(1670) K^-)$	LHCb [885]	$0.03 \pm 0.14 \pm 0.10$	0.03 ± 0.17
$A_{CP}(\Xi^-_b \to \Sigma(1775) K^-)$	LHCb [885]	$-0.47 \pm 0.26 \pm 0.14$	-0.47 ± 0.30
$A_{CP}(\Xi^-_b \to \Sigma(1915) K^-)$	LHCb [885]	$0.11 \pm 0.26 \pm 0.22$	0.11 ± 0.34

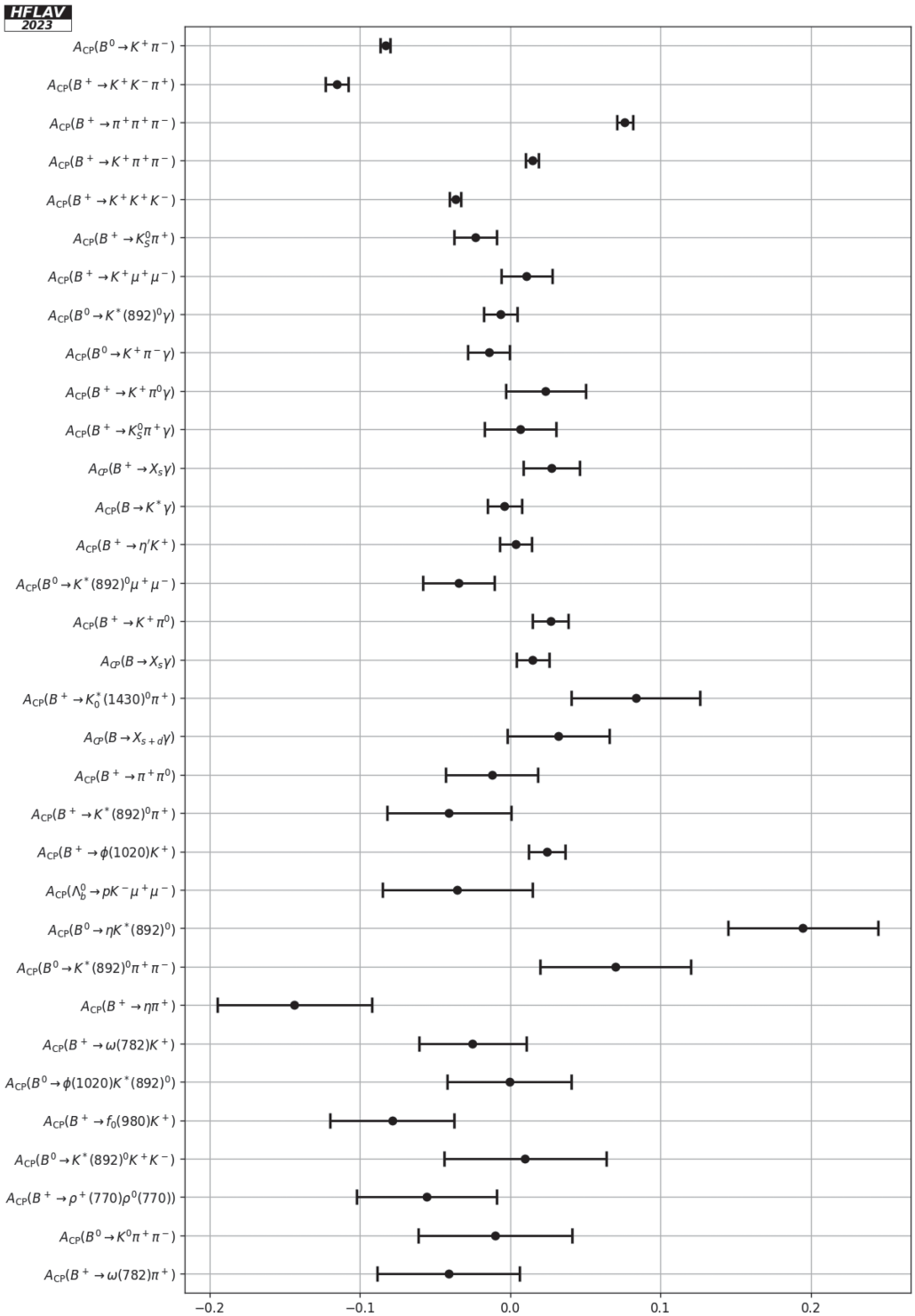


FIG. 41. A selection among the most precise direct *CP* asymmetries (A_{CP}) measured in charmless B^+ and B^0 decay modes.

decays to the same final states with an intermediate charmed baryon.

H. Polarization measurements in b-hadron decays

In this section, compilations of polarization measurements in b-hadron decays are given. Tables 236, 237, and 238 detail measurements of the longitudinal polarization fraction f_L in B^+ B^0, and B_s^0 decays, respectively. They are followed by Tables 239, 240, and 241, which list polarization fractions and CP parameters measured in full angular analyses of B^+, B^0 and B_s^0 decays. Figures 42 and 43 show graphic representations of a selection of results shown in this section.

Most of the final states considered in the tables are pairs of vector mesons and thus, we detail below the corresponding definitions. For specific definitions, for example regarding vector-tensor final states or vector recoiling against dispin-half states, please refer to the articles. In the decay of a pseudoscalar meson into two vector mesons, momentum conservation allows for three helicity configurations: $H_0, H_{\pm 1}$. They can be expressed in terms of longitudinal polarization amplitudes, $A_0 = H_0$, and transverse polarization amplitudes, $A_\perp = (H_{+1} - H_{-1})/\sqrt{2}$ and $A_\parallel = (H_{+1} + H_{-1})/\sqrt{2}$. The corresponding amplitudes for the charge conjugate decays are denoted $\overline{A_0}$, $\overline{A_\parallel}$, and $\overline{A_\perp}$. Using the definition

$$F_{k=0,\parallel,\perp} = \frac{|A_k|^2}{|A_0|^2 + |A_\perp|^2 + |A_\parallel|^2},$$
$$\bar{F}_{k=0,\parallel,\perp} = \frac{|\overline{A_k}|^2}{|\overline{A_0}|^2 + |\overline{A_\perp}|^2 + |\overline{A_\parallel}|^2}, \tag{129}$$

the following CP conserving and CP violating observables, which are used in our tables, are defined

$$f_{k=0,\parallel,\perp} = \frac{1}{2}(F_k + \overline{F_k}), \qquad A_{CP}^{k=0,\perp} = \frac{F_k - \overline{F_k}}{F_k + \overline{F_k}}. \tag{130}$$

TABLE 236. Longitudinal polarization fraction, f_L, in B^+ decays.

Parameter	Measurements		Average
$f_L(B^+ \to \omega(782)K^*(892)^+)$	*BABAR* [724]	$0.41 \pm 0.18 \pm 0.05$	0.41 ± 0.19
$f_L(B^+ \to \omega(782)K_2^*(1430)^+)$	*BABAR* [724]	$0.56 \pm 0.10 \pm 0.04$	0.56 ± 0.11
$f_L(B^+ \to K^*(892)^+\bar{K}^*(892)^0)$	*BABAR* [758]	$0.75^{+0.16}_{-0.26} \pm 0.03$	$0.82^{+0.13}_{-0.17}$
	Belle [757]	$1.06 \pm 0.30 \pm 0.14$	
$f_L(B^+ \to \phi(1020)K^*(892)^+)$	*BABAR* [763][b]	$0.49 \pm 0.05 \pm 0.03$	0.50 ± 0.05
	Belle [1049]	$0.52 \pm 0.08 \pm 0.03$	
	Belle II [760][a]	$0.58 \pm 0.23 \pm 0.02$	
$f_L(B^+ \to \phi(1020)K_1(1270)^+)$	*BABAR* [765]	$0.46^{+0.12\,+0.06}_{-0.13\,-0.07}$	0.46 ± 0.14
$f_L(B^+ \to \phi(1020)K_2^*(1430)^+)$	*BABAR* [765]	$0.80^{+0.09}_{-0.10} \pm 0.03$	0.80 ± 0.10
$f_L(B^+ \to K^*(892)^+\rho^0(770))$	*BABAR* [741]	$0.78 \pm 0.12 \pm 0.03$	0.78 ± 0.12
$f_L(B^+ \to K^*(892)^0\rho^+(770))$	*BABAR* [744]	$0.52 \pm 0.10 \pm 0.04$	0.48 ± 0.08
	Belle [745][c]	$0.43 \pm 0.11^{+0.05}_{-0.02}$	
$f_L(B^+ \to \rho^+(770)\rho^0(770))$	*BABAR* [779]	$0.950 \pm 0.015 \pm 0.006$	0.949 ± 0.015
	Belle II [780][a]	$0.943^{+0.035}_{-0.033} \pm 0.027$	
	Belle [781]	$0.948 \pm 0.106 \pm 0.021$	
$f_L(B^+ \to \omega(782)\rho^+(770))$	*BABAR* [724]	$0.90 \pm 0.05 \pm 0.03$	0.90 ± 0.06
$f_L(B^+ \to p\bar{p}K^*(892)^+)$	Belle [859]	$0.32 \pm 0.17 \pm 0.09$	0.32 ± 0.19

[a]Preliminary result.

[b]Combination of two final states of the $K^*(892)^\pm$, $K_S^0\pi^\pm$ and $K^\pm\pi^0$. In addition to the combined results, the paper reports separately the results for each individual final state.

[c]See also Ref. [747].

TABLE 237. Longitudinal polarization fraction, f_L, in B^0 decays.

Parameter	Measurements		Average
$f_L(B^0 \to \omega(782)K^*(892)^0)$	*BABAR* [724]	$0.72 \pm 0.14 \pm 0.02$	0.69 ± 0.11
	LHCb [1062]	$0.68 \pm 0.17 \pm 0.16$	
	Belle [800]	$0.56 \pm 0.29^{+0.18}_{-0.08}$	
$f_L(B^0 \to \omega(782)K_2^*(1430)^0)$	*BABAR* [724]	$0.45 \pm 0.12 \pm 0.02$	0.45 ± 0.12
$f_L(B^0 \to K^*(892)^0\bar{K}^*(892)^0)$	LHCb [831]	$0.724 \pm 0.051 \pm 0.016$	0.73 ± 0.05
	BABAR [832]	$0.80^{+0.10}_{-0.12} \pm 0.06$	
$f_L(B^0 \to \phi(1020)K^*(892)^0)$	LHCb [1063]	$0.497 \pm 0.019 \pm 0.015$	0.497 ± 0.017
	Belle [825]	$0.499 \pm 0.030 \pm 0.018$	
	BABAR [824]	$0.494 \pm 0.034 \pm 0.013$	
	Belle II [760][a]	$0.57 \pm 0.20 \pm 0.04$	
$f_L(B^0 \to \phi(1020)K_2^*(1430)^0)$	Belle [825]	$0.918^{+0.029}_{-0.060} \pm 0.012$	$0.912^{+0.032}_{-0.046}$
	BABAR [824]	$0.901^{+0.046}_{-0.058} \pm 0.037$	
$f_L(B^0 \to K^*(892)^0\rho^0(770))$	LHCb [1062]	$0.164 \pm 0.015 \pm 0.022$	0.173 ± 0.026
	BABAR [814]	$0.40 \pm 0.08 \pm 0.11$	
$f_L(B^0 \to K^*(892)^+\rho^-(770))$	*BABAR* [814]	$0.38 \pm 0.13 \pm 0.03$	0.38 ± 0.13
$f_L(B^0 \to \rho^+(770)\rho^-(770))$	Belle [848]	$0.988 \pm 0.012 \pm 0.023$	0.985 ± 0.018
	BABAR [849]	$0.992 \pm 0.024^{+0.026}_{-0.013}$	
	Belle II [850][a]	$0.956 \pm 0.035 \pm 0.033$	
$f_L(B^0 \to \rho^0(770)\rho^0(770))$[b]	LHCb [829]	$0.745^{+0.048}_{-0.058} \pm 0.034$	0.71 ± 0.06
	BABAR [845]	$0.75^{+0.11}_{-0.14} \pm 0.04$	
	Belle [844]	$0.21^{+0.18}_{-0.22} \pm 0.15$	
$f_L(B^0 \to a_1(1260)^+a_1(1260)^-)$	*BABAR* [852]	$0.31 \pm 0.22 \pm 0.10$	0.31 ± 0.24
$f_L(B^0 \to p\bar{p}K^*(892)^0)$	Belle [859]	$1.01 \pm 0.13 \pm 0.03$	1.01 ± 0.13
$f_L(B^0 \to \Lambda^0\bar{\Lambda}^0K^*(892)^0)$	Belle [482][c,d]	$0.60 \pm 0.22 \pm 0.08$	0.60 ± 0.23
$f_L(B^0 \to K^{*0}\mu^+\mu^-), 0.04 < q^2 < 6.0\ \mathrm{GeV}^2/c^4$	ATLAS [1034]	$0.50 \pm 0.06 \pm 0.04$	0.50 ± 0.07
$f_L(B^0 \to K^{*0}e^+e^-), 0.002 < q^2 < 1.120\ \mathrm{GeV}^2/c^4$	LHCb [1064]	$0.16 \pm 0.06 \pm 0.03$	0.16 ± 0.07

[a]Preliminary result.
[b]The PDG uncertainty includes a scale factor.
[c]The charmonium mass regions are vetoed.
[d]$m_{\Lambda^0\overline{\Lambda^0}} < 2.85\ \mathrm{GeV}/c^2$.

TABLE 238. Longitudinal polarization fraction, f_L, in B_s^0 decays.

Parameter	Measurements		Average
$f_L(B_s^0 \to \phi(1020)\phi(1020))$	LHCb [840]	$0.381 \pm 0.007 \pm 0.012$	0.378 ± 0.013
	CDF [893]	$0.348 \pm 0.041 \pm 0.021$	
$f_L(B_s^0 \to K^*(892)^0\bar{K}^*(892)^0)$	LHCb [831]	$0.240 \pm 0.031 \pm 0.025$	0.24 ± 0.04
$f_L(B_s^0 \to \phi(1020)\bar{K}^*(892)^0)$	LHCb [826]	$0.51 \pm 0.15 \pm 0.07$	0.51 ± 0.17
$f_L(B_s^0 \to \bar{K}_2^*(1430)^0K^*(892)^0)$	LHCb [1065]	$0.911 \pm 0.020 \pm 0.165$	0.91 ± 0.17
$f_L(B_s^0 \to K_2^*(1430)^0\bar{K}^*(892)^0)$	LHCb [1065]	$0.62 \pm 0.16 \pm 0.25$	0.62 ± 0.30
$f_L(B_s^0 \to K_2^*(1430)^0\bar{K}_2^*(1430)^0)$	LHCb [1065]	$0.25 \pm 0.14 \pm 0.18$	0.25 ± 0.23

TABLE 239. Results of full angular analyses of B^+ decays.

Parameter	Measurements		Average
$f_\perp(B^+ \to \phi(1020)K^*(892)^+)$	*BABAR* [763][a]	$0.21 \pm 0.05 \pm 0.02$	0.20 ± 0.05
	Belle [1049]	$0.19 \pm 0.08 \pm 0.02$	

[a]Combination of two final states of the $K^*(892)^\pm$, $K^0_S\pi^\pm$ and $K^\pm\pi^0$. In addition to the combined results, the paper reports separately the results for each individual final state.

TABLE 240. Results of full angular analyses of B^0 decays.

Parameter	Measurements		Average
$f_\perp(B^0 \to \phi(1020)K^*(892)^0)$	LHCb [1063]	$0.221 \pm 0.016 \pm 0.013$	0.224 ± 0.015
	Belle [825]	$0.238 \pm 0.026 \pm 0.008$	
	BABAR [824]	$0.212 \pm 0.032 \pm 0.013$	
$f_\perp(B^0 \to \phi(1020)K_2^*(1430)^0)$[a]	*BABAR* [824]	$0.002^{+0.018}_{-0.002} \pm 0.031$	$0.029^{+0.024}_{-0.026}$
	Belle [825]	$0.056^{+0.050}_{-0.035} \pm 0.009$	

[a]The PDG uncertainty includes a scale factor.

TABLE 241. Results of full angular analyses of B^0_s decays.

Parameter	Measurements		Average
$f_\perp(B^0_s \to \phi(1020)\phi(1020))$	LHCb [840]	$0.290 \pm 0.008 \pm 0.007$	0.293 ± 0.010
	CDF [893]	$0.365 \pm 0.044 \pm 0.027$	
$f_\parallel(B^0_s \to \phi(1020)\bar{K}^*(892)^0)$	LHCb [826]	$0.21 \pm 0.11 \pm 0.02$	0.21 ± 0.11
$f_\perp(B^0_s \to K^*(892)^0\bar{K}^*(892)^0)$	LHCb [831]	$0.526 \pm 0.032 \pm 0.019$	0.526 ± 0.037
$f_\parallel(B^0_s \to K^*(892)^0\bar{K}^*(892)^0)$	LHCb [831]	$0.234 \pm 0.025 \pm 0.010$	0.23 ± 0.03

Note that, in the literature, f_0 and f_L are used interchangeably to denote the longitudinal polarization fraction.

Measurements that are not included in the tables (the definitions of observables can be found in the corresponding experimental papers):

(i) In the angular analysis of $B^0 \to \phi K^*(892)^0$ decays [1063], in addition to the results quoted in Table 240, LHCb reports observables related to the S-wave component contributing the final state $K^+K^-K^+\pi^-$: $f_S(K\pi)$, $f_S(KK)$, $\delta_s(K\pi)$, $\delta_s(KK)$, $\mathcal{A}_S(K\pi)^{CP}$, $\mathcal{A}_S(KK)^{CP}$, $\delta_S(K\pi)^{CP}$, $\delta_S(KK)^{CP}$.

(ii) In the amplitude analysis of $B^0_s \to \phi\phi$ decays, in addition to the results quoted in Table 241, LHCb, in Ref. [840], extracts the CP-violating phase $\phi_s^{s\bar{s}s}$ and the CP-violating parameter $|\lambda|$ from a decay-time-dependent and polarization independent fit. The CP-violating phases $\phi_{s,\parallel}$ and $\phi_{s,\perp}$ are obtained in a polarization-dependent fit. A time-integrated fit is performed to extract the triple-product asymmetries A_U and A_V. CDF, in Ref. [893] also reports the triple-product asymmetries A_U and A_V.

(iii) In Ref. [1065], LHCb presents a flavor-tagged, decay-time-dependent amplitude analysis of $B^0_s \to (K^+\pi^-)(K^-\pi^+)$ decays in the $K^\pm\pi^\mp$ mass range from 750 to 1600 MeV/c^2. The paper includes measurements of 19 CP-averaged amplitude parameters corresponding to scalar, vector and tensor final states as well as the first measurement of the CP-violating phase $\phi_s^{d\bar{d}}$.

(iv) Reference [1062] presents an amplitude analysis of $B^0 \to \rho K^*(892)^0$ realized by LHCb. Scalar (S) and vector (V) contributions to the final state $(\pi^+\pi^+)(K^+\pi^-)$ are considered through partial waves sharing the same angular dependence (VV, SS, SV, VS) and the corresponding amplitudes are extracted for each case. Triple product asymmetries are also reported.

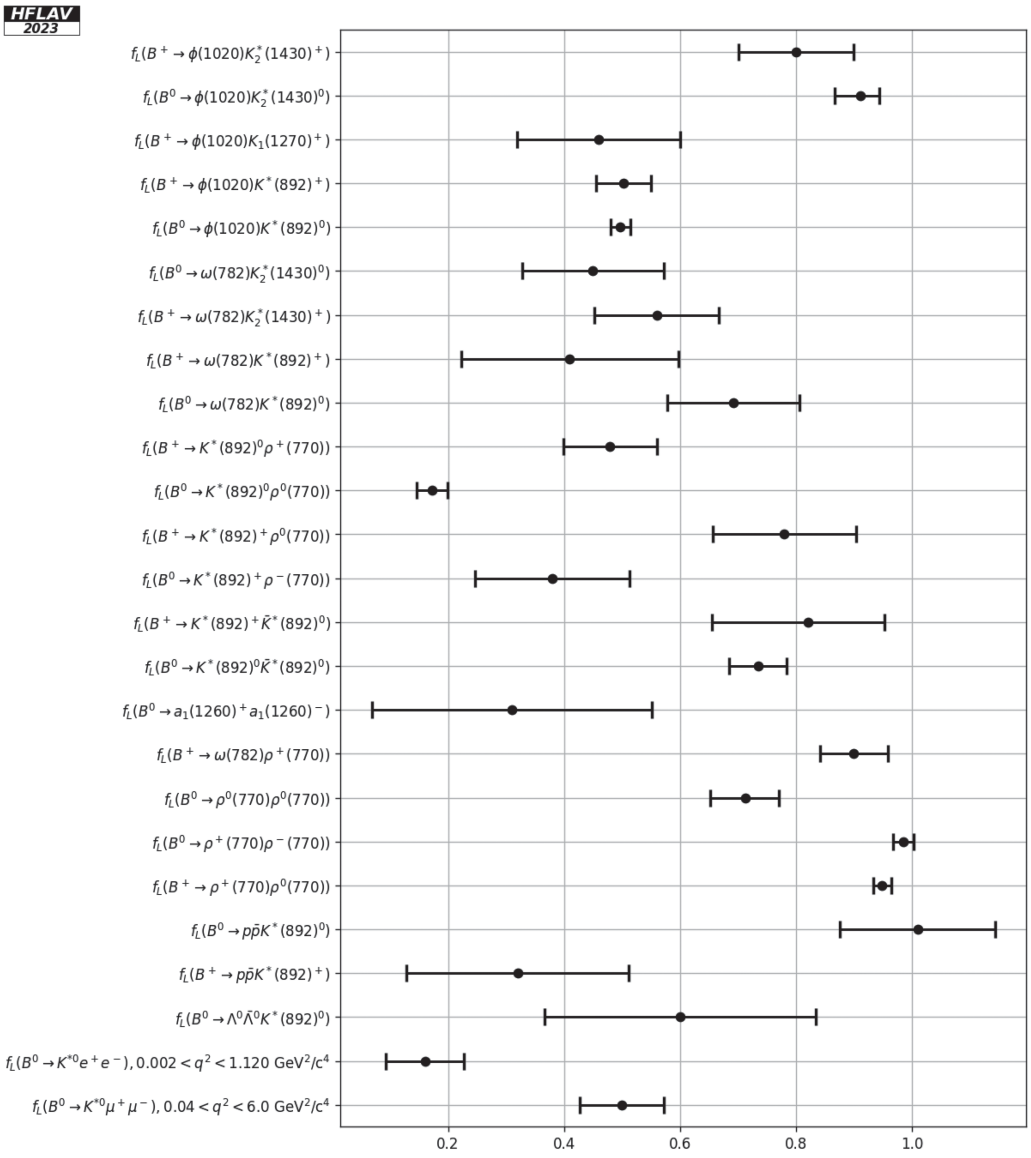


FIG. 42. Longitudinal polarization fraction in charmless B decays.

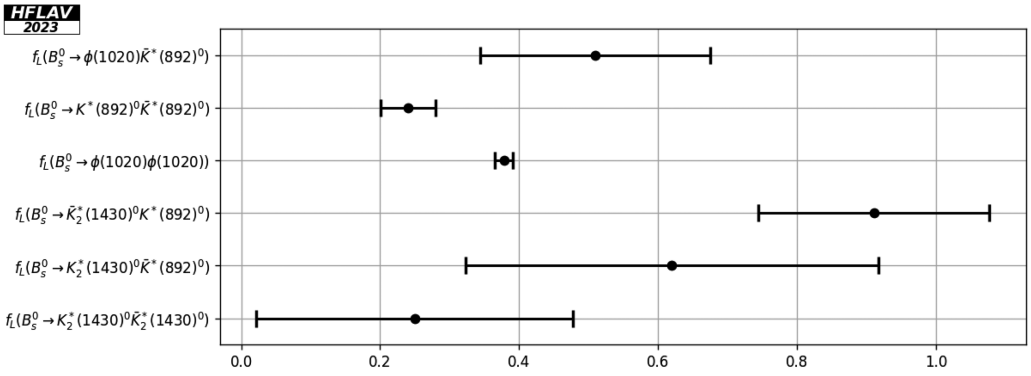


FIG. 43. Longitudinal polarization fraction in charmless B_s^0 decays.

IX. CHARM MIXING AND *CP* VIOLATION

A. D^0-$\bar{D}^0$ mixing and *CP* violation

1. Introduction

The first evidence for D^0-$\bar{D}^0$ oscillations, indicating mixing, was obtained in 2007 by Belle [1066] and *BABAR* [1067]. These results were confirmed later that year by CDF [1068] and, in 2013 with improved precision, by LHCb [1069]. There are now numerous measurements of D^0-$\bar{D}^0$ mixing with various levels of sensitivity. In 2021, LHCb measured the mixing parameters x and y (see below) with much higher precision [1070] than that of previous measurements. All these measurements, plus others, are input into a "global fit" reported here to determine world-average values for mixing parameters, *CP* violation (*CPV*) parameters, and strong phase differences.

Our notation is as follows. We use the phase convention $CP|D^0\rangle = -|\bar{D}^0\rangle$ and $CP|\bar{D}^0\rangle = -|D^0\rangle$ [1071] and denote the mass eigenstates as

$$D_1 = p|D^0\rangle - q|\bar{D}^0\rangle \tag{131}$$

$$D_2 = p|D^0\rangle + q|\bar{D}^0\rangle. \tag{132}$$

Our phase convention corresponds to the following: for $p = q$ (i.e., no indirect *CP* violation), D_1 is *CP*-even and D_2 is *CP*-odd. The mixing parameters are defined as $x \equiv (m_1 - m_2)/\Gamma$ and $y \equiv (\Gamma_1 - \Gamma_2)/(2\Gamma)$, where m_1, m_2 and Γ_1, Γ_2 are the masses and decay widths, respectively, of the mass eigenstates, and $\Gamma \equiv (\Gamma_1 + \Gamma_2)/2$.

We perform a global fit to determine central values and uncertainties for ten underlying parameters. These parameters, in addition to x and y, are as follows:

(i) *CPV* parameters $|q/p|$ and $\mathrm{Arg}(q/p) \equiv \phi$, which give rise to indirect *CPV* (see Sec. IX B for a discussion of indirect and direct *CPV*). Here we assume that indirect *CPV* (when present) is "universal," i.e., independent of the final state f in the decay $D^0 \to f$.

(ii) direct *CPV* asymmetries

$$A_D \equiv \frac{\Gamma(D^0 \to K^+\pi^-) - \Gamma(\bar{D}^0 \to K^-\pi^+)}{\Gamma(D^0 \to K^+\pi^-) + \Gamma(\bar{D}^0 \to K^-\pi^+)}$$
$$A_K \equiv \frac{\Gamma(D^0 \to K^+K^-) - \Gamma(\bar{D}^0 \to K^-K^+)}{\Gamma(D^0 \to K^+K^-) + \Gamma(\bar{D}^0 \to K^-K^+)}$$
$$A_\pi \equiv \frac{\Gamma(D^0 \to \pi^+\pi^-) - \Gamma(\bar{D}^0 \to \pi^-\pi^+)}{\Gamma(D^0 \to \pi^+\pi^-) + \Gamma(\bar{D}^0 \to \pi^-\pi^+)},$$

where, as indicated, the decay rates are for the pure D^0 and $\bar{D}^0$ flavor eigenstates.

(iii) the ratio of doubly Cabibbo-suppressed (DCS) to Cabibbo-favored (CF) decay rates

$$R_D \equiv \frac{\Gamma(D^0 \to K^+\pi^-) + \Gamma(\bar{D}^0 \to K^-\pi^+)}{\Gamma(D^0 \to K^-\pi^+) + \Gamma(\bar{D}^0 \to K^+\pi^-)}.$$

(iv) the strong phase difference δ between the amplitudes $\mathcal{A}(\bar{D}^0 \to K^-\pi^+)$ and $\mathcal{A}(D^0 \to K^-\pi^+)$; and

(v) the strong phase difference $\delta_{K\pi\pi}$ between the amplitudes $\mathcal{A}(\bar{D}^0 \to K^-\rho^+)$ and $\mathcal{A}(D^0 \to K^-\rho^+)$.

There are 63 measurements of 18 observables used in the fit. The measurements are based on the following Cabibbo-suppressed decays[17]: $D^0 \to K^{(*)+}\ell^-\bar{\nu}$, $D^0 \to K^+K^-$, $D^0 \to \pi^+\pi^-$, $D^0 \to K^+\pi^-$, $D^0 \to K^+\pi^-\pi^0$, $D^0 \to K^0_S\pi^+\pi^-$, $D^0 \to \pi^0\pi^+\pi^-$, $D^0 \to K^0_S K^+K^-$, and $D^0 \to K^+\pi^-\pi^+\pi^-$. The fit also uses measurements of mixing parameters and strong phases determined using quantum correlations and double-tagged branching fractions measured in $e^+e^- \to \Psi(3770) \to D\bar{D}$ reactions. The relationships between measured observables and fitted parameters are given in Table 242. Correlations among measured observables are accounted for by using covariance matrices provided by the experimental collaborations. Uncertainties are assumed to be Gaussian, and systematic uncertainties among different experiments are assumed to be uncorrelated unless specific correlations have been identified. We have compared this method with a second method that adds together three-dimensional log-likelihood functions for x, y, and δ obtained from several independent measurements; this combination accounts for non-Gaussian uncertainties. When both methods are applied to the same set of measurements, equivalent results are obtained. We have furthermore compared the results to those obtained from an independent fit based on the GAMMACOMBO framework [1072] and found excellent agreement.

Mixing in the heavy flavor B^0 and B^0_s systems is governed by a short-distance box diagram. In the D^0 system, however, this box diagram is both doubly-Cabibbo-suppressed and GIM-suppressed [1073], and thus the short-distance mixing rate is tiny. As a consequence, D^0-$\bar{D}^0$ mixing is dominated by long-distance processes. These are difficult to calculate, and theoretical estimates for x and y range over three orders of magnitude, up to the percent level [1074–1077].

Most experimental analyses besides that of the $\psi(3770) \to \bar{D}D$ measurements identify the flavor of the D^0 or $\bar{D}^0$ when produced by reconstructing the decay $D^{*+} \to D^0\pi^+$ or $D^{*-} \to \bar{D}^0\pi^-$. The charge of the pion, which has low momentum in the lab frame relative to that of the D^0 daughters and is often referred to as the "soft" pion, identifies the D^0 flavor. For $D^{*+} \to D^0\pi^+$,

[17]Charge-conjugate modes are implicitly included.

TABLE 242. Left column: decay modes used to determine the fitted parameters x, y, δ, $\delta_{K\pi\pi}$, R_D, A_D, A_K, A_π, $|q/p|$, and ϕ. Middle column: measured observables for each decay mode. Right column: relationships between the measured observables and the fitted parameters. The symbol $\langle t \rangle$ denotes the mean reconstructed decay time for $D^0 \to K^+K^-$ or $D^0 \to \pi^+\pi^-$ decays.

Decay Mode	Observables	Relationship
$D^0 \to K^+K^-/\pi^+\pi^-$	y_{CP} A_Γ	$2y_{CP} = (\lvert q/p\rvert + \lvert p/q\rvert)y\cos\phi - (\lvert q/p\rvert - \lvert p/q\rvert)x\sin\phi$ $2A_\Gamma = (\lvert q/p\rvert - \lvert p/q\rvert)y\cos\phi - (\lvert q/p\rvert + \lvert p/q\rvert)x\sin\phi$
$D^0 \to K^0_S\pi^+\pi^-$	x y $\lvert q/p\rvert$ ϕ	
$D^0 \to K^{(*)+}\ell^-\bar{\nu}$	R_M	$R_M = \frac{x^2+y^2}{2}$
$D^0 \to K^+\pi^-\pi^0$ (Dalitz plot analysis)	x'' y''	$x'' = x\cos\delta_{K\pi\pi} + y\sin\delta_{K\pi\pi}$ $y'' = y\cos\delta_{K\pi\pi} - x\sin\delta_{K\pi\pi}$
"Double-tagged" branching fractions measured in $\psi(3770) \to DD$ decays	R_M y R_D $\sqrt{R_D}\cos\delta$	$R_M = \frac{x^2+y^2}{2}$
$D^0 \to K^+\pi^-$	x'^2, y' x'^{2+}, x'^{2-} y'^+, y'^-	$x' = x\cos\delta + y\sin\delta$ $y' = y\cos\delta - x\sin\delta$ $x'^{\pm} = \lvert q/p\rvert^{\pm 1}(x'\cos\phi \pm y'\sin\phi)$ $y'^{\pm} = \lvert q/p\rvert^{\pm 1}(y'\cos\phi \mp x'\sin\phi)$
$D^0 \to K^+\pi^-/K^-\pi^+$ (time-integrated)	R_D A_D	
$D^0 \to K^+K^-/\pi^+\pi^-$ (time-integrated)	$\frac{\Gamma(D^0 \to K^+K^-) - \Gamma(\bar{D}^0 \to K^+K^-)}{\Gamma(D^0 \to K^+K^-) + \Gamma(\bar{D}^0 \to K^+K^-)}$ $\frac{\Gamma(D^0 \to \pi^+\pi^-) - \Gamma(\bar{D}^0 \to \pi^+\pi^-)}{\Gamma(D^0 \to \pi^+\pi^-) + \Gamma(\bar{D}^0 \to \pi^+\pi^-)}$	$A_K + \frac{\langle t\rangle}{\tau_D}\mathcal{A}_{CP}^{\text{indirect}}$ $(\mathcal{A}_{CP}^{\text{indirect}} \approx -A_\Gamma)$ $A_\pi + \frac{\langle t\rangle}{\tau_D}\mathcal{A}_{CP}^{\text{indirect}}$ $(\mathcal{A}_{CP}^{\text{indirect}} \approx -A_\Gamma)$

$M_{D^*} - M_{D^0} - M_{\pi^+} \equiv Q \approx 6$ MeV/c^2; this value is close to the kinematic threshold. Thus, analyses typically require that the reconstructed Q be less than some value (e.g., 20 MeV/c^2) to suppress backgrounds. In some analyses, LHCb identifies the flavor of the D^0 by partially reconstructing $\bar{B} \to D^{(*)}\mu^- X$ and $B \to \bar{D}^{(*)}\mu^+ X$ decays; in this case the charge of the $\mu^\mp$ identifies the flavor of the D^0 or $\bar{D}^0$.

For time-dependent measurements, the D^0 decay time is calculated as $t = M_{D^0}(\vec{d}\cdot\hat{p})/p$, where $\vec{d}$ is the displacement vector from the D^0 production vertex to the D^0 decay vertex, $\hat{p}$ is the direction of the D^0 momentum, and p is its magnitude. At e^+e^- experiments, the D^{*+} vertex position is typically taken as the intersection of the D^0 momentum vector with the beam spot profile. At pp and $\bar{p}p$ experiments, the D^{*+} decay vertex is taken to be at a primary interaction vertex.

2. Input measurements

The global fit determines central values and uncertainties for the above ten parameters by minimizing a χ^2 statistic. All input measurements are listed in Tables 243–248. In the $D^0 \to K^+\pi^-\pi^0$ Dalitz plot analysis [1078], the phases of intermediate resonances are fitted relative to the phase of $\mathcal{A}(D^0 \to K^+\rho^-)$, and the phases of resonances in $\bar{D}^0 \to K^+\pi^-\pi^0$ are fitted relative to the phase of $\mathcal{A}(\bar{D}^0 \to K^+\rho^-)$. The phase difference $\delta_{K\pi\pi} \equiv \text{Arg}[\mathcal{A}(\bar{D}^0 \to K^+\rho^-)/\mathcal{A}(D^0 \to K^+\rho^-)]$ cannot be determined from these fits but can be constrained in the global fit and is included as a fitted parameter.

Three inputs to the fit are themselves world averages of relevant measurements:

$$R_M = \frac{x^2+y^2}{2} \tag{133}$$

TABLE 243. Measurements of $R_M = (x^2 + y^2)/2$ from "wrong-sign" semileptonic $D^0 \to K^{(*)+}\ell^-\bar{\nu}$ decays measured relative to "right-sign" $D^0 \to K^{(*)-}\ell^+\nu$ decays. The weighted average is used in the global fit.

Experiment	$R_M(\%)$	Comment
FNAL E791 (1996) [1081]	$0.11^{+0.30+0.00}_{-0.27-0.014}$	500 GeV $\pi^- N$ interactions (2×10^{10} events)
CLEO II (2005) [1082]	$0.16 \pm 0.29 \pm 0.29$	9.0 fb^{-1} near $\Upsilon(4S)$ resonance
BABAR (2004) [1083]	$0.23 \pm 0.12 \pm 0.04$	87 fb^{-1} near $\Upsilon(4S)$ resonance
BABAR (2007) [1084]	$0.004^{+0.070}_{-0.060}$	344 fb^{-1} near $\Upsilon(4S)$ resonance; tag side reconstructed + D^* tag (decays are "double-tagged")
Belle (2008) [1085]	$0.013 \pm 0.022 \pm 0.020$	492 fb^{-1} near $\Upsilon(4S)$ resonance
Weighted average	0.0130 ± 0.0269	Stat. and syst. errors taken to be uncorrelated; *BABAR* 2004 result not included due to unknown correlation with *BABAR* 2007

TABLE 244. Measurements of y_{CP} using singly Cabibbo-suppressed decays $D^0 \to K^+K^-$, $D^0 \to \pi^+\pi^-$, $D^0 \to K^0_S h(h = \pi^0, \eta, \omega)$, $D^0 \to K^0_S\pi^0\pi^0$, and $D^0 \to K^0_S K^+K^-$. The weighted average is used in the global fit.

Experiment	Final state	$y_{CP}(\%)$	Comment
FNAL E791 (1999) [1086]	K^+K^-	$0.73 \pm 2.89 \pm 1.03$	$\pi^- N$ interactions (2×10^{10} events)
FOCUS (2000) [1087]	K^+K^-	$3.42 \pm 1.39 \pm 0.74$	γN interactions (1×10^6 events)
CLEO II (2002) [1088]	$K^+K^-, \pi^+\pi^-$	$-1.2 \pm 2.5 \pm 1.4$	9.0 fb^{-1} near $\Upsilon(4S)$ resonance
Belle (2009) [1089]	$K^0_S K^+K^-$	$0.11 \pm 0.61 \pm 0.52$	673 fb^{-1} near $\Upsilon(4S)$ resonance
BABAR (2012) [1090]	$K^+K^-, \pi^+\pi^-$	$0.72 \pm 0.18 \pm 0.12$	468 fb^{-1} near $\Upsilon(4S)$ resonance
BES III (2015) [1091]	$K^+K^-, \pi^+\pi^-, K^0_S\pi^0, K^0_S\eta, K^0_S\omega, K^0_S\pi^0\pi^0$	$-2.0 \pm 1.3 \pm 0.7$	2.92 fb^{-1} near $\psi(3770)$ resonance
Belle (2016) [1092]	$K^+K^-, \pi^+\pi^-$	$1.11 \pm 0.22 \pm 0.09$	976 fb^{-1} near $\Upsilon(4S)$ resonance
LHCb (2019) [1093]	$K^+K^-, \pi^+\pi^-$	$0.57 \pm 0.13 \pm 0.09$	3 fb^{-1} at $\sqrt{s} = 7, 8$ TeV; B flavortag
Belle (2020) [1094]	$K^0_S\omega$	$0.96 \pm 0.91^{+0.64}_{-0.62}$	976 fb^{-1} near $\Upsilon(4S)$ resonance
LHCb (2022) [1095]	$K^+K^-, \pi^+\pi^-$	$y_{CP} - y_{CP}(K^-\pi^+) = 0.696 \pm 0.026 \pm 0.013$	6 fb^{-1} at $\sqrt{s} = 13$ TeV; D^* flavor tag
Weighted average		0.697 ± 0.028	

$$y_{CP} = \frac{1}{2}\left(\left|\frac{q}{p}\right| + \left|\frac{p}{q}\right|\right) y\cos\phi - \frac{1}{2}\left(\left|\frac{q}{p}\right| - \left|\frac{p}{q}\right|\right) x\sin\phi \qquad (134)$$

$$A_\Gamma = \frac{1}{2}\left(\left|\frac{q}{p}\right| - \left|\frac{p}{q}\right|\right) y\cos\phi - \frac{1}{2}\left(\left|\frac{q}{p}\right| + \left|\frac{p}{q}\right|\right) x\sin\phi. \qquad (135)$$

The world average for R_M is calculated from measurements of $D^0 \to K^{(*)+}\ell^-\bar{\nu}$ decays relative to $D^0 \to K^{(*)-}\ell^+\nu$ decays, as listed in Table 243. A measurement of R_M using $D^0 \to K^+\pi^-\pi^+\pi^-$ decays [1105] is input separately to the global fit. The world averages for y_{CP} and A_Γ are calculated from measurements of $D^0 \to K^+K^-$, $D^0 \to \pi^+\pi^-$, $D^0 \to K^0_S h(h = \pi^0, \eta, \omega)$, $D^0 \to K^0_S\pi^0\pi^0$, and $D^0 \to K^0_S K^+K^-$ decays, as listed in Tables 244 and 245. The most recent measurement of y_{CP} from LHCb is sufficiently precise such that the small value of $y^{K\pi}_{CP}$ for Cabibbo-favored $D^0 \to K^-\pi^+$ decays, which is also used for the measurement, must be taken into account (i.e., subtracted) [1079]. The $y^{K\pi}_{CP}$ correction we use for the global fit is from Ref. [1080].

The $D^0 \to K^+\pi^-$ measurements used are from Belle [1108,1109], *BABAR* [1067], CDF [1110], and LHCb [1111,1112]; earlier measurements are either superseded or have significantly less precision and are not used. The observables from $D^0 \to K^0_S\pi^+\pi^-$ decays are measured in two ways: assuming CP conservation (D^0 and $\bar{D}^0$ decays

TABLE 245. Measurements of A_Γ using singly Cabibbo-suppressed decays $D^0 \to K^+K^-$ and $D^0 \to \pi^+\pi^-$. The weighted average is used in the global fit.

Experiment	Final state	$A_\Gamma(\times 10^{-3})$	Comment
BABAR (2012) [1090]	$K^+K^- + \pi^+\pi^-$	$0.9 \pm 2.6 \pm 0.6$	468 fb^{-1} near $\Upsilon(4S)$ resonance
CDF (2014) [1096]	$K^+K^- + \pi^+\pi^-$	-1.2 ± 1.2	9.7 fb^{-1} at $\sqrt{s} = 2.0$ TeV
	K^+K^-	$-1.9 \pm 1.5 \pm 0.4$	
	$\pi^+\pi^-$	$-0.1 \pm 1.8 \pm 0.3$	
Belle (2016) [1092]	$K^+K^- + \pi^+\pi^-$	$-0.3 \pm 2.0 \pm 0.7$	976 fb^{-1} near $\Upsilon(4S)$ resonance
LHCb (2021) [1097]	$K^+K^- + \pi^+\pi^-$	$0.10 \pm 0.11 \pm 0.03$	8.4 fb^{-1} at $\sqrt{s} = 7$, 8, 13 TeV
	K^+K^-	$0.03 \pm 0.13 \pm 0.03$	$D^* + B$ flavor tags
	$\pi^+\pi^-$	$0.36 \pm 0.24 \pm 0.04$	
Weighted average		0.089 ± 0.113	

combined), and allowing for CP violation (D^0 and $\bar{D}^0$ decays fitted separately). The no-CPV measurements are from Belle [1098], *BABAR* [1103], and LHCb [1099]; for the CPV-allowed case, only Belle [1098] and LHCb [1070,1100] measurements are available. The $D^0 \to K^+\pi^-\pi^0$, $D^0 \to K^0_S K^+K^-$, and $D^0 \to \pi^0\pi^+\pi^-$ results are from *BABAR* [1078,1104]; the $D^0 \to K^+\pi^-\pi^+\pi^-$ result is from LHCb [1105]; and the $\psi(3770) \to \bar{D}D$ results are from CLEOc [1106]. Measurements of the strong phase δ by BES III [1107,1119] based on $\psi(3770) \to \bar{D}D$ events use HFLAV's world averages for R_D and y as external inputs; thus, we do not include these results in the global fit. However, a BES III measurement [1107] of the asymmetry between CP-even-tagged and CP-odd-tagged $D^0 \to K^-\pi^+$ decays, denoted $A^{CP}_{K\pi}$, is included. To lowest order in the mixing parameters, $A^{CP}_{K\pi} = (2\sqrt{R_D}\cos\delta + y)/(1 + R)$, where $R = R_D + \sqrt{R_D}(y\cos\delta - x\sin\delta) + (x^2 + y^2)/2$.

For each set of correlated observables, we construct a difference vector $\vec{V}$ between the measured values and those calculated from the fitted parameters using the relations of Table 242. For example, for $D^0 \to K^0_S\pi^+\pi^-$ decays, $\vec{V} = (\Delta x, \Delta y, \Delta|q/p|, \Delta\phi)$, where $\Delta x \equiv x_{\text{measured}} - x_{\text{fitted}}$ and similarly for $\Delta y, \Delta|q/p|$, and $\Delta\phi$. The contribution of a set of observables to the fit χ^2 is calculated as $\vec{V} \cdot (M^{-1}) \cdot \vec{V}^T$, where M^{-1} is the inverse of the covariance matrix for the measured observables. Covariance matrices are constructed from the correlation coefficients among the observables. These correlation coefficients are furnished by the experiments and listed in Tables 246 and 247.

3. Fit results

The global fitter uses MINUIT with the MIGRAD minimizer, and all uncertainties are obtained from MINOS [1120]. Three categories of fits are performed:

(1) One-parameter description of indirect CP violation

This parametrization is based on two simplifications: (1) subleading amplitudes in CF and DCS decays are neglected; and (2) subleading amplitudes in singly Cabibbo-suppressed (SCS) decays are neglected in indirect CP violation observables, as their contribution is suppressed by the mixing parameters x and y. These simplifications imply there is no direct CP violation in CF or DCS decays ($A_D = 0$), and that all indirect CP violation can be parametrized in terms of the phase difference between M_{12} and Γ_{12}, the off-diagonal elements of the mass and decay matrices, respectively, for the D^0-$\bar{D}^0$ system. This difference, $\text{Arg}(M_{12}/\Gamma_{12}) \equiv \phi_{12}$, is independent of phase convention. For the phase convention in which the dominant $\Delta(U\text{-spin}) = 2$ amplitudes are aligned with the real axis, $\text{Arg}(\Gamma_{12}) = 0$, and thus $\phi_{12} = \text{Arg}(M_{12})$. Neglecting subleading amplitudes, it can be shown that $\tan\phi = (1 - |q/p|^2)/(1 + |q/p|^2)(x/y)$, i.e., only three of the four parameters $(x, y, |q/p|, \phi)$ are independent. This relation was first derived by Ciuchini *et al.* [1121] and later, independently, by Kagan and Sokoloff [1122]. Defining alternative mixing parameters $x_{12} \equiv 2|M_{12}|/\Gamma$ and $y_{12} \equiv |\Gamma_{12}|/\Gamma$, the traditional parameters $(x, y, |q/p|, \phi)$ can be expressed in terms of $(x_{12}, y_{12}, \phi_{12})$ as follows [1122,1123]:

$$x = \left[\frac{x_{12}^2 - y_{12}^2 + \sqrt{(x_{12}^2 + y_{12}^2)^2 - 4x_{12}^2 y_{12}^2 \sin^2\phi_{12}}}{2}\right]^{1/2} \tag{136}$$

$$y = \left[\frac{y_{12}^2 - x_{12}^2 + \sqrt{(x_{12}^2 + y_{12}^2)^2 - 4x_{12}^2 y_{12}^2 \sin^2\phi_{12}}}{2}\right]^{1/2} \tag{137}$$

$$\left|\frac{q}{p}\right| = \left(\frac{x_{12}^2 + y_{12}^2 + 2x_{12}y_{12}\sin\phi_{12}}{x_{12}^2 + y_{12}^2 - 2x_{12}y_{12}\sin\phi_{12}}\right)^{1/4} \tag{138}$$

TABLE 246. Measurements used in the global fit, except those from time-dependent $D^0 \to K^+\pi^-$ measurements (listed in Table 247) and those from direct CPV measurements (listed in Table 248).

Mode	Observable	Values	Correlation coefficients
$D^0 \to K^+K^-/\pi^+\pi^-$, ϕK^0_S	$y_{CP} - y_{CP}(K\pi)$	$(0.697 \pm 0.028)\%$	
	A_Γ	$(0.0089 \pm 0.0113)\%$	
$D^0 \to K^0_S\pi^+\pi^-$ [1098] (Belle: no CPV)	x	$(0.56 \pm 0.19^{+0.067}_{-0.127})\%$	$+0.012$
	y	$(0.30 \pm 0.15^{+0.050}_{-0.078})\%$	
$D^0 \to K^0_S\pi^+\pi^-$ [1098] (Belle: no direct CPV)	x	$(0.56 \pm 0.19^{+0.067}_{-0.127})\%$	$\begin{Bmatrix} 10.054 & -0.074 & -0.031 \\ 1 & 0.034 & -0.019 \\ & 1 & 0.044 \\ & & 1 \end{Bmatrix}$
	y	$(0.30 \pm 0.15^{+0.050}_{-0.078})\%$	
	$\lvert q/p\rvert$	$0.90^{+0.16+0.078}_{-0.15-0.064}$	
	ϕ	$(-6 \pm 11^{+4.2}_{-5.0})$ degrees	
$D^0 \to K^0_S\pi^+\pi^-$ [1098] (Belle: direct CPV allowed)	x	$(0.58 \pm 0.19^{+0.0734}_{-0.1177})\%$	same as above
	y	$(0.27 \pm 0.16^{+0.0546}_{-0.0854})\%$	
	$\lvert q/p\rvert$	$0.82^{+0.20+0.0807}_{-0.18-0.0645}$	
	ϕ	$(-13^{+12+4.15}_{-13-4.77})$ degrees	
$D^0 \to K^0_S\pi^+\pi^-$ [1099] (LHCb: 1 fb^{-1} no CPV)	x	$(-0.86 \pm 0.53 \pm 0.17)\%$	$+0.37$
	y	$(0.03 \pm 0.46 \pm 0.13)\%$	
$D^0 \to K^0_S\pi^+\pi^-$ [1100] (LHCb: 3 fb^{-1} CPV allowed)	x_{CP}	$(0.27 \pm 0.16 \pm 0.04)\%$	$\begin{Bmatrix} 1 & (-0.17+0.15) & (0.04+0.01) & (-0.02-0.02) \\ & 1 & (-0.03-0.05) & (0.01-0.03) \\ & & 1 & (-0.13+0.14) \\ & & & 1 \end{Bmatrix}$ Notation: above coefficients are (statistical + systematic). For $(x, y, \lvert q/p\rvert, \phi) \to (x_{CP}, y_{CP}, \Delta x, \Delta y)$ mapping, see [1101].
	y_{CP}	$(0.74 \pm 0.36 \pm 0.11)\%$	
	Δx	$(-0.053 \pm 0.070 \pm 0.022)\%$	
	Δy	$(0.06 \pm 0.16 \pm 0.03)\%$	
$D^0 \to K^0_S\pi^+\pi^-$ [1102] (LHCb: 5.4 fb^{-1} CPV allowed)	x_{CP}	$(0.401 \pm 0.045 \pm 0.020)\%$	$\begin{Bmatrix} 1 & (0.121+0.13) & (-0.018+0.01) & (-0.016+0.01) \\ & 1 & (-0.012-0.02) & (-0.058+0.01) \\ & & 1 & (0.069+0.31) \\ & & & 1 \end{Bmatrix}$
	y_{CP}	$(0.551 \pm 0.116 \pm 0.059)\%$	
	Δx	$(-0.029 \pm 0.018 \pm 0.001)\%$	
	Δy	$(0.031 \pm 0.035 \pm 0.013)\%$	
$D^0 \to K^0_S\pi^+\pi^-$ [1103] $K^0_SK^+K^-$ (*BABAR*: no CPV)	x	$(0.16 \pm 0.23 \pm 0.12 \pm 0.08)\%$	$+0.0615$
	y	$(0.57 \pm 0.20 \pm 0.13 \pm 0.07)\%$	
$D^0 \to \pi^0\pi^+\pi^-$ [1104] (*BABAR*: no CPV)	x	$(1.5 \pm 1.2 \pm 0.6)\%$	-0.006
	y	$(0.2 \pm 0.9 \pm 0.5)\%$	
$D^0 \to K^+\ell^-\bar{\nu}$	R_M	$(0.0130 \pm 0.0269)\%$	
$D^0 \to K^+\pi^-\pi^0$ [1078]	x''	$(2.61^{+0.57}_{-0.68} \pm 0.39)\%$	-0.75
	y''	$(-0.06^{+0.55}_{-0.64} \pm 0.34)\%$	
$D^0 \to K^+\pi^-\pi^+\pi^-$ [1105] (LHCb)	$R_M/2$	$(4.8 \pm 1.8) \times 10^{-5}$	
$\psi(3770) \to \bar{D}D$ [1106] (CLEOc)	R_D	$(0.533 \pm 0.107 \pm 0.045)\%$	$\begin{Bmatrix} 1 & 0 & 0 & -0.42 & 0.01 \\ & 1 & -0.73 & 0.39 & 0.02 \\ & & 1 & -0.53 & -0.03 \\ & & & 1 & 0.04 \\ & & & & 1 \end{Bmatrix}$
	x^2	$(0.06 \pm 0.23 \pm 0.11)\%$	
	y	$(4.2 \pm 2.0 \pm 1.0)\%$	
	$\cos\delta$	$0.81^{+0.22+0.07}_{-0.18-0.05}$	
	$\sin\delta$	$-0.01 \pm 0.41 \pm 0.04$	
$\psi(3770) \to \bar{D}D$ [1107] (BES III)	$A_{CP}(K\pi)$	$0.132 \pm 0.011 \pm 0.007$	

TABLE 247. Time-dependent $D^0 \to K^+\pi^-$ observables used for the global fit. The observables R_D^+ and R_D^- are related to parameters R_D and A_D via $R_D^\pm = R_D(1 \pm A_D)$.

Mode	Observable	Values	Correlation coefficients
$D^0 \to K^+\pi^-$ [1067] (*BABAR* 384 fb^{-1})	R_D	$(0.303 \pm 0.0189)\%$	$\begin{Bmatrix} 1 & 0.77 & -0.87 \\ & 1 & -0.94 \\ & & 1 \end{Bmatrix}$
	x'^{2+}	$(-0.024 \pm 0.052)\%$	
	y'^{+}	$(0.98 \pm 0.78)\%$	
$\bar{D}^0 \to K^-\pi^+$ [1067] (*BABAR* 384 fb^{-1})	A_D	$(-2.1 \pm 5.4)\%$	$\begin{Bmatrix} 1 & 0.77 & -0.87 \\ & 1 & -0.94 \\ & & 1 \end{Bmatrix}$
	x'^{2-}	$(-0.020 \pm 0.050)\%$	
	y'^{-}	$(0.96 \pm 0.75)\%$	
$D^0 \to K^+\pi^-$ [1108] (Belle 976 fb^{-1} No *CPV*)	R_D	$(0.353 \pm 0.013)\%$	$\begin{Bmatrix} 1 & 0.737 & -0.865 \\ & 1 & -0.948 \\ & & 1 \end{Bmatrix}$
	x'^{2}	$(0.009 \pm 0.022)\%$	
	y'	$(0.46 \pm 0.34)\%$	
$D^0 \to K^+\pi^-$ [1109] (Belle 400 fb^{-1} *CPV*-allowed)	R_D	$(0.364 \pm 0.018)\%$	$\begin{Bmatrix} 1 & 0.655 & -0.834 \\ & 1 & -0.909 \\ & & 1 \end{Bmatrix}$
	x'^{2+}	$(0.032 \pm 0.037)\%$	
	y'^{+}	$(-0.12 \pm 0.58)\%$	
$\bar{D}^0 \to K^-\pi^+$ [1109] (Belle 400 fb^{-1} *CPV*-allowed)	A_D	$(+2.3 \pm 4.7)\%$	$\begin{Bmatrix} 1 & 0.655 & -0.834 \\ & 1 & -0.909 \\ & & 1 \end{Bmatrix}$
	x'^{2-}	$(0.006 \pm 0.034)\%$	
	y'^{-}	$(0.20 \pm 0.54)\%$	
$D^0 \to K^+\pi^-$ [1110] (CDF 9.6 fb^{-1} No *CPV*)	R_D	$(0.351 \pm 0.035)\%$	$\begin{Bmatrix} 1 & 0.90 & -0.97 \\ & 1 & -0.98 \\ & & 1 \end{Bmatrix}$
	x'^{2}	$(0.008 \pm 0.018)\%$	
	y'	$(0.43 \pm 0.43)\%$	
$D^0 \to K^+\pi^-$ [1111] (LHCb 3.0 fb^{-1} $B \to D^*\mu X$ tag *CPV*-allowed)	R_D^+	$(0.338 \pm 0.0161)\%$	$\begin{Bmatrix} 1 & 0.823 & -0.920 \\ & 1 & -0.962 \\ & & 1 \end{Bmatrix}$
	x'^{2+}	$(-0.0019 \pm 0.0447)\%$	
	y'^{+}	$(0.581 \pm 0.526)\%$	
$\bar{D}^0 \to K^-\pi^+$ [1111] (LHCb 3.0 fb^{-1} $B \to D^*\mu X$ tag *CPV*-allowed)	R_D^-	$(0.360 \pm 0.0166)\%$	$\begin{Bmatrix} 1 & 0.812 & -0.918 \\ & 1 & -0.956 \\ & & 1 \end{Bmatrix}$
	x'^{2-}	$(0.0079 \pm 0.0433)\%$	
	y'^{-}	$(0.332 \pm 0.523)\%$	
$D^0 \to K^+\pi^-$ [1112] (LHCb 5.0 fb^{-1} D^* tag *CPV*-allowed)	R_D^+	$(0.3454 \pm 0.0045)\%$	$\begin{Bmatrix} 1 & 0.843 & -0.935 \\ & 1 & -0.963 \\ & & 1 \end{Bmatrix}$
	x'^{2+}	$(0.0061 \pm 0.0037)\%$	
	y'^{+}	$(0.501 \pm 0.074)\%$	
$\bar{D}^0 \to K^-\pi^+$ [1112] (LHCb 5.0 fb^{-1} D^* tag *CPV*-allowed)	R_D^-	$(0.3454 \pm 0.0045)\%$	$\begin{Bmatrix} 1 & 0.846 & -0.935 \\ & 1 & -0.964 \\ & & 1 \end{Bmatrix}$
	x'^{2-}	$(0.0016 \pm 0.0039)\%$	
	y'^{-}	$(0.554 \pm 0.074)\%$	

$$\tan 2\phi = -\frac{\sin 2\phi_{12}}{\cos 2\phi_{12} + (y_{12}/x_{12})^2}. \quad (139)$$

Based on this formalism, three separate fits are performed:

(a) float x, y, and ϕ and use the Ciuchini/Kagan formula to derive $|q/p|$; this yields (MINOS) errors for (x, y, ϕ).

(b) float x, y, and $|q/p|$ and use the Ciuchini/Kagan formula to derive ϕ; this yields (MINOS) errors for $(x, y, |q/p|)$.

(c) fit for the parameters x_{12}, y_{12}, and ϕ_{12}.

(2) Two-parameter description of indirect *CP* violation

In this parametrization, subleading amplitudes in CF and DCS decays are neglected as in Fit #1, and thus $A_D = 0$. However, subleading amplitudes in SCS decays are taken into account in indirect *CP* violation observables. There is one simplification: final-state-dependent effects for $D^0 \to K^+K^-$ and $D^0 \to \pi^+\pi^-$ are neglected in A_Γ, as they cancel at leading-order in U-spin breaking. The subleading SCS amplitudes contribute to both M_{12} and Γ_{12}, and thus $\mathrm{Arg}(\Gamma_{12})$ can be nonzero. To account for this,

TABLE 248. Measurements of time-integrated CP asymmetries. The observable $A_{CP}(f) = [\Gamma(D^0 \to f) - \Gamma(\bar{D}^0 \to f)]/[\Gamma(D^0 \to f) + \Gamma(\bar{D}^0 \to f)]$. The symbol $\Delta\langle t\rangle$ denotes the difference between the mean reconstructed decay times for $D^0 \to K^+K^-$ and $D^0 \to \pi^+\pi^-$ decays due to different trigger and reconstruction efficiencies.

Mode	Observable	Values	$\Delta\langle t\rangle/\tau_D$
$D^0 \to h^+h^-$ [1113]	$A_{CP}(K^+K^-)$	$(+0.00 \pm 0.34 \pm 0.13)\%$	0
(*BABAR* 386 fb^{-1})	$A_{CP}(\pi^+\pi^-)$	$(-0.24 \pm 0.52 \pm 0.22)\%$	
$D^0 \to h^+h^-$ [1114]	$A_{CP}(K^+K^-)$	$(-0.43 \pm 0.30 \pm 0.11)\%$	0
(Belle 540 fb^{-1})	$A_{CP}(\pi^+\pi^-)$	$(+0.43 \pm 0.52 \pm 0.12)\%$	
$D^0 \to h^+h^-$ [1115,1116] (CDF 9.7 fb^{-1})	$A_{CP}(K^+K^-) - A_{CP}(\pi^+\pi^-)$	$(-0.62 \pm 0.21 \pm 0.10)\%$	0.27 ± 0.01
	$A_{CP}(K^+K^-)$	$(-0.32 \pm 0.21)\%$	
	$A_{CP}(\pi^+\pi^-)$	$(+0.31 \pm 0.22)\%$	
$D^0 \to h^+h^-$ [1117] (LHCb 8.9 fb^{-1}, $D^{*+} \to D^0\pi^+ + \bar{B} \to D^0\mu^- X$ tags combined)	$A_{CP}(K^+K^-) - A_{CP}(\pi^+\pi^-)$	$(-0.154 \pm 0.029)\%$	0.115 ± 0.002
$D^0 \to K^+K^-$ [1118] (LHCb 5.7 fb^{-1}, $D^{*+} \to D^0\pi^+$ tag)	$A_{CP}(K^+K^-)$	$(0.068 \pm 0.054 \pm 0.016)\%$	$\frac{\langle t\rangle_K}{\tau_D} = \frac{(701.5 \pm 1.1)}{(410.3 \pm 1.0)} = 1.7097 \pm 0.0050$

TABLE 249. Results of the global fit for different assumptions regarding CPV. The χ^2/d.o.f. are considered satisfactory, although care should be taken when interpreting them in terms of probability due to unknown systematic uncertainties.

Parameter	No subleading ampl. in indirect CPV (Fit #1)	No subleading ampl. for CF/DCS decays (Fit #2)	all CPV allowed (Fit #3)	95% CL Interval (from [1]: Fit #1, [2]: Fit #2, [3]: Fit #3)
$x(\%)$	0.407 ± 0.044	…	0.407 ± 0.044	$[0.320, 0.493]^3$
$y(\%)$	$0.643^{+0.024}_{-0.023}$	…	$0.645^{+0.024}_{-0.023}$	$[0.600, 0.692]^3$
$\delta_{K\pi}(^\circ)$	$11.3^{+3.6}_{-3.8}$	$10.9^{+3.6}_{-3.8}$	$11.4^{+3.5}_{-3.8}$	$[3.7, 18.2]^3$
$R_D(\%)$	0.344 ± 0.002	0.344 ± 0.002	0.344 ± 0.002	$[0.340, 0.347]^3$
$A_D(\%)$	…	…	-0.77 ± 0.35	$[-1.46, -0.08]^3$
$\lvert q/p\rvert$	1.005 ± 0.007	…	$0.994^{+0.016}_{-0.015}$	$[0.96, 1.02]^3$
$\phi(^\circ)$	-0.19 ± 0.26	…	$-2.6^{+1.1}_{-1.2}$	$[-4.88, -0.37]^3$
$\delta_{K\pi\pi}(^\circ)$	$24.5^{+21.4}_{-22.5}$	$24.4^{+21.5}_{-22.5}$	$24.6^{+21.4}_{-22.5}$	$[-20.1, 65.7]^3$
$A_\pi(\%)$	0.202 ± 0.059	0.200 ± 0.059	0.218 ± 0.060	$[0.10, 0.34]^3$
$A_K(\%)$	0.045 ± 0.053	0.043 ± 0.053	0.062 ± 0.054	$[-0.04, 0.17]^3$
$x_{12}(\%)$	0.407 ± 0.044	0.407 ± 0.044	…	$[0.321, 0.494]^2$
$y_{12}(\%)$	$0.643^{+0.024}_{-0.023}$	$0.641^{+0.024}_{-0.023}$	…	$[0.595, 0.687]^2$
$\phi_{12}(^\circ)$	$0.65^{+0.92}_{-0.90}$	…	…	$[-1.13, 2.49]^1$
$\phi_2^M(^\circ)$	…	-0.48 ± 0.92	…	$[-1.35, 2.32]^2$
$\phi_2^\Gamma(^\circ)$	…	$2.40^{+1.55}_{-1.54}$	…	$[-0.61, 5.45]^2$
χ^2/d.o.f.	$68.9/(63-8) = 1.25$	$66.5/(63-9) = 1.23$	$65.4/(63-10) = 1.23$	

we fit for four parameters: $(x_{12}, y_{12}, \phi_2^M, \phi_2^\Gamma)$, where ϕ_2^M and ϕ_2^Γ are the phases of M_{12} and Γ_{12}, respectively, relative to that of the dominant $\Delta(U\text{-spin}) = 2$ dispersive and absorptive amplitudes. This parametrization is discussed by Kagan and Silvestrini [1123]. The relationships between $(x, y, |q/p|)$ and $(x_{12}, y_{12}, \phi_2^M, \phi_2^\Gamma)$ remain as given in Eqs. (136)–(138), now with $\phi_{12} = \phi_2^M - \phi_2^\Gamma$,

while Eq. (139) is replaced by

$$\tan 2\phi = -\frac{x_{12}^2 \sin 2\phi_2^M + y_{12}^2 \sin 2\phi_2^\Gamma}{x_{12}^2 \cos 2\phi_2^M + y_{12}^2 \cos 2\phi_2^\Gamma}.$$

(3) Allowing all *CP* violation

We allow for direct *CP* violation in DCS decays by relaxing the constraint $A_D = 0$. Thus, we now fit for all ten parameters: x, y, δ, R_D, A_D, $\delta_{K\pi\pi}$, $|q/p|$, ϕ, A_K, and A_π.

All fit results are listed in Table 249. The χ^2 for the most general Fit #3 (all *CPV* allowed) is 65.4 for $63 - 10 = 53$ degrees of freedom. Individual contributions to the χ^2 are listed in Table 250. Confidence contours in the two dimensions (x, y) or $(|q/p|, \phi)$ are obtained by finding the minimum χ^2 for each fixed point in the two-dimensional plane. The resulting $1\sigma - 5\sigma$ contours are shown in Fig. 44 for Fits #1 and #2, and in Fig. 45 for Fit #3. These contours are determined from the increase of the χ^2 above the overall minimum value: $\Delta\chi^2 = \chi^2 - \chi^2_{\rm min}$. For the all-*CPV*-allowed Fit #3, $\Delta\chi^2 = 2631$ at the no-mixing point $(x, y) = (0, 0)$; this corresponds to a statistical significance for two degrees of freedom of greater than 11.5σ, and the no-mixing hypothesis is excluded at this high level. In the $(|q/p|, \phi)$ plot (Fig. 45, bottom), $\Delta\chi^2 = 6.49$ at the no-*CPV* point $(|q/p|, \phi) = (1, 0)$; this corresponds to a statistical significance of 2.1σ. For Fit #2, $\Delta\chi^2 = 3.40$ at the no-*CPV* point $(\phi_2^M, \phi_2^\Gamma) = (0, 0)$; this corresponds to a statistical significance of only 1.3σ. This significance is less than that for Fit #3 because the constraint $A_D = 0$ increases the minimum χ^2 value.

One-dimensional likelihood curves for individual parameters are obtained by finding the minimum χ^2 for fixed values of the parameter of interest. The resulting functions $\Delta\chi^2 = \chi^2 - \chi^2_{\rm min}$ ($\chi^2_{\rm min}$ is the overall minimum value) are shown in Fig. 46. The points where $\Delta\chi^2 = 3.84$ determine 95% CL intervals for the parameters. These intervals are listed in Table 249. The value of $\Delta\chi^2$ at $x = 0$ is 82.8 (Fig. 46, upper left), and the value of $\Delta\chi^2$ at $y = 0$ is 1227 (Fig. 46, upper right). These correspond to statistical significances of 9.1σ and 35σ, respectively. These large values demonstrate that neutral D mesons undergo both dispersive ($\Delta M \neq 0$) and absorptive ($\Delta\Gamma \neq 0$) mixing.

4. Conclusions

From the results listed in Table 249 and shown in Figs. 45 and 46, we conclude the following:

(i) The experimental data consistently demonstrate D^0-$\bar{D}^0$ mixing. The no-mixing point $x = y = 0$ is excluded at more than 11.5σ. The parameter x differs from zero with a significance of 9.1σ, and y differs from zero with a significance of 35σ. Within the SM, mixing at the observed level is too large to be

TABLE 250. Individual contributions to the χ^2 for the all-*CPV*-allowed Fit #3.

Observable	χ^2	$\sum\chi^2$
y_{CP} ($K^+K^-, \pi^+\pi^-$) World Average	0.15	0.15
A_Γ World Average	0.24	0.39
$x_{K^0\pi^+\pi^-}$ Belle [1098]	0.60	0.99
$y_{K^0\pi^+\pi^-}$ Belle [1098]	4.28	5.28
$\lvert q/p\rvert_{K^0\pi^+\pi^-}$ Belle [1098]	0.65	5.92
$\phi_{K^0\pi^+\pi^-}$ Belle [1098]	0.63	6.56
$x_{CP}(K^0\pi^+\pi^-)$ LHCb 3 fb^{-1} [1100]	0.69	7.25
$y_{CP}(K^0\pi^+\pi^-)$ LHCb 3 fb^{-1} [1100]	0.06	7.31
$\Delta x(K^0\pi^+\pi^-)$ LHCb 3 fb^{-1} [1100]	0.08	7.39
$\Delta y(K^0\pi^+\pi^-)$ LHCb 3 fb^{-1} [1100]	0.03	7.42
$x_{CP}(K^0\pi^+\pi^-)$ LHCb 5.4 fb^{-1} [1102]	0.02	7.44
$y_{CP}(K^0\pi^+\pi^-)$ LHCb 5.4 fb^{-1} [1102]	0.52	7.96
$\Delta x(K^0\pi^+\pi^-)$ LHCb 5.4 fb^{-1} [1102]	0.03	7.98
$\Delta y(K^0\pi^+\pi^-)$ LHCb 5.4 fb^{-1} [1102]	0.14	8.12
$x_{K^0h^+h^-}$ *BABAR* [1103]	0.83	8.95
$y_{K^0h^+h^-}$ *BABAR* [1103]	0.06	9.01
$x_{\pi^0\pi^+\pi^-}$ *BABAR* [1104]	0.67	9.67
$y_{\pi^0\pi^+\pi^-}$ *BABAR* [1104]	0.18	9.86
$(x^2 + y^2)_{K^{(*)+}\ell^-\nu}$ World Average	0.14	10.00
$x_{K^+\pi^-\pi^0}$ *BABAR* [1078]	7.08	17.08
$y_{K^+\pi^-\pi^0}$ *BABAR* [1078]	3.88	20.96
$(x/y/R_D/\cos\delta/\sin\delta)$ CLEOc [1106]	10.49	31.45
$R_D^+/x'^{2+}/y'^+$ *BABAR* [1067]	8.46	39.90
$R_D^-/x'^{2-}/y'^-$ *BABAR* [1067]	4.26	44.16
$R_D^+/x'^{2+}/y'^+$ Belle [1109]	1.92	46.08
$R_D^-/x'^{2-}/y'^-$ Belle [1109]	2.34	48.43
$R_D/x'^2/y'$ CDF [1110]	1.22	49.65
$R_D^+/x'^{2+}/y'^+$ LHCb (D^* tag) [1112]	1.15	50.80
$R_D^-/x'^{2-}/y'^-$ LHCb (D^* tag) [1112]	0.19	51.00
$R_D^+/x'^{2+}/y'^+$ LHCb (B tag) [1111]	0.62	51.62
$R_D^-/x'^{2-}/y'^-$ LHCb (B tag) [1111]	1.67	53.28
$A_{KK}/A_{\pi\pi}$ *BABAR* [1113]	0.63	53.92
$A_{KK}/A_{\pi\pi}$ Belle [1114]	2.42	56.33
$A_{KK}/A_{\pi\pi}$ CDF [1115,1116]	4.56	60.90
$A_{KK} - A_{\pi\pi}$ LHCb ($D^* + B^0 \to D^0\mu X$ tags) [1117]	0.03	60.93
A_{KK} only LHCb (D^* tag) [1118]	0.29	61.22
$(x^2 + y^2)_{K^+\pi^-\pi^+\pi^-}$ LHCb [1105]	3.45	64.68
$A_{CP}(K^+\pi^-)$ BES III [1107]	0.72	65.40

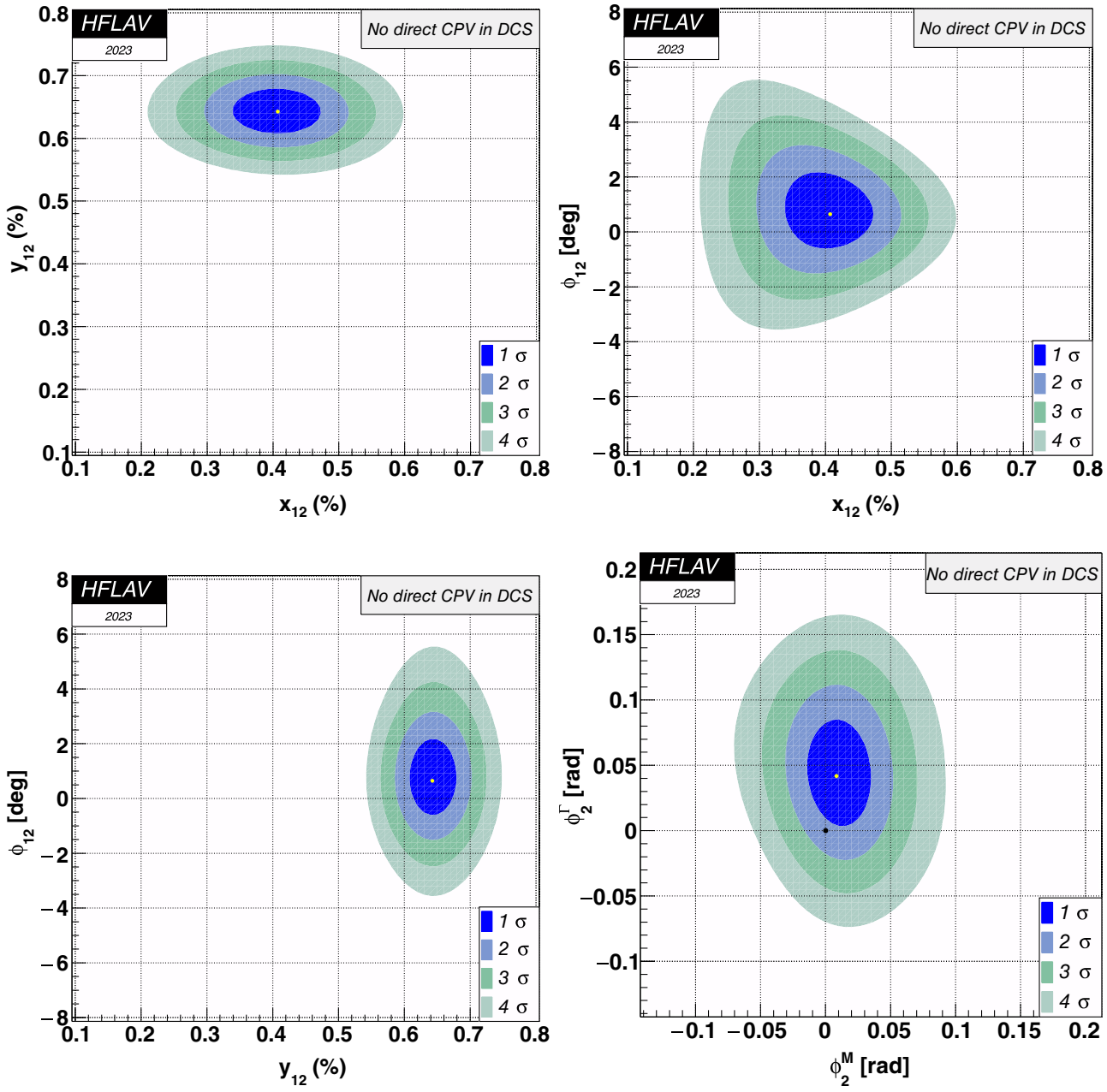


FIG. 44. Two-dimensional contours for parameters (x_{12}, y_{12}) (top left), (x_{12}, ϕ_{12}) (top right), and (y_{12}, ϕ_{12}) (bottom left), resulting from Fit #1. Contours for $(\phi_2^M, \phi_2^\Gamma)$ resulting from Fit #2 are shown in the bottom right.

accounted for by short-distance amplitudes and must be dominated by long-distance processes, which are difficult to calculate.

(ii) Since y_{CP} is positive, the mostly CP-even state is shorter-lived, as in the K^0-$\bar{K}^0$ system. However, since x is positive, the mostly CP-even state is heavier, unlike in the K^0-$\bar{K}^0$ system.

(iii) There is no significant evidence for indirect CPV arising from $D^0 - \bar{D}^0$ mixing ($|q/p| \neq 1$) or arising from interference between a mixed amplitude and a direct decay amplitude ($\phi \neq 0$). The fitted values for these parameters differ from the no-CPV case with a significance of 2.1σ, and more data is needed to establish whether indirect CPV is present. We note that small *direct CPV* (at the level of 0.15%) has been observed in time-integrated $D^0 \to K^+K^-, \pi^+\pi^-$ decays by LHCb [1117], as listed in Table 248. Several theory calculations indicate this value is consistent with Standard Model expectations, although new physics contributions cannot be excluded. Direct CP asymmetries are discussed in Sec. IX B.

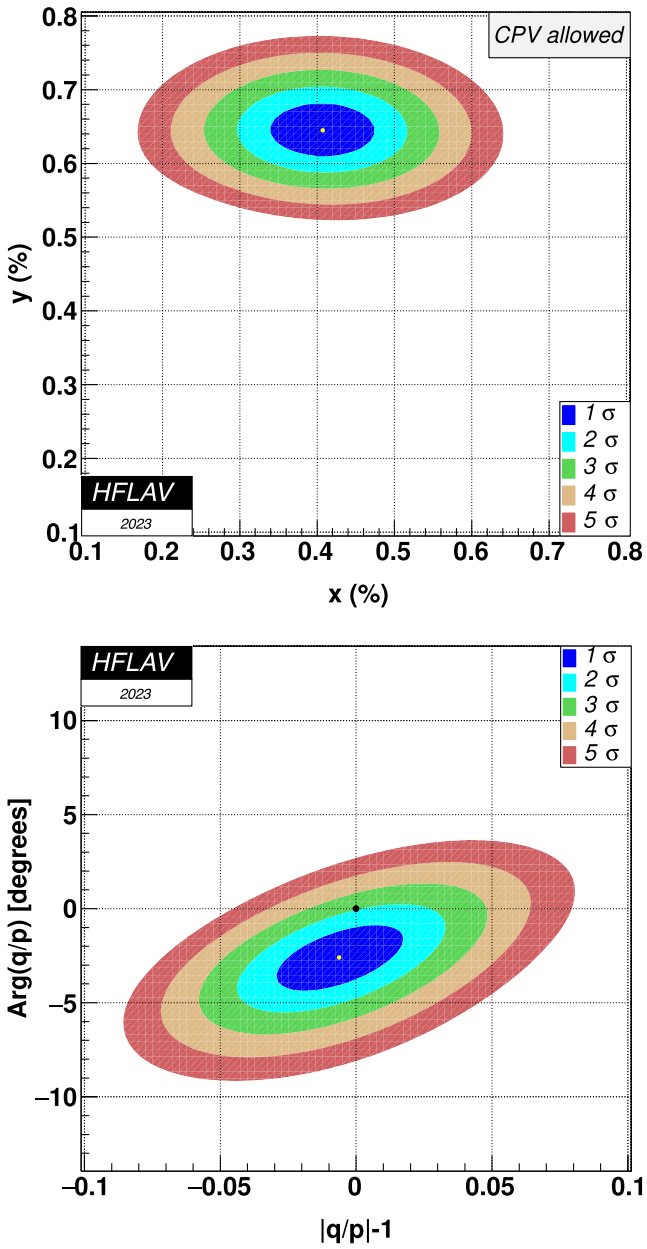


FIG. 45. Two-dimensional contours for parameters (x, y) (upper) and $(|q/p| - 1, \phi)$ (lower), allowing for *CPV* (Fit #3).

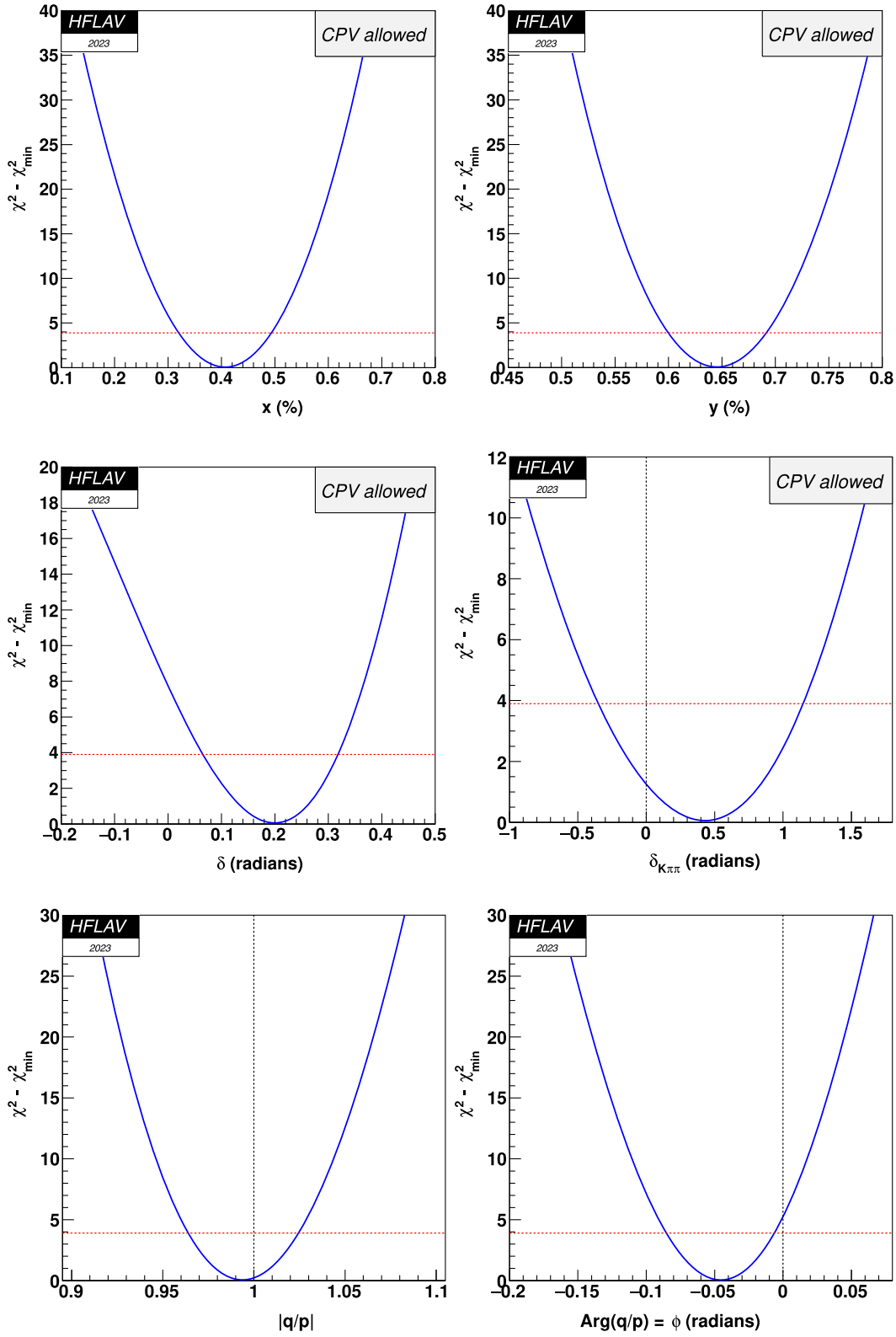


FIG. 46. The function $\Delta\chi^2 = \chi^2 - \chi^2_{\rm min}$ for parameters $x, y, \delta, \delta_{K\pi\pi}, |q/p|$, and ϕ, from Fit #3. The points where $\Delta\chi^2 = 3.84$ (denoted by dashed horizontal lines) determine 95% CL intervals.

B. *CP* asymmetries

1. Introduction

One manifestation of CP violation is a difference in decay rates between that of a particle and that of its CP-conjugate anti-particle [1124]. Such phenomena can be classified into two broad categories: *direct* CP violation and *indirect* CP violation [1125].

Direct CP violation refers to charm-changing $\Delta C = 1$ processes and can occur in both charged and neutral charm hadron decays. It results from interference between at least two different decay amplitudes, e.g., a penguin amplitude and a tree amplitude, that have different weak and strong phases. The weak phase difference between the interfering amplitudes ($\Delta\phi$) has opposite signs for $D \to f$ and $\bar{D} \to \bar{f}$ decays, while the strong phase difference ($\Delta\delta$) has the same sign. As a result, squaring the total amplitudes to obtain the decay rates gives an interference term proportional to $\cos(\Delta\phi + \Delta\delta)$ for $D \to f$ decays, and proportional to $\cos(-\Delta\phi + \Delta\delta)$ for $\bar{D} \to \bar{f}$ decays. Thus, the decay rates differ. This difference is time-independent and can be measured in time-integrated measurements.

In the Standard Model (SM), the strong-phase difference can arise due to differences in the final-state interactions (FSI) [1126], isospin amplitudes, intermediate-resonance contributions, or partial waves of the interfering decay amplitudes. A difference in weak phases arises from different CKM vertex factors, as is often the case for tree and penguin diagrams. Within the SM, direct CP violation is expected only in singly Cabibbo-suppressed (SCS) charm decays, as only these decays receive a non-negligible contribution from the penguin amplitude. At a short distance, the $c \to u$ penguin amplitude is severely suppressed by CKM factors and the GIM mechanism [1073]. Long-distance effects can lift the GIM cancellation between d- and s-quark loops, and increase the penguin contribution. Direct CP violation depends on the decay mode, and the CP asymmetries can reach the permille level.

Indirect CP violation refers to $\Delta C = 2$ processes and arises in D^0 decays due to D^0-$\bar{D}^0$ mixing. It can occur as an asymmetry in the mixing itself, or result from interference between a decay amplitude following mixing and a non-mixed amplitude. Thus, the final state must be reachable from both D^0 and $\bar{D}^0$ decays. Within the SM, charm indirect CP violation is expected to be universal, i.e., independent of final state. Current experimental limits on indirect CP violation are discussed in Sec. IX A.

The time-integrated CP asymmetry A_{CP} is defined as the difference between D and $\bar{D}$ partial widths to a final state f divided by their sum

$$A_{CP} = \frac{\Gamma(D \to f) - \Gamma(\bar{D} \to f)}{\Gamma(D \to f) + \Gamma(\bar{D} \to f)}. \tag{140}$$

In the case of D^+ and D_s^+ decays, A_{CP} measures direct CP violation; in the case of D^0 decays, A_{CP} measures direct and indirect CP violation combined (see also Sec. IX D). Given experimental constraints on A_Γ (see Table 245), a contribution from indirect CP violation would be negligible compared to current A_{CP} sensitivities.

In multi-body decays, which usually proceed via intermediate states, strong phase differences typically vary over the phase space. Thus, local CP asymmetries, i.e., those corresponding to a local region of phase space or those involving specific intermediate states, can offer better sensitivity to CP violation than a global asymmetry. Probing the multi-body phase space is often done in a model-dependent way by employing a Dalitz-plot analysis or, more generally, an amplitude analysis, separately for D and $\bar{D}$ decays. A CP asymmetry is then determined for each contributing amplitude. The CP-violating observables are asymmetries in the magnitudes and phases of CP-conjugate amplitudes, as well as asymmetries in the amplitude fit fractions.

For multi-body decays, some experiments use model-independent techniques to search for local CP asymmetries. One approach, the so-called Miranda technique (see Refs. [1127,1128]) uses a binned χ^2 approach to compare the relative density in a bin of phase space for $D \to f$ with that of the CP-conjugate decay. Another technique (the *Energy Test* technique [1129]) uses a test statistic variable (T) to determine the average distance between events in phase space. If the distribution of events in two CP-conjugate samples are identical (the CP-symmetric case), T will fluctuate around a value close to zero. Both techniques yield a p-value for the no-CP violation hypothesis and identifies CP-asymmetric phase-space regions.

2. Nuisance asymmetries

In each experiment, care must be taken to correct for production and detection asymmetries, as they can reach the percent level. To take into account differences in production rates between D and $\bar{D}$, which would affect the number of respective decays observed, some experiments (such as E791 and FOCUS) normalize A_{CP} to that measured in a Cabibbo-favored (CF) mode. This method relies on the absence of CP violation in this so-called normalization mode. Explicitly, the CP asymmetry is calculated as

$$A_{CP} = \frac{\eta(D) - \eta(\bar{D})}{\eta(D) + \eta(\bar{D})}, \tag{141}$$

where (considering, for example, $D^0 \to K^+K^-$)

$$\eta(D) = \frac{N(D^0 \to K^+K^-)}{N(D^0 \to K^-\pi^+)}, \tag{142}$$

$$\eta(\bar{D}) = \frac{N(\bar{D}^0 \to K^- K^+)}{N(\bar{D}^0 \to K^+ \pi^-)}, \tag{143}$$

and $N(D \to f)$ is the number of $D \to f$ decays reconstructed. This method has the additional advantage that most corrections due to reconstruction inefficiencies cancel out, reducing systematic uncertainties. Possible detection asymmetries between the $K^-\pi^+$ and $K^+\pi^+$ systems, which are introduced in this approach without further corrections, are negligible compared to the limited statistical sensitivities of these past experiments.

Other experiments (such as Belle and LHCb) determine A_{CP} via the relation

$$A_{\text{meas}} = A_{CP} + A_{\text{prod}} + A_{\text{det}}, \tag{144}$$

where A_{meas} is the measured (raw) asymmetry, A_{prod} is the asymmetry in the charm hadron production, and A_{det} is due to a difference in detection efficiencies between positively and negatively charged hadrons. The production asymmetry at the LHC arises from a charge asymmetry of the colliding particles: in pp collisions more charm baryons are produced than anti-baryons, and, as a result, charm mesons are less abundantly produced than anti-charm mesons. Though not yet experimentally confirmed [1130,1130], such a production asymmetry is expected to be dependent on the kinematics of the produced charm hadrons. The production asymmetry in e^+e^- collisions appears as a forward-backward (FB) asymmetry caused by an interference of the off-shell photon and Z^0 contributions. The detection asymmetries typically arise from differences in hadron interactions with detector material. In particular, the interaction cross sections for K^+ and K^- significantly differ, with the differences being dependent on the kaon momentum.

The B-factory strategy to separate the production and CP asymmetries relies on the former being odd, while the latter being even, with respect to the center-of-mass production polar angle (θ^*). The A_{meas} is measured in $|\cos\theta^*|$ bins and subsequently averaged; this removes the A_{prod} contribution. The soft π detection asymmetry is estimated by Belle by comparing A_{meas} for D^*-tagged $D^0 \to K^-\pi^+$ decays with that for untagged $D^0 \to K^-\pi^+$ decays, both measured in $|\cos\theta^*|$ bins.

At LHCb, the production asymmetry is removed by measuring A_{meas} for D^*-tagged $D^0 \to K^-\pi^+$ decays; this also corrects for the soft π detection asymmetry. Subsequently, $D^+ \to K^-\pi^+\pi^+$ decays are used to correct for the detection asymmetry introduced by the $K^-\pi^+$ system itself, and $D^+ \to K_S\pi^+$ decays are then used to remove the asymmetries in D^+ production and π^+ detection. Finally, the asymmetry related to the neutral kaon [1131], i.e., from regeneration and different interactions of K^0 and $\bar{K}^0$ with the detector, as well as from CP violation occurring in the K^0-$\bar{K}^0$ mixing, is calculated. Put together, this gives

$$A_{CP}(K^+K^-) = A_{\text{meas}}(K^+K^-) - A_{\text{meas}}(K^-\pi^+) + A_{\text{meas}}(K^-\pi^+\pi^+) - A_{\text{meas}}(K_S\pi^+) + A(\bar{K}^0 - K^0). \tag{145}$$

For some decays, typically the ones with lower statistics, one corrects for nuisance asymmetries by measuring A_{CP} relative to some well-measured reference channel, for instance

$$A_{CP}(D^+ \to \eta'\pi^+) = A_{\text{meas}}(D^+ \to \eta'\pi^+) - A_{\text{meas}}(D^+ \to \phi\pi^+) + A_{CP}(D^+ \to \phi\pi^+). \tag{146}$$

The uncertainty of the reference A_{CP}, here $A_{CP}(D^+ \to \phi\pi^+)$, is treated as an external-input uncertainty. $A_{CP}(D^+ \to \phi\pi^+)$ itself is precisely measured by LHCb exploiting $D^+ \to K_S\pi^+$ reference channel, in which CP violation is expected only due to the neutral kaon. Therefore one gets

$$A_{CP}(D^+ \to \phi\pi^+) = A_{\text{meas}}(D^+ \to \phi\pi^+) - A_{\text{meas}}(D^+ \to K_S\pi^+) + A(\bar{K}^0 - K^0). \tag{147}$$

BESIII performed measurements of A_{CP} for $D^+_{(s)}$ decays using e^+e^- collision data collected at the $D_{(s)}\bar{D}_{(s)}$ threshold. Employing the double-tag technique, where both charm mesons produced are reconstructed, results in quite a limited statistical sensitivity. Therefore any impact of the production asymmetry, expected to be smaller than at the B-factories, would have a negligible impact and is not corrected for.

3. Measurements for charmed mesons

Measurements of A_{CP} *differences*, denoted ΔA_{CP}, are often easier to interpret theoretically than individual A_{CP} measurements. The most important difference is that for $D^0 \to K^+K^-$ and $D^0 \to \pi^+\pi^-$ decays, which is discussed in Sec. IX D. Notably, its measurement by LHCb, $\Delta A_{CP} = (-15.4 \pm 2.9) \times 10^{-4}$, constitutes the first observation of CP violation in the charm sector [1117]. We note

that, in the limit of U-spin symmetry, direct CP violation in $D^0 \to K^+K^-$ and $D^0 \to \pi^+\pi^-$ decays is expected to have equal magnitude but opposite sign [1132]; thus the measurement of ΔA_{CP} would *double* the effect. The measured ΔA_{CP} value is at the upper end of the SM predictions. This triggers many interpretations, some involve new physics origins [1133–1135], while others explain the experimental observation by enhanced long-distance effects [1136–1142].

Results of measurements of A_{CP} for D^+, D^0 and D_s^+ decays are listed in Tables 251–258. Overall, CP asymmetries have been measured for more than 60 charm decay modes, and in several modes the uncertainty on A_{CP} is well below 5×10^{-3}. CP violation has been observed only in the

TABLE 251. CP asymmetries $A_{CP} = [\Gamma(D^+) - \Gamma(D^-)]/[\Gamma(D^+) + \Gamma(D^-)]$ for two-body $D^\pm$ decays. For each entry, the first uncertainty is statistical, and the second is systematic.

Mode	Year	Collaboration	A_{CP}
$D^+ \to \mu^+\nu$	2008	CLEO [1143]	$+0.08 \pm 0.08$
$D^+ \to \pi^+\pi^0$	2021	LHCb [1144]	$-0.013 \pm 0.009 \pm 0.006$
	2018	Belle [1145]	$+0.0231 \pm 0.0124 \pm 0.0023$
	2010	CLEO [1146]	$+0.029 \pm 0.029 \pm 0.003$
		HFLAV average	$+0.004 \pm 0.008$
$D^+ \to \pi^+\eta$	2022	LHCb [1147]	$+0.0013 \pm 0.0050 \pm 0.0018$
	2011	Belle [1148]	$+0.0174 \pm 0.0113 \pm 0.0019$
	2010	CLEO [1146]	$-0.020 \pm 0.023 \pm 0.003$
		HFLAV average	$+0.0031 \pm 0.0047$
$D^+ \to \pi^+\eta'$	2022	LHCb [1147]	$+0.0043 \pm 0.0017 \pm 0.0010$
	2011	Belle [1148]	$-0.0012 \pm 0.0112 \pm 0.0017$
	2010	CLEO [1146]	$-0.040 \pm 0.034 \pm 0.003$
		HFLAV average	$+0.0040 \pm 0.0020$
$D^+ \to K^+\pi^0$	2021	LHCb [1144]	$-0.032 \pm 0.047 \pm 0.021$
	2010	CLEO [1146]	$-0.035 \pm 0.107 \pm 0.009$
		HFLAV average	-0.033 ± 0.046
$D^+ \to K^+\eta$	2021	LHCb [1144]	$-0.06 \pm 0.10 \pm 0.04$
$D^+ \to K_S\pi^+$	2014	CLEO [1149]	$-0.011 \pm 0.006 \pm 0.002$
	2012	Belle [1150]	$-0.00363 \pm 0.00094 \pm 0.00067$
	2011	*BABAR* [1151]	$-0.0044 \pm 0.0013 \pm 0.0010$
	2002	FOCUS [1152]	$-0.016 \pm 0.015 \pm 0.009$
		HFLAV average	-0.0041 ± 0.0009
$D^+ \to \phi\pi^+$	2019	LHCb [1153]	$+0.00003 \pm 0.00040 \pm 0.00029$
$D^+ \to K_S K^+$	2018	BESIII [1156]	$-0.018 \pm 0.027 \pm 0.016$
	2013	*BABAR* [1154]	$+0.0013 \pm 0.0036 \pm 0.0025$
	2013	Belle [1155]	$-0.0025 \pm 0.0028 \pm 0.0014$
	2010	CLEO [1146]	$-0.002 \pm 0.015 \pm 0.009$
	2002	FOCUS [1152]	$+0.071 \pm 0.061 \pm 0.012$
		HFLAV average	-0.0011 ± 0.0025
$D^+ \to K_L K^+$	2018	BESIII [1156]	$-0.042 \pm 0.032 \pm 0.012$
$D^+ \to (\bar{K}^0/K^0)K^+$	2019	LHCb [1153]	$-0.00004 \pm 0.00061 \pm 0.00045$
	2013	*BABAR* [1154]	$+0.0046 \pm 0.0036 \pm 0.0025$
	2013	Belle [1155]	$-0.0008 \pm 0.0028 \pm 0.0014$
		HFLAV average	$+0.0001 \pm 0.0007$

TABLE 252. CP asymmetries $A_{CP} = [\Gamma(D^+) - \Gamma(D^-)]/[\Gamma(D^+) + \Gamma(D^-)]$ for three- and four-body $D^\pm$ decays. For each entry, the first uncertainty is statistical, and the second (if quoted) is systematic.

Mode	Year	Collaboration	A_{CP}
$D^+ \to K_L e^+ \nu_e$	2015	BESIII [1157]	$-0.0059 \pm 0.0060 \pm 0.0148$
$D^+ \to \pi^+\pi^-\pi^+$	2022	BESIII [1158]	$+0.012 \pm 0.021 \pm 0.006$
	2014	LHCb [1159]	Model independent technique, no evidence for CPV
	1997	E791 [1160]	-0.017 ± 0.042 (stat.)
		HFLAV average	$+0.006 \pm 0.019$
$D^+ \to \pi^+\pi^0\pi^0$	2022	BESIII [1158]	$+0.060 \pm 0.027 \pm 0.005$
$D^+ \to K^-\pi^+\pi^+$	2023	LHCb [1161]	Model independent technique, no evidence for CPV
	2014	D0 [1162]	$-0.0016 \pm 0.0015 \pm 0.0009$
	2014	CLEO [1149]	$-0.003 \pm 0.002 \pm 0.004$
		HFLAV average	-0.0018 ± 0.0016
$D^+ \to K_S\pi^+\pi^0$	2014	CLEO [1149]	$-0.001 \pm 0.007 \pm 0.002$
$D^+ \to K_S\pi^+\eta$	2020	BESIII [1163]	$-0.009 \pm 0.029 \pm 0.010$
$D^+ \to K_S K^+\pi^0$	2018	BESIII [1156]	$+0.014 \pm 0.037 \pm 0.024$
$D^+ \to K_L K^+\pi^0$	2018	BESIII [1156]	$-0.006 \pm 0.041 \pm 0.017$
$D^+ \to K^+K^-\pi^+$	2014	CLEO [1149]	$-0.001 \pm 0.009 \pm 0.004$
	2013	*BABAR* [1164]	$+0.0037 \pm 0.0030 \pm 0.0015$
	2011	LHCb [1165]	Model independent technique, no evidence for CPV
	2008	CLEO [1166]	Dalitz plot analysis, no evidence for CPV
	2000	FOCUS [1167]	$+0.006 \pm 0.011 \pm 0.005$
	1997	E791 [1160]	-0.014 ± 0.029 (stat.)
		HFLAV average	$+0.0032 \pm 0.0031$
$D^+ \to K^+K^-K^+$	2023	LHCb [1161]	Model independent technique, no evidence for CPV
$D^+ \to K^-\pi^+\pi^+\pi^0$	2014	CLEO [1149]	$-0.003 \pm 0.006 \pm 0.004$
$D^+ \to K_S\pi^+\pi^+\pi^-$	2014	CLEO [1149]	$+0.000 \pm 0.012 \pm 0.003$
$D^+ \to K_S K^+\pi^+\pi^-$	2005	FOCUS [1168]	$-0.042 \pm 0.064 \pm 0.022$
$D^+ \to \pi^+\pi^+\pi^-\pi^0$	2022	BESIII [1158]	$+0.004 \pm 0.018 \pm 0.008$
$D^+ \to \pi^+\pi^+\pi^-\eta$	2020	BESIII [1163]	$0.025 \pm 0.050 \pm 0.016$
$D^+ \to K^+\pi^+\pi^-\pi^0$	2020	BESIII [1169]	$-0.0004 \pm 0.0006 \pm 0.0001$
$D^+ \to \pi^+\pi^+\pi^-\pi^0\pi^0$	2022	BESIII [1158]	$-0.042 \pm 0.038 \pm 0.013$

difference of $A_C P$ asymmetries of the modes $D^0 \to K^+K^-$ and $D^0 \to \pi^+\pi^-$. The most recent LHCb measurement [1118] of the individual CP asymmetries for these decays leads to an evidence of CP violation in $D^0 \to \pi^+\pi^-$, $A_{CP}(D^0 \to \pi^+\pi^-) = (+2.32 \pm 0.61) \times 10^{-3}$. Interestingly, the sum of the direct CP asymmetries for $D^0 \to K^+K^-$ and $D^0 \to \pi^+\pi^-$ decays is non-zero at 2.7σ, giving an evidence for U-spin symmetry breaking.

Modes with a single K_S meson in the final state can exhibit a CP asymmetry due to CP violation in K^0-$\bar{K}^0$ mixing [1131]; i.e., the rate for $\bar{K}^0 \to K_S$ differs slightly from that for $K^0 \to K_S$. The CP asymmetry observed for the mode $D^+ \to K_S\pi^+$ (see Table 251) is consistent with that expected from K^0-$\bar{K}^0$ mixing [1131]. Thus, it is not attributed to direct CP violation in charm but to the K^0-$\bar{K}^0$ mixing. For modes indicated with a K^0 or $\bar{K}^0$ in the final

TABLE 253. *CP* asymmetries $A_{CP} = [\Gamma(D^0) - \Gamma(\bar{D}^0)]/[\Gamma(D^0) + \Gamma(\bar{D}^0)]$ for two-body $D^0, \bar{D}^0$ decays. In each entry, the first uncertainty is statistical, and the second (if quoted) is systematic, unless explicitly stated that they have been combined. The third uncertainty in the Belle and LHCb $A_{CP}(D^0 \to K_S K_S)$ measurements is due to A_{CP} of the normalization channels $D^0 \to K_S\pi^0$ (Belle) and $D^0 \to K^+K^-$ (LHCb).

Mode	Year	Collaboration	A_{CP}
$D^0 \to \pi^+\pi^-$	2022	LHCb [1118]	$+0.00232 \pm 0.00061$ (stat. and syst. combined)
	2012	CDF [1170]	$+0.0022 \pm 0.0024 \pm 0.0011$
	2008	*BABAR* [1113]	$-0.0024 \pm 0.0052 \pm 0.0022$
	2012	Belle [1114]	$+0.0043 \pm 0.0052 \pm 0.0012$
	2002	CLEO [1088]	$+0.019 \pm 0.032 \pm 0.008$
	2000	FOCUS [1167]	$+0.048 \pm 0.039 \pm 0.025$
	1998	E791 [1171]	$-0.049 \pm 0.078 \pm 0.030$
		HFLAV average	$+0.00230 \pm 0.00059$
$D^0 \to \pi^0\pi^0$	2014	Belle [1172]	$-0.0003 \pm 0.0064 \pm 0.0010$
	2001	CLEO [1173]	$+0.001 \pm 0.048$ (stat. and syst. combined)
		HFLAV average	-0.0003 ± 0.0064
$D^0 \to K^-\pi^+$	2014	CLEO [1149]	$+0.003 \pm 0.003 \pm 0.006$
$D^0 \to K_S\pi^0$	2014	Belle [1172]	$-0.0021 \pm 0.0016 \pm 0.0007$
	2001	CLEO [1173]	$+0.001 \pm 0.013$ (stat. and syst. combined)
		HFLAV average	-0.0020 ± 0.0017
$D^0 \to K_S\eta$	2011	Belle [1174]	$+0.0054 \pm 0.0051 \pm 0.0016$
$D^0 \to K_L\eta$	2022	BESIII [1175]	$+0.028 \pm 0.029 \pm 0.004$
$D^0 \to \phi\eta$	2021	Belle [1176]	$-0.019 \pm 0.044 \pm 0.006$
$D^0 \to K_S\eta'$	2011	Belle [1174]	$+0.0098 \pm 0.0067 \pm 0.0014$
$D^0 \to K_L\eta'$	2022	BESIII [1175]	$-0.022 \pm 0.025 \pm 0.004$
$D^0 \to K_L\omega$	2022	BESIII [1175]	$+0.034 \pm 0.019 \pm 0.006$
$D^0 \to K_L\phi$	2022	BESIII [1175]	$+0.027 \pm 0.054 \pm 0.007$
$D^0 \to K_S K_S$	2021	LHCb [1177]	$-0.031 \pm 0.012 \pm 0.004 \pm 0.002$
	2017	Belle [1178]	$-0.0002 \pm 0.0153 \pm 0.0002 \pm 0.0017$
	2001	CLEO [1173]	-0.23 ± 0.19 (stat. and syst. combined)
		HFLAV average	-0.019 ± 0.010
$D^0 \to K^+K^-$	2022	LHCb [1118]	$+0.00077 \pm 0.00057$ (stat. and syst. combined)
	2012	CDF [1170]	$-0.0024 \pm 0.0022 \pm 0.0009$
	2008	*BABAR* [1113]	$+0.0000 \pm 0.0034 \pm 0.0013$
	2012	Belle [1114]	$-0.0043 \pm 0.0030 \pm 0.0011$
	2002	CLEO [1088]	$+0.000 \pm 0.022 \pm 0.008$
	2000	FOCUS [1167]	$-0.001 \pm 0.022 \pm 0.015$
	1998	E791 [1171]	$-0.010 \pm 0.049 \pm 0.012$
		HFLAV average	$+0.00044 \pm 0.00054$

state, the table entries are already corrected for this effect. This correction, denoted in Eq. (145) as $A(\bar{K}^0\text{-}K^0)$, is at the level of $10^{-4} - 10^{-3}$ and has the negative sign. For a given experiment, the value of this correction depends on the experimental conditions, such as measured distributions of the momentum and decay-time of K_S mesons. Some of the BESIII measurements are for final states involving K_L [1156,1201], which makes them unique. The asymmetry

TABLE 254. CP asymmetries $A_{CP} = [\Gamma(D^0) - \Gamma(\bar{D}^0)]/[\Gamma(D^0) + \Gamma(\bar{D}^0)]$ for three- and four-body $D^0, \bar{D}^0$ decays. In each entry, the first uncertainty is statistical, and the second (if quoted) is systematic, unless explicitly stated that they have been combined.

Mode	Year	Collaboration	A_{CP}
$D^0 \to \pi^+\pi^-\pi^0$	2023	LHCb [1179]	Model-independent method, no evidence for CPV
	2022	BESIII [1158]	$+0.006 \pm 0.009 \pm 0.004$
	2015	LHCb [1180]	Model-independent method, no evidence for CPV
	2008	*BABAR* [1127]	$+0.0031 \pm 0.0041 \pm 0.0017$
	2008	Belle [1181]	$+0.0043 \pm 0.0130$ (stat. and syst. combined)
	2005	CLEO [1182]	$+0.01^{+0.09}_{-0.07} \pm 0.05$
		HFLAV average	$+0.0037 \pm 0.0039$
$D^0 \to \pi^+\pi^-\eta$	2021	Belle [1176]	$+0.009 \pm 0.012 \pm 0.005$
$D^0 \to K^-\pi^+\pi^0$	2014	CLEO [1149]	$+0.001 \pm 0.003 \pm 0.004$
$D^0 \to K^-\pi^+\eta$	2020	BESIII [1163]	$-0.019 \pm 0.013 \pm 0.010$
$D^0 \to K^+\pi^-\pi^0$	2005	Belle [1183]	-0.006 ± 0.053 (stat.)
	2001	CLEO [1184]	$+0.09^{+0.25}_{-0.22}$ (stat.)
		HFLAV average	-0.0014 ± 0.0517
$D^0 \to K_S\pi^+\pi^-$	2012	CDF [1185]	$-0.0005 \pm 0.0057 \pm 0.0054$
	2004	CLEO [1186]	$-0.009 \pm 0.021^{+0.016}_{-0.057}$
		HFLAV average	-0.0008 ± 0.0077
$D^0 \to K_S\pi^0\eta$	2020	BESIII [1163]	$-0.039 \pm 0.032 \pm 0.008$
$D^0 \to K_SK^-\pi^+$	2023	LHCb [1187]	Model-independent method, no evidence for CPV
	2016	LHCb [1188]	Amplitude analysis, no evidence for CPV
$D^0 \to K_SK^+\pi^-$	2023	LHCb [1187]	Model-independent method, no evidence for CPV
	2016	LHCb [1188]	Amplitude analysis, no evidence for CPV
$D^0 \to K^+K^-\pi^0$	2008	*BABAR* [1127]	$-0.0100 \pm 0.0167 \pm 0.0025$
$D^0 \to K^+K^-\eta$	2021	Belle [1176]	$-0.014 \pm 0.033 \pm 0.011$
$D^0 \to \pi^+\pi^-\pi^+\pi^-$	2017	LHCb [1189]	Model-independent method, no evidence for CPV
	2013	LHCb [1190]	Model-independent method, no evidence for CPV
$D^0 \to \pi^+\pi^-\pi^0\pi^0$	2022	BESIII [1158]	$-0.026 \pm 0.019 \pm 0.007$
$D^0 \to \pi^+\pi^-\pi^0\eta$	2020	BESIII [1163]	$-0.055 \pm 0.052 \pm 0.024$
$D^0 \to K^-\pi^+\pi^+\pi^-$	2014	CLEO [1149]	$+0.002 \pm 0.003 \pm 0.004$
$D^0 \to K^-\pi^+\pi^0\eta$	2020	BESIII [1163]	$-0.079 \pm 0.048 \pm 0.025$
$D^0 \to K^+\pi^-\pi^+\pi^-$	2005	Belle [1183]	-0.018 ± 0.044 (stat.)
$D^0 \to K^+K^-\pi^+\pi^-$	2018	Belle [1191]	$+0.0034 \pm 0.0036 \pm 0.0006$
	2018	LHCb [1192]	Amplitude analysis, no evidence for CPV
	2013	LHCb [1190]	Model-independent method, no evidence for CPV
	2012	CLEO [1193]	Amplitude analysis, no evidence for CPV
	2005	FOCUS [1168]	$-0.082 \pm 0.056 \pm 0.047$
		HFLAV average	$+0.0032 \pm 0.0036$
$D^0 \to K_SK_S\pi^+\pi^-$	2022	Belle [1194]	$-0.0251 \pm 0.0144^{+0.0035}_{-0.0052}$

TABLE 255. *CP* asymmetries $A_{CP} = [\Gamma(D^0) - \Gamma(\bar{D}^0)]/[\Gamma(D^0) + \Gamma(\bar{D}^0)]$ for rare $D^0, \bar{D}^0$ decays. In each entry, the first uncertainty is statistical, and the second is systematic.

Mode	Year	Collaboration	A_{CP}
$D^0 \to \bar{K}^{*0}[\to K^-\pi^+]\gamma$	2016	Belle [1195]	$-0.003 \pm 0.020 \pm 0.000$
$D^0 \to \phi[\to K^+K^-]\gamma$	2016	Belle [1195]	$-0.094 \pm 0.066 \pm 0.001$
$D^0 \to \rho^0[\to \pi^+\pi^-]\gamma$	2016	Belle [1195]	$+0.056 \pm 0.152 \pm 0.006$
$D^0 \to K^+K^-\mu^+\mu^-$	2022	LHCb [1196]	$-0.023 \pm 0.063 \pm 0.006$
$D^0 \to \pi^+\pi^-\mu^+\mu^-$	2022	LHCb [1196]	$+0.029 \pm 0.021 \pm 0.004$

TABLE 256. *CP* asymmetries of $D^0, \bar{D}^0 \to h^+h^-\mu^+\mu^-$ decays in different dimuon invariant mass ranges, measured by LHCb. In each entry, the first uncertainty is statistical, and the second is systematic. Measurements are not performed for mass intervals with insignificant signal yields.

Mode	$m(\mu^+\mu^-)$ [MeV/c^2]	A_{CP}
$D^0 \to \pi^+\pi^-\mu^+\mu^-$ [1196]	< 525	$+0.28 \pm 0.13 \pm 0.01$
	$525 \div 565$	...
	$565 \div 780$	$-0.027 \pm 0.041 \pm 0.004$
	$780 \div 950$	$-0.019 \pm 0.058 \pm 0.004$
	$950 \div 1020$	$+0.005 \pm 0.037 \pm 0.004$
	$1020 \div 1100$	$+0.042 \pm 0.034 \pm 0.004$
$D^0 \to K^+K^-\mu^+\mu^-$ [1196]	< 525	$+0.04 \pm 0.15 \pm 0.01$
	$525 \div 565$	...
	> 565	$-0.025 \pm 0.068 \pm 0.006$

TABLE 257. *CP* asymmetries $A_{CP} = [\Gamma(D_s^+) - \Gamma(D_s^-)]/[\Gamma(D_s^+) + \Gamma(D_s^-)]$ for two-body $D_s^\pm$ decays. In each entry, the first uncertainty is statistical and the second is systematic.

Mode	Year	Collaboration	A_{CP}
$D_s^+ \to \mu^+\nu$	2009	CLEO [1197]	$+0.048 \pm 0.061$
$D_s^+ \to \pi^+\eta$	2022	LHCb [1147]	$+0.0048 \pm 0.0042 \pm 0.0017$
	2021	Belle [1198]	$+0.002 \pm 0.003 \pm 0.003$
	2013	CLEO [1199]	$+0.011 \pm 0.030 \pm 0.008$
		HFLAV average	$+0.0034 \pm 0.0031$
$D_s^+ \to \pi^+\eta'$	2022	LHCb [1147]	$-0.0004 \pm 0.0011 \pm 0.0009$
	2013	CLEO [1199]	$-0.022 \pm 0.022 \pm 0.006$
		HFLAV average	-0.0005 ± 0.0014
$D_s^+ \to K_S\pi^+$	2013	*BABAR* [1154]	$+0.006 \pm 0.020 \pm 0.003$
	2010	Belle [1200]	$+0.0545 \pm 0.0250 \pm 0.0033$
	2010	CLEO [1146]	$+0.163 \pm 0.073 \pm 0.003$
		HFLAV average	$+0.0311 \pm 0.0154$

(Table continued)

TABLE 257. *(Continued)*

Mode	Year	Collaboration	A_{CP}
$D_s^+ \to (\bar{K}^0/K^0)\pi^+$	2019	LHCb [1153]	$+0.0016 \pm 0.0017 \pm 0.0005$
	2013	*BABAR* [1154]	$+0.003 \pm 0.020 \pm 0.003$
		HFLAV average	$+0.0016 \pm 0.0018$
$D_s^+ \to K_S K^+$	2019	BESIII [1201]	$+0.006 \pm 0.028 \pm 0.006$
	2013	CLEO [1199]	$+0.026 \pm 0.015 \pm 0.006$
	2013	*BABAR* [1154]	$-0.0005 \pm 0.0023 \pm 0.0024$
	2010	Belle [1200]	$+0.0012 \pm 0.0036 \pm 0.0022$
		HFLAV average	$+0.0008 \pm 0.0026$
$D_s^+ \to K_L K^+$	2019	BESIII [1201]	$-0.011 \pm 0.026 \pm 0.006$
$D_s^+ \to K^+\pi^0$	2021	LHCb [1144]	$-0.008 \pm 0.039 \pm 0.012$
	2021	Belle [1198]	$+0.064 \pm 0.044 \pm 0.011$
	2010	CLEO [1146]	$+0.266 \pm 0.228 \pm 0.009$
		HFLAV average	$+0.020 \pm 0.030$
$D_s^+ \to K^+\eta$	2021	Belle [1198]	$+0.021 \pm 0.021 \pm 0.004$
	2021	LHCb [1144]	$+0.009 \pm 0.037 \pm 0.011$
	2010	CLEO [1146]	$+0.093 \pm 0.152 \pm 0.009$
		HFLAV average	$+0.019 \pm 0.019$
$D_s^+ \to K^+\eta'$	2010	CLEO [1146]	$+0.060 \pm 0.189 \pm 0.009$

TABLE 258. CP asymmetries $A_{CP} = [\Gamma(D_s^+) - \Gamma(D_s^-)]/[\Gamma(D_s^+) + \Gamma(D_s^-)]$ for multi-body $D_s^\pm$ decays. In each entry, the first uncertainty is statistical, and the second is systematic.

Mode	Year	Collaboration	A_{CP}
$D_s^+ \to \pi^+\pi^+\pi^-$	2014	LHCb [1159]	Model independent technique, no evidence for CPV
	2013	CLEO [1199]	$-0.007 \pm 0.030 \pm 0.006$
$D_s^+ \to \pi^+\pi^0\eta$	2013	CLEO [1199]	$-0.005 \pm 0.039 \pm 0.020$
$D_s^+ \to \pi^+\pi^0\eta'$	2013	CLEO [1199]	$-0.004 \pm 0.074 \pm 0.019$
$D_s^+ \to K_S K^+\pi^0$	2013	CLEO [1199]	$-0.016 \pm 0.060 \pm 0.011$
$D_s^+ \to K_S K_S\pi^+$	2013	CLEO [1199]	$+0.031 \pm 0.052 \pm 0.006$
$D_s^+ \to K^+\pi^+\pi^-$	2013	CLEO [1199]	$+0.045 \pm 0.048 \pm 0.006$
$D_s^+ \to K^+K^-\pi^+$	2023	LHCb [1161]	Model independent technique, no evidence for CPV
	2013	CLEO [1199]	$-0.005 \pm 0.008 \pm 0.004$
$D_s^+ \to K^+K^-K^+$	2023	LHCb [1161]	Model independent technique, no evidence for CPV
$D_s^+ \to K_S K^-\pi^+\pi^+$	2013	CLEO [1199]	$+0.041 \pm 0.027 \pm 0.009$
$D_s^+ \to K_S K^+\pi^+\pi^-$	2013	CLEO [1199]	$-0.057 \pm 0.053 \pm 0.009$
$D_s^+ \to K^+K^-\pi^+\pi^0$	2013	CLEO [1199]	$+0.000 \pm 0.027 \pm 0.012$

for the DCS decay $D^0 \to K^+\pi^-$ is not included in these tables, as it is a by-product of charm-mixing measurements and thus is discussed in Sec. IX A (where it is referred to as A_D).

The asymmetries for three- and four-body decays (Tables 252, 254, and 258) are given for their observed final state, i.e., resonant substructure is implicitly included but not considered separately. Most asymmetries measured for three- and four-body channels are still only global asymmetries. The reported model-independent tests, which attempt to probe the decay phase space, yield p-values typically at the level of a few percent or higher and thus are consistent with no CP violation. The lowest p-value of 0.6%, corresponding to a significance for CP violation of 2.7σ, is obtained for the P-odd (parity-odd) test of $D^0 \to \pi^+\pi^-\pi^+\pi^-$ decay [1190]. This implies that the effect, if not a statistical fluctuation, originates in a P-odd amplitude such as $D^0 \to [\rho^0\rho^0]_{L=1}$. For $D^0 \to K^+K^-\pi^+\pi^-$ decay [1192], a model-dependent amplitude analysis was performed, and CP asymmetries were measured for 25 intermediate amplitudes. The uncertainties on these asymmetries ranged from 1% to 15% and were dominated by statistical errors. No significant CP violation was observed, and the most significant asymmetry of 2.8σ was observed for the phase of the P-odd amplitude $D^0 \to [\phi(1020)\rho(1450)^0]_{L=1}$. CP violation arising through P violation is discussed further in Sec. IX C. LHCb is still analyzing many multi-body decays, some with yields of the order of 10^8 events.

CP asymmetries have also been measured for decays classified as rare: the radiative modes $D^0 \to V\gamma$, with $V = \bar{K}^{*0}, \phi(1020), \rho^0$, as well as the dimuon decays $D^0 \to \pi^+\pi^-\mu^+\mu^-$ and $D^0 \to K^+K^-\mu^+\mu^-$ (see Table 255). For the dimuon modes, in addition to their global asymmetries listed in Table 254, CP asymmetries in bins of the dimuon invariant mass have been measured by LHCb for the ranges with significant signal yields. They are given in Table 256. Asymmetries for mass regions away from $\mu^+\mu^-$ production via $\eta, \rho-\omega$ or ϕ decays still have very limited sensitivities, with uncertainties ranging from 12% to 26%. These nonresonant regions are particularly important for new physics searches (see Sec. X F).

4. Measurements for charmed baryons

In the charm baryon sector, there is no evidence of CP violation. Until recently, there were only two measurements for Λ_c^+; these were performed by CLEO [1202] and FOCUS [1203] and had limited sensitivity. The CLEO measurement used the semileptonic decay $\Lambda_c^+ \to \Lambda e^+\nu_e$, while the FOCUS measurement used the CF decay $\Lambda_c^+ \to \Lambda\pi^+$. Both searched for CP violation through an angular analysis. Exploiting the Λ helicity angle, CP violation was probed by comparing the P asymmetry in decays of Λ_c^+ and $\bar{\Lambda}_c^-$. This was done by measuring the weak-asymmetry parameter α_{Λ_c}, defined for Λ_c^+ decays as

$$\alpha_{\Lambda_c} = \frac{\sum_{\lambda_2}|H_{\lambda_1=+\frac{1}{2},\lambda_2}|^2 - |H_{\lambda_1=-\frac{1}{2},\lambda_2}|^2}{\sum_{\lambda_2}|H_{\lambda_1=+\frac{1}{2},\lambda_2}|^2 + |H_{\lambda_1=-\frac{1}{2},\lambda_2}|^2}, \tag{148}$$

and the corresponding parameter $\alpha_{\bar{\Lambda}_c}$ defined for $\bar{\Lambda}_c^-$ decays. H_{λ_1,λ_2} in Eq. (148) is the helicity amplitude with λ_1 denoting the helicity of Λ baryon and λ_2 denoting the helicity of the accompanying particle, i.e., π^+ in $\Lambda_c^+ \to \Lambda\pi^+$ decays and $W^+ \to e^+\nu_e$ in the semileptonic decays. Thus α_{Λ_c} ($\alpha_{\bar{\Lambda}_c}$) describes a longitudinal polarization of the Λ ($\bar{\Lambda}$) baryon.

The α_{Λ_c} parameter is measured from the angular distribution for the decay chain $\Lambda_c^+ \to \Lambda\pi^+$ followed by $\Lambda \to p\pi^-$,

$$\frac{d\Gamma}{d\cos\theta_p} \simeq 1 + \alpha_{\Lambda_c}\alpha_\Lambda\cos\theta_p, \tag{149}$$

where θ_p is the Λ helicity angle, defined as the angle between the proton momentum and the vector opposite to the Λ_c^+ momentum, both in the Λ rest frame. A weak-asymmetry parameter for $\Lambda \to p\pi^-$ decays, α_Λ, is defined similar to Eq. (148) but with λ_1 denoting the proton helicities of $\pm\frac{1}{2}$ and λ_2 being the π^- helicity. The angular distribution in Eq. (149) for the charge conjugate process, $\bar{\Lambda}_c^- \to \bar{\Lambda}\pi^-$ with $\bar{\Lambda} \to \bar{p}\pi^+$, involves $\alpha_{\bar{\Lambda}_c}$ and $\alpha_{\bar{\Lambda}}$. The weak-asymmetry parameters for the Λ and $\bar{\Lambda}$ decays are well measured [9] and used as external parameters in the fits for α_{Λ_c} and $\alpha_{\bar{\Lambda}_c}$. The angular distribution of the semileptonic decays $\Lambda_c^+ \to \Lambda e^+\nu_e$ is more complicated, owing to contribution from one more weakly-decaying system, $W^+ \to e^+\nu_e$ (see Sec. X A). Therefore, in addition to the Λ helicity angle, it also depends on the W^+ helicity angle, the angle between the decay planes of the W^+ and Λ, as well as $q^2 \equiv m^2(e^+\nu_e)$, making the CLEO measurement a four-dimensional analysis [1202].

As $\alpha_{\Lambda_c} = -\alpha_{\bar{\Lambda}_c}$ in the case of P-parity conservation, the CP-violating asymmetry is defined as

$$A_{CP}^{\alpha} = \frac{\alpha_{\Lambda_c} + \alpha_{\bar{\Lambda}_c}}{\alpha_{\Lambda_c} - \alpha_{\bar{\Lambda}_c}}. \tag{150}$$

Recently, A_{CP}^{α} has been measured by Belle [1204] for the SCS decays $\Lambda_c^+ \to \Lambda K^+$ and $\Lambda_c^+ \to \Sigma^0 K^+$, $\Sigma^0 \to \Lambda\gamma$. The method of accessing CP violation occurring through P violation has also been applied by Belle [1205] to the channel $\Xi_c^0 \to \Xi^-\pi^+, \Xi^- \to \Lambda\pi^-$. All the measurements of α-induced CP asymmetry are summarized in Table 259.

The first CPV measurement with charm baryons and precision reaching the 1% level was performed by LHCb, who measured A_{CP} difference for the SCS decays

TABLE 259. CP asymmetries A_{CP}^{α} induced through the weak-asymmetry parameter α, for decays of charmed baryons and anti-baryons. For each entry, the first uncertainty is statistical, and the second is systematic. The third uncertainty in the CLEO measurement is related to the uncertainty of the Λ weak-asymmetry parameter.

Mode	Year	Collaboration	A_{CP}^{α}
$\Lambda_c^+ \to \Lambda e^+ \nu_e$	2005	CLEO [1202]	$0.00 \pm 0.03 \pm 0.01 \pm 0.02$
$\Lambda_c^+ \to \Lambda \pi^+$	2006	FOCUS [1202]	$-0.07 \pm 0.19 \pm 0.12$
$\Lambda_c^+ \to \Lambda K^+$	2022	Belle [1204]	$-0.023 \pm 0.086 \pm 0.071$
$\Lambda_c^+ \to \Sigma^0 K^+$	2022	Belle [1204]	$+0.08 \pm 0.35 \pm 0.14$
$\Xi_c^0 \to \Xi^- \pi^+$	2021	Belle [1205]	$+0.024 \pm 0.052 \pm 0.014$

TABLE 260. CP asymmetries A_{CP} of decay widths for decays of charmed baryons and anti-baryons. For each entry, the first uncertainty is statistical, and the second is systematic.

Mode	Year	Collaboration	A_{CP}
$\Lambda_c^+ \to \Lambda K^+$	2022	Belle [1204]	$+0.021 \pm 0.026 \pm 0.001$
$\Lambda_c^+ \to \Sigma^0 K^+$	2022	Belle [1204]	$+0.025 \pm 0.054 \pm 0.004$

$\Lambda_c^+ \to p K^+ K^-$ and $\Lambda_c^+ \to p \pi^+ \pi^-$ [1206], obtaining the result

$$\Delta A_{CP}(\Lambda_c^+ \to p h^+ h^-) \equiv A_{CP}(p K^+ K^-) - A_{CP}(p \pi^+ \pi^-) = 0.003 \pm 0.009 \pm 0.006.$$

However, the U-spin argument which motivated measuring the ΔA_{CP} for $D^0 \to K^+ K^-$ and $D^0 \to \pi^+ \pi^-$ decays does not exist for $\Lambda_c^+ \to p K^+ K^-$ and $\Lambda_c^+ \to p \pi^+ \pi^-$ decays. The measurement, performed in a phase-space-integrated manner, has limited sensitivity and does not facilitate an interpretation. Nevertheless, the production asymmetry between Λ_c^+ and $\bar{\Lambda}_c^-$ baryons cancels in this difference. Given the potentially rich dynamics of these decays in their five-dimensional phase space,[18] ΔA_{CP} measured in phase-space regions or a model-dependent measurement of intermediate amplitude asymmetries would be very desirable. The first A_{CP} measurements for Λ_c^+ decays have been only recently performed by Belle; they are summarized in Table 260.

5. Sum rules

For charm decays, one can construct various SU(3)-based sum rules which, in addition to testing SU(3) symmetry itself, are also useful for performing model-independent tests of the SM. Particularly useful are sum rules exploiting SU(3) subgroups such as U-spin or isospin (I), as they involve fewer decays and offer more precise tests. While U-spin symmetry in charm decays is broken by a non-negligible amount due to the s-quark mass, isospin symmetry holds at the $(m_u - m_d)$ level and thus is very precise. Important for consideration are sum rules that relate individual CP asymmetries of isospin-related processes; such rules allow for tests to be performed that have reduced uncertainty arising from strong interaction effects.

Such a sum rule has been proposed for $D \to \pi\pi$ decays in Ref. [1207]. Following the phase convention of [1207], the isospin decomposition of $D \to \pi\pi$ amplitudes gives

$$A_{\pi^+\pi^-} = \sqrt{2}\mathcal{A}_3 + \sqrt{2}\mathcal{A}_1, \tag{151}$$

$$A_{\pi^0\pi^0} = 2\mathcal{A}_3 - \mathcal{A}_1, \tag{152}$$

$$A_{\pi^+\pi^0} = 3\mathcal{A}_3, \tag{153}$$

where $\mathcal{A}_1$ and $\mathcal{A}_3$ are amplitudes corresponding to the $\Delta I = 1/2$ and $\Delta I = 3/2$ transitions, respectively (i.e., transitions to $\pi\pi$ final states with $I = 0$ and $I = 2$). From this, one can get an amplitude isospin sum rule

$$\frac{1}{\sqrt{2}} A_{\pi^+\pi^-} + A_{\pi^0\pi^0} - A_{\pi^+\pi^0} = 0. \tag{154}$$

[18] For unpolarized Λ_c, the decay phase space reduces to a two-dimensional Dalitz distribution.

Probing such a sum requires knowledge of strong phases, which are accessible only at charm-threshold experiments. However, even without this knowledge, the sum of differences of decay rates for D and $\bar{D}$ decays can be measured

$$|A_{\pi^+\pi^-}|^2 - |\bar{A}_{\pi^+\pi^-}|^2 + |A_{\pi^0\pi^0}|^2 - |\bar{A}_{\pi^0\pi^0}|^2 - \frac{2}{3}(|A_{\pi^+\pi^0}|^2 - |\bar{A}_{\pi^-\pi^0}|^2) = 3(|\mathcal{A}_1|^2 - |\bar{\mathcal{A}}_1|^2). \quad (155)$$

This equation suggests several SM tests. As the penguin amplitude is, to excellent approximation within the SM, purely $\Delta I = 1/2$, it does not contribute to $D^+ \to \pi^+\pi^0$. This decay is therefore expected to be CP symmetric within the SM. Any CP asymmetry observed in $D^+ \to \pi^+\pi^0$ would be a sign of new physics, which would be associated with the $\Delta I = 3/2$ amplitude.

If the sum in Eq. (155), depending only on $\mathcal{A}_1$, is found to be non-zero, this would mean that CP violation arises from the $\Delta I = 1/2$ transitions. Moreover, a scenario in which the sum in Eq. (155) is zero and individual asymmetries are non-zero would suggest new physics contributing to the $\Delta I = 3/2$ amplitude.

To facilitate an experimental test, one can exploit also the combination of decay rates

$$|A_{\pi^+\pi^-}|^2 + |\bar{A}_{\pi^+\pi^-}|^2 + |A_{\pi^0\pi^0}|^2 + |\bar{A}_{\pi^0\pi^0}|^2 - \frac{2}{3}(|A_{\pi^+\pi^0}|^2 + |\bar{A}_{\pi^-\pi^0}|^2) = 3(|\mathcal{A}_1|^2 + |\bar{\mathcal{A}}_1|^2). \quad (156)$$

Dividing Eq. (155) by Eq. (156) gives

$$R \equiv \frac{|A_{\pi^+\pi^-}|^2 - |\bar{A}_{\pi^+\pi^-}|^2 + |A_{\pi^0\pi^0}|^2 - |\bar{A}_{\pi^0\pi^0}|^2 - \frac{2}{3}(|A_{\pi^+\pi^0}|^2 - |\bar{A}_{\pi^-\pi^0}|^2)}{|A_{\pi^+\pi^-}|^2 + |\bar{A}_{\pi^+\pi^-}|^2 + |A_{\pi^0\pi^0}|^2 + |\bar{A}_{\pi^0\pi^0}|^2 - \frac{2}{3}(|A_{\pi^+\pi^0}|^2 + |\bar{A}_{\pi^-\pi^0}|^2)}. \quad (157)$$

Note that the last term of the denominator enters with the sign opposite compared to the one in the sum tested in Refs. [1144,1145]. An advantage of the ratio in Eq. (157) is that, unlike the sum in Refs. [1144,1145], it corresponds to the CP asymmetry in the $\Delta I = 1/2$ process and has no dependence on the $\Delta I = 3/2$ amplitude, which facilitates an interpretation.

Relating the amplitude, the branching fraction, the lifetime, and the asymmetry with $|A|^2 \propto \mathcal{B}/\tau_D$ and $|A|^2 - |\bar{A}|^2 = A_{CP}(|A|^2 + |\bar{A}|^2)$, we rewrite Eq. (157) as

$$R = \frac{A_{CP}(D^0 \to \pi^+\pi^-)}{1 + \frac{\tau_{D^0}}{\mathcal{B}_{+-}}(\frac{\mathcal{B}_{00}}{\tau_{D^0}} - \frac{2}{3}\frac{\mathcal{B}_{+0}}{\tau_{D^+}})} + \frac{A_{CP}(D^0 \to \pi^0\pi^0)}{1 + \frac{\tau_{D^0}}{\mathcal{B}_{00}}(\frac{\mathcal{B}_{+-}}{\tau_{D^0}} - \frac{2}{3}\frac{\mathcal{B}_{+0}}{\tau_{D^+}})} + \frac{A_{CP}(D^+ \to \pi^+\pi^0)}{1 - \frac{3}{2}\frac{\tau_{D^+}}{\mathcal{B}_{+0}}(\frac{\mathcal{B}_{00}}{\tau_{D^0}} + \frac{\mathcal{B}_{+-}}{\tau_{D^0}})}, \quad (158)$$

where $\mathcal{B}_{+-}$, $\mathcal{B}_{00}$, and $\mathcal{B}_{+0}$ denote the branching fractions for $D^0 \to \pi^+\pi^-$, $D^0 \to \pi^0\pi^0$, and $D^+ \to \pi^+\pi^0$, respectively. The sum R is calculated using our averages for CP asymmetries (Tables 251 and 253) and PDG averages [9] for branching fractions and lifetimes. The result is

$$R = (+0.86 \pm 3.09) \times 10^{-3}, \quad (159)$$

which is consistent with zero. In addition, all the individual asymmetries contributing to R are consistent with zero. The uncertainty on R is dominated by the uncertainties on individual asymmetries.

The analogous sum rule for $D \to \bar{K}K$ decays involves full SU(3) considerations and thus is imprecise. Reference [1207] proposes a set of isospin sum rules for $D \to \rho\pi$ or $D \to \bar{K}^{(*)}K^{(*)}\pi$, but testing these sum rules requires a number of experimental measurements that have not yet been performed. A number of U-spin sum rules for three-body decays of charmed baryons is proposed in Ref. [1208].

C. T-odd asymmetries

Measuring T-odd asymmetries provides a complementary way to search for CP violation in the charm sector, exploiting CPT invariance. T-odd asymmetries are measured using triple-products of the form $\vec{a} \cdot (\vec{b} \times \vec{c})$, where a, b, and c are spins or momenta. This combination is odd under time reversal (T). Because triple products are T-odd, measuring a nonzero value for them was originally proposed as a way to search for T violation [1209,1210].

If a triple product is formed using *both* spin and momenta, i.e.,

$$\vec{s_1} \cdot (\vec{p_2} \times \vec{p_3}),$$

it can be even under P-conjugation. However, if only momenta are used, i.e.,

$$\vec{p_1} \cdot (\vec{p_2} \times \vec{p_3}),$$

it is odd under P-conjugation. Thus, in this case the T-odd method becomes P-odd and allows one to probe CP violation occurring via P violation. This type of CPV, arising in P-odd amplitudes, can be studied in decays of mesons into final states with at least four spinless particles. Two- and three-body hadronic decays of charm mesons to spinless particles do not provide T-odd or P-odd

TABLE 261. Measurements of the T-odd CP asymmetry $\mathcal{A}_T = (A_T - \bar{A}_T)/2$.

Mode	Year	Collaboration	$\mathcal{A}_T$
$D^0 \to K^+K^-\pi^+\pi^-$	2018	Belle [1191]	$+0.0052 \pm 0.0037 \pm 0.0007$
	2014	LHCb [1218]	$+0.0018 \pm 0.0029 \pm 0.0004$
	2010	*BABAR* [1219]	$+0.0010 \pm 0.0051 \pm 0.0044$
	2005	FOCUS [1168]	$+0.010 \pm 0.057 \pm 0.037$
		HFLAV average	$+0.0035 \pm 0.0021$
$D^0 \to K_S\pi^+\pi^-\pi^0$	2017	Belle [1216]	$-0.00028 \pm 0.00138^{+0.00023}_{-0.00076}$
$D^0 \to K_SK_S\pi^+\pi^-$	2022	Belle [1194]	$-0.0195 \pm 0.0142^{+0.0014}_{-0.0012}$
$D^+ \to K_SK^+\pi^+\pi^-$	2023	Belle [1220]	$+0.0034 \pm 0.0087 \pm 0.0032$
	2011	*BABAR* [1221]	$-0.0120 \pm 0.0100 \pm 0.0046$
	2005	FOCUS [1168]	$+0.023 \pm 0.062 \pm 0.022$
		HFLAV average	-0.0027 ± 0.0070
$D^+ \to K^+K^-K_S\pi^+$	2023	Belle [1220]	$-0.0334 \pm 0.0266 \pm 0.0035$
$D^+ \to K^+K^-\pi^+\pi^0$	2023	Belle [1217]	$+0.026 \pm 0.066 \pm 0.013$
$D^+ \to K^+\pi^-\pi^+\pi^0$	2023	Belle [1217]	$-0.013 \pm 0.042 \pm 0.001$
$D^+ \to K^-\pi^+\pi^+\pi^0$	2023	Belle [1217]	$+0.002 \pm 0.015 \pm 0.008$
$D_s^+ \to K_SK^+\pi^+\pi^-$	2023	Belle [1220]	$-0.0046 \pm 0.0063 \pm 0.0038$
	2011	*BABAR* [1221]	$-0.0136 \pm 0.0077 \pm 0.0034$
	2005	FOCUS [1168]	$-0.036 \pm 0.067 \pm 0.023$
		HFLAV average	-0.0087 ± 0.0055
$D_s^+ \to K^+K^-\pi^+\pi^0$	2023	Belle [1217]	$+0.022 \pm 0.033 \pm 0.043$
$D_s^+ \to K^+\pi^-\pi^+\pi^0$	2023	Belle [1217]	$-0.011 \pm 0.022 \pm 0.001$

observables,[19] thus only CP violation occurring through C-violation can be probed for them.

Taking as an example the decay mode $D^0 \to K^+K^-\pi^+\pi^-$, involving spinless particles only, one forms a triple-product correlation using momenta of the final-state particles in the D^0 center-of-mass frame.[20] Defining the T-odd (and P-odd) correlation for D^0

$$C_T \equiv \vec{p}_{K^+} \cdot (\vec{p}_{\pi^+} \times \vec{p}_{\pi^-}), \tag{160}$$

and the corresponding quantity for $\overline{D}^0$

$$\bar{C}_T \equiv \vec{p}_{K^-} \cdot (\vec{p}_{\pi^-} \times \vec{p}_{\pi^+}), \tag{161}$$

one can construct the asymmetry for the D^0 decays as

$$A_T = \frac{\Gamma(C_T > 0) - \Gamma(C_T < 0)}{\Gamma(C_T > 0) + \Gamma(C_T < 0)}, \tag{162}$$

and for their CP-conjugate decays as

$$\bar{A}_T = \frac{\Gamma(-\bar{C}_T > 0) - \Gamma(-\bar{C}_T < 0)}{\Gamma(-\bar{C}_T > 0) + \Gamma(-\bar{C}_T < 0)}. \tag{163}$$

In these expressions, Γ represents a partial width, and the following applies:

$$P(C_T) = -C_T, \quad C(C_T) = \overline{C_T}, \quad CP(A_T) = \overline{A}_T. \tag{164}$$

The asymmetries A_T and $\bar{A}_T$ depend on angular distributions of the daughter particles and may be nonzero due to final-state interactions or P violation in weak decays. Given Eq. (164), one can construct the CP-violating, i.e. CP-odd (and P-odd, T-odd) asymmetry

[19]They can be fully described with P-even variables, such as invariant masses or helicity angles.

[20]For momentum-only triple products, at least four-daughter final states are required to give a nonzero correlation, as only three out of four momenta are independent. For three-body decays, the daughters are in a plane and the triple product is zero.

$$\mathcal{A}_T \equiv \frac{A_T - \bar{A}_T}{2}; \tag{165}$$

where a nonzero value indicates *CP* violation (see Refs. [1210–1215]). This asymmetry is also referred to in the literature by other names: $A_{T\text{viol}}$, a_{CP}^{P}, and $a_{CP}^{T\text{-odd}}$.

Values of $\mathcal{A}_T$ for D^+, D_s^+, and D^0 decay modes are listed in Table 261. Despite relatively high precision ($< 1\%$), there is no evidence for *CP* violation. In order to increase sensitivity to *CP* violation (see Sec. IX B), some of the measurements in Table 261 are also performed locally in phase-space regions. Decay phase space is divided according to two- or three-body invariant mass (for $D^0 \to K_S\pi^+\pi^-\pi^0$ decays in Ref. [1216], and $D_{(s)}^+ \to K^+K^-\pi^+\pi^0$ and $D_{(s)}^+ \to K^+\pi^-\pi^+\pi^0$ decays in Ref. [1217]), helicity angles of the two-body systems ($D^0 \to K^+K^-\pi^+\pi^-$ in Ref. [1191]), or using both mass and angular observables ($D^0 \to K^+K^-\pi^+\pi^-$ in Ref. [1218]). None of the local $\mathcal{A}_T$ asymmetries are found to be significant.

All *P*-even contributions contributing to $\mathcal{A}_T$ cancel out in the difference. Thus, $\mathcal{A}_T$ is only sensitive to *P*-odd amplitudes or to interference between *P*-odd and *P*-even ones. The cancellation typically applies also to detection asymmetries and, at the hadron-collider experiments, the production asymmetry, making this is a significant advantage of the *T*-odd method.

Another way to probe *P*-odd amplitudes is through amplitude analysis using *P*-odd variables. One example is $\sin\Phi$, where Φ is the angle in the D^0 frame between the K^+K^- decay plane and the $\pi^+\pi^-$ decay plane for the decay $D^0 \to K^+K^-\pi^+\pi^-$ [1192]. It can be shown that $\sin\Phi$ is proportional to the triple product as in Eqs. (161) or (163) [1210]. However, *P*-odd amplitudes in four-body decays of charm mesons, for instance $D \to [VV]_{L=1}$, i.e. final states involving two vector mesons in a *P*-wave state, are typically quite suppressed ($< 10\%$) [1192,1222]. This makes searches for *CP* violation in these amplitudes challenging. As discussed in Sec. IX B, no significant *CP* violation was observed for any of the amplitudes contributing into the $D^0 \to K^+K^-\pi^+\pi^-$ decays studied by LHCb [1192]. The most significant asymmetry of 2.8σ was observed for the phase of the *P*-odd amplitude $D^0 \to [\phi(1020)\rho(1450)^0]_{L=1}$. In another method, the model-independent technique used to search for *CP* asymmetries in $D^0 \to \pi^+\pi^-\pi^+\pi^-$ decays (see Sec. IX B) has been carried out separately for *P*-odd and *P*-even contributions, separated out using a triple product [1190]. The *p*-value of 0.6%, corresponding to a significance for *CP* violation of 2.7σ, was obtained for the *P*-odd test of $D^0 \to \pi^+\pi^-\pi^+\pi^-$ decays.

Decays of charm baryons also offer access to *P*-odd amplitudes, e.g., Λ_c^+ decays with a weakly-decaying baryon in the final state, such as $\Lambda_c^+ \to \Lambda\pi^+$. Moreover, for polarized charm baryons, e.g., Λ_c produced weakly in Λ_b decays, one can build a triple product using the Λ_c spin. Recently, the topic of symmetries has been revisited (see Refs. [1223,1224]), with the suggestion to exploit additional asymmetries constructed from triple products in multi-body decays.

D. Interplay between direct and indirect *CP* violation

In decays of D^0 mesons, *CP* asymmetry measurements have contributions from both direct and indirect *CP* violation, as discussed in Sec. IX A. The contribution from indirect *CP* violation depends on the decay-time distribution of the data sample [1122]. This section describes a combination of measurements that allows the determination of the individual contributions of the two types of *CP* violation. At the same time, the level of agreement for a no-*CP*-violation hypothesis is tested.

The first observable is

$$A_\Gamma \equiv \frac{\hat{\tau}(\bar{D}^0 \to f) - \hat{\tau}(D^0 \to f)}{\hat{\tau}(\bar{D}^0 \to f) + \hat{\tau}(D^0 \to f)}, \tag{166}$$

where f can be K^+K^- or $\pi^+\pi^-$ and $\hat{\tau}(D^0 \to f)$ indicates the effective D^0 lifetime, measured with an exponential approximation in the decay to f. More recently, the related observable [1123]

$$\Delta Y \equiv \frac{\hat{\Gamma}(\bar{D}^0 \to f) - \hat{\Gamma}(D^0 \to f)}{2}, \tag{167}$$

has been measured [1097] instead of A_Γ, where $\hat{\Gamma}$ denotes the effective decay width and is the inverse of the effective lifetime. They are related by

$$A_\Gamma = \frac{-\Delta Y}{1 + y_{CP}}. \tag{168}$$

The second observable is

$$\Delta A_{CP} \equiv A_{CP}(K^+K^-) - A_{CP}(\pi^+\pi^-), \tag{169}$$

where A_{CP} are time-integrated *CP* asymmetries. The underlying theoretical parameters are

$$a_{CP}^{\text{dir}} \equiv \frac{|\mathcal{A}_{D^0\to f}|^2 - |\mathcal{A}_{\bar{D}^0\to f}|^2}{|\mathcal{A}_{D^0\to f}|^2 + |\mathcal{A}_{\bar{D}^0\to f}|^2},$$
$$a_{CP}^{\text{ind}} \equiv \frac{1}{2}\left[\left(\left|\frac{q}{p}\right| + \left|\frac{p}{q}\right|\right) x \sin\phi - \left(\left|\frac{q}{p}\right| - \left|\frac{p}{q}\right|\right) y \cos\phi\right], \tag{170}$$

where $\mathcal{A}_{D\to f}$ is the amplitude for $D \to f$ [1225]. The observables are related to the underlying parameters via [1226]

TABLE 262. Inputs to the fit for direct and indirect CP violation. The first uncertainty listed is statistical and the second is systematic. The uncertainties on $\Delta\langle t\rangle/\tau$ and $\langle t\rangle/\tau$ are ≤ 0.01 and are not quoted here.

Year	Experiment	Results	$\Delta\langle t\rangle/\tau$	$\langle t\rangle/\tau$	Reference
2012	*BABAR*	$A_\Gamma = (+0.09 \pm 0.26 \pm 0.06)\%$	⋯	⋯	[1090]
2014	CDF	$A_\Gamma = (-0.12 \pm 0.12)\%$	⋯	⋯	[1096]
2015	Belle	$A_\Gamma = (-0.03 \pm 0.20 \pm 0.07)\%$	⋯	⋯	[1092]
2021	LHCb	$\Delta Y(KK) = (-0.003 \pm 0.013 \pm 0.003)\%$	⋯	⋯	[1097]
		$\Delta Y(\pi\pi) = (-0.036 \pm 0.024 \pm 0.004)\%$	⋯	⋯	
2008	*BABAR*	$A_{CP}(KK) = (+0.00 \pm 0.34 \pm 0.13)\%$			
		$A_{CP}(\pi\pi) = (-0.24 \pm 0.52 \pm 0.22)\%$	0.00	1.00	[1113]
2012	CDF	$\Delta A_{CP} = (-0.62 \pm 0.21 \pm 0.10)\%$	0.25	2.58	[1116]
2014	LHCb SL	$\Delta A_{CP} = (+0.14 \pm 0.16 \pm 0.08)\%$	0.01	1.07	[1227]
2016	LHCb prompt	$\Delta A_{CP} = (-0.10 \pm 0.08 \pm 0.03)\%$	0.12	2.10	[1228]
2019	LHCb SL2	$\Delta A_{CP} = (-0.09 \pm 0.08 \pm 0.05)\%$	0.00	1.21	[1117]
2019	LHCb prompt2	$\Delta A_{CP} = (-0.182 \pm 0.032 \pm 0.009)\%$	0.13	1.74	[1117]

$$\Delta Y = -A_\Gamma(1 + y_{CP}) = a_{CP}^{\rm ind} + a_{CP}^{\rm dir} y_{CP} \approx a_{CP}^{\rm ind}, \quad (171)$$

$$\Delta A_{CP} = \Delta a_{CP}^{\rm dir}\left(1 + y_{CP}\frac{\overline{\langle t\rangle}}{\tau}\right) + a_{CP}^{\rm ind}\frac{\Delta\langle t\rangle}{\tau} + \overline{a_{CP}^{\rm dir}} y_{CP}\frac{\Delta\langle t\rangle}{\tau},$$
$$\approx \Delta a_{CP}^{\rm dir}\left(1 + y_{CP}\frac{\overline{\langle t\rangle}}{\tau}\right) + a_{CP}^{\rm ind}\frac{\Delta\langle t\rangle}{\tau}. \quad (172)$$

Equation (171) shows that ΔY constrains mostly indirect CP violation. The direct CP violation contribution can differ for different final states. However, the $a_{CP}^{\rm dir}$ term is neglected as it is suppressed by y_{CP} and not directly accessible in the fit below. In Eq. (172), $\langle t\rangle/\tau$ denotes the mean decay time in units of the D^0 lifetime; $\Delta X = X_{KK} - X_{\pi\pi}$ denotes the difference in quantity X between the K^+K^- and $\pi^+\pi^-$ final states; and $\bar{X} = (X_{KK} + X_{\pi\pi})/2$ denotes the average for quantity X. We neglect the term $\overline{a_{CP}^{\rm dir}} y_{CP}\frac{\Delta\langle t\rangle}{\tau}$ in Eq. (172), as the factors constituting it make it negligible with respect to the other two terms.

We perform a χ^2 fit to extract $\Delta a_{CP}^{\rm dir}$ and $a_{CP}^{\rm ind}$. The value for y_{CP} is taken to be $y_{CP} = (0.655 \pm 0.028)\%$, obtained by taking $y_{CP} - y_{CP}(K\pi) = (0.697 \pm 0.028)\%$ (see Table 246) and subtracting $y_{CP}(K\pi) = -4.19 \times 10^{-4}$ [1080]. The input measurements are listed in Table 262. For the *BABAR* measurements of $A_{CP}(K^+K^-)$ and $A_{CP}(\pi^+\pi^-)$, we calculate ΔA_{CP} adding all uncertainties in quadrature. This may overestimate the systematic uncertainty for the difference, as it neglects correlated uncertainties. However, the result is conservative, and the effect is small, as all measurements are statistically limited. For all measurements, statistical and systematic uncertainties are added in quadrature when calculating the χ^2. In this fit, $A_\Gamma(KK)$ and $A_\Gamma(\pi\pi)$ are assumed to be identical but are plotted separately in Fig. 47 to visualize their level of agreement. This approximation, which holds in the SM, is supported by all measurements to date. An alternative assessment that avoids relying on this approximation by analyzing only the KK final state is presented below. The inclusion of these measurements in the fit excludes a significant contribution to ΔA_{CP} that is due to final-state-dependent A_Γ values and different mean decay times, corresponding to a contribution from the term proportional to $a_{CP}^{\rm ind}$ in Eq. (172). The latest LHCb measurement in the fit measures ΔY [1097], which is approximately equal to $-A_\Gamma$ up to a fractional difference of y_{CP}.

The fit results are shown in Fig. 47. From the fit, the change in χ^2 from the minimum value for the no-CPV point (0,0) is 33.0, which corresponds to a CL of 6.7×10^{-8} for two degrees of freedom or 5.4 standard deviations. The central values and $\pm 1\sigma$ uncertainties for the individual parameters are

$$a_{CP}^{\rm ind} = (-0.010 \pm 0.012)\%$$
$$\Delta a_{CP}^{\rm dir} = (-0.159 \pm 0.029)\%. \quad (173)$$

Relative to the average reported in our previous report [1], the results remain approximately unchanged, with the main update being the value of y_{CP}, which only plays a minor role. The average clearly demonstrates direct CP violation in the singly Cabibbo-suppressed decays to two charged hadrons.

A new combination with respect to the previous report is performed to extract the parameters for the KK final state alone. This fit avoids the assumption of universal indirect

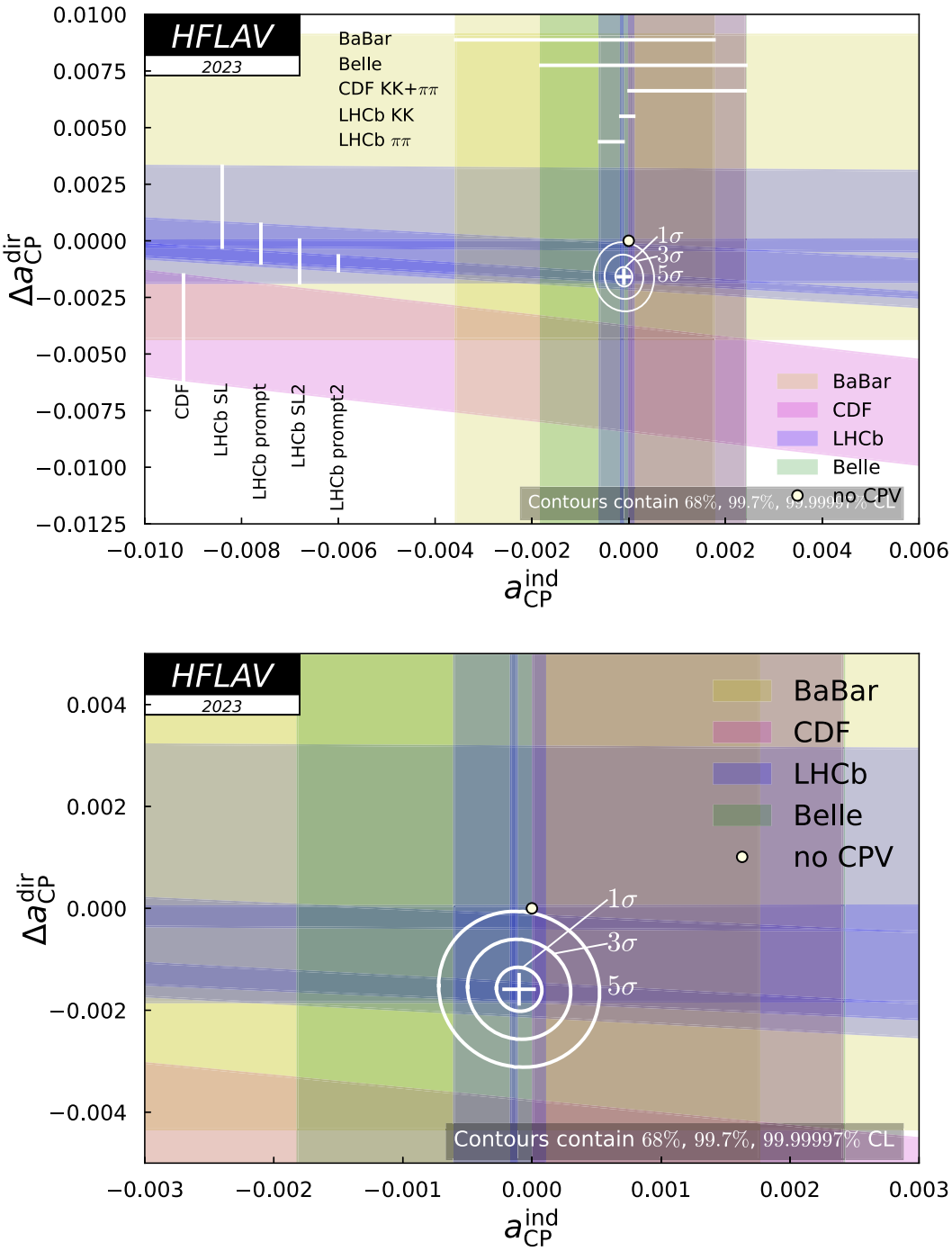


FIG. 47. Top: plot of all data and the fit result for $\Delta a_{CP}^{\mathrm{dir}}$ and a_{CP}^{ind}. Individual measurements are plotted as bands showing their $\pm 1\sigma$ range. The no-*CPV* point (0,0) is shown as a filled circle, and the best fit value is indicated by a cross showing the one-dimensional uncertainties. Two-dimensional 1σ (68.3% CL), 3σ (99.7% CL), and 5σ (99.99997% CL) regions are plotted as ellipses. Bottom: zoom of the same plot, highlighting the best fit region.

TABLE 263. Inputs to the fit for direct and indirect CP violation in the KK final state. The first uncertainty listed is statistical and the second is systematic. The uncertainties on $\langle t\rangle/\tau$ are ≤ 0.01 and are not quoted here.

Year	Experiment	Results	$\langle t\rangle/\tau$	Reference
2014	CDF	$A_\Gamma(KK) = (-0.19 \pm 0.15 \pm 0.04)\%$	⋯	[1096]
2021	LHCb	$\Delta Y(KK) = (-0.003 \pm 0.013 \pm 0.003)\%$	⋯	[1097]
2008	*BABAR*	$A_{CP}(KK) = (+0.00 \pm 0.34 \pm 0.13)\%$	1.00	[1113]
2008	Belle	$A_{CP}(KK) = (-0.43 \pm 0.30 \pm 0.11)\%$	1.00	[1114]
2023	LHCb	$A_{CP}(KK) = (0.068 \pm 0.054 \pm 0.016)\%$	1.75	[1118]

CP violation. As not all measurements were published with a separate result for the KK final state, only the results in Table 263 are used. Compared to the fits above, the second term in Eq. (171) is no longer neglected, resulting in the time-dependent measurements being represented by sloped bands, although the smallness of y_{CP} suppresses this effect so they still appear as vertical bands in Fig. 48. The value for y_{CP} is also extracted from the KK final state alone, for which the only available measurement is that of the LHCb collaboration, $y_{CP}(KK) - y_{CP}(K\pi) = (0.708 \pm 0.033)\%$ [1095], corrected for $y_{CP}(K\pi)$ as described above to yield $y_{CP}(KK) = (0.666 \pm 0.033)\%$. The time integrated asymmetry enters the fit according to the equation

$$A_{CP} \approx a_{CP}^{\rm dir} + a_{CP}^{\rm ind}\frac{\langle t\rangle}{\tau}. \tag{174}$$

The fit results are shown in Fig. 48. From the fit, the change in χ^2 from the minimum value for the no-CPV point (0,0) is 1.44, which corresponds to a CL of 0.49 for two degrees of freedom or 0.7 standard deviations. The central values and $\pm 1\sigma$ uncertainties for the individual parameters are

$$\begin{aligned} a_{CP}^{\rm ind}(KK) &= (-0.001 \pm 0.013)\% \\ a_{CP}^{\rm dir}(KK) &= (0.054 \pm 0.060)\%. \end{aligned} \tag{175}$$

The results are in agreement with CP symmetry in $D^0 \to K^+K^-$ decays. The result for $a_{CP}^{\rm ind}(KK)$ is in agreement with that obtained with the fit above assuming universality of indirect CP violation [see Eq. (173)] and hence supports this assumption. The result for $a_{CP}^{\rm dir}(KK)$ indicates that the CP violation observed in Δa_{CP} is driven by $D^0 \to \pi^+\pi^-$ decays.

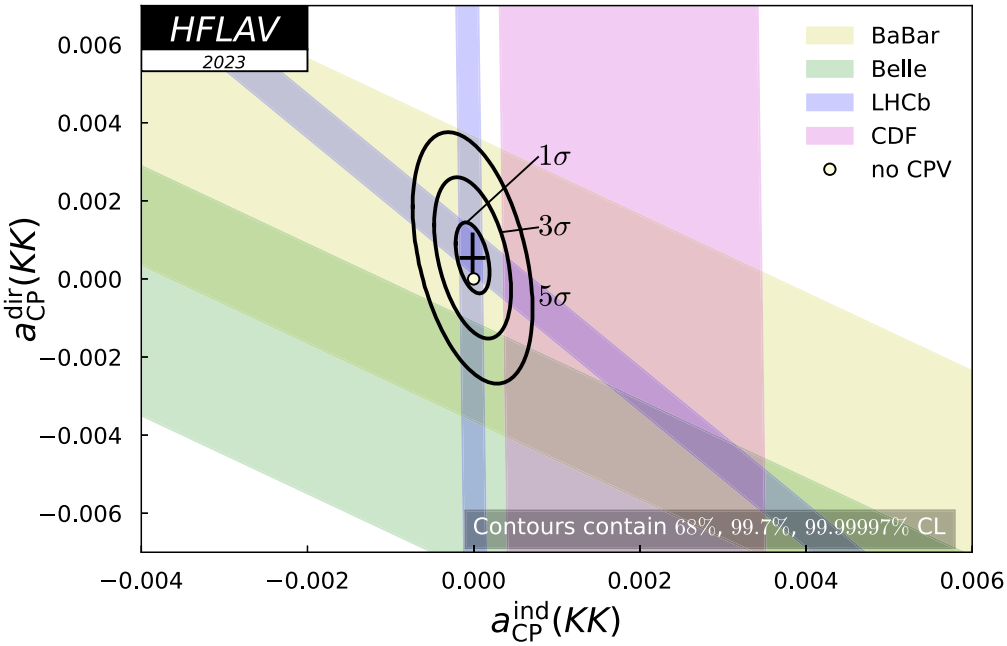


FIG. 48. Plot of data and the fit result for $a_{CP}^{\rm dir}(KK)$ and $a_{CP}^{\rm ind}(KK)$. Individual measurements are plotted as bands showing their $\pm 1\sigma$ range. The no-CPV point (0,0) is shown as a filled circle, and the best fit value is indicated by a cross showing the one-dimensional uncertainties. Two-dimensional 1σ (68.3% CL), 3σ (99.7% CL), and 5σ (99.99997% CL) regions are plotted as ellipses.

X. CHARM DECAYS

A. Semileptonic decays

Semileptonic D decays involve the interaction of a leptonic current with a hadronic current. The latter is nonperturbative and is usually parametrized in terms of form factors. The transition matrix element is written as

$$\mathcal{M} = -i\frac{G_F}{\sqrt{2}} V_{cq} L^\mu H_\mu, \tag{176}$$

where G_F is the Fermi constant and V_{cq} is a CKM matrix element. The leptonic current L^μ is evaluated directly from the lepton spinors and has a simple structure; this allows one to extract information about the form factors (in H_μ) from data on semileptonic decays [1229]. Conversely, because there are no strong final-state interactions between the leptonic and hadronic systems, semileptonic decays for which the form factors can be calculated allow one to determine $|V_{cq}|$ [3]. In experiment, one determines the form factors after taking the $|V_{cq}|$ from the standard model global fit as input; or determines the $|V_{cq}|$ after taking the form factors calculated by theory as input.

1. $D \to P\ell^+\nu_\ell$ decays and $|V_{cq}|$

Theoretical formula. When the final state hadron is a pseudoscalar, the hadronic current is given by [1230]

$$\begin{aligned} H_\mu &= \langle P(p)|\bar{q}\gamma_\mu c|D(p')\rangle \\ &= f_+(q^2)\left[(p'+p)_\mu - \frac{m_D^2 - m_P^2}{q^2} q_\mu\right] \\ &\quad + f_0(q^2)\frac{m_D^2 - m_P^2}{q^2} q_\mu, \end{aligned} \tag{177}$$

where m_D and p' are the mass and four momentum of the parent D meson, m_P and p are those of the daughter meson, $f_+(q^2)$ and $f_0(q^2)$ are the form factors, and $q = p' - p$. Kinematics require that $f_+(0) = f_0(0)$. The contraction $L^\mu q_\mu$ results in terms proportional to m_ℓ [1231], and thus for $\ell = e$ the terms proportional to q_μ in Eq. (177) are negligible and only the $f_+(q^2)$ vector form factor is relevant. The corresponding differential partial width is

$$\frac{d\Gamma(D \to Pe^+\nu_e)}{dq^2 d\cos\theta_e} = \frac{G_F^2 |V_{cq}|^2}{32\pi^3} p^{*3} |f_+(q^2)|^2 \sin\theta_e^2, \tag{178}$$

where $p^* = \frac{[(m_D^2 - (m_P+q))^2 (m_D^2 - (m_P-q))]^{1/2}}{2m_D}$ is the magnitude of the momentum of the final state hadron in the D rest frame, and θ_e is the angle of the electron in the $e\nu$ rest frame with respect to the direction of the pseudoscalar meson in the D rest frame.

The form factor is traditionally parametrized with an explicit pole and a sum of effective poles

$$f_+(q^2) = \frac{f_+(0)}{(1-\alpha)}\left[\left(\frac{1}{1 - q^2/m_{\text{pole}}^2}\right) + \sum_{k=1}^{N} \frac{\rho_k}{1 - q^2/(\gamma_k m_{\text{pole}}^2)}\right], \tag{179}$$

where ρ_k and γ_k are expansion parameters and α is a parameter that normalizes the form factor at $q^2 = 0$, $f_+(0)$. The parameter m_{pole} is the mass of the lowest-lying $c\bar{q}$ resonance with the vector quantum numbers; this is expected to provide the largest contribution to the form factor for the $c \to q$ transition. The sum over N gives the contribution of higher mass states. For example, for $D \to \pi$ transitions the dominant resonance is expected to be the $D^*(2010)$, and thus $m_{\text{pole}} = m_{D^*(2010)}$. For $D \to K$ transitions, the dominant resonance is expected to be the $D_s^*(2112)$, and thus $m_{\text{pole}} = m_{D_s^*(2112)}$.

Equation (179) can be simplified by neglecting the sum over effective poles, leaving only the explicit vector meson pole. This approximation is referred to as "nearest pole dominance" or "vector-meson dominance." The resulting parametrization is

$$f_+(q^2) = \frac{f_+(0)}{(1 - q^2/m_{\text{pole}}^2)}. \tag{180}$$

However, values of m_{pole} that give a good fit to the data do not agree with the expected vector meson masses [1230]. To address this problem, the "modified pole" or Becirevic-Kaidalov (BK) parametrization [1232] was introduced. In this parametrization $m_{\text{pole}}/\sqrt{\alpha_{\text{BK}}}$ is interpreted as the mass of an effective pole higher than m_{pole}, i.e., it is expected that $\alpha_{\text{BK}} < 1$. The parametrization takes the form

$$f_+(q^2) = \frac{f_+(0)}{(1 - q^2/m_{\text{pole}}^2)} \frac{1}{(1 - \alpha_{\text{BK}} \frac{q^2}{m_{\text{pole}}^2})}, \tag{181}$$

where α_{BK} is a free parameter that takes into account contributions from higher states in the form of an effective pole. This phenomenological parametrization is used by several experiments to determine form factor parameters.

Alternatively, a power series expansion around some value $q^2 = t_0$ can be used to parametrize $f_+(q^2)$ [1229,1233–1235]. This parametrization is model-independent and correctly incorporates the branch points associated with m_D and m_P. The expansion is given in terms of a complex parameter z, which is the analytic continuation of q^2 into the complex plane

$$z(q^2, t_0) = \frac{\sqrt{t_+ - q^2} - \sqrt{t_+ - t_0}}{\sqrt{t_+ - q^2} + \sqrt{t_+ - t_0}}, \tag{182}$$

where $t_0 = t_+(1 - \sqrt{1 - t_-/t_+})$ and $t_\pm \equiv (m_D \pm m_P)^2$. In this parametrization, $q^2 = t_0$ corresponds to $z = 0$, and the

physical region extends in either direction up to $\pm|z|_{\rm max} = \pm 0.051$ for $D \to K\ell^+\nu_\ell$ decays, and up to ± 0.17 for $D \to \pi\ell^+\nu_\ell$ decays.

The form factor is expressed as

$$f_+(q^2) = \frac{1}{P(q^2)\phi(q^2,t_0)} \sum_{k=0}^{\infty} a_k(t_0)[z(q^2,t_0)]^k, \quad (183)$$

where the Blaschke factor $P(q^2)$ is used to remove subthreshold poles, for instance, $P(q^2) = 1$ for $D \to \pi$ and $P(q^2) = z(q^2, M^2_{D_s^*})$ for $D \to K$. The "outer" function $\phi(t,t_0)$ can be any analytic function, but a preferred choice (see, e.g., Refs. [1233,1234,1236]), obtained from the operator product expansion (OPE), is

$$\phi(q^2,t_0) = \alpha\left(\sqrt{t_+ - q^2} + \sqrt{t_+ - t_0}\right) \times \frac{t_+ - q^2}{(t_+ - t_0)^{1/4}} \frac{(\sqrt{t_+ - q^2} + \sqrt{t_+ - t_-})^{3/2}}{(\sqrt{t_+ - q^2} + \sqrt{t_+})^5}, \quad (184)$$

with $\alpha = \sqrt{\pi m_c^2/3}$. The OPE analysis provides a constraint upon the expansion coefficients, $\sum_{k=0}^{N} a_k^2 \le 1$. These coefficients receive $1/M_D$ corrections, and thus the constraint is only approximate. However, the expansion is expected to converge rapidly since $|z| < 0.051(0.17)$ for $D \to K$ ($D \to \pi$) over the entire physical q^2 range, and Eq. (183) remains a useful parametrization. As a major advantage, the z-expansion complies with the analytic structure of the form factors predicted by general principles of quantum field theory. The main disadvantage as compared to phenomenological approaches is that there is no physical interpretation of the fitted coefficients a_K.

Experimental results of $D \to K\ell^+\nu_\ell$ and $D \to \pi\ell^+\nu_\ell$. Various techniques have been used by several experiments to measure semileptonic D decays with a pseudoscalar particle in the final state. The most recent results are provided by the *BABAR* [1237] and BESIII [1157,1238] collaborations. Belle [1239], *BABAR* [1240], and CLEO-c [1241,1242] have all previously reported results. Belle fully reconstructs $e^+e^- \to D\bar{D}X$ events from the continuum under the $\Upsilon(4S)$ resonance, achieving very good q^2 resolution (15 MeV^2) and a low background level but with a low efficiency. Using 282 fb^{-1} of data, about 1300 $D \to K\ell^+\nu_\ell$ (Cabibbo-favored) and 115 $D \to \pi\ell^+\nu_\ell$ (Cabibbo-suppressed) decays are reconstructed, considering the electron and muon channels together. The *BABAR* experiment uses a partial reconstruction technique in which the semileptonic decays are tagged via $D^{*+} \to D^0\pi^+$ decays. The D direction and neutrino energy are obtained using information from the rest of the event. With 75 fb^{-1} of data, 74000 signal events in the $D^0 \to K^-e^+\nu_e$ mode are obtained. This technique provides a large signal yield but also a high background level and a poor q^2 resolution (ranging from 66 to 219 MeV^2). In this case, the measurement of the branching fraction is obtained by normalizing to the $D^0 \to K^-\pi^+$ decay channel; thus the measurement would benefit from future improvements in the determination of the branching fraction for this reference channel. The Cabibbo-suppressed mode has been measured using the same technique and 350 fb^{-1} data. For this measurement, 5000 $D^0 \to \pi^-e^+\nu_e$ signal events were reconstructed [1237].

The CLEO-c experiment uses two different methods to measure charm semileptonic decays. The *tagged* analyses [1241] rely on the full reconstruction of $\psi(3770) \to D\bar{D}$ events. One of the D mesons is reconstructed in a hadronic decay mode, and the other in the semileptonic channel. The only missing particle is the neutrino, and thus the q^2 resolution is very good and the background level very low. With the entire CLEO-c data sample of 818 pb^{-1}, 14123 and 1374 signal events are reconstructed for the $D^0 \to K^-e^+\nu_e$ and $D^0 \to \pi^-e^+\nu_e$ channels, respectively, and 8467 and 838 are reconstructed for the $D^+ \to \bar{K}^0e^+\nu_e$ and $D^+ \to \pi^0e^+\nu_e$ decays, respectively. An alternative method that does not tag the D decay in a hadronic mode (referred to as *untagged* analyses) has also been used by CLEO-c [1242]. In this method, the entire missing energy and momentum in an event are associated with the neutrino four momentum, with the penalty of larger backgrounds as compared to the tagged method.

Using the tagged method, the BESIII experiment measures the $D^0 \to K^-e^+\nu_e$ and $D^0 \to \pi^-e^+\nu_e$ decay channels. With 2.93 fb^{-1} of data, they fully reconstruct 70700 and 6300 signal events, respectively, for the two channels [1238]. In a separate analysis, BESIII measures the semileptonic decay $D^+ \to K_L^0e^+\nu_e$ [1157], with about 20100 semileptonic candidates. Since 2016, BESIII has reported additional measurements of $D \to \bar{K}\ell^+\nu_\ell$ and $\pi\ell^+\nu_\ell$. The signal yields are 26008, 5013, 47100, 20714, 3402, 2265, and 1335 events for $D^+ \to \bar{K}^0(\pi^+\pi^-)e^+\nu_e$, $D^+ \to \bar{K}^0(\pi^0\pi^0)e^+\nu_e$, $D^0 \to K^-\mu^+\nu_\mu$, $D^+ \to \bar{K}^0(\pi\pi)\mu^+\nu_\mu$, $D^+ \to \pi^0e^+\nu_e$, $D^0 \to \pi^-\mu^+\nu_\mu$, and $D^+ \to \pi^0\mu^+\nu_\mu$ [1243–1247], respectively. The branching fractions or hadronic form factors are determined with good precision.

Results of the hadronic form factor parameters, $m_{\rm pole}$ and $\alpha_{\rm BK}$, obtained from the measurements discussed above, are given in Tables 264 and 265. The z-expansion formalism has been used by *BABAR* [1237,1240], BESIII [1157,1238,1243,1244] and CLEO-c [1241,1242]. Their fits use the first three terms of the expansion, and the results for the ratios $r_1 \equiv a_1/a_0$ and $r_2 \equiv a_2/a_0$ are listed in Tables 266 and 267.

TABLE 264. Results for $m_{\rm pole}$ and $\alpha_{\rm BK}$ from various experiments for $D^0 \to K^-\ell^+\nu_\ell$ ($\ell = e$ or μ) and $D^+ \to \bar{K}^0\ell^+\nu_\ell$ decays. The last two rows list results for other $c \to se^+\nu_e$ decays, for comparison, because some lattice calculations [1248,1249] find that the form factors are possibly insensitive to the spectator quarks.

Experiment	Mode	Ref.	$m_{\rm pole}$ (GeV/c^2)	$\alpha_{\rm BK}$
CLEO III	$D^0 \to K^-\ell^+\nu_\ell$	[1250]	$1.89 \pm 0.05^{+0.04}_{-0.03}$	$0.36 \pm 0.10^{+0.03}_{-0.07}$
FOCUS	$D^0 \to K^-\mu^+\nu_\mu$	[1251]	$1.93 \pm 0.05 \pm 0.03$	$0.28 \pm 0.08 \pm 0.07$
Belle	$D^0 \to K^-\ell^+\nu_\ell$	[1239]	$1.82 \pm 0.04 \pm 0.03$	$0.52 \pm 0.08 \pm 0.06$
BABAR	$D^0 \to K^-e^+\nu_e$	[1240]	$1.88 \pm 0.01 \pm 0.02$	$0.38 \pm 0.02 \pm 0.03$
CLEO-c (tagged)	$D^{0,+} \to K^-/\bar{K}^0\ell^+\nu_\ell$	[1241]	$1.93 \pm 0.02 \pm 0.01$	$0.30 \pm 0.03 \pm 0.01$
CLEO-c (untagged)	$D^0 \to K^-e^+\nu_e$	[1242]	$1.97 \pm 0.03 \pm 0.01$	$0.21 \pm 0.05 \pm 0.03$
CLEO-c (untagged)	$D^+ \to \bar{K}^0e^+\nu_e$	[1242]	$1.96 \pm 0.04 \pm 0.02$	$0.22 \pm 0.08 \pm 0.03$
BESIII	$D^0 \to K^-e^+\nu_e$	[1238]	$1.92 \pm 0.01 \pm 0.01$	$0.31 \pm 0.02 \pm 0.01$
BESIII	$D^+ \to K^0_Le^+\nu_e$	[1157]	$1.95 \pm 0.04 \pm 0.04$	$0.24 \pm 0.08 \pm 0.07$
BESIII	$D^+ \to K^0_Se^+\nu_e$	[1243]	$1.94 \pm 0.02 \pm 0.01$	$0.29 \pm 0.03 \pm 0.01$
BESIII	$D_s^+ \to \eta e^+\nu_e$	[1252]	$1.90 \pm 0.04 \pm 0.01$	$0.37 \pm 0.08 \pm 0.03$
BESIII	$D_s^+ \to \eta' e^+\nu_e$	[1252]	$1.67 \pm 0.22 \pm 0.04$	$0.73 \pm 0.50 \pm 0.12$

Determinations of $|V_{cs}|$ *and* $|V_{cd}|$. Results and world averages for the products $f_+^{D\to K}(0)|V_{cs}|$ and $f_+^{D\to\pi}(0)|V_{cd}|$ as measured by CLEO-c, Belle, *BABAR*, and BESIII are summarized in Tables 268 and 269, and plotted in Fig. 49. When calculating these world averages, the systematic uncertainties of the BESIII analyses are conservatively taken to be fully correlated.

Assuming unitarity of the CKM matrix, the values of the CKM matrix elements entering in charm semileptonic decays are evaluated as [302]

$$|V_{cs}| = 0.97349 \pm 0.00016,$$
$$|V_{cd}| = 0.22486 \pm 0.00067. \quad (185)$$

The unitarity assumption means that the measurement of charm decays themselves have insignificant influence on these averages, and they can thus be used to give a determination of the form factors under the unitarity assumption. Using the world average values of $f_+^K(0)|V_{cs}|$ and $f_+^\pi(0)|V_{cd}|$ from Tables 268 and 269 leads to the form factor values

TABLE 265. Results for $m_{\rm pole}$ and $\alpha_{\rm BK}$ from various experiments for $D^0 \to \pi^-\ell^+\nu_\ell$ and $D^+ \to \pi^0\ell^+\nu_\ell$ decays. The last two rows list results for other $c \to de^+\nu_e$ decays, for comparison, because some lattice calculations [1248,1249] find that the form factors are possibly insensitive to the spectator quarks.

Experiment	Mode	Refs.	$m_{\rm pole}$ (GeV/c^2)	$\alpha_{\rm BK}$
CLEO III	$D^0 \to \pi^-\ell^+\nu_\ell$	[1250]	$1.86^{+0.10+0.07}_{-0.06-0.03}$	$0.37^{+0.20}_{-0.31} \pm 0.15$
FOCUS	$D^0 \to \pi^-\mu^+\nu_\mu$	[1251]	$1.91^{+0.30}_{-0.15} \pm 0.07$	...
Belle	$D^0 \to \pi^-\ell^+\nu_\ell$	[1239]	$1.97 \pm 0.08 \pm 0.04$	$0.10 \pm 0.21 \pm 0.10$
CLEO-c (tagged)	$D^{0,+} \to \pi^{-,0}\ell^+\nu_\ell$	[1241]	$1.91 \pm 0.02 \pm 0.01$	$0.21 \pm 0.07 \pm 0.02$
CLEO-c (untagged)	$D^0 \to \pi^-\ell^+\nu_\ell$	[1242]	$1.87 \pm 0.03 \pm 0.01$	$0.37 \pm 0.08 \pm 0.03$
CLEO-c (untagged)	$D^+ \to \pi^0\ell^+\nu_\ell$	[1242]	$1.97 \pm 0.07 \pm 0.02$	$0.14 \pm 0.16 \pm 0.04$
BESIII	$D^0 \to \pi^-\ell^+\nu_\ell$	[1238]	$1.91 \pm 0.01 \pm 0.01$	$0.28 \pm 0.04 \pm 0.01$
BABAR	$D^0 \to \pi^-\ell^+\nu_\ell$	[1237]	$1.91 \pm 0.03 \pm 0.02$	$0.27 \pm 0.07 \pm 0.06$
BESIII	$D^+ \to \pi^0\ell^+\nu_\ell$	[1243]	$1.90 \pm 0.02 \pm 0.01$	$0.29 \pm 0.06 \pm 0.01$
CLEO-c	$D^+ \to \eta e^+\nu_e$	[1253]	$1.87 \pm 0.24 \pm 0.00$	$0.21 \pm 0.44 \pm 0.05$
BESIII	$D^+ \to \eta e^+\nu_e$	[1254]	$1.73 \pm 0.17 \pm 0.03$	$0.50 \pm 0.54 \pm 0.08$

TABLE 266. Results for r_1 and r_2 from various experiments for $D^0 \to K^-\ell^+\nu_\ell$ and $D^+ \to \bar{K}^0\ell^+\nu_\ell$ decays. Some lattice calculations [1248,1249] find that the form factors are possibly insensitive to the spectator quarks. For comparison, the last four rows list results for $c \to se^+\nu_e$ decays in which only the first two terms of the z expansion were used.

Experiment	Mode	Refs.	r_1	r_2
BABAR	$D^0 \to K^-e^+\nu_e$	[1240]	$-2.5 \pm 0.2 \pm 0.2$	$1 \pm 6 \pm 5$
CLEO-c (tagged)	$D^{0,+} \to K^-/\bar{K}^0e^+\nu_e$	[1241]	$-2.3 \pm 0.3 \pm 0.1$	$3 \pm 7 \pm 1$
CLEO-c (untagged)	$D^0 \to K^-e^+\nu_e$	[1242]	$-2.4 \pm 0.4 \pm 0.1$	$21 \pm 11 \pm 2$
CLEO-c (untagged)	$D^+ \to \bar{K}^0e^+\nu_e$	[1242]	$-2.8 \pm 6.0 \pm 2.0$	$32 \pm 18 \pm 4$
BESIII	$D^0 \to K^-e^+\nu_e$	[1238]	$-2.3 \pm 0.2 \pm 0.1$	$3 \pm 4 \pm 2$
BESIII	$D^+ \to K_L^0e^+\nu_e$	[1157]	$-2.2 \pm 0.4 \pm 0.5$	$11 \pm 9 \pm 9$
BESIII	$D^0 \to K^-\mu^+\nu_\mu$	[1244]	$-1.9 \pm 0.2 \pm 0.1$	…
BESIII	$D^+ \to K_S^0e^+\nu_e$	[1243]	$-1.8 \pm 0.3 \pm 0.1$	…
BESIII	$D_s^+ \to \eta e^+\nu_e$	[1252]	$-2.6 \pm 0.4 \pm 0.1$	…
BESIII	$D_s^+ \to \eta' e^+\nu_e$	[1252]	$-6.3 \pm 4.0 \pm 1.0$	…
BESIII	$D_s^+ \to \eta\mu^+\nu_\mu$	[1255]	$-2.9 \pm 0.6 \pm 0.3$	…
BESIII	$D_s^+ \to \eta'\mu^+\nu_\mu$	[1255]	$-10.6 \pm 5.3 \pm 1.3$	…

TABLE 267. Results for r_1 and r_2 from various experiments for $D^0 \to \pi^-\ell^+\nu_\ell$ and $D^+ \to \pi^0\ell^+\nu_\ell$ decays. Some lattice calculations [1248,1249] find that the form factors are possibly insensitive to the spectator quarks. For comparison, the last three rows list results for $c \to de^+\nu_e$ decays in which only the first two terms of the z expansion were used.

Experiment	Mode	Refs.	r_1	r_2
CLEO-c (tagged)	$D^{0,+} \to \pi^{-,0}e^+\nu_e$	[1241]	$-2.8 \pm 0.5 \pm 0.0$	$3 \pm 3 \pm 0$
CLEO-c (untagged)	$D^0 \to \pi^-e^+\nu_e$	[1242]	$-2.1 \pm 0.7 \pm 0.3$	$-1 \pm 5 \pm 2$
CLEO-c (untagged)	$D^+ \to \pi^0e^+\nu_e$	[1242]	$-0.2 \pm 1.5 \pm 0.4$	$-10 \pm 9 \pm 2$
BESIII	$D^0 \to \pi^-e^+\nu_e$	[1238]	$-1.8 \pm 0.2 \pm 0.1$	$-1 \pm 2 \pm 1$
BABAR	$D^0 \to \pi^-e^+\nu_e$	[1237]	$-1.3 \pm 0.7 \pm 0.4$	$-4 \pm 4 \pm 2$
BESIII	$D^+ \to \pi^0e^+\nu_e$	[1243]	$-2.2 \pm 0.4 \pm 0.1$	…
CLEO-c	$D^+ \to \eta e^+\nu_e$	[1253]	$1.8 \pm 2.2 \pm 0.3$	…
BESIII	$D^+ \to \eta e^+\nu_e$	[1254]	$-7.3 \pm 1.7 \pm 0.4$	…
BESIII	$D^+ \to \eta\mu^+\nu_\mu$	[1256]	$-0.9 \pm 2.7 \pm 0.2$	…

TABLE 268. Results for $f_+^{D\to K}(0)|V_{cs}|$ from various experiments. *BABAR* 2007 [1240] and Belle 2006 [1239] only reported $f_+^{D\to K}(0)$ values. The listed $f_+^{D\to K}(0)|V_{cs}|$ values of these two experiments are obtained by multiplying $f_+^{D\to K}(0)$ with their quoted $|V_{cs}|$.

Experiment	Mode	$f_+^{D\to K}(0)\lvert V_{cs}\rvert$	Comment
BESIII 2019 [1244]	$D^0 \to K^-\mu^+\nu_\mu$	0.7133(38)(30)	z expansion, 2 terms
BESIII 2017 [1243]	$D^+ \to K_S^0e^+\nu_e$	0.6983(56)(112)	z expansion, 3 terms
BESIII 2015B [1157]	$D^+ \to K_L^0e^+\nu_e$	0.7370(60)(90)	z expansion, 3 terms
BESIII 2015A [1238]	$D^0 \to K^-e^+\nu_e$	0.7195(35)(41)	z expansion, 3 terms
CLEO-c 2009 [1241]	$D^{0,+} \to K^-/\bar{K}^0e^+\nu_e$	0.7189(64)(48)	z expansion, 3 terms
BABAR 2007 [1240]	$D^0 \to K^-e^+\nu_e$	0.7211(69)(85)	Fitted pole mass + modified pole ansatze; $\lvert V_{cs}\rvert = 0.9729 \pm 0.0003$; corrected for $\mathcal{B}(D^0 \to K^-\pi^+)$
Belle 2006 [1239]	$D^0 \to K^-\ell^+\nu_\ell$	0.6762(68)(214)	$\lvert V_{cs}\rvert = 0.97296 \pm 0.00024$ (PDG 2006 w/unitarity)
World average		**0.7180(33)**	BESIII syst. fully correlated

TABLE 269. Results for $f_+^{D\to\pi}(0)|V_{cd}|$ from various experiments.

Experiment	Mode	$f_+^{D\to\pi}(0)\|V_{cd}\|$	Comment
BESIII 2017 [1243]	$D^+ \to \pi^0 e^+ \nu_e$	0.1413(35)(12)	z expansion, 3 terms
BESIII 2015A [1238]	$D^0 \to \pi^- e^+ \nu_e$	0.1420(24)(10)	z expansion, 3 terms
CLEO-c 2009 [1241]	$D^{0,+} \to \pi^{-,0} e^+ \nu_e$	0.1500(40)(10)	z expansion, 3 terms
BABAR 2015 [1237]	$D^0 \to \pi^- e^+ \nu_e$	0.1374(38)(24)	z expansion, 3 terms
Belle 2006 [1239]	$D^{0,+} \to \pi^{-,0} e^+ \nu_e$	0.1417(45)(68)	$\|V_{cd}\| = 0.2271 \pm 0.0010$ (PDG 2006 w/unitarity)
World average		**0.1426(18)**	BESIII syst. fully correlated

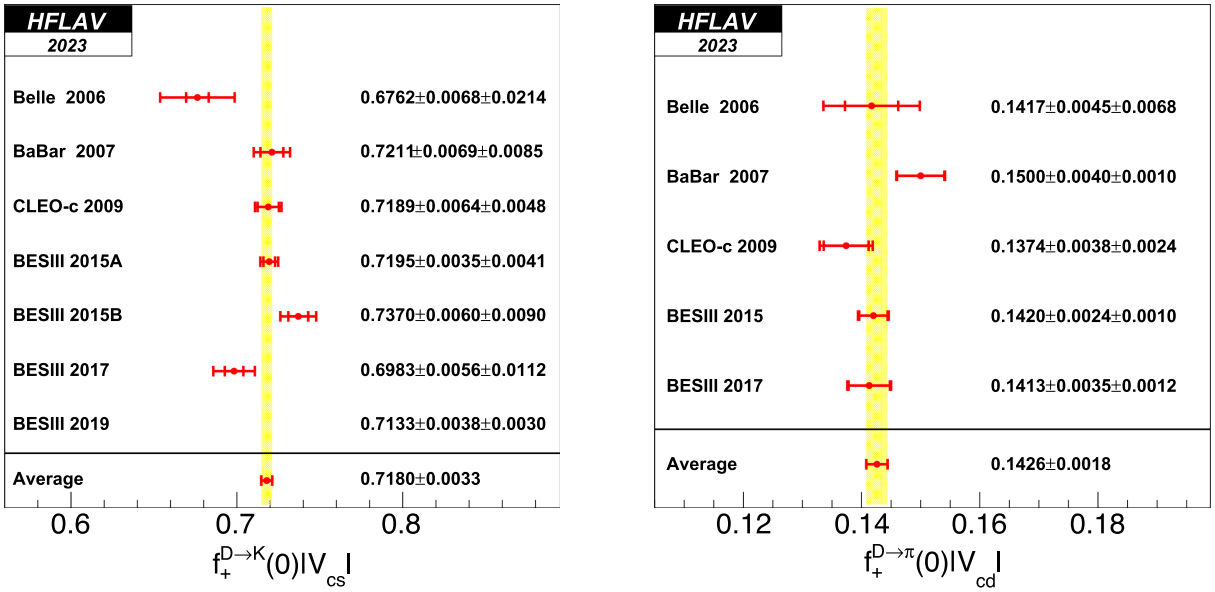


FIG. 49. Comparison of the experimental results of $f_+^{D\to K}(0)|V_{cs}|$ and $f_+^{D\to\pi}(0)|V_{cd}|$.

$$f_+^{D\to K}(0) = 0.7376 \pm 0.0034,$$
$$f_+^{D\to\pi}(0) = 0.6342 \pm 0.0082.$$

Table 270 summarizes $f_+^{D\to\pi}(0)$ and $f_+^{D\to K}(0)$ results based on $N_f = 2+1+1$ flavor lattice QCD of the ETM [1257], HPQCD [1258], and Fermilab Lattice and MILC [1259] Collaborations. The weighted averages are $f_+^{D\to K}(0) = 0.7449 \pm 0.0025$ and $f_+^{D\to\pi}(0) = 0.6296 \pm 0.0050$. The experimental averages of $f_+^{D\to K}(0)$ and $f_+^{D\to\pi}(0)$ agree with the corresponding lattice QCD calculations within 2σ.

Alternatively, if one assumes the lattice QCD form factor values, the averages in Tables 268 and 269 give

TABLE 270. Summary of the latest LQCD calculations of $f_+^{D\to\pi}(0)$ and $f_+^{D\to K}(0)$ from the Fermilab/MILC, ETM, and HPQCD collaborations.

Collaboration	$f_+^{D\to\pi}(0)$	$f_+^{D\to K}(0)$
Fermilab Lattice and MILC$(2+1+1)$ [1259]	0.6300 ± 0.0051	0.7452 ± 0.0031
ETM$(2+1+1)$ [1257]	0.612 ± 0.035	0.765 ± 0.031
HPQCD$(2+1+1)$ [1258]	...	0.7441 ± 0.0040
Average	0.6296 ± 0.0050	0.7449 ± 0.0025

TABLE 271. Results for $f_+^{D_s^+\to\eta}(0)|V_{cs}|$ from various experiments.

Experiment	Mode	$f_+^{D_s^+\to\eta}(0)\|V_{cs}\|$	Comment
BESIII [1252]	$D_s^+ \to \eta e^+\nu_e$	0.452(07)(07)	z expansion, 2 terms
BESIII [1255]	$D_s^+ \to \eta\mu^+\nu_\mu$	0.452(10)(07)	z expansion, 2 terms
World average		**0.452(09)**	Syst. fully correlated

TABLE 272. Results for $f_+^{D_s^+\to\eta'}(0)|V_{cs}|$ from various experiments.

Experiment	Mode	$f_+^{D_s^+\to\eta'}(0)\|V_{cs}\|$	Comment
BESIII [1252]	$D_s^+ \to \eta' e^+\nu_e$	0.525(24)(09)	z expansion, 2 terms
BESIII [1255]	$D_s^+ \to \eta'\mu^+\nu_\mu$	0.504(37)(12)	z expansion, 2 terms
World average		**0.519(10)**	Syst. fully correlated

TABLE 273. Results for $f_+^{D\to\eta}(0)|V_{cd}|$ from various experiments.

Experiment	Mode	$\|V_{cd}\|f_+^{D\to\eta}(0)$	Comment
BESIII 2020 [1256]	$D^+ \to \eta\mu^+\nu_\mu$	0.087(8)(2)	z expansion, 2 terms
BESIII 2018 [1254]	$D^+ \to \eta e^+\nu_e$	0.079(6)(2)	z expansion, 2 terms
CLEO-c 2009 [1253]	$D^+ \to \eta e^+\nu_e$	0.085(6)(1)	z expansion, 2 terms
World average		**0.083(4)**	BESIII syst. fully correlated

$$|V_{cs}| = 0.9639 \pm 0.0044(\text{exp}) \pm 0.0032(\text{LQCD}),$$
$$|V_{cd}| = 0.2265 \pm 0.0029(\text{exp}) \pm 0.0018(\text{LQCD}).$$

Here, the uncertainties are dominated by the lattice QCD calculations.

Experimental results of other $D_{(s)} \to P\ell^+\nu_\ell$ decays. In the past two decades, rapid progress in lattice QCD calculations of $f_+^{D\to K(\pi)}(0)$ has been achieved, motivated by much improved experimental measurements of $D \to \bar{K}\ell^+\nu_\ell$ and $D \to \pi\ell^+\nu_\ell$. However, in contrast, progress in theoretical calculations of form factors in other $D_{(s)} \to P\ell^+\nu_\ell$ decays has been slow, and experimental measurements sparse. Before BESIII, only CLEO reported a measurement of $f_+^{D\to\eta}(0)$ [1253]. For this analysis both tagged and untagged methods were used. In 2018 and 2019, BESIII reported measurements of $f_+^{D\to\eta}(0)$, $f_+^{D_s\to\eta^{(\prime)}}(0)$, and $f_+^{D_s\to K}(0)$ with a tagged method. The former one was measured by using 2.93 fb^{-1} of e^+e^- collision data taken at $\sqrt{s} =$ 3.773 GeV [1254,1256], and the latter two were measured by analyzing 3.19 fb^{-1} of e^+e^- collision data taken at $\sqrt{s} = 4.178$ GeV [1260,1261]. In 2023, BESIII reported the updated measurements of $f_+^{D_s\to\eta'}(0)$ with the same method, by analyzing the $D_s^+ \to \eta^{(\prime)}e^+\nu_e$ [1252] and $D_s^+ \to \eta^{(\prime)}\mu^+\nu_\mu$ [1255] decays from 7.33 fb^{-1} of e^+e^- collision data taken at $\sqrt{s} = 4.128$–4.226 GeV. These measurements greatly expand experimental knowledge of hadronic form factors in $D \to P\ell^+\nu_\ell$ decays. To date, there is still no measurement of $f_+^{D\to\eta'}(0)$ due to the small amount of data available.

The results and world averages of the products $f_+^{D_s^+\to\eta}(0)|V_{cs}|$, $f_+^{D_s^+\to\eta'}(0)|V_{cs}|$, and $f_+^{D\to\eta}(0)|V_{cd}|$, which have been measured by BESIII and CLEO-c, are summarized in Tables 271, 271, and 273 and plotted in Fig. 50. In averaging, the systematic uncertainties of the two BESIII analyses are conservatively taken to be fully correlated.

2. $D \to V\ell^+\nu_\ell$ decays

Theoretical formula. When the final state hadron is a vector meson, the decay can proceed through both vector and axial vector currents, and four form factors are needed. The hadronic current is $H_\mu = V_\mu + A_\mu$, where [1231]

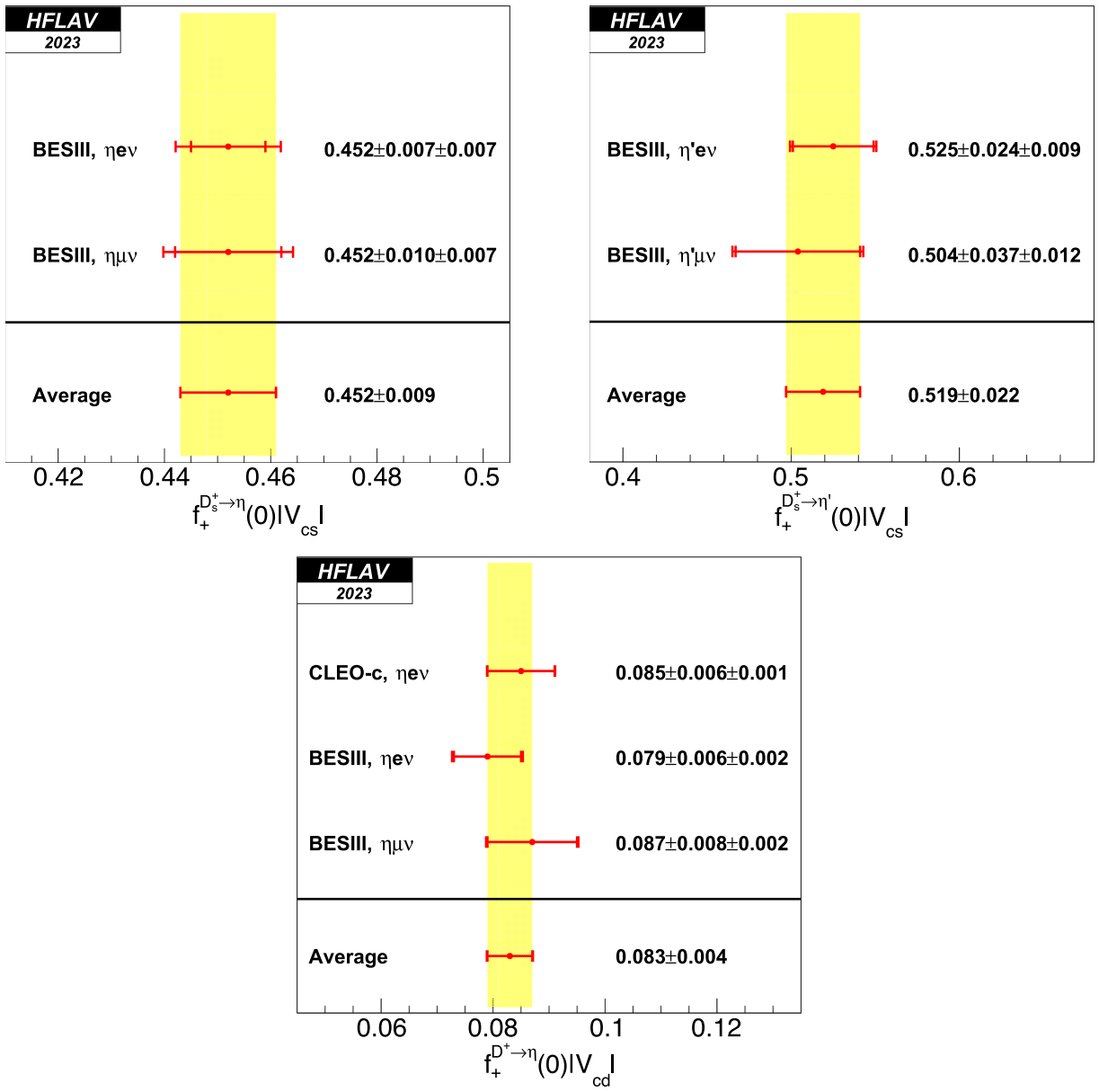


FIG. 50. Comparison of the experimental results of $f_+^{D_s^+\to\eta}(0)|V_{cs}|$, $f_+^{D_s^+\to\eta'}(0)|V_{cs}|$ and $f_+^{D^+\to\eta}(0)|V_{cd}|$.

$$V_\mu = \langle V(p,\varepsilon)|\bar{q}\gamma_\mu c|D(p')\rangle = \frac{2V(q^2)}{m_D+m_V}\varepsilon_{\mu\nu\rho\sigma}\varepsilon^{*\nu}p'^{\rho}p^{\sigma}, \tag{186}$$

$$\begin{aligned} A_\mu = \langle V(p,\varepsilon)|-\bar{q}\gamma_\mu\gamma_5 c|D(p')\rangle &= -i(m_D+m_V)A_1(q^2)\varepsilon_\mu^* \\ &+ i\frac{A_2(q^2)}{m_D+m_V}(\varepsilon^*\cdot q)(p'+p)_\mu \\ &+ i\frac{2m_V}{q^2}(A_3(q^2)-A_0(q^2))[\varepsilon^*\cdot(p'+p)]q_\mu. \end{aligned} \tag{187}$$

In this expression, m_V is the invariant mass of the daughter particles of the V meson and

$$A_3(q^2) = \frac{m_D+m_V}{2m_V}A_1(q^2) - \frac{m_D-m_V}{2m_V}A_2(q^2). \tag{188}$$

To avoid divergence of the $i\frac{2m_V}{q^2}(A_3(q^2)-A_0(q^2))$ item, kinematics require that $A_3(0)=A_0(0)$. Terms proportional to q_μ are important for the τ case. Thus, only the three form factors $A_1(q^2)$, $A_2(q^2)$ and $V(q^2)$ are relevant for charm decays. Usually, the q^2 dependent hadronic form factors $A_{1/2}(q^2)$ and $V(q^2)$ take simple pole forms, $A_{1/2}(q^2) = A_{1/2}(0)/(1-q^2/M_A^2)$ and $V(q^2) = V(0)/(1-q^2/M_V^2)$, with pole masses of $M_V = M_{D^*(1^-)} \backsimeq 2.1\ \mathrm{GeV}/c^2$ and $M_A = M_{D^*(1^+)} \backsimeq 2.5\ \mathrm{GeV}/c^2$, respectively.

The differential decay rate is

$$\frac{d\Gamma(D \to V\overline{\ell}\nu_\ell)}{dq^2 d\cos\theta_\ell} = \frac{G_F^2|V_{cq}|^2}{128\pi^3 m_D^2} p^* q^2 \times \left[\frac{(1-\cos\theta_\ell)^2}{2}|H_-|^2 + \frac{(1+\cos\theta_\ell)^2}{2}|H_+|^2 + \sin^2\theta_\ell |H_0|^2\right], \tag{189}$$

where $H_\pm$ and H_0 are helicity amplitudes, corresponding to helicities of the vector (V) meson. The helicity amplitudes can be expressed in terms of the form factors as

$$H_\pm = \frac{1}{m_D + m_V}[(m_D + m_V)^2 A_1(q^2) \mp 2m_D p^* V(q^2)], \tag{190}$$

$$H_0 = \frac{1}{|q|}\frac{m_D^2}{2m_V(m_D+m_V)} \times \left[\left(1 - \frac{m_V^2 - q^2}{m_D^2}\right)(m_D+m_V)^2 A_1(q^2) - 4p^{*2}A_2(q^2)\right]. \tag{191}$$

Here p^* is the magnitude of the three-momentum of the V system as measured in the D rest frame, and θ_ℓ is the angle of the lepton momentum with respect to the direction opposite that of the D in the W rest frame (see Fig. 51 for the electron case, θ_e). The left-handed nature of the quark current manifests itself as $|H_-| > |H_+|$. The differential decay rate for $D \to V\ell^+\nu_\ell$ followed by the vector meson decaying into two pseudoscalars is

$$\begin{aligned}\frac{d\Gamma(D \to V\overline{\ell}\nu, V \to P_1P_2)}{dq^2 d\cos\theta_V d\cos\theta_\ell d\chi} = {} & \frac{3G_F^2}{2048\pi^4}|V_{cq}|^2 \frac{p^*(q^2)q^2}{m_D^2}\mathcal{B}(V \to P_1P_2) \\ & \times \{(1+\cos\theta_\ell)^2 \sin^2\theta_V |H_+(q^2)|^2 + (1-\cos\theta_\ell)^2 \sin^2\theta_V |H_-(q^2)|^2 \\ & + 4\sin^2\theta_\ell \cos^2\theta_V |H_0(q^2)|^2 \\ & - 4\sin\theta_\ell(1+\cos\theta_\ell)\sin\theta_V\cos\theta_V\cos\chi H_+(q^2)H_0(q^2) \\ & + 4\sin\theta_\ell(1-\cos\theta_\ell)\sin\theta_V\cos\theta_V\cos\chi H_-(q^2)H_0(q^2) \\ & - 2\sin^2\theta_\ell\sin^2\theta_V\cos 2\chi H_+(q^2)H_-(q^2)\},\end{aligned} \tag{192}$$

where the helicity angles θ_ℓ, θ_V, and acoplanarity angle χ are defined as shown in Fig. 51. Inclusion of the S-wave $D \to K\pi\ell^+\nu_\ell$ contribution, denoted an S-wave form factor $h_0(q^2)$, leads to an interference term between them. Usually, the ratios of the form factors at $q^2 = 0$ are defined as

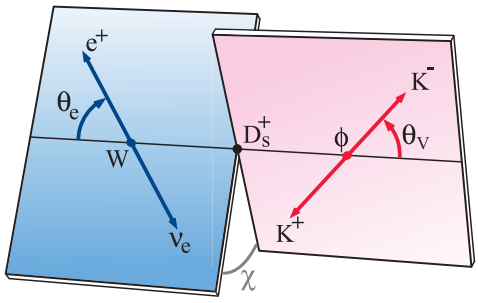


FIG. 51. Decay angles θ_V, θ_ℓ and χ. Note that the angle χ between the decay planes is defined in the D-meson reference frame, whereas the angles θ_V and θ_ℓ are defined in the V meson and W reference frames, respectively.

$$r_V \equiv \frac{V(0)}{A_1(0)}, \tag{193}$$

$$r_2 \equiv \frac{A_2(0)}{A_1(0)}. \tag{194}$$

From the experimental point of view, these ratios can be obtained without any assumption about the total decay rates or the CKM matrix elements.

Experimental results. In 2002 FOCUS reported an asymmetry in the observed $\cos(\theta_V)$ distribution in $D^+ \to K^-\pi^+\mu^+\nu_\mu$ decays [1262]. This was interpreted as evidence for an S-wave $K^-\pi^+$ component in the decay amplitude. It should be noted that $H_0(q^2)$ is equal to zero at $q^2 = q^2_{\rm max}$ but dominated over a wide range of q^2 [1263]. The distribution given by Eq. (192) is, after integration over χ, roughly proportional to $\cos^2\theta_V$. Inclusion of a constant S-wave amplitude of the form $Ae^{i\delta}$ leads to an interference term proportional to $|AH_0 \sin\theta_\ell \cos\theta_V|$ which then causes an asymmetry in $\cos(\theta_V)$. When FOCUS fit their data including this S-wave amplitude, they obtained $A = 0.330 \pm 0.022 \pm 0.015\,\text{GeV}^{-1}$ and $\delta = 0.68 \pm 0.07 \pm 0.05$

[1264]. Both *BABAR* [1265] and CLEO-c [1266] have also found evidence for an $f_0 \to K^+K^-$ component in semileptonic D_s decays.

The CLEO-c collaboration extracted the form factors $H_+(q^2)$, $H_-(q^2)$, and $H_0(q^2)$ from 11000 $D^+ \to K^-\pi^+\ell^+\nu_\ell$ events with purity greater than 96% in a model-independent fashion directly as functions of q^2 [1267]. They also determined the S-wave form factor $h_0(q^2)$ via the interference term, despite the fact that the $K\pi$ mass distribution appears dominated by the vector $K^*(892)$ state. The transverse form factor,

$$H_t(q^2) = \frac{M_D K}{m_{K\pi}\sqrt{q^2}}\left[(M_D + m_{K\pi})A_1(q^2) - \frac{(M_D^2 - m_{K\pi}^2 + q^2)}{M_D + m_{K\pi}}A_2(q^2) + \frac{2q^2}{M_D + m_{K\pi}}A_3(q^2)\right], \quad (195)$$

which can be related to $A_3(q^2)$, is small compared to LQCD calculations and suggests that the form factor ratio $r_3 \equiv A_3(0)/A_1(0)$ is large and negative.

The *BABAR* collaboration selected a large sample of 244×10^3 $D^+ \to K^-\pi^+e^+\nu_e$ candidates with a ratio $S/B \sim 2.3$ from an integrated luminosity of 347 fb^{-1} [1268]. With four particles emitted in the final state, the differential decay rate depends on five variables. In addition to the four variables defined in previous sections there is also m^2, the mass squared of the $K\pi$ system. To analyze the $D^+ \to K^-\pi^+e^+\nu_e$ decay channel, it was assumed that all form factors have a q^2 variation given by the simple pole model, and an effective pole mass of $m_A = (2.63 \pm 0.10 \pm 0.13)$ GeV/c^2 is fitted. This value is compatible with expectations when comparing to the mass of $J^P = 1^+$ charm mesons. For the mass dependence of the form factors, a Breit-Wigner with a mass-dependent width and a Blatt-Weisskopf damping factor is used. For the S-wave amplitude, a polynomial below the $\bar{K}_0^*(1430)$, and a Breit-Wigner distribution above, are used [1268]. These are consistent with measurements of $D^+ \to K^-\pi^+\pi^+$ decays. For the polynomial part, a linear term is sufficient to fit the data. It is verified that the variation of the S-wave phase is compatible with expectations from elastic $K\pi$ scattering [938,1269] (after correcting for $\delta^{3/2}$) according to the Watson theorem [1270]. As compared with elastic $K^-\pi^+$ scattering, there is an additional negative sign between the S- and P-waves. Contributions from other spin-1 and spin-2 resonances decaying into $K^-\pi^+$ are also considered.

From an e^+e^- collision data sample corresponding to an integrated luminosity of 2.92 fb^{-1} taken at $\sqrt{s} = 3.773$ GeV, the BESIII Collaboration obtained an almost background free sample which contains 18262 $D^+ \to K^-\pi^+e^+\nu_e$ events [1271], benefiting from double-tag technique. A partial wave analysis on this sample reveals that the $D^+ \to K^-\pi^+e^+\nu_e$ decay is dominated by $D^+ \to \bar{K}^*(892)^0e^+\nu_e$ with a $K\pi$ S-wave component with a fraction of $(6.05 \pm 0.22 \pm 0.18)\%$, and possible contributions from the $\bar{K}^*(1410)^0$ and $\bar{K}_2^*(1430)^0$ are negligible. The parametrizations of hadronic form factors follow those of the *BABAR* collaboration [1268]. The hadronic transition form factor ratios (r_V and r_2) for $D^+ \to \bar{K}^*(892)^0e^+\nu_e$ are extracted with the vector pole mass m_V floated or fixed at 2.0 GeV/c^2; and the pole mass of the axial form factor is free. The obtained results in different cases are consistent with each other. The S-wave phase variation with $m_{K\pi}$ is measured in a model-independent way, and it agrees with the partial wave analysis results based on the parametrization in the LASS scattering experiment [938]. A model-independent measurement of the q^2 dependence of the helicity basis form factors is also reported and the obtained results are consistent with the CLEO-c result. From the same data sample, BESIII obtained 3112 $D^0 \to K_S^0\pi^-e^+\nu_e$ events [1272] with background fraction of 0.6%. Based on the first amplitude analysis on the $D^0 \to K_S^0\pi^-e^+\nu_e$ sample, the hadronic form factor ratios for $D^0 \to \bar{K}^*(892)^-e^+\nu_e$ are extracted.

In 2013, the CLEO-c experiment reported a measurement of the $D^{0(+)} \to \rho^{-(0)}e^+\nu_e$ decay dynamics [1273] from the analysis of 0.818 fb^{-1} of data taken at $\sqrt{s} = 3.774$ GeV. Unlike the other measurements, the $\pi\pi$ invariant mass is not used in their amplitude analysis. Based on several hundreds of signal events, the hadronic form factor ratios for $D^{0(+)} \to \rho^{-(0)}e^+\nu_e$ are determined for the first time. In the measurement, the interference term between a possible S-wave $\pi\pi$ component and the ρ amplitude has not been included, and its absence is treated as a source of systematic uncertainty.

Later, the BESIII Collaboration reported the analysis of the decay dynamics of $D^0 \to \pi^-\pi^0e^+\nu_e$ and $D^+ \to \pi^+\pi^-e^+\nu_e$ [1274] by using 2.92 fb^{-1} of data taken at $\sqrt{s} = 3.773$ GeV. The signal yields for D^0 and D^+ decays are 1498 and 2017 with background fractions of 33% and 24%, respectively. The hadronic system in $D^+ \to \pi^+\pi^-e^+\nu_e$ is found to be dominated by the P wave, which is mostly from ρ^0 contribution along with much smaller ω contribution. Additionally, the S-wave component of $D^+ \to f_0(500)e^+\nu_e$ is observed for the first time with a relative contribution of $(25.7 \pm 1.6 \pm 1.1)\%$. Meanwhile, the P-wave component of $D^0 \to \rho^-e^+\nu_e$ dominates in the $\pi^-\pi^0$ system of $D^0 \to \pi^-\pi^0e^+\nu_e$, but no significant S-wave component is observed. Based on the same data sample, BESIII also presented the amplitude analysis of $D^+ \to \omega e^+\nu_e$ with hundreds of signal events after ignoring the non-ω component due to limited statistics. In these two measurements, the hadronic form factor ratios for $D^{0(+)} \to \rho^{-(0)}e^+\nu_e$ and $D^+ \to \omega e^+\nu_e$ are measured.

TABLE 274. Results for r_V and r_2 from various experiments. Experiments marked with * did not consider a separate S-wave contribution.

Experiment	Refs.	r_V	r_2
$D^+ \to \bar{K}^{*0}\ell^+\nu_\ell$			
E691*	[1276]	$2.0 \pm 0.6 \pm 0.3$	$0.0 \pm 0.5 \pm 0.2$
E653*	[1277]	$2.00 \pm 0.33 \pm 0.16$	$0.82 \pm 0.22 \pm 0.11$
E687*	[1278]	$1.74 \pm 0.27 \pm 0.28$	$0.78 \pm 0.18 \pm 0.11$
E791 (e)*	[1279]	$1.84 \pm 0.11 \pm 0.08$	$0.71 \pm 0.08 \pm 0.09$
E791 (μ)*	[1280]	$1.84 \pm 0.11 \pm 0.09$	$0.75 \pm 0.08 \pm 0.09$
Beatrice*	[1281]	$1.45 \pm 0.23 \pm 0.07$	$1.00 \pm 0.15 \pm 0.03$
FOCUS	[1264]	$1.50 \pm 0.06 \pm 0.04$	$0.88 \pm 0.05 \pm 0.06$
BABAR (e)	[1268]	$1.46 \pm 0.02 \pm 0.03$	$0.80 \pm 0.02 \pm 0.02$
BESIII (e)	[1271]	$1.41 \pm 0.06 \pm 0.02$	$0.78 \pm 0.04 \pm 0.02$
$D^0 \to \bar{K}^0\pi^-\ell^+\nu_\ell$			
FOCUS (μ)	[1282]	$1.71 \pm 0.68 \pm 0.34$	$0.91 \pm 0.37 \pm 0.10$
BESIII (e)	[1272]	$1.46 \pm 0.07 \pm 0.02$	$0.67 \pm 0.06 \pm 0.01$
$D^+ \to \omega e^+\nu_e$			
BESIII	[1283]	$1.24 \pm 0.09 \pm 0.06$	$1.06 \pm 0.15 \pm 0.05$
$D^{0,+} \to \rho e\nu_e$			
CLEO-c	[1273]	$1.48 \pm 0.15 \pm 0.05$	$0.83 \pm 0.11 \pm 0.04$
BESIII	[1274]	$1.70 \pm 0.08 \pm 0.05$	$0.85 \pm 0.06 \pm 0.04$
$D_s^+ \to \phi e^+\nu_e$			
BABAR	[1265]	$1.85 \pm 0.06 \pm 0.10$	$0.76 \pm 0.07 \pm 0.07$
$D_s^+ \to \phi\mu^+\nu_\mu$			
BESIII*	[1275]	$1.58 \pm 0.17 \pm 0.02$	$0.71 \pm 0.14 \pm 0.02$
$D_s^+ \to K^{*0}e^+\nu_e$			
BESIII*	[1261]	$1.67 \pm 0.34 \pm 0.16$	$0.77 \pm 0.28 \pm 0.07$

Using 3.19 fb^{-1} of e^+e^- collision data taken at $\sqrt{s} = 4.178$ GeV, the BESIII Collaboration presented the first amplitude analysis of $D_s^+ \to K^+\pi^-e^+\nu_e$ with only about one hundred of signal events [1261]. In 2023, by analyzing 7.33 fb^{-1} of data sample taken at in the energy region of $\sqrt{s} = 4.188$–4.226 GeV, BESIII reported an amplitude analysis of $D_s^+ \to K^+K^-e^+\nu_e$ [1275]. The obtained $D_s^+ \to K^+K^-e^+\nu_e$ sample contains about one thousand of signal events with background fraction of 10%. The former and latter channels are found to be dominated by $D_s^+ \to K^*(892)^0e^+\nu_e$ and $D_s^+ \to \phi e^+\nu_e$, while the S-wave component is found to be negligible in both two measurements. Based on these, the hadronic form factor ratios for $D_s^+ \to K^*(892)^0e^+\nu_e$ and $D_s^+ \to \phi e^+\nu_e$ are determined.

Table 274 lists the obtained results of r_V and r_2 from different experiments. The measured form factors are important to test different theoretical calculations based on quark model, QCD sum rule, and lattice QCD. The list of references is huge and see a recent review of theoretical calculations [1263] for example.

3. $D \to S\ell^+\nu_\ell$ decays

In 2018, BESIII reported measurements of semileptonic D decays into a scalar meson, $D \to S\ell^+\nu_\ell$. The experiment measured $D^{0,+} \to a_0(980)e^+\nu_e$, with $a_0(980) \to \eta\pi$. Signal yields of $25.7^{+6.4}_{-5.7}$ events for $D^0 \to a_0(980)^-e^+\nu_e$, and $10.2^{+5.0}_{-4.1}$ events for $D^+ \to a_0(980)^0e^+\nu_e$, were obtained, resulting in statistical significances of greater than 6.5σ and 3.0σ, respectively [1284]. As the branching fraction for $a_0(980) \to \eta\pi$ is not well measured, BESIII reports the product branching fractions

$$\mathcal{B}(D^0 \to a_0(980)^-e^+\nu_e) \times \mathcal{B}(a_0(980)^- \to \eta\pi^-) = (1.33^{+0.33}_{-0.29} \pm 0.09) \times 10^{-4}, \quad (196)$$

$$\mathcal{B}(D^+ \to a_0(980)^0 e^+\nu_e) \times \mathcal{B}(a_0(980)^0 \to \eta\pi^0) = (1.66^{+0.81}_{-0.66} \pm 0.11) \times 10^{-4}. \quad (197)$$

The ratio of these values can be compared to a prediction based on QCD light-cone sum rules [1285] Taking the lifetimes of the D^0 and D^+ into account, and assuming $\mathcal{B}(a_0(980)^- \to \eta\pi^-) = \mathcal{B}(a_0(980)^0 \to \eta\pi^0)$, the ratio of the partial widths is

$$\frac{\Gamma(D^0 \to a_0(980)^- e^+\nu_e)}{\Gamma(D^+ \to a_0(980)^0 e^+\nu_e)} = 2.03 \pm 0.95 \pm 0.06. \quad (198)$$

This value is consistent with the prediction based on isospin symmetry.

In 2021, BESIII searched for the semileptonic decay of $D_s^+ \to a_0(980) e^+\nu_e$, with $a_0(980)^0 \to \eta\pi^0$. No significant signal is observed. The product branching fraction upper limit at the 90% confidence level is $\mathcal{B}(D_s^+ \to a_0(980) e^+\nu_e) \times \mathcal{B}(a_0(980)^0 \to \eta\pi^0) < 1.2 \times 10^{-4}$ [1286].

In 2022, BESIII reported the studies of $D_s^+ \to \pi^0\pi^0 e^+\nu_e$ and $D_s^+ \to K_S^0 K_S^0 e^+\nu_e$ [1287], by analyzing 6.32 fb^{-1} of data taken at 4.178–4.226 GeV. The $f_0(980)$ is clearly observed in the $\pi^0\pi^0$ mass spectrum and the product branching fraction is determined to be $\mathcal{B}(D_s^+ \to f_0(980) e^+\nu_e)\mathcal{B}(f_0(980) \to \pi^0\pi^0) = (7.9 \pm 1.4 \pm 0.4) \times 10^{-4}$. No significant signal of $D_s^+ \to f_0(500) e^+\nu_e$ and $D_s^+ \to K_S^0 K_S^0 e^+\nu_e$ is observed. The (product) branching fraction upper limits at the 90% confidence level are $\mathcal{B}(D_s^+ \to f_0(500) e^+\nu_e) \times \mathcal{B}(f_0(500) \to \pi^0\pi^0) < 7.3 \times 10^{-4}$ and $\mathcal{B}(D_s^+ \to K_S^0 K_S^0 e^+\nu_e) < 3.8 \times 10^{-4}$, respectively.

In 2023, BESIII reported the studies of $D_s^+ \to \pi^+\pi^- e^+\nu_e$ [1288], by analyzing 7.33 fb^{-1} of data taken at 4.126–4.226 GeV. The $f_0(980)$ is observed in the $\pi^+\pi^-$ mass spectrum and the product branching fraction is determined to be $\mathcal{B}(D_s^+ \to f_0(980) e^+\nu_e)\mathcal{B}(f_0(980) \to \pi^0\pi^0) = (1.72 \pm 0.13 \pm 0.10) \times 10^{-3}$. From the studies of the dynamics of the $D_s^+ \to f_0(980) e^+\nu_e$ decay, the product of the form factor $f_+^{D_s \to f_0}(0)$ and the $c \to s$ Cabibbo-Kobayashi-Maskawa matrix element $|V_{cs}|$ is determined for the first time to be $f_+^{D_s \to f_0}(0)|V_{cs}| = 0.504 \pm 0.017 \pm 0.035$.

4. $D \to A\ell^+\nu_\ell$ decays

Experimental studies of semileptonic D decays into an axial-vector (A) meson $D \to A\ell^+\nu_\ell$ are challenging due to low statistics and high backgrounds. In 2007, CLEO-c reported first evidence for the Cabibbo-favored decay $D^0 \to K_1(1270)^- e^+\nu_e$ with a statistical significance of 4σ [1289]. The branching fraction was measured to be $\mathcal{B}(D^0 \to K_1(1270)^- e^+\nu_e) = (7.6^{+4.1}_{-3.0} \pm 0.6 \pm 0.7) \times 10^{-4}$. In 2019, BESIII reported the first observation of $D^+ \to \bar{K}_1(1270)^0 e^+\nu_e$, with statistical significance greater than 10σ [1290]. The branching fraction was measured to be $\mathcal{B}(D^+ \to \bar{K}_1(1270)^0 e^+\nu_e) = (23.0 \pm 2.6^{+1.8}_{-2.1} \pm 2.5) \times 10^{-4}$. In 2021, the $D^0 \to K_1(1270)^- e^+\nu_e$ decay was observed for the first time by BESIII with a statistical significance greater than 10σ [1291]. The reported branching fraction is $\mathcal{B}(D^+ \to \bar{K}_1(1270)^0 e^+\nu_e) = (10.9 \pm 1.3^{+0.9}_{-1.3} \pm 1.2) \times 10^{-4}$. Here, the third errors listed arise from the branching fraction for $K_1(1270) \to K\pi\pi$. The obtained branching fractions are consistent with the theoretical calculations with the K_1 mixing angle of 33° or 57°. Taking the lifetimes of D^0 and D^+ into account, the ratio of the partial widths is

$$\frac{\Gamma(D^+ \to \bar{K}_1(1270)^0 e^+\nu_e)}{\Gamma(D^0 \to K_1(1270)^- e^+\nu_e)} = 1.20 \pm 0.20 \pm 0.15. \quad (199)$$

This value agrees with unity as predicted by isospin symmetry.

In 2020, BESIII searched for the Cabibbo-suppressed semileptonic decays $D^+ \to b_1(1235)^0 e^+\nu_e$ and $D^0 \to b_1(1235)^0 e^+\nu_e$, by analyzing 2.93 fb^{-1} of data taken at 3.773 GeV. No significant signal is observed. The product branching fraction upper limits at the 90% confidence level are $\mathcal{B}(D^+ \to b_1(1235)^0 e^+\nu_e) \times \mathcal{B}(b_1(1235)^0 \to \omega\pi^0) < 1.12 \times 10^{-4}$ and $\mathcal{B}(D^0 \to b_1(1235)^- e^+\nu_e) \times \mathcal{B}(b_1(1235)^0 \to \omega\pi^0) < 1.75 \times 10^{-4}$, respectively [1292].

In 2023, BESIII searched for $D_s^+ \to K_1(1270)^0 e^+\nu_e$ and $D_s^+ \to b_1(1235)^0 e^+\nu_e$, by analyzing 7.33 fb^{-1} of data taken at 4.128–4.226 GeV. Also, no significant signal is observed. The product branching fraction upper limits at the 90% confidence level are $\mathcal{B}(D_s^+ \to K_1(1270)^0 e^+\nu_e) < 4.1 \times 10^{-4}$ and $\mathcal{B}(D_s^+ \to b_1(1235)^0 e^+\nu_e) \times \mathcal{B}(b_1(1235)^0 \to \omega\pi^0) < 6.4 \times 10^{-4}$, respectively [1293].

5. Test of e-μ lepton flavor universality

In the Standard Model (SM), the couplings between the three families of leptons and gauge bosons are expected to be equal; this is known as lepton flavor universality (LFU). The semileptonic decays of pseudoscalar mesons are well understood in the SM and thus offer a robust way to test LFU and search for new physics. Various tests of LFU with B semileptonic decays have been reported by *BABAR*, Belle, and LHCb. The average of the ratio of the branching fractions $\mathcal{B}_{B \to \bar{D}^{(*)}\tau^+\nu_\tau}/\mathcal{B}_{B \to \bar{D}^{(*)}\ell^+\nu_\ell}$ ($\ell = \mu$, e) deviates from the SM prediction by 3.1σ (see Sec. VI F). Precision measurements of the semileptonic D decays also test LFU, and in a manner complimentary to that of B decays [1294]. Within the SM, the ratios $\mathcal{B}_{D \to \bar{K}\mu^+\nu_\mu}/\mathcal{B}_{D \to \bar{K}e^+\nu_e}$ and $\mathcal{B}_{D \to \pi\mu^+\nu_\mu}/\mathcal{B}_{D \to \pi e^+\nu_e}$ are predicted to be 0.975 ± 0.001 and 0.985 ± 0.002, respectively [1295]. The ratios are expected to be close to unity with negligible uncertainty mainly due to high correlation of the corresponding hadronic form factors [1295].

In the SM, the semimuonic D decays are expected to have lower branching fraction than their semielectronic counterparts. Before BESIII, however, the information

TABLE 275. Comparison of the branching fractions of the semileptonic D decays.

Decay mode	$\mathcal{B}_\mu$ (%)	$\mathcal{B}_e$ (%)	$\mathcal{B}_\mu/\mathcal{B}_e$
$D^0 \to K^-\ell^+\nu_\ell$	$3.413 \pm 0.019 \pm 0.035$ [1244]	$3.505 \pm 0.014 \pm 0.033$ [1238]	0.974 ± 0.014 [1244]
$D^0 \to \pi^-\ell^+\nu_\ell$	$0.272 \pm 0.008 \pm 0.006$ [1247]	$0.295 \pm 0.004 \pm 0.003$ [1238]	0.922 ± 0.037 [1247]
$D^+ \to \bar{K}^0\ell^+\nu_\ell$	$8.72 \pm 0.07 \pm 0.18$ [1245]	8.72 ± 0.09 [302]	1.000 ± 0.024
$D^+ \to \pi^0\ell^+\nu_\ell$	$0.350 \pm 0.011 \pm 0.010$ [1247]	$0.363 \pm 0.008 \pm 0.005$ [1243]	0.964 ± 0.045 [1247]
$D^+ \to \omega\ell^+\nu_\ell$	$0.177 \pm 0.018 \pm 0.011$ [1296]	0.169 ± 0.011 [302]	1.05 ± 0.14
$D^+ \to \eta\ell^+\nu_\ell$	$0.104 \pm 0.010 \pm 0.005$ [1256]	0.111 ± 0.007 [302]	0.94 ± 0.12
$D_s^+ \to \phi\ell^+\nu_\ell$	$2.25 \pm 0.09 \pm 0.07$ [1275]	2.39 ± 0.16 [302]	0.94 ± 0.08 [1275]
$D_s^+ \to \eta\ell^+\nu_\ell$	$2.235 \pm 0.051 \pm 0.052$ [1255]	$2.255 \pm 0.039 \pm 0.051$ [1252]	0.984 ± 0.032 [1255]
$D_s^+ \to \eta'\ell^+\nu_\ell$	$0.801 \pm 0.055 \pm 0.028$ [1255]	$0.810 \pm 0.038 \pm 0.024$ [1252]	0.989 ± 0.089 [1255]

related to the semimuonic D decays is relatively poor, mainly due to higher backgrounds caused due to difficulty of distinguishing muon and charged pions. In the charmed meson sector, only $D^0 \to K^-\mu^+\nu_\mu$, $D^0 \to K^{*-}\mu^+\nu_\mu$, $D^0 \to \pi^-\mu^+\nu_\mu$, $D^+ \to \bar{K}^0\mu^+\nu_\mu$, $D^+ \to \rho^0\mu^+\nu_\mu$, and $D^+ \to \bar{K}^{*0}\mu^+\nu_\mu$ have been investigated in experiments previously. Except for $D^+ \to \bar{K}^{*0}\mu^+\nu_\mu$, all measurements of the other decays are dominated by FOCUS and Belle experiments and the existing measurements suffer from large uncertainties.

Since 2016, BESIII performed a series of studies of semimuonic D decays, including improved measurements of $D^+ \to \bar{K}^0\mu^+\nu_\mu$ [1245], $D^0 \to \pi^-\mu^+\nu_\mu$ [1247], and $D^0 \to K^-\mu^+\nu_\mu$ [1244], and the first observations of $D^+ \to \pi^0\mu^+\nu_\mu$ [1247], $D^+ \to \omega\mu^+\nu_\mu$ [1296], $D^+ \to \eta\mu^+\nu_\mu$ [1256]. All these analyses used the tagged method and 2.93 fb^{-1} of data taken at 3.773 GeV. The reported branching fractions are summarized in the second column of Table 275. Combining these results with previous BESIII measurements of their counterparts of the semielectronic decays using the same data sample or the world average values, the ratios of branching fractions are obtained, as shown in the last column of Table 275.

In 2018, using 0.482 fb^{-1} of data taken at the center-of-mass energy of 4.009 GeV, BESIII reported measurements of the branching fractions for semileptonic decays $D_s^+ \to \phi\mu^+\nu_\mu$, $D_s^+ \to \eta\mu^+\nu_\mu$, and $D_s^+ \to \eta'\mu^+\nu_\mu$ [1297]. In 2023, BESIII reported the precision measurements of the branching fractions of $D_s^+ \to \phi\mu^+\nu_\mu$ [1275], $D_s^+ \to \eta\mu^+\nu_\mu$, and $D_s^+ \to \eta'\mu^+\nu_\mu$ [1255], from analyses of 7.33 fb^{-1} of data taken at center-of-mass energies between 4.128 and 4.226 GeV, Combining these results with the world average value of the branching fraction of $D_s^+ \to \phi e^+\nu_e$ [302], and those of $D_s^+ \to \eta e^+\nu_e$, and $D_s^+ \to \eta' e^+\nu_e$ reported in Ref. [1252]. The obtained branching fractions, the comparison with their counterparts of the semielectronic decays using the same data sample or the world average value are also given in Table 275.

These results indicate that any $e-\mu$ LFU violation in semileptonic D decays has to be at the level of a few percent or less. BESIII also tested $e-\mu$ LFU in separate q^2 intervals using $D^{0,+} \to \pi^{-(0)}\ell^+\nu_\ell$ [1247], $D^0 \to K^-\ell^+\nu_\ell$ [1244], and $D_s^+ \to \eta^{(\prime)}\mu^+\nu_\mu$ [1255] decays. No indication of LFU above the 2σ level was found.

B. Leptonic decays

Purely leptonic decays of D^+ and D_s^+ mesons are among the simplest and best understood probes of $c \to d$ and $c \to s$ quark flavor-changing transitions. The amplitude of purely leptonic decays consists of the annihilation of the initial quark-antiquark pair ($c\bar{d}$ or $c\bar{s}$) into a virtual W^+ that subsequently materializes as an antilepton-neutrino pair ($\ell^+\nu_\ell$). The Standard Model (SM) branching fraction is given by

$$\mathcal{B}(D_q^+ \to \ell^+\nu_\ell) = \frac{G_F^2}{8\pi}\tau_{D_q} f_{D_q}^2 |V_{cq}|^2 m_{D_q} m_\ell^2 \left(1 - \frac{m_\ell^2}{m_{D_q}^2}\right)^2, \tag{200}$$

where m_{D_q} is the D_q meson mass, τ_{D_q} is its lifetime, m_ℓ is the charged lepton mass, $|V_{cq}|$ is the magnitude of the relevant CKM matrix element, and G_F is the Fermi coupling constant. The parameter f_{D_q} is the D_q meson decay constant and parametrizes the overlap of the wave functions of the constituent quark and anti-quark. This formulas and the similar formulas later do not include QED corrections. In view of the small errors quoted later these corrections may be relevant. The decay constants have been calculated using several methods, the most accurate and robust being that of lattice QCD (LQCD). Using the $N_f = 2+1+1$ flavor LQCD calculations of f_{D^+} and $f_{D_s^+}$ from the ETM [1298] and FNAL/MILC [1299] Collaborations, the Flavor Lattice Averaging Group (FLAG) calculates world average values [328]

$$f_{D^+}^{\mathrm{FLAG}} = 212.0 \pm 0.7 \text{ MeV}, \tag{201}$$

$$f_{D_s^+}^{\mathrm{FLAG}} = 249.9 \pm 0.5 \text{ MeV}, \tag{202}$$

and the ratio

$$\left(\frac{f_{D_s^+}}{f_{D^+}}\right)^{\mathrm{FLAG}} = 1.1783 \pm 0.0016. \tag{203}$$

These values are used within this section to determine the magnitudes $|V_{cd}|$ and $|V_{cs}|$ from the measured branching fractions of $D^+ \to \ell^+\nu_\ell$ and $D_s^+ \to \ell^+\nu_\ell$.

The leptonic decays of pseudoscalar mesons are helicity-suppressed, meaning their decay rates are proportional to the square of the charged lepton mass. Thus, decays to $\tau^+\nu_\tau$ are favored over decays to $\mu^+\nu_\mu$, and decays to $e^+\nu_e$, with an expected $\mathcal{B} \lesssim 10^{-7}$, are not yet experimentally observable. The ratio of $\tau^+\nu_\tau$ to $\mu^+\nu_\tau$ decays is given by

$$R_{\tau/\mu}^{D_q} \equiv \frac{\mathcal{B}(D_q^+ \to \tau^+\nu_\tau)}{\mathcal{B}(D_q^+ \to \mu^+\nu_\mu)} = \left(\frac{m_\tau^2}{m_\mu^2}\right)\frac{(m_{D_q}^2 - m_\tau^2)^2}{(m_{D_q}^2 - m_\mu^2)^2}, \tag{204}$$

and equals 9.75 ± 0.01 for D_s^+ decays and 2.67 ± 0.01 for D^+ decays, based on the well-measured values of m_μ, m_τ, and $m_{D_{(s)}}$ [302]. A significant deviation from this expectation would be interpreted as LFU violation in charged currents [1300].

In this section we present world average values for the product $f_{D_q}|V_{cq}|$, where $q = d,\ s$. For these averages, correlations between measurements and dependencies on input parameters are taken into account.

1. Recent experimental results

In 2019, BESIII reported the first observation of $D^+ \to \tau^+\nu_\tau$ with a statistical significance of 5.1σ from analysis of 2.93 fb^{-1} of e^+e^- collision data taken at the center-of-mass energy of 3.773 GeV. [1301]. In the same year, BESIII reported a measurement of $D_s^+ \to \mu^+\nu_\mu$ [1302], by analyzing 3.19 fb^{-1} of e^+e^- collision data taken at a center-of-mass energy of 4.178 GeV, in which this analysis used the muon counter to identify μ^+ lepton, and thereby obtained low background.

In 2021, BESIII reported an updated measurement of $D_s^+ \to \mu^+\nu_\mu$ [1303] without using the muon counter, the measurements of $D_s^+ \to \tau^+\nu_\tau$ with $\tau^+ \to \pi^+\bar{\nu}_\tau$ [1303], $\tau^+ \to \rho^+\bar{\nu}_\tau$ [1304] and $\tau^+ \to e^+\nu_e\bar{\nu}_\tau$ [1305] decays, by analyzing 6.32 fb^{-1} of e^+e^- collision data taken at center-of-mass energies of 4.178–4.226 GeV. Compared to Ref. [1302], there are much higher backgrounds in the measurement of $D_s^+ \to \mu^+\nu_\mu$ [1303] due to not using the muon counter. The updated measurement of $D_s^+ \to \mu^+\nu_\mu$ in Ref. [1303] supersedes that reported in Ref. [1302].

In 2023, BESIII reported a further updated measurement of $D_s^+ \to \mu^+\nu_\mu$ [1306] by using the muon counter, an updated measurement of $\tau^+ \to \pi^+\bar{\nu}_\tau$ [1307] with a multivariate analysis method, and a measurement of $\tau^+ \to \mu^+\nu_\mu\bar{\nu}_\tau$ [1308], based on the analysis of 7.33 fb^{-1} of e^+e^- collision data taken at center-of-mass energies of 4.128–4.226 GeV. The latest measurements of $D_s^+ \to \mu^+\nu_\mu$ and $D_s^+ \to \tau^+\nu_\tau$ with $\tau^+ \to \pi^+\bar{\nu}_\tau$ reported in Refs. [1306,1307] supersede those reported in Ref. [1303].

2. $D^+ \to \ell^+\nu_\ell$ decays and $|V_{cd}|$

The branching fraction $\mathcal{B}(D^+ \to \mu^+\nu_\mu)$ has been determined by CLEO-c [1143] and BESIII [1309]. These lead to the world average (WA) value

$$\mathcal{B}^{\mathrm{WA}}(D^+ \to \mu^+\nu_\mu) = (3.77 \pm 0.18) \times 10^{-4}. \tag{205}$$

For $D^+ \to \tau^+\nu_\tau$, the recent BESIII measurement [1301] gives

$$\mathcal{B}^{\mathrm{WA}}(D^+ \to \tau^+\nu_\tau) = (1.20 \pm 0.27) \times 10^{-3}. \tag{206}$$

Based on these two branching fractions and using the most recent values for m_τ, m_D, and τ_D [302], we determine the products of the decay constant and $|V_{cd}|$ to be

$$f_D|V_{cd}| = (46.2 \pm 1.0 \pm 0.3 \pm 0.1) \text{ MeV} \tag{207}$$

and

$$f_D|V_{cd}| = (50.5 \pm 5.1 \pm 2.5 \pm 0.1) \text{ MeV}, \tag{208}$$

respectively. These give the weighted product of the decay constant and $|V_{cd}|$ to be

$$f_D|V_{cd}| = (46.3 \pm 1.0) \text{ MeV}. \tag{209}$$

The uncertainty listed includes the uncertainty on $\mathcal{B}^{\mathrm{WA}}(D^+ \to \mu^+\nu_\mu)$, and also uncertainties on the external parameters m_μ, m_D, and τ_D [302] needed to extract $f_D|V_{cd}|$ from the branching fraction via Eq. (200). Using the LQCD value for f_D from FLAG [Eq. (201)], we calculate the magnitude of the CKM matrix element V_{cd} to be

$$|V_{cd}| = 0.2186 \pm 0.0049(\mathrm{exp}) \pm 0.0007(\mathrm{LQCD}), \tag{210}$$

where the first and second uncertainties are from experiment and from LQCD, respectively. All input values and the resulting world average are summarized in Table 276 and plotted in Fig. 52 (left).

Using the WA values of the branching fractions $\mathcal{B}(D^+ \to \mu^+\nu_\mu)$ and $\mathcal{B}(D^+ \to \tau^+\nu_\tau)$ [Eq. (205) and Eq. (213)], the ratio of these two branching fractions is determined to be

TABLE 276. Experimental results and world averages for $\mathcal{B}(D^+ \to \ell^+\nu_\ell)$ and $f_D|V_{cd}|$. The first uncertainties are statistical and the second are experimental systematic. The third uncertainties in the case of $f_{D^+}|V_{cd}|$ are due to external inputs (dominated by the uncertainty on τ_D). Here, we take the unconstrained result from CLEO-c.

Mode	$\mathcal{B}$ (10^{-4})	$f_D\|V_{cd}\|$ (MeV)	Reference	
$\mu^+\nu_\mu$	$3.95 \pm 0.35 \pm 0.09$	$47.3 \pm 2.1 \pm 0.5 \pm 0.1$	CLEO-c	[1143]
	$3.71 \pm 0.19 \pm 0.06$	$45.9 \pm 1.2 \pm 0.4 \pm 0.1$	BESIII	[1309]
	$3.77 \pm 0.17 \pm 0.05$	**$46.2 \pm 1.0 \pm 0.3 \pm 0.1$**	**Average**	
$\tau^+\nu_\tau$	$12.0 \pm 2.4 \pm 1.2$	$50.5 \pm 5.1 \pm 2.5 \pm 0.1$	BESIII	[1301]
$\mu^+\nu_\mu + \tau^+\nu_\tau$		**$46.3 \pm 1.0 \pm 0.3 \pm 0.1$**	**Average**	
$e^+\nu_e$	< 0.088 at 90% CL		CLEO-c	[1143]

$$R^{D^+}_{\tau/\mu} = 3.18 \pm 0.73, \tag{211}$$

which is consistent with the ratio expected in the SM.

3. $D_s^+ \to \ell^+\nu_\ell$ decays and $|V_{cs}|$

We use the measurements of the branching fraction $\mathcal{B}(D_s^+ \to \mu^+\nu_\mu)$ from CLEO-c [1197], *BABAR* [1311], Belle [1312], and BESIII [1306,1310] to obtain a WA value of

$$\mathcal{B}^{\rm WA}(D_s^+ \to \mu^+\nu_\mu) = (5.36 \pm 0.12) \times 10^{-3}. \tag{212}$$

The WA value for $\mathcal{B}(D_s^+ \to \tau^+\nu_\tau)$ is calculated from the CLEO-c, *BABAR*, Belle, and BESIII measurements. For the CLEO-c experiment, the separate measurements of $\mathcal{B}(D_s^+ \to \tau^+\nu_\tau)$ were performed with the $\tau^+ \to e^+\nu_e\bar{\nu}_\tau$ [1313], $\tau^+ \to \pi^+\bar{\nu}_\tau$ [1197], and $\tau^+ \to \rho^+\bar{\nu}_\tau$ decays [1314]. The Belle measurement was based on the tau decay modes of $\tau^+ \to e^+\nu_e\bar{\nu}_\tau$, $\tau^+ \to \mu^+\nu_\mu\bar{\nu}_\tau$, and $\tau^+ \to \pi^+\bar{\nu}_\tau$ [1312]; while the *BABAR* measurement was only based on the $\tau^+ \to e^+\nu_e\bar{\nu}_\tau$ and $\tau^+ \to \mu^+\nu_\mu\bar{\nu}_\tau$ decays were adopted [1311]; The BESIII Collaboration reported individual measurements of $\mathcal{B}(D_s^+ \to \tau^+\nu_\tau)$ by using the $\tau^+ \to \pi^+\bar{\nu}_\tau$ [1307,1310], $\tau^+ \to \rho^+\bar{\nu}_\tau$ [1304], $\tau^+ \to e^+\nu_e\bar{\nu}_\tau$ [1305] and $\tau^+ \to \mu^+\nu_\mu\bar{\nu}_\tau$ [1308] decays. Combining all these results and accounting for correlations, we obtain a WA value of

$$\mathcal{B}^{\rm WA}(D_s^+ \to \tau^+\nu_\tau) = (5.33 \pm 0.12) \times 10^{-2}. \tag{213}$$

The ratio of branching fractions is found to be

$$R^{D_s}_{\tau/\mu} = 10.01 \pm 0.29, \tag{214}$$

which is consistent with the ratio expected in the SM.

Taking the average of $\mathcal{B}^{\rm WA}(D_s^+ \to \mu^+\nu_\mu)$ and $\mathcal{B}^{\rm WA}(D_s^+ \to \tau^+\nu_\tau)$ [Eqs. (212) and (213)], and using the most recent values for m_τ, m_{D_s}, and τ_{D_s} [302], the products of the D_s decay constant and $|V_{cs}|$ are determined to be

$$f_{D_s}|V_{cs}| = (243.2 \pm 2.1 \pm 1.6 \pm 1.0)\ \text{MeV} \tag{215}$$

and

$$f_{D_s}|V_{cs}| = (246.5 \pm 1.5 \pm 1.7 \pm 1.0)\ \text{MeV}, \tag{216}$$

respectively. The average of these two results is

$$f_{D_s}|V_{cs}| = (245.1 \pm 2.0)\ \text{MeV}, \tag{217}$$

where the uncertainty is due to the uncertainties on $\mathcal{B}^{\rm WA}(D_s^+ \to \mu^+\nu_\mu)$, $\mathcal{B}^{\rm WA}(D_s^+ \to \tau^+\nu_\tau)$, and the external inputs. All input values and the resulting world average are summarized in Table 277 and plotted in Fig. 52 (right). To calculate this average, we take into account correlations within each experiment[21] for uncertainties related to normalization, tracking, particle identification, signal and background parametrizations, and peaking background contributions.

Using the LQCD value for f_{D_s} from FLAG [Eq. (202)], we calculate the magnitude of the CKM matrix element V_{cs} to be

$$|V_{cs}| = 0.9808 \pm 0.0079(\text{exp}) \pm 0.0020(\text{LQCD}), \tag{218}$$

where the first and second uncertainties are from experiment and from lattice calculations, respectively.

4. Comparison with other determinations of $|V_{cd}|$ and $|V_{cs}|$

Table 278 summarizes, and Fig. 53 displays, all determinations of the magnitudes $|V_{cd}|$ and $|V_{cs}|$. The table and figure show that, currently, the most precise direct determinations are from leptonic D^+ and D_s^+ decays. The obtained $|V_{cd}|$ and $|V_{cs}|$ values are in agreement within

[21] In the case of *BABAR*, we use the covariance matrix from the Errata of Ref. [1311].

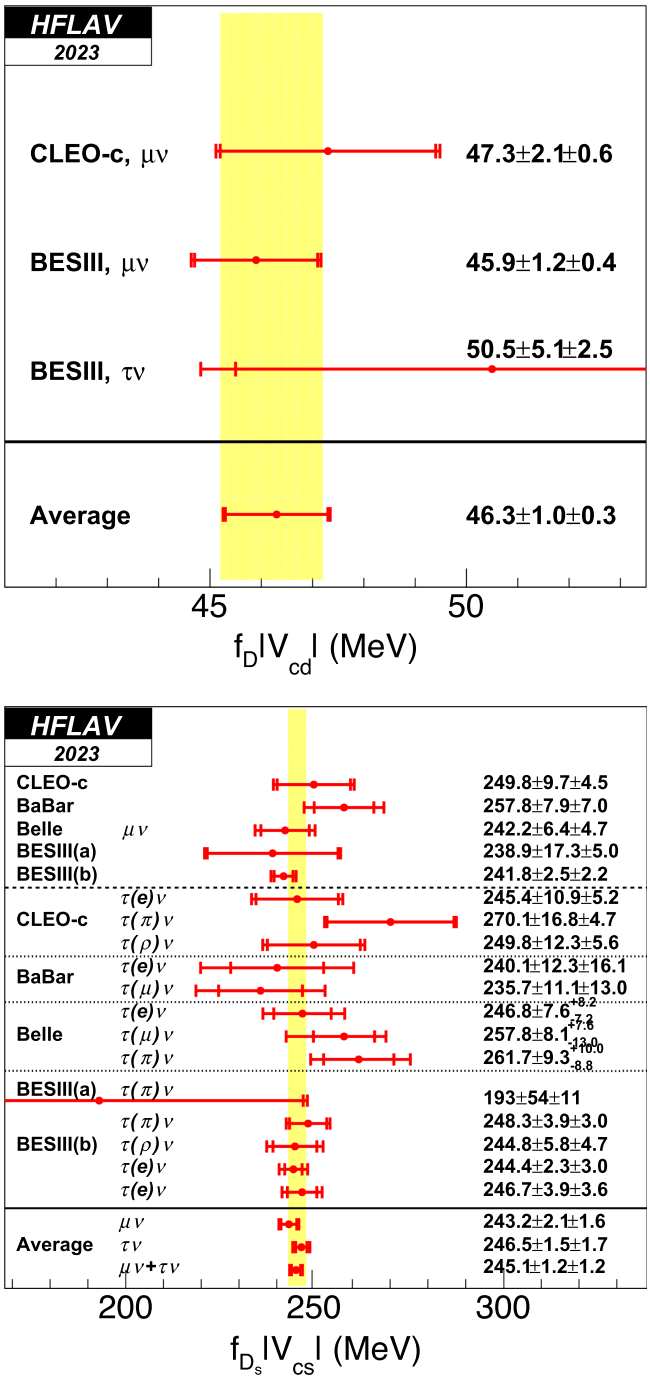


FIG. 52. WA values for $f_D|V_{cd}|$ (top) and $f_{D_s}|V_{cs}|$ (bottom). For each point, the first errors are statistical and the second errors are systematic. BESIII(a) represents results based on 0.48 fb^{-1} of data recorded at $\sqrt{s} = 4.009$ GeV [1310], and BESIII(b) represents results based on 7.33 (or 6.32) fb^{-1} of data recorded at $\sqrt{s} = 4.128$–4.226 GeV [1304,1305,1307,1308].

TABLE 277. Experimental results and world averages for $\mathcal{B}(D_s^+ \to \ell^+\nu_\ell)$ and $f_{D_s}|V_{cs}|$. The first uncertainties are statistical and the second are experimental systematic. The third uncertainties in the case of $f_{D_s}|V_{cs}|$ are due to external inputs (dominated by the uncertainty on τ_{D_s}). We have adjusted the $\mathcal{B}(D_s^+ \to \tau^+\nu_\tau)$ values quoted by CLEO-c and *BABAR* to account for the most recent values of $\mathcal{B}(\tau^+ \to \pi^+\bar{\nu}_\tau)$, $\mathcal{B}(\tau^+ \to \mu^+\nu_\mu\bar{\nu}_\tau)$, and $\mathcal{B}(\tau^+ \to e^+\nu_e\bar{\nu}_\tau)$ [302]. CLEO-c and *BABAR* include the uncertainty in the number of D_s tags (denominator in the calculation of the branching fraction) in the statistical uncertainty of $\mathcal{B}$; however, we subtract this uncertainty from the statistical one and include it in the systematic uncertainty. When averaging the BESIII results of $\mathcal{B}(D_s^+ \to \tau^+\nu_\tau)$, small correlations among various measurements have been taken into account.

Mode	$\mathcal{B}$ (10^{-2})	$f_{D_s}\|V_{cs}\|$ (MeV)	References	
	$0.565 \pm 0.044 \pm 0.020$	$249.8 \pm 9.7 \pm 4.4 \pm 1.0$	CLEO-c	[1197]
	$0.602 \pm 0.037 \pm 0.032$	$257.8 \pm 7.9 \pm 6.9 \pm 1.0$	*BABAR*	[1311]
$\mu^+\nu_\mu$	$0.531 \pm 0.028 \pm 0.020$	$242.2 \pm 6.4 \pm 4.6 \pm 1.0$	Belle	[1312]
	$0.517 \pm 0.075 \pm 0.021$	$238.9 \pm 17.3 \pm 4.9 \pm 0.9$	BESIII	[1310]
	$0.5294 \pm 0.0108 \pm 0.0085$	$241.8 \pm 2.5 \pm 2.2 \pm 1.0$	BESIII	[1306]
	$\mathbf{0.5358 \pm 0.0094 \pm 0.0072}$	$\mathbf{243.2 \pm 2.1 \pm 1.6 \pm 1.0}$	**Average**	
$\tau^+(e^+)\nu_\tau$	$5.32 \pm 0.47 \pm 0.22$	$245.4 \pm 10.9 \pm 5.1 \pm 1.0$	CLEO-c	[1314]
$\tau^+(\pi^+)\nu_\tau$	$6.47 \pm 0.80 \pm 0.22$	$270.1 \pm 16.8 \pm 4.6 \pm 1.1$	CLEO-c	[1197]
$\tau^+(\rho^+)\nu_\tau$	$5.50 \pm 0.54 \pm 0.24$	$249.8 \pm 12.3 \pm 5.5 \pm 1.0$	CLEO-c	[1313]
$\tau^+\nu_\tau$	$5.59 \pm 0.32 \pm 0.14$	$251.7 \pm 7.2 \pm 3.2 \pm 1.0$	CLEO-c	
$\tau^+(e^+)\nu_\tau$	$5.09 \pm 0.52 \pm 0.68$	$240.1 \pm 12.3 \pm 16.1 \pm 1.0$	*BABAR*	[1311]
$\tau^+(\mu^+)\nu_\tau$	$4.90 \pm 0.46 \pm 0.54$	$235.7 \pm 11.1 \pm 13.0 \pm 1.0$		
$\tau^+\nu_\tau$	$4.96 \pm 0.37 \pm 0.57$	$237.1 \pm 8.8 \pm 13.6 \pm 1.0$	*BABAR*	
$\tau^+(e^+)\nu_\tau$	$5.38 \pm 0.33^{+0.35}_{-0.31}$	$246.8 \pm 7.6^{+8.1}_{-7.1} \pm 1.0$	Belle	[1312]
$\tau^+(\mu^+)\nu_\tau$	$5.86 \pm 0.37^{+0.34}_{-0.59}$	$257.8 \pm 8.1^{+7.5}_{-13.0} \pm 1.0$		
$\tau^+(\pi^+)\nu_\tau$	$6.05 \pm 0.43^{+0.46}_{-0.40}$	$261.7 \pm 9.3^{+10.0}_{-8.7} \pm 1.0$		
$\tau^+\nu_\tau$	$5.70 \pm 0.21 \pm 0.31$	$254.1 \pm 4.7 \pm 6.9 \pm 1.0$	Belle	
$\tau^+(\pi^+)\nu_\tau$	$3.28 \pm 1.83 \pm 0.37$	$193 \pm 54 \pm 11 \pm 1$	BESIII	[1310]
$\tau^+(\pi^+)\nu_\tau$	$5.21 \pm 0.25 \pm 0.17$	$243.0 \pm 5.8 \pm 4.0 \pm 1.0$	BESIII	[1307]
$\tau^+(\rho^+)\nu_\tau$	$5.44 \pm 0.17 \pm 0.13$	$248.3 \pm 3.9 \pm 3.0 \pm 1.0$	BESIII	[1304]
$\tau^+(e^+)\nu_\tau$	$5.27 \pm 0.10 \pm 0.12$	$244.4 \pm 2.3 \pm 2.8 \pm 1.0$	BESIII	[1305]
$\tau^+(\mu^+)\nu_\tau$	$5.37 \pm 0.17 \pm 0.15$	$246.7 \pm 3.9 \pm 3.6 \pm 1.0$	BESIII	[1308]
$\tau^+\nu_\tau$	$5.33 \pm 0.07 \pm 0.08$	$245.7 \pm 1.7 \pm 1.8 \pm 1.0$	BESIII	
	$\mathbf{5.362 \pm 0.064 \pm 0.073}$	$\mathbf{246.5 \pm 1.5 \pm 1.7 \pm 1.0}$	**Average**	
$\boldsymbol{\mu^+\nu_\mu + \tau^+\nu_\tau}$		$\mathbf{245.1 \pm 1.2 \pm 1.2 \pm 1.0}$	**Average**	
$e^+\nu_e$	< 0.0083 at 90% CL		Belle	[1312]

TABLE 278. Averages of the magnitudes of CKM matrix elements $|V_{cd}|$ and $|V_{cs}|$, as determined from leptonic and semileptonic $D_{(s)}$ decays. In calculating these averages, we conservatively assume that uncertainties due to LQCD are fully correlated. For comparison, values determined from neutrino scattering, from W decays, and from a global fit to the CKM matrix assuming unitarity [1315] are also listed.

Method	References	Value
		$\lvert V_{cd}\rvert$
$D \to \ell\nu_\ell$	This section	$0.2186 \pm 0.0049(\text{exp}) \pm 0.0007(\text{LQCD})$
$D \to \pi\ell\nu_\ell$	Sec. X A	$0.2265 \pm 0.0029(\text{exp}) \pm 0.0018(\text{LQCD})$
$D \to \ell\nu_\ell$ $D \to \pi\ell\nu_\ell$	**Average**	0.2240 ± 0.0028
νN	PDG [302]	0.230 ± 0.011
Global CKM Fit	CKMFitter [1315]	0.22486 ± 0.00067
		$\lvert V_{cs}\rvert$
$D_s \to \ell\nu_\ell$	This section	$0.9808 \pm 0.0079(\text{exp}) \pm 0.0020(\text{LQCD})$
$D \to K\ell\nu_\ell$	Sec. X A	$0.9639 \pm 0.0044(\text{exp}) \pm 0.0032(\text{LQCD})$
$D_s \to \ell\nu_\ell$ $D \to K\ell\nu_\ell$	**Average**	0.9691 ± 0.0045
$W \to c\bar{s}$	PDG [302]	$0.94^{+0.32}_{-0.26} \pm 0.13$
Global CKM Fit	CKMFitter [1315]	0.97349 ± 0.00016

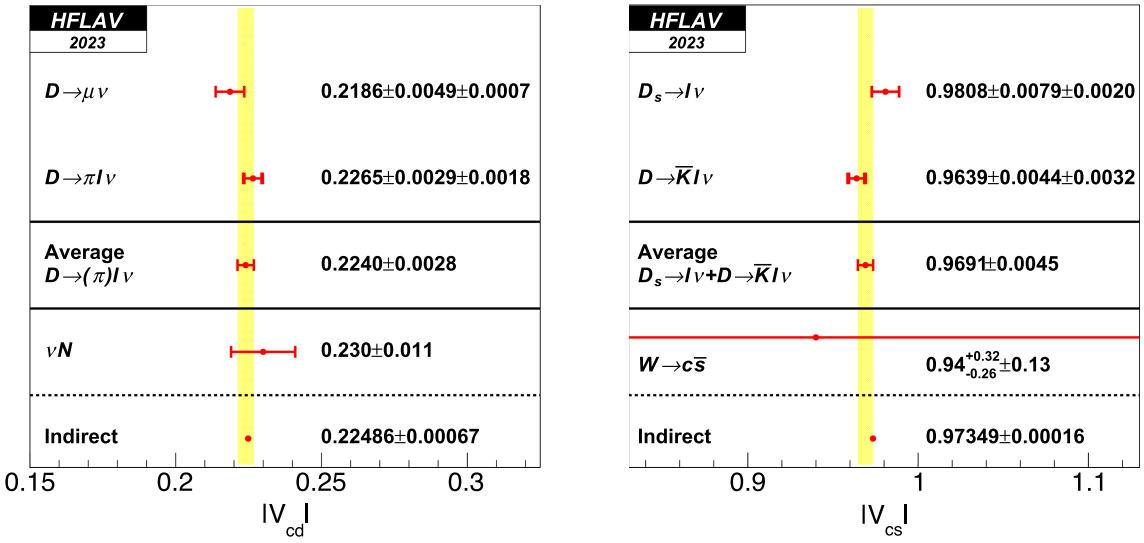


FIG. 53. Comparison of magnitudes of CKM matrix elements $|V_{cd}|$ (left) and $|V_{cs}|$ (right), as determined from leptonic and semileptonic $D_{(s)}$ decays. Also listed are results from neutrino scattering, from W decays, and from a global fit of the CKM matrix assuming unitarity [1315].

uncertainties with that obtained from a global fit assuming CKM unitarity [1315].

5. Extraction of $D_{(s)}$ meson decay constants

As listed in Table 278 (and plotted in Fig. 53), the values of $|V_{cs}|$ and $|V_{cd}|$ can be determined from a global fit of the CKM matrix assuming unitarity [1315]. These values can be used to extract the D^+ and D_s^+ decay constants from the world average values of $f_D|V_{cd}|$ and $f_{D_s}|V_{cs}|$ given in Eqs. (209) and (217). The results are

$$f_D^{\rm exp} = (206.0 \pm 4.7)\ \text{MeV}, \tag{219}$$

$$f_{D_s}^{\rm exp} = (251.8 \pm 2.0)\ \text{MeV}, \tag{220}$$

and the ratio of the decay constants is

$$\frac{f_{D_s}^{\rm exp}}{f_D^{\rm exp}} = 1.223 \pm 0.030. \tag{221}$$

These values are in agreement within their uncertainties with the LQCD values given by FLAG [Eqs. (201)–(203)].

C. Hadronic D^0 decays and final state radiation

Measurements of the branching fractions for the decays $D^0 \to K^{\mp}\pi^{\pm}$, $D^0 \to \pi^+\pi^-$, and $D^0 \to K^+K^-$ have reached sufficient precision to allow averages with $\mathcal{O}(1\%)$ relative uncertainties. At this precision, QED final state radiation (FSR) must be treated correctly and consistently across the input measurements for the accuracy of the averages to match the precision. The sensitivity of measurements to FSR arises because of a tail in the distribution of radiated energy that extends to the kinematic limit. The tail beyond $\sum E_\gamma \approx 30$ MeV causes typical selection variables like the hadronic invariant mass to shift outside the selection range dictated by experimental resolution, as shown in Fig. 54. While the differential rate for the tail is small, the integrated rate amounts to several percent of the total $h^+h^-(n\gamma)$ rate because of the tail's extent. The tail therefore translates directly into a several percent loss in experimental efficiency.

All measurements that include an FSR correction have a correction based on the use of PHOTOS [1316–1320] within the experiment's Monte Carlo (MC) simulation. PHOTOS itself, however, has evolved over the period spanning the set of measurements [1319]. In particular, the incorporation of interference between radiation from the two separate mesons has proceeded in stages: it was first available for particle-antiparticle pairs in version 2.00 (1993), extended to any two-body, all-charged, final states in version 2.02 (1999), and further extended to multi-body final states in version 2.15 (2005). The effects of interference are clearly visible, as shown in Fig. 54, and cause a roughly 30% increase in the integrated rate into the high

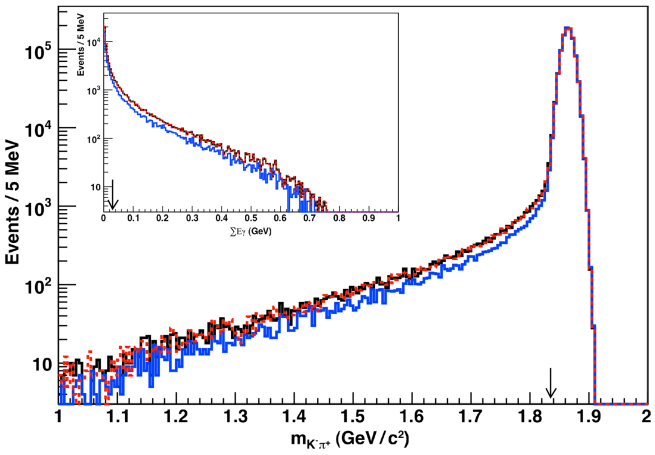


FIG. 54. The $K\pi$ invariant mass distribution for equally-sized samples of $D^0 \to K^-\pi^+(n\gamma)$ decays. The three curves correspond to three different configurations of PHOTOS for modeling FSR: version 2.02 without interference (blue/gray), version 2.02 with interference (red dashed) and version 2.15 with interference (black). The true invariant mass has been smeared with a typical experimental resolution of 10 MeV/c^2. Inset: The corresponding spectrum of total energy radiated per event. The arrow indicates the $\sum E_\gamma$ value that begins to shift kinematic quantities outside of the range typically accepted in a measurement.

energy photon tail. To evaluate the FSR correction incorporated into a given measurement, we must therefore note whether any correction was made, the version of PHOTOS used in correction, and whether the interference terms in PHOTOS were turned on. Also worth noting, an exponentiated multiple-photon mode was introduced in PHOTOS version 2.09, which allows PHOTOS to also simulate photons with low energies; this mode can be switched on or off.

1. Updates to the branching fractions

Before averaging the measured branching fractions, the published results are updated, as necessary, to the FSR prediction of PHOTOS 2.15 with interference included and exponentiated multiple-photon mode turned on. The update will always shift a branching fraction to a higher value: with no FSR correction or an FSR correction suboptimally modeled, the experimental efficiency determination will be biased high, and therefore the branching fraction will be biased low.

Most of the branching fraction analyses used the kinematic quantity sensitive to FSR in the candidate selection criteria. For the analyses at the $\psi(3770)$, this variable was ΔE, the difference between the candidate D^0 energy and the beam energy (e.g., $E_K + E_\pi - E_{\rm beam}$ for $D^0 \to K^-\pi^+$). In the remainder of the analyses, the relevant quantity was the reconstructed hadronic two-body mass $m_{h^+h^-}$. To make an FSR correction, we need to evaluate the fraction of decays that FSR moves outside of the range accepted for the analysis. The corrections were evaluated

using an event generator (EVTGEN [1321,1322]) that incorporates PHOTOS to simulate the portions of the decay process most relevant to the correction.

We compared corrections determined both with and without smearing to account for experimental resolution; for the analyses using $m_{h^+h^-}$ as the kinematic quantity sensitive to FSR, the differences were negligible, typically of $\mathcal{O}(1\%)$ of the correction itself. The immunity of the correction to resolution effects comes about because most of the long FSR-induced tail in the $m_{h^+h^-}$ distribution resides well away from the selection boundaries. The smearing from resolution, on the other hand, mainly affects the distribution of events right at the boundary. For the analyses using ΔE however, events with low energy photons are found to substantially move events across the selection boundary; thus PHOTOS versions with exponentiated multiple-photon mode turned on and off, respectively, can give substantially different FSR corrections. In the case that this mode is on, smearing of the events with low energy photons increases the amount of the FSR correction by about 10%. This is well within the uncertainty on the FSR correction, as discussed later in this section, and thus ignored.

For measurements incorporating an FSR correction that did not include interference and/or use exponentiated multiple-photon mode, we update by assessing the FSR-induced efficiency loss for both the PHOTOS version and configuration used in the analysis and our nominal version 2.15 (with interference included and exponentiated multiple-photon mode turned on). For measurements that published their sensitivity to FSR, our generator-level predictions for the original efficiency loss agreed to within a few percent of the correction. This agreement lends additional credence to the procedure.

Once the event loss from FSR in the most sensitive kinematic quantity is accounted for, the event loss in other quantities is typically very small. For example, analyses using D^{*+} tags show very little sensitivity to FSR in the reconstructed $D^{*+} - D^0$ mass difference, i.e., in $m_{h^+h^-\pi^+} - m_{h^+h^-}$. In this case, the effect of FSR tends to cancel in the difference of reconstructed masses. In the $\psi(3770)$ analyses, the beam-constrained mass distributions (e.g. $\sqrt{E^2_{\rm beam} - |\vec{p}_K + \vec{p}_\pi|^2}$) have some sensitivity, but provide negligible independent sensitivity after the ΔE selection.

The FOCUS [1323] analysis of the branching fraction ratios $\mathcal{B}(D^0 \to \pi^+\pi^-)/\mathcal{B}(D^0 \to K^-\pi^+)$ and $\mathcal{B}(D^0 \to K^+K^-)/\mathcal{B}(D^0 \to K^-\pi^+)$ obtained yields using fits to the two-body mass distributions. FSR will both distort the low end of the signal mass peak, and will contribute a signal component to the low side tail used to estimate the background. The fitting procedure is not sensitive to signal events out in the FSR tail, which would be counted as part of the background.

A more complex toy MC procedure was required to analyze the effect of FSR on the fitted yields, which were published with no FSR corrections applied. Determining the update involved an iterative procedure in which samples of similar size to the FOCUS sample were generated and then fit using the FOCUS signal and background parametrizations. The MC parametrizations were tuned based on differences between the fits to the toy MC data and the FOCUS fits, and the procedure was repeated. These steps were iterated until the fit parameters matched the original FOCUS parameters.

The toy MC samples for the first iteration were based on the generator-level distributions of $m_{K^-\pi^+}$, $m_{\pi^+\pi^-}$, and $m_{K^+K^-}$, including the effects of FSR, smeared according to the original FOCUS resolution function, and on backgrounds generated using the parametrization from the final FOCUS fits. For each iteration, 400 to 1600 individual data-sized samples were generated and fit. The central values of the parameters from these fits determined the corrections to the generator parameters for the following iteration. The ratio between the number of signal events generated and the final signal yield provides the required FSR correction in the final iteration. Only a few iterations were required in each mode. Figure 55 shows the FOCUS data, the published FOCUS fits, and the final toy MC parametrizations. The toy MC provides an excellent description of the data.

The corrections obtained to the individual FOCUS yields were 1.0298 ± 0.0001 for $K^-\pi^+$, 1.062 ± 0.001 for $\pi^+\pi^-$, and 1.0183 ± 0.0003 for K^+K^-. These corrections tend to cancel in the branching ratios, leading to corrections (update shifts) of 1.031 ± 0.001 (3.10%) for $\mathcal{B}(D^0 \to \pi^+\pi^-)/\mathcal{B}(D^0 \to K^-\pi^+)$, and 0.9888 ± 0.0003 (-1.12%) for $\mathcal{B}(D^0 \to K^+K^-)/\mathcal{B}(D^0 \to K^-\pi^+)$.

Table 279 summarizes the updated branching fractions. The published FSR-related modeling uncertainties have been replaced with a new, common estimate; this estimate is based on the assumption that the dominant uncertainty in the FSR corrections comes from the fact that the mesons are treated as structureless particles. No contributions from structure-dependent terms in the decay process (e.g., radiation from individual quarks) are included in PHOTOS. Internal studies performed by various experiments (reconstructing decays including FSR photons) have indicated that in $K\pi$ decays, the PHOTOS corrections agree with data at the 20%–30% level. We therefore attribute a 25% uncertainty to the (updated) FSR correction from potential structure-dependent contributions. For the other two modes, the only difference in structure is the final state valence quark content. While radiative corrections typically enter with a $1/M$ dependence, the additional contribution from the structure terms enters on a timescale shorter than the hadronization timescale. Thus, this contribution corresponds to $M \sim \Lambda_{\rm QCD}$ rather than that of the quark masses and would be the same for all three modes. We make this assumption when treating the correlations among measurements. We also assume that the PHOTOS amplitudes and any missing structure amplitudes interfere constructively.

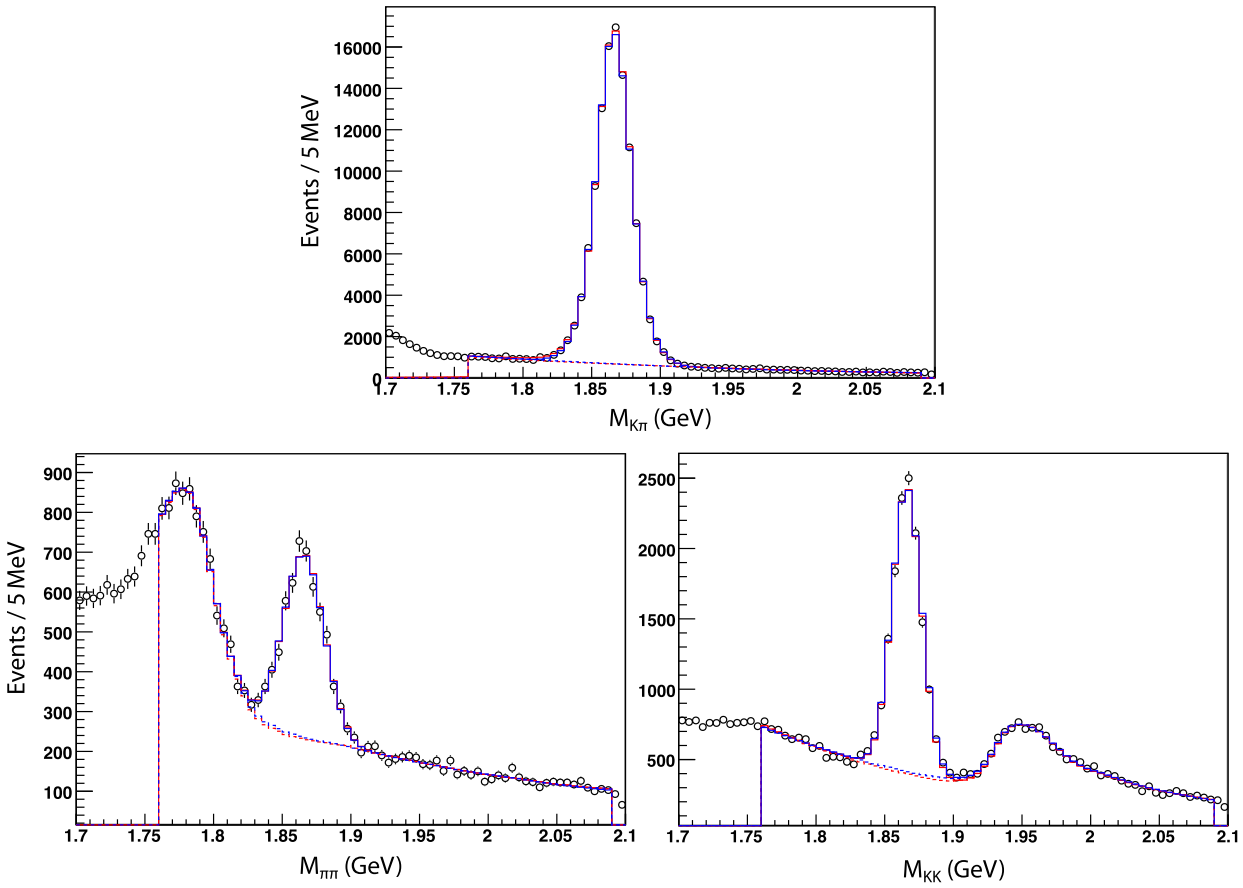


FIG. 55. FOCUS data (dots), original fits (blue) and toy MC parametrization (red) for $D^0 \to K^-\pi^+$ (top), $D^0 \to \pi^+\pi^-$ (bottom left), and $D^0 \to \pi^+\pi^-$ (bottom right).

The uncertainties largely cancel in the branching fraction ratios. For the final average branching fractions, the FSR uncertainty on $K\pi$ is as large as the uncertainty due to other systematic effects. Note that because of the relative sizes of FSR in the different modes, the $\pi\pi/K\pi$ branching ratio uncertainty from FSR is positively correlated with that for the $K\pi$ branching fraction, while the $KK/K\pi$ branching ratio FSR uncertainty is negatively correlated.

The $\mathcal{B}(D^0 \to K^-\pi^+)$ measurement of Ref. [1332] (CLEO II), the $\mathcal{B}(D^0 \to \pi^+\pi^-)/\mathcal{B}(D^0 \to K^-\pi^+)$ measurements of Refs. [1171] (E791) and [1088] (CLEO II.V), and the $\mathcal{B}(D^0 \to K^+K^-)/\mathcal{B}(D^0 \to K^-\pi^+)$ measurement of Ref. [1088] are excluded from the branching fraction averages presented here. These measurements appear not to have incorporated any FSR corrections, and insufficient information is available to determine the 2%–3% update shifts that would be required.

2. Average branching fractions for $D^0 \to K^-\pi^+$, $D^0 \to \pi^+\pi^-$ and $D^0 \to K^+K^-$

The average branching fractions for $D^0 \to K^-\pi^+$, $D^0 \to \pi^+\pi^-$ and $D^0 \to K^+K^-$ decays are obtained from a single χ^2 minimization procedure, in which the three branching fractions are floating parameters and the measurements listed in Table 279 are the inputs. The central values are obtained from a fit in which the full covariance matrix, accounting for all statistical, systematic (excluding FSR), and FSR measurement uncertainties, is used. Table 280 presents the correlation matrix for this nominal fit. We then obtain the three reported uncertainties on those central values as follows: The statistical uncertainties are obtained from a fit using only the statistical covariance matrix. The systematic uncertainties are obtained by subtracting (in quadrature) the statistical uncertainties from the uncertainties determined via a fit using a covariance matrix that accounts for both statistical and systematic measurement uncertainties. The FSR uncertainties are obtained by subtracting (in quadrature) the uncertainties determined via a fit using a covariance matrix that accounts for both statistical and systematic measurement uncertainties from the uncertainties determined via the fit using the full covariance matrix.

In forming the full covariance matrix, the FSR uncertainties are treated as fully correlated (or anti-correlated) as described above. For the covariance matrices involving systematic measurement uncertainties, ALEPH's systematic uncertainties in the θ_{D^*} parameter are treated as fully

TABLE 279. The experimental measurements relating to $\mathcal{B}(D^0 \to K^-\pi^+)$, $\mathcal{B}(D^0 \to \pi^+\pi^-)$, and $\mathcal{B}(D^0 \to K^+K^-)$ after updating them to the common version and configuration of PHOTOS. The uncertainties are statistical and total systematic, with the FSR-related systematic estimated in this procedure shown in parentheses. Also listed are the percent shifts in the results from those with the original correction (if any), in the case an update is applied here, as well as the original PHOTOS and interference configuration for each publication.

Experiment (acronym)	Result (rescaled)	Update shift	PHOTOS
$D^0 \to K^-\pi^+$			
BESIII 18 (BE18) [1324]	$3.931 \pm 0.006 \pm 0.067(44)\%$	1.25	2.03/Yes
CLEO-c 14 (CC14) [1149]	$3.934 \pm 0.021 \pm 0.061(31)\%$	⋯	2.15/Yes
BABAR 07 (BA07) [1325]	$4.035 \pm 0.037 \pm 0.074(24)\%$	0.69	2.02/No
CLEO II 98 (CL98) [1326]	$3.917 \pm 0.154 \pm 0.167(27)\%$	2.80	None
ALEPH 97 (AL97) [1327]	$3.931 \pm 0.091 \pm 0.124(27)\%$	0.79	2.0/No
ARGUS 94 (AR94) [1328]	$3.490 \pm 0.123 \pm 0.287(20)\%$	2.33	None
CLEO II 93 (CL93) [1329]	$3.965 \pm 0.080 \pm 0.171(13)\%$	0.38	2.0/No
ALEPH 91 (AL91) [1330]	$3.733 \pm 0.351 \pm 0.455(28)\%$	3.12	None
$D^0 \to \pi^+\pi^-$			
BESIII 18 [1324]	$0.1529 \pm 0.0018 \pm 0.0032(23)\%$	1.39	2.03/Yes
$D^0 \to \pi^+\pi^-/D^0 \to K^-\pi^+$			
CLEO-c 10 (CC10) [1146]	$0.0370 \pm 0.0006 \pm 0.0009(02)$	⋯	2.15/Yes
CDF 05 (CD05) [1331]	$0.03594 \pm 0.00054 \pm 0.00043(15)$	⋯	2.15/Yes
FOCUS 02 (FO02) [1323]	$0.0364 \pm 0.0012 \pm 0.0006(02)$	3.10	None
$D^0 \to K^+K^-$			
BESIII 18 [1324]	$0.4271 \pm 0.0021 \pm 0.0069(27)\%$	0.89	2.03/Yes
$D^0 \to K^+K^-/D^0 \to K^-\pi^+$			
CLEO-c 10 [1146]	$0.1041 \pm 0.0011 \pm 0.0012(03)$	⋯	2.15/Yes
CDF 05 [1331]	$0.0992 \pm 0.0011 \pm 0.0012(01)$	⋯	2.15/Yes
FOCUS 02 [1323]	$0.0982 \pm 0.0014 \pm 0.0014(01)$	−1.12	None

correlated between the ALEPH 97 and ALEPH 91 measurements. Similarly, the tracking efficiency uncertainties in the CLEO II 98 and the CLEO II 93 measurements are treated as fully correlated. For the three BESIII 18 results, both tracking and particle identification efficiencies for any particles shared between decay modes are treated as fully correlated. Finally, the BESIII 18 results also have a fully correlated statistical dependence on the number of $D^0\bar{D}^0$ pairs produced.

The averaging procedure results in a final χ^2 of 36.0 for 13 $(16-3)$ degrees of freedom (p-value $= 5.9 \times 10^{-4}$). The branching fractions obtained are

$$\mathcal{B}(D^0 \to K^-\pi^+) = (3.999 \pm 0.006 \pm 0.031 \pm 0.032)\%, \tag{222}$$

$$\mathcal{B}(D^0 \to \pi^+\pi^-) = (0.1490 \pm 0.0012 \pm 0.0015 \pm 0.0019)\%, \tag{223}$$

$$\mathcal{B}(D^0 \to K^+K^-) = (0.4113 \pm 0.0017 \pm 0.0041 \pm 0.0025)\%. \tag{224}$$

The uncertainties, estimated as described above, are statistical, systematic (excluding FSR), and FSR modeling. The correlation coefficients from the fit using the total uncertainties are

	$K^-\pi^+$	$\pi^+\pi^-$	K^+K^-
$K^-\pi^+$	1.00	0.77	0.76
$\pi^+\pi^-$	0.77	1.00	0.58
K^+K^-	0.76	0.58	1.00

These results are explained in detail as follows. As Fig. 56 shows, the average value for $\mathcal{B}(D^0 \to K^-\pi^+)$ and the input branching fractions agree very well. For the $\mathcal{B}(D^0 \to K^-\pi^+)$ measurements only, the partial χ^2 is 4.9 in the final fit. With the estimated uncertainty in the FSR modeling used here, the FSR uncertainty dominates the statistical uncertainty in the average, suggesting that experimental work in the near future should focus on verification of FSR with $\sum E_\gamma \gtrsim 100$ MeV. Note that the systematic uncertainty excluding FSR has now approached the level of the FSR uncertainty; in the most precise

TABLE 280. The correlation matrix corresponding to the full covariance matrix. Subscripts $h \in \{\pi, K\}$ denote which of the $D^0 \to h^+h^-$ decay results from a single experiment is represented in that row or column.

	BE18	CC14	BA07	CL98	AL97	AR94	CL93	AL91	$BE18_\pi$	$CC10_\pi$	$CD05_\pi$	$FO02_\pi$	$BE18_K$	$CC10_K$	$CD05_K$	$FO02_K$
BE18	1.0000	0.3143	0.1897	0.0777	0.1148	0.0419	0.0450	0.0319	0.6534	0.0930	0.1401	0.0948	0.5839	−0.1153	−0.0437	−0.0259
CC14	0.3143	1.0000	0.1394	0.0571	0.0844	0.0308	0.0331	0.0234	0.3023	0.0683	0.1029	0.0697	0.1788	−0.0847	−0.0321	−0.0191
BA07	0.1897	0.1394	1.0000	0.0345	0.0509	0.0186	0.0200	0.0141	0.1825	0.0413	0.0621	0.0421	0.1079	−0.0511	−0.0194	−0.0115
CL98	0.0777	0.0571	0.0345	1.0000	0.0209	0.0076	0.0082	0.0058	0.0748	0.0169	0.0255	0.0172	0.0442	−0.0209	−0.0079	−0.0047
AL97	0.1148	0.0844	0.0509	0.0209	1.0000	0.0112	0.0121	0.1156	0.1104	0.0250	0.0376	0.0254	0.0653	−0.0309	−0.0117	−0.0070
AR94	0.0419	0.0308	0.0186	0.0076	0.0112	1.0000	0.0044	0.0031	0.0403	0.0091	0.0137	0.0093	0.0238	−0.0113	−0.0043	−0.0025
CL93	0.0450	0.0331	0.0200	0.0082	0.0121	0.0044	1.0000	0.0034	0.0433	0.0098	0.0147	0.0100	0.0256	−0.0121	−0.0046	−0.0027
AL91	0.0319	0.0234	0.0141	0.0058	0.1156	0.0031	0.0034	1.0000	0.0306	0.0069	0.0104	0.0071	0.0181	−0.0086	−0.0033	−0.0019
$BE18_\pi$	0.6534	0.3023	0.1825	0.0748	0.1104	0.0403	0.0433	0.0306	1.0000	0.0895	0.1347	0.0912	0.4334	−0.1109	−0.0421	−0.0249
$CC10_\pi$	0.0930	0.0683	0.0413	0.0169	0.0250	0.0091	0.0098	0.0069	0.0895	1.0000	0.0305	0.0206	0.0529	−0.0251	−0.0095	−0.0056
$CD05_\pi$	0.1401	0.1029	0.0621	0.0255	0.0376	0.0137	0.0147	0.0104	0.1347	0.0305	1.0000	0.0310	0.0797	−0.0378	−0.0143	−0.0085
$FO02_\pi$	0.0948	0.0697	0.0421	0.0172	0.0254	0.0093	0.0100	0.0071	0.0912	0.0206	0.0310	1.0000	0.0539	−0.0255	−0.0097	−0.0057
$BE18_K$	0.5839	0.1788	0.1079	0.0442	0.0653	0.0238	0.0256	0.0181	0.4334	0.0529	0.0797	0.0539	1.0000	−0.0656	−0.0249	−0.0148
$CC10_K$	−0.1153	−0.0847	−0.0511	−0.0209	−0.0309	−0.0113	−0.0121	−0.0086	−0.1109	−0.0251	−0.0378	−0.0255	−0.0656	1.0000	0.0118	0.0070
$CD05_K$	−0.0437	−0.0321	−0.0194	−0.0079	−0.0117	−0.0043	−0.0046	−0.0033	−0.0421	−0.0095	−0.0143	−0.0097	−0.0249	0.0118	1.0000	0.0027
$FO02_K$	−0.0259	−0.0191	−0.0115	−0.0047	−0.0070	−0.0025	−0.0027	−0.0019	−0.0249	−0.0056	−0.0085	−0.0057	−0.0148	0.0070	0.0027	1.0000

measurements of these branching fractions, the competing uncertainty is the uncertainty on the tracking efficiency.

The $\mathcal{B}(D^0 \to K^+K^-)$ and $\mathcal{B}(D^0 \to \pi^+\pi^-)$ measurements inferred from the branching ratio measurements do not agree as well (Fig. 57). There is some tension among the results when all measurements related to $\mathcal{B}(D^0 \to K^+K^-)$ and $\mathcal{B}(D^0 \to \pi^+\pi^-)$ are included in the average together. For the measurements related to $\mathcal{B}(D^0 \to K^+K^-)$ [$\mathcal{B}(D^0 \to \pi^+\pi^-)$] only, the partial χ^2 is 15.7 [6.0] in the final fit.

The $\mathcal{B}(D^0 \to K^-\pi^+)$ average obtained here is approximately two standard deviations higher than the PDG 2023 update average [302]. Table 281 shows the evolution from a fit similar to the PDG fit (no FSR updates or correlations, Ref. [1332] included) to the average presented here. There are three main contributions to the difference. The branching fraction in Ref. [1332] is low, and its exclusion shifts the result upward. A subsequently larger shift (+0.035%) is due to the FSR updates, which as expected shift the result upward. The largest shift (+0.050%) occurs as all of the measurements related to $\mathcal{B}(D^0 \to K^+K^-)$ and $\mathcal{B}(D^0 \to \pi^+\pi^-)$ are included in the average together with the $\mathcal{B}(D^0 \to K^-\pi^+)$ measurements.

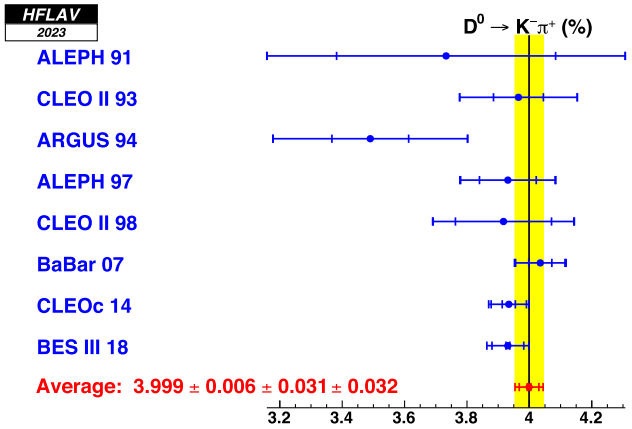


FIG. 56. Comparison of measurements of $\mathcal{B}(D^0 \to K^-\pi^+)$ (blue) with the average branching fraction obtained here (red and yellow band). For these measurements only, the partial χ^2 is 4.9 in the final fit.

3. Average branching fraction for $D^0 \to K^+\pi^-$

There is no reason to presume that the effects of FSR should be different in $D^0 \to K^+\pi^-$ and $D^0 \to K^-\pi^+$ decays, as both decay to one charged kaon and one charged pion; indeed, for the same version of PHOTOS the FSR simulations of these decays are identical. Measurements of the relative branching fraction ratio between the doubly Cabibbo-suppressed decay $D^0 \to K^+\pi^-$ and the Cabibbo-favored decay $D^0 \to K^-\pi^+$ (R_D, determined in Sec. IX A) have now approached $\mathcal{O}(1\%)$ relative uncertainties. This makes it worthwhile to combine our R_D average with the $\mathcal{B}(D^0 \to K^-\pi^+)$ average obtained in Eq. (222), to provide a measurement of the branching fraction

$$\mathcal{B}(D^0 \to K^+\pi^-) = (1.376 \pm 0.017) \times 10^{-4}. \quad (225)$$

Note that, by definition of R_D, these branching fractions do not include any contribution from Cabibbo-favored $\bar{D}^0 \to K^+\pi^-$ decays. Our result is more precise than the PDG 2023 value of $(1.363 \pm 0.025) \times 10^{-4}$ [302] due to our using a more precise value for the ratio R_D (obtained from a global fit to a range of mixing data, see Sec. IX A).

4. Consideration of PHOTOS++

The versions of PHOTOS that existing measurements were performed with are now well over a decade out of

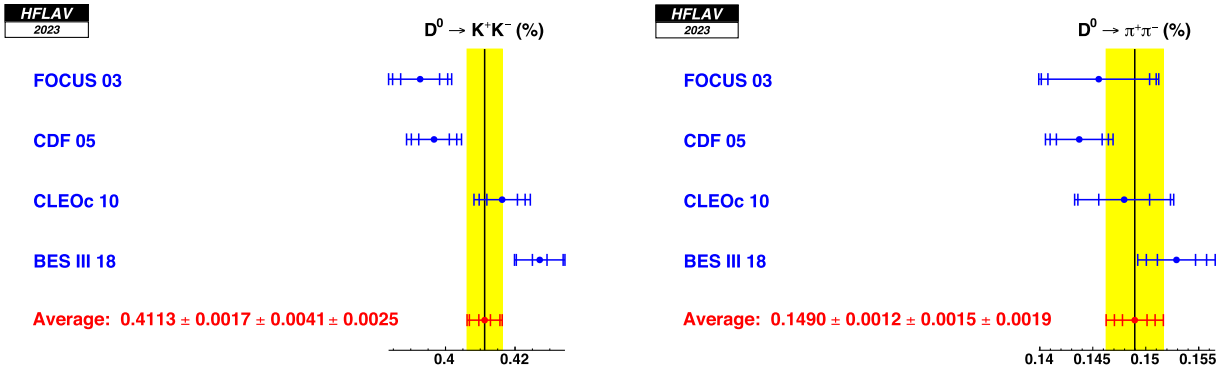


FIG. 57. The $\mathcal{B}(D^0 \to K^+K^-)$ (left) and $\mathcal{B}(D^0 \to \pi^+\pi^-)$ (right) values obtained either from absolute measurements or by scaling the measured branching ratios with the $\mathcal{B}(D^0 \to K^-\pi^+)$ branching fraction average obtained here. For the measurements (blue points), the error bars correspond to the statistical, systematic and either the $K\pi$ normalization uncertainties or, in case of an absolute measurement, the FSR modeling uncertainty. The average obtained here (red point, yellow band) lists the statistical, systematics excluding FSR, and the FSR systematic. For the measurements related to $\mathcal{B}(D^0 \to K^+K^-)$ [$\mathcal{B}(D^0 \to \pi^+\pi^-)$] only, the partial χ^2 is 15.7 [6.0] in the final fit.

date. The newest version, PHOTOS++ 3.61 [1333], is now fully based on C++ instead of the original FORTRAN. None of the measurements used in our branching fraction averages use PHOTOS++, so we have not yet undertaken an effort to update all results to this newest version. However, at this time it is worth continuing our procedure to evaluate whether there is any continued low bias in the branching fractions, due to sub-optimal modeling of FSR.

We find that the FSR spectra for PHOTOS 2.15, with interference included and exponentiated multiple-photon mode turned on, and PHOTOS++ (in its default mode) are compatible. The distributions of $m_{K\pi}$ for simulated D mesons from $B \to D^*X$ decays produced at $\Upsilon(4S)$ threshold are nearly identical. As an example, the *BABAR* 07 selection criteria were applied to decays simulated with PHOTOS++ and our nominal version of PHOTOS 2.15; both produce identical FSR corrections to within 0.01%.

The distributions of ΔE for simulated D mesons produced at $\psi(3770)$ threshold also are nearly identical. As an example, for the BESIII 18 $D^0 \to K^-\pi^+$, $D^0 \to \pi^+\pi^-$, and $D^0 \to K^+K^-$ branching fraction results, the additional update shifts required to correct from our nominal version of PHOTOS 2.15 to PHOTOS++ are less than or equal to 0.02%. However, if smearing is applied with the BESIII 18 ΔE resolution, while the update for $D^0 \to K^-\pi^+$ remains negligible, the update shifts for $D^0 \to \pi^+\pi^-$ and $D^0 \to K^+K^-$ are modest at −0.25% and 0.19%, respectively; this level of shifts are well within the systematic uncertainty of our averages.

D. Excited $D_{(s)}$ mesons

Excited "open" charm mesons have received increased attention since the first observation of low mass, narrow D_{sJ} states that were inconsistent with QCD predictions [1334–1337]. Their properties can be measured in both prompt analyses as well as in amplitude analyses of multi-body B decays. Tables 282–284 summarize the measurements of masses and widths of excited D and D_s states. If a preferred assignment of spin and parity was measured, it is listed in the column J^P, where the label "natural" denotes $P = (-1)^J$ $(J^P = 0^+, 1^-, 2^+ \ldots)$ and "unnatural" denotes $P = (-1)^{J+1}$ $(J^P = 0^-, 1^+, 2^- \ldots)$. In some studies, it was possible to identify only whether the

TABLE 281. Evolution of the $D^0 \to K^-\pi^+$ branching fraction from a fit with no FSR updates or correlations (similar to the average in the PDG 2023 update [302]) to the nominal fit presented here.

Modes fit	Description	$\mathcal{B}(D^0 \to K^-\pi^+)$ (%)	χ^2/(deg. of freedom)
$K^-\pi^+$	PDG 2023 [302] equivalent	$3.910 \pm 0.006 \pm 0.033$	$5.1/(9-1) = 0.64$
$K^-\pi^+$	drop Ref. [1332]	$3.913 \pm 0.006 \pm 0.033$	$5.1/(8-1) = 0.73$
$K^-\pi^+$	add FSR updates	$3.948 \pm 0.006 \pm 0.032 \pm 0.019$	$3.5/(8-1) = 0.50$
$K^-\pi^+$	add FSR correlations	$3.949 \pm 0.006 \pm 0.032 \pm 0.033$	$3.7/(8-1) = 0.53$
all	add CLEO-c, CDF, and FOCUS h^+h^-	$3.956 \pm 0.006 \pm 0.032 \pm 0.033$	$11.1/(14-3) = 1.01$
all	add BESIII h^+h^-	$3.999 \pm 0.006 \pm 0.031 \pm 0.032$	$36.0/(16-3) = 2.77$

state has natural or unnatural spin-parity, but not the values of the quantum numbers.

For states in which multiple measurements are available, an average mass and width are calculated; these are listed in the gray shaded rows. For simplicity, when calculating averages we neglect possible correlations among individual measurements. All averaged masses and widths are summarized in Fig. 58. The resonances listed in the tables and figures are as they appear in the respective publications. In some cases, it is unclear whether separately listed states are in fact distinct or are the same resonance. An example is the $D_1^*(2680)^0$ state [1351], which has parameters close to those of the $D^*(2650)^0$. Further measurements are needed to resolve these ambiguities. Additionally, subsequent measurements can change the average value such as to change the relative masses of states, which may be in contradiction with the naming. An example is the $D_1(2430)^0$ state, whose average mass has been lowered by the latest LHCb measurement [1340] to become smaller than the average mass of the $D_1(2420)$ states.

The masses and widths of narrow ($\Gamma < 50$ MeV) orbitally excited D mesons (1P states), both neutral and charged, are well-established. Measurements of broad states ($\Gamma \sim 200$–400 MeV) are less abundant, as identifying the signal is more challenging. The measured masses and widths, as well as the J^P values, are in agreement with theoretical predictions based on potential models [304,1368–1370]. Following precise measurements from LHCb, recent studies based on unitarized chiral perturbation theory and lattice QCD propose a two-pole structure of the $D^*(2300)^0$ and predict the existence of a lighter state $D^*(2100)^0$ [312,314].

The spectroscopic assignment of heavier states remains less clear. Further theoretical studies taking into account the experimentally observed mesons suggest the identity of some 2S and 1D states [1371,1372] and tentatively discuss possible 1F, 3S and 2P states. Possible new states to be found in the future were suggested in Refs. [1372,1373]. In the region around 3000 MeV, the state $D_2^*(3000)^0$ has been observed by LHCb [1351] and is explained as potentially a 2P or 1F state [1374]. A pseudoscalar state $D(2900)$ is predicted in this region along with its decay channels [1375], laying out the path for further experimental investigations.

Tables 285–287 summarize the branching fractions of B meson decays to excited D and D_s states, respectively. The measurements listed are the products of the B meson branching fraction and the daughter D meson branching fraction. It is notable that the branching fractions for B mesons decaying to a narrow D^* state and a pion are similar for charged and neutral B initial states, while the branching fractions to a broad D^* state and π^+ are much larger for B^+ than for B^0. This may be due to the fact that color-suppressed amplitudes contribute only to the B^+ decay and not to the B^0 decay (for a theoretical discussion, see Refs. [1376,1377]). Values for the branching fractions of the D mesons are difficult to extract due to the unknown (and difficult to calculate) $B \to D^* X$ branching fractions. Recently, BESIII produced the first absolute branching fraction measurement of $D_{s0}^*(2317)^- \to D_s^- \pi^0$ [1356].

The discoveries of the $D_{s0}^*(2317)^\pm$ and $D_{s1}(2460)^\pm$ have triggered increased interest in properties of, and searches for, excited D_s mesons. While the masses and widths of the $D_{s1}(2536)^\pm$ and $D_{s2}^*(2573)^\pm$ states are in relatively good agreement with potential model predictions, the masses of the $D_{s0}^*(2317)^\pm$ and $D_{s1}(2460)^\pm$ states are significantly lower than expected (see Ref. [1381] for a discussion of $c\bar{s}$ models). Moreover, the mass splitting between these two states greatly exceeds that between the $D_{s1}(2536)^\pm$ and $D_{s2}(2573)^\pm$. The internal structure of the $D_{s0}^*(2317)^\pm$ and $D_{s1}(2460)^\pm$ remains a subject of intense study to this date. The unexpected properties have led to interpretations as exotic four-quark states [1382,1383]. A molecule-like (DK) interpretation of these states [1382,1383] that can account for their low masses and isospin-breaking decay modes, or a mixture or molecular and $c\bar{s}$ states, are among the most prominent models in recent works [1384–1389]. A study of the states in an unquenched quark model shows that the best match is a model with a DK component around 53% [1390]. Searches for charged and neutral isospin partners of these states have so far yielded negative results. A crucial tool to test the molecular picture is also measuring the partial decay widths, particularly isospin-breaking hadronic decays which would have a much larger width in a hadronic molecule approach. Another prominent test would be measuring rates for the radiative processes $D_{s0}^*(2317)^\pm / D_{s1}(2460)^\pm \to D_s^{(*)}\gamma$ and comparing to theoretical predictions. The predicted rates, however, are below the sensitivity of current experiments. A step toward this recent goal is the branching fraction measurement of $D_{s0}^*(2317)^- \to D_s^- \pi^0$ by BESIII [1356]. A study of the transition $D_{s1}(2460)^+ \to D_s^+ \pi^+ \pi^-$ indicates that in a molecular scenario, the $\pi^+\pi^-$ invariant mass would show a double bump structure which is not present in a compact state scenario [1388], thus offering another potentially discriminating variable for experimental studies. Future measurements with more statistics are expected to shed further light on the topic of a molecular interpretation.

Another model successful in explaining the total widths and the $D_{s0}^*(2317)^\pm - D_{s1}(2460)^\pm$ mass splitting is based on the assumption that these states are chiral partners of the ground states D_s^+ and D_s^* [1391]. While some measured branching fraction ratios agree with predicted values, further experimental tests with better sensitivity are needed to confirm or refute this scenario. A summary of the mass difference measurements is given in Table 288.

Measurements by *BABAR* [1394] and LHCb [1395] first indicated the existence of the $D_{sJ}^*(2860)^\pm$ meson. An LHCb study of $B_s^0 \to \bar{D}^0 K^- \pi^+$ decays, in which they

TABLE 282. Measurements of masses and widths for excited D mesons. The column J^P lists the assignment of spin and parity. If possible, an average mass or width is calculated. Table 1 of 2.

Resonance	J^P	Decay mode	Mass [MeV/c^2]	Width [MeV]	Measured by	References
$D_0^*(2300)^0$	0^+	$D^+\pi^-$	$2297 \pm 8 \pm 20$	$273 \pm 12 \pm 48$	*BABAR*	[585]
		$D^+\pi^-$	$2308 \pm 17 \pm 32$	$276 \pm 21 \pm 63$	Belle	[586]
		$D^+\pi^-$	$2407 \pm 21 \pm 35$	$240 \pm 55 \pm 59$	FOCUS	[1338]
			2318.2 ± 16.9	267.4 ± 35.6	Our average	
$D_0^*(2300)^\pm$	0^+	$D^0\pi^+$	$2360 \pm 15 \pm 12 \pm 28$	$255 \pm 26 \pm 20 \pm 47$	LHCb	[1339]
		$D^0\pi^+$	$2349 \pm 6 \pm 1 \pm 4$	$217 \pm 13 \pm 5 \pm 12$	LHCb	[454]
		$D^0\pi^+$	$2403 \pm 14 \pm 35$	$283 \pm 24 \pm 34$	FOCUS(m & Γ) + Belle(J^P)	[455]
			2351.3 ± 7.0	229.9 ± 16.1	Our average	
$D_1(2420)^0$	1^+	$D^{*+}\pi^-$	$2424.8 \pm 0.1 \pm 0.7$	$33.6 \pm 0.3 \pm 2.7$	LHCb	[1340]
		$D^{*+}\pi^-$	$2419.6 \pm 0.1 \pm 0.7$	$35.2 \pm 0.4 \pm 0.9$	LHCb	[1341]
		$D^{*+}\pi^-$	$2423.1 \pm 1.5^{+0.4}_{-0.7}$	$38.8 \pm 5^{+1.9}_{-5.4}$	ZEUS	[1342]
		$D^{*+}\pi^-$	$2420.1 \pm 0.1 \pm 0.8$	$31.4 \pm 0.5 \pm 1.3$	*BABAR*	[1343]
		$D^{*+}\pi^-$		$20 \pm 1.7 \pm 1.3$	CDF	[1344]
		$D^{*+}\pi^-$	$2421.4 \pm 1.5 \pm 0.9$	$23.7 \pm 2.7 \pm 4$	Belle	[586]
		$D^0\pi^+\pi^-$	$2426 \pm 3 \pm 1$	$24 \pm 7 \pm 8$	Belle	[476]
		$D^{*+}\pi^-$	$2421^{+1}_{-2} \pm 2$	$20^{+6}_{-5} \pm 3$	CLEO	[1345]
		$D^{*+}\pi^-$	$2422 \pm 2 \pm 2$	$15 \pm 8 \pm 4$	E387	[1346]
		$D^{*+}\pi^-$	$2414 \pm 2 \pm 5$	$13 \pm 6^{+10}_{-5}$	ARGUS	[1347]
		$D^{*+}\pi^-$	$2428 \pm 3 \pm 2$	23^{+8+10}_{-6-4}	CLEO	[1348]
		$D^{*+}\pi^-$	$2428 \pm 8 \pm 5$	$58 \pm 14 \pm 20$	TPS	[1349]
			2421.8 ± 0.4	31.8 ± 0.7	Our average	
$D_1(2420)^\pm$	1^+	$D^{*0}\pi^+$	$2421.9 \pm 4.7^{+3.4}_{-1.2}$		ZEUS	[1342]
		$D^+\pi^-\pi^+$	$2421 \pm 2 \pm 1$	$21 \pm 5 \pm 8$	Belle	[476]
		$D^{*0}\pi^+$	$2425 \pm 2 \pm 2$	$26^{+8}_{-7} \pm 4$	CLEO	[1350]
		$D^{*0}\pi^+$	$2443 \pm 7 \pm 5$	$41 \pm 19 \pm 8$	TPS	[1349]
			2423.2 ± 1.6	25.0 ± 6.0	Our average	
$D_1(2430)^0$	1^+	$D^{*+}\pi^-$	$2411 \pm 3 \pm 9$	$309 \pm 9 \pm 28$	LHCb	[1340]
		$D^{*+}\pi^-$	$2427 \pm 26 \pm 25$	$384^{+107}_{-75} \pm 74$	Belle	[586]
			2412.0 ± 9.2	312.6 ± 28.6	Our average	
$D_2^*(2460)^0$	2^+	$D^+\pi^-$	$2463.7 \pm 0.4 \pm 0.4 \pm 0.6$	$47 \pm 0.8 \pm 0.9 \pm 0.3$	LHCb	[1351]
		$D^+\pi^-$	$2460.4 \pm 0.1 \pm 0.1$	$45.6 \pm 0.4 \pm 1.1$	LHCb	[1341]
		$D^{*+}\pi^-$	$2464 \pm 1.4 \pm 0.5 \pm 0.2$	$43.8 \pm 2.9 \pm 1.7 \pm 0.6$	LHCb	[590]
		$D^{*+}\pi^-$, $D^+\pi^-$	$2462.5 \pm 2.4^{+1.3}_{-1.1}$	$46.6 \pm 8.1^{+5.9}_{-3.8}$	ZEUS	[1342]
		$D^+\pi^-$	$2462.2 \pm 0.1 \pm 0.8$	$50.5 \pm 0.6 \pm 0.7$	*BABAR*	[1343]
		$D^+\pi^-$	$2460.4 \pm 1.2 \pm 2.2$	$41.8 \pm 2.5 \pm 2.9$	*BABAR*	[585]
		$D^+\pi^-$		$49.2 \pm 2.3 \pm 1.3$	CDF	[1344]
		$D^+\pi^-$	$2461.6 \pm 2.1 \pm 3.3$	$45.6 \pm 4.4 \pm 6.7$	Belle	[586]
		$D^+\pi^-$	$2464.5 \pm 1.1 \pm 1.9$	$38.7 \pm 5.3 \pm 2.9$	FOCUS	[1338]
		$D^+\pi^-$	$2465 \pm 3 \pm 3$	$28^{+8}_{-7} \pm 6$	CLEO	[1345]
		$D^+\pi^-$	$2455 \pm 3 \pm 5$	15^{+13+5}_{-10-10}	ARGUS	[1352]
		$D^+\pi^-$	$2459 \pm 3 \pm 2$	$20 \pm 10 \pm 5$	TPS	[1349]
		$D^{*+}\pi^-$	$2461 \pm 3 \pm 1$	$20^{+9\ +9}_{-12-10}$	CLEO	[1348]
			$2453 \pm 3 \pm 2$	$25 \pm 10 \pm 5$	E687	[1346]
			2460.6 ± 0.1	47.6 ± 0.6	Our average	

TABLE 283. Measurements of masses and widths for excited D mesons. The column J^P lists the assignment of spin and parity. If possible, an average mass or width is calculated. Table 2 of 2.

Resonance	J^P	Decay mode	Mass [MeV/c^2]	Width [MeV]	Measured by	References
$D_2^*(2460)^\pm$	2^+	$D^0\pi^+$	$2463.1 \pm 0.2 \pm 0.6$	$48.6 \pm 1.3 \pm 1.9$	LHCb	[1341]
		$D^0\pi^+$	$2465.6 \pm 1.8 \pm 0.5 \pm 1.2$	$46 \pm 3.4 \pm 1.4 \pm 2.9$	LHCb	[1339]
		$D^0\pi^+$	$2468.6 \pm 0.6 \pm 0.0 \pm 0.3$	$47.3 \pm 1.5 \pm 0.3 \pm 0.6$	LHCb	[454]
		$D^{*0}\pi^+$, $D^0\pi^+$	$2460.6 \pm 4.4^{+3.6}_{-0.8}$		ZEUS	[1342]
		$D^0\pi^+$	$2465.4 \pm 0.2 \pm 1.1$		*BABAR*	[1343]
		$D^0\pi^+$	$2465.7 \pm 1.8^{+1.4}_{-4.8}$	$49.7 \pm 3.8 \pm 6.4$	Belle	[445]
		$D^0\pi^+$	$2467.6 \pm 1.5 \pm 0.8$	$34.1 \pm 6.5 \pm 4.2$	FOCUS	[1338]
		$D^0\pi^+$	$2463 \pm 3 \pm 3$	$27^{+11}_{-8} \pm 5$	CLEO	[1350]
		$D^0\pi^+$	$2453 \pm 3 \pm 2$	$23 \pm 9 \pm 5$	E687	[1346]
		$D^0\pi^+$	$2469 \pm 4 \pm 6$		ARGUS	[1353]
			2465.6 ± 0.4	46.7 ± 1.2	Our average	
$D(2550)^0$	0^-	$D^{*+}\pi^-$	$2518 \pm 2 \pm 7$	$199 \pm 5 \pm 17$	LHCb	[1340]
		$D^{*+}\pi^-$	$2539.4 \pm 4.5 \pm 6.8$	$130 \pm 12 \pm 13$	*BABAR*	[1343]
			2527.5 ± 5.4	164.4 ± 12.5	Our average	
$D(2580)^0$	Unnatural	$D^{*+}\pi^-$	$2579.5 \pm 3.4 \pm 5.5$	$117.5 \pm 17.8 \pm 46$	LHCb	[1341]
$D^*(2600)^0$	1^-	$D^{*+}\pi^-$	$2641.9 \pm 1.8 \pm 4.5$	$149 \pm 4 \pm 20$	LHCb	[1340]
		$D^+\pi^-$	$2608.7 \pm 2.4 \pm 2.5$	$93 \pm 6 \pm 13$	*BABAR*	[1343]
			2619.9 ± 2.8	111.5 ± 11.7	Our average	
$D^*(2600)^\pm$	Natural	$D^0\pi^+$	$2621.3 \pm 3.7 \pm 4.2$		*BABAR*	[1343]
$D^*(2640)^\pm$	1^-	$D^{*+}\pi^+\pi^-$	$2637.0 \pm 2 \pm 6$		Delphi	[1354]
$D^*(2650)^0$	Natural	$D^{*+}\pi^-$	$2649.2 \pm 3.5 \pm 3.5$	$140.2 \pm 17.1 \pm 18.6$	LHCb	[1341]
$D^*(2680)^0$	1^-	$D^+\pi^-$	$2681.1 \pm 5.6 \pm 4.9 \pm 13.1$	$186.7 \pm 8.5 \pm 8.6 \pm 8.2$	LHCb	[1351]
$D_2(2740)^0$	2^-	$D^{*+}\pi^-$	$2751 \pm 3 \pm 7$	$102 \pm 6 \pm 26$	LHCb	[1340]
		$D^{*+}\pi^-$	$2737.0 \pm 3.5 \pm 11.2$	$73.2 \pm 13.4 \pm 25$	LHCb	[1341]
			2746.9 ± 6.4	88.5 ± 19.4	Our average	
$D_3^*(2750)^0$	3^-	$D^{*+}\pi^-$	$2753 \pm 4 \pm 6$	$66 \pm 10 \pm 14$	LHCb	[1340]
		$D^{*+}\pi^-$	$2752.4 \pm 1.7 \pm 2.7$	$71 \pm 6 \pm 11$	*BABAR*	[1343]
			2752.5 ± 2.9	69.3 ± 10.1	Our average	
$D^*(2760)^0$	1^-	$D^+\pi^-$	$2781 \pm 18 \pm 11 \pm 6$	$177 \pm 32 \pm 20 \pm 7$	LHCb	[590]
		$D^{*+}\pi^-$	$2761.1 \pm 5.1 \pm 6.5$	$74.4 \pm 3.4 \pm 37$	LHCb	[1341]
		$D^+\pi^-$	$2760.1 \pm 1.1 \pm 3.7$	$74.4 \pm 3.4 \pm 19.1$	LHCb	[1341]
		$D^+\pi^-$	$2763.3 \pm 2.3 \pm 2.3$	$60.9 \pm 5.1 \pm 3.6$	*BABAR*	[1343]
			2762.1 ± 2.4	65.1 ± 5.8	Our average	
$D_3^*(2760)^0$	3^-	$D^+\pi^-$	$2775.5 \pm 4.5 \pm 4.5 \pm 4.7$	$95.3 \pm 9.6 \pm 7.9 \pm 33.1$	LHCb	[1351]
$D_3^*(2760)^\pm$	3^-	$D^0\pi^+$	$2771.7 \pm 1.7 \pm 3.8$	$66.7 \pm 6.6 \pm 10.5$	LHCb	[1341]
		$D^0\pi^+$	$2798 \pm 7 \pm 1 \pm 7$	$105 \pm 18 \pm 6 \pm 23$	LHCb	[454]
		$D^0\pi^+$	$2769.7 \pm 3.8 \pm 1.5$		*BABAR*	[1343]
			2772.8 ± 2.8	72.3 ± 11.5	Our average	
$D_2^*(3000)^0$	2^+	$D^+\pi^-$	$3214 \pm 29 \pm 33 \pm 36$	$186 \pm 38 \pm 34 \pm 63$	LHCb	[1351]

TABLE 284. Measurements of masses and widths for excited D_s mesons. The column J^P lists the of spin and parity. If possible, an average mass or width is calculated.

Resonance	J^P	Decay mode	Mass [MeV/c^2]		Measured by	References
$D^*_{s0}(2317)^\pm$	0^+	$D_s^+\pi^0$	$2319.6 \pm 0.2 \pm 1.4$		*BABAR*	[1355]
		$D_s^+\pi^0$	$2317.3 \pm 0.4 \pm 0.8$		*BABAR*	[1337]
		$D_s^+\pi^0$	$2318.3 \pm 1.2 \pm 1.2$		BESIII	[1356]
			2318.0 ± 0.7		Our average	
$D_{s1}(2460)^\pm$	1^+	$D_s^{*+}\pi^0, D_s^+\pi^0\Gamma, D_s^+\Gamma, D_s^+\pi^+\pi^-$	$2460.1 \pm 0.2 \pm 0.8$		*BABAR*	[1355]
		$D_s^+\pi^0\Gamma$	$2458 \pm 1 \pm 1$		*BABAR*	[1337]
			459.6 ± 0.7		Our average	
$D_{s1}(2536)^\pm$	1^+		$2537.7 \pm 0.5 \pm 3.1$	$1.7 \pm 1.2 \pm 0.6$	BESIII	[1357]
		$D^{*+}K_S^0$		$0.92 \pm 0.03 \pm 0.04$	*BABAR*	[1358]
		$D^{*+}K_S^0$	$2535.7 \pm 0.6 \pm 0.5$		DØ	[1359]
		$D^{*+}K_S^0, D^{*0}K^+$	$2534.78 \pm 0.31 \pm 0.4$		*BABAR*	[502]
		$D_s^+\pi^+\pi^-$	$2534.6 \pm 0.3 \pm 0.7$		*BABAR*	[1355]
		$D^{*+}K_S^0, D^{*0}K^+$	$2535.0 \pm 0.6 \pm 1.0$		E687	[1346]
		$D^{*0}K^+$	$2535.3 \pm 0.2 \pm 0.5$		CLEO	[1360]
		$D^{*+}K_S^0$	$2534.8 \pm 0.6 \pm 0.6$		CLEO	[1360]
		$D^{*0}K^+$	$2535.2 \pm 0.5 \pm 1.5$		ARGUS	[1361]
		$D^{*+}K_S^0$	$2535.6 \pm 0.7 \pm 0.4$		CLEO	[1348]
		$D^{*+}K_S^0$	$2535.9 \pm 0.6 \pm 2.0$		ARGUS	[1362]
			2535.1 ± 0.3	0.9 ± 0.0	Our average	
$D^*_{s2}(2573)^\pm$	2^+		$2570.7 \pm 2.0 \pm 1.7$	$17.2 \pm 3.6 \pm 1.1$	BESIII	[1357]
		$D^0K^+, D^{*+}K_S^0$	$2568.39 \pm 0.29 \pm 0.26$	$16.9 \pm 0.5 \pm 0.6$	LHCb	[1363]
		$D^+K_S^0, D^0K^+$	$2569.4 \pm 1.6 \pm 0.5$	$12.1 \pm 4.5 \pm 1.6$	LHCb	[1364]
		$D^+K_S^0, D^0K^+$	$2572.2 \pm 0.3 \pm 1.0$	$27.1 \pm 0.6 \pm 5.6$	*BABAR*	[1365]
		D^0K^+	$2574.25 \pm 3.3 \pm 1.6$	$10.4 \pm 8.3 \pm 3.0$	ARGUS	[1366]
		D^0K^+	$2573.2^{+1.7}_{-1.6} \pm 0.9$	$16^{+5}_{-4} \pm 3$	CLEO	[1367]
			2569.1 ± 0.3	16.9 ± 0.7	Our average	
$D_{s0}(2590)^\pm$	0^-	$D^+K^+\pi^-$	$2591 \pm 6.0 \pm 7$	$89 \pm 16 \pm 12$	LHCb	[1399]
$D^*_{s1}(2700)^\pm$	1^-	$D^{*+}K_S^0, D^{*0}K^+$	$2732.3 \pm 4.3 \pm 5.8$	$136 \pm 19 \pm 34$	LHCb	[1397]
		D^0K^+	2699^{+14}_{-7}	127^{+24}_{-19}	*BABAR*	[1380]
		$D^{*+}K_S^0, D^{*0}K^+$	$2709.2 \pm 1.9 \pm 4.5$	$115.8 \pm 7.3 \pm 12.1$	LHCb	[1395]
		DK, D^*K	$2710 \pm 2^{+11}_{-10}$	$149 \pm 7^{+39}_{-52}$	*BABAR*	[1394]
		D^0K^+	$2708 \pm 9^{+11}_{-10}$	$108 \pm 2^{+36}_{-31}$	Belle	[604]
			2713.0 ± 3.5	120.9 ± 10.3	Our average	
$D^*_{s1}(2860)^\pm$	1	D^0K^+	$2859 \pm 12 \pm 24$	$159 \pm 23 \pm 77$	LHCb	[1396]
$D^*_{s2}(2860)^\pm$	3^-	$D^{*+}K_S^0, D^{*0}K^+$	$2867.1 \pm 4.3 \pm 1.9$	$50 \pm 11 \pm 13$	LHCb	[1397]
		D^0K^+	$2860.5 \pm 2.6 \pm 6.5$	$53 \pm 7 \pm 7$	LHCb	[1396]
			2865.0 ± 3.9	52.2 ± 8.6	Our average	
$D_{sJ}(3040)^\pm$	Unnatural	D^0K	3044^{+30}_{-5}	$239 \pm 35^{+46}_{-42}$	*BABAR* (m & Γ) + LHCb(J^P)	[1394]

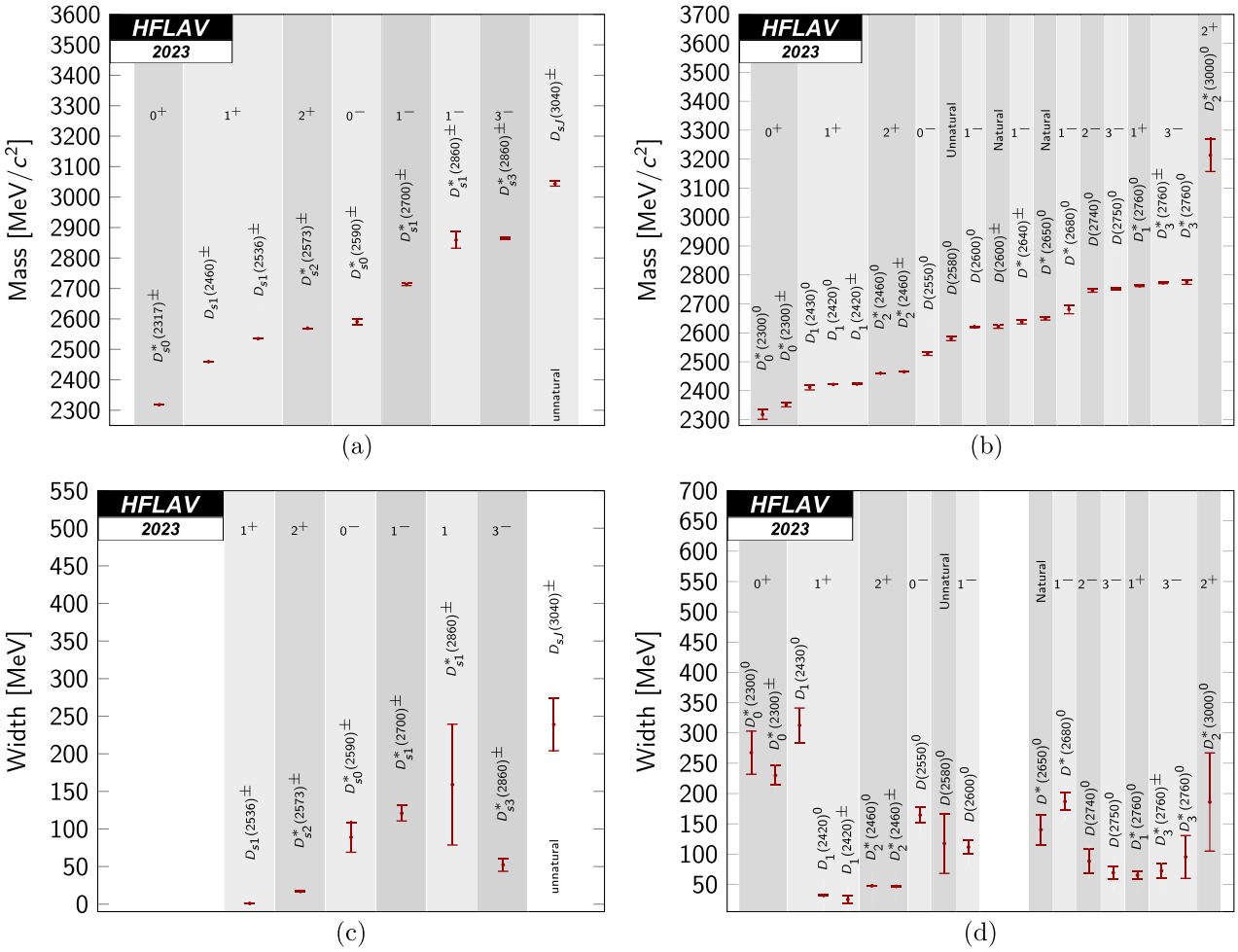


FIG. 58. (a) Average masses for excited D_s mesons; (b) average masses for excited D mesons; (c) average widths for excited D_s mesons; (d) average widths for excited D mesons. The vertical shaded regions distinguish between different spin-parity states.

searched for excited D_s mesons [1396], showed with 10σ significance that this state comprises two different particles, one of spin 1 and one of spin 3. This represents the first measurement of a heavy flavored spin-3 particle, and the first observation of B meson decays to spin-3 particles. A subsequent study of $D_{sJ}^{(*)}$ mesons by the LHCb collaboration [1397] supports the natural parity assignment for these states. This study also shows weak evidence for a further structure at a mass around 3040 MeV/c^2 with unnatural parity, which was first hinted at by a *BABAR* analysis [1394]. The second observation of a spin-3 charm meson was a subsequent LHCb analysis of $B^0 \to \bar{D}^0\pi^+\pi^-$ decays, which measured the spin-parity assignment of the state $D_3^*(2760)^\pm$ to be $J^P = 3^-$ [454]. This resonance was in fact observed previously by *BABAR* [1343] and LHCb [1341]. The measurement suggests a spectroscopic assignment of $^3D_3$. Recently, also the corresponding neutral state was observed by LHCb, the $D_3^*(2760)^0$ [1351].

Other observed excited D_s states include $D_{s1}^*(2700)^\pm$ and $D_{s2}^*(2573)^\pm$. The properties of both (mass, width, J^P) have been measured and determined in several analyses. A theoretical discussion [1398] investigates the possibility that the $D_{s1}(2700)^\pm$ could represent radial excitations of the $D_s^{*\pm}$. Similarly, the $D_{s1}^*(2860)^\pm$ and $D_{sJ}(3040)^\pm$ could be excitations of $D_{s0}^*(2317)^\pm$ and $D_{s1}(2460)^\pm$ or $D_{s1}(2536)^\pm$, respectively. The most recently discovered state is denoted as $D_{s0}(2590)^\pm$, and is a strong candidate to be the missing 2^1S_0 state, the radial excitation of the pseudoscalar ground-state D_s^+ meson [1399]. Matching newly observed states to theoretical predictions is not always trivial, as the predicted widths often heavily depend on the assumed mass. In this particular case, however, a recalculation of the width at the experimentally measured mass nevertheless remains inconclusive as to the interpretation of the $D_{s0}(2590)^\pm$ as the 2^1S_0 state [1400].

Table 289 summarizes measurements of the helicity parameter A_D (also referred to as the polarization parameter). In decays of orbitally excited charm mesons (D^{**}) to $D^*\pi$, $D^* \to D\pi$, the helicity distribution varies like $1 + A_D \cos^2\theta_H$, where θ_H is the angle in the D^* rest frame

TABLE 285. Product of the B meson branching fraction and the daughter (excited) D meson branching fraction. Table 1 of 2.

Resonance	Decay	$\mathcal{B}[10^{-4}]$	Measured by	References
$D_0^*(2300)^0$	$B^- \to D_0^*(2300)^0(\to D^+\pi^-)\pi^-$	$6.1 \pm 0.6 \pm 1.8$	Belle	[586]
		$6.8 \pm 0.3 \pm 2.0$	*BABAR*	[585]
		6.4 ± 1.4	Our average	
	$B^- \to D_0^*(2300)^0(\to D^+\pi^-)l^-\bar{\nu}_l$	$5.4 \pm 2.2 \pm 0.5$	Belle	[303]
		$26 \pm 5 \pm 4$	*BABAR*	[309]
		$24 \pm 4 \pm 6$	Belle	[1378]
		9.0 ± 2.0	Our average	
	$B^- \to D_0^*(2300)^0(\to D^+\pi^-)K^-$	$0.061 \pm 0.019 \pm 0.015$	LHCb	[590]
$D_0^*(2300)^\pm$	$\bar{B}^0 \to D_0^*(2300)^+(\to D^0\pi^+)\pi^-$	$0.77 \pm 0.05 \pm 0.06$	LHCb	[454]
		$0.60 \pm 0.13 \pm 0.27$	Belle	[445]
		0.76 ± 0.07	Our average	
	$\bar{B}^0 \to D_0^*(2300)^+(\to D^0\pi^+)l^-\bar{\nu}_l$	$44 \pm 8 \pm 6$	*BABAR*	[309]
		$20 \pm 7 \pm 5$	Belle	[1378]
		30 ± 7	Our average	
	$\bar{B}^0 \to D_0^*(2300)^+(\to D^0\pi^+)K^-$	$0.177 \pm 0.026 \pm 0.072$	LHCb	[1339]
$D_1(2420)^0$	$B^- \to D_1(2420)^0(\to D^{*+}\pi^-)\pi^-$	$6.8 \pm 0.7 \pm 1.3$	Belle	[586]
		$8.42 \pm 0.08 \pm 1.46$	LHCb	[1340]
		7.6 ± 1.0	Our average	
	$B^- \to D_1(2420)^0(\to D^0\pi^+\pi^-)\pi^-$	$1.85 \pm 0.29 \pm 0.35^{+0.0}_{-0.46}$	Belle	[476]
	$B^- \to D_1(2420)^0(\to D^{*+}\pi^-)l^-\bar{\nu}_l$	$24.9 \pm 2.3 \pm 1.4$	Belle	[303]
		$29.7 \pm 1.7 \pm 1.7$	*BABAR*	[310]
		$29 \pm 3 \pm 3$	*BABAR*	[309]
		$42 \pm 7 \pm 7$	Belle	[1378]
		28.2 ± 1.6	Our average	
	$B^- \to D_1(2420)^0(\to D^0\pi^+\pi^-)l^-\bar{\nu}_l$	$10.5 \pm 1.1 \pm 0.8$	Belle	[303]
	$\bar{B}^0 \to D_1(2420)^0(\to D^{*+}\pi^-)\omega$	$0.7 \pm 0.2^{+0.1}_{-0.0} \pm 0.1$	Belle	[450]
$D_1(2420)^\pm$	$\bar{B}^0 \to D_1(2420)^+(\to D^+\pi^-\pi^+)\pi^-$	$0.89 \pm 0.15 \pm 0.17^{+0.0}_{-0.26}$	Belle	[476]
	$\bar{B}^0 \to D_1(2420)^+(\to D^{*0}\pi^+)l^-\bar{\nu}_l$	$30.6 \pm 5.0 \pm 2.8$	Belle	[303]
		$27.8 \pm 2.4 \pm 2.5$	*BABAR*	[310]
		$27 \pm 4 \pm 3$	*BABAR*	[309]
		$54 \pm 19 \pm 9$	Belle	[1378]
		28.5 ± 2.5	Our average	
	$\bar{B}^0 \to D_1(2420)^+(\to D^+\pi^+\pi^-)l^-\bar{\nu}_l$	$10.2 \pm 1.3 \pm 0.9$	Belle	[303]
$D_1(2430)^0$	$B^- \to D_1(2430)^0(\to D^{*+}\pi^-)\pi^-$	$5.0 \pm 0.4 \pm 1.08$	Belle	[586]
		$3.51 \pm 0.06 \pm 0.61$	LHCb	[1340]
		4.5 ± 0.7	Our average	
	$\bar{B}^0 \to D_1(2430)^0(\to D^{*+}\pi^-)\omega$	$2.5 \pm 0.4^{+0.7+0.4}_{-0.2-0.1}$	Belle	[450]
	$B^- \to D_1(2430)^0(\to D^{*+}\pi^-)l^-\bar{\nu}_l$	$13.8 \pm 3.6 \pm 0.8$	Belle	[303]
		$27 \pm 4 \pm 5$	*BABAR*	[309]
		17.0 ± 3.2	Our average	

TABLE 286. Product of the B meson branching fraction and the daughter (excited) D meson branching fraction. Table 2 of 2.

Resonance	Decay	$\mathcal{B}[10^{-4}]$	Measured by	References
$D_1(2430)^{\pm}$	$\bar{B}^0 \to D_1(2430)^+(\to D^{*0}\pi^+)l^-\bar{\nu}_l$	$20.6 \pm 6.8 \pm 2.5$	Belle	[303]
		$31 \pm 7 \pm 5$	*BABAR*	[309]
		24.9 ± 5.5	Our average	
$D_2^*(2460)^0$	$B^- \to D_2^*(2460)^0(\to D^+\pi^-)\pi^-$	$3.4 \pm 0.3 \pm 0.7$	Belle	[586]
		$3.5 \pm 0.2 \pm 0.5$	*BABAR*	[585]
		$3.62 \pm 0.06 \pm 0.30$	LHCb	[1351]
		3.57 ± 0.25	Our average	
	$B^- \to D_2^*(2460)^0(\to D^{*+}\pi^-)\pi^-$	$1.8 \pm 0.3 \pm 0.4$	Belle	[586]
		$2.08 \pm 0.03 \pm 0.37$	LHCb	[1340]
		1.98 ± 0.30	Our average	
	$\bar{B}^0 \to D_2^*(2460)^0(\to D^{*+}\pi^-)\omega$	$0.4 \pm 0.1^{+0.0}_{-0.1} \pm 0.1$	Belle	[450]
	$B^- \to D_2^*(2460)^0(\to D^+\pi^-)K^-$	$0.232 \pm 0.011 \pm 0.02$	LHCb	[590]
	$B^- \to D_2^*(2460)^0(\to D^{(*)+}\pi^-)l^-\bar{\nu}_l$	$30.0 \pm 2.8 \pm 1.1$	Belle	[303]
		$22.9 \pm 2.3 \pm 2.1$	*BABAR*	[310]
		$15 \pm 2 \pm 1$	*BABAR*	[309]
		$22 \pm 3 \pm 4$	Belle	[1378]
		21.1 ± 1.5	Our average	
$D_2^*(2460)^{\pm}$	$\bar{B}^0 \to D_2^*(2460)^+(\to D^0\pi^+)\pi^-$	$2.44 \pm 0.07 \pm 0.16$	LHCb	[454]
		$2.15 \pm 0.17 \pm 0.31$	Belle	[445]
		2.38 ± 0.16	Our average	
	$\bar{B}^0 \to D_2^*(2460)^+(\to D^0\pi^+)K^-$	$0.212 \pm 0.010 \pm 0.029$	LHCb	[1339]
	$\bar{B}^0 \to D_2^*(2460)^+(\to D^0\pi^+)l^-\bar{\nu}_l$	$20.8 \pm 4.3 \pm 1.1$	Belle	[303]
		$17.7 \pm 2.6 \pm 1.1$	*BABAR*	[310]
		$7 \pm 3 \pm 1$	*BABAR*	[309]
		$22 \pm 4 \pm 4$	Belle	[1378]
		15.2 ± 1.8	Our average	
$D_0(2550)^0$	$B^- \to D_0(2550)^0(\to D^{*+}\pi^-)\pi^-$	$0.72 \pm 0.01 \pm 0.14$	LHCb	[1340]
$D_1^*(2600)^0$	$B^- \to D_1^*(2600)^0(\to D^{*+}\pi^-)\pi^-$	$0.68 \pm 0.01 \pm 0.13$	LHCb	[1340]
$D_1^*(2680)^0$	$B^- \to D_1^*(2680)^0(\to D^+\pi^-)\pi^-$	$0.84 \pm 0.06 \pm 0.20$	LHCb	[1351]
$D_2(2740)^0$	$B^- \to D_2(2740)^0(\to D^{*+}\pi^-)\pi^-$	$0.33 \pm 0.02 \pm 0.15$	LHCb	[1340]
$D_1^*(2760)^0$	$B^- \to D_1^*(2760)^0(\to D^+\pi^-)K^-$	$0.036 \pm 0.009 \pm 0.008$	LHCb	[590]
$D_3^*(2760)^0$	$\bar{B}^- \to D_3^*(2760)^0(\to D^+\pi^-)\pi^-$	$0.10 \pm 0.01 \pm 0.02$	LHCb	[1351]
	$\bar{B}^- \to D_3^*(2760)^0(\to D^{*+}\pi^-)\pi^-$	$0.11 \pm 0.01 \pm 0.03$	LHCb	[1340]
$D_3^*(2760)^{\pm}$	$\bar{B}^0 \to D_3^*(2760)^+(\to D^0\pi^+)\pi^-$	$0.103 \pm 0.016 \pm 0.011$	LHCb	[454]
$D_2^*(3000)^0$	$\bar{B}^0 \to D_2^*(3000)^0(\to D^+\pi^-)\pi^-$	$0.02 \pm 0.01 \pm 0.01$	LHCb	[1351]

TABLE 287. Product of the B meson branching fraction and the daughter (excited) D_s meson branching fraction.

Resonance	Decay	$\mathcal{B}[10^{-4}]$	Measured by	References
$D_{s0}^*(2317)^\pm$	$B^0 \to D_{s0}^*(2317)^+(\to D_s^+\pi^0)D^-$	$8.6^{+3.3}_{-2.6} \pm 2.6$	Belle	[501]
		$18.0 \pm 4.0^{+6.7}_{-5.0}$	*BABAR*	[500]
		$10.1^{+1.3}_{-1.2} \pm 1.0 \pm 0.4$	Belle	[499]
		10.2 ± 1.5	Our average	
	$B^+ \to D_{s0}^*(2317)^+(\to D_s^+\pi^0)\bar{D}^0$	$8.0^{+1.3}_{-1.2} \pm 1.0 \pm 0.4$	Belle	[499]
	$B^0 \to D_{s0}^*(2317)^+(\to D_s^+\pi^0)K^-$	$0.53^{+0.15}_{-0.13} \pm 0.16$	Belle	[477]
$D_{s1}(2460)^\pm$	$B^0 \to D_{s1}(2460)^+(\to D_s^{*+}\pi^0)D^-$	$22.7^{+7.3}_{-6.2} \pm 6.8$	Belle	[501]
		$28.0 \pm 8.0^{+11.2}_{-7.8}$	*BABAR*	[500]
		24.7 ± 7.6	Our average	
	$B^0 \to D_{s1}(2460)^+(\to D_s^{*+}\gamma)D^-$	$8.2^{+2.2}_{-1.9} \pm 2.5$	Belle	[501]
		$8.0 \pm 2.0^{+3.2}_{-2.3}$	*BABAR*	[500]
		8.1 ± 2.3	Our average	
	$D_{s1}(2460)^+ \to D_s^{*+}\pi^0$	$(56 \pm 13 \pm 9)\%$	*BABAR*	[495]
	$D_{s1}(2460)^+ \to D_s^{*+}\gamma$	$(16 \pm 4 \pm 3)\%$	*BABAR*	[495]
$D_{s1}(2536)^\pm$	$B^0 \to D_{s1}(2536)^+(\to D^*(2007)^0\mathrm{K}^+)K^-$	$0.051 \pm 0.002 \pm 0.006$	LHCb	[1379]
	$B^0 \to D_{s1}(2536)^+(\to D^{*0}K^+)D^-$	$1.71 \pm 0.48 \pm 0.32$	*BABAR*	[502]
	$B^0 \to D_{s1}(2536)^+(\to D^{*+}K^0)D^-$	$2.61 \pm 1.03 \pm 0.31$	*BABAR*	[502]
	$B^0 \to D_{s1}(2536)^+(\to D^{*0}K^+)D^{*-}$	$3.32 \pm 0.88 \pm 0.66$	*BABAR*	[502]
	$B^0 \to D_{s1}(2536)^+(\to D^{*+}K^0)D^{*-}$	$5.00 \pm 1.51 \pm 0.67$	*BABAR*	[502]
	$B_s^0 \to D_{s1}(2536)^+(\to D^*(2007)^0\mathrm{K}^+)K^-$	$0.249 \pm 0.011 \pm 0.028$	LHCb	[1379]
	$B^+ \to D_{s1}(2536)^+(\to D^{*0}K^+)\bar{D}^0$	$2.16 \pm 0.52 \pm 0.45$	*BABAR*	[502]
	$B^+ \to D_{s1}(2536)^+(\to D^{*+}K^0)\bar{D}^0$	$2.30 \pm 0.98 \pm 0.43$	*BABAR*	[502]
	$B^+ \to D_{s1}(2536)^+(\to D^{*0}K^+)\bar{D}^{*0}$	$5.46 \pm 1.17 \pm 1.04$	*BABAR*	[502]
	$B^+ \to D_{s1}(2536)^+(\to D^{*+}K^0)\bar{D}^{*0}$	$3.92 \pm 2.46 \pm 0.83$	*BABAR*	[502]
$D_{s2}^*(2573)^\pm$	$B^0 \to D_{s2}^*(2573)(\to D^0K^+)D^-$	$0.34 \pm 0.17 \pm 0.05$	*BABAR*	[1380]
	$B^+ \to D_{s2}^*(2573)(\to D^0K^+)\bar{D}^0$	$0.08 \pm 14 \pm 0.05$	*BABAR*	[1380]
$D_{s1}{}^*(2700)^\pm$	$B^+ \to D_{s1}{}^*(2700)^+(\to D^0K^+)\bar{D}^0$	$11.3 \pm 2.2^{+1.4}_{-2.8}$	Belle	[604]
		$5.02 \pm 0.71 \pm 0.93$	*BABAR*	[1380]
		5.83 ± 1.09	Our average	
	$B^0 \to D_{s1^*}(2700)^+(\to D^0K^+)D^-$	$7.14 \pm 0.96 \pm 0.69$	*BABAR*	[1380]

TABLE 288. Measurements of mass differences for excited D mesons.

Resonance	Relative to	Δm [MeV/c^2]	Measured by	Reference
$D_1^*(2420)^0$	D^{*+}	$410.2 \pm 2.1 \pm 0.9$	ZEUS	[1392]
		$411.7 \pm 0.7 \pm 0.4$	CDF	[1344]
		411.5 ± 0.8	Our average	
$D_1(2420)^{\pm}$	$D_1^*(2420)^0$	$4^{+2}_{-3} \pm 3$	CLEO	[1350]
$D_2^*(2460)^0$	D^+	$593.9 \pm 0.6 \pm 0.5$	CDF	[1344]
	D^{*+}	$458.8 \pm 3.7^{+1.2}_{-1.3}$	ZEUS	[1392]
$D_2^*(2460)^{\pm}$	$D_2^*(2460)^0$	$3.1 \pm 1.9 \pm 0.9$	FOCUS	[1338]
		$-2 \pm 4 \pm 4$	CLEO	[1350]
		$14 \pm 5 \pm 8$	ARGUS	[1353]
		3.0 ± 1.9	Our average	
$D_{s0}^*(2317)^{\pm}$	$D_s^{\pm}$	$348.7 \pm 0.5 \pm 0.7$	Belle	[1336]
		$350.0 \pm 1.2 \pm 1.0$	CLEO	[1335]
		$351.3 \pm 2.1 \pm 1.9$	Belle	[501]
		346.2 ± 0.7	Our average	
$D_{s1}(2460)^{\pm}$	$D_s^{*\pm}$	$344.1 \pm 1.3 \pm 1.1$	Belle	[1336]
		$351.2 \pm 1.7 \pm 1.0$	CLEO	[1335]
		$346.8 \pm 1.6 \pm 1.9$	Belle	[501]
		347.1 ± 1.1	Our average	
	$D_s^{\pm}$	$491.0 \pm 1.3 \pm 1.9$	Belle	[1336]
		$491.4 \pm 0.9 \pm 1.5$	Belle	[1336]
		491.3 ± 1.4	Our average	
$D_{s1}(2536)^{\pm}$	$D^*(2010)^{\pm}$	$524.83 \pm 0.01 \pm 0.04$	*BABAR*	[1358]
		$525.30^{+0.44}_{-0.41} \pm 0.10$	ZEUS	[1392]
		$525.3 \pm 0.6 \pm 0.1$	ALEPH	[1393]
		524.84 ± 0.04	Our average	
	$D^*(2007)^0$	$528.7 \pm 1.9 \pm 0.5$	ALEPH	[1393]
$D_{s2}^*(2573)^{\pm}$	D^0	$704 \pm 3 \pm 1$	ALEPH	[1393]

between the two pions emitted by the decays $D^{**} \to D^*\pi$ and $D^* \to D\pi$. The parameter is sensitive to possible S-wave contributions in the decay. In the case of a D meson decaying purely via D-wave, the helicity parameter is predicted to give $A_D = 3$. Studies of the $D_1(2420)^0$ meson by the ZEUS and *BABAR* collaborations suggest that there is an S-wave admixture in the decay, which is contrary to the expectation based on heavy quark effective theory [266,1401].

E. Excited charmed baryons

In this section we summarize the present status of excited charmed baryons decaying strongly or electromagnetically. We list their masses (or the mass difference between the excited baryon and the corresponding ground state), natural widths, decay modes, and assigned quantum numbers. The present ground-state measurements are: $M(\Lambda_c^+) = (2286.46 \pm 0.14)$ MeV/c^2 measured by *BABAR* [1402], $M(\Xi_c^0) = (2470.90^{+0.22}_{-0.29})$ MeV/c^2 and

TABLE 289. Measurements of polarization amplitudes for excited D mesons.

Resonance	A_D	Measured by	References
$D_1(2420)^0$	$7.8^{+6.7+4.6}_{-2.7-1.8}$	ZEUS	[1342]
	5.72 ± 0.25	*BABAR*	[1343]
	$5.9^{+3.0+2.4}_{-1.7-1.0}$	ZEUS	[1392]
	$3.8 \pm 0.6 \pm 0.8$	*BABAR*	[310]
	5.61 ± 0.24	Our average	
$D_1(2420)^{\pm}$	$3.8 \pm 0.6 \pm 0.8$	*BABAR*	[310]
$D_2^*(2460)^0$	-1.16 ± 0.35 (stat.)	ZEUS	[1342]
$D(2750)^0$	-0.33 ± 0.28 (stat.)	*BABAR*	[1343]

$M(\Xi_c^+) = (2467.94^{+0.17}_{-0.20})$ MeV/c^2, both dominated by CDF [147], and $M(\Omega_c^0) = (2695.2 \pm 1.7)$ MeV/c^2, dominated by Belle [1403]. Should these values change, so will many of the values for the masses of the excited states.

Table 290 summarizes the excited Λ_c^+ baryons. The first two states listed, namely the $\Lambda_c(2595)^+$ and $\Lambda_c(2625)^+$, are well-established. The measured masses and decay patterns suggest that they are orbitally excited Λ_c^+ baryons with total angular momentum of the light quarks $L = 1$. Thus their quantum numbers are assigned to be $J^P = \frac{1}{2}^-$ and $J^P = \frac{3}{2}^-$, respectively. Their mass measurements are dominated by CDF [1404]: $M(\Lambda_c(2595)^+) = (2592.25 \pm 0.28)$ MeV/c^2 and $M(\Lambda_c(2625)^+) = (2628.11 \pm 0.19)$ MeV/c^2. Earlier measurements did not fully take into account the restricted phase-space of the $\Lambda_c(2595)^+$ decays.

The next two states, $\Lambda_c(2765)^+$ and $\Lambda_c(2880)^+$, were discovered by CLEO [1405] in the $\Lambda_c^+\pi^+\pi^-$ final state. CLEO found that a significant fraction of the $\Lambda_c(2880)^+$ decays proceeds via an intermediate $\Sigma_c(2445)^{++,0}\pi^{-,+}$. Later, *BABAR* [1406] observed that this state has also a D^0p decay mode. This was the first example of an excited charmed baryon decaying into a charm meson plus a baryon; previously all excited charmed baryons were found via hadronic transitions into lower lying charmed baryons. In the same analysis, *BABAR* observed for the first time an additional state, $\Lambda_c(2940)^+$, decaying into D^0p. Studying the D^+p final state, *BABAR* found no signal and this implies that the $\Lambda_c(2880)^+$ and $\Lambda_c(2940)^+$ are Λ_c^+ excited states rather than Σ_c excitations. Belle reported the result of an angular analysis that favors 5/2 for the $\Lambda_c(2880)^+$ spin hypothesis [1407]. Moreover, the measured ratio of branching fractions $\mathcal{B}(\Lambda_c(2880)^+ \to \Sigma_c(2520)\pi^{\pm})/\mathcal{B}(\Lambda_c(2880)^+ \to \Sigma_c(2455)\pi^{\pm}) = 0.225 \pm 0.062 \pm 0.025$, combined with theoretical predictions based on HQS [304,1408], favor even parity. However this prediction is only valid if the P-wave portion of $\Sigma_c(2520)\pi$ is suppressed. LHCb [700] have analyzed the D^0p system in the resonant substructure of Λ_b decays. They confirm the $\frac{5}{2}^+$ identification of the $\Lambda_c(2880)^+$. In addition they find evidence for a further, wider, state they name the $\Lambda_c(2860)^+$, with $J^P = \frac{3}{2}^+$ (the parity is measured with respect to that of the $\Lambda_c(2880)^+$). The explanation for these states in the heavy quark-light diquark model is that they are a pair of orbital D-wave excitations. Furthermore, LHCb [700] find evidence for the spin-parity of the $\Lambda_c(2940)^+$ to be $\frac{3}{2}^-$, and improve the world average measurements of both the mass and width of this particle.

The Belle analysis that measured the $\Lambda_c(2880)$ spin [1407] also showed a statistically significant excess in the $\Sigma_c\pi$ mass distribution between the $\Lambda_c(2880)$ and $\Lambda_c(2940)$ states. Further information was lacking until 2022 when Belle analyzed the decay $B \to \Sigma_c\pi p$ [1409]. Here in the $\Sigma_c\pi$ mass spectrum, no signals for the $\Lambda_c(2880)$ or $\Lambda_c(2940)$ resonances were observed, but a large, wide peak spanning the region and centered at a mass of

TABLE 290. Summary of excited Λ_c^+ baryons. The uncertainties are the total of the statistical and systematic uncertainties.

Charmed baryon excited state	Mode	Mass (MeV/c^2)	Natural width (MeV)	J^P
$\Lambda_c(2595)^+$	$\Lambda_c^+\pi^+\pi^-$, $\Sigma_c(2455)\pi$	2592.25 ± 0.28	2.59 ± 0.57	$\frac{1}{2}^-$
$\Lambda_c(2625)^+$	$\Lambda_c^+\pi^+\pi^-$	2628.11 ± 0.19	< 0.97	$\frac{3}{2}^-$
$\Lambda_c(2765)^+$	$\Lambda_c^+\pi^+\pi^-$, $\Sigma_c(2455)\pi$	2766.6 ± 2.4	50	?
$\Lambda_c(2860)^+$	D^0p	$2856.1^{+2.3}_{-5.6}$	$67.6^{+11.8}_{-21.6}$	$\frac{3}{2}^+$
$\Lambda_c(2880)^+$	$\Lambda_c^+\pi^+\pi^-$, $\Sigma_c(2455)\pi$, $\Sigma_c(2520)\pi$, D^0p	2881.63 ± 0.24	$5.6^{+11.3}_{-10.0}$	$\frac{5}{2}^+$
$\Lambda_c(2910)^+$	$\Sigma_c(2455)\pi$,	$2913.8 \pm 5.6 \pm 3.8$	$51.8 \pm 20.3 \pm 18.8$	?
$\Lambda_c(2940)^+$	D^0p, $\Sigma_c(2455)\pi$	$2939.6^{+1.3}_{-1.5}$	20^{+6}_{-5}	?

TABLE 291. Summary of the excited $\Sigma_c^{++,+,0}$ baryon family. The mass difference is given with respect to the Λ_c^+.

Charmed baryon excited state	Mode	Mass Difference (MeV/c^2)	Natural width (MeV)	J^P
$\Sigma_c(2455)^{++}$	$\Lambda_c^+\pi^+$	167.510 ± 0.17	$1.89^{+0.09}_{-0.18}$	$\frac{1}{2}^+$
$\Sigma_c(2455)^{+}$	$\Lambda_c^+\pi^0$	166.4 ± 0.4	< 4.6 @ 90% CL	$\frac{1}{2}^+$
$\Sigma_c(2455)^{0}$	$\Lambda_c^+\pi^-$	167.29 ± 0.17	$1.83^{+0.11}_{-0.19}$	$\frac{1}{2}^+$
$\Sigma_c(2520)^{++}$	$\Lambda_c^+\pi^+$	$231.95^{+0.17}_{-0.12}$	$14.78^{+0.30}_{-0.40}$	$\frac{3}{2}^+$
$\Sigma_c(2520)^{+}$	$\Lambda_c^+\pi^0$	231.0 ± 2.3	< 17 @ 90% CL	$\frac{3}{2}^+$
$\Sigma_c(2520)^{0}$	$\Lambda_c^+\pi^-$	$232.02^{+0.15}_{-0.14}$	$15.3^{+0.4}_{-0.5}$	$\frac{3}{2}^+$
$\Sigma_c(2800)^{++}$	$\Lambda_c^+\pi^+$	514^{+4}_{-6}	75^{+22}_{-17}	$\frac{3}{2}^-$?
$\Sigma_c(2800)^{+}$	$\Lambda_c^+\pi^0$	505^{+15}_{-5}	62^{+64}_{-44}	
$\Sigma_c(2800)^{0}$	$\Lambda_c^+\pi^-$	519^{+5}_{-7}	72^{+22}_{-15}	
	$\Lambda_c^+\pi^-$	560 ± 13	86^{+33}_{-22}	

2910 MeV/c^2. They conjecture that this peak could be due to a $J^P = \frac{1}{2}^-$, $2P$ state. However, we must also be aware that this could be the overlap of two or more particles as has been seen in Ξ_c production from B decays, and it is clearly an area that requires more investigation.

A current open question concerns the nature of the $\Lambda_c(2765)^+$ state. However, it has now been experimentally shown by Belle [1410] to be a Λ_c rather than a Σ_c, and implicit in this analysis is that the data can be explained by one resonance. The state has also been observed, but not measured, by LHCb [1411].

Table 291 summarizes the excited $\Sigma_c^{++,+,0}$ baryons. The ground state isotriplets of $\Sigma_c(2455)^{++,+,0}$ and $\Sigma_c(2520)^{++,+,0}$ baryons are well-established. Belle [1412] precisely measured the mass differences and widths of the doubly charged and neutral members of this triplet. The short list of excited Σ_c baryons is completed by the triplet of $\Sigma_c(2800)$ states observed by Belle [1413]. Based on the measured masses and theoretical predictions [1414,1415], these states are thought by some to be members of the predicted $\Sigma_{c2}\,\frac{3}{2}^-$ triplet, where the subscript 2 refers to the total spin of the light quark degrees of freedom. From a study of resonant substructure in $B^- \to \Lambda_c^+ \bar{p}\pi^-$ decays, *BABAR* found a significant signal in the $\Lambda_c^+\pi^-$ final state with a mean value higher than measured for the $\Sigma_c(2800)$ by Belle by about 3σ (Table 291). The decay widths measured by Belle and *BABAR* are consistent, but it is an open question if the observed state is the same as the Belle state. It is possible that the present excesses will prove to be due to two or more overlapping states. Circumstantial evidence for this can be found by comparing with the Ξ_c and Ω_c states of similar excitation energies.

Table 292 summarizes the excited $\Xi_c^{+,0}$. The list of excited Ξ_c baryons has many states, of unknown quantum numbers, having masses above 2900 MeV/c^2 and decaying through three different types of modes: $\Lambda_c K n\pi$ or $\Sigma_c K n\pi$, $\Xi_c n\pi$, and ΛD. Some of these states ($\Xi_c(2970)^+$, $\Xi_c(3055)$ and $\Xi_c(3080)^{+,0}$) have been observed by both Belle [1416–1418] and *BABAR* [561], are produced in the charm continuum, and are considered well-established. Recently LHCb [1419] reported three narrow states in $\Lambda_c^+ K^-$. The masses of two of these states, named the $\Xi_c(2923)$ and $\Xi_c(2939)$ bookend the already discovered, wide $\Xi_c(2930)^0$. This latter state, also decaying into $\Lambda_c^+ K^-$, was found in B decays by *BABAR* [1420]. It was also observed by Belle [634], who in addition observed a similar charged state. Table 292 shows the parameters measured by Belle, who allow for interference and other possible resonances in their analysis. However, given the low statistics of these observations in e^+e^- annihilation, it seems likely that the LHCb data explains the peaks found by Belle and *BABAR* as the manifestation of the two states seen by LHCb overlapping, and thus there are no distinct $\Xi_c(2930)$ states. They are thus not included in Table 292.

LHCb [1419] note that there may well be a fourth resonance at a lower mass of ≈2880 MeV/c^2. This was then confirmed, albeit still with low statistical precision, in a subsequent LHCb paper [1421] using low statistics decays from B decays. The authors note that the pattern of masses of these states bears a remarkable similarity to that of the excited Ω_c masses, implying the same underlying spin-structure of the quarks. The highest mass of the LHCb Ω_c quintuplet does not appear to have an analogous state here. This state had the lowest signal of the five in the LHCb data and was not confirmed by Belle, so this may imply that it is of a completely different nature to the other four. Alternatively there may exist an equivalent state in the excited $\Lambda_c^+ K^-$ data but it cannot be seen because of its large width and alternative decay modes. The highest-mass of the new Ξ_c states reported by LHCb is very close in mass to the $\Xi_c(2970)$; formerly named by the PDG as the $\Xi_c(2980)$. A recent analysis by Belle [1422] reveals that the favored spin-parity of this state is $J^P = \frac{1}{2}^+$, which corresponds to it being a (2S) radial excitation. The $\Xi_c(2765)$ and $\Xi_c(2970)$ properties seem to differ by enough to be able to say with reasonable confidence that they are completely different states, though the confusion due to their similar masses might help explain the poor consistency of the historical measurements of the $\Xi_c(2970)$. The properties of the $\Xi_c(2970)$ can be seen to have similarities to the $\Lambda_c(2765)$, not only in its mass difference with respect to the ground state, but also its decay pattern and large production cross-section in e^+e^- annihilation data. This strengthens the confidence in their identification as Roper-like resonances [1423], that is, as the charmed

TABLE 292. Summary of excited $\Xi_c^{+,0}$ states. For the first four isodoublets, it is the mass difference with respect to the ground state to which they decay that is quoted as this avoids uncertainties in the ground state masses. For the remaining cases, the uncertainty on the measurement of the excited state itself dominates.

Charmed baryon excited state	Mode	Mass difference (MeV/c^2)	Natural width (MeV)	J^P
$\Xi_c'^+$	$\Xi_c^+\gamma$	110.5 ± 0.4		$\frac{1}{2}^+$
$\Xi_c'^0$	$\Xi_c^0\gamma$	108.3 ± 0.4		$\frac{1}{2}^+$
$\Xi_c(2645)^+$	$\Xi_c^0\pi^+$	174.7 ± 0.1	2.1 ± 0.2	$\frac{3}{2}^+$
$\Xi_c(2645)^0$	$\Xi_c^+\pi^-$	178.5 ± 0.1	2.4 ± 0.2	$\frac{3}{2}^+$
$\Xi_c(2790)^+$	$\Xi_c'^0\pi^+$	320.7 ± 0.5	9 ± 1	$\frac{1}{2}^-$
$\Xi_c(2790)^0$	$\Xi_c'^+\pi^-$	323.8 ± 0.5	10 ± 1	$\frac{1}{2}^-$
$\Xi_c(2815)^+$	$\Xi_c(2645)^0\pi^+$	348.8 ± 0.1	2.43 ± 0.23	$\frac{3}{2}^-$
$\Xi_c(2815)^0$	$\Xi_c(2645)^+\pi^-$,$\Xi_c^0\gamma$	349.4 ± 0.1	2.54 ± 0.23	$\frac{3}{2}^-$
Charmed baryon excited state	Mode	Mass (MeV/c^2)	Natural width (MeV)	J^P
$\Xi_c(2880)^0$	$\Lambda_c^+K^-$	$2881.8 \pm 3.1 \pm 8.5$	$12.4 \pm 5.3 \pm 5.8$	?
$\Xi_c(2923)^0$	$\Lambda_c^+K^-$	2923.2 ± 0.34	6.2 ± 1.3	?
$\Xi_c(2939)^0$	$\Lambda_c^+K^-$	2938.55 ± 0.30	10.2 ± 1.4	?
$\Xi_c(2965)^0$	$\Lambda_c^+K^-$	2964.88 ± 0.33	14.1 ± 1.6	?
$\Xi_c(2970)^+$	$\Lambda_c^+K^-\pi^+$, $\Sigma_c^{++}K^-$, $\Xi_c(2645)^0\pi^+$	2967.2 ± 0.8	21 ± 3	?
$\Xi_c(2970)^0$	$\Xi_c(2645)^+\pi^-$	2970.4 ± 0.8	28 ± 3	?
$\Xi_c(3055)^+$	$\Sigma_c^{++}K^-$, ΛD	3055.7 ± 0.4	8.0 ± 1.9	?
$\Xi_c(3055)^0$	ΛD	3059.0 ± 0.8	6.2 ± 2.4	?
$\Xi_c(3080)^+$	$\Lambda_c^+K^-\pi^+$, $\Sigma_c^{++}K^-$, $\Sigma_c(2520)^{++}K^-$, ΛD	3077.8 ± 0.3	3.6 ± 0.7	?
$\Xi_c(3080)^0$	$\Lambda_c^+K_S^0\pi^-$, $\Sigma_c^0K_S^0$, $\Sigma_c(2520)^0K_S^0$	3079.9 ± 1.0	5.6 ± 2.2	?

TABLE 293. Summary of excited Ω_c^0 baryons. For the $\Omega_c(2770)^0$, the mass difference with respect to the ground state is given, as the uncertainty is dominated by the uncertainty in the ground state mass. In the remaining cases the total mass is shown, though the uncertainty in the Ξ_c^+ mass (the last uncertainty quoted) makes an important contribution to the total uncertainty. The latest LHCb results supercede their initial ones and the Belle result can no longer contribute significantly to the average values.

Charmed baryon excited state	Mode	Mass difference (MeV/c^2)	Natural width (MeV)	J^P
$\Omega_c(2770)^0$	$\Omega_c^0\gamma$	$70.7^{+0.8}_{-0.9}$		$\frac{3}{2}^+$
Charmed baryon excited state	Mode	Mass (MeV/c^2)	Natural width (MeV)	J^P
$\Omega_c(3000)^0$	$\Xi_c^+K^-$	$3000.44 \pm 0.07^{+0.07}_{-0.13} \pm 0.23$	$3.83 \pm 0.23^{+1.50}_{-0.29}$	?
$\Omega_c(3050)^0$	$\Xi_c^+K^-$	$3050.18 \pm 0.04^{+0.06}_{-0.06} \pm 0.23$	$0.67 \pm 0.17^{+0.64}_{-0.72}$	?
$\Omega_c(3065)^0$	$\Xi_c^+K^-$	$3065.63 \pm 0.06 \pm 0.06 \pm 0.23$	$3.79 \pm 0.20^{+0.38}_{-0.47}$	?
$\Omega_c(3090)^0$	$\Xi_c^+K^-$	$3090.16 \pm 0.11^{+0.06}_{-0.10} \pm 0.23$	$8.48 \pm 0.44^{+0.61}_{-1.62}$	?
$\Omega_c(3120)^0$	$\Xi_c^+K^-$	$3118.98 \pm 0.12^{+0.09}_{-0.23} \pm 0.23$	$0.60 \pm 0.63^{+0.90}_{-1.05}$	?
$\Omega_c(3185)^0$	$\Xi_c^+K^-$	$3185.1 \pm 1.7^{+7.4}_{-0.9} \pm 0.2$	$50 \pm 7^{+10}_{-20}$	?
$\Omega_c(3327)^0$	$\Xi_c^+K^-$	$3327.1 \pm 1.2^{+0.1}_{-1.3} \pm 0.2$	$20 \pm 5^{+13}_{-1}$	?

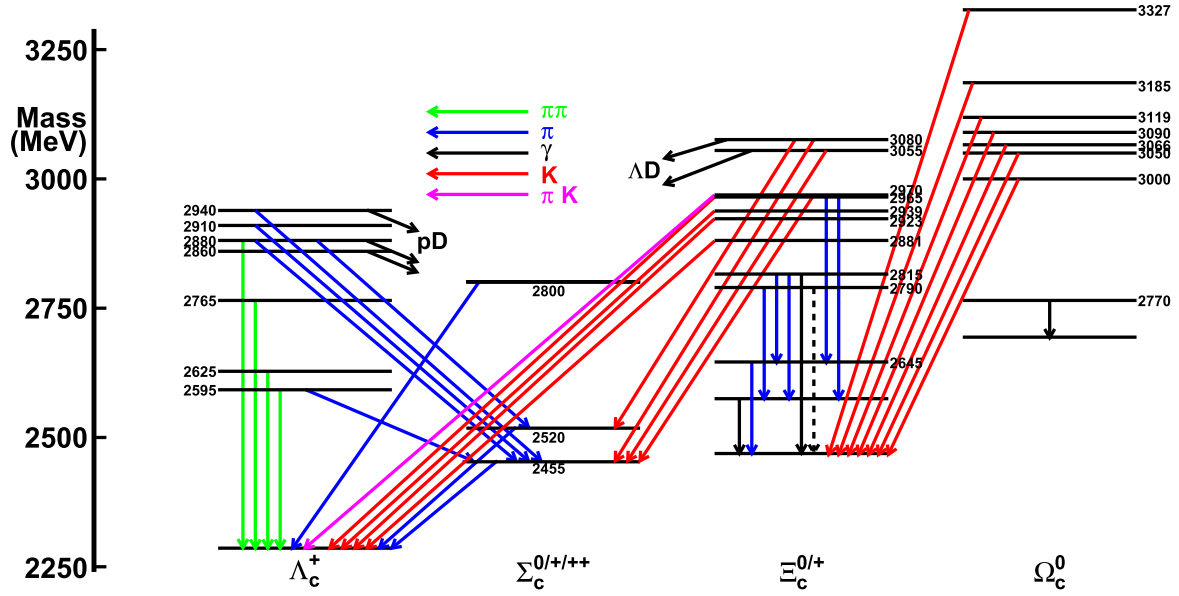


FIG. 59. Level diagram for multiplets and transitions for excited charm baryons.

equivalents of the light quark $P_{11}(1440)$ which is often identified as a radial excitation.

In addition to the $\Xi_c(2970)$, Belle [1424] has analyzed large samples of Ξ_c', $\Xi_c(2645)$, $\Xi_c(2790)$, and $\Xi_c(2815)$ decays. From this analysis they obtain the most precise mass measurements of all five isodoublets, and the first significant width measurements of the $\Xi_c(2645)$, $\Xi_c(2790)$ and $\Xi_c(2815)$. Though the spin-parity of these particles have not been directly measured, there seems little controversy that the simple quark-diquark model can explain the data. We note that the precision of the mass measurements allows for added information from the isospin mass-splitting to be used in identifying the underlying structure. In addition, the recent observation by Belle [1425] of photon transitions to the ground state from the neutral (but not charged) $\Xi_c(2815)$, and probably also the $\Xi_c(2790)$, can be interpreted as confirmation of the standard quark interpretation.

Several of the width and mass measurements for the $\Xi_c(3055)$ and $\Xi_c(3080)$ isodoublets are only in marginal agreement between experiments and decay modes. However, there seems little doubt that the differing measurements are of the same particle. The masses do indicate that their spin-parity might match those of the $\Lambda_c(2860)$ and $\Lambda_c(2880)$.

The $\Xi_c(3123)^+$ reported by *BABAR* [561] in the $\Sigma_c(2520)^{++}\pi^-$ final state has not been confirmed by Belle [1417] with twice the statistics; thus its existence is in doubt and it is omitted from Table 292 which summarizes the present situation in the excited Ξ_c sector.

The Ω_c^{*0} doubly-strange charmed baryon has been seen by both *BABAR* [1426] and Belle [1403]. The mass differences $\Delta M = M(\Omega_c^{*0}) - M(\Omega_c^0)$ measured by the experiments are in good agreement and are also consistent with most theoretical predictions [1427–1430]. LHCb [1431] has found a family of five excited Ω_c^0 baryons decaying into $\Xi_c^+ K^-$. A natural explanation is that they are the five states with $L = 1$ between the heavy quark and the light (ss) diquark; however, there is no consensus as to which state is which, and this overall interpretation is controversial. Four of the five states were confirmed by Belle [1432]. These same four states were then confirmed by LHCb in the decays of the Ω_b [1433]. The lack of confirmation of the $\Omega_c(3120)^0$ in these latter two production mechanisms indicate that it might well belong to a different multiplet—for instance a ρ excitation where the $L = 1$ is between the two lighter quarks. Further data from LHCb [1434] added two more clear observations. One, the $\Omega_c(3185)$ is copiously produced and wide, and the other, of width ≈20 MeV at a considerably higher mass.

Figure 59 shows the levels of excited charm baryons along with corresponding transitions between them, and also transitions to the ground states. We note that Belle and *BABAR* discovered that transitions between "families" of baryons are possible, i.e., between the charmed-strange (Ξ_c) and charmed-nonstrange (Λ_c^+ and Σ_c) families of excited charmed baryons [561,1416], and that highly excited states are found to decay into a non-charmed baryon and a D meson [1406,1418]. Transitions of the ground state Ξ_c^0 to the Λ_c^+, corresponding to the weak decay of the stange quark, were observed first by Belle [1412], and then studied and measured by LHCb [1435].

F. Rare and forbidden decays

This section provides a summary of searches for rare and forbidden charm decays in tabular form. The decay modes can be categorized as flavor-changing neutral currents,

including decays with and without hadrons in the final state, and radiative, lepton-flavor-violating, lepton-number-violating, and both baryon- and lepton-number-violating decays. Figures 60–63 plot the upper limits for D^0, D^+, D_s^+, D^{*0}, D_s^{*+}, and Λ_c^+ decay branching fractions. Tables 294–298 give the corresponding numerical

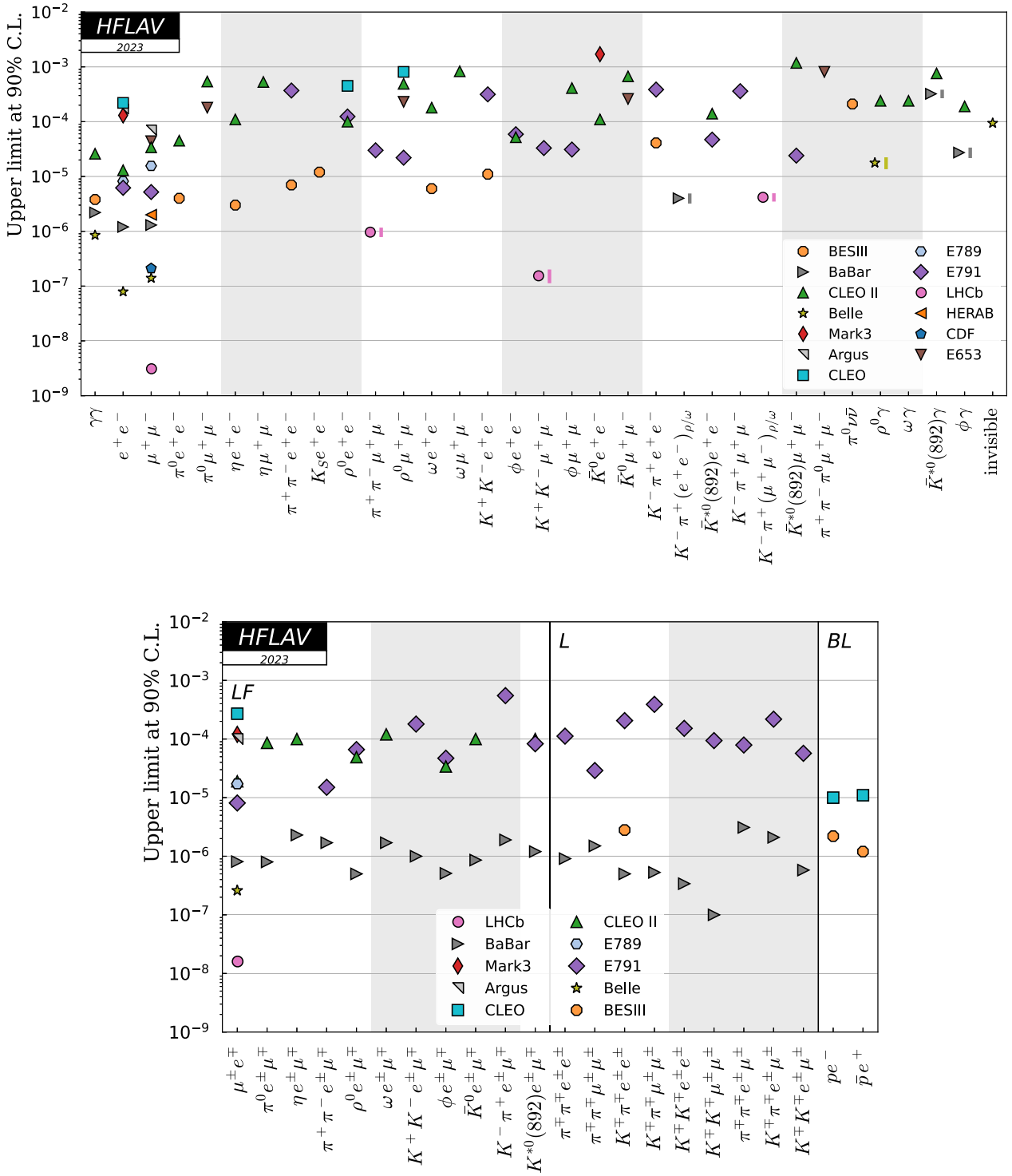


FIG. 60. Upper limits at 90% CL for D^0 decay branching fractions. The top plot shows flavor-changing neutral current and radiative decays, and the bottom plot shows lepton-flavor-changing (LF), lepton-number-changing (L), and both baryon- and lepton-number-changing (BL) decays.

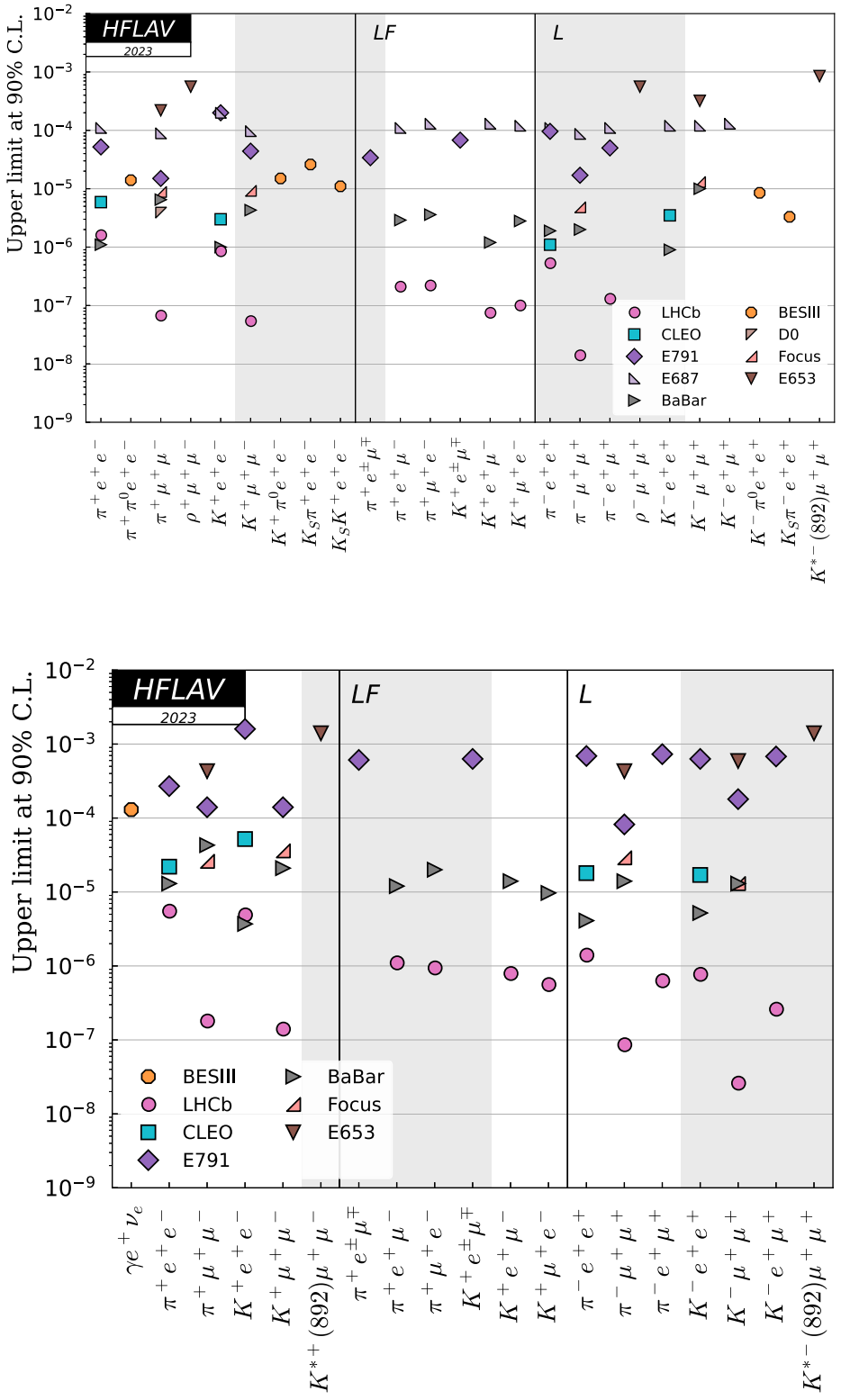


FIG. 61. Upper limits at 90% CL for D^+ (top) and D_s^+ (bottom) decay branching fractions. Each plot shows flavor-changing neutral current and rare decays, lepton-flavor-changing decays (LF), and lepton-number-changing (L) decays.

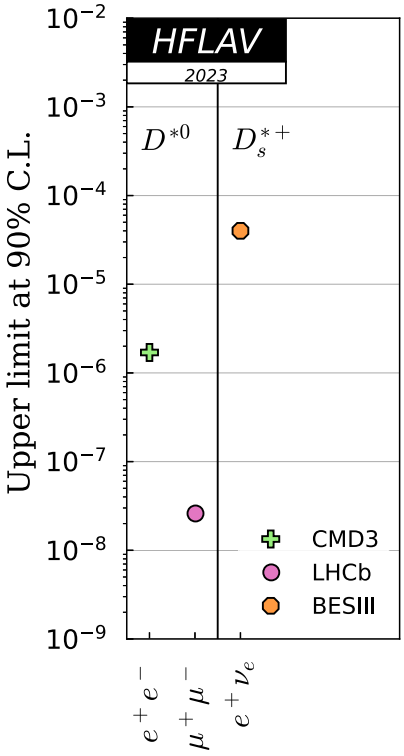


FIG. 62. Upper limits at 90% CL for D^{*0} and D_s^{*+} decay branching fractions.

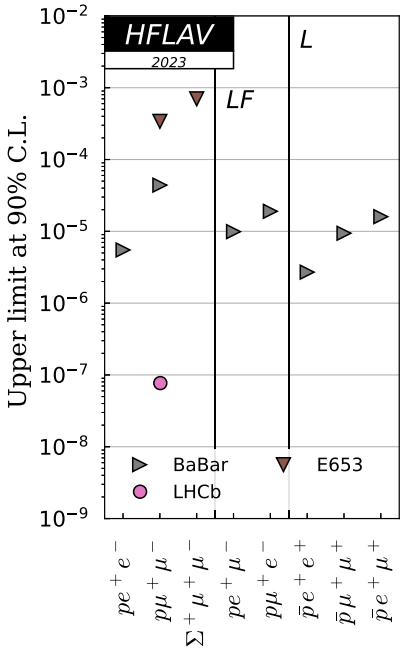


FIG. 63. Upper limits at 90% CL for Λ_c^+ decay branching fractions. Shown are flavor-changing neutral current decays, lepton-flavor-changing (LF) decays, and lepton-number-changing (L) decays.

TABLE 294. Upper limits for branching fractions at 90% CL for D^0 decay branching fractions. Where values are quoted with uncertainties, these refer to observed branching fractions, with the first uncertainty being statistical and all others being systematic, as detailed in the corresponding reference.

Decay	BF $\times 10^6$	Experiment	References
$\gamma\gamma$	26.0	CLEO II	[1452]
	3.8	BESIII	[1453]
	2.2	*BABAR*	[1454]
	0.85	Belle	[1455]
e^+e^-	220.0	CLEO	[1456]
	170.0	Argus	[1457]
	130.0	Mark3	[1458]
	13.0	CLEO II	[1459]
	8.19	E789	[1460]
	6.2	E791	[1461]
	1.2	*BABAR*	[1462]
	0.079	Belle	[1463]
$\mu^+\mu^-$	70.0	Argus	[1457]
	44.0	E653	[1464]
	34.0	CLEO II	[1459]
	15.6	E789	[1460]
	5.2	E791	[1461]
	2.0	HERAb	[1465]
	1.3	*BABAR*	[1462]
	0.21	CDF	[1466]
	0.14	Belle	[1463]
	0.0031	LHCb	[1467]
$\pi^0e^+e^-$	45.0	CLEO II	[1459]
	4.0	BESIII	[1468]
$\pi^0\mu^+\mu^-$	540.0	CLEO II	[1459]
	180.0	E653	[1464]
ηe^+e^-	110.0	CLEO II	[1459]
	3.0	BESIII	[1468]
$\eta\mu^+\mu^-$	530.0	CLEO II	[1459]
$\pi^+\pi^-e^+e^-$	370.0	E791	[1469]
	7.0	BESIII	[1468]
$K_Se^+e^-$	12.0	BESIII	[1468]
$\rho^0e^+e^-$	450.0	CLEO	[1456]
	124.0	E791	[1469]
	100.0	CLEO II	[1459]
$\pi^+\pi^-\mu^+\mu^-$	30.0	E791	[1469]
	$0.964 \pm 0.048 \pm 0.051 \pm 0.097$	LHCb	[1470]

(Table continued)

TABLE 294. *(Continued)*

Decay	BF $\times 10^6$	Experiment	References
$\rho^0\mu^+\mu^-$	810.0	CLEO	[1456]
	490.0	CLEO II	[1459]
	230.0	E653	[1464]
	22.0	E791	[1469]
ωe^+e^-	180.0	CLEO II	[1459]
	6.0	BESIII	[1468]
$\omega\mu^+\mu^-$	830.0	CLEO II	[1459]
$K^+K^-e^+e^-$	315.0	E791	[1469]
	11.0	BESIII	[1468]
ϕe^+e^-	59.0	E791	[1469]
	52.0	CLEO II	[1459]
$K^+K^-\mu^+\mu^-$	33.0	E791	[1469]
	$0.154 \pm 0.027 \pm 0.009 \pm 0.016$	LHCb	[1470]
$\phi\mu^+\mu^-$	410.0	CLEO II	[1459]
	31.0	E791	[1469]
$\bar{K}^0e^+e^-$	1700.0	Mark3	[1471]
	110.0	CLEO II	[1459]
$\bar{K}^0\mu^+\mu^-$	670.0	CLEO II	[1459]
	260.0	E653	[1464]
$K^-\pi^+e^+e^-$	385.0	E791	[1469]
	41.0	BESIII	[1468]
$K^-\pi^+(e^+e^-)_{\rho/\omega}$	$4.0 \pm 0.5 \pm 0.2 \pm 0.1$	*BABAR*	[1472]
$\bar{K}^{*0}(892)e^+e^-$	140.0	CLEO II	[1459]
	47.0	E791	[1469]
$K^-\pi^+\mu^+\mu^-$	360.0	E791	[1469]
$K^-\pi^+(\mu^+\mu^-)_{\rho/\omega}$	$4.17 \pm 0.12 \pm 0.40$	LHCb	[1473]
$\bar{K}^{*0}(892)\mu^+\mu^-$	1180.0	CLEO II	[1459]
	24.0	E791	[1469]
$\pi^+\pi^-\pi^0\mu^+\mu^-$	810.0	E653	[1464]
$\pi^0\nu\bar{\nu}$	210.0	BESIII	[1474]
$\rho^0\gamma$	240.0	CLEO II	[1475]
	$17.7 \pm 3.0 \pm 0.7$	Belle	[1195]
$\omega\gamma$	240.0	CLEO II	[1475]
$\bar{K}^{*0}(892)\gamma$	760.0	CLEO II	[1475]
	$322.0 \pm 20.0 \pm 27.0$	*BABAR*	[1476]

(Table continued)

TABLE 294. *(Continued)*

Decay	BF $\times 10^6$	Experiment	References
$\phi\gamma$	190.0	CLEO II	[1475]
	$27.3 \pm 3.0 \pm 2.6$	*BABAR*	[1476]
invisible	94.0	Belle	[1477]
$\mu^\pm e^\mp$	270.0	CLEO	[1456]
	120.0	Mark3	[1478]
	100.0	Argus	[1457]
	19.0	CLEO II	[1459]
	17.2	E789	[1460]
	8.1	E791	[1461]
	0.81	*BABAR*	[1462]
	0.26	Belle	[1463]
	0.016	LHCb	[1479]
$\pi^0e^\pm\mu^\mp$	86.0	CLEO II	[1459]
	0.80	*BABAR*	[1480]
$\eta e^\pm\mu^\mp$	100.0	CLEO II	[1459]
	2.3	*BABAR*	[1480]
$\pi^+\pi^-e^\pm\mu^\mp$	15.0	E791	[1469]
	1.7	*BABAR*	[1481]
$\rho^0e^\pm\mu^\mp$	66.0	E791	[1469]
	49.0	CLEO II	[1459]
	0.5	*BABAR*	[1480]
$\omega e^\pm\mu^\mp$	120.0	CLEO II	[1459]
	1.7	*BABAR*	[1480]
$K^+K^-e^\pm\mu^\mp$	180.0	E791	[1469]
	1.0	*BABAR*	[1481]
$\phi e^\pm\mu^\mp$	47.0	E791	[1469]
	34.0	CLEO II	[1459]
	0.51	*BABAR*	[1480]
$\bar{K}^0e^\pm\mu^\mp$	100.0	CLEO II	[1459]
	0.86	*BABAR*	[1480]
$K^-\pi^+e^\pm\mu^\mp$	550.0	E791	[1469]
	1.9	*BABAR*	[1481]
$K^{*0}(892)e^\pm\mu^\mp$	100.0	CLEO II	[1459]
	83.0	E791	[1469]
	1.2	*BABAR*	[1480]
$\pi^\mp\pi^\mp e^\pm e^\pm$	112.0	E791	[1469]
	0.91	*BABAR*	[1481]
$\pi^\mp\pi^\mp\mu^\pm\mu^\pm$	29.0	E791	[1469]
	1.5	*BABAR*	[1481]

(Table continued)

TABLE 294. *(Continued)*

Decay	BF $\times 10^6$	Experiment	References
$K^{\mp}\pi^{\mp}e^{\pm}e^{\pm}$	206.0	E791	[1469]
	2.8	BESIII	[1482]
	0.5	*BABAR*	[1481]
$K^{\mp}\pi^{\mp}\mu^{\pm}\mu^{\pm}$	390.0	E791	[1469]
	0.53	*BABAR*	[1481]
$K^{\mp}K^{\mp}e^{\pm}e^{\pm}$	152.0	E791	[1469]
	0.34	*BABAR*	[1481]
$K^{\mp}K^{\mp}\mu^{\pm}\mu^{\pm}$	94.0	E791	[1469]
	0.10	*BABAR*	[1481]
$\pi^{\mp}\pi^{\mp}e^{\pm}\mu^{\pm}$	79.0	E791	[1469]
	3.1	*BABAR*	[1481]
$K^{\mp}\pi^{\mp}e^{\pm}\mu^{\pm}$	218.0	E791	[1469]
	2.1	*BABAR*	[1481]
$K^{\mp}K^{\mp}e^{\pm}\mu^{\pm}$	57.0	E791	[1469]
	0.58	*BABAR*	[1481]
pe^{-}	10.0	CLEO	[1483]
	2.2	BESIII	[1484]
$\bar{p}e^{+}$	11.0	CLEO	[1483]
	1.2	BESIII	[1484]

TABLE 295. Upper limits at 90% CL for D^+ decay branching fractions.

Decay	Limit $\times 10^6$	Experiment	References
$\pi^+e^+e^-$	110.0	E687	[1485]
	52.0	E791	[1461]
	5.9	CLEO	[1486]
	1.6	LHCb	[1487]
	1.1	*BABAR*	[1488]
$\pi^+\pi^0e^+e^-$	14.0	BESIII	[1468]
$\pi^+\mu^+\mu^-$	220.0	E653	[1464]
	89.0	E687	[1485]
	15.0	E791	[1461]
	8.8	Focus	[1489]
	6.5	*BABAR*	[1488]
	3.9	D0	[1490]
	0.067	LHCb	[1487]
$\rho^+\mu^+\mu^-$	560.0	E653	[1464]

(Table continued)

TABLE 295. *(Continued)*

Decay	Limit $\times 10^6$	Experiment	References
$K^+e^+e^-$	200.0	E687	[1485]
	3.0	CLEO	[1486]
	1.0	*BABAR*	[1488]
	0.85	LHCb	[1487]
$K^+\mu^+\mu^-$	97.0	E687	[1485]
	44.0	E791	[1461]
	9.2	Focus	[1489]
	4.3	*BABAR*	[1488]
	0.054	LHCb	[1487]
$K^+\pi^0e^+e^-$	15.0	BESIII	[1468]
$K_S\pi^+e^+e^-$	26.0	BESIII	[1468]
$K_SK^+e^+e^-$	11.0	BESIII	[1468]
$\pi^+e^{\pm}\mu^{\mp}$	34.0	E791	[1461]
$\pi^+e^+\mu^-$	110.0	E687	[1485]
	2.9	*BABAR*	[1488]
	0.21	LHCb	[1487]
$\pi^+\mu^+e^-$	130.0	E687	[1485]
	3.6	*BABAR*	[1488]
	0.22	LHCb	[1487]
$K^+e^{\pm}\mu^{\mp}$	68.0	E791	[1461]
$K^+e^+\mu^-$	130.0	E687	[1485]
	1.2	*BABAR*	[1488]
	0.075	LHCb	[1487]
$K^+\mu^+e^-$	120.0	E687	[1485]
	2.8	*BABAR*	[1488]
	0.10	LHCb	[1487]
$\pi^-e^+e^+$	110.0	E687	[1485]
	96.0	E791	[1461]
	1.9	*BABAR*	[1488]
	1.1	CLEO	[1486]
	0.53	LHCb	[1487]
$\pi^-\mu^+\mu^+$	87.0	E687	[1485]
	17.0	E791	[1461]
	4.8	Focus	[1489]
	2.0	*BABAR*	[1488]
	0.014	LHCb	[1487]
$\pi^-e^+\mu^+$	110.0	E687	[1485]
	50.0	E791	[1461]
	0.13	LHCb	[1487]
$\rho^-\mu^+\mu^+$	560.0	E653	[1464]

(Table continued)

TABLE 295. *(Continued)*

Decay	Limit $\times 10^6$	Experiment	References
$K^-e^+e^+$	120.0	E687	[1485]
	3.5	CLEO	[1486]
	0.89	*BABAR*	[1488]
$K^-\mu^+\mu^+$	320.0	E653	[1464]
	120.0	E687	[1485]
	13.0	Focus	[1489]
	10.0	*BABAR*	[1488]
$K^-e^+\mu^+$	130.0	E687	[1485]
$K^-\pi^0e^+e^+$	8.5	BESIII	[1482]
$K_S\pi^-e^+e^+$	3.3	BESIII	[1482]
$K^{*-}(892)\mu^+\mu^+$	850.0	E653	[1464]

TABLE 296. Upper limits at 90% CL for D_s^+ decay branching fractions.

Decay	Limit $\times 10^6$	Experiment	References
$\gamma e^+\nu_e$	130.0	BESIII	[1491]
$\pi^+e^+e^-$	270.0	E791	[1461]
	22.0	CLEO	[1486]
	13.0	*BABAR*	[1488]
	5.5	LHCb	[1487]
$\pi^+\mu^+\mu^-$	430.0	E653	[1464]
	140.0	E791	[1461]
	43.0	*BABAR*	[1488]
	26.0	Focus	[1489]
	0.18	LHCb	[1487]
$K^+e^+e^-$	1600.0	E791	[1461]
	52.0	CLEO	[1486]
	4.9	LHCb	[1487]
	3.7	*BABAR*	[1488]
$K^+\mu^+\mu^-$	140.0	E791	[1461]
	36.0	Focus	[1489]
	21.0	*BABAR*	[1488]
	0.14	LHCb	[1487]
$K^{*+}(892)\mu^+\mu^-$	1400.0	E653	[1464]
$\pi^+e^\pm\mu^\mp$	610.0	E791	[1461]
$\pi^+e^+\mu^-$	12.0	*BABAR*	[1488]
	1.1	LHCb	[1487]

(Table continued)

TABLE 296. *(Continued)*

Decay	Limit $\times 10^6$	Experiment	References
$\pi^+\mu^+e^-$	20.0	*BABAR*	[1488]
	0.94	LHCb	[1487]
$K^+e^\pm\mu^\mp$	630.0	E791	[1461]
$K^+e^+\mu^-$	14.0	*BABAR*	[1488]
	0.79	LHCb	[1487]
$K^+\mu^+e^-$	9.7	*BABAR*	[1488]
	0.56	LHCb	[1487]
$\pi^-e^+e^+$	690.0	E791	[1461]
	18.0	CLEO	[1486]
	4.1	*BABAR*	[1488]
	1.4	LHCb	[1487]
$\pi^-\mu^+\mu^+$	430.0	E653	[1464]
	82.0	E791	[1461]
	29.0	Focus	[1489]
	14.0	*BABAR*	[1488]
	0.086	LHCb	[1487]
$\pi^-e^+\mu^+$	730.0	E791	[1461]
	0.63	LHCb	[1487]
$K^-e^+e^+$	630.0	E791	[1461]
	17.0	CLEO	[1486]
	5.2	*BABAR*	[1488]
	0.77	LHCb	[1487]
$K^-\mu^+\mu^+$	590.0	E653	[1464]
	180.0	E791	[1461]
	13.0	*BABAR*	[1488]
	0.026	LHCb	[1487]
$K^-e^+\mu^+$	680.0	E791	[1461]
	0.26	LHCb	[1487]
$K^{*-}(892)\mu^+\mu^+$	1400.0	E653	[1464]

TABLE 297. Upper limits at 90% CL for D^{*0} and D_s^{*+} decay branching fractions.

Decay	Limit $\times 10^6$	Experiment	References
e^+e^-	1.7	CMD-3	[1492]
$\mu^+\mu^-$	0.026	LHCb	[1493]
$e^+\nu_e$	40.0	BESIII	[1494]

TABLE 298. Upper limits at 90% CL for Λ_c^+ decay branching fractions.

Decay	Limit $\times 10^6$	Experiment	References
pe^+e^-	5.5	*BABAR*	[1488]
$p\mu^+\mu^-$	340.0	E653	[1464]
	44.0	*BABAR*	[1488]
	0.077	LHCb	[1495]
$\Sigma^+\mu^+\mu^-$	700.0	E653	[1464]
$pe^+\mu^-$	9.9	*BABAR*	[1488]
$p\mu^+e^-$	19.0	*BABAR*	[1488]
$\bar{p}e^+e^+$	2.7	*BABAR*	[1488]
$\bar{p}\mu^+\mu^+$	9.4	*BABAR*	[1488]
$\bar{p}e^+\mu^+$	16.0	*BABAR*	[1488]

results. Some theoretical predictions are given in Refs. [1436–1451].

Some D^0 decay modes have been observed and are quoted as branching fractions with uncertainties in the tables and shown as a symbol with a line representing the 68% CL interval in the plots.

In several cases the rare-decay final states have been observed with the dilepton pair being the decay product of a vector meson. For these measurements the quoted limits are those expected for the non-resonant dilepton spectrum. For the extrapolation to the full spectrum a phase-space distribution of the non-resonant component has been assumed. This applies to the CLEO measurement of the decays $D_{(s)}^+ \to (K^+, \pi^+)e^+e^-$ [1486], to the D0 measurements of the decays $D_{(s)}^+ \to \pi^+\mu^+\mu^-$ [1490], and to the *BABAR* measurements of the decays $D_{(s)}^+ \to (K^+, \pi^+)e^+e^-$ and $D_{(s)}^+ \to (K^+, \pi^+)\mu^+\mu^-$, where the contribution from $\phi \to l^+l^-$ ($l = e, \mu$) has been excluded. In the case of the LHCb measurements of the decays $D^0 \to \pi^+\pi^-\mu^+\mu^-$ [1496] as well as the decays $D_{(s)}^+ \to \pi^+\mu^+\mu^-$ [1497] the contributions from $\phi \to l^+l^-$ as well as from $\rho, \omega \to l^+l^-$ ($l = e, \mu$) have been excluded.

For the D^{*0} meson, the limit for the e^+e^- final state was obtained by searching for the meson's on-shell production in e^+e^- collisions by the CMD-3 experiment. The D_s^{*+} limit for the final state $e^+\nu_e$ seemingly refers to a Cabibbo-favored weak decay. However, the limit on its partial width is comparable to that of other rare decays. This is due to its total width being among the smallest of any excited meson state.

XI. TAU LEPTON PROPERTIES

This section reports the averages of the τ mass (Sec. XI A) and lifetime (Sec. XI B), and a global fit of the available measurements of the τ branching fractions (Sec. XI C). When the averaged measurements have asymmetric uncertainties, they are symmetrized using the quadratic average, i.e., the square root of the mean of the squares of the positive and negative uncertainties. The fit results are used in Sec. XI D to test the lepton-flavor universality of the charged-current weak interaction. A "universality-improved" [1498] branching fraction $\mathcal{B}_e = \mathcal{B}(\tau \to e\nu\bar{\nu})$ and the ratio between the hadronic branching fraction and $\mathcal{B}_e$ are obtained in Sec. XI E. The value of the Cabibbo-Kobayashi-Maskawa (CKM) matrix element $|V_{us}|$ obtained from τ decays is given in Sec. XI F. Combinations of upper limits on lepton-flavor-violating τ branching fractions are computed in Sec. XI G. We use measurements reported through September 2023 and the following ones that were made available at a later time:

(i) $\mathcal{B}(\tau^- \to \mu^-\bar{\nu}_\mu\nu_\tau)/\mathcal{B}(\tau^- \to e^-\bar{\nu}_e\nu_\tau)$ by the Belle II experiment [1499],
(ii) $\mathcal{B}(\tau^- \to \mu^-\mu^+\mu^-)$ by the CMS experiment [1500],
(iii) $\mathcal{B}(\tau^- \to \mu^-\mu^+\mu^-)$ by the Belle II experiment [1501],
(iv) $\mathcal{B}(\tau^- \to \pi^-\Lambda)$ by the Belle II experiment [1502], and
(v) $\mathcal{B}(\tau^- \to \pi^-\bar{\Lambda})$ by the Belle II experiment [1502].

A. τ mass

A total of 10 τ mass measurements are averaged. The fit has $\chi^2/\text{d.o.f.} = 8.2/9$, corresponding to a confidence level CL = 51%. We include recent measurements by Belle II [1503] and KEDR [1504], which were not included in the 2022 edition and 2023 update of the Review of Particle Physics [302]. Table 299 and Fig. 64 report the experimental inputs and the calculated average, which are also available at [1505].

TABLE 299. τ mass measurements and their average.

τ mass [MeV]	Experiment	References
$1776.30 \pm 2.40 \pm 1.40$	ARGUS	[1506]
$1776.68 \pm 0.12 \pm 0.41$	*BABAR*	[1507]
$1776.61 \pm 0.13 \pm 0.35$	Belle	[1508]
$1777.09 \pm 0.08 \pm 0.11$	Belle II	[1503]
$1776.96^{+0.18+0.25}_{-0.21-0.17}$	BES	[1509]
$1776.91 \pm 0.12^{+0.10}_{-0.13}$	BES3	[1510]
$1778.20 \pm 0.80 \pm 1.20$	CLEO	[1511]
$1783.00^{+3.00}_{-4.00} \pm 0.00$	DELCO	[1512]
$1776.69^{+0.17}_{-0.19} \pm 0.15$	KEDR	[1504]
$1775.10 \pm 1.60 \pm 1.00$	OPAL	[1513]
1776.94 ± 0.09	HFLAV average	

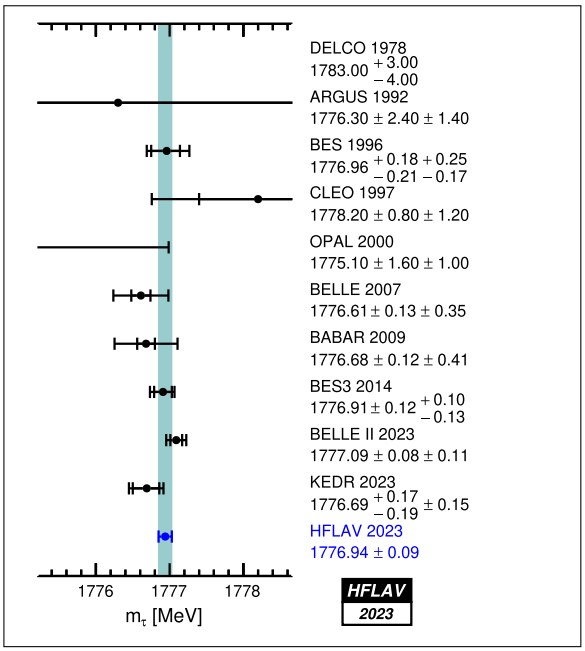


FIG. 64. τ mass measurements and their average.

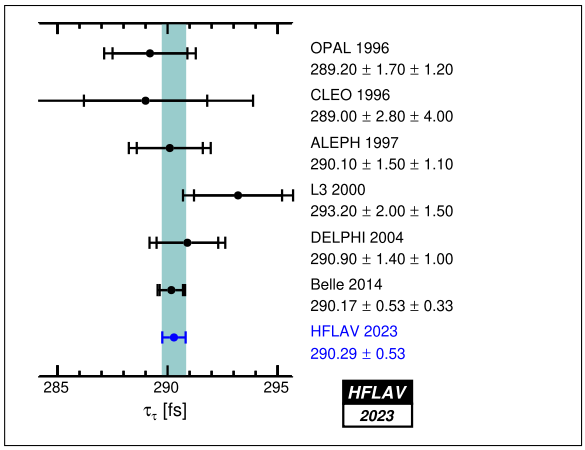


FIG. 65. τ lifetime measurements and their average.

B. τ lifetime

A total of 6τ lifetime measurements are averaged. All are included in the 2022 edition and 2023 update of the Review of Particle Physics [302]. The fit has $\chi^2/\text{d.o.f.} = 1.87/5$, corresponding to a confidence level CL = 87%. Table 300 and Fig. 65 report the experimental inputs and the calculated average, which are also available at [1505].

C. Branching fraction fit

A fit of the available experimental measurements is used to determine the τ branching fractions. All relevant published statistical and systematic correlations among the measurements are used. In addition, for a selection of measurements, particularly the most precise and the most recent ones, the documentation on the systematic uncertainties' contributions is examined to determine how they depend on parameters such as other τ branching fractions or other external parameters, e.g., η and ω meson branching fractions and the cross-section $\sigma(e^+e^- \to \tau^+\tau^-)$. We follow the procedures detailed in Sec. III A to adjust the measurements' values and uncertainties to account for the updated values and uncertainties of the external parameters, which are taken from the Review of Particle Physics [302]. The measurements' correlations are adjusted to account for the dependence of different measurement on the same parameters.

Following a convention established in the Review of Particle Physics, τ branching fractions are often labeled with the final state content of $\pi^\pm$, π^0, $K^\pm$, γ, implicitly including decay chains that involve intermediate particles, e.g., $K^0_S \to \pi^+\pi^-$, and η, ω, ϕ decays. When measurements exclude the contribution of some or all the known intermediate particles, the branching fraction notation flags this information by adding, e.g., "ex. K^0."

Each measurement is modeled with one fit parameter that is either a τ decay branching fraction, labeled $\mathcal{B}_i$, or a ratio of two τ decay branching fractions, labeled $\mathcal{B}_{i/j} = \mathcal{B}_i/\mathcal{B}_j$. Some branching fractions are linear combinations of other branching fractions: for instance $\mathcal{B}_8 = \mathcal{B}(\tau^- \to h^-\nu_\tau)$ is the sum of $\mathcal{B}_9 = \mathcal{B}(\tau^- \to \pi^-\nu_\tau)$ and $\mathcal{B}_{10} = \mathcal{B}(\tau^- \to K^-\nu_\tau)$, with the symbol h referring to a π or a K. In some cases, constraints arise from approximate relations that nevertheless hold within the present experimental precision and are treated as exact. For instance, the constraint $\mathcal{B}(\tau^- \to K^-K^-K^+\nu_\tau) = \mathcal{B}(\tau^- \to K^-\phi\nu_\tau) \times \mathcal{B}(\phi \to K^+K^-)$ is justified according to the current experimental evidence. The constraint equations depend on uncertain quantities, such as $\mathcal{B}(\phi \to K^+K^-)$ in this example. The uncertainties associated with these constraints are typically smaller in relative value than the uncertainties on the τ branching fractions. Therefore, we neglect all of them except for the poorly known branching fraction $\mathcal{B}_{980} = \mathcal{B}(a_1^- \to \pi^-\gamma)$, which is modeled with a nuisance

TABLE 300. τ lifetime measurements and their average.

τ lifetime [fs]	Experiment	References
$290.10 \pm 1.50 \pm 1.10$	ALEPH	[1514]
$290.17 \pm 0.53 \pm 0.33$	Belle	[1515]
$289.00 \pm 2.80 \pm 4.00$	CLEO	[1516]
$290.90 \pm 1.40 \pm 1.00$	DELPHI	[1517]
$293.20 \pm 2.00 \pm 1.50$	L3	[1518]
$289.20 \pm 1.70 \pm 1.20$	OPAL	[1519]
290.29 ± 0.53	HFLAV average	

fit parameter, based on the value and uncertainty estimated by the ALEPH collaboration [1520]. All the constraints are listed in Sec. XI C 4.

The fit χ^2 is constructed following Eq. (1)

$$\chi^2 = \sum_{ijkl}(m_i - M_{ik}q_k)(V^{-1})_{ij}(m_j - M_{jl}q_l) + \sum_r \frac{(n_r - p_r)^2}{\sigma^2_{n_r}}, \quad (226)$$

where m_i is a measurement result, q_k is a fit parameter, V_{ij} is the covariance matrix that describes the measurements' uncertainties and correlations, M_{ik} is a model matrix that specifies the linear combination of the fit parameters corresponding to the measurement m_i, p_r is a nuisance fit parameter, and n_r and σ_{n_r} are, respectively, the value and uncertainty that summarize the existing prior knowledge on p_r. In the current fit, the second sum includes just one nuisance fit parameter.

The χ^2 is minimized varying all fit parameters while respecting all constraints, using the technique of the Lagrange multipliers (see Sec. III).

In performing the fit, a scale factor of 5.44 was applied to the published uncertainties of the two severely inconsistent measurements of $\mathcal{B}_{96} = \mathcal{B}(\tau^- \to K^-K^-K^+\nu_\tau)$ by *BABAR* and Belle. The scale-factor value was chosen using the PDG procedure, i.e., it is such that $\chi^2/\text{d.o.f.} = 1$ when fitting just the two $\mathcal{B}_{96}$ measurements.

1. Changes with respect to the previous report

The 2021 HFLAV report [1] used the ALEPH 2006 estimate of $\mathcal{B}_{805} = \mathcal{B}(\tau^- \to a_1^-(\pi^-\gamma)\nu_\tau)$ [1520] and treated it as an experimental measurement, therefore $\mathcal{B}_{805} = \mathcal{B}(\tau^- \to a_1^-(\pi^-\gamma)\nu_\tau)$ was determined using $\mathcal{B}_{980} = \mathcal{B}(a_1^- \to \pi^-\gamma)$ and the values of $\mathcal{B}_{62} = \mathcal{B}(\tau^- \to \pi^-\pi^+\pi^-\nu_\tau\,(\text{ex. } K^0, \omega))$ and $\mathcal{B}_{20} = \mathcal{B}(\tau^- \to \pi^-2\pi^0\nu_\tau\,(\text{ex. } K^0))$ as known at the time of the ALEPH 2006 publication. In this edition, we use an estimate of $\mathcal{B}_{980}$ in a constraint equation that defines $\mathcal{B}_{805}$, and $\mathcal{B}_{980}$ is optimized in the τ branching fraction fit as nuisance fit parameter. With the current procedure, $\mathcal{B}_{805}$ is determined using $\mathcal{B}_{980}$ and the fit values of $\mathcal{B}_{62}$ and $\mathcal{B}_{20}$. The fit returns $\mathcal{B}_{805} = (0.38 \pm 0.15) \times 10^{-3}$, while the HFLAV 2021 report [1] had $\mathcal{B}_{805} = (0.40 \pm 0.20) \times 10^{-3}$ (the ALEPH estimate [1520]). The other τ branching fractions averages are not affected by this modification of the fit procedure.

We include in the τ branching fraction fit measurements the recently published measurement of the ratio of the τ leptonic branching fractions:

$$\frac{\mathcal{B}(\tau^- \to \mu^-\bar{\nu}_\mu\nu_\tau)}{\mathcal{B}(\tau^- \to e^-\bar{\nu}_e\nu_\tau)} = 0.9675 \pm 0.0007 \pm 0.0036 \quad (227)$$

by the Belle II experiment [1499]. Since this result is the most precise measurement from a single experiment to date, the precision of the fitted leptonic branching fractions is also improved.

We also report the results from a unitarity-constrained fit, along with the results from the non-unitarity-constrained fit. The results from the unitarity-constrained fit are required as inputs for tau-decay Monte Carlo event generators, such as Tauola [1521], and were not included in the previous reports.

The parameters used to update the measurements' systematic biases and the parameters appearing in the constraint equations in Sec. XI C 4 have been updated to values reported in the Review of Particle Physics 2022 and 2023 update [302].

2. Differences with respect to the PDG fit

The τ branching fraction fit provided by HFLAV for the 2024 edition of the Review of Particle Physics reports as in the past editions only the unitarity-constrained fit results, and includes all the updates of this report, except the recent Belle II measurement of the ratio of the τ leptonic branching fractions, which was published later than the new literature publication deadline.

3. Fit results

We use a total of 171 τ branching fractions and ratios measurements and 1 nuisance fit parameter measurement to optimize 137 fit parameters and 1 nuisance fit parameter, while respecting 91 equality constraints. When considering just the τ branching fractions, omitting the nuisance fit parameter, the fit has $\chi^2/\text{d.o.f.} = 138/125$, corresponding to a confidence level CL = 20.2%. The fitted parameters' values and uncertainties corresponding to τ branching fractions measurements are listed in Table 301, for both the universality-constrained fit and the unconstrained fit. The table also includes:

(i) $\mathcal{B}_{110} = \mathcal{B}(\tau^- \to X_s^-\nu_\tau)$, the total measured branching fraction of τ decays to final states with net strangeness;
(ii) $\mathcal{B}_{\text{all}}$, the total branching fraction of the τ into any known final state according to measurements, defined by its constraint equation in Sec. XI C 4;
(iii) $\mathcal{B}_{\text{ur}} = 1 - \mathcal{B}_{\text{all}}$, the τ decay unitarity residual.

When no unitarity constraint is applied, we find that $\mathcal{B}_{\text{ur}}$ is consistent with 0. The nuisance fit parameter's value and uncertainty are listed in Table 302. All resulting fit parameters, their input measurements, and their correlation matrix are available at [1505].

4. Equality constraints

The constraints on the τ branching-fractions used in the fit are listed in the following equations.

TABLE 301. Fit averages and measurements of τ branching fractions and ratios of branching fractions. The label "u.c." indicates the results from the unitarity-constrained fit.

Fit parameter	Experiment	References
$\mathcal{B}_1 = \mathcal{B}(\tau^- \to \text{particle}^- \geq 0 \text{ neutrals } \geq 0\, K^0 \nu_\tau)$		
0.8518 ± 0.0011	Average	
0.8524 ± 0.0006	Average with u.c.	
$\mathcal{B}_2 = \mathcal{B}(\tau^- \to \text{particle}^- \geq 0 \text{ neutrals } \geq 0\, K_L^0 \nu_\tau)$		
0.8452 ± 0.0010	Average	
0.8458 ± 0.0006	Average with u.c.	
$\mathcal{B}_3 = \mathcal{B}(\tau^- \to \mu^- \bar{\nu}_\mu \nu_\tau)$		
0.17360 ± 0.00037	Average	
0.17366 ± 0.00036	Average with u.c.	
$0.17319 \pm 0.00070 \pm 0.00032$	ALEPH	[1520]
$0.17325 \pm 0.00095 \pm 0.00077$	DELPHI	[1522]
$0.17342 \pm 0.00110 \pm 0.00067$	L3	[1523]
$0.17340 \pm 0.00090 \pm 0.00060$	OPAL	[1524]
$\mathcal{B}_{3/5} = \frac{\mathcal{B}(\tau^- \to \mu^- \bar{\nu}_\mu \nu_\tau)}{\mathcal{B}(\tau^- \to e^- \bar{\nu}_e \nu_\tau)}$		
0.9730 ± 0.0022	Average	
0.9730 ± 0.0022	Average with u.c.	
$0.9970 \pm 0.0350 \pm 0.0400$	ARGUS	[1525]
$0.9796 \pm 0.0016 \pm 0.0036$	*BABAR*	[1526]
$0.9675 \pm 0.0007 \pm 0.0036$	Belle II	[1499]
$0.9777 \pm 0.0063 \pm 0.0087$	CLEO	[1511]
$\mathcal{B}_5 = \mathcal{B}(\tau^- \to e^- \bar{\nu}_e \nu_\tau)$		
0.1784 ± 0.0004	Average	
0.1785 ± 0.0004	Average with u.c.	
$0.1784 \pm 0.0007 \pm 0.0004$	ALEPH	[1520]
$0.1776 \pm 0.0006 \pm 0.0017$	CLEO	[1511]
$0.1788 \pm 0.0011 \pm 0.0011$	DELPHI	[1522]
$0.1781 \pm 0.0010 \pm 0.0008$	L3	[1523]
$0.1781 \pm 0.0009 \pm 0.0006$	OPAL	[1527]
$\mathcal{B}_7 = \mathcal{B}(\tau^- \to h^- \geq 0\, K_L^0 \nu_\tau)$		
0.1202 ± 0.0005	Average	
0.1203 ± 0.0005	Average with u.c.	
$0.1240 \pm 0.0070 \pm 0.0070$	DELPHI	[1528]
$0.1247 \pm 0.0026 \pm 0.0043$	L3	[1529]
$0.1210 \pm 0.0070 \pm 0.0050$	OPAL	[1530]
$\mathcal{B}_8 = \mathcal{B}(\tau^- \to h^- \nu_\tau)$		
0.1150 ± 0.0005	Average	
0.1151 ± 0.0005	Average with u.c.	
$0.1152 \pm 0.0005 \pm 0.0012$	CLEO	[1511]
$0.1157 \pm 0.0012 \pm 0.0011$	DELPHI	[1531]
$0.1198 \pm 0.0013 \pm 0.0016$	OPAL	[1532]
$\mathcal{B}_{8/5} = \frac{\mathcal{B}(\tau^- \to h^- \nu_\tau)}{\mathcal{B}(\tau^- \to e^- \bar{\nu}_e \nu_\tau)}$		
0.6448 ± 0.0032	Average	
0.6450 ± 0.0032	Average with u.c.	

(Table continued)

TABLE 301. *(Continued)*

Fit parameter	Experiment	References
$\mathcal{B}_9 = \mathcal{B}(\tau^- \to \pi^- \nu_\tau)$		
0.1081 ± 0.0005	Average	
0.1082 ± 0.0005	Average with u.c.	
$0.1083 \pm 0.0007 \pm 0.0008$	ALEPH	[1520]
$\mathcal{B}_{9/5} = \frac{\mathcal{B}(\tau^- \to \pi^- \nu_\tau)}{\mathcal{B}(\tau^- \to e^- \bar{\nu}_e \nu_\tau)}$		
0.6058 ± 0.0032	Average	
0.6060 ± 0.0031	Average with u.c.	
$0.5945 \pm 0.0014 \pm 0.0061$	*BABAR*	[1526]
$\mathcal{B}_{10} = \mathcal{B}(\tau^- \to K^- \nu_\tau)$		
0.00696 ± 0.00010	Average	
0.00697 ± 0.00010	Average with u.c.	
$0.00696 \pm 0.00025 \pm 0.00014$	ALEPH	[1533]
$0.00660 \pm 0.00070 \pm 0.00090$	CLEO	[1534]
$0.00850 \pm 0.00180 \pm 0.00000$	DELPHI	[1535]
$0.00658 \pm 0.00027 \pm 0.00029$	OPAL	[1536]
$\mathcal{B}_{10/5} = \frac{\mathcal{B}(\tau^- \to K^- \nu_\tau)}{\mathcal{B}(\tau^- \to e^- \bar{\nu}_e \nu_\tau)}$		
0.03901 ± 0.00054	Average	
0.03903 ± 0.00054	Average with u.c.	
$0.03882 \pm 0.00032 \pm 0.00057$	*BABAR*	[1526]
$\mathcal{B}_{10/9} = \frac{\mathcal{B}(\tau^- \to K^- \nu_\tau)}{\mathcal{B}(\tau^- \to \pi^- \nu_\tau)}$		
0.0644 ± 0.0009	Average	
0.0644 ± 0.0009	Average with u.c.	
$\mathcal{B}_{11} = \mathcal{B}(\tau^- \to h^- \geq 1 \text{ neutrals } \nu_\tau)$		
0.3698 ± 0.0010	Average	
0.3700 ± 0.0009	Average with u.c.	
$\mathcal{B}_{12} = \mathcal{B}(\tau^- \to h^- \geq 1\pi^0 \nu_\tau \, (\text{ex. } K^0))$		
0.3648 ± 0.0010	Average	
0.3650 ± 0.0009	Average with u.c.	
$\mathcal{B}_{13} = \mathcal{B}(\tau^- \to h^- \pi^0 \nu_\tau)$		
0.25917 ± 0.00090	Average	
0.25926 ± 0.00089	Average with u.c.	
$0.25670 \pm 0.00010 \pm 0.00390$	Belle	[1537]
$0.25870 \pm 0.00120 \pm 0.00420$	CLEO	[1538]
$0.25740 \pm 0.00201 \pm 0.00138$	DELPHI	[1531]
$0.25050 \pm 0.00350 \pm 0.00500$	L3	[1529]
$0.25890 \pm 0.00170 \pm 0.00290$	OPAL	[1532]
$\mathcal{B}_{14} = \mathcal{B}(\tau^- \to \pi^- \pi^0 \nu_\tau)$		
0.2548 ± 0.0009	Average	
0.2549 ± 0.0009	Average with u.c.	
$0.2547 \pm 0.0010 \pm 0.0008$	ALEPH	[1520]
$\mathcal{B}_{16} = \mathcal{B}(\tau^- \to K^- \pi^0 \nu_\tau)$		
0.004321 ± 0.000148	Average	

(Table continued)

TABLE 301. *(Continued)*

Fit parameter	Experiment	References
0.004328 ± 0.000148	Average with u.c.	
$0.004440 \pm 0.000260 \pm 0.000240$	ALEPH	[1533]
$0.004160 \pm 0.000030 \pm 0.000180$	*BABAR*	[1539]
$0.005100 \pm 0.001000 \pm 0.000700$	CLEO	[1534]
$0.004710 \pm 0.000590 \pm 0.000230$	OPAL	[1540]
$\mathcal{B}_{17} = \mathcal{B}(\tau^- \to h^- \geq 2\,\pi^0 \nu_\tau)$		
0.1079 ± 0.0010	Average	
0.1081 ± 0.0009	Average with u.c.	
$0.0991 \pm 0.0031 \pm 0.0027$	OPAL	[1532]
$\mathcal{B}_{18} = \mathcal{B}(\tau^- \to h^- 2\,\pi^0 \nu_\tau)$		
0.0946 ± 0.0010	Average	
0.0948 ± 0.0010	Average with u.c.	
$\mathcal{B}_{19} = \mathcal{B}(\tau^- \to h^- 2\,\pi^0 \nu_\tau\,(\text{ex. } K^0))$		
0.0931 ± 0.0010	Average	
0.0932 ± 0.0010	Average with u.c.	
$0.0950 \pm 0.0032 \pm 0.0027$	DELPHI	[1531]
$0.0888 \pm 0.0037 \pm 0.0042$	L3	[1529]
$\mathcal{B}_{19/13} = \frac{\mathcal{B}(\tau^- \to h^- 2\pi^0 \nu_\tau\,(\text{ex. } K^0))}{\mathcal{B}(\tau^- \to h^- \pi^0 \nu_\tau)}$		
0.359 ± 0.005	Average	
0.360 ± 0.004	Average with u.c.	
$0.342 \pm 0.006 \pm 0.016$	CLEO	[1541]
$\mathcal{B}_{20} = \mathcal{B}(\tau^- \to \pi^- 2\,\pi^0 \nu_\tau\,(\text{ex. } K^0))$		
0.0925 ± 0.0010	Average	
0.0926 ± 0.0010	Average with u.c.	
$0.0924 \pm 0.0009 \pm 0.0009$	ALEPH	[1520]
$\mathcal{B}_{23} = \mathcal{B}(\tau^- \to K^- 2\,\pi^0 \nu_\tau\,(\text{ex. } K^0))$		
0.00063 ± 0.00022	Average	
0.00065 ± 0.00022	Average with u.c.	
$0.00056 \pm 0.00020 \pm 0.00015$	ALEPH	[1533]
$0.00090 \pm 0.00100 \pm 0.00030$	CLEO	[1534]
$\mathcal{B}_{24} = \mathcal{B}(\tau^- \to h^- \geq 3\,\pi^0 \nu_\tau)$		
0.0134 ± 0.0007	Average	
0.0134 ± 0.0007	Average with u.c.	
$\mathcal{B}_{25} = \mathcal{B}(\tau^- \to h^- \geq 3\,\pi^0 \nu_\tau\,(\text{ex. } K^0))$		
0.0125 ± 0.0007	Average	
0.0126 ± 0.0007	Average with u.c.	
$0.0140 \pm 0.0021 \pm 0.0022$	DELPHI	[1531]
$\mathcal{B}_{26} = \mathcal{B}(\tau^- \to h^- 3\,\pi^0 \nu_\tau)$		
0.0117 ± 0.0007	Average	
0.0118 ± 0.0007	Average with u.c.	
$0.0170 \pm 0.0024 \pm 0.0038$	L3	[1529]

(Table continued)

TABLE 301. *(Continued)*

Fit parameter	Experiment	References
$\mathcal{B}_{26/13} = \frac{\mathcal{B}(\tau^- \to h^- 3\pi^0 \nu_\tau)}{\mathcal{B}(\tau^- \to h^- \pi^0 \nu_\tau)}$		
0.0453 ± 0.0028	Average	
0.0454 ± 0.0028	Average with u.c.	
$0.0440 \pm 0.0030 \pm 0.0050$	CLEO	[1541]
$\mathcal{B}_{27} = \mathcal{B}(\tau^- \to \pi^- 3\,\pi^0 \nu_\tau\,(\text{ex. } K^0))$		
0.0104 ± 0.0007	Average	
0.0104 ± 0.0007	Average with u.c.	
$0.0098 \pm 0.0007 \pm 0.0006$	ALEPH	[1520]
$\mathcal{B}_{28} = \mathcal{B}(\tau^- \to K^- 3\,\pi^0 \nu_\tau\,(\text{ex. } K^0, \eta))$		
$(0.46 \pm 0.21) \times 10^{-3}$	Average	
$(0.48 \pm 0.21) \times 10^{-3}$	Average with u.c.	
$(0.37 \pm 0.21 \pm 0.11) \times 10^{-3}$	ALEPH	[1533]
$\mathcal{B}_{29} = \mathcal{B}(\tau^- \to h^- 4\,\pi^0 \nu_\tau\,(\text{ex. } K^0))$		
0.0016 ± 0.0004	Average	
0.0016 ± 0.0004	Average with u.c.	
$0.0016 \pm 0.0005 \pm 0.0005$	CLEO	[1541]
$\mathcal{B}_{30} = \mathcal{B}(\tau^- \to h^- 4\,\pi^0 \nu_\tau\,(\text{ex. } K^0, \eta))$		
0.00112 ± 0.00039	Average	
0.00112 ± 0.00039	Average with u.c.	
$0.00112 \pm 0.00037 \pm 0.00035$	ALEPH	[1520]
$\mathcal{B}_{31} = \mathcal{B}(\tau^- \to K^- \geq 0\,\pi^0 \geq 0\,K^0 \geq 0\,\gamma \nu_\tau)$		
0.01548 ± 0.00029	Average	
0.01552 ± 0.00029	Average with u.c.	
$0.01700 \pm 0.00120 \pm 0.00190$	CLEO	[1534]
$0.01540 \pm 0.00240 \pm 0.00000$	DELPHI	[1535]
$0.01528 \pm 0.00039 \pm 0.00040$	OPAL	[1536]
$\mathcal{B}_{32} = \mathcal{B}(\tau^- \to K^- \geq 1(\pi^0 \text{ or } K^0 \text{ or } \gamma)\nu_\tau)$		
0.00856 ± 0.00028	Average	
0.00859 ± 0.00028	Average with u.c.	
$\mathcal{B}_{33} = \mathcal{B}(\tau^- \to K^0_S(\text{particle } s)^- \nu_\tau)$		
0.00937 ± 0.00029	Average	
0.00943 ± 0.00028	Average with u.c.	
$0.00970 \pm 0.00058 \pm 0.00062$	ALEPH	[1542]
$0.00970 \pm 0.00090 \pm 0.00060$	OPAL	[1543]
$\mathcal{B}_{34} = \mathcal{B}(\tau^- \to h^- \bar{K}^0 \nu_\tau)$		
0.00986 ± 0.00014	Average	
0.00987 ± 0.00014	Average with u.c.	
$0.00855 \pm 0.00036 \pm 0.00073$	CLEO	[1544]
$\mathcal{B}_{35} = \mathcal{B}(\tau^- \to \pi^- \bar{K}^0 \nu_\tau)$		
0.008375 ± 0.000139	Average	
0.008384 ± 0.000138	Average with u.c.	
$0.009280 \pm 0.000450 \pm 0.000340$	ALEPH	[1533]
$0.008320 \pm 0.000025 \pm 0.000150$	Belle	[1545]

(Table continued)

TABLE 301. *(Continued)*

Fit parameter	Experiment	References
$0.009500 \pm 0.001500 \pm 0.000600$	L3	[1546]
$0.009330 \pm 0.000680 \pm 0.000490$	OPAL	[1547]
$\mathcal{B}_{37} = \mathcal{B}(\tau^- \to K^- K^0 \nu_\tau)$		
0.001486 ± 0.000034	Average	
0.001486 ± 0.000034	Average with u.c.	
$0.001580 \pm 0.000420 \pm 0.000170$	ALEPH	[1542]
$0.001620 \pm 0.000210 \pm 0.000110$	ALEPH	[1533]
$0.001478 \pm 0.000022 \pm 0.000040$	*BABAR*	[1548]
$0.001480 \pm 0.000013 \pm 0.000055$	Belle	[1545]
$0.001510 \pm 0.000210 \pm 0.000220$	CLEO	[1544]
$\mathcal{B}_{38} = \mathcal{B}(\tau^- \to K^- K^0 \geq 0\,\pi^0 \nu_\tau)$		
0.00298 ± 0.00007	Average	
0.00299 ± 0.00007	Average with u.c.	
$0.00330 \pm 0.00055 \pm 0.00039$	OPAL	[1547]
$\mathcal{B}_{39} = \mathcal{B}(\tau^- \to h^- \bar{K}^0 \pi^0 \nu_\tau)$		
0.00531 ± 0.00013	Average	
0.00532 ± 0.00013	Average with u.c.	
$0.00562 \pm 0.00050 \pm 0.00048$	CLEO	[1544]
$\mathcal{B}_{40} = \mathcal{B}(\tau^- \to \pi^- \bar{K}^0 \pi^0 \nu_\tau)$		
0.003810 ± 0.000129	Average	
0.003817 ± 0.000129	Average with u.c.	
$0.002940 \pm 0.000730 \pm 0.000370$	ALEPH	[1542]
$0.003470 \pm 0.000530 \pm 0.000370$	ALEPH	[1533]
$0.003860 \pm 0.000031 \pm 0.000135$	Belle	[1545]
$0.004100 \pm 0.001200 \pm 0.000300$	L3	[1546]
$\mathcal{B}_{42} = \mathcal{B}(\tau^- \to K^- K^0 \pi^0 \nu_\tau)$		
0.001499 ± 0.000070	Average	
0.001500 ± 0.000070	Average with u.c.	
$0.001520 \pm 0.000760 \pm 0.000210$	ALEPH	[1542]
$0.001430 \pm 0.000250 \pm 0.000150$	ALEPH	[1533]
$0.001496 \pm 0.000019 \pm 0.000073$	Belle	[1545]
$0.001450 \pm 0.000360 \pm 0.000200$	CLEO	[1544]
$\mathcal{B}_{43} = \mathcal{B}(\tau^- \to \pi^- \bar{K}^0 \geq 1\,\pi^0 \nu_\tau)$		
0.00404 ± 0.00026	Average	
0.00408 ± 0.00025	Average with u.c.	
$0.00324 \pm 0.00074 \pm 0.00066$	OPAL	[1547]
$\mathcal{B}_{44} = \mathcal{B}(\tau^- \to \pi^- \bar{K}^0 2\pi^0 \nu_\tau\,(\text{ex. } K^0))$		
$(0.23 \pm 0.23) \times 10^{-3}$	Average	
$(0.26 \pm 0.23) \times 10^{-3}$	Average with u.c.	
$(0.26 \pm 0.24 \pm 0.00) \times 10^{-3}$	ALEPH	[1549]
$\mathcal{B}_{46} = \mathcal{B}(\tau^- \to \pi^- K^0 \bar{K}^0 \nu_\tau)$		
0.00152 ± 0.00025	Average	
0.00155 ± 0.00024	Average with u.c.	

(Table continued)

TABLE 301. *(Continued)*

Fit parameter	Experiment	References
$\mathcal{B}_{47} = \mathcal{B}(\tau^- \to \pi^- K_S^0 K_S^0 \nu_\tau)$		
$(234.8 \pm 6.5) \times 10^{-6}$	Average	
$(234.9 \pm 6.5) \times 10^{-6}$	Average with u.c.	
$(260.0 \pm 100.0 \pm 50.0) \times 10^{-6}$	ALEPH	[1542]
$(231.0 \pm 4.0 \pm 8.0) \times 10^{-6}$	*BABAR*	[1550]
$(233.0 \pm 3.3 \pm 9.3) \times 10^{-6}$	Belle	[1545]
$(230.0 \pm 50.0 \pm 30.0) \times 10^{-6}$	CLEO	[1544]
$\mathcal{B}_{48} = \mathcal{B}(\tau^- \to \pi^- K_S^0 K_L^0 \nu_\tau)$		
0.00105 ± 0.00025	Average	
0.00108 ± 0.00024	Average with u.c.	
$0.00101 \pm 0.00023 \pm 0.00013$	ALEPH	[1542]
$\mathcal{B}_{49} = \mathcal{B}(\tau^- \to \pi^- \pi^0 K^0 \bar{K}^0 \nu_\tau)$		
$(0.35 \pm 0.12) \times 10^{-3}$	Average	
$(0.36 \pm 0.12) \times 10^{-3}$	Average with u.c.	
$\mathcal{B}_{50} = \mathcal{B}(\tau^- \to \pi^- K_S^0 K_S^0 \pi^0 \nu_\tau)$		
$(18.2 \pm 2.1) \times 10^{-6}$	Average	
$(18.2 \pm 2.1) \times 10^{-6}$	Average with u.c.	
$(16.0 \pm 2.0 \pm 2.2) \times 10^{-6}$	*BABAR*	[1550]
$(20.0 \pm 2.2 \pm 2.0) \times 10^{-6}$	Belle	[1545]
$\mathcal{B}_{51} = \mathcal{B}(\tau^- \to \pi^- K_S^0 K_L^0 \pi^0 \nu_\tau)$		
$(0.32 \pm 0.12) \times 10^{-3}$	Average	
$(0.32 \pm 0.12) \times 10^{-3}$	Average with u.c.	
$(0.31 \pm 0.11 \pm 0.05) \times 10^{-3}$	ALEPH	[1542]
$\mathcal{B}_{53} = \mathcal{B}(\tau^- \to \bar{K}^0 h^- h^- h^+ \nu_\tau)$		
$(0.22 \pm 0.20) \times 10^{-3}$	Average	
$(0.22 \pm 0.20) \times 10^{-3}$	Average with u.c.	
$(0.23 \pm 0.19 \pm 0.07) \times 10^{-3}$	ALEPH	[1542]
$\mathcal{B}_{54} = \mathcal{B}(\tau^- \to h^- h^- h^+ \geq 0\,\text{neutrals} \geq 0\, K_L^0 \nu_\tau)$		
0.1519 ± 0.0006	Average	
0.1520 ± 0.0006	Average with u.c.	
$0.1500 \pm 0.0040 \pm 0.0030$	CELLO	[1551]
$0.1440 \pm 0.0060 \pm 0.0030$	L3	[1552]
$0.1510 \pm 0.0080 \pm 0.0060$	TPC	[1553]
$\mathcal{B}_{55} = \mathcal{B}(\tau^- \to h^- h^- h^+ \geq 0\,\text{neutrals}\, \nu_\tau\, (\text{ex.}\, K^0))$		
0.1454 ± 0.0006	Average	
0.1455 ± 0.0006	Average with u.c.	
$0.1456 \pm 0.0010 \pm 0.0008$	L3	[1554]
$0.1496 \pm 0.0009 \pm 0.0022$	OPAL	[1555]
$\mathcal{B}_{56} = \mathcal{B}(\tau^- \to h^- h^- h^+ \nu_\tau)$		
0.0979 ± 0.0005	Average	
0.0980 ± 0.0005	Average with u.c.	

(Table continued)

TABLE 301. *(Continued)*

Fit parameter	Experiment	References
$\mathcal{B}_{57} = \mathcal{B}(\tau^- \to h^-h^-h^+\nu_\tau\,(\text{ex. } K^0))$		
0.0945 ± 0.0005	Average	
0.0945 ± 0.0005	Average with u.c.	
$0.0951 \pm 0.0007 \pm 0.0020$	CLEO	[1556]
$0.0932 \pm 0.0009 \pm 0.0008$	DELPHI	[1531]
$\mathcal{B}_{57/55} = \frac{\mathcal{B}(\tau^- \to h^-h^-h^+\nu_\tau\,(\text{ex. } K^0))}{\mathcal{B}(\tau^- \to h^-h^-h^+ \geq 0\,\text{neutrals}\,\nu_\tau\,(\text{ex. } K^0))}$		
0.6496 ± 0.0031	Average	
0.6498 ± 0.0031	Average with u.c.	
$0.6600 \pm 0.0040 \pm 0.0140$	OPAL	[1555]
$\mathcal{B}_{58} = \mathcal{B}(\tau^- \to h^-h^-h^+\nu_\tau\,(\text{ex. } K^0, \omega))$		
0.0942 ± 0.0005	Average	
0.0942 ± 0.0005	Average with u.c.	
$\mathcal{B}_{59} = \mathcal{B}(\tau^- \to \pi^-\pi^+\pi^-\nu_\tau)$		
0.0930 ± 0.0005	Average	
0.0931 ± 0.0005	Average with u.c.	
$\mathcal{B}_{60} = \mathcal{B}(\tau^- \to \pi^-\pi^+\pi^-\nu_\tau\,(\text{ex. } K^0))$		
0.09010 ± 0.00052	Average	
0.09016 ± 0.00051	Average with u.c.	
$0.08830 \pm 0.00010 \pm 0.00130$	*BABAR*	[1557]
$0.08420 \pm 0.00000^{+0.00260}_{-0.00250}$	Belle	[1558]
$0.09130 \pm 0.00050 \pm 0.00460$	CLEO3	[1559]
$\mathcal{B}_{62} = \mathcal{B}(\tau^- \to \pi^-\pi^+\pi^-\nu_\tau\,(\text{ex. } K^0, \omega))$		
0.0898 ± 0.0005	Average	
0.0899 ± 0.0005	Average with u.c.	
$0.0904 \pm 0.0006 \pm 0.0008$	ALEPH	[1520]
$\mathcal{B}_{63} = \mathcal{B}(\tau^- \to h^-h^-h^+ \geq 1\,\text{neutrals}\,\nu_\tau)$		
0.0529 ± 0.0005	Average	
0.0529 ± 0.0005	Average with u.c.	
$\mathcal{B}_{64} = \mathcal{B}(\tau^- \to h^-h^-h^+ \geq 1\,\pi^0\nu_\tau\,(\text{ex. } K^0))$		
0.0509 ± 0.0005	Average	
0.0509 ± 0.0005	Average with u.c.	
$\mathcal{B}_{65} = \mathcal{B}(\tau^- \to h^-h^-h^+\pi^0\nu_\tau)$		
0.0476 ± 0.0005	Average	
0.0476 ± 0.0005	Average with u.c.	
$\mathcal{B}_{66} = \mathcal{B}(\tau^- \to h^-h^-h^+\pi^0\nu_\tau\,(\text{ex. } K^0))$		
0.0457 ± 0.0005	Average	
0.0457 ± 0.0005	Average with u.c.	
$0.0423 \pm 0.0006 \pm 0.0022$	CLEO	[1556]
$0.0454 \pm 0.0011 \pm 0.0010$	DELPHI	[1531]
$\mathcal{B}_{67} = \mathcal{B}(\tau^- \to h^-h^-h^+\pi^0\nu_\tau\,(\text{ex. } K^0, \omega))$		
0.0279 ± 0.0007	Average	
0.0279 ± 0.0007	Average with u.c.	

(Table continued)

TABLE 301. *(Continued)*

Fit parameter	Experiment	References
$\mathcal{B}_{68} = \mathcal{B}(\tau^- \to \pi^-\pi^+\pi^-\pi^0\nu_\tau)$		
0.0462 ± 0.0005	Average	
0.0462 ± 0.0005	Average with u.c.	
$\mathcal{B}_{69} = \mathcal{B}(\tau^- \to \pi^-\pi^+\pi^-\pi^0\nu_\tau\,(\text{ex. } K^0))$		
0.0449 ± 0.0005	Average	
0.0449 ± 0.0005	Average with u.c.	
$0.0460 \pm 0.0006 \pm 0.0006$	ALEPH	[1520]
$0.0419 \pm 0.0010 \pm 0.0021$	CLEO	[1560]
$\mathcal{B}_{70} = \mathcal{B}(\tau^- \to \pi^-\pi^+\pi^-\pi^0\nu_\tau\,(\text{ex. } K^0, \omega))$		
0.0274 ± 0.0007	Average	
0.0274 ± 0.0007	Average with u.c.	
$\mathcal{B}_{74} = \mathcal{B}(\tau^- \to h^-h^-h^+ \geq 2\,\pi^0\nu_\tau\,(\text{ex. } K^0))$		
0.00515 ± 0.00031	Average	
0.00517 ± 0.00031	Average with u.c.	
$0.00561 \pm 0.00068 \pm 0.00095$	DELPHI	[1531]
$\mathcal{B}_{75} = \mathcal{B}(\tau^- \to h^-h^-h^+2\,\pi^0\nu_\tau)$		
0.00504 ± 0.00031	Average	
0.00505 ± 0.00031	Average with u.c.	
$\mathcal{B}_{76} = \mathcal{B}(\tau^- \to h^-h^-h^+2\pi^0\nu_\tau\,(\text{ex. } K^0))$		
0.00494 ± 0.00031	Average	
0.00495 ± 0.00031	Average with u.c.	
$0.00435 \pm 0.00030 \pm 0.00035$	ALEPH	[1520]
$\mathcal{B}_{76/54} = \frac{\mathcal{B}(\tau^- \to h^-h^-h^+2\pi^0\nu_\tau\,(\text{ex. } K^0))}{\mathcal{B}(\tau^- \to h^-h^-h^+ \geq 0\,\text{neutrals} \geq 0 K_L^0\nu_\tau)}$		
0.0325 ± 0.0020	Average	
0.0326 ± 0.0020	Average with u.c.	
$0.0340 \pm 0.0020 \pm 0.0030$	CLEO	[1561]
$\mathcal{B}_{77} = \mathcal{B}(\tau^- \to h^-h^-h^+2\,\pi^0\nu_\tau\,(\text{ex. } K^0, \omega, \eta))$		
0.0010 ± 0.0004	Average	
0.0010 ± 0.0004	Average with u.c.	
$\mathcal{B}_{78} = \mathcal{B}(\tau^- \to h^-h^-h^+3\,\pi^0\nu_\tau)$		
$(212 \pm 30) \times 10^{-6}$	Average	
$(213 \pm 30) \times 10^{-6}$	Average with u.c.	
$(220 \pm 30 \pm 40) \times 10^{-6}$	CLEO	[1562]
$\mathcal{B}_{79} = \mathcal{B}(\tau^- \to K^-h^-h^+ \geq 0\,\text{neutrals}\,\nu_\tau)$		
0.00628 ± 0.00014	Average	
0.00629 ± 0.00014	Average with u.c.	
$\mathcal{B}_{80} = \mathcal{B}(\tau^- \to K^-\pi^-h^+\nu_\tau\,(\text{ex. } K^0))$		
0.00436 ± 0.00007	Average	
0.00437 ± 0.00007	Average with u.c.	
$\mathcal{B}_{80/60} = \frac{\mathcal{B}(\tau^- \to K^-\pi^-h^+\nu_\tau\,(\text{ex. } K^0))}{\mathcal{B}(\tau^- \to \pi^-\pi^+\pi^-\nu_\tau\,(\text{ex. } K^0))}$		
0.0484 ± 0.0008	Average	
0.0485 ± 0.0008	Average with u.c.	

(Table continued)

TABLE 301. *(Continued)*

Fit parameter	Experiment	References
$0.0544 \pm 0.0021 \pm 0.0053$	CLEO	[1563]
$\mathcal{B}_{81} = \mathcal{B}(\tau^- \to K^-\pi^- h^+ \pi^0 \nu_\tau \,(\text{ex. } K^0))$		
$(0.85 \pm 0.12) \times 10^{-3}$	Average	
$(0.86 \pm 0.12) \times 10^{-3}$	Average with u.c.	
$\mathcal{B}_{81/69} = \frac{\mathcal{B}(\tau^- \to K^-\pi^- h^+ \pi^0 \nu_\tau \,(\text{ex. } K^0))}{\mathcal{B}(\tau^- \to \pi^-\pi^+\pi^-\pi^0 \nu_\tau \,(\text{ex. } K^0))}$		
0.0189 ± 0.0026	Average	
0.0191 ± 0.0026	Average with u.c.	
$0.0261 \pm 0.0045 \pm 0.0042$	CLEO	[1563]
$\mathcal{B}_{82} = \mathcal{B}(\tau^- \to K^-\pi^-\pi^+ \geq 0\,\text{neutrals}\,\nu_\tau)$		
0.00476 ± 0.00014	Average	
0.00477 ± 0.00014	Average with u.c.	
$0.00580^{+0.00150}_{-0.00130} \pm 0.00120$	TPC	[1564]
$\mathcal{B}_{83} = \mathcal{B}(\tau^- \to K^-\pi^-\pi^+ \geq 0\,\pi^0 \nu_\tau \,(\text{ex. } K^0))$		
0.00372 ± 0.00013	Average	
0.00373 ± 0.00013	Average with u.c.	
$\mathcal{B}_{84} = \mathcal{B}(\tau^- \to K^-\pi^-\pi^+ \nu_\tau)$		
0.00344 ± 0.00007	Average	
0.00345 ± 0.00007	Average with u.c.	
$\mathcal{B}_{85} = \mathcal{B}(\tau^- \to K^-\pi^+\pi^- \nu_\tau \,(\text{ex. } K^0))$		
0.002930 ± 0.000068	Average	
0.002933 ± 0.000068	Average with u.c.	
$0.002140 \pm 0.000370 \pm 0.000290$	ALEPH	[1565]
$0.002730 \pm 0.000020 \pm 0.000090$	*BABAR*	[1557]
$0.003300 \pm 0.000010^{+0.000160}_{-0.000170}$	Belle	[1558]
$0.003840 \pm 0.000140 \pm 0.000380$	CLEO3	[1559]
$0.004150 \pm 0.000530 \pm 0.000400$	OPAL	[1540]
$\mathcal{B}_{85/60} = \frac{\mathcal{B}(\tau^- \to K^-\pi^+\pi^- \nu_\tau \,(\text{ex. } K^0))}{\mathcal{B}(\tau^- \to \pi^-\pi^+\pi^- \nu_\tau \,(\text{ex. } K^0))}$		
0.0325 ± 0.0007	Average	
0.0325 ± 0.0007	Average with u.c.	
$\mathcal{B}_{87} = \mathcal{B}(\tau^- \to K^-\pi^-\pi^+\pi^0 \nu_\tau)$		
0.00131 ± 0.00012	Average	
0.00131 ± 0.00012	Average with u.c.	
$\mathcal{B}_{88} = \mathcal{B}(\tau^- \to K^-\pi^-\pi^+\pi^0 \nu_\tau \,(\text{ex. } K^0))$		
$(0.79 \pm 0.12) \times 10^{-3}$	Average	
$(0.80 \pm 0.12) \times 10^{-3}$	Average with u.c.	
$(0.61 \pm 0.39 \pm 0.18) \times 10^{-3}$	ALEPH	[1565]
$(0.74 \pm 0.08 \pm 0.11) \times 10^{-3}$	CLEO3	[1566]
$\mathcal{B}_{89} = \mathcal{B}(\tau^- \to K^-\pi^-\pi^+\pi^0 \nu_\tau \,(\text{ex. } K^0, \eta))$		
$(0.75 \pm 0.12) \times 10^{-3}$	Average	
$(0.76 \pm 0.12) \times 10^{-3}$	Average with u.c.	
$\mathcal{B}_{92} = \mathcal{B}(\tau^- \to \pi^- K^- K^+ \geq 0\,\text{neutrals}\,\nu_\tau)$		
0.001495 ± 0.000033	Average	

(Table continued)

TABLE 301. *(Continued)*

Fit parameter	Experiment	References
0.001496 ± 0.000033	Average with u.c.	
$0.001590 \pm 0.000530 \pm 0.000200$	OPAL	[1567]
$0.001500^{+0.000900}_{-0.000700} \pm 0.000300$	TPC	[1564]
$\mathcal{B}_{93} = \mathcal{B}(\tau^- \to \pi^- K^- K^+ \nu_\tau)$		
0.001434 ± 0.000027	Average	
0.001435 ± 0.000027	Average with u.c.	
$0.001630 \pm 0.000210 \pm 0.000170$	ALEPH	[1565]
$0.001346 \pm 0.000010 \pm 0.000036$	*BABAR*	[1557]
$0.001550 \pm 0.000010^{+0.000060}_{-0.000050}$	Belle	[1558]
$0.001550 \pm 0.000060 \pm 0.000090$	CLEO3	[1559]
$\mathcal{B}_{93/60} = \frac{\mathcal{B}(\tau^- \to \pi^- K^- K^+ \nu_\tau)}{\mathcal{B}(\tau^- \to \pi^- \pi^+ \pi^- \nu_\tau \,(\text{ex. } K^0))}$		
0.01592 ± 0.00030	Average	
0.01592 ± 0.00030	Average with u.c.	
$0.01600 \pm 0.00150 \pm 0.00300$	CLEO	[1563]
$\mathcal{B}_{94} = \mathcal{B}(\tau^- \to \pi^- K^- K^+ \pi^0 \nu_\tau)$		
$(61 \pm 18) \times 10^{-6}$	Average	
$(61 \pm 18) \times 10^{-6}$	Average with u.c.	
$(750 \pm 290 \pm 150) \times 10^{-6}$	ALEPH	[1565]
$(55 \pm 14 \pm 12) \times 10^{-6}$	CLEO3	[1566]
$\mathcal{B}_{94/69} = \frac{\mathcal{B}(\tau^- \to \pi^- K^- K^+ \pi^0 \nu_\tau)}{\mathcal{B}(\tau^- \to \pi^- \pi^+ \pi^- \pi^0 \nu_\tau \,(\text{ex. } K^0))}$		
0.0014 ± 0.0004	Average	
0.0014 ± 0.0004	Average with u.c.	
$0.0079 \pm 0.0044 \pm 0.0016$	CLEO	[1563]
$\mathcal{B}_{96} = \mathcal{B}(\tau^- \to K^- K^- K^+ \nu_\tau)$		
$(21.7 \pm 8.0) \times 10^{-6}$	Average	
$(21.7 \pm 8.0) \times 10^{-6}$	Average with u.c.	
$(15.8 \pm 1.3 \pm 1.2) \times 10^{-6}$	*BABAR*	[1557]
$(32.9 \pm 1.7^{+1.9}_{-2.0}) \times 10^{-6}$	Belle	[1558]
$\mathcal{B}_{102} = \mathcal{B}(\tau^- \to 3h^- 2h^+ \geq 0\,\text{neutrals}\,\nu_\tau \,(\text{ex. } K^0))$		
0.00099 ± 0.00004	Average	
0.00099 ± 0.00004	Average with u.c.	
$0.00097 \pm 0.00005 \pm 0.00011$	CLEO	[1568]
$0.00102 \pm 0.00029 \pm 0.00000$	HRS	[1569]
$0.00170 \pm 0.00022 \pm 0.00026$	L3	[1554]
$\mathcal{B}_{103} = \mathcal{B}(\tau^- \to 3h^- 2h^+ \nu_\tau \,(\text{ex. } K^0))$		
$(828 \pm 31) \times 10^{-6}$	Average	
$(829 \pm 31) \times 10^{-6}$	Average with u.c.	
$(720 \pm 90 \pm 120) \times 10^{-6}$	ALEPH	[1520]
$(640 \pm 230 \pm 100) \times 10^{-6}$	ARGUS	[1570]
$(770 \pm 50 \pm 90) \times 10^{-6}$	CLEO	[1568]
$(970 \pm 150 \pm 50) \times 10^{-6}$	DELPHI	[1531]
$(510 \pm 200 \pm 0) \times 10^{-6}$	HRS	[1569]

(Table continued)

TABLE 301. *(Continued)*

Fit parameter	Experiment	References
$(910 \pm 140 \pm 60) \times 10^{-6}$	OPAL	[1571]
$\mathcal{B}_{104} = \mathcal{B}(\tau^- \to 3h^- 2h^+ \pi^0 \nu_\tau \,(\text{ex. } K^0))$		
$(165 \pm 11) \times 10^{-6}$	Average	
$(165 \pm 11) \times 10^{-6}$	Average with u.c.	
$(210 \pm 70 \pm 90) \times 10^{-6}$	ALEPH	[1520]
$(170 \pm 20 \pm 20) \times 10^{-6}$	CLEO	[1562]
$(160 \pm 120 \pm 60) \times 10^{-6}$	DELPHI	[1531]
$(270 \pm 180 \pm 90) \times 10^{-6}$	OPAL	[1571]
$\mathcal{B}_{106} = \mathcal{B}(\tau^- \to (5\pi)^- \nu_\tau)$		
0.0078 ± 0.0005	Average	
0.0078 ± 0.0005	Average with u.c.	
$\mathcal{B}_{110} = \mathcal{B}(\tau^- \to X_s^- \nu_\tau)$		
0.0291 ± 0.0005	Average	
0.0292 ± 0.0004	Average with u.c.	
$\mathcal{B}_{126} = \mathcal{B}(\tau^- \to \pi^- \pi^0 \eta \nu_\tau)$		
0.001386 ± 0.000072	Average	
0.001389 ± 0.000072	Average with u.c.	
$0.001800 \pm 0.000400 \pm 0.000200$	ALEPH	[1572]
$0.001350 \pm 0.000030 \pm 0.000070$	Belle	[1573]
$0.001700 \pm 0.000200 \pm 0.000200$	CLEO	[1574]
$\mathcal{B}_{128} = \mathcal{B}(\tau^- \to K^- \eta \nu_\tau)$		
$(155 \pm 8) \times 10^{-6}$	Average	
$(155 \pm 8) \times 10^{-6}$	Average with u.c.	
$(290^{+130}_{-120} \pm 70) \times 10^{-6}$	ALEPH	[1572]
$(142 \pm 11 \pm 7) \times 10^{-6}$	*BABAR*	[1575]
$(158 \pm 5 \pm 9) \times 10^{-6}$	Belle	[1573]
$(260 \pm 50 \pm 50) \times 10^{-6}$	CLEO	[1576]
$\mathcal{B}_{130} = \mathcal{B}(\tau^- \to K^- \pi^0 \eta \nu_\tau)$		
$(48 \pm 12) \times 10^{-6}$	Average	
$(48 \pm 12) \times 10^{-6}$	Average with u.c.	
$(46 \pm 11 \pm 4) \times 10^{-6}$	Belle	[1573]
$(177 \pm 56 \pm 71) \times 10^{-6}$	CLEO	[1577]
$\mathcal{B}_{132} = \mathcal{B}(\tau^- \to \pi^- \bar{K}^0 \eta \nu_\tau)$		
$(94 \pm 15) \times 10^{-6}$	Average	
$(94 \pm 15) \times 10^{-6}$	Average with u.c.	
$(88 \pm 14 \pm 6) \times 10^{-6}$	Belle	[1573]
$(220 \pm 70 \pm 22) \times 10^{-6}$	CLEO	[1577]
$\mathcal{B}_{136} = \mathcal{B}(\tau^- \to \pi^- \pi^+ \pi^- \eta \nu_\tau \,(\text{ex. } K^0))$		
$(220 \pm 13) \times 10^{-6}$	Average	
$(220 \pm 13) \times 10^{-6}$	Average with u.c.	
$\mathcal{B}_{149} = \mathcal{B}(\tau^- \to h^- \omega \geq 0 \,\text{neutrals}\, \nu_\tau)$		
0.0240 ± 0.0008	Average	

(Table continued)

TABLE 301. *(Continued)*

Fit parameter	Experiment	References
0.0240 ± 0.0008	Average with u.c.	
$\mathcal{B}_{150} = \mathcal{B}(\tau^- \to h^- \omega \nu_\tau)$		
0.0199 ± 0.0006	Average	
0.0199 ± 0.0006	Average with u.c.	
$0.0191 \pm 0.0007 \pm 0.0006$	ALEPH	[1572]
$0.0160 \pm 0.0027 \pm 0.0041$	CLEO	[1578]
$\mathcal{B}_{150/66} = \frac{\mathcal{B}(\tau^- \to h^- \omega \nu_\tau)}{\mathcal{B}(\tau^- \to h^- h^- h^+ \pi^0 \nu_\tau \,(\text{ex. } K^0))}$		
0.435 ± 0.014	Average	
0.435 ± 0.014	Average with u.c.	
$0.431 \pm 0.033 \pm 0.000$	ALEPH	[1579]
$0.464 \pm 0.016 \pm 0.017$	CLEO	[1556]
$\mathcal{B}_{151} = \mathcal{B}(\tau^- \to K^- \omega \nu_\tau)$		
$(0.41 \pm 0.09) \times 10^{-3}$	Average	
$(0.41 \pm 0.09) \times 10^{-3}$	Average with u.c.	
$(0.41 \pm 0.06 \pm 0.07) \times 10^{-3}$	CLEO3	[1566]
$\mathcal{B}_{152} = \mathcal{B}(\tau^- \to h^- \pi^0 \omega \nu_\tau)$		
0.0041 ± 0.0004	Average	
0.0041 ± 0.0004	Average with u.c.	
$0.0043 \pm 0.0006 \pm 0.0005$	ALEPH	[1572]
$\mathcal{B}_{152/54} = \frac{\mathcal{B}(\tau^- \to h^- \omega \pi^0 \nu_\tau)}{\mathcal{B}(\tau^- \to h^- h^- h^+ \geq 0 \,\text{neutrals} \geq 0 K_L^0 \nu_\tau)}$		
0.0268 ± 0.0028	Average	
0.0269 ± 0.0028	Average with u.c.	
$\mathcal{B}_{152/76} = \frac{\mathcal{B}(\tau^- \to h^- \omega \pi^0 \nu_\tau)}{\mathcal{B}(\tau^- \to h^- h^- h^+ 2\pi^0 \nu_\tau \,(\text{ex. } K^0))}$		
0.82 ± 0.08	Average	
0.82 ± 0.08	Average with u.c.	
$0.81 \pm 0.06 \pm 0.06$	CLEO	[1561]
$\mathcal{B}_{167} = \mathcal{B}(\tau^- \to K^- \phi \nu_\tau)$		
$(44 \pm 16) \times 10^{-6}$	Average	
$(44 \pm 16) \times 10^{-6}$	Average with u.c.	
$\mathcal{B}_{168} = \mathcal{B}(\tau^- \to K^- \phi(K^+ K^-) \nu_\tau)$		
$(22 \pm 8) \times 10^{-6}$	Average	
$(22 \pm 8) \times 10^{-6}$	Average with u.c.	
$\mathcal{B}_{169} = \mathcal{B}(\tau^- \to K^- \phi(K_S^0 K_L^0) \nu_\tau)$		
$(15 \pm 6) \times 10^{-6}$	Average	
$(15 \pm 6) \times 10^{-6}$	Average with u.c.	
$\mathcal{B}_{800} = \mathcal{B}(\tau^- \to \pi^- \omega \nu_\tau)$		
0.0195 ± 0.0006	Average	
0.0195 ± 0.0006	Average with u.c.	
$\mathcal{B}_{802} = \mathcal{B}(\tau^- \to K^- \pi^- \pi^+ \nu_\tau \,(\text{ex. } K^0, \omega))$		
0.00292 ± 0.00007	Average	
0.00293 ± 0.00007	Average with u.c.	

(Table continued)

TABLE 301. *(Continued)*

Fit parameter	Experiment	References
$\mathcal{B}_{803} = \mathcal{B}(\tau^- \to K^-\pi^-\pi^+\pi^0\nu_\tau\,(\text{ex. } K^0, \omega, \eta))$		
$(0.39 \pm 0.14) \times 10^{-3}$	Average	
$(0.39 \pm 0.14) \times 10^{-3}$	Average with u.c.	
$\mathcal{B}_{804} = \mathcal{B}(\tau^- \to \pi^- K_L^0 K_L^0 \nu_\tau)$		
$(235 \pm 6) \times 10^{-6}$	Average	
$(235 \pm 6) \times 10^{-6}$	Average with u.c.	
$\mathcal{B}_{805} = \mathcal{B}(\tau^- \to a_1^-(\pi^-\gamma)\nu_\tau)$		
$(0.38 \pm 0.15) \times 10^{-3}$	Average	
$(0.40 \pm 0.15) \times 10^{-3}$	Average with u.c.	
$\mathcal{B}_{806} = \mathcal{B}(\tau^- \to \pi^- K_L^0 K_L^0 \pi^0 \nu_\tau)$		
$(18.2 \pm 2.1) \times 10^{-6}$	Average	
$(18.2 \pm 2.1) \times 10^{-6}$	Average with u.c.	
$\mathcal{B}_{810} = \mathcal{B}(\tau^- \to 2\pi^-\pi^+ 3\pi^0 \nu_\tau\,(\text{ex. } K^0))$		
$(194 \pm 30) \times 10^{-6}$	Average	
$(194 \pm 30) \times 10^{-6}$	Average with u.c.	
$\mathcal{B}_{811} = \mathcal{B}(\tau^- \to \pi^- 2\pi^0 \omega \nu_\tau)$		
$(72 \pm 16) \times 10^{-6}$	Average	
$(72 \pm 16) \times 10^{-6}$	Average with u.c.	
$(73 \pm 12 \pm 12) \times 10^{-6}$	*BABAR*	[1580]
$\mathcal{B}_{812} = \mathcal{B}(\tau^- \to 2\,\pi^-\pi^+ 3\,\pi^0 \nu_\tau\,(\text{ex. } K^0, \eta, \omega, f_1))$		
$(14 \pm 27) \times 10^{-6}$	Average	
$(14 \pm 27) \times 10^{-6}$	Average with u.c.	
$(10 \pm 8 \pm 30) \times 10^{-6}$	*BABAR*	[1580]
$\mathcal{B}_{820} = \mathcal{B}(\tau^- \to 3\,\pi^- 2\,\pi^+ \nu_\tau\,(\text{ex. } K^0, \omega))$		
$(826 \pm 31) \times 10^{-6}$	Average	
$(827 \pm 31) \times 10^{-6}$	Average with u.c.	
$\mathcal{B}_{821} = \mathcal{B}(\tau^- \to 3\,\pi^- 2\,\pi^+ \nu_\tau\,(\text{ex. } K^0, \omega, f_1))$		
$(774 \pm 30) \times 10^{-6}$	Average	
$(775 \pm 30) \times 10^{-6}$	Average with u.c.	
$(768 \pm 4 \pm 40) \times 10^{-6}$	*BABAR*	[1580]
$\mathcal{B}_{822} = \mathcal{B}(\tau^- \to K^- 2\,\pi^- 2\,\pi^+ \nu_\tau\,(\text{ex. } K^0))$		
$(0.6 \pm 1.2) \times 10^{-6}$	Average	
$(0.6 \pm 1.2) \times 10^{-6}$	Average with u.c.	
$(0.6 \pm 0.5 \pm 1.1) \times 10^{-6}$	*BABAR*	[1580]
$\mathcal{B}_{830} = \mathcal{B}(\tau^- \to 3\,\pi^- 2\,\pi^+ \pi^0 \nu_\tau\,(\text{ex. } K^0))$		
$(163 \pm 11) \times 10^{-6}$	Average	
$(164 \pm 11) \times 10^{-6}$	Average with u.c.	
$\mathcal{B}_{831} = \mathcal{B}(\tau^- \to 2\,\pi^-\pi^+ \omega \nu_\tau\,(\text{ex. } K^0))$		
$(84 \pm 6) \times 10^{-6}$	Average	
$(84 \pm 6) \times 10^{-6}$	Average with u.c.	
$(84 \pm 4 \pm 6) \times 10^{-6}$	*BABAR*	[1580]

(Table continued)

TABLE 301. *(Continued)*

Fit parameter	Experiment	References
$\mathcal{B}_{832} = \mathcal{B}(\tau^- \to 3\pi^- 2\pi^+\pi^0\nu_\tau\,(\text{ex. } K^0, \eta, \omega, f_1))$		
$(37.7 \pm 8.7) \times 10^{-6}$	Average	
$(37.7 \pm 8.7) \times 10^{-6}$	Average with u.c.	
$(36.0 \pm 3.0 \pm 9.0) \times 10^{-6}$	*BABAR*	[1580]
$\mathcal{B}_{833} = \mathcal{B}(\tau^- \to K^- 2\pi^- 2\pi^+\pi^0\nu_\tau\,(\text{ex. } K^0))$		
$(1.1 \pm 0.6) \times 10^{-6}$	Average	
$(1.1 \pm 0.6) \times 10^{-6}$	Average with u.c.	
$(1.1 \pm 0.4 \pm 0.4) \times 10^{-6}$	*BABAR*	[1580]
$\mathcal{B}_{910} = \mathcal{B}(\tau^- \to 2\pi^-\pi^+\eta(3\pi^0)\nu_\tau\,(\text{ex. } K^0))$		
$(72 \pm 4) \times 10^{-6}$	Average	
$(72 \pm 4) \times 10^{-6}$	Average with u.c.	
$(83 \pm 9 \pm 8) \times 10^{-6}$	*BABAR*	[1580]
$\mathcal{B}_{911} = \mathcal{B}(\tau^- \to \pi^- 2\pi^0\eta(\pi^+\pi^-\pi^0)\nu_\tau\,(\text{ex. } K^0))$		
$(45 \pm 9) \times 10^{-6}$	Average	
$(45 \pm 9) \times 10^{-6}$	Average with u.c.	
$(46 \pm 8 \pm 5) \times 10^{-6}$	*BABAR*	[1580]
$\mathcal{B}_{920} = \mathcal{B}(\tau^- \to \pi^- f_1(2\pi^- 2\pi^+)\nu_\tau)$		
$(52.4 \pm 4.4) \times 10^{-6}$	Average	
$(52.4 \pm 4.4) \times 10^{-6}$	Average with u.c.	
$(52.0 \pm 3.1 \pm 3.7) \times 10^{-6}$	*BABAR*	[1580]
$\mathcal{B}_{930} = \mathcal{B}(\tau^- \to 2\pi^-\pi^+\eta(\pi^+\pi^-\pi^0)\nu_\tau\,(\text{ex. } K^0))$		
$(50.7 \pm 3.0) \times 10^{-6}$	Average	
$(50.7 \pm 3.0) \times 10^{-6}$	Average with u.c.	
$(53.9 \pm 2.7 \pm 4.1) \times 10^{-6}$	*BABAR*	[1580]
$\mathcal{B}_{944} = \mathcal{B}(\tau^- \to 2\pi^-\pi^+\eta(\gamma\gamma)\nu_\tau\,(\text{ex. } K^0))$		
$(86.6 \pm 5.1) \times 10^{-6}$	Average	
$(86.8 \pm 5.1) \times 10^{-6}$	Average with u.c.	
$(82.6 \pm 3.5 \pm 5.1) \times 10^{-6}$	*BABAR*	[1580]
$\mathcal{B}_{945} = \mathcal{B}(\tau^- \to \pi^- 2\pi^0\eta\nu_\tau\,(\text{ex. } K^0))$		
$(0.19 \pm 0.04) \times 10^{-3}$	Average	
$(0.19 \pm 0.04) \times 10^{-3}$	Average with u.c.	
$\mathcal{B}_{\text{ur}} = \mathcal{B}(\tau^-\text{unitarity residual})$		
0.0007 ± 0.0011	Average	
0.0	Average with u.c.	
$\mathcal{B}_{\text{all}} = \mathcal{B}(\tau^- \to \text{all modes})$		
0.9993 ± 0.0011	Average	
1.0	Average with u.c.	

The equations involve fit parameters associated to τ branching fractions, nuisance fit parameters, external parameters corresponding to non-τ branching fractions (like $\mathcal{B}_{K_S\to\pi^0\pi^0}$), probabilities corresponding to squared moduli of amplitudes of quantum state mixtures, such as K^0, $\bar{K}^0$, K_S, K_L. The probabilities are denoted with, e.g., $\mathcal{B}_{\langle K^0|K_S\rangle} = |\langle K^0|K_S\rangle|^2$. The values of all non-$\tau$ quantities are taken from the PDG 2022 and 2023 update [302] averages.

TABLE 302. Nuisance fit parameter of the τ branching fractions fit.

Nuisance fit parameter	Experiment	Reference
$\mathcal{B}_{980} = \mathcal{B}(a_1^- \to \pi^-\gamma)$		
0.0021 ± 0.0008	Average	
$0.0021 \pm 0.0008 \pm 0.0000$	ALEPH	[1520]

$$
\begin{aligned}
\mathcal{B}_1 &= \mathcal{B}_3 + \mathcal{B}_5 + \mathcal{B}_9 + \mathcal{B}_{10} + \mathcal{B}_{14} + \mathcal{B}_{16} + \mathcal{B}_{20} + \mathcal{B}_{23} + \mathcal{B}_{27} + \mathcal{B}_{28} + \mathcal{B}_{30} + \mathcal{B}_{35} + \mathcal{B}_{40} + \mathcal{B}_{44} + \mathcal{B}_{37} \\
&\quad + \mathcal{B}_{42} + \mathcal{B}_{47} + \mathcal{B}_{48} + \mathcal{B}_{804} + \mathcal{B}_{50} + \mathcal{B}_{51} + \mathcal{B}_{806} + \mathcal{B}_{126}\cdot\mathcal{B}_{\eta\to\text{neutral}} + \mathcal{B}_{128}\cdot\mathcal{B}_{\eta\to\text{neutral}} \\
&\quad + \mathcal{B}_{130}\cdot\mathcal{B}_{\eta\to\text{neutral}} + \mathcal{B}_{132}\cdot\mathcal{B}_{\eta\to\text{neutral}} + \mathcal{B}_{800}\cdot\mathcal{B}_{\omega\to\pi^0\gamma} + \mathcal{B}_{151}\cdot\mathcal{B}_{\omega\to\pi^0\gamma} + \mathcal{B}_{152}\cdot\mathcal{B}_{\omega\to\pi^0\gamma} + \mathcal{B}_{167}\cdot\mathcal{B}_{\phi\to K_SK_L} \\
\mathcal{B}_2 &= \mathcal{B}_3 + \mathcal{B}_5 + \mathcal{B}_9 + \mathcal{B}_{10} + \mathcal{B}_{14} + \mathcal{B}_{16} + \mathcal{B}_{20} + \mathcal{B}_{23} + \mathcal{B}_{27} + \mathcal{B}_{28} + \mathcal{B}_{30} + \mathcal{B}_{35}\cdot(\mathcal{B}_{\langle\bar{K}^0|K_S\rangle}\cdot\mathcal{B}_{K_S\to\pi^0\pi^0} + \mathcal{B}_{\langle\bar{K}^0|K_L\rangle}) \\
&\quad + \mathcal{B}_{40}\cdot(\mathcal{B}_{\langle\bar{K}^0|K_S\rangle}\cdot\mathcal{B}_{K_S\to\pi^0\pi^0} + \mathcal{B}_{\langle\bar{K}^0|K_L\rangle}) + \mathcal{B}_{44}\cdot(\mathcal{B}_{\langle\bar{K}^0|K_S\rangle}\cdot\mathcal{B}_{K_S\to\pi^0\pi^0} + \mathcal{B}_{\langle\bar{K}^0|K_L\rangle}) \\
&\quad + \mathcal{B}_{37}\cdot(\mathcal{B}_{\langle\bar{K}^0|K_S\rangle}\cdot\mathcal{B}_{K_S\to\pi^0\pi^0} + \mathcal{B}_{\langle\bar{K}^0|K_L\rangle}) + \mathcal{B}_{42}\cdot(\mathcal{B}_{\langle\bar{K}^0|K_S\rangle}\cdot\mathcal{B}_{K_S\to\pi^0\pi^0} + \mathcal{B}_{\langle\bar{K}^0|K_L\rangle}) + \mathcal{B}_{47}\cdot(\mathcal{B}_{K_S\to\pi^0\pi^0}\cdot\mathcal{B}_{K_S\to\pi^0\pi^0}) \\
&\quad + \mathcal{B}_{48}\cdot\mathcal{B}_{K_S\to\pi^0\pi^0} + \mathcal{B}_{804} + \mathcal{B}_{50}\cdot(\mathcal{B}_{K_S\to\pi^0\pi^0}\cdot\mathcal{B}_{K_S\to\pi^0\pi^0}) + \mathcal{B}_{51}\cdot\mathcal{B}_{K_S\to\pi^0\pi^0} + \mathcal{B}_{806} + \mathcal{B}_{126}\cdot\mathcal{B}_{\eta\to\text{neutral}} \\
&\quad + \mathcal{B}_{128}\cdot\mathcal{B}_{\eta\to\text{neutral}} + \mathcal{B}_{130}\cdot\mathcal{B}_{\eta\to\text{neutral}} + \mathcal{B}_{132}\cdot(\mathcal{B}_{\eta\to\text{neutral}}\cdot(\mathcal{B}_{\langle\bar{K}^0|K_S\rangle}\cdot\mathcal{B}_{K_S\to\pi^0\pi^0} + \mathcal{B}_{\langle\bar{K}^0|K_L\rangle})) \\
&\quad + \mathcal{B}_{800}\cdot\mathcal{B}_{\omega\to\pi^0\gamma} + \mathcal{B}_{151}\cdot\mathcal{B}_{\omega\to\pi^0\gamma} + \mathcal{B}_{152}\cdot\mathcal{B}_{\omega\to\pi^0\gamma} + \mathcal{B}_{167}\cdot(\mathcal{B}_{\phi\to K_SK_L}\cdot\mathcal{B}_{K_S\to\pi^0\pi^0}) \\
\mathcal{B}_{3/5} &= \frac{\mathcal{B}_3}{\mathcal{B}_5} \\
\mathcal{B}_7 &= \mathcal{B}_{35}\cdot\mathcal{B}_{\langle\bar{K}^0|K_L\rangle} + \mathcal{B}_9 + \mathcal{B}_{804} + \mathcal{B}_{37}\cdot\mathcal{B}_{\langle K^0|K_L\rangle} + \mathcal{B}_{10} \\
\mathcal{B}_8 &= \mathcal{B}_9 + \mathcal{B}_{10} \\
\mathcal{B}_{8/5} &= \frac{\mathcal{B}_8}{\mathcal{B}_5} \\
\mathcal{B}_{9/5} &= \frac{\mathcal{B}_9}{\mathcal{B}_5} \\
\mathcal{B}_{10/5} &= \frac{\mathcal{B}_{10}}{\mathcal{B}_5} \\
\mathcal{B}_{10/9} &= \frac{\mathcal{B}_{10}}{\mathcal{B}_9} \\
\mathcal{B}_{11} &= \mathcal{B}_{14} + \mathcal{B}_{16} + \mathcal{B}_{20} + \mathcal{B}_{23} + \mathcal{B}_{27} + \mathcal{B}_{28} + \mathcal{B}_{30} + \mathcal{B}_{35}\cdot(\mathcal{B}_{\langle K^0|K_S\rangle}\cdot\mathcal{B}_{K_S\to\pi^0\pi^0}) + \mathcal{B}_{37}\cdot(\mathcal{B}_{\langle K^0|K_S\rangle}\cdot\mathcal{B}_{K_S\to\pi^0\pi^0}) \\
&\quad + \mathcal{B}_{40}\cdot(\mathcal{B}_{\langle K^0|K_S\rangle}\cdot\mathcal{B}_{K_S\to\pi^0\pi^0}) + \mathcal{B}_{42}\cdot(\mathcal{B}_{\langle K^0|K_S\rangle}\cdot\mathcal{B}_{K_S\to\pi^0\pi^0}) + \mathcal{B}_{47}\cdot(\mathcal{B}_{K_S\to\pi^0\pi^0}\cdot\mathcal{B}_{K_S\to\pi^0\pi^0}) \\
&\quad + \mathcal{B}_{50}\cdot(\mathcal{B}_{K_S\to\pi^0\pi^0}\cdot\mathcal{B}_{K_S\to\pi^0\pi^0}) + \mathcal{B}_{126}\cdot\mathcal{B}_{\eta\to\text{neutral}} + \mathcal{B}_{128}\cdot\mathcal{B}_{\eta\to\text{neutral}} + \mathcal{B}_{130}\cdot\mathcal{B}_{\eta\to\text{neutral}} \\
&\quad + \mathcal{B}_{132}\cdot(\mathcal{B}_{\langle K^0|K_S\rangle}\cdot\mathcal{B}_{K_S\to\pi^0\pi^0}\cdot\mathcal{B}_{\eta\to\text{neutral}}) + \mathcal{B}_{151}\cdot\mathcal{B}_{\omega\to\pi^0\gamma} + \mathcal{B}_{152}\cdot\mathcal{B}_{\omega\to\pi^0\gamma} + \mathcal{B}_{800}\cdot\mathcal{B}_{\omega\to\pi^0\gamma} \\
\mathcal{B}_{12} &= \mathcal{B}_{128}\cdot\mathcal{B}_{\eta\to3\pi^0} + \mathcal{B}_{30} + \mathcal{B}_{23} + \mathcal{B}_{28} + \mathcal{B}_{14} + \mathcal{B}_{16} + \mathcal{B}_{20} + \mathcal{B}_{27} + \mathcal{B}_{126}\cdot\mathcal{B}_{\eta\to3\pi^0} + \mathcal{B}_{130}\cdot\mathcal{B}_{\eta\to3\pi^0} \\
\mathcal{B}_{13} &= \mathcal{B}_{14} + \mathcal{B}_{16} \\
\mathcal{B}_{17} &= \mathcal{B}_{128}\cdot\mathcal{B}_{\eta\to3\pi^0} + \mathcal{B}_{30} + \mathcal{B}_{23} + \mathcal{B}_{28} + \mathcal{B}_{35}\cdot(\mathcal{B}_{\langle K^0|K_S\rangle}\cdot\mathcal{B}_{K_S\to\pi^0\pi^0}) + \mathcal{B}_{40}\cdot(\mathcal{B}_{\langle K^0|K_S\rangle}\cdot\mathcal{B}_{K_S\to\pi^0\pi^0}) \\
&\quad + \mathcal{B}_{42}\cdot(\mathcal{B}_{\langle K^0|K_S\rangle}\cdot\mathcal{B}_{K_S\to\pi^0\pi^0}) + \mathcal{B}_{20} + \mathcal{B}_{27} + \mathcal{B}_{47}\cdot(\mathcal{B}_{K_S\to\pi^0\pi^0}\cdot\mathcal{B}_{K_S\to\pi^0\pi^0}) + \mathcal{B}_{50}\cdot(\mathcal{B}_{K_S\to\pi^0\pi^0}\cdot\mathcal{B}_{K_S\to\pi^0\pi^0}) \\
&\quad + \mathcal{B}_{126}\cdot\mathcal{B}_{\eta\to3\pi^0} + \mathcal{B}_{37}\cdot(\mathcal{B}_{\langle K^0|K_S\rangle}\cdot\mathcal{B}_{K_S\to\pi^0\pi^0}) + \mathcal{B}_{130}\cdot\mathcal{B}_{\eta\to3\pi^0}
\end{aligned}
$$

$$\mathcal{B}_{18} = \mathcal{B}_{23} + \mathcal{B}_{35} \cdot (\mathcal{B}_{\langle K^0|K_S\rangle} \cdot \mathcal{B}_{K_S\to\pi^0\pi^0}) + \mathcal{B}_{20} + \mathcal{B}_{37} \cdot (\mathcal{B}_{\langle K^0|K_S\rangle} \cdot \mathcal{B}_{K_S\to\pi^0\pi^0})$$

$$\mathcal{B}_{19} = \mathcal{B}_{23} + \mathcal{B}_{20}$$

$$\mathcal{B}_{19/13} = \frac{\mathcal{B}_{19}}{\mathcal{B}_{13}}$$

$$\mathcal{B}_{24} = \mathcal{B}_{27} + \mathcal{B}_{28} + \mathcal{B}_{30} + \mathcal{B}_{40} \cdot (\mathcal{B}_{\langle K^0|K_S\rangle} \cdot \mathcal{B}_{K_S\to\pi^0\pi^0}) + \mathcal{B}_{42} \cdot (\mathcal{B}_{\langle K^0|K_S\rangle} \cdot \mathcal{B}_{K_S\to\pi^0\pi^0}) + \mathcal{B}_{47} \cdot (\mathcal{B}_{K_S\to\pi^0\pi^0} \cdot \mathcal{B}_{K_S\to\pi^0\pi^0}) + \mathcal{B}_{50} \cdot (\mathcal{B}_{K_S\to\pi^0\pi^0} \cdot \mathcal{B}_{K_S\to\pi^0\pi^0}) + \mathcal{B}_{126} \cdot \mathcal{B}_{\eta\to 3\pi^0} + \mathcal{B}_{128} \cdot \mathcal{B}_{\eta\to 3\pi^0} + \mathcal{B}_{130} \cdot \mathcal{B}_{\eta\to 3\pi^0} + \mathcal{B}_{132} \cdot (\mathcal{B}_{\langle K^0|K_S\rangle} \cdot \mathcal{B}_{K_S\to\pi^0\pi^0} \cdot \mathcal{B}_{\eta\to 3\pi^0})$$

$$\mathcal{B}_{25} = \mathcal{B}_{128} \cdot \mathcal{B}_{\eta\to 3\pi^0} + \mathcal{B}_{30} + \mathcal{B}_{28} + \mathcal{B}_{27} + \mathcal{B}_{126} \cdot \mathcal{B}_{\eta\to 3\pi^0} + \mathcal{B}_{130} \cdot \mathcal{B}_{\eta\to 3\pi^0}$$

$$\mathcal{B}_{26} = \mathcal{B}_{128} \cdot \mathcal{B}_{\eta\to 3\pi^0} + \mathcal{B}_{28} + \mathcal{B}_{40} \cdot (\mathcal{B}_{\langle K^0|K_S\rangle} \cdot \mathcal{B}_{K_S\to\pi^0\pi^0}) + \mathcal{B}_{42} \cdot (\mathcal{B}_{\langle K^0|K_S\rangle} \cdot \mathcal{B}_{K_S\to\pi^0\pi^0}) + \mathcal{B}_{27}$$

$$\mathcal{B}_{26/13} = \frac{\mathcal{B}_{26}}{\mathcal{B}_{13}}$$

$$\mathcal{B}_{29} = \mathcal{B}_{30} + \mathcal{B}_{126} \cdot \mathcal{B}_{\eta\to 3\pi^0} + \mathcal{B}_{130} \cdot \mathcal{B}_{\eta\to 3\pi^0}$$

$$\mathcal{B}_{31} = \mathcal{B}_{128} \cdot \mathcal{B}_{\eta\to\text{neutral}} + \mathcal{B}_{23} + \mathcal{B}_{28} + \mathcal{B}_{42} + \mathcal{B}_{16} + \mathcal{B}_{37} + \mathcal{B}_{10} + \mathcal{B}_{167} \cdot (\mathcal{B}_{\phi\to K_S K_L} \cdot \mathcal{B}_{K_S\to\pi^0\pi^0})$$

$$\mathcal{B}_{32} = \mathcal{B}_{16} + \mathcal{B}_{23} + \mathcal{B}_{28} + \mathcal{B}_{37} + \mathcal{B}_{42} + \mathcal{B}_{128} \cdot \mathcal{B}_{\eta\to\text{neutral}} + \mathcal{B}_{130} \cdot \mathcal{B}_{\eta\to\text{neutral}} + \mathcal{B}_{167} \cdot (\mathcal{B}_{\phi\to K_S K_L} \cdot \mathcal{B}_{K_S\to\pi^0\pi^0})$$

$$\mathcal{B}_{33} = \mathcal{B}_{35} \cdot \mathcal{B}_{\langle \bar{K}^0|K_S\rangle} + \mathcal{B}_{40} \cdot \mathcal{B}_{\langle \bar{K}^0|K_S\rangle} + \mathcal{B}_{42} \cdot \mathcal{B}_{\langle K^0|K_S\rangle} + \mathcal{B}_{47} + \mathcal{B}_{48} + \mathcal{B}_{50} + \mathcal{B}_{51} + \mathcal{B}_{37} \cdot \mathcal{B}_{\langle K^0|K_S\rangle} + \mathcal{B}_{132} \cdot (\mathcal{B}_{\langle \bar{K}^0|K_S\rangle} \cdot \mathcal{B}_{\eta\to\text{neutral}}) + \mathcal{B}_{44} \cdot \mathcal{B}_{\langle \bar{K}^0|K_S\rangle} + \mathcal{B}_{167} \cdot \mathcal{B}_{\phi\to K_S K_L}$$

$$\mathcal{B}_{34} = \mathcal{B}_{35} + \mathcal{B}_{37}$$

$$\mathcal{B}_{38} = \mathcal{B}_{42} + \mathcal{B}_{37}$$

$$\mathcal{B}_{39} = \mathcal{B}_{40} + \mathcal{B}_{42}$$

$$\mathcal{B}_{43} = \mathcal{B}_{40} + \mathcal{B}_{44}$$

$$\mathcal{B}_{46} = \mathcal{B}_{48} + \mathcal{B}_{47} + \mathcal{B}_{804}$$

$$\mathcal{B}_{49} = \mathcal{B}_{50} + \mathcal{B}_{51} + \mathcal{B}_{806}$$

$$\mathcal{B}_{54} = \mathcal{B}_{35} \cdot (\mathcal{B}_{\langle K^0|K_S\rangle} \cdot \mathcal{B}_{K_S\to\pi^+\pi^-}) + \mathcal{B}_{37} \cdot (\mathcal{B}_{\langle K^0|K_S\rangle} \cdot \mathcal{B}_{K_S\to\pi^+\pi^-}) + \mathcal{B}_{40} \cdot (\mathcal{B}_{\langle K^0|K_S\rangle} \cdot \mathcal{B}_{K_S\to\pi^+\pi^-}) + \mathcal{B}_{42} \cdot (\mathcal{B}_{\langle K^0|K_S\rangle} \cdot \mathcal{B}_{K_S\to\pi^+\pi^-}) + \mathcal{B}_{47} \cdot (2 \cdot \mathcal{B}_{K_S\to\pi^+\pi^-} \cdot \mathcal{B}_{K_S\to\pi^0\pi^0}) + \mathcal{B}_{48} \cdot \mathcal{B}_{K_S\to\pi^+\pi^-} + \mathcal{B}_{50} \cdot (2 \cdot \mathcal{B}_{K_S\to\pi^+\pi^-} \cdot \mathcal{B}_{K_S\to\pi^0\pi^0}) + \mathcal{B}_{51} \cdot \mathcal{B}_{K_S\to\pi^+\pi^-} + \mathcal{B}_{53} \cdot (\mathcal{B}_{\langle \bar{K}^0|K_S\rangle} \cdot \mathcal{B}_{K_S\to\pi^0\pi^0} + \mathcal{B}_{\langle \bar{K}^0|K_L\rangle}) + \mathcal{B}_{62} + \mathcal{B}_{70} + \mathcal{B}_{77} + \mathcal{B}_{78} + \mathcal{B}_{93} + \mathcal{B}_{94} + \mathcal{B}_{126} \cdot \mathcal{B}_{\eta\to\text{charged}} + \mathcal{B}_{128} \cdot \mathcal{B}_{\eta\to\text{charged}} + \mathcal{B}_{130} \cdot \mathcal{B}_{\eta\to\text{charged}} + \mathcal{B}_{132} \cdot (\mathcal{B}_{\langle \bar{K}^0|K_L\rangle} \cdot \mathcal{B}_{\eta\to\pi^+\pi^-\pi^0} + \mathcal{B}_{\langle \bar{K}^0|K_S\rangle} \cdot \mathcal{B}_{K_S\to\pi^0\pi^0} \cdot \mathcal{B}_{\eta\to\pi^+\pi^-\pi^0} + \mathcal{B}_{\langle \bar{K}^0|K_S\rangle} \cdot \mathcal{B}_{K_S\to\pi^+\pi^-} \cdot \mathcal{B}_{\eta\to 3\pi^0}) + \mathcal{B}_{151} \cdot (\mathcal{B}_{\omega\to\pi^+\pi^-\pi^0} + \mathcal{B}_{\omega\to\pi^+\pi^-}) + \mathcal{B}_{152} \cdot (\mathcal{B}_{\omega\to\pi^+\pi^-\pi^0} + \mathcal{B}_{\omega\to\pi^+\pi^-}) + \mathcal{B}_{167} \cdot (\mathcal{B}_{\phi\to K^+K^-} + \mathcal{B}_{\phi\to K_S K_L} \cdot \mathcal{B}_{K_S\to\pi^+\pi^-}) + \mathcal{B}_{802} + \mathcal{B}_{803} + \mathcal{B}_{800} \cdot (\mathcal{B}_{\omega\to\pi^+\pi^-\pi^0} + \mathcal{B}_{\omega\to\pi^+\pi^-})$$

$$\begin{aligned}
\mathcal{B}_{55} &= \mathcal{B}_{128}\cdot\mathcal{B}_{\eta\to\text{charged}} + \mathcal{B}_{152}\cdot(\mathcal{B}_{\omega\to\pi^+\pi^-\pi^0}+\mathcal{B}_{\omega\to\pi^+\pi^-}) + \mathcal{B}_{78} + \mathcal{B}_{77} + \mathcal{B}_{94} + \mathcal{B}_{62} + \mathcal{B}_{70} + \mathcal{B}_{93}\\
&\quad + \mathcal{B}_{126}\cdot\mathcal{B}_{\eta\to\text{charged}} + \mathcal{B}_{802} + \mathcal{B}_{803} + \mathcal{B}_{800}\cdot(\mathcal{B}_{\omega\to\pi^+\pi^-\pi^0}+\mathcal{B}_{\omega\to\pi^+\pi^-}) + \mathcal{B}_{151}\cdot(\mathcal{B}_{\omega\to\pi^+\pi^-\pi^0}+\mathcal{B}_{\omega\to\pi^+\pi^-})\\
&\quad + \mathcal{B}_{130}\cdot\mathcal{B}_{\eta\to\text{charged}} + \mathcal{B}_{168}\\
\mathcal{B}_{56} &= \mathcal{B}_{35}\cdot(\mathcal{B}_{\langle K^0|K_S\rangle}\cdot\mathcal{B}_{K_S\to\pi^+\pi^-}) + \mathcal{B}_{62} + \mathcal{B}_{93} + \mathcal{B}_{37}\cdot(\mathcal{B}_{\langle K^0|K_S\rangle}\cdot\mathcal{B}_{K_S\to\pi^+\pi^-}) + \mathcal{B}_{802} + \mathcal{B}_{800}\cdot\mathcal{B}_{\omega\to\pi^+\pi^-}\\
&\quad + \mathcal{B}_{151}\cdot\mathcal{B}_{\omega\to\pi^+\pi^-} + \mathcal{B}_{168}\\
\mathcal{B}_{57} &= \mathcal{B}_{62} + \mathcal{B}_{93} + \mathcal{B}_{802} + \mathcal{B}_{800}\cdot\mathcal{B}_{\omega\to\pi^+\pi^-} + \mathcal{B}_{151}\cdot\mathcal{B}_{\omega\to\pi^+\pi^-} + \mathcal{B}_{167}\cdot\mathcal{B}_{\phi\to K^+K^-}\\
\mathcal{B}_{57/55} &= \frac{\mathcal{B}_{57}}{\mathcal{B}_{55}}\\
\mathcal{B}_{58} &= \mathcal{B}_{62} + \mathcal{B}_{93} + \mathcal{B}_{802} + \mathcal{B}_{167}\cdot\mathcal{B}_{\phi\to K^+K^-}\\
\mathcal{B}_{59} &= \mathcal{B}_{35}\cdot(\mathcal{B}_{\langle K^0|K_S\rangle}\cdot\mathcal{B}_{K_S\to\pi^+\pi^-}) + \mathcal{B}_{62} + \mathcal{B}_{800}\cdot\mathcal{B}_{\omega\to\pi^+\pi^-}\\
\mathcal{B}_{60} &= \mathcal{B}_{62} + \mathcal{B}_{800}\cdot\mathcal{B}_{\omega\to\pi^+\pi^-}\\
\mathcal{B}_{63} &= \mathcal{B}_{40}\cdot(\mathcal{B}_{\langle K^0|K_S\rangle}\cdot\mathcal{B}_{K_S\to\pi^+\pi^-}) + \mathcal{B}_{42}\cdot(\mathcal{B}_{\langle K^0|K_S\rangle}\cdot\mathcal{B}_{K_S\to\pi^+\pi^-}) + \mathcal{B}_{47}\cdot(2\cdot\mathcal{B}_{K_S\to\pi^+\pi^-}\cdot\mathcal{B}_{K_S\to\pi^0\pi^0})\\
&\quad + \mathcal{B}_{50}\cdot(2\cdot\mathcal{B}_{K_S\to\pi^+\pi^-}\cdot\mathcal{B}_{K_S\to\pi^0\pi^0}) + \mathcal{B}_{70} + \mathcal{B}_{77} + \mathcal{B}_{78} + \mathcal{B}_{94} + \mathcal{B}_{126}\cdot\mathcal{B}_{\eta\to\text{charged}} + \mathcal{B}_{128}\cdot\mathcal{B}_{\eta\to\text{charged}}\\
&\quad + \mathcal{B}_{130}\cdot\mathcal{B}_{\eta\to\text{charged}} + \mathcal{B}_{132}\cdot(\mathcal{B}_{\langle\bar{K}^0|K_S\rangle}\cdot\mathcal{B}_{K_S\to\pi^+\pi^-}\cdot\mathcal{B}_{\eta\to\text{neutral}} + \mathcal{B}_{\langle\bar{K}^0|K_S\rangle}\cdot\mathcal{B}_{K_S\to\pi^0\pi^0}\cdot\mathcal{B}_{\eta\to\text{charged}})\\
&\quad + \mathcal{B}_{151}\cdot\mathcal{B}_{\omega\to\pi^+\pi^-\pi^0} + \mathcal{B}_{152}\cdot(\mathcal{B}_{\omega\to\pi^+\pi^-\pi^0}+\mathcal{B}_{\omega\to\pi^+\pi^-}) + \mathcal{B}_{800}\cdot\mathcal{B}_{\omega\to\pi^+\pi^-\pi^0} + \mathcal{B}_{803}\\
\mathcal{B}_{64} &= \mathcal{B}_{78} + \mathcal{B}_{77} + \mathcal{B}_{94} + \mathcal{B}_{70} + \mathcal{B}_{126}\cdot\mathcal{B}_{\eta\to\pi^+\pi^-\pi^0} + \mathcal{B}_{128}\cdot\mathcal{B}_{\eta\to\pi^+\pi^-\pi^0} + \mathcal{B}_{130}\cdot\mathcal{B}_{\eta\to\pi^+\pi^-\pi^0} + \mathcal{B}_{800}\cdot\mathcal{B}_{\omega\to\pi^+\pi^-\pi^0}\\
&\quad + \mathcal{B}_{151}\cdot\mathcal{B}_{\omega\to\pi^+\pi^-\pi^0} + \mathcal{B}_{152}\cdot(\mathcal{B}_{\omega\to\pi^+\pi^-\pi^0}+\mathcal{B}_{\omega\to\pi^+\pi^-}) + \mathcal{B}_{803}\\
\mathcal{B}_{65} &= \mathcal{B}_{40}\cdot(\mathcal{B}_{\langle K^0|K_S\rangle}\cdot\mathcal{B}_{K_S\to\pi^+\pi^-}) + \mathcal{B}_{42}\cdot(\mathcal{B}_{\langle K^0|K_S\rangle}\cdot\mathcal{B}_{K_S\to\pi^+\pi^-}) + \mathcal{B}_{70} + \mathcal{B}_{94} + \mathcal{B}_{128}\cdot\mathcal{B}_{\eta\to\pi^+\pi^-\pi^0}\\
&\quad + \mathcal{B}_{151}\cdot\mathcal{B}_{\omega\to\pi^+\pi^-\pi^0} + \mathcal{B}_{152}\cdot\mathcal{B}_{\omega\to\pi^+\pi^-} + \mathcal{B}_{800}\cdot\mathcal{B}_{\omega\to\pi^+\pi^-\pi^0} + \mathcal{B}_{803}
\end{aligned}$$

$$\begin{aligned}
\mathcal{B}_{66} &= \mathcal{B}_{70} + \mathcal{B}_{94} + \mathcal{B}_{128}\cdot\mathcal{B}_{\eta\to\pi^+\pi^-\pi^0} + \mathcal{B}_{151}\cdot\mathcal{B}_{\omega\to\pi^+\pi^-\pi^0} + \mathcal{B}_{152}\cdot\mathcal{B}_{\omega\to\pi^+\pi^-} + \mathcal{B}_{800}\cdot\mathcal{B}_{\omega\to\pi^+\pi^-\pi^0} + \mathcal{B}_{803}\\
\mathcal{B}_{67} &= \mathcal{B}_{70} + \mathcal{B}_{94} + \mathcal{B}_{128}\cdot\mathcal{B}_{\eta\to\pi^+\pi^-\pi^0} + \mathcal{B}_{803}\\
\mathcal{B}_{68} &= \mathcal{B}_{40}\cdot(\mathcal{B}_{\langle K^0|K_S\rangle}\cdot\mathcal{B}_{K_S\to\pi^+\pi^-}) + \mathcal{B}_{70} + \mathcal{B}_{152}\cdot\mathcal{B}_{\omega\to\pi^+\pi^-} + \mathcal{B}_{800}\cdot\mathcal{B}_{\omega\to\pi^+\pi^-\pi^0}\\
\mathcal{B}_{69} &= \mathcal{B}_{152}\cdot\mathcal{B}_{\omega\to\pi^+\pi^-} + \mathcal{B}_{70} + \mathcal{B}_{800}\cdot\mathcal{B}_{\omega\to\pi^+\pi^-\pi^0}\\
\mathcal{B}_{74} &= \mathcal{B}_{152}\cdot\mathcal{B}_{\omega\to\pi^+\pi^-\pi^0} + \mathcal{B}_{78} + \mathcal{B}_{77} + \mathcal{B}_{126}\cdot\mathcal{B}_{\eta\to\pi^+\pi^-\pi^0} + \mathcal{B}_{130}\cdot\mathcal{B}_{\eta\to\pi^+\pi^-\pi^0}\\
\mathcal{B}_{75} &= \mathcal{B}_{152}\cdot\mathcal{B}_{\omega\to\pi^+\pi^-\pi^0} + \mathcal{B}_{47}\cdot(2\cdot\mathcal{B}_{K_S\to\pi^+\pi^-}\cdot\mathcal{B}_{K_S\to\pi^0\pi^0}) + \mathcal{B}_{77} + \mathcal{B}_{126}\cdot\mathcal{B}_{\eta\to\pi^+\pi^-\pi^0} + \mathcal{B}_{130}\cdot\mathcal{B}_{\eta\to\pi^+\pi^-\pi^0}\\
\mathcal{B}_{76} &= \mathcal{B}_{152}\cdot\mathcal{B}_{\omega\to\pi^+\pi^-\pi^0} + \mathcal{B}_{77} + \mathcal{B}_{126}\cdot\mathcal{B}_{\eta\to\pi^+\pi^-\pi^0} + \mathcal{B}_{130}\cdot\mathcal{B}_{\eta\to\pi^+\pi^-\pi^0}\\
\mathcal{B}_{76/54} &= \frac{\mathcal{B}_{76}}{\mathcal{B}_{54}}\\
\mathcal{B}_{78} &= \mathcal{B}_{810} + \mathcal{B}_{50}\cdot(2\cdot\mathcal{B}_{K_S\to\pi^+\pi^-}\cdot\mathcal{B}_{K_S\to\pi^0\pi^0}) + \mathcal{B}_{132}\cdot(\mathcal{B}_{\langle\bar{K}^0|K_S\rangle}\cdot\mathcal{B}_{K_S\to\pi^+\pi^-}\cdot\mathcal{B}_{\eta\to 3\pi^0})\\
\mathcal{B}_{79} &= \mathcal{B}_{37}\cdot(\mathcal{B}_{\langle K^0|K_S\rangle}\cdot\mathcal{B}_{K_S\to\pi^+\pi^-}) + \mathcal{B}_{42}\cdot(\mathcal{B}_{\langle K^0|K_S\rangle}\cdot\mathcal{B}_{K_S\to\pi^+\pi^-}) + \mathcal{B}_{93} + \mathcal{B}_{94} + \mathcal{B}_{128}\cdot\mathcal{B}_{\eta\to\text{charged}}\\
&\quad + \mathcal{B}_{151}\cdot(\mathcal{B}_{\omega\to\pi^+\pi^-\pi^0}+\mathcal{B}_{\omega\to\pi^+\pi^-}) + \mathcal{B}_{168} + \mathcal{B}_{802} + \mathcal{B}_{803}
\end{aligned}$$

$$\mathcal{B}_{80} = \mathcal{B}_{93} + \mathcal{B}_{802} + \mathcal{B}_{151} \cdot \mathcal{B}_{\omega\to\pi^+\pi^-}$$
$$\mathcal{B}_{80/60} = \frac{\mathcal{B}_{80}}{\mathcal{B}_{60}}$$
$$\mathcal{B}_{81} = \mathcal{B}_{128} \cdot \mathcal{B}_{\eta\to\pi^+\pi^-\pi^0} + \mathcal{B}_{94} + \mathcal{B}_{803} + \mathcal{B}_{151} \cdot \mathcal{B}_{\omega\to\pi^+\pi^-\pi^0}$$
$$\mathcal{B}_{81/69} = \frac{\mathcal{B}_{81}}{\mathcal{B}_{69}}$$
$$\mathcal{B}_{82} = \mathcal{B}_{128} \cdot \mathcal{B}_{\eta\to\text{charged}} + \mathcal{B}_{42} \cdot (\mathcal{B}_{\langle K^0|K_S\rangle} \cdot \mathcal{B}_{K_S\to\pi^+\pi^-}) + \mathcal{B}_{802} + \mathcal{B}_{803} + \mathcal{B}_{151} \cdot (\mathcal{B}_{\omega\to\pi^+\pi^-\pi^0} + \mathcal{B}_{\omega\to\pi^+\pi^-}) + \mathcal{B}_{37} \cdot (\mathcal{B}_{\langle K^0|K_S\rangle} \cdot \mathcal{B}_{K_S\to\pi^+\pi^-})$$
$$\mathcal{B}_{83} = \mathcal{B}_{128} \cdot \mathcal{B}_{\eta\to\pi^+\pi^-\pi^0} + \mathcal{B}_{802} + \mathcal{B}_{803} + \mathcal{B}_{151} \cdot (\mathcal{B}_{\omega\to\pi^+\pi^-\pi^0} + \mathcal{B}_{\omega\to\pi^+\pi^-})$$
$$\mathcal{B}_{84} = \mathcal{B}_{802} + \mathcal{B}_{151} \cdot \mathcal{B}_{\omega\to\pi^+\pi^-} + \mathcal{B}_{37} \cdot (\mathcal{B}_{\langle K^0|K_S\rangle} \cdot \mathcal{B}_{K_S\to\pi^+\pi^-})$$
$$\mathcal{B}_{85} = \mathcal{B}_{802} + \mathcal{B}_{151} \cdot \mathcal{B}_{\omega\to\pi^+\pi^-}$$
$$\mathcal{B}_{85/60} = \frac{\mathcal{B}_{85}}{\mathcal{B}_{60}}$$
$$\mathcal{B}_{87} = \mathcal{B}_{42} \cdot (\mathcal{B}_{\langle K^0|K_S\rangle} \cdot \mathcal{B}_{K_S\to\pi^+\pi^-}) + \mathcal{B}_{128} \cdot \mathcal{B}_{\eta\to\pi^+\pi^-\pi^0} + \mathcal{B}_{151} \cdot \mathcal{B}_{\omega\to\pi^+\pi^-\pi^0} + \mathcal{B}_{803}$$

$$\mathcal{B}_{88} = \mathcal{B}_{128} \cdot \mathcal{B}_{\eta\to\pi^+\pi^-\pi^0} + \mathcal{B}_{803} + \mathcal{B}_{151} \cdot \mathcal{B}_{\omega\to\pi^+\pi^-\pi^0}$$
$$\mathcal{B}_{89} = \mathcal{B}_{803} + \mathcal{B}_{151} \cdot \mathcal{B}_{\omega\to\pi^+\pi^-\pi^0}$$
$$\mathcal{B}_{92} = \mathcal{B}_{94} + \mathcal{B}_{93}$$
$$\mathcal{B}_{93/60} = \frac{\mathcal{B}_{93}}{\mathcal{B}_{60}}$$
$$\mathcal{B}_{94/69} = \frac{\mathcal{B}_{94}}{\mathcal{B}_{69}}$$
$$\mathcal{B}_{96} = \mathcal{B}_{167} \cdot \mathcal{B}_{\phi\to K^+K^-}$$
$$\mathcal{B}_{102} = \mathcal{B}_{103} + \mathcal{B}_{104}$$
$$\mathcal{B}_{103} = \mathcal{B}_{820} + \mathcal{B}_{822} + \mathcal{B}_{831} \cdot \mathcal{B}_{\omega\to\pi^+\pi^-}$$
$$\mathcal{B}_{104} = \mathcal{B}_{830} + \mathcal{B}_{833}$$
$$\mathcal{B}_{106} = \mathcal{B}_{30} + \mathcal{B}_{44} \cdot \mathcal{B}_{\langle \bar{K}^0|K_S\rangle} + \mathcal{B}_{47} + \mathcal{B}_{53} \cdot \mathcal{B}_{\langle K^0|K_S\rangle} + \mathcal{B}_{77} + \mathcal{B}_{103} + \mathcal{B}_{126} \cdot (\mathcal{B}_{\eta\to 3\pi^0} + \mathcal{B}_{\eta\to\pi^+\pi^-\pi^0}) + \mathcal{B}_{152} \cdot \mathcal{B}_{\omega\to\pi^+\pi^-\pi^0}$$
$$\mathcal{B}_{110} = \mathcal{B}_{10} + \mathcal{B}_{16} + \mathcal{B}_{23} + \mathcal{B}_{28} + \mathcal{B}_{35} + \mathcal{B}_{40} + \mathcal{B}_{128} + \mathcal{B}_{802} + \mathcal{B}_{803} + \mathcal{B}_{151} + \mathcal{B}_{130} + \mathcal{B}_{132} + \mathcal{B}_{44} + \mathcal{B}_{53} + \mathcal{B}_{168} + \mathcal{B}_{169} + \mathcal{B}_{822} + \mathcal{B}_{833}$$
$$\mathcal{B}_{149} = \mathcal{B}_{152} + \mathcal{B}_{800} + \mathcal{B}_{151}$$
$$\mathcal{B}_{150} = \mathcal{B}_{800} + \mathcal{B}_{151}$$
$$\mathcal{B}_{150/66} = \frac{\mathcal{B}_{150}}{\mathcal{B}_{66}}$$
$$\mathcal{B}_{152/54} = \frac{\mathcal{B}_{152}}{\mathcal{B}_{54}}$$
$$\mathcal{B}_{152/76} = \frac{\mathcal{B}_{152}}{\mathcal{B}_{76}}$$
$$\mathcal{B}_{168} = \mathcal{B}_{167} \cdot \mathcal{B}_{\phi\to K^+K^-}$$

$$
\begin{aligned}
\mathcal{B}_{169} &= \mathcal{B}_{167}\cdot\mathcal{B}_{\phi\to K_S K_L}\\
\mathcal{B}_{804} &= \mathcal{B}_{47}\cdot((\mathcal{B}_{\langle K^0|K_L\rangle}\cdot\mathcal{B}_{\langle\bar{K}^0|K_L\rangle})/(\mathcal{B}_{\langle K^0|K_S\rangle}\cdot\mathcal{B}_{\langle\bar{K}^0|K_S\rangle}))\\
\mathcal{B}_{805} &= \mathcal{B}_{980}/(1-\mathcal{B}_{980})\cdot(\mathcal{B}_{20}+\mathcal{B}_{62})\\
\mathcal{B}_{806} &= \mathcal{B}_{50}\cdot((\mathcal{B}_{\langle K^0|K_L\rangle}\cdot\mathcal{B}_{\langle\bar{K}^0|K_L\rangle})/(\mathcal{B}_{\langle K^0|K_S\rangle}\cdot\mathcal{B}_{\langle\bar{K}^0|K_S\rangle}))\\
\mathcal{B}_{810} &= \mathcal{B}_{910}+\mathcal{B}_{911}+\mathcal{B}_{811}\cdot\mathcal{B}_{\omega\to\pi^+\pi^-\pi^0}+\mathcal{B}_{812}\\
\mathcal{B}_{820} &= \mathcal{B}_{920}+\mathcal{B}_{821}\\
\mathcal{B}_{830} &= \mathcal{B}_{930}+\mathcal{B}_{831}\cdot\mathcal{B}_{\omega\to\pi^+\pi^-\pi^0}+\mathcal{B}_{832}\\
\mathcal{B}_{910} &= \mathcal{B}_{136}\cdot\mathcal{B}_{\eta\to 3\pi^0}\\
\mathcal{B}_{911} &= \mathcal{B}_{945}\cdot\mathcal{B}_{\eta\to\pi^+\pi^-\pi^0}\\
\mathcal{B}_{930} &= \mathcal{B}_{136}\cdot\mathcal{B}_{\eta\to\pi^+\pi^-\pi^0}\\
\mathcal{B}_{944} &= \mathcal{B}_{136}\cdot\mathcal{B}_{\eta\to\gamma\gamma}\\
\mathcal{B}_{\rm ur} &= 1-\mathcal{B}_{\rm all}\\
\mathcal{B}_{\rm all} &= \mathcal{B}_3+\mathcal{B}_5+\mathcal{B}_9+\mathcal{B}_{10}+\mathcal{B}_{14}+\mathcal{B}_{16}+\mathcal{B}_{20}+\mathcal{B}_{23}+\mathcal{B}_{27}+\mathcal{B}_{28}+\mathcal{B}_{30}+\mathcal{B}_{35}+\mathcal{B}_{37}+\mathcal{B}_{40}+\mathcal{B}_{42}\\
&\quad+\mathcal{B}_{47}\cdot(1+((\mathcal{B}_{\langle K^0|K_L\rangle}\cdot\mathcal{B}_{\langle\bar{K}^0|K_L\rangle})/(\mathcal{B}_{\langle K^0|K_S\rangle}\cdot\mathcal{B}_{\langle\bar{K}^0|K_S\rangle})))+\mathcal{B}_{48}+\mathcal{B}_{62}+\mathcal{B}_{70}+\mathcal{B}_{77}+\mathcal{B}_{811}+\mathcal{B}_{812}\\
&\quad+\mathcal{B}_{93}+\mathcal{B}_{94}+\mathcal{B}_{832}+\mathcal{B}_{833}+\mathcal{B}_{126}+\mathcal{B}_{128}+\mathcal{B}_{802}+\mathcal{B}_{803}+\mathcal{B}_{800}+\mathcal{B}_{151}+\mathcal{B}_{130}+\mathcal{B}_{132}+\mathcal{B}_{44}+\mathcal{B}_{53}\\
&\quad+\mathcal{B}_{50}\cdot(1+((\mathcal{B}_{\langle K^0|K_L\rangle}\cdot\mathcal{B}_{\langle\bar{K}^0|K_L\rangle})/(\mathcal{B}_{\langle K^0|K_S\rangle}\cdot\mathcal{B}_{\langle\bar{K}^0|K_S\rangle})))+\mathcal{B}_{51}+\mathcal{B}_{167}\cdot(\mathcal{B}_{\phi\to K^+K^-}+\mathcal{B}_{\phi\to K_S K_L})\\
&\quad+\mathcal{B}_{152}+\mathcal{B}_{920}+\mathcal{B}_{821}+\mathcal{B}_{822}+\mathcal{B}_{831}+\mathcal{B}_{136}+\mathcal{B}_{945}+\mathcal{B}_{805}
\end{aligned}
$$

D. Tests of lepton universality

Lepton universality tests probe the Standard-Model prediction that the weak charged-current interaction has the same coupling for all lepton generations. Beginning with our 2014 report [1581], the precision of such tests was significantly improved thanks to the Belle τ lifetime measurement [1515]. The most significant improvement of the τ branching fraction fit results comes from the recent Belle II measurement [1499]. We perform the universality tests by using ratios of the partial widths of a heavier lepton $\mathcal{L}$ decaying to a lighter lepton ℓ [1582],

$$
\begin{aligned}
\Gamma(\mathcal{L}\to\nu_{\mathcal{L}}\ell\bar{\nu}_\ell(\gamma)) &= \frac{\mathcal{B}(\mathcal{L}\to\nu_{\mathcal{L}}\ell\bar{\nu}_\ell)}{\tau_{\mathcal{L}}}\\
&= \frac{G_{\mathcal{L}}G_\ell m_{\mathcal{L}}^5}{192\pi^3} f\left(\frac{m_\ell^2}{m_{\mathcal{L}}^2}\right) R_W^{\mathcal{L}\ell} R_\gamma^{\mathcal{L}}, \qquad (228)
\end{aligned}
$$

where

$$
G_\ell = \frac{g_\ell^2}{4\sqrt{2}M_W^2}, \qquad f(x) = 1-8x+8x^3-x^4-12x^2\ln x, \qquad (229)
$$

$$
\begin{aligned}
R_W^{\mathcal{L}\ell} &= 1+\frac{3}{5}\frac{m_{\mathcal{L}}^2}{M_W^2}+\frac{9}{5}\frac{m_\ell^2}{M_W^2} \quad [1583\text{–}1585],\\
R_\gamma^{\mathcal{L}} &= 1+\frac{\alpha(m_{\mathcal{L}})}{2\pi}\left(\frac{25}{4}-\pi^2\right). \qquad (230)
\end{aligned}
$$

The equation holds at leading perturbative order (with some corrections being computed at next-to-leading order) for branching fractions to final states that include a soft photon, as detailed in the notation. The inclusion of soft photons is not explicitly mentioned in the branching fractions notation used in this section, but is implicitly assumed, since experimental measurements do include soft photons. For most measurements of τ branching fractions, soft photons are not experimentally reconstructed but accounted for in the simulations used to estimate the experimental efficiency. We use $R_\gamma^\tau = 1\text{–}43.2\times10^{-4}$, $R_\gamma^\mu = 1\text{–}42.4\times10^{-4}$ [1582] and take the averages for the τ mass, lifetime and branching fractions from this report. We use the CODATA 2018 report [1585] for the electron and muon masses, and PDG 2022 and 2023 update [302] for the muon lifetime, the $\pi^\pm$ and $K^\pm$ meson masses and lifetimes, and the W boson mass.

Using pure leptonic processes we obtain the coupling ratios

$$\left(\frac{g_\tau}{g_\mu}\right)_\tau = 1.0016 \pm 0.0014, \tag{231}$$

$$\left(\frac{g_\tau}{g_e}\right)_\tau = 1.0018 \pm 0.0014, \tag{232}$$

$$\left(\frac{g_\mu}{g_e}\right)_\tau = 1.0002 \pm 0.0011. \tag{233}$$

Under the assumption that the muon and electron charged weak couplings are equal, we average $\mathcal{B}_e = \mathcal{B}(\tau \to e\bar{\nu}_e\nu_\tau)$ and its prediction from $\mathcal{B}_\mu = \mathcal{B}(\tau \to \mu\bar{\nu}_\mu\nu_\tau)$,

$$\mathcal{B}_e^{\mathcal{B}_\mu} = \mathcal{B}_\mu \frac{f(m_e^2/m_\tau^2)}{f(m_\mu^2/m_\tau^2)} \frac{R_W^{\tau e}}{R_W^{\tau\mu}}, \tag{234}$$

to obtain $\mathcal{B}'_e$, a measurement of the τ electronic branching fraction that summarizes the experimental information on the electron and the muon couplings from the measurements of B_e and B_μ. We test the universality of the couplings of the lighter leptons with respect to the τ by comparing $\mathcal{B}'_e$ to the predicted τ electronic branching fraction from the measurement of the τ lifetime

$$\mathcal{B}_e^{\tau_\tau} = \mathcal{B}(\mu \to e\bar{\nu}_e\nu_\mu) \frac{\tau_\tau}{\tau_\mu} \frac{m_\tau^5}{m_\mu^5} \frac{f(m_e^2/m_\tau^2)}{f(m_e^2/m_\mu^2)} \frac{R_W^{\tau e}}{R_W^{\mu e}} \frac{R_\gamma^\tau}{R_\gamma^\mu}. \tag{235}$$

In Fig. 66, the plot shows the measured $\mathcal{B}'_e$, the measured τ lifetime, and a band corresponding to $\mathcal{B}_e^{\tau_\tau}$ as function of the τ lifetime, whose width depends primarily on the uncertainty on the τ mass, which has been reduced thanks to the recent Belle measurement [1503].

An additional universality test is obtained using the measurements of semileptonic branching fractions of pseudoscalar mesons, using [1586]

$$\left(\frac{g_\tau}{g_\mu}\right)_h^2 = \frac{\mathcal{B}(\tau \to h\nu_\tau)}{\mathcal{B}(h \to \mu\bar{\nu}_\mu)} \frac{2m_h m_\mu^2 \tau_h}{(1+\delta_{\tau/h}) m_\tau^3 \tau_\tau} \left(\frac{1-m_\mu^2/m_h^2}{1-m_h^2/m_\tau^2}\right)^2, \tag{236}$$

where $h = \pi$ or K. The radiative corrections $\delta_{\tau/\pi}$ and $\delta_{\tau/K}$ have been recently updated with an improved estimation of their uncertainties and their values are $(0.18 \pm 0.57)\%$ and $(0.97 \pm 0.58)\%$ [1587], respectively. Using $\mathcal{B}(\pi \to \mu\bar{\nu}_\mu)$ and $\mathcal{B}(K \to \mu\bar{\nu}_\mu)$ from the Review of Particle Physics 2022 edition and 2023 update [302], we obtain

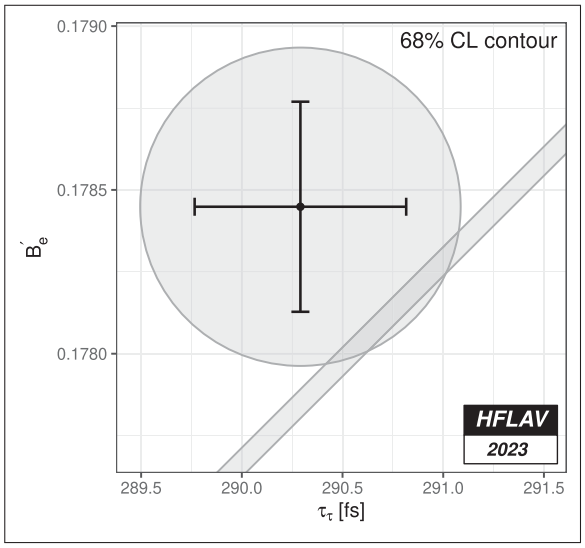


FIG. 66. Test of the universality of the couplings of the lighter leptons e and μ, assumed to be the same, and of the τ lepton. The plot shows values and uncertainties of the τ lifetime and of $\mathcal{B}'_e$, a determination of the electronic τ branching fractions obtained from the direct measurements of the electronic and the muonic τ branching fractions. The contour delimits the 68% CL region. The oblique band shows the Standard Model prediction of $\mathcal{B}'_e$ as a function of the τ lifetime, and its width is mainly determined by the uncertainty on the τ mass.

$$\left(\frac{g_\tau}{g_\mu}\right)_\pi = 0.996 \pm 0.004, \quad \left(\frac{g_\tau}{g_\mu}\right)_K = 0.989 \pm 0.008. \tag{237}$$

The largest contribution to the uncertainties of these tests are the uncertainty on $\delta_{\tau/\pi}$ for $(g_\tau/g_\mu)_\pi$ and the uncertainty on the τ branching fraction for $(g_\tau/g_\mu)_K$. Similar tests can be performed using measurements of decay modes with electrons, but are less precise, since the meson decays to electrons are helicity suppressed and have less precise experimental measurements. Averaging the three g_τ/g_μ ratios we obtain

$$\left(\frac{g_\tau}{g_\mu}\right)_{\tau+\pi+K} = 1.0011 \pm 0.0014, \tag{238}$$

accounting for correlations and assuming that the $\delta_{\tau/\pi}$ and $\delta_{\tau/K}$ uncertainties are uncorrelated, as they are estimated to be with good approximation [1587]. Table 303 reports the correlation coefficients for the fitted coupling ratios.

Since $(g_\tau/g_\mu)_\tau = (g_\tau/g_e)_\tau/(g_\mu/g_e)_\tau$, the correlation matrix is expected to be positive semi-definite, with one eigenvalue equal to zero. A numerical calculation of the eigenvalues returns the values 1.804, 1.329, 0.959, 0.907, 2.887×10^{-15}.

TABLE 303. Universality coupling ratios correlation coefficients (%).

$\left(\frac{g_\tau}{g_e}\right)_\tau$	67			
$\left(\frac{g_\mu}{g_e}\right)_\tau$	−41	40		
$\left(\frac{g_\tau}{g_\mu}\right)_\pi$	18	19	1	
$\left(\frac{g_\tau}{g_\mu}\right)_K$	12	12	−1	7
	$\left(\frac{g_\tau}{g_\mu}\right)_\tau$	$\left(\frac{g_\tau}{g_e}\right)_\tau$	$\left(\frac{g_\mu}{g_e}\right)_\tau$	$\left(\frac{g_\tau}{g_\mu}\right)_\pi$

E. Universality-improved values of $\mathcal{B}(\tau \to e\bar{\nu}_e\nu_\tau)$ and $R_{\rm had}$

Following Ref. [1498], we compute the experimental value of $\mathcal{B}_e = \mathcal{B}(\tau \to e\bar{\nu}_e\nu_\tau)$ assuming the Standard Model lepton universality by averaging:

(i) the $\mathcal{B}_e$ fit value $\mathcal{B}_5$,
(ii) the $\mathcal{B}_e$ determination from the $\mathcal{B}_\mu = \mathcal{B}(\tau \to \mu\bar{\nu}_\mu\nu_\tau)$ fit value $\mathcal{B}_3$ assuming that $g_\mu/g_e = 1$ [Eq. (234)],
(iii) the $\mathcal{B}_e$ determination from the τ lifetime assuming that $g_\tau/g_\mu = 1$ [Eq. (235)].

Accounting for correlations, we obtain

$$\mathcal{B}_e^{\rm uni} = (17.815 \pm 0.023)\%. \tag{239}$$

We compute the sum of all *measured* branching fractions to hadrons and the experimental value of the ratio between the τ hadronic and electronic widths assuming the Standard Model lepton universality:

$$\mathcal{B}_{\rm had} = (64.73 \pm 0.11)\%, \tag{240}$$

$$R_{\rm had}^{\rm uni} = \frac{\Gamma(\tau \to {\rm hadrons}\nu_\tau)}{\Gamma^{\rm uni}(\tau \to e\bar{\nu}_e\nu_\tau)} = \frac{\mathcal{B}_{\rm had}}{\mathcal{B}_e^{\rm uni}} = 3.634 \pm 0.008. \tag{241}$$

An alternative definition of $\mathcal{B}_{\rm had}$ uses the unitarity of the sum of all branching fractions, resulting in:

$$\mathcal{B}_{\rm had}^{\rm uni,lept} = 1 - \mathcal{B}_e - \mathcal{B}_\mu = (64.80 \pm 0.06)\%, \tag{242}$$

$$R_{\rm had}^{\rm uni,lept} = \frac{1 - \mathcal{B}_e - \mathcal{B}_\mu}{\mathcal{B}_e^{\rm uni}} = 3.637 \pm 0.008. \tag{243}$$

A third definition of $\mathcal{B}_{\rm had}$ uses the unitarity of the sum of all τ branching fractions, $1 = \mathcal{B}_e + \mathcal{B}_\mu + \mathcal{B}_{\rm had}$, the Standard Model prediction of $\mathcal{B}_\mu$ from $\mathcal{B}_e$ in Eq. (234) and $\mathcal{B}_e^{\rm uni}$ to define:

$$\mathcal{B}_{\rm had}^{\rm uni,SM} = 1 - \mathcal{B}_e^{\rm uni} - \mathcal{B}_e^{\rm uni} \cdot f(m_\mu^2/m_\tau^2)/f(m_e^2/m_\tau^2) = (64.86 \pm 0.05)\%, \tag{244}$$

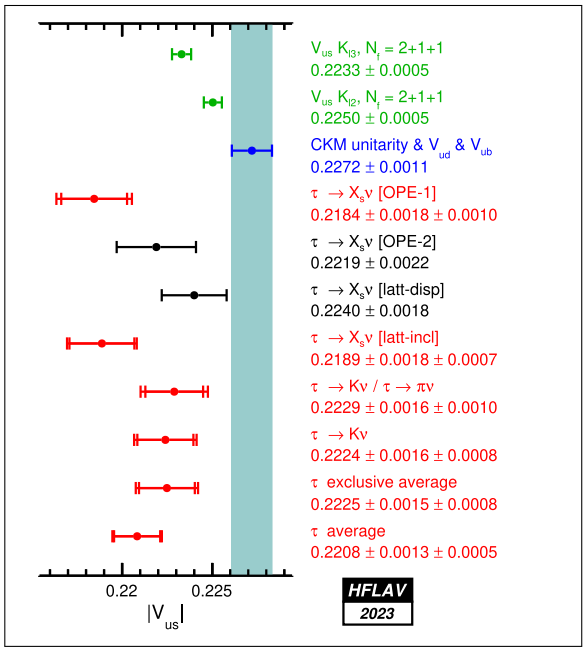


FIG. 67. $|V_{us}|$ determinations. The values of $|V_{us}|_{K\ell 3}$, $|V_{us}|_{K\ell 2}$ and the expected $|V_{us}|$ from the CKM matrix unitarity are taken from Ref. [1589]. The other reported $|V_{us}|$ values are documented in the text. When two uncertainties are reported, the first one accounts for the uncertainties of the HFLAV-Tau fit results, and the second one accounts for the uncertainties of the theory and the other inputs that are used for the $|V_{us}|$ determinations.

$$R_{\rm had}^{\rm uni,SM} = \frac{1 - \mathcal{B}_e^{\rm uni} - \mathcal{B}_e^{\rm uni} \cdot f(m_\mu^2/m_\tau^2)/f(m_e^2/m_\tau^2)}{\mathcal{B}_e^{\rm uni}} = 3.641 \pm 0.007. \tag{245}$$

Although $\mathcal{B}_{\rm had}^{\rm uni,lept}$ and $\mathcal{B}_{\rm had}^{\rm uni,SM}$ are more precise than $\mathcal{B}_{\rm had}^{\rm uni}$, the precision of $R_{\rm had}{}^{\rm uni,lept}$ and $R_{\rm had}{}^{\rm uni,SM}$ is comparable to the one of $R_{\rm had}{}^{\rm uni}$ because there are larger correlations between $\mathcal{B}_{\rm had}^{\rm uni,lept}$, $\mathcal{B}_{\rm had}^{\rm uni,SM}$ and $\mathcal{B}_e^{\rm uni}$ than between $\mathcal{B}_{\rm had}$ and $\mathcal{B}_e^{\rm uni}$.

F. Measurements of $|V_{us}|$

The CKM matrix element magnitude $|V_{us}|$ is most precisely determined from kaon decays [1588] (see Fig. 67), and its precision is limited by the uncertainties of the lattice QCD estimates of the meson form factor $f_+^{K\pi}(0)$ and decay-constant ratio $f_{K\pm}/f_{\pi\pm}$. The following sections report alternative determinations of $|V_{us}|$ based on the experimental measurements of the τ branching fractions.

1. $|V_{us}|$ from $\mathcal{B}(\tau \to X_s\nu)$

$|V_{us}|$ is computed using the inclusive τ branching fraction to strange hadronic final states as [1590,1591]

TABLE 304. A summary of the averaged τ branching fractions to strange final states.

Branching fraction	HFLAV 2023 fit (%)
$\mathcal{B}(\tau^- \to K^-\nu_\tau)$	0.6959 ± 0.0096
$\mathcal{B}(\tau^- \to K^-\pi^0\nu_\tau)$	0.4321 ± 0.0148
$\mathcal{B}(\tau^- \to K^-2\pi^0\nu_\tau(\text{ex.}K^0))$	0.0634 ± 0.0219
$\mathcal{B}(\tau^- \to K^-3\pi^0\nu_\tau(\text{ex.}K^0,\eta))$	0.0465 ± 0.0213
$\mathcal{B}(\tau^- \to \pi^-\bar{K}^0\nu_\tau)$	0.8375 ± 0.0139
$\mathcal{B}(\tau^- \to \pi^-\bar{K}^0\pi^0\nu_\tau)$	0.3810 ± 0.0129
$\mathcal{B}(\tau^- \to \pi^-\bar{K}^0 2\pi^0\nu_\tau(\text{ex.}K^0))$	0.0234 ± 0.0231
$\mathcal{B}(\tau^- \to \bar{K}^0 h^- h^- h^+\nu_\tau)$	0.0222 ± 0.0202
$\mathcal{B}(\tau^- \to K^-\eta\nu_\tau)$	0.0155 ± 0.0008
$\mathcal{B}(\tau^- \to K^-\pi^0\eta\nu_\tau)$	0.0048 ± 0.0012
$\mathcal{B}(\tau^- \to \pi^-\bar{K}^0\eta\nu_\tau)$	0.0094 ± 0.0015
$\mathcal{B}(\tau^- \to K^-\omega\nu_\tau)$	0.0410 ± 0.0092
$\mathcal{B}(\tau^- \to K^-\phi(K^+K^-)\nu_\tau)$	0.0022 ± 0.0008
$\mathcal{B}(\tau^- \to K^-\phi(K_S^0K_L^0)\nu_\tau)$	0.0015 ± 0.0006
$\mathcal{B}(\tau^- \to K^-\pi^-\pi^+\nu_\tau(\text{ex.}K^0,\omega))$	0.2924 ± 0.0068
$\mathcal{B}(\tau^- \to K^-\pi^-\pi^+\pi^0\nu_\tau(\text{ex.}K^0,\omega,\eta))$	0.0388 ± 0.0142
$\mathcal{B}(\tau^- \to K^-2\pi^-2\pi^+\nu_\tau(\text{ex.}K^0))$	0.0001 ± 0.0001
$\mathcal{B}(\tau^- \to K^-2\pi^-2\pi^+\pi^0\nu_\tau(\text{ex.}K^0))$	0.0001 ± 0.0001
$\mathcal{B}(\tau^- \to X_s^-\nu_\tau)$	2.9078 ± 0.0478

$$|V_{us}|_{\tau\text{-OPE-1}} = \sqrt{R_{us}/\left[\frac{R_{ud}}{|V_{ud}|^2} - \delta R_{\tau\text{-}SU(3)\text{-break}}\right]} = 0.2184 \pm 0.0021, \quad (246)$$

where $R_{us} = \mathcal{B}_{us}/\mathcal{B}_e^{\text{uni}} = 0.1632 \pm 0.0027$, $\mathcal{B}_{us} = 2.908 \pm 0.048$ is the inclusive τ branching fraction to strange hadronic final states (see also Table 304), $R_{ud} = R_{\text{had}}^{\text{uni}} - R_{us} = 3.470 \pm 0.008$, and $|V_{ud}| = 0.97384 \pm 0.00026$ is taken from a recent average of measurements of superallowed nuclear β decays, neutron decay measurements [1589], and the correction $\delta R_{\tau\text{-}SU(3)\text{-break}}$ accounts for the $SU(3)$-breaking effects due to the difference between the strange, up and down quark masses. $\delta R_{\tau\text{-}SU(3)\text{-break}}$ is determined using perturbative QCD and experimental low energy scattering measurements [1592–1594]. In this report, we compute $\delta R_{\tau\text{-}SU(3)\text{-break}} = 0.239 \pm 0.032$ using Ref. [1592] and the s-quark mass $m_s = 93 \pm 7$ MeV [302]. Reference [1592] estimates a $\delta R_{\tau\text{-}SU(3)\text{-break}}$ uncertainty that is intermediate with respect to the other two assessments [1593,1594]. The uncertainty on $\delta R_{\tau\text{-}SU(3)\text{-break}}$ contributes a 0.47% systematic contribution on $|V_{us}|_{\tau\text{-OPE-1}}$. The above-mentioned $\delta R_{\tau\text{-}SU(3)\text{-break}}$ calculations have been criticized for falling short in dealing with the biases and uncertainties in the low-energy regime of QCD [1595]. However, the community has not reached yet a consensus on the matter. In order to obtain more reliable QCD uncertainties, alternative procedures for computing $|V_{us}|$ using τ decays have been proposed, which involve the τ spectral functions [1595] and lattice QCD methods [1596]. Because of the complexity of these two last proposed procedures, the effort that is required to use them to compute $|V_{us}|$ using the current HFLAV-Tau branching fractions exceeds the scope of this report. Therefore, we just report the most recent updates:

$$|V_{us}|_{\tau\text{-OPE-2}} = 0.2219(22) \quad [1597, 1598] \quad (247)$$

$$|V_{us}|_{\tau\text{-latt-disp}} = 0.2240(18) \quad [1596, 1598] \quad (248)$$

We also use a recently reported lattice QCD calculation of the inclusive τ hadronic decay rate [1599] to compute an additional determination of $|V_{us}|$,

$$|V_{us}|_{\tau\text{-latt-incl}} = \sqrt{\left(\frac{|V_{us}|^2}{R_{us}}\right)_{\text{latt-incl}} \cdot R_{us}} = 0.2189 \pm 0.0019, \quad (249)$$

where $(R_{us}/|V_{us}|^2)_{\text{latt-incl}} = 3.407 \pm 0.022$ [1599]. It is worth noting that all calculations of the τ inclusive decay rate to hadrons are not presently including the long-distance isospin-breaking corrections [1599].

In several of the past determinations of $|V_{us}|$, such as the 2009 HFLAV report [1600], the total hadronic branching fraction was computed using unitarity as $\mathcal{B}_{\text{had}}^{\text{uni}} = 1 - \mathcal{B}_e - \mathcal{B}_\mu$, and $\mathcal{B}_{ud}$ was obtained from $\mathcal{B}_{\text{had}}^{\text{uni}} - \mathcal{B}_{us}$. Here we rather use the direct experimental determination of $\mathcal{B}_{ud}$ for two reasons. First, both methods result in comparable uncertainties on $|V_{us}|$, since the better precision on $\mathcal{B}_{\text{had}}^{\text{uni}} = 1 - \mathcal{B}_e - \mathcal{B}_\mu$ with respect to $\mathcal{B}_{\text{had}}$ equal to the sum of all τ hadronic branching fractions is offset by increased correlations when considering $R_{\text{had}}{}^{\text{uni}} = \mathcal{B}_{\text{had}}/\mathcal{B}_e^{\text{uni}}$ and similar expressions in the $|V_{us}|$ calculation. Second, if there are unobserved τ hadronic decay modes, they will affect $\mathcal{B}_{ud}$ and $\mathcal{B}_{us}$ in a more asymmetric way when using $\mathcal{B}_{\text{had}}^{\text{uni}}$.

The values of $|V_{us}|_{\tau\text{-OPE-1}}$ and $|V_{us}|_{\tau\text{-latt-incl}}$ are respectively 3.6σ and 3.7σ lower than the value $|V_{us}|_{\text{uni}} = 0.2272 \pm 0.0011$ predicted from the CKM unitarity relation $(|V_{us}|_{\text{uni}})^2 = 1 - |V_{ud}|^2 - |V_{ub}|^2$, with $|V_{ub}| = 0.00382 \pm 0.00020$ [302]. Using Eqs. (246) and (249) we also compute $|V_{us}|/|V_{ud}|_{\tau\text{-OPE-1}} = 0.2243 \pm 0.0022$ and $|V_{us}|/|V_{ud}|_{\tau\text{-latt-incl}} = 0.2248 \pm 0.0020$.

2. $|V_{us}|$ from $\mathcal{B}(\tau \to K\nu)/\mathcal{B}(\tau \to \pi\nu)$

We also compute $|V_{us}|/|V_{ud}|$ from the ratio of branching fractions $\mathcal{B}_{10/9} = \mathcal{B}(\tau^- \to K^-\nu_\tau)/\mathcal{B}(\tau^- \to \pi^-\nu_\tau) = 0.0644 \pm 0.0009$ (Table 301) using the equation [1601]:

$$\frac{\mathcal{B}(\tau^- \to K^- \nu_\tau)}{\mathcal{B}(\tau^- \to \pi^- \nu_\tau)} = \frac{f_{K\pm}^2 |V_{us}|^2}{f_{\pi\pm}^2 |V_{ud}|^2} \frac{(m_\tau^2 - m_K^2)^2}{(m_\tau^2 - m_\pi^2)^2} (1 + \delta_{\tau K/\tau\pi}), \tag{250}$$

where $\delta_{\tau K/\tau\pi} = (0.10 \pm 0.80)\%$ [1587] is the radiative correction for the ratio of partial widths $\Gamma(\tau \to K\nu_\tau[\gamma])/\Gamma(\tau \to \pi\nu_\tau[\gamma])$. Using the ratio of decay constants $f_{K\pm}/f_{\pi\pm} = 1.1934 \pm 0.0019$ from the 2023 web update of the FLAG 2021 lattice QCD averages with $N_f = 2 + 1 + 1$ [1298,1299,1602–1606], we obtain $|V_{us}|/|V_{ud}| = 0.2289 \pm 0.0019$. By using the above-mentioned $|V_{ud}|$ value, we compute $|V_{us}|_{\tau K/\pi} = 0.2229 \pm 0.0019$, which is 2.0σ below the CKM unitarity prediction.

3. $|V_{us}|$ from $\mathcal{B}(\tau \to K\nu)$

We also determine $|V_{us}|$ from the branching fraction $\mathcal{B}(\tau^- \to K^- \nu_\tau)$ using

$$\mathcal{B}(\tau^- \to K^- \nu_\tau) = \frac{G_F^2}{16\pi\hbar} f_{K\pm}^2 |V_{us}|^2 \tau_\tau m_\tau^3 \left(1 - \frac{m_K^2}{m_\tau^2}\right)^2 \times S_{\rm EW}^{\tau h}(1 + \delta_{\tau K}). \tag{251}$$

We use $f_{K\pm} = 155.7 \pm 0.3$ MeV from the 2023 web update of the FLAG 2021 lattice QCD averages with $N_f = 2 + 1 + 1$ [1298,1602–1604,1606,1607]. The universal short-distance electroweak correction for τ hadronic decays is $S_{\rm EW}^{\tau h} = S_{\rm EW}^{R\tau h} \cdot S_{\rm EW}^{\rm sub,lep} = 1.01910 \pm 0.00030$, where the radiative correction for the tau spectral functions is $S_{\rm EW}^{R\tau h} = 1.02350 \pm 0.00030$ [1586,1608,1609] and the sub-leading universal short-distance correction for the τ leptonic decays is $S_{\rm EW}^{\rm sub,lep} = 0.9957$ [1608]. The long-distance radiative correction for $\mathcal{B}(\tau^- \to K^- \nu_\tau)$ is $\delta_{\tau K} = (-0.15 \pm 0.57)\%$ [1587]. The physical constants G_F and $\hbar$ are taken from CODATA 2018 [1585]. We obtain $|V_{us}|_{\tau K} = 0.2224 \pm 0.0017$, which is 2.3σ below the CKM unitarity prediction.

4. Summary of $|V_{us}|$ from τ decays

We summarize the $|V_{us}|$ determinations that we updated using the present HFLAV-Tau averages by reporting the values, the discrepancy with respect to the $|V_{us}|$ determination from CKM unitarity, and an illustration of the measurement method

$$|V_{us}|_{\rm uni} = 0.2272 \pm 0.0011 \quad 0.0\sigma \quad [\sqrt{1 - |V_{ud}|^2 - |V_{ub}|^2} \quad \text{(CKM unitarity)}], \tag{252}$$

$$|V_{us}|_{K\ell 3} = 0.2233 \pm 0.0005 \quad 3.2\sigma \quad [\mathcal{B}_{K\ell 3} \quad [1591]], \tag{253}$$

$$|V_{us}|_{K\ell 2} = 0.2250 \pm 0.0005 \quad 1.7\sigma \quad [\mathcal{B}_{K\ell 2} \quad [1591]], \tag{254}$$

$$|V_{us}|_{\tau\text{-OPE-1}} = 0.2184 \pm 0.0021 \quad 3.6\sigma \quad [\mathcal{B}(\tau^- \to X_s^- \nu_\tau)], \tag{255}$$

$$|V_{us}|_{\tau\text{-latt-incl}} = 0.2189 \pm 0.0019 \quad 3.7\sigma \quad [\mathcal{B}(\tau^- \to X_s^- \nu_\tau)], \tag{256}$$

$$|V_{us}|_{\tau K/\pi} = 0.2229 \pm 0.0019 \quad 2.0\sigma \quad [\mathcal{B}(\tau^- \to K^- \nu_\tau)/\mathcal{B}(\tau^- \to \pi^- \nu_\tau)], \tag{257}$$

$$|V_{us}|_{\tau K} = 0.2224 \pm 0.0017 \quad 2.3\sigma \quad [\mathcal{B}(\tau^- \to K^- \nu_\tau)]. \tag{258}$$

Averaging the two $|V_{us}|$ determinations that rely on exclusive τ branching fractions [Eqs. (257), (258)], we obtain

$$|V_{us}|_{\tau\,\rm excl} = 0.2225 \pm 0.0017 \quad 2.3\sigma \quad [\text{average of } \tau \text{ exclusive measurements}]. \tag{259}$$

Averaging the τ inclusive and exclusive $|V_{us}|$ determinations [Eqs. (255)–(258)], we obtain

$$|V_{us}|_{\tau} = 0.2208 \pm 0.0014 \quad 3.6\sigma \quad [\text{average of 4}|V_{us}|\tau \text{ measurements}]. \tag{260}$$

In calculating the averages, all correlations arising from using the τ branching fractions fit results and common external inputs are accounted for. The systematic uncertainties of $|V_{us}|_{\tau\text{-OPE-1}}$ and $|V_{us}|_{\tau\text{-latt-incl}}$ have been assumed to be uncorrelated. The correlation between $f_{K\pm}$ and $f_{K\pm}/f_{\pi\pm}$ is conservatively set to 100%. For the purpose of estimating the correlations between $\delta_{\tau K}$, $\delta_{\tau\pi}$ and $\delta_{\tau K/\tau\pi}$, we use the information [1587] that the uncertainties on $\delta_{\tau K}$ and $\delta_{\tau\pi}$ are uncorrelated to a good approximation, and that $\delta_{\tau K/\tau\pi} = \delta_{\tau K} - \delta_{\tau\pi}$.

All $|V_{us}|$ determinations based on measured τ branching fractions are lower than both the kaon and the CKM-unitarity determinations. This is correlated with the fact that the direct measurements of the three largest τ branching fractions to kaons [$\mathcal{B}(\tau^- \to K^- \nu_\tau)$, $\mathcal{B}(\tau^- \to \pi^0 \nu_\tau)$ and $\mathcal{B}(\tau^- \to \pi^- \bar{K}^0 \nu_\tau)$] yield lower values than their SM predictions based on the branching fractions of leptonic kaon decays [1586,1610,1611].

Figure 67 reports our $|V_{us}|$ determinations using the present HFLAV-Tau averages, two additional $|V_{us}|$ determinations using partially different τ measurements inputs [1596–1598], two determinations based on kaon data [1589], and the $|V_{us}|$ value obtained from $|V_{ud}|$ using the CKM-matrix unitarity [1589].

G. Combination of upper limits on τ lepton-flavor-violating branching fractions

The Standard Model prediction for the τ lepton-flavor-violating (LFV) branching fractions are of order 10^{-54} [1612,1613], which are too small to be measured experimentally. Recently, the contributions due to finite neutrino masses for $\tau^- \to \ell_i^- \ell_j^+ \ell_a^-$ decays (where $a = i$ or j, and i may or may not be equal to j), were re-scrutinized and also found to be in the range of $[10^{-56}, 10^{-54}]$ [1614,1615]. However, these branching fractions are expected to be of the order of 10^{-10}–10^{-9} in several new physics scenarios [1616–1620], which is just below the current experimental sensitivity. Several searches have been performed to observe neutrino-less τ decays to final states categorized as $\ell\gamma$, ℓP^0, ℓV^0, ℓS^0, $\ell\ell\ell$, ℓhh, including decays that are also baryon-number-violating (BNV). In Table 305 and Fig. 68, we report the observed upper limits on these branching fractions published by the *B*-factories *BABAR* and Belle and the LHC experiments. Weaker upper limits (mainly from CLEO) have been omitted from Table 305, but are shown in Fig. 68, to document the historical progress. For channels where multiple results of similar strengths are available, we also report the combined upper limits, following the prescription described below. No preliminary results are included in this report.

We combine the reported upper limits by first averaging the central values of the corresponding branching-fraction measurements to obtain the average branching fraction $\bar{\mathcal{B}}$ and its uncertainty $\delta\bar{\mathcal{B}}$,

$$\bar{\mathcal{B}} = \frac{\sum w_i \mathcal{B}_i}{\sum w_i}, \qquad \delta\bar{\mathcal{B}} = \sqrt{\frac{1}{\sum w_i}}, \tag{261}$$

where $\mathcal{B}_i$ is the central value for the branching fraction of measurement i and $w_i = 1/\delta\mathcal{B}_i^2$ is the inverse of square of its uncertainty. We then compute the 90% confidence level

TABLE 305. Experimental upper limits on lepton flavor violating τ decays. The modes are grouped according to the properties of their final states. Modes with baryon number violation are labeled with "BNV". The combinations of upper limits are reported in the rows with label "Comb." in the "Experiment / Reference" column. The measurements used to compute the combinations are tagged with an asterisk attached to their reference. Where available, additional information is reported about the number of τ decays used in the search, the efficiency of the selection, the expected background and the number of observed events, or the central value of branching fractions.

Decay mode	90% CL limit	Exp./Ref.	$N_\tau(10^6)$	$\varepsilon(\%)$	$N_{\rm bkg}$	$N_{\rm obs}$
$\ell\gamma$ category						
	3.3×10^{-8}	*BABAR* [1622]*	963	3.90 ± 0.30	1.60 ± 0.40	0
$\mathcal{B}(\tau^- \to e^-\gamma)$	5.6×10^{-8}	*BABAR* [1623]*	1824	2.90 ± 0.19	5.50 ± 4.65	5
	2.6×10^{-8}	Comb.				
	4.4×10^{-8}	*BABAR* [1622]*	963	6.10 ± 0.50	3.60 ± 0.70	2
$\mathcal{B}(\tau^- \to \mu^-\gamma)$	4.2×10^{-8}	*BABAR* [1623]*	1824	3.70 ± 0.21	5.30 ± 2.75	5
	2.7×10^{-8}	Comb.				
ℓP^0 category						
	1.3×10^{-7}	*BABAR* [1624]*	623	2.80 ± 0.25	0.17 ± 0.04	0
$\mathcal{B}(\tau^- \to e^-\pi^0)$	8.0×10^{-8}	*BABAR* [1625]*	737	3.88 ± 0.17	0.20 ± 0.20	0
	6.4×10^{-8}	Comb.				
	1.1×10^{-7}	*BABAR* [1624]*	623	4.69 ± 0.37	1.33 ± 0.15	1
$\mathcal{B}(\tau^- \to \mu^-\pi^0)$	1.2×10^{-7}	*BABAR* [1625]*	737	4.48 ± 0.20	0.58 ± 0.34	1
	8.1×10^{-8}	Comb.				
	3.3×10^{-8}	*BABAR* [1626]*	862	9.40 ± 0.20	1.00 ± 0.40	1
$\mathcal{B}(\tau^- \to e^-K_S^0)$	2.6×10^{-8}	*BABAR* [1627]*	1234	7.06 ± 0.47	0.18 ± 0.18	0
	2.0×10^{-8}	Comb.				
	4.0×10^{-8}	*BABAR* [1626]*	862	7.00 ± 0.39	5.30 ± 2.20	2
$\mathcal{B}(\tau^- \to \mu^-K_S^0)$	2.3×10^{-8}	*BABAR* [1627]*	1234	7.40 ± 0.50	0.35 ± 0.21	0
	1.8×10^{-8}	Comb.				

(Table continued)

TABLE 305. *(Continued)*

Decay mode	90% CL limit	Exp./Ref.	$N_\tau(10^6)$	$\varepsilon(\%)$	$N_{\rm bkg}$	$N_{\rm obs}$
	1.6×10^{-7}	*BABAR* [1624]*	623	2.12 ± 0.20	0.22 ± 0.05	0
$\mathcal{B}(\tau^-\to e^-\eta)$	9.2×10^{-8}	*BABAR* [1625]*	737	2.87 ± 0.14	0.78 ± 0.59	0
	7.4×10^{-8}	Comb.				
	1.5×10^{-7}	*BABAR* [1624]*	623	3.59 ± 0.41	0.75 ± 0.08	1
$\mathcal{B}(\tau^-\to \mu^-\eta)$	6.5×10^{-8}	*BABAR* [1625]*	737	4.08 ± 0.20	0.64 ± 0.38	0
	6.1×10^{-8}	Comb.				
	2.4×10^{-7}	*BABAR* [1624]*	623	1.53 ± 0.16	0.12 ± 0.03	0
$\mathcal{B}(\tau^-\to e^-\eta'(958))$	1.6×10^{-7}	*BABAR* [1625]*	737	2.15 ± 0.11	0.57 ± 0.41	0
	1.3×10^{-7}	Comb.				
	1.4×10^{-7}	*BABAR* [1624]*	623	2.18 ± 0.26	0.49 ± 0.04	0
$\mathcal{B}(\tau^-\to \mu^-\eta'(958))$	1.3×10^{-7}	*BABAR* [1625]*	737	2.45 ± 0.13	0.46 ± 0.33	0
	8.6×10^{-8}	Comb.				
ℓS^0 category						
$\mathcal{B}(\tau^-\to e^-f_0(980))$	6.8×10^{-8}	*BABAR* [1628]	1233	2.90 ± 0.33	0.10 ± 0.07	0
$\mathcal{B}(\tau^-\to \mu^-f_0(980))$	6.4×10^{-8}	*BABAR* [1628]	1233	3.01 ± 0.33	0.11 ± 0.08	0
ℓV^0 category						
	4.6×10^{-8}	*BABAR* [1629]*	829	7.31 ± 0.18	1.32 ± 0.17	1
$\mathcal{B}(\tau^-\to e^-\rho^0)$	2.2×10^{-8}	*BABAR* [1630]*	1796	8.49 ± 0.37	0.80 ± 0.27	1
	2.0×10^{-8}	Comb.				
	2.6×10^{-8}	*BABAR* [1629]*	829	4.52 ± 0.41	2.04 ± 0.19	0
$\mathcal{B}(\tau^-\to \mu^-\rho^0)$	1.7×10^{-8}	*BABAR* [1630]*	1796	7.78 ± 0.36	0.95 ± 0.25	0
	1.3×10^{-8}	Comb.				
	1.1×10^{-7}	*BABAR* [1631]*	706	2.61 ± 0.11	0.35 ± 0.06	0
$\mathcal{B}(\tau^-\to e^-\omega)$	2.4×10^{-8}	*BABAR* [1630]*	1796	5.41 ± 0.24	0.74 ± 0.43	0
	2.2×10^{-8}	Comb.				
	1.0×10^{-7}	*BABAR* [1631]*	706	2.26 ± 0.14	0.73 ± 0.03	0
$\mathcal{B}(\tau^-\to \mu^-\omega)$	3.9×10^{-8}	*BABAR* [1630]*	1796	3.27 ± 0.16	0.32 ± 0.30	0
	3.4×10^{-8}	Comb.				
	5.9×10^{-8}	*BABAR* [1629]*	829	8.00 ± 0.19	1.65 ± 0.23	2
$\mathcal{B}(\tau^-\to e^-K^*(892))$	1.9×10^{-8}	*BABAR* [1630]*	1796	6.94 ± 0.28	0.54 ± 0.26	0
	1.9×10^{-8}	Comb.				
	1.7×10^{-7}	*BABAR* [1629]*	829	4.57 ± 0.36	1.79 ± 0.21	4
$\mathcal{B}(\tau^-\to \mu^-K^*(892))$	2.9×10^{-8}	*BABAR* [1630]*	1796	4.52 ± 0.19	0.84 ± 0.40	0
	3.3×10^{-8}	Comb.				
	4.6×10^{-8}	*BABAR* [1629]*	829	7.76 ± 0.18	2.76 ± 0.28	2
$\mathcal{B}(\tau^-\to e^-\bar{K}^*(892))$	1.7×10^{-8}	*BABAR* [1630]*	1796	7.45 ± 0.31	0.25 ± 0.11	0
	1.5×10^{-8}	Comb.				
	7.3×10^{-8}	*BABAR* [1629]*	829	4.11 ± 0.32	1.72 ± 0.17	1
$\mathcal{B}(\tau^-\to \mu^-\bar{K}^*(892))$	4.3×10^{-8}	*BABAR* [1630]*	1796	4.58 ± 0.20	0.58 ± 0.21	1
	3.7×10^{-8}	Comb.				

(Table continued)

TABLE 305. *(Continued)*

Decay mode	90% CL limit	Exp./Ref.	$N_\tau(10^6)$	$\varepsilon(\%)$	$N_{\rm bkg}$	$N_{\rm obs}$
	3.1×10^{-8}	*BABAR* [1629]*	829	6.43 ± 0.16	0.68 ± 0.12	0
$\mathcal{B}(\tau^-\to e^-\phi)$	2.0×10^{-8}	*BABAR* [1630]*	1796	6.45 ± 0.29	0.38 ± 0.21	0
	1.6×10^{-8}	Comb.				
	1.9×10^{-7}	*BABAR* [1629]*	829	5.18 ± 0.27	2.76 ± 0.16	6
$\mathcal{B}(\tau^-\to \mu^-\phi)$	2.3×10^{-8}	*BABAR* [1630]*	1796	5.59 ± 0.27	0.47 ± 0.16	0
	2.6×10^{-8}	Comb.				
***ℓℓℓ* category**						
	2.9×10^{-8}	*BABAR* [1632]*	860	8.60 ± 0.20	0.12 ± 0.02	0
$\mathcal{B}(\tau^-\to e^-e^+e^-)$	2.7×10^{-8}	*BABAR* [1633]*	1437	6.00 ± 0.59	0.21 ± 0.15	0
	1.9×10^{-8}	Comb.				
	3.2×10^{-8}	*BABAR* [1632]*	860	6.40 ± 0.40	0.54 ± 0.14	0
$\mathcal{B}(\tau^-\to e^-\mu^+\mu^-)$	2.7×10^{-8}	*BABAR* [1633]*	1437	6.10 ± 0.58	0.10 ± 0.04	0
	2.0×10^{-8}	Comb.				
	2.6×10^{-8}	*BABAR* [1632]*	860	10.20 ± 0.60	0.03 ± 0.02	0
$\mathcal{B}(\tau^-\to \mu^-e^+\mu^-)$	1.7×10^{-8}	*BABAR* [1633]*	1437	10.10 ± 0.77	0.02 ± 0.02	0
	1.4×10^{-8}	Comb.				
	2.2×10^{-8}	*BABAR* [1632]*	860	8.80 ± 0.50	0.64 ± 0.19	0
$\mathcal{B}(\tau^-\to \mu^-e^+e^-)$	1.8×10^{-8}	*BABAR* [1633]*	1437	9.30 ± 0.73	0.04 ± 0.04	0
	1.3×10^{-8}	Comb.				
	1.8×10^{-8}	*BABAR* [1632]*	860	12.70 ± 0.70	0.34 ± 0.12	0
$\mathcal{B}(\tau^-\to e^-\mu^+e^-)$	1.5×10^{-8}	*BABAR* [1633]*	1437	11.50 ± 0.89	0.01 ± 0.01	0
	1.1×10^{-8}	Comb.				
	3.8×10^{-7}	ATLAS [1634]				
	3.3×10^{-8}	*BABAR* [1632]*	860	6.60 ± 0.60	0.44 ± 0.17	0
	2.1×10^{-8}	*BABAR* [1633]*	1437	7.60 ± 0.56	0.13 ± 0.20	0
$\mathcal{B}(\tau^-\to \mu^-\mu^+\mu^-)$	1.9×10^{-8}	Belle II[1501]*	777	20.42 ± 0.93	0.70 ± 0.56	1
	2.9×10^{-8}	CMS [1500]*		$\mathcal{B}=5.1\times10^{-9}$		
	4.6×10^{-8}	LHCb [1621]*		$\mathcal{B}=2.3\times10^{-8}$		
	1.6×10^{-8}	Comb.				
***ℓhh* category**						
	1.2×10^{-7}	*BABAR* [1635]*	407	3.30 ± 0.15	0.81 ± 0.13	0
$\mathcal{B}(\tau^-\to e^-\pi^+\pi^-)$	2.3×10^{-8}	*BABAR* [1636]*	1564	5.45 ± 0.31	0.55 ± 0.23	0
	2.1×10^{-8}	Comb.				
$\mathcal{B}(\tau^-\to e^+\pi^-\pi^-)$	2.7×10^{-7}	*BABAR* [1635]	407	3.40 ± 0.15	0.41 ± 0.10	1
	2.0×10^{-8}	*BABAR* [1636]	1564	6.56 ± 0.36	0.37 ± 0.19	0
$\mathcal{B}(\tau^-\to \mu^-\pi^+\pi^-)$	2.9×10^{-7}	*BABAR* [1635]	407	3.40 ± 0.19	2.99 ± 0.41	3
	2.1×10^{-8}	*BABAR* [1636]	1564	5.83 ± 0.33	0.63 ± 0.23	0
	7.0×10^{-8}	*BABAR* [1635]*	407	3.30 ± 0.18	1.46 ± 0.27	0
$\mathcal{B}(\tau^-\to \mu^+\pi^-\pi^-)$	3.9×10^{-8}	*BABAR* [1636]*	1564	6.55 ± 0.37	0.33 ± 0.16	1
	3.5×10^{-8}	Comb.				

(Table continued)

TABLE 305. *(Continued)*

Decay mode	90% CL limit	Exp./Ref.	$N_\tau(10^6)$	$\varepsilon(\%)$	$N_{\rm bkg}$	$N_{\rm obs}$
	3.2×10^{-7}	*BABAR* [1635]*	407	3.10 ± 0.13	0.14 ± 0.06	1
$\mathcal{B}(\tau^-\to e^-\pi^+K^-)$	3.7×10^{-8}	*BABAR* [1636]*	1564	3.97 ± 0.25	0.18 ± 0.13	0
	3.8×10^{-8}	Comb.				
	1.7×10^{-7}	*BABAR* [1635]*	407	3.08 ± 0.13	0.32 ± 0.08	0
$\mathcal{B}(\tau^-\to e^-K^+\pi^-)$	3.1×10^{-8}	*BABAR* [1636]*	1564	4.07 ± 0.25	0.55 ± 0.31	0
	2.9×10^{-8}	Comb.				
	1.8×10^{-7}	*BABAR* [1635]*	407	3.19 ± 0.14	0.16 ± 0.06	0
$\mathcal{B}(\tau^-\to e^+\pi^-K^-)$	3.2×10^{-8}	*BABAR* [1636]*	1564	4.00 ± 0.25	0.46 ± 0.21	0
	3.1×10^{-8}	Comb.				
$\mathcal{B}(\tau^-\to e^-K^0_SK^0_S)$	7.1×10^{-8}	*BABAR* [1627]	1234	2.79 ± 0.31	0.07 ± 0.07	0
	1.4×10^{-7}	*BABAR* [1635]*	407	3.77 ± 0.16	0.22 ± 0.06	0
$\mathcal{B}(\tau^-\to e^-K^+K^-)$	3.4×10^{-8}	*BABAR* [1636]*	1564	4.29 ± 0.29	0.17 ± 0.10	0
	3.3×10^{-8}	Comb.				
	1.5×10^{-7}	*BABAR* [1635]*	407	3.85 ± 0.16	0.04 ± 0.04	0
$\mathcal{B}(\tau^-\to e^+K^-K^-)$	3.3×10^{-8}	*BABAR* [1636]*	1564	4.64 ± 0.30	0.06 ± 0.06	0
	3.2×10^{-8}	Comb.				
	2.6×10^{-7}	*BABAR* [1635]*	407	2.87 ± 0.16	1.04 ± 0.18	1
$\mathcal{B}(\tau^-\to \mu^-\pi^+K^-)$	8.6×10^{-8}	*BABAR* [1636]*	1564	2.72 ± 0.17	0.72 ± 0.28	1
	8.2×10^{-8}	Comb.				
	3.2×10^{-7}	*BABAR* [1635]*	407	2.97 ± 0.16	1.67 ± 0.29	2
$\mathcal{B}(\tau^-\to \mu^-K^+\pi^-)$	4.5×10^{-8}	*BABAR* [1636]*	1564	2.62 ± 0.15	0.64 ± 0.23	0
	4.6×10^{-8}	Comb.				
	2.2×10^{-7}	*BABAR* [1635]*	407	2.85 ± 0.16	1.54 ± 0.25	1
$\mathcal{B}(\tau^-\to \mu^+\pi^-K^-)$	4.8×10^{-8}	*BABAR* [1636]*	1564	2.55 ± 0.16	0.56 ± 0.21	0
	4.5×10^{-8}	Comb.				
$\mathcal{B}(\tau^-\to \mu^-K^0_SK^0_S)$	8.0×10^{-8}	*BABAR* [1627]	1234	2.43 ± 0.27	0.12 ± 0.08	0
	2.5×10^{-7}	*BABAR* [1635]*	407	2.16 ± 0.12	0.24 ± 0.07	0
$\mathcal{B}(\tau^-\to \mu^-K^+K^-)$	4.4×10^{-8}	*BABAR* [1636]*	1564	2.85 ± 0.17	0.51 ± 0.19	0
	4.2×10^{-8}	Comb.				
	4.8×10^{-7}	*BABAR* [1635]	407	2.06 ± 0.11	0.07 ± 0.10	1
$\mathcal{B}(\tau^-\to \mu^+K^-K^-)$	4.7×10^{-8}	*BABAR* [1636]	1564	2.98 ± 0.18	0.25 ± 0.13	0
BNV category						
	7.2×10^{-8}	Belle [1637]*	283	7.48 ± 0.68	1.70 ± 0.80	0
$\mathcal{B}(\tau^-\to \pi^-\Lambda)$	4.7×10^{-8}	Belle II [1502]*	669	9.50 ± 0.26	1.00 ± 1.20	0
	3.0×10^{-8}	Comb.				
	1.4×10^{-7}	Belle [1637]*	283	7.54 ± 0.69	1.70 ± 0.80	1
$\mathcal{B}(\tau^-\to \pi^-\bar\Lambda)$	4.3×10^{-8}	Belle II [1502]*	669	9.90 ± 0.28	0.50 ± 0.60	0
	3.8×10^{-8}	Comb.				
$\mathcal{B}(\tau^-\to \bar p e^+e^-)$	3.0×10^{-8}	Belle [1638]	1682	7.80 ± 0.39	0.50 ± 0.35	1
$\mathcal{B}(\tau^-\to p e^-e^-)$	3.0×10^{-8}	Belle [1638]	1682	8.00 ± 0.40	0.23 ± 0.07	1
$\mathcal{B}(\tau^-\to \bar p e^+\mu^-)$	2.0×10^{-8}	Belle [1638]	1682	6.50 ± 0.33	0.22 ± 0.06	0

(Table continued)

TABLE 305. *(Continued)*

Decay mode	90% CL limit	Exp./Ref.	$N_\tau(10^6)$	$\varepsilon(\%)$	$N_{\rm bkg}$	$N_{\rm obs}$
$\mathcal{B}(\tau^- \to \bar{p}e^-\mu^+)$	1.8×10^{-8}	Belle [1638]	1682	6.90 ± 0.34	0.40 ± 0.28	0
$\mathcal{B}(\tau^- \to p\mu^-\mu^-)$	4.0×10^{-8}	Belle [1638]	1682	4.60 ± 0.23	1.30 ± 0.46	1
	4.4×10^{-7}	LHCb [1639]				
$\mathcal{B}(\tau^- \to \bar{p}\mu^+\mu^-)$	1.8×10^{-8}	Belle [1638]	1682	5.00 ± 0.25	1.14 ± 0.43	0
	3.3×10^{-7}	LHCb [1639]				

(CL) upper limit as $\overline{\mathcal{B}^{90}} = \bar{\mathcal{B}} + 1.645\delta\bar{\mathcal{B}}$, assuming a Gaussian uncertainty. The majority of published limits do not have reported values for $\mathcal{B}_i$ and w_i. In such cases, we take the central value to be $\mathcal{B}_i = (N^i_{\rm obs} - N^i_{\rm bkg})/(N^i_\tau \varepsilon^i)$, where $N^i_{\rm obs}$ is the number of observed events, $N^i_{\rm bkg}$ is the number of expected background events, N^i_τ is the number of τ decays in the data sample, and ε^i is the signal reconstruction efficiency in the signal region. Additional information for central value of $\mathcal{B}(\tau^- \to \mu^-\mu^+\mu^-)$ are obtained from the CMS [1500] and LHCb [1621] collaborations, respectively, and are listed in Table 305 for future reference.

The uncertainty $\delta\mathcal{B}_i$ is computed assuming that the reported 90% CL limit corresponds to $\mathcal{B}^{90}_i = \mathcal{B}_i + 1.645\,\delta\mathcal{B}_i$. Using this combination procedure, the resulting upper limit may be weaker than the most stringent input limit, but always corresponds to a more precise branching fraction, obtained by averaging multiple measurements. Since there is negligible gain in combining limits of very different strength, the combinations do not include the limits that are more than 10 times larger than the strictest limit in the respective channel. This excludes limits of the CLEO and ATLAS searches and the LHCb searches for τ decays into proton and two muons. We report in Table 305 and Fig. 68 the observed upper limits on the τ lepton-flavor-violating decays and their combinations.

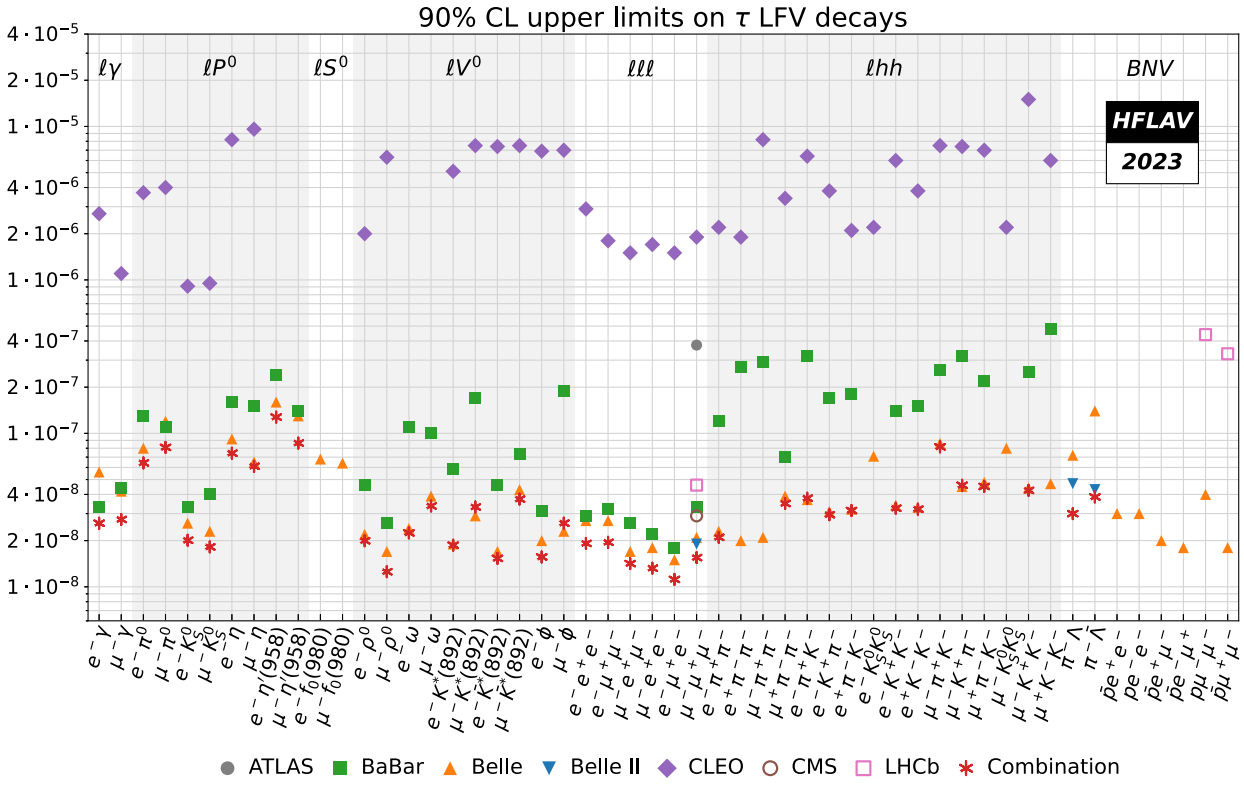


FIG. 68. Tau lepton-flavor-violating branching fraction upper limits and combinations. In order to appreciate the physics reach improvement over time, the plot includes also the CLEO upper limits reported by PDG 2022 [302].

ACKNOWLEDGMENTS

We thank Lu Cao, Mirco Dorigo, Sevda Esen, Alessandro Gaz, Carla Göbel, Yuval Grossman, Judd Harrison, Tobias Huber, Gianluca Inguglia, Martin Jung, Alexander Lenz, Ryan Mitchell, Ulrich Nierste, Emilie Passemar, and Keri Vos for their careful review of the text in preparation of this paper for publication. We also thank all past members of HFLAV and coauthors previous HFLAV reports. We are grateful for the strong support of the ATLAS, *BABAR*, Belle, Belle II, BES III, CLEO, CDF, CMS, D0 and LHCb collaborations, without whom this compilation of results and world averages would not have been possible. The success of these experiments was made possible by the excellent performance and operation of the BEPC-II, CESR, KEKB, LHC, PEP-II, SuperKEKB, and Tevatron colliders. We recognize the interplay between theoretical and experimental communities that has provided a stimulus for many of the measurements in this document. We thank CERN for providing computing resources to HFLAV. Members of HFLAV are supported by the following funding agencies: Australian Research Council (Australia); Ministry of Science and Technology, National Natural Science Foundation, Key Research Program of Frontier Sciences of the Chinese Academy of Sciences (China); European Research Council; CNRS/IN2P3 (France); Deutsche Forschungsgemeinschaft (Germany); Israel Science Foundation, US-Israel Binational Science Fund (Israel); Istituto Nazionale di Fisica Nucleare (Italy); Ministry of Education, Culture, Sports, Science and Technology, Japan Society for the Promotion of Science (Japan); National Agency for Academic Exchange, Ministry of Science and Higher Education, National Science Centre (Poland); MCINN, XuntaGal, and InTalent-Inditex (Spain); Swiss National Science Foundation (Switzerland); Science and Technology Facilities Council (UK); and Department of Energy (USA).

DATA AVAILABILITY

The data that support the findings of this article are not publicly available upon publication because it is not technically feasible and/or the cost of preparing, depositing, and hosting the data would be prohibitive within the terms of this research project. The data are available from the authors upon reasonable request.

[1] Y. S. Amhis *et al.* (HFLAV Collaboration), Averages of b-hadron, c-hadron, and τ-lepton properties as of 2021, Phys. Rev. D **107**, 052008 (2023).
[2] N. Cabibbo, Unitary symmetry and leptonic decays, Phys. Rev. Lett. **10**, 531 (1963).
[3] M. Kobayashi and T. Maskawa, *CP* violation in the renormalizable theory of weak interaction, Prog. Theor. Phys. **49**, 652 (1973).
[4] D. Abbaneo *et al.*, Combined results on b-hadron production rates, lifetimes, oscillations and semileptonic decays, Report No. CERN-EP-2000-096, arXiv:hep-ex/0009052; Combined results on b-hadron production rates and decay properties, Report No. CERN-EP-2001-050, arXiv:hep-ex/0112028.
[5] HFLAV web page, https://hflav.web.cern.ch.
[6] O. Schneider and H. Seywerd, COMBOS: A program to COMbine results from B OScillations analyses, https://gitlab.cern.ch/hflav/shared-material/-/blob/main/combos.pdf (1999).
[7] E. Bertholet and T. Kuhr, HFLAV averaging, 10.5281/zenodo.6632075 (2022).
[8] A. C. Aitken, On least squares and linear combination of observations, Proc. R. Soc. Edinburgh, Sect. A **55**, 42 (1936).
[9] P. A. Zyla *et al.* (Particle Data Group), Review of particle physics, Prog. Theor. Exp. Phys. **2020**, 083C01 (2020).
[10] R. Barlow, Asymmetric statistical errors, arXiv:physics/0406120.
[11] J. P. Alexander *et al.* (CLEO Collaboration), Measurement of the relative branching fraction of $\Upsilon(4S)$ to charged and neutral B meson pairs, Phys. Rev. Lett. **86**, 2737 (2001).
[12] B. Aubert *et al.* (*BABAR* Collaboration), Measurement of branching fractions and charge asymmetries for exclusive B decays to charmonium, Phys. Rev. Lett. **94**, 141801 (2005).
[13] S. Choudhury *et al.* (Belle Collaboration), Measurement of the B^+/B^0 production ratio in e^+e^- collisions at the $\Upsilon(4S)$ resonance using $B \to J/\psi(\ell\ell)K$ decays at Belle, Phys. Rev. D **107**, L031102 (2023).
[14] S. B. Athar *et al.* (CLEO Collaboration), Measurement of the ratio of branching fractions of the $\Upsilon(4S)$ to charged and neutral B mesons, Phys. Rev. D **66**, 052003 (2002).
[15] N. C. Hastings *et al.* (Belle Collaboration), Studies of $B^0 - \bar{B}^0$ mixing properties with inclusive dilepton events, Phys. Rev. D **67**, 052004 (2003).
[16] B. Aubert *et al.* (*BABAR* Collaboration), Measurement of the branching fraction of $\Upsilon(4S) \to B^0\bar{B}^0$, Phys. Rev. Lett. **95**, 042001 (2005).
[17] B. Barish *et al.* (CLEO Collaboration), Measurements of the B semileptonic branching fraction with lepton tags, Phys. Rev. Lett. **76**, 1570 (1996).
[18] B. Aubert *et al.* (*BABAR* Collaboration), Study of hadronic transitions between Upsilon states and observation of $\Upsilon(4S) \to \eta\Upsilon(1S)$ decay, Phys. Rev. D **78**, 112002 (2008).
[19] E. Guido *et al.* (Belle Collaboration), Study of η and dipion transitions in $\Upsilon(4S)$ decays to lower bottomonia, Phys. Rev. D **96**, 052005 (2017).

[20] E. Guido *et al.* (Belle Collaboration), Observation of $\Upsilon(4S) \to \eta'\Upsilon(1S)$, Phys. Rev. Lett. **121**, 062001 (2018).

[21] U. Tamponi *et al.* (Belle Collaboration), First observation of the hadronic transition $\Upsilon(4S) \to \eta h_b(1P)$ and new measurement of the $h_b(1P)$ and $\eta_b(1S)$ parameters, Phys. Rev. Lett. **115**, 142001 (2015).

[22] J. Chay, H. Georgi, and B. Grinstein, Lepton energy distributions in heavy meson decays from QCD, Phys. Lett. B **247**, 399 (1990).

[23] M. Gronau, Y. Grossman, and J. L. Rosner, Isospin in B decays and the $(B^0\bar{B}^0)/(B^+B^-)$ production ratio, Phys. Rev. D **73**, 057501 (2006).

[24] M. Jung, Branching ratio measurements and isospin violation in B-meson decays, Phys. Lett. B **753**, 187 (2016).

[25] F. Bernlochner, M. Jung, M. Khan, G. Landsberg, and Z. Ligeti, Novel approaches to determine $B^{\pm}$ and B^0 meson production fractions, Phys. Rev. D **110**, 014007 (2024).

[26] A. E. Bondar, A. I. Milstein, R. V. Mizuk, and S. G. Salnikov, Effects of isospin violation in the $e^+e^- \to B^{(*)}\bar{B}^{(*)}$ cross sections, J. High Energy Phys. 05 (2022) 170.

[27] R. Mizuk *et al.* (Belle Collaboration), Measurement of the energy dependence of the $e^+e^- \to B\bar{B}$, $B\bar{B}^*$ and $B^*\bar{B}^*$ exclusive cross sections, J. High Energy Phys. 06 (2021) 137.

[28] Belle Collaboration, Measurement of the energy dependence of the $e^+e^- \to B\bar{B}$, $B\bar{B}^*$, and $B^*\bar{B}^*$ cross sections at Belle II, J. High Energy Phys. 10 (2024) 114.

[29] B. Aubert *et al.* (*BABAR* Collaboration), Measurement of the mass difference $m(B^0) - m(B^+)$, Phys. Rev. D **78**, 011103 (2008).

[30] S. Esen *et al.* (Belle Collaboration), Precise measurement of the branching fractions for $B_s \to D_s^{(*)+}D_s^{(*)-}$ and first measurement of the $D_s^{*+}D_s^{*-}$ polarization using e^+e^- collisions, Phys. Rev. D **87**, 031101 (2013).

[31] A. Garmash *et al.* (Belle Collaboration), Observation of $Z_b(10610)$ and $Z_b(10650)$ decaying to B mesons, Phys. Rev. Lett. **116**, 212001 (2016).

[32] A. Drutskoy *et al.* (Belle Collaboration), Measurement of $\Upsilon(5S)$ decays to B^0 and B^+ mesons, Phys. Rev. D **81**, 112003 (2010).

[33] V. Zhukova *et al.* (Belle Collaboration), Measurement of the $e^+e^- \to B_s^0\bar{B}_s^0X$ cross section in the energy range from 10.63 to 11.02 GeV using inclusive D_s^+ and D^0 production, J. High Energy Phys. 08 (2023) 131.

[34] B. Wang *et al.* (Belle Collaboration), Measurement of $\mathcal{B}(B_s \to D_sX)$ with B_s semileptonic tagging, Phys. Rev. D **105**, 012004 (2022).

[35] G. S. Huang *et al.* (CLEO Collaboration), Measurement of $\mathcal{B}(\Upsilon(5S) \to B_s^{(*)}\bar{B}_s^{(*)})$ using ϕ mesons, Phys. Rev. D **75**, 012002 (2007).

[36] J. P. Lees *et al.* (*BABAR* Collaboration), A measurement of the semileptonic branching fraction of the B_s^0 meson, Phys. Rev. D **85**, 011101 (2012).

[37] A. Garmash *et al.* (Belle Collaboration), Amplitude analysis of $e^+e^- \to \Upsilon(nS)\pi^+\pi^-$ at $\sqrt{s} = 10.865$ GeV, Phys. Rev. D **91**, 072003 (2015).

[38] P. Krokovny *et al.* (Belle Collaboration), First observation of the $Z_b(10610)^0$ in a Dalitz analysis of $\Upsilon(10860) \to \Upsilon(\mathrm{nS})\pi^0\pi^0$, Phys. Rev. D **88**, 052016 (2013).

[39] I. Adachi *et al.* (Belle Collaboration), First observation of the P-wave spin-singlet bottomonium states $h_b(1P)$ and $h_b(2P)$, Phys. Rev. Lett. **108**, 032001 (2012).

[40] X. H. He *et al.* (Belle Collaboration), Observation of $e^+e^- \to \pi^+\pi^-\pi^0\chi_{bJ}$ and search for $X_b \to \omega\Upsilon(1S)$ at $\sqrt{s} = 10.867$ GeV, Phys. Rev. Lett. **113**, 142001 (2014).

[41] U. Tamponi *et al.* (Belle Collaboration), Inclusive study of bottomonium production in association with an η meson in e^+e^- annihilations near $\Upsilon(5S)$, Eur. Phys. J. C **78**, 633 (2018).

[42] R. Louvot, Study of B_s meson production and measurement of B_s decays into a $D_s^{(*)-}$ and a light meson in e^+e^- collisions at $\sqrt{s} = 10.87$ GeV, Ph.D. thesis #5213, EPFL, Lausanne, 2012.

[43] Y. S. Amhis *et al.* (HFLAV Collaboration), Averages of b-hadron, c-hadron, and τ-lepton properties as of 2018, Eur. Phys. J. C **81**, 226 (2021).

[44] M. A. Shifman and M. B. Voloshin, Hierarchy of lifetimes of charmed and beautiful hadrons, Sov. Phys. JETP **64**, 698 (1986).

[45] I. I. Bigi, N. G. Uraltsev, and A. I. Vainshtein, Nonperturbative corrections to inclusive beauty and charm decays: QCD versus phenomenological models, Phys. Lett. B **293**, 430 (1992); **297**, 477(E) (1992).

[46] K. G. Wilson, Nonlagrangian models of current algebra, Phys. Rev. **179**, 1499 (1969).

[47] J. Albrecht, F. Bernlochner, A. Lenz, and A. Rusov, Lifetimes of b-hadrons and mixing of neutral B-mesons: Theoretical and experimental status, Eur. Phys. J. Spec. Top. **233**, 359 (2024).

[48] A. Lenz, Lifetimes and heavy quark expansion, Int. J. Mod. Phys. A **30**, 1543005 (2015).

[49] M. A. Shifman, Quark-hadron duality, in *At The Frontier of Particle Physics* (World Scientific, 2001), p. 1447.

[50] I. I. Y. Bigi and N. Uraltsev, A vademecum on quark hadron duality, Int. J. Mod. Phys. A **16**, 5201 (2001).

[51] T. Jubb, M. Kirk, A. Lenz, and G. Tetlalmatzi-Xolocotzi, On the ultimate precision of meson mixing observables, Nucl. Phys. **B915**, 431 (2017).

[52] M. B. Voloshin, Relations between inclusive decay rates of heavy baryons Phys. Rep. **320**, 275 (1999); B. Guberina, B. Melic, and H. Stefancic, Enhancement of preasymptotic effects in inclusive beauty decays, Phys. Lett. B **469**, 253 (1999); M. Neubert and C. T. Sachrajda, Spectator effects in inclusive decays of beauty hadrons, Nucl. Phys. **B483**, 339 (1997); I. I. Y. Bigi, M. A. Shifman, and N. Uraltsev, Aspects of heavy quark theory, Annu. Rev. Nucl. Part. Sci. **47**, 591 (1997).

[53] F. Gabbiani, A. I. Onishchenko, and A. A. Petrov, Spectator effects and lifetimes of heavy hadrons, Phys. Rev. D **70**, 094031 (2004).

[54] A. Lenz and U. Nierste, Numerical updates of lifetimes and mixing parameters of B mesons, arXiv:1102.4274.

[55] A. Lenz and U. Nierste, Theoretical update of $B_s - \bar{B}_s$ mixing, J. High Energy Phys. 06 (2007) 072.

[56] M. Beneke *et al.*, The $B^+ - B_d^0$ lifetime difference beyond leading logarithms, Nucl. Phys. **B639**, 389 (2002).

[57] E. Franco, V. Lubicz, F. Mescia, and C. Tarantino, Lifetime ratios of beauty hadrons at the next-to-leading order in QCD, Nucl. Phys. **B633**, 212 (2002).

[58] A. Lenz and T. Rauh, D-meson lifetimes within the heavy quark expansion, Phys. Rev. D **88**, 034004 (2013).

[59] T. Mannel, D. Moreno, and A. Pivovarov, Heavy quark expansion for heavy hadron lifetimes: Completing the $1/m_b^3$ corrections, J. High Energy Phys. 08 (2020) 089.

[60] A. Lenz, M. L. Piscopo, and A. V. Rusov, Contribution of the Darwin operator to non-leptonic decays of heavy quarks, J. High Energy Phys. 12 (2020) 199.

[61] G. Finauri and P. Gambino, The q^2 moments in inclusive semileptonic B decays, J. High Energy Phys. 02 (2024) 206.

[62] M. Bordone, B. Capdevila, and P. Gambino, Three loop calculations and inclusive V_{cb}, Phys. Lett. B **822**, 136679 (2021).

[63] F. Bernlochner, M. Fael, K. Olschewsky, E. Persson, R. van Tonder, K. Keri Vos, and M. Welsch, First extraction of inclusive V_{cb} from q^2 moments, J. High Energy Phys. 10 (2022) 068.

[64] M. Kirk, A. Lenz, and T. Rauh, Dimension-six matrix elements for meson mixing and lifetimes from sum rules, J. High Energy Phys. 12 (2017) 068; 06 (2020) 162(E).

[65] D. King, A. Lenz, and T. Rauh, SU(3) breaking effects in B and D meson lifetimes, J. High Energy Phys. 06 (2022) 134.

[66] J. Gratrex, A. Lenz, B. Melić, I. Nišandžić, M. L. Piscopo, and A. V. Rusov, Quark-hadron duality at work: Lifetimes of bottom baryons, J. High Energy Phys. 04 (2023) 034.

[67] A. Lenz, M. L. Piscopo, and A. V. Rusov, Disintegration of beauty: A precision study, J. High Energy Phys. 01 (2023) 004.

[68] M. Black *et al.*, Using gradient flow to renormalise matrix elements for meson mixing and lifetimes, Proc. Sci. LATTICE2023 (**2024**) 263 [arXiv:2310.18059].

[69] J. Lin, W. Detmold, and S. Meinel, Lattice study of spectator effects in b-hadron decays, Proc. Sci. LATTICE2022 (**2023**) 417 [arXiv:2212.09275].

[70] D. King, A. Lenz, M. L. Piscopo, T. Rauh, A. V. Rusov, and C. Vlahos, Revisiting inclusive decay widths of charmed mesons, J. High Energy Phys. 08 (2022) 241.

[71] J. Abdallah *et al.* (DELPHI Collaboration), A precise measurement of the B^+, B^0 and mean b-hadron lifetime with the DELPHI detector at LEP1, Eur. Phys. J. C **33**, 307 (2004).

[72] R. Barate *et al.* (ALEPH Collaboration), Measurement of the $\bar{B}^0$ and B^- meson lifetimes, Phys. Lett. B **492**, 275 (2000).

[73] D. Buskulic *et al.* (ALEPH Collaboration), Improved measurement of the $\bar{B}^0$ and B^- meson lifetimes, Z. Phys. C **71**, 31 (1996).

[74] P. Abreu *et al.* (DELPHI Collaboration), A measurement of B^+ and B^0 lifetimes using $\bar{D}\ell^+$ events, Z. Phys. C **68**, 13 (1995).

[75] W. Adam *et al.* (DELPHI Collaboration), Lifetimes of charged and neutral B hadrons using event topology, Z. Phys. C **68**, 363 (1995).

[76] P. Abreu *et al.* (DELPHI Collaboration), A precise measurement of the B_d^0 meson lifetime using a new technique, Z. Phys. C **74**, 19 (1997); **75**, 579(E) (1997).

[77] M. Acciarri *et al.* (L3 Collaboration), Upper limit on the lifetime difference of shortlived and longlived B_s^0 mesons, Phys. Lett. B **438**, 417 (1998).

[78] R. Akers *et al.* (OPAL Collaboration), Improved measurements of the B^0 and B^+ meson lifetimes, Z. Phys. C **67**, 379 (1995).

[79] G. Abbiendi *et al.* (OPAL Collaboration), Measurement of the B^+ and B^0 lifetimes and search for $CP(T)$ violation using reconstructed secondary vertices, Eur. Phys. J. C **12**, 609 (2000).

[80] G. Abbiendi *et al.* (OPAL Collaboration), Measurement of the B^0 lifetime and oscillation frequency using $\bar{B}^0 \to D^{*+}\ell^-\bar{\nu}$ decays, Phys. Lett. B **493**, 266 (2000).

[81] K. Abe *et al.* (SLD Collaboration), Measurement of the B^+ and B^0 lifetimes using topological reconstruction of inclusive and semileptonic decays, Phys. Rev. Lett. **79**, 590 (1997).

[82] F. Abe *et al.* (CDF Collaboration), Improved measurement of the B^- and $\bar{B}^0$ meson lifetimes using semileptonic decays, Phys. Rev. D **58**, 092002 (1998).

[83] D. Acosta *et al.* (CDF Collaboration), Measurement of B meson lifetimes using fully reconstructed B decays produced in $p\bar{p}$ collisions at $\sqrt{s} = 1.8$ TeV, Phys. Rev. D **65**, 092009 (2002).

[84] T. Aaltonen *et al.* (CDF Collaboration), Measurement of b hadron lifetimes in exclusive decays containing a J/ψ in $p\bar{p}$ collisions at $\sqrt{s} = 1.96$ TeV, Phys. Rev. Lett. **106**, 121804 (2011).

[85] V. M. Abazov *et al.* (D0 Collaboration), Measurement of the angular and lifetime parameters of the decays $B_d^0 \to J/\psi K^{*0}$ and $B_s^0 \to J/\psi\phi$, Phys. Rev. Lett. **102**, 032001 (2009).

[86] V. M. Abazov *et al.* (D0 Collaboration), Measurement of the Λ_b^0 lifetime in the exclusive decay $\Lambda_b^0 \to J/\psi\Lambda^0$ in $p\bar{p}$ collisions at $\sqrt{s} = 1.96$ TeV, Phys. Rev. D **85**, 112003 (2012).

[87] V. M. Abazov *et al.* (D0 Collaboration), Measurement of the B_s^0 lifetime in the flavor-specific decay channel $B_s^0 \to D_s^-\mu^+\nu X$, Phys. Rev. Lett. **114**, 062001 (2015).

[88] B. Aubert *et al.* (*BABAR* Collaboration), Measurement of the B^0 and B^+ meson lifetimes with fully reconstructed hadronic final states, Phys. Rev. Lett. **87**, 201803 (2001).

[89] B. Aubert *et al.* (*BABAR* Collaboration), Measurement of the B^0 lifetime with partially reconstructed $B^0 \to D^{*-}\ell^+\nu_\ell$ decays, Phys. Rev. Lett. **89**, 011802 (2002); **89**, 169903 (E) (2002).

[90] B. Aubert *et al.* (*BABAR* Collaboration), Simultaneous measurement of the B^0 meson lifetime and mixing frequency with $B^0 \to D^{*-}\ell^+\nu_\ell$ decays, Phys. Rev. D **67**, 072002 (2003).

[91] B. Aubert *et al.* (*BABAR* Collaboration), Measurement of the B^0 meson lifetime with partial reconstruction of $B^0 \to D^{*-}\pi^+$ and $B^0 \to D^{*-}\rho^+$ decays, Phys. Rev. D **67**, 091101 (2003).

[92] B. Aubert *et al.* (*BABAR* Collaboration), Measurement of the $\bar{B}^0$ lifetime and the $B^0\bar{B}^0$ oscillation frequency using

partially reconstructed $\bar{B}^0 \to D^{*+}\ell^-\bar{\nu}_\ell$ decays, Phys. Rev. D **73**, 012004 (2006).
[93] K. Abe *et al.* (Belle Collaboration), Improved measurement of *CP*-violation parameters $\sin(2\phi_1)$ and $|\lambda|$, B meson lifetimes, and $B^0 - \bar{B}^0$ mixing parameter Δm_d, Phys. Rev. D **71**, 072003 (2005); **71**, 079903(E) (2005).
[94] G. Aad *et al.* (ATLAS Collaboration), Measurement of the Λ_b lifetime and mass in the ATLAS experiment, Phys. Rev. D **87**, 032002 (2013).
[95] A. M. Sirunyan *et al.* (CMS Collaboration), Measurement of b hadron lifetimes in pp collisions at $\sqrt{s} = 8$ TeV, Eur. Phys. J. C **78**, 457 (2018); **78**, 561(E) (2018).
[96] R. Aaij *et al.* (LHCb Collaboration), Measurements of the B^+, B^0, B_s^0 meson and Λ_b^0 baryon lifetimes, J. High Energy Phys. 04 (2014) 114.
[97] R. Aaij *et al.* (LHCb Collaboration), Effective lifetime measurements in the $B_s^0 \to K^+K^-$, $B^0 \to K^+\pi^-$ and $B_s^0 \to \pi^+K^-$ decays, Phys. Lett. B **736**, 446 (2014).
[98] F. Abudinén *et al.* (Belle II Collaboration), Measurement of the B^0 lifetime and flavor-oscillation frequency using hadronic decays reconstructed in 2019–2021 Belle II data, Phys. Rev. D **107**, L091102 (2023).
[99] T. Aaltonen *et al.* (CDF Collaboration), Measurement of the B^- lifetime using a simulation free approach for trigger bias correction, Phys. Rev. D **83**, 032008 (2011).
[100] V. M. Abazov *et al.* (D0 Collaboration), Measurement of the ratio of B^+ and B^0 meson lifetimes, Phys. Rev. Lett. **94**, 182001 (2005).
[101] R. Aaij *et al.* (LHCb Collaboration), Determination of the sign of the decay width difference in the B_s^0 system, Phys. Rev. Lett. **108**, 241801 (2012).
[102] A. Lenz and G. Tetlalmatzi-Xolocotzi, Model-independent bounds on new physics effects in non-leptonic tree-level decays of B-mesons, J. High Energy Phys. 07 (2020) 177.
[103] M. Artuso, G. Borissov, and A. Lenz, *CP* violation in the B_s^0 system, Rev. Mod. Phys. **88**, 045002 (2016).
[104] S. Laplace, Z. Ligeti, Y. Nir, and G. Perez, Implications of the *CP* asymmetry in semileptonic B decay, Phys. Rev. D **65**, 094040 (2002).
[105] M. Ciuchini, V. Lubicz, C. Tarantino, E. Franco, and F. Mescia, Lifetime differences and *CP* violation parameters of neutral B mesons at the next-to-leading order in QCD, J. High Energy Phys. 08 (2003) 031.
[106] M. Beneke, G. Buchalla, A. Lenz, and U. Nierste, *CP* asymmetry in flavor specific B decays beyond leading logarithms, Phys. Lett. B **576**, 173 (2003).
[107] K. Hartkorn and H. G. Moser, A new method of measuring $\Delta\Gamma/\Gamma$ in the $B_s^0 - \bar{B}_s^0$ system, Eur. Phys. J. C **8**, 381 (1999).
[108] I. Dunietz, R. Fleischer, and U. Nierste, In pursuit of new physics with B_s decays, Phys. Rev. D **63**, 114015 (2001).
[109] R. Fleischer and R. Knegjens, Effective lifetimes of B_s decays and their constraints on the $B_s^0 - \bar{B}_s^0$ mixing parameters, Eur. Phys. J. C **71**, 1789 (2011).
[110] R. Aaij *et al.* (LHCb Collaboration), Measurement of the *CP*-violating phase ϕ_s from $B_s^0 \to J/\psi\pi^+\pi^-$ decays in 13 TeV pp collisions, Phys. Lett. B **797**, 134789 (2019).
[111] R. Barate *et al.* (ALEPH Collaboration), Study of B_s^0 oscillations and lifetime using fully reconstructed D_s^- decays, Eur. Phys. J. C **4**, 367 (1998).
[112] P. Abreu *et al.* (DELPHI Collaboration), Study of $B_s^0 - \bar{B}_s^0$ oscillations and B_s^0 lifetimes using hadronic decays of B_s^0 mesons, Eur. Phys. J. C **18**, 229 (2000).
[113] K. Ackerstaff *et al.* (OPAL Collaboration), A measurement of the B_s^0 lifetime using reconstructed D_s^- mesons, Eur. Phys. J. C **2**, 407 (1998).
[114] D. Buskulic *et al.* (ALEPH Collaboration), Study of the $B_s^0 - \bar{B}_s^0$ oscillation frequency using $D_s^-\ell^+$ combinations in Z decays, Phys. Lett. B **377**, 205 (1996).
[115] F. Abe *et al.* (CDF Collaboration), Measurement of the B_s^0 meson lifetime using semileptonic decays, Phys. Rev. D **59**, 032004 (1999).
[116] P. Abreu *et al.* (DELPHI Collaboration), Measurement of the B_s^0 lifetime and study of $B_s^0 - \bar{B}_s^0$ oscillations using $D_s\ell$ events, Eur. Phys. J. C **16**, 555 (2000).
[117] K. Ackerstaff *et al.* (OPAL Collaboration), Measurements of the B_s^0 and Λ_b^0 lifetimes, Phys. Lett. B **426**, 161 (1998).
[118] T. Aaltonen *et al.* (CDF Collaboration), Measurement of the B_s^0 lifetime in fully and partially reconstructed $B_s^0 \to D_s^-(\phi\pi^-)X$ decays in $\bar{p}p$ collisions at $\sqrt{s} = 1.96$ TeV, Phys. Rev. Lett. **107**, 272001 (2011).
[119] R. Aaij *et al.* (LHCb Collaboration), Measurement of the $\bar{B}_s^0 \to D_s^-D_s^+$ and $\bar{B}_s^0 \to D^-D_s^+$ effective lifetimes, Phys. Rev. Lett. **112**, 111802 (2014).
[120] R. Aaij *et al.* (LHCb Collaboration), Measurement of the $\bar{B}_s^0$ meson lifetime in $D_s^+\pi^-$ decays, Phys. Rev. Lett. **113**, 172001 (2014).
[121] R. Aaij *et al.* (LHCb Collaboration), Measurement of B_s^0 and D_s^- meson lifetimes, Phys. Rev. Lett. **119**, 101801 (2017).
[122] F. Abe *et al.* (CDF Collaboration), Measurement of B hadron lifetimes using J/ψ final states at CDF, Phys. Rev. D **57**, 5382 (1998).
[123] V. M. Abazov *et al.* (D0 Collaboration), Measurement of the B_s^0 lifetime in the exclusive decay channel $B_s^0 \to J/\psi\phi$, Phys. Rev. Lett. **94**, 042001 (2005).
[124] R. Aaij *et al.* (LHCb Collaboration), Analysis of neutral B-meson decays into two muons, Phys. Rev. Lett. **128**, 041801 (2022); Measurement of the $B_s^0 \to \mu^+\mu^-$ decay properties and search for the $B^0 \to \mu^+\mu^-$ and $B_s^0 \to \mu^+\mu^-\gamma$ decays, Phys. Rev. D **105**, 012010 (2022).
[125] A. Tumasyan *et al.* (CMS Collaboration), Measurement of the $B_s^0 \to \mu^+\mu^-$ decay properties and search for the $B^0 \to \mu^+\mu^-$ decay in proton-proton collisions at $\sqrt{s} = 13$ TeV, Phys. Lett. B **842**, 137955 (2023).
[126] G. Aad *et al.* (ATLAS Collaboration), Measurement of the $B_s^0 \to \mu\mu$ effective lifetime with the ATLAS detector, J. High Energy Phys. 09 (2023) 199.
[127] R. Barate *et al.* (ALEPH Collaboration), A study of the decay width difference in the $B_s^0 - \bar{B}_s^0$ system using $\phi\phi$ correlations, Phys. Lett. B **486**, 286 (2000).
[128] R. Aaij *et al.* (LHCb Collaboration), Measurement of the effective $B_s^0 \to K^+K^-$ lifetime, Phys. Lett. B **707**, 349 (2012).
[129] R. Aaij *et al.* (LHCb Collaboration), Measurement of the $B_s^0 \to J/\psi\eta$ lifetime, Phys. Lett. B **762**, 484 (2016).

[130] R. Aaij *et al.* (LHCb Collaboration), Measurement of τ_L using the $B_s^0 \to J/\psi\eta$ decay mode, Eur. Phys. J. C **83**, 629 (2023).

[131] R. Aaij *et al.* (LHCb Collaboration), Measurement of the effective $B_s^0 \to J/\psi K_S^0$ lifetime, Nucl. Phys. **B873**, 275 (2013).

[132] A. Hayrapetyan *et al.* (CMS Collaboration), Measurement of the $B_s^0 \to J/\psi K_S^0$ effective lifetime from proton-proton collisions at $\sqrt{s} = 13$ TeV, J. High Energy Phys. 10 (2024) 247.

[133] T. Aaltonen *et al.* (CDF Collaboration), Measurement of branching ratio and B_s^0 lifetime in the decay $B_s^0 \to J/\psi f_0(980)$ at CDF, Phys. Rev. D **84**, 052012 (2011).

[134] V. M. Abazov *et al.* (D0 Collaboration), B_s^0 lifetime measurement in the CP-odd decay channel $B_s^0 \to J/\psi f_0(980)$, Phys. Rev. D **94**, 012001 (2016).

[135] R. Aaij *et al.* (LHCb Collaboration), Measurement of CP violation and the B_s^0 meson decay width difference with $B_s^0 \to J/\psi K^+K^-$ and $B_s^0 \to J/\psi\pi^+\pi^-$ decays, Phys. Rev. D **87**, 112010 (2013).

[136] R. Aaij *et al.* (LHCb Collaboration), Measurement of the $\bar{B}^0 - B^0$ and $\bar{B}_s^0 - B_s^0$ production asymmetries in pp collisions at $\sqrt{s} = 7$ TeV, Phys. Lett. B **739**, 218 (2014).

[137] R. Aleksan, A. Le Yaouanc, L. Oliver, O. Pène, and J.-C. Raynal, Estimation of $\Delta\Gamma$ for the $B_s - \bar{B}_s$ system: Exclusive decays and the parton model, Phys. Lett. B **316**, 567 (1993).

[138] F. Abe *et al.* (CDF Collaboration), Observation of the B_c meson in $p\bar{p}$ collisions at $\sqrt{s} = 1.8$ TeV, Phys. Rev. Lett. **81**, 2432 (1998).

[139] A. Abulencia *et al.* (CDF Collaboration), Measurement of the B_c^+ meson lifetime using $B_c^+ \to J/\psi e^+\nu_e$, Phys. Rev. Lett. **97**, 012002 (2006).

[140] V. M. Abazov *et al.* (D0 Collaboration), Measurement of the lifetime of the $B_c^\pm$ meson in the semileptonic decay channel, Phys. Rev. Lett. **102**, 092001 (2009).

[141] T. Aaltonen *et al.* (CDF Collaboration), Measurement of the B_c^- meson lifetime in the decay $B_c^- \to J/\psi\pi^-$, Phys. Rev. D **87**, 011101 (2013).

[142] R. Aaij *et al.* (LHCb Collaboration), Measurement of the B_c^+ meson lifetime using $B_c^+ \to J/\psi\mu^+\nu_\mu X$ decays, Eur. Phys. J. C **74**, 2839 (2014).

[143] R. Aaij *et al.* (LHCb Collaboration), Measurement of the lifetime of the B_c^+ meson using the $B_c^+ \to J/\psi\pi^+$ decay mode, Phys. Lett. B **742**, 29 (2015).

[144] M. Beneke and G. Buchalla, The B_c meson lifetime, Phys. Rev. D **53**, 4991 (1996).

[145] J. Aebischer and B. Grinstein, Standard model prediction of the B_c lifetime, J. High Energy Phys. 07 (2021) 130.

[146] S. Schael *et al.* (ALEPH, CDF, DELPHI, L3, OPAL, and SLD Collaborations, LEP Electroweak Working Group, SLD Electroweak and Heavy Flavor Working Groups), Precision electroweak measurements on the Z resonance, Phys. Rep. **427**, 257 (2006).

[147] T. A. Aaltonen *et al.* (CDF Collaboration), Mass and lifetime measurements of bottom and charm baryons in $p\bar{p}$ collisions at $\sqrt{s} = 1.96$ TeV, Phys. Rev. D **89**, 072014 (2014).

[148] R. Barate *et al.* (ALEPH Collaboration), Measurement of the b baryon lifetime and branching fractions in Z decays, Eur. Phys. J. C **2**, 197 (1998).

[149] P. Abreu *et al.* (DELPHI Collaboration), Measurement of the lifetime of b baryons, Eur. Phys. J. C **10**, 185 (1999).

[150] P. Abreu *et al.* (DELPHI Collaboration), Determination of the average lifetime of b baryons, Z. Phys. C **71**, 199 (1996).

[151] R. Akers *et al.* (OPAL Collaboration), Measurement of the average b baryon lifetime and the product branching ratio $f(b \to \Lambda_b) \times \mathrm{BR}(\Lambda_b \to \Lambda\ell^-\bar{\nu}X)$, Z. Phys. C **69**, 195 (1996).

[152] D. Buskulic *et al.* (ALEPH Collaboration), Strange b baryon production and lifetime in Z decays, Phys. Lett. B **384**, 449 (1996).

[153] P. Abreu *et al.* (DELPHI Collaboration), Production of strange B-baryons decaying into $\Xi^\mp -$ lepton$^\mp$ pairs at LEP, Z. Phys. C **68**, 541 (1995).

[154] J. Abdallah *et al.* (DELPHI Collaboration), Production of Ξ_c^0 and Ξ_b in Z decays and lifetime measurement of Ξ_b, Eur. Phys. J. C **44**, 299 (2005).

[155] F. Abe *et al.* (CDF Collaboration), Measurement of Λ_b^0 lifetime using $\Lambda_b^0 \to \Lambda_c^+\ell^-\bar{\nu}$, Phys. Rev. Lett. **77**, 1439 (1996).

[156] V. M. Abazov *et al.* (D0 Collaboration), Measurement of the Λ_b^0 lifetime using semileptonic decays, Phys. Rev. Lett. **99**, 182001 (2007).

[157] T. Aaltonen *et al.* (CDF Collaboration), Measurement of the Λ_b lifetime in $\Lambda_b \to \Lambda_c^+\pi^-$ decays in $p\bar{p}$ collisions at $\sqrt{s} = 1.96$ TeV, Phys. Rev. Lett. **104**, 102002 (2010).

[158] S. Chatrchyan *et al.* (CMS Collaboration), Measurement of the Λ_b^0 lifetime in pp collisions at $\sqrt{s} = 7$ TeV, J. High Energy Phys. 07 (2013) 163.

[159] R. Aaij *et al.* (LHCb Collaboration), Precision measurement of the ratio of the Λ_b^0 to $\bar{B}^0$ lifetimes, Phys. Lett. B **734**, 122 (2014).

[160] R. Aaij *et al.* (LHCb Collaboration), Measurement of the Ξ_b^- and Ω_b^- baryon lifetimes, Phys. Lett. B **736**, 154 (2014).

[161] R. Aaij *et al.* (LHCb Collaboration), Precision measurement of the mass and lifetime of the Ξ_b^- baryon, Phys. Rev. Lett. **113**, 242002 (2014).

[162] R. Aaij *et al.* (LHCb Collaboration), Precision measurement of the Ξ_b^- baryon lifetime, Phys. Rev. D **110**, 072002 (2024).

[163] R. Aaij *et al.* (LHCb Collaboration), Precision measurement of the mass and lifetime of the Ξ_b^0 baryon, Phys. Rev. Lett. **113**, 032001 (2014).

[164] R. Aaij *et al.* (LHCb Collaboration), Measurement of the mass and lifetime of the Ω_b^- baryon, Phys. Rev. D **93**, 092007 (2016).

[165] G. Altarelli, G. Martinelli, S. Petrarca, and F. Rapuano, Failure of local duality in inclusive nonleptonic heavy flavor decays, Phys. Lett. B **382**, 409 (1996).

[166] H.-Y. Cheng, A phenomenological analysis of heavy hadron lifetimes, Phys. Rev. D **56**, 2783 (1997).

[167] T. Ito, M. Matsuda, and Y. Matsui, New possibility of solving the problem of lifetime ratio $\tau(\Lambda_b)/\tau(B_d)$, Prog. Theor. Phys. **99**, 271 (1998).

[168] M. Beneke, G. Buchalla, and I. Dunietz, Width difference in the $B_s - \bar{B}_s$ system, Phys. Rev. D **54**, 4419 (1996); **83**, 119902(E) (2011).

[169] M. Beneke, G. Buchalla, C. Greub, A. Lenz, and U. Nierste, Next-to-leading order QCD corrections to the lifetime difference of B_s mesons, Phys. Lett. B **459**, 631 (1999).

[170] M. Gerlach, U. Nierste, V. Shtabovenko, and M. Steinhauser, Width difference in the $B - \bar{B}$ system at next-to-next-to-leading order of QCD, Phys. Rev. Lett. **129**, 102001 (2022).

[171] A. Bazavov *et al.* (Fermilab Lattice and MILC Collaborations), $B^0_{(s)}$-mixing matrix elements from lattice QCD for the Standard Model and beyond, Phys. Rev. D **93**, 113016 (2016).

[172] A. G. Grozin, R. Klein, T. Mannel, and A. A. Pivovarov, $B^0 - \bar{B}^0$ mixing at next-to-leading order, Phys. Rev. D **94**, 034024 (2016).

[173] P. A. Boyle *et al.* (RBC and UKQCD Collaborations), SU(3)-breaking ratios for $D_{(s)}$ and $B_{(s)}$ mesons, arXiv: 1812.08791.

[174] D. King, A. Lenz, and T. Rauh, B_s mixing observables and $|V_{td}/V_{ts}|$ from sum rules, J. High Energy Phys. 05 (2019) 034.

[175] R. J. Dowdall *et al.*, Neutral B-meson mixing from full lattice QCD at the physical point, Phys. Rev. D **100**, 094508 (2019).

[176] C. T. H. Davies, J. Harrison, G. Peter Lepage, C. J. Monahan, J. Shigemitsu, and M. Wingate (HPQCD Collaboration), Lattice QCD matrix elements for the $B^0_s - \bar{B}^0_s$ width difference beyond leading order, Phys. Rev. Lett. **124**, 082001 (2020).

[177] D. Buskulic *et al.* (ALEPH Collaboration), Improved measurement of the $B^0_d - \bar{B}^0_d$ oscillation frequency, Z. Phys. C **75**, 397 (1997).

[178] P. Abreu *et al.* (DELPHI Collaboration), Measurement of $B^0_d - \bar{B}^0_d$ oscillations, Z. Phys. C **76**, 579 (1997).

[179] J. Abdallah *et al.* (DELPHI Collaboration), Search for $B^0_s - \bar{B}^0_s$ oscillations and a measurement of $B^0_d - \bar{B}^0_d$ oscillations using events with an inclusively reconstructed vertex, Eur. Phys. J. C **28**, 155 (2003).

[180] M. Acciarri *et al.* (L3 Collaboration), Measurement of the $B^0_d - \bar{B}^0_d$ oscillation frequency, Eur. Phys. J. C **5**, 195 (1998).

[181] K. Ackerstaff *et al.* (OPAL Collaboration), An updated study of B meson oscillations using dilepton events, Z. Phys. C **76**, 417 (1997).

[182] K. Ackerstaff *et al.* (OPAL Collaboration), A study of B meson oscillations using hadronic Z^0 decays containing leptons, Z. Phys. C **76**, 401 (1997).

[183] G. Alexander *et al.* (OPAL Collaboration), A measurement of the B^0_d oscillation frequency using leptons and $D^{*\pm}$ mesons, Z. Phys. C **72**, 377 (1996).

[184] F. Abe *et al.* (CDF Collaboration), Measurement of the $B^0 - \bar{B}^0$ oscillation frequency using πB meson charge-flavor correlations in $p\bar{p}$ collisions at $\sqrt{s} = 1.8$ TeV, Phys. Rev. Lett. **80**, 2057 (1998); Measurement of the $B^0_d - \bar{B}^0_d$ flavor oscillation frequency and study of same side flavor tagging of B mesons in $p\bar{p}$ collisions, Phys. Rev. D **59**, 032001 (1998).

[185] F. Abe *et al.* (CDF Collaboration), Measurement of the $B^0_d - \bar{B}^0_d$ oscillation frequency using dimuon data in $p\bar{p}$ collisions at $\sqrt{s} = 1.8$ TeV, Phys. Rev. D **60**, 051101 (1999).

[186] F. Abe *et al.* (CDF Collaboration), Measurement of $B^0 - \bar{B}^0$ flavor oscillations using jet-charge and lepton flavor tagging in $p\bar{p}$ collisions at $\sqrt{s} = 1.8$ TeV, Phys. Rev. D **60**, 072003 (1999).

[187] T. Affolder *et al.* (CDF Collaboration), Measurement of the $B^0 - \bar{B}^0$ oscillation frequency using $\ell^- D^{*+}$ pairs and lepton flavor tags, Phys. Rev. D **60**, 112004 (1999).

[188] V. M. Abazov *et al.* (D0 Collaboration), Measurement of B_d mixing using opposite-side flavor tagging, Phys. Rev. D **74**, 112002 (2006).

[189] B. Aubert *et al.* (*BABAR* Collaboration), Measurement of $B^0 - \bar{B}^0$ flavor oscillations in hadronic B^0 decays, Phys. Rev. Lett. **88**, 221802 (2002); A study of time dependent CP-violating asymmetries and flavor oscillations in neutral B decays at the $\Upsilon(4S)$, Phys. Rev. D **66**, 032003 (2002).

[190] B. Aubert *et al.* (*BABAR* Collaboration), Measurement of the $B^0 - \bar{B}^0$ oscillation frequency with inclusive dilepton events, Phys. Rev. Lett. **88**, 221803 (2002).

[191] Y. Zheng *et al.* (Belle Collaboration), Measurement of the $B^0 - \bar{B}^0$ mixing rate with $B^0(\bar{B}^0) \to D^{*\mp}\pi^{\pm}$ partial reconstruction, Phys. Rev. D **67**, 092004 (2003).

[192] LHCb Collaboration, Measurement of Δm_d in $B^0 \to D^-(K^+\pi^-\pi^-)\pi^+$, Report No. LHCb-CONF-2011-010, 2011, https://cdsweb.cern.ch/record/1331124; this result has been published in Ref. [235].

[193] R. Aaij *et al.* (LHCb Collaboration), Measurement of the $B^0_s - \bar{B}^0_s$ oscillation frequency Δm_s in $B^0_s \to D^-_s(3)\pi$ decays, Phys. Lett. B **709**, 177 (2012).

[194] R. Aaij *et al.* (LHCb Collaboration), Measurement of the $B^0 - \bar{B}^0$ oscillation frequency Δm_d with the decays $B^0 \to D^-\pi^+$ and $B^0 \to J/\psi K^{*0}$, Phys. Lett. B **719**, 318 (2013).

[195] R. Aaij *et al.* (LHCb Collaboration), Observation of $B^0_s - \bar{B}^0_s$ mixing and measurement of mixing frequencies using semileptonic B decays, Eur. Phys. J. C **73**, 2655 (2013).

[196] R. Aaij *et al.* (LHCb Collaboration), A precise measurement of the B^0 meson oscillation frequency, Eur. Phys. J. C **76**, 412 (2016).

[197] H. Albrecht *et al.* (ARGUS Collaboration), A new determination of the $B^0 - \bar{B}^0$ oscillation strength, Z. Phys. C **55**, 357 (1992); A study of $\bar{B}^0 \to D^{*+}\ell^-\bar{\nu}$ and $B^0\bar{B}^0$ mixing using partial D^{*+} reconstruction, Phys. Lett. B **324**, 249 (1994).

[198] J. E. Bartelt *et al.* (CLEO Collaboration), Two measurements of $B^0 - \bar{B}^0$ mixing, Phys. Rev. Lett. **71**, 1680 (1993).

[199] B. H. Behrens *et al.* (CLEO Collaboration), Precise measurement of $B^0\bar{B}^0$ mixing parameters at the $\Upsilon(4S)$, Phys. Lett. B **490**, 36 (2000).

[200] B. Aubert *et al.* (*BABAR* Collaboration), Limits on the decay-rate difference of neutral B mesons and on CP, T, and CPT violation in $B^0 - \bar{B}^0$ oscillations, Phys. Rev. Lett. **92**, 181801 (2004); Limits on the decay-rate difference of neutral B mesons and on CP, T, and CPT violation in $B^0 - \bar{B}^0$ oscillations, Phys. Rev. D **70**, 012007 (2004).

[201] T. Higuchi *et al.* (Belle Collaboration), Search for time-dependent CPT violation in hadronic and semileptonic B decays, Phys. Rev. D **85**, 071105 (2012).

[202] T. Gershon, $\Delta\Gamma_d$: A forgotten null test of the standard model, J. Phys. G **38**, 015007 (2011); **42**, 119501(E) (2015).

[203] M. Aaboud *et al.* (ATLAS Collaboration), Measurement of the relative width difference of the $B^0 - \bar{B}^0$ system with the ATLAS detector, J. High Energy Phys. 06 (2016) 081.

[204] J. Charles *et al.*, Current status of the Standard Model CKM fit and constraints on $\Delta F = 2$ new physics, Phys. Rev. D **91**, 073007 (2015);. with updated results and plots available at http://ckmfitter.in2p3.fr

[205] M. Bona *et al.* (UTfit Collaboration), New UTfit analysis of the unitarity triangle in the Cabibbo-Kobayashi-Maskawa scheme, Rend. Lincei Sci. Fis. Nat. **34**, 37 (2023); with updated results and plots available at http://www.utfit.org.

[206] V. M. Abazov *et al.* (D0 Collaboration), Study of CP-violating charge asymmetries of single muons and like-sign dimuons in $p\bar{p}$ collisions, Phys. Rev. D **89**, 012002 (2014).

[207] U. Nierste, Effect of $\Delta\Gamma$ on the dimuon asymmetry in B decays, *Talk Presented at the 8th International Workshop on the CKM Unitarity Triangle (CKM 2014)* (2014).

[208] T. Aaltonen *et al.* (CDF Collaboration), Measurement of the bottom-strange meson mixing phase in the full CDF data set, Phys. Rev. Lett. **109**, 171802 (2012).

[209] V. M. Abazov *et al.* (D0 Collaboration), Measurement of the CP-violating phase $\phi_s^{J/\psi\phi}$ using the flavor-tagged decay $B_s^0 \to J/\psi\phi$ in 8 fb^{-1} of $p\bar{p}$ collisions, Phys. Rev. D **85**, 032006 (2012).

[210] G. Aad *et al.* (ATLAS Collaboration), Flavour tagged time dependent angular analysis of the $B_s \to J/\psi\phi$ decay and extraction of $\Delta\Gamma$ and the weak phase ϕ_s in ATLAS, Phys. Rev. D **90**, 052007 (2014).

[211] G. Aad *et al.* (ATLAS Collaboration), Measurement of the CP-violating phase ϕ_s and the B_s^0 meson decay width difference with $B_s^0 \to J/\psi\phi$ decays in ATLAS, J. High Energy Phys. 08 (2016) 147.

[212] G. Aad *et al.* (ATLAS Collaboration), Measurement of the CP-violating phase ϕ_s in $B_s^0 \to J/\psi\phi$ decays in ATLAS at 13 TeV, Eur. Phys. J. C **81**, 342 (2021).

[213] V. Khachatryan *et al.* (CMS Collaboration), Measurement of the CP-violating weak phase ϕ_s and the decay width difference $\Delta\Gamma_s$ using the $B_s^0 \to J/\psi\phi(1020)$ decay channel in pp collisions at $\sqrt{s} = 8$ TeV, Phys. Lett. B **757**, 97 (2016).

[214] CMS Collaboration, Measurement of time-dependent CP violation in $B_s^0 \to J/\psi\phi(1020)$ decays with the CMS detector, Report No. CMS PAS BPH-23-004, https://cds.cern.ch/record/2894821/files/BPH-23-004-pas.pdf.

[215] R. Aaij *et al.* (LHCb Collaboration), Precision measurement of CP violation in $B_s^0 \to J/\psi K^+K^-$ decays, Phys. Rev. Lett. **114**, 041801 (2015).

[216] R. Aaij *et al.* (LHCb Collaboration), Resonances and CP violation in B_s^0 and $\bar{B}_s^0 \to J/\psi K^+K^-$ decays in the mass region above the $\phi(1020)$, J. High Energy Phys. 08 (2017) 037.

[217] R. Aaij *et al.* (LHCb Collaboration), First study of the CP -violating phase and decay-width difference in $B_s^0 \to \psi(2S)\phi$ decays, Phys. Lett. B **762**, 253 (2016).

[218] R. Aaij *et al.* (LHCb Collaboration), First measurement of the CP-violating phase in $B_s^0 \to J/\psi(\to e^+e^-)\phi$ decays, Eur. Phys. J. C **81**, 1026 (2021).

[219] R. Aaij *et al.* (LHCb Collaboration), Improved measurement of CP violation parameters in $B_s^0 \to J/\psi K^+K^-$ decays in the vicinity of the $\phi(1020)$ resonance, Phys. Rev. Lett. **132**, 051802 (2024).

[220] R. Aaij *et al.* (LHCb Collaboration), A measurement of $\Delta\Gamma_s$, J. High Energy Phys. 05 (2024) 253.

[221] M. Gerlach *et al.*, NNLO QCD corrections to $\Delta\Gamma_s$ in the $B_s - \bar{B}_s$ system, in *Proceedings of the 12th International Workshop on the CKM Unitarity Triangle* (2024), arXiv:2403.08316.

[222] A. Lenz, Theoretical update of B-mixing and lifetimes, arXiv:1205.1444.

[223] S. Esen *et al.* (Belle Collaboration), Observation of $B_s^0 \to D_s^{(*)+}D_s^{(*)-}$ using e^+e^- collisions and a determination of the $B_s - \bar{B}_s$ width difference $\Delta\Gamma_s$, Phys. Rev. Lett. **105**, 201802 (2010).

[224] V. M. Abazov *et al.* (D0 Collaboration), Evidence for decay $B_s^0 \to D_s^{(*)}D_s^{(*)}$ and a measurement of $\Delta\Gamma_s^{CP}/\Gamma_s$, Phys. Rev. Lett. **102**, 091801 (2009).

[225] T. Aaltonen *et al.* (CDF Collaboration), First observation of the decay $B_s^0 \to D_s^-D_s^+$ and measurement of its branching ratio, Phys. Rev. Lett. **100**, 021803 (2008).

[226] T. Aaltonen *et al.* (CDF Collaboration), Measurement of $B_s^0 \to D_s^{(*)+}D_s^{(*)-}$ branching ratios, Phys. Rev. Lett. **108**, 201801 (2012).

[227] A. Heister *et al.* (ALEPH Collaboration), Improved search for $B_s^0 - \bar{B}_s^0$ oscillations, Eur. Phys. J. C **29**, 143 (2003).

[228] J. Abdallah *et al.* (DELPHI Collaboration), Search for $B_s^0 - \bar{B}_s^0$ oscillations in DELPHI using high-p_t leptons, Eur. Phys. J. C **35**, 35 (2004).

[229] G. Abbiendi *et al.* (OPAL Collaboration), A study of B_s^0 meson oscillation using hadronic Z^0 decays containing leptons, Eur. Phys. J. C **11**, 587 (1999).

[230] G. Abbiendi *et al.* (OPAL Collaboration), A study of B_s meson oscillation using D_s-lepton correlations, Eur. Phys. J. C **19**, 241 (2001).

[231] K. Abe *et al.* (SLD Collaboration), Search for time-dependent $B_s^0 - \bar{B}_s^0$ oscillations using a vertex charge dipole technique, Phys. Rev. D **67**, 012006 (2003).

[232] K. Abe *et al.* (SLD Collaboration), A search for time-dependent $B_s^0 - \bar{B}_s^0$ oscillations using exclusively reconstructed $D_s^{\pm}$ mesons, Phys. Rev. D **66**, 032009 (2002).

[233] F. Abe *et al.* (CDF Collaboration), A search for $B_s^0 - \bar{B}_s^0$ oscillations using the semileptonic decay $B_s^0 \to \phi\ell^+X\nu$, Phys. Rev. Lett. **82**, 3576 (1999).

[234] V. M. Abazov *et al.* (D0 Collaboration), First direct two-sided bound on the B_s^0 oscillation frequency, Phys. Rev. Lett. **97**, 021802 (2006).

[235] A. Abulencia *et al.* (CDF Collaboration), Observation of $B_s^0 - \bar{B}_s^0$ oscillations, Phys. Rev. Lett. **97**, 242003 (2006).

[236] R. Aaij *et al.* (LHCb Collaboration), Precision measurement of the $B_s^0 - \bar{B}_s^0$ oscillation frequency with the decay $B_s^0 \to D_s^-\pi^+$, New J. Phys. **15**, 053021 (2013).

[237] R. Aaij *et al.* (LHCb Collaboration), Measurement of the CKM angle γ and $B_s^0 - \bar{B}_s^0$ mixing frequency with $B_s^0 \to D_s^{\mp} h^{\pm}\pi^{\pm}\pi^{\mp}$ decays, J. High Energy Phys. 03 (2021) 137.

[238] R. Aaij *et al.* (LHCb Collaboration), Precise determination of the $B_s^0 - \bar{B}_s^0$ oscillation frequency, Nat. Phys. **18**, 1 (2022).

[239] L. Di Luzio, M. Kirk, A. Lenz, and T. Rauh, ΔM_s theory precision confronts flavour anomalies, J. High Energy Phys. 12 (2019) 009.

[240] S. Aoki *et al.* (FLAG Collaboration), FLAG review 2019, Eur. Phys. J. C **80**, 113 (2020).

[241] D. E. Jaffe *et al.* (CLEO Collaboration), Bounds on the *CP* asymmetry in like sign dileptons from $B^0\bar{B}^0$ meson decays, Phys. Rev. Lett. **86**, 5000 (2001).

[242] J. P. Lees *et al.* (*BABAR* Collaboration), Study of *CP* asymmetry in $B^0 - \bar{B}^0$ mixing with inclusive dilepton events, Phys. Rev. Lett. **114**, 081801 (2015).

[243] F. Abe *et al.* (CDF Collaboration), Measurement of $b\bar{b}$ production correlations, $B^0\bar{B}^0$ mixing, and a limit on $\epsilon(B)$ in $p\bar{p}$ collisions at $\sqrt{s} = 1.8$ TeV, Phys. Rev. D **55**, 2546 (1997).

[244] R. Barate *et al.* (ALEPH Collaboration), Investigation of inclusive *CP* asymmetries in B^0 decays, Eur. Phys. J. C **20**, 431 (2001).

[245] J. P. Lees *et al.* (*BABAR* Collaboration), Search for *CP* violation in $B^0 - \bar{B}^0$ mixing using partial reconstruction of $B^0 \to D^{*-}X\ell^+\nu_\ell$ and a kaon tag, Phys. Rev. Lett. **111**, 101802 (2013); **111**, 159901(E) (2013).

[246] B. Aubert *et al.* (*BABAR* Collaboration), Search for *T*, *CP* and *CPT* violation in $B^0 - \bar{B}^0$ mixing with inclusive dilepton events, Phys. Rev. Lett. **96**, 251802 (2006).

[247] E. Nakano *et al.* (Belle Collaboration), Charge asymmetry of same-sign dileptons in $B^0 - \bar{B}^0$ mixing, Phys. Rev. D **73**, 112002 (2006).

[248] M. Beneke, G. Buchalla, and I. Dunietz, Mixing induced *CP* asymmetries in inclusive *B* decays, Phys. Lett. B **393**, 132 (1997); I. Dunietz, *CP* asymmetries in semiinclusive B^0 decays, Eur. Phys. J. C **7**, 197 (1999).

[249] V. M. Abazov *et al.* (D0 Collaboration), Measurement of the semileptonic charge asymmetry in B^0 meson mixing with the D0 detector, Phys. Rev. D **86**, 072009 (2012).

[250] R. Aaij *et al.* (LHCb Collaboration), Measurement of the semileptonic *CP* asymmetry in $B^0 - \bar{B}^0$ mixing, Phys. Rev. Lett. **114**, 041601 (2015).

[251] V. M. Abazov *et al.* (D0 Collaboration), Measurement of the *CP*-violation parameter of B^0 mixing and decay with $p\bar{p} \to \mu\mu X$ data, Phys. Rev. D **74**, 092001 (2006).

[252] Y. Amhis *et al.*, Averages of *b*-hadron, *c*-hadron, and τ-lepton properties as of early, arXiv:1207.1158.

[253] V. M. Abazov *et al.* (D0 Collaboration), Measurement of the semileptonic charge asymmetry using $B_s^0 \to D_s\mu X$ decays, Phys. Rev. Lett. **110**, 011801 (2013).

[254] R. Aaij *et al.* (LHCb Collaboration), Measurement of the *CP* asymmetry in $B_s^0 - \bar{B}_s^0$ mixing, Phys. Rev. Lett. **117**, 061803 (2016).

[255] A. Lenz (private communication).

[256] S. Descotes-Genon and J. F. Kamenik, A possible explanation of the D0 like-sign dimuon charge asymmetry, Phys. Rev. D **87**, 074036 (2013); **92**, 079903(E) (2015).

[257] M. Aaboud *et al.* (ATLAS Collaboration), Measurements of charge and *CP* asymmetries in *b*-hadron decays using top-quark events collected by the ATLAS detector in *pp* collisions at $\sqrt{s} = 8$ TeV, J. High Energy Phys. 02 (2017) 071.

[258] R. Aaij *et al.* (LHCb Collaboration), Measurement of the *CP*-violating phase ϕ_s in $\bar{B}_s^0 \to J/\psi\pi^+\pi^-$ decays, Phys. Lett. B **736**, 186 (2014).

[259] R. Aaij *et al.* (LHCb Collaboration), Analysis of the resonant components in $B_s \to J/\psi\pi^+\pi^-$, Phys. Rev. D **86**, 052006 (2012).

[260] R. Aaij *et al.* (LHCb Collaboration), Measurement of the *CP*-violating phase ϕ_s in $\bar{B}_s^0 \to D_s^+D_s^-$ decays, Phys. Rev. Lett. **113**, 211801 (2014).

[261] R. Aaij *et al.* (LHCb Collaboration), Measurement of *CP* violation in $B^0 \to D^+D^-$ and $B_s^0 \to D_s^+D_s^-$ decays, J. High Energy Phys. 01 (2025) 061.

[262] P. Frings, U. Nierste, and M. Wiebusch, Penguin contributions to *CP* phases in $B_{d,s}$ decays to charmonium, Phys. Rev. Lett. **115**, 061802 (2015).

[263] R. Aaij *et al.* (LHCb Collaboration), Measurement of the *CP*-violating phase β in $B^0 \to J/\psi\pi^+\pi^-$ decays and limits on penguin effects, Phys. Lett. B **742**, 38 (2015).

[264] R. Aaij *et al.* (LHCb Collaboration), Measurement of *CP* violation parameters and polarisation fractions in $B_s^0 \to J/\psi\bar{K}^{*0}$ decays, J. High Energy Phys. 11 (2015) 082.

[265] R. Aaij *et al.* (LHCb Collaboration), Determination of γ and $-2\beta_s$ from charmless two-body decays of beauty mesons, Phys. Lett. B **741**, 1 (2015).

[266] M. Neubert, Heavy quark symmetry, Phys. Rep. **245**, 259 (1994).

[267] A. Sirlin, Large m_W, m_Z behavior of the $O(\alpha)$ corrections to semileptonic processes mediated by *W*, Nucl. Phys. **B196**, 83 (1982).

[268] D. Buskulic *et al.* (ALEPH Collaboration), Measurements of $|V_{cb}|$, form factors and branching fractions in the decays $\bar{B}^0 \to D* + \ell^-\bar{\nu}_l$ and $\bar{B}^0 \to D + \ell^-\bar{\nu}_l$, Phys. Lett. B **395**, 373 (1997).

[269] G. Abbiendi *et al.* (OPAL Collaboration), Measurement of $|V_{cb}|$ using $\bar{B}^0 \to D^{*+}\ell^-\bar{\nu}$ decays, Phys. Lett. B **482**, 15 (2000).

[270] P. Abreu *et al.* (DELPHI Collaboration), Measurement of V_{cb} from the decay process $\bar{B}^0 \to D^{*+}\ell^-\bar{\nu}$, Phys. Lett. B **510**, 55 (2001).

[271] J. Abdallah *et al.* (DELPHI Collaboration), Measurement of $|V_{cb}|$ using the semileptonic decay $\bar{B}_d^0 \to D^{*+}\ell^-\overline{\nu_\ell}$, Eur. Phys. J. C **33**, 213 (2004).

[272] N. E. Adam *et al.* (CLEO Collaboration), Determination of the $\bar{B} \to D^*\ell\bar{\nu}$ decay width and $|V_{cb}|$. ((B)), Phys. Rev. D **67**, 032001 (2003).

[273] E. Waheed *et al.* (Belle Collaboration), Measurement of the CKM matrix element $|V_{cb}|$ from $B^0 \to D^{*-}\ell^+\nu_\ell$ at Belle, Phys. Rev. D **100**, 052007 (2019); **103**, 079901(E) (2021).

[274] B. Aubert *et al.* (*BABAR* Collaboration), Determination of the form-factors for the decay $B^0 \to D^{*-}\ell^+\nu_l$ and of the CKM matrix element $|V_{cb}|$, Phys. Rev. D **77**, 032002 (2008).

[275] B. Aubert *et al.* (*BABAR* Collaboration), A measurement of the branching fractions of exclusive $\bar{B} \to D^{(*)}\ (\pi)\ \ell^- \bar{\nu}_\ell$ decays in events with a fully reconstructed B meson, Phys. Rev. Lett. **100**, 151802 (2008).

[276] I. Adachi *et al.* (Belle-II Collaboration), Determination of $|V_{cb}|$ using $\bar{B}^0 \to D^{*+}\ell^-\bar{\nu}_\ell$ decays with Belle II, Phys. Rev. D **108**, 092013 (2023).

[277] F. Abudinén *et al.* (Belle-II Collaboration), Measurement of the $B^0 \to D^{*-}\ell^+\nu_\ell$ branching ratio and $|V_{cb}|$ with a fully reconstructed accompanying B meson in 2019-2021 Belle II data, arXiv:2301.04716.

[278] B. Aubert *et al.* (*BABAR* Collaboration), Measurement of the decay $B^- \to D^*0e^-\bar{\nu}(e)$, Phys. Rev. Lett. **100**, 231803 (2008).

[279] D. Atwood and W. J. Marciano, Radiative corrections and semileptonic B decays, Phys. Rev. D **41**, 1736 (1990).

[280] M. T. Prim *et al.* (Belle Collaboration), Measurement of differential distributions of $B \to D^{*\ell}\bar{\nu}_\ell$ and implications on $|V_{cb}|$, Phys. Rev. D **108**, 012002 (2023).

[281] Heavy Flavor Averaging Group, Average of exclusive B to D* l nu, Zenodo, 10.5281/zenodo.12696548 (2024).

[282] C. G. Boyd, B. Grinstein, and R. F. Lebed, Precision corrections to dispersive bounds on form-factors, Phys. Rev. D **56**, 6895 (1997).

[283] B. Grinstein and A. Kobach, Model-independent extraction of $|V_{cb}|$ from $\bar{B} \to D^*\ell\bar{\nu}$, Phys. Lett. B **771**, 359 (2017).

[284] D. Bigi, P. Gambino, and S. Schacht, A fresh look at the determination of $|V_{cb}|$ from $B \to D^*\ell\nu$, Phys. Lett. B **769**, 441 (2017).

[285] A. Bazavov *et al.* (MILC, Fermilab Lattice, and MILC Collaborations), Semileptonic form factors for $B \to D^*\ell\nu$ at nonzero recoil from $2+1$-flavor lattice QCD, Eur. Phys. J. C **82**, 1141 (2022); **83**, 21(E) (2023).

[286] J. Harrison and C. T. H. Davies (HPQCD Collaboration), $B \to D^*$ and $B_s \to D_s^*$ vector, axial-vector and tensor form factors for the full q^2 range from lattice QCD, Phys. Rev. D **109**, 094515 (2024).

[287] Y. Aoki, B. Colquhoun, H. Fukaya, S. Hashimoto, T. Kaneko, R. Kellermann, J. Koponen, and E. Kou (JLQCD Collaboration), $B \to D^*\ell\nu\ell$ semileptonic form factors from lattice QCD with Möbius domain-wall quarks, Phys. Rev. D **109**, 074503 (2024).

[288] E. J. Eichten and C. Quigg, Mesons with beauty and charm: Spectroscopy, Phys. Rev. D **49**, 5845 (1994).

[289] F. U. Bernlochner, Z. Ligeti, and D. J. Robinson, $N = 5, 6, 7, 8$: Nested hypothesis tests and truncation dependence of $|V_{cb}|$, Phys. Rev. D **100**, 013005 (2019).

[290] J. E. Bartelt *et al.* (CLEO Collaboration), Measurement of the $B \to D\ell\nu$ branching fractions and form factor, Phys. Rev. Lett. **82**, 3746 (1999).

[291] B. Aubert *et al.* (*BABAR* Collaboration), Measurement of $|V_{cb}|$ and the form-factor slope in $\bar{B} \to D\ell^-\bar{\nu}$ decays in events tagged by a fully reconstructed B meson, Phys. Rev. Lett. **104**, 011802 (2010).

[292] R. Glattauer *et al.* (Belle Collaboration), Measurement of the decay $B \to D\ell\nu_\ell$ in fully reconstructed events and determination of the Cabibbo-Kobayashi-Maskawa matrix element $|V_{cb}|$, Phys. Rev. D **93**, 032006 (2016).

[293] F. Abudinén *et al.* (Belle-II Collaboration), Determination of $|V_{cb}|$ from $B \to D\ell\nu$ decays using 2019-2021 Belle II data, arXiv:2210.13143.

[294] J. A. Bailey *et al.* (MILC Collaboration), $B \to D\ell\nu$ form factors at nonzero recoil and $|V_{cb}|$ from $2+1$-flavor lattice QCD, Phys. Rev. D **92**, 034506 (2015).

[295] H. Na *et al.* (HPQCD Collaboration), $B \to Dl\nu$ form factors at nonzero recoil and extraction of $|V_{cb}|$, Phys. Rev. D **92**, 054510 (2015); **93**, 119906(E) (2016).

[296] C. J. Monahan, H. Na, C. M. Bouchard, G. Peter Lepage, and J. Shigemitsu, $B_s \to D_s\ell\nu$ form factors and the fragmentation fraction ratio f_s/f_d, Phys. Rev. D **95**, 114506 (2017).

[297] Y. Aoki *et al.* (Flavour Lattice Averaging Group (FLAG)), FLAG review 2021, Eur. Phys. J. C **82**, 869 (2022).

[298] R. Aaij *et al.* (LHCb Collaboration), Measurement of $|V_{cb}|$ with $B_s^0 \to D_s^{(*)-}\mu^+\nu_\mu$ decays, Phys. Rev. D **101**, 072004 (2020).

[299] E. McLean, C. T. H. Davies, A. T. Lytle, and J. Koponen, Lattice QCD form factor for $B_s \to D_s^* l\nu$ at zero recoil with non-perturbative current renormalisation, Phys. Rev. D **99**, 114512 (2019).

[300] E. McLean, C. T. H. Davies, J. Koponen, and A. T. Lytle, $B_s \to D_s\ell\nu$ form factors for the full q^2 range from lattice QCD with non-perturbatively normalized currents, Phys. Rev. D **101**, 074513 (2020).

[301] R. Aaij *et al.* (LHCb Collaboration), Precise measurement of the f_s/f_d ratio of fragmentation fractions and of B_s^0 decay branching fractions, Phys. Rev. D **104**, 032005 (2021).

[302] R. L. Workman *et al.* (Particle Data Group), Review of particle physics, Prog. Theor. Exp. Phys. **2022**, 083C01 (2022).

[303] F. Meier *et al.* (Belle Collaboration), First observation of $B \to \bar{D}_1(\to \bar{D}\pi^+\pi^-)\ell^+\nu_\ell$ and measurement of the $B \to \bar{D}^{(*)}\pi\ell^+\nu_\ell$ and $B \to \bar{D}^{(*)}\pi^+\pi^-\ell^+\nu_\ell$ branching fractions with hadronic tagging at Belle, Phys. Rev. D **107**, 092003 (2023).

[304] N. Isgur and M. B. Wise, Spectroscopy with heavy quark symmetry, Phys. Rev. Lett. **66**, 1130 (1991).

[305] D. Buskulic *et al.* (ALEPH Collaboration), Production of orbitally excited charm mesons in semileptonic B decays, Z. Phys. C **73**, 601 (1997).

[306] G. Abbiendi *et al.* (OPAL Collaboration), A measurement of semileptonic B decays to narrow orbitally-excited charm mesons, Eur. Phys. J. C **30**, 467 (2003).

[307] A. Anastassov *et al.* (CLEO Collaboration), Investigation of semileptonic B meson decay to P-wave charm mesons, Phys. Rev. Lett. **80**, 4127 (1998).

[308] V. M. Abazov *et al.* (D0 Collaboration), Measurement of semileptonic branching fractions of B mesons to narrow D^{**} states, Phys. Rev. Lett. **95**, 171803 (2005).

[309] B. Aubert *et al.* (*BABAR* Collaboration), Measurement of the branching fractions of $\bar{B} \to D^{**}\ell^-\bar{\nu}_\ell$ decays in events tagged by a fully reconstructed B meson, Phys. Rev. Lett. **101**, 261802 (2008).

[310] B. Aubert *et al.* (*BABAR* Collaboration), Measurement of semileptonic B decays into orbitally-excited charmed mesons, Phys. Rev. Lett. **103**, 051803 (2009).

[311] J. Abdallah *et al.* (DELPHI Collaboration), Determination of heavy quark non-perturbative parameters from spectral moments in semileptonic B decays, Eur. Phys. J. C **45**, 35 (2006).

[312] M. Albaladejo, P. Fernandez-Soler, F.-K. Guo, and J. Nieves, Two-pole structure of the $D_0^*(2400)$, Phys. Lett. B **767**, 465 (2017).

[313] M.-L. Du, M. Albaladejo, P. Fernandez-Soler, F.-K. Guo, C. Hanhart, U.-G. Meißner, J. Nieves, and D.-L. Yao, Towards a new paradigm for heavy-light meson spectroscopy, Phys. Rev. D **98**, 094018 (2018).

[314] M.-L. Du, F.-K. Guo, C. Hanhart, B. Kubis, and U.-G. Meißner, Where is the lightest charmed scalar meson?, Phys. Rev. Lett. **126**, 192001 (2021).

[315] I. I. Y. Bigi, M. A. Shifman, N. Uraltsev, and A. I. Vainshtein, High power n of m_b in beauty widths and $n = 5 \to \infty$ limit, Phys. Rev. D **56**, 4017 (1997).

[316] M. Fael, T. Mannel, and K. Keri Vos, V_{cb} determination from inclusive $b \to c$ decays: An alternative method, J. High Energy Phys. 02 (2019) 177.

[317] C. W. Bauer, Z. Ligeti, M. Luke, A. V. Manohar, and M. Trott, Global analysis of inclusive B decays, Phys. Rev. D **70**, 094017 (2004).

[318] F. Abudinén *et al.* (Belle-II Collaboration), Measurement of lepton mass squared moments in $B \to X_c \ell \bar{\nu}_\ell$ decays with the Belle II experiment, Phys. Rev. D **107**, 072002 (2023).

[319] B. Aubert *et al.* (*BABAR* Collaboration), Measurement and interpretation of moments in inclusive semileptonic decays $\bar{B} \to X_c \ell^- \overline{\nu u}$, Phys. Rev. D **81**, 032003 (2010).

[320] B. Aubert *et al.* (*BABAR* Collaboration), Measurement of the electron energy spectrum and its moments in inclusive $B \to Xe\nu$ decays, Phys. Rev. D **69**, 111104 (2004).

[321] P. Urquijo *et al.* (Belle Collaboration), Moments of the electron energy spectrum and partial branching fraction of $B \to X_c e\nu$ decays at Belle, Phys. Rev. D **75**, 032001 (2007).

[322] C. Schwanda *et al.* (Belle Collaboration), Moments of the hadronic invariant mass spectrum in $B \to X_c \ell \nu$ decays at Belle, Phys. Rev. D **75**, 032005 (2007).

[323] R. van Tonder *et al.* (Belle Collaboration), Measurements of q^2 moments of inclusive $B \to X_c \ell^+ \nu_\ell$ decays with hadronic tagging, Phys. Rev. D **104**, 112011 (2021).

[324] D. E. Acosta *et al.* (CDF Collaboration), Measurement of the moments of the hadronic invariant mass distribution in semileptonic B decays, Phys. Rev. D **71**, 051103 (2005).

[325] S. E. Csorna *et al.* (CLEO Collaboration), Moments of the B meson inclusive semileptonic decay rate using neutrino reconstruction, Phys. Rev. D **70**, 032002 (2004).

[326] P. Gambino and C. Schwanda, Inclusive semileptonic fits, heavy quark masses, and V_{cb}, Phys. Rev. D **89**, 014022 (2014).

[327] A. Alberti, P. Gambino, K. J. Healey, and S. Nandi, Precision determination of the Cabibbo-Kobayashi-Maskawa element V_{cb}, Phys. Rev. Lett. **114**, 061802 (2015).

[328] S. Aoki *et al.* (FLAG Collaboration), FLAG review 2019, Eur. Phys. J. C **80**, 113 (2020).

[329] M. Fael, K. Schönwald, and M. Steinhauser, Kinetic heavy quark mass to three loops, Phys. Rev. Lett. **125**, 052003 (2020).

[330] M. Fael, K. Schönwald, and M. Steinhauser, Third order corrections to the semileptonic $b \to c$ and the muon decays, Phys. Rev. D **104**, 016003 (2021).

[331] M. Fael and F. Herren, NNLO QCD corrections to the q^2 spectrum of inclusive semileptonic B-meson decays, J. High Energy Phys. 05 (2024) 287.

[332] B. O. Lange, M. Neubert, and G. Paz, Theory of charmless inclusive B decays and the extraction of V_{ub}, Phys. Rev. D **72**, 073006 (2005).

[333] R. Aaij *et al.* (LHCb Collaboration), Determination of the quark coupling strength $|V_{ub}|$ using baryonic decays, Nat. Phys. **11**, 743 (2015).

[334] R. Aaij *et al.* (LHCb Collaboration), First observation of the decay $B_s^0 \to K^- \mu^+ \nu_\mu$ and measurement of $|V_{ub}|/|V_{cb}|$, Phys. Rev. Lett. **126**, 081804 (2021).

[335] H. Ha *et al.* (Belle Collaboration), Measurement of the decay $B^0 \to \pi^- \ell^+ \nu$ and determination of $|V_{ub}|$, Phys. Rev. D **83**, 071101 (2011).

[336] A. Sibidanov *et al.* (Belle Collaboration), Study of exclusive $B \to X_u \ell \nu$ decays and extraction of $\|V_{ub}\|$ using full reconstruction tagging at the Belle experiment, Phys. Rev. D **88**, 032005 (2013).

[337] P. del Amo Sanchez *et al.* (*BABAR* Collaboration), Study of $B \to \pi \ell \nu$ and $B \to \rho \ell \nu$ decays and determination of $|V_{ub}|$, Phys. Rev. D **83**, 032007 (2011).

[338] J. P. Lees *et al.* (*BABAR* Collaboration), Branching fraction and form-factor shape measurements of exclusive charmless semileptonic B decays, and determination of $|V_{ub}|$, Phys. Rev. D **86**, 092004 (2012).

[339] G. D'Agostini, On the use of the covariance matrix to fit correlated data, Nucl. Instrum. Methods Phys. Res., Sect. A **346**, 306 (1994).

[340] G. Cowan, Statistical models with uncertain error parameters, Eur. Phys. J. C **79**, 133 (2019).

[341] C. Bourrely, I. Caprini, and L. Lellouch, Model-independent description of $B \to \pi \ell \nu$ decays and a determination of $|V_{ub}|$, Phys. Rev. D **79**, 013008 (2009); **82**, 099902(E) (2010).

[342] Y. Aoki *et al.* (Flavour Lattice Averaging Group (FLAG)), Web Update http://flag.unibe.ch/2021/Media?action=AttachFile&do=get&target=FLAG_webupdate_February2024.pdf (2024).

[343] J. A. Bailey *et al.*, $|V_{ub}|$ from $B \to \pi \ell \nu$ decays and $(2 + 1)$-flavor lattice QCD, Phys. Rev. D **92**, 014024 (2015).

[344] J. M. Flynn, T. Izubuchi, T. Kawanai, C. Lehner, A. Soni, R. S. Van de Water, and O. Witzel, $B \to \pi \ell \nu$ and $B_s \to K \ell \nu$ form factors and $|V_{ub}|$ from $2 + 1$-flavor lattice QCD with domain-wall light quarks and relativistic heavy quarks, Phys. Rev. D **91**, 074510 (2015).

[345] B. Colquhoun, S. Hashimoto, T. Kaneko, and J. Koponen (JLQCD Collaboration), Form factors of $B \to \pi \ell \nu$ and a determination of $|V_{ub}|$ with Möbius domain-wall fermions, Phys. Rev. D **106**, 054502 (2022).

[346] B. H. Behrens *et al.* (CLEO Collaboration), Measurement of $B \to \rho \ell \nu$ decay and $|V_{ub}|$, Phys. Rev. D **61**, 052001 (2000).

[347] N. E. Adam *et al.* (CLEO Collaboration), A study of exclusive charmless semileptonic B decay and $|V_{ub}|$, Phys. Rev. Lett. **99**, 041802 (2007).

[348] T. Hokuue *et al.* (Belle Collaboration), Measurements of branching fractions and q^2 distributions for $B \to \pi \ell \nu$ and $B \to \rho \ell \nu$ decays with $B \to D^{(*)} \ell \nu$ decay tagging, Phys. Lett. B **648**, 139 (2007).

[349] C. Schwanda *et al.* (Belle Collaboration), Evidence for $B^+ \to \omega \ell^+ \nu$, Phys. Rev. Lett. **93**, 131803 (2004).

[350] J. P. Lees *et al.* (*BABAR* Collaboration), Branching fraction measurement of $B^+ \to \omega \ell^+ \nu$ decays, Phys. Rev. D **87**, 032004 (2013).

[351] J. P. Lees *et al.* (*BABAR* Collaboration), Measurement of the $B^+ \to \omega \ell^+ \nu$ branching fraction with semileptonically tagged B mesons, Phys. Rev. D **88**, 072006 (2013).

[352] A. Bharucha, D. M. Straub, and R. Zwicky, $B \to V \ell^+ \ell^-$ in the standard model from light-cone sum rules, J. High Energy Phys. 08 (2016) 098.

[353] R. Gray *et al.* (CLEO Collaboration), A study of exclusive charmless semileptonic B decays and extraction of $|V_{ub}|$ at CLEO, Phys. Rev. D **76**, 012007 (2007).

[354] B. Aubert *et al.* (*BABAR* Collaboration), Measurement of the $B^+ \to \omega \ell^+ \nu$ and $B^+ \to \eta \ell^+ \nu$ branching fractions, Phys. Rev. D **79**, 052011 (2009).

[355] B. Aubert *et al.* (*BABAR* Collaboration), Measurements of $B \to \{\pi, \eta, \eta'\} \ell \nu_\ell$ branching fractions and determination of $|V_{ub}|$ with semileptonically tagged B mesons, Phys. Rev. Lett. **101**, 081801 (2008).

[356] C. Beleño *et al.* (Belle Collaboration), Measurement of the decays $\boldsymbol{B \to \eta \ell \nu_\ell}$ and $\boldsymbol{B \to \eta' \ell \nu_\ell}$ in fully reconstructed events at Belle, Phys. Rev. D **96**, 091102 (2017).

[357] U. Gebauer *et al.* (Belle Collaboration), Measurement of the branching fractions of the $B^+ \to \eta \ell^+ \nu_\ell$ and $B^+ \to \eta' \ell^+ \nu_\ell$ decays with signal-side only reconstruction in the full q^2 range, Phys. Rev. D **106**, 032013 (2022).

[358] W. Detmold, C. Lehner, and S. Meinel, $\Lambda_b \to p \ell^- \bar{\nu}_\ell$ and $\Lambda_b \to \Lambda_c \ell^- \bar{\nu}_\ell$ form factors from lattice QCD with relativistic heavy quarks, Phys. Rev. D **92**, 034503 (2015).

[359] A. Khodjamirian and A. V. Rusov, $B_s \to K \ell \nu_\ell$ and $B_{(s)} \to \pi(K) \ell^+ \ell^-$ decays at large recoil and CKM matrix elements, J. High Energy Phys. 08 (2017) 112.

[360] C. M. Bouchard *et al.*, $B_s \to K \ell \nu$ form factors from lattice QCD, Phys. Rev. D **90**, 054506 (2014).

[361] A. Bazavov *et al.* (Fermilab Lattice and MILC Collaborations), $B_s \to K \ell \nu$ decay from lattice QCD, Phys. Rev. D **100**, 034501 (2019).

[362] J. M. Flynn, R. C. Hill, A. Jüttner, A. Soni, J. T. Tsang, and O. Witzel (RBC/UKQCD Collaboration), Exclusive semileptonic $B_s \to K \ell \nu$ decays on the lattice, Phys. Rev. D **107**, 114512 (2023).

[363] C. Bolognani, D. van Dyk, and K. K. Vos, New determination of $|V_{ub}/V_{cb}|$ from $B_s^0 \to \{K^-, D_s^-\} \mu^+ \nu$, J. High Energy Phys. 11 (2023) 082.

[364] P. Urquijo *et al.* (Belle Collaboration), Measurement Of $|V_{ub}|$ from inclusive charmless semileptonic B decays, Phys. Rev. Lett. **104**, 021801 (2010).

[365] J. P. Lees *et al.* (*BABAR* Collaboration), Study of $\bar{B} \to X_u \ell \bar{\nu}$ decays in $B\bar{B}$ events tagged by a fully reconstructed B-meson decay and determination of $\|V_{ub}\|$, Phys. Rev. D **86**, 032004 (2012).

[366] J. P. Lees *et al.* (*BABAR* Collaboration), Measurement of the inclusive electron spectrum from B meson decays and determination of $|V_{ub}|$, Phys. Rev. D **95**, 072001 (2017).

[367] R. V. Kowalewski and S. Menke, Complementary observables for the determination of $|V_{ub}|$ in inclusive semileptonic B decays, Phys. Lett. B **541**, 29 (2002).

[368] B. Aubert *et al.* (*BABAR* Collaboration), Determination of $|V_{ub}|$ from measurements of the electron and neutrino momenta in inclusive semileptonic B decays, Phys. Rev. Lett. **95**, 111801 (2005).

[369] A. Bornheim *et al.* (CLEO Collaboration), Improved measurement of $|V_{ub}|$ with inclusive semileptonic B decays, Phys. Rev. Lett. **88**, 231803 (2002).

[370] A. Limosani *et al.* (Belle Collaboration), Measurement of inclusive charmless semileptonic B-meson decays at the endpoint of the electron momentum spectrum, Phys. Lett. B **621**, 28 (2005).

[371] H. Kakuno *et al.* (Belle Collaboration), Measurement of $|V_{ub}|$ using inclusive $B \to X_u \ell \nu$ decays with a novel X_u reconstruction method, Phys. Rev. Lett. **92**, 101801 (2004).

[372] L. Cao *et al.* (Belle Collaboration), Measurements of partial branching fractions of inclusive $B \to X_u \ell^+ \nu_\ell$ decays with hadronic tagging, Phys. Rev. D **104**, 012008 (2021).

[373] M. Neubert, Analysis of the photon spectrum in inclusive $B \to X_s \gamma$ decays, Phys. Rev. D **49**, 4623 (1994).

[374] A. K. Leibovich, I. Low, and I. Z. Rothstein, Extracting V_{ub} without recourse to structure functions, Phys. Rev. D **61**, 053006 (2000).

[375] B. O. Lange, M. Neubert, and G. Paz, A two-loop relation between inclusive radiative and semileptonic B decay spectra, J. High Energy Phys. 10 (2005) 084.

[376] U. Aglietti, F. Di Lodovico, G. Ferrera, and G. Ricciardi, Inclusive measure of $|V_{ub}|$ with the analytic coupling model, Eur. Phys. J. C **59**, 831 (2009).

[377] C. W. Bauer, Z. Ligeti, and M. E. Luke, Precision determination of $|V_{ub}|$ from inclusive decays, Phys. Rev. D **64**, 113004 (2001).

[378] S. W. Bosch, B. O. Lange, M. Neubert, and G. Paz, Factorization and shape-function effects in inclusive B-meson decays, Nucl. Phys. **B699**, 335 (2004).

[379] S. W. Bosch, M. Neubert, and G. Paz, Subleading shape functions in inclusive B decays, J. High Energy Phys. 11 (2004) 073.

[380] M. Neubert, Impact of four-quark shape functions on inclusive B decay spectra, Eur. Phys. J. C **44**, 205 (2005).

[381] M. Neubert, Two-loop relations for heavy-quark parameters in the shape-function scheme, Phys. Lett. B **612**, 13 (2005).

[382] M. Neubert, Advanced predictions for moments of the $\bar{B} \to X_s \gamma$ photon spectrum, Phys. Rev. D **72**, 074025 (2005).

[383] J. R. Andersen and E. Gardi, Inclusive spectra in charmless semileptonic B decays by dressed gluon exponentiation, J. High Energy Phys. 01 (2006) 097.

[384] I. R. Blokland, A. Czarnecki, M. Misiak, M. Ślusarczyk, and F. Tkachov, The Electromagnetic dipole operator effect on $\bar{B} \to X_s \gamma$ at $O(\alpha^2 - s)$, Phys. Rev. D **72**, 033014 (2005).

[385] P. Gambino and P. Giordano, Normalizing inclusive rare B decays, Phys. Lett. B **669**, 69 (2008).

[386] P. Gambino, P. Giordano, G. Ossola, and N. Uraltsev, Inclusive semileptonic B decays and the determination of $|V_{ub}|$, J. High Energy Phys. 10 (2007) 058.

[387] D. Bigi and P. Gambino, Revisiting $B \to D\ell\nu$, Phys. Rev. D **94**, 094008 (2016).

[388] M. Bordone, M. Jung, and D. van Dyk, Theory determination of $\bar{B} \to D^{(*)}\ell^-\bar{\nu}$ form factors at $\mathcal{O}(1/m_c^2)$, Eur. Phys. J. C **80**, 74 (2020).

[389] G. Martinelli, S. Simula, and L. Vittorio, $|V_{cb}|$ and $R(D^{(*)})$ using lattice QCD and unitarity, Phys. Rev. D **105**, 034503 (2022).

[390] F. U. Bernlochner, Z. Ligeti, M. Papucci, M. T. Prim, D. J. Robinson, and C. Xiong, Constrained second-order power corrections in HQET: $R(D^{(*)})$, $|V_{cb}|$, and new physics, Phys. Rev. D **106**, 096015 (2022).

[391] I. Ray and S. Nandi, Test of new physics effects in $\bar{B} \to (D^{(*)}, \pi)\ell^-\bar{\nu}_\ell$ decays with heavy and light leptons, J. High Energy Phys. 01 (2024) 022.

[392] J. P. Lees *et al.* (*BABAR* Collaboration), Extraction of form factors from a four-dimensional angular analysis of $\bar{B} \to D^*\ell^-\bar{\nu}_\ell$, Phys. Rev. Lett. **123**, 091801 (2019).

[393] P. Gambino, M. Jung, and S. Schacht, The V_{cb} puzzle: An update, Phys. Lett. B **795**, 386 (2019).

[394] G. Martinelli, S. Simula, and L. Vittorio, Exclusive determinations of $|V_{cb}|$ and $R(D^*)$ through unitarity, Eur. Phys. J. C **82**, 1083 (2022).

[395] S. Aoki *et al.*, Review of lattice results concerning low-energy particle physics, Eur. Phys. J. C **77**, 112 (2017); see also http://flag.unibe.ch/.

[396] M. Neubert, Z. Ligeti, and Y. Nir, QCD sum rule analysis of the subleading Isgur-Wise form-factor $X_2(v \cdot v')$, Phys. Lett. B **301**, 101 (1993).

[397] M. Neubert, Z. Ligeti, and Y. Nir, The subleading Isgur-Wise form-factor $\chi_3(v, v')$ to order α_s in QCD sum rules, Phys. Rev. D **47**, 5060 (1993).

[398] Z. Ligeti, Y. Nir, and M. Neubert, The subleading Isgur-Wise form-factor $\Xi_3(v \cdot v')$ and its implications for the decays $\bar{B} \to D*$ lepton anti-neutrino, Phys. Rev. D **49**, 1302 (1994).

[399] N. Gubernari, A. Kokulu, and D. van Dyk, $B \to P$ and $B \to V$ form factors from B-meson light-cone sum rules beyond leading twist, J. High Energy Phys. 01 (2019) 150.

[400] A. V. Avilés-Casco *et al.* (Fermilab Lattice and MILC Collaborations), The $B \to D^*\ell\nu$ semileptonic decay at nonzero recoil and its implications for $|V_{cb}|$ and $R(D^*)$, Proc. Sci. LATTICE2019 (**2019**) 049 [arXiv:1912.05886].

[401] A. Abdesselam *et al.* (Belle Collaboration), Precise determination of the CKM matrix element $|V_{cb}|$ with $\bar{B}^0 \to D^{*+}\ell^-\bar{\nu}_\ell$ decays with hadronic tagging at Belle, arXiv:1702.01521.

[402] G. Martinelli, S. Simula, and L. Vittorio, Updates on the determination of $|V_{cb}|, R(D^*)$ and $|V_{ub}|/|V_{cb}|$, Eur. Phys. J. C **84**, 400 (2024).

[403] A. Matyja *et al.* (Belle Collaboration), Observation of $B^0 \to D^{*-}\tau^+\nu_\tau$ decay at Belle, Phys. Rev. Lett. **99**, 191807 (2007).

[404] B. Aubert *et al.* (*BABAR* Collaboration), Observation of the semileptonic decays $B \to D^*\tau^-\bar{\nu}_\tau$ and evidence for $B \to D\tau^-\bar{\nu}_\tau$, Phys. Rev. Lett. **100**, 021801 (2008).

[405] A. Bozek *et al.* (Belle Collaboration), Observation of $B^+ \to \bar{D}^{*0}\tau^+\nu_\tau$ and Evidence for $B^+ \to \bar{D}^0\tau^+\nu_\tau$ at Belle, Phys. Rev. D **82**, 072005 (2010).

[406] J. P. Lees *et al.* (*BABAR* Collaboration), Evidence for an excess of $\bar{B} \to D^{(*)}\tau^-\bar{\nu}_\tau$ decays, Phys. Rev. Lett. **109**, 101802 (2012).

[407] J. P. Lees *et al.* (*BABAR* Collaboration), Measurement of an excess of $\bar{B} \to D^{(*)}\tau^-\bar{\nu}_\tau$ decays and implications for charged Higgs bosons, Phys. Rev. D **88**, 072012 (2013).

[408] M. Huschle *et al.* (Belle Collaboration), Measurement of the branching ratio of $\bar{B} \to D^{(*)}\tau^-\bar{\nu}_\tau$ relative to $\bar{B} \to D^{(*)}\ell^-\bar{\nu}_\ell$ decays with hadronic tagging at Belle, Phys. Rev. D **92**, 072014 (2015).

[409] S. Hirose *et al.* (Belle Collaboration), Measurement of the τ lepton polarization and $R(D^*)$ in the decay $\bar{B} \to D^*\tau^-\bar{\nu}_\tau$, Phys. Rev. Lett. **118**, 211801 (2017).

[410] G. Caria *et al.* (Belle Collaboration), Measurement of $\mathcal{R}(D)$ and $\mathcal{R}(D^*)$ with a semileptonic tagging method, Phys. Rev. Lett. **124**, 161803 (2020).

[411] Y. Sato *et al.* (Belle Collaboration), Measurement of the branching ratio of $\bar{B}^0 \to D^{*+}\tau^-\bar{\nu}_\tau$ relative to $\bar{B}^0 \to D^{*+}\ell^-\bar{\nu}_\ell$ decays with a semileptonic tagging method, Phys. Rev. D **94**, 072007 (2016).

[412] R. Aaij *et al.* (LHCb Collaboration), Measurement of the ratios of branching fractions $\mathcal{R}(D^*)$ and $\mathcal{R}(D^0)$, Phys. Rev. Lett. **131**, 111802 (2023).

[413] R. Aaij *et al.* (LHCb Collaboration), Measurement of the ratio of branching fractions $\mathcal{B}(\bar{B}^0 \to D^{*+}\tau^-\bar{\nu}_\tau)/\mathcal{B}(\bar{B}^0 \to D^{*+}\mu^-\bar{\nu}_\mu)$, Phys. Rev. Lett. **115**, 111803 (2015); **115**, 159901(E) (2015).

[414] R. Aaij *et al.* (LHCb Collaboration), Measurement of the ratio of the $B^0 \to D^{*-}\tau^+\nu_\tau$ and $B^0 \to D^{*-}\mu^+\nu_\mu$ branching fractions using three-prong τ-lepton decays, Phys. Rev. Lett. **120**, 171802 (2018).

[415] R. Aaij *et al.* (LHCb Collaboration), Test of lepton flavor universality using $B^0 \to D^{*-}\tau^+\nu_\tau$ decays with hadronic τ channels, Phys. Rev. D **108**, 012018 (2023).

[416] R. Aaij *et al.* (LHCb Collaboration), Measurement of the branching fraction ratios $R(D^+)$ and $R(D^{*+})$ using muonic τ decays, Phys. Rev. Lett. **134**, 061801 (2025).

[417] I. Adachi *et al.* (Belle-II Collaboration), A test of lepton flavor universality with a measurement of $R(D^*)$ using hadronic B tagging at the Belle II experiment, Phys. Rev. D **110**, 072020 (2024).

[418] R. Aaij *et al.* (LHCb Collaboration), Test of lepton flavor universality by the measurement of the $B^0 \to D^{*-}\tau^+\nu_\tau$ branching fraction using three-prong τ decays, Phys. Rev. D **97**, 072013 (2018).

[419] R. Aaij *et al.* (LHCb Collaboration), Measurement of the ratio of branching fractions $\mathcal{B}(B_c^+ \to J/\psi\tau^+\nu_\tau)/\mathcal{B}(B_c^+ \to J/\psi\mu^+\nu_\mu)$, Phys. Rev. Lett. **120**, 121801 (2018).

[420] J. Harrison, C. T. H. Davies, and A. Lytle (LATTICE-HPQCD Collaboration), $R(J/\psi)$ and $B_c^- \to J/\psi\ell^-\bar{\nu}_\ell$ lepton flavor universality violating observables from lattice QCD, Phys. Rev. Lett. **125**, 222003 (2020).

[421] R. Aaij *et al.* (LHCb Collaboration), Observation of the decay $\Lambda_b^0 \to \Lambda_c^+\tau^-\bar{\nu}_\tau$, Phys. Rev. Lett. **128**, 191803 (2022).

[422] F. U. Bernlochner, Z. Ligeti, D. J. Robinson, and W. L. Sutcliffe, Precise predictions for $\Lambda_b \to \Lambda_c$ semileptonic decays, Phys. Rev. D **99**, 055008 (2019).

[423] I. Adachi *et al.* (Belle-II Collaboration), First measurement of $R(X_{\tau/\ell})$ as an inclusive test of the $b \to c\tau\nu$ anomaly, Phys. Rev. Lett. **132**, 211804 (2024).

[424] Z. Ligeti, M. Luke, and F. J. Tackmann, Theoretical predictions for inclusive $B \to X_u \tau \bar{\nu}$ decay, Phys. Rev. D **105**, 073009 (2022).

[425] M. Rahimi and K. K. Vos, Standard Model predictions for lepton flavour universality ratios of inclusive semileptonic B decays, J. High Energy Phys. 11 (2022) 007.

[426] S. K. Choi *et al.* (Belle Collaboration), Observation of a narrow charmonium—like state in exclusive $B^{\pm} \to K^{\pm}\pi^{+}pi^{-}J/\psi$ decays, Phys. Rev. Lett. **91**, 262001 (2003).

[427] R. Aaij *et al.* (LHCb Collaboration), Quantum numbers of the $X(3872)$ state and orbital angular momentum in its $\rho^0 J/\psi$ decay, Phys. Rev. D **92**, 011102 (2015).

[428] S. K. Choi *et al.* (Belle Collaboration), Observation of a resonance-like structure in the $pi^{\pm}\psi'$ mass distribution in exclusive $B \to K\pi^{\pm}\psi'$ decays, Phys. Rev. Lett. **100**, 142001 (2008).

[429] R. Aaij *et al.* (LHCb Collaboration), Observation of the resonant character of the $Z(4430)^-$ state, Phys. Rev. Lett. **112**, 222002 (2014).

[430] R. Aaij *et al.* (LHCb Collaboration), Observation of $J/\psi p$ Resonances Consistent with Pentaquark States in $\Lambda_b^0 \to J/\psi K^- p$ Decays, Phys. Rev. Lett. **115**, 072001 (2015).

[431] Hflav web page on hadronic b decays into open or hidden charm, https://hflav.web.cern.ch/content/b-hadron-decays-open-or-hidden-charm-hadronsour web page.

[432] K. De Bruyn, R. Fleischer, R. Knegjens, P. Koppenburg, M. Merk, and N. Tuning, Branching ratio measurements of B_s decays, Phys. Rev. D **86**, 014027 (2012).

[433] B. Aubert *et al.* (*BABAR* Collaboration), Branching fraction measurement of $B^0 \to D^{(*)+}\pi^-$, $B^- \to D^{(*)0}\pi^-$ and isospin analysis of $\bar{B} \to D^{(*)}\pi$ decays, Phys. Rev. D **75**, 031101 (2007).

[434] B. Aubert *et al.* (*BABAR* Collaboration), Measurement of the absolute branching fractions $B \to D\pi$, $D^*\pi$, $D^{**}\pi$ with a missing mass method, Phys. Rev. D **74**, 111102 (2006).

[435] K. Abe *et al.* (Belle Collaboration), Observation of Cabibbo suppressed $B \to D^{(*)}K^-$ decays at Belle, Phys. Rev. Lett. **87**, 111801 (2001).

[436] A. Abulencia *et al.* (CDF Collaboration), Measurement of the ratios of branching fractions $B(B_s^0 \to D_s^-\pi^+)/B(B^0 \to D^-\pi^+)$ and $B(B^+ \to \bar{D}^0\pi^+)/B(B^0 \to D^-\pi^+)$, Phys. Rev. Lett. **96**, 191801 (2006).

[437] A. Abulencia *et al.* (CDF Collaboration), Measurement of the ratios of branching fractions $\mathcal{B}(B_s^0 \to D_s^-\pi^+\pi^+\pi^-)/\mathcal{B}(B^0 \to D^-\pi^+\pi^+\pi^-)$ and $\mathcal{B}(B_s^0 \to D_s^-\pi^+)/\mathcal{B}(B^0 \to D^-\pi^+)$, Phys. Rev. Lett. **98**, 061802 (2007).

[438] A. Abulencia *et al.* (CDF Collaboration), Measurement of $\sigma(\Lambda_b^0)/\sigma(\bar{B}^0) \times \mathrm{BR}(\Lambda_b^0 \to \Lambda_c^+\pi^-)/\mathrm{BR}(\bar{B}^0 \to D^+\pi^-)$ in $p\bar{p}$ collisions at $\sqrt{s} = 1.96$-TeV., Phys. Rev. Lett. **98**, 122002 (2007).

[439] R. Aaij *et al.* (LHCb Collaboration), Measurements of the branching fractions for $B_{(s)} \to D_{(s)}\pi\pi\pi$ and $\Lambda_b^0 \to \Lambda_c^+\pi\pi\pi$, Phys. Rev. D **84**, 092001 (2011).

[440] R. Aaij *et al.* (LHCb Collaboration), Measurement of the fragmentation fraction ratio f_s/f_d and its dependence on B meson kinematics, J. High Energy Phys. 04 (2013) 001; with numerical results and full covariance matrix available at http://cdsweb.cern.ch/record/1507868.

[441] R. Aaij *et al.* (LHCb Collaboration), Determination of the branching fractions of $\mathrm{B}_s^0 \to \mathrm{D}_s^{\mp}\mathrm{K}^{\pm}$ and $\mathrm{B}^0 \to \mathrm{D}_s^-\mathrm{K}^+$, J. High Energy Phys. 05 (2015) 019.

[442] R. Aaij *et al.* (LHCb Collaboration), Study of the kinematic dependences of Λ_b^0 production in pp collisions and a measurement of the $\Lambda_b^0 \to \Lambda_c^+\pi^-$ branching fraction, J. High Energy Phys. 08 (2014) 143.

[443] R. Aaij *et al.* (LHCb Collaboration), First observation of the decays $\bar{B}^0 \to D^+K^-\pi^+\pi^-$ and $B^- \to D^0K^-\pi^+\pi^-$, Phys. Rev. Lett. **108**, 161801 (2012).

[444] J.-F. Krohn *et al.* (Belle Collaboration), Measurements of the branching fractions $\mathcal{B}(\bar{B}^0 \to D^{*+}\pi^-)$ and $\mathcal{B}(\bar{B}^0 \to D^{*+}K^-)$ and tests of QCD factorization, Phys. Rev. D **107**, 012003 (2023).

[445] A. Kuzmin *et al.* (Belle Collaboration), Study of $\bar{B}^0 \to D^0\pi^+\pi^-$ decays, Phys. Rev. D **76**, 012006 (2007).

[446] B. Aubert *et al.* (*BABAR* Collaboration), Measurement of branching fractions and resonance contributions for $B^0 \to \bar{D}^0K^+\pi^-$ and search for $B^0 \to D^0K^+\pi^-$ decays, Phys. Rev. Lett. **96**, 011803 (2006).

[447] R. Aaij *et al.* (LHCb Collaboration), Study of $B^0 \to D^{*-}\pi^+\pi^-\pi^+$ and $B^0 \to D^{*-}K^+\pi^-\pi^+$ decays, Phys. Rev. D **87**, 092001 (2013).

[448] J. P. Lees *et al.* (*BABAR* Collaboration), Measurement of the $B^0 \to D^{*-}\pi^+\pi^-\pi^+$ branching fraction, Phys. Rev. D **94**, 091101 (2016).

[449] G. Majumder *et al.* (Belle Collaboration), Observation of $B^0 \to D^{*-}(5\pi)^+$, $B^+ \to D^{*-}(4\pi)^{++}$ and $B^+ \to \bar{D}^{*0}(5\pi)^+$, Phys. Rev. D **70**, 111103 (2004).

[450] D. Matvienko *et al.* (Belle Collaboration), Study of D^{**} production and light hadronic states in the $\bar{B}^0 \to D^{*+}\omega\pi^-$ decay, Phys. Rev. D **92**, 012013 (2015).

[451] B. Aubert *et al.* (*BABAR* Collaboration), Study of the decay $\bar{B}^0 \to D^{*+}\omega\pi^-$, Phys. Rev. D **74**, 012001 (2006).

[452] J. P. Lees *et al.* (*BABAR* Collaboration), Branching fraction measurements of the color-suppressed decays $\bar{B}^0 \to D^{(*)0}\pi^0$, $D^{(*)0}\eta$, $D^{(*)0}\omega$, and $D^{(*)0}\eta'$ and measurement of the polarization in the decay $\bar{B}^0 \to D^{*0}\omega$, Phys. Rev. D **84**, 112007 (2011).

[453] S. Blyth *et al.* (Belle Collaboration), Improved measurements of color-suppressed decays $\bar{B}^0 \to D^0\pi^0$, $D^0\eta$, $D^0\omega$, $D^{*0}\pi^0$, $D^{*0}\eta$ and $D^{*0}\omega$, Phys. Rev. D **74**, 092002 (2006).

[454] R. Aaij *et al.* (LHCb Collaboration), Dalitz plot analysis of $B^0 \to \bar{D}^0\pi^+\pi^-$ decays, Phys. Rev. D **92**, 032002 (2015).

[455] R. Aaij *et al.* (LHCb Collaboration), Measurement of the branching fractions of the decays $B_s^0 \to \bar{D}^0K^-\pi^+$ and $B^0 \to \bar{D}^0K^+\pi^-$, Phys. Rev. D **87**, 112009 (2013).

[456] R. Aaij *et al.* (LHCb Collaboration), Observation of the decay $B_s^0 \to \bar{D}^0K^+K^-$, Phys. Rev. D **98**, 072006 (2018).

[457] A. Satpathy *et al.* (Belle Collaboration), Study of $\bar{B}^0 \to D^{0(*)}\pi^+\pi^-$ decays, Phys. Lett. B **553**, 159 (2003).

[458] R. Aaij *et al.* (LHCb Collaboration), Observation of the $B^0 \to \bar{D}^{*0}K^+\pi^-$ and $B_s^0 \to \bar{D}^{*0}K^-\pi^+$ decays, Phys. Rev. D **105**, 072005 (2022).

[459] R. Aaij *et al.* (LHCb Collaboration), First observation of the decay $\bar{B}_s^0 \to D^0 K^{*0}$ and a measurement of the ratio of branching fractions $\frac{\mathcal{B}(\bar{B}_s^0 \to D^0 K^{*0})}{\mathcal{B}(\bar{B}^0 \to D^0 \rho^0)}$, Phys. Lett. B **706**, 32 (2011).

[460] M. Kumar *et al.* (Belle Collaboration), Search for rare decays $B^+ \to D_s^{(*)+}\eta$, $D_s^{(*)+}K^0$, $D^+\eta$, and D^+K^0, Phys. Rev. D **107**, L031101 (2023).

[461] J. Schumann *et al.* (Belle Collaboration), Observation of $\bar{B}^0 \to D^0\eta'$ and $\bar{B}^0 \to D^{*0}\eta'$, Phys. Rev. D **72**, 011103 (2005).

[462] B. Aubert *et al.* (*BABAR* Collaboration), Measurement of branching fraction and Dalitz distribution for $B^0 \to D^{(*)\pm}K^0\pi^\mp$ decays, Phys. Rev. Lett. **95**, 171802 (2005).

[463] I. Adachi *et al.* (Belle-II Collaboration), Measurement of the branching fractions of $\bar{B} \to D^{(*)}K^-K_{(S)}^{(*)0}$ and $\bar{B} \to D^{(*)}D_s^-$ decays at Belle II, J. High Energy Phys. 08 (2024) 206.

[464] A. Drutskoy *et al.* (Belle Collaboration), Observation of $B \to D^{(*)}K^-K^{0(*)}$ decays, Phys. Lett. B **542**, 171 (2002).

[465] B. Aubert *et al.* (*BABAR* Collaboration), Measurement of $\bar{B}^0 \to D^{(*)0}\bar{K}^{(*)0}$ branching fractions, Phys. Rev. D **74**, 031101 (2006).

[466] P. Krokovny *et al.* (Belle Collaboration), Observation of $\bar{B}^0 \to D^0\bar{K}^0$ and $\bar{B}^0 \to D^0\bar{K}^{*0}$ decays, Phys. Rev. Lett. **90**, 141802 (2003).

[467] R. Aaij *et al.* (LHCb Collaboration), Observation of the decay $B_s^0 \to \bar{D}^0\phi$, Phys. Lett. B **727**, 403 (2013).

[468] R. Aaij *et al.* (LHCb Collaboration), Evidence for the decays $B^0 \to \bar{D}^{(*)0}\phi$ and updated measurements of the branching fractions of the $B_s^0 \to \bar{D}^{(*)0}\phi$ decays, J. High Energy Phys. 10 (2023) 123.

[469] A. Das *et al.* (Belle Collaboration), Measurements of branching fractions for $B^0 \to D_s^+\pi^-$ and $\bar{B}^0 \to D_s^+K^-$, Phys. Rev. D **82**, 051103 (2010).

[470] B. Aubert *et al.* (*BABAR* Collaboration), Measurement of the branching fractions of the rare decays $B^0 \to D_s^{(*)+}\pi^-$, $B^0 \to D_s^{(*)+}\rho^-$, and $B^0 \to D_s^{(*)-}K^{(*)+}$, Phys. Rev. D **78**, 032005 (2008).

[471] N. J. Joshi *et al.* (Belle Collaboration), Measurement of the branching fractions for $B^0 \to D_s^{*+}\pi^-$ and $B^0 \to D_s^{*-}K^+$ decays, Phys. Rev. D **81**, 031101 (2010).

[472] B. Aubert *et al.* (*BABAR* Collaboration), Search for the rare decays $B^0 \to D_s^{(*)+}a_{0(2)}^-$, Phys. Rev. D **73**, 071103 (2006).

[473] B. Aubert *et al.* (*BABAR* Collaboration), Observation of tree-level B decays with $s\bar{s}$ production from gluon radiation., Phys. Rev. Lett. **100**, 171803 (2008).

[474] R. Aaij *et al.* (LHCb Collaboration), First observation of the decays $\bar{B}_{(s)}^0 \to D_s^+K^-\pi^+\pi^-$ and $\bar{B}_s^0 \to D_{s1}(2536)^+\pi^-$, Phys. Rev. D **86**, 112005 (2012).

[475] B. Aubert *et al.* (*BABAR* Collaboration), Measurement of the $B^0 \to D^{*-}D_s^{*+}$ and $D_s^+ \to \phi\pi^+$ branching fractions, Phys. Rev. D **71**, 091104 (2005).

[476] K. Abe *et al.* (Belle Collaboration), Observation of the $D_1(2420) \to D\pi^+\pi^-$ decays, Phys. Rev. Lett. **94**, 221805 (2005).

[477] A. Drutskoy *et al.* (Belle Collaboration), Observation of $\bar{B}^0 \to D_{sJ}^*(2317)^+K^-$ decay, Phys. Rev. Lett. **94**, 061802 (2005).

[478] P. del Amo Sanchez *et al.* (*BABAR* Collaboration), Observation and study of the baryonic B-meson decays $B \to D^{(*)}p\bar{p}(\pi)(\pi)$, Phys. Rev. D **85**, 092017 (2012).

[479] K. Abe *et al.* (Belle Collaboration), Observation of $\bar{B}^0 \to D^{0(*)}p\bar{p}$, Phys. Rev. Lett. **89**, 151802 (2002).

[480] T. Medvedeva *et al.* (Belle Collaboration), Observation of the decay $\bar{B}^0 \to D_s^+\Lambda\bar{p}$, Phys. Rev. D **76**, 051102 (2007).

[481] J. P. Lees *et al.* (*BABAR* Collaboration), Evidence for the baryonic decay $\bar{B}^0 \to D^0\Lambda\bar{\Lambda}$, Phys. Rev. D **89**, 112002 (2014).

[482] Y.-W. Chang *et al.* (Belle Collaboration), Observation of $B^0 \to \Lambda\bar{\Lambda}K^0$ and $B^0 \to \Lambda\bar{\Lambda}K^{*0}$ at Belle, Phys. Rev. D **79**, 052006 (2009).

[483] Y. Y. Chang *et al.* (Belle Collaboration), Observation of $B^0 \to p\bar{\Lambda}D^{(*)-}$, Phys. Rev. Lett. **115**, 221803 (2015).

[484] M. Rohrken *et al.* (Belle Collaboration), Measurements of branching fractions and time-dependent CP violating asymmetries in $B^0 \to D^{(*)\pm}D^\mp$ decays, Phys. Rev. D **85**, 091106 (2012).

[485] B. Aubert *et al.* (*BABAR* Collaboration), Measurement of branching fractions and CP-violating charge asymmetries for B meson decays to $D^{(*)}\bar{D}^{(*)}$, and implications for the CKM angle γ, Phys. Rev. D **73**, 112004 (2006).

[486] R. Aaij *et al.* (LHCb Collaboration), First observations of $\bar{B}_s^0 \to D^+D^-$, $D_s^+D^-$ and $D^0\bar{D}^0$ decays, Phys. Rev. D **87**, 092007 (2013).

[487] B. Kronenbitter *et al.* (Belle Collaboration), First observation of CP violation and improved measurement of the branching fraction and polarization of $B^0 \to D^{*+}D^{*-}$ decays, Phys. Rev. D **86**, 071103 (2012).

[488] R. Aaij *et al.* (LHCb Collaboration), Observation of the $B_s^0 \to D^{*+}D^{*-}$ decay, J. High Energy Phys. 07 (2023) 119.

[489] I. Adachi *et al.* (Belle Collaboration), Measurement of the branching fraction and charge asymmetry of the decay $B^+ \to D^+\bar{D}^0$ and search for $B^0 \to D^0\bar{D}^0$, Phys. Rev. D **77**, 091101 (2008).

[490] P. del Amo Sanchez *et al.* (*BABAR* Collaboration), Measurement of the $B \to \bar{D}^{(*)}D^{(*)}K$ branching fractions, Phys. Rev. D **83**, 032004 (2011).

[491] B. Aubert *et al.* (*BABAR* Collaboration), Measurement of the branching fraction and time-dependent CP asymmetry in the decay $B^0 \to D^{*+}D^{*-}K_S^0$, Phys. Rev. D **74**, 091101 (2006).

[492] J. Dalseno *et al.* (Belle Collaboration), Measurement of branching fraction and time-dependent CP asymmetry parameters in $B^0 \to D^{*+}D^{*-}K_s^0$ decays, Phys. Rev. D **76**, 072004 (2007).

[493] G. Gokhroo *et al.* (Belle Collaboration), Observation of a near-threshold $D^0\bar{D}^0\pi^0$ enhancement in $B \to D^0\bar{D}^0\pi^0K$ decay, Phys. Rev. Lett. **97**, 162002 (2006).

[494] A. Zupanc *et al.*, Improved measurement of $\bar{B}^0 \to D_s^-D^+$ and search for $\bar{B}^0 \to D_s^+D_s^-$ at Belle, Phys. Rev. D **75**, 091102 (2007).

[495] B. Aubert *et al.* (*BABAR* Collaboration), Study of $B \to D^{(*)}D^{(*)}$ (s(J)) decays and measurement of D_s^- and D_{sJ} (2460)—branching fractions, Phys. Rev. D **74**, 031103 (2006).

[496] R. Aaij *et al.* (LHCb Collaboration), Study of beauty hadron decays into pairs of charm hadrons, Phys. Rev. Lett. **112**, 202001 (2014).

[497] B. Aubert *et al.* (*BABAR* Collaboration), Measurement of $B^0 \to D_s^{(*)+} D^{*-}$ branching fractions and $B^0 \to D_s^{(*)+} D^{*-}$ polarization with a partial reconstruction technique, Phys. Rev. D **67**, 092003 (2003).

[498] B. Aubert *et al.* (*BABAR* Collaboration), Search for the W^- exchange decays $B^0 \to D_s^{(*)-} D_s^{(*)+}$, Phys. Rev. D **72**, 111101 (2005).

[499] S.-K. Choi *et al.* (Belle Collaboration), Measurements of $B \to \bar{D} D_{s0}^{*+}(2317)$ decay rates and a search for isospin partners of the $D_{s0}^{*+}(2317)$, Phys. Rev. D **91**, 092011 (2015); **92**, 039905(E) (2015).

[500] B. Aubert *et al.* (*BABAR* Collaboration), Study of $B \to D_{sJ}^{(*)+} \bar{D}^{(*)}$ decays, Phys. Rev. Lett. **93**, 181801 (2004).

[501] P. Krokovny *et al.* (Belle Collaboration), Observation of the $D_{sJ}(2317)$ and $D_{sJ}(2457)$ in B decays, Phys. Rev. Lett. **91**, 262002 (2003).

[502] B. Aubert *et al.* (*BABAR* Collaboration), Study of resonances in exclusive B decays to anti-D(*) D(*) K, Phys. Rev. D **77**, 011102 (2008).

[503] T. Aushev *et al.* (Belle Collaboration), Study of the decays $B \to D_{s1}(2536)^+ \bar{D}^{(*)}$, Phys. Rev. D **83**, 051102 (2011).

[504] S. Choudhury *et al.* (Belle Collaboration), Test of lepton flavor universality and search for lepton flavor violation in $B \to K\ell\ell$ decays, J. High Energy Phys. 03 (2021) 105.

[505] K. Abe *et al.* (Belle Collaboration), Measurement of branching fractions and charge asymmetries for two-body B meson decays with charmonium, Phys. Rev. D **67**, 032003 (2003).

[506] F. Abe *et al.* (CDF Collaboration), Reconstruction of $B^0 \to J/\psi K_s^0$ and measurement of ratios of branching ratios involving $B \to J/\psi K^*$, Phys. Rev. Lett. **76**, 2015 (1996).

[507] B. Aubert *et al.* (*BABAR* Collaboration), Branching fraction measurements of $B \to \eta_c K$ decays, Phys. Rev. D **70**, 011101 (2004).

[508] K. Chilikin *et al.* (Belle Collaboration), Evidence for $B^+ \to h_c K^+$ and observation of $\eta_c(2S) \to p\bar{p}\pi^+\pi^-$, Phys. Rev. D **100**, 012001 (2019).

[509] F. Abe *et al.* (CDF Collaboration), Ratios of bottom meson branching fractions involving J/ψ mesons and determination of b quark fragmentation fractions, Phys. Rev. D **54**, 6596 (1996).

[510] R. Aaij *et al.* (LHCb Collaboration), Measurement of the $B_s^0 \to J/\psi K_S^0$ branching fraction, Phys. Lett. B **713**, 172 (2012).

[511] R. Aaij *et al.* (LHCb Collaboration), Observation of the $B_s^0 \to J/\psi K_s^0 K^\pm \pi^\mp$ decay, J. High Energy Phys. 07 (2014) 140.

[512] K. Chilikin *et al.* (Belle Collaboration), Observation of a new charged charmoniumlike state in $\bar{B}^0 \to J/\psi K^- \pi^+$ decays, Phys. Rev. D **90**, 112009 (2014).

[513] R. Aaij *et al.* (LHCb Collaboration), Evidence for an $\eta_c(1S)\pi^-$ resonance in $B^0 \to \eta_c(1S) K^+ \pi^-$ decays, Eur. Phys. J. C **78** (2018) 1019,

[514] F. Abe *et al.* (CDF Collaboration), Observation of $B^+ \to \psi(2S) K^+$ and $B^0 \to \psi(2S) K^{*0}(892)$ decays and measurements of B meson branching fractions into J/ψ and $\psi(2S)$ final states, Phys. Rev. D **58**, 072001 (1998).

[515] R. Aaij *et al.* (LHCb Collaboration), Measurement of relative branching fractions of B decays to $\psi(2S)$ and J/ψ mesons, Eur. Phys. J. C **72**, 2118 (2012).

[516] T. Affolder *et al.* (CDF Collaboration), A study of $B^0 \to J/\psi K^{(*)0} \pi^+ \pi^-$ decays with the collider detector at Fermilab, Phys. Rev. Lett. **88**, 071801 (2002).

[517] P. del Amo Sanchez *et al.* (*BABAR* Collaboration), Evidence for the decay $X(3872) \to J/\psi\omega$, Phys. Rev. D **82**, 011101 (2010).

[518] B. Aubert *et al.* (*BABAR* Collaboration), Rare B decays into states containing a J/ψ meson and a meson with $s\bar{s}$ quark content, Phys. Rev. Lett. **91**, 071801 (2003).

[519] K. Abe *et al.* (Belle Collaboration), Observation of $B \to J/\psi K_1(1270)$, Phys. Rev. Lett. **87**, 161601 (2001).

[520] T. Iwashita *et al.* (Belle Collaboration), Measurement of branching fractions for $B \to J/\psi\eta K$ decays and search for a narrow resonance in the $J/\psi\eta$ final state, Prog. Theor. Exp. Phys. **2014**, 43C01 (2014).

[521] B. Aubert *et al.* (*BABAR* Collaboration), Observation of the decay $B \to J/\psi\eta K$ and search for $X(3872) \to J/\psi\eta$, Phys. Rev. Lett. **93**, 041801 (2004).

[522] V. Bhardwaj *et al.* (Belle Collaboration), Evidence of a new narrow resonance decaying to $\chi_{c1}\gamma$ in $B \to \chi_{c1}\gamma K$, Phys. Rev. Lett. **111**, 032001 (2013).

[523] R. Mizuk *et al.* (Belle Collaboration), Dalitz analysis of $B \to K\pi^+\psi'$ decays and the $Z(4430)^+$, Phys. Rev. D **80**, 031104 (2009).

[524] R. Aaij *et al.* (LHCb Collaboration), Observation of the decay $\bar{B}_s^0 \to \psi(2S) K^+ \pi^-$, Phys. Lett. B **747**, 484 (2015).

[525] B. Aubert *et al.* (*BABAR* Collaboration), Evidence for the $B^0 \to p\bar{p}K^{*0}$ and $B^+ \to \eta_c K^{*+}$ decays and study of the decay dynamics of B meson decays into $p\bar{p}h$ final states, Phys. Rev. D **76**, 092004 (2007).

[526] F. Fang *et al.* (Belle Collaboration), Measurement of branching fractions for $B \to \eta_c K^{(*)}$ decays, Phys. Rev. Lett. **90**, 071801 (2003).

[527] B. Aubert *et al.* (*BABAR* Collaboration), Study of B-meson decays to $\eta_c K^{(*)}$, $\eta_c(2S) K^{(*)}$ and $\eta_c\gamma K^{(*)}$, Phys. Rev. D **78**, 012006 (2008).

[528] B. Aubert *et al.* (*BABAR* Collaboration), Search for factorization-suppressed $B \to \chi_c K^{(*)}$ decays, Phys. Rev. Lett. **94**, 171801 (2005).

[529] B. Aubert *et al.* (*BABAR* Collaboration), Observation of $B^0 \to \chi_{c0} K^{*0}$ and evidence for $B^+ \to \chi_{c0} K^{*+}$, Phys. Rev. D **78**, 091101 (2008).

[530] V. Bhardwaj *et al.* (Belle Collaboration), Observation of $X(3872) \to J/\psi\gamma$ and search for $X(3872) \to \psi'\gamma$ in B decays, Phys. Rev. Lett. **107**, 091803 (2011).

[531] B. Aubert *et al.* (*BABAR* Collaboration), Evidence for $X(3872) \to \psi_{2S}\gamma$ in $B^\pm \to X_{3872} K^\pm$ decays, and a study of $B \to c\bar{c}\gamma K$, Phys. Rev. Lett. **102**, 132001 (2009).

[532] V. Bhardwaj *et al.* (Belle Collaboration), Inclusive and exclusive measurements of B decays to χ_{c1} and χ_{c2} at Belle, Phys. Rev. D **93**, 052016 (2016).

[533] J. P. Lees *et al.* (*BABAR* Collaboration), Search for the $Z_1(4050)^+$ and $Z_2(4250)^+$ states in $\bar{B}^0 \to \chi_{c1} K^- \pi^+$ and $B^+ \to \chi_{c1} K_S^0 \pi^+$, Phys. Rev. D **85**, 052003 (2012).

[534] N. Soni *et al.* (Belle Collaboration), Measurement of branching fractions for $B \to \chi_{c1(2)} K(K^*)$ at Belle, Phys. Lett. B **634**, 155 (2006).

[535] B. Aubert *et al.* (*BABAR* Collaboration), Evidence for *CP* violation in $B^0 \to J/\psi \pi^0$ decays, Phys. Rev. Lett. **101**, 021801 (2008).

[536] B. Aubert *et al.* (*BABAR* Collaboration), A measurement of the $B^0 \to J/\psi \pi^+ \pi^-$ branching fraction, Phys. Rev. Lett. **90**, 091801 (2003).

[537] R. Aaij *et al.* (LHCb Collaboration), Observations of $B_s^0 \to \psi(2S)\eta$ and $B_{(s)}^0 \to \psi(2S)\pi^+\pi^-$ decays, Nucl. Phys. **B871**, 403 (2013).

[538] B. Aubert *et al.* (*BABAR* Collaboration), Branching fraction and charge asymmetry measurements in $B \to J/\psi\pi\pi$ decays, Phys. Rev. D **76**, 031101 (2007).

[539] R. Aaij *et al.* (LHCb Collaboration), Evidence for the decay $B^0 \to J/\psi\omega$ and measurement of the relative branching fractions of B_s^0 meson decays to $J/\psi\eta$ and $J/\psi\eta'$, Nucl. Phys. **B867**, 547 (2013).

[540] M. C. Chang *et al.*, Measurement of $B^0 \to J/\psi\eta^{(\prime)}$ and constraint on the $\eta - \eta'$ mixing angle, Phys. Rev. D **85**, 091102 (2012).

[541] R. Aaij *et al.* (LHCb Collaboration), Study of $\eta - \eta'$ mixing from measurement of $B_{(s)}^0 \to J/\psi\eta^{(\prime)}$ decay rates, J. High Energy Phys. 01 (2015) 024.

[542] R. Aaij *et al.* (LHCb Collaboration), Analysis of the resonant components in $B^0 \to J/\psi\pi^+\pi^-$, Phys. Rev. D **87**, 052001 (2013).

[543] R. Aaij *et al.* (LHCb Collaboration), Observation of $B_{(s)}^0 \to J/\psi f_1(1285)$ decays and measurement of the $f_1(1285)$ mixing angle, Phys. Rev. Lett. **112**, 091802 (2014).

[544] R. Aaij *et al.* (LHCb Collaboration), First observation of $\bar{B}^0 \to J/\psi K^+ K^-$ and search for $\bar{B}^0 \to J/\psi\phi$ decays, Phys. Rev. D **88**, 072005 (2013).

[545] Y. Liu *et al.* (Belle Collaboration), Search for $B^0 \to J/\psi\phi$ decays, Phys. Rev. D **78**, 011106 (2008).

[546] R. Kumar *et al.* (Belle Collaboration), Evidence for $B^0 \to \chi_{c1}\pi^0$ at Belle, Phys. Rev. D **78**, 091104 (2008).

[547] R. Aaij *et al.* (LHCb Collaboration), Search for the rare decays $B^0 \to J/\psi\gamma$ and $B_s^0 \to J/\psi\gamma$, Phys. Rev. D **92**, 112002 (2015).

[548] B. Aubert *et al.* (*BABAR* Collaboration), Search for the decay $B^0 \to J/\psi\gamma$, Phys. Rev. D **70**, 091104 (2004).

[549] R. Aaij *et al.* (LHCb Collaboration), Observation of $B_{(s)}^0 \to J/\psi p\bar{p}$ decays and precision measurements of the $B_{(s)}^0$ masses, Phys. Rev. Lett. **122**, 191804 (2019).

[550] R. Aaij *et al.* (LHCb Collaboration), Searches for $B_{(s)}^0 \to J/\psi p\bar{p}$ and $B^+ \to J/\psi p\bar{p}\pi^+$ decays, J. High Energy Phys. 09 (2013) 006.

[551] Q. L. Xie *et al.* (Belle Collaboration), Observation of $B^- \to J/\psi\Lambda\bar{p}$ and searches for $B^- \to J/\psi\Sigma^0\bar{p}$ and $B^0 \to J/\psi p\bar{p}$ decays, Phys. Rev. D **72**, 051105 (2005).

[552] B. Aubert *et al.* (*BABAR* Collaboration), Evidence for $B^+ \to J/\psi p\bar{\Lambda}$ and search for $B^0 \to J/\psi p\bar{p}$, Phys. Rev. Lett. **90**, 231801 (2003).

[553] B. Aubert *et al.* (*BABAR* Collaboration), Search for $B \to J/\psi D$ decays, Phys. Rev. D **71**, 091103 (2005).

[554] L. M. Zhang *et al.* (Belle Collaboration), Search for $B^0 \to J/\psi\bar{D}^0$ and $B^+ \to J/\psi\bar{D}^0\pi^+$ decays, Phys. Rev. D **71**, 091107 (2005).

[555] B. Aubert *et al.* (*BABAR* Collaboration), Observation of the decay $\bar{B}^0 \to \Lambda_c^+ \bar{p}\pi^0$, Phys. Rev. D **82**, 031102 (2010).

[556] J. P. Lees *et al.* (*BABAR* Collaboration), Study of the decay $\bar{B}^0 \to \Lambda_c^+ \bar{p}\pi^+\pi^-$ and its intermediate states, Phys. Rev. D **87**, 092004 (2013).

[557] N. Gabyshev *et al.* (Belle Collaboration), Study of exclusive *B* decays to charmed baryons at Belle, Phys. Rev. D **66**, 091102 (2002).

[558] K. S. Park *et al.* (Belle Collaboration), Study of the charmed baryonic decays $\bar{B}^0 \to \Sigma_c^{++}\bar{p}\pi^-$ and $\bar{B}^0 \to \Sigma_c^0 \bar{p}\pi^+$, Phys. Rev. D **75**, 011101 (2007).

[559] Y. Uchida *et al.* (Belle Collaboration), Search for $\bar{B}^0 \to \Lambda_c^+\Lambda_c^-$ decay at Belle, Phys. Rev. D **77**, 051101 (2008).

[560] K. Abe *et al.* (Belle Collaboration), Observation of $B^+ \to \Lambda_c^+\Lambda_c^- K^+$ and $B^0 \to \Lambda_c^+\Lambda_c^- K^0$ decays, Phys. Rev. Lett. **97**, 202003 (2006).

[561] B. Aubert *et al.* (*BABAR* Collaboration), A study of excited charm-strange baryons with evidence for new baryons $\Xi_c(3055)^+$ and $\Xi_c(3123)^+$, Phys. Rev. D **77**, 012002 (2008).

[562] R. Chistov *et al.* (Belle Collaboration), Observation of $B^+ \to \bar{\Xi}_c^0\Lambda_c^+$ and evidence for $B^0 \to \bar{\Xi}_c^-\Lambda_c^+$, Phys. Rev. D **74**, 111105 (2006).

[563] J. P. Lees *et al.* (*BABAR* Collaboration), Observation of the baryonic decay $\bar{B}^0 \to \Lambda_c^+ \bar{p}K^- K^+$, Phys. Rev. D **91**, 031102 (2015).

[564] B. Aubert *et al.* (*BABAR* Collaboration), Measurements of $\mathcal{B}(\bar{B}^0 \to \Lambda_c^+ \bar{p})$ and $\mathcal{B}(B^- \to \Lambda_c^+ \bar{p}\pi^-)$ and studies of $\Lambda_c^+\pi^-$ resonances, Phys. Rev. D **78**, 112003 (2008).

[565] N. Gabyshev *et al.* (Belle Collaboration), Observation of $\bar{B}^0 \to \Lambda_c^+ \bar{p}$ decay, Phys. Rev. Lett. **90**, 121802 (2003).

[566] B. Aubert *et al.* (*BABAR* Collaboration), Observation of the baryonic *B*-decay $\bar{B}^0 \to \Lambda_c^+ \bar{p}K^-\pi^+$, Phys. Rev. D **80**, 051105 (2009).

[567] J. P. Lees *et al.* (*BABAR* Collaboration), Observation of the baryonic *B* decay $\bar{B}^0 \to \Lambda_c^+ \bar{\Lambda} K^-$, Phys. Rev. D **84**, 071102 (2011).

[568] J. P. Lees *et al.* (*BABAR* Collaboration), Search for the decay $\bar{B}^0 \to \Lambda_c^+ \bar{p}p\bar{p}$, Phys. Rev. D **89**, 071102 (2014).

[569] S.-K. Choi *et al.* (Belle Collaboration), Bounds on the width, mass difference and other properties of $X(3872) \to \pi^+\pi^- J/\psi$ decays, Phys. Rev. D **84**, 052004 (2011).

[570] B. Aubert *et al.* (*BABAR* Collaboration), A study of $B \to X(3872)K$, with $X_{3872} \to J/\Psi\pi^+\pi^-$, Phys. Rev. D **77**, 111101 (2008).

[571] A. Bala *et al.* (Belle Collaboration), Observation of $X(3872)$ in $B \to X(3872)K\pi$ decays, Phys. Rev. D **91**, 051101 (2015).

[572] R. Mizuk *et al.* (Belle Collaboration), Observation of two resonance-like structures in the $\pi^+\chi_{c1}$ mass distribution in exclusive $\bar{B}^0 \to K^-\pi^+\chi_{c1}$ decays, Phys. Rev. D **78**, 072004 (2008).

[573] B. Aubert *et al.* (*BABAR* Collaboration), Measurements of the absolute branching fractions of $B^\pm \to K^\pm X(c\bar{c})$, Phys. Rev. Lett. **96**, 052002 (2006).

[574] B. Aubert *et al.* (*BABAR* Collaboration), Search for a charged partner of the $X(3872)$ in the B meson decay $B \to X^- K$, $X^- \to J/\psi\pi^-\pi^0$, Phys. Rev. D **71**, 031501 (2005).

[575] B. Aubert *et al.* (*BABAR* Collaboration), Search for the $Z(4430)^-$ at *BABAR*, Phys. Rev. D **79**, 112001 (2009).

[576] Y. Kato *et al.* (Belle Collaboration), Measurements of the absolute branching fractions of $B^+ \to X_{c\bar{c}}K^+$ and $B^+ \to \bar{D}^{(*)0}\pi^+$ at Belle, Phys. Rev. D **97**, 012005 (2018).

[577] B. Aubert *et al.* (*BABAR* Collaboration), Measurement of the branching fractions and CP-asymmetry of $B^- \to D^0_{(CP)}K^-$ decays with the *BABAR* detector, Phys. Rev. Lett. **92**, 202002 (2004).

[578] Y. Horii *et al.* (Belle Collaboration), Study of the suppressed B meson decay $B^- \to DK^-$, $D \to K^+\pi^-$, Phys. Rev. D **78**, 071901 (2008).

[579] S. K. Swain *et al.* (Belle Collaboration), Measurement of branching fraction ratios and CP asymmetries in $B^\pm \to D_{CP}K^\pm$, Phys. Rev. D **68**, 051101 (2003).

[580] R. Aaij *et al.* (LHCb Collaboration), Measurement of CP observables in $B^\pm \to DK^\pm$ and $B^\pm \to D\pi^\pm$ with two- and four-body D decays, Phys. Lett. B **760**, 117 (2016).

[581] R. Aaij *et al.* (LHCb Collaboration), Measurement of CP observables in $B^\pm \to D^{(*)}K^\pm$ and $B^\pm \to D^{(*)}\pi^\pm$ decays using two-body D final states, J. High Energy Phys. 04 (2021) 081.

[582] I. Adachi *et al.* (Belle-II Collaboration), Measurement of the branching fraction of the decay $B^- \to D^0\rho(770)^-$ at Belle II, Phys. Rev. D **109**, L111103 (2024).

[583] R. Aaij *et al.* (LHCb Collaboration), Measurement of CP observables in $B^\pm \to D^{(*)}K^\pm$ and $B^\pm \to D^{(*)}\pi^\pm$ decays, Phys. Lett. B **777**, 16 (2018).

[584] B. Aubert *et al.* (*BABAR* Collaboration), Measurement of the ratio $B(B^- \to D^{*0}K^-)/B(B^- \to D^{*0}\pi^-)$ and of the CP asymmetry of $B^- \to D^{*0}_{CP+}K^-$ decays, Phys. Rev. D **71**, 031102 (2005).

[585] B. Aubert *et al.* (*BABAR* Collaboration), Dalitz plot analysis of $B^- \to D^+\pi^-\pi^-$, Phys. Rev. D **79**, 112004 (2009).

[586] K. Abe *et al.* (Belle Collaboration), Study of $B^- \to D^{**0}\pi^-(D^{**0} \to D^{(*)+}\pi^-)$ decays, Phys. Rev. D **69**, 112002 (2004).

[587] R. Aaij *et al.* (LHCb Collaboration), Observation of the $B^+ \to D^{*-}K^+\pi^+$ decay, Phys. Rev. D **96**, 011101 (2017).

[588] B. Aubert *et al.* (*BABAR* Collaboration), Measurement of the $B^- \to D^0K^{*-}$ branching fraction, Phys. Rev. D **73**, 111104 (2006).

[589] B. Aubert *et al.* (*BABAR* Collaboration), Measurement of the branching fraction and polarization for the decay $B^- \to D^{0*}K^{*-}$, Phys. Rev. Lett. **92**, 141801 (2004).

[590] R. Aaij *et al.* (LHCb Collaboration), First observation and amplitude analysis of the $B^- \to D^+K^-\pi^-$ decay, Phys. Rev. D **91**, 092002 (2015); **93**, 119901(E) (2016).

[591] P. del Amo Sanchez *et al.* (*BABAR* Collaboration), Search for $B^+ \to D^+K^0$ and $B^+ \to D^+K^{*0}$ decays, Phys. Rev. D **82**, 092006 (2010).

[592] R. Aaij *et al.* (LHCb Collaboration), First observation of the rare $B^+ \to D^+K^+\pi^-$ decay, Phys. Rev. D **93**, 051101 (2016); **93**, 119902(E) (2016).

[593] B. Aubert *et al.* (*BABAR* Collaboration), Search for the rare decays $B^+ \to D^{(*)+}K^0_S$, Phys. Rev. D **72**, 011102 (2005).

[594] M. Iwabuchi *et al.* (Belle Collaboration), Search for $B^+ \to D^{*+}\pi^0$ decay, Phys. Rev. Lett. **101**, 041601 (2008).

[595] J. Wiechczynski *et al.* (Belle Collaboration), Measurement of $B \to D^{(*)}_s K\pi$ branching fractions, Phys. Rev. D **80**, 052005 (2009).

[596] B. Aubert *et al.* (*BABAR* Collaboration), Evidence for the rare decay $B^+ \to D^+_s\pi^0$, Phys. Rev. Lett. **98**, 171801 (2007).

[597] R. Aaij *et al.* (LHCb Collaboration), First observation of $B^+ \to D^+_s K^+K^-$ decays and a search for $B^+ \to D^+_s\phi$ decays, J. High Energy Phys. 01 (2018) 131.

[598] B. Aubert *et al.* (*BABAR* Collaboration), Search for rare quark-annihilation decays, $B^- \to D^{(*)-}_s\phi$, Phys. Rev. D **73**, 011103 (2006).

[599] P. Chen *et al.* (Belle Collaboration), Observation of $B^- \to \bar{p}\Lambda D^0$ at Belle, Phys. Rev. D **84**, 071501 (2011).

[600] O. Seon *et al.* (Belle Collaboration), Search for lepton-number-violating $B^+ \to D^-l^+l'^+$ decays, Phys. Rev. D **84**, 071106 (2011).

[601] R. Aaij *et al.* (LHCb Collaboration), Search for B^+_c decays to two charm mesons, Nucl. Phys. **B930**, 563 (2018).

[602] R. Aaij *et al.* (LHCb Collaboration), Measurements of CP asymmetries and branching fractions of B^- decays to two charm mesons, J. High Energy Phys. 09 (2023) 202.

[603] G. Majumder *et al.* (Belle Collaboration), Evidence for $B^0 \to D^+D^-$ and observation of $B^- \to D^0D^-$ and $B^- \to D^0D^{*-}$ decays, Phys. Rev. Lett. **95**, 041803 (2005).

[604] J. Brodzicka *et al.* (Belle Collaboration), Observation of a new D_{sJ} meson in $B^+ \to \bar{D}^0D^0K^+$ decays, Phys. Rev. Lett. **100**, 092001 (2008).

[605] K. Abe *et al.* (Belle Collaboration), Observation of $B^+ \to \psi(3770)K^+$, Phys. Rev. Lett. **93**, 051803 (2004).

[606] R. Aaij *et al.* (LHCb Collaboration), First observation of the $B^+ \to D^+_s D^-_s K^+$ decay, Phys. Rev. D **108**, 034012 (2023).

[607] C.-H. Wu *et al.* (Belle Collaboration), Study of $J/\psi \to p\bar{p}$, $\Lambda\bar{\Lambda}$ and observation of $\eta_c \to \Lambda\bar{\Lambda}$ at Belle, Phys. Rev. Lett. **97**, 162003 (2006).

[608] B. Aubert *et al.* (*BABAR* Collaboration), Measurement of the $B^+ \to p\bar{p}K^+$ branching fraction and study of the decay dynamics, Phys. Rev. D **72**, 051101 (2005).

[609] B. Aubert *et al.* (*BABAR* Collaboration), Study of $B^\pm \to J/\psi\pi^\pm$ and $B^\pm \to J/\psi K^\pm$ decays: Measurement of the ratio of branching fractions and search for direct CP violation, Phys. Rev. Lett. **92**, 241802 (2004).

[610] K. Abe *et al.* (Belle Collaboration), Observation of $B^+ \to \chi_{c0}K^+$, Phys. Rev. Lett. **88**, 031802 (2002).

[611] F. Abe *et al.* (CDF Collaboration), Measurement of the branching fraction $B(B^+_u \to J/\psi\pi^+)$ and search for $B^+_c \to J/\psi\pi^+$, Phys. Rev. Lett. **77**, 5176 (1996).

[612] A. Abulencia (CDF Collaboration), Measurement of the ratio of branching fractions $B(B^+ \to J/\psi\pi^+)/B(B^+ \to J/\psi K^+)$, Phys. Rev. D **79**, 112003 (2009).

[613] V. Khachatryan *et al.* (CMS Collaboration), Measurement of the ratio of the production cross sections times

branching fractions of $B_c^{\pm} \to J/\psi\pi^{\pm}$ and $B^{\pm} \to J/\psi K^{\pm}$ and $\mathcal{B}(B_c^{\pm} \to J/\psi\pi^{\pm}\pi^{\pm}\pi^{\mp})/\mathcal{B}(B_c^{\pm} \to J/\psi\pi^{\pm})$ in pp collisions at $\sqrt{s} = 7$ TeV, J. High Energy Phys. 01 (2015) 063.

[614] V. M. Abazov *et al.* (D0 Collaboration), Relative rates of B meson decays into ψ_{2S} and J/ψ mesons, Phys. Rev. D **79**, 111102 (2009).

[615] R. Aaij *et al.* (LHCb Collaboration), Measurements of B_c^+ production and mass with the $B_c^+ \to J/\psi\pi^+$ decay, Phys. Rev. Lett. **109**, 232001 (2012).

[616] R. Aaij *et al.* (LHCb Collaboration), Measurements of the branching fractions of $B^+ \to p\bar{p}K^+$ decays, Eur. Phys. J. C **73**, 2462 (2013).

[617] R. Aaij *et al.* (LHCb Collaboration), Measurement of B_c^+ production in proton-proton collisions at $\sqrt{s} = 8$ TeV, Phys. Rev. Lett. **114**, 132001 (2015).

[618] K. Abe *et al.* (Belle Collaboration), Measurements of branching fractions and decay amplitudes in $B \to J/\psi K^*$ decays, Phys. Lett. B **538**, 11 (2002).

[619] H. Guler *et al.* (Belle Collaboration), Study of the $K^+\pi^+\pi^-$ Final State in $B^+ \to J/\psi K^+\pi^+\pi^-$ and $B^+ \to \psi' K^+\pi^+\pi^-$, Phys. Rev. D **83**, 032005 (2011).

[620] B. Aubert *et al.* (*BABAR* Collaboration), Study of the $B \to J/\psi K^-\pi^+\pi^-$ decay and measurement of the $B \to X(3872)K^-$ branching fraction, Phys. Rev. D **71**, 071103 (2005).

[621] D. Acosta *et al.* (CDF Collaboration), Branching ratio measurements of exclusive B^+ decays to charmonium with the Collider Detector at Fermilab, Phys. Rev. D **66**, 052005 (2002).

[622] V. M. Abazov *et al.* (D0 Collaboration), Search for the $X(4140)$ state in $B^+ \to J/\psi\phi K^+$ decays with the D0 detector, Phys. Rev. D **89**, 012004 (2014).

[623] R. Aaij *et al.* (LHCb Collaboration), Observation of $J/\psi\phi$ structures consistent with exotic states from amplitude analysis of $B^+ \to J/\psi\phi K^+$ decays, Phys. Rev. Lett. **118**, 022003 (2017).

[624] R. Aaij *et al.* (LHCb Collaboration), Observation of the $B^+ \to J/\psi\eta' K^+$ decay, J. High Energy Phys. 08 (2023) 174; 10 (2023) 150(E).

[625] V. Khachatryan *et al.* (CMS Collaboration), Observation of the decay $B^+ \to \psi(2S)\phi(1020)K^+$ in pp collisions at $\sqrt{s} = 8$ TeV, Phys. Lett. B **764**, 66 (2017).

[626] A. Vinokurova *et al.* (Belle Collaboration), Study of $B^{\pm} \to K^{\pm}(K_S K\pi)^0$ decay and determination of eta_c and $eta_c(2S)$ parameters, Phys. Lett. B **706**, 139 (2011).

[627] F. Fang *et al.* (Belle Collaboration), Search for the h_c meson in $B^{\pm} \to h_c K^{\pm}$, Phys. Rev. D **74**, 012007 (2006).

[628] B. Aubert *et al.* (*BABAR* Collaboration), Dalitz plot analysis of the decay $B^{\pm} \to K^{\pm}K^{\pm}K^{\mp}$, Phys. Rev. D **74**, 032003 (2006).

[629] R. Kumar *et al.* (Belle Collaboration), Observation of $B^{\pm} \to \chi_{c1}\pi^{\pm}$ and search for direct CP violation, Phys. Rev. D **74**, 051103 (2006).

[630] R. Aaij *et al.* (LHCb Collaboration), Measurements of the branching fractions and CP asymmetries of $B^+ \to J/\psi\pi^+$ and $B^+ \to \psi(2S)\pi^+$ decays, Phys. Rev. D **85**, 091105 (2012).

[631] R. Aaij *et al.* (LHCb Collaboration), Measurement of the branching fraction and CP asymmetry in $B^+ \to J/\psi\rho^+$ decays, Eur. Phys. J. C **79**, 537 (2018).

[632] B. Aubert *et al.* (*BABAR* Collaboration), An amplitude analysis of the decay $B^{\pm} \to \pi^{\pm}\pi^{\pm}\pi^{\mp}$, Phys. Rev. D **72**, 052002 (2005).

[633] V. M. Abazov *et al.* (D0 Collaboration), Measurement of direct CP violation parameters in $B^{\pm} \to J/\psi K^{\pm}$ and $B^{\pm} \to J/\psi\pi^{\pm}$ decays with 10.4 fb^{-1} of Tevatron data, Phys. Rev. Lett. **110**, 241801 (2013).

[634] Y. B. Li *et al.* (Belle Collaboration), Observation of $\Xi_c(2930)^0$ and updated measurement of $B^- \to K^-\Lambda_c^+\bar{\Lambda}_c^-$ at Belle, Eur. Phys. J. C **78**, 252 (2018).

[635] J. P. Lees *et al.* (*BABAR* Collaboration), Study of the baryonic B decay $B^- \to \Sigma_c^{++}\bar{p}\pi^-\pi^-$, Phys. Rev. D **86**, 091102 (2012).

[636] J. P. Lees *et al.* (*BABAR* Collaboration), Measurements of the absolute branching fractions of $B^{\pm} \to K^{\pm}X_{c\bar{c}}$, Phys. Rev. Lett. **124**, 152001 (2020).

[637] B. Aubert *et al.* (*BABAR* Collaboration), Search for $B^+ \to X(3872)K^+$, $X_{3872} \to J/\psi\gamma$, Phys. Rev. D **74**, 071101 (2006).

[638] B. Aubert *et al.* (*BABAR* Collaboration), Study of $J/\psi\pi^+\pi^-$ states produced in $B^0 \to J/\psi\pi^+\pi^-K^0$ and $B^- \to J/\psi\pi^+\pi^-K^-$, Phys. Rev. D **73**, 011101 (2006).

[639] R. Aaij *et al.* (LHCb Collaboration), Measurement of the polarization amplitudes in $B^0 \to J/\psi K^*(892)^0$ decays, Phys. Rev. D **88**, 052002 (2013).

[640] B. Aubert *et al.* (*BABAR* Collaboration), Measurement of decay amplitudes of $B \to J/\psi K^*, \psi(2S)K^*$, and $\chi_{c1}K^*$ with an angular analysis, Phys. Rev. D **76**, 031102 (2007).

[641] R. Itoh *et al.* (Belle Collaboration), Studies of CP violation in $B \to J/\psi K^*$ decays, Phys. Rev. Lett. **95**, 091601 (2005).

[642] T. Aushev *et al.* (Belle Collaboration), Study of the $B \to X(3872)(D^{*0}\bar{D}^0)K$ decay, Phys. Rev. D **81**, 031103 (2010).

[643] K. Abe *et al.* (Belle Collaboration), Observation of a near-threshold $\omega J/\psi$ mass enhancement in exclusive $B \to K\omega J/\psi$ decays, Phys. Rev. Lett. **94**, 182002 (2005).

[644] R. Aaij *et al.* (LHCb Collaboration), Measurements of the branching fractions of the decays $B_s^0 \to D_s^{\mp}K^{\pm}$ and $B_s^0 \to D_s^-\pi^+$, J. High Energy Phys. 06 (2012) 115.

[645] R. Louvot *et al.* (Belle Collaboration), Measurement of the decay $B_s^0 \to D_s^-\pi^+$ and evidence for $B_s^0 \to D_s^{\mp}K^{\pm}$ in e^+e^- annihilation at $\sqrt{s} \simeq 10.87$ GeV, Phys. Rev. Lett. **102**, 021801 (2009).

[646] T. Aaltonen *et al.* (CDF Collaboration), First observation of $\bar{B}_s^0 \to D_s^{\pm}K^{\mp}$ and measurement of the ratio of branching fractions $\mathcal{B}(\bar{B}_s^0 \to D_s^{\pm}K^{\mp})/\mathcal{B}(\bar{B}_s^0 \to D_s^+\pi^-)$, Phys. Rev. Lett. **103**, 191802 (2009).

[647] R. Louvot *et al.* (Belle Collaboration), Observation of $B_s^0 \to D_s^{*-}\pi^+$, $B_s^0 \to D_s^{(*)-}\rho^+$ decays and measurement of $B_s^0 \to D_s^{*-}\rho^+$ polarization, Phys. Rev. Lett. **104**, 231801 (2010).

[648] R. Aaij *et al.* (LHCb Collaboration), First observation and measurement of the branching fraction for the decay $B_s^0 \to D_s^{*\mp}K^{\pm}$, J. High Energy Phys. 06 (2015) 130.

[649] R. Aaij *et al.* (LHCb Collaboration), Observation of $B_s^0 \to \bar{D}^0 K_S^0$ and evidence for $B_s^0 \to \bar{D}^{*0} K_S^0$ decays, Phys. Rev. Lett. **116**, 161802 (2016).

[650] R. Aaij *et al.* (LHCb Collaboration), Search for the decay $B_s^0 \to D^{*\mp}\pi^{\pm}$, Phys. Rev. D **87**, 071101 (2013).

[651] R. Aaij *et al.* (LHCb Collaboration), Search for the decay $B_s^0 \to \bar{D}^0 f_0(980)$, J. High Energy Phys. 08 (2015) 005.

[652] R. Aaij *et al.* (LHCb Collaboration), Measurement of the $B_s^0 \to D_s^{(*)+} D_s^{(*)-}$ branching fractions, Phys. Rev. D **93**, 092008 (2016).

[653] R. Aaij *et al.* (LHCb Collaboration), Amplitude analysis and the branching fraction measurement of $\bar{B}_s^0 \to J/\psi K^+ K^-$, Phys. Rev. D **87**, 072004 (2013).

[654] F. Thorne *et al.* (Belle Collaboration), Measurement of the decays $B_s^0 \to J/\psi\phi(1020)$, $B_s^0 \to J/\psi f_2'(1525)$ and $B_s^0 \to J/\psi K^+ K^-$ at Belle, Phys. Rev. D **88**, 114006 (2013).

[655] A. Abulencia *et al.* (CDF Collaboration), Observation of $B_s^0 \to \psi(2S)\phi$ and measurement of ratio of branching fractions $B(B_s^0 \to \psi(2S)\phi)/B(B_s^0 \to J/\psi\phi)$, Phys. Rev. Lett. **96**, 231801 (2006).

[656] V. Khachatryan *et al.* (CMS Collaboration), Measurement of the ratio $\mathcal{B}(\mathrm{B}_s^0 \to \mathrm{J}/\psi \mathrm{f}_0(980))/\mathcal{B}(\mathrm{B}_s^0 \to \mathrm{J}/\psi\phi(1020))$ in pp collisions at $\sqrt{s} = 7$ TeV, Phys. Lett. B **756**, 84 (2016).

[657] V. M. Abazov *et al.* (D0 Collaboration), Measurement of the relative branching ratio of $B_s^0 \to J/\psi f_0(980) to B_s^0 \to J/\psi\phi$, Phys. Rev. D **85**, 011103 (2012).

[658] V. M. Abazov *et al.* (D0 Collaboration), Study of the decay $B_s^0 \to J/\psi f_2'(1525)$ in $\mu^+\mu^- K^+ K^-$ final states, Phys. Rev. D **86**, 092011 (2012).

[659] R. Aaij *et al.* (LHCb Collaboration), Observation of $B_s \to J/\psi f_2'(1525)$ in $J/\psi K^+ K^-$ final states, Phys. Rev. Lett. **108**, 151801 (2012).

[660] R. Aaij *et al.* (LHCb Collaboration), Observation of the $B_s^0 \to J/\psi\phi\phi$ decay, J. High Energy Phys. 03 (2016) 040.

[661] R. Aaij *et al.* (LHCb Collaboration), First observation of $B_s^0 \to J/\psi f_0(980)$ decays, Phys. Lett. B **698**, 115 (2011).

[662] J. Li *et al.* (Belle Collaboration), First observation of $B_s^0 \to J/\psi\eta$ and $B_s^0 \to J/\psi\eta'$, Phys. Rev. Lett. **108**, 181808 (2012).

[663] T. Aaltonen *et al.* (CDF Collaboration), Observation of $B_s^0 \to J/\psi K^{*0}(892)$ and $B_s^0 \to J/\psi K_S^0$ decays, Phys. Rev. D **83**, 052012 (2011).

[664] J. Li *et al.* (Belle Collaboration), Observation of $B_s^0 \to J/\psi f_0(980)$ and evidence for $B_s^0 \to J/\psi f_0(1370)$, Phys. Rev. Lett. **106**, 121802 (2011).

[665] R. Aaij *et al.* (LHCb Collaboration), Measurement of resonant and CP components in $\bar{B}_s^0 \to J/\psi\pi^+\pi^-$ decays, Phys. Rev. D **89**, 092006 (2014).

[666] R. Aaij *et al.* (LHCb Collaboration), Study of $B_s^0 \to J\psi\pi^+\pi^- K^+ K^-$ decays, J. High Energy Phys. 02 (2021) 024; 04 (2021) 170(E).

[667] R. Aaij *et al.* (LHCb Collaboration), Observation of the $\mathrm{B}_s^0 \to \chi_{c1}(3872)\pi^+\pi^-$ decay, J. High Energy Phys. 07 (2023) 084.

[668] R. Aaij *et al.* (LHCb Collaboration), Observation of the decay $\bar{B}_s^0 \to \chi_{c2} K^+ K^-$ in the ϕ mass region, J. High Energy Phys. 08 (2018) 191.

[669] E. Solovieva *et al.* (Belle Collaboration), Evidence for $\bar{B}_s^0 \to \Lambda_c^+ \bar{\Lambda}\pi^-$, Phys. Lett. B **726**, 206 (2013).

[670] R. Aaij *et al.* (LHCb Collaboration), Observation of $B_c^+ \to D^0 K^+$ decays, Phys. Rev. Lett. **118**, 111803 (2017).

[671] R. Aaij *et al.* (LHCb Collaboration), Study of B_c^+ decays to the $K^+ K^-\pi^+$ final state and evidence for the decay $B_c^+ \to \chi_{c0}\pi^+$, Phys. Rev. D **94**, 091102 (2016).

[672] R. Aaij *et al.* (LHCb Collaboration), Observation of $B_c^+ \to J/\psi D_s^+$ and $B_c^+ \to J/\psi D_s^{*+}$ decays, Phys. Rev. D **87**, 112012 (2013).

[673] G. Aad *et al.* (ATLAS Collaboration), Study of the $B_c^+ \to J/\psi D_s^+$ and $B_c^+ \to J/\psi D_s^{*+}$ decays with the ATLAS detector, Eur. Phys. J. C **76**, 4 (2016).

[674] R. Aaij *et al.* (LHCb Collaboration), First observation of the decay $B_c^+ \to J/\psi\pi^+\pi^-\pi^+$, Phys. Rev. Lett. **108**, 251802 (2012).

[675] R. Aaij *et al.* (LHCb Collaboration), Observation of $B_c^+ \to J/\psi D^{(*)} K^{(*)}$ decays, Phys. Rev. D **95**, 032005 (2017).

[676] R. Aaij *et al.* (LHCb Collaboration), First observation of the decay $B_c^+ \to J/\psi K^+$, J. High Energy Phys. 09 (2013) 075.

[677] R. Aaij *et al.* (LHCb Collaboration), Observation of the decay $B_c \to J/\psi K^+ K^-\pi^+$, J. High Energy Phys. 11 (2013) 094.

[678] R. Aaij *et al.* (LHCb Collaboration), Measurement of the branching fraction ratio $\mathcal{B}(B_c^+ \to \psi(2S)\pi^+)/\mathcal{B}(B_c^+ \to J/\psi\pi^+)$, Phys. Rev. D **92**, 072007 (2015).

[679] R. Aaij *et al.* (LHCb Collaboration), Observation of the decay $B_c^+ \to B_s^0\pi^+$, Phys. Rev. Lett. **111**, 181801 (2013).

[680] R. Aaij *et al.* (LHCb Collaboration), Studies of beauty baryon decays to $D^0 p h^-$ and $\Lambda_c^+ h^-$ final states, Phys. Rev. D **89**, 032001 (2014).

[681] R. Aaij *et al.* (LHCb Collaboration), First observation and branching fraction measurement of the $\Lambda_b^0 \to D_s^- p$ decay, J. High Energy Phys. 07 (2023) 075.

[682] R. Aaij *et al.* (LHCb Collaboration), Study of the production of Λ_b^0 and $\bar{B}^0$ hadrons in pp collisions and first measurement of the $\Lambda_b^0 \to J/\psi p K^-$ branching fraction, Chin. Phys. C **40**, 011001 (2016).

[683] R. Aaij *et al.* (LHCb Collaboration), Observation of the $\Lambda_b^0 \to J/\psi p\pi^-$ decay, J. High Energy Phys. 07 (2014) 103.

[684] R. Aaij *et al.* (LHCb Collaboration), Observation of $\Lambda_b^0 \to \psi(2S) p K^-$ and $\Lambda_b^0 \to J/\psi\pi^+\pi^- p K^-$ decays and a measurement of the Λ_b^0 baryon mass, J. High Energy Phys. 05 (2016) 132.

[685] R. Aaij *et al.* (LHCb Collaboration), Evidence for exotic hadron contributions to $\Lambda_b^0 \to J/\psi p\pi^-$ decays, Phys. Rev. Lett. **117**, 082003 (2016); **117**, 109902(A) (2016); **118**, 119901(A) (2017).

[686] R. Aaij *et al.* (LHCb Collaboration), Observation of the decays $\Lambda_b^0 \to \chi_{c1} p K^-$ and $\Lambda_b^0 \to \chi_{c2} p K^-$, Phys. Rev. Lett. **119**, 062001 (2017).

[687] F. Abe *et al.* (CDF Collaboration), Observation of $\Lambda_b^0 \to J/\psi\Lambda$ at the Fermilab proton antiproton collider, Phys. Rev. D **55**, 1142 (1997).

[688] G. Aad *et al.* (ATLAS Collaboration), Measurement of the branching ratio $\Gamma(\Lambda_b^0 \to \psi(2S)\Lambda^0)/\Gamma(\Lambda_b^0 \to J/\psi\Lambda^0)$ with the ATLAS detector, Phys. Lett. B **751**, 63 (2015).

[689] T. Aaltonen *et al.* (CDF Collaboration), Observation of the Ω_b^- baryon and measurement of the properties of the Ξ_b^- and Ω_b^- baryons, Phys. Rev. D **80**, 072003 (2009).

[690] R. Aaij *et al.* (LHCb Collaboration), Measurement of the ratio of branching fractions of the decays $\Lambda_b^0 \to \psi(2S)\Lambda$ and $\Lambda_b^0 \to J/\psi\Lambda$, J. High Energy Phys. 03 (2019) 126.

[691] V. M. Abazov *et al.* (D0 Collaboration), Measurement of the production fraction times branching fraction $f(b \to \Lambda_b) \cdot \mathcal{B}(\Lambda_b \to J/\psi\Lambda)$, Phys. Rev. D **84**, 031102 (2011).

[692] R. Aaij *et al.* (LHCb Collaboration), Observation of the decay $\Lambda_b^0 \to \psi(2S)p\pi^-$, J. High Energy Phys. 08 (2018) 131.

[693] R. Aaij *et al.* (LHCb Collaboration), Observation of the $\Lambda_b^0 \to \chi_{c1}(3872)pK^-$ decay, J. High Energy Phys. 09 (2019) 028.

[694] A. M. Sirunyan *et al.* (CMS Collaboration), Measurement of the Λ_b polarization and angular parameters in $\Lambda_b \to J/\psi\Lambda$ decays from pp collisions at $\sqrt{s} = 7$ and 8 TeV, Phys. Rev. D **97**, 072010 (2018).

[695] G. Aad *et al.* (ATLAS Collaboration), Measurement of the parity-violating asymmetry parameter α_b and the helicity amplitudes for the decay $\Lambda_b^0 \to J/\psi + \Lambda^0$ with the ATLAS detector, Phys. Rev. D **89**, 092009 (2014).

[696] R. Aaij *et al.* (LHCb Collaboration), Measurements of the $\Lambda_b^0 \to J/\psi\Lambda$ decay amplitudes and the Λ_b^0 polarisation in pp collisions at $\sqrt{s} = 7$ TeV, Phys. Lett. B **724**, 27 (2013).

[697] T. Aaltonen *et al.* (CDF Collaboration), Measurement of the branching fraction $\mathcal{B}(\Lambda_b^0 \to \Lambda_c^+\pi^-\pi^+\pi^-)$ at CDF, Phys. Rev. D **85**, 032003 (2012).

[698] R. Aaij *et al.* (LHCb Collaboration), Observation of the decay $\Lambda_b^0 \to \Lambda_c^+ p\bar{p}\pi^-$, Phys. Lett. B **784**, 101 (2018).

[699] R. Aaij *et al.* (LHCb Collaboration), Evidence for the strangeness-changing weak decay $\Xi_b^- \to \Lambda_b^0\pi^-$, Phys. Rev. Lett. **115**, 241801 (2015).

[700] R. Aaij *et al.* (LHCb Collaboration), Study of the D^0p amplitude in $\Lambda_b^0 \to D^0p\pi^-$ decays, J. High Energy Phys. 05 (2017) 030.

[701] HFLAV rare B decays web page, https://hflav.web.cern.ch/content/rare-b-decays.

[702] Y.-T. Duh *et al.* (Belle Collaboration), Measurements of branching fractions and direct CP asymmetries for $B \to K\pi$, $B \to K\pi\pi$ and $B \to KK$ decays, Phys. Rev. D **87**, 031103 (2013).

[703] I. Adachi *et al.* (Belle-II Collaboration), Measurement of branching fractions and direct CP asymmetries for $B \to K\pi$ and $B \to \pi\pi$ decays at Belle II, Phys. Rev. D **109**, 012001 (2024).

[704] B. Aubert *et al.* (*BABAR* Collaboration), Observation of $B^+ \to \bar{K}^0K^+$ and $B^0 \to K^0\bar{K}^0$, Phys. Rev. Lett. **97**, 171805 (2006).

[705] A. Bornheim *et al.* (CLEO Collaboration), Measurements of charmless hadronic two body B meson decays and the ratio $\mathcal{B}(B \to DK)/\mathcal{B}(B \to D\pi)$, Phys. Rev. D **68**, 052002 (2003); **75**, 119907(E) (2007).

[706] R. Aaij *et al.* (LHCb Collaboration), Branching fraction and CP asymmetry of the decays $B^+ \to K_S^0\pi^+$ and $B^+ \to K_S^0K^+$, Phys. Lett. B **726**, 646 (2013).

[707] B. Aubert *et al.* (*BABAR* Collaboration), Study of $B^0 \to \pi^0\pi^0$, $B^\pm \to \pi^\pm\pi^0$, and $B^\pm \to K^\pm\pi^0$ decays, and isospin analysis of $B \to \pi\pi$ decays, Phys. Rev. D **76**, 091102 (2007).

[708] B. Aubert *et al.* (*BABAR* Collaboration), B meson decays to charmless meson pairs containing η or η' mesons, Phys. Rev. D **80**, 112002 (2009).

[709] J. Schumann *et al.* (Belle Collaboration), Evidence for $B \to \eta'\pi$ and improved measurements for $B \to \eta'K$, Phys. Rev. Lett. **97**, 061802 (2006).

[710] F. Abudinén *et al.* (Belle-II Collaboration), Measurement of the branching fractions of $B \to \eta'K$ decays using 2019/2020 Belle II data, arXiv:2104.06224.

[711] I. Adachi *et al.* (Belle Collaboration), Search for resonant $B^\pm \to K^\pm h \to K^\pm\gamma\gamma$ decays at Belle, Phys. Lett. B **662**, 323 (2008).

[712] S. J. Richichi *et al.* (CLEO Collaboration), Two-body B meson decays to η and η': Observation of $B \to \eta K^*$, Phys. Rev. Lett. **85**, 520 (2000).

[713] R. Aaij *et al.* (LHCb Collaboration), Observation of the $B_s^0 \to \eta'\eta'$ decay, Phys. Rev. Lett. **115**, 051801 (2015).

[714] P. del Amo Sanchez *et al.* (*BABAR* Collaboration), B-meson decays to $\eta'\rho$, $\eta' f_0$, and $\eta' K^*$, Phys. Rev. D **82**, 011502 (2010).

[715] J. Schumann *et al.* (Belle Collaboration), Search for B decays into $\eta'\rho$, $\eta'K^*$, $\eta'\phi$, $\eta'\omega$ and $\eta'\eta^{(\prime)}$ at Belle, Phys. Rev. D **75**, 092002 (2007).

[716] C. T. Hoi *et al.* (Belle Collaboration), Evidence for direct CP violation in $B^\pm \to \eta h^\pm$ and observation of $B^0 \to \eta K^0$, Phys. Rev. Lett. **108**, 031801 (2012).

[717] B. Aubert *et al.* (*BABAR* Collaboration), Measurement of branching fractions and charge asymmetries in B decays to an η meson and a K^* meson, Phys. Rev. Lett. **97**, 201802 (2006).

[718] C. H. Wang *et al.* (Belle Collaboration), Measurement of charmless B Decays to ηK^* and $\eta\rho$, Phys. Rev. D **75**, 092005 (2007).

[719] B. Aubert *et al.* (*BABAR* Collaboration), Study of B meson decays with excited η and η' mesons, Phys. Rev. Lett. **101**, 091801 (2008).

[720] J. P. Lees *et al.* (*BABAR* Collaboration), Study of CP violation in Dalitz-plot analyses of $B^0 \to K^+K^-K_S^0$, $B^+ \to K^+K^-K^+$, and $B^+ \to K_S^0K_S^0K^+$, Phys. Rev. D **85**, 112010 (2012).

[721] V. Chobanova *et al.* (Belle Collaboration), Measurement of branching fractions and CP violation parameters in $B \to \omega K$ decays with first evidence of CP violation in $B^0 \to \omega K_S^0$, Phys. Rev. D **90**, 012002 (2014).

[722] B. Aubert *et al.* (*BABAR* Collaboration), Branching fraction and CP-violation charge asymmetry measurements for B-meson decays to $\eta K^\pm$, $\eta\pi^\pm$, $\eta'K$, $\eta'\pi^\pm$, ωK, and $\omega\pi^\pm$, Phys. Rev. D **76**, 031103 (2007).

[723] C. P. Jessop *et al.* (CLEO Collaboration), Study of charmless hadronic B meson decays to pseudoscalar vector final states, Phys. Rev. Lett. **85**, 2881 (2000).

[724] B. Aubert *et al.* (*BABAR* Collaboration), Observation of B meson decays to ωK^* and improved measurements for $\omega\rho$ and ωf_0, Phys. Rev. D **79**, 052005 (2009).

[725] B. Aubert *et al.* (*BABAR* Collaboration), Search for B-meson decays to two-body final states with $a_0(980)$ mesons, Phys. Rev. D **70**, 111102 (2004).

[726] B. Aubert *et al.* (*BABAR* Collaboration), Evidence for direct CP violation from Dalitz-plot analysis of $B^{\pm} \to K^{\pm}\pi^{\mp}\pi^{\pm}$, Phys. Rev. D **78**, 012004 (2008).

[727] A. Garmash *et al.* (Belle Collaboration), Evidence for large direct CP violation in $B^{\pm} \to \rho^0(770)K^{\pm}$ from analysis of the three-body charmless $B^{\pm} \to K^{\pm}\pi^{+}\pi^{-}$ decay, Phys. Rev. Lett. **96**, 251803 (2006).

[728] J. P. Lees *et al.* (*BABAR* Collaboration), Evidence for CP violation in $B^+ \to K^*(892)^+\pi^0$ from a Dalitz plot analysis of $B^+ \to K^0_S\pi^+\pi^0$ decays, Phys. Rev. D **96**, 072001 (2017).

[729] J. P. Lees *et al.* (*BABAR* Collaboration), Observation of the rare decay $B^+ \to K^+\pi^0\pi^0$ and measurement of the quasi-two body contributions $B^+ \to K^*(892)^+\pi^0$, $B^+ \to f_0(980)K^+$ and $B^+ \to \chi_{c0}K^+$, Phys. Rev. D **84**, 092007 (2011).

[730] R. Aaij *et al.* (LHCb Collaboration), Measurement of the relative branching fractions of $B^+ \to h^+h'^+h'^-$ decays, Phys. Rev. D **102**, 112010 (2020).

[731] F. Abudinén *et al.* (Belle-II Collaboration), Measurements of branching fractions and CP-violating charge asymmetries in multibody charmless B decays reconstructed in 2019-2020 Belle II data, arXiv:2109.10807.

[732] B. Aubert *et al.* (*BABAR* Collaboration), Dalitz-plot analysis of the decays $B^{\pm} \to K^{\pm}\pi^{\mp}\pi^{\pm}$, Phys. Rev. D **72**, 072003 (2005); **74**, 099903(E) (2006).

[733] A. Garmash *et al.* (Belle Collaboration), Dalitz analysis of the three-body charmless decays $B^+ \to K^+\pi^+\pi^-$ and $B^+ \to K^+K^+K^-$, Phys. Rev. D **71**, 092003 (2005).

[734] R. Aaij *et al.* (LHCb Collaboration), Search for the suppressed decays $B^+ \to K^+K^+\pi^-$ and $B^+ \to \pi^+\pi^+K^-$, Phys. Lett. B **765**, 307 (2017).

[735] B. Aubert *et al.* (*BABAR* Collaboration), Search for the highly suppressed decays $B^- \to K^+\pi^-\pi^-$ and $B^- \to K^-K^-\pi^+$, Phys. Rev. D **78**, 091102 (2008).

[736] A. Garmash *et al.* (Belle Collaboration), Study of B meson decays to three body charmless hadronic final states, Phys. Rev. D **69**, 012001 (2004).

[737] T. Bergfeld *et al.* (CLEO Collaboration), A search for nonresonant $B^+ \to h^+h^-h^+$ decays, Phys. Rev. Lett. **77**, 4503 (1996).

[738] B. Aubert *et al.* (*BABAR* Collaboration), Measurement of branching fractions of B decays to $K_1(1270)\pi$ and $K_1(1400)\pi$ and determination of the CKM angle α from $B^0 \to a_1(1260)^{\pm}\pi^{\mp}$, Phys. Rev. D **81**, 052009 (2010).

[739] E. Eckhart *et al.* (CLEO Collaboration), Observation of $B \to K^0_S\pi^+\pi^-$ and evidence for $B \to K^{*\pm}\pi^{\mp}$, Phys. Rev. Lett. **89**, 251801 (2002).

[740] B. Aubert *et al.* (*BABAR* Collaboration), Branching fraction measurements of charged B decays to $K^{*+}K^+K^-$, $K^{*+}\pi^+K^-$, $K^{*+}K^+\pi^-$ and $K^{*+}\pi^+\pi^-$ final states, Phys. Rev. D **74**, 051104 (2006).

[741] P. del Amo Sanchez *et al.* (*BABAR* Collaboration), Measurements of branching fractions, polarizations, and direct CP-violation asymmetries in $B^+ \to \rho^0K^{*+}$ and $B^+ \to f_0(980)K^{*+}$ decays, Phys. Rev. D **83**, 051101 (2011).

[742] B. Aubert *et al.* (*BABAR* Collaboration), Observation of $B^+ \to a_1^+(1260)K^0$ and $B^0 \to a_1^-(1260)K^+$, Phys. Rev. Lett. **100**, 051803 (2008).

[743] B. Aubert *et al.* (*BABAR* Collaboration), Observation of $B^+ \to b_1^+K^0$ and search for B-meson decays to $b_1^0K^0$ and $b_1\pi^0$, Phys. Rev. D **78**, 011104 (2008).

[744] B. Aubert *et al.* (*BABAR* Collaboration), Measurements of branching fractions, polarizations, and direct CP-violation asymmetries in $B \to \rho K^*$ and $B \to f_0(980)K^*$ decays, Phys. Rev. Lett. **97**, 201801 (2006).

[745] J. Zhang *et al.* (Belle Collaboration), Measurements of branching fractions and polarization in $B \to K^*\rho$ decays, Phys. Rev. Lett. **95**, 141801 (2005).

[746] H. Albrecht *et al.* (ARGUS Collaboration), Search for $b \to s$ gluon in B meson decays, Phys. Lett. B **254**, 288 (1991).

[747] J. Zhang *et al.* (Belle Collaboration), Measurements of branching fraction and polarization in $B^+ \to \rho^+K^{*0}$ decay, arXiv:hep-ex/0505039.

[748] B. Aubert *et al.* (*BABAR* Collaboration), Observation of B-meson decays to $b_1\pi$ and b_1K, Phys. Rev. Lett. **99**, 241803 (2007).

[749] B. Aubert *et al.* (*BABAR* Collaboration), Search for B-meson decays to $b_1\rho$ and b_1K^*, Phys. Rev. D **80**, 051101 (2009).

[750] A. B. Kaliyar *et al.* (Belle Collaboration), Measurements of branching fraction and direct CP asymmetry in $B^{\pm} \to K^0_SK^0_SK^{\pm}$ and a search for $B^{\pm} \to K^0_SK^0_S\pi^{\pm}$, Phys. Rev. D **99**, 031102 (2019).

[751] B. Aubert *et al.* (*BABAR* Collaboration), Search for the decay $B^+ \to K^0_SK^0_S\pi^+$, Phys. Rev. D **79**, 051101 (2009).

[752] C.-L. Hsu *et al.* (Belle Collaboration), Angular analysis of the low K^+K^- invariant mass enhancement in $B^+ \to K^+K^-\pi^+$ decays, Phys. Rev. D **107**, 032013 (2023).

[753] B. Aubert *et al.* (*BABAR* Collaboration), Observation of the decay $B^+ \to K^+K^-\pi^+$, Phys. Rev. Lett. **99**, 221801 (2007).

[754] R. Aaij *et al.* (LHCb Collaboration), Amplitude analysis of $B^{\pm} \to \pi^{\pm}K^+K^-$ decays, Phys. Rev. Lett. **123**, 231802 (2019).

[755] B. Aubert *et al.* (*BABAR* Collaboration), Search for the decay $B^+ \to \bar{K}^{*0}(892)K^+$, Phys. Rev. D **76**, 071103 (2007).

[756] M.-Z. Wang *et al.* (Belle Collaboration), Study of the baryon-antibaryon low-mass enhancements in charmless three-body baryonic B decays, Phys. Lett. B **617**, 141 (2005).

[757] Y. M. Goh *et al.* (Belle Collaboration), Search for the decay $B^+ \to \bar{K}^{*0}K^{*+}$ at Belle, Phys. Rev. D **91**, 071101 (2015).

[758] B. Aubert *et al.* (*BABAR* Collaboration), Evidence for $B^+ \to \bar{K}^{*0}K^{*+}$, Phys. Rev. D **79**, 051102 (2009).

[759] R. Aaij *et al.* (LHCb Collaboration), Observation of the decay $\Xi_b^- \to pK^-K^-$, Phys. Rev. Lett. **118**, 071801 (2017).

[760] F. Abudinén *et al.* (Belle-II Collaboration), Rediscovery of $B \to \phi K^{(*)}$ decays and measurement of the longitudinal polarization fraction f_L in $B \to \phi K^*$ decays using the Summer 2020 Belle II dataset, arXiv:2008.03873.

[761] D. Acosta *et al.* (CDF Collaboration), First evidence for $B_s^0 \to \phi\phi$ decay and measurements of branching ratio and A_{CP} for $B^+ \to \phi K^+$, Phys. Rev. Lett. **95**, 031801 (2005).

[762] R. A. Briere *et al.* (CLEO Collaboration), Observation of $B \to \phi K$ and $B \to \phi K^*$, Phys. Rev. Lett. **86**, 3718 (2001).

[763] B. Aubert *et al.* (*BABAR* Collaboration), Amplitude analysis of the $B^\pm \to \phi K^*(892)^\pm$ decay, Phys. Rev. Lett. **99**, 201802 (2007).

[764] K. F. Chen *et al.* (Belle Collaboration), Measurement of branching fractions and polarization in $B \to \phi K^{(*)}$ decays, Phys. Rev. Lett. **91**, 201801 (2003).

[765] B. Aubert *et al.* (*BABAR* Collaboration), Observation and polarization measurements of $B^\pm \to \phi K_1^\pm$ and $B^\pm \to \phi K_2^{*\pm}$, Phys. Rev. Lett. **101**, 161801 (2008).

[766] P. del Amo Sanchez *et al.* (*BABAR* Collaboration), Search for B^+ meson decay to $a_1^+(1260)K^{*0}(892)$, Phys. Rev. D **82**, 091101 (2010).

[767] J. P. Lees *et al.* (*BABAR* Collaboration), Measurements of branching fractions and CP asymmetries and studies of angular distributions for $B \to \phi\phi K$ decays, Phys. Rev. D **84**, 012001 (2011).

[768] H.-C. Huang *et al.* (Belle Collaboration), Evidence for $B \to \phi\phi K$, Phys. Rev. Lett. **91**, 241802 (2003).

[769] B. Aubert *et al.* (*BABAR* Collaboration), Search for B meson decays to $\eta'\eta' K$, Phys. Rev. D **74**, 031105 (2006).

[770] C. Liu *et al.* (Belle Collaboration), Search for the X(1812) in $B^\pm \to K^\pm\omega\phi$, Phys. Rev. D **79**, 071102 (2009).

[771] R. Ammar *et al.* (CLEO Collaboration), Search for the familon via $B^\pm \to \pi^\pm X^0$, $B^\pm \to K^\pm X^0$, and $B^0 \to K_S^0 X^0$ decays, Phys. Rev. Lett. **87**, 271801 (2001).

[772] B. Aubert *et al.* (*BABAR* Collaboration), Dalitz plot analysis of $B^\pm \to \pi^\pm\pi^\pm\pi^\mp$ Decays, Phys. Rev. D **79**, 072006 (2009).

[773] R. Aaij *et al.* (LHCb Collaboration), Observation of several sources of CP violation in $B^+ \to \pi^+\pi^+\pi^-$ decays, Phys. Rev. Lett. **124**, 031801 (2020).

[774] A. Gordon *et al.* (Belle Collaboration), Study of $B \to \rho\pi$ decays at BELLE, Phys. Lett. B **542**, 183 (2002).

[775] R. Aaij *et al.* (LHCb Collaboration), Amplitude analysis of the $B^+ \to \pi^+\pi^+\pi^-$ decay, Phys. Rev. D **101**, 012006 (2020).

[776] Y.-T. Lai *et al.* (Belle Collaboration), First Measurement of the $B^+ \to \pi^+\pi^0\pi^0$ branching fraction and CP asymmetry, Phys. Rev. Lett. **130**, 181804 (2023).

[777] H. Albrecht *et al.* (ARGUS Collaboration), Search for hadronic $b \to u$ decays, Phys. Lett. B **241**, 278 (1990).

[778] B. Aubert *et al.* (*BABAR* Collaboration), Measurement of the $B^\pm \to \rho^\pm\pi^0$ branching fraction and direct CP asymmetry, Phys. Rev. D **75**, 091103 (2007).

[779] B. Aubert *et al.* (*BABAR* Collaboration), Improved measurement of $B^+ \to \rho^+\rho^0$ and determination of the quark-mixing phase angle α, Phys. Rev. Lett. **102**, 141802 (2009).

[780] F. Abudinén *et al.* (Belle-II Collaboration), Angular analysis of $B^+ \to \rho^+\rho^0$ decays reconstructed in 2019, 2020, and 2021 Belle II data, arXiv:2206.12362.

[781] J. Zhang *et al.* (Belle Collaboration), Observation of $B^+ \to \rho^+\rho^0$, Phys. Rev. Lett. **91**, 221801 (2003).

[782] B. Aubert *et al.* (*BABAR* Collaboration), Evidence for charged B meson decays to $a_1^\pm(1260)\pi^0$ and $a_1^0(1260)\pi^\pm$, Phys. Rev. Lett. **99**, 261801 (2007).

[783] C.-M. Jen *et al.* (Belle Collaboration), Improved measurements of branching fractions and CP partial rate asymmetries for $B \to \omega K$ and $B \to \omega\pi$, Phys. Rev. D **74**, 111101 (2006).

[784] B. Aubert *et al.* (*BABAR* Collaboration), Observation of $B^+ \to \eta\rho^+$ and search for B^0 decays to $\eta'\eta$, $\eta\pi^0$, $\eta\,'\,\pi^0$, and $\omega\pi^0$, Phys. Rev. D **78**, 011107 (2008).

[785] B. Aubert *et al.* (*BABAR* Collaboration), Search for $B^+ \to \phi\pi^+$ and $B^0 \to \phi\pi^0$ Decays, Phys. Rev. D **74**, 011102 (2006).

[786] J. H. Kim *et al.* (Belle Collaboration), Search for $B \to \phi\pi$ decays, Phys. Rev. D **86**, 031101 (2012).

[787] B. Aubert *et al.* (*BABAR* Collaboration), Searches for B meson decays to $\phi\phi$, $\phi\rho$, $\phi f_0(980)$, and $f_0(980)f_0(980)$ final states, Phys. Rev. Lett. **101**, 201801 (2008).

[788] D. Bortoletto *et al.* (CLEO Collaboration), A search for $b \to u$ transitions in exclusive hadronic B meson decays, Phys. Rev. Lett. **62**, 2436 (1989).

[789] B. Aubert *et al.* (*BABAR* Collaboration), Improved measurements of the branching fractions for $B^0 \to \pi^+\pi^-$ and $B^0 \to K^+\pi^-$, and a search for $B^0 \to K^+K^-$, Phys. Rev. D **75**, 012008 (2007).

[790] T. Aaltonen *et al.* (CDF Collaboration), Observation of new charmless decays of bottom hadrons, Phys. Rev. Lett. **103**, 031801 (2009).

[791] T. Aaltonen *et al.* (CDF Collaboration), Measurements of direct CP violating asymmetries in charmless decays of strange bottom mesons and bottom baryons, Phys. Rev. Lett. **106**, 181802 (2011).

[792] T. Aaltonen *et al.* (CDF Collaboration), Evidence for the charmless annihilation decay mode $B_s^0 \to \pi^+\pi^-$, Phys. Rev. Lett. **108**, 211803 (2012).

[793] R. Aaij *et al.* (LHCb Collaboration), Measurement of b-hadron branching fractions for two-body decays into charmless charged hadrons, J. High Energy Phys. 10 (2012) 037.

[794] R. Aaij *et al.* (LHCb Collaboration), Observation of the annihilation decay mode $B^0 \to K^+K^-$, Phys. Rev. Lett. **118**, 081801 (2017).

[795] J. P. Lees *et al.* (*BABAR* Collaboration), Measurement of CP asymmetries and branching fractions in charmless two-body B-meson decays to pions and kaons, Phys. Rev. D **87**, 052009 (2013).

[796] R. Aaij *et al.* (LHCb Collaboration), Search for the $\Lambda_b^0 \to \Lambda\eta'$ and $\Lambda_b^0 \to \Lambda\eta$ decays with the LHCb detector, J. High Energy Phys. 09 (2015) 006.

[797] S. Sato *et al.* (Belle Collaboration), Observation of the decay $B^0 \to \eta' K^*(892)^0$, Phys. Rev. D **90**, 072009 (2014).

[798] A. Valassi, Combining correlated measurements of several different physical quantities, Nucl. Instrum. Methods Phys. Res., Sect. A **500**, 391 (2003).

[799] B. Aubert *et al.* (*BABAR* Collaboration), Search for neutral B-meson decays to $a^0\pi$, a^0K, $\eta\rho^0$, and ηf^0, Phys. Rev. D **75**, 111102 (2007).

[800] P. Goldenzweig *et al.* (Belle Collaboration), Evidence for neutral B meson decays to ωK^{*0}, Phys. Rev. Lett. **101**, 231801 (2008).

[801] J. P. Lees *et al.* (*BABAR* Collaboration), Amplitude analysis of $B^0 \to K^+\pi^-\pi^0$ and evidence of direct CP violation in $B \to K^*\pi$ decays, Phys. Rev. D **83**, 112010 (2011).

[802] P. Chang *et al.* (Belle Collaboration), Observation of the decays $B^0 \to K^+\pi^-\pi^0$ and $B^0 \to \rho^- K^+$, Phys. Lett. B **599**, 148 (2004).

[803] B. Aubert *et al.* (*BABAR* Collaboration), Dalitz plot analysis of the decay $B^0(\bar{B}^0) \to K^\pm\pi^\mp\pi^0$, Phys. Rev. D **78**, 052005 (2008).

[804] B. Aubert *et al.* (*BABAR* Collaboration), Time-dependent amplitude analysis of $B^0 \to K^0_S\pi^+\pi^-$, Phys. Rev. D **80**, 112001 (2009).

[805] A. Garmash *et al.* (Belle Collaboration), Dalitz analysis of three-body charmless $B^0 \to K^0\pi^+\pi^-$ decay, Phys. Rev. D **75**, 012006 (2007).

[806] R. Aaij *et al.* (LHCb Collaboration), Searches for Λ^0_b and Ξ^0_b decays to $K^0_S p\pi^-$ and $K^0_S pK^-$ final states with first observation of the $\Lambda^0_b \to K^0_S p\pi^-$ decay, J. High Energy Phys. 04 (2014) 087.

[807] R. Aaij *et al.* (LHCb Collaboration), First observation of the decay $B^0_s \to K^0_S K^*(892)^0$ at LHCb, J. High Energy Phys. 01 (2016) 012.

[808] R. Aaij *et al.* (LHCb Collaboration), Updated branching fraction measurements of $B^0_{(s)} \to K^0_S h^+ h'^-$ decays, J. High Energy Phys. 11 (2017) 027.

[809] R. Aaij *et al.* (LHCb Collaboration), Amplitude analysis of the decay $\bar{B}^0 \to K^0_S\pi^+\pi^-$ and first observation of the CP asymmetry in $\bar{B}^0 \to K^*(892)^-\pi^+$, Phys. Rev. Lett. **120**, 261801 (2018).

[810] R. Aaij *et al.* (LHCb Collaboration), Observation of $B^0_s \to K^{*\pm}K^\mp$ and evidence for $B^0_s \to K^{*-}\pi^+$ decays, New J. Phys. **16**, 123001 (2014).

[811] W. Adam *et al.* (DELPHI Collaboration), Study of rare b decays with the DELPHI detector at LEP, Z. Phys. C **72**, 207 (1996).

[812] S.-H. Kyeong *et al.* (Belle Collaboration), Measurements of charmless hadronic $b \to s$ penguin decays in the $\pi^+\pi^-K^+\pi^-$ final state and observation of $B^) \to \rho^0 K^+\pi^-$, Phys. Rev. D **80**, 051103 (2009).

[813] B. Aubert *et al.* (*BABAR* Collaboration), Measurements of the branching fractions of $B^0 \to \mathrm{K}^*0K^+K^-$, $B^0 \to \mathrm{K}^*0\pi^+K^-$, $B^0 \to \mathrm{K}^*0K^+\pi^-$, and $B^0 \to \mathrm{K}^*0\pi^+\pi^-$, Phys. Rev. D **76**, 071104 (2007).

[814] J. P. Lees *et al.* (*BABAR* Collaboration), B^0 meson decays to $\rho^0 K^{*0}$, $f_0 K^{*0}$, and $\rho^- K^{*+}$, including higher K^* resonances, Phys. Rev. D **85**, 072005 (2012).

[815] Y. T. Lai *et al.* (Belle Collaboration), Measurement of branching fraction and final-state asymmetry for the $\bar{B}^0 \to K^0_S K^\mp\pi^\pm$ decay, Phys. Rev. D **100**, 011101 (2019).

[816] P. del Amo Sanchez *et al.* (*BABAR* Collaboration), Observation of the rare decay $B^0 \to K^0_S K^\pm\pi^\mp$, Phys. Rev. D **82**, 031101 (2010).

[817] B. Aubert *et al.* (*BABAR* Collaboration), Search for the decay of a B^0 or $\bar{B}^0$ meson to $\bar{K}^{*0}K^0$ or $K^{*0}\bar{K}^0$, Phys. Rev. D **74**, 072008 (2006).

[818] V. Gaur *et al.* (Belle Collaboration), Evidence for the decay $B^0 \to K^+K^-\pi^0$, Phys. Rev. D **87**, 091101 (2013).

[819] B. Aubert *et al.* (*BABAR* Collaboration), Search for B^0 meson decays to $\pi^0 K^0_S K^0_S$, $\eta K^0_S K^0_S$, and $\eta' K^0_S K^0_S$, Phys. Rev. D **80**, 011101 (2009).

[820] R. Aaij *et al.* (LHCb Collaboration), Observation of the $\Lambda^0_b \to \Lambda\phi$ decay, Phys. Lett. B **759**, 282 (2016).

[821] R. Aaij *et al.* (LHCb Collaboration), Measurement of the branching fraction of the decay $B^0_s \to K^0_S K^0_S$, Phys. Rev. D **102**, 012011 (2020).

[822] J. P. Lees *et al.* (*BABAR* Collaboration), Amplitude analysis and measurement of the time-dependent CP asymmetry of $B^0 \to K^0_S K^0_S K^0_S$ decays, Phys. Rev. D **85**, 054023 (2012).

[823] B. Aubert *et al.* (*BABAR* Collaboration), Search for the decay $B^0 \to K^0_s K^0_s K^0_L$, Phys. Rev. D **74**, 032005 (2006).

[824] B. Aubert *et al.* (*BABAR* Collaboration), Time-dependent and time-integrated angular analysis of $B \to \phi K^0_S\pi^0$ and $B \to \phi K^\pm\pi^\mp$, Phys. Rev. D **78**, 092008 (2008).

[825] M. Prim *et al.* (Belle Collaboration), Angular analysis of $B^0 \to \phi K^*$ decays and search for CP violation at Belle, Phys. Rev. D **88**, 072004 (2013).

[826] R. Aaij *et al.* (LHCb Collaboration), First observation of the decay $B^0_s \to \phi\bar{K}^{*0}$, J. High Energy Phys. 11 (2013) 092.

[827] R. Aaij *et al.* (LHCb Collaboration), Measurement of CP asymmetries and polarisation fractions in $B^0_s \to K^{*0}\bar{K}^{*0}$ decays, J. High Energy Phys. 07 (2015) 166.

[828] R. Aaij *et al.* (LHCb Collaboration), Measurement of the $B^0_s \to \phi\phi$ branching fraction and search for the decay $B^0 \to \phi\phi$, J. High Energy Phys. 10 (2015) 053.

[829] R. Aaij *et al.* (LHCb Collaboration), Observation of the $B^0 \to \rho^0\rho^0$ decay from an amplitude analysis of $B^0 \to (\pi^+\pi^-)(\pi^+\pi^-)$ decays, Phys. Lett. B **747**, 468 (2015).

[830] C.-C. Chiang *et al.* (Belle Collaboration), Search for $B^0 \to K^{*0}\bar{K}^{*0}$, $B^0 \to K^{*0}K^{*0}$ and $B^0 \to K^+\pi^-K^\mp\pi^\pm$ decays, Phys. Rev. D **81**, 071101 (2010).

[831] R. Aaij *et al.* (LHCb Collaboration), Amplitude analysis of the $B^0_{(s)} \to K^{*0}\bar{K}^{*0}$ decays and measurement of the branching fraction of the $B^0 \to K^{*0}\bar{K}^{*0}$ decay, J. High Energy Phys. 07 (2019) 032.

[832] B. Aubert *et al.* (*BABAR* Collaboration), Observation of $B^0 \to K^{*0}\bar{K}^{*0}$ and search for $B^0 \to K^{*0}K^{*0}$, Phys. Rev. Lett. **100**, 081801 (2008).

[833] B. Aubert *et al.* (*BABAR* Collaboration), Search for $B^0 \to K^{*+}K^{*-}$, Phys. Rev. D **78**, 051103 (2008).

[834] B. Aubert *et al.* (*BABAR* Collaboration), Search for $B^0 \to \phi(K^+\pi^-)$ decays with large $K^+\pi^-$ invariant mass, Phys. Rev. D **76**, 051103 (2007).

[835] T. Julius *et al.* (Belle Collaboration), Measurement of the branching fraction and CP asymmetry in $B^0 \to \pi^0\pi^0$ decays, and an improved constraint on ϕ_2, Phys. Rev. D **96**, 032007 (2017).

[836] F. Abudinén *et al.* (Belle-II Collaboration), Measurement of the branching fraction and CP asymmetry of $B^0 \to \pi^0\pi^0$ decays using 2019-2021 Belle II data, Phys. Rev. D **107**, 112009 (2023).

[837] B. Pal *et al.* (Belle Collaboration), Evidence for the decay $B^0 \to \eta\pi^0$, Phys. Rev. D **92**, 011101 (2015).

[838] J. P. Lees *et al.* (*BABAR* Collaboration), Evidence for the decay $B^0 \to \omega\omega$ and search for $B^0 \to \omega\phi$, Phys. Rev. D **89**, 051101 (2014).

[839] R. Aaij *et al.* (LHCb Collaboration), Observation of the decay $B_s^0 \to \phi\pi^+\pi^-$ and evidence for $B^0 \to \phi\pi^+\pi^-$, Phys. Rev. D **95**, 012006 (2017).

[840] R. Aaij *et al.* (LHCb Collaboration), Measurement of *CP* violation in the $B_s^0 \to \phi\phi$ decay and search for the $B^0 \to \phi\phi$ decay, J. High Energy Phys. 12 (2019) 155.

[841] A. Kusaka *et al.* (Belle Collaboration), Measurement of *CP* asymmetries and branching fractions in a time-dependent Dalitz analysis of $B^0 \to (\rho\pi)^0$ and a constraint on the quark mixing angle ϕ_2, Phys. Rev. D **77**, 072001 (2008).

[842] B. Aubert *et al.* (*BABAR* Collaboration), Measurement of branching fractions and charge asymmetries in $B^\pm \to \rho^\pm\pi^0$ and $B^\pm \to \rho^0\pi^\pm$ decays, and search for $B^0 \to \rho^0\pi^0$, Phys. Rev. Lett. **93**, 051802 (2004).

[843] B. Aubert *et al.* (*BABAR* Collaboration), Measurements of branching fractions and *CP*-violating asymmetries in $B^0 \to \rho^\pm h^\mp$ decays, Phys. Rev. Lett. **91**, 201802 (2003).

[844] I. Adachi *et al.* (Belle Collaboration), Study of $B^0 \to \rho^0\rho^0$ decays, implications for the CKM angle ϕ_2 and search for other B^0 decay modes with a four-pion final state, Phys. Rev. D **89**, 072008 (2014); **89**, 119903(E) (2014).

[845] B. Aubert *et al.* (*BABAR* Collaboration), Measurement of the branching fraction, polarization, and *CP* asymmetries in $B^0 \to \rho^0\rho^0$ decay, and implications for the CKM angle α, Phys. Rev. D **78**, 071104 (2008).

[846] J. Dalseno *et al.* (Belle Collaboration), Measurement of branching fraction and first evidence of *CP* violation in $B^0 \to a_1^\pm(1260)\pi^\mp$ decays, Phys. Rev. D **86**, 092012 (2012).

[847] B. Aubert *et al.* (*BABAR* Collaboration), Observation of B^0 meson decay to $a_1(1260)^\pm\pi^\mp$, Phys. Rev. Lett. **97**, 051802 (2006).

[848] P. Vanhoefer *et al.* (Belle Collaboration), Study of $B^0 \to \rho^+\rho^-$ decays and implications for the CKM angle ϕ_2, Phys. Rev. D **93**, 032010 (2016); **94**, 099903(A) (2016).

[849] B. Aubert *et al.* (*BABAR* Collaboration), A study of $B^0 \to \rho^+\rho^-$ decays and constraints on the CKM angle α, Phys. Rev. D **76**, 052007 (2007).

[850] F. Abudinén *et al.* (Belle-II Collaboration), Measurement of branching fraction and longitudinal polarization in $B^0 \to \rho^+\rho^-$ decays at Belle II, arXiv:2208.03554.

[851] B. Aubert *et al.* (*BABAR* Collaboration), Search for the decay $B^0 \to a_1^\pm\rho^\pm$, Phys. Rev. D **74**, 031104 (2006).

[852] B. Aubert *et al.* (*BABAR* Collaboration), Observation and polarization measurement of $B^0 \to a_1(1260)^+a_1(1260)^-$ decay, Phys. Rev. D **80**, 092007 (2009).

[853] C. Hadjivasiliou *et al.* (Belle Collaboration), Search for B^0 meson decays into Λ and missing energy with a hadronic tagging method at Belle, Phys. Rev. D **105**, L051101 (2022).

[854] K.-N. Chu *et al.* (Belle Collaboration), Study of $B^+ \to p\bar{n}\pi^0$, Phys. Rev. D **108**, 112007 (2023).

[855] J. T. Wei *et al.* (Belle Collaboration), Study of $B^+ \to p\bar{p}K^+$ and $B^+ \to p\bar{p}\pi^+$, Phys. Lett. B **659**, 80 (2008).

[856] R. Aaij *et al.* (LHCb Collaboration), Evidence for *CP* violation in $B^+ \to p\bar{p}K^+$ decays, Phys. Rev. Lett. **113**, 141801 (2014).

[857] K. Chu *et al.* (Belle Collaboration), Study of $B \to p\bar{p}\pi\pi$, Phys. Rev. D **101**, 052012 (2020).

[858] H. Albrecht *et al.* (ARGUS Collaboration), Observation of the charmless B meson decays, Phys. Lett. B **209**, 119 (1988).

[859] J. H. Chen *et al.* (Belle Collaboration), Observation of $B^0 \to p\bar{p}K^{*0}$ with a large K^{*0} polarization, Phys. Rev. Lett. **100**, 251801 (2008).

[860] R. Aaij *et al.* (LHCb Collaboration), Evidence for the two-body charmless baryonic decay $B^+ \to p\bar{\Lambda}$, J. High Energy Phys. 04 (2017) 162.

[861] Y.-T. Tsai *et al.* (Belle Collaboration), Search for $B^0 \to p\bar{p}$, $\Lambda\bar{\Lambda}$ and $B^+ \to p\bar{\Lambda}$ at Belle, Phys. Rev. D **75**, 111101 (2007).

[862] M.-Z. Wang *et al.* (Belle Collaboration), Study of $B^+ \to p\bar{\Lambda}\gamma$, $p\bar{\Lambda}\pi^0$ and $B^0 \to p\bar{\Lambda}\pi^-$, Phys. Rev. D **76**, 052004 (2007).

[863] P. Chen *et al.* (Belle Collaboration), Observation of $B^+ \to p\bar{\Lambda}\pi^+\pi^-$ at Belle, Phys. Rev. D **80**, 111103 (2009).

[864] P.-C. Lu *et al.* (Belle Collaboration), Observation of $B^+ \to p\bar{\Lambda}K^+K^-$ and $B^+ \to \bar{p}\Lambda K^+K^+$, Phys. Rev. D **99**, 032003 (2019).

[865] R. Aaij *et al.* (LHCb Collaboration), Search for the rare hadronic decay $B_s^0 \to p\bar{p}$, Phys. Rev. D **108**, 012007 (2023).

[866] B. Aubert *et al.* (*BABAR* Collaboration), Search for the decay $B^0 \to p\bar{p}$, Phys. Rev. D **69**, 091503 (2004).

[867] R. Aaij *et al.* (LHCb Collaboration), Observation of charmless baryonic decays $B_{(s)}^0 \to p\bar{p}h^+h'^-$, Phys. Rev. D **96**, 051103 (2017).

[868] B. Pal *et al.* (Belle Collaboration), Evidence for the decay $B^0 \to p\bar{p}\pi^0$, Phys. Rev. D **99**, 091104 (2019).

[869] J. P. Lees *et al.* (*BABAR* Collaboration), Search for the decay mode $B^0 \to pp\bar{p}\,\bar{p}$, Phys. Rev. D **98**, 071102 (2018).

[870] C.-Y. Chang *et al.* (Belle Collaboration), Evidence for $B^0 \to p\bar{\Sigma}^0\pi^-$ at Belle, Phys. Rev. D **108**, 052011 (2023).

[871] B. Aubert *et al.* (*BABAR* Collaboration), Measurement of the branching fraction and $\bar{\Lambda}$ polarization in $B^0 \to \bar{\Lambda}p\pi^-$, Phys. Rev. D **79**, 112009 (2009).

[872] M. Z. Wang *et al.* (Belle Collaboration), Observation of $B^0 \to p\bar{\Lambda}\pi^-$, Phys. Rev. Lett. **90**, 201802 (2003).

[873] R. Aaij *et al.* (LHCb Collaboration), Measurement of the branching fractions $\mathcal{B}(B^0 \to p\bar{p}p\bar{p})$ and $\mathcal{B}(B_s^0 \to p\bar{p}p\bar{p})$, Phys. Rev. Lett. **131**, 091901 (2023).

[874] R. Aaij *et al.* (LHCb Collaboration), Angular moments of the decay $\Lambda_b^0 \to \Lambda\mu^+\mu^-$ at low hadronic recoil, J. High Energy Phys. 09 (2018) 146.

[875] R. Aaij *et al.* (LHCb Collaboration), Search for baryon-number violating Ξ_b^0 oscillations, Phys. Rev. Lett. **119**, 181807 (2017).

[876] R. Aaij *et al.* (LHCb Collaboration), Measurement of the photon polarization in $\Lambda_b^0 \to \Lambda\gamma$ decays, Phys. Rev. D **105**, L051104 (2022).

[877] R. Aaij *et al.* (LHCb Collaboration), Measurement of the differential branching fraction of the decay $\Lambda_b^0 \to \Lambda\mu^+\mu^-$, Phys. Lett. B **725**, 25 (2013).

[878] T. Aaltonen *et al.* (CDF Collaboration), Observation of the baryonic flavor-changing neutral current decay $\Lambda_b \to \Lambda\mu^+\mu^-$, Phys. Rev. Lett. **107**, 201802 (2011).

[879] R. Aaij *et al.* (LHCb Collaboration), Observation of the suppressed decay $\Lambda_b^0 \to p\pi^-\mu^+\mu^-$, J. High Energy Phys. 04 (2017) 029.

[880] R. Aaij *et al.* (LHCb Collaboration), Test of lepton universality with $\Lambda_b^0 \to pK^-\ell^+\ell^-$ decays, J. High Energy Phys. 05 (2020) 040.

[881] R. Aaij *et al.* (LHCb Collaboration), First observation of the radiative decay $\Lambda_b^0 \to \Lambda\gamma$, Phys. Rev. Lett. **123**, 031801 (2019).

[882] R. Aaij *et al.* (LHCb Collaboration), Observations of $\Lambda_b^0 \to \Lambda K^+\pi^-$ and $\Lambda_b^0 \to \Lambda K^+K^-$ decays and searches for other Λ_b^0 and Ξ_b^0 decays to $\Lambda h^+h'^-$ final states, J. High Energy Phys. 05 (2016) 081.

[883] R. Aaij *et al.* (LHCb Collaboration), Measurement of branching fractions of charmless four-body Λ_b^0 and Ξ_b^0 decays, J. High Energy Phys. 02 (2018) 098.

[884] R. Aaij *et al.* (LHCb Collaboration), Differential branching fraction and angular analysis of $\Lambda_b^0 \to \Lambda\mu^+\mu^-$ decays, J. High Energy Phys. 06 (2015) 115; 09 (2018) 145(E).

[885] R. Aaij *et al.* (LHCb Collaboration), Search for CP violation in $\Xi_b^- \to pK^-K^-$ decays, Phys. Rev. D **104**, 052010 (2021).

[886] R. Aaij *et al.* (LHCb Collaboration), Search for the radiative $\Xi_b^- \to \Xi^-\gamma$ decay, J. High Energy Phys. 01 (2022) 069.

[887] C.-C. Peng *et al.* (Belle Collaboration), Search for $B_s^0 -> hh$ decays at the $\Upsilon(5S)$ resonance, Phys. Rev. D **82**, 072007 (2010).

[888] J. Borah *et al.* (Belle Collaboration), Search for the decay $B_s^0 \to \pi^0\pi^0$ at Belle, Phys. Rev. D **107**, L051101 (2023).

[889] M. Acciarri *et al.* (L3 Collaboration), Search for neutral charmless B decays at LEP, Phys. Lett. B **363**, 127 (1995).

[890] B. Bhuyan *et al.* (Belle Collaboration), Search for the decay $B_s^0 \to \eta\eta$, Phys. Rev. D **105**, 012007 (2022).

[891] K. Abe *et al.* (SLD Collaboration), Search for charmless hadronic decays of B mesons with the SLD detector, Phys. Rev. D **62**, 071101 (2000).

[892] R. Aaij *et al.* (LHCb Collaboration), Search for the $B_s^0 \to \eta'\phi$ decay, J. High Energy Phys. 05 (2017) 158.

[893] T. Aaltonen *et al.* (CDF Collaboration), Measurement of polarization and search for CP-violation in $B_s^0 \to \phi\phi$ decays, Phys. Rev. Lett. **107**, 261802 (2011).

[894] B. Pal *et al.* (Belle Collaboration), Observation of the decay $B_s^0 \to K^0\bar{K}^0$, Phys. Rev. Lett. **116**, 161801 (2016).

[895] R. Aaij *et al.* (LHCb Collaboration), Amplitude analysis of $B_s^0 \to K_S^0 K^\pm\pi^\mp$ decays, J. High Energy Phys. 06 (2019) 114.

[896] R. Aaij *et al.* (LHCb Collaboration), First observation of a baryonic B_s^0 decay, Phys. Rev. Lett. **119**, 041802 (2017).

[897] D. Dutta *et al.* (Belle Collaboration), Search for $B_s^0 \to \gamma\gamma$ and a measurement of the branching fraction for $B_s^0 \to \phi\gamma$, Phys. Rev. D **91**, 011101 (2015).

[898] R. Aaij *et al.* (LHCb Collaboration), Measurement of the ratio of branching fractions $\mathrm{BR}(B_0 \to K^{\star 0}\gamma)/\mathrm{BR}(B_{s0} \to \phi\gamma)$ and the direct CP asymmetry in $B_0 \to K^{\star 0}\gamma$, Nucl. Phys. **B867**, 1 (2013).

[899] R. Aaij *et al.* (LHCb Collaboration), Search for the rare decays $B_s^0 \to e^+e^-$ and $B^0 \to e^+e^-$, Phys. Rev. Lett. **124**, 211802 (2020).

[900] T. Aaltonen *et al.* (CDF Collaboration), Search for the decays $B_s^0 \to e^+\mu^-$ and $B_s^0 \to e^+e^-$ in CDF Run II, Phys. Rev. Lett. **102**, 201801 (2009).

[901] S. Watanuki *et al.* (Belle Collaboration), Search for the lepton flavour violating decays $B^+ \to K^+\tau^\pm\ell^\mp$ ($\ell = e, \mu$) at Belle, Phys. Rev. Lett. **130**, 261802 (2023).

[902] R. Aaij *et al.* (LHCb Collaboration), Search for the decays $B_s^0 \to \tau^+\tau^-$ and $B^0 \to \tau^+\tau^-$, Phys. Rev. Lett. **118**, 251802 (2017).

[903] R. Aaij *et al.* (LHCb Collaboration), Measurement of the $B_s^0 \to \mu^+\mu^-$ decay properties and search for the $B^0 \to \mu^+\mu^-$ and $B_s^0 \to \mu^+\mu^-\gamma$ decays, Phys. Rev. D **105**, 012010 (2022).

[904] R. Aaij *et al.* (LHCb Collaboration), Searches for rare B_s^0 and B^0 decays into four muons, J. High Energy Phys. 03 (2022) 109.

[905] R. Aaij *et al.* (LHCb Collaboration), Branching fraction measurements of the rare $B_s^0 \to \phi\mu^+\mu^-$ and $B_s^0 \to f_2'(1525)\mu^+\mu^-$- decays, Phys. Rev. Lett. **127**, 151801 (2021).

[906] R. Aaij *et al.* (LHCb Collaboration), Evidence for the decay $B_S^0 \to \bar{K}^{*0}\mu^+\mu^-$, J. High Energy Phys. 07 (2018) 020.

[907] R. Aaij *et al.* (LHCb Collaboration), Study of the rare B_s^0 and B^0 decays into the $\pi^+\pi^-\mu^+\mu^-$ final state, Phys. Lett. B **743**, 46 (2015).

[908] R. Aaij *et al.* (LHCb Collaboration), Search for the lepton-flavour violating decays $\mathrm{B}_{(s)}^0 \to e^\pm\mu^\mp$, J. High Energy Phys. 03 (2018) 078.

[909] L. Nayak *et al.* (Belle Collaboration), Search for $B_s^0 \to \ell^\mp\tau^\pm$ with the semi-leptonic tagging method at Belle, J. High Energy Phys. 08 (2023) 178.

[910] R. Aaij *et al.* (LHCb Collaboration), Search for the lepton-flavour-violating decays $B_s^0 \to \tau^\pm\mu^\mp$ and $B^0 \to \tau^\pm\mu^\mp$, Phys. Rev. Lett. **123**, 211801 (2019).

[911] R. Aaij *et al.* (LHCb Collaboration), Search for the lepton-flavour violating decays $B^0 \to K^{*0}\mu^\pm e^\mp$ and $B_s^0 \to \phi\mu^\pm e^\mp$, J. High Energy Phys. 06 (2023) 073.

[912] R. Aaij *et al.* (LHCb Collaboration), Search for the baryon- and lepton-number violating decays $B^0 \to p\mu^-$ and $B_s^0 \to p\mu^-$, Phys. Rev. D **108**, 012021 (2023).

[913] N. K. Nisar *et al.* (Belle Collaboration), Search for the decay $B_s^0 \to \eta'\eta$, Phys. Rev. D **104**, L031101 (2021).

[914] S. Dubey *et al.* (Belle Collaboration), Search for $B_s^0 \to \eta' X_{s\bar{s}}$ at Belle using a semi-inclusive method, Phys. Rev. D **104**, 012007 (2021).

[915] T. Pang *et al.* (Belle Collaboration), Search for the decay $B_s^0 \to \eta' K_S^0$, Phys. Rev. D **106**, L051103 (2022).

[916] R. Aaij *et al.* (LHCb Collaboration), Study of charmonium production in b-hadron decays and first evidence for the decay $B_s^0 \to \phi\phi\phi$, Eur. Phys. J. C **77**, 609 (2017).

[917] R. Aaij *et al.* (LHCb Collaboration), Angular analysis of the rare decay $B_s^0 \to \phi\mu^+\mu^-$, J. High Energy Phys. 11 (2021) 043.

[918] R. Aaij *et al.* (LHCb Collaboration), First experimental study of photon polarization in radiative B_s^0 decays, Phys. Rev. Lett. **118**, 021801 (2017).

[919] Working group on heavy flavour physics at the lhc, https://lpcc.web.cern.ch/content/lhc-hf-wg-wg-heavy-flavour-physics-lhc.

[920] M. Aaboud *et al.* (ATLAS Collaboration), Study of the rare decays of B_s^0 and B^0 mesons into muon pairs using data collected during 2015 and 2016 with the ATLAS detector, J. High Energy Phys. 04 (2019) 098.

[921] R. Aaij *et al.* (LHCb Collaboration), Search for B_c^+ decays to the $p\bar{p}\pi^+$ final state, Phys. Lett. B **759**, 313 (2016).

[922] T. Horiguchi *et al.* (Belle Collaboration), Evidence for isospin violation and measurement of *CP* asymmetries in $B \to K^*(892)\gamma$, Phys. Rev. Lett. **119**, 191802 (2017).

[923] B. Aubert *et al.* (*BABAR* Collaboration), Measurement of branching fractions and *CP* and isospin asymmetries in $B \to K^*(892)\gamma$ decays, Phys. Rev. Lett. **103**, 211802 (2009).

[924] F. Abudinén *et al.* (Belle II Collaboration), Measurements of the branching fractions for $B \to K^*\gamma$ decays at Belle II, arXiv:2110.08219.

[925] T. E. Coan *et al.* (CLEO Collaboration), Study of exclusive radiative B meson decays, Phys. Rev. Lett. **84**, 5283 (2000).

[926] P. del Amo Sanchez *et al.* (*BABAR* Collaboration), Time-dependent analysis of $B^0 \to K_S^0\pi^-\pi^+\gamma$ decays and studies of the $K^+\pi^-\pi^+$ system in $B^+ \to K^+\pi^-\pi^+\gamma$ decays, Phys. Rev. D **93**, 052013 (2016).

[927] H. Yang *et al.* (Belle Collaboration), Observation of $B^+ \to K_1(1270)^+\gamma$, Phys. Rev. Lett. **94**, 111802 (2005).

[928] B. Aubert *et al.* (*BABAR* Collaboration), Branching fractions and *CP*-violating asymmetries in radiative B decays to $\eta K\gamma$, Phys. Rev. D **79**, 011102 (2009).

[929] S. Nishida *et al.* (Belle Collaboration), Observation of $B^+ \to K^+\eta\gamma$, Phys. Lett. B **610**, 23 (2005).

[930] R. Wedd *et al.* (Belle Collaboration), Evidence for $B \to K\eta'\gamma$ decays at Belle, Phys. Rev. D **81**, 111104 (2010).

[931] B. Aubert *et al.* (*BABAR* Collaboration), Measurement of branching fractions in radiative B decays to $\eta K\gamma$ and search for B decays to $\eta' K\gamma$, Phys. Rev. D **74**, 031102 (2006).

[932] H. Sahoo *et al.* (Belle Collaboration), First observation of radiative $B^0 \to \phi K^0\gamma$ decays and measurements of their time-dependent *CP* violation, Phys. Rev. D **84**, 071101 (2011).

[933] B. Aubert *et al.* (*BABAR* Collaboration), Measurement of B decays to $\phi K\gamma$, Phys. Rev. D **75**, 051102 (2007).

[934] S. Nishida *et al.* (Belle Collaboration), Radiative B meson decays into $K\pi\gamma$ and $K\pi\pi\gamma$ final states, Phys. Rev. Lett. **89**, 231801 (2002).

[935] B. Aubert *et al.* (*BABAR* Collaboration), Measurement of branching fractions and mass spectra of $B \to K\pi\pi\gamma$, Phys. Rev. Lett. **98**, 211804 (2007); **100**, 189903(E) (2008); **100**, 199905(E) (2008).

[936] B. Aubert *et al.* (*BABAR* Collaboration), Measurement of the $B^0 \to K_2^*(1430)^0\gamma$ and $B^+ \to K_2^*(1430)^+\gamma$ branching fractions, Phys. Rev. D **70**, 091105 (2004).

[937] H. Albrecht *et al.* (ARGUS Collaboration), Search for $b \to s\gamma$ in exclusive decays of B mesons, Phys. Lett. B **229**, 304 (1989).

[938] D. Aston *et al.*, A study of $K^-\pi^+$ scattering in the reaction $K^-p \to K^-\pi + n$ at 11 GeV/c, Nucl. Phys. **B296**, 493 (1988).

[939] N. Taniguchi *et al.* (Belle Collaboration), Measurement of branching fractions, isospin and *CP*-violating asymmetries for exclusive $b \to d\gamma$ modes, Phys. Rev. Lett. **101**, 111801 (2008); **101**, 129904(E) (2008).

[940] B. Aubert *et al.* (*BABAR* Collaboration), Measurements of branching fractions for $B^+ \to \rho^+\gamma$, $B^0 \to \rho^0\gamma$, and $B^0 \to \omega\gamma$, Phys. Rev. D **78**, 112001 (2008).

[941] Y.-J. Lee *et al.* (Belle Collaboration), Observation of $B^+ \to p\bar{\Lambda}\gamma$, Phys. Rev. Lett. **95**, 061802 (2005).

[942] J.-T. Wei *et al.* (Belle Collaboration), Search for $B \to \pi\ell^+\ell^-$ decays at Belle, Phys. Rev. D **78**, 011101 (2008).

[943] J. P. Lees *et al.* (*BABAR* Collaboration), Search for the rare decays $B \to \pi\ell^+\ell^-$ and $B^0 \to \eta\ell^+\ell^-$, Phys. Rev. D **88**, 032012 (2013).

[944] R. Aaij *et al.* (LHCb Collaboration), First measurement of the differential branching fraction and *CP* asymmetry of the $B^\pm \to \pi^\pm\mu^+\mu^-$ decay, J. High Energy Phys. 10 (2015) 034.

[945] J. Grygier *et al.* (Belle Collaboration), Search for $\boldsymbol{B \to h\nu\bar{\nu}}$ decays with semileptonic tagging at Belle, Phys. Rev. D **96**, 091101 (2017); **97**, 099902(A) (2018).

[946] B. Aubert *et al.* (*BABAR* Collaboration), A search for the decay $B^+ \to K^+\nu\bar{\nu}$, Phys. Rev. Lett. **94**, 101801 (2005).

[947] B. Aubert *et al.* (*BABAR* Collaboration), Direct *CP*, lepton flavor and isospin asymmetries in the decays $B \to K^{(*)}\ell^+\ell^-$, Phys. Rev. Lett. **102**, 091803 (2009).

[948] R. Aaij *et al.* (LHCb Collaboration), Differential branching fractions and isospin asymmetries of $B \to K^{(*)}\mu^+\mu^-$ decays, J. High Energy Phys. 06 (2014) 133.

[949] J. P. Lees *et al.* (*BABAR* Collaboration), Search for $B^+ \to K^+\tau^+\tau^-$ at the *BABAR* experiment, Phys. Rev. Lett. **118**, 031802 (2017).

[950] J. P. Lees *et al.* (*BABAR* Collaboration), Search for $B \to K^{(*)}\nu\bar{\nu}$ and invisible quarkonium decays, Phys. Rev. D **87**, 112005 (2013).

[951] F. Abudinén *et al.* (Belle-II Collaboration), Search for $B^+ \to K^+\nu\bar{\nu}$ decays using an inclusive tagging method at Belle II, Phys. Rev. Lett. **127**, 181802 (2021).

[952] J.-T. Wei *et al.* (Belle Collaboration), Measurement of the differential branching fraction and forward-backward asymmetry for $B \to K^{(*)}\ell^+\ell^-$, Phys. Rev. Lett. **103**, 171801 (2009).

[953] O. Lutz *et al.* (Belle Collaboration), Search for $B \to h^{(*)}\nu\bar{\nu}$ with the full Belle $\Upsilon(4S)$ data sample, Phys. Rev. D **87**, 111103 (2013).

[954] R. Aaij *et al.* (LHCb Collaboration), First observations of the rare decays $B^+ \to K^+\pi^+\pi^-\mu^+\mu^-$ and $B^+ \to \phi K^+\mu^+\mu^-$, J. High Energy Phys. 10 (2014) 064.

[955] J. P. Lees *et al.* (*BABAR* Collaboration), Search for $B^- \to \Lambda\bar{p}\nu\bar{\nu}$ with the *BABAR* experiment, Phys. Rev. D **100**, 111101 (2019).

[956] H. J. Hyun *et al.* (Belle Collaboration), Search for a low mass particle decaying into $\mu^+\mu^-$ in $B^0 \to K^{*0}X$ and $B^0 \to \rho^0 X$ at Belle, Phys. Rev. Lett. **105**, 091801 (2010).

[957] H. B. Jeon *et al.* (Belle Collaboration), Search for the radiative penguin decays $B^0 \to K_S^0 K_S^0\gamma$ in the Belle experiment, Phys. Rev. D **106**, 012006 (2022).

[958] Z. King *et al.* (Belle Collaboration), Search for the decay $B^0 \to \phi\gamma$, Phys. Rev. D **93**, 111101 (2016).

[959] B. Aubert *et al.* (*BABAR* Collaboration), Search for the radiative decay $B \to \phi\gamma$, Phys. Rev. D **72**, 091103 (2005).

[960] Y. T. Lai *et al.* (Belle Collaboration), Search for $B^0 \to p\bar{\Lambda}\pi^-\gamma$ at Belle, Phys. Rev. D **89**, 051103 (2014).

[961] R. Aaij *et al.* (LHCb Collaboration), Measurements of the S-wave fraction in $B^0 \to K^+\pi^-\mu^+\mu^-$ decays and the $B^0 \to K^*(892)^0\mu^+\mu^-$ differential branching fraction, J. High Energy Phys. 11 (2016) 047; 04 (2017) 142(E).

[962] T. V. Dong *et al.* (Belle Collaboration), Search for the decay $B^0 \to K^{*0}\tau^+\tau^-$ at the Belle experiment, Phys. Rev. D **108**, L011102 (2023).

[963] B. Aubert *et al.* (*BABAR* Collaboration), Search for the rare decay $B \to \pi l^+ l^-$, Phys. Rev. Lett. **99**, 051801 (2007).

[964] B. Aubert *et al.* (*BABAR* Collaboration), Measurements of branching fractions, rate asymmetries, and angular distributions in the rare decays $B \to K\ell^+\ell^-$ and $B \to K^*\ell^+\ell^-$, Phys. Rev. D **73**, 092001 (2006).

[965] S. Sandilya *et al.* (Belle Collaboration), Search for the lepton-flavor-violating decay $B^0 \to K^{*0}\mu^\pm e^\mp$, Phys. Rev. D **98**, 071101 (2018).

[966] P. del Amo Sanchez *et al.* (*BABAR* Collaboration), Searches for the baryon- and lepton-number violating decays $B^0 \to \Lambda_c^+\ell^-$, $B^- \to \Lambda\ell^-$, and $B^- \to \bar{\Lambda}\ell^-$, Phys. Rev. D **83**, 091101 (2011).

[967] R. Aaij *et al.* (LHCb Collaboration), Search for the decay $B^0 \to \phi\mu^+\mu^-$, J. High Energy Phys. 05 (2022) 067.

[968] A. Limosani *et al.* (Belle Collaboration), Measurement of inclusive radiative B-meson decays with a photon energy threshold of 1.7-GeV, Phys. Rev. Lett. **103**, 241801 (2009).

[969] J. P. Lees *et al.* (*BABAR* Collaboration), Precision measurement of the $B \to X_s\gamma$ photon energy spectrum, branching fraction, and direct CP asymmetry $A_{CP}(B \to X_{s+d}\gamma)$, Phys. Rev. Lett. **109**, 191801 (2012).

[970] T. Saito *et al.* (Belle Collaboration), Measurement of the $\bar{B} \to X_s\gamma$ branching fraction with a sum of exclusive decays, Phys. Rev. D **91**, 052004 (2015).

[971] J. P. Lees *et al.* (*BABAR* Collaboration), Exclusive measurements of $b \to s\gamma$ transition rate and photon energy spectrum, Phys. Rev. D **86**, 052012 (2012).

[972] S. Chen *et al.* (CLEO Collaboration), Branching fraction and photon energy spectrum for $b \to s\gamma$, Phys. Rev. Lett. **87**, 251807 (2001).

[973] F. Abudinén *et al.* (Belle-II Collaboration), Measurement of the photon-energy spectrum in inclusive $B \to X_s\gamma$ decays identified using hadronic decays of the recoil B meson in 2019–2021 Belle II data, arXiv:2210.10220.

[974] B. Aubert *et al.* (*BABAR* Collaboration), Measurement of the $B \to X_s\gamma$ branching fraction and photon energy spectrum using the recoil method, Phys. Rev. D **77**, 051103 (2008).

[975] P. del Amo Sanchez *et al.* (*BABAR* Collaboration), Study of $B \to X\gamma$ decays and determination of $|V_{td}/V_{ts}|$, Phys. Rev. D **82**, 051101 (2010).

[976] J. P. Lees *et al.* (*BABAR* Collaboration), Measurement of the $B \to X_s l^+ l^-$ branching fraction and search for direct CP violation from a sum of exclusive final states, Phys. Rev. Lett. **112**, 211802 (2014).

[977] M. Iwasaki *et al.* (Belle Collaboration), Improved measurement of the electroweak penguin process $B \to X_s l^+ l^-$, Phys. Rev. D **72**, 092005 (2005).

[978] O. Buchmuller and H. Flacher, Fit to moment from $B \to X_c\ell\bar{\nu}$ and $B \to X_s\gamma$ decays using heavy quark expansions in the kinetic scheme, Phys. Rev. D **73**, 073008 (2006).

[979] F. Abudinén *et al.* (Belle-II Collaboration), Measurement of the branching fraction for the decay $B \to K^*(892)\ell^+\ell^-$ at Belle II, arXiv:2206.05946.

[980] J. P. Lees *et al.* (*BABAR* Collaboration), Measurement of branching fractions and rate asymmetries in the rare decays $B \to K^{(*)} l^+ l^-$, Phys. Rev. D **86**, 032012 (2012).

[981] K. W. Edwards *et al.* (CLEO Collaboration), Search for lepton flavor violating decays of B mesons, Phys. Rev. D **65**, 111102 (2002).

[982] N. Satoyama *et al.* (Belle Collaboration), A search for the rare leptonic decays $B^+ \to \mu^+\nu_\mu$ and $B^+ \to e^+\nu_e$, Phys. Lett. B **647**, 67 (2007).

[983] B. Aubert *et al.* (*BABAR* Collaboration), Search for the rare leptonic decays $B^+ \to l^+\nu_l$ ($l = e, \mu$), Phys. Rev. D **79**, 091101 (2009).

[984] M. T. Prim *et al.* (Belle Collaboration), Search for $B^+ \to \mu^+\nu_\mu$ and $B^+ \to \mu^+ N$ with inclusive tagging, Phys. Rev. D **101**, 032007 (2020).

[985] A. Sibidanov *et al.* (Belle Collaboration), Search for $B^- \to \mu^-\bar{\nu}_\mu$ decays at the Belle experiment, Phys. Rev. Lett. **121**, 031801 (2018).

[986] I. Adachi *et al.* (Belle Collaboration), Evidence for $B^- \to \tau^-\bar{\nu}_\tau$ with a hadronic tagging method using the full data sample of Belle, Phys. Rev. Lett. **110**, 131801 (2013).

[987] B. Kronenbitter *et al.* (Belle Collaboration), Measurement of the branching fraction of $B^+ \to \tau^+\nu_\tau$ decays with the semileptonic tagging method, Phys. Rev. D **92**, 051102 (2015).

[988] J. P. Lees *et al.* (*BABAR* Collaboration), Evidence of $B^+ \to \tau^+\nu$ decays with hadronic B tags, Phys. Rev. D **88**, 031102 (2013).

[989] B. Aubert *et al.* (*BABAR* Collaboration), A search for $B^+ \to \ell^+\nu_\ell$ recoiling against $B^- \to D^0\ell^-\bar{\nu}X$, Phys. Rev. D **81**, 051101 (2010).

[990] M. Gelb *et al.* (Belle Collaboration), Search for the rare decay of $B^+ \to \ell^+\nu_\ell\gamma$ with improved hadronic tagging, Phys. Rev. D **98**, 112016 (2018).

[991] B. Aubert *et al.* (*BABAR* Collaboration), A model-independent search for the decay $B^+ \to l^+\nu_l\gamma$, Phys. Rev. D **80**, 111105 (2009).

[992] P. del Amo Sanchez *et al.* (*BABAR* Collaboration), Search for the decay $B^0 \to \gamma\gamma$, Phys. Rev. D **83**, 032006 (2011).

[993] S. Villa *et al.* (Belle Collaboration), Search for the decay $B^0 \to \gamma\gamma$, Phys. Rev. D **73**, 051107 (2006).

[994] B. Aubert *et al.* (*BABAR* Collaboration), Search for decays of $B^0 \to$ mesons into e^+e^-, $\mu^+\mu^-$, and $e^\pm\mu^\mp$ final states, Phys. Rev. D **77**, 032007 (2008).

[995] M. C. Chang *et al.* (Belle Collaboration), Search for $B^0 \to \ell^+\ell^-$ at BELLE, Phys. Rev. D **68**, 111101 (2003).

[996] B. Aubert *et al.* (*BABAR* Collaboration), Search for the decays $B^0 \to e^+e^-\gamma$ and $B^0 \to \mu^+\mu^-\gamma$, Phys. Rev. D **77**, 011104 (2008).

[997] R. Aaij *et al.* (LHCb Collaboration), Search for decays of neutral beauty mesons into four muons, J. High Energy Phys. 03 (2017) 001.

[998] B. Aubert *et al.* (*BABAR* Collaboration), A search for the rare decay $B^0 \to \tau^+\tau^-$ at *BABAR*, Phys. Rev. Lett. **96**, 241802 (2006).

[999] J. P. Lees *et al.* (*BABAR* Collaboration), Improved limits on B^0 decays to invisible final states and to $\nu\bar{\nu}\gamma$, Phys. Rev. D **86**, 051105 (2012).

[1000] Y. Ku *et al.* (Belle Collaboration), Search for B^0 decays to invisible final states $(+\gamma)$ at Belle, Phys. Rev. D **102**, 012003 (2020).

[1001] R. Aaij *et al.* (LHCb Collaboration), Search for the rare decay $B^+ \to \mu^+\mu^-\mu^+\nu_\mu$, Eur. Phys. J. C **79**, 675 (2019).

[1002] R. Aaij *et al.* (LHCb Collaboration), Measurement of lepton universality parameters in $B^+ \to K^+\ell^+\ell^-$ and $B^0 \to K^{*0}\ell^+\ell^-$ decays, Phys. Rev. D **108**, 032002 (2023).

[1003] R. Aaij *et al.* (LHCb Collaboration), Tests of lepton universality using $B^0 \to K^0_S\ell^+\ell^-$ and $B^+ \to K^{*+}\ell^+\ell^-$ decays, Phys. Rev. Lett. **128**, 191802 (2022).

[1004] A. Abdesselam *et al.* (Belle Collaboration), Test of lepton-flavor universality in $B \to K^*\ell^+\ell^-$ decays at Belle, Phys. Rev. Lett. **126**, 161801 (2021).

[1005] K. Nishimura *et al.* (Belle Collaboration), First measurement of inclusive $B \to X_s\eta$ decays, Phys. Rev. Lett. **105**, 191803 (2010).

[1006] T. E. Browder *et al.* (CLEO Collaboration), Observation of high momentum η' production in B decay, Phys. Rev. Lett. **81**, 1786 (1998).

[1007] B. Aubert *et al.* (*BABAR* Collaboration), Study of high momentum η' production in $B \to \eta' X_s$, Phys. Rev. Lett. **93**, 061801 (2004).

[1008] G. Bonvicini *et al.* (CLEO Collaboration), Study of the charmless inclusive $B \to \eta' X$ decay, Phys. Rev. D **68**, 011101 (2003).

[1009] P. del Amo Sanchez *et al.* (*BABAR* Collaboration), Measurement of partial branching fractions of inclusive charmless B meson decays to K^+, K^0, and π^+, Phys. Rev. D **83**, 031103 (2011).

[1010] S. Watanuki *et al.* (Belle Collaboration), Measurements of isospin asymmetry and difference of direct CP asymmetries in inclusive $B \to X_s\gamma$ decays, Phys. Rev. D **99**, 032012 (2019).

[1011] B. Aubert *et al.* (*BABAR* Collaboration), Measurements of the $B \to X_s\gamma$ branching fraction and photon spectrum from a sum of exclusive final states, Phys. Rev. D **72**, 052004 (2005).

[1012] J. P. Lees *et al.* (*BABAR* Collaboration), A search for the decay modes $B^\pm \to h^\pm\tau^\pm l^\mp$, Phys. Rev. D **86**, 012004 (2012).

[1013] R. Aaij *et al.* (LHCb Collaboration), Search for lepton-flavor violating decays $B^+ \to K^+\mu^\pm e^\mp$, Phys. Rev. Lett. **123**, 241802 (2019).

[1014] R. Aaij *et al.* (LHCb Collaboration), Search for the lepton flavour violating decay $B^+ \to K^+\mu^-\tau^+$ using B^{*0}_{s2} decays, J. High Energy Phys. 06 (2020) 129.

[1015] J. P. Lees *et al.* (*BABAR* Collaboration), Search for lepton-number violating processes in $B^+ \to h^- l^+ l^+$ decays, Phys. Rev. D **85**, 071103 (2012).

[1016] R. Aaij *et al.* (LHCb Collaboration), Search for Majorana neutrinos in $B^- \to \pi^+\mu^-\mu^-$ decays, Phys. Rev. Lett. **112**, 131802 (2014).

[1017] J. P. Lees *et al.* (*BABAR* Collaboration), Search for lepton-number violating $B^+ \to X^-\ell^+\ell'^+$ decays, Phys. Rev. D **89**, 011102 (2014).

[1018] R. Aaij *et al.* (LHCb Collaboration), Search for the lepton number violating decays $B^+ \to \pi^-\mu^+\mu^+$ and $B^+ \to K^-\mu^+\mu^+$, Phys. Rev. Lett. **108**, 101601 (2012).

[1019] R. Aaij *et al.* (LHCb Collaboration), Searches for Majorana neutrinos in B^- decays, Phys. Rev. D **85**, 112004 (2012).

[1020] R. Aaij *et al.* (LHCb Collaboration), Search for the lepton-flavour violating decays $B^0 \to K^{*0}\tau^\pm\mu^\mp$, J. High Energy Phys. 06 (2023) 143.

[1021] H. Atmacan *et al.* (Belle Collaboration), Search for $B^0 \to \tau^\pm\ell^\mp$ $(\ell = e, \mu)$ with a hadronic tagging method at Belle, Phys. Rev. D **104**, L091105 (2021).

[1022] B. Aubert *et al.* (*BABAR* Collaboration), Searches for the decays $B^0 \to \ell^\pm\tau^\mp$ and $B^+ \to \ell^+\nu$ $(\mathrm{l} = \mathrm{e}, \mu)$ using hadronic tag reconstruction, Phys. Rev. D **77**, 091104 (2008).

[1023] R. Aaij *et al.* (LHCb Collaboration), Observation of photon polarization in the $b \to s\gamma$ transition, Phys. Rev. Lett. **112**, 161801 (2014).

[1024] R. Aaij *et al.* (LHCb Collaboration), Angular analysis of charged and neutral $B \to K\mu^+\mu^-$ decays, J. High Energy Phys. 05 (2014) 082.

[1025] R. Aaij *et al.* (LHCb Collaboration), Strong constraints on the $b \to s\gamma$ photon polarisation from $B^0 \to K^{*0}e^+e^-$ decays, J. High Energy Phys. 12 (2020) 081.

[1026] R. Aaij *et al.* (LHCb Collaboration), Measurement of the $B^0 \to K^{*0}e^+e^-$ branching fraction at low dilepton mass, J. High Energy Phys. 05 (2013) 159.

[1027] A. Abdesselam *et al.* (Belle Collaboration), Angular analysis of $B^0 \to K^*(892)^0\ell^+\ell^-$, in LHC Ski 2016: A First Discussion of 13 TeV Results (2016), arXiv:1604.04042.

[1028] S. Wehle *et al.* (Belle Collaboration), Lepton-flavor-dependent angular analysis of $B \to K^*\ell^+\ell^-$, Phys. Rev. Lett. **118**, 111801 (2017).

[1029] J. P. Lees *et al.* (*BABAR* Collaboration), Measurement of angular asymmetries in the decays $B \to K^*\ell^+\ell^-$, Phys. Rev. D **93**, 052015 (2016).

[1030] R. Aaij *et al.* (LHCb Collaboration), Angular analysis of the $B^0 \to K^{*0}\mu^+\mu^-$ decay using 3 fb^{-1} of integrated luminosity, J. High Energy Phys. 02 (2016) 104.

[1031] R. Aaij *et al.* (LHCb Collaboration), Measurement of CP-averaged observables in the $B^0 \to K^{*0}\mu^+\mu^-$ decay, Phys. Rev. Lett. **125**, 011802 (2020).

[1032] V. Khachatryan *et al.* (CMS Collaboration), Angular analysis of the decay $B^0 \to K^{*0}\mu^+\mu^-$ from pp collisions at $\sqrt{s} = 8$ TeV, Phys. Lett. B **753**, 424 (2016).

[1033] A. M. Sirunyan *et al.* (CMS Collaboration), Measurement of angular parameters from the decay $\mathrm{B}^0 \to \mathrm{K}^{*0}\mu^+\mu^-$ in proton-proton collisions at $\sqrt{s} = 8$ TeV, Phys. Lett. B **781**, 517 (2018).

[1034] M. Aaboud *et al.* (ATLAS Collaboration), Angular analysis of $B^0_d \to K^*\mu^+\mu^-$ decays in pp collisions at $\sqrt{s} = 8$ TeV with the ATLAS detector, J. High Energy Phys. 10 (2018) 047.

[1035] R. Aaij *et al.* (LHCb Collaboration), Angular analysis of the $B^+ \to K^{*+}\mu^+\mu^-$ decay, Phys. Rev. Lett. **126**, 161802 (2021).

[1036] A. M. Sirunyan *et al.* (CMS Collaboration), Angular analysis of the decay $B^+ \to K^{*+}(892)\mu^+\mu^-$ in proton-proton collisions at $\sqrt{s} = 8$ TeV, J. High Energy Phys. 04 (2021) 124.

[1037] Y. Sato *et al.* (Belle Collaboration), Measurement of the lepton forward-backward asymmetry in $B \to X_s\ell^+\ell^-$ decays with a sum of exclusive modes, Phys. Rev. D **93**, 032008 (2016); **93**, 059901(A) (2016).

[1038] R. Aaij *et al.* (LHCb Collaboration), Differential branching fraction and angular moments analysis of the decay $B^0 \to K^+\pi^-\mu^+\mu^-$ in the $K^*_{0,2}(1430)^0$ region, J. High Energy Phys. 12 (2016) 065.

[1039] R. Aaij *et al.* (LHCb Collaboration), Measurement of the phase difference between short- and long-distance amplitudes in the $B^+ \to K^+\mu^+\mu^-$ decay, Eur. Phys. J. C **77**, 161 (2017).

[1040] A. M. Sirunyan *et al.* (CMS Collaboration), Angular analysis of the decay $B^+ \to K^+\mu^+\mu^-$ in proton-proton collisions at $\sqrt{s} = 8$ TeV, Phys. Rev. D **98**, 112011 (2018).

[1041] R. Aaij *et al.* (LHCb Collaboration), Search for hidden-sector bosons in $B^0 \to K^{*0}\mu^+\mu^-$ decays, Phys. Rev. Lett. **115**, 161802 (2015).

[1042] R. Aaij *et al.* (LHCb Collaboration), Search for long-lived scalar particles in $B^+ \to K^+\chi(\mu^+\mu^-)$ decays, Phys. Rev. D **95**, 071101 (2017).

[1043] R. Aaij *et al.* (LHCb Collaboration), Measurement of the $\Lambda_b^0 \to \Lambda(1520)\mu^+\mu^-$ differential branching fraction, Phys. Rev. Lett. **131**, 151801 (2023).

[1044] I. Adachi *et al.* (Belle-II Collaboration), Search for a long-lived spin-0 mediator in $b \to s$ transitions at the Belle II experiment, Phys. Rev. D **108**, L111104 (2023).

[1045] S. Chen *et al.* (CLEO Collaboration), Measurement of charge asymmetries in charmless hadronic in B meson decays, Phys. Rev. Lett. **85**, 525 (2000).

[1046] R. Aaij *et al.* (LHCb Collaboration), Measurement of CP violation in the decay $B^+ \to K^+\pi^0$, Phys. Rev. Lett. **126**, 091802 (2021).

[1047] R. Aaij *et al.* (LHCb Collaboration), Direct CP violation in charmless three-body decays of $B^\pm$ mesons, Phys. Rev. D **108**, 012008 (2023).

[1048] R. Aaij *et al.* (LHCb Collaboration), Measurements of CP violation in the three-body phase space of charmless $B^\pm$ decays, Phys. Rev. D **90**, 112004 (2014).

[1049] K.-F. Chen *et al.* (Belle Collaboration), Measurement of polarization and triple-product correlations in $B \to \phi K^*$ decays, Phys. Rev. Lett. **94**, 221804 (2005).

[1050] R. Aaij *et al.* (LHCb Collaboration), Measurement of CP asymmetries in the decays $B^0 \to K^{*0}\mu^+\mu^-$ and $B^+ \to K^+\mu^+\mu^-$, J. High Energy Phys. 09 (2014) 177.

[1051] R. Aaij *et al.* (LHCb Collaboration), Observation of CP violation in two-body $B^0_{(s)}$-meson decays to charged pions and kaons, J. High Energy Phys. 03 (2021) 075.

[1052] T. A. Aaltonen *et al.* (CDF Collaboration), Measurements of direct CP-violating asymmetries in charmless decays of bottom baryons, Phys. Rev. Lett. **113**, 242001 (2014).

[1053] R. Aaij *et al.* (LHCb Collaboration), Measurement of CP asymmetries in two-body $B^0_{(s)}$-meson decays to charged pions and kaons, Phys. Rev. D **98**, 032004 (2018).

[1054] J. Dalseno *et al.* (Belle Collaboration), Time-dependent Dalitz plot measurement of CP parameters in $B^0 \to K^0_S\pi^+\pi^-$ decays, Phys. Rev. D **79**, 072004 (2009).

[1055] J. P. Lees *et al.* (*BABAR* Collaboration), Measurements of direct CP asymmetries in $B \to X_s\gamma$ decays using sum of exclusive decays, Phys. Rev. D **90**, 092001 (2014).

[1056] L. Pesántez *et al.* (Belle Collaboration), Measurement of the direct CP asymmetry in $\bar{B} \to X_{s+d}\gamma$ decays with a lepton tag, Phys. Rev. Lett. **114**, 151601 (2015).

[1057] R. Aaij *et al.* (LHCb Collaboration), Search for CP violation in $\Lambda_b^0 \to pK^-$ and $\Lambda_b^0 \to p\pi^-$ decays, Phys. Lett. B **787**, 124 (2018).

[1058] R. Aaij *et al.* (LHCb Collaboration), Measurement of matter-antimatter differences in beauty baryon decays, Nat. Phys. **13**, 391 (2017).

[1059] R. Aaij *et al.* (LHCb Collaboration), Observation of the decay $\Lambda_b^0 \to pK^-\mu^+\mu^-$ and a search for CP violation, J. High Energy Phys. 06 (2017) 108.

[1060] R. Aaij *et al.* (LHCb Collaboration), Search for CP violation using triple product asymmetries in $\Lambda_b^0 \to pK^-\pi^+\pi^-$, $\Lambda_b^0 \to pK^-K^+K^-$ and $\Xi_b^0 \to pK^-K^-\pi^+$ decays, J. High Energy Phys. 08 (2018) 039.

[1061] R. Aaij *et al.* (LHCb Collaboration), Measurements of CP asymmetries in charmless four-body Λ_b^0 and Ξ_b^0 decays, Eur. Phys. J. C **79**, 745 (2019).

[1062] R. Aaij *et al.* (LHCb Collaboration), Study of the $B^0 \to \rho(770)^0K^*(892)^0$ decay with an amplitude analysis of $B^0 \to (\pi^+\pi^-)(K^+\pi^-)$ decays, J. High Energy Phys. 05 (2019) 026.

[1063] R. Aaij *et al.* (LHCb Collaboration), Measurement of polarization amplitudes and CP asymmetries in $B^0 \to \phi K^*(892)^0$, J. High Energy Phys. 05 (2014) 069.

[1064] R. Aaij *et al.* (LHCb Collaboration), Angular analysis of the $B^0 \to K^{*0}e^+e^-$ decay in the low-q^2 region, J. High Energy Phys. 04 (2015) 064.

[1065] R. Aaij *et al.* (LHCb Collaboration), First measurement of the CP-violating phase $\phi_s^{d\bar{d}}$ in $B_s^0 \to (K^+\pi^-)(K^-\pi^+)$ decays, J. High Energy Phys. 03 (2018) 140.

[1066] M. Staric *et al.* (Belle Collaboration), Evidence for $D^0 - \bar{D}^0$ mixing, Phys. Rev. Lett. **98**, 211803 (2007).

[1067] B. Aubert *et al.* (*BABAR* Collaboration), Evidence for $D^0 - -\bar{D}^0$ mixing, Phys. Rev. Lett. **98**, 211802 (2007).

[1068] T. Aaltonen *et al.* (CDF Collaboration), Evidence for $D^0 - \bar{D}^0$ mixing using the CDF II detector, Phys. Rev. Lett. **100**, 121802 (2008).

[1069] R. Aaij *et al.* (LHCb Collaboration), Observation of $D^0 - \bar{D}^0$ oscillations, Phys. Rev. Lett. **110**, 101802 (2013).

[1070] R. Aaij *et al.* (LHCb Collaboration), Observation of the mass difference between neutral charm-meson eigenstates, Phys. Rev. Lett. **127**, 111801 (2021).

[1071] S. Bergmann, Y. Grossman, Z. Ligeti, Y. Nir, and A. A. Petrov, Lessons from CLEO and FOCUS measurements of $D^0 - \bar{D}^0$ mixing parameters, Phys. Lett. B **486**, 418 (2000).

[1072] R. Aaij *et al.* (LHCb Collaboration), Measurement of the CKM angle γ from a combination of LHCb results, J. High Energy Phys. 12 (2016) 087.

[1073] S. L. Glashow, J. Iliopoulos, and L. Maiani, Weak interactions with lepton-hadron symmetry, Phys. Rev. D **2**, 1285 (1970).

[1074] I. I. Y. Bigi and N. G. Uraltsev, $D^0\bar{D}^0$ oscillations as a probe of quark-hadron duality, Nucl. Phys. **B592**, 92 (2001).

[1075] A. A. Petrov, Charm physics: Theoretical review, arXiv: hep-ph/0311371.

[1076] A. A. Petrov, Mixing and *CP*-violation in charm, Nucl. Phys. Proc. Suppl. **142**, 333 (2005).

[1077] A. F. Falk, Y. Grossman, Z. Ligeti, Y. Nir, and A. A. Petrov, The $D^0 - -\bar{D}^0$ mass difference from a dispersion relation, Phys. Rev. D **69**, 114021 (2004).

[1078] B. Aubert *et al.* (*BABAR* Collaboration), Measurement of $D^0 - \bar{D}^0$ mixing from a time- dependent amplitude analysis of $D^0 \to K^+\pi^-\pi^0$ decays, Phys. Rev. Lett. **103**, 211801 (2009).

[1079] T. Pajero and M. J. Morello, Mixing and *CP* violation in $D^0 \to K^-\pi^+$ decays, J. High Energy Phys. 03 (2022) 162.

[1080] A. J. Schwartz, Effect of $D^0 - \bar{D}^0$ mixing upon Cabibbo-favored D^0 decays, arXiv:2207.11867.

[1081] E. M. Aitala *et al.* (E791 Collaboration), Search for D^0-anti-D^0 mixing in semileptonic decay modes, Phys. Rev. Lett. **77**, 2384 (1996).

[1082] C. Cawlfield *et al.* (CLEO Collaboration), Limits on neutral D mixing in semileptonic decays, Phys. Rev. D **71**, 077101 (2005).

[1083] B. Aubert *et al.* (*BABAR* Collaboration), Search for $D^0 - \bar{D}^0$ mixing using semileptonic decay modes, Phys. Rev. D **70**, 091102 (2004).

[1084] B. Aubert *et al.* (*BABAR* Collaboration), Search for D^0-anti-D^0 mixing using doubly flavor tagged semileptonic decay modes, Phys. Rev. D **76**, 014018 (2007).

[1085] U. Bitenc *et al.* (Belle Collaboration), Improved search for D^0-anti-D^0 mixing using semileptonic decays at Belle, Phys. Rev. D **77**, 112003 (2008).

[1086] E. M. Aitala *et al.* (E791 Collaboration), Measurements of lifetimes and a limit on the lifetime difference in the neutral D meson system, Phys. Rev. Lett. **83**, 32 (1999).

[1087] J. M. Link *et al.* (FOCUS Collaboration), A measurement of lifetime differences in the neutral D meson system, Phys. Lett. B **485**, 62 (2000).

[1088] S. E. Csorna *et al.* (CLEO Collaboration), Lifetime differences, direct *CP* violation and partial widths in D^0 meson decays to K^+K^- and $\pi^+\pi^-$, Phys. Rev. D **65**, 092001 (2002).

[1089] A. Zupanc *et al.* (Belle Collaboration), Measurement of $y(CP)$ in D^0 meson decays to the $K^0_S K^+K^-$ final state, Phys. Rev. D **80**, 052006 (2009).

[1090] J. P. Lees *et al.* (*BABAR* Collaboration), Measurement of $D^0 - \bar{D}^0$ mixing and *CP* violation in two-body D^0 decays, Phys. Rev. D **87**, 012004 (2013).

[1091] M. Ablikim *et al.* (BESIII Collaboration), Measurement of y_{CP} in $D^0 - \bar{D}^0$ oscillation using quantum correlations in $e^+e^- \to D^0\bar{D}^0$ at $\sqrt{s} = 3.773$ GeV, Phys. Lett. B **744**, 339 (2015).

[1092] M. Starič *et al.* (Belle Collaboration), Measurement of $D^0 - \bar{D}^0$ mixing and search for *CP* violation in $D^0 \to K^+K^-, \pi^+\pi^-$ decays with the full Belle data set, Phys. Lett. B **753**, 412 (2016).

[1093] R. Aaij *et al.* (LHCb Collaboration), Measurement of the charm-mixing parameter y_{CP}, Phys. Rev. Lett. **122**, 011802 (2019).

[1094] M. Nayak *et al.* (Belle Collaboration), Measurement of the charm-mixing parameter y_{CP} in $D^0 \to K^0_S\omega$ decays at Belle, Phys. Rev. D **102**, 071102 (2020).

[1095] R. Aaij *et al.* (LHCb Collaboration), Measurement of the charm mixing parameter $y_{CP} - y_{CP}^{K\pi}$ using two-body D^0 meson decays, Phys. Rev. D **105**, 092013 (2022).

[1096] T. A. Aaltonen *et al.* (CDF Collaboration), Measurement of indirect *CP*-violating asymmetries in $D^0 \to K^+K^-$ and $D^0 \to \pi^+\pi^-$ decays at CDF, Phys. Rev. D **90**, 111103 (2014).

[1097] R. Aaij *et al.* (LHCb Collaboration), Search for time-dependent *CP* violation in $D^0 \to K^+K^-$ and $D^0 \to \pi^+\pi^-$ decays, Phys. Rev. D **104**, 072010 (2021).

[1098] T. Peng *et al.* (Belle Collaboration), Measurement of D^0–$\bar{D}^0$ mixing and search for indirect *CP* violation using $D^0 \to K^0_S\pi^+\pi^-$ decays, Phys. Rev. D **89**, 091103 (2014).

[1099] R. Aaij *et al.* (LHCb Collaboration), Model-independent measurement of mixing parameters in $D^0 \to K^0_S\pi^+\pi^-$ decays, J. High Energy Phys. 04 (2016) 033.

[1100] R. Aaij *et al.* (LHCb Collaboration), Measurement of the mass difference between neutral charm-meson eigenstates, Phys. Rev. Lett. **122**, 231802 (2019).

[1101] A. Di Canto, J. Garra Ticó, T. Gershon, N. Jurik, M. Martinelli, T. Pilař, S. Stahl, and D. Tonelli, Novel method for measuring charm-mixing parameters using multibody decays, Phys. Rev. D **99**, 012007 (2019).

[1102] R. Aaij *et al.* (LHCb Collaboration), Model-independent measurement of charm mixing parameters in $B \to D^0(\to K^0_S\pi^+\pi^-)\mu^-\bar{\nu}_\mu X$ decays, Phys. Rev. D **108**, 052005 (2023).

[1103] P. del Amo Sanchez *et al.* (*BABAR* Collaboration), Measurement of D^0–$\bar{D}^0$ mixing parameters using $D^0 \to K^0_S\pi^+\pi^-$ and $D^0 \to K^0_S K^+K^-$ decays, Phys. Rev. Lett. **105**, 081803 (2010).

[1104] J. P. Lees *et al.* (*BABAR* Collaboration), Measurement of the neutral D meson mixing parameters in a time-dependent amplitude analysis of the $D^0 \to \pi^+\pi^-\pi^0$ decay, Phys. Rev. D **93**, 112014 (2016).

[1105] R. Aaij *et al.* (LHCb Collaboration), First observation of $D^0 - \bar{D}^0$ oscillations in $D^0 \to K^+\pi^-\pi^+\pi^-$ decays and measurement of the associated coherence parameters, Phys. Rev. Lett. **116**, 241801 (2016).

[1106] D. M. Asner *et al.* (CLEO Collaboration), Updated measurement of the strong phase in $D^0 \to K^+\pi^-$ decay using quantum correlations in $e^+e^- \to D^0\bar{D}^0$ at CLEO, Phys. Rev. D **86**, 112001 (2012).

[1107] M. Ablikim *et al.* (BESIII Collaboration), Improved measurement of the strong-phase difference $\delta_D^{K\pi}$ in quantum-correlated $D\bar{D}$ decays, Eur. Phys. J. C **82**, 1009 (2022).

[1108] B. R. Ko *et al.* (Belle Collaboration), Observation of $D^0 - \bar{D}^0$ mixing in e^+e^- collisions, Phys. Rev. Lett. **112**, 111801 (2014).

[1109] L. M. Zhang *et al.* (Belle Collaboration), Improved constraints on $D^0 - \bar{D}^0$ mixing in $D^0 \to K^+\pi^-$ decays at Belle, Phys. Rev. Lett. **96**, 151801 (2006).

[1110] T. A. Aaltonen *et al.* (CDF Collaboration), Observation of $D^0 - \bar{D}^0$ mixing using the CDF II detector, Phys. Rev. Lett. **111**, 231802 (2013).

[1111] R. Aaij *et al.* (LHCb Collaboration), Measurements of charm mixing and CP violation using $D^0 \to K^\pm\pi^\mp$ decays, Phys. Rev. D **95**, 052004 (2017); **96**, 099907 (E) (2017).

[1112] R. Aaij *et al.* (LHCb Collaboration), Updated determination of D^0-$\bar{D}^0$ mixing and CP violation parameters with $D^0 \to K^+\pi^-$ decays, Phys. Rev. D **97**, 031101 (2018).

[1113] B. Aubert *et al.* (*BABAR* Collaboration), Search for CP violation in the decays $D^0 \to K^-K^+$ and $D^0 \to \pi^-\pi^+$, Phys. Rev. Lett. **100**, 061803 (2008).

[1114] M. Staric *et al.* (Belle Collaboration), Measurement of CP asymmetry in Cabibbo suppressed D^0 decays, Phys. Lett. B **670**, 190 (2008).

[1115] CDF Collaboration, Improved measurement of the difference between time-integrated CP asymmetries in $D^0 \to K^+K^-$ and $D^0 \to \pi^+\pi^-$ decays at CDF, CDF Note 10784, 2012.

[1116] T. Aaltonen *et al.* (CDF Collaboration), Measurement of the difference of CP–violating asymmetries in $D^0 \to K^+K^-$ and $D^0 \to \pi^+\pi^-$ decays at CDF, Phys. Rev. Lett. **109**, 111801 (2012).

[1117] R. Aaij *et al.* (LHCb Collaboration), Observation of CP violation in charm decays, Phys. Rev. Lett. **122**, 211803 (2019).

[1118] R. Aaij *et al.* (LHCb Collaboration), Measurement of the time-integrated CP asymmetry in $D^0 \to K^-K^+$ decays, Phys. Rev. Lett. **131**, 091802 (2023).

[1119] M. Ablikim *et al.* (BESIII Collaboration), Measurement of the $D \to K^-\pi^+$ strong phase difference in $\psi(3770) \to D^0\bar{D}^0$, Phys. Lett. B **734**, 227 (2014).

[1120] F. James, MINUIT—Function Minimization and Error Analysis, Reference Manual Version 94.1, CERN Program Library Long Writeup D506, 1994.

[1121] M. Ciuchini, E. Franco, D. Guadagnoli, V. Lubicz, M. Pierini, V. Porretti, and L. Silvestrini, D-$\bar{D}$ mixing and new physics: General considerations and constraints on the MSSM, Phys. Lett. B **655**, 162 (2007).

[1122] A. L. Kagan and M. D. Sokoloff, On indirect CP violation and implications for $D^0 - -\bar{D}^0$ and $B_s - -\bar{B}_s$ mixing, Phys. Rev. D **80**, 076008 (2009).

[1123] A. L. Kagan and L. Silvestrini, Dispersive and absorptive CP violation in $D^0 - \overline{D^0}$ mixing, Phys. Rev. D **103**, 053008 (2021).

[1124] I. I. Y. Bigi and A. I. Sanda, CP violation, Cambridge Monogr. Part. Phys., Nucl. Phys., Cosmol. **9**, 1 (2000).

[1125] Y. Nir, CP violation in and beyond the standard model, arXiv:hep-ph/9911321.

[1126] F. Buccella, M. Lusignoli, G. Miele, A. Pugliese, and P. Santorelli, Nonleptonic weak decays of charmed mesons, Phys. Rev. D **51**, 3478 (1995).

[1127] B. Aubert *et al.* (*BABAR* Collaboration), Search for CP violation in neutral D meson Cabibbo- suppressed three-body decays, Phys. Rev. D **78**, 051102 (2008).

[1128] I. Bediaga, I. I. Bigi, A. Gomes, G. Guerrer, J. Miranda, and A. C. dos Reis, On a CP anisotropy measurement in the Dalitz plot, Phys. Rev. D **80**, 096006 (2009).

[1129] B. Aslan and G. Zech, New test for the multivariate two-sample problem based on the concept of minimum energy, J. Stat. Comput. Simul. **75**, 109 (2005).

[1130] R. Aaij *et al.* (LHCb Collaboration), Measurement of the $D^\pm$ production asymmetry in 7 TeV pp collisions, Phys. Lett. B **718**, 902 (2013).

[1131] Y. Grossman and Y. Nir, CP violation in $\tau \to \nu\pi K_S$ and $D \to \pi K_S$: The importance of $K_S - K_L$ interference, J. High Energy Phys. 04 (2012) 002.

[1132] J. Brod, Y. Grossman, A. L. Kagan, and J. Zupan, A consistent picture for large penguins in $D \to \pi^+\pi^-$, K^+K^-, J. High Energy Phys. 10 (2012) 161.

[1133] M. Chala, A. Lenz, A. V. Rusov, and J. Scholtz, ΔA_{CP} within the standard model and beyond, J. High Energy Phys. 07 (2019) 161.

[1134] A. Dery and Y. Nir, Implications of the LHCb discovery of CP violation in charm decays, J. High Energy Phys. 12 (2019) 104.

[1135] R. Bause, H. Gisbert, M. Golz, and G. Hiller, Exploiting CP-asymmetries in rare charm decays, Phys. Rev. D **101**, 115006 (2020).

[1136] Y. Grossman and S. Schacht, The emergence of the $\Delta U = 0$ rule in charm physics, J. High Energy Phys. 07 (2019) 020.

[1137] F. Buccella, A. Paul, and P. Santorelli, $SU(3)_F$ breaking through final state interactions and CP asymmetries in $D \to PP$ decays, Phys. Rev. D **99**, 113001 (2019).

[1138] H.-Y. Cheng and C.-W. Chiang, Revisiting CP violation in $D \to PP$ and VP decays, Phys. Rev. D **100**, 093002 (2019).

[1139] S. Schacht and A. Soni, Enhancement of charm CP violation due to nearby resonances, Phys. Lett. B **825**, 136855 (2022).

[1140] I. Bediaga, T. Frederico, and P. C. Magalhães, Enhanced charm CP asymmetries from final state interactions, Phys. Rev. Lett. **131**, 051802 (2023).

[1141] A. Pich, E. Solomonidi, and L. Vale Silva, Final-state interactions in the CP asymmetries of charm-meson two-body decays, Phys. Rev. D **108**, 036026 (2023).

[1142] M. Gavrilova, Y. Grossman, and S. Schacht, Determination of the $D \to \pi\pi$ ratio of penguin over tree diagrams, Phys. Rev. D **109**, 033011 (2024).

[1143] B. I. Eisenstein *et al.* (CLEO Collaboration), Precision measurement of $B(D^+ \to \mu^+\nu)$ and the pseudoscalar decay constant f_+^D, Phys. Rev. D **78**, 052003 (2008).

[1144] R. Aaij *et al.* (LHCb Collaboration), Search for CP violation in $D^+_{(s)} \to h^+\pi^0$ and $D^+_{(s)} \to h^+\eta$ decays, J. High Energy Phys. 06 (2021) 019.

[1145] V. Babu *et al.* (Belle Collaboration), Search for CP violation in the $D^+ \to \pi^+\pi^0$ decay at Belle, Phys. Rev. D **97**, 011101 (2018).

[1146] H. Mendez *et al.* (CLEO Collaboration), Measurements of D meson decays to two pseudoscalar mesons, Phys. Rev. D **81**, 052013 (2010).

[1147] R. Aaij *et al.* (LHCb Collaboration), Measurement of CP asymmetries in $D^+_{(s)} \to \eta\pi^+$ and $D^+_{(s)} \to \eta'\pi^+$ decays, J. High Energy Phys. 04 (2023) 081.

[1148] E. Won *et al.* (Belle Collaboration), Observation of $D^+ \to K^+\eta^{(\prime)}$ and search for CP violation in $D^+ \to \pi^+\eta^{(\prime)}$ decays, Phys. Rev. Lett. **107**, 221801 (2011).

[1149] G. Bonvicini *et al.* (CLEO Collaboration), Updated measurements of absolute D^+ and D^0 hadronic branching fractions and $\sigma(e^+e^- \to D\bar{D})$ at $E_{cm} = 3774$ MeV, Phys. Rev. D **89**, 072002 (2014).

[1150] B. R. Ko *et al.* (Belle Collaboration), Evidence for CP violation in the decay $D^+ \to K^0_S\pi^+$, Phys. Rev. Lett. **109**, 021601 (2012).

[1151] P. del Amo Sanchez *et al.* (*BABAR* Collaboration), Search for CP violation in the decay $D^\pm \to K_S\pi^\pm$, Phys. Rev. D **83**, 071103 (2011).

[1152] J. M. Link *et al.* (FOCUS Collaboration), Search for CP violation in the decays $D^+ \to K_S\pi^+$ and $D^+ \to K_SK^+$, Phys. Rev. Lett. **88**, 041602 (2002); **88**, 159903(E) (2002).

[1153] R. Aaij *et al.* (LHCb Collaboration), Search for CP violation in $D_s^+ \to K^0_S\pi^+$, $D^+ \to K^0_SK^+$ and $D^+ \to \phi\pi^+$ decays, Phys. Rev. Lett. **122**, 191803 (2019).

[1154] J. P. Lees *et al.* (*BABAR* Collaboration), Search for CP violation in the decays $D^\pm \to K^0_sK^\pm$, $D_s^\pm \to K^0_sK^\pm$, and $D_s^\pm \to K^0_s\pi^\pm$, Phys. Rev. D **87**, 052012 (2013).

[1155] B. R. Ko *et al.* (Belle Collaboration), Search for CP violation in the decay $D^+ \to K^0_S\pi+$, J. High Energy Phys. 02 (2013) 098.

[1156] M. Ablikim *et al.* (BESIII Collaboration), Measurements of the absolute branching fractions and CP asymmetries for $D^+ \to K^0_{S,L}K^+(\pi^0)$, Phys. Rev. D **99**, 032002 (2019).

[1157] M. Ablikim *et al.* (BESIII Collaboration), Study of decay dynamics and CP asymmetry in $D^+ \to K^0_Le^+\nu_e$ decay, Phys. Rev. D **92**, 112008 (2015).

[1158] M. Ablikim *et al.* (BESIII Collaboration), Absolute measurements of branching fractions of Cabibbo-suppressed hadronic $D^{0(+)}$ decays involving multiple pions, Phys. Rev. D **106**, 092005 (2022).

[1159] R. Aaij *et al.* (LHCb Collaboration), Search for CP violation in the decay $D^+ \to \pi^-\pi^+\pi^+$, Phys. Lett. B **728**, 585 (2014).

[1160] E. M. Aitala *et al.* (Fermilab E791 Collaboration), Search for CP violation in charged D meson decays, Phys. Lett. B **403**, 377 (1997).

[1161] R. Aaij *et al.* (LHCb Collaboration), Search for CP violation in $D^+_{(s)} \to K^-K^+K^+$ decays, J. High Energy Phys. 07 (2023) 067.

[1162] V. M. Abazov *et al.* (D0 Collaboration), Measurement of the direct CP-violating parameter A_{CP} in the decay $D^+ \to K^-\pi^+\pi^+$, Phys. Rev. D **90**, 111102 (2014).

[1163] M. Ablikim *et al.* (BESIII Collaboration), Measurements of absolute branching fractions of fourteen exclusive hadronic D decays to η, Phys. Rev. Lett. **124**, 241803 (2020).

[1164] J. P. Lees *et al.* (*BABAR* Collaboration), Search for direct CP Violation in singly Cabibbo-suppressed $D^\pm \to K^+K^-\pi^\pm$ decays, Phys. Rev. D **87**, 052010 (2013).

[1165] R. Aaij *et al.* (LHCb Collaboration), Search for CP violation in $D^+ \to K^-K^+\pi^+$ decays, Phys. Rev. D **84**, 112008 (2011).

[1166] P. Rubin *et al.* (CLEO Collaboration), Search for CP violation in the Dalitz-plot analysis of $D^\pm \to K^+K^-\pi^\pm$, Phys. Rev. D **78**, 072003 (2008).

[1167] J. M. Link *et al.* (FOCUS Collaboration), Search for CP violation in D^0 and D^+ decays, Phys. Lett. B **491**, 232 (2000).

[1168] J. M. Link *et al.* (FOCUS Collaboration), Search for T violation in charm meson decays, Phys. Lett. B **622**, 239 (2005).

[1169] M. Ablikim *et al.* (BESIII Collaboration), Observation of the doubly Cabibbo-suppressed decay $D^+ \to K^+\pi^+\pi^-\pi^0$ and evidence for $D^+ \to K^+\omega$, Phys. Rev. Lett. **125**, 141802 (2020).

[1170] T. Aaltonen *et al.* (CDF Collaboration), Measurement of CP–violating asymmetries in $D^0 \to \pi^+\pi^-$ and $D^0 \to K^+K^-$ decays at CDF, Phys. Rev. D **85**, 012009 (2012).

[1171] E. M. Aitala *et al.* (Fermilab E791 Collaboration), Branching fractions for $D^0 \to K^+K^-$ and $D^0 \to \pi^+\pi^-$, and a search for CP violation in D^0 decays, Phys. Lett. B **421**, 405 (1998).

[1172] N. K. Nisar *et al.* (Belle Collaboration), Search for CP violation in $D^0 \to \pi^0\pi^0$ decays, Phys. Rev. Lett. **112**, 211601 (2014).

[1173] G. Bonvicini *et al.* (CLEO Collaboration), Search for CP violation in $D^0 \to K^0_S\pi^0$ and $D^0 \to \pi^0\pi^0$ and $D^0 \to K^0_SK^0_S$ decays, Phys. Rev. D **63**, 071101 (2001).

[1174] B. R. Ko *et al.* (Belle Collaboration), Search for CP violation in the decays $D^0 \to K^0_S\pi^0$, Phys. Rev. Lett. **106**, 211801 (2011).

[1175] M. Ablikim *et al.* (BESIII Collaboration), Measurements of absolute branching fractions of $D^0 \to K^0_L\phi$, $K^0_L\eta$, $K^0_L\omega$, and $K^0_L\eta'$, Phys. Rev. D **105**, 092010 (2022).

[1176] L. K. Li *et al.* (Belle Collaboration), Measurement of branching fractions and search for CP violation in $D^0 \to \pi^+\pi^-\eta$, $D^0 \to K^+K^-\eta$, and $D^0 \to \phi\eta$ at Belle, J. High Energy Phys. 09 (2021) 075.

[1177] R. Aaij *et al.* (LHCb Collaboration), Measurement of CP asymmetry in $D^0 \to K^0_SK^0_S$ decays, Phys. Rev. D **104**, L031102 (2021).

[1178] N. Dash *et al.*, Search for CP violation and measurement of the branching fraction in the decay $D^0 \to K^0_SK^0_S$, Phys. Rev. Lett. **119**, 171801 (2017).

[1179] R. Aaij *et al.* (LHCb Collaboration), Search for CP violation in the phase space of $D^0 \to \pi^-\pi^+\pi^0$ decays with the energy test, J. High Energy Phys. 09 (2023) 129.

[1180] R. Aaij *et al.* (LHCb Collaboration), Search for CP violation in $D^0 \to \pi^-\pi^+\pi^0$ decays with the energy test, Phys. Lett. B **740**, 158 (2015).

[1181] K. Arinstein (Belle Collaboration), Measurement of the ratio $B(D^0 \to \pi^+\pi^-\pi^0)/B(D^0 \to K^-\pi^+\pi^0)$ and the time-integrated CP asymmetry in $D^0 \to \pi^+\pi^-\pi^0$, Phys. Lett. B **662**, 102 (2008).

[1182] D. Cronin-Hennessy *et al.* (CLEO Collaboration), Searches for CP violation and $\pi\pi S$-wave in the Dalitz-plot of $D^0 \to \pi^+\pi^-\pi^0$, Phys. Rev. D **72**, 031102 (2005).

[1183] X. C. Tian *et al.* (Belle Collaboration), Measurement of the wrong-sign decays $D^0 \to K^+\pi^-(\pi^0, \pi^+\pi^-)$ and search for CP violation, Phys. Rev. Lett. **95**, 231801 (2005).

[1184] G. Brandenburg *et al.* (CLEO Collaboration), Rate measurement of $D^0 \to K^+\pi^-\pi^0$ and constraints on $D^0\bar{D}^0$ mixing, Phys. Rev. Lett. **87**, 071802 (2001).

[1185] T. Aaltonen *et al.* (CDF Collaboration), Measurement of CP-violation asymmetries in $D^0 \to K_S\pi^+\pi^-$, Phys. Rev. D **86**, 032007 (2012).

[1186] D. M. Asner *et al.* (CLEO Collaboration), Search for CP violation in $D^0 \to K^0_S\pi^+\pi^-$, Phys. Rev. D **70**, 091101 (2004).

[1187] R. Aaij *et al.* (LHCb Collaboration), Search for CP violation in the phase space of $D^0 \to K^0_S K^\pm\pi^\mp$ decays with the energy test, J. High Energy Phys. 03 (2024) 107.

[1188] R. Aaij *et al.* (LHCb Collaboration), Studies of the resonance structure in $D^0 \to K^0_S K^\pm\pi^\mp$ decays, Phys. Rev. D **93**, 052018 (2016).

[1189] R. Aaij *et al.* (LHCb Collaboration), Search for CP violation in the phase space of $D^0 \to \pi^+\pi^-\pi^+\pi^-$ decays, Phys. Lett. B **769**, 345 (2017).

[1190] R. Aaij *et al.* (LHCb Collaboration), Model-independent search for CP violation in $D^0 \to \pi^-\pi + \pi^+\pi^-$ and $D^0 \to K^-K^+\pi^-\pi^+$ decay, Phys. Lett. B **726**, 623 (2013).

[1191] J. B. Kim *et al.* (Belle Collaboration), Search for CP violation with kinematic asymmetries in the $D^0 \to K^+K^-\pi^+\pi^-$ decay, Phys. Rev. D **99**, 011104 (2019).

[1192] R. Aaij *et al.* (LHCb Collaboration), Search for CP violation through an amplitude analysis of $D^0 \to K^+K^-\pi^+\pi^-$ decays, J. High Energy Phys. 02 (2019) 126.

[1193] M. Artuso *et al.* (CLEO Collaboration), Amplitude analysis of $D^0 \to K^-K^+\pi^-\pi^+$, Phys. Rev. D **85**, 122002 (2012).

[1194] A. Sangal *et al.* (Belle Collaboration), Measurement of the branching fraction and search for CP violation in $D^0 \to K^0_S K^0_S\pi^+\pi^-$ decays at Belle, Phys. Rev. D **107**, 052001 (2023).

[1195] A. Abdesselam *et al.* (Belle Collaboration), Observation of $D^0 \to \rho^0\gamma$ and search for CP violation in radiative charm decays, Phys. Rev. Lett. **118**, 051801 (2017).

[1196] R. Aaij *et al.* (LHCb Collaboration), Angular analysis of $D^0 \to \pi^+\pi^-\mu^+\mu^-$ and $D^0 \to K^+K^-\mu^+\mu^-$ decays and search for CP violation, Phys. Rev. Lett. **128**, 221801 (2022).

[1197] J. P. Alexander *et al.* (CLEO Collaboration), Measurement of $BD^+_s \to \ell^+\nu$ and the decay constant fD^+_s From $600/pb^{-1}$ of $e^\pm$ annihilation data near 4170 MeV, Phys. Rev. D **79**, 052001 (2009).

[1198] Y. Guan *et al.* (Belle Collaboration), Measurement of branching fractions and CP asymmetries for $D^+_s \to K^+(\eta, \pi^0)$ and $D^+_s \to \pi^+(\eta, \pi^0)$ decays at Belle, Phys. Rev. D **103**, 112005 (2021).

[1199] P. U. E. Onyisi *et al.* (CLEO Collaboration), Improved measurement of absolute hadronic branching fractions of the D^+_s meson, Phys. Rev. D **88**, 032009 (2013).

[1200] B. R. Ko *et al.* (Belle Collaboration), Search for CP violation in the decays $D^+_{(s)} \to K^0_S\pi^+$ and $D^+_{(s)} \to K^0_S K^+$, Phys. Rev. Lett. **104**, 181602 (2010).

[1201] M. Ablikim *et al.* (BESIII Collaboration), Study of the decays $D^+_s \to K^0_S K^+$ and $K^0_L K^+$, Phys. Rev. D **99**, 112005 (2019).

[1202] J. W. Hinson *et al.* (CLEO Collaboration), Improved measurement of the form-factors in the decay $\Lambda^+_c \to \Lambda e^+\nu_e$, Phys. Rev. Lett. **94**, 191801 (2005).

[1203] J. M. Link *et al.* (FOCUS Collaboration), Study of the decay asymmetry parameter and CP violation parameter in the $\Lambda^+_c \to \Lambda\pi^+$ decay, Phys. Lett. B **634**, 165 (2006).

[1204] L. K. Li *et al.* (Belle Collaboration), Search for CP violation and measurement of branching fractions and decay asymmetry parameters for $\Lambda^+_c \to \Lambda h^+$ and $\Lambda^+_c \to \Sigma^0 h^+ (h = K, \pi)$, Sci. Bull. **68**, 583 (2023).

[1205] Y. B. Li *et al.* (Belle Collaboration), Measurements of the branching fractions of the semileptonic decays $\Xi^0_c \to \Xi^-\ell^+\nu_\ell$ and the asymmetry parameter of $\Xi^0_c \to \Xi^-\pi^+$, Phys. Rev. Lett. **127**, 121803 (2021).

[1206] R. Aaij *et al.* (LHCb Collaboration), A measurement of the CP asymmetry difference in $\Lambda^+_c \to pK^-K^+$ and $p\pi^-\pi^+$ decays, J. High Energy Phys. 03 (2018) 182.

[1207] Y. Grossman, A. L. Kagan, and J. Zupan, Testing for new physics in singly Cabibbo suppressed D decays, Phys. Rev. D **85**, 114036 (2012).

[1208] Y. Grossman and S. Schacht, U-spin sum rules for CP asymmetries of three-body charmed baryon decays, Phys. Rev. D **99**, 033005 (2019).

[1209] A. Datta and D. London, Triple-product correlations in $B \to V_1V_2$ decays and new physics, Int. J. Mod. Phys. A **19**, 2505 (2004).

[1210] M. Gronau and J. L. Rosner, Triple product asymmetries in K, $D_{(s)}$ and $B_{(s)}$ decays, Phys. Rev. D **84**, 096013 (2011).

[1211] E. Golowich and G. Valencia, Triple product correlations in semileptonic $B^\pm$ decays, Phys. Rev. D **40**, 112 (1989).

[1212] I. I. Y. Bigi, Charm physics—like botticelli in the sistine chapel, arXiv:hep-ph/0107102.

[1213] W. Bensalem, A. Datta, and D. London, New-physics effects on triple-product correlations in Λ_b decays, Phys. Rev. D **66**, 094004 (2002).

[1214] W. Bensalem and D. London, T odd triple product correlations in hadronic b decays, Phys. Rev. D **64**, 116003 (2001).

[1215] W. Bensalem, A. Datta, and D. London, T-violating triple-product correlations in charmless Λ_b decays, Phys. Lett. B **538**, 309 (2002).

[1216] K. Prasanth *et al.* (Belle Collaboration), First measurement of $\boldsymbol{T}$-odd moments in $\boldsymbol{D^0 \to K^0_S\pi^+\pi^-\pi^0}$ decays, Phys. Rev. D **95**, 091101 (2017).

[1217] L. K. Li *et al.* (Belle Collaboration), Search for CP violation using T-odd correlations in $D^+_{(s)} \to K^+K^-\pi^+\pi^0$, $D^+_{(s)} \to K^+\pi^-\pi^+\pi^0$, and $D^+ \to K^-\pi^+\pi^+\pi^0$ decays, arXiv:2305.12806.

[1218] R. Aaij *et al.* (LHCb Collaboration), Search for CP violation using T-odd correlations in $D^0 \to K^+K^-\pi^+\pi^-$ decays, J. High Energy Phys. 10 (2014) 005.

[1219] P. del Amo Sanchez *et al.* (*BABAR* Collaboration), Search for CP violation using T-odd correlations in $D^0 \to K^+K^-\pi^+\pi^-$ decays, Phys. Rev. D **81**, 111103 (2010).

[1220] H. K. Moon *et al.* (Belle Collaboration), Search for CP violation in $D^+_{(s)} \to K^+K^0_S h^+h^-(h = K, \pi)$ decays and

observation of the Cabibbo-suppressed decay $D_s^+ \to K^+K^-K_S^0\pi^+$, Phys. Rev. D **108**, L111102 (2023).
[1221] J. P. Lees *et al.* (*BABAR* Collaboration), Search for *CP* violation using *T*-odd correlations in $D^+ \to K^+K_S^0\pi^+\pi^-$ and $D_s^+ \to K^+K_S^0\pi^+\pi^-$ decays, Phys. Rev. D **84**, 031103 (2011).
[1222] R. Aaij *et al.* (LHCb Collaboration), Studies of the resonance structure in $D^0 \to K^\mp\pi^\pm\pi^\pm\pi^\mp$ decays, Eur. Phys. J. C **78**, 443 (2018).
[1223] A. J. Bevan, *C*, *P*, and *CP* asymmetry observables based on triple product asymmetries, arXiv:1506.04246.
[1224] G. Durieux and Y. Grossman, Probing *CP* violation systematically in differential distributions, Phys. Rev. D **92**, 076013 (2015).
[1225] Y. Grossman, A. L. Kagan, and Y. Nir, New physics and *CP* violation in singly Cabibbo suppressed *D* decays, Phys. Rev. D **75**, 036008 (2007).
[1226] M. Gersabeck, M. Alexander, S. Borghi, V. V. Gligorov, and C. Parkes, On the interplay of direct and indirect *CP* violation in the charm sector, J. Phys. G **39**, 045005 (2012).
[1227] R. Aaij *et al.* (LHCb Collaboration), Measurement of *CP* asymmetry in $D^0 \to K^-K^+$ and $D^0 \to \pi^-\pi^+$ decays, J. High Energy Phys. 07 (2014) 041.
[1228] R. Aaij *et al.* (LHCb Collaboration), Measurement of the difference of time-integrated *CP* asymmetries in $D^0 \to K^-K^+$ and $D^0 \to \pi^-\pi^+$ decays, Phys. Rev. Lett. **116**, 191601 (2016).
[1229] T. Becher and R. J. Hill, Comment on form-factor shape and extraction of $|V_{ub}|$ from $B \to \pi\ell\nu$, Phys. Lett. B **633**, 61 (2006).
[1230] R. J. Hill, The modern description of semileptonic meson form factors, eConf **C060409**, 027 (2006).
[1231] F. J. Gilman and R. L. Singleton, Analysis of semileptonic decays of mesons containing heavy quarks, Phys. Rev. D **41**, 142 (1990).
[1232] D. Becirevic and A. B. Kaidalov, Comment on the heavy to light form-factors, Phys. Lett. B **478**, 417 (2000).
[1233] C. G. Boyd, B. Grinstein, and R. F. Lebed, Constraints on form-factors for exclusive semileptonic heavy to light meson decays, Phys. Rev. Lett. **74**, 4603 (1995).
[1234] C. G. Boyd and M. J. Savage, Analyticity, shapes of semileptonic form-factors, and $\bar{B} \to pi\ell\bar{\nu}$, Phys. Rev. D **56**, 303 (1997).
[1235] M. C. Arnesen, B. Grinstein, I. Z. Rothstein, and I. W. Stewart, A precision model independent determination of $|V_{ub}|$ from $B \to \pi\ell\nu$, Phys. Rev. Lett. **95**, 071802 (2005).
[1236] C. Bourrely, B. Machet, and E. de Rafael, Semileptonic decays of pseudoscalar particles ($M \to M'\ell\nu_\ell$) and short distance behavior of quantum chromodynamics, Nucl. Phys. **B189**, 157 (1981).
[1237] J. P. Lees *et al.* (*BABAR* Collaboration), Measurement of the $D^0 \to \pi^-e^+\nu_e$ differential decay branching fraction as a function of q^2 and study of form factor parametrizations, Phys. Rev. D **91**, 052022 (2015).
[1238] M. Ablikim *et al.* (BESIII Collaboration), Study of dynamics of $D^0 \to K^-e^+\nu_e$ and $D^0 \to \pi^-e^+\nu_e$ decays, Phys. Rev. D **92**, 072012 (2015).
[1239] L. Widhalm *et al.* (Belle Collaboration), Measurement of $D^0 \to \pi l\nu(Kl\nu)$ form factors and absolute branching fractions, Phys. Rev. Lett. **97**, 061804 (2006).
[1240] B. Aubert *et al.* (*BABAR* Collaboration), Measurement of the hadronic form-factor in $D^0 \to K^-e^+\nu_e$ decays, Phys. Rev. D **76**, 052005 (2007).
[1241] D. Besson *et al.* (CLEO Collaboration), Improved measurements of *D* meson semileptonic decays to π and *K* mesons, Phys. Rev. D **80**, 032005 (2009).
[1242] S. Dobbs *et al.* (CLEO Collaboration), A study of the semileptonic charm decays $D^0 \to \pi^-e^+\nu_e$, $D^+ \to \pi^0e^+\nu_e$, $D^0 \to K^-e^+\nu_e$, and $D^+ \to \bar{K}^0e^+\nu_e$, Phys. Rev. D **77**, 112005 (2008).
[1243] M. Ablikim *et al.* (BESIII Collaboration), Analysis of $D^+ \to \bar{K}^0e^+\nu_e$ and $D^+ \to \pi^0e^+\nu_e$ semileptonic decays, Phys. Rev. D **96**, 012002 (2017).
[1244] M. Ablikim *et al.* (BESIII Collaboration), Study of the $D^0 \to K^-\mu^+\nu_\mu$ dynamics and test of lepton flavor universality with $D^0 \to K^-\ell^+\nu_\ell$ decays, Phys. Rev. Lett. **122**, 011804 (2019).
[1245] M. Ablikim *et al.* (BESIII Collaboration), Improved measurement of the absolute branching fraction of $D^+ \to \bar{K}^0\mu^+\nu_\mu$, Eur. Phys. J. C **76**, 369 (2016).
[1246] M. Ablikim *et al.* (BESIII Collaboration), Measurement of the absolute branching fraction of $D^+ \to \bar{K}^0e^+\nu_e$ via $\bar{K}^0 \to \pi^0\pi^0$, Chin. Phys. C **40**, 113001 (2016).
[1247] M. Ablikim *et al.* (BESIII Collaboration), Measurement of the branching fraction for the semi-leptonic decay $D^{0(+)} \to \pi^{-(0)}\mu^+\nu_\mu$ and test of lepton universality, Phys. Rev. Lett. **121**, 171803 (2018).
[1248] J. Koponen *et al.* (HPQCD Collaboration), $D \to K$ and $D \to \pi$ semileptonic form factors from lattice QCD, arXiv:1208.6242.
[1249] J. Koponen *et al.* (HPQCD Collaboration), The shape of the $D \to K$ semileptonic form factor from full lattice QCD and V_{cs}, arXiv:1305.1462.
[1250] G. S. Huang *et al.* (CLEO Collaboration), Study of semileptonic charm decays $D^0 \to \pi^-\ell^+\nu$ and $D^0 \to K^-\ell^+\nu$, Phys. Rev. Lett. **94**, 011802 (2005).
[1251] J. M. Link *et al.* (FOCUS Collaboration), Measurements of the q^2 dependence of the $D^0 \to K^-\mu^+\nu$ and $D^0 \to \pi^-\mu^+\nu$ form factors, Phys. Lett. B **607**, 233 (2005).
[1252] M. Ablikim *et al.* (BESIII Collaboration), Precision measurements of $D_s^+ \to \eta e^+\nu_e$ and $D_s^+ \to \eta' e^+\nu_e$, Phys. Rev. D **108**, 092003 (2023).
[1253] J. Yelton *et al.* (CLEO Collaboration), Studies of $D^+ \to \{\eta, \eta', \phi\}e^+\nu_e$, Phys. Rev. D **84**, 032001 (2011).
[1254] M. Ablikim *et al.* (BESIII Collaboration), Study of the decays $D^+ \to \eta^{(\prime)}e^+\nu_e$, Phys. Rev. D **97**, 092009 (2018).
[1255] M. Ablikim *et al.* (BESIII Collaboration), Observation of $D_s^+ \to \eta'\mu^+\nu_\mu$, precision test of lepton flavor universality with $D_s^+ \to \eta^{(\prime)}l^+\nu_l$, and first measurements of $D_s^+ \to \eta^{(\prime)}\mu^+\nu_\mu$ decay dynamics, Phys. Rev. Lett. **132**, 091802 (2024).
[1256] M. Ablikim *et al.* (BESIII Collaboration), First observation of $D^+ \to \eta\mu^+\nu_\mu$ and measurement of its decay dynamics, Phys. Rev. Lett. **124**, 231801 (2020).

[1257] V. Lubicz *et al.* (ETM Collaboration), Scalar and vector form factors of $D \to \pi(K)\ell\nu$ decays with $N_f = 2 + 1 + 1$ twisted fermions, Phys. Rev. D **96**, 054514 (2017).

[1258] W. G. Parrott, C. Bouchard, and C. T. H. Davies (HPQCD Collaboration), $B \to K$ and $D \to K$ form factors from fully relativistic lattice QCD, Phys. Rev. D **107**, 014510 (2023).

[1259] A. Bazavov *et al.* (Fermilab Lattice and MILC Collaborations), D-meson semileptonic decays to pseudoscalars from four-flavor lattice QCD, Phys. Rev. D **107**, 094516 (2023).

[1260] M. Ablikim *et al.* (BESIII Collaboration), Measurement of the dynamics of the decays $D_s^+ \to \eta^{(\prime)} e^+ \nu_e$, Phys. Rev. Lett. **122**, 121801 (2019).

[1261] M. Ablikim *et al.* (BESIII Collaboration), First measurement of the form factors in $D_s^+ \to K^0 e^+ \nu_e$ and $D_s^+ \to K^{*0} e^+ \nu_e$ decays, Phys. Rev. Lett. **122**, 061801 (2019).

[1262] J. M. Link *et al.* (FOCUS Collaboration), Evidence for new interference phenomena in the decay $D^+ \to K^- \pi^+ \mu^+ \nu$, Phys. Lett. B **535**, 43 (2002).

[1263] M. A. Ivanov, J. G. Körner, J. N. Pandya, P. Santorelli, N. R. Soni, and C. T. Tra, Exclusive semileptonic decays of D and D_s mesons in the covariant confining quark model, Front. Phys. **14**, 64401 (2019).

[1264] J. M. Link *et al.* (FOCUS Collaboration), New measurements of the $D^+ \to \bar{K}^{*0} \mu^+ \nu$ form-factor ratios, Phys. Lett. B **544**, 89 (2002).

[1265] B. Aubert *et al.* (*BABAR* Collaboration), Study of the decay $D_s^+ \to K^+ K^- e^+ \nu_e$, Phys. Rev. D **78**, 051101 (2008).

[1266] K. M. Ecklund *et al.* (CLEO Collaboration), Study of the semileptonic decay $D_s^+ \to f_0(980) e^+ \nu$ and implications for $B_s \to J/\psi f_0$, Phys. Rev. D **80**, 052009 (2009).

[1267] R. A. Briere *et al.* (CLEO Collaboration), Analysis of $D^+ \to K^- pi^+ e^+ \nu_e$ and $D^+ \to K^- \pi^+ \mu^+ \nu_\mu$ semileptonic decays, Phys. Rev. D **81**, 112001 (2010).

[1268] P. del Amo Sanchez *et al.* (*BABAR* Collaboration), Analysis of the $D^+ \to K^- \pi^+ e^+ \nu_e$ decay channel, Phys. Rev. D **83**, 072001 (2011).

[1269] P. Estabrooks *et al.*, Study of $K\pi$ scattering using the reactions $K^\pm p \to K^\pm \pi^+ n$ and $K^\pm p \to K^\pm \pi^- \Delta^{++}$ at 13-GeV/c, Nucl. Phys. **B133**, 490 (1978).

[1270] K. M. Watson, Some general relations between the photoproduction and scattering of pi mesons, Phys. Rev. **95**, 228 (1954).

[1271] M. Ablikim *et al.* (BESIII Collaboration), Study of $D^+ \to K^- \pi^+ e^+ \nu_e$, Phys. Rev. D **94**, 032001 (2016).

[1272] M. Ablikim *et al.* (BESIII Collaboration), Study of the decay $D^0 \to \bar{K}^0 \pi^- e^+ \nu_e$, Phys. Rev. D **99**, 011103 (2019).

[1273] S. Dobbs *et al.* (CLEO Collaboration), First measurement of the form factors in the decays $D^0 \to \rho^- e^+ \nu_e$ and $D^+ \to \rho^0 e^+ \nu_e$, Phys. Rev. Lett. **110**, 131802 (2013).

[1274] M. Ablikim *et al.* (BESIII Collaboration), First observation of $D^+ \to f_0(500) e^+ \nu_e$ and improved measurements of $D \to \rho e^+ \nu_e$, Phys. Rev. Lett. **122**, 062001 (2019).

[1275] M. Ablikim *et al.* (BESIII Collaboration), Studies of the decay $D_s^+ \to K^+ K^- \mu^+ \nu_\mu$, J. High Energy Phys. 12 (2023) 072.

[1276] J. C. Anjos *et al.* (Fermilab E691 Collaboration), Measurement of the form-factors in the decay $D^+ \to \bar{K}^{*0} e^+ \nu_e$, Phys. Rev. Lett. **65**, 2630 (1990).

[1277] K. Kodama *et al.* (Fermilab E653 Collaboration), Measurement of the form-factor ratios in the decay $D^+ \to \bar{K}^{*0}(892) \mu^+ \nu$, Phys. Lett. B **274**, 246 (1992).

[1278] P. L. Frabetti *et al.* (Fermilab E687 Collaboration), Analysis of the decay mode $D^+ \to \bar{K}^{*0} \mu^+ \nu$, Phys. Lett. B **307**, 262 (1993).

[1279] E. M. Aitala *et al.* (Fermilab E791 Collaboration), Measurement of the form-factor ratios for $D^+ \to \bar{K}^{*0} e^+ \nu_e$, Phys. Rev. Lett. **80**, 1393 (1998).

[1280] E. M. Aitala *et al.* (Fermilab E791 Collaboration), Measurement of the form-factor ratios for $D^+ \to \bar{K}^{*0} \ell^+ \nu_\ell$, Phys. Lett. B **440**, 435 (1998).

[1281] M. Adamovich *et al.* (BEATRICE Collaboration), A measurement of the form-factor ratios in the decay $D^+ \to \bar{K}^{*0} \mu^+ \nu_\mu$, Eur. Phys. J. C **6**, 35 (1999).

[1282] J. M. Link *et al.* (FOCUS Collaboration), Analysis of the semileptonic decay $D^0 \to \bar{K}^0 \pi^- \mu^+ \nu$, Phys. Lett. B **607**, 67 (2005).

[1283] M. Ablikim *et al.* (BESIII Collaboration), Measurement of the form factors in the decay $D^+ \to \omega e^+ \nu_e$ and search for the decay $D^+ \to \phi e^+ \nu_e$, Phys. Rev. D **92**, 071101 (2016).

[1284] M. Ablikim *et al.* (BESIII Collaboration), Observation of the semileptonic decay $D^0 \to a_0(980)^- e^+ \nu_e$ and evidence for $D^+ \to a_0(980)^0 e^+ \nu_e$, Phys. Rev. Lett. **121**, 081802 (2018).

[1285] X.-D. Cheng, H.-B. Li, B. Wei, Y.-G. Xu, and M.-Z. Yang, Study of $D \to a_0(980) e^+ \nu_e$ decay in the light-cone sum rules approach, Phys. Rev. D **96**, 033002 (2017).

[1286] M. Ablikim *et al.* (BESIII Collaboration), Search for the decay $D_s^+ \to a_0(1270)^0 e^+ \nu_e$, Phys. Rev. D **103**, 092004 (2021).

[1287] M. Ablikim *et al.* (BESIII Collaboration), Study of light scalar mesons through $D_s^+ \to \pi^0 \pi^0 e^+ \nu_e$ and $K_S^0 K_S^0 e^+ \nu_e$ decays, Phys. Rev. D **105**, L031101 (2022).

[1288] M. Ablikim *et al.* (BESIII Collaboration), Study of the $f_0(980)$ through the decay $D_s^+ \to \pi^+ \pi^- e^+ \nu_e$, Phys. Rev. Lett. **132**, 141901 (2024).

[1289] M. Artuso *et al.* (CLEO Collaboration), Evidence for the decay $D^0 \to K^- \pi^+ \pi^- e^+ \nu_e$, Phys. Rev. Lett. **99**, 191801 (2007).

[1290] M. Ablikim *et al.* (BESIII Collaboration), Observation of the semileptonic D^+ transition into an axial-vector meson $\bar{K}_1(1270)^0$, Phys. Rev. Lett. **123**, 231801 (2019).

[1291] M. Ablikim *et al.* (BESIII Collaboration), Observation of $D^0 \to K_1(1270)^- e^+ \nu_e$, Phys. Rev. Lett. **127**, 131801 (2021).

[1292] M. Ablikim *et al.* (BESIII Collaboration), Search for the semileptonic decays $D^+ \to b_1(1235)^0 e^+ \nu_e$ and $D^0 \to b_1(1235)^- e^+ \nu_e$, Phys. Rev. D **102**, 112005 (2020).

[1293] M. Ablikim *et al.* (BESIII Collaboration), Search for the semileptonic decays $D_s^+ \to K_1(1270) e^+ \nu_e$ and $D_s^+ \to b_1(1235)^0 e^+ \nu_e$, Phys. Rev. D **108**, 112002 (2023).

[1294] S. Fajfer, I. Nišandžić, and U. Rojec, Discerning new physics in charm meson leptonic and semileptonic decays, Phys. Rev. D **91**, 094009 (2015).

[1295] L. Riggio, G. Salerno, and S. Simula, Scalar and vector form factors of $D \to \pi(K)\ell\nu$ decays with $N_f = 2+1+1$ twisted fermions, Eur. Phys. J. C **78**, 501 (2018).

[1296] M. Ablikim *et al.* (BESIII Collaboration), Observation of the semimuonic decay $D^+ \to \omega\mu^+\nu_\mu$, Phys. Rev. D **101**, 072005 (2020).

[1297] M. Ablikim *et al.* (BESIII Collaboration), Measurements of the branching fractions for the semi-leptonic decays $D_s^+ \to \phi e^+\nu_e$, $\phi\mu^+\nu_\mu$, $\eta\mu^+\nu_\mu$, and $\eta'\mu^+\nu_\mu$, Phys. Rev. D **97**, 012006 (2018).

[1298] N. Carrasco *et al.* (ETM Collaboration), Leptonic decay constants f_K, f_D, and f_{D_s} with $N_f = 2+1+1$ twisted-mass lattice QCD, Phys. Rev. D **91**, 054507 (2015).

[1299] A. Bazavov *et al.* (Fermilab Lattice and MILC Collaborations), B- and D-meson leptonic decay constants from four-flavor lattice QCD, Phys. Rev. D **98**, 074512 (2018).

[1300] A. Filipuzzi, J. Portoles, and M. Gonzalez-Alonso, $U(2)^5$ flavor symmetry and lepton universality violation in $W \to \tau\nu_\tau$, Phys. Rev. D **85**, 116010 (2012).

[1301] M. Ablikim *et al.* (BESIII Collaboration), Observation of the leptonic decay $D^+ \to \tau^+\nu_\tau$, Phys. Rev. Lett. **123**, 211802 (2019).

[1302] M. Ablikim *et al.* (BESIII Collaboration), Determination of the pseudoscalar decay constant $f_{D_s^+}$ via $D_s^+ \to \mu^+\nu_\mu$, Phys. Rev. Lett. **122**, 071802 (2019).

[1303] M. Ablikim *et al.* (BESIII Collaboration), Measurement of the absolute branching fractions for purely leptonic D_s^+ decays, Phys. Rev. D **104**, 052009 (2021).

[1304] M. Ablikim *et al.* (BESIII Collaboration), Measurement of the branching fraction of leptonic decay $D_s^+ \to \tau^+\nu_\tau$ via $\tau^+ \to \pi^+\pi^0\bar{\nu}_\tau$, Phys. Rev. D **104**, 032001 (2021).

[1305] M. Ablikim *et al.* (BESIII Collaboration), Measurement of the absolute branching fraction of $D_s^+ \to \tau^+\nu_\tau$ via $\tau^+ \to e^+\nu_e\bar{\nu}_\tau$, Phys. Rev. Lett. **127**, 171801 (2021).

[1306] M. Ablikim *et al.* (BESIII Collaboration), Improved measurement of the branching fraction of $D_s^+ \to \mu^+\nu_\mu$, Phys. Rev. D **108**, 112001 (2023).

[1307] M. Ablikim *et al.* (BESIII Collaboration), Updated measurement of the branching fraction of $D_s^+ \to \tau^+\nu_\tau$ via $\tau^+ \to \pi^+ bar\nu_\tau$, Phys. Rev. D **108**, 092014 (2023).

[1308] M. Ablikim *et al.* (BESIII Collaboration), Measurement of the branching fraction of $D_s^+ \to \tau^+\nu_\tau$ via $\tau^+ \to \mu^+\nu_\mu\bar{\nu}_\tau$, J. High Energy Phys. 09 (2023) 124.

[1309] M. Ablikim *et al.* (BESIII Collaboration), Precision measurements of $B(D^+ \to \mu^+\nu_\mu)$, the pseudoscalar decay constant f_{D^+}, and the quark mixing matrix element $|V_{cd}|$, Phys. Rev. D **89**, 051104 (2014).

[1310] M. Ablikim *et al.* (BESIII Collaboration), Measurement of the $D_s^+ \to \ell^+\nu_\ell$ branching fractions and the decay constant $f_{D_s^+}$, Phys. Rev. D **94**, 072004 (2016).

[1311] P. del Amo Sanchez *et al.* (*BABAR* Collaboration), Measurement of the absolute branching fractions for $D_s^- \to \ell^-\bar{\nu}_\ell$ and extraction of the decay constant f_{D_s}, Phys. Rev. D **82**, 091103 (2010); **91**, 019901(E) (2015).

[1312] A. Zupanc *et al.* (Belle Collaboration), Measurements of branching fractions of leptonic and hadronic D_s^+ meson decays and extraction of the D_s^+ meson decay constant, J. High Energy Phys. 09 (2013) 139.

[1313] P. Naik *et al.* (CLEO Collaboration), Measurement of the pseudoscalar decay constant f_{D_s} using $D_s^+ \to \tau^+\nu$, $\tau^+ \to \rho^+\bar{\nu}$ decays, Phys. Rev. D **80**, 112004 (2009).

[1314] P. U. E. Onyisi *et al.* (CLEO Collaboration), Improved measurement of absolute branching fraction of $D_s^+ \to \tau^+\nu_\tau$, Phys. Rev. D **79**, 052002 (2009).

[1315] J. Charles *et al.*, *CP* violation and the CKM matrix: Assessing the impact of the asymmetric B factories, Eur. Phys. J. C **41**, 1 (2005), updated results and plots available at: http://ckmfitter.in2p3.fr

[1316] E. Barberio, B. van Eijk, and Z. Was, PHOTOS: A universal Monte Carlo for QED radiative corrections in decays, Comput. Phys. Commun. **66**, 115 (1991).

[1317] E. Barberio and Z. Was, PHOTOS: A universal Monte Carlo for QED radiative corrections. Version 2.0, Comput. Phys. Commun. **79**, 291 (1994).

[1318] P. Golonka and Z. Was, PHOTOS Monte Carlo: A precision tool for QED corrections in Z and W decays, Eur. Phys. J. C **45**, 97 (2006).

[1319] P. Golonka, B. Kersevan, T. Pierzchała, E. Richter-Wąs, Z. Wąs, and M. Worek, The Tauola photos F environment for the TAUOLA and PHOTOS packages: Release. 2., Comput. Phys. Commun. **174**, 818 (2006).

[1320] P. Golonka and Z. Was, Next to leading logarithms and the PHOTOS Monte Carlo, Eur. Phys. J. C **50**, 53 (2007).

[1321] A. Ryd *et al.*, EvtGen: A Monte Carlo generator for B-physics, Report No. EVTGEN-V00-11-07, 2005.

[1322] D. J. Lange, The EvtGen particle decay simulation package, Nucl. Instrum. Methods Phys. Res., Sect. A **462**, 152 (2001).

[1323] J. M. Link *et al.* (FOCUS Collaboration), Study of the Cabibbo-suppressed decay modes $D^0 \to \pi^-\pi^+$ and $D^0 \to K^-K^+$, Phys. Lett. B **555**, 167 (2003).

[1324] M. Ablikim *et al.* (BESIII Collaboration), Measurements of absolute branching fractions for D mesons decays into two pseudoscalar mesons, Phys. Rev. D **97**, 072004 (2018).

[1325] B. Aubert *et al.* (*BABAR* Collaboration), Measurement of the absolute branching fraction of $D^0 \to K^-\pi^+$, Phys. Rev. Lett. **100**, 051802 (2008).

[1326] M. Artuso *et al.* (CLEO Collaboration), Measurement of $\mathrm{Br}(D^0 \to K^-\pi^+)$ using partial reconstruction of $\bar{B} \to D^{*+}X\ell^-\bar{n}u$, Phys. Rev. Lett. **80**, 3193 (1998).

[1327] R. Barate *et al.* (ALEPH Collaboration), Measurement of the branching fraction for $D^0 \to K^-\pi^+$, Phys. Lett. B **403**, 367 (1997).

[1328] H. Albrecht *et al.* (ARGUS Collaboration), Measurement of the absolute branching fractions for D^0 decays into $K^-\pi^+$, $K^-\pi^+\pi^+\pi^-$, $\bar{K}^0\pi^+\pi^-$, Phys. Lett. B **340**, 125 (1994).

[1329] D. S. Akerib *et al.* (CLEO Collaboration), Measurement of the absolute branching fraction for $D^0 \to K^-\pi^+$, Phys. Rev. Lett. **71**, 3070 (1993).

[1330] D. Decamp *et al.* (ALEPH Collaboration), Production and decay of charmed mesons at the Z resonance, Phys. Lett. B **266**, 218 (1991).

[1331] D. E. Acosta *et al.* (CDF Collaboration), Measurement of partial widths and search for direct *CP* violation in D^0 meson decays to K^-K^+ and $\pi^-\pi^+$, Phys. Rev. Lett. **94**, 122001 (2005).

[1332] T. E. Coan *et al.* (CLEO Collaboration), Flavor-specific inclusive B decays to charm, Phys. Rev. Lett. **80**, 1150 (1998).

[1333] N. Davidson, T. Przedzinski, and Z. Was, PHOTOS interface in C++: Technical and physics documentation, Comput. Phys. Commun. **199**, 86 (2016), and online update at http://photospp.web.cern.ch.

[1334] B. Aubert *et al.* (*BABAR* Collaboration), Observation of a narrow meson decaying to $D_s^+\pi^0$ at a mass of $2.32-\mathrm{GeV}/c^2$, Phys. Rev. Lett. **90**, 242001 (2003).

[1335] D. Besson *et al.* (CLEO Collaboration), Observation of a narrow resonance of mass $2.46-\mathrm{GeV}/c^2$ decaying to $D_s^{*+}\pi^0$ and confirmation of the $D_{sJ}^*(2317)$ state, Phys. Rev. D **68**, 032002 (2003); **75**, 119908(E) (2007).

[1336] K. Abe *et al.* (Belle Collaboration), Measurements of the D_{sJ} resonance properties, Phys. Rev. Lett. **92**, 012002 (2004).

[1337] B. Aubert *et al.* (*BABAR* Collaboration), Observation of a narrow meson decaying to $D_s^+\pi^0\gamma$ at a mass of $2.458\ \mathrm{GeV}/c^2$, Phys. Rev. D **69**, 031101 (2004).

[1338] J. M. Link *et al.* (FOCUS Collaboration), Measurement of masses and widths of excited charm mesons D_2^* and evidence for broad states, Phys. Lett. B **586**, 11 (2004).

[1339] R. Aaij *et al.* (LHCb Collaboration), Amplitude analysis of $B^0 \to \bar{D}^0 K^+\pi^-$ decays, Phys. Rev. D **92**, 012012 (2015).

[1340] R. Aaij *et al.* (LHCb Collaboration), Determination of quantum numbers for several excited charmed mesons observed in $B^- \to D^{*+}\pi^-\pi^-$ decays, Phys. Rev. D **101**, 032005 (2020).

[1341] R. Aaij *et al.* (LHCb Collaboration), Study of D_J meson decays to $D^+\pi^-$, $D^0\pi^+$ and $D^{*+}\pi^-$ final states in pp collision, J. High Energy Phys. 09 (2013) 145.

[1342] H. Abramowicz *et al.* (ZEUS Collaboration), Production of the excited charm mesons D_1 and D_2^* at HERA, Nucl. Phys. **B866**, 229 (2013).

[1343] P. del Amo Sanchez *et al.* (*BABAR* Collaboration), Observation of new resonances decaying to $D\pi$ and $D^*\pi$ in inclusive e^+e^- collisions near $\sqrt{s}=10.58\,\mathrm{GeV}$, Phys. Rev. D **82**, 111101 (2010).

[1344] A. Abulencia *et al.* (CDF Collaboration), Measurement of mass and width of the excited charmed meson states D_1^0 and D_2^{*0} at CDF, Phys. Rev. D **73**, 051104 (2006).

[1345] P. Avery *et al.* (CLEO Collaboration), Production and decay of $D_1^0(2420)$ and $D_2^{*0}(2460)$, Phys. Lett. B **331**, 236 (1994).

[1346] P. L. Frabetti *et al.* (Fermilab E687 Collaboration), Measurement of the masses and widths of $L=1$ charm mesons, Phys. Rev. Lett. **72**, 324 (1994).

[1347] H. Albrecht *et al.* (ARGUS Collaboration), Resonance decomposition of the $D^{*0}(2420)$ through a decay angular analysis, Phys. Lett. B **232**, 398 (1989).

[1348] P. Avery *et al.* (CLEO Collaboration), P wave charmed mesons in e^+e^- annihilation, Phys. Rev. D **41**, 774 (1990).

[1349] J. C. Anjos *et al.* (Tagged Photon Spectrometer Collaboration), Observation of excited charmed mesons, Phys. Rev. Lett. **62**, 1717 (1989).

[1350] T. Bergfeld *et al.* (CLEO Collaboration), Observation of $D_1^+(2420)$ and $D_2^{*+}(2460)$, Phys. Lett. B **340**, 194 (1994).

[1351] R. Aaij *et al.* (LHCb Collaboration), Amplitude analysis of $B^- \to D^+\pi^-\pi^-$ decays, Phys. Rev. D **94**, 072001 (2016).

[1352] H. Albrecht *et al.* (ARGUS Collaboration), Observation of the $D^{*0}(2459)$ in e^+e^- annihilation, Phys. Lett. B **221**, 422 (1989).

[1353] H. Albrecht *et al.* (ARGUS Collaboration), Observation of the charged isospin partner of the $D^*0(2459)$, Phys. Lett. B **231**, 208 (1989).

[1354] P. Abreu *et al.* (DELPHI Collaboration), First evidence for a charm radial excitation, D^*, Phys. Lett. B **426**, 231 (1998).

[1355] B. Aubert *et al.* (*BABAR* Collaboration), A study of the $D_{sJ}^*(2317)$ and $D_{sJ}(2460)$ mesons in inclusive $c\bar{c}$ production near $\sqrt{s}=10.6$ GeV, Phys. Rev. D **74**, 032007 (2006).

[1356] M. Ablikim *et al.* (BESIII Collaboration), Measurement of the absolute branching fraction of $D_{s0}^{*\pm}(2317)\to \pi^0 D_s^\pm$, Phys. Rev. D **97**, 051103 (2018).

[1357] M. Ablikim *et al.* (BESIII Collaboration), Observation of $e^+e^- \to D_s^+\bar{D}^{(*)0}K^-$ and study of the P-wave D_s mesons, Chin. Phys. C **43**, 031001 (2019).

[1358] J. P. Lees *et al.* (*BABAR* Collaboration), Measurement of the mass and width of the $D_{s1}(2536)^+$ meson, Phys. Rev. D **83**, 072003 (2011).

[1359] V. M. Abazov *et al.* (D0 Collaboration), Measurement of the B_s^0 semileptonic branching ratio to an orbitally excited D_s state, $\mathrm{Br}(B_s^0 \to D_{s1}^-(2536)\mu^+\nu X)$, Phys. Rev. Lett. **102**, 051801 (2009).

[1360] J. P. Alexander *et al.* (CLEO Collaboration), Production and decay of the $D_{s1}^+(2536)$, Phys. Lett. B **303**, 377 (1993).

[1361] H. Albrecht *et al.* (ARGUS Collaboration), Observation of the decay $D_{s1}^+(2536) \to D^{*0}K^+$, Phys. Lett. B **297**, 425 (1992).

[1362] H. Albrecht *et al.* (ARGUS Collaboration), Observation of a new charmed—strange meson, Phys. Lett. B **230**, 162 (1989).

[1363] R. Aaij *et al.* (LHCb Collaboration), Dalitz plot analysis of $B_s^0 \to \bar{D}^0 K^-\pi^+$ decays, Phys. Rev. D **90**, 072003 (2014).

[1364] R. Aaij *et al.* (LHCb Collaboration), First observation of $\bar{B}_s^0 \to D_{s2}^{*+}X\mu^-\bar{\nu}$ decays, Phys. Lett. B **698**, 14 (2011).

[1365] B. Aubert *et al.* (*BABAR* Collaboration), Observation of a new D_s meson decaying to DK at a mass of $2.86\ \mathrm{GeV}/c^2$, Phys. Rev. Lett. **97**, 222001 (2006).

[1366] H. Albrecht *et al.* (ARGUS Collaboration), Measurement of the decay $D_{s2}^{*+} \to D^0K^+$, Z. Phys. C **69**, 405 (1996).

[1367] Y. Kubota *et al.* (CLEO Collaboration), Observation of a new charmed strange meson, Phys. Rev. Lett. **72**, 1972 (1994).

[1368] S. Godfrey and N. Isgur, Mesons in a relativized quark model with chromodynamics, Phys. Rev. D **32**, 189 (1985).

[1369] S. Godfrey and R. Kokoski, The properties of p wave mesons with one heavy quark, Phys. Rev. D **43**, 1679 (1991).

[1370] P. Schweitzer, S. Boffi, and M. Radici, Polynomiality of unpolarized off forward distribution functions and the D term in the chiral quark soliton model, Phys. Rev. D **66**, 114004 (2002).

[1371] B. Chen, X. Liu, and A. Zhang, Combined study of $2S$ and $1D$ open-charm mesons with natural spin-parity, Phys. Rev. D **92**, 034005 (2015).

[1372] S. Godfrey and K. Moats, Properties of excited charm and charm-strange mesons, Phys. Rev. D **93**, 034035 (2016).

[1373] A. M. Badalian and B. L. G. Bakker, The charmed mesons in the region above 3.0 GeV, Phys. At. Nucl. **84**, 354 (2021).

[1374] Q.-T. Song, D.-Y. Chen, X. Liu, and T. Matsuki, Higher radial and orbital excitations in the charmed meson family, Phys. Rev. D **92**, 074011 (2015).

[1375] B. B. Malabarba, K. P. Khemchandani, and A. M. Torres, Decay processes of a pseudoscalar $D(2900)$, Phys. Rev. D **104**, 116002 (2021).

[1376] F. Jugeau, A. Le Yaouanc, L. Oliver, and J.-C. Raynal, The decays $\bar{B} \to D^{**}\pi$ and the Isgur-Wise functions $\tau_{1/2}(w)$, $\tau_{3/2}(w)$, Phys. Rev. D **72**, 094010 (2005).

[1377] P. Colangelo, F. De Fazio, and R. Ferrandes, Excited charmed mesons: Observations, analyses and puzzles, Mod. Phys. Lett. A **19**, 2083 (2004).

[1378] D. Liventsev *et al.* (Belle Collaboration), Study of $B \to D^{**}l\nu$ with full reconstruction tagging, Phys. Rev. D **77**, 091503 (2008).

[1379] R. Aaij *et al.* (LHCb Collaboration), Observation of the decays $B^0_{(s)} \to D_{s1}(2536)^{\mp}K^{\pm}$, J. High Energy Phys. 10 (2023) 106.

[1380] J. P. Lees *et al.* (*BABAR* Collaboration), Dalitz plot analyses of $B^0 \to D^-D^0K^+$ and $B^+ \to \bar{D}^0D^0K^+$ decays, Phys. Rev. D **91**, 052002 (2015).

[1381] R. N. Cahn and J. D. Jackson, Spin orbit and tensor forces in heavy quark light quark mesons: Implications of the new D_s state at 2.32-GeV, Phys. Rev. D **68**, 037502 (2003).

[1382] T. Barnes, F. E. Close, and H. J. Lipkin, Implications of a DK molecule at 2.32-GeV, Phys. Rev. D **68**, 054006 (2003).

[1383] H. J. Lipkin, New predictions for multiquark hadron masses, Phys. Lett. B **580**, 50 (2004).

[1384] M. Cleven, H. W. Grießhammer, F.-K. Guo, C. Hanhart, and U.-G. Meißner, Strong and radiative decays of the $D^*_{s0}(2317)$ and $D_{s1}(2460)$, Eur. Phys. J. A **50**, 149 (2014).

[1385] L. Liu *et al.*, Interactions of charmed mesons with light pseudoscalar mesons from lattice QCD and implications on the nature of the $D^*_{s0}(2317)$, Phys. Rev. D **87**, 014508 (2013).

[1386] F.-K. Guo, C. Hanhart, U.-G. Meißner, Q. Wang, Q. Zhao, and B.-S. Zou, Hadronic molecules, Rev. Mod. Phys. **90**, 015004 (2018); **94**, 029901(E) (2022).

[1387] H.-L. Fu, H. W. Grießhammer, F.-K. Guo, C. Hanhart, and U.-G. Meißner, Update on strong and radiative decays of the $D^*_{s0}(2317)$ and $D_{s1}(2460)$ and their bottom cousins, Eur. Phys. J. A **58**, 70 (2022).

[1388] M.-N. Tang, Y.-H. Lin, F.-K. Guo, C. Hanhart, and U.-G. Meißner, Isospin-conserving hadronic decay of the $D_{s1}(2460)$ into $D_s\pi^+\pi^-$, Commun. Theor. Phys. **75**, 055203 (2023).

[1389] F. Gil-Domínguez and R. Molina, Quark mass dependence of the $D^*_{s0}(2317)$ and $D_{s1}(2460)$ resonances, Phys. Rev. D **109**, 096002 (2024).

[1390] Y. Tan and J. Ping, $D^*_{s0}(2317)$ and $D_{s1}(2460)$ in an unquenched quark model, Phys. Rev. D **111**, 096023 (2025).

[1391] W. A. Bardeen, E. J. Eichten, and C. T. Hill, Chiral multiplets of heavy—light mesons, Phys. Rev. D **68**, 054024 (2003).

[1392] S. Chekanov *et al.* (ZEUS Collaboration), Production of excited charm and charm-strange mesons at HERA, Eur. Phys. J. C **60**, 25 (2009).

[1393] A. Heister *et al.* (ALEPH Collaboration), Production of D_s^{**} mesons in hadronic Z decays, Phys. Lett. B **526**, 34 (2002).

[1394] B. Aubert *et al.* (*BABAR* Collaboration), Study of D_{sJ} decays to D^*K in inclusive e^+e^- interactions, Phys. Rev. D **80**, 092003 (2009).

[1395] R. Aaij *et al.* (LHCb Collaboration), Study of D_{sJ} decays to $D^+K^0_S$ and D^0K^+ final states in pp collisions, J. High Energy Phys. 10 (2012) 151.

[1396] R. Aaij *et al.* (LHCb Collaboration), Observation of overlapping spin-1 and spin-3 $\bar{D}^0K^-$ resonances at mass 2.86 GeV$/c^2$, Phys. Rev. Lett. **113**, 162001 (2014).

[1397] R. Aaij *et al.* (LHCb Collaboration), Study of $D^{(*)?+}_{sJ}$ mesons decaying to $D^{*+}K^0_S$ and $D^{*0}K^+$ final states, J. High Energy Phys. 02 (2016) 133.

[1398] T. Matsuki, T. Morii, and K. Sudoh, Radial excitations of heavy mesons, Eur. Phys. J. A **31**, 701 (2007).

[1399] R. Aaij *et al.* (LHCb Collaboration), Observation of a new excited D_s^+ meson in $B^0 \to D^-D^+K^+\pi^-$ decays, Phys. Rev. Lett. **126**, 122002 (2021).

[1400] G.-L. Wang, W. Li, T.-F. Feng, Y.-L. Wang, and Y.-B. Liu, The newly observed state $D_{s0}(2590)^+$ and width of $D^*(2007)^0$, Eur. Phys. J. C **82**, 267 (2022).

[1401] N. Isgur and M. B. Wise, Weak decays of heavy mesons in the static quark approximation, Phys. Lett. B **232**, 113 (1989).

[1402] B. Aubert *et al.* (*BABAR* Collaboration), A precision measurement of the Λ_c^+ baryon mass, Phys. Rev. D **72**, 052006 (2005).

[1403] E. Solovieva *et al.* (Belle Collaboration), Study of Ω_c^0 and Ω_c^{*0} baryons at Belle, Phys. Lett. B **672**, 1 (2009).

[1404] T. Aaltonen *et al.* (CDF Collaboration), Measurements of the properties of $\Lambda_c(2595)$, $\Lambda_c(2625)$, $\Sigma_c(2455)$, and $\Sigma_c(2520)$ baryons, Phys. Rev. D **84**, 012003 (2011).

[1405] M. Artuso *et al.* (CLEO Collaboration), Observation of new states decaying into $Lambda_c^+\pi^-\pi^+$, Phys. Rev. Lett. **86**, 4479 (2001).

[1406] B. Aubert *et al.* (*BABAR* Collaboration), Observation of a charmed baryon decaying to D^0p at a mass near 2.94 – GeV$/c^2$, Phys. Rev. Lett. **98**, 012001 (2007).

[1407] K. Abe *et al.* (Belle Collaboration), Experimental constraints on the possible J^P quantum numbers of the $\Lambda_c(2880)^+$, Phys. Rev. Lett. **98**, 262001 (2007).

[1408] H.-Y. Cheng and C.-K. Chua, Strong decays of charmed baryons in heavy hadron chiral perturbation theory, Phys. Rev. D **75**, 014006 (2007).

[1409] Y. B. Li *et al.* (Belle Collaboration), Evidence of a new excited charmed baryon decaying to $\Sigma_c(2455)^{0,++}\pi^{\pm}$, Phys. Rev. Lett. **130**, 031901 (2023).

[1410] K. Tanida *et al.* (Belle Collaboration), Experimental determination of the isospin of $\Lambda_c(2765)^+/\Sigma_c(2765)^+$, in *Proceedings of the 18th International Conference on Hadron Spectroscopy and Structure* (2019), arXiv:1908.06235.

[1411] R. Aaij *et al.* (LHCb Collaboration), Measurement of the shape of the $\Lambda_b^0 \to \Lambda_c^+\mu^-\bar{\nu}_\mu$ differential decay rate, Phys. Rev. D **96**, 112005 (2017).

[1412] S. H. Lee *et al.* (Belle Collaboration), Measurements of the masses and widths of the $\Sigma_c(2455)^{0/++}$ and $\Sigma_c(2520)^{0/++}$ baryons, Phys. Rev. D **89**, 091102 (2014).

[1413] R. Mizuk *et al.* (Belle Collaboration), Observation of an isotriplet of excited charmed baryons decaying to $\Lambda_c^+\pi$, Phys. Rev. Lett. **94**, 122002 (2005).

[1414] L. A. Copley, N. Isgur, and G. Karl, Charmed baryons in a quark model with hyperfine interactions, Phys. Rev. D **20**, 768 (1979); **23**, 817(E) (1981).

[1415] D. Pirjol and T.-M. Yan, Predictions for s wave and p wave heavy baryons from sum rules and constituent quark model. 1. Strong interactions, Phys. Rev. D **56**, 5483 (1997).

[1416] R. Chistov *et al.* (Belle Collaboration), Observation of new states decaying into $\Lambda_c^+K^-\pi^+$ and $\Lambda_c^+K_S^0\pi^-$, Phys. Rev. Lett. **97**, 162001 (2006).

[1417] Y. Kato *et al.* (Belle Collaboration), Search for doubly charmed baryons and study of charmed strange baryons at Belle, Phys. Rev. D **89**, 052003 (2014).

[1418] Y. Kato *et al.* (Belle Collaboration), Studies of charmed baryons in the $\Lambda - D$ final state at Belle, Phys. Rev. D **94**, 032002 (2016).

[1419] R. Aaij *et al.* (LHCb Collaboration), Observation of new Ξ_c^0 baryons decaying to $\Lambda_c^+K^-$, Phys. Rev. Lett. **124**, 222001 (2020).

[1420] B. Aubert *et al.* (*BABAR* Collaboration), A study of $\bar{B} \to \Xi_c\bar{\Lambda}_c^-$ and $\bar{B} \to \Lambda_c^+\bar{\Lambda}_c^-\bar{K}$ decays at *BABAR*, Phys. Rev. D **77**, 031101 (2008).

[1421] R. Aaij *et al.* (LHCb Collaboration), Study of the $B^- \to \Lambda_c^+\bar{\Lambda}_c^-K^-$ decay, Phys. Rev. D **108**, 012020 (2023).

[1422] T. J. Moon *et al.* (Belle Collaboration), First determination of the spin and parity of a charmed-strange baryon, $\Xi_c(2970)^+$, Phys. Rev. D **103**, L111101 (2021).

[1423] L. D. Roper, Evidence for a P-11 pion-nucleon resonance at 556 MeV, Phys. Rev. Lett. **12**, 340 (1964).

[1424] J. Yelton *et al.* (Belle Collaboration), Study of excited Ξ_c states decaying into Ξ_c^0 and Ξ_c^+ baryons, Phys. Rev. D **94**, 052011 (2016).

[1425] J. Yelton *et al.* (Belle Collaboration), Study of electromagnetic decays of orbitally excited Ξ_c baryons, Phys. Rev. D **102**, 071103 (2020).

[1426] B. Aubert *et al.* (*BABAR* Collaboration), Observation of an excited charm baryon Ω_c^* decaying to $\Omega_c^0\gamma$, Phys. Rev. Lett. **97**, 232001 (2006).

[1427] J. L. Rosner, Charmed baryons with $J = 3/2$, Phys. Rev. D **52**, 6461 (1995).

[1428] L. Y. Glozman and D. O. Riska, The Charm and bottom hyperons and chiral dynamics, Nucl. Phys. **A603**, 326 (1996); **A620**, 510(E) (1997).

[1429] E. E. Jenkins, Heavy baryon masses in the $1/m_Q$ and $1/N_c$ expansions, Phys. Rev. D **54**, 4515 (1996).

[1430] L. Burakovsky, J. T. Goldman, and L. P. Horwitz, New quadratic baryon mass relations, Phys. Rev. D **56**, 7124 (1997).

[1431] R. Aaij *et al.* (LHCb Collaboration), Observation of five new narrow Ω_c^0 states decaying to $\Xi_c^+K^-$, Phys. Rev. Lett. **118**, 182001 (2017).

[1432] J. Yelton *et al.* (Belle Collaboration), Observation of excited Ω_c charmed baryons in e^+e^- collisions, Phys. Rev. D **97**, 051102 (2018).

[1433] R. Aaij *et al.* (LHCb Collaboration), Observation of excited Ω_c^0 baryons in $\Omega_b^- \to \Xi_c^+K^-\pi^-$ decays, Phys. Rev. D **104**, L091102 (2021).

[1434] R. Aaij *et al.* (LHCb Collaboration), Observation of new Ω_c^0 states decaying to the $\Xi_c^+K^-$ final state, Phys. Rev. Lett. **131**, 131902 (2023).

[1435] R. Aaij *et al.* (LHCb Collaboration), First branching fraction measurement of the suppressed decay $\Xi_c^0 \to \pi^-\Lambda_c^+$, Phys. Rev. D **102**, 071101 (2020).

[1436] G. Burdman, E. Golowich, J. L. Hewett, and S. Pakvasa, Rare charm decays in the Standard Model and beyond, Phys. Rev. D **66**, 014009 (2002).

[1437] S. Fajfer, A. Prapotnik, S. Prelovšek, P. Singer, and J. Zupan, The rare decays of D mesons, Nucl. Phys. B, Proc. Suppl. **115**, 93 (2003).

[1438] S. Fajfer, N. Kosnik, and S. Prelovsek, Updated constraints on new physics in rare charm decays, Phys. Rev. D **76**, 074010 (2007).

[1439] E. Golowich, J. Hewett, S. Pakvasa, and A. A. Petrov, Relating $D^0 - \bar{D}^0$ mixing and $D^0 \to \ell^+\ell^-$ with new physics, Phys. Rev. D **79**, 114030 (2009).

[1440] A. Paul, I. I. Bigi, and S. Recksiegel, $D^0 \to \gamma\gamma$ and $D^0 \to \mu^+\mu^-$ rates on an unlikely impact of the littlest Higgs model with T-parity, Phys. Rev. D **82**, 094006 (2010); **83**, 019901(E) (2011).

[1441] A. V. Borisov, Lepton-number violating meson decays in theories beyond the standard model, arXiv:1112.3269.

[1442] R.-M. Wang, J.-H. Sheng, J. Zhu, Y.-Y. Fan, and Y. Gao, Studying the lepton number and lepton flavor violating $D^0 \to e^{\pm}\mu^{\mp}$ and $D_{d/s}^+ \to \pi(K)^+e^{\pm}\mu^{\mp}$ decays, Int. J. Mod. Phys. A **29**, 1450169 (2014).

[1443] S. de Boer and G. Hiller, Flavor and new physics opportunities with rare charm decays into leptons, Phys. Rev. D **93**, 074001 (2016).

[1444] S. Fajfer and N. Košnik, Prospects of discovering new physics in rare charm decays, Eur. Phys. J. C **75**, 567 (2015).

[1445] S. Sahoo and R. Mohanta, New physics effects in charm meson decays involving $c \to ul^+l^-(l_i^{\mp}l_j^{\pm})$ transitions, Eur. Phys. J. C **77**, 344 (2017).

[1446] S. de Boer and G. Hiller, Rare radiative charm decays within the standard model and beyond, J. High Energy Phys. 08 (2017) 091.

[1447] S. De Boer and G. Hiller, Null tests from angular distributions in $D \to P_1P_2l^+l^-$, $l = e, \mu$ decays on and off peak, Phys. Rev. D **98**, 035041 (2018).

[1448] R. Bause, M. Golz, G. Hiller, and A. Tayduganov, The new physics reach of null tests with $D \to \pi\ell\ell$ and

$D_s \to K\ell\ell$ decays, Eur. Phys. J. C **80**, 65 (2020); **81**, 219 (E) (2021).

[1449] R. Bause, H. Gisbert, M. Golz, and G. Hiller, Rare charm $c \to u\nu\bar{\nu}$ dineutrino null tests for e^+e^- machines, Phys. Rev. D **103**, 015033 (2021).

[1450] B. Bhattacharya, C. M. Grant, and A. A. Petrov, Invisible widths of heavy mesons, Phys. Rev. D **99**, 093010 (2019).

[1451] S. Fajfer and A. Novosel, Coloured scalars mediated rare charm meson decays to invisible fermions, Phys. Rev. D **104**, 015014 (2021).

[1452] T. E. Coan *et al.* (CLEO Collaboration), First search for the flavor changing neutral current decay $D^0 \to \gamma\gamma$, Phys. Rev. Lett. **90**, 101801 (2003).

[1453] M. Ablikim *et al.* (BESIII Collaboration), Search for $D^0 \to \gamma\gamma$ and improved measurement of the branching fraction for $D^0 \to \pi^0\pi^0$, Phys. Rev. D **91**, 112015 (2015).

[1454] J. P. Lees *et al.* (*BABAR* Collaboration), Search for the decay $D^0 \to \gamma\gamma$ and measurement of the branching fraction for $D^0 \to \pi^0\pi^0$, Phys. Rev. D **85**, 091107 (2012).

[1455] N. K. Nisar *et al.* (Belle Collaboration), Search for the rare decay $D^0 \to \gamma\gamma$ at Belle, Phys. Rev. D **93**, 051102 (2016).

[1456] P. Haas *et al.* (CLEO Collaboration), Upper limits on charm changing neutral current interactions, Phys. Rev. Lett. **60**, 1614 (1988).

[1457] H. Albrecht *et al.* (ARGUS Collaboration), Search for D^0 decays into lepton pairs, Phys. Lett. B **209**, 380 (1988).

[1458] J. Adler *et al.* (MARK-III Collaboration), A search for the decay $D^0 \to e^+e^-$, Phys. Rev. D **37**, 2023 (1988); **40**, 3788(E) (1989).

[1459] A. Freyberger *et al.* (CLEO Collaboration), Limits on flavor changing neutral currents in D^0 meson decays, Phys. Rev. Lett. **76**, 3065 (1996).

[1460] D. Pripstein *et al.* (Fermilab E789 Collaboration), Search for flavor changing neutral currents and lepton family number violation in two-body D^0 decays, Phys. Rev. D **61**, 032005 (2000).

[1461] E. M. Aitala *et al.* (Fermilab E791 Collaboration), Search for rare and forbidden dilepton decays of the D^+, D_s^+, and D^0 charmed mesons, Phys. Lett. B **462**, 401 (1999).

[1462] B. Aubert *et al.* (*BABAR* Collaboration), Search for flavor-changing neutral current and lepton flavor violating decays of $D^0 \to \ell^+\ell^-$, Phys. Rev. Lett. **93**, 191801 (2004).

[1463] M. Petric *et al.* (Belle Collaboration), Search for leptonic decays of D^0 mesons, Phys. Rev. D **81**, 091102 (2010).

[1464] K. Kodama *et al.* (Fermilab E653 Collaboration), Upper limits of charm hadron decays to two muons plus hadrons, Phys. Lett. B **345**, 85 (1995).

[1465] I. Abt *et al.* (HERA-B Collaboration), Search for the flavor changing neutral current decay $D^0 \to \mu^+\mu^-$ with the HERA-B detector, Phys. Lett. B **596**, 173 (2004).

[1466] T. Aaltonen *et al.* (CDF Collaboration), Updated search for the flavor-changing neutral-current decay $D^0 \to \mu^+\mu^-$, Phys. Rev. D **82**, 091105 (2010).

[1467] R. Aaij *et al.* (LHCb Collaboration), Search for rare decays of D0 mesons into two muons, Phys. Rev. Lett. **131**, 041804 (2023).

[1468] M. Ablikim *et al.* (BESIII Collaboration), Search for the rare decays $D \to h(h')e^+e^-$, Phys. Rev. D **97**, 072015 (2018).

[1469] E. M. Aitala *et al.* (Fermilab E791 Collaboration), Search for rare and forbidden charm meson decays $D^0 \to V\ell^+\ell^-$ and $hh\ell\ell$, Phys. Rev. Lett. **86**, 3969 (2001).

[1470] R. Aaij *et al.* (LHCb Collaboration), Observation of D^0 meson decays to $\pi^+\pi^-\mu^+\mu^-$ and $K^+K^-\mu^+\mu^-$ final states, Phys. Rev. Lett. **119**, 181805 (2017).

[1471] J. Adler *et al.* (MARK-III Collaboration), A search for the decay $D^0 \to \bar{K}^0e^+e^-$, Phys. Rev. D **40**, 906 (1989).

[1472] J. P. Lees *et al.* (*BABAR* Collaboration), Observation of the decay $D^0 \to K^-\pi^+e^+e^-$, Phys. Rev. Lett. **122**, 081802 (2019).

[1473] R. Aaij *et al.* (LHCb Collaboration), First observation of the decay $D^0 \to K^-\pi^+\mu^+\mu^-$ in the $\rho^0 - \omega$ region of the dimuon mass spectrum, Phys. Lett. B **757**, 558 (2016).

[1474] M. Ablikim *et al.* (BESIII Collaboration), Search for the decay $D^0 \to \pi^0\nu\bar{\nu}$, Phys. Rev. D **105**, L071102 (2022).

[1475] D. M. Asner *et al.* (CLEO Collaboration), Radiative decay modes of the D^0 meson, Phys. Rev. D **58**, 092001 (1998).

[1476] B. Aubert *et al.* (*BABAR* Collaboration), Measurement of the branching fractions of the radiative charm decays $D^0 \to \bar{K} * 0\gamma$ and $D^0 \to \phi\gamma$, Phys. Rev. D **78**, 071101 (2008).

[1477] Y.-T. Lai *et al.* (Belle Collaboration), Search for D^0 decays to invisible final states at Belle, Phys. Rev. D **95**, 011102 (2017).

[1478] J. Becker *et al.* (MARK-III Collaboration), A search for the lepton family number violating decay $D^0 \to \mu e$, Phys. Lett. B **193**, 147 (1987).

[1479] R. Aaij *et al.* (LHCb Collaboration), Search for the lepton-flavour violating decay $D^0 \to e^\pm\mu^\mp$, Phys. Lett. B **754**, 167 (2016).

[1480] J. P. Lees *et al.* (*BABAR* Collaboration), Search for lepton-flavor-violating decays $D^0 \to X^0e^\pm\mu^\mp$, Phys. Rev. D **101**, 112003 (2020).

[1481] J. P. Lees *et al.* (*BABAR* Collaboration), Search for rare or forbidden decays of the D^0 meson, Phys. Rev. Lett. **124**, 071802 (2020).

[1482] M. Ablikim *et al.* (BESIII Collaboration), Search for heavy Majorana neutrino in lepton number violating decays of $D \to K\pi e^+e^+$, Phys. Rev. D **99**, 112002 (2019).

[1483] P. Rubin *et al.* (CLEO Collaboration), Search for $D^0 \to \bar{p}e^+$ and $D^0 \to pe^-$, Phys. Rev. D **79**, 097101 (2009).

[1484] M. Ablikim *et al.* (BESIII Collaboration), Search for baryon- and lepton-number violating decays $D^0 \to \bar{p}e^+$ and $D^0 \to pe^-$, Phys. Rev. D **105**, 032006 (2022).

[1485] P. L. Frabetti *et al.* (Fermilab E687 Collaboration), Search for rare and forbidden decays of the charmed meson D^+, Phys. Lett. B **398**, 239 (1997).

[1486] P. Rubin *et al.* (CLEO Collaboration), Search for rare and forbidden decays of charm and charmed-strange mesons to final states $h^+ - e^- + e^+$, Phys. Rev. D **82**, 092007 (2010).

[1487] R. Aaij *et al.* (LHCb Collaboration), Searches for 25 rare and forbidden decays of D^+ and D_s^+ mesons, J. High Energy Phys. 06 (2021) 44.

[1488] J. P. Lees *et al.* (*BABAR* Collaboration), Searches for rare or forbidden semileptonic charm decays, Phys. Rev. D **84**, 072006 (2011).

[1489] J. M. Link *et al.* (FOCUS Collaboration), Search for rare and forbidden three body dimuon decays of the charmed mesons D^+ and $D_s{}^+$, Phys. Lett. B **572**, 21 (2003).

[1490] V. M. Abazov *et al.* (D0 Collaboration), Search for flavor-changing-neutral-current D meson decays, Phys. Rev. Lett. **100**, 101801 (2008).

[1491] M. Ablikim *et al.* (BESIII Collaboration), Search for the decay $D_s^+ \to \gamma e^+ \nu_e$, Phys. Rev. D **99**, 072002 (2019).

[1492] D. N. Shemyakin (CMD-3 collaboration), Search for the process $e^+e^- \to D^*(2007)^0$ with the CMD-3 detector, Phys. At. Nucl. **83**, 954 (2020).

[1493] R. Aaij *et al.* (LHCb Collaboration), Search for $D^*(2007)^0 \to \mu^+\mu^-$ in $B^- \to \pi^-\mu^+\mu^-$ decays, Eur. Phys. J. C **83**, 666 (2023).

[1494] M. Ablikim *et al.* (BESIII Collaboration), First experimental study of the purely leptonic decay $D_s^{*+} \to e^+\nu e$, Phys. Rev. Lett. **131**, 141802 (2023).

[1495] R. Aaij *et al.* (LHCb Collaboration), Search for the rare decay $\Lambda_c^+ \to p\mu^+\mu^-$, Phys. Rev. D **97**, 091101 (2018).

[1496] R. Aaij *et al.* (LHCb Collaboration), Search for the decay $D^0 \to \pi^+\pi^-\mu^+\mu^-$, Phys. Lett. B **728**, 234 (2014).

[1497] R. Aaij *et al.* (LHCb Collaboration), Search for $D_{(s)}^+ \to \pi^+\mu^+\mu^-$ and $D_{(s)}^+ \to \pi^-\mu^+\mu^+$ decays, Phys. Lett. B **724**, 203 (2013).

[1498] M. Davier, A. Hocker, and Z. Zhang, The physics of hadronic tau decays, Rev. Mod. Phys. **78**, 1043 (2006).

[1499] I. Adachi *et al.* (Belle-II Collaboration), Test of light-lepton universality in τ decays with the Belle II experiment, J. High Energy Phys. 08 (2024) 205.

[1500] A. Hayrapetyan *et al.* (CMS Collaboration), Search for the lepton flavor violating $\tau \to 3\mu$ decay in proton-proton collisions at $\sqrt{s} = 13$ TeV, Phys. Lett. B **853**, 138633 (2024).

[1501] I. Adachi *et al.* (Belle-II Collaboration), Search for lepton-flavor-violating $\tau \to \mu\mu\mu$ decays at Belle II, J. High Energy Phys. 09 (2024) 062.

[1502] I. Adachi *et al.* (Belle-II Collaboration), Search for the baryon number and lepton number violating decays $\tau^- \to \Lambda\pi^-$ and $\tau^- \to \bar{\Lambda}\pi^-$ at Belle II, Phys. Rev. D **110**, 112003 (2024).

[1503] I. Adachi *et al.* (Belle II Collaboration), Measurement of the τ-lepton mass with the Belle II experiment, Phys. Rev. D **108**, 032006 (2023).

[1504] V. V. Anashin *et al.*, Experiments with the KEDR detector at the e^+e^- collider VEPP-4M in the energy range $\sqrt{s} = 1.84$–3.88 GeV, Phys. Part. Nucl. **54**, 185 (2023).

[1505] Heavy Flavor Averaging Group, HFLAV Tau averages, Zenodo, 10.5281/zenodo.13989054 (2024).

[1506] H. Albrecht *et al.* (ARGUS Collaboration), A measurement of the τ mass, Phys. Lett. B **292**, 221 (1992).

[1507] B. Aubert *et al.* (*BABAR* Collaboration), Measurements of the τ mass and the mass difference of the τ^+ and τ^- at *BABAR*, Phys. Rev. D **80**, 092005 (2009).

[1508] K. Abe *et al.* (Belle Collaboration), Measurement of the mass of the tau-lepton and an upper limit on the mass difference between τ^+ and τ^-, Phys. Rev. Lett. **99**, 011801 (2007).

[1509] J. Z. Bai *et al.* (BES Collaboration), Measurement of the mass of the τ lepton, Phys. Rev. D **53**, 20 (1996).

[1510] M. Ablikim *et al.* (BESIII Collaboration), Precision measurement of the mass of the τ lepton, Phys. Rev. D **90**, 012001 (2014).

[1511] A. Anastassov *et al.* (CLEO Collaboration), Experimental test of lepton universality in τ decay, Phys. Rev. D **55**, 2559 (1997); **58**, 119903(E) (1998).

[1512] W. Bacino *et al.*, Measurement of the threshold behavior of $\tau^+\tau^-$ production in e^+e^- annihilation, Phys. Rev. Lett. **41**, 13 (1978).

[1513] G. Abbiendi *et al.* (OPAL Collaboration), A measurement of the τ mass and the first CPT test with τ leptons, Phys. Lett. B **492**, 23 (2000).

[1514] R. Barate *et al.* (ALEPH Collaboration), Updated measurement of the τ lepton lifetime, Phys. Lett. B **414**, 362 (1997).

[1515] K. Belous *et al.* (Belle Collaboration), Measurement of the τ-lepton lifetime at Belle, Phys. Rev. Lett. **112**, 031801 (2014).

[1516] R. Balest *et al.* (CLEO Collaboration), Measurement of the τ lepton lifetime, Phys. Lett. B **388**, 402 (1996).

[1517] J. Abdallah *et al.* (DELPHI Collaboration), A precise measurement of the τ lifetime, Eur. Phys. J. C **36**, 283 (2004).

[1518] M. Acciarri *et al.* (L3 Collaboration), Measurement of the lifetime of the τ lepton, Phys. Lett. B **479**, 67 (2000).

[1519] G. Alexander *et al.* (OPAL Collaboration), Improved measurement of the lifetime of the τ lepton, Phys. Lett. B **374**, 341 (1996).

[1520] S. Schael *et al.* (ALEPH Collaboration), Branching ratios and spectral functions of τ decays: Final ALEPH measurements and physics implications, Phys. Rep. **421**, 191 (2005).

[1521] S. Banerjee, D. Biswas, T. Przedzinski, and Z. Was, Monte Carlo event generator updates, for τ pair events at Belle II energies, in *Proceedings of the 16th International Workshop on Tau Lepton Physics* (2021), arXiv:2111.05914.

[1522] P. Abreu *et al.* (DELPHI Collaboration), Measurements of the leptonic branching fractions of the τ, Eur. Phys. J. C **10**, 201 (1999).

[1523] M. Acciarri *et al.* (L3 Collaboration), Measurement of the τ branching fractions into leptons, Phys. Lett. B **507**, 47 (2001).

[1524] G. Abbiendi *et al.* (OPAL Collaboration), A measurement of the $\tau^- \to \mu^-\bar{\nu}_\mu\nu_\tau$ branching ratios, Phys. Lett. B **551**, 35 (2003).

[1525] H. Albrecht *et al.* (ARGUS Collaboration), Measurement of exclusive one prong and inclusive three prong branching ratios of the τ lepton, Z. Phys. C **53**, 367 (1992).

[1526] B. Aubert *et al.* (*BABAR* Collaboration), Measurements of charged current lepton universality and $|V_{us}|$ using tau lepton decays to $e^-\bar{\nu}_e\nu_\tau$, $\mu^-\bar{\nu}_\mu\nu_\tau$, $\pi^-\nu_\tau$ and $K^-\nu_\tau$, Phys. Rev. Lett. **105**, 051602 (2010).

[1527] G. Abbiendi *et al.* (OPAL Collaboration), A measurement of the $\tau^- \to e^-\bar{\nu}_e\nu_\tau$ branching ratio, Phys. Lett. B **447**, 134 (1999).

[1528] P. Abreu *et al.* (DELPHI Collaboration), A study of the decays of τ leptons produced on the Z resonance at LEP, Z. Phys. C **55**, 555 (1992).

[1529] M. Acciarri *et al.* (L3 Collaboration), Measurement of exclusive branching fractions of hadronic one space prong τ decays, Phys. Lett. B **345**, 93 (1995).

[1530] G. Alexander *et al.* (OPAL Collaboration), Measurement of branching ratios and τ polarization from $\tau \to e\nu\bar{\nu}$, $\tau \to \mu\nu\bar{\nu}$, and $\tau \to \pi(K)\nu$ decays at LEP, Phys. Lett. B **266**, 201 (1991).

[1531] J. Abdallah *et al.* (DELPHI Collaboration), A measurement of the τ hadronic branching ratios, Eur. Phys. J. C **46**, 1 (2006).

[1532] K. Ackerstaff *et al.* (OPAL Collaboration), Measurement of the one prong hadronic τ branching ratios at LEP, Eur. Phys. J. C **4**, 193 (1998).

[1533] R. Barate *et al.* (ALEPH Collaboration), One-prong τ decays with kaons, Eur. Phys. J. C **10**, 1 (1999).

[1534] M. Battle *et al.* (CLEO Collaboration), Measurement of Cabibbo suppressed decays of the τ lepton, Phys. Rev. Lett. **73**, 1079 (1994).

[1535] P. Abreu *et al.* (DELPHI Collaboration), Charged kaon production in τ decays at LEP, Phys. Lett. B **334**, 435 (1994).

[1536] G. Abbiendi *et al.* (OPAL Collaboration), A study of one-prong τ decays with a charged kaon, Eur. Phys. J. C **19**, 653 (2001).

[1537] M. Fujikawa *et al.* (Belle Collaboration), High-statistics study of the $\tau^- \to \pi^-\pi^0\nu_\tau$ decay, Phys. Rev. D **78**, 072006 (2008).

[1538] M. Artuso *et al.* (CLEO Collaboration), A measurement of the branching fraction $B(\tau^- \to h^-\pi^0\nu_\tau)$, Phys. Rev. Lett. **72**, 3762 (1994).

[1539] B. Aubert *et al.* (*BABAR* Collaboration), Measurement of the $\tau^- \to K^-\pi^0\nu_\tau$ branching fraction, Phys. Rev. D **76**, 051104 (2007).

[1540] G. Abbiendi *et al.* (OPAL Collaboration), Measurement of the strange spectral function in hadronic τ decays, Eur. Phys. J. C **35**, 437 (2004).

[1541] M. Procario *et al.* (CLEO Collaboration), Tau decays with one charged particle plus multiple π^0's, Phys. Rev. Lett. **70**, 1207 (1993).

[1542] R. Barate *et al.* (ALEPH Collaboration), K_S^0 production in τ decays, Eur. Phys. J. C **4**, 29 (1998).

[1543] R. Akers *et al.* (OPAL Collaboration), Measurements of the inclusive branching ratios of τ leptons to K_S^0 and charged $K^*(892)$, Phys. Lett. B **339**, 278 (1994).

[1544] T. E. Coan *et al.* (CLEO Collaboration), Decays of τ leptons to final states containing K_S^0 mesons, Phys. Rev. D **53**, 6037 (1996).

[1545] S. Ryu *et al.* (Belle Collaboration), Measurements of branching fractions of τ lepton decays with one or more K_S^0, Phys. Rev. D **89**, 072009 (2014).

[1546] M. Acciarri *et al.* (L3 Collaboration), One prong τ decays with neutral kaons, Phys. Lett. B **352**, 487 (1995).

[1547] G. Abbiendi *et al.* (OPAL Collaboration), Tau decays with neutral kaons, Eur. Phys. J. C **13**, 213 (2000).

[1548] J. P. Lees *et al.* (*BABAR* Collaboration), Measurement of the spectral function for the $\tau^- \to K^-K_S\nu_\tau$ decay, Phys. Rev. D **98**, 032010 (2018).

[1549] R. Barate *et al.* (ALEPH Collaboration), Study of τ decays involving kaons, spectral functions and determination of the strange quark mass, Eur. Phys. J. C **11**, 599 (1999).

[1550] J. P. Lees *et al.* (*BABAR* Collaboration), The branching fraction of $\tau^- \to \pi^-K_S^0K_S^0(\pi^0)\nu_\tau$ decays, Phys. Rev. D **86**, 092013 (2012).

[1551] H. J. Behrend *et al.* (CELLO Collaboration), Tau production and decay with the CELLO detector at PETRA, Phys. Lett. B **222**, 163 (1989).

[1552] B. Adeva, O. Adriani, M. Aguilar-Benitez, H. Akbari, J. Alcaraz, A. Aloisio, G. Alverson, M. G. Alviggi, and G. Ambrosi (L3 Collaboration), Decay properties of τ leptons measured at the Z^0 resonance, Phys. Lett. B **265**, 451 (1991).

[1553] H. Aihara *et al.* (TPC/Two Gamma Collaboration), Measurement of τ branching ratios, Phys. Rev. D **35**, 1553 (1987).

[1554] P. Achard *et al.* (L3 Collaboration), Measurement of the topological branching fractions of the τ lepton at LEP, Phys. Lett. B **519**, 189 (2001).

[1555] R. Akers *et al.* (OPAL Collaboration), Measurement of the $\tau^- \to h^-h^+h^-\nu_\tau$ and $\tau^- \to h^-h^+h^- \geq 1\pi^0\nu_\tau$ branching ratios, Z. Phys. C **68**, 555 (1995).

[1556] R. Balest *et al.* (CLEO Collaboration), Measurements of the decays $\tau^- \to h^-h^+h^-\nu_\tau$ and $\tau^- \to h^-h^+h^-\pi^0\nu_\tau$, Phys. Rev. Lett. **75**, 3809 (1995).

[1557] B. Aubert *et al.* (*BABAR* Collaboration), Exclusive branching fraction measurements of semileptonic τ decays into three charged hadrons, $\tau^- \to \phi\pi^-\nu_\tau$ and $\tau^- \to \phi K^-\nu_\tau$, Phys. Rev. Lett. **100**, 011801 (2008).

[1558] M. J. Lee *et al.* (Belle Collaboration), Measurement of the branching fractions and the invariant mass distributions for $\tau^- \to h^-h^+h^-\nu_\tau$ decays, Phys. Rev. D **81**, 113007 (2010).

[1559] R. A. Briere *et al.* (CLEO Collaboration), Branching fractions of τ leptons decays to three charged hadrons, Phys. Rev. Lett. **90**, 181802 (2003).

[1560] K. W. Edwards *et al.* (CLEO Collaboration), Resonant structure of $\tau \to 3\pi\pi^0\nu_\tau$ and $\tau \to \omega\pi\nu_\tau$ decays, Phys. Rev. D **61**, 072003 (2000).

[1561] D. Bortoletto *et al.* (CLEO Collaboration), Measurement of the decay $\tau^- \to \pi^-\pi^+\pi^-2\pi^0\nu_\tau$, Phys. Rev. Lett. **71**, 1791 (1993).

[1562] A. Anastassov *et al.* (CLEO Collaboration), Study of τ decays to six pions and neutrino, Phys. Rev. Lett. **86**, 4467 (2001).

[1563] S. J. Richichi *et al.* (CLEO Collaboration), Study of 3-prong hadronic τ decays with charged kaons, Phys. Rev. D **60**, 112002 (1999).

[1564] D. A. Bauer *et al.* (TPC/Two Gamma Collaboration), Measurement of the kaon content of three-prong τ decays, Phys. Rev. D **50**, R13 (1994).

[1565] R. Barate *et al.* (ALEPH Collaboration), Three-prong τ decays with charged kaons, Eur. Phys. J. C **1**, 65 (1998).

[1566] K. Arms *et al.* (CLEO Collaboration), Study of τ decays to four-hadron final states with kaons, Phys. Rev. Lett. **94**, 241802 (2005).

[1567] G. Abbiendi *et al.* (OPAL Collaboration), A study of three-prong τ decays with charged kaons, Eur. Phys. J. C **13**, 197 (2000).

[1568] D. Gibaut *et al.* (CLEO Collaboration), Study of the five charged pion decay of the τ lepton, Phys. Rev. Lett. **73**, 934 (1994).

[1569] B. G. Bylsma *et al.*, Limit on τ decay to seven charged particles, Phys. Rev. D **35**, 2269 (1987).

[1570] H. Albrecht *et al.* (ARGUS Collaboration), An improved upper limit on the τ-neutrino mass from the decay $\tau^- \to \pi^-\pi^-\pi^-\pi^+\pi^+\nu_\tau$, Phys. Lett. B **202**, 149 (1988).

[1571] K. Ackerstaff *et al.* (OPAL Collaboration), Measurement of τ branching ratios to five charged hadrons, Eur. Phys. J. C **8**, 183 (1999).

[1572] D. Buskulic *et al.* (ALEPH Collaboration), A study of τ decays involving η and omega mesons, Z. Phys. C **74**, 263 (1997).

[1573] K. Inami *et al.* (Belle Collaboration), Precise measurement of hadronic τ-decays with an η meson, Phys. Lett. B **672**, 209 (2009).

[1574] M. Artuso *et al.* (CLEO Collaboration), Measurement of τ decays involving η mesons, Phys. Rev. Lett. **69**, 3278 (1992).

[1575] P. del Amo Sanchez *et al.* (*BABAR* Collaboration), Studies of $\tau^- \to \eta K^-\nu_\tau$ and $\tau^- \to \eta\pi^-\nu_\tau$ at *BABAR* and a search for a second-class current, Phys. Rev. D **83**, 032002 (2011).

[1576] J. E. Bartelt *et al.* (CLEO Collaboration), First observation of the decay $\tau^- \to K^-\eta\nu_\tau$, Phys. Rev. Lett. **76**, 4119 (1996).

[1577] M. Bishai *et al.* (CLEO Collaboration), First observation of the decay $\tau^- \to K^{*-}\eta\nu_\tau$, Phys. Rev. Lett. **82**, 281 (1999).

[1578] P. S. Baringer *et al.* (CLEO Collaboration), Production of η and ω mesons in τ decay and a search for second class currents, Phys. Rev. Lett. **59**, 1993 (1987).

[1579] D. Buskulic *et al.* (ALEPH Collaboration), Tau hadronic branching ratios, Z. Phys. C **70**, 579 (1996).

[1580] J. P. Lees *et al.* (*BABAR* Collaboration), Study of high-multiplicity 3-prong and 5-prong τ decays at *BABAR*, Phys. Rev. D **86**, 092010 (2012).

[1581] Y. Amhis *et al.*, Averages of b-hadron, c-hadron, and τ-lepton properties as of summer 2014, arXiv:1412.7515.

[1582] W. J. Marciano and A. Sirlin, Electroweak radiative corrections to τ decay, Phys. Rev. Lett. **61**, 1815 (1988).

[1583] A. Ferroglia, C. Greub, A. Sirlin, and Z. Zhang, Contributions of the W-boson propagator to μ and τ leptonic decay rates, Phys. Rev. D **88**, 033012 (2013).

[1584] M. Fael, L. Mercolli, and M. Passera, W-propagator corrections to μ and τ leptonic decays, Phys. Rev. D **88**, 093011 (2013).

[1585] E. Tiesinga, P. J. Mohr, D. B. Newell, and B. N. Taylor, CODATA recommended values of the fundamental physical constants: 2018, Rev. Mod. Phys. **93**, 025010 (2021), Database developed by J. Baker, M. Douma, and S. Kotochigova. Available at http://physics.nist.gov/constants, National Institute of Standards and Technology, Gaithersburg, MD 20899.

[1586] A. Pich, Precision tau physics, Prog. Part. Nucl. Phys. **75**, 41 (2014).

[1587] M. A. Arroyo-Ureña, G. Hernández-Tomé, G. López-Castro, P. Roig, and I. Rosell, Radiative corrections to $\tau \to \pi(K)\nu_\tau[\gamma]$: A reliable new physics test, Phys. Rev. D **104**, L091502 (2021).

[1588] M. Antonelli *et al.*, An evaluation of $|V_{us}|$ and precise tests of the standard model from world data on leptonic and semileptonic kaon decays, Eur. Phys. J. C **69**, 399 (2010).

[1589] V. Cirigliano, A. Crivellin, M. Hoferichter, and M. Moulson, Scrutinizing CKM unitarity with a new measurement of the $K_{\mu3}/K_{\mu2}$ branching fraction, Phys. Lett. B **838**, 137748 (2023).

[1590] E. Gámiz, J. Prades, M. Jamin, F. Schwab, and A. Pich, Determination of m_s and $|V_{us}|$ from hadronic tau decays, J. High Energy Phys. 01 (2003) 060.

[1591] E. Gamiz, M. Jamin, A. Pich, J. Prades, and F. Schwab, $|V_{us}|$ and m_s from hadronic τ decays, Phys. Rev. Lett. **94**, 011803 (2005).

[1592] E. Gamiz, M. Jamin, A. Pich, J. Prades, and F. Schwab, $|V_{us}|$ and m_s from hadronic τ decays, Nucl. Phys. Proc. Suppl. **169**, 85 (2007).

[1593] E. Gamiz *et al.*, Theoretical progress on the V_{us} determination from τ decays, Proc. Sci., KAON2008 (**2008**) 008 [arXiv:0709.0282].

[1594] K. Maltman, A critical look at V_{us} determinations from hadronic τ decay data, Nucl. Phys. Proc. Suppl. **218**, 146 (2011).

[1595] R. J. Hudspith, R. Lewis, K. Maltman, and J. Zanotti, A resolution of the inclusive flavor-breaking $\tau|V_{us}|$ puzzle, Phys. Lett. B **781**, 206 (2018).

[1596] P. Boyle, R. James Hudspith, T. Izubuchi, A. Jüttner, C. Lehner, R. Lewis, K. Maltman, H. Ohki, A. Portelli, and M. Spraggs (RBC and UKQCD Collaborations), Novel $|V_{us}|$ determination using inclusive strange τ decay and lattice hadronic vacuum polarization functions, Phys. Rev. Lett. **121**, 202003 (2018).

[1597] K. Maltman *et al.*, A resolution of the inclusive flavor-breaking sum rule τV_{us} puzzle, Proc. Sci. LATTICE2015 (**2016**) 260 [arXiv:1510.06954].

[1598] K. Maltman *et al.*, Current Status of inclusive hadronic τ determinations of $|V_{us}|$, SciPost Phys. Proc. **1**, 006 (2019).

[1599] C. Alexandrou *et al.* (Extended Twisted Mass Collaboration), Inclusive hadronic decay rate of the τ lepton from lattice QCD: The $\overline{us}$ flavor channel and the Cabibbo angle, Phys. Rev. Lett. **132**, 261901 (2024).

[1600] D. Asner *et al.*, Averages of b-hadron, c-hadron, and τ-lepton properties, arXiv:1010.1589.

[1601] S. Banerjee (*BABAR* Collaboration), Lepton universality, $|V_{us}|$ and search for second class current in τ decays, in *Proceedings of the 34th International Conference on High Energy Physics* (2008), arXiv:0811.1429.

[1602] Y. Aoki *et al.*, FLAG review 2021, arXiv:2111.09849.

[1603] S. Aoki *et al.*, Flag review 2023 web update, http://flag.unibe.ch/2021/Media?-action=AttachFile&do=get&target=FLAG_2023_webupdate.pdf (2023).

[1604] C. Alexandrou *et al.* (Extended Twisted Mass Collaboration), Ratio of kaon and pion leptonic decay constants with $N_f = 2 + 1 + 1$ Wilson-clover twisted-mass fermions, Phys. Rev. D **104**, 074520 (2021).

[1605] N. Miller *et al.*, F_K/F_π from Möbius domain-wall fermions solved on gradient-flowed HISQ ensembles, Phys. Rev. D **102**, 034507 (2020).

[1606] R. J. Dowdall, C. T. H. Davies, G. P. Lepage, and C. McNeile (HPQCD Collaboration), V_{us} from π and K decay constants in full lattice QCD with physical u, d, s and c quarks, Phys. Rev. D **88**, 074504 (2013).

[1607] A. Bazavov *et al.* (Fermilab Lattice and MILC Collaborations), Charmed and light pseudoscalar meson decay constants from four-flavor lattice QCD with physical light quarks, Phys. Rev. D **90**, 074509 (2014).

[1608] M. Davier, S. Eidelman, A. Hocker, and Z. Zhang, Confronting spectral functions from e^+e^- annihilation and tau decays: Consequences for the muon magnetic moment, Eur. Phys. J. C **27**, 497 (2003).

[1609] M. Davier, A. Hoecker, A.-M. Lutz, B. Malaescu, and Z. Zhang, Tensions in $e^+e^- \to \pi^+\pi^-(\gamma)$ measurements: The new landscape of data-driven hadronic vacuum polarization predictions for the muon $g-2$, Eur. Phys. J. C **84**, 721 (2024).

[1610] M. Jamin, A. Pich, and J. Portoles, What can be learned from the Belle spectrum for the decay $\tau^- \to \nu_\tau K_S \pi^-$, Phys. Lett. B **664**, 78 (2008).

[1611] M. Antonelli, V. Cirigliano, A. Lusiani, and E. Passemar, Predicting the τ strange branching ratios and implications for V_{us}, J. High Energy Phys. 10 (2013) 070.

[1612] B. W. Lee and R. E. Shrock, Natural suppression of symmetry violation in gauge theories: Muon—lepton and electron lepton number nonconservation, Phys. Rev. D **16**, 1444 (1977).

[1613] S. T. Petcov, The processes $\mu \to e+\gamma, \mu \to e+\bar{e},\nu' \to \nu+\gamma$ in the Weinberg-Salam model with neutrino mixing, Yad. Fiz. **25**, 1336(E) (1977); **25**, 340 (1977); **25**, 698 (E) (1977).

[1614] G. Hernández-Tomé, G. López Castro, and P. Roig, Flavor violating leptonic decays of τ and μ leptons in the standard model with massive neutrinos, Eur. Phys. J. C **79**, 84 (2019); **80**, 438(E) (2020).

[1615] P. Blackstone, M. Fael, and E. Passemar, $\tau \to \mu\mu\mu$ at a rate of one out of 10^{14} tau decays?, Eur. Phys. J. C **80**, 506 (2020).

[1616] A. Ilakovac and A. Pilaftsis, Flavor violating charged lepton decays in seesaw-type models, Nucl. Phys. **B437**, 491 (1995).

[1617] M. Raidal *et al.*, Flavour physics of leptons and dipole moments, Eur. Phys. J. C **57**, 13 (2008).

[1618] A. de Gouvea and P. Vogel, Lepton flavor and number conservation, and physics beyond the standard model, Prog. Part. Nucl. Phys. **71**, 75 (2013).

[1619] I. Doršner, S. Fajfer, A. Greljo, J. F. Kamenik, and N. Košnik, Physics of leptoquarks in precision experiments and at particle colliders, Phys. Rep. **641**, 1 (2016).

[1620] M. Ardu and G. Pezzullo, Introduction to charged lepton flavor violation, Universe **8**, 299 (2022).

[1621] R. Aaij *et al.* (LHCb Collaboration), Search for the lepton flavour violating decay $\tau^- \to \mu^-\mu^+\mu^-$, J. High Energy Phys. 02 (2015) 121.

[1622] B. Aubert *et al.* (*BABAR* Collaboration), Searches for lepton flavor violation in the decays $\tau^\pm \to e^\pm\gamma$ and $\tau^\pm \to \mu^\pm\gamma$, Phys. Rev. Lett. **104**, 021802 (2010).

[1623] A. Abdesselam *et al.* (Belle Collaboration), Search for lepton-flavor-violating tau-lepton decays to $\ell\gamma$ at Belle, J. High Energy Phys. 10 (2021) 19.

[1624] B. Aubert *et al.* (*BABAR* Collaboration), Search for lepton flavor violating decays $\tau^\pm \to \ell^\pm\pi^0$, $\ell^\pm\eta$, $\ell^\pm\eta'$, Phys. Rev. Lett. **98**, 061803 (2007).

[1625] Y. Miyazaki *et al.* (Belle Collaboration), Search for lepton flavor violating τ^- decays into $\ell^-\eta$, $\ell^-\eta'$ and $\ell^-\pi^0$, Phys. Lett. B **648**, 341 (2007).

[1626] B. Aubert *et al.* (*BABAR* Collaboration), Search for lepton flavor violating decays $\tau \to \ell^- K_S^0$ with the *BABAR* experiment, Phys. Rev. D **79**, 012004 (2009).

[1627] Y. Miyazaki *et al.* (Belle Collaboration), Search for lepton flavor violating τ^- decays into $\ell^- K_s^0$ and $\ell^- K_s^0 K_s^0$, Phys. Lett. B **692**, 4 (2010).

[1628] Y. Miyazaki *et al.* (Belle Collaboration), Search for lepton-flavor-violating τ decays into a lepton and an $f_0(980)$ meson, Phys. Lett. B **672**, 317 (2009).

[1629] B. Aubert *et al.* (*BABAR* Collaboration), Improved limits on lepton flavor violating τ decays to $\ell\phi$, $\ell\rho$, ℓK^* and $\ell\bar{K}^*$, Phys. Rev. Lett. **103**, 021801 (2009).

[1630] N. Tsuzuki *et al.* (Belle Collaboration), Search for lepton-flavor-violating τ decays into a lepton and a vector meson using the full Belle data sample, J. High Energy Phys. 06 (2023) 118.

[1631] B. Aubert *et al.* (*BABAR* Collaboration), Search for lepton flavor violating decays $\tau^\pm \to \ell^\pm\omega(\ell = e,\mu)$, Phys. Rev. Lett. **100**, 071802 (2008).

[1632] J. P. Lees *et al.* (*BABAR* Collaboration), Limits on τ lepton-flavor violating decays in three charged leptons, Phys. Rev. D **81**, 111101 (2010).

[1633] K. Hayasaka *et al.* (Belle Collaboration), Search for lepton-flavor-violating τ decays into three leptons with 719 million produced $\tau^+\tau^-$ pairs, Phys. Lett. B **687**, 139 (2010).

[1634] G. Aad *et al.* (ATLAS Collaboration), Probing lepton flavour violation via neutrinoless $\tau \to 3\mu$ decays with the ATLAS detector, Eur. Phys. J. C **76**, 232 (2016).

[1635] B. Aubert *et al.* (*BABAR* Collaboration), Search for lepton-flavor and lepton-number violation in the decay $\tau^- \to \ell^\mp h^\pm h'^-$, Phys. Rev. Lett. **95**, 191801 (2005).

[1636] Y. Miyazaki *et al.* (Belle Collaboration), Search for lepton-flavor-violating and lepton-number-violating $\tau \to \ell hh'$ decay modes, Phys. Lett. B **719**, 346 (2013).

[1637] Y. Miyazaki *et al.* (Belle Collaboration), Search for lepton and baryon number violating τ^- decays into $\bar{\Lambda}\pi^-$ and $\Lambda\pi^-$, Phys. Lett. B **632**, 51 (2006).

[1638] D. Sahoo *et al.* (Belle Collaboration), Search for lepton-number- and baryon-number-violating tau decays at Belle, Phys. Rev. D **102**, 111101 (2020).

[1639] R. Aaij *et al.* (LHCb Collaboration), Searches for violation of lepton flavour and baryon number in tau lepton decays at LHCb, Phys. Lett. B **724**, 36 (2013).